FINAL REPORT

MITIGATING THE IMPACTS OF UNCONTROLLED AIR FLOW ON INDOOR ENVIRONMENTAL QUALITY AND ENERGY DEMAND IN NON-RESIDENTIAL BUILDINGS

NYSERDA Agreement #6770
DOE Contract #DE-FC-36-02GO12012

April 26, 2007

Submitted to:

New York State Energy Research and Development Authority
17 Columbia Circle
Albany, NY 12203-6399

Submitted by:

Hugh I Henderson, Jr.
Adam Walburger
CDH Energy Corp.
PO Box 641
132 Albany Street
Cazenovia, NY 13035
(315) 655-1063

James B. Cummings
Chuck Withers
Lixing Gu
Florida Solar Energy Center
1679 Clearlake Road
Cocoa, FL 32922-5703
(321) 638-1403

Jensen Zhang
Mark Bomberg
Mikael Salonvaara
Syracuse University
Link Hall
Syracuse, NY 13244
(315) 443-1366

Terry Brennan
Mike Clarkin
Camroden Associates, Inc.
7240 East Carter Rd.
Westmoreland, NY 13490
(315) 336-7955

EXECUTIVE SUMMARY

This multi-faceted study evaluated several aspects of uncontrolled air flows in commercial buildings in both Northern and Southern climates. Field data were collected from 25 small commercial buildings in New York State to understand baseline conditions for Northern buildings.

Laboratory wall assembly testing was completed at Syracuse University to understand the impact of typical air leakage pathways on heat and moisture transport within wall assemblies for both Northern and Southern building applications. The experimental data from the laboratory tests were used to verify detailed heat and moisture (HAM) simulation models that could be used to evaluate a wider array of building applications and situations.

Whole building testing at FSEC's Building Science Laboratory (BSL) systematically evaluated the energy and IAQ impacts of duct leakage with various attic and ceiling configurations. This systematic test carefully controlled all aspects of building performance to quantify the impact of duct leakage and unbalanced flow. The newest features of the EnergyPlus building simulation tool were used to model the combined impacts of duct leakage, ceiling leakage, unbalanced flows, and air conditioner performance. The experimental data provided the basis to validate the simulation model so it could be used to study the impact of duct leakage over a wide range of climates and applications.

Field Test Results

CDH Energy and Camroden Associates tested 25 small commercial buildings in NY to establish a baseline. The sample of buildings in this field study were larger on average than the 69 Florida buildings in the study completed by Cummings et al (1996). However, the range of building types included in this sample were generally in line with the distribution of building types identified in the 1999 CBECS study for the Northeast region.

The average ACH50 for NY buildings was 11.4 air changes per hour, compared to 16.7 air changes per hour in the Florida study. The lower ACH50 for the NY buildings appears to have been due to the smaller number of buildings without an air barrier at the ceiling or roof (16% in NY compared to 42% in Florida). The average building in this study was depressurized by about 1.1 Pa, which is very similar to the FSEC findings for Florida Buildings.

Duct leakage measurements were taken on 14 different systems from 8 different NY buildings. The average and median duct leakage (ELA-25) normalized for air conditioner tonnage was 12.8 and 7 in^2 per ton. The average values from the Florida and California field studies (Delp et al 1998) were 12.1 and 17.1, respectively. The NY buildings showed a wide degree of variation in duct leakage rates, similar to what had been observed in the other field studies.

At three of the tested buildings we identified and implemented improvements to reduce energy use and/or improve comfort. The impact of these improvements was quantified by continuously monitoring building energy use and analyzing monthly utility bills.

A major lesson from all the tested buildings was to confirm the importance of designing and implementing an effective air barrier for the building. At a few of these buildings that were relatively new, seemingly-minor decisions made during construction had a significant impact on building energy use. For instance, installing gypsum board (or some other air barrier) above the t-bar ceiling at Sites 1, 2, 21 and 22 during construction would have created an effective air barrier at the ceiling for a modest cost. Once construction was complete and the building is occupied – with the ceiling tiles and electrical/mechanical systems in place – it is prohibitively disruptive and expensive to install an air barrier.

A somewhat surprising finding from the three mitigated buildings in this section was significant energy savings that can be provided by relatively minor, low-cost improvements. At two single-story commercial buildings, replacing and/or repositioning fiberglass batts in the ceiling had significant energy impacts. The annual heating energy savings from fixing major voids in the building envelope were 44% at Site 1 and 37% at Site 2. We found missing or fallen fiberglass batts in two of 25 sites, or 8% of the buildings in this New York sample. At an historic, 3-story building, we used spray foam as a low-cost way to seal air leaks in a poorly-insulated attic floor and the mechanical room above an elevator shaft. These modest, low-cost improvements resulted in annual heating energy savings of about 25%.

<u>Wall Assembly Testing and Analysis</u>

The laboratory testing and analysis at Syracuse University evaluated the impact of air leakage on the performance of various wall assemblies. Performance issues include understanding the impact of leakage on the thermal performance of the wall assembly as well as durability and IAQ issues related to condensation risk and mold formation inside the wall.

Two different wall assemblies were selected based on the field experiences in NY and Florida – steel frame and concrete masonry units. Care was taken to construct the wall assemblies to be representative of normal construction practices, including workmanship related to window installation and sealing. The wall assemblies were tested in the Full-Scale Coupled Indoor/Outdoor Environmental Simulator (C-I/O-ES) at Syracuse University. Indoor and outdoor environmental conditions were imposed on the wall to represent climatic conditions typical of Northern and Southern small commercial buildings. The laboratory measurements focused on understanding the impact of air leakage on temperature and humidity conditions inside the wall assembly.

The laboratory testing demonstrated that detail elements within the wall assembly contributed significantly to thermal bridging. Steel studs – especially those in exposed areas such as window sill or plate – can significantly affect the temperature profile within the assembly. Changing the airflow direction within the wall (by changing the direction of pressurization) can have a significant impact localized temperatures within the wall assembly.

Although, the impact of airflows within the wall does not significantly change the surface temperature of the steel studs, it significantly affects the conditions within the wall assembly and can result in the high relative humidities within the insulation cavity. As warm moisture laden air flows through the wall, surfaces can be cooled below the dew point so that condensation occurs.

The thermal mass effect within a masonry wall appears to be very small. The temperature measurements indicated that steady state conditions were achieved relatively quickly.

The simulation model LATENITE was used to predict the impact of air leakage on temperature and humidity conditions within a wall assembly for a wide array of climatic conditions. The simulations confirmed that walls with steel studs have more condensation risk at locations where the thermal bridging occurs at lower indoor air temperatures under summer conditions. In the winter, moisture intends to accumulate closer to the exterior side of the wall assemblies. Leaky walls with an impermeable interior surface such as vinyl wall paper can have excessive moisture accumulation behind the interior surface material, resulting in favorable conditions for mold growth.

Whole Building Testing and Analysis

Whole building testing at FSEC's Building Science Laboratory (BSL) systematically evaluated the airtightness, infiltration, relative humidity, energy, and peak demand impacts of duct leakage – during the cooling season – with various attic and ceiling space configurations. The two primary independent variables were the amount of attic venting and the amount of duct leakage. Data were collected with the building and ductwork in 16 different configurations. Half the configurations used an unvented attic while the other half used a vented attic. Duct leaks of 0, 15 and 30% were imposed on both the return and supply sides of the air distribution system. Test data were collected over several hundred days during 2004, 2005, and 2006.

The building was moderately airtight with the unvented attic configuration (ACH50 of 5.2) and much leakier with the vented attic configuration (ACH50 of 29). With no attic venting, the average infiltration rate was about 0.15 ach, with or without duct leakage. With the attic vented, the average infiltration rate was about 0.5 ach without duct leakage and 1.5 ach with 30% duct leakage (both supply and return).

The attic dry bulb temperature was about 1^{o}F warmer with the unvented attic configuration. Attic humidity levels were dramatically impacted by attic venting. The attic dew point temperature averaged 54^{o}F when unvented and 72^{o}F when vented. Indoor dew point temperatures were 55^{o}F for unvented attic case and 60^{o}F in the vented configuration.

Cooling energy use increased as a result of attic venting and as a result of duct leakage. Attic venting increased cooling energy use by an average of 12% for a range of duct leak configurations. Duct leakage increased cooling energy use by 20% to 35% for various duct leaks for the unvented attic. Duct leakage increased cooling energy use by 20% to 50% for various duct leaks for the vented attic. Peak cooling demand increased by 10% to 40% for the unvented attic and by 12% to 58% for the vented attic, for various duct leak configurations.

The AirflowNetwork model was recently incorporated into Version 1.3 of EnergyPlus as part of this project. This new feature provides the means to simulate the impacts of duct leakage, unbalanced air flows, and attic space interactions in an air conditioned building. An EnergyPlus model of the laboratory building was developed to simulate the performance of duct leakage under the various tested scenarios. The simulation model compared reasonably well with the experimental data, properly predicting space and attic humidity levels as well as air conditioner energy use. The model was then used to simulate the impacts of various levels of supply and return duct leakage for vented and unvented attics in prototypical 2,000 ft^2 office building located in several different climates (Tampa, Miami, Houston, New Orleans). The simulation results confirmed the findings from the laboratory testing. This new model provides the means to evaluate a wider array of building options in the future.

Recommendations

A common theme from the field study portion of the project is the need create an effective air barrier at a modest cost with minimal disruption to the building occupants. Weatherization and insulation contractors need better information, approaches and diagnostic tools to identify and address air barrier problems. New commercially-available materials – such as small polyurethane spray foam kits (with 200-500 board feet of foam) – offer the potential to cost effectively address these issues. Developing practical and cost effective ways to use these new materials can provide significant energy savings in existing buildings.

There also may be potential to use lower cost diagnostic tools, such as infrared thermometers, to diagnose and identify problem areas in buildings instead of more expensive tools such as infrared cameras. Developing low cost means to quickly diagnose and identify opportunities to improve building performance will be of great use to building practitioners.

Both the wall assembly and whole building testing efforts were complemented by efforts to develop and validate computer simulation approaches. In both cases these simulation models can be used in future work to understand the impact of uncontrolled air flows in other building applications. The LATENITE model can be used to quantify the impact of air leakage on the durability, IAQ risks, and energy performance of wall assemblies in wide array of applications. Similarly, the newly developed AirflowNetwork features of EnergyPlus provide the means to evaluate the impacts of duct leakage and unbalanced flows in a wide array of commercial and residential building applications.

GLOSSARY

ACH50	Air change rate (ACH) per hour when building is pressurized by 50 Pascals (Pa).
ADS	Air Distribution System. An early version of the AirflowNetwork model developed for EnergyPlus and used for the simulation analysis in Section 7.
BEESL	Building Energy and Environmental Systems Laboratory at Syracuse University.
BSL	Building Science Laboratory at the Florida Solar Energy Center.
CBECS	Commercial Building Energy Consumption Survey. National survey completed by Energy Information Agency every 4 years.
C-I/O-ES	Coupled Indoor/Outdoor Environmental Simulator in the BEESL at Syracuse University.
CFM50	Air flow rate (in cfm) when pressurized by 50 Pascals (Pa) with respect to outdoors. Usually applied to building envelopes.
CFM25	Air flow rate (in cfm) when pressurized by 25 Pascals (Pa) with respect to surroundings. Usually applied to ducts.
CMU	Concrete Masonry Unit. Also concrete block.
ELA	Equivalent leakage area (in square inches). Area of a single orifice opening that provides equivalent air flow rate at pressure difference of 4 Pa. See equation 2-5.
ELA-25	Similar to ELA above but with a reference pressure of 25 Pa, which is more representative of ductwork.
FSEC	Florida Solar Energy Center
IEQ	Indoor environmental quality
IAQ	Indoor air quality
J	Joule
MBtu	1000 Btu
MMBtu	1,000,000 Btu
OSB	Oriented Strand Board. Sheathing commonly used for building walls. Comes in 4 ft by 8 f t sheets.
Pa	Pascal (unit of pressure)
RH	Relative Humidity
RTF	Runtime Fraction. Portion of a period when equipment (air conditioner, fan or furnace) operates. 0 or 0% = off, 1 or 100% = operates continuously.
SPF	Spray Polyurethane Foam. Closed cell foam used to seal air leaks.
UAF	Uncontrolled air flow. Alternatively Unplanned or Unintended air flow.

TABLE OF CONTENTS

LIST OF FIGURES

LIST OF TABLES

1. Introduction

1.1. Background

This project builds on previous field research in Florida that has demonstrated the significant impact that uncontrolled air flows (UAFs) have on indoor environmental quality (IEQ) and energy use in small commercial buildings – a large but poorly understood segment of the nation's building stock. The goal of this project was to extend that research to a national scale by assessing the importance of UAFs in a sample of 25 commercial buildings in New York State. The differences in climate and construction techniques between New York and Florida are expected to bound the range conditions typically found on a national basis. The project also completed a series of carefully-controlled full-scale laboratory experiments and computer simulations to further understand the nature and impact of UAFs on air quality, occupant comfort, and energy use. The research results from this project provide the basis for developing improved construction and diagnostic techniques that will ultimately result in higher quality and more energy efficient buildings that result in lower peak demand on the nation's electric system.

Research at the Florida Solar Energy Center (FSEC) has shown that commercial buildings are three times "leakier" than residential buildings and that unintended interactions between the forced air systems, the building envelope, and the interior zones have substantial impacts on IEQ. Florida's research found that 69 of the 70 non-residential buildings tested exhibited substantial "uncontrolled air flow" that resulted in building problems (Cummings et al 1996). Repair of 20 of these buildings resulted in cooling energy savings and demand reductions of 15%, and in many cases substantial improvement of indoor temperature and relative humidity.

This project extended the Florida work to a national basis by completing a similar field survey of small commercial buildings in NY State. New York buildings are expected to exhibit some differences in construction details that are typical of buildings in the Northern US. Furthermore, it is expected that there will be substantial differences in the magnitude and form that uncontrolled airflow takes in New York compared to Florida because of climate. It is important, therefore, to characterize the building envelope and HVAC system elements of New York construction that contribute to uncontrolled air flow, and perform field testing and monitoring to reveal the climate-specific response.

The research also used newly-constructed laboratory facilities at FSEC and Syracuse University (SU) to carefully quantify the physical mechanisms driving UAFs as well as their impacts on energy use, IEQ and building durability. FSEC's whole-building test lab focuses on interactions between the HVAC system, ductwork, and the building envelope. SU's Coupled Indoor/Outdoor Environmental Simulator (C-I/O-ES) test facility focuses on the dynamic impacts of UAFs in built-up wall assemblies. The experimental tests in both facilities were designed and evaluated considering the building characteristics and measured results observed in the New York and Florida field surveys. Both whole building and wall assembly computer simulations were developed and verified using the experimental results in order to extend the findings over a wider array of climates and configurations.

The results of this research were disseminated to the building industry by refining the practitioner training programs already underway at FSEC. The training materials were adapted for use in New York to further the practical application of this research. Two one-day seminars were given in April 2006.

1.2. Project Objectives

The overall objective of this project was to transfer work and knowledge that has been done on uncontrolled air flow in non-residential buildings in Florida to a national basis.

This objective was implemented by means of four tasks:

- Field testing and monitoring of uncontrolled air flow in a sample of New York buildings
- Detailed wall assembly laboratory measurements and modeling
- Whole building experiments and simulation of uncontrolled air flows
- Develop and implement training on uncontrolled air flows for Practitioners in New York State.

1.3. Report Organization

This report is organized into the following sections:

Part II – Field Testing
Section 2 describes the field testing that was completed at 25 commercial buildings in NY. Section 3 describes improvements that were implemented at 3 of these buildings to mitigate the impact of UAFs. Measured performance data are used to show the energy and IAQ impact of these retrofits.

Part III – Wall Assembly Performance
Section 4 describes the laboratory testing that was completed in the C-I/O-ES at Syracuse University to quantify the performance of wall assemblies. Section 5 presents simulation results related to wall assembly performance.

Part IV – Whole Building Performance
Section 6 describes the whole building testing that was completed at the Building Science Laboratory (BSL) at FSEC. Section 7 presents simulated performance results using the Air Distribution System model that has recently been added to EnergyPlus.

Part V – Conclusions and Recommendations
Section 8 describes the training that was developed for New York.

Section 9 provides overall conclusions for this study and makes recommendations for future work.

1.4. References

Cummings, J.B., C.R. Withers, N. Moyer, P. Fairey, and B. McKendry. 1996. "Uncontrolled Air Flow in Non-Residential Buildings; Final Report", FSEC-CR-878-96, Florida Solar Energy Center, Cocoa, FL, April, 1996.

2. Field Testing Commercial Buildings

This section describes the field testing that that was completed at 25 commercial buildings in New York State. The testing protocols completed in these buildings were very similar to the FSEC study (Cummings et al 1996).

2.1. Overview

The purpose of field testing was to collect "baseline" data on small commercial buildings that are typical of the building stock in the Northeastern U.S. Previous studies of building airflows, envelope leakage, and duct leakage have been concentrated in Florida (Cummings et al 1996) and California (Delp et al 1998). Building construction practices in the Northeast are thought to be different than in these other regions since heating is the predominant concern.

The 1999 CBECS[1] database was used gauge the distribution of commercial buildings that should be included in the field test. The goal was to understand the range of small commercial buildings that are typical in Northeast Region, which includes New York, New Jersey, Pennsylvania, and the New England States. This study focused on commercial buildings under 20,000 ft^2.

Buildings under 20,000 ft^2 in the Northeast are generally older and tend to have more floors than other US regions. Of all small commercial buildings in the US, about 30% have been constructed since 1980. In the Northeast this portion of the population drops to 23%. Table 2-1 summarizes the percentage for each building type determined for small commercial buildings in the CBECS Northeast region. Figure 2-1 summarizes the distribution graphically also indicates building age. Based on these percentages, we established targets for types of buildings to recruit for this field study. Table 2-1 also lists the ACTUAL test sites that were included in this study. Generally, the buildings recruited for this study reasonably reflected the targeted categories. Though the sample did include more offices and less retail buildings than we had originally targeted.

[1] CBECS stands for Commercial Building Energy Consumption Survey. The 1999 survey included 5430 commercial buildings, or which 903 were in the Northeast. More details about CBECS is available at www.eia.doe.gov/emeu/cbecs/contents.html.

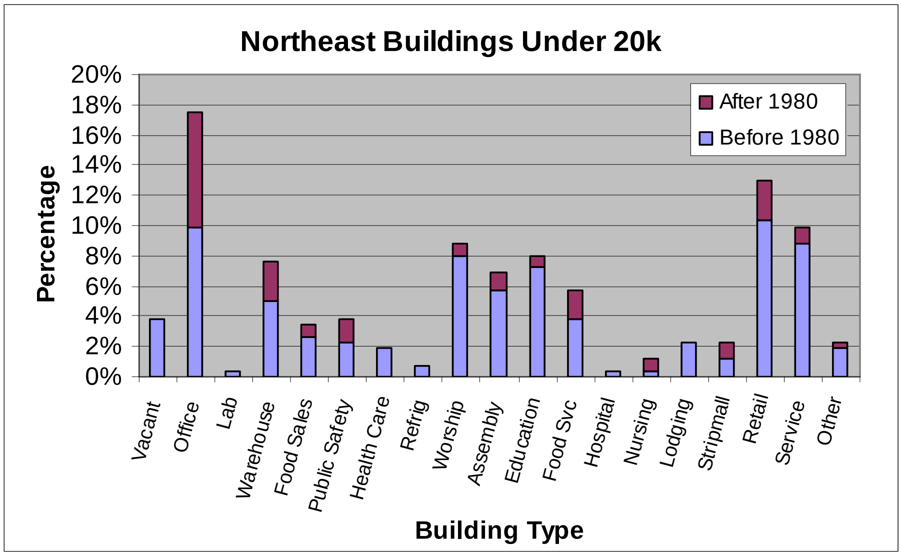

Figure 2-1. Distribution of Buildings Under 20,000 ft^2 in Northeast (CBECS 1999)

Table 2-1. Comparison of Target and Actual Test Sites

Category (% of buildings constructed since 1980)	TARGET No. of Test Sites	ACTUAL No. of Test Sites	CBECS Subcategory (PBA+)
Offices (34%)	8-9	11 (44%)	Administrative/Professional office, Bank/Financial, Doctor/Dentist office, Government office, Other office
Retail/Strip Mall (17%)	4-5	2 (8%)	Auto dealership/Showroom, Other retail, Store, Strip shopping center
Warehouse (12%)	3-4	1 (4%)	Non-refrigerated warehouse
Food Service (8%)	2-3	3 (12%)	Restaurant/Bar/Fast food/Cafeteria
Public Safety (7%)	2-3	2 (8%)	Fire station/Police station, Other public order and safety
Service (5%)	1	1 (4%)	Auto service/Auto repair, Dry cleaner/Laundromat, Other service, Repair shop
Assembly (5%)	1	2 (8%)	Entertainment (Theater/Sports arena/Nightclub), Library/Museum, Other public assembly, Recreation (Gymnasium/Bowling alley/Health club), Social meeting center/Convention center
Worship (3%)	0-1	1 (4%)	Religious worship
Education (3%)	0-1		College/University, Elementary/Middle/High school, Other education, Preschool/Daycare
Food Sales (3%)	0-1	1 (4%)	Grocery store/Food market, Other food sales or service
Nursing (3%)	0-1	1 (4%)	Nursing home/Assisted living
Total	25	25	

Notes: All the subcategories listed above were found in the database for Northeast buildings at least once.
We combined the Retail and Strip Mall CBECS categories

2.2. *Field Measurements and Testing Approach*

This section describes the data collection, analysis and reduction techniques used at the 25 test sites included in this field study. It was not always possible to complete each of the test protocols described below at every test site.

2.2.1. Blower Door Testing

Blower door testing was used to establish the relationship of flow and pressure for the building envelope. From this flow-pressure data, various leakage statistics can be determined. At a test site, one of more blower doors was installed depressurize the building. For a test we typically:

- closed all exterior doors and windows,
- opened all interior doors,
- turned off HVAC equipment and exhaust fans,
- block off fresh air intakes.

In this study we typically used two BD3 series blower doors from the Energy Conservatory (owned by CDH Energy and Camroden Associates) that were each capable of providing up to 6,000 cfm of airflow. Each BD3 had an A, B or C ring to provide lower airflow rates. We typically used a two-channel DG700 micromanometer from Energy Conservatory (owned by CDH) to measure pressures and convert them to airflows.

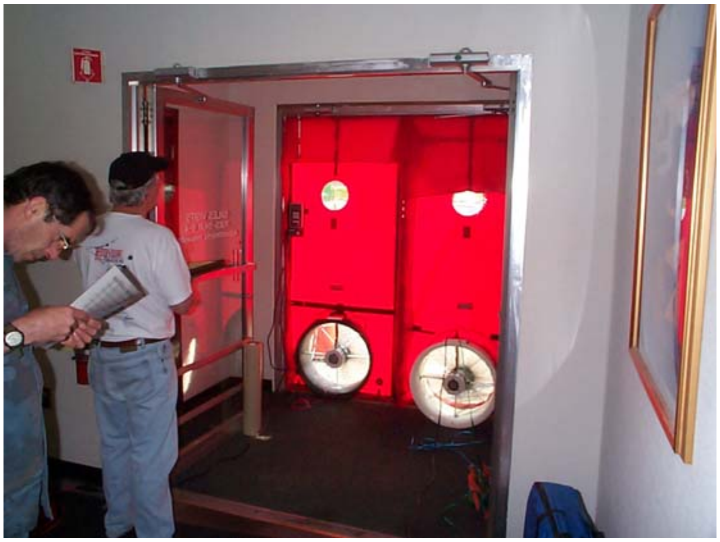

Figure 2-2. Two Blower Doors Setup to Measured Building Leakage (Site 4)

The blower door is used to depressurize the building to various levels by changing the fan speed. At each fan speed, the airflow and building pressure (relative to outdoors) is recorded. By collecting multiple readings, sufficient data can be collected and fit to a function of the form:

$$Q = K(\Delta p)^n \quad \text{(eqn. 2-1)}$$

Where Q is the airflow rate (cfm) and Δp the building pressure (Pa). The measured data were fit to the function using linear regression by transforming equation 2-1 into linear form with a log-log transform on the data:

$$\log(Q) = \log(K) + n \cdot \log(\Delta p) \qquad \text{(eqn. 2-2)}$$

or

$$\mathrm{Y} \quad = \quad \mathrm{b} \quad + \mathrm{m} \cdot \mathrm{X}$$

Linear regression analysis in a spreadsheet can then be used to determine the model coefficients K and n and shown in Figure 2-3 below.

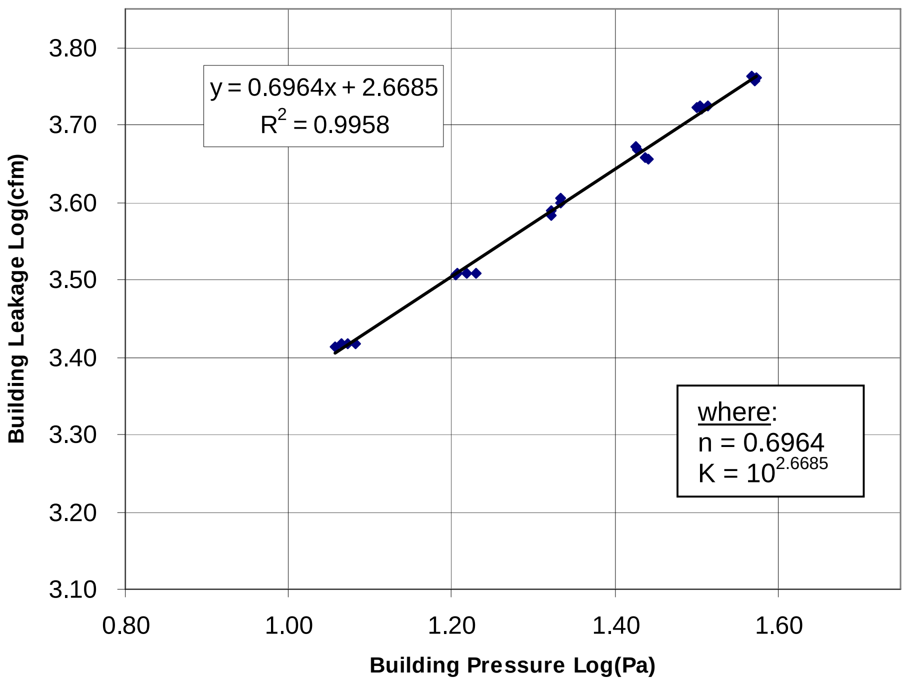

Figure 2-3. Example of Linear Regression Analysis of Log-Log Data to Determine K and n

Once K and n are known for a given building, the following air leakage statistics can be determined:

Air Changes per Hour at 50 Pa (ACH50). The air changes per hour of a building at pressure difference of 50 Pa. This metric indicates the relative leakiness of the building envelope at a pressure much higher than is typically seen with normal building operation. This equation can be used to estimate the leakage rate at 50 Pa even if that pressure could not be achieved during the test.

$$ACH50 = \frac{60 \cdot K(50)^n}{V} \qquad \text{(eqn. 2-3)}$$

Equivalent Leakage Area (ELA). The area of a single "hole" or opening – equivalent to a square edge orifice with an exponent of 0.5 – that would provide the same leakage flow rate as all the leaks in a building at the reference pressure difference (e.g., 4 Pa). The ELA is defined by:

$$Q = ELA \cdot \sqrt{\frac{2\Delta p_{ref}}{\rho}} \cdot \left(\frac{\Delta p}{\Delta p_{ref}} \right)^{n} \qquad \text{(eqn. 2-4)}$$

Where Δp_{ref} is the reference pressure corresponding the ELA (usually 4 Pa for a building; 25 Pa for ductwork). Equation 2-5 below finds the ELA from K, n and Δp_{ref} by combining equations 2-1 and 2-4. The ELA equation below is in units of square inches and assumes K (and Q) are in units of cfm with air near 60ºF.

$$ELA = 0.7316 \cdot K (\Delta p_{ref})^{n-0.5} \sqrt{\frac{1.2}{2}} \qquad \text{(eqn. 2-5)}$$

Significant confusion occurs when relating these statistics to building volume and building surface area. Our conventions for this field study are summarized below:

- Building Volume. The building volume is the gross, occupied volume of the building, minus the exterior wall thickness. Basements and attics are only included when they are conditioned, occupied spaces.

- Building Surface Area. The surface area of the gross, occupied volume of the building. Only above-ground surfaces are included.

2.2.2. Other Methods to Estimate Envelope Leakage

At some of the test sites, it was not possible to shut down the HVAC system to complete a building pressurization test. In other cases the building was simply too big to perform a blower door test. In these cases, we were sometimes able to use a single measured data point, and obtain a value for K by assuming a value for "n" in equation 2-1 (we usually assumed n=0.65). The technique was used to find the leakage statistics at Sites 6, 7, 9 and 24, where we were able to accurately measure the net air airflows into the building as well as the operating pressure.

2.2.3. Pressure Mapping

A key aspect of determining the impact of uncontrolled air flows is to understand the distribution of pressures in a building. Pressure mapping provides qualitative and quantitative information on the driving pressures in a building. We also used pressure mapping when the building was depressurized with the blower door to qualitatively indicate the location of leaks within the building. Each of these approaches is described below. We typically used to DG700 (owned by CDH) or a DG2 (owned by Camroden) for these measurements.

Pressure Mapping with Blower Door ON. To implement this test, the building is normally depressurized with all the interior doors open in order ensure uniform pressure differences are maintained across the building envelope. The first step in pressure mapping is to measure pressures at various locations on the exterior to confirm uniform pressures are maintained across the envelope. The next step is to close interior doors, one at a time, and measure the pressure difference across each door (see Figure 2-4). This technique provides the means to understand where the major leakage paths are located. If the pressure difference between the main zone and the sub-zone are large relative to the building pressure, that indicates that the zone is closer to ambient pressure and probably contains major leakage paths. This process is repeated for each building zone as well as for the ceiling plenum, attic space and other sections of the building.

Pressure Mapping with Normal Building Operation. Pressure mapping can also be used to quantify the driving pressures when the building operates “normally”. Normal operation means that HVAC equipment is configured to provide ventilation and space conditioning as required, and the exhaust fans and AHUs are set to their normal operating state. In many commercial buildings there can be multiple operating states depending on building occupancy, process operations, economizer operation, or the degree of thermal loading. Generally we attempted to measure pressures with the building in the one or two most common operating states for the day of testing. We typically closed interior doors to understand the degree of supply-return flow imbalance with the doors closed.

Taking pressure readings under a closed office door (Site 12)

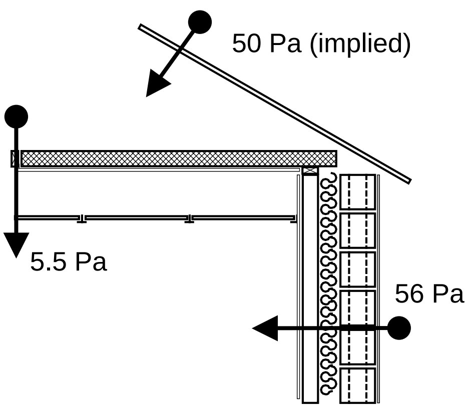

Measured pressure differences across walls and ceiling while depressurized (Site 4)

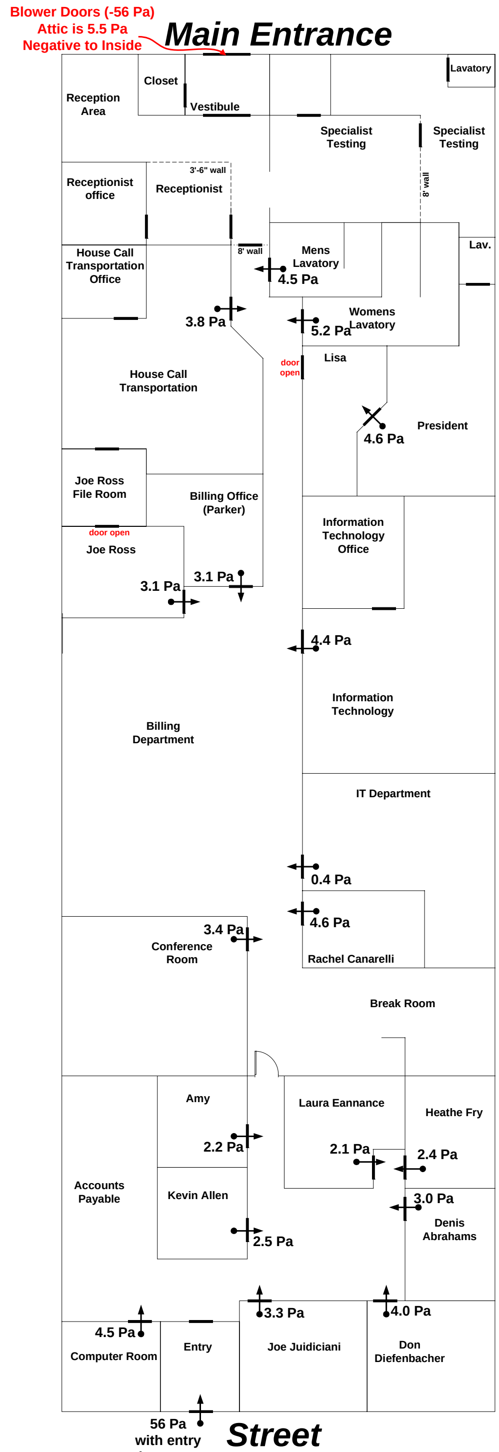

Measured pressure differences while depressurized (Site 4)

Figure 2-4. Pressure Mapping with Blower Door Depressurizing Building

2.2.4. Measuring Airflow Rates

Another goal of this project was to quantify the airflow rates in each building. The flow rates of interest included supply airflows, returns airflows, ventilation airflows (outdoor air), and exhaust airflows. For each building we attempted to measure the net ventilation rate of the building (ventilation minus exhaust) as well as total supply and return airflow rates. Several methods were used to determine airflow rates, which are listed below. We also measured fan power where possible in order to determine the fan power per unit airflow for the different HVAC systems.

Flow Hood Measurements. A Shortridge compensated flow hood (see Figure 2-5) was used to measure airflows at supply and return diffusers up to 2,500 cfm. The compensated hood includes a restricting mechanism to impose a known pressure drop inside the hood. By taking two flow readings the hood is able to predict the diffuser flow with zero static pressure at the flow hood inlet. This process "compensates" for the flow restriction imposed by adding the hood over a diffuser. In all cases we used the compensated flow reading.

Using compensated flow hood to measure return air flow rates (Site 2, portion of register is blocked off)

Figure 2-5. Air Flow Measurements with Compensated Flow Hood

Velocity Measurements by Equal Area Method. In many instances we measured air flows in a duct using a hot-wire anemometer (TSI VelciCalc 8360). This method requires that holes be drilled in the duct (see Figure 2-6) to take velocity readings at multiple points according to the equal area method. The TSI probe in this case records the velocity in standard feet per minute so the resulting airflow in is standard cfm. The figure below shows two examples where this method was used.

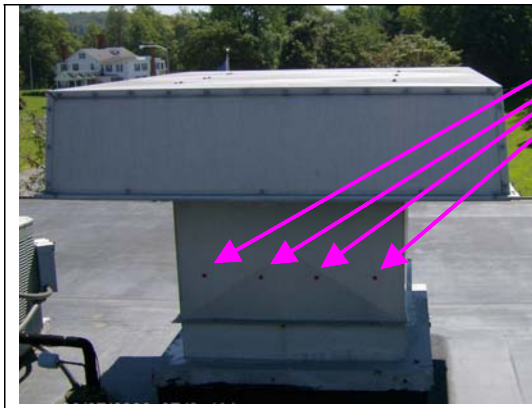

Multiple velocity readings taken with hot-wire anemometer according to the equal area method (Site 24)

Building Section:	Green
MUA Unit #	2
Duct Length	34 in
Duct Width	34 in

	4 1/4"	12 3/4"	21 1/4"	29 3/4"	Average
4 1/4"	135	65	125	50	93.8
12 3/4"	230	200	210	55	173.8
21 1/4"	120	210	120	60	127.5
29 3/4"	85	205	45	45	95
					122.5 ft/min
					983.4 SCFM

Cardboard "shroud" added to ventilation inlet to measure airflow with hot wire anemometer by equal area method (Site 6). Measurement holes drilled in cardboard. In this case the cardboard "shroud" was only 6-8 inches deep, so the reading only provided an approximate indication of the ventilation flow (without greatly impacting the inlet geometry).

Ventilation Airflow		
Opening width	33 inches	Sep-03
Opening height	73 inches	Test 1
		Time Const. = 1

	4.5"	12.5"	20.5"	28.5"
5.5"	850	730	680	480
13.5"	780	515	390	350
21.5"	575	500	420	300
29.5"	815	490	410	470
37.5"	900	490	410	420
45.5"	870	480	440	390
53.5"	825	600	420	460
61.5"	940	580	430	440
69.5"	900	825	530	520

Average	572.9 SFPM
Area	16.7 ft^2
Air Flow	**9584 SCFM**

Figure 2-6. Air Flows Determined from Multiple Velocity Measurements by Equal Area Method

<u>Air Flow Readings Determined with "Duct Blaster"</u>. In many applications it is only possible to measure the air flow using a calibrated fan known as a duct blaster. Figure 2-7 shows two different examples. For the exhaust fan, a capture tent with a calibrated fan is added to over the fan outlet. The fan flow is varied until the pressure inside the tent is near zero (in some cases we were able to measure fan current and confirm that the same current was achieved with and without the tent installed). For airflow into a rooftop ventilation intake, we first measured the pressure at a location inside the fresh air hood, and then added the calibrated fan and varied its speed until the same pressure was achieved at the same point. Figure 2-7 shows an example of the flow-pressure curve developed in this case.

Roof-mounted exhaust fan (Site 7)

Same exhaust fan covered with "Capture Tent" with calibrated fans installed to measure flow-pressure response

Pressure in ventilation hood is measured before fan is installed. Then with fan installed, speed is varied to determine flow over a range of pressures (Site 6)

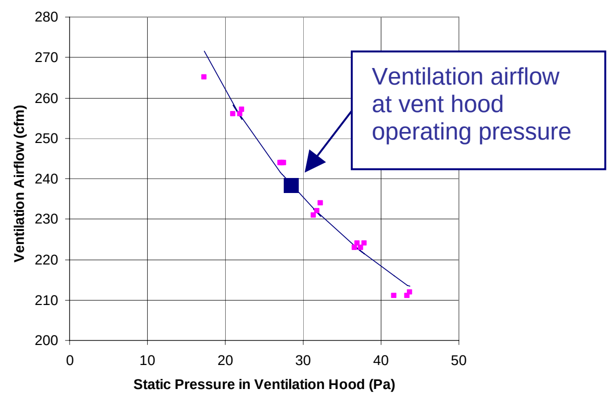

Figure 2-7. Air Flows Determined Using Calibrated Fan

2.2.5. Duct Leakage Testing

One of the most important factors driving uncontrolled air flows is duct leakage. For this study we sought to gather duct leakage data from number of the test sites. Duct leakage testing was one of the most time-consuming and difficult elements of this field test study. Therefore, we typically limited duct leakage testing to sites where testing was easily implemented and would provide clear results. Many cases we only tested a subset of the HVAC units at a site. In other cases, we tested duct leakage on units where all the ductwork was in the conditioned space (and would have no energy implications) in order to gather base line data.

Duct leakage testing is similar to building envelope testing except the focus is on the ductwork. Duct mask was installed to block all the diffusers. Depending on the system arrangement, the supply and return sides of the duct system were tested separately, or all the ductwork was tested together. In many cases the air handler unit (AHU) cabinet is included with the supply or return ductwork, in some cases it was included with both. The measured flow and pressure data were fit to equation 2-1 to determine K and n for each section of the ductwork. From these parameters it is possible to determine the air leakage rate and the leakage area (hole size) at the reference conditions. Generally, the reference pressure used for duct leakage is 25 Pa. However, the concept of a reference pressure does not work as well for ductwork. While the pressure inside a house is relatively uniform, the operating pressure in duct is maximum (or minimum) near the mechanical equipment (e.g., the fan) and near zero at the diffuser. Therefore it is difficult to use a single reference pressure in determining duct leakage. In practice a leak located near mechanical equipment is much more important than a leak near the diffuser. The commonly used leak statistics for ductwork ignore this issue applying equal importance to all leaks regardless of location. The leakage statistics commonly used for ductwork are summarized below.

Leakage at 25 Pa (cfm25 or Q_{25}). The duct leakage at 25 Pa is determined from K and n using a reference pressure of 25 Pa. The leakage value of Q_{25} is often normalized based on the surface area of the duct (cfm25 per 100 ft^2 of duct area) or per floor area (cfm25 per 1,000 ft^2 of floor area).

Equivalent Leakage Area at 25 Pa (ELA-25). The equivalent leakage area at 25 Pa is determined using equation 2-5 with a reference pressure of 25 Pa. The ELA-25 is expressed in square inches and can be normalized by dividing by the duct surface area (ELA-25 per 100 ft^2 of duct area).

SMACNA Leakage Class. SMACNA has defined a metric of duct leakage that is appropriate for high pressure duct. It uses a reference pressure of 1 inch (249 Pa) and divides by the duct surface area (Q_{249} per 100 ft^2 of duct area). The SMACNA Leakage Class is most appropriate for supply ducts in high pressure supply ducts, such as in a VAV system.

2.2.6. Measurements of Space Conditions

At many sites we installed battery-powered HOBO data loggers to measure temperature and humidity in the space. T/RH loggers were usually installed in 1 to 3 zones. Loggers were also installed to measure CO_2 levels in one of more locations. The CO_2 sensors were calibrated at several times throughout the study using a 0 ppm and 800 ppm reference gas. The T/RH and CO_2 loggers were typically configured to collect data at 15-minute intervals for the several weeks.

The data from these temperature sensors were used to verify temperature set points as well as to determine heating setback and cooling setup schedules. The T/RH data were used to track humidity levels in the space, which was of particular interest in the summer period. At many sites, outdoor humidity data from a nearby airport weather station was compared to the indoor humidity data to determine the humidity response characteristic.

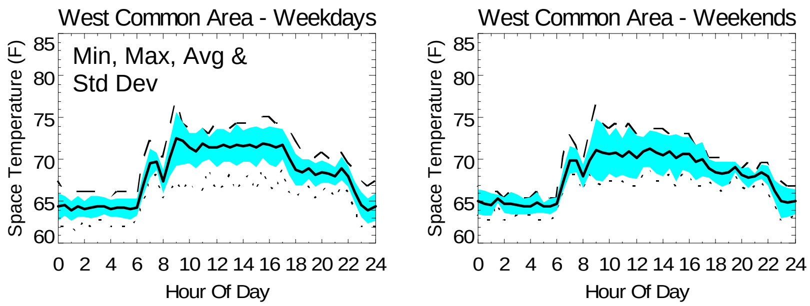

Space temperature data showing thermostat setback (Site 1)

HOBO T/RH battery-powered data logger

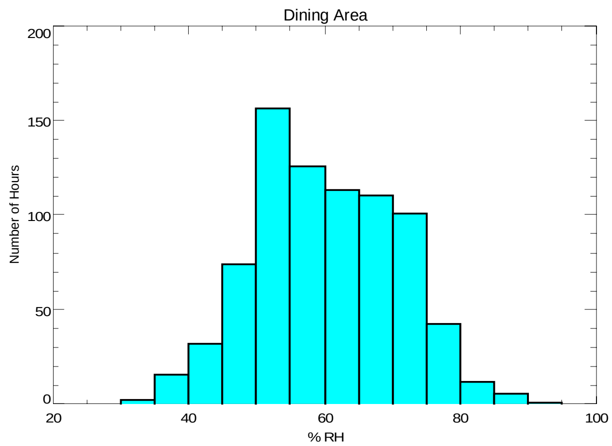

Distribution of space relative humidity levels in a summer period (Site 7)

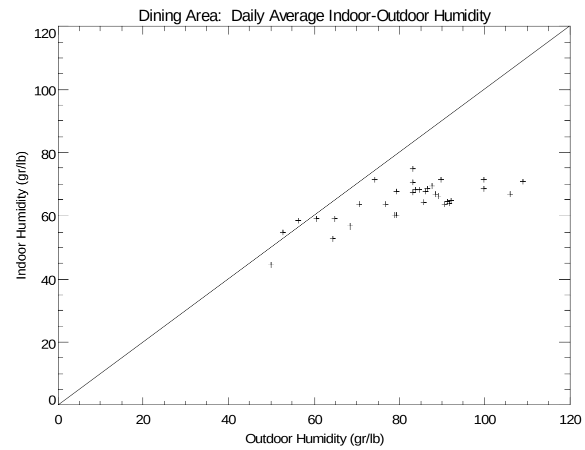

Comparing indoor and outdoor (absolute) humidity on a daily basis (Site 7)

Figure 2-8. Measuring and Analyzing Space Conditions (Temperature and Humidity)

2.2.7. Using CO_2 as a Tracer Gas

With data loggers installed to measure CO_2 concentration at 15-minute intervals, it was possible to infer the local infiltration rate by quantifying the CO_2 decay rate at some sites. For a CO_2 decay to accurately represent the infiltration or ventilation rate in a space, the following criteria must be met:

- the space is well mixed, with a uniformly decreasing CO_2 concentration,
- the CO_2 concentration starts from a high enough value to provide a strong signal,
- there is no occupancy (or additional CO_2 generation) during the decay period,
- all infiltration or ventilation comes from outdoors (i.e., not adjacent space).

If these criteria are met, then the decay rate is representative of the building air change rate. CO_2 can be added to the space by a large occupancy event or by artificially seeding the space with CO_2. The decay can be represented as

$$\frac{(C - C_o)}{(C_i - C_o)} = e^{-t \cdot \alpha} \qquad \text{(eqn. 2-6)}$$

Where C_i is the initial CO_2 concentration in the space and C_o is the concentration outdoors (or the final indoor concentration after several hours). Applying a log transformation, the data become linear and the coefficient α becomes the slope of the line, which can be determined by linear regression analysis of the data.

$1/\alpha$ is defined as the mean age of the air at the sensor location. If the all the criteria listed above are met, then α is effectively the air change rate per hour (ACH) of the space due to ventilation and/or infiltration.

Figure 2-9 shows the results of a CO_2 decay where the space was initially seeded with "industrial grade" CO_2 (obtained from a welding supply store). Care was taken to distribute the CO_2 though-out the space. The resulting ACH from the regression analysis was 0.35 air changes per hour, or 156 cfm, in this case. The ventilation rate measured for this space with a flow hood was 150 cfm.

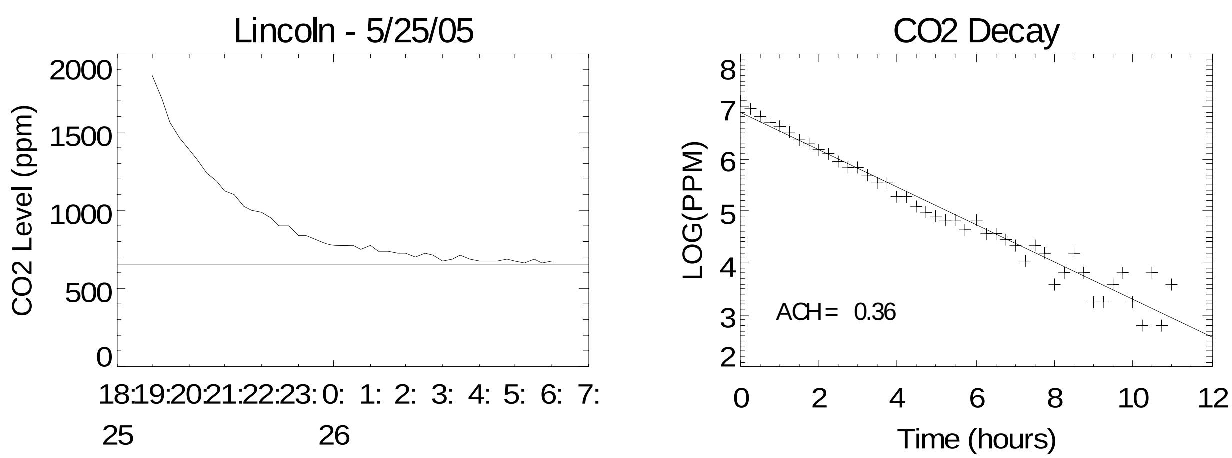

Figure 2-9. Using CO_2 as a Tracer Gas to Determine the Infiltration Rate (Site 16)

2.2.8. Utility Bill Analysis

Where possible we also gathered utility bill data from the site to determine building load lines as well as the annual energy use intensity per square foot of floor area. Load lines were developed by using daily average temperature data from the National Climatic Data Center (NCDC) to determine the average outdoor temperature for the utility billing period. NCDC data weather data were taken from the nearest weather station. Figure 2-10 shows how gas use varies with ambient temperature at a facility in Syracuse (Site 17). Daily weather temperature data from the Syracuse Airport were used to predict the temperature corresponding to each gas meter reading. The load line indicates significant information about the facility. Gas use shows a strong linear trend with temperature. Heating is required until the average daily temperature reaches 61°F or 62ºF. The facility also has baseline gas use of 4 therms per day for cooking and water heating.

Projecting the data to 0ºF, the facility uses about 110 therms per day, or 458 MBtu/h. At –20ºF, the linear model predicts that gas use increases to144 therms per day, or 600 MBtu/h (which is still only about ½ the boiler capacity at this site).

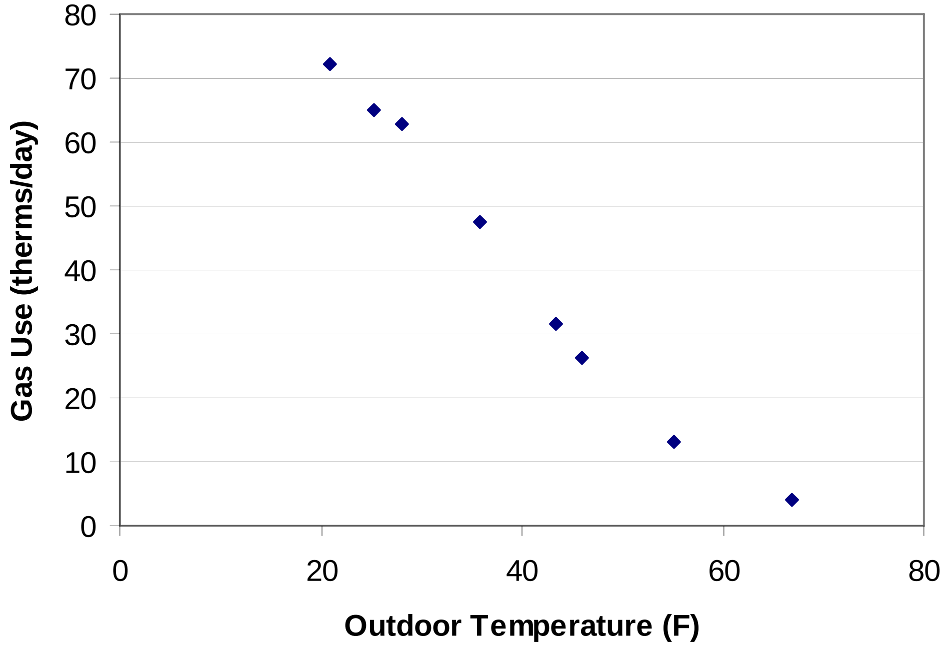

Figure 2-10. Heating Load Line for a Building with Gas Boiler (Site 17)

2.3. Summary of Building Characteristics

Twenty five different buildings were recruited to be part of this study. Buildings were recruited based on the following criteria:

- Satisfying the targeted building types from Table 2-1,
- Providing geographic diversity from around New York (excluding the metro NY areas),
- The building owner's willingness to participate in the study.

The sites were usually recruited by personnel from the project team (CDH Energy, Camroden, NYIEQ Center, etc.). In many cases the site personnel had a professional relationship with the team staff from past projects. We usually provided the site with a summary of their test results as well as any recommendations about changes or improvements they could make in their facility.

A detailed description and results summary for each test site is included as Appendix A in this report. The summary for each site includes from 10 to 60 pages and is identified by the page numbering system. For instance page A5-3 refers to the 3rd page of the summary for Test Site 5. Figures and tables in each site summary are also uniquely identified. The sites that were retrofitted or remediated also have information about that process in the written summary.

The first part of Appendix A (section A0) includes summary tables of the building characteristics data and measured results collected as part of this study. The tables in this section are in a format similar to the results in Appendix B of the FSEC Study (Cummings et al 1996).

Table 2-2 summarizes the key characteristics of the test buildings and compares them to the averages from the FSEC study. The tested buildings ranged up to 136,000 ft^2 of gross floor area. The average building size was 20,852 ft^2 and the median building size was 9,200 ft^2. Four of the tested buildings exceeded the upper range of 20,000 ft^2 that was originally envisioned for this study. Site 18 was effectively two distinct buildings, so that site is included as two entries in the table to make a total of 26 unique buildings in Table 2-2. The buildings in New York were generally larger than the buildings in the FSEC study (5030 ft^2 average floor area). Figure 2-11 through Figure 2-13 graphically show the distribution of floor area, normalized gas use, and normalized electric use for the sample of tested buildings. Energy use in commercial buildings is mostly a function of the building type. Figure 2-14 and Figure 2-15 show the average normalized energy use for NY buildings grouped according to the main CBECS categories identified in Table 2-1 and Table 2-2.

Table 2-2. Key Characteristics of Tested Commercial Buildings

Site	Description	CBECS Category	Location	Year Built	Renovated	Age (yrs)	Building Floor Area (ft^2)	Gas Use ($MBtu/ft^2$-year)	Electricity Use (kWh/ft^2-year)
1	Office Building	office	Utica, NY	1987		17	5,040	56.5	7.8
2	Office Building	office	Cazenovia, NY	1980	1996	8	1,443	74.3	4.0
3	Restaurant	restaurant	Cazenovia, NY	1992		12	1,034	616.0	26.5
4	Office Building	office	New Hartford, NY	1932	1960	44	6,974	34.7	26.2
5	Office Building/Training Ctr	office	Syracuse, NY	1974		30	17,819	26.4	29.7
6	Supermarket	food	Hauppauge, NY	2002		2	57,000	41.0	39.3
7	Fast Food Restaurant	restaurant	Herkimer, NY	2002		2	3,300	431.2	116.1
8	Church	worship	Rome, NY	1991		13	8,607	58.5	2.4
9	Fast Food Restaurant	restaurant	Lockport, NY	2002		2	3,300	486.0	105.1
10	Office Building	office	Ithaca, NY	1960	2000	4	14,400	83.1	6.5
11	Office Section Only	office	Ithaca, NY	1995		9	3,289		
12	Office Building (2 story)	office	Cazenovia, NY	1998		6	12,700		
13	Fire Department	public	Cazenovia, NY	1989		15	9,800	37.5	2.8
14	Office Building	public	Ithaca, NY	2004			12,600	104.9	12.8
15	Office Building (2 story)	office	Ithaca, NY	1980	2001	3	10,391	38.8	8.9
16	Office Building	office	Ithaca, NY	1980	2001	3	2,451	50.2	10.4
17	Social Club (3 story)	assembly	Syracuse, NY	1853	1893	111	14,694	61.4	4.2
18a	Office		Syracuse, NY	1940	1986	18	6,021		
18c	Warehouse	warehouse	Syracuse, NY	1986		18	10,700		
19	Office Building	office	New Hartford, NY	1985		19	13,720	29.0	3.4
20	Movie Theater	assembly	Rochester, NY	1996		8	96,214		
21	Retail / Auto Service	service	Clinton, NY	1985		19	3,332	70.9	6.1
22	Retail Garage	retail	Clinton, NY	1996		8	3,994		
23	Retail	retail	Oneonta, NY	2005			132,000		
24	Nursing Home (2 story)	nursing	Waterville, NY	1970		34	88,000	93.8	7.2
25	Office & Apartment	office	Cazenovia, NY	1900	1997	7	3,323		
Average				**1976**		**16**	**20,852**	**133.0**	**23.3**
Median						**9**	**9,204**	**60.0**	**8.3**
Average from FSEC Study (1996)						**21**	**5,030**		

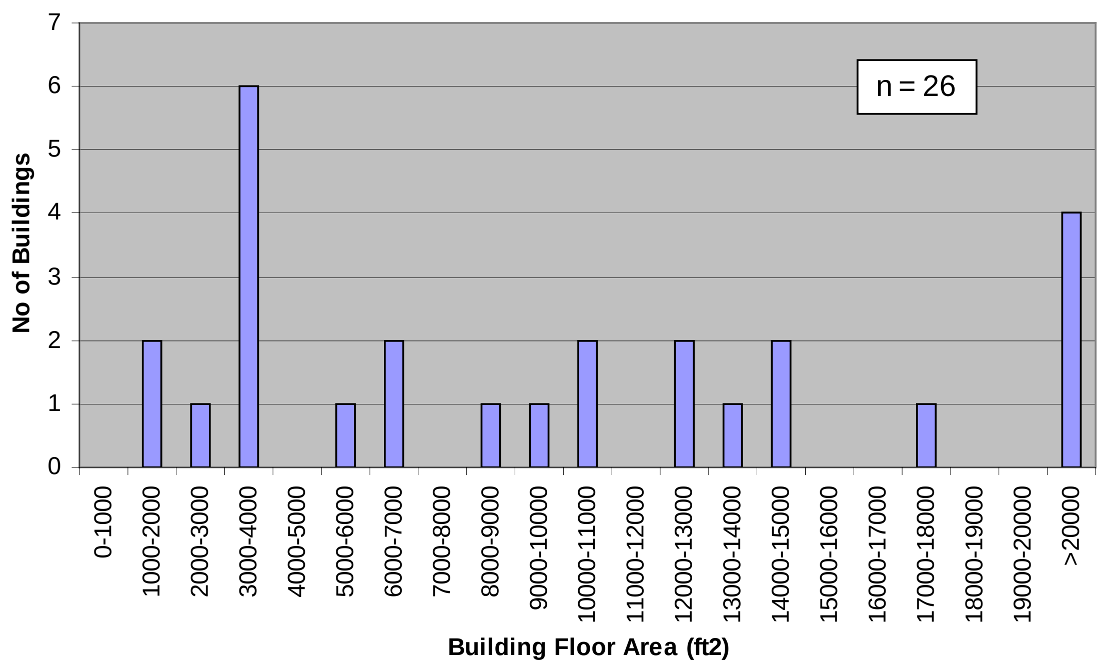

Figure 2-11. Histogram Showing Distribution of Floor Area for Tested Buildings

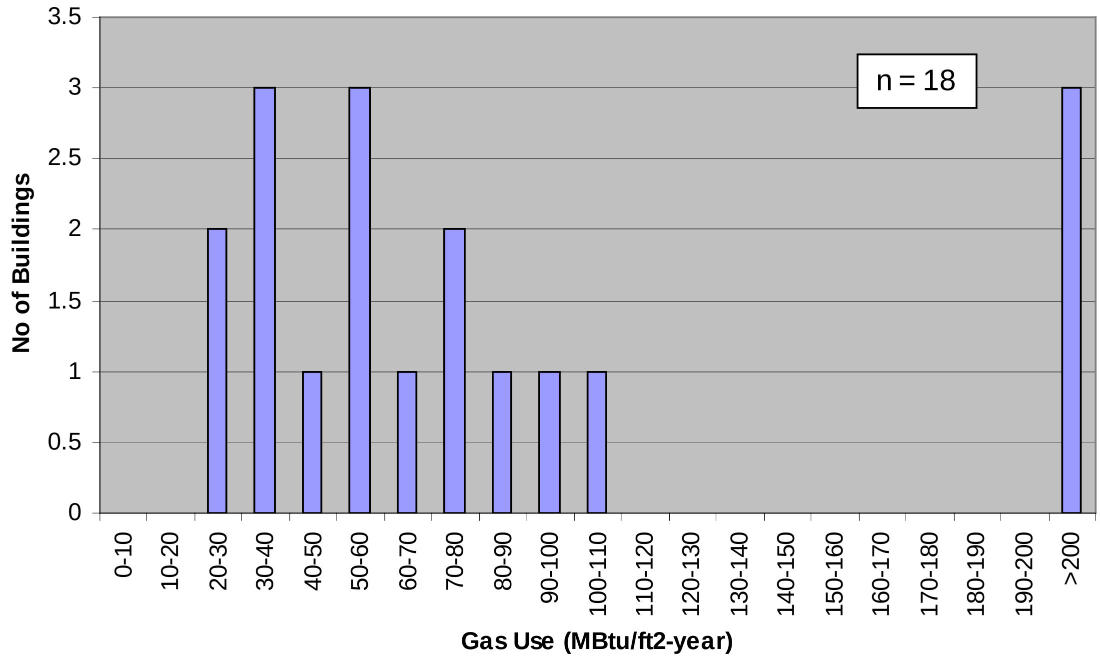

Figure 2-12. Histogram Showing Distribution of Normalized Gas Use for Tested Buildings

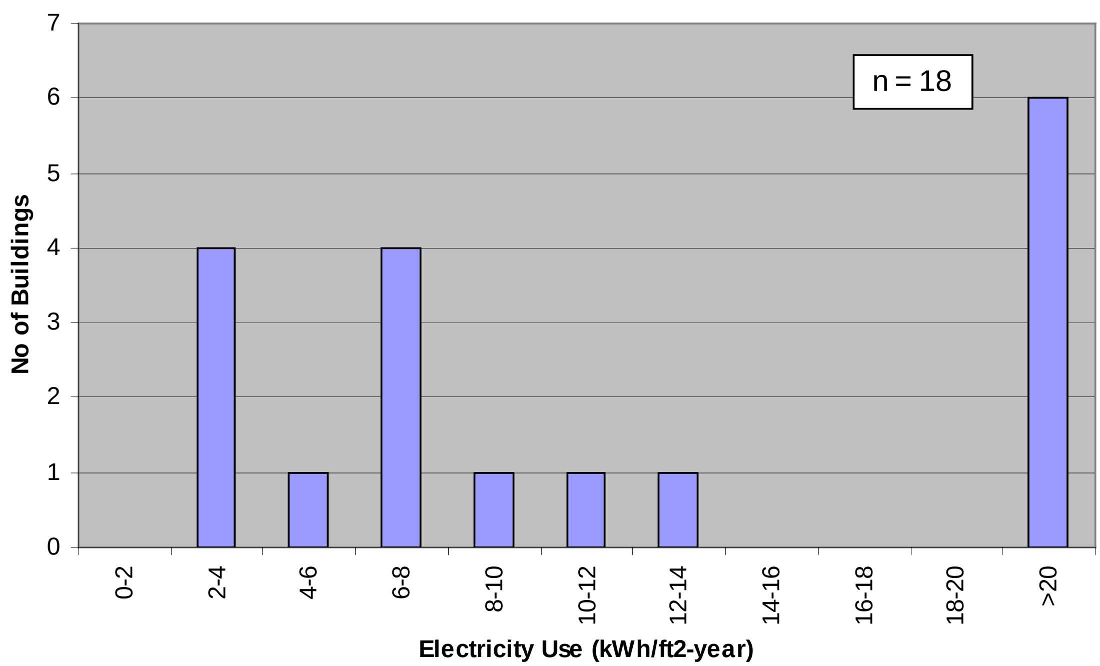

Figure 2-13. Histogram Showing Distribution of Normalized Electric Use for Tested Buildings

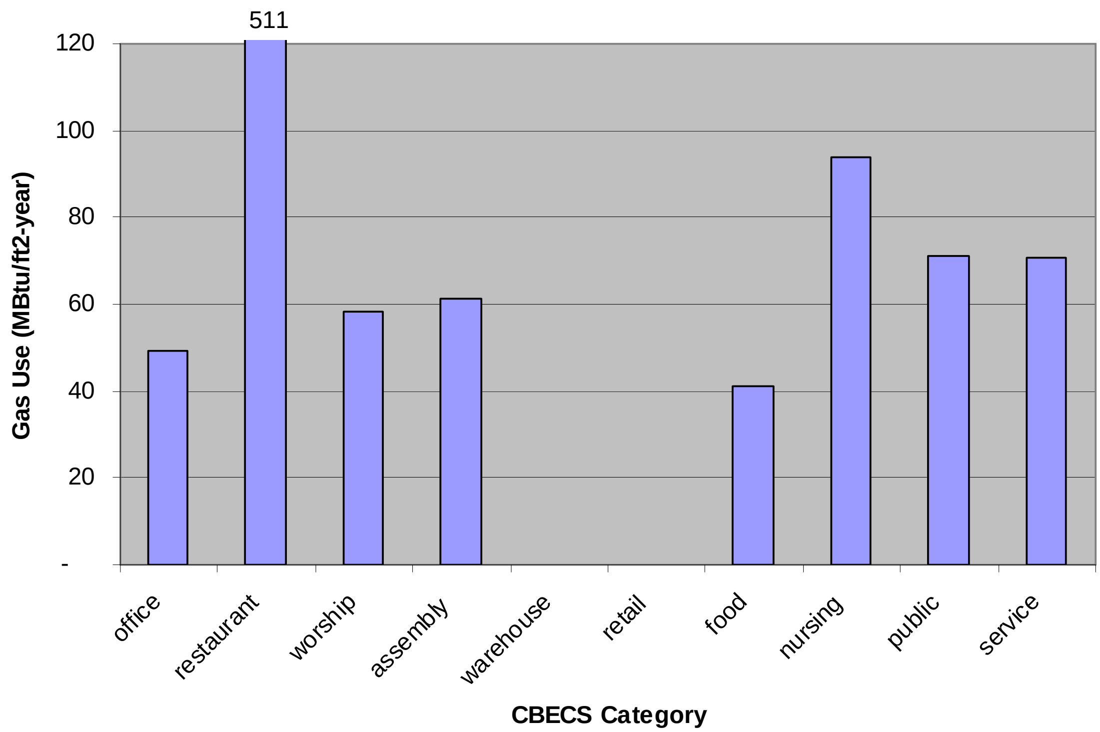

Figure 2-14. Average Gas Use by Building Type for Tested Buildings

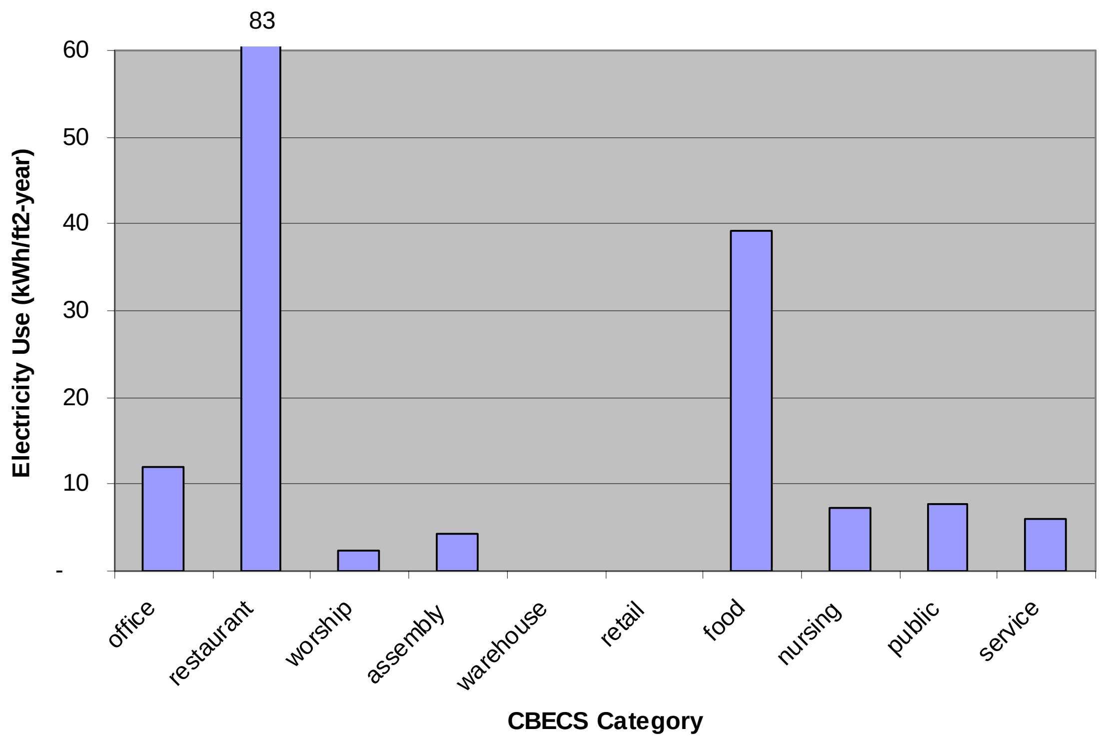

Figure 2-15. Average Electric Use by Building Type for Tested Buildings

2.4. Measured Building Envelope Results

Table 2-3 summarizes the building leakage results along with the "Ceiling Configuration" code defined by Cummings et al (1996). The Ceiling Configuration codes are defined at the bottom of Figure 2-16, which compares the mix of buildings in the New York and Florida studies. The average and median results for the NY sample of buildings are given in the table. On average, the 25 buildings from NY had a lower ACH50 (11.4) than the 68 buildings from the FSEC Study (16.7). Part of the difference in airtightness between the Florida and New York buildings can be attributed to building size. In general, larger buildings are less likely to have a vented attic space above a suspended T-bar ceiling, and are therefore much more likely to have a relatively tight exterior envelope.

Table 2-3. Summary of Envelope Leakage Results for Commercial Buildings

		Building Envelope					
Site	Description	FSEC Ceiling Config	CFM50	ACH50	Infiltration: AHUs Operating Normally (ACH)	Power Law Exponent n	ELA per 100 sq ft Envelope Area (sq-in @ 4 Pa)
1	Office Building	7	20,988	31.2	0.42	0.528	19.3
2	Office Building	7	6,807	33.0	0.44	0.579	15.7
3	Restaurant	8	4,169	25.0		0.556	12.6
4	Office Building	6	7,394	6.8	0.18	0.653	3.2
5	Office Building/Training Ctr	2	16,902	3.9	0.44	0.704	3.0
6	Supermarket	1	27,232	2.0		0.600	2.4
7	Fast Food Restaurant	2	6,332	13.8		0.620	6.2
8	Church	8	12,467	7.6	0.24	0.700	5.1
9	Fast Food Restaurant	2	6,969	15.2		0.600	7.2
10	Office Building	2	13,090	6.5		0.870	2.1
11	Office Section Only	2	3,934	7.6	0.25	0.661	3.1
12	Office Building (2 story)	2	5,687	3.4	0.23	0.501	3.2
13	Fire Department	8	8,188	4.0		0.795	2.1
14	Office Building	8	9,279	4.5		0.661	2.5
15	Office Building (2 story)	2	14,088	7.4		0.603	4.3
16	Office Building	2	1,819	3.4	0.36	0.802	1.2
17	Social Club (3 story)	8	32,068	14.3	0.80	0.620	15.9
18a	Office	2	8,680	7.9		0.632	4.9
18c	Warehouse	1	24,628	4.8		0.487	9.0
19	Office Building	8	3,676	1.7		0.612	2.1
20	Movie Theater	2	33,955	0.8		0.500	1.7
21	Retail / Auto Service	7	18,929	38.6		0.620	20.3
22	Retail Garage	7	11,907	17.9		0.620	10.6
23	Retail	1					
24	Nursing Home (2 story)	2	68,772	5.9	1.40	0.600	3.7
25	Office & Apartment	8	7,094	17.1		0.696	6.7
Average			**15,002**	**11.4**	**0.48**	**0.650**	**6.7**
Median			**9,279**	**7.4**	**0.39**	**0.653**	**4.3**
Average from FSEC Study (1996)				**16.7**	**1.25**	**0.61**	

Note: Shaded exponents were specified instead of determined from regression so they were excluded from average and median.

This difference in ACH between the two studies may also be explained by the fact that several of the vented ceiling configurations common in Florida – namely ceiling configurations 4 and 5 – were not found at all in NY. Overall, the vented configurations without an air barrier (configurations 4, 5 and 7) accounted for 29 of the 68 building in Florida (or 42%). In NY there were only 4 buildings that were vented (i.e., configuration 7), or 16% of the sample. The 4 vented buildings in NY generally attempted to incorporate some degrees of air barrier (e.g., using paper-faced fiberglass batts). Though, the air barrier was in most cases unsuccessful due to either poor implementation and/or poor design. It seems probable that vented configurations 4, 5 and 7 are used less often in NY because occupant comfort issues are more likely arise in this more severe climate.

Figure 2-16 compares the ACH50 for the New York and Florida buildings by ceiling configuration. The average ACH50 of all the vented-attic buildings in Florida (configuration 4, 5 and 7) was 25.2, which is close to the average of 30.2 for the NY vented-attic buildings.

This study included 7 buildings with a gypsum board ceiling similar to residential construction (Some of these included a suspended t-bar ceiling below the gypsum board). The ACH50 for these 7 buildings was 10.6, which was much leakier than the one building in this category for the FSEC sample, but was similar to average ACH50 of 10 that FSEC has found for residential construction (Cummings et al 1996). Figure 2-17 shows the distribution of ACH50 for the buildings. Figure 2-18 shows the distribution of Equivalent Leakage Area (ELA) per 100 ft^2 of surface area of the building envelope. Roughly speaking, there are three groupings of buildings by airtightness:

- one group of 16 buildings is tight, with an ACH50 of 8 or less,
- a second group of five moderately leaky buildings with 12 to 18 ACH50,
- a third group of four very leaky buildings, with leakage in the range of 24 to 40 ACH50.

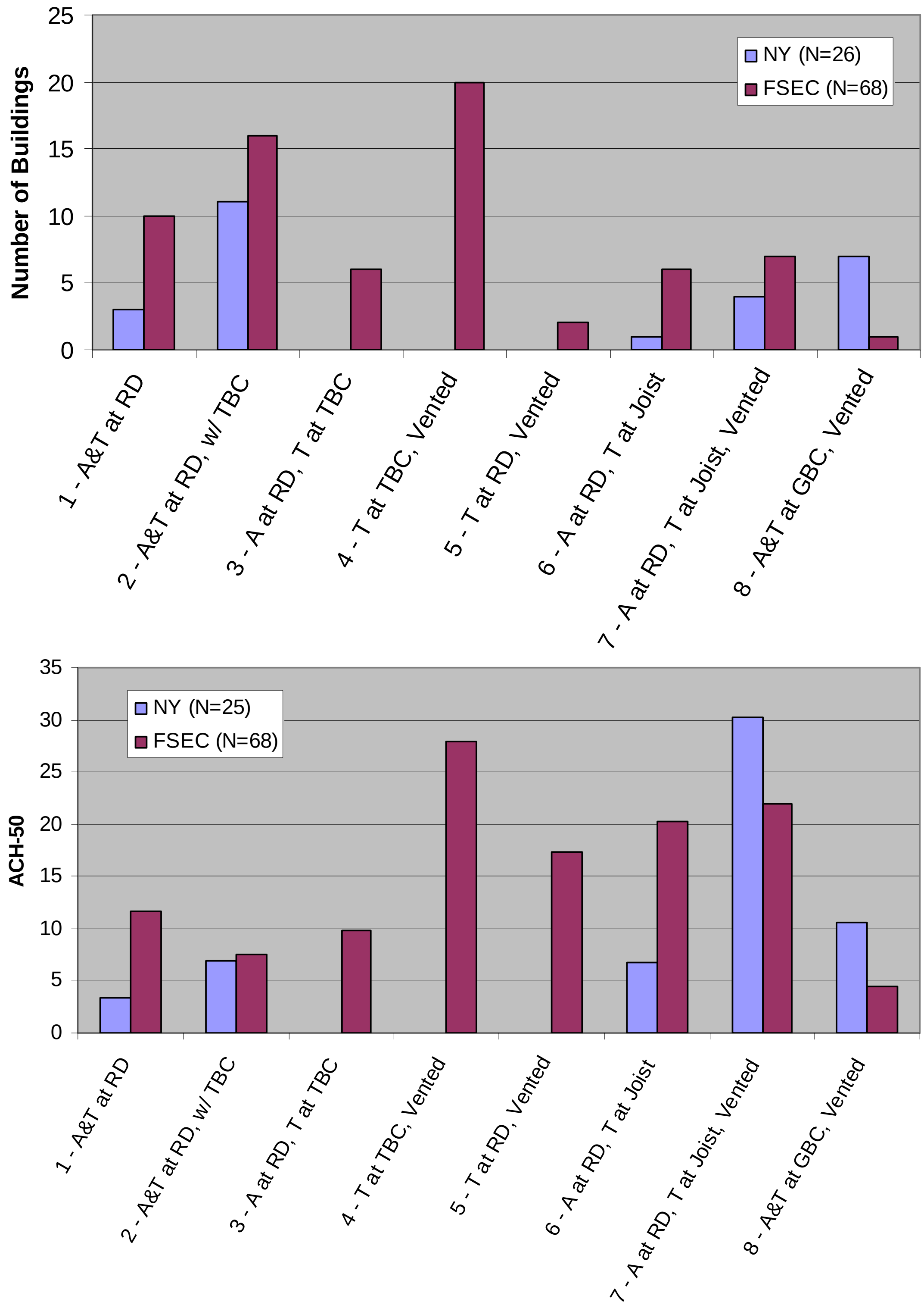

A – Air Barrier, T – Thermal Barrier (or insulation)
RD – Roof Deck, TBC – T-Bar Ceiling, GBC – Gypsum Board Ceiling
"Joist" refers to the bottom cord of the roof joist. "Vented" refers to the attic space (attic is unvented otherwise)

Figure 2-16. Comparing Ceiling Configuration of NY Buildings and Buildings from 1996 FSEC Study

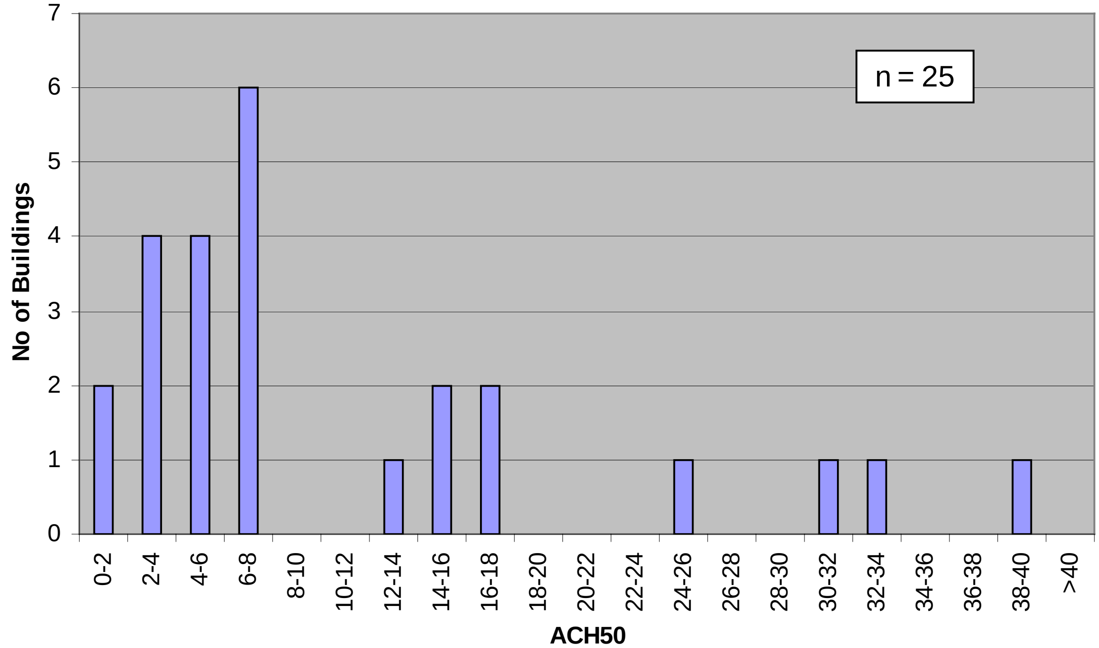

Figure 2-17. Histogram Showing Distribution of ACH50 for Tested Buildings

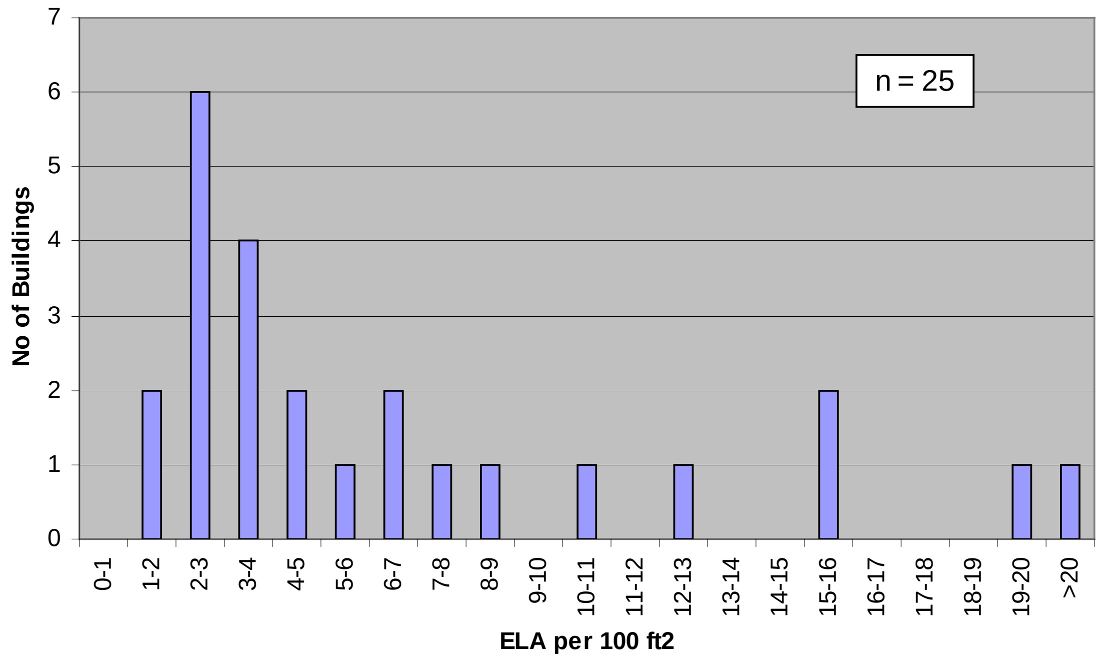

Figure 2-18. Histogram Showing Distribution of ELA per 100 ft^2 of Surface Area for Tested Buildings

ELA per surface area and ACH50 are similar measures of building leakiness. Figure 2-19 shows that these two metrics are very comparable for most buildings. The two buildings that deviate farthest from the overall trend are the 3-story social club (Site 17) and 30 ft high-bay warehouse (Site 18c).

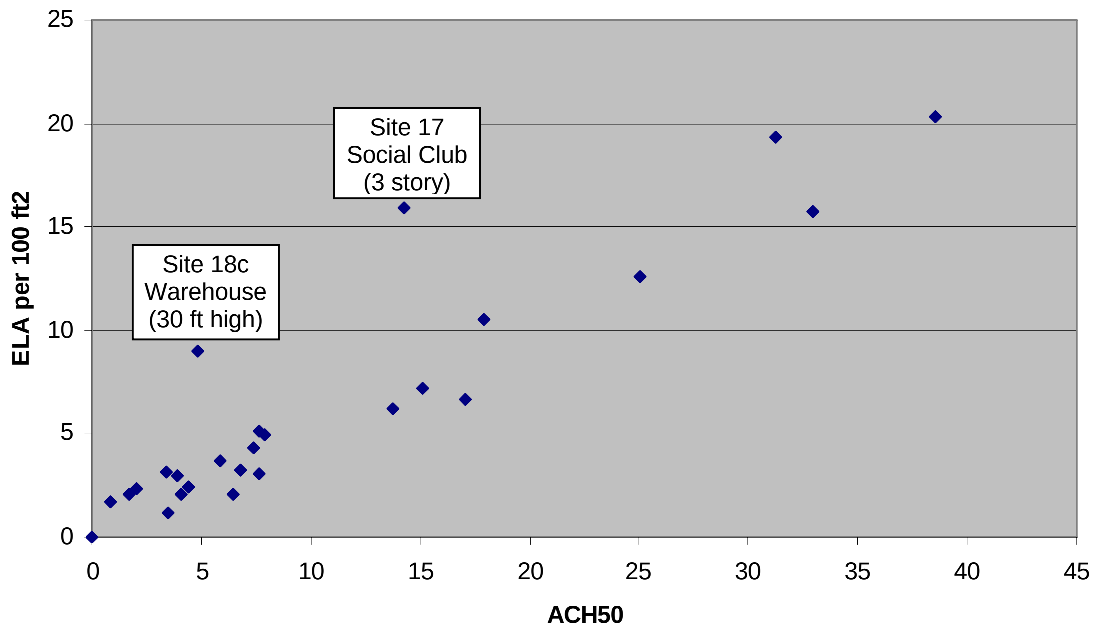

Figure 2-19. Comparing ACH50 and ELA per 100 ft^2 of Surface Area

Another key metric of building air tightness is the exponent of the flow-pressure curve (from equation 2-1). The value of the flow exponent has physical meaning. For turbulent flow through an orifice, the exponent should be 0.5. Flow through a long, narrow passage in laminar flow should result in an exponent of 1.0. In most buildings the exponent is expected to be around 0.6. The average exponent from the FSEC study was 0.61. Figure 2-20 shows that the distribution of the exponent was determined from the regression analysis. The average and median (from Table 2-3) exponents were 0.65 for the 17 tested New York buildings.

In theory one might expect that the exponent should be closer to 0.5 for leaky buildings – which might be expected to have larger holes. Similarly, tight buildings should have smaller, narrower openings, so the exponent should be nearer to 1.0. Figure 2-21 compares the exponent to the ACH50 for 17 buildings. While there is significant scatter, the data demonstrates a slight trend of the exponent decreasing for buildings with a higher ACH50 – or in other words, larger leaks (as indicated by smaller exponents) result in greater air change rates.

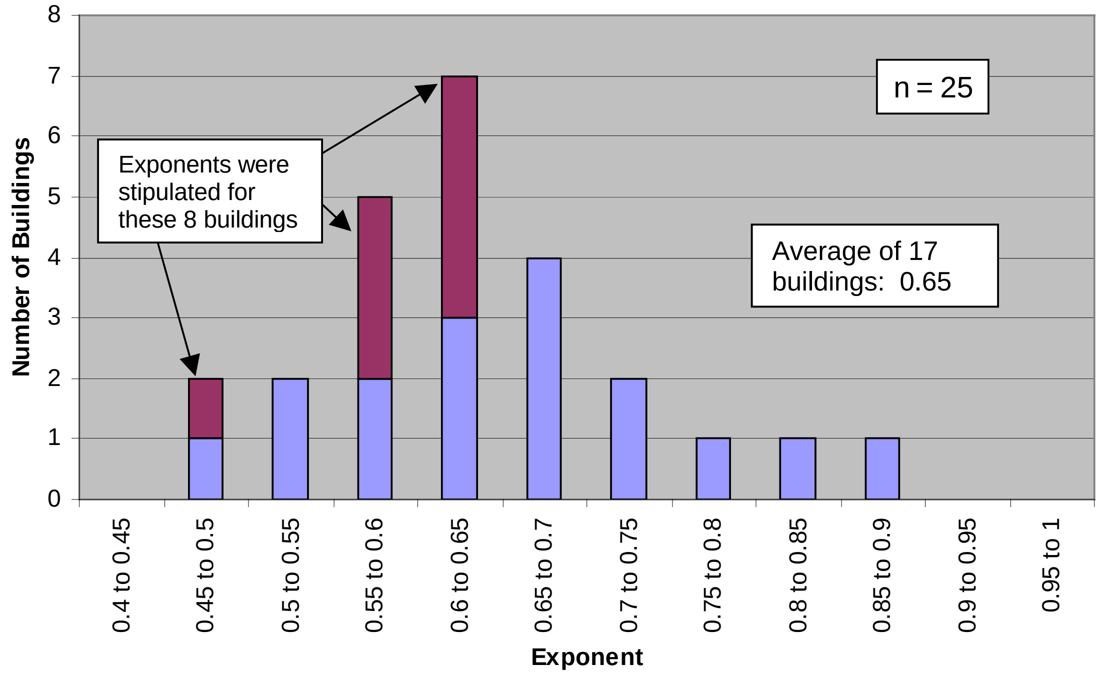

Figure 2-20. Histogram Showing Distribution of Exponent (n) for Tested Buildings

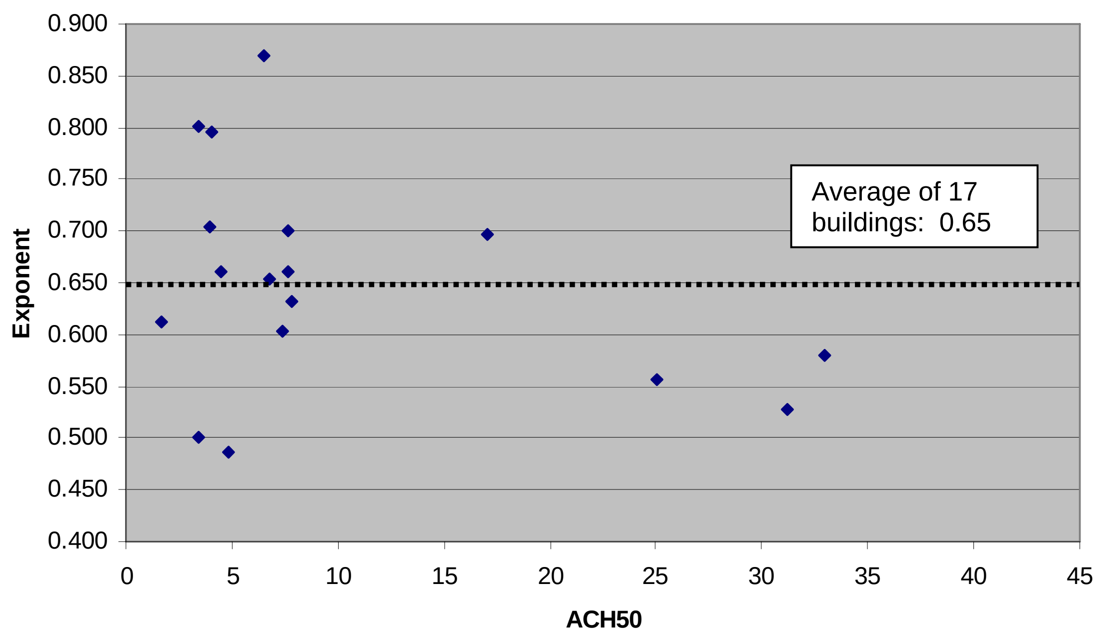

Figure 2-21. Variation of Exponent (n) with ACH50 for Tested Buildings

2.5. Measured Building Pressurization Results

Figure 2-22 shows the distribution of building pressures (with respect to outdoors). Of the 26 buildings (Site 18 is included as two buildings), 19 were depressurized while 7 operated at a pressure greater than zero. At least one of the 7 pressurized buildings (Site 6) was operating at a positive pressure because an exhaust fan was broken. The majority of the buildings were only slightly depressurized by 1 to 3 Pa. The median pressure was -1.2 Pa, which compares well to the average pressure of –1.1 Pa from the FSEC study. One building not shown on the plot (but included in the sample) is Site 2, a takeout restaurant with a large exhaust fan. At this site the pressure with all doors shut was -41 Pa. As a result, the restaurant staff generally kept the kitchen door open (there was screen door) in all but coldest weather.

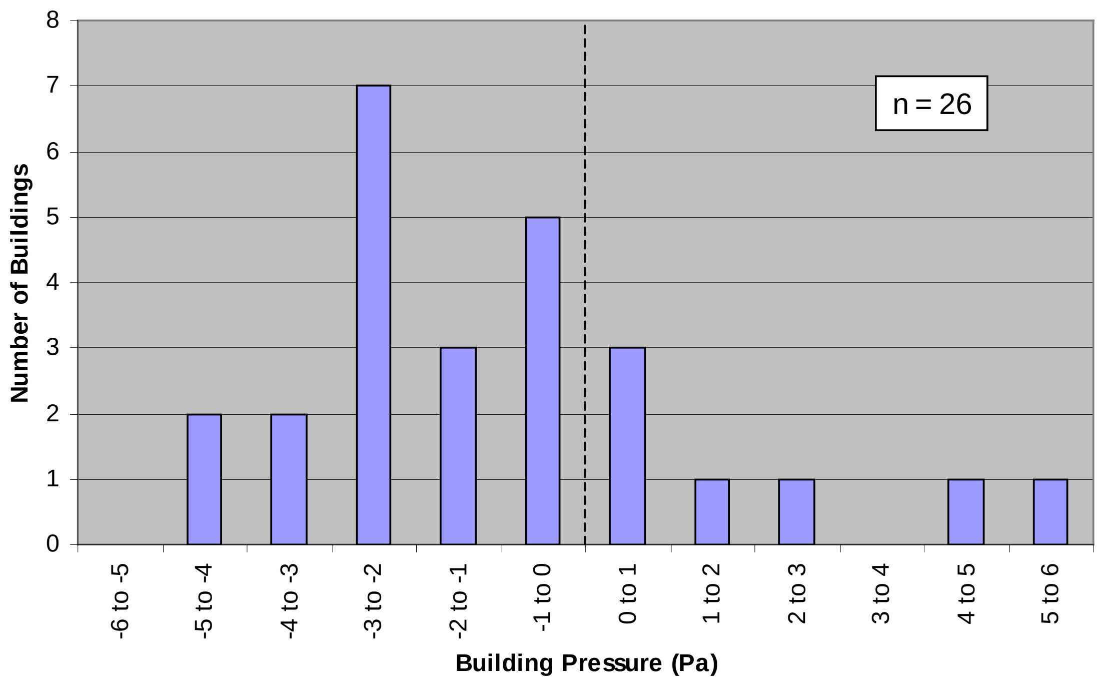

Figure 2-22. Histogram Showing Distribution of Building Pressure for Tested Buildings

2.6. Measured AHU Fan Power

At several of the sites we were able to determine the air flow for each air handler unit (AHU) as well as its fan power. From this data the normalized fan power was determined. The industry rule of thumb is that the Watts per cfm are in the range 0.35 to 0.5. The DOE Test procedure to determine SEER (Federal Register 1979) assumes 0.35 Watts per cfm for residential evaporator coils sold without fans. Commercial systems are often assumed to use about 0.5 Watts per cfm. Recent field testing of residential systems by Proctor and Parker (2000) found the normalized fan power to be closer to 0.5 Watts per cfm.

Figure 2-23 and Figure 2-24 show the range of normalized fan power measured for 27 different AHUs from 11 different sites. Table 2-4 lists the data for each site. The average fan power is near 0.5 W/cfm for all of the units. Somewhat surprisingly, very little of the variation can be explained by the size of AC of the unit. The one exception was a large Variable Air Volume (VAV) unit (Site 5, AHU-VAV) that was modulated down to a fraction of its total airflow. This high static pressure unit required about 3 Watts per actual cfm of airflow. The other constant volume units were generally in line with expectations except for a unit dedicated to providing ventilation air (Site 12, ERV), which had a very high airflow rate relative to its cooling capacity.

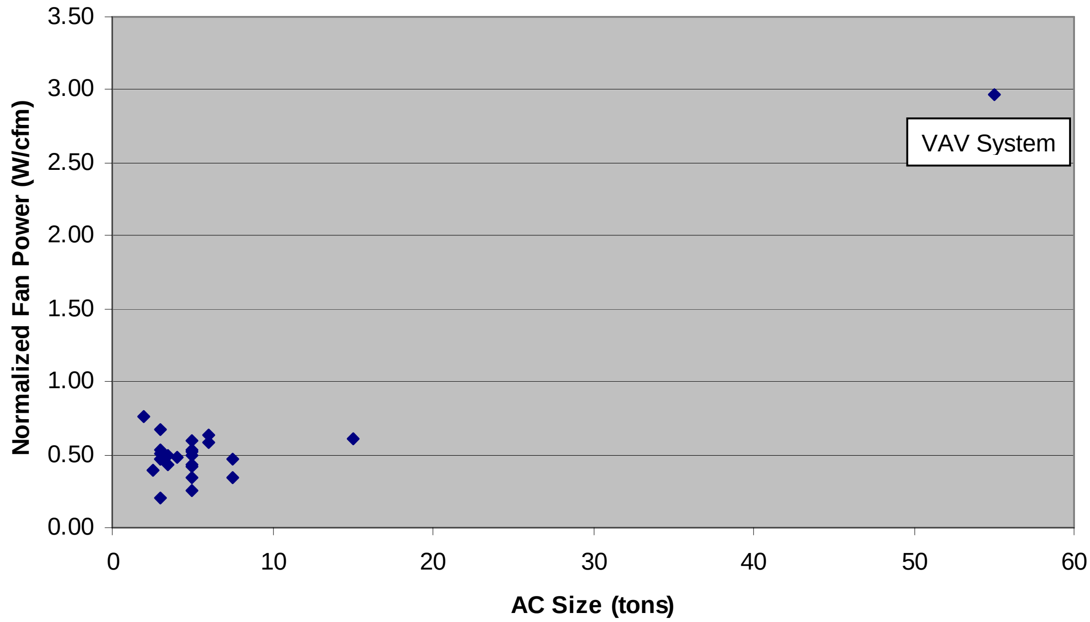

Figure 2-23. Variation of Normalized Fan Power with Unit Size

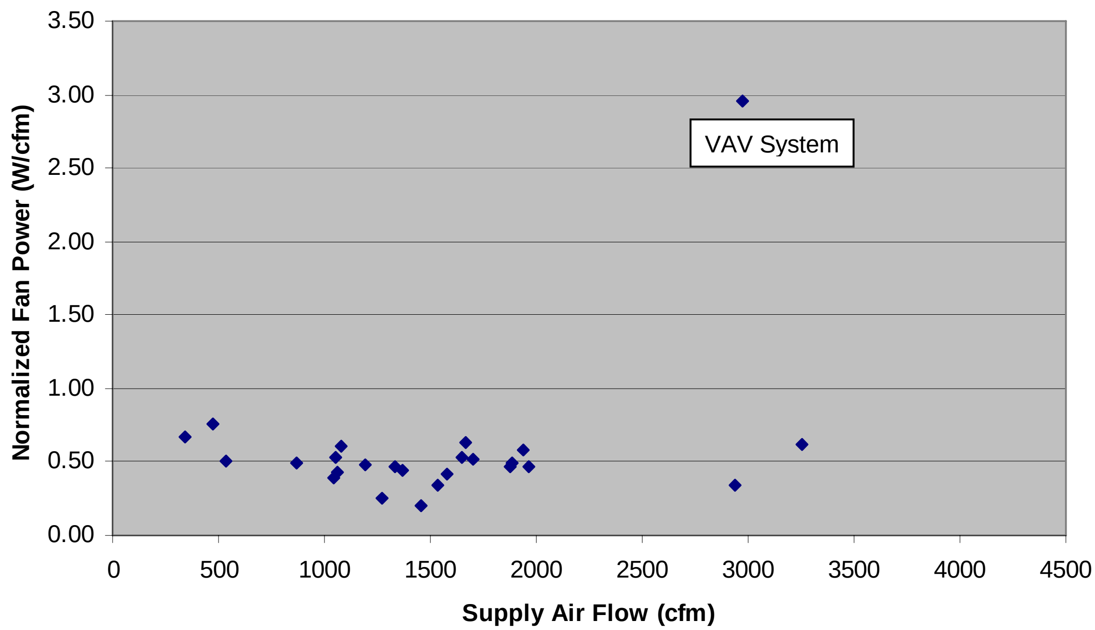

Figure 2-24. Variation of Normalized Fan Power with Supply Air Flow

Table 2-4. Summary of Airflow and Fan Power Data (27 AHUs)

Site	Unit Name	AC Unit Size (tons)	Served Floor Area (ft^2)	Supply Fan Power (kW)	Supply Airflow (cfm)	Norm. Airflow (cfm/ton)	Area per ton (ft^2/ton)	Norm. Fan Power (W/cfm)	Norm. Airflow (cfm/ft^2)	Unit Static: Supply -Return (Pa)
2	AHU	2.5	1,443	0.41	1048	419	577	0.39	0.73	83
4	AHU #2	5	1,875	0.32	1268	254	375	0.25	0.68	39
5	AHU-VAV	55	18,000	8.8	2971	54	327	2.96	0.17	
7	RTU-3	6	825	1.13	1942	324	138	0.58	2.35	275
7	RTU-4	6	825	1.05	1668	278	138	0.63	2.02	339
8	F-3	5	1,536	0.66	1575	315	307	0.42	1.03	40
8	F-6	3	921	0.62	1333	444	307	0.47	1.45	77
9	RTU-1	5	611	0.88	1652	330	122	0.53	2.70	112
9	RTU-2	5	611	0.94	1884	377	122	0.50	3.08	107
9	RTU-3	5	611	0.88	1699	340	122	0.52	2.78	94
10	RTU-1	7.5	2,919	0.99	2936	391	389	0.34	1.01	129
10	RTU-4	8.5	3,308		2426	285	389		0.73	213
13	AC-1	2	841	0.36	473	237	420	0.76	0.56	49
14	AHU-2	15	3,830	2.50	4062	271	255	0.61	1.06	
4	AHU #1	5	1,875	0.60	1372	274	375	0.44	0.73	
4	AHU #3	5	1,875	0.65	1081	216	375	0.60	0.58	
4	AHU #4	5	1,875	0.53	1537	307	375	0.34	0.82	
8	F-4	3	921	0.56	1057	352	307	0.53	1.15	
8	F-5	4	1,229	0.58	1195	299	307	0.49	0.97	
12	ERV	3	12,700	0.91	1962	654	4233	0.46	0.15	
14	AHU-1	15	5,250	2.00	3253	217	350	0.61	0.62	
15	AHU-1	3	1,873	0.27	534	178	624	0.51	0.29	
15	AHU-2	3	1,873	0.29	1460	487	624	0.20	0.78	
15	AHU-3	3	1,873	0.23	341	114	624	0.67	0.18	
15	RTU	7.5	4,682	0.87	1876	250	624	0.46	0.40	
16	AGE	3.5	1,250	0.46	1060	303	357	0.43	0.85	
16	AGW	3.5	1,250	0.43	871	249	357	0.49	0.70	
Average		**7.2**	**2,840**	**1.07**	**1649**	**304**	**501**	**0.59**	**1.06**	**130**
Median		**5.0**	**1,873**	**0.64**	**1537**	**299**	**357**	**0.50**	**0.78**	**100**

Figure 2-25 compares the normalized fan power to normalized airflow for all units excluding the two exceptions mentioned above. The remaining 25 AHUs show a very linear trend. The linear regression model that fits the data is:

$$W/cfm = 0.743 - 0.00085 \times [cfm/ton]$$

So at the nominal airflow rate of 400 cfm per ton, the model predicts a normalized fan power of 0.4 W/cfm.

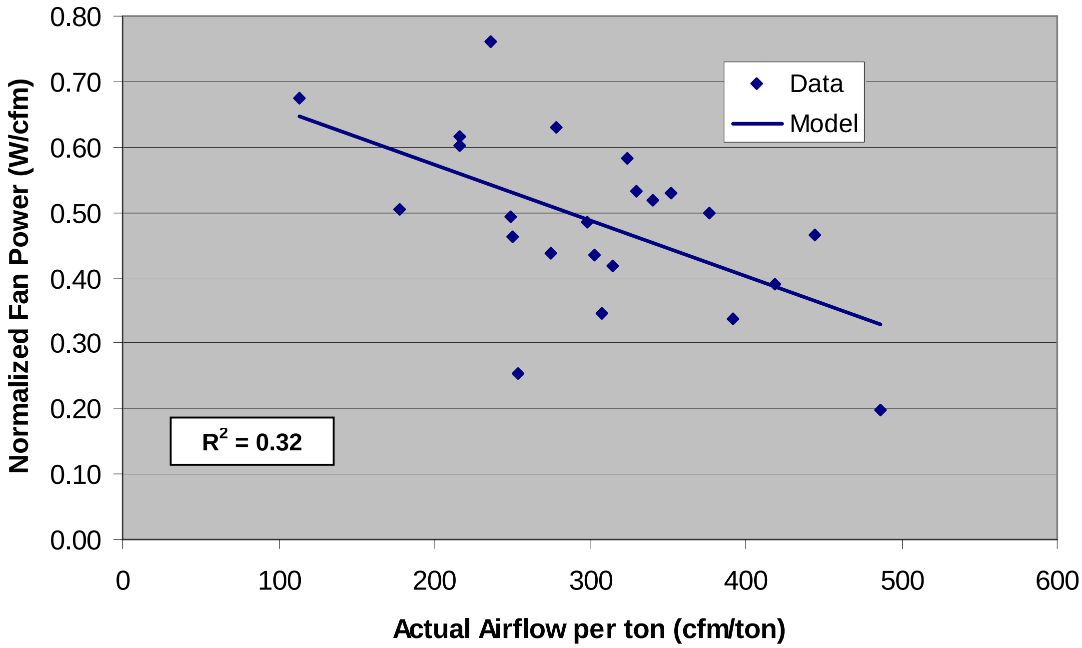

Figure 2-25. Variation of Normalized Fan Power (W/cfm) with Normalized Airflow (cfm/ton)

One likely explanation for this trend is that unit designs are optimized to provide airflow near 400 cfm per ton. At lower airflow rates the fan efficiency falls off and fan power per cfm increases. Therefore, AHUs installed with restrictive ductwork tend to operate below the optimized point on the fan curve and require more energy per unit airflow.

2.7. Measured Duct Leakage Results

The duct leakage data was measured at a subset of the of the test sites. Duct leakage testing was a time-intensive process, Therefore, we typically limited our efforts to sites where testing was easily implemented with minimal impact of the occupants and would provide clear results. At many sites, we only tested a portion of the HVAC units at a site. In other cases, we tested duct leakage on units where all the ductwork was in the conditioned space (and would have no energy implications) in order to gather base line data.

Table 2-5, Table 2-6, and Table 2-7 summarize the duct leakage testing that was completed on 14 different HVAC units in 8 different buildings. The unit size and building details for each unit are listed above in Table 2-4 (the first 14 units). In many cases the supply and return sides of the HVAC system and ductwork could be separately tested. Measured data and statistics for the supply ducts are given in Table 2-5 and the return duct data are summarized in Table 2-6. The air handler cabinet was usually included in either the return or the supply side (but not both). Data and statistics for the supply and return sides of the ductwork combined (i.e., the total duct work) are in Table 2-7. In most cases these values are the sum of the supply and return side of the system. In three cases the total ductwork was tested together so an exponent (n) and coefficient (K) are available for the combined system. The leakage rate was determined using the nominal pressure of 25 Pa as well as using the average operating pressure in the ductwork (i.e., ½ the operating pressure (OP) measured at the air handler unit). The "Actual Leakage %" divides the Actual Leakage airflow rate (at ½ the operating pressure) by the measured diffuser airflow rate.

Table 2-5. Summary of Duct Leakage Data and Statistics – Supply Duct

		Supply													
Site	Unit Name	Diffuser Air Flow (cfm)	Duct Area (ft^2)	Coef K	Exp n	Operating Press (OP) in Duct (Pa)	Actual Leakage (cfm @ OP/2)	Leakage @ 25Pa (CFM25)	Ductwork ELA-25 (in2 @ 25Pa)	ELA-25 per Duct Area (in^2 per 100 ft^2)	CFM25 per Duct Area (cfm per 100 ft^2)	SMACNA Leakage Class (cfm per 100 ft^2 @ 1-in water)	CFM25 per Floor Area (cfm per 1000 ft2)	Supply CFM per Duct Area (cfm/ft^2)	Actual Leakage %
2	AHU	1048	503	97.3	0.557	25.5	402	584	66	13.2	116	418	405	2.1	38%
4	AHU #2	1268	518	88.8	0.566	26.4	383	549	62	12.0	106	389	293	2.4	30%
5	AHU-VAV	2971	2941	165.1	0.542	485.0	3,238	945	107	3.6	32	112	52	1.0	109%
7	RTU-3	1942	229	13.7	0.940	163.9	862	282	32	14.0	123	1,070	342	8.5	44%
7	RTU-4	1668	229	49.2	0.577	200.0	701	315	36	15.6	138	519	382	7.3	42%
8	F-3	1575	671	69.2	0.569	21.0	264	432	49	7.3	64	238	281	2.3	17%
8	F-6	1333	166	76.7	0.546	47.0	430	445	50	30.4	268	940	483	8.0	32%
9	RTU-1	1652	150	7.9	0.580	42.7	47	51	6	3.9	34	130	84	11.1	3%
9	RTU-2	1884	204	4.8	0.718	44.4	44	48	5	2.7	24	124	79	9.2	2%
9	RTU-3	1699	205	4.8	0.763	28.6	37	56	6	3.1	27	158	92	8.3	2%
10	RTU-1	2936	657	65	0.611	95.0	688	465	53	8.0	71	288	159	4.5	23%
10	RTU-4	2426	932	57	0.543	114.7	514	327	37	4.0	35	122	99	2.6	21%
13	AC-1	473	302			32.5								1.6	0%
14	AHU-2	4062	1946	50.5	0.635			390	44	2.3	20	86	102	2.1	0%
Average		**1924**	**689**	**57.7**	**0.627**	**102.1**	**543**	**349**	**40**	**8.6**	**76**	**328**	**204**	**5.1**	**26%**
Median		**1684**	**403**	**57.0**	**0.577**	**44.4**	**392**	**359**	**41**	**5.6**	**50**	**198**	**130**	**3.5**	**22%**

Table 2-6. Summary of Duct Leakage Data and Statistics – Return Duct

		Return												
Site	Unit Name	Diffuser Air Flow (cfm)	Duct Area (ft^2)	Coef K	Exp n	Operating Press (OP) in Duct (Pa)	Actual Leakage (cfm @ OP/2)	Leakage @ 25Pa (CFM25)	Ductwork ELA-25 (in2 @ 25Pa)	ELA-25 per Duct Area (in^2 per 100 ft^2)	CFM25 per Duct Area (cfm per 100 ft^2)	SMACNA Leakage Class (cfm per 100 ft^2 @ 1-in water)	CFM25 per Floor Area (cfm per 1000 ft2)	Actual Leakage %
2	AHU	820	380	77.7	0.573	57.5	532	491	56	14.7	129	483	341	65%
4	AHU #2	993				12.4								
5	AHU-VAV													
7	RTU-3	1286	94	31.5	0.775	111	708	382	43	46.0	406	2,412	463	55%
7	RTU-4	1540	94	55.2	0.559	139.4	592	334	38	40.2	355	1,283	405	38%
8	F-3	998	656	125.8	0.584	19.3	473	824	93	14.2	126	481	537	47%
8	F-6	1111	49	52.0	0.551	30	231	306	35	70.9	625	2,219	333	21%
9	RTU-1	1443	63.1	22.9	0.535	68.8	152	128	15	23.0	203	695	210	11%
9	RTU-2	1226	63.1	5.3	0.900	62.4	117	96	11	17.2	152	1,205	157	10%
9	RTU-3	1504	110	11.3	0.616	65.2	97	82	9	8.4	74	307	134	6%
10	RTU-1					34								
10	RTU-4					98								
13	AC-1	386	347	18.4	0.587	16.8	64	122	14	4.0	35	135	145	17%
14	AHU-2	2957	913	71.3	0.555			426	48	5.3	47	167	111	
Average		**1297**	**277**	**47.1**	**0.624**	**59.567**	**212**	**228**	**26**	**17.4**	**154**	**671**	**202**	**30%**
Median		**1226**	**102**	**41.8**	**0.579**	**59.95**	**107**	**125**	**14**	**11.3**	**100**	**394**	**151**	**21%**

Table 2-7. Summary of Duct Leakage Data and Statistics – Supply & Return Ducts Combined

Site	Unit Name	All Ductwork (Supply & Return)									
		Coef K	Exp n	Actual Leakage (cfm @ OP/2)	Leakage @ 25Pa (CFM25)	Ductwork ELA-25 (in2 @ 25Pa)	ELA-25 per Duct Area (in^2 per 100 ft^2)	CFM25 per Duct Area (cfm per 100 ft^2)	SMACNA Leakage Class (cfm per 100 ft2 @ 1-in water)	CFM25 per Floor Area (cfm per 1000 ft2)	Duct ELA-25 per Unit Size (in^2/ton)
2	AHU	122.0	0.584	934	1076	122	13.8	122	446	746	48.8
4	AHU #2	127.0	0.606	383	549	62	12.0	106	389	293	12.4
5	AHU-VAV			3238	945	107	3.6	32	112	52	1.9
7	RTU-3			1570	664	75	23.3	206	1461	805	12.5
7	RTU-4			1293	649	74	22.8	201	741	787	12.3
8	F-3			736	1256	142	10.7	95	358	818	28.5
8	F-6			661	751	85	39.6	349	1232	815	28.4
9	RTU-1			199	179	20	9.6	84	297	293	4.1
9	RTU-2			162	144	16	6.1	54	379	236	3.3
9	RTU-3			133	138	16	5.0	44	210	226	3.1
10	RTU-1			688	465	53	8.0	71	288	159	7.0
10	RTU-4			514	327	37	4.0	35	122	99	4.4
13	AC-1	39.2	0.590	64	122	14	2.1	19	72	145	6.9
14	AHU-2				815	92	3.2	29	112	213	6.2
Average		**96.1**	**0.593**	**813**	**577**	**65**	**11.7**	**103**	**444**	**406**	**12.8**
Median		**122.0**	**0.590**	**661**	**599**	**68**	**8.8**	**78**	**328**	**265**	**7.0**

Figure 2-26 shows an analysis from Delp et al (1998) comparing duct leakage testing results from California buildings to the results from the FSEC study. They developed a linear regression model to fit the FSEC results. Figure 2-27 compares the duct leakage results from this study of NY buildings to that regression model for the Florida buildings. They calculated that the ELA-25 per nominal ton was 12.1 sq in per ton (78 cm^2 per ton) for the Florida buildings and 17.1 sq in per ton (110 cm^2 per ton) for the California buildings. The corresponding average and median values from Table 2-7 are 12.8 and 7.0, respectively. Generally the data from the NY buildings have a similar degree of scatter as well as a similar average as the FSEC study.

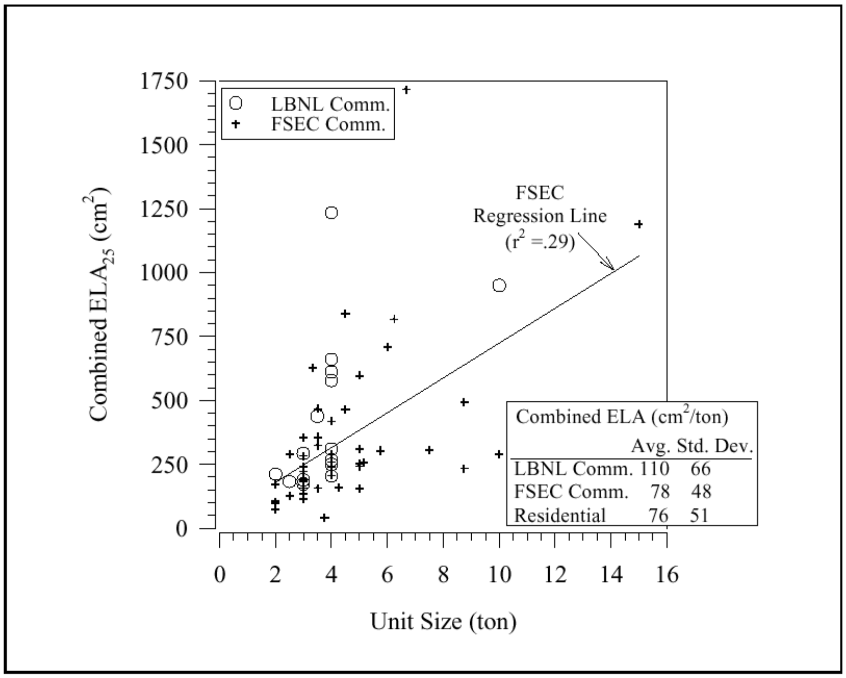

Figure 6. Combined leakage area (ELA_{25}) -vs- unit size using the current LBNL and FSEC (Cummings, et al., 1996) commercial data along with residential (Jump, et al., 1996) summary information. Combined leakage area includes both supply and return leakage. The FSEC unit size is derived from the total installed capacity in the building divided by the number of units.

Figure 2-26. Duct Leakage Results from FSEC and LBNL Field Tests (from Delp et al. 1998)

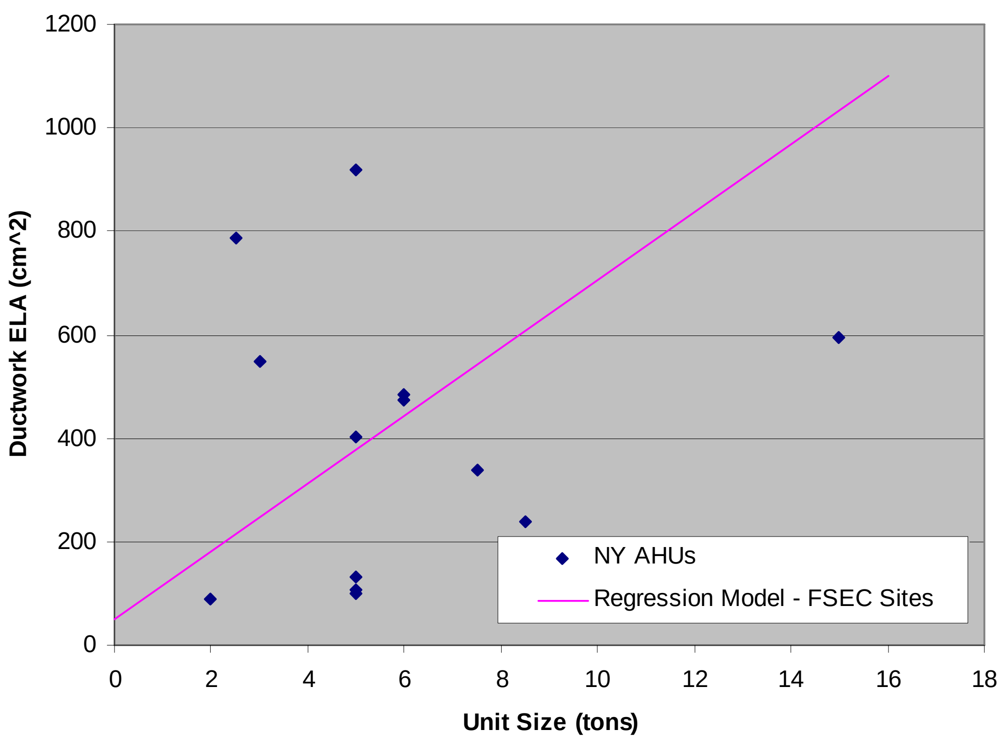

Figure 2-27. Comparing Duct Leakage Results to FSEC Regression Model (Delp et al. 1998 & Figure 2-26)

Several other normalization methods are have been used for duct leakage data, including normalizing ELA-25 or CFM25 per 100 ft^2 of duct surface area or per 1000 ft^2 of floor area. FSEC reported an average of 341 CFM25 per 1000 ft^2 of floor area for the Florida buildings (Cummings et al 1996). The corresponding average and median values from the New York buildings (Table 2-7 are 406 and 265, respectively. Table 2-8 provides a summary comparison of the duct leakage statistics. The plots below show histograms of the New York duct leakage data normalized by these various means.

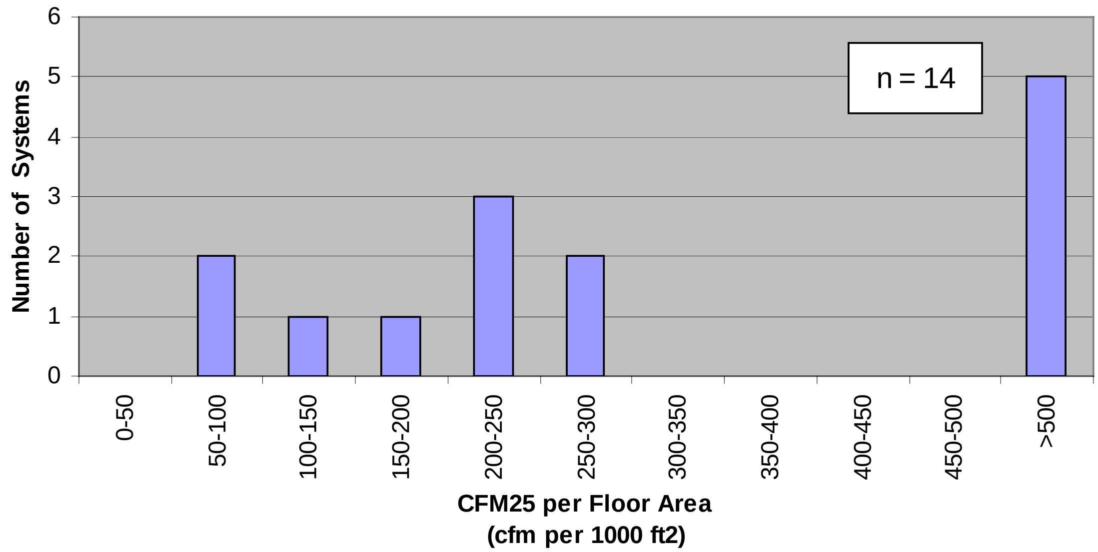

Figure 2-28. Histogram of Ductwork CFM25 per Floor Area

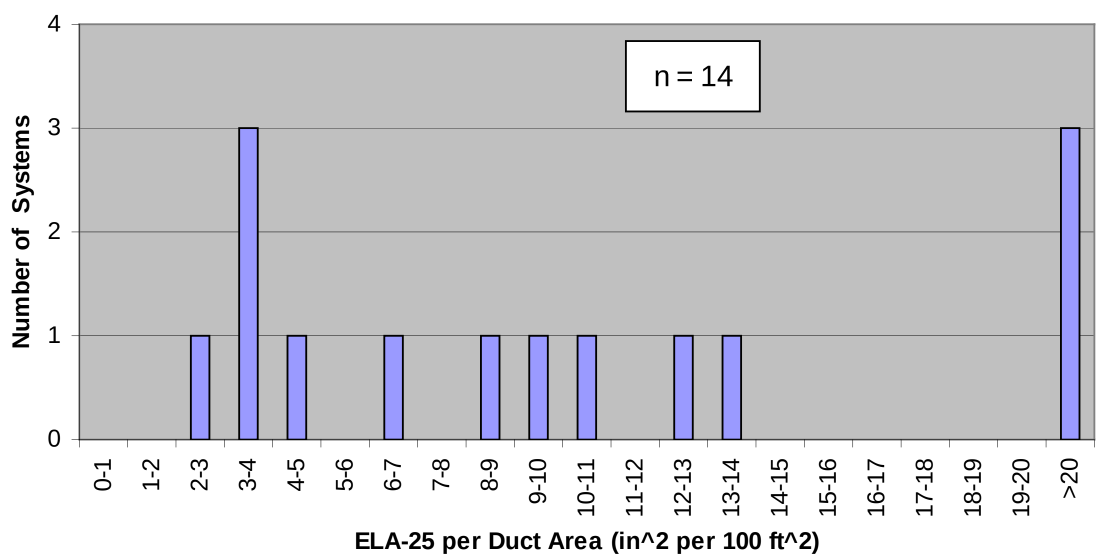

Figure 2-29. Histogram of Ductwork ELA-25 per Ductwork Surface Area

Table 2-8. Comparison Duct Leakage Statistics from Previous Studies

	NY Buildings Avg / Median	Florida Buildings[1] Average	California Buildings[2] Average
ELA-25 (sq in) per Nominal AC Size (ton)	12.8 / 7	12.1	17.1
CFM-25 per 1000 ft^2 of floor area	406 / 265	341	na

Notes: 1 – Florida buildings from Cummings et al (1996),
2 – California buildings from Delp et al (1998)

2.8. Summary

The field test results from the 25 small commercial buildings in New York identified some differences and some similarities compared to the Florida (Cummings et al 1996) and California (Delp et al 1998) field studies. The sample of 25 buildings in this study were larger on average than the 69 Florida buildings (median floor area of 9,204 ft^2 in NY compared to an average of 5,030 ft^2 in Florida). Generally, the range of building types included in the sample were in line with the distribution of building types identified in the 1999 CBECS study for the Northeast region (with the exception that the field study sample included slightly more offices and fewer retail buildings than the CBECS study)

The average ACH50 for NY buildings was 11.4 air changes per hour, compared to 16.7 air changes per hour in the Florida study. The lower ACH50 for the NY buildings appears to primarily driven by the smaller number of buildings without an air barrier at the ceiling or roof (16% in NY compared to 42% in Florida). We generally found that larger buildings – which tend to have flat, built-up roofs and unvented attics – were usually tighter than smaller buildings with a more residential building design.

The exponent determined from the blower door tests at 17 buildings averaged 0.65, which is in line with the FSEC study (with average of 0.61) as well as other industry experience. The exponent did show a slight trend with air tightness, implying that leakier buildings are more likely to have larger holes with exponents closer to 0.5.

The average building in this study was depressurized by about 1.1 Pa, which is very similar to the FSEC findings for Florida Buildings. Only 7 of the 26 buildings operated at positive pressure; one of these buildings was positively pressurized because it had a failed exhaust fan.

The normalized fan power (Watts per cfm) was determined for several air handlers ranging from 2.5 to 55 tons. The average fan power was 0.59 W/cfm, which is in line with findings from other field studies (Proctor and Parker 2000). While we could not detect any variation in normalized fan power as function of unit size or airflow, the data did show a modest trend of higher normalized fan power for units operating at a lower normalized air flow (cfm per ton).

Duct leakage measurements were taken on 14 different systems from 8 different NY buildings. The average and median duct leakage (ELA-25) normalized for air conditioner tonnage was 12.8 and 7 in^2 per ton. The average values from the Florida and California field studies were 12.1 and 17.1, respectively. The NY buildings showed a wide degree of variation in duct leakage rates, similar to what had been observed in the other field studies.

2.9. References

Cummings, J.B., C.R. Withers, N. Moyer, P. Fairey, and B. McKendry. 1996. "Uncontrolled Air Flow in Non-Residential Buildings; Final Report", FSEC-CR-878-96, Florida Solar Energy Center, Cocoa, FL, April, 1996.

Delp, Wm. Woody, Nance E. Matson, Eric Tschudy, Mark P. Modera and Richard C. Diamond. 1998. "Field Investigation of Duct System Performance in California Light Commercial Buildings". Report LBNL# 40102. Lawrence Berkeley Laboratory.

Federal Register. 1979. Test procedures for central air conditioners including heat pumps. Federal Register Vol. 44, No. 249. pp 76700-76723. December 27, 1979.

Proctor, John, and Danny Parker. 2000. "Hidden Power Drains: Residential Heating and Cooling Fan Power Demand." In Proceedings of the ACEEE 2000 Summer Study on Buildings, 1.225–1.234. Washington, D.C.: American Council for an Energy-Efficient Economy.

Sherman, M. 1998. The Use of Blower Door Data. Report LBL #35173. Lawrence Berkeley Laboratory. March 13.

3. Monitoring the Energy Impacts of Mitigating UAFs

At three of the twenty-five tested buildings, improvements were implemented to correct or mitigate the impact of uncontrolled airflows. At these sites we installed monitoring equipment or evaluated utility bills to quantify the impact of these improvements on building energy use.

3.1. Buildings Selected for Mitigation

At many test sites we identified potential opportunities to fix UAF problems and improve building performance. These ideas and suggestions were typically communicated to the site personnel via phone conversations along with a brief summary report (see the Detailed Summary for each site in Appendix A). At some of the sites, the proposed improvements were capital intensive (e.g., apply 2-3 inches of spray foam on the underside of the roof deck to seal and insulate the attic space). While we tried to convince some of the sites that comprehensive and capital-intensive improvements were cost effective, we were ultimately unsuccessful. However, at three of the sites we were able to implement lower-cost improvements that significantly reduced uncontrolled airflows and energy use.

Table 3-1 summarizes the buildings that were recommended for remediation to mitigate UAFs and reduce energy use. In many of these cases the proposed improvement was a capital intensive project that was difficult for the site owner to undertake. The three buildings where improvements were ultimately implemented and monitored – Sites 1, 2 and 17 – are shaded as gray in the table. These improvements were all relatively low-cost improvements that were implemented with 1 or 2 man-days of labor for a few thousand dollars. At the other sites we presented our ideas to the site owner but were ultimately unable to convince them to implement the proposed project. The measured impacts of the improvements at these 3 sites are discussed individually in the sections that follow.

Table 3-1. UAF Mitigation Improvements Considered and Proposed At Sites

Site	Issue and Proposed Improvement	Status
Site 1 Office Utica	Issue: This office has a very leaky ceiling insulation with no air barrier above t-bar ceiling. Many insulation batts had been knocked down by efforts to remove a squirrel nest. Proposed Improvement: 1) reposition batts, 2) apply spray foam to underside of roof deck; seal attic to make it airtight.	The site staff replaced/repositioned the fiberglass batts themselves in late 2004, but was not interested in fully insulating the attic
Site 2 Office Cazenovia	Issue: This office has a very leaky ceiling insulation with no air barrier above t-bar ceiling. Uninsulated return duct goes above the insulation into the attic. Proposed Improvement: Eliminate the return duct system and provide door under-cuts and door vents to allow air to return back to the air handler. Use spray foam to seal large leaks in the insulation barrier	The site reluctant to eliminate the return duct system due to concerns about maintaining privacy in each office. Compromise solution was to spray foam the surface of the return duct to provide some insulation and air sealing. Also replaced fiberglass batts and sealed major leaks with foam to improve air barrier.
Site 4 Office New Hartford	Issue: Loose insulation is above the t-bar ceiling between attic and conditioned space. Several penetrations in insulation barrier for wiring, HVAC, etc. AHUs are located in unconditioned attic. Several major duct leaks. Building is reasonably airtight, but air barrier is effectively at uninsulated roof deck. As a result the building has problems with ice dams. Proposed Improvement: Apply spray foam insulation to the underside of the roof deck. Bring the HVAC units inside the thermal boundary.	The site was not interested in investing the capital required for a spray foam insulation project. The large leak in the ductwork was fixed.
Site 10 Public Office Ithaca	Issue: Energy Recovery Ventilator (ERV) was providing too much ventilation to the space. Proposed Improvement: Rebalance airflows to provide proper ventilation	The site was interested but could not obtain approvals in time to complete the work required for this study
Site 17 Social Club Syracuse	Issue: 3 story historic building was fairly leaky. Attic floor was uninsulated or poorly insulated. Vintage elevator shaft from 1st floor to attic represented a significant leakage path for stack-driven airflows. Infrared camera analysis revealed significant air leaks into the attic around penetrations (fireplaces, structural elements, etc.). Elevator room in the attic was very leaky. Proposed Improvement: Use spray foam to seal air leaks in attic floor. Caulk and weather-strip elevator mechanical room to reduce stack effect.	The site agreed to let CDH staff apply spray foam to seal leaks in the attic and seal the mechanical room.
Site 21 Retail / Auto Service Clinton	Issue: Steel panels were used as an interior covering / air barrier in the shop area. Sales area at front of the building had no air barrier above drop ceiling, resulting in significant airflow through fiberglass batts. Hatch in rear of the building was open. Building had ice dam problems. Proposed Improvement: Install gypsum board or steel panels in front of the building above drop ceiling to air barrier	This change would significantly disrupt the showroom area. May be appropriate when building is remodeled.

3.2. Measured Impacts: Site 1 – Utica Office

Site 1 was a 5,000 ft^2 office in Utica. This site had a very leaky building envelope due to the lack of an air barrier above the t-bar ceiling. Problems were exacerbated because the ceiling space (space between the ceiling and insulation) was also used as the return air path and many insulation batts had been knocked down, providing a clear air path from the conditioned space to the attic. We proposed several ideas to the site to solve these problems. While this not-for-profit institution was not able to obtain funding to implement the capital improvements, they did replace the fallen fiberglass batts around January 2005. The impact of this simple improvement is discussed below. A comprehensive description of the site and the measured impacts is given in Appendix A1.

3.2.1. Implemented Improvements

When Site 1 was blower door tested in April 2004, the ACH50 for building was 31.2 air changes per hour. This high leakage rate was due to the fact that many of the fiberglass batts had fallen from between the roof trusses. Figure 3-1 shows the locations of the fallen fiberglass batts. The batts had fallen in November 2003 when a worker had gone into the attic to remove a squirrel and its nest. In the process, several batts had been dislodged, leaving large openings between the ceiling plenum and the attic. In total, about 60 linear feet of fiberglass batts had been knocked down, mostly in the front part of the building.

In January 2005 we had reported the problem with the fallen fiberglass batts and suggested several improvements. Shortly after receiving our report, the site fixed the fallen insulation.

3.2.2. Measured Results

Combining the monthly utility bill readings with temperature data from a nearby weather station (Syracuse) demonstrated the large impact that the fallen batts had on heating energy use. Figure 3-2 shows that the heating load line was much different from December 2003 to January 2005 when the insulation batts were down. After the batts were put back in place, the heating load line resumed the trend that had been seen before December 2003.

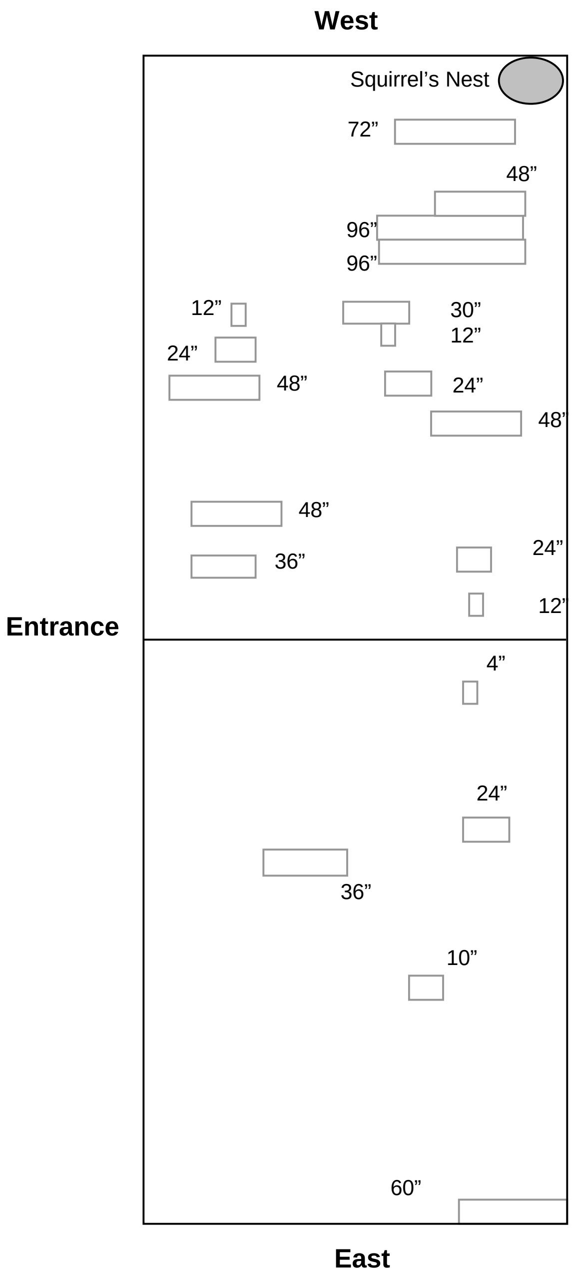

Total Length of Fallen Batts:

West/Front Area: 52.5 ft
East/Rear Area: 11.2 ft

Figure 3-1. Location of Fallen Fiberglass Batts at Site 1 (in March 2004)

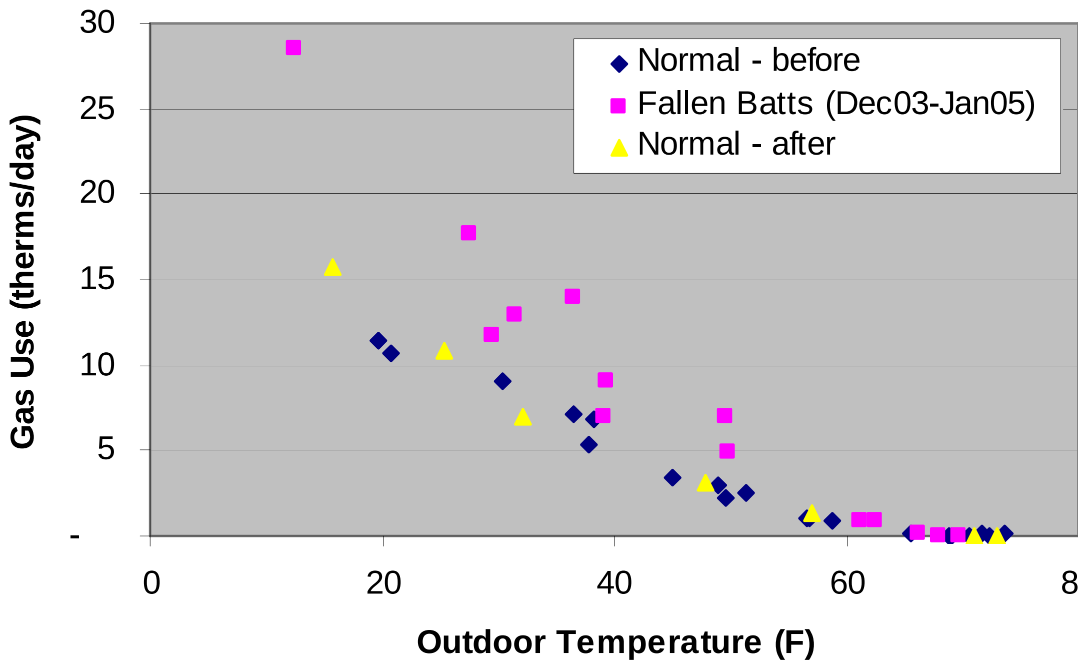

Figure 3-2. Impact of Fallen Fiberglass Batts on Heating Load Line

Table 3-2 summarizes the impact of the fallen fiberglass batts on the annual gas use (normalized per square foot of floor area). Annual gas use was higher by 70-80% for the period when the batts were down (December 2003 through January 2005). The energy use impact was considerably greater on the front (or west) section of the building because nearly 80% of the fallen batts were located in this area. With the batts in place (July 2002 through June 2003) the gas use intensity was 32 MBtu per square foot per year, which is more inline with expectations for this type of building.

Table 3-2. Summary of Impact Fiberglass Batts on Annual Gas Use Index

	Gas Use Index (MBtu/ft^2-yr)		
	East	West	Total
Jul-02 - Jun-03	28.0	35.9	32.0
Jul-03 - Jun-04	46.0	63.8	54.9
Jul-04 - Jun-05	25.9	51.7	38.8
Insul Down	47.1	65.9	56.5

Note: The "Insul Down" period corresponds to December 2003 to January 2005

The insulation breach in 2004 had no perceptible impact on cooling energy use as shown in Figure 3-3 below. Electric use in the cooling months was not as strongly affected by the large ceiling leak. This implies that stack-driven heat loss into the attic was the primary loss mechanism. Apparently induced leakage from the AHU fan depressurizing the ceiling plenum – which should impact both heat and cooling operation – had much less impact.

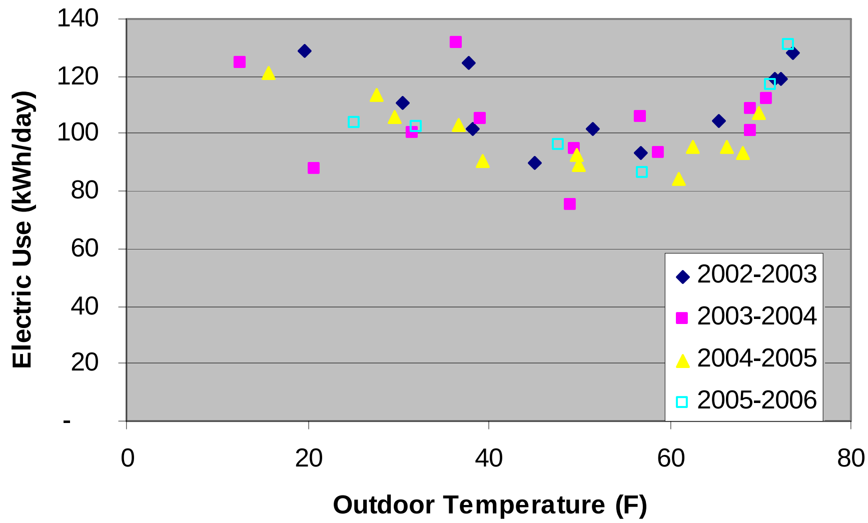

Figure 3-3. Variation of Electric Use for Different Periods

We were never able to repeat the blower door testing at the building after the fiberglass batts were replaced because the organization had sublet part of the space to another tenant in 2006.

3.3. Measured Impacts: Site 2 – Cazenovia Office

Site 2 was a 1,440 ft^2 office in Cazenovia, NY. This site had a very leaky building envelope due to the lack of an air barrier above the ceiling. While the ceiling space had 12 inches fiberglass insulation (stapled to the bottom of the trusses), many of paper-face fiberglass batts were poorly secured and had fallen down. The energy performance of the building was further degraded because the uninsulated metal return duct was in the attic above the insulation. We proposed a range of building envelope improvements to owner which CDH implemented. Monitoring equipment was installed in the building to measure the impact of the changes. The following provides a brief description of the implemented changes and the measured impact of these improvements. A comprehensive description of the site and the measured impacts is given in Appendix A2.

3.3.1. Implemented Improvements

When Site 2 was blower door tested in April 2004, the ACH50 for building was 33 air changes per hour. This high leakage rate was due to the fact that the fiberglass batts were installed above the t-bar ceiling without an air barrier. The energy use intensity in this building was also much higher than the other similarly-constructed offices at 74 MBtu per squared foot of floor area per year.

The HVAC system in this small accounting office was unique in that it included separate return ducts to each of the 6 to 8 private offices and rooms in the building. This more complicated design approach had been used to maintain privacy in all of the offices (i.e., it eliminated the need for door undercuts and transfer grills to return air back to the air handler/furnace). However, due to the limited space between the ceiling and the insulation, only the supply ducts were located below the insulation; the return ducts had to be located above the insulation in the attic. As result, return air was pre-cooled as it traveled through the uninsulated return duct in the winter (and preheated in the summer).

Our initial proposal to the building owners was to eliminate the return duct. However, they were concerned that increasing door undercuts and vents that would affect office privacy. As a compromise, we agreed to a complete the following steps: 1) replace fiberglass batts and fill obvious voids in the ceiling insulation, and 2) apply spray foam on top of the return duct in the attic to seal and insulate it. The major remediation dates are summarized below.

February 19, 2006	CDH staff completes process of reposition batts and filling large voids.
March 11, 2006	CDH staff applies spray foam insulation to top and side of the return duct; fixes some additional voids in the ceiling insulation.

<u>Envelope Sealing</u>

The first step in addressing the leakage issue with the building was to evaluate and repair the ceiling batts, and seal any major envelope leaks. Some of the 12-inch fiberglass batts that had been installed during the building remodeling (in 1996) had fallen through the framing trusses, leaving large areas of the drop ceiling exposed directly to the attic space. The fiberglass batts act as both the thermal and air barrier in this building, with no sheathing on the underside of the trusses. The batts were originally installed with a friction fit, with no support underneath.

These large leaks allow conditioned air to escape into the vented attic space, warming the attic in the winter and causing large ice dams to form (Figure 3-4). The leakage into the attic also results in additional heating and cooling energy consumption.

As a low cost way to mitigate these gross envelope leaks, we removed the ceiling tiles, identified and replaced any batts which had fallen down, and supported the batts from underneath with furring strips, attached to the underside of the truss (see Figure 3-5). We also sealed the perimeter of the building and other large voids with expandable spray foam.

Figure 3-4. Ice Dams Formed from Leakage to the Attic

Figure 3-5. Furring Strip Installed to Support Fiberglass Batts from Underneath

Duct Insulation and Air Sealing

The un-insulated return ductwork in the attic also contributed to the ice dam issue by transferring heat from the space to the attic. These duct losses were magnified by the decrease in attic temperature after the envelope was sealed on February 19, 2006. To mitigate these losses, the return ductwork was sprayed with expandable foam. Approximately ½ to 1 inch of foam coating was added to seal air leaks in the ductwork and provide some insulation from the unconditioned attic.

Figure 3-6 shows a section of the ductwork before and after the foam was applied. The typical foam depth was between ½-inch and 1-inch thick, resulting in an applied insulation level of R2.5 to R5. The transitions between the sheet metal return plenum and flexible duct takeoffs were coated, overlapping slightly onto the flexible duct.

Existing Return Ductwork | Return Ductwork with Spray Foam Insulation

Figure 3-6. Return Ductwork in Attic Space

During this work, a few additional gaps were identified in the fiberglass insulation and these were closed in the same manner as the previous fix (supporting the batts from below using furring strips).

Estimated Retrofit Costs

The retrofit work at Site 2 was completed by CDH staff. The labor and material costs to complete the retrofit are summarized below:

	Labor	Materials
February 19 (reposition batts, fill voids)	2 man-days	$100
March 11 (spray foam duct, fill voids)	2 man-days	$500

Assuming a fully-burdened labor rate of $50 per hour for a weatherization contractor, the total retrofit cost would have been approximately $2,200-2,500 depending on the markup.

3.3.2. Measured Results

A Campbell CR10 datalogger was installed to characterize the heating load and remediation impacts by measuring the furnace runtime. Return and space temperatures were also monitored to determine impact of return duct leakage on the heating load. The schematic in Figure 3-7 shows the location of measured points.

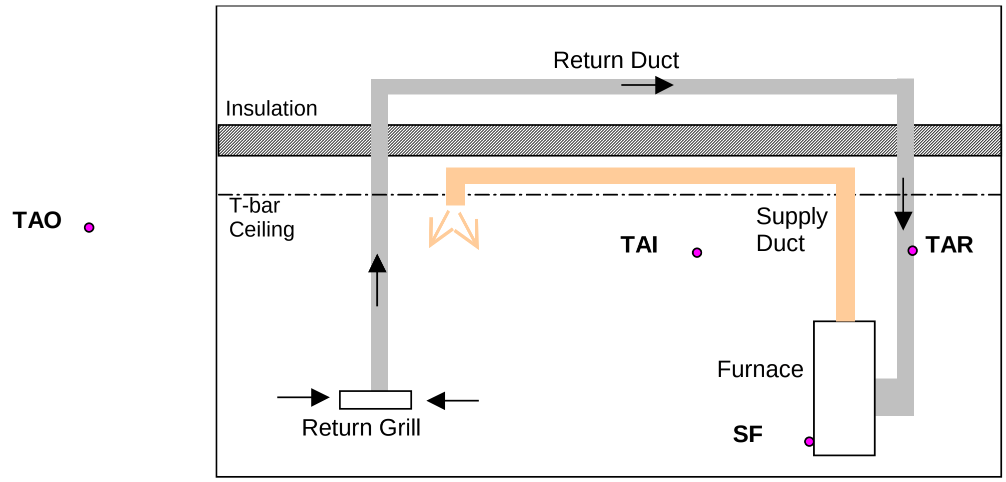

TAR – Return Air Temperature Entering Furnace
TAI – Indoor Temperature (F)
SF – Furnace Runtime (F)
TAO – Ambient Temperature (F) (from Syracuse Airport)

Figure 3-7. Locations of Monitored Data Points Installed at Site 2 to Measure Remediation Impact

The measured runtime of the furnace was compared to the gas meter readings for the building to determine the typical fuel input for the furnace. A heating value of 1,020 Btu/cu ft was used to convert the gas meter readings to energy input. The gas meter is read to the nearest 100 cu ft, which resulted in a typical error of ±0.02 therm/h in the table below. The fuel input to the furnace averaged 0.712 therm/h or 71.2 MBtu/h. This agrees well with the nominal size of the furnace (75 MBtu/h input).

Table 3-3. Comparing Measured Furnace Runtime to Gas Meter Readings

Start Date	End Date	Start Meter Reading (cu ft)	End Meter Reading (cu ft)	Furnace Runtime (hours)	Gas Use (therms)	Furnace Input (Therm/h)
Jan 6, 2006	Jan 18, 2006	9,528	9,593	93.1	66.3	0.712
Jan 18, 2006	Feb 17, 2006	9,593	9,732	199.5	141.8	0.711
Feb 17, 2006	Feb 27, 2006	9,732	9,785	77.4	54.1	0.698
Feb 27, 2006	Mar 8, 2006	9,785	9,826	60.7	41.8	0.689
Mar 8, 2006	Apr 17, 2006	9,826	9,919	129.3	94.6	0.731
Totals/Average				***560.0***	***398.5***	***0.712 (0.69 – 0.73)***

Using the calculated fuel input and the measured daily runtime of the furnace, the thermal load line for the building after remediation was calculated, and compared to the historic building load line. Compared to the heating load line for 2002-2003, the building is using approximately 285 therms per year less (24% less) than the building did in 2002-2003. However, this change may include other factors such as the use of a more aggressive thermostat setback in the post period. The sections below attempt to normalize for thermostat control changes as well as discern the separate impacts of the envelope sealing and duct leakage.

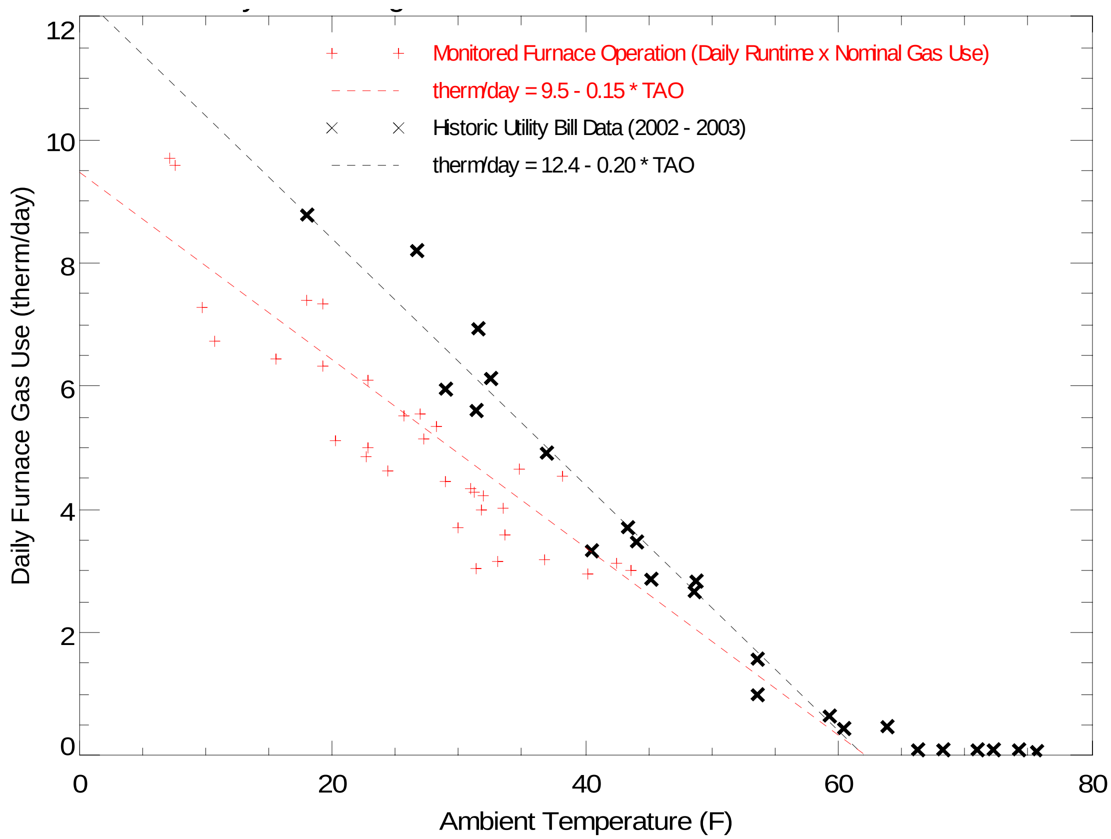

Figure 3-8. Comparing Monitored Gas Use (Based On Furnace Runtime) and Historic Utility Bill Data

Figure 3-9 shows the data collected for the base period before the remediation. The return temperature (TAR) is consistently lower than the space temperature (TAI), indicating a combination of thermal conduction loss from the return duct, as well as air leakage into the depressurized duct.

The return temperature is typically 5-8°F lower than the space temperature. For some periods the return temperature is as much as 15°F lower than the space.

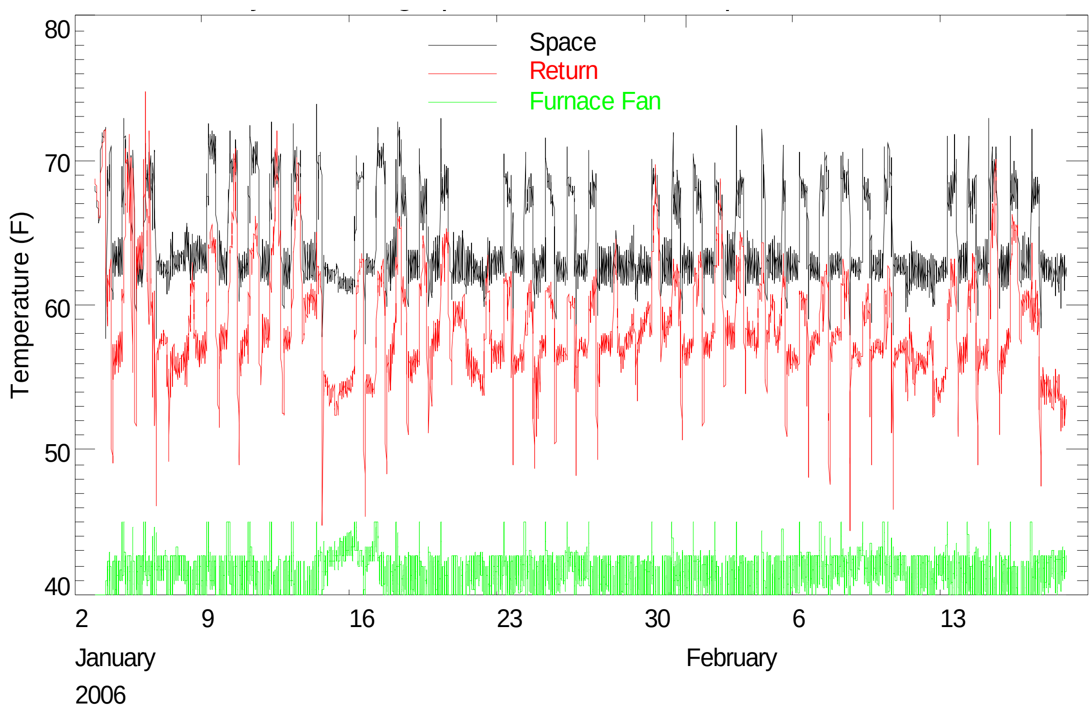

Figure 3-9. Space and Return Conditions For Base Building

Figure 3-10 shows this temperature data for one day. The transition period from the occupied setpoint to the setback temperature around 6 PM is of particular interest. During this period when the furnace fan remained off for a couple of hours, the return temperature approaches the outdoor temperature rather than approaching the space temperature. The return temperature sensor is located in the un-insulated return plenum (near the furnace) in the conditioned space. This trend implies that air is continuing to move down into the return plenum even while the fan is off. As a result, thermal losses continue to occur when the system is off. If the air were stagnant in the return plenum, the return temperature would be expected to approach the space temperature.

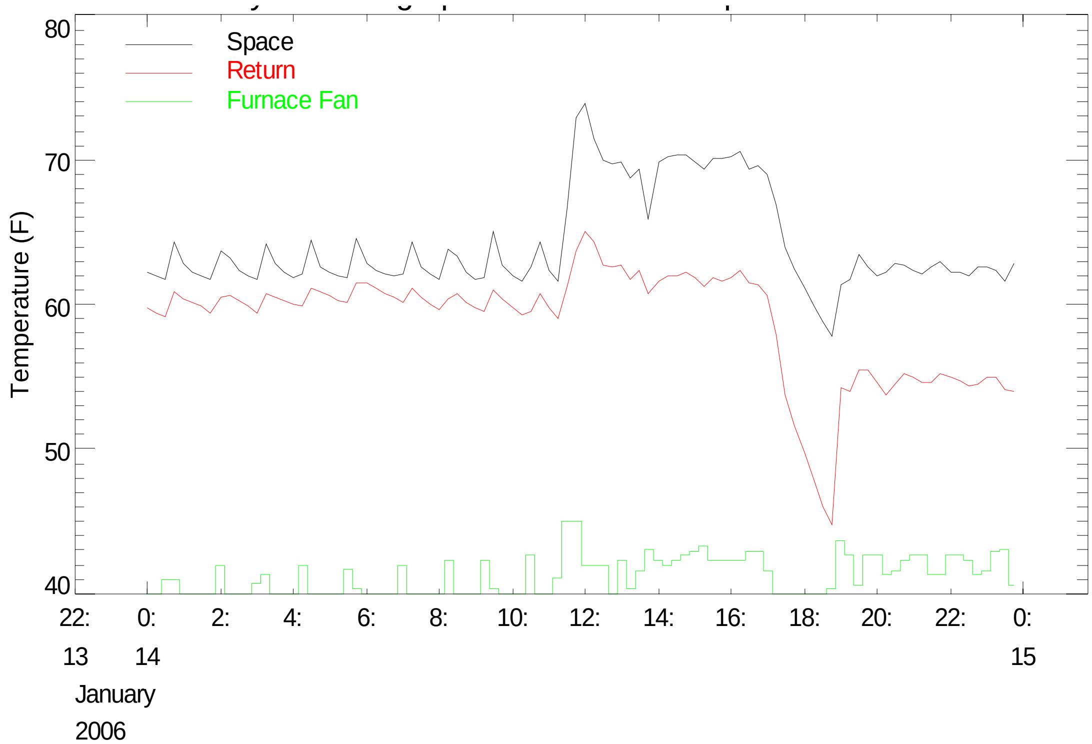

Figure 3-10. Space and Return Conditions For Base Building Typical Day with Setback

This remediation had a multifaceted impact on the building. With less leakage of air into the attic, the building uses less energy to maintain the space at the heating setpoint, providing energy and cost savings. The potential for ice damming has decreased, as the tighter building envelope lowers temperatures in attic. However, the decrease in attic temperatures caused an increase in the return duct losses, as shown in Figure 3-11. The temperature drop in the return duct (TAI-TAR) increased by an average of 1.3°F after the envelope was sealed on February 19 – implying that the attic temperature is colder.

When the return duct was insulated on March 11, the return duct temperature drop (TAI-TAR) decreased to just below the original levels observed in the base period. Figure 3-12 shows that return duct temperature drop decreased by an average of 1.7ºF when the duct was insulated.

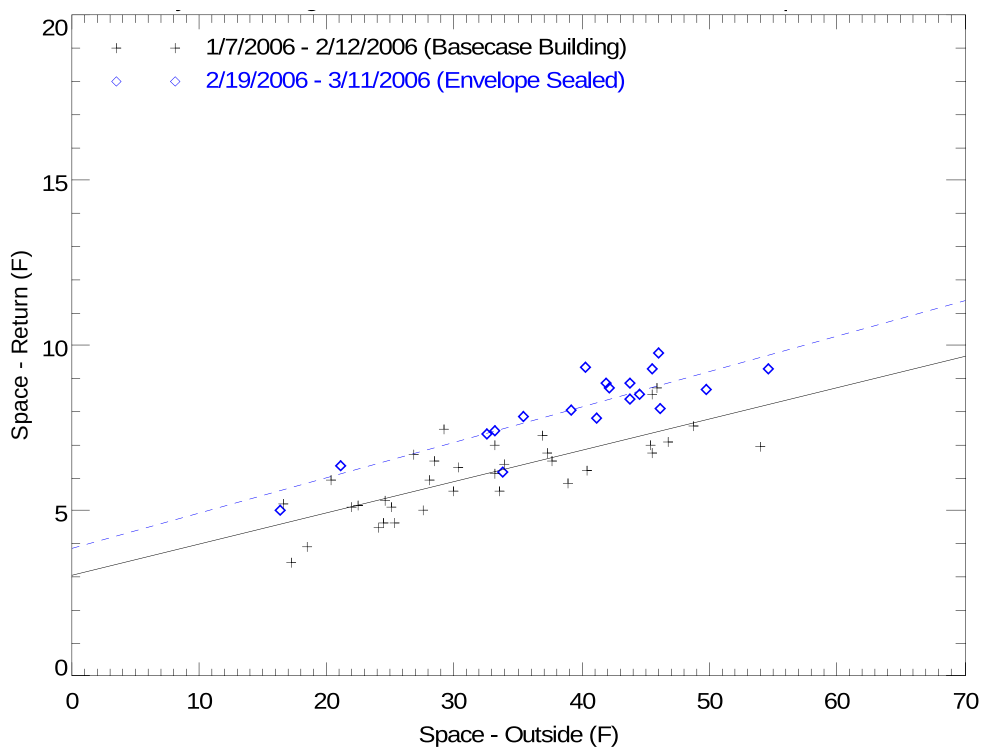

Figure 3-11. Change in Return Duct Temperature Drop Resulting From Tightening the Envelope

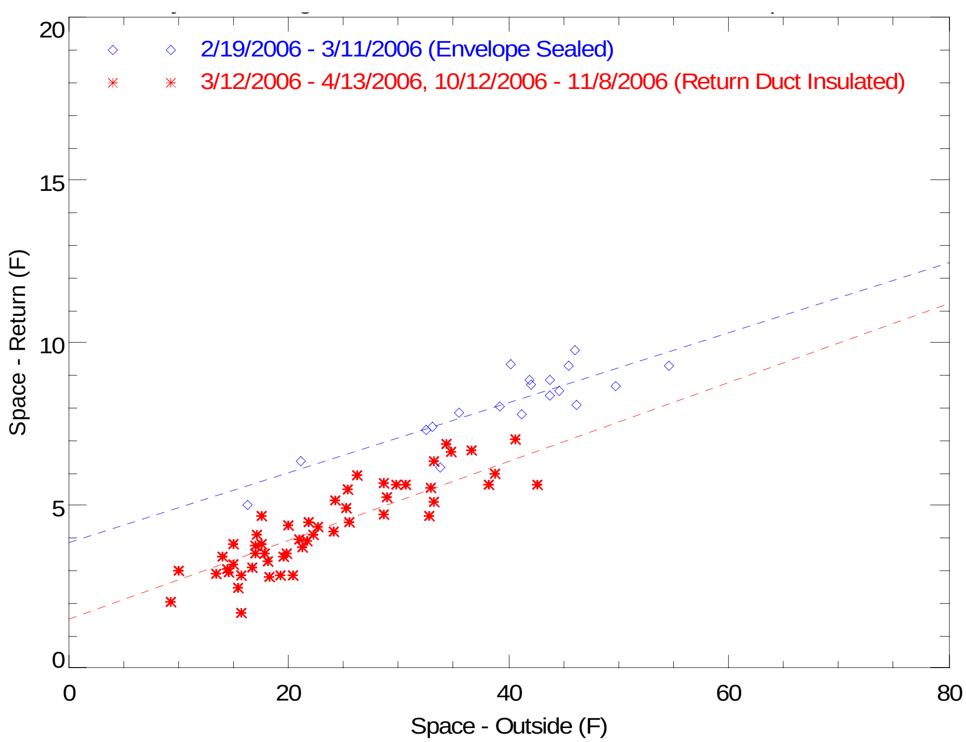

Figure 3-12. Change in Return Duct Temperature Drop Resulting From Adding Duct Insulation

Using the trends above with typical meteorological year (TMY) data for Syracuse, NY provided the means to estimate the total losses through the return ductwork. The thermal losses were calculated by using the temperature drop in the duct and the measured furnace airflow. The heat loss was determined by multiplying by the daily furnace runtime fraction (RTF). This represents the lower bound of the duct losses. The upper bound assumes that losses occur continuously, without considering furnace runtime. The actual level of losses is probably somewhere between these two extremes, since the temperature data imply that some air continues to move through the ductwork when the furnace fan is off.

Table 3-4 and Table 3-5 display bin calculations using daily relations for the temperature drop in the return duct and the daily furnace runtime fraction. In Table 3-5 the daily runtime fraction is set to 1.0 to simulate constant losses from the ductwork. Table 3-4 assumes losses only occur when the furnace fan is on. The annual impact of duct losses on the base case building under these two scenarios ranged from 98 to 453 therms/year. Assuming that off-cycle losses are on the order of 25% of continuous fan operation, the annual duct losses for the base building would be about 190 therms/year.

Table 3-4. Duct Loss Calculation – Base Case Building with Furnace RTF (lower bound of losses)

[1]	[2]	[3]	[4]	[5]	[6] = 3.03 + 0.095*[5]	[7] = [6]*1.08 * 1,035 SCFM / 1000	[8] = (1.17 + 0.738 * [5])/100	[9] = [4]*[7]*[8]*24
Syracuse TMY2 Bin Data								
Bin Low	Bin High	Bin Med	Number of Days	Average Space Outdoor Temp Diff	Temp Drop Through Duct	Steady State Losses	Daily Furnace RTF	Acutal Losses
(F)	(F)	(F)	(days)	(F)	(F)	(MBtu/h)	(-)	(MBtu)
-25	-20	-22.0	0	-	-	-	-	-
-20	-15	-17.0	0	-	-	-	-	-
-15	-10	-12.0	0	-	-	-	-	-
-10	-5	-7.0	0	-	-	-	-	-
-5	0	-2.0	0	-	-	-	-	-
0	5	2.0	3	58	8.5	9.5	0.44	300.6
5	10	7.0	4	56	8.3	9.3	0.42	378.7
10	15	12.0	5	51	7.9	8.8	0.39	407.8
15	20	17.0	14	45	7.3	8.2	0.34	938.4
20	25	22.0	21	41	6.9	7.7	0.31	1,219.9
25	30	27.0	22	35	6.4	7.1	0.27	1,007.8
30	35	32.0	39	30	5.9	6.6	0.23	1,427.3
35	40	37.0	29	24	5.3	5.9	0.19	776.6
40	45	42.0	32	20	4.9	5.5	0.16	671.4
45	50	47.0	28	14	4.4	4.9	0.11	375.3
50	55	52.0	23	10	4.0	4.5	0.09	209.3
55	60	57.0	32	5	3.5	3.9	0.05	145.9
60	65	62.0	37	0	-	-	-	-
65	70	67.0	34	-4	-	-	-	-
70	75	72.0	25	-9	-	-	-	-
75	80	77.0	14	-14	-	-	-	-
80	85	82.0	3	-17	-	-	-	-
85	90	87.0	0	-	-	-	-	-

No days in temperature bin	**Total MBtu**	**7,859.0**
Assumes no losses untill 10 F below space temperature	**therms @ 80% EFF**	**98.2**

Note: Columns 6 and 8 were derived from a linear regression analysis of the data presented in the figures above.

Table 3-5. Duct Loss Calculation – Base Case Building with Constant Furnace RTF (upper bound of losses)

[1]	[2]	[3]	[4]	[5]	[6] = 3.03 + 0.095*[5]	[7] = [6]*1.08 * 1,035 SCFM / 1000	[8] = 1 (continuous)	[9] = [4]*[7]*[8]*24
Syracuse TMY2 Bin Data								
Bin Low	Bin High	Bin Med	Number of Days	Average Space Outdoor Temp Diff	Temp Drop Through Duct	Steady State Losses	Daily Furnace RTF	Acutal Losses
(F)	(F)	(F)	(days)	(F)	(F)	(MBtu/h)	(-)	(MBtu)
-25	-20	-22.0	0	-	-	-	-	-
-20	-15	-17.0	0	-	-	-	-	-
-15	-10	-12.0	0	-	-	-	-	-
-10	-5	-7.0	0	-	-	-	-	-
-5	0	-2.0	0	-	-	-	-	-
0	5	2.0	3	58	8.5	9.5	1.00	686.6
5	10	7.0	4	56	8.3	9.3	1.00	895.1
10	15	12.0	5	51	7.9	8.8	1.00	1,055.3
15	20	17.0	14	45	7.3	8.2	1.00	2,741.4
20	25	22.0	21	41	6.9	7.7	1.00	3,898.5
25	30	27.0	22	35	6.4	7.1	1.00	3,748.6
30	35	32.0	39	30	5.9	6.6	1.00	6,149.5
35	40	37.0	29	24	5.3	5.9	1.00	4,130.4
40	45	42.0	32	20	4.9	5.5	1.00	4,232.3
45	50	47.0	28	14	4.4	4.9	1.00	3,276.2
50	55	52.0	23	10	4.0	4.5	1.00	2,457.3
55	60	57.0	32	5	3.5	3.9	1.00	3,012.1
60	65	62.0	37	0	-	-	-	-
65	70	67.0	34	-4	-	-	-	-
70	75	72.0	25	-9	-	-	-	-
75	80	77.0	14	-14	-	-	-	-
80	85	82.0	3	-17	-	-	-	-
85	90	87.0	0	-	-	-	-	-

No days in temperature bin

Assumes no losses untill 10 F below space temperature

Total MBtu **36,283.3**

therms @ 80% EFF **453.5**

Note: Columns 6 and 8 were derived from a linear regression analysis of the data presented in the figures above.

Net Energy Impact of Remediation

The net impact of the building remediation is observed in the change in furnace operation (and hence energy consumption). Due to the number of drastic thermostat setpoint changes observed during monitoring, direct comparison of the different periods was not possible. Therefore energy use data from before and after the remediation steps was compared to the daily indoor to outdoor temperature differential.

Figure 3-13 displays the daily furnace runtime to the average indoor-outdoor temperature difference. The percentage on the plot legend indicates the average reduction in furnace runtime from each stage of the remediation efforts.

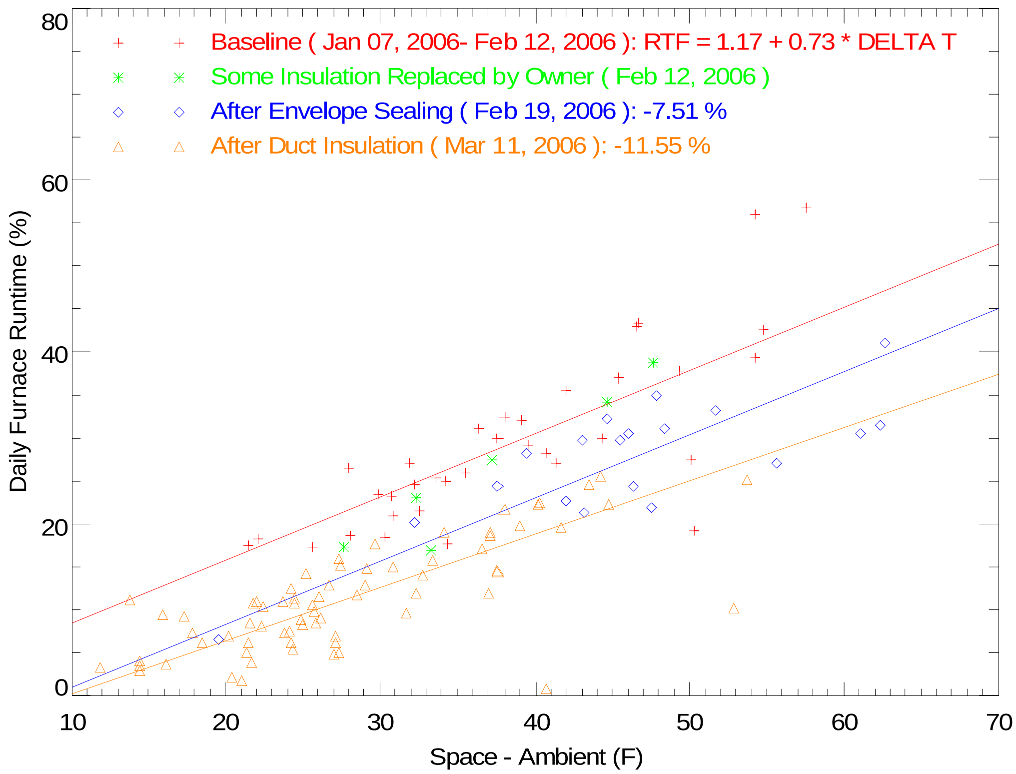

Figure 3-13. Impact of Remediation Efforts on Daily Furnace Runtime

By using the TMY2 data for Syracuse and a consistent space temperature/thermostat schedule, the annual impact of the remediation could be determined by means of modeling. The space temperature was set to be 70°F from 8:00 AM to 5:00 PM on weekdays, and 65°F for all other hours. Replacing the insulation reduced furnace runtime (and gas consumption) by 37%. Adding the duct insulation (and further sealing of the envelope) reduced the furnace runtime by an additional 13%.

Table 3-6. Annual Impact of Remediation Efforts

	Hours	Gas Input @ 0.712 Therm/h (therms)	Savings (therms)	Savings (%)
Base case Heating Hours	1203	856.7	N/A	N/A
Sealed Envelope Heating Hours	754	536.9	319.8	37%
Sealed Envelope + Duct Insulation Heating Hours	606	431.5	425.3	50%

Annual energy savings from the remediation are 425 therm/year, and at a typical cost of natural gas of $1.50/therm, provides a cost savings of $638/year. Assuming a cost of $2,500 to implement this retrofit, the simple payback for remediation was 4 years.

Impact of Remediation on Building Airtightness

The blower door tests were repeated in November 2006 after remediation was complete to assess the impact on building leakage. The test was repeated with the same conditions as the original test (AHU closet closed, exhaust fans sealed). Then the supply and return grills were covered and the test was repeated (to estimate the ducts leakage). Table 3-7 compares these newest test results to the original tests. The remediation efforts reduced the equivalent leakage area (ELA) by 57 square inches (13%). The exponent changed from 0.58 to 0.65, implying that many large holes had been fixed. The ACH50 did not change appreciably (and actually increased slightly) after the remediation. This somewhat surprising result indicates the uncertainty associated with extrapolating blower door data to 50 Pa.

Table 3-7. Summary of Blower Door Test Results – Before and After Remediation

			Building Envelope			Ducts
	Flow Coeff. K	Exp. n	ELA@4 (sq in)	ELA / 100 sq ft (sq in/sq ft)	ACH_{50}	ELA@25 (sq in)
Before Remediation (Fig A2-8, Table A2-2)	706	0.579	447	10.42	33.0	
After Remediation	560	0.647	389	9.08	34.1	509
After Remediation (duct diffusers sealed)	553	0.637		8.84	32.3	487
			57			23

Notes: In the last column, only the difference in the ELA @ 25 Pa is meaningful (i.e., it provides an indication of duct leakage)

The second blower door test was conducted with the supply and return grills sealed with duct mask in order to estimate the duct leakage to outdoors. The ELA at 25 Pa is also shown in Table 3-7 to provide an indication of the duct leakage. The effective duct leakage to outdoors (ELA-25) after the remediation was 23 square inches, compared to a total duct leakage (ELA-25) of 56 square inches determined for the return ducts before the remediation with duct blaster (See Appendix A2).

3.4. Measured Impacts: Site 17 – Syracuse Social Club

The Social Club in Syracuse is an 18,000 ft^2, 3-story historic building that is a social club with dining facilities. The gas use intensity in this building was fairly high at 61 MBtu per square foot of floor area per year. The ACH50 for this building was 14.3 air changes per hour.
The attic floor was uninsulated or poorly insulated. A vintage elevator shaft from 1st floor to attic was significant leakage path for stack-driven airflows. Appendix A17 provides a full description of the implemented changes and the measured impact of these improvements.

3.4.1. Implemented Improvements

On February 23, 2006 the attic was surveyed with a thermal imaging camera. Several large leakage areas were identified along the perimeter attic wall (where the attic floor meets the brick wall), around each of the five chimney penetrations, and around each of the roof support braces.

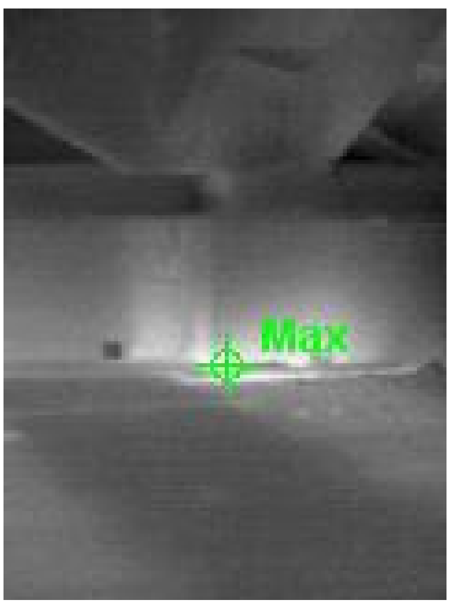

Leak along perimeter wall

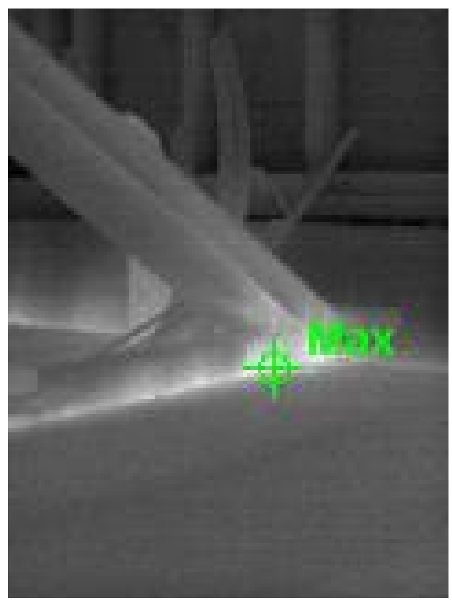

Leak along ceiling support brace

Figure 3-14. Thermal Imaging Camera Results Showing Air Leaks in Attic at Site 17

Based on the observations from the imaging camera, it was decided that a low cost way to mitigate these losses to the attic would be to spray expandable foam at the location of each leak. It was also determined that the small room housing the mechanical equipment for the elevator (located in the attic) was an additional source of leakage. The elevator mechanical room is constructed out of exterior wood framing, sheathed with mineral board with no insulation, and is not well sealed from the attic space (Figure 3-15). Calking and weather-stripping were added to this room to help seal it from the attic and reduce the impact of stack effect driving conditioned air up the elevator shaft into the attic

On March 23, 2006, we returned to the building to implement these improvements.

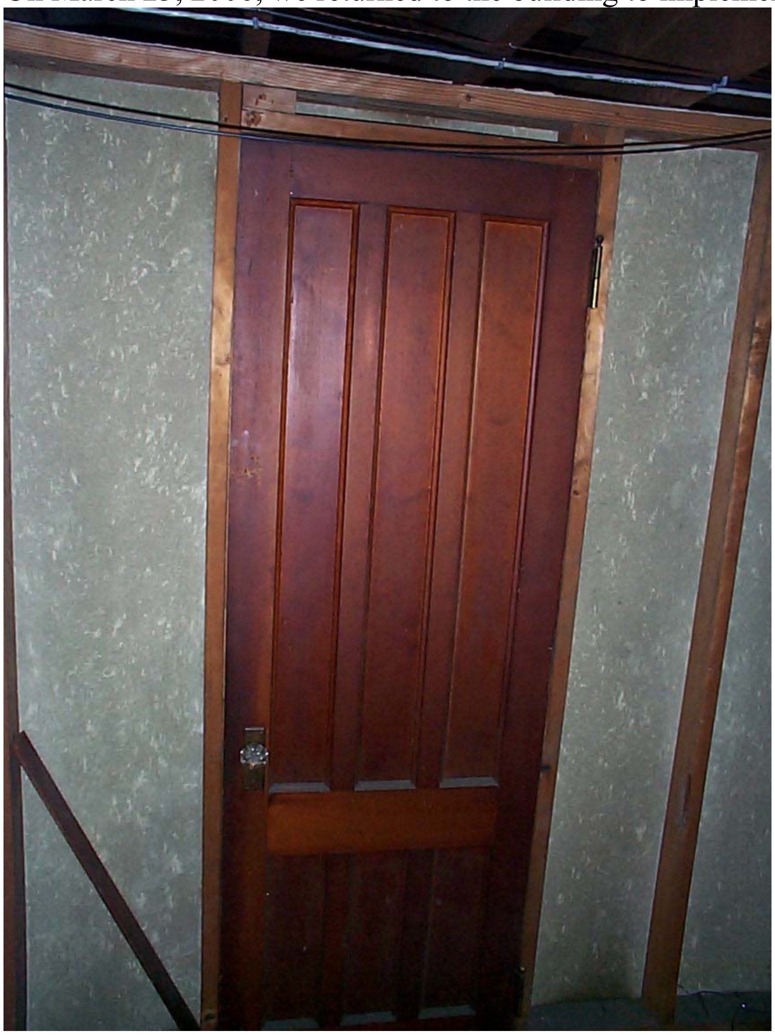

Figure 3-15. Exterior of Elevator Mechanical Room (Viewed from Attic)

Prior to spraying the expandable foam, areas of extreme leakage were identified using an infrared thermometer. The typical attic floor temperature away from a leak was near 41ºF, but areas where leaks occurred had a much higher surface temperature. Some areas were as high as 57ºF (see Figure 3-16). Areas where leaks were identified were marked with orange paint.

The entire perimeter of the attic was sprayed with expandable foam. The foam was applied with the spray tip flush with the crack between floor deck and the wall, to ensure the foam expanded downward into the crack. In other areas, the foam was applied to both surfaces (the wall and the floor) to seal the surfaces together.

Figure 3-17 displays typical areas where leaks were identified and filled with foam.


Attic Floor Temperature away from Leak


Attic Floor Temperature at Leak


Marking Leaks Areas before Spraying


Leakage Area Sealed with Foam

Figure 3-16. Diagnosing and Sealing Perimeter Leaks in the Attic

Around Chimney Penetration

Entire Perimeter

Roof Bracing

Large Area Leak Around Drain Plumbing

Figure 3-17. Different Types of Leaks Sealed with Expandable Urethane Foam

The elevator mechanical room was sealed using clear silicone adhesive caulk, which was wet mopped into each seam in the mineral board. The joints between the ceiling and wall, and floor and wall were also caulked. A closed cell foam rubber weather striping was applied to the mechanical room doorway. Figure 3-18 shows work performed on the mechanical room.

Caulking and Weather Striping

Corner Joints and Butt Joints Caulked

Figure 3-18. Sealing the Elevator Mechanical Room in Attic at Site 17

The impact of sealing the elevator shaft was confirmed measuring the pressure across the door before and after remediation. Prior to remediation, the pressure difference between the attic and the elevator room was 1.2 Pa (determined with the DG700 digital micromanometer). After the remediation (with approximately the same indoor to outdoor temperature differential), the pressure difference increased to 2.5 Pa, implying that sealing had created a greater flow restriction.

Estimated Retrofit Costs

The retrofit work at Site 17 was completed by CDH staff. The labor and material costs to complete the retrofit are summarized below:

	Labor	Materials
Apply Spray Foam (200 board ft), Caulk Elevator Room	1 ½ man-days	$600

Assuming a fully-burdened labor rate of $50 per hour for a weatherization contractor, the total retrofit cost would have been approximately $1,200-1,500 depending on the markup.

3.4.2. Measured Results

A CR10 Campbell Scientific data logger was installed at the site 15 days before the remediation was completed (March 8, 2006). Sensors were installed to determine the variation in boiler runtime and compared it with ambient temperature. The boiler is a modular boiler with three sections. Each section has an input of 400 MBtu/h for a total of 1.2 MMBtu/h, however the three sections operate in unison providing only a single stage of heating capacity. The runtime of the boiler was monitored using a current status switch on the 24 VAC control circuit for the natural gas valve (Figure 3-19).

Figure 3-19. Current Status Switch on 24 VAC Control Transformer for Boiler Natural Gas Train

Figure 3-20 displays the monitored boiler runtime data for before and after the remediation was completed. Multiplying the baseline boiler runtime trend (before building remediation) by the nominal boiler input (1.2 MMBtu/h) agrees well with the historic natural gas data. At 20°F ambient temperature, the historic gas consumption indicates a gas use of approximately 70 therm/day. The calculated baseline boiler gas use at this temperature based on 6 hours/day of runtime is 72 therm/day (6 hrs × 1.2 MMBtu/h × 10 therm/MMBtu).

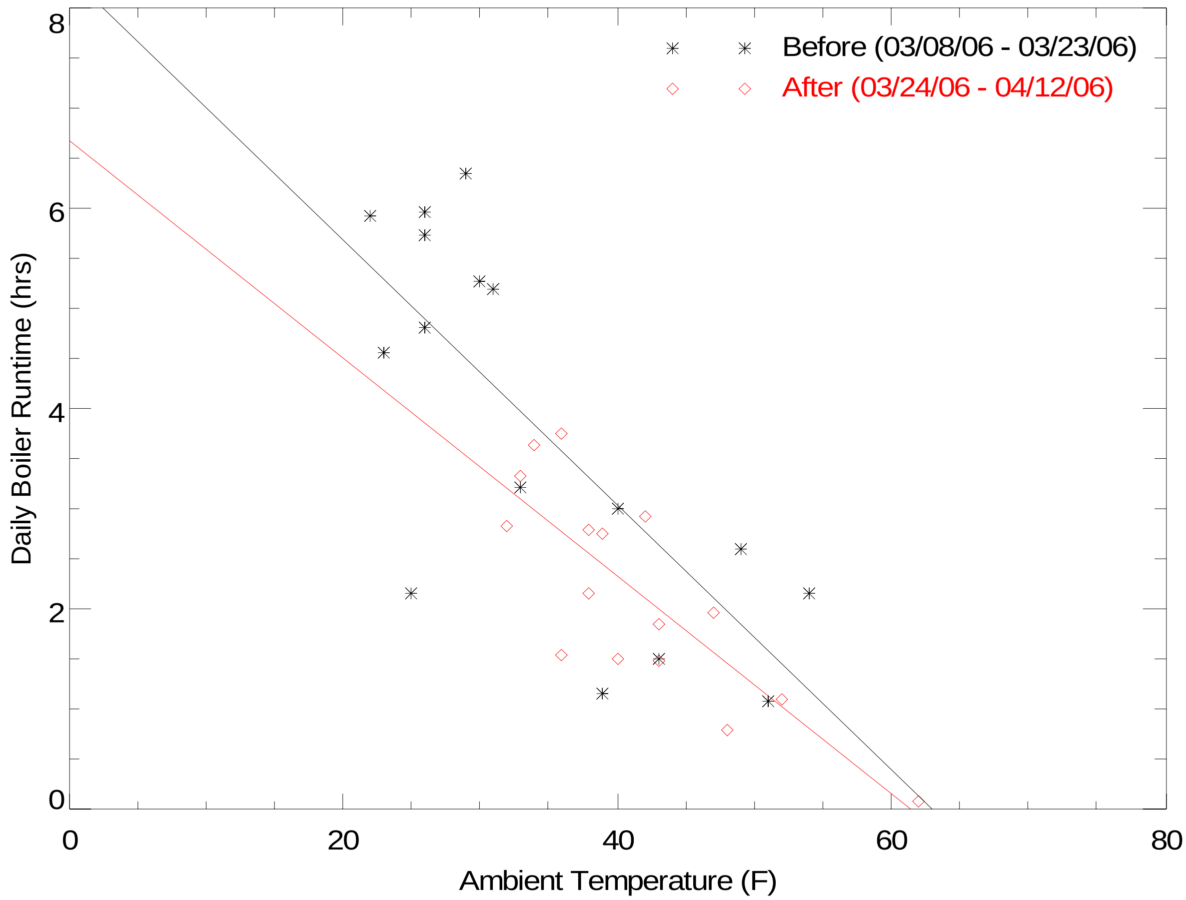

Figure 3-20. Boiler Runtime Variation with Ambient

The best-fit trendlines indicate that after the remediation, the boiler is operating 1.6 hours/day less at 0°F ambient. The impact is lower at milder conditions, and both trends converge at approximately the same point near 62°F.

Comparison of daily boiler runtime with the indoor-outdoor temperature difference (which compensates for variations in thermostat set point) imply similar results. The trends indicate that at a 70°F temperature difference to outdoors (approximately 0°F ambient), the boiler will operate 2.1 hours/day less after the remediation.

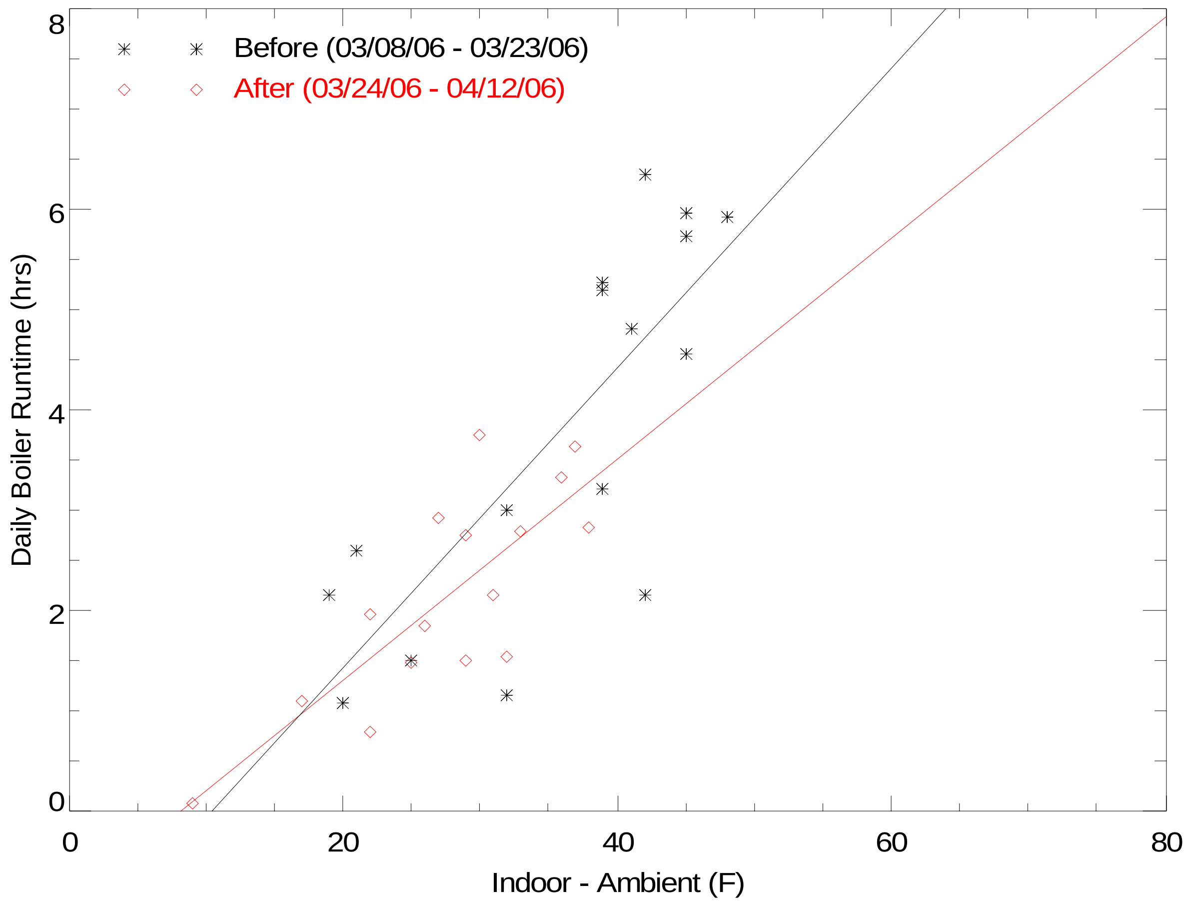

Figure 3-21. Boiler Runtime Variation with Indoor – Ambient Temperature Difference

Using the boiler runtime trends for the baseline and remediation periods, and bin data of the daily average temperature for Syracuse (from the Syracuse TMY2 file), the annual savings was calculated. Annually the boiler runtime was reduced by 199 hours, resulting in 2,389 therms of natural gas savings. Using natural gas costs of $1.50 per therm, the estimated annual cost savings are about $3,600/year.

Table 3-8. Annual Energy Savings Calculated for Remediation at Site 17

[1]	[2]	[3]	[4]	[5] = [8.33 - 0.133*[3]] * [4]	[6] = [6.68 - 0.109*[3]] * [4]	[7] = [6] - [5]	[8] = -4.35 + 1.06*[6]
Syracuse TMY2 Bin Data							
Bin Low (F)	**Bin High (F)**	**Bin Med (F)**	**Number of Days (days)**	**Baseline Boiler Runtime (hours)**	**Remediated Boiler Runtime (hours)**	**Runtime Reduction (hours)**	**Boiler Gas Savings @ 1.2 MMBtu/h Input (therms)**
-25	-20	-22.0	0	-	-	-	-
-20	-15	-17.0	0	-	-	-	-
-15	-10	-12.0	0	-	-	-	-
-10	-5	-7.0	0	-	-	-	-
-5	0	-2.0	0	-	-	-	-
0	5	2.0	3	24.2	19.4	4.8	58
5	10	7.0	4	29.6	23.7	5.9	71
10	15	12.0	5	33.7	26.8	6.8	82
15	20	17.0	14	85.1	67.6	17.5	210
20	25	22.0	21	113.7	89.9	23.8	286
25	30	27.0	22	104.5	82.2	22.3	268
30	35	32.0	39	159.4	124.4	35.0	420
35	40	37.0	29	99.3	76.7	22.6	271
40	45	42.0	32	88.4	67.2	21.2	254
45	50	47.0	28	58.8	43.6	15.2	183
50	55	52.0	23	33.1	23.2	9.8	118
55	60	57.0	32	24.8	14.9	9.9	118
60	65	62.0	37	4.1	-	4.1	50
65	70	67.0	34	-	-	-	-
70	75	72.0	25	-	-	-	-
75	80	77.0	14	-	-	-	-
80	85	82.0	3	-	-	-	-
85	90	87.0	0	-	-	-	-
Totals				**858.6**	**659.6**	**199.1** **23%**	**2,389**

At the end of November 2006, the monthly gas bills were compared to weather data to develop gas use load lines for before and after the remediation (on March 24, 2006). Figure 3-22 shows this data from with linear regression models fit to the data with daily average temperatures over 60°F. The most recent months of October and November (shown as yellow diamonds) returned to the pre-remediation trend. When we visited the site on November 29, 2006, we found the door to elevator room in the attic was not full closed. We theorize that door had been opened to service the elevator during the summer. This anecdotal experience demonstrates the large impact that the stack effect can have in a three-story building. Its appears that efforts to seal the elevator room most-likely accounted for the large portion of the energy savings.

Table 3-9 uses the same bin data from Table 3-8 with the load lines based on gas use from Figure 3-22. The predicted savings from this analysis are very similar to savings predicted from the boiler runtime data. Annual gas savings are 2,711 therms (25%) compared the analysis using boiler runtime that predicted 2,389 therms (23%).

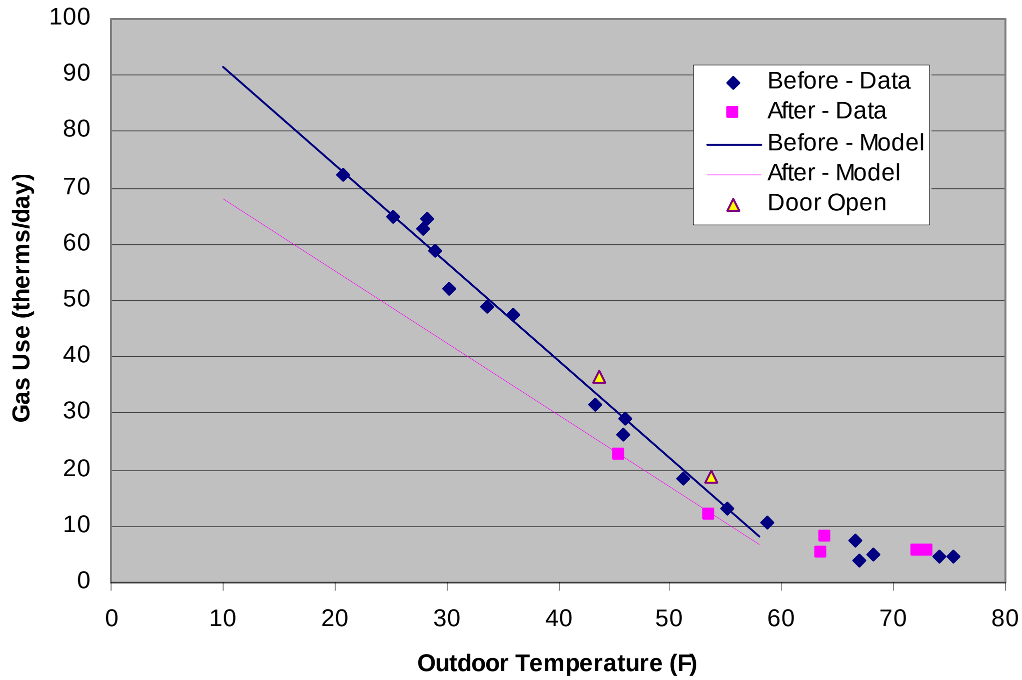

Figure 3-22. Monthly Gas Use vs. Ambient Temperature

Table 3-9. Annual Energy Savings Calculated Using Gas Bills for Site 17

Temp Bin (F)	No of Days			After		Savings
		therms/day	therms	therms/day	therms	therms
2.5	3	104.7	314.0	77.8	233.5	80.5
7.5	4	96.0	383.9	71.4	285.6	98.3
12.5	5	87.3	436.3	65.0	324.9	111.4
17.5	14	78.6	1,099.9	58.6	819.9	280.0
22.5	21	69.9	1,467.1	52.1	1,095.0	372.1
27.5	22	61.2	1,345.5	45.7	1,005.9	339.6
32.5	39	52.5	2,045.9	39.3	1,532.8	513.1
37.5	29	43.8	1,269.0	32.9	953.6	315.4
42.5	32	35.1	1,121.8	26.5	846.9	275.0
47.5	28	26.4	738.0	20.0	561.3	176.7
52.5	23	17.7	406.1	13.6	313.4	92.7
57.5	32	9.0	286.5	7.2	230.6	55.9
Totals:	***252***		***10,914***		***8,203***	***2,711***
						25%

On November 29, 2006, we repeated the blower door test to evaluate if the remediation had changed the building air tightness. The test was completed in the morning when the winds were very calm and the ambient temperature was about 45-50ºF. The blower door test was repeated with the kitchen exhaust fan running (exhausting 3655 cfm). For this test we were able to depressurize the building to -17 Pa (compared to -7.2 Pa for the previous test). The building pressure before testing was about -1.5 Pa. Table 3-10 compares air leakage statistics before and after the remediation (the "before" data is taken from Table A17-2). The leakage area decreased by about 800 square inches (about 5.5 square feet) due to the spraying foam to fill air gaps between the attic and the conditioned space. Both the leakage area and the air change rate at 50 Pa decreased by about 40% as a result of the remediation.

Table 3-10. Impact of Remediation on Building Airtightness

	Flow Coeff. K	Exp. n	ELA (sq in)	ELA / 100 sq ft (sq in/sq ft)	Flow @ 50 Pa (cfm_{50})	ACH_{50}
Before	2,836.0	0.620	1898	12.34	32,068	14.3
After	1,608.4	0.637	1101	7.16	19,404	8.6
			58%			61%

3.5. Summary and Lessons from Measured Impacts

A major lesson from the 25 tested buildings is to confirm the importance of designing and implementing an effective air barrier for the building. At a few of these buildings that were relatively new, seemingly-minor decisions made during construction had a significant impact on building energy use. For instance, installing gypsum board (or some other air barrier) above the t-bar ceiling at Sites 1, 2, 21 and 22 during construction would have created an effective air barrier at the ceiling for a modest cost. Once construction is complete and building is occupied – with the ceiling tiles, electrical and mechanical system in place – it is often prohibitively disruptive and expensive to install an air barrier.

A somewhat surprising finding from the three mitigated buildings in this section was significant energy savings that can be provided by relatively minor, low-cost improvements. At Sites 1 and 2, replacing and/or repositioning fiberglass batts in the ceiling had significant energy impacts. The annual heating energy savings from fixing major voids in the building envelope were 44% at Site 1 and 37% at Site 2. We found missing or fallen batts in two of 25 sites, or 8% of the buildings in this New York sample.

At Site 17 we used spray foam as a low-cost way to seal air leaks in a poorly-insulated attic floor. We also carefully sealed the elevator shaft in this 3-story historic building. These modest, low-cost improvements resulted in annual heating energy savings of about 25%.

The common theme from this field study is the need create an effective air barrier at modest cost with minimal disruption to the building occupants. Weatherization contractors need better information and diagnostic tools to identify and address air barrier problems. New commercial materials, such 200-600 board feet spray foam kits, offer the potential to cost effectively address these issues.

4. Laboratory Testing of Wall Assembly Performance

Air flows through building envelope have a significant effect on moisture transport and energy performance in buildings.

VanBronkhorst (1995) reviewed a case of estimating the national energy cost of air leakage. The results show that infiltration accounts for roughly 15% of the heating load in all office buildings nationwide, and a higher percentage in recently constructed buildings.

Air leakage may influence the moisture transport greatly. Desmarais (1998) investigated the impact of the initial air leakage characteristics on the hygrothermal performance of insulated walls retrofitted with rigid insulation added either on the warm side or on the cold side of the wood studs. Through the graphic representation of the results, it was seen that there is indeed a correlation between the moisture distribution pattern and the air leakage path, and between the temperature profiles and the air leakage path. The moisture accumulation patterns, as well as the temperature profiles, follow the expected air path inside the assembly. It was recommended that the air leakage patterns be integrated into heat, air and moisture transfer modeling and compare simulation results with experimental ones.

In New York State, many buildings have had moisture condensation issues and poor energy performance in the winter. In Florida, many hotels and homes have had moisture damage in the building envelope. In this uncontrolled air flow (UAF) project for small commercial buildings, steel frame wall has been identified as a common structure in New York State and concrete wall in Florida. In order to identify the potential problems in steel frame and concrete walls in various conditions, and to understand the response of the walls to changes in climatic conditions, it is important to quantify the effect of air flows both through simulations and experiments.

This section of the project report provides information on the air flow effects of heat, moisture and energy performances in wall assemblies observed in laboratory experiments. Section 5 describes how the hygrothermal simulation model LATENITE was used to analyze the moisture performance of wall assemblies. The simulation model was used to predict the behavior of wall sections to be tested in the full-scale chamber. The results were used in designing the experiments.

4.1. Overview

The objectives of this task were:

1. To experimentally determine and demonstrate the effects of leakage airflows on the temperature and humidity distribution in wall assemblies.
2. To generate a set of experimental data that can be compared with numerical simulations both qualitatively and quantitatively.

4.2. Test Facility

The information collected from the NY field testing (Section 2) and the previous field survey in Florida was used to identify two typical wall assemblies for testing in Syracuse University's laboratory facility. One of the wall assemblies was selected to represent typical NY construction in small commercial buildings while the other assembly reflected Florida construction practices. The wall assemblies were fully instrumented to measure the temperature and humidity levels at numerous positions within the assembly. Since the quality of the wall construction (workmanship) impacts its thermal and moisture performance, attempts were made to construct the wall test sections to mimic construction quality typically found in the field. Local builders were hired to construct the test walls.

The wall assemblies were tested using the Full-Scale Coupled Indoor/Outdoor Environmental Simulator (C-I/O-ES) at Syracuse University. The facility consists of an environmental chamber (16 ft by 12 ft by 10 ft high) composed of two equally sized compartments separated by the test wall. One compartment (IEQ chamber) is capable of simulating a conditioned full-scale interior room. The other side of the test wall is exposed to a climate chamber (6.5 ft by 12 ft by 10 ft high) capable of simulating dynamic outdoor conditions (temperature, humidity and wind pressure). A removable section of the chamber separates the two compartments and serves as a support frame for the "test wall". A desired test wall can be constructed to simulate any interior/exterior wall with inclusion of fenestrations such as doors and windows.

The environmental chamber (i.e., IEQ chamber) has an independent HVAC system with direct digital controls to provide accurate simulation of an array of indoor temperature, relative humidity, internal heat load, airflow rate and air distribution conditions. The climate (i.e., outdoor) chamber, also equipped with direct digital controls, can simulate weather conditions from low winter (down to –13ºF) to high summer (up to 100ºF) temperature. A wide range of humidity conditions can also be maintained in either chamber. Some limitations in relative humidity control arise at low temperatures. Care had to be taken to avoid excessively high relative humidity as these can lead to ice formation on the cooling coils. A photo of the chamber facility is shown in Figure 4-1.

Figure 4-1. The Coupled Indoor/Outdoor Environmental Simulator (C-I/O-ES) at the Building Energy and Environmental Systems Laboratory

4.3. Wall Construction

Two wall sections were assembled and tested side-by-side at the same climatic conditions in the full-scale C-I/O-ES facility of Syracuse University at the Building Energy and Environmental Systems Laboratory.

The following section describes the sequence of construction for the two walls. Figure 4-2 shows the dimensions of the two assemblies constructed for testing. Both walls were constructed in the same test frame assembly and both walls were exposed simultaneously to the same climatic conditions during the tests.

Table 4-1 summarizes the construction materials used in the two wall assemblies.

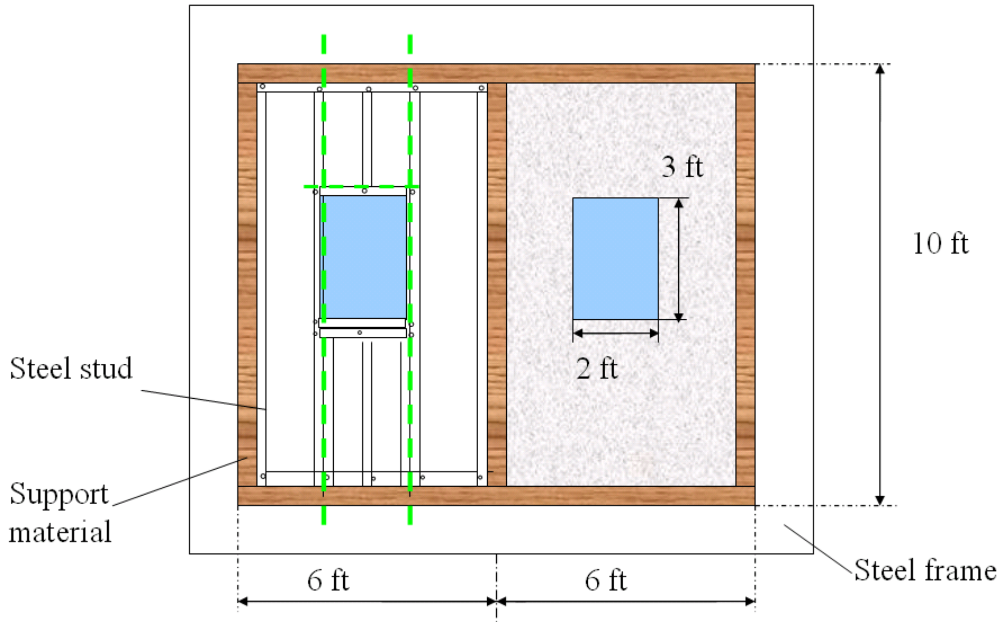

Figure 4-2. Schematic Shows the Two Walls Mounted Side by Side in the Frame Assembly for Testing

Table 4-1. List of Construction Materials Used in Fabrication of the Two Wall Assemblies for Testing

Steel Frame Wall	Concrete Wall
▪ Gypsum board	▪ Gypsum board
▪ Fiber glass insulation, 6”	▪ Concrete block, 8”
▪ Extruded polystyrene	▪ Stucco
▪ Air cavity	▪ Air cavity
▪ Plywood sill	▪ Rigid insulation (foil faced expanded polystyrene), ½”
▪ Steel framing	
▪ Polyethylene sheet	

4.3.1. Steel Frame Wall

The wall structure is as follows starting from the exterior to the interior side:

- ½ inch Exterior Grade Gypsum board
- ¾ inch extruded polystyrene insulation
- 6 inch Mineral wool insulation
- Polyethylene vapor retarder (6 mil)
- 5/8 inch Interior gypsum board

The sequence of construction began with a fabrication of 2 inch by 6 inch steel stud frame wall. Extruded polystyrene insulation was installed using screws on the outside of the frame and exterior grade gypsum board (dense glass gold) was installed on the exterior side of the wall. The frame was filled with 6 inches of mineral wool insulation. A 6 mil polyethylene vapor retarder was installed on the interior side of the frame and a interior gypsum board was mounted on the interior side. Both were attached using self-taping dry wall screws. The perimeter of the wall was sprayed with high density SPF foam to impart airtightness and reduce errors resulting from air infiltrating or exfiltrating at the perimeter of the frame wall or bypassing the frame wall all together.

The dimensions of the window measured 2 feet by 3 feet in length and height respectively. The rough opening was ½ inch larger in both directions. The wall window interface (the distance between the window and the rough opening) was approximately ¼ inch in width. The window for the steel frame wall was installed fairly carefully and the net result was a reasonably air tight seal (see Section 4.11 below for the resulting leakage rates).

4.3.2. Concrete Wall

The concrete wall structure consists of the following components from the exterior to interior side:

- ½ inch stucco
- Concrete block 8 inch x 18 inch (two open cores per block)
- Furring strips (1/2 inch thickness and installed 16 inch O.C.) creating an air space
- 1/2 inch extruded polystyrene (foil faced)
- 5/8 inch interior gypsum board.

The heavy weight of the concrete wall required that the wall be constructed construction with the wall holding assembly in place (i.e., installed between the two chambers).

Figure 4-3 shows the cross-section of the concrete block wall. The sequence of construction began with an installation of a horizontally leveled support (OSB on the chamber frame for walls) for erecting the concrete block wall. The block wall was erected in two phases. Half of the wall height (equivalent to 7 courses of block) was erected in the first day and allowed to cure for a period of 72 hours. The remainder of the block was installed following a 72 hour period so that the dead load from the upper section of the load could be transferred without creating load bearing stress cracks. The top of the wall, i.e., the space between the block and the frame of the test chamber was filled with a strip of oriented strand board (OSB). The strip was secured in place with a high density spray polyurethane foam (SPF) to impart airtightness around the perimeter of the test assembly.

The mason that built the block wall was also in charge of installing the window. The dimensions of the window measured 2 feet by 3 feet in length and height respectively. The rough opening was ½ inch larger in both directions. The interface between the window and the rough opening was approximately ¼ inch in width. The window installed in this wall assembly was much leakier than for the steel frame wall above because the mason did not use caulk. Section 4.11 below provides the resulting leakage rate measured for this portion of the wall assembly.

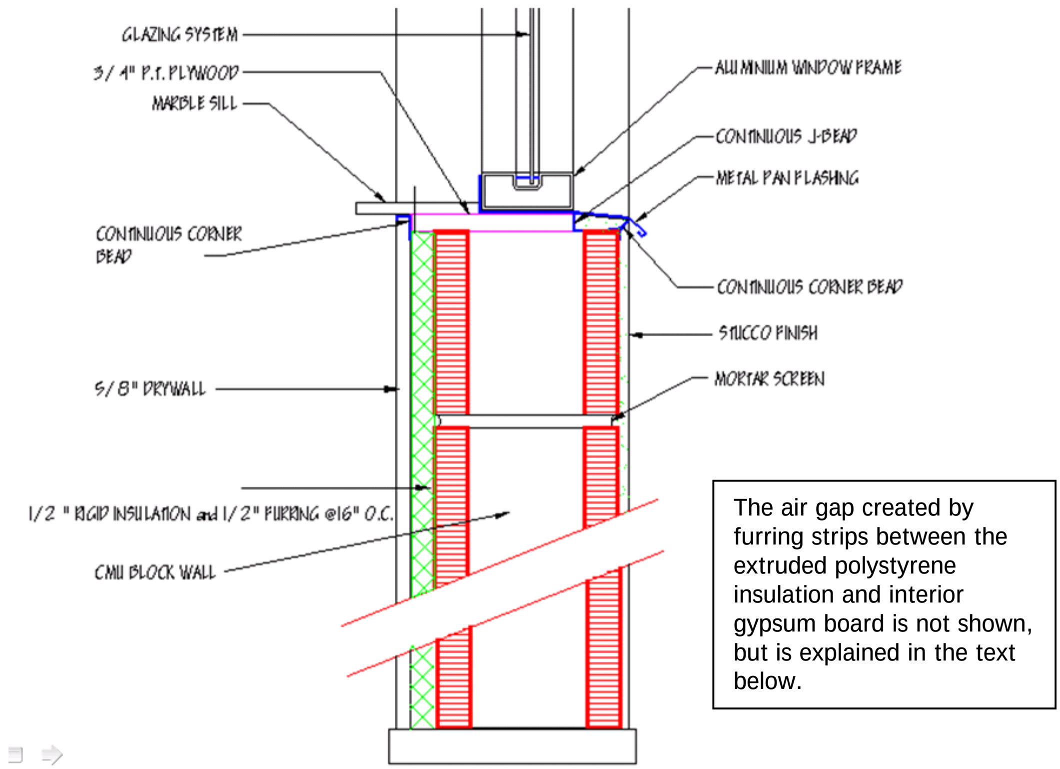

Figure 4-3. Cross Section of the CMU block Wall Showing the Different Layers and the Wall Window Interface

The exterior surface of the wall was finished with ½ inch thick two-coat stucco. On the interior side of the block wall ½ inch thick foil faced extruded insulation was installed on top of 1/2 inch furring strips (not shown in Figure 4-3 above). A 5/8 inch thick gypsum board was installed as the finishing layer. The cores of block were not grouted allowing for easy access of air movement between the blocks.

The floor/wall junction detail in the experimental set up was not representative of typical construction practice. Since the blocks were installed on top of an OSB board, a connecting concrete floor base could not have been built in the chambers. Thus the concrete block/OSB interface was one air leakage path.

The wall was allowed to cure and was monitored for 4 weeks after installation to ensure that the initial conditions in the wall were dry enough allowing measurements to show effects of air leakage flows on moisture conditions. Due to time constraints of the chamber and the time needed for curing the wall, the tests aimed at examining the climatic effects on the walls were performed in July 2006.

4.4. *Measurements and Analysis*

The walls were instrumented to measure temperature, relative humidity and air pressure differentials at multiple locations inside the walls, on the surfaces and in the outdoor and indoor chambers, as applicable.

4.4.1. Sensor Locations

Figure 4-4 through Figure 4-6 as well as Table 4-2, Table 4-3 and Table 4-4 indicate the location of thermocouples, temperature/relative humidity sensors, and pressure sensors. Figure 4-4 shows the location of all the sensors (also see Table 4-3). Figure 4-5 shows the locations of thermocouples on the steel frame surfaces and within the concrete masonry unit (CMU) blocks (see Table 4-2). Figure 4-6 shows the locations of the temperature/relative humidity sensors in the CMU block wall. Sensors were placed in the air cavities of the CMU blocks as well as in the mortar joints and between layers (also see Table 4-3).

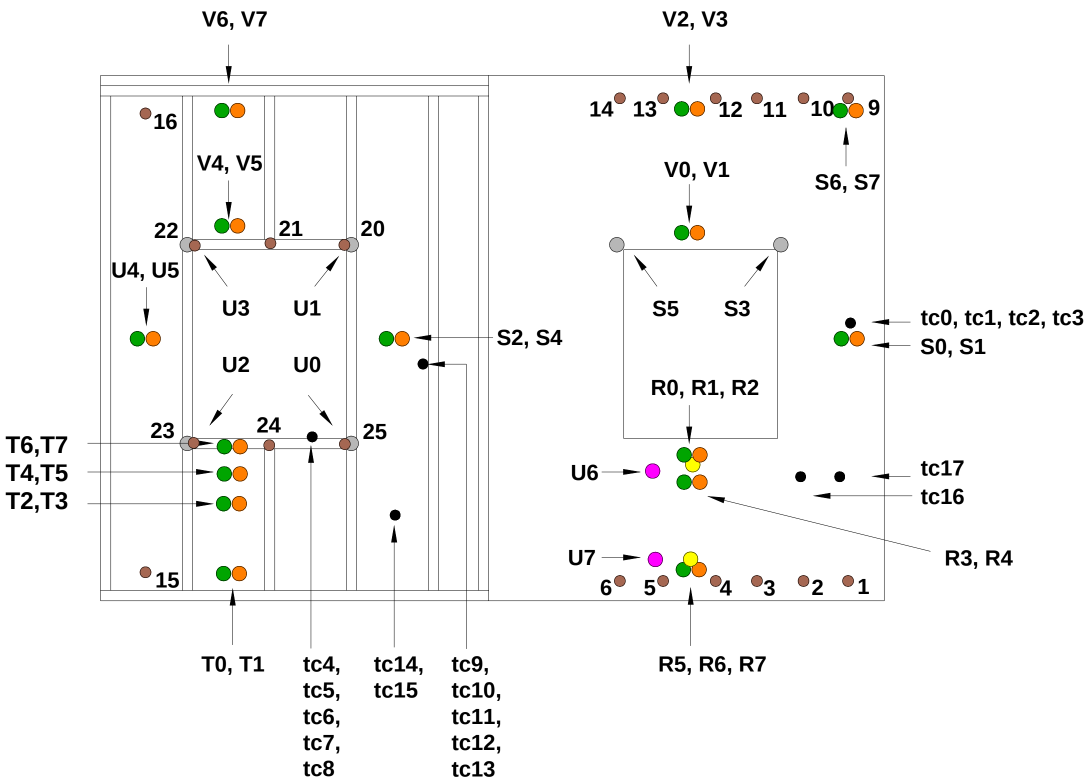

The sensors are grouped to sets of 8 temperature/relative humidity sensors for each letter designation R, S, T, U and V. The green/orange sensors are placed on different sides of the insulated cavity or the air cavity in the CMU-block; odd numbered sensors are on the climate chamber side. Yellow sensors placed on the stick (in the middle of the cavity in CMU-block). Grey sensors are T/RH sensors placed in the middle of air cavity in the window. Pink sensors are in the air cavity between the interior foam insulation and the interior gypsum board. Black sensors are thermocouples (tcnn). Numbered Brown sensors are pressure transducers. More details about sensor locations are given in Figure 4-5

Figure 4-4. Locations of the Thermocouples and Pressure Sensors on the Walls

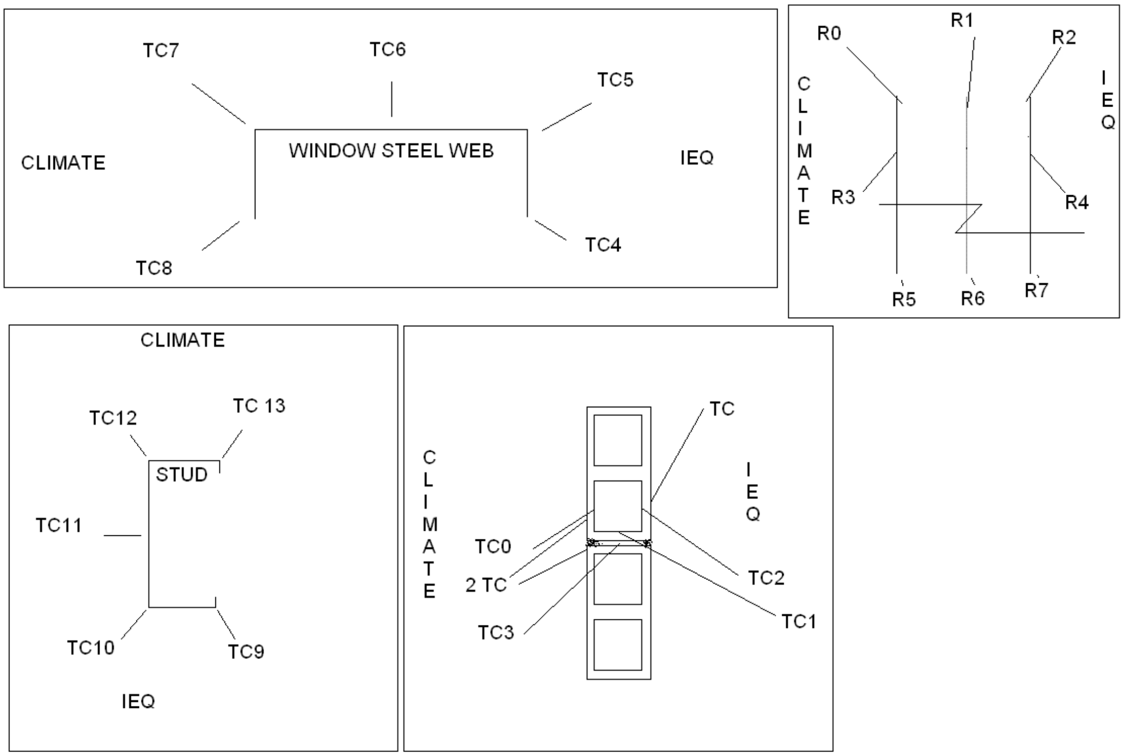

Figure 4-5. Detailed Thermocouple Locations in the Steel Frame and CMU Block Wall

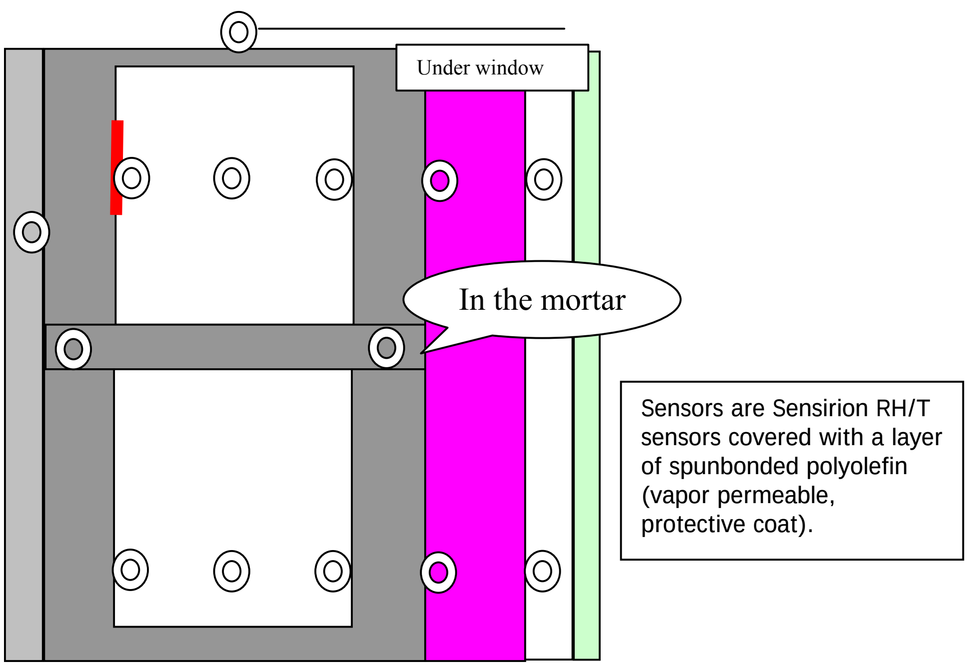

Figure 4-6. Schematics of the Sensor Locations in the CMU Block Wall Vertically

Table 4-2. Locations of Thermocouples (TC0 – TC17)

Location of thermocouples

Sensor Code	Sensor Type	Wall Type	Location in the Wall			Parameter measured
			Cavity No.	Height Location	Depth Location	
TC0	Thermocouple	CMU Block	-	Middle	Climate side	Temperature
TC1	Thermocouple	CMU Block	-	Middle	Middle	Temperature
TC2	Thermocouple	CMU Block	-	Middle	Indoor side (IEQ)	Temperature
TC3	Thermocouple	CMU Block	-	Middle	Middle	Temperature
TC4	Thermocouple	Steel frame	5	Equidistant b/w middle-bottom	Indoor side (IEQ)	Temperature
TC5	Thermocouple	Steel frame	5	Equidistant b/w middle-bottom	Indoor side (IEQ)	Temperature
TC6	Thermocouple	Steel frame	5	Equidistant b/w middle-bottom	Middle	Temperature
TC7	Thermocouple	Steel frame	5	Equidistant b/w middle-bottom	Climate side	Temperature
TC8	Thermocouple	Steel frame	5	Equidistant b/w middle-bottom	Climate side	Temperature
TC9	Thermocouple	Steel frame	6	Equidistant b/w middle-bottom	Indoor side (IEQ)	Temperature
TC10	Thermocouple	Steel frame	6	Equidistant b/w middle-bottom	Indoor side (IEQ)	Temperature
TC11	Thermocouple	Steel frame	6	Equidistant b/w middle-bottom	Middle	Temperature
TC12	Thermocouple	Steel frame	6	Equidistant b/w middle-bottom	Climate side	Temperature
TC13	Thermocouple	Steel frame	6	Equidistant b/w middle-bottom	Climate side	Temperature
TC14	Thermocouple	Steel frame	5	Bottom		Temperature
TC15	Thermocouple	Steel frame	5	Bottom		Temperature
TC16	Thermocouple	CMU Block	-	Middle		Temperature
TC17	Thermocouple	CMU Block	-	Middle		Temperature

Table 4-3. Locations of Combined (Sensirion) Temperature/Relative Humidity Sensors (Series R, S, T, U, V)

Location of Sensirion sensor

Series Code	Sensor Code	Sensor Type	Wall Type	Location in the Wall			Parameter measured
				Cavity No.	Height Location	Depth Location	
R Series	R0	Sensirion	Steel frame	3	Bottom	Climate side	Temp & RH
	R1	Sensirion	Steel frame	3	Bottom	Middle	Temp & RH
	R2	Sensirion	Steel frame	3	Middle	Indoor side (IEQ)	Temp & RH
	R3	Sensirion	Steel frame	3	Middle	Climate side	Temp & RH
	R4	Sensirion	Steel frame	3	Middle	Indoor side (IEQ)	Temp & RH
	R5	Sensirion	Steel frame	3	Middle	Climate side	Temp & RH
	R6	Sensirion	Steel frame	3	Middle	Middle	Temp & RH
	R7	Sensirion	Steel frame	3	Middle	Indoor side (IEQ)	Temp & RH
S Series	S0	Sensirion	CMU Block	-	Middle	Climate side	Temp & RH
	S1	Sensirion	CMU Block	-	Middle	Indoor side (IEQ)	Temp & RH
	S3	Sensirion	CMU Block	-	Top 'R' window corner	Middle	Temp & RH
	S5	Sensirion	CMU Block	-	Top 'L' window corner	Middle	Temp & RH
	S6	Sensirion	CMU Block	-	Bottom	Climate side	Temp & RH
	S7	Sensirion	CMU Block	-	Bottom	Indoor side (IEQ)	Temp & RH
T Series	T0	Sensirion	Steel frame	-	Bottom	Indoor side (IEQ)	Temp & RH
	T1	Sensirion	Steel frame	-	Bottom	Climate side	Temp & RH
	T2	Sensirion	Steel frame	-	Middle	Indoor side (IEQ)	Temp & RH
	T3	Sensirion	Steel frame	-	Middle	Climate side	Temp & RH
	T4	Sensirion	Steel frame	-	Middle	Indoor side (IEQ)	Temp & RH
	T5	Sensirion	Steel frame	-	Middle	Climate side	Temp & RH
	T6	Sensirion	Steel frame	-	Below window	Indoor side (IEQ)	Temp & RH
	T7	Sensirion	Steel frame	-	Below window	Climate side	Temp & RH
U Series	U0	Sensirion	Steel frame	-	Bottom 'R' window corner	Middle	Temp & RH
	U1	Sensirion	Steel frame	-	Top 'R' window corner	Middle	Temp & RH
	U2	Sensirion	Steel frame	-	Bottom 'L' window corner	Middle	Temp & RH
	U3	Sensirion	Steel frame	-	Top 'L' window corner	Middle	Temp & RH
	U4	Sensirion	Steel frame	1	Middle	Indoor side (IEQ)	Temp & RH
	U5	Sensirion	Steel frame	1	Middle	Climate side	Temp & RH
	U6	Sensirion	CMU Block	-	Middle	Indoor side (IEQ)	Temp & RH
	U7	Sensirion	CMU Block	-	Bottom	Indoor side (IEQ)	Temp & RH
V Series	V0	Sensirion	CMU Block	-	Middle Window	Indoor side (IEQ)	Temp & RH
	V1	Sensirion	CMU Block	-	Middle Window	Climate side	Temp & RH
	V2	Sensirion	CMU Block	-	Top	Indoor side (IEQ)	Temp & RH
	V3	Sensirion	CMU Block	-	Top	Climate side	Temp & RH
	V4	Sensirion	Steel frame	3	Middle	Indoor side (IEQ)	Temp & RH
	V5	Sensirion	Steel frame	3	Middle	Climate side	Temp & RH
	V6	Sensirion	Steel frame	3	Top	Indoor side (IEQ)	Temp & RH
	V7	Sensirion	Steel frame	3	Top	Climate side	Temp & RH

Table 4-4. Locations of Pressure Transducers (P1-P25)

Location of Pressure Points

Sensor Code	Sensor Type	Wall Type	Location in the Wall			Parameter measured
			Note	Height Location	Depth Location	
1	Pressure Transducer	CMU Block	-	Bottom	Middle	Pressure
2	Pressure Transducer	CMU Block	-	Bottom	Middle	Pressure
3	Pressure Transducer	CMU Block	-	Bottom	Middle	Pressure
4	Pressure Transducer	CMU Block	-	Bottom	Middle	Pressure
5	Pressure Transducer	CMU Block	-	Bottom	Middle	Pressure
6	Pressure Transducer	CMU Block	-	Bottom	Middle	Pressure
7	Pressure Transducer	CMU Block		Climate chamber	-	Pressure
8	Pressure Transducer	Steel frame		Middle height	Middle	Pressure
9	Pressure Transducer	CMU Block	-	Top	Middle	Pressure
10	Pressure Transducer	CMU Block	-	Top	Middle	Pressure
11	Pressure Transducer	CMU Block	-	Top	Middle	Pressure
12	Pressure Transducer	CMU Block	-	Top	Middle	Pressure
13	Pressure Transducer	CMU Block	-	Top	Middle	Pressure
14	Pressure Transducer	CMU Block	-	Top	Middle	Pressure
15	Pressure Transducer	Steel frame		Bottom	Middle	Pressure
16	Pressure Transducer	Steel frame		Top	Middle	Pressure
17	Pressure Transducer	Steel frame	2	Bottom	Middle	Pressure
18	Pressure Transducer	Steel frame	2	Middle	Middle	Pressure
19	Pressure Transducer	Steel frame	2	Top	Middle	Pressure
20	Pressure Transducer	Steel frame	-	Top 'R' window corner	Middle	Pressure
21	Pressure Transducer	Steel frame	-	Top 'M' window corner	Middle	Pressure
22	Pressure Transducer	Steel frame	-	Top 'L' window corner	Middle	Pressure
23	Pressure Transducer	Steel frame	-	Bottom 'L' window corner	Middle	Pressure
24	Pressure Transducer	Steel frame	-	Bottom 'M' window corner	Middle	Pressure
25	Pressure Transducer	Steel frame	-	Bottom 'R' window corner	Middle	Pressure

4.5. Climatic Conditions in Chambers

Planned climatic conditions to which the test walls were subjected for testing included:

- Hot and humid (FL/NY summer condition) - Outdoor: 30ºC (86ºF) & 70% RH
  Indoor : 22ºC (72ºF) & 50% RH
- Cold and dry (NY winter condition) Outdoor: -10ºC (14ºF) (humidity can float)
  Indoor: 22ºC (72ºF) & 50% RH
- Low vs. High wind pressure: with or without pressure difference across wall between climate chambers.

The actual climatic conditions that were imposed for the tests are shown in Figure 4-7. Due to some unexpected chamber maintenance needs, the conditions achieved were not exactly as planned; nevertheless they were representative of the conditions outlined above.

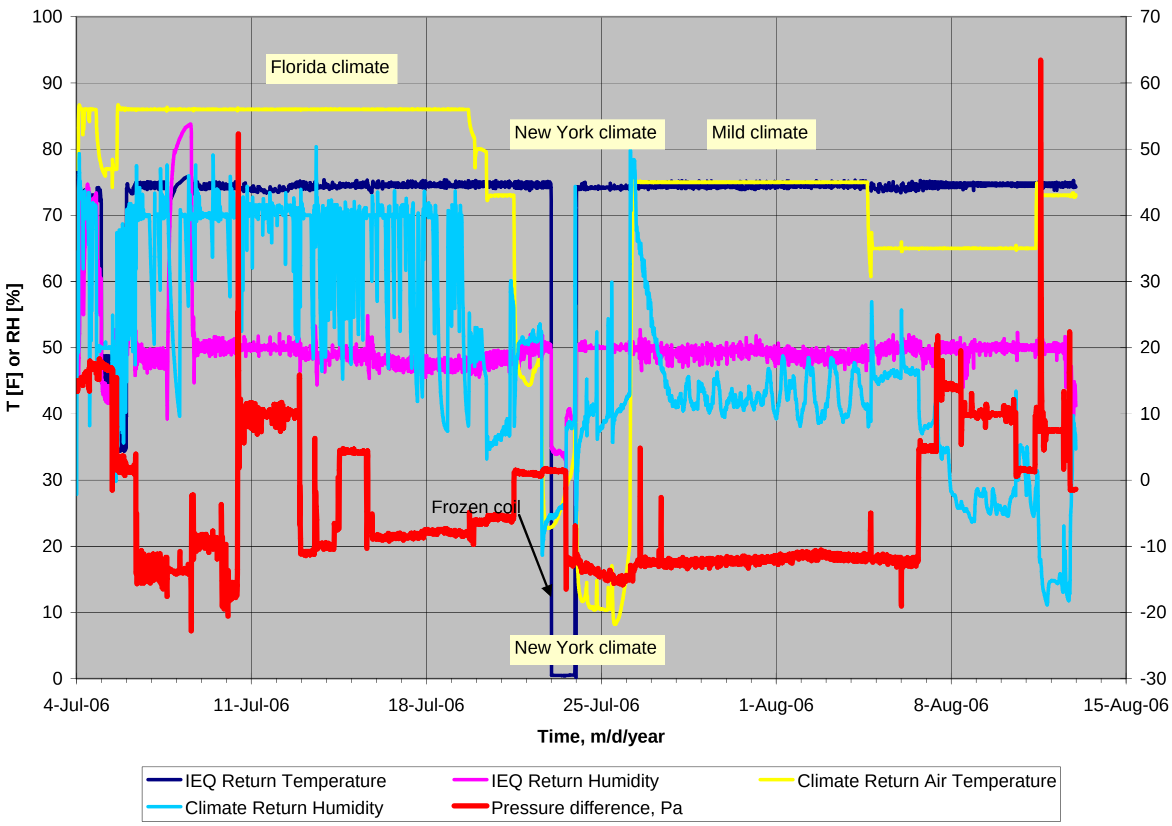

Figure 4-7. Temperature and Relative Humidity in the Climate and Indoor Environment Chamber during the Test Periods in July. (Temperature conversion: 87F = 30.5ºC, 10F = -12ºC; T[ºC] = (T[F]-32)*5/9)

4.6. Results for Steel Frame Wall – New York Weather

As a first step, the temperatures measured by thermocouples at different locations in steel stud frame wall and masonry wall are evaluated. The locations of the sensors are shown (highlighted) in Figure 4-5. The sensors denoted as TC4, TC5, TC6, TC7, and TC8 (which correspond to the steel web under the window) should indicate a pattern of decreasing temperature under winter conditions. Similarly, the sensors denoted as TC9, TC10, TC11, TC12 and TC13 (which correspond to the steel stud) should also indicate the same pattern. Table 4-2 lists temperatures corresponding to these sensors at two distinct winter conditions (test data from July 22nd at 2:40 am, and July 23rd 10:40 am). These time periods have been selected for comparison because at those times the data points indicate a relatively flat portion of the curve (~steady-state), thus making the data comparison much simpler.

Table 4-5. Temperature of Steel Stud and Steel Web – Winter Conditions (°C/F)

	Date and time of reading	
	7/22/2006	7/23/2006
	2:40 AM	10:40 AM
Outdoor Indoor	6.8 / 44.2 24.0 / 75.2	-3.3 /26.1 22.7/72.9
Steel Web under Window		
TC4	19.7/67.5	17.1/62.8
TC5	19.2/66.6	17.0/62.6
TC6	18.2/64.8	15.0/59.0
TC7	16.8/62.2	13.2/55.8
TC8	16.8/62.2	12.8/55.0
Steel Stud		
TC9	20.5/68.9	17.2/63.0
TC10	20.5/68.9	17.2/63.2
TC11	19.1/66.4	15/59.0
TC12	18.1/64.6	13.7/56.7
TC13	17.9/64.2	13.3/55.9

The data confirms this assumption (hypothesis). However, since the steel web is an excellent conductor, the temperatures in the steel web are quite comparable to each other. Temperature comparison can also be performed between TC7, TC8 and TC12, TC13 sensors. It is expected that the temperatures would be similar, and in fact they are. There is a difference in temperature between thermocouples denoted as TC7, TC8 and TC12, TC13 on July 22 (the more moderate outdoor condition). It is likely that the window steel web has a higher (greater) degree of exposure to the indoor climate in comparison to the web of a steel stud located within the cavity.

Table 4-6 shows the measured temperatures, relative humidities, and the corresponding vapor pressures (calculated from measured temperature and relative humidity) in locations below the window in the steel frame wall. It can be clearly seen that the sensors farthest away from the thermal bridges (T2, T3) have the largest temperature difference.

Table 4-6. Measured Temperatures and Relative Humidities (and the Calculated Vapor Pressures) for the Locations Below the Steel Frame Window

	07/22/06 2:40AM		07/23/06 10:40AM	
Indoor	24 / 75.2		27 / 80.6	
Outdoor	6.8 / 44.2		-3.3 / 26.	
Temperature	ºC/F			
T7	15.1/59.2	T6-T7	6.7/44.1	T6-T7
T6	16.5/61.7	1.4/2.5	8.4/47.1	1.7/3.1
T5	12.4/54.3	T4-T5	1.3/34.3	T4-T5
T4	14.6/58.3	2.1/3.8	3.6/38.5	2.3/4.1
T3	11.6/52.9	T2-T3	0.9/33.6	T2-T3
T2	14.1/57.4	2.5/4.5	3.2/37.8	2.2/4.0
Relative Humidity	%			
T7	40.2	T6-T7	69.1	T6-T7
T6	41.1	0.9	55.7	-13.4
T5	47.3	T4-T5	60.0	T4-T5
T4	43.7	-3.6	52.8	-7.2
T3	50.7	T2-T3	60.4	T2-T3
T2	44.0	-6.7	54.2	-6.2
Vapor pressure	Pa			
T7	688	T6-T7	677	T6-T7
T6	772	83	614	-63
T5	684	T4-T5	402	T4-T5
T4	725	41	417	14
T3	691	T2-T3	395	T2-T3
T2	706	15	416	21
U4				
T, ºC/F	22.1/71.8		20.1/68.2	
RH, %	21.8		6.9	
Pv, Pa	580		162	
U5				
T, ºC/F	13.1/55.6		5.6/42.1	
RH, %	38.5		21.1	
Pv, Pa	579		192	

Figure 4-8 shows the temperatures as a function of time during the period when two different changes occurred in the climatic conditions: First the outdoor temperature dropped from approximately 9ºC (48F) to about -6ºC (21F) and followed by a constant temperature level. During this first stage the air pressure difference was in the direction of the indoor environmental chamber (from outdoors to indoors). During the latter stage the temperatures were maintained constant, but the air pressure difference was reversed so that the indoor environmental chamber became pressurized with respect to the climate chamber (from indoors to outdoors). From these results it can be seen that similar conditions inside the wall can result from two completely different climatic conditions for some locations in the wall. Figure 4-8 clearly depicts the effects of air flows on the thermal conditions in the wall. Figure 4-9 shows the vapor pressures of the same locations and for the same time period as Figure 4-8. Again, very strong effects of air flows can be seen.

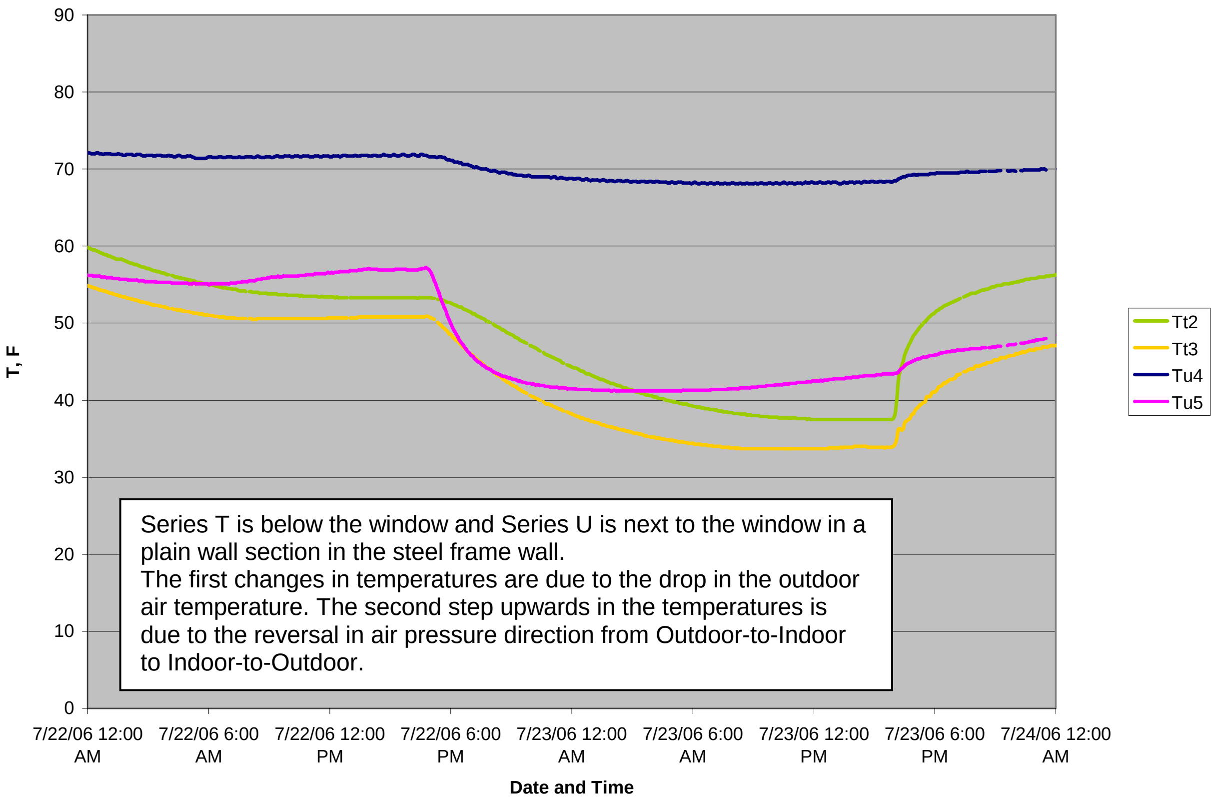

Figure 4-8. Temperatures of Sensors T2, T3, U4 and U5. (Temperature conversion T[°C] = (T[F]-32)*5/9). Even numbered sensors (T2 and U4) are on the indoor side.

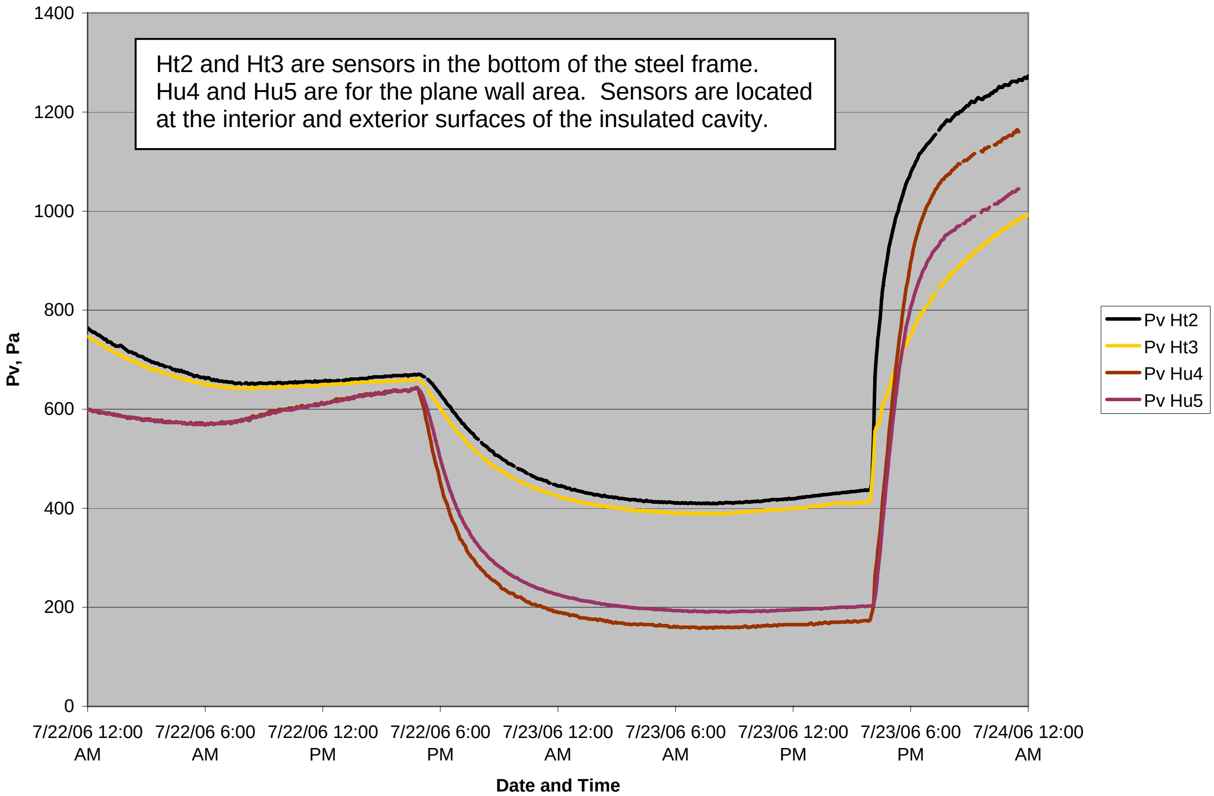

Figure 4-9. Vapor Pressure as a Function of Time for Wall Sensors

4.7. Results for Steel Frame Wall - Florida Weather

The spot relative humidities measured by sensors located on the perimeter of the rough opening were investigated. The data shown represents averaged data for short time periods that were approximately at steady state conditions. Table 4-7 shows spot relative humidities measured at various locations within the steel stud frame wall during two test periods (July 7th and July 9th). Table 4-8 shows the corresponding averaged climatic conditions for the same period. Note that the values for climatic conditions represent averages for the steady state portion of the test. The initial transient condition has not been accounted for in the averaging.

Table 4-7. Spot Relative Humidities for the Perimeter of Rough Opening in Steel Frame Wall

Date & Time	7/7/2006 12:00 AM	7/9/2006 10:00 AM
Sensor No.	RH [%]	RH [%]
U0	77.9	76.9
U1	75.3	74.5
U2	75.8	62.8
U3	73.2	69.9
U4	81.5	81.6
U5	66.4	65.7

Date & Time	7/7/2006 12:00 AM	7/9/2006 10:00 AM
Sensor No.	RH [%]	RH [%]
T0	50.1	46.6
T1	50.7	48
T2	51.4	48.5
T3	51.9	49.5
T4	53.1	51.4
T5	59	55.5
T6	63.6	63.4
T7	65.6	65.3

Table 4-8 lists the climatic conditions during the high temperature and high humidity test stage. Figure 4-10 shows the climatic conditions in the course of time. In Table 4-8, conditions are listed during the steady-state stage of the test i.e., excluding the initial 1.5 days of transient data. The table lists temperature, relative humidity on both sides of the wall, i.e., inside the IEQ chamber (interior side), and climatic chamber (exterior side). In addition the table lists calculated vapor pressure, which corresponds to the temperatures and relative humidities in both chambers. The values indicate driving potential for vapor transport in the direction of the interior (from climatic chamber to IEQ chamber). The vapor pressure inside the climatic chamber was slightly greater than twice the vapor pressure inside the IEQ chamber. Furthermore, differential air pressure is also listed. The negative value indicates that the air pressure was acting in the direction of the climatic chamber.

Table 4-8. Climatic Conditions Corresponding to Analysis in Table 4-7

	7/7/2006	7/9/2006
	Climate side	Climate side
T, [F/C]	86.0/30.0	86.0/30.0
RH, [%]	92.5	91.8
Pv, [Pa]	2929	2884
	IEQ side	IEQ side
T, [F]	73.2/22.9	73.4/23.0
RH, [%]	48.6	59.7
Pv, [Pa]	1432	1755
Diff Pres. Direction	-10.4 From IEQ to climate	

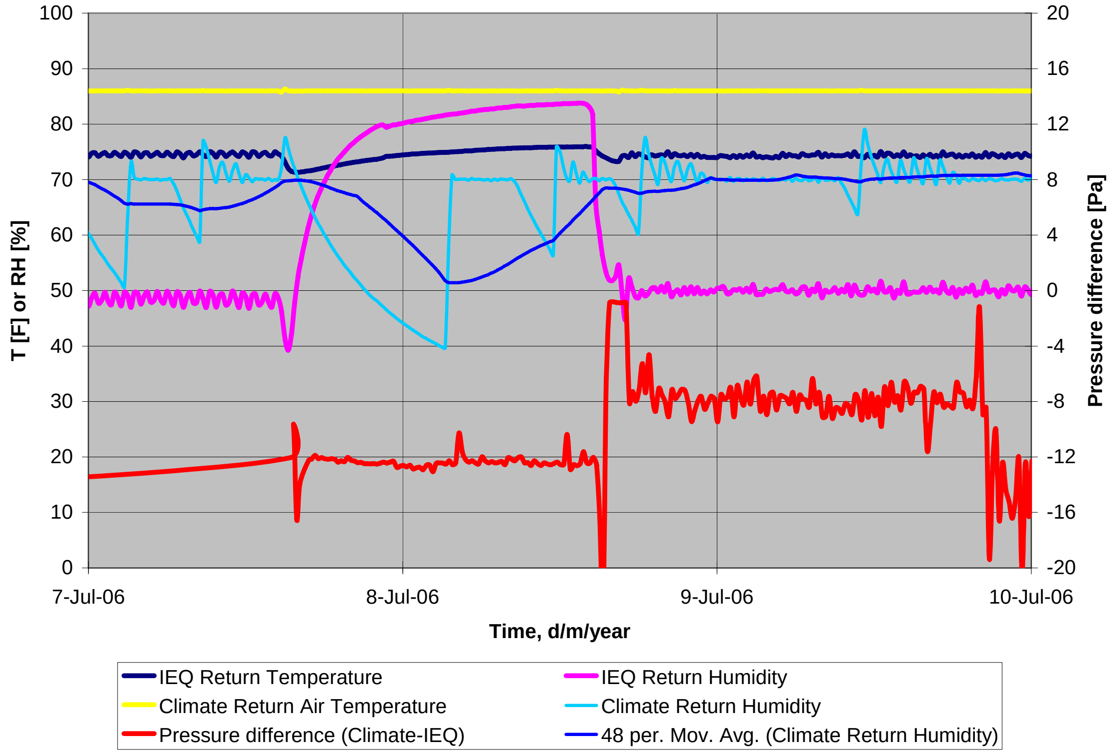

Figure 4-10. Climatic Conditions During the July 7-9 Period (Temperature conversion T[°C] = (T[F]-32)*5/9)

Figure 4-11 shows how the air pressure difference and air leaks drove humidity into the steel frame wall cavity. The wall had a polyethylene vapor retarder on the interior side; however, the wall cavity experienced high increase in humidity when the indoor humidity increased rapidly. This effect can only be due to air leaks, since the temperatures remained constant during this period.

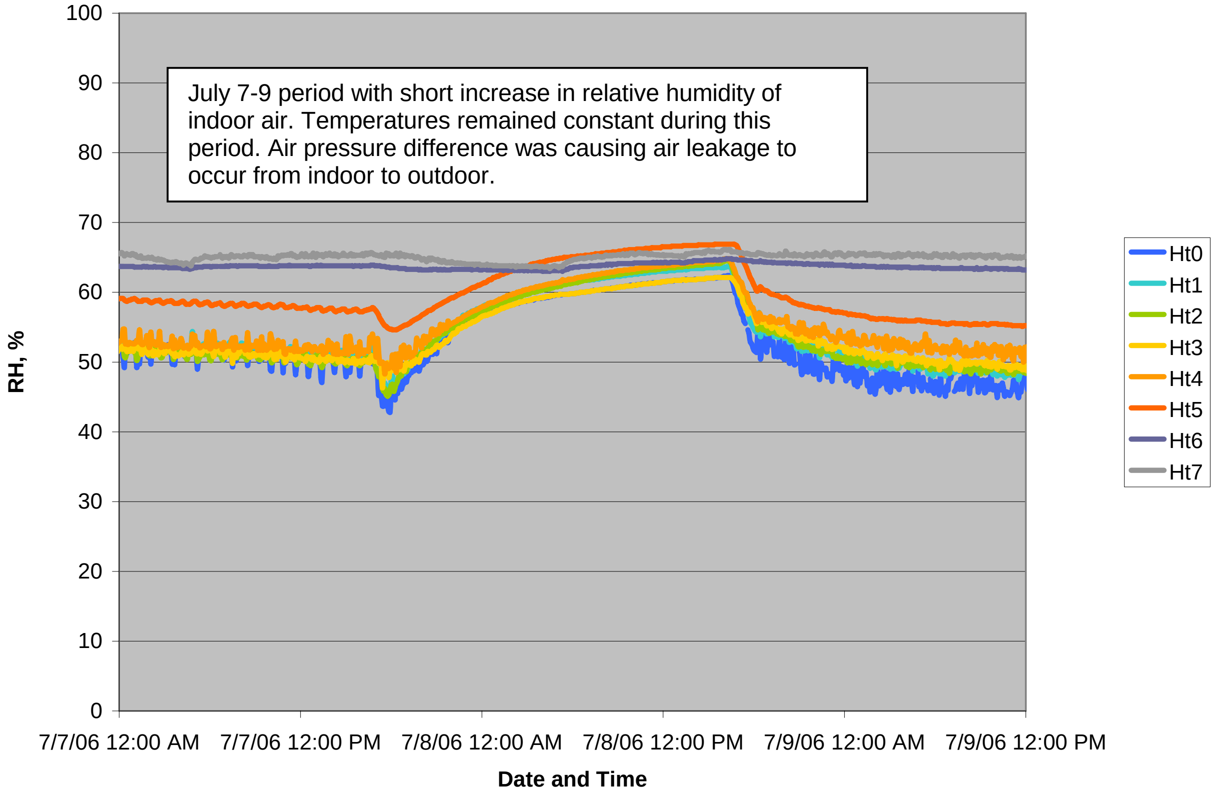

Figure 4-11. Relative Humidity at Different Locations under the Window in the Steel Frame Wall During the July 7-9 Period

There are number of interesting findings shown in Table 4-7

1. Generally, there is a reduction in relative humidities between July 7th and July 9th as indicated by both groups of sensors U and T. This is an effect that could be attributed to the direction of air pressure gradient. Although, the vapor pressure is much higher on the hot and humid side of the test assembly (wall), the relative humidity inside the wall decreases due to air exfiltration. A sudden increase in the relative humidity of the indoor environmental chamber increases the humidities inside the wall. When the indoor humidity decreased again the humidities in the wall followed and decreased accordingly. Note that the steel frame wall has a vapor retarder; however, the response is quick which is an indicator of air leakage (exfiltration effect).
2. Comparison of relative humidity readings for July 7th and July 9th for each sensor in group T shows greater changes in relative humidity in sensors imbedded deeper inside the wall. It is likely the conditions on the interior of the wall take longer time to equilibrate. Sensors mounted closer to the surface i.e., T6 and T7, shows very small change in comparison to sensor T0, T1, T2, T3, T4 and T5. It is postulated that conditions at those locations change faster i.e., within first several hours.
3. Sensors in group U also indicate similar pattern.

Similar procedures were also conducted and data was examined for the stage of reversed air pressure. Similarly, relative humidity, temperature, and air pressure were measured. Table 4-9 lists corresponding relative humidities for two time instances during this stage of testing. Table 4-10 lists averaged exposure conditions i.e.: temperatures, relative humidities and air pressure difference on both sides of the tested wall. This time the air pressure was comparable in magnitude (approximately 11.1 Pa) but acting in the opposite direction. The vapor pressure gradient was lower in magnitude (-40%) when air pressure was lower in the climate chamber than in the indoor chamber but vapor pressure difference acted still in the same direction as in the previous stage of testing.

Table 4-9. Measured Relative Humidity and Temperature at Various Locations in the Walls During Air Pressure Reversal

Date & Time	7/11/2006 12:30 PM	7/13/2006 4:00 PM
Sensor	RH [%]	RH [%]
U0	77.1	59.6
U1	80.1	57.2
U2	73.8	52.1
U3	77.4	54.2
U4	91.8	61
U5	72.8	49.6

Date & Time	7/11/2006 12:30 PM	7/13/2006 4:00 PM
Sensor	RH [%]	RH [%]
T0	67.7	45.7
T1	67.6	48.8
T2	67.6	49.8
T3	66.4	49.5
T4	68.4	51
T5	70.6	52.9
T6	69.7	59.2
T7	70.5	60.3

Table 4-10. Climatic Conditions for the Time of Spot Measurements (Table 4-9)

	Climatic conditions	
	Climate side 07/11/2006	Climate side 07/13/2006
T, [F/C]	86.0/30.0	86.0/30.0
RH, [%]	93.5	69.6
Pv, [Pa]	3963	2951
	IEQ side	IEQ side
T, [F/C]	73.9/23.3	73.8/23.2
RH, [%]	50.0	50.0
Pv, [Pa]	1427	1424
Diff Pres. Direction	11.1 to -8.4 (+) = Climate to IEQ	

In this stage of testing the air pressure and vapor pressure gradient both acted in the same direction (from outdoors to indoors). The data shows that before the reversal of air pressure (i.e., on July 11) the relative humidities measured by the U series sensors were fairly high, with the U4 sensor approaching the dangerously-high level of 92% RH (Table 4-9). These are also shown by results from sensors near the bottom of the window. The relative humidities are on average 20% lower than those measured during the previous test stage in which the air pressure gradient was acting toward the interior side (cold side of the wall). The steel frame wall did not experience as high humidity as the CMU block wall (Figure 4-12). The gradient across the wall cavity was much less than in the CMU block wall. These effects are likely due to the fact that the steel frame wall was better insulated with part of the R-value in the exterior sheathing. The exterior surface relative humidity sensors in the insulation cavity below window (sensors HT7 and HT5, in the order of magnitude of humidity variation) react to the climate chamber humidity variations when the air pressure difference is from climate to indoor chamber and the climate chamber humidity fluctuates (Figure 4-13). This shows that the air leakage is occurring around the window frame.

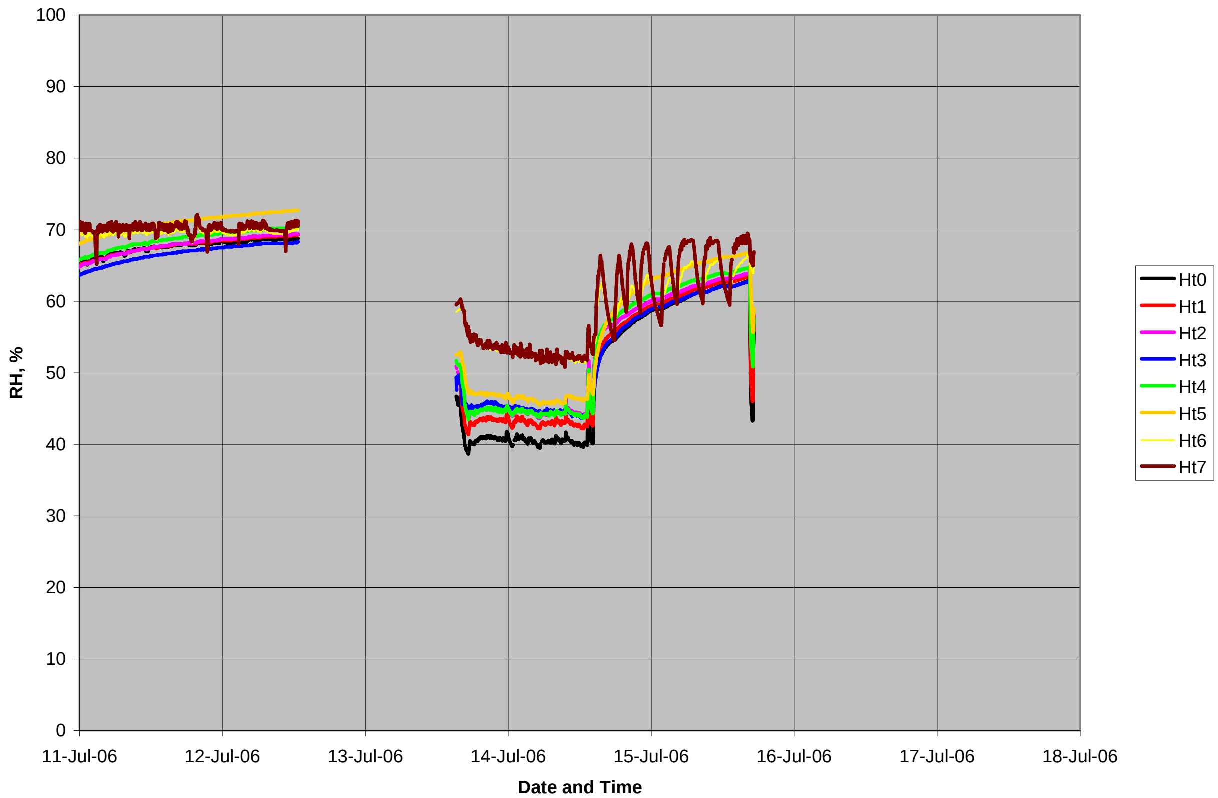

Figure 4-12. Relative Humidities of Sensor Series T in the steel frame wall during the Pressure Reversal (unfortunately the computer was down during the transient stage on July 12-13)

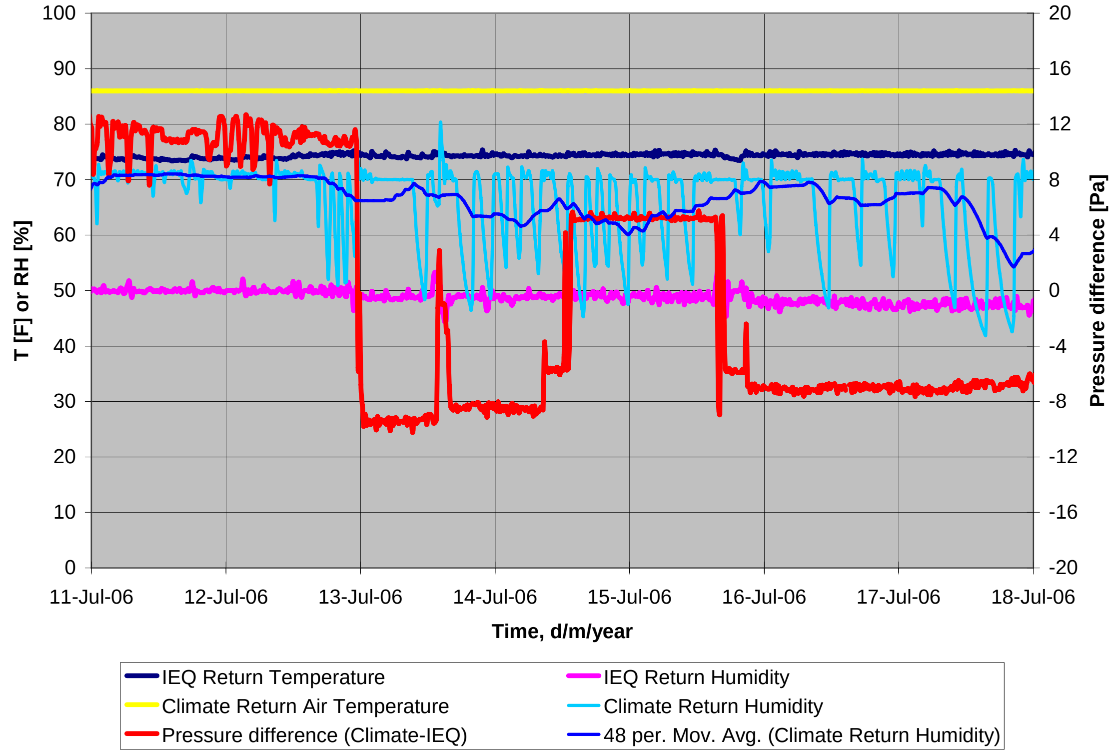

Figure 4-13. Climatic Conditions in the Full-Scale Chamber for the Period July 11-18, 2006. (Temperature conversion T[°C] = (T[F]-32)*5/9)

4.8. Results for CMU Block Wall – New York Weather

Similar comparison of temperatures was also performed for the masonry wall. The same phenomenon was postulated and observed in the masonry wall. Table 4-11 below lists the sensors in order of expected decreasing temperature (the expectation is assumed based on the location of the sensor within the web). The values for the corresponding sensors decrease.

Table 4-11. Temperature (°C/F) of the Masonry Web (Thermocouple locations shown in Figure 4-14).

	Date and time of reading	
	7/22/2006	7/23/2006
	2:40 AM	10:40 AM
TC2	12.1/53.8	3.2/37.8
TC1	11.4/52.5	2.4/36.3
TC3	11.0/51.8	1.8/35.2
TC0	10.3/50.5	0.9/33.6

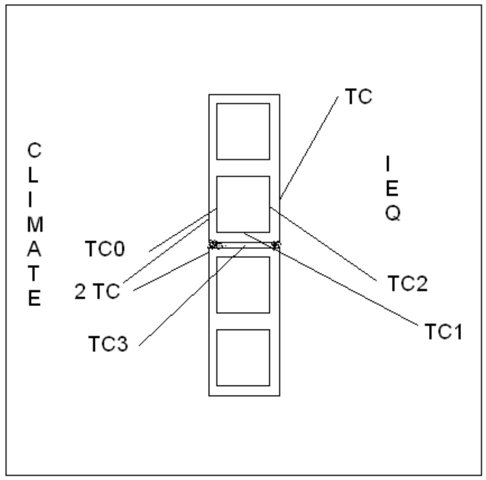

Figure 4-14. Thermocouple Locations in the CMU Block Wall

The masonry wall was tested simultaneously with the steel stud frame wall in the previous sections. The masonry wall was subjected to the same test protocol and exposure conditions. Table 4-8 and Table 4-10 (in previous section) respectively show the relative humidity and exposure conditions. Table 4-12 summarizes the relative humidity measurements in the masonry wall assembly.

Table 4-12. Relative Humidity Conditions in the CMU Block Wall During Spot Measurements on July 7 and July 9

Date & Time	7/7/2006 12:00 AM	7/9/2006 10:00 AM
Sensor	RH [%]	RH [%]
S0	66.3	65.7
S1	68.4	67.8
S3	68.8	65.0
S5	78.7	72.7
S6	72.1	64.4
S7	59.0	55.4

Date & Time	7/7/2006 12:00 AM	7/9/2006 10:00 AM
Sensor	RH [%]	RH [%]
R0	73.6	70.1
R1	81.2	78.2
R2	65.6	62.8
R3	79.7	76.8
R4	65.6	62.9
R5	77.4	74.4
R6	72.2	69.4
R7	76.3	73.2

With the air pressure gradient acting in the opposite direction of the vapor pressure gradient, a similar pattern of response was observed as in the steel stud frame wall. The relative humidities are reduced. Following the increase in indoor humidity there was an increase in relative humidity as denoted by sensors S0, S1, S7, and sensors R0, R1, R2, and R3. Figure 4-15 and Figure 4-16 show the transient response of the S series and R series humidity sensors during this test. Table 4-13 compares humidity measurements for key moments pressure reversal. The positive air pressure from the indoor to outdoor chamber allows the introduction of hot moisture laden air into the cavities, thus increasing moisture load. This behavior was very similar in both types of wall construction.

Table 4-13. Measured Relative Humidities in the CMU Block Wall During the Air Pressure Reversal

Date & Time	7/11/2006 12:30 PM	7/13/2006 4:00 PM
Sensor	RH [%]	RH [%]
S0	71.5	61.6
S1	72.9	63.4
S3	72	59.8
S5	84.5	53.3
S6	73.8	53
S7	71.8	54.6

Date & Time	7/11/2006 12:30 PM	7/13/2006 4:00 PM
Sensor	RH [%]	RH [%]
R0	82.5	52.7
R1	90.7	56.8
R2	73.7	47.8
R3	89.0	56.8
R4	73.1	48.1
R5	86.2	56
R6	79.6	53.2
R7	83.9	56

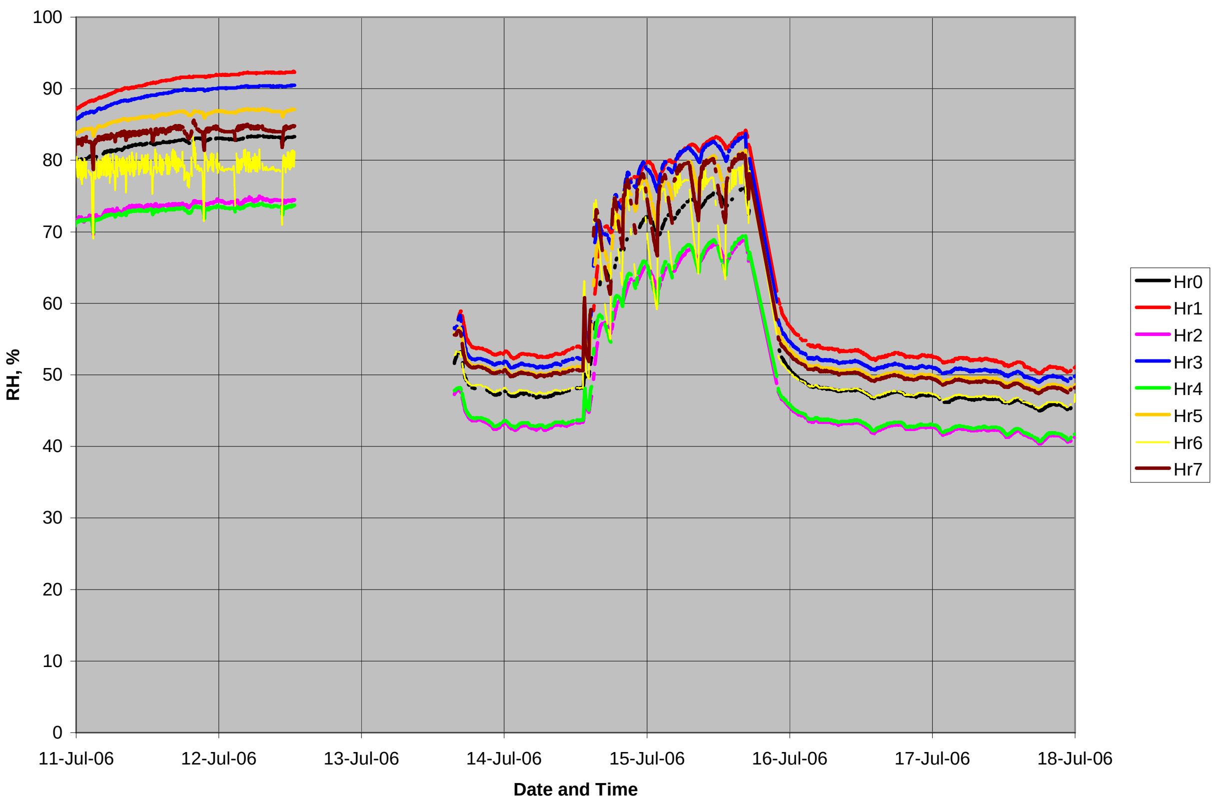

Figure 4-15. Relative Humidities of Sensor Series R During the Pressure Reversal (unfortunately the computer was down during the transient stage on July 12-13)

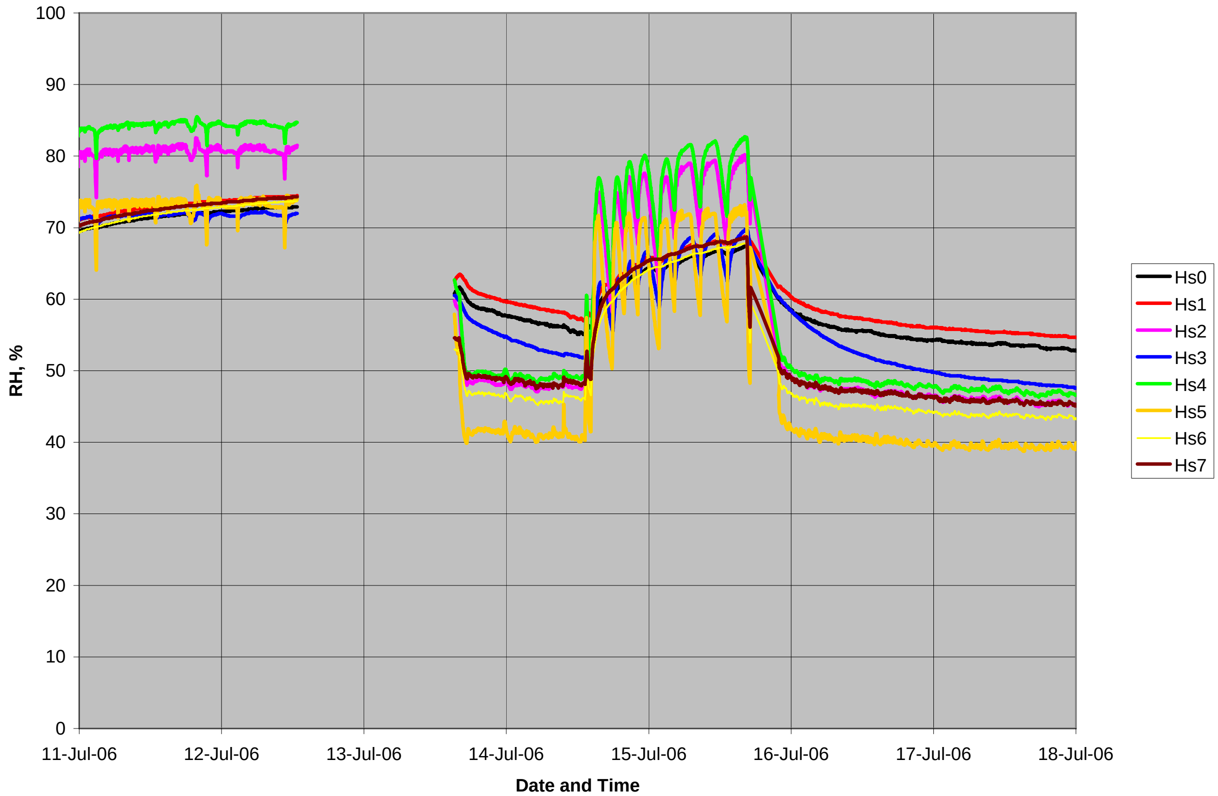

Figure 4-16. Relative Humidities of Sensor Series S During the Pressure Reversal (unfortunately the computer was down during the transient stage on July 12-13)

4.9. Results for Steel Frame Wall – Transition from Hot to Cold Weather

A similar exercise was also repeated in an instance of testing under winter conditions i.e., low temperatures on the climatic side.

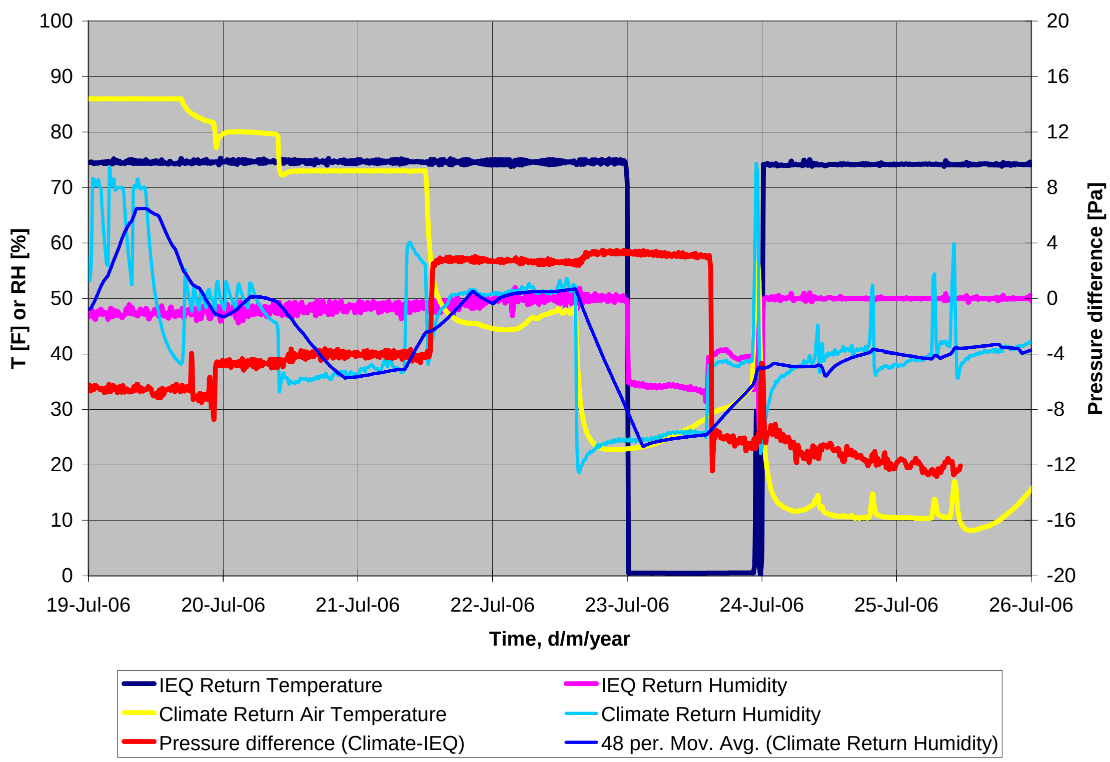

Figure 4-17. Climatic Conditions in the Full-Scale Chamber During the Cold Climate Transition. Note missing data for indoor temperature (IEQ) for July 23.

Table 4-14 and Table 4-15 list respectively relative humidities for one set of sensors (denoted T series) and climatic conditions (the U series were not reading properly for this test). Figure 4-18, Figure 4-19 and Figure 4-20 graphically show the trends of temperature, relative humidity and vapor pressure during the test. The results in Table 4-14 shows a startling effect. The results indicate that initially the relative humidities are low in a range between 40% and 52%. With the transition to very low temperatures (to approximately 10F or -12ºC) and reversal of air pressure gradient in the direction of climatic chamber, moisture laden air from the interior side was transported through the assembly, dramatically increasing the relative humidity during the first 34 hours. Relative humidities in excess of 90% were recorded in two locations. Following an additional 24 hour period of testing, relative humidity continued to increase with 4 locations above 90% relative humidity. The climatic conditions for this period indicate a high vapor pressure difference in excess of 1300 Pa, and a 12 Pa air pressure gradient superimposed, both acting in the direction of the outdoor chamber. Moisture laden air condenses on colder surfaces when the dew point is reached, thus resulting in moisture accumulation.

Table 4-14. Spot Relative Humidities for Sensor Series T in Steel Frame Wall During the Transition to Cold Weather

Date & Time	7/22/2006 5:30 AM	7/24/2006 3:30 PM	7/25/2006 3:30 PM
Sensor	RH [%]	RH [%]	RH [%]
T0	51.8	89.4	90.1
T1	48.1	94.9	97.6
T2	44.7	83	85.6
T3	50.9	91	91.1
T4	44.5	88.4	91.2
T5	47.6	70.9	72.5
T6	40.7	82.2	86.4
T7	40.8	61.9	65.6

Table 4-15. Climatic Conditions During the Spot Measurements in Table 4-14

	Climatic conditions		
	7/22/2006	7/24/2006	7/25/2006
	Climate side	Climate side	Climate side
T, [F/C]	45.0/7.2	10.6/-11.9	9/-12.8
RH, [%]	51.9	40.7	40.4
Pv, [Pa]	522	106	98
	IEQ side	IEQ side	IEQ side
T, [F/C]	74.9/23.8	74.2/23.4	74.1/23.4
RH, [%]	48.7	49.8	50.1
Pv, [Pa]	1450	1458	1448
Diff Pres.	2.6	-12	-11.3
Direction	Climate to IEQ	IEQ to climate	IEQ to climate

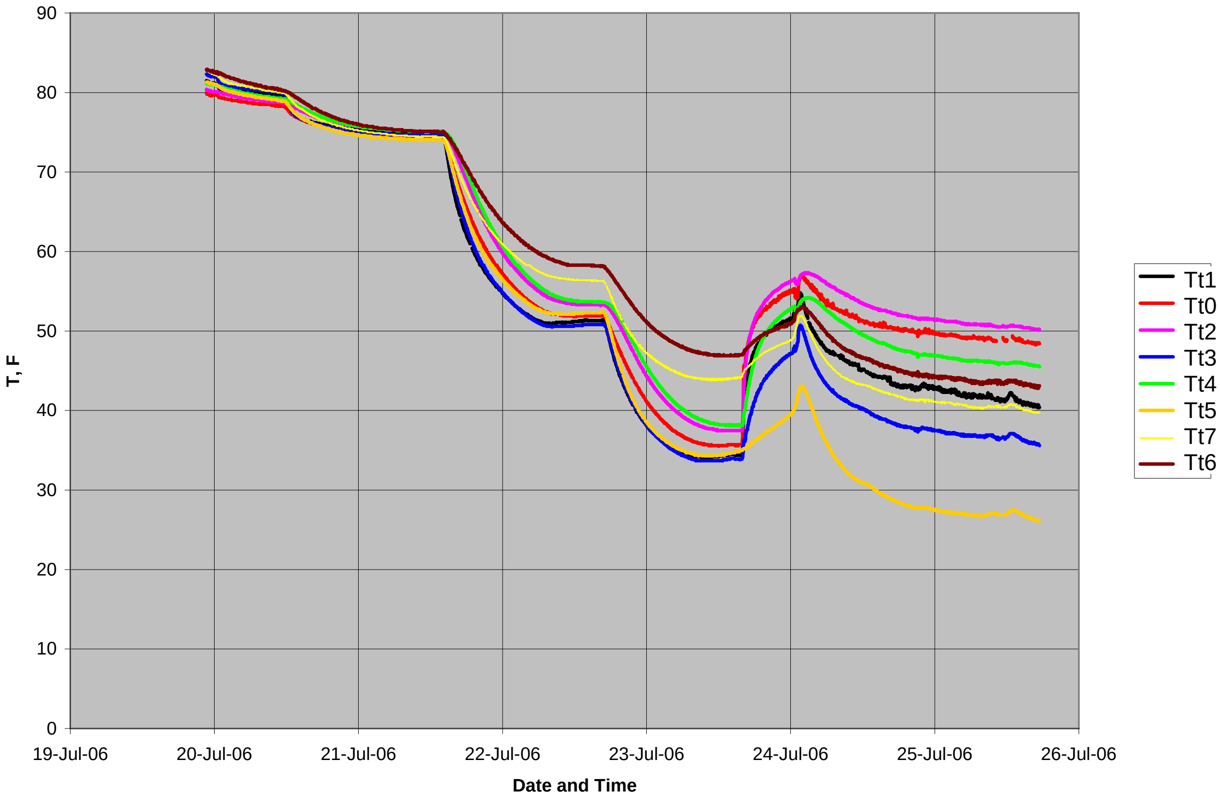

Figure 4-18. Temperatures of Sensor Series T in the Steel Frame Wall (under the window) During the Transition to Cold Weather (Temperature conversion T[C]=(Tj[F]-32)*5/9)

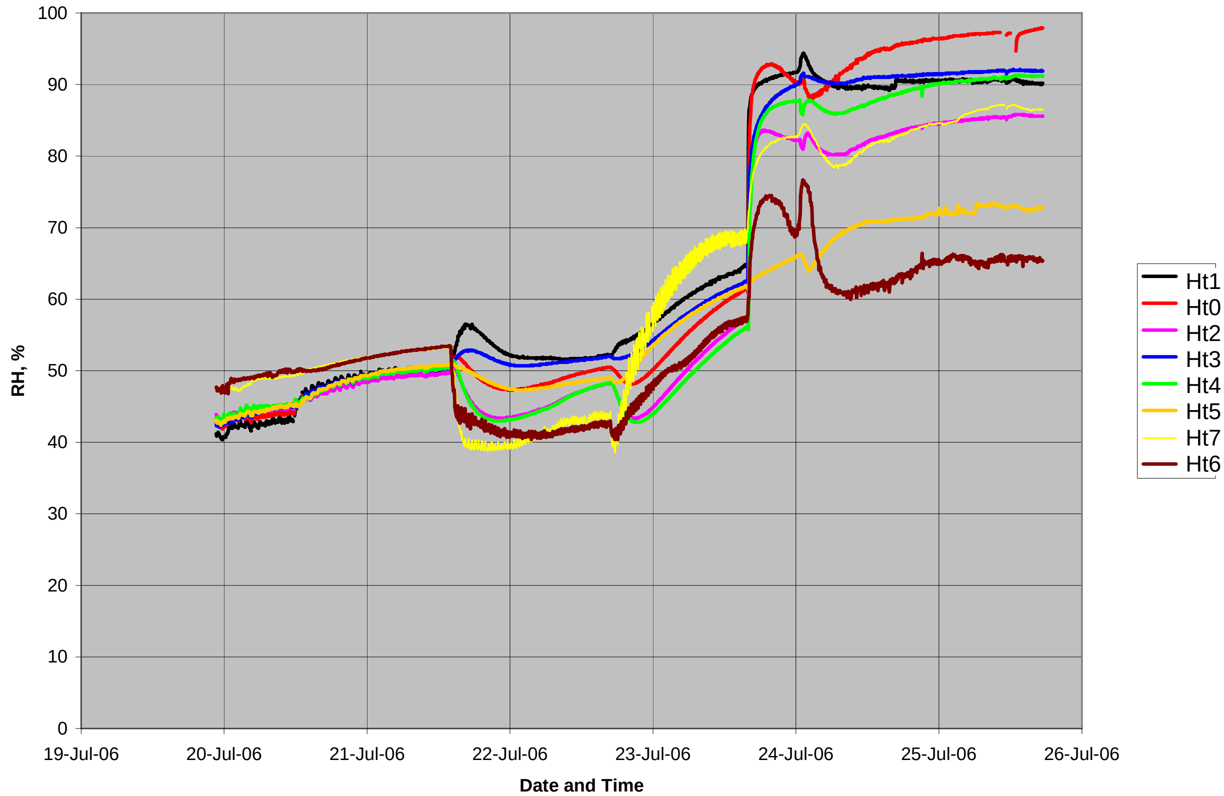

Figure 4-19. Relative Humidities of Sensor Series T in the Steel Frame Wall (under the window) During the Transition to Cold Weather

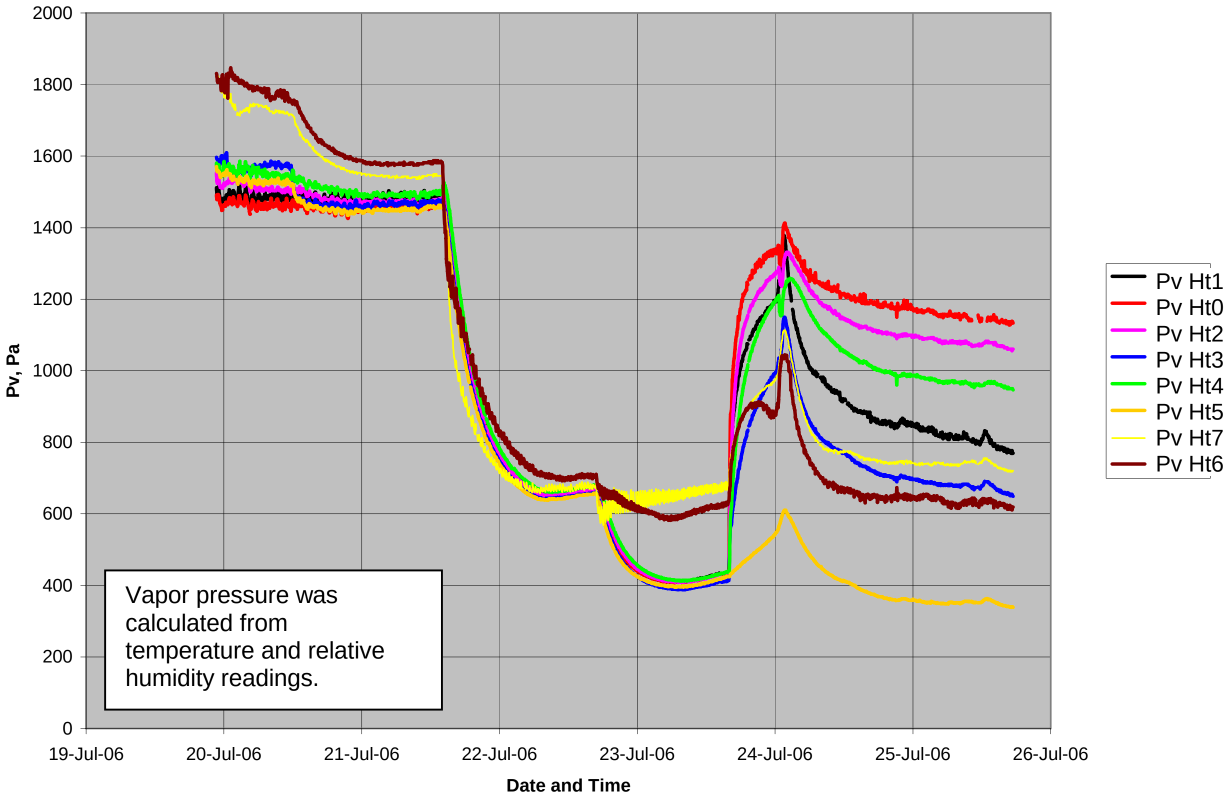

Figure 4-20. Vapor Pressure at the Locations of Sensor Series T in the Steel Frame Wall (under the window) during the Transition to Cold Weather

4.10. Results for CMU Wall – Transition from Hot to Cold Weather

The same comparison was also made for the masonry wall to examine the effect of warm exfiltrating air on conditions within the cavity. The results are shown in Table 4-16 as well as Figure 4-21, Figure 4-22 and Figure 4-23. Climatic conditions were the same as for the steel frame results in the previous section. A similar pattern of increased relative humidities was observed in the masonry wall. For the masonry wall, both groups of sensors were in a working condition. The sensors mounted on the surface of the concrete block on the cold side of cavity show conditions well in excess of 90% relative humidity (sensors R0, R3, and R5). However, the humidity increase for the other sensors R1, R2, R4 and R7 was not as large. An even more puzzling observation was the slight decrease in relative humidity during the 24 hour transition from July 24th to 25th.

Table 4-16. Spot Relative Humidities for Sensor Series R and S in Masonry Wall during the Cold Weather Changes

Date & Time	7/22/2006 5:30 AM	7/24/2006 3:30 PM	7/25/2006 3:30 PM
Sensor	RH [%]	RH [%]	RH [%]
S0	48.3	70.4	74.6
S1	44.4	56.8	60.8
S3	36.2	80.2	90.7
S5	34.5	95.7	86.5
S6	46.3	68.4	70.7
S7	43.7	57.6	58.9

Date & Time	7/22/2006 5:30 AM	7/24/2006 3:30 PM	7/25/2006 3:30 PM
Sensor	RH [%]	RH [%]	RH [%]
R0	38.8	91.7	91.9
R1	26.8	52.7	52.4
R5	37.4	92.6	93.4
R4	24	40.4	38.7
R3	39.6	93.6	94.2
R2	25.3	43.2	41.9
R6	32.2	61.5	61.7
R7	25.2	42.1	40.9

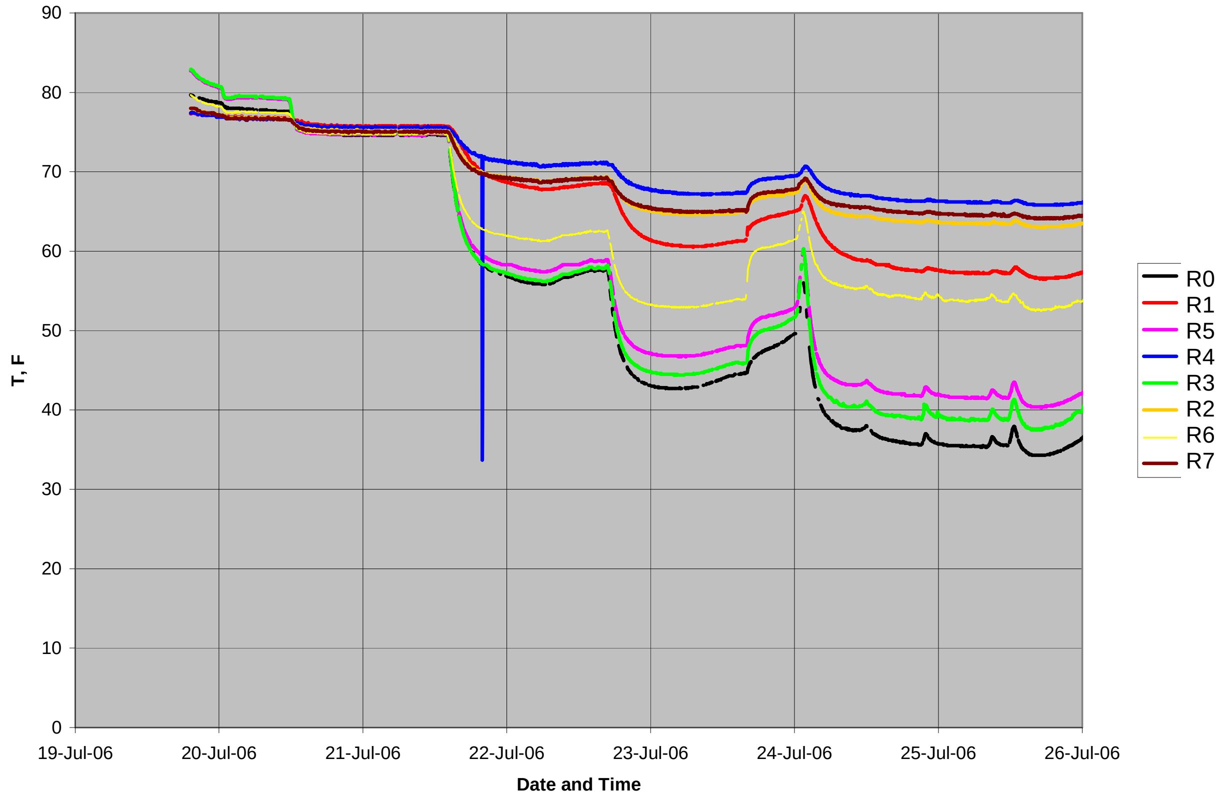

Figure 4-21. Temperature at the Locations of Sensor Series R in the CMU Block Wall (under the window) During the Cold Weather Transition (Temperature conversion T[C]=(Tj[F]-32)*5/9).

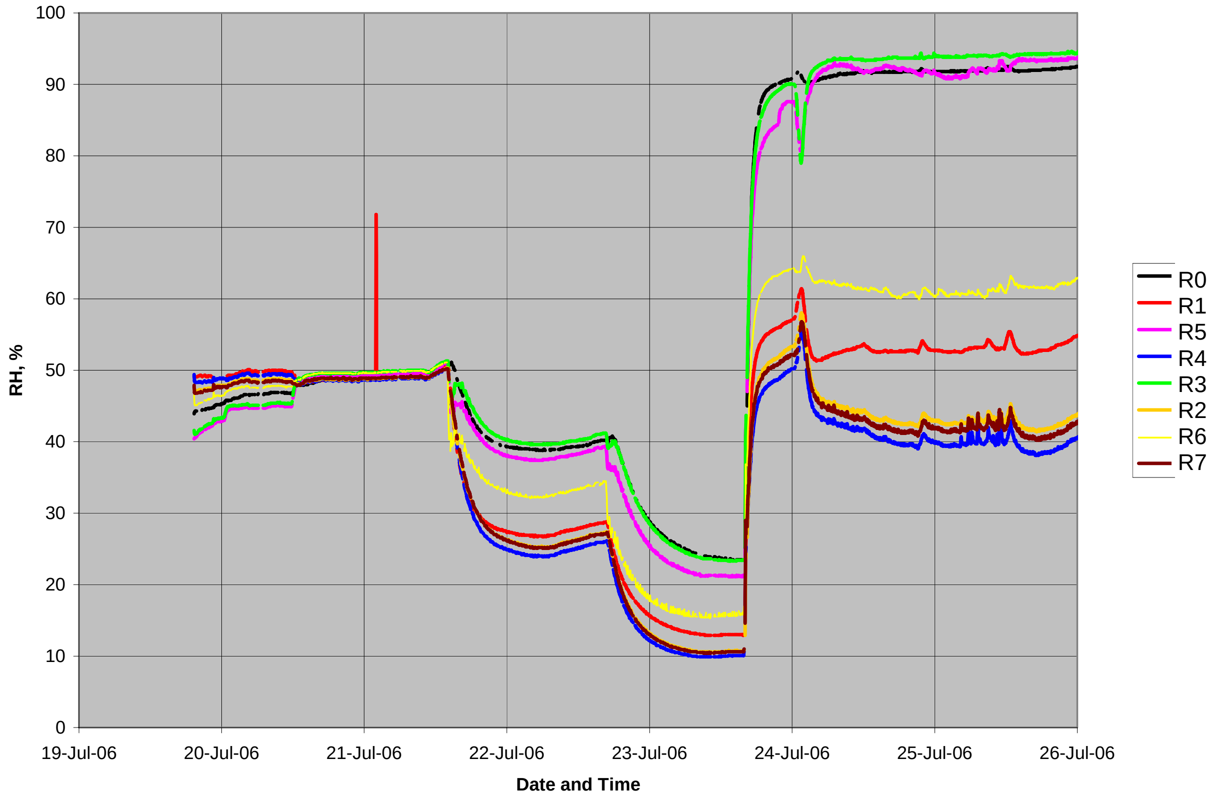

Figure 4-22. Relative Humidity at the Locations of Sensor Series R in the CMU Block Wall (under the window) During the Cold Weather Transition

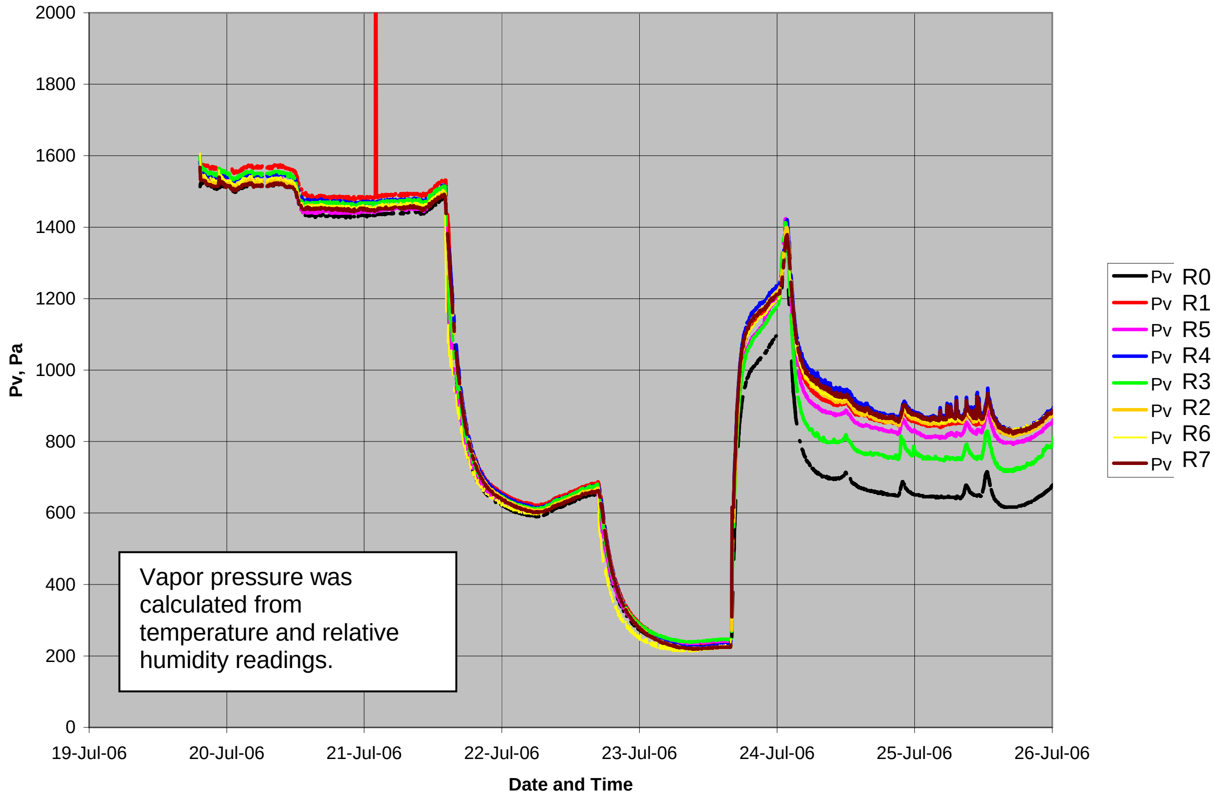

Figure 4-23. Vapor Pressure at the Locations of Sensor Series R in the CMU Block Wall (under the window) During the Cold Weather Transition

4.11. Air Leakage Testing of Measured Walls

Measurements were made to determine the air leakage paths and overall air tightness of each of the two walls using specially designed boxes to cover leakage sites on the wall (Figure 4-24).

Figure 4-24. Experimental Setup to Measure Air Leakage for Various Wall Sections

The measurement method characterized the local air leaks using a fan assisted box to isolate the airflows through the area covered by the box. The fan placed on the tube is controlled in such a way that the pressure inside the box becomes the same as in the chamber outside the box. The airflow rate through the tube is measured using an orifice plate and pressure measurements across the orifice. For high flow rates (leak through the window edges in the CMU block wall) a larger tube with a velocimeter to measure the centerline air velocity in the tube was used.

Full-scale testing of the walls under different air pressure differences across the wall indicated that the walls had significant air leakage. Eliminating the pressure difference between the box and the chamber guarantees that there are no parallel flows in the wall or leaks in the box affected by the measuring device itself. A picture of the system in use is shown in Figure 4-24 and the schematic of the measuring system is presented in Figure 4-25. The air flow rate leaking the surface/section of the wall that is covered with box (attached with a gasket to the wall) can be determined from the equation of the orifice plate correlating the pressure difference across the orifice plate and the flow rate.

The air leaks were characterized for the locations shown in Figure 4-25.

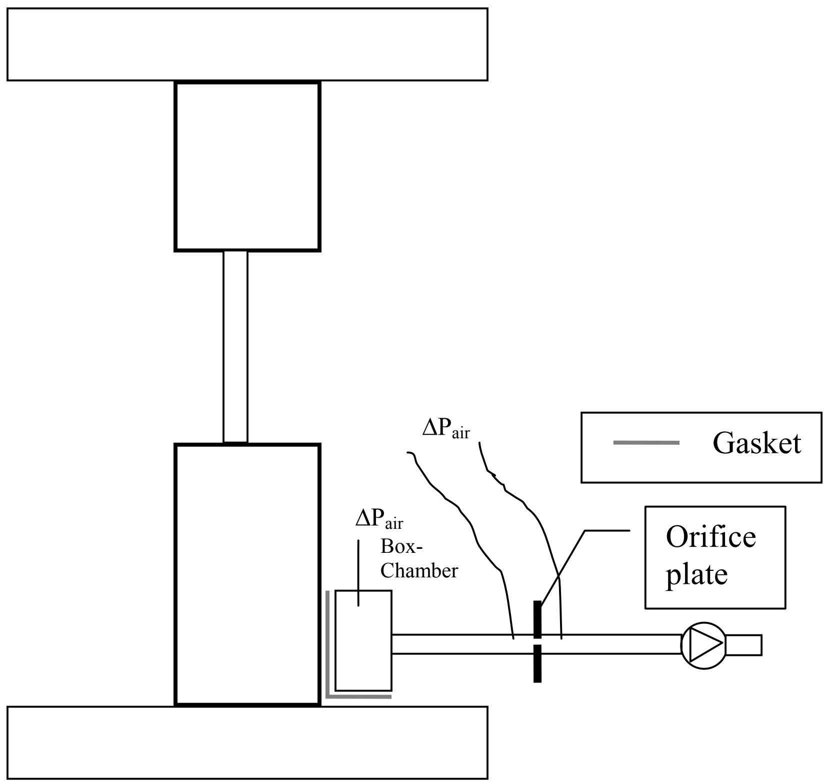

Figure 4-25. Schematic of the Wall Section and the Air Leakage Measurement Device

Two sizes of orifice plates were used, ½” and ¾” inner diameter. The estimated flow-pressure correlations are shown in Figure 4-26. The maximum pressure difference that could be measured with the pressure transducers was 62 Pa which at the same time limited the maximum air flow rate that could be determined. The orifice plates were sufficient for the bottom and top leaks in the walls (through the joint between the wall board and the bottom/top plate), but for the window leaks it was necessary to use a larger 4” pipe and determine the flow rate by measuring the air velocity in the pipe (Model: TSI Velocicalc).

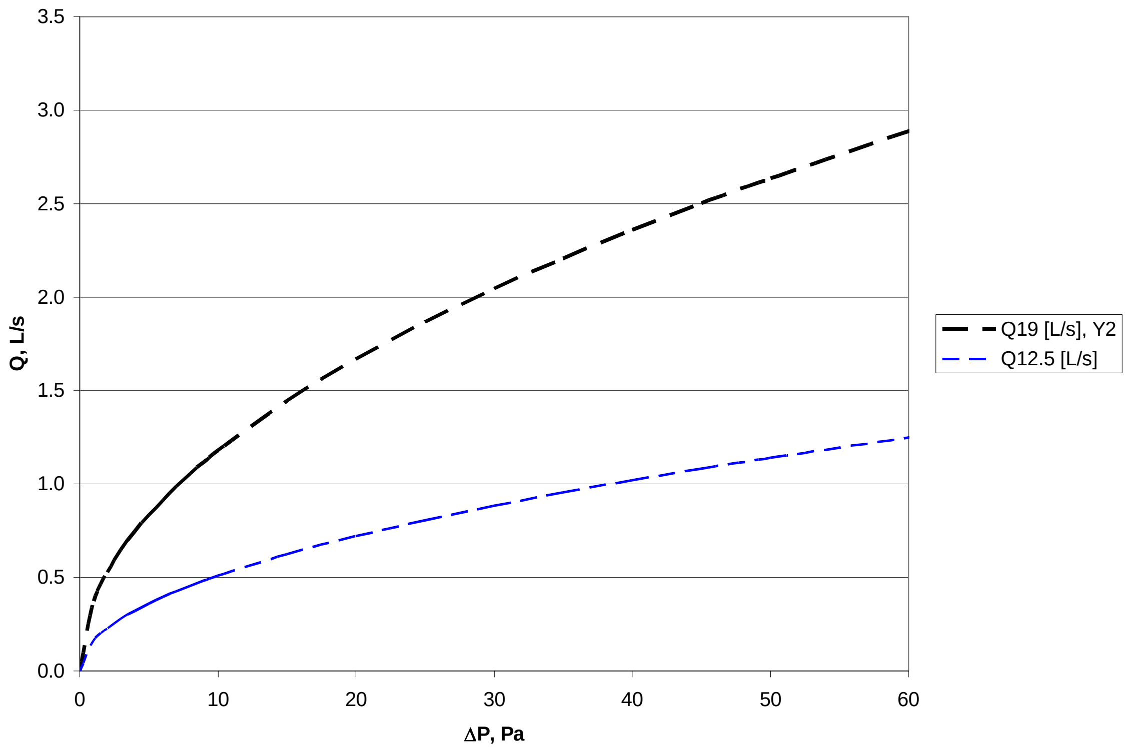

Figure 4-26. The Estimated Flow-Pressure Correlation for the Two Orifice Plates

The air leakage testing showed that the window in the CMU-block wall was not well sealed and the leakage through the frame was very large. However, the window in the steel frame wall had been installed reasonably tightly.

The flow rates through the window in the CMU block wall at different pressure differences across the whole wall are shown in Table 4-17.

Table 4-17. Flow-Pressure Correlation of the Leakage Through the Window in the CMU Block Wall

Pressure difference across the wall, Pa	Flow rate, L/s
4.1	4.0
7.3	6.3
10.2	8.5
12.3	10.2

The pressure difference across the wall was fluctuating during the measurements and the pressures and flow rates are to be considered approximate values.

The air leakage rates through the steel frame wall window could be measured using the orifice plate system with the larger ¾" orifice in place.

The air leakage through the main leakage locations in the walls – window wall interface, bottom and top wall to floor/ceiling interface – could only be measured to indicate the magnitude of the flow. The set of data was not robust enough to predict the flow exponents i.e. whether the flow is laminar or turbulent along the flow path.

Finally Table 4-18 summarizes the air leakage tests for the top and bottom parts of the CMU block and steel frame wall.

Table 4-18. Air Leakage vs. Pressure in the CMU Block and Steel Frame Wall

Wall/Location (Orifice size, in)	Pressure across the wall, Pa	Pressure across the orifice, Pa	Estimated flow rate, L/s
Steel/Top (½" orifice)	8.56	60	0.47
Window/Steel (½" orifice)	7.5	56.6	0.44
Steel/Bottom (¾" orifice)	7.5	6.24	1.02
Window/CMU (3/4" orifice)	11.7	10.7	1.28
CMU/Top ½" orifice	10.6	59	0.53
CMU/Bottom ¾" orifice	9.4	59.7	1.14

The effective leakage area for the leak locations were approximate 1-2 cm^2 (except for the CMU block wall window). These leak locations produced air leakage that is within the suggested air leakage for 'air tight' walls in real buildings – the suggested range for air tightness is 1-2 $L/s\text{-}m^2$ at 75 Pa i.e. these walls are representative to walls in practice.

4.12. Discussion and Conclusions

The tested walls responded strongly to air pressure differentials across the wall even though the walls were not especially leaky with estimated airflow rates of 1-2 $L/s\text{-}m^2$ at 75 Pa. The conditions inside the wall changed rapidly and by a large amount when the airflow changed direction. The measurements focused on the insulation cavity and air cavity conditions and therefore the data was not greatly affected by the thermal and hygric mass. Furthermore the tests were short term tests – only a couple of days for each condition – and the final steady-state conditions (if they existed) were not reached. Therefore the tests do not allow for estimating whether there were any serious moisture problems to be expected in any of the test cases in the long run. The moisture content of the materials within the wall assembly did not likely change much; the relative humidity was high when the temperature was low and the vapor pressures reflected mainly the changes in air humidity and variations in temperature. The steel frame wall assembly had very little hygroscopic mass which in large part explains the fast response to air flow direction, temperature and humidity changes in climatic chambers. The concrete wall has higher hygroscopic mass but moisture transport in concrete is fairly slow and as explained above the longer term performance could not be reached within this short time period. Also the thermal mass did not show up in the measurements for the masonry wall. The temperatures in the wall changed quickly to a steady value after the excitations in the surrounding environments.

The tests revealed what was expected based on the preliminary simulations: the airflow effects are quite local and most effects are happening in the areas where the air is entering and exiting the wall structure i.e. where the air is moving across the heat flux isolines. Thermal bridges in the structures may hide some of the effects and the most pronounced effects are found in well insulated areas such as in the insulated cavity.

In summary the following conclusion can be drawn from the test results:

1. Detail elements can contribute significantly to thermal bridging. Steel studs especially those in exposed areas such as window sill or plate can significantly affect the temperature profile of the construction.
2. Change in airflow (reversal of air flow direction) from the exterior to the interior of side (from cold to warm side) can have a significant localized temperature effects within the assembly
3. Although, the effect of airflows does not significantly affect the surface temperature of the steel studs, this effect is pronounced and highly affects the conditions within the assembly and more specifically the relative humidity within the insulation cavity. This in actuality becomes counter positive. As warm moisture laden air flows through the wall cold surfaces can cause the flowing air to be cooled. If cooled significantly below the dew point then condensation can take place.
4. The thermal mass effect in the masonry wall appears to be very small. The sensors indicate that the appearance of steady state is reached relatively soon.

4.13. References

Desmarais, G., D, Derome, and P. Fazio. (1998). "Experimental setup for the study of air leakage patterns." Thermal Performance of the Exterior Envelopes of Buildings VII, ASHRAE / BETEC /CIBSE/ ORNL/ USDOE/ NRCC, December 7-11, Clearwater Beach Florida, pp 99-108.

Hukka, A. and Viitanen, H.A. (1999). "A Mathematical Model of Mold Growth on Wooden Material", Wood Science and Technology, 33: 475–485.

VanBronkhorst D.A, A K Persily, S J Emrnerich (1995). "Energy Impacts of Air Leakage in US Office Buildings Implementing the Results of Ventilation Research." 16th AIVC Conference, Palm Springs, USA 19-22 September, 1995

5. Computer Modeling Wall Assembly Performance

5.1. Modeling Approach

LATENITE is a multi-dimensional heat, air, and moisture transport (HAM) in building envelope systems developed by Salonvaara & Karagiozis during the collaboration between VTT Building Technology (One of the institutes of Technical Research Center of Finland) and National Research Council of Canada in the middle of 1990s. The model has been validated in several projects in the past as well as during the IEA Annex 24 (International Energy Agency). The common benchmark tests and model capabilities are listed in the final reports of the Annex by Hens (1993). The model is also described in 'Moisture Analysis and Condensation Control in Building Envelopes' (ASTM MNL40, 2001). Further model verification is being carried out in another project at Syracuse University. VTT Building Technology is continuously improving the model and only some of the features are used in this analysis. The LATENITE model is described in more detail in Salonvaara, M (1994, 1999) and Hukka (1999).

The governing equations in the model are

Moisture balance

$$\rho_0 \frac{\partial u}{\partial t} = \nabla \cdot (\delta_p \nabla P_v) + \nabla \cdot (\rho_0 D_w \nabla u) - \nabla v \rho_v \qquad \text{(eqn. 5-1)}$$

Energy balance

$$c\rho_{eff} \frac{\partial T}{\partial t} = \nabla \cdot (\lambda \nabla T) + L_v \nabla \cdot (\delta_p \nabla P_v) - \nabla \cdot (\rho_a v c T) \qquad \text{(eqn. 5-2)}$$

Mass balance for airflow

$$\nabla \cdot (\rho_a \vec{v}) = 0 \qquad \text{(eqn. 5-3)}$$

The air velocity is calculated using the Darcy-flow equation including buoyancy effects

$$\vec{v} = -\frac{K}{\eta}(\nabla P - \rho_a g) \qquad \text{(eqn. 5-4)}$$

where

ρ_a	- Air density, kg/m^3
$c\rho_{eff}$	- Volumetric heat capacity of moist porous materials, J/m^{3}-K
ρ_0	- Air density, kg/m^3
u	- Moisture content, kg/kg
T	- Absolute temperature, K
t	- Time, s
c	- Specific heat, J/kg-K
λ	- Thermal conductivity, W/m-K
L_v	- Latent heat of vapor phase change, J/kg
δ_p	- Vapor permeability, kg/m-s-Pa

D_w	- Liquid moisture diffusivity, m^2/s
K	- Air permeability, m^2
v	- Velocity vector, m/s
V	- Volume, m^3
η	- Dynamic viscosity, Pa-s
P	- Pressure, Pa
ρ_v	- Water vapor concentration, kg/m^3
P_v	- Water vapor pressure, Pa

Two major simplifications were made in this analysis:

1. Focus in the study is on the interface between the window sill and floor section of the wall assembly. Air leakage across the window-sill is a key leakage element in the wall assembly based on the results of full-scale wall assembly test. At the same time, the connection between the wall and roof or floor can vary greatly in actual field practice. In this wall experimental setup, the sections between the roof-wall and floor-wall details are the same. Therefore, our objective is to focus on modeling the window sill and floor section of the wall assembly.

2. Two-dimensional flow between the window sill and floor section of the wall assembly was assumed. Significant efforts are needed in using computational fluid dynamic (CFD) simulation model to investigate true 3D flow effects of airflow on heat and moisture transport. The open slots of steel studs are large enough to equalize the pressure between the wall cavities. Two dimensional flows give in many cases as much information about the behavior of the wall structure with air leakage: most significant effects of airflows on heat and moisture performance happen at areas where air flows are flowing the same direction as heat flow, less pronounced effects are found when air is moving along the heat flux isolines. Therefore, as practical compromise we will use a 2D model to evaluate the impact of air flow on heat and moisture performance in the wall assembly.

Two different base simulation cases, modeled with LATENITE, have been setup in this analysis. The cases are as shown below (Figure 5-1) for steel frame and (Figure 5-2) for block masonry wall. Flow Path A is representative of airflow through a wall driven by wind or mechanically-created pressure differences. Flow Path B is representative of stack-driven airflow effects.

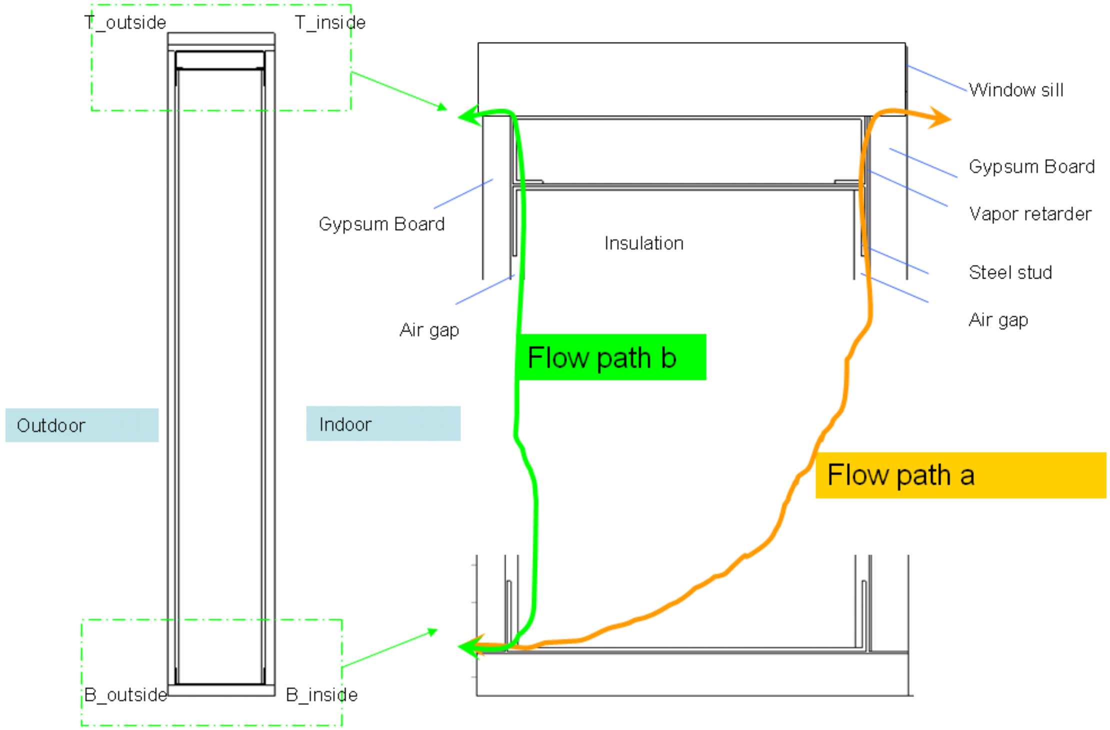

Figure 5-1. Flow Path Considerations for the Steel Frame Wall in the Simulations

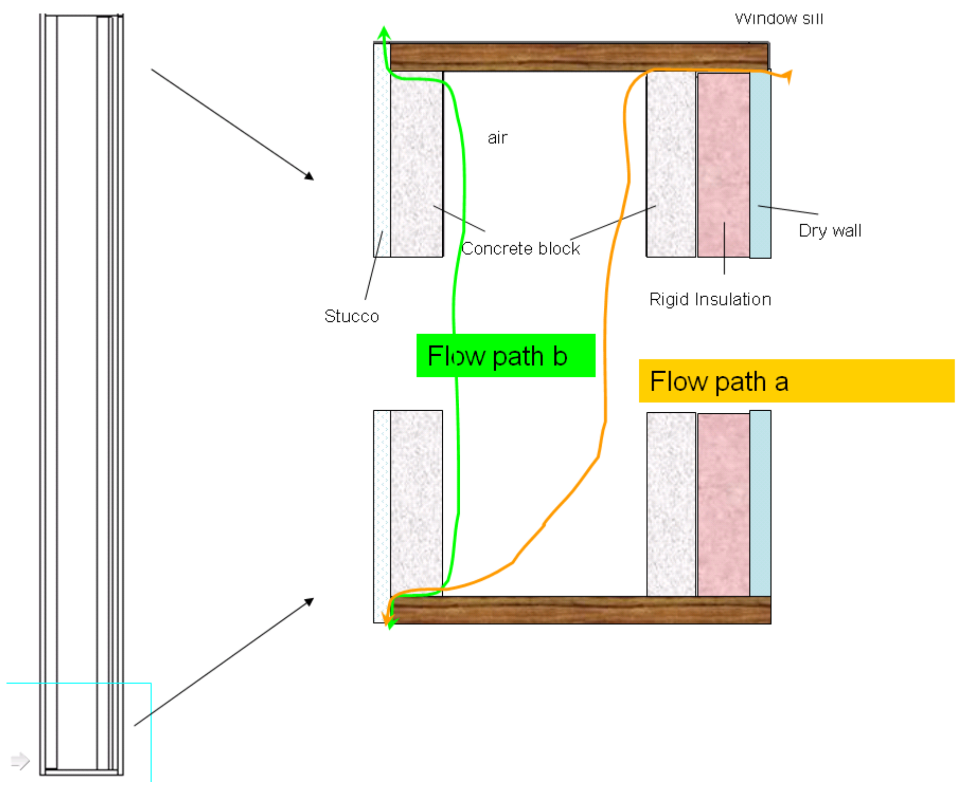

Figure 5-2. Flow Path Considerations for the CMU Block Wall for Simulation Purposes

Only the interior wall section was modeled in this analysis i.e., the exterior cladding was not included in the modeling. The aim was to isolate the effects of diffusion and air leakage. Therefore wind-driven rain or solar radiation effects were not taken into account in this analysis. The wall performance is representative of a wall section sheltered from rain and oriented to North. The effects of wind induced pressure changes on the exterior wall surface as well as stack effects due to temperature difference between indoor and outdoor were taken into account in the air leakage calculations.

The initial conditions selected for the wall simulation in both cases were 23ºC (73.4F) for temperature and RH=50% relative humidity. The selected boundary conditions on the top and bottom section of the wall were assumed to be adiabatic and impermeable i.e.: there is no heat and mass transfer occurring through the frame. There are no wind effects and there are no heat and moisture sources. The neutral pressure plane is selected at a height of 1 m from the bottom of the wall.

5.2. Steady State Simulations of Steel Frame Wall

5.2.1. Effects of Flow Rate on Moisture Accumulation Under Summer Conditions for Flow Path A

In the following simulation the effects of air flow path during summer conditions were examined. The simulation was performed for three distinct flow rates. The results in Figure 5-3 show the effect of flow rate on relative humidity (moisture accumulation) in wall assemblies. Relative humidity contours below indicate that higher flow rates (7 and 14 m^3/h-m^2) results in lower relative humidity inside the assembly. The reason for this can be seen in Figure 5-4 which presents the temperature contours for the same air leakage cases. When the airflow rate is higher, the temperature behind the drywall is also higher. Higher airflow rates allow greater quantities of moisture transport and storage into the wall. This moisture however cannot condense and/or accumulate because the air flowing out of the wall to the indoors can also carry more moisture out of the wall due to higher temperature at the exit. Saturation vapor pressure increases exponentially as a function of temperature and therefore the temperature has a stronger effect on the performance than the linear effect of airflow rate on moisture ingress into the wall. 7 m^3/h-m^2 means about 2 L/s-m^2 airflow rate which is already past the 'optimum' for moisture accumulation. The high airflow rate affects the temperatures and the higher interior surface temperature reduces the potential for moisture accumulation. In the contour plots red color indicates high temperature and high relative humidity and blue color low values.

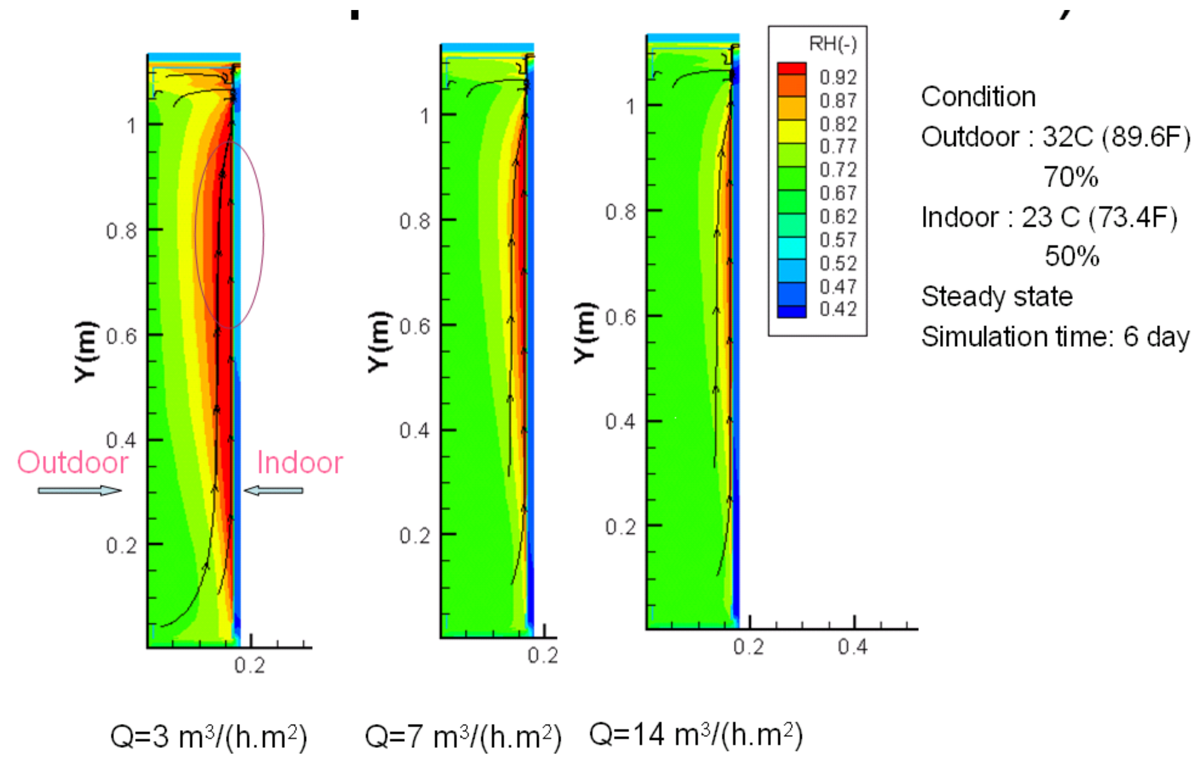

Figure 5-3. Relative Humidity Contour of Steel Frame Wall in Summer Conditions with Air Infiltration (flow from outdoors to indoors)

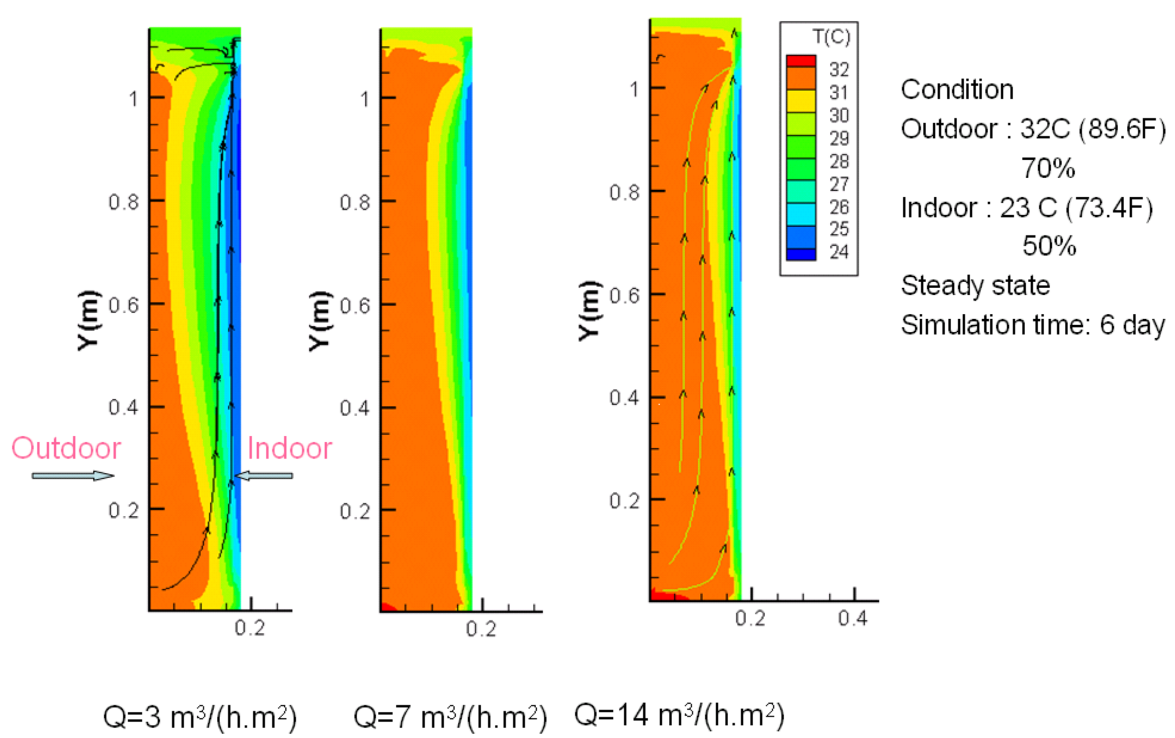

Figure 5-4. Temperature Contour of Steel Frame Wall in Summer Condition (flow from outdoors to indoors)

5.2.2. Effects of Flow Rate on Moisture Accumulation Under Winter Conditions for Flow Path A

The same case was also examined under winter conditions. Simulation was repeated for the same air flow rates as the previous section but with airflow a reverse direction. As is shown in Figure 5-5, when Q=3 m^3/h-m^2, condensation may occur near the exterior surface. When the airflow rate is increased to Q= 14 m^3/h-m^2, more moisture is transported out of the wall cavity due to high air flow leakage rate and there is a resulting increase in temperature. The sections of the cavity near the exterior surface become significantly warmer as indicated by the contours in Figure 5-6.

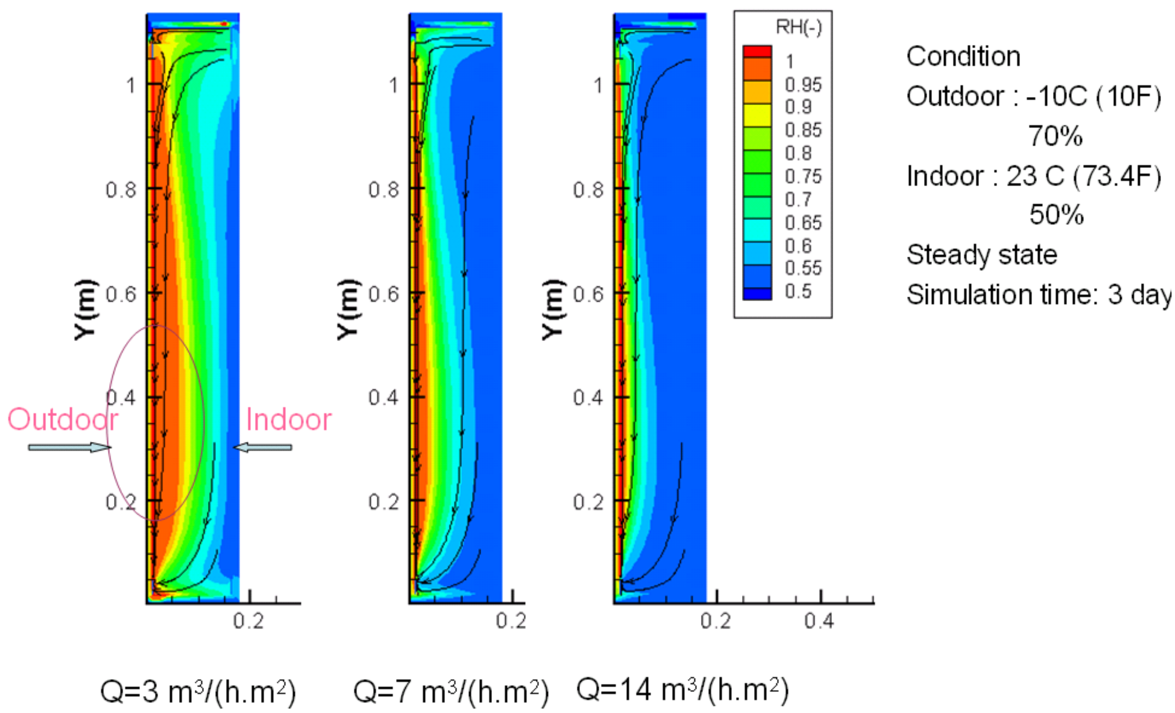

Figure 5-5. Relative Humidity Contour of Steel Frame Wall in Winter Conditions with Air Exfiltration (flow from indoors to outdoors)

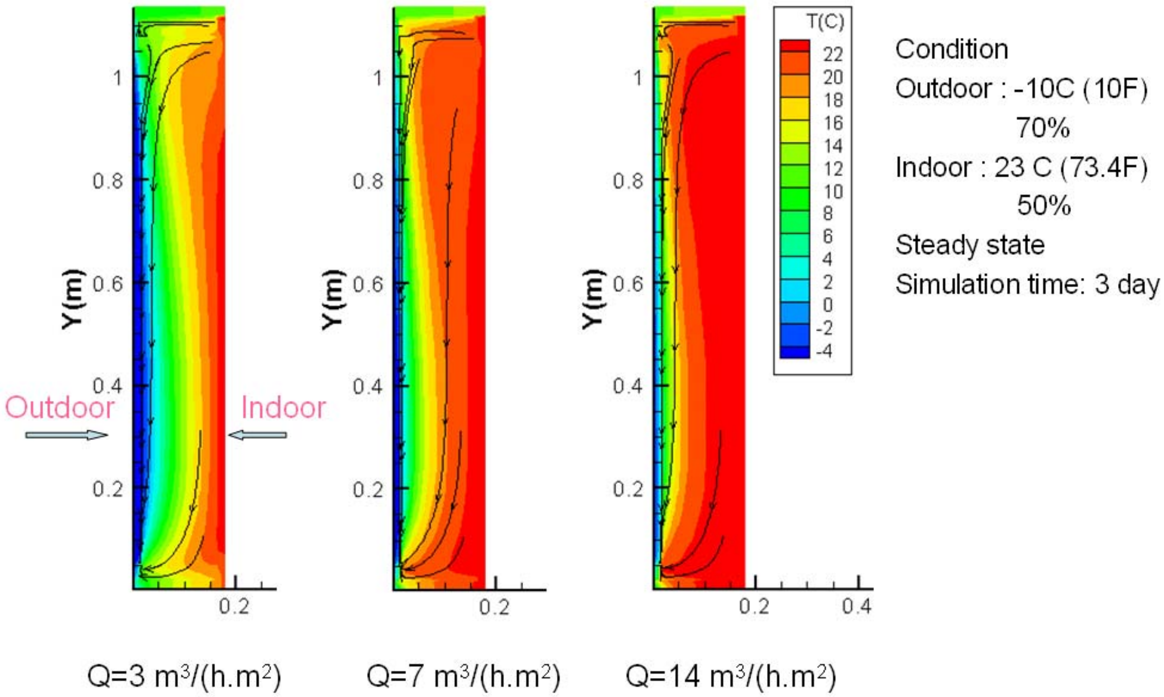

Figure 5-6. Temperature Contour of Steel Frame Wall in Winter Condition (flow from indoors to outdoors)

5.2.3. Effects of Flow Rate on Moisture Accumulation Under Winter Conditions for Flow Path B

The simulation was repeated to examine a path B air flow regime. In this case the cold outdoor air enters at the bottom of the wall, and is carried to the top of the cavity. The temperature of the air increases as it flows along the wall cavity to the top of the cavity. At the top of the cavity the air exits to the outdoors i.e. there is only very little flow through the wall system. The cold air entering the cavity has low moisture content (cold air) and as the air warms up the relative humidity goes down. The cold air entering the cavity has such low moisture content that increasing its temperature results in small changes in relative humidity. The pressure difference across the wall did not change the performance much since the flow through the wall was very small.

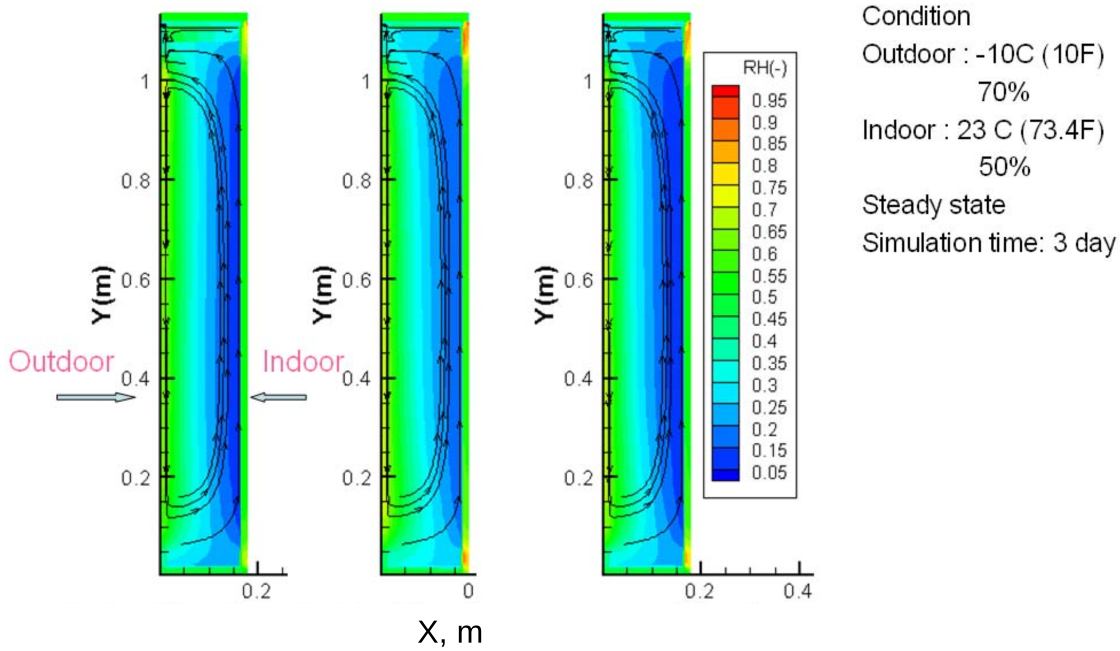

Pressure difference ΔP = 0, 2 and 4 Pa across the wall (outdoor to indoor).

Figure 5-7. Effect of Flow Path B on RH Contours in the Winter

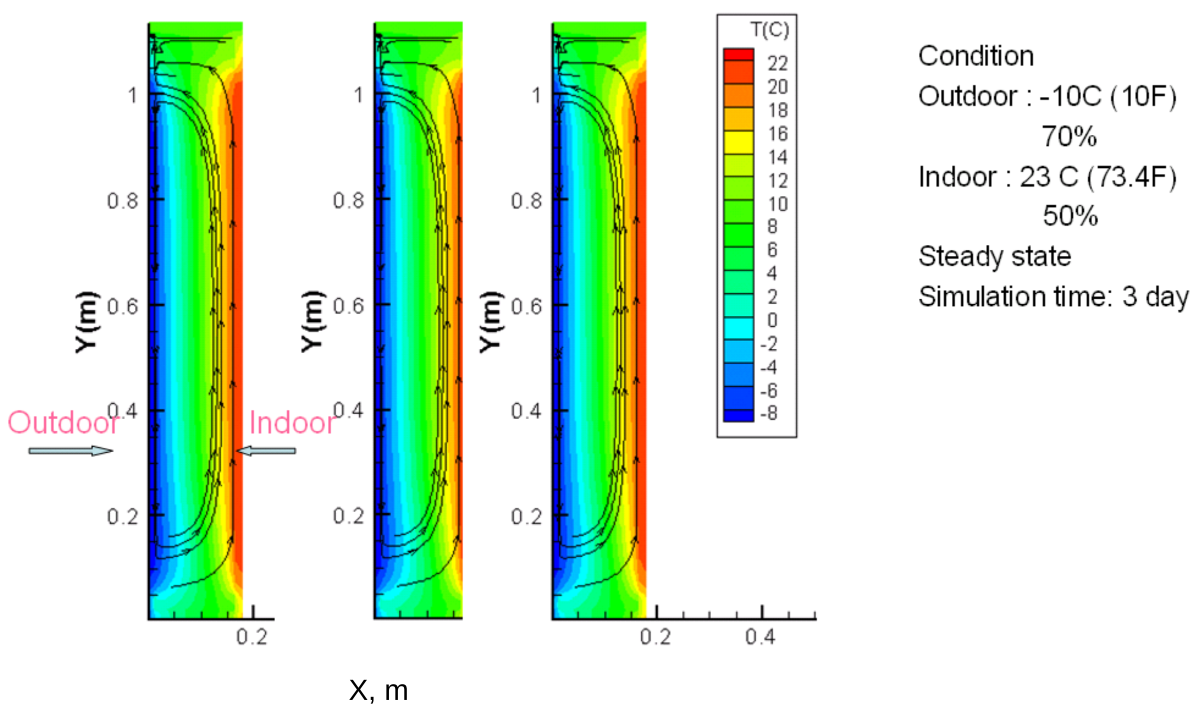

Pressure difference ΔP = 0, 2 and 4 Pa across the wall (outdoor to indoor).

Figure 5-8. Effect Flow Path B on Temperature Contours in the Winter

5.2.4. Prediction of Mold Growth

The mold growth model and involved mathematical equations are presented in a more detailed manner in another publication (Hukka & Viitanen, 1999) and only short introduction is given here. Quantification of mold growth in the model is based on the mold index used in the experiments for visual inspection. The mold growth model is based on mathematical relations for growth rate of mold index in different conditions including the effects of exposure time, temperature, relative humidity and dry periods. The model is purely mathematical in nature. As mold growth is only investigated with the use of visual inspection, it does not have any connection to the biology in the form of modeling the number of live cells. Also it must be noted that the results of calculations of mold index do not reflect the visual appearance of the surface under study, because traces of mold growth remain on wood surface for a long period of time. The way to interpret these results requires realizing that the mold index represents the possible activity of the mold fungi on the wood surface.

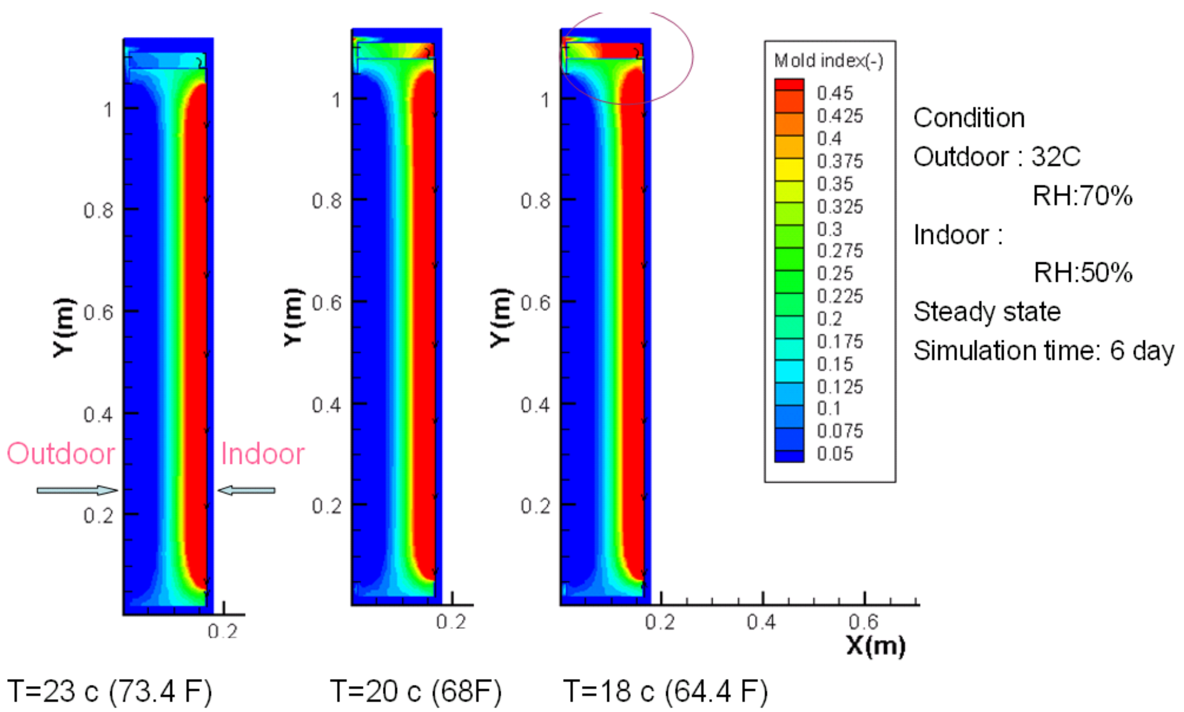

Figure 5-9. Indoor Temperature Effect on the Mold Growth in the Summer (no air leakage)

The model allows the possibility of calculating the development of mold growth on the surface of small wooden samples exposed to fluctuating temperature and humidity conditions including dry periods. The numerical values of the parameters included in the model are fitted for pine and spruce sapwood, but the functional form of the model can be reasoned to be valid also for other wood-based materials. The mold index scale is described in more detail in Table 5-1.

Table 5-1. Mold Index Values and Their Meaning

Index	Descriptive meaning
0	No growth
1	some growth detected only with microscope
2	moderate growth detected with microscope
3	some growth detected visually
4	visually detected coverage more than 10%
5	visually detected coverage more than 50%
6	visually detected coverage 100%

Increasing the duration of the simulation increases, the mold index as well. Figure 5-9 had only six-day simulation period, therefore the mold index is small compared to the table value. It is obvious that there will be more moisture condensation in the wall cavity at T=18 ºC (64.4F) than T=23 ºC 73.4F). This explains the slightly larger area with higher mold index in the simulation results shown in Figure 5-10 below.

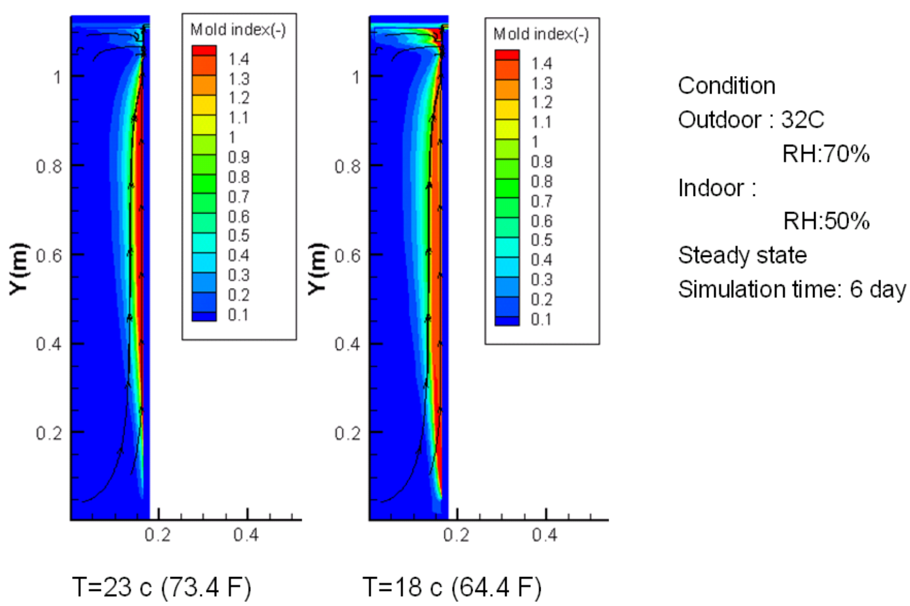

Figure 5-10. Indoor Temperature Effect on the Mold Growth in the Summer (Leakage Path A).

For the configuration with Leakage Path A in the wall assembly under summer conditions (Figure 5-10), more moisture condenses at the window sill near the interior surface when the indoor temperature is low 18°C. The possible reason for this occurrence is that the steel studs near the window sill have a lower temperature differential while they form a thermal bridge in the wall cavity balancing the temperature difference across the insulated cavity. When the indoor temperature becomes lower the critical temperature in the stud is finally reached and condensation starts forming on the studs. In effect the reduced temperature at this location leads to greater condensation. The wall area below the window without thermal bridges becomes lower in temperature on the interior side already at higher indoor temperature (23°C) and condensation occurs earlier.

5.3. Yearly Simulation of Steel Frame Wall with Weather Data

Yearly simulations of steel frame wall were also performed to examine the potential for moisture related risks and problems in the wall assembly. As is shown in Figure 5-11, measured Syracuse weather data were used for input into the simulation. Three pressure gradients acting across the wall (0, 2 and 4 Pa) were simulated to examine their influence on the heat and moisture transport through the assemblies (e.g., pressures caused by ventilation system). Wind and stack pressures caused additional pressure differentials depending on the time and weather. These pressure differences generated the same magnitude of air leakage rate as in the field. Therefore this simulation was used to predict actual wall performance with regard to the weather data. The simulations in this case considered a steel frame wall with brick cladding (slightly different than the walls from the full-scale testing).

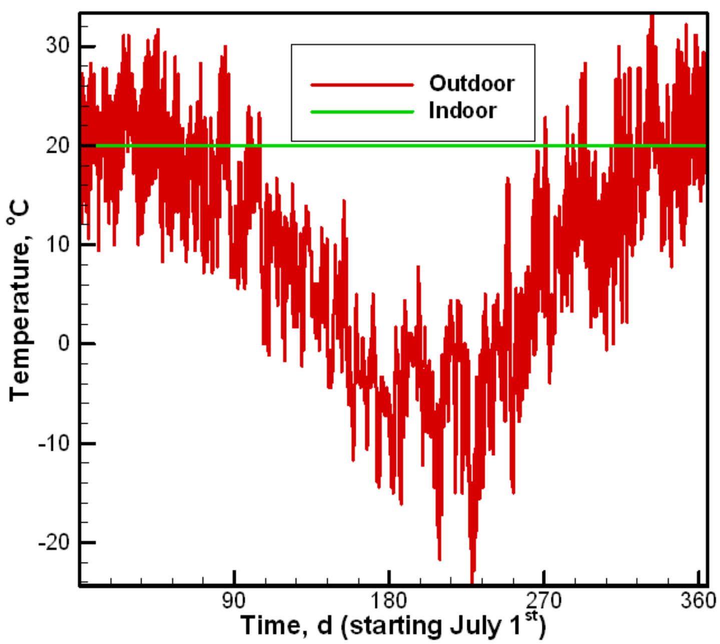

Figure 5-11. Yearly Simulation Weather in Syracuse, NY

With a positive pressure difference between the indoor and outdoor environment (either induced by wind or mechanical ventilation), moisture accumulates in the insulation inside the cavity. Figure 5-12 shows the impact of imposing forced pressure differences of 0, 2 or 4 Pa across the wall by mechanical means. Wind induced airflows are present in all the cases. For the 0 Pa case the airflow direction (from indoors to outdoors vs. outdoors to indoors) is fluctuating depending on the wind and stack effects. The long term average airflow rate through the wall is close to zero for the 0 Pa case. However, even with 0 Pa pressure difference (on average) the air leaks through the wall leave moisture in the wall cavity. Airflow from warm indoors to cold outdoors leaves moisture in the wall cavity. When the airflow is reversed from cold outdoors to indoors, the air cannot always transport the moisture from the cold side of the wall back to indoors because it may be nearly saturated (e.g., its high relative humidity with respect to the outdoor air temperature limits the capacity to pick-up moisture in insulation). With forced pressure differences of 2 and 4 Pa, the primary airflow direction is from indoors to outdoors and the wall exhibits more moisture accumulation with more airflows towards the outdoors.

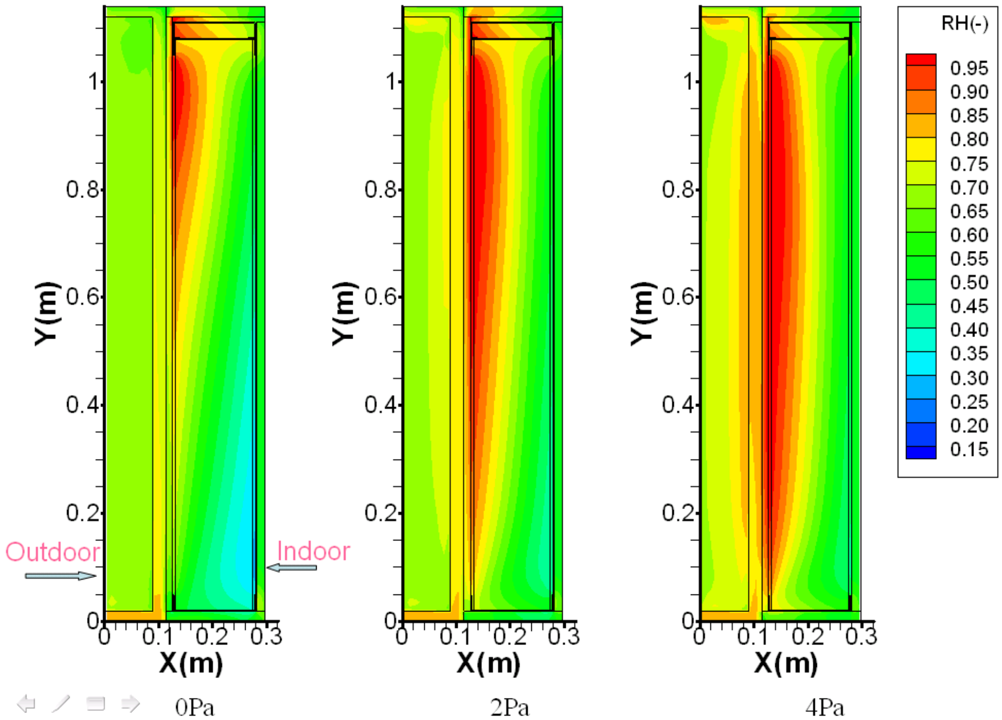

Figure 5-12a – RH contour

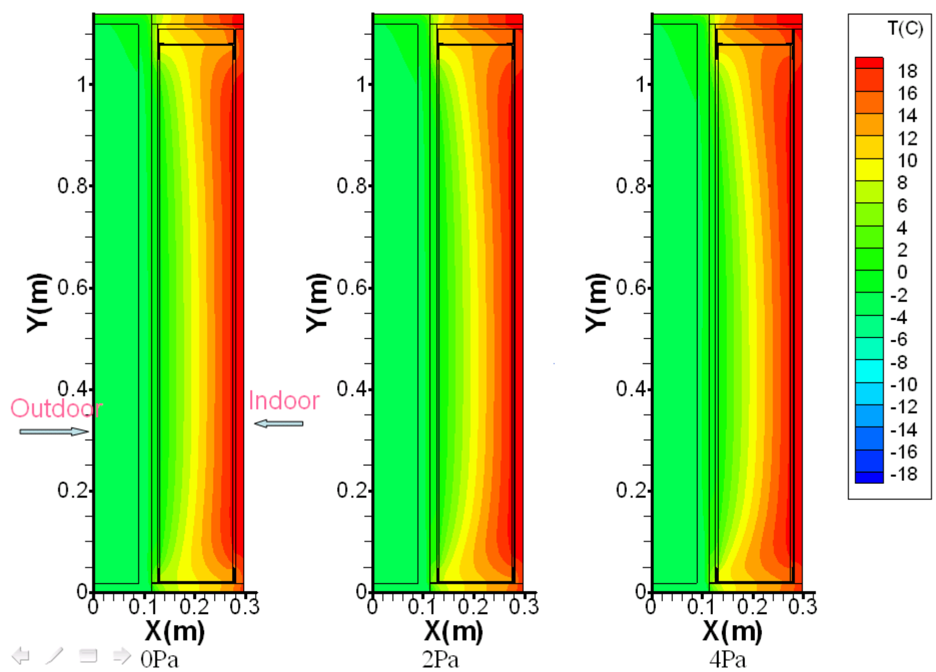

Figure 5-12b – temperature contour

Figure 5-12. Relative Humidity and Temperature Contours in December for the Steel Frame Wall (including brick and air gap) with Different Ventilation-Forced Pressures (0, 2 & 4 Pa)

Figure 5-13 shows RH contours for 0 Pa case but with airflow patterns corresponding to a wind pressure of 4 Pa. Short term, wind-induced pressure fluctuations imposed on the 0 Pa case cause airflows through the wall. The direction and magnitude of the airflow at a certain time depends on the instantaneous total pressure difference caused by the forced and wind-induced pressure across the wall. In the case with 0 Pa forced pressure difference the effects of air leakage are clear. Moisture accumulates at the top of the wall where the warm air enters the wall depositing moisture on the cold side of the insulation cavity. Occasional reversed flows keep the bottom of the wall dry. With forced pressure differences 2 and 4 Pa the airflow path is the same but the airflow rates towards the outside are higher and the direction is more often from indoors to outdoors resulting in higher moisture accumulation along the whole wall height.

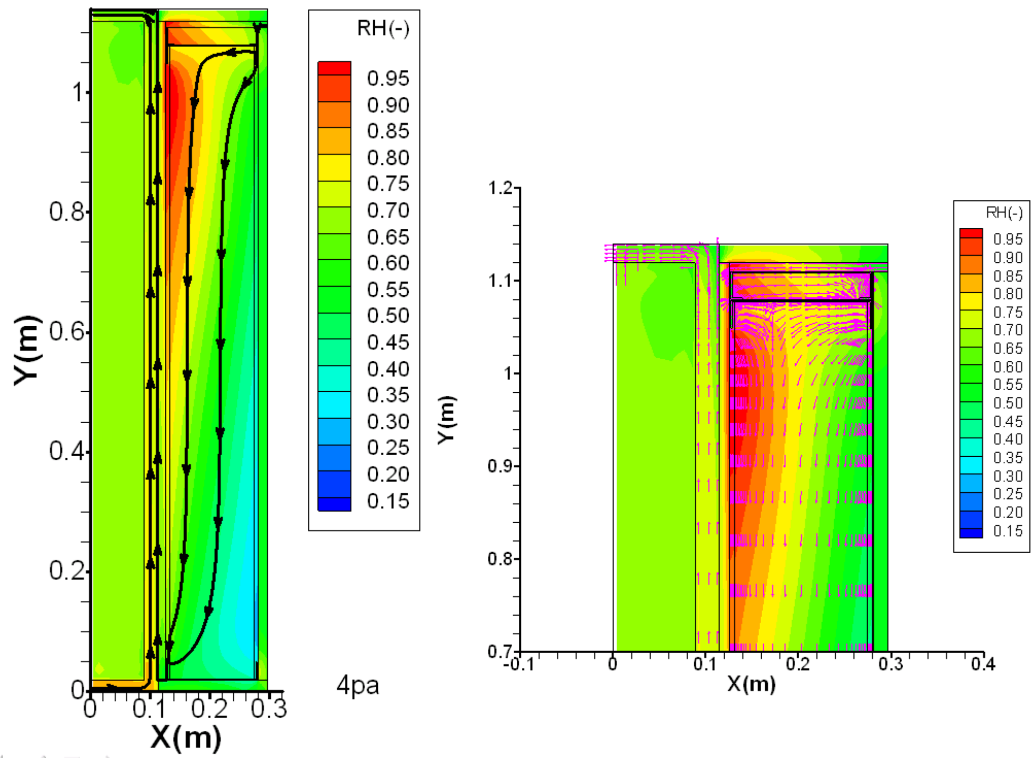

Figure 5-13. Air Leakage Paths and the Detailed Airflow Pattern for 0 Pa Case (i.e., no mechanical ventilation) with 4 Pa of Wind Pressure

With a higher rate of moisture accumulation occurring on the insulation materials within the cavity of the wall, the potential risk of mold growth increases as well. The mold index indicates a substantial section in which the mold index is 5 or above. This translates to visually detected mold coverage on 50% of the area. This constitutes a very probable risk for mold growth.

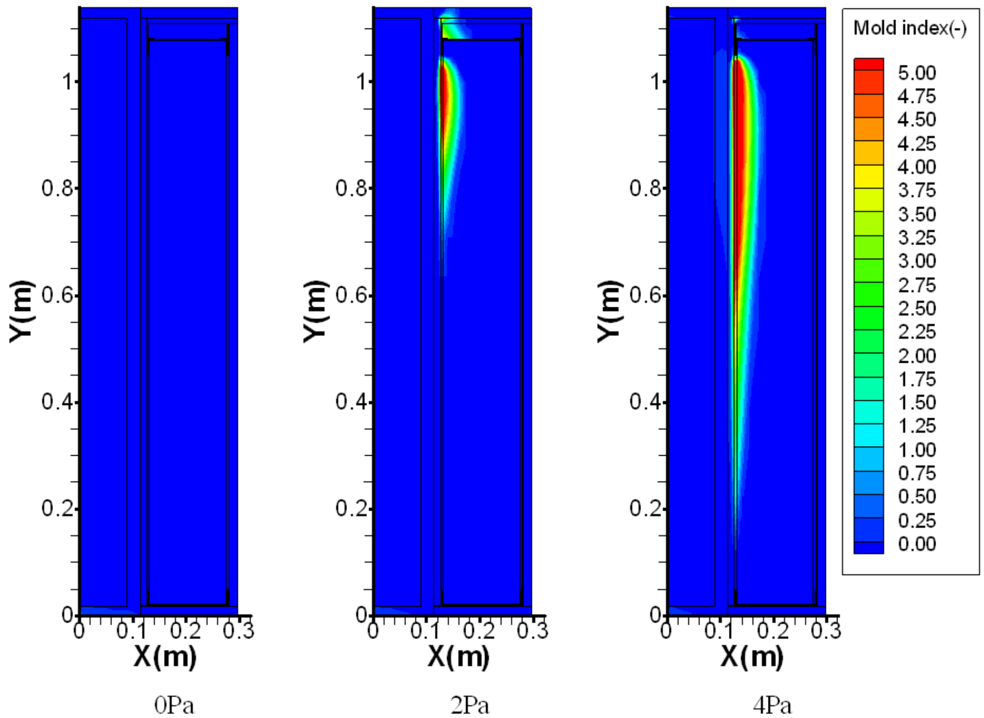

Figure 5-14. Mold Index Contour in December

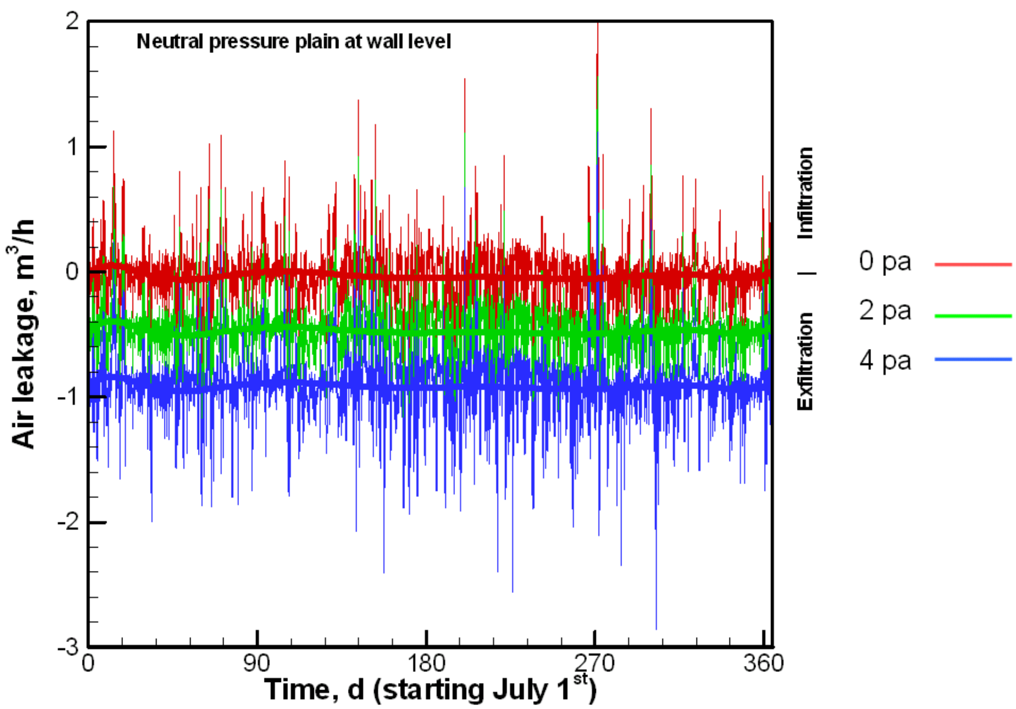

Figure 5-15. Air Leakage Flow Rate When There is 0, 2, 4 Pa Pressure Difference Across the Wall Assembly

The 4 Pa pressure difference can result in volumetric air leakage rate equivalent to 0.7 m^3/h, which is much higher than the air leakage rates occurring at 2 Pa and 0 Pa. For the 2 Pa pressure difference the airflow rates are approximately half of those at 4 Pa, and zero pressure difference produces only the fluctuating airflows resulting in the long term average of the airflow of about 0 m^3/h.

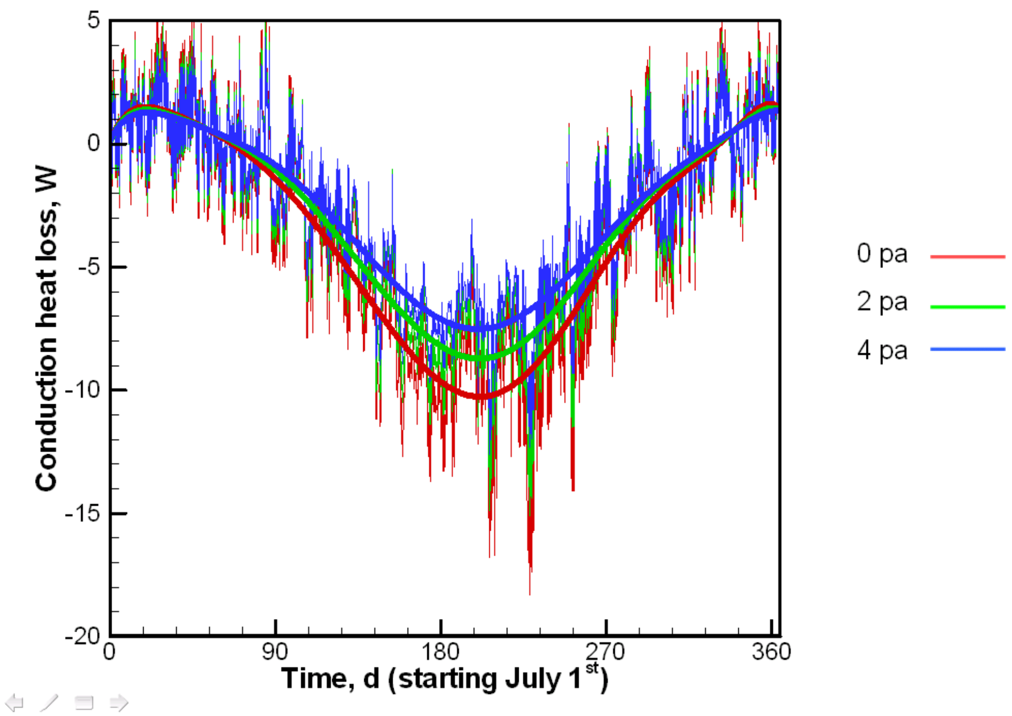

Figure 5-16. Conduction Heat Loss When There is 0, 2, 4 Pa Pressure Difference Across the Wall Assembly

With a 4 Pa pressure difference, the conduction heat losses were smallest because the heat transfer transported by air leakage was the dominant effect. Airflow rate of 0.7 m^3/h is equivalent to a U-value of 0.16 W/m^2K (RSI=6.17 m^2K/W) which equals to R=35 $ft^2 \cdot °F \cdot h/Btu$. In well insulated 2”x6” wall this amount of airflow increases the total heat loss approximately 40%. The relative increase depends on the thermal bridges in the structure; if the thermal resistance of the wall is low, the relative increase of heat losses caused by the airflow is low. For walls with high R-value, the relative increase becomes significant.

5.4. Steady State Simulations of Concrete Block Wall

5.4.1. Effects of Flow Rate on Moisture Accumulation Under Summer Conditions for Flow Path A

Steady state simulations with three respective air leakage rates of 3 $m^3/h\text{-}m^2$; 8 $m^3/h\text{-}m^2$; 12 $m^3/h\text{-}m^2$ were performed on the concrete block wall (Figure 5-17). It can be observed that the condensation of moisture occurring at Q=12 $m^3/h\text{-}m^2$ is much higher than in simulations performed with 3 $m^3/h\text{-}m^2$ and 8 $m^3/h\text{-}m^2$ air leakage rates. Moisture accumulation occurs near the indoor surface due to cooler indoor conditions. With the building at negative pressure (wrt outdoors), the warm and humid outdoor air travels through the open cores in the concrete blocks resulting in moisture condensation and accumulation on the interior surfaces of the concrete block cores. The CMU block wall is poorly insulated and conduction heat losses are much higher than for the steel frame wall. This makes the airflow effects on the temperature less pronounced for the concrete wall than for the steel frame wall

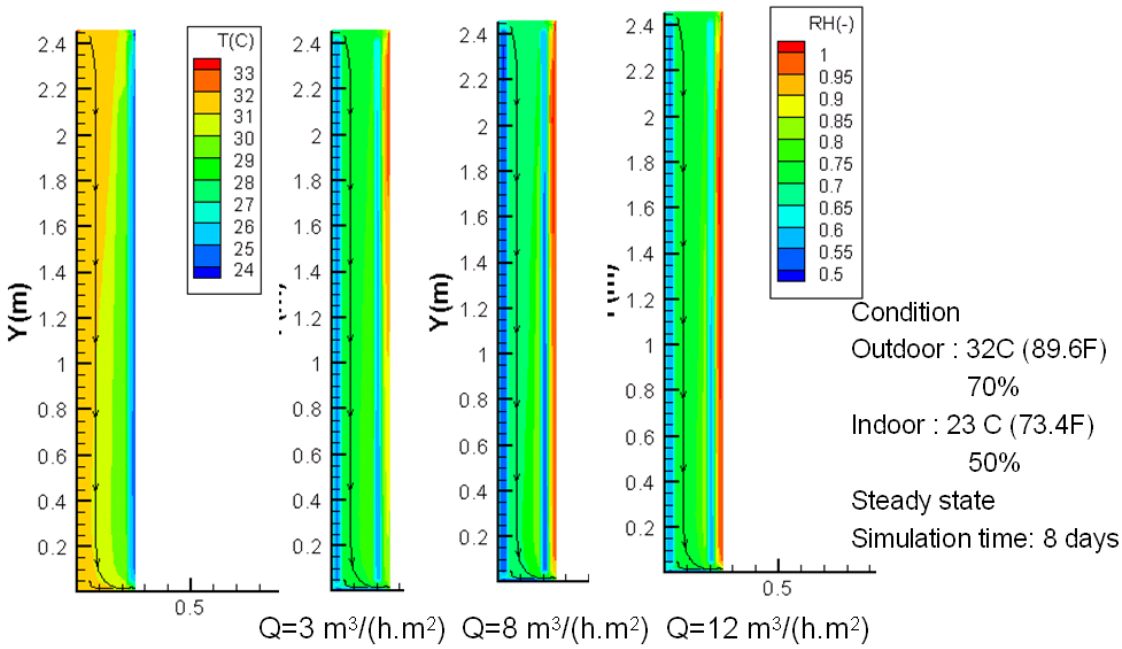

Figure 5-17. RH/T Contour of Concrete Wall in the Summer (Flow Path A)

5.4.2. Effects of Flow Rate on Moisture Accumulation Under Summer Conditions for Flow Path B

The case was repeated for the air flow path B configuration. The airflow rate for this case depends on the stack pressure between the CMU block cavity and outdoor air and the resulting airflow rate was therefore much smaller (~0.3 $m^3/h\text{-}m^2$) than in the flow through cases described above. The results indicate that there is no risk of condensation occurring inside the cavity. The relative humidity at top of the cavity, near the entry point of air leakage into the cavity reaches approximately 70% RH. Even for the short simulation period of 8 days it was observed that this condition remained seemingly constant. The airflow rate along the leakage path was naturally much smaller and the capacity of the concrete to store the moisture was large, so that there was not a rapid increase in relative humidity inside the wall. 'Wind washing' i.e. flow into and out of the wall may cause moisture accumulation in the wall in the long run but this type of air flow is likely less common than flow through the wall, except near corners and section around the building were wind can cause pressure differences on different sides of the façade.

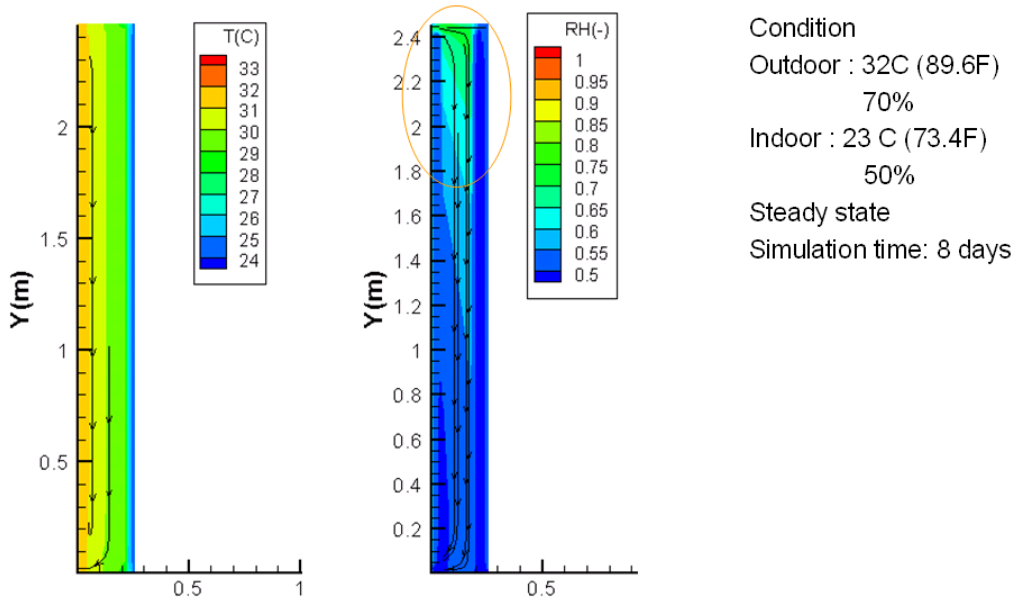

Figure 5-18. RH/T Contour of Concrete Wall in the Summer (Flow Path B)

5.4.3. Moisture Accumulation Under Summer Conditions with Air Impermeable Interior Layer (paint or vinyl)

Simulation was performed to examine the effect of a tight, highly-impermeable interior finish such as vinyl wall paper or paint. This time the simulation time was extended to 70 days to examine in more detail the effect if any of moisture accumulation

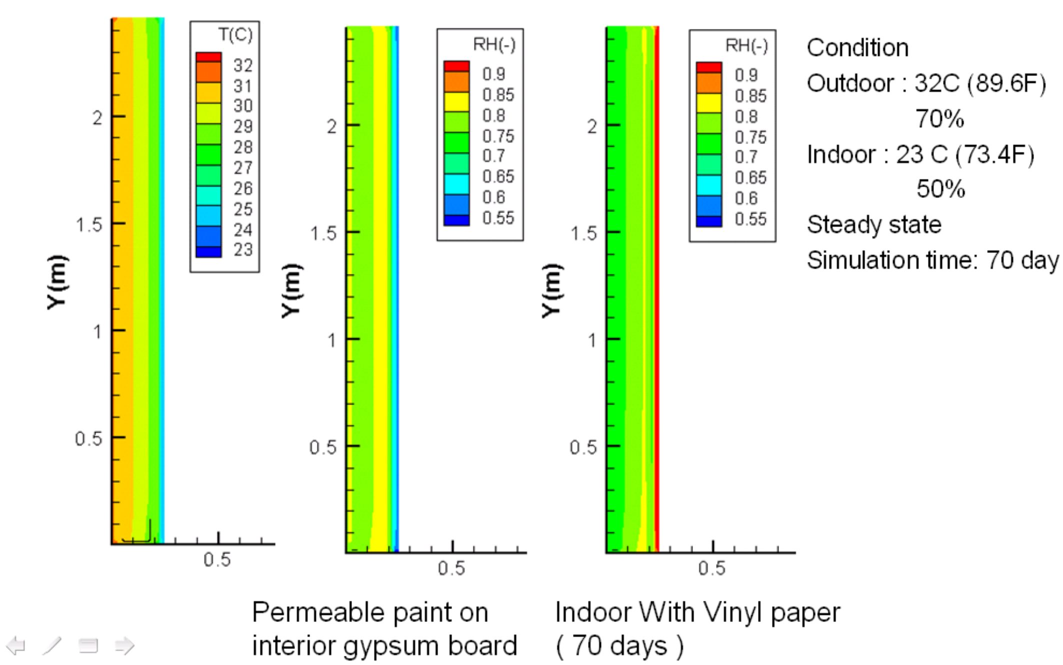

Figure 5-19. RH/T Contour of Different Indoor Surface Materials: Paint vs. Vinyl Paper

By simulating 70 days, it is obvious that most moisture accumulated near the vinyl paper surface. The vapor tight interior surface in hot and humid climate, which prevents inward drying, is often the reason why in practice a lot of mold growth has been found behind the wall paper.

5.5. Conclusions

The following conclusions may be drawn from the work presented in this report section:

- The significance of air leakage from wall assemblies and whole building is different. More leakage from the whole buildings does not necessarily mean more leakage from the wall assemblies per unit area. Larger buildings can have larger volume-to-surface area ratio meaning that smaller whole building leakage rate does not necessarily tell what air leakage the building envelope is exposed to.
- For steel frame structure, more condensation will occur at the place where the thermal bridge exists when the indoor air temperature is lower.
- Moisture accumulation in the wall assemblies has been simulated for several severe situations. For example, in the steel frame wall, the moisture tends to accumulate closer to the interior side of wall assemblies when the air leakage flow comes from outside in the summer. In the winter, the moisture intends to accumulate closer to the exterior side of wall assemblies. Too much cooling can cause severe moisture condensation problems on the interior side of the walls in hot and humid climates, especially when a vapor barrier is located on the cold side of the wall assembly
- The steel frame wall had a polyethylene vapor retarder and the wall was not very leaky. However, the air pressure differences across the wall resulted in significant effects inside the wall cavity.
- Under hot and humid summer conditions, walls with an impermeable interior surface such as vinyl wall paper but otherwise leakage can lead excessive moisture accumulation behind the interior surface material, resulting favorable conditions for mold growth.

5.6. References

Andrew Persily, (1999). “Airtightness of Commercial and Institutional Buildings: Blowing Holes in the Myth of Tight Buildings”, NIST.

Heinz R. Trechsel (2001) Moisture Analysis and Condensation Control in Building Envelopes, pp 179 ASTM MNL40.

Hens, H. & Janssens (1993). “A. Inquiry on HAMCAT CODES, International Energy Agency, Heat, Air and Moisture Transfer in Insulated Envelope Parts”, Report Annex 24, Task 1, Modeling, Karagiozis, A., (1997) "Moisture Engineer," 7th Conference on Building Science and Technology, pp 93-112.

Salonvaara, M and Karagiozis, A., (1999), Proceedings, Performance of Exterior Envelopes of Buildings, Thermal VII, pp 179-188.

Salonvaara, M. and Karagiozis, A., (1994) "Moisture Transport in Building Envelopes using Approximate Factorization Solution Method," CFD Society of Canada, Toronto, 1-3 June 1994

6. Whole Building Laboratory Testing

6.1. Introduction

This task was implemented by means of experiments carried out in FSEC's Building Science Laboratory (BSL). This lab was constructed in 1999 with the purpose of allowing the examination of building airflow issues (air flow, air pressure, airtightness) in a carefully controlled environment. Previous field survey work in Florida had identified the interactions between ceiling spaces and HVAC ductwork as one of the most significant sources of uncontrolled airflow in commercial buildings (Cummings et al 1996).

The objective of the whole building laboratory experiments has been to characterize the seasonal energy, peak demand, relative humidity (RH), and infiltration impacts of various levels of return and supply duct leakage with two ceiling space (attic) configurations – unvented attic with insulation on the ceiling tiles (hot and dry) and vented attic with insulation on the ceiling tiles (hot and humid).

The BSL is a fully instrumented building that includes various calibrated "leaks" (in the envelope, HVAC system, and ducts) that can be set to duplicate many conditions that have been observed in actual buildings. The facility allows for the characterization of the energy, demand, humidity, and ventilation impacts of duct leakage with various ceiling space configurations. Use of this unoccupied lab building allowed control over building systems, internal heat and moisture loads, building ventilation, and building occupancy parameters.

6.2. Experiment Overview

The experimental work performed at the BSL characterized the energy, humidity, and ventilation impacts of duct leakage as a function of two common ceiling space configurations:

- <u>Hot and dry configuration</u>. An unvented attic with insulation at the ceiling. Ceiling space environmental conditions will be "hot and dry. The building has a nearly flat roof with a dark exterior surface. Insulation (R19 batts) is located on top of the suspended T-bar ceiling.

- <u>Hot and humid configuration</u>. A vented attic space with insulation at the ceiling. Ceiling space environmental conditions will be "hot and humid" with dry bulb and dew point temperatures that will depend upon the outdoor conditions (including wind), the type and amount of duct leakage, and heat flux into the attic through the roof and through attic vents.

The focus was primarily on hot and humid weather conditions since these conditions are most prevalent in Florida. Data from all but the most hot/humid Florida days are similar to design conditions for New York State during peak summer conditions. Testing during portions of the fall, winter, and spring in Florida can be considered similar to "average" NY State summer conditions.

Table 6-1. Duct Leak and Ceiling Space Configurations for Completed Lab Experiments Showing Dates & Julian Day

Test	Attic	RL (%)	SL (%)	Periods of Data Collection (Red is 2004. Blue is 2005. Orange is 2006)					Total Days
1	Hot/dry	0	0	May 27-Jun 2 148-154	Jul 27-Aug 4 209-17	Jan 13-Mar 10 013-59, 063-70	Sep30-Oct31 274-296,300-303	Jun17-Jul 4 168-185	116
2	Hot/dry	15	0	Jun 26-Jul 6 178-188	Mar 24-31 084-91	Apr 29-May 10 119-130			31
3	Hot/dry	30	0	Jul 7-16 189-198	Mar 11-22 071-82	May 12- 21 132-141			32
4	Hot/dry	0	15	Jun 10-17 162-169	Aug 16-25 228-237	Nov 29 – Dec 8 333-342	Dec12-15 346-349		32
5	Hot/dry	0	30	Jun 3-9 155-161	Sep 7-16 250 - 259	Nov 11-27 315-331	Sep 14-Oct5 257-278		56
6	Hot/dry	15	15	Jun 18-25 170-177	Aug 27-Sep 6 239-249	Dec 17 – Jan 3 351-004	May 23-June 4 143-155		51
7	Hot/dry	30	30	Jul 17-26 199-208	May 11-26 132-134,139-147	Jan 5 – 18 004-018			37
8	Hot/dry	30*	30*	Jun25-July 176-185	Sep 17-30 260-273	Nov 1-9 305-313	Jan 18-Jan 30 018-030	Jun 6-15 157-166	56
9	Hot/humid	0	0	Aug 13-26 226-239	Nov 9-29 314-330,332-334	Apr 11-20 101-110	Aug 5-9 217-221		49
10	Hot/humid	15	0	Sep 30-Oct 9 274-283	Nov 30-Dec 9 335-337,341-344	Apr 21-May 1 111-121	July7-14 188-195		36
11	Hot/humid	30	0	Aug 27-Sep3 240-247	Dec 10- Jan 10 344, 345,5-10	Apr 5-10;May 2-5 095-100; 122-125	April 11-27 101-117		43
12	Hot/humid	0	15	Oct 23-Nov 8 297-313	Jan 11 – Mar 3 12-13, 48, 52-55	May 6-12 126-132	Aug 2-14 214-226		44
13	Hot/humid	0	30	Aug 10-12 223-225	Sep 11-15 255-259	March 21-27 080-86	Mar 22-April 9 081-099		34
14	Hot/humid	15	15	Oct 10-22 284-296	Mar 4-17 66-67, 73-75	July16-24 197-205	Mar 11- Mar 21 070-080		38
15	Hot/humid	30	30	Sep 16-24 260-268	Mar 28-Apr 4 087-094	Feb 23-Mar 9 054-068	July 6-23 187-204		50
16	Hot/humid	30*	30*	May 14-22 134-142	Jun10-12, 21-23 161-163,172-174	Jan 31–Feb 21 031-052	July 25-Aug 3 206-215		47

Notes:
* - These duct leak experiments differ from other configurations in that the return and supply leaks are located in close proximity (<8 feet), whereas other configurations will have the return leak and supply separated by substantial distance (>25 feet).
"Total # Days" are good days based on weather, data quality, systems operational, etc.

A variety of duct leakage configurations (both the supply and return leaks) were tested with the two indicated ceiling space configurations. In total, 16 duct leak configurations were tested. The duct leak/ceiling space configurations implemented are shown in Table 6-1. Approximately 30 to 50 days of data was collected for each experimental configuration, or about twice as much as indicated in the contract statement of work.

6.2.1. Lab Building Preparation

Instrumentation was installed to characterize the temperature and humidity of the occupied space, the ceiling space, and outdoors. Other data points were collected as well. Table 6-2 contains a listing of temperature and humidity sensors. Figure 6-1 and Figure 6-2 show the location of these sensors in the building, in the occupied space and also in the ceiling space that houses the air distribution system.

Table 6-2. Number and Location of Temperature and RH Measurement Probes in the BSL

Location	Temperature	Relative Humidity
Main room	4	4
Mechanical room	1	1
SW room	1	1
Storage room	1	1
Rest room	1	1
NE room	1	1
Ceiling space (main)	6	6
Ceiling space (east zone)	2	2
Entering air handler	2	2
Leaving air handler	2	2

In addition to the data points of Table 6-2, the following parameters were monitored.

- Heat pump energy use
- Air flow rate in the main supply
- Condensate measurement (redundant with a tipping bucket and positive displacement pump in series)
- Pressure in the occupied space with respect to outdoors
- Pressure drop across the ceiling

The weather station at FSEC also measured outdoor temperature, dew point, solar radiation (global horizontal), wind speed, and wind direction. In total, 72 channels of data were collected for over 2 years at 15-minute time steps.

6.2.2. Calibration of Instrumentation

Temperatures were measured by means of T-type thermocouples. Relative humidity was measured by means of Energy Conservatory RH probes and Vaisala RH probes. They were calibrated in the following manner. The thermocouples were grouped together in an insulated cooler and evaluated at temperatures ranging from 75^{o}F to 87^{o}F. All thermocouples agreed to within +/- 0.1 degree F. A General Eastern Hygro M4 was used as a reference for the lab sensor calibration. The M4 measures drybulb temperature using a thermocouple and dew point temperature using a chilled mirror. Based on these two measurements, relative humidity is calculated. The M4 was taken around to areas (such as into the ceiling space) where temperature and RH sensors were located for a comparison under the typical conditions that the sensors would be measuring. The Energy Conservatory RH sensors agreed within the manufacture specification of +/-3% and the Vaisala RH sensor agreed within +/-2%.

Condensate was measured by means of a Texas Electronics, Inc. Tipping Bucket and a Fluid Metering Inc. Model QV100 Positive Displacement pump. They were calibrated in the following manner. Water was pumped using the displacement pump into a container on a Mettler PJ 3000 electronic mass scale with a resolution to 0.01 grams. The mass pumped was used with the pump pulse output to calibrate the water flow in grams per pulse. The displacement pump measurements agreed to within 0.7% difference on average. A graduated cylinder was used to pour water into the tipping bucket at rates similar to that expected from condensate drain-off. The tipping bucket was calibrated using the total number of tips for a given mass flow. Several trials were conducted for each measurement device. During the experiments, tipping bucket and positive displacement pump were placed in series allowing their measurements to be compared.

6.2.3. Lab Building Setup

The lab building has both a 3.5-ton heat pump and a 5.0-ton heat pump. It was determined that the 2000 square foot lab building could be cooled using only the 3.5 ton unit, in the absence of uncontrolled air flows. However, when various duct leaks are added, especially with the attic space vented, the building cooling load would increase significantly (the amount of increase is actually one of the primary experimental objectives). Our best estimate was that the 5-ton system would be sufficient to meet the building plus UAF-induced cooling loads. Therefore, it was determined that we should use the five-ton cooling system for these experiments. In fact, peak cooling loads matched but did not exceed the capacity of the 5-ton system. As it turned out, the 5-ton capacity was just sufficient to meet the cooling load on the hottest days with the most extreme test configurations (e.g., 30% supply and 30% return leaks with vented attic).

During periods with less duct leakage, the AC system would be considerably oversized. In order to reduce the potential impacts related to over sizing of the cooling system (during periods with smaller duct leak configurations), a Honeywell PC8900 thermostat was installed. It has the capability to adjust the maximum number of cycles per hour (Nmax). We set the thermostat cycle rate to 2 cycles per hour (at 50% load factor). The reason this is important is that oversized equipment tends to produce shorter "on" cycles. Reducing the cycling rate will tend to counteract this by lengthening the "on" periods and therefore more provide effective dehumidification. For example, under 50% load factor, Nmax=3 will produce "on" and "off" cycles of 10 minutes, while using Nmax=2 produces "on" and "off" cycles of 15 minutes. Since a cooling system does not reach steady state performance until 3 to 5 minutes after start-up, the longer cycle will provide more consistent dehumidification performance at part load conditions.

A 77°F thermostat setting was used throughout the year, which produced an average 75.0°F in the building. No experiments were specifically designed for the heating season. In Central Florida, the heating season is rather short (~700 HDD), and intermittent, and therefore it was determined that attempting to obtain heating season effects from UAF would be difficult and uncertain. The cooling experiments continued, therefore, throughout the entire year. During periods when heating was required, the building was typically heated to 72°F. The primary purpose for our providing this heating was to keep the building from become overly cold, so that when the weather warmed up and cooling was again required (usually several days later), the amount of negative cooling load stored in the building mass would be limited. Even with this implemented, cooling loads for one or two days following cold periods were significantly reduced because of the stored "coldness" in the building walls, floors, etc. Stored heat or cold in the building mass, carrying over from one day to the next, is one of a significant source of variability in daily cooling energy.

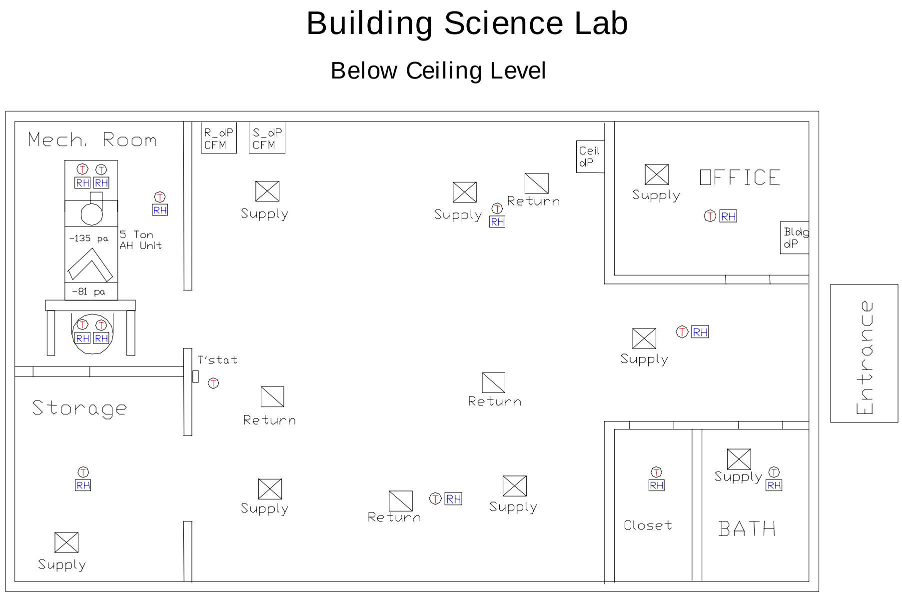

Figure 6-1. **Floor Plan of Building Science Lab Building Showing Sensor Locations**

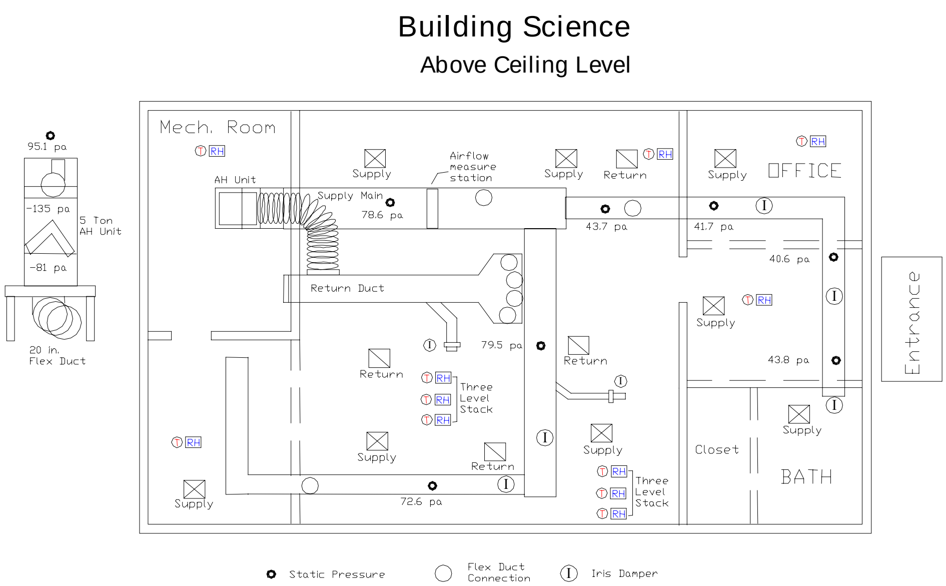

Figure 6-2. Floor Plan of the Attic of the Building Science Lab Building Showing Sensor Locations

Sensible and latent internal loads that would be typical of a small office environment were installed. The sensible load (2000 W to represent 5 people and office equipment) was implemented by means of an electric space heater and hot plate. Three banks of lights were also used to provide typical sensible loads. Including the lights, the total internal sensible load was 3080 W.

The latent load was implemented by the following means. Condensate collected from the air conditioner was pumped into a 15-gallon reservoir. Water from this reservoir was delivered by means of another positive displacement pump to an evaporation surface that was heated by the hot plate. The internal latent load was 799.1 Btu/hour (345.2 grams per hour). All sensible and latent loads, including lighting, were controlled by the same Campbell datalogger that collected data from 70+ sensors and meters, turning these loads on at 7:30 AM and turning them off at 5:10 PM (EST). Every day had the same schedule, treating the building occupancy schedule as if there were no weekends or holidays.

The air handler is located in a mechanical room that previously had acted as a return plenum. Ducted return air was installed for these experiments. Intentional duct leaks of 15% and 30% were created on both the return and supply sides of the air distribution system. The leaks were created by inserting duct sections into the main return and supply ducts. These inserted duct sections were then open to the attic space. In effect, these duct leaks were like having a return duct drawing from the attic and a supply duct delivering air to the attic. The return leak was located about 20 feet from the supply leak (except for Test Configurations 8 and 16). However, since the supply leak air was being discharged with considerable velocity away from the return leak location, the effective distance between return and supply was more like 30 feet. For Test Configurations 8 and 16, the supply leak was relocated to about 8 feet from the return leak, and the direction of supply leak air discharge was generally toward the return leak location. The purpose of these latter two configurations was to identify the magnitude of “regain”, a topic of some interest in ASHRAE Standard 152.

In order to allow calibration of the duct leakage flow rates, and to allow repeated flipping back and forth between various duct leakage amounts, iris dampers (with precision control) were installed in the return and supply leak ducts. Calibration of the duct leaks was based on a TSI Wind Tunnel. Interior doors were kept open, with the exception of doors to the bathroom and a storage closet.

No outdoor ventilation air was provided to this building. Instead, all fresh air was introduced into the building passively via infiltration. We believe this scenario is most representative of a typical 2,000 square foot office building. Of the 70 small commercial buildings that we tested in Florida during a 1993-1996 study, only 26 had outdoor air directly provided through the HVAC system. The remaining 44 (or 63%) provided ventilation air only by means of infiltration. Therefore, we concluded that our base building be representative of actual practice, instead of less-commonly-implemented ventilation code requirements.

Furthermore, we concluded that introducing ventilation air into the BSL would also create several practical and experimental difficulties that would take away from the main focus of the test, which was to quantify the impact of duct leakage on energy use and IAQ.

1. When duct leaks are added to the building, indoor humidity will increase (with the vented ceiling space). Addition of ventilation air in a building with a fully ventilated attic would create even higher indoor humidity, and this elevated humidity could lead to mold damage in our lab building. Addition of 100 cfm of ventilation air (equivalent to an office space with 5 people) would add about 2/3 of one ton of cooling load to this building. Given that the lab building had a 5.0-ton split system air conditioner available for these experiments, the addition of the OA would likely push the total cooling load beyond 5.0 tons. This would have forced us to discard data from some of the hottest days when space conditions could not be maintained.
2. To obtain predictable ventilation through the AC unit requires continuous fan operation. With DX systems, continuous fan operation greatly compromises the dehumidification performance of the system due to off-cycle moisture evaporation from the coil. This would increase space humidity levels at lower runtime fractions and confound the testing.

6.2.4. Tested Characteristics of the Lab Building

Blower Door Testing

Blower door tests were performed to characterize the airtightness of the building envelope. Ten standard multi-point blower door tests were performed. Leakage of the entire building envelope was measured with vented ceiling space and unvented ceiling space, and with various duct leak test configurations (Table 6-3).

Only 10 of the 16 experimental configurations were tested, three with unvented attic and seven with vented attic.

Unvented Attic. Only three tests were done with the attic unvented because it was clear, after three tests, that addition of duct leaks caused almost no change in building envelope airtighness. Because the ductwork is located completely within the air boundary of the building envelope (with unvented attic), CFM50 increased only 3% with the addition of large duct leaks (Test Configuration 7). The primary air boundary was also identified. With the conditioned space at –50 Pa (wrt outdoors), pressure drop across the ceiling was only 0.9 Pa, meaning that the pressure in the attic was –49.1 Pa wrt outdoors. This also means that the primary air boundary of the building was the roof deck and exterior walls above the ceiling.

V*ented Attic*. Seven of the 8 test configurations were tested. With twenty-three 8”x 16” attic vents open, the leakage of the building envelope increased by a factor of 5.5 to 8224 CFM50 (Configuration 9). This is consistent with the fact that suspended T-bar ceilings are very leaky. Previous testing had found that suspended T-bar ceilings have leakage of about 5 CFM50 per square foot. (Note that the T-bar ceiling in this building consists of 2’ x 4’ ceiling tiles.) Therefore, if the attic were wide open to outdoors (no roof, for example), then the building leakage would be about 10,300 CFM50 (9500 CFM50 in the ceiling and about 800 CFM50 in the building below the ceiling level).

Table 6-3. Blower Door Test Results for Various Duct Leak and Attic Configurations

Test Configuration		Pressure drop across ceiling with occupied space @50 Pa wrt out	CFM50	ACH50
1	0% RL, 0% SL; unvented attic	0.9	1501	5.1
5	30% RL, 0% SL, unvented attic	0.8	1541	5.2
7	30% RL, 30% SL, unvented attic	0.7	1548	5.2
9	0% RL, 0% SL; vented attic	40.4	8224	27.8
10	15% RL, 0% SL, vented attic	38.4	8323	28.2
11	30% RL, 0% SL, vented attic	39.6	8688	29.4
12	0% RL, 15% SL, vented attic	40.5	8497	28.8
13	0% RL, 30% SL, vented attic	39.9	8666	29.3
14	15% RL, 15% SL, vented attic	38.4	8671	29.3
15	30% RL, 30% SL, vented attic	38.3	8948	30.3

TEST 1 airtightness equation: $Q = 141.9\ (dP)^{0.60}$
TEST 9 airtightness equation: $Q = 841.2\ (dP)^{0.58}$

Addition of duct leak openings caused substantial increase in the building envelope leakage when the attic was vented. Building CFM50 increased 8.8% (from 8224 to 8948) with the addition of the 30% return and 30% supply duct leaks (Test Configuration 15). With the conditioned space depressurized to –50 Pa (wrt outdoors), pressure drop across the ceiling ranged from 38.4 Pa to 40.5 Pa for the seven tested configurations. When the pressure in the occupied space was at –50 Pa wrt outdoors, pressure in the attic was at about –11 Pa wrt outdoors. Because the greatest pressure drop was across the suspended T-bar ceiling, the primary air boundary of the building was therefore the ceiling. For the vented attic tests, the ductwork and the duct leaks are located outside the primary air boundary of the building. For the unvented attic tests, the ductwork and the duct leaks are located inside the primary air boundary of the building, thereby allowing much greater regain of energy lost from duct leakage.

When a suspended T-bar ceiling, with leakage of 5 CFM50 per square foot is the “primary air boundary”, then the building has, in effect, no air barrier. The Florida Building Code, for example, requires that the ceiling plane of a building have leakage no greater than 0.5 CFM25 per square foot, and it specifically disallows use of a suspended T-bar ceiling as the air barrier between the conditioned space and outdoors.

Three additional blower door tests were done to disaggregate the leakage for the conditioned space, the unvented attic, and the vented attic. Blower door fans were set up in two locations, an exterior doorway in the occupied space and an exterior doorway located above the ceiling (most buildings don’t have an exterior doorway in the attic). The test was carried out in the following manner. The occupied space and the attic space were simultaneously taken to –50 Pa (all pressures in this discussion are to outdoors, unless otherwise stated) so that the pressure across the ceiling was measured as 0.0 Pa. The airflows through the respective blower doors were then equal to the CFM50 leakage (to outdoors) for each space. Table 6-4 presents the leakage characteristics of the occupied space and the attic space.

Table 6-4. Building and Attic Airtightness (leakage) with Respect to Outdoors

	CFM50	Airflow Coefficient C	Airflow Exponent n	Correlation Coefficient r
Conditioned space (excluding ceiling)	805	99.27	0.54	0.9996
Unvented attic (excluding ceiling)	831	55.25	0.69	0.9906
Vented attic (excluding ceiling)	20,230	2704	0.51	0.9695

While CFM50 is an airflow rate measured at the specified pressure of 50 Pa, it is more accurate to think of it as the equivalent cumulative hole size when all leaks in the envelope are added together. There is a rule of thumb used to convert CFM50 to square inches of equivalent hole area; divide CFM50 by 8 to get square inches. Alternatively, one can use equation 2-5 to calculate ELA (see Section 2). Therefore, for the attic space, the equivalent hole size is about 2529 square inches, or 17.6 square feet. Note that the gross area of the twenty-three 8" x 16" openings is 20.9 square feet (careful measurements found gross opening area of 131.0 square inches per vent). To account for the free area of the insect screen used in the attic vents, a sample piece of screen was measured to the tenth millimeter and found 74% net free area fraction. It was observed that the aluminum screen fibers do vary in distance between each other (much more so than nylon type screens) in any given section making an accurate assessment more difficult. Based on 74% free area, the net vent openings would be 15.5 square feet. Since there are about 100 square inches of leakage in the non-vent areas of the attic, the equivalent hole size of the 23 vent openings predicted by the blower door test is 16.9 square feet, or 9% greater than the measured net vent opening area. Simply using the blower door tests of the vented and unvented measurements, the acting free area of the screens may be as much as 81%. This is calculated as follows: 20,230 – 831 = 19,399 CFM50 vent leakage in attic (19,399 CFM50/ 8 = 2424.9 sq. in. (16.8 square feet); 16.8/20.9 =80.6%).

Duct System Airtightness

Prior to beginning these experiments, inspection and airtightening of the duct system was performed. The objective was to achieve essentially airtight ducts. Duct airtightness tests were performed. The duct system was physically split between the supply and return side by sealing off the top of the air handler where the supply duct connects. Two duct-test fans (Duct Blasters) were installed, one on each side of the system (return and supply), and all registers/grills were carefully sealed off. Both test fans were operated at the same time to maintain equal test pressures during the test with nine points measured to create a multi-point generated best-fit calculation of duct tightness on each side. With no intentional duct leaks in place, we found $Q_{25,total}$ to be 36 cfm on the return side and 31 cfm on the supply side of the system.

Table 6-5. Duct System Airtightness Test Results: Combined Leakage to Outdoors and Indoors

	$Q_{25,total}$	Airflow Coefficient C	Airflow Exponent n	Correlation Coefficient r
Return	36	4.27	0.66	0.9985
Supply	31	3.79	0.65	0.9992

These results indicate that this system is tight enough to be considered "substantially airtight" according to IECC residential standards. This designation does not, of course, guarantee that there is no significant leakage particularly if the test leakage is concentrated in areas of highest pressure. It is expected that the leakage measured is distributed at various locations throughout the system and not concentrated at high-pressure locations. The areas of highest pressure around the air handler were sealed using tape and putty, and remained sealed throughout the 2+ years of experiments. Tracer gas testing allowed us to determine that the return side leakage was 3% of system airflow.

Unexpected Duct Failure

During the winter/spring of 2004, an unexpected duct leak occurred. This leak was discovered on May 10, 2004. A hissing/flapping noise was detected in the attic space, near a flex duct that had been installed in November 2003. Upon inspection, we found the interior liner of a 10" round flex return duct had fallen apart, and as a result, considerable return leakage was occurring. The leak was repaired before testing could be performed to determine the size of the leakage. However, by examining temperature data collected from December 2003 through May 10, 2004 at the return grilles (as represented by three room air temperatures about 3 feet below the ceiling) versus temperatures in the main return duct about 8 feet from the air handler, we were able to determine that the return leakage was about 10% of system air flow.

Examination of the leak site found that a portion of the inner liner equal to about 1.5 square feet of area had separated into individual strips. The nature of this failure can be understood by understanding how these flex ducts are fabricated. Strips of plastic are overlapped, one upon the other, and onto the metal coil that gives structure to the flex duct. A combination of adhesives and/or heat is applied to cause the overlapped plastic strips to adhere and form a presumably airtight seal. We have now observed, in at least three different situations, that the adhesive has failed on flex ductwork, causing significant leakage. This seems, in part, to be precipitated in vertical installations over six feet when a flex duct turns about 90 degrees downward and the weight of the duct pulls on the inner liner. SMACNA Standards for duct support were known at the time of installation, however there is a practical difficulty in supporting vertical flexible ducts. There must be enough force upward without having the support around the duct causing significant constriction in the insulation or air duct.

We were aware of this problem (in general) based on an experience earlier in this project. We had installed a 20-inch flex duct (at the beginning of the project) to run about 25 feet from the attic return to the air handler. One day (before the experiments were under way) we found that the 20-inch duct had shrunk in, like a narrow waistline. Upon disassembly, we found that the inner liner had disintegrated in a several foot section of this duct. The negative pressure that was supposed to be contained inside the inner liner of the duct had spilled outward into the outer jacket. Subsequently, we replaced this failed section of flex by ductboard duct.

The more difficult task was to determine when the leak occurred, so that we could determine the amount of experimental data that would have to be discarded. We had carefully sealed all joints and connections in the entire duct system in the fall of 2003, and tested the entire duct system at the same time. Subsequently, we installed the 6-foot long section of 12-inch flex duct that later failed. Considerable effort was put into trying to determine when the leakage failure initiated. We examined room and return duct temperatures all the way back into December 2003 when the experiments began in order to determine when the leakage occurred. By examining the rise in air temperature from the return grills to where it enters the air handler, and simultaneously knowing the attic air temperature (approximating where the return leak was occurring), we could identify a change in the mix of air streams in the return ductwork.

A major problem with this examination was the comparability of the room air temperature (representing the return grills) with the return duct temperatures. The return duct temperatures are recorded only when the air handler is operating, so that cooling system output could be calculated. The room temperatures are recorded during the entire 15-minute period. Because of this difference, this analysis could only be performed on data when the air handler was running for the entire 15-minute period. Back in February, March, and much of April, the system rarely ran for the full 15-minute period. Consequently, there are relatively few 15-minute periods when this analysis can be performed to assess return leakage amount. We were able to determine that the leak in this duct did not occur before March 24. We also had clear evidence that the duct failure had occurred by April 15. As a consequence, we had to discard all of our experimental data for the period March 24 through May 10.

Infiltration Testing

An important task of this project was to understand the infiltration impacts of duct leakage with vented and unvented attic. Tracer gas decay testing was used to characterize these infiltration impacts. Tests were done for a variety of wind speeds, and with and without the air handler operating. Tests were performed during December 2004 and January/February 2005. A total of 110 hours of tracer gas decay tests were performed. Outdoor temperatures were moderately cool, generally in the range of 60^{o}F to 80^{o}F. Wind speed and direction are indicated in the table.

Infiltration with Attic Vents Open

Wind speed has significant effect upon the infiltration rate, especially for the vented attic. Testing was repeated for some duct leak configurations during different wind speeds to better understand wind impacts upon ventilation. The best example occurs for the five tracer gas decay tests for the 30% supply leak. In Table 6-6, a clear pattern of increasing infiltration with increasing wind speed can be observed. For tests with wind speed of 8 mph and above, infiltration averaged 1.31 ach. For tests with wind speed of 4 mph and lower, infiltration averaged 0.94 ach. The primary influence of the wind speed is the rate of entry of attic ventilation air. With 23 vents open, air can flow fairly readily through the attic space. The supply leak has the effect of taking air from the conditioned space and delivering it into the attic space. Simultaneously, depressurization of the conditioned space (as a result of the supply leakage) draws air from the attic into the conditioned space. As wind speeds increase, the attic venting increases, carrying away a larger portion of the supply air that spilled into the attic space. Under light winds, more of the spilled supply air can be "re-captured" by being drawn through the ceiling into the conditioned space. With stronger winds, less of the spilled supply air can be "re-captured" by being drawn through the ceiling into the conditioned space.

Table 6-6. Air Infiltration Rate for Various Duct Leakage Configurations with Vented Attic

Description	Test Configuration	Average wind speed (mph)	Avg. wind direction	Air changes per hour
15% Return leak	10	10.8	NNW	1.24
30% Return leak	11	7.6	NNW	1.71
30% Return leak	11	7.3	ESE	1.55
30% Return leak	11	7.4	ESE	1.51
30% Return leak	11	7.2	SE	1.59
Average		7.4		1.59
15% Supply leak	12	6.9	NW	1.08
15% Supply leak	12	10.4	SE	1.14
Average				1.11
30% Supply leak	13	8.5	ESE	1.21
30% Supply leak	13	3.7	ESE	1.05
30% Supply leak	13	2.2	N	0.83
30% Supply leak	13	9.7	SE	1.42
30% Supply leak	13	5.5	N	1.26
Average		5.9		1.15
15% Supply, 15% Return leak	14	9.8	N	1.26
30% Supply, 30% Return leak	15	6.7	NNW	1.54
AVERAGE (all)				1.31

Return leaks produce higher infiltration rates than supply leaks. This can be observed by comparing 30% return leaks to 30% supply leaks. This is most accurately assessed by comparing tests with comparable wind speeds. If we compared, for example, the four 30% return leak tests (average 7.4 mph) to the three 30% supply leak tests with the higher wind speeds (average 7.9 mph), we find that the return leaks generate 1.59 ach while the supply leaks generate 1.20 ach. Return leaks appear to generate infiltration about 33% higher than supply leaks. The attic space can be thought of as having a mixture of unconditioned and conditioned air. In the case of a vented attic it will mostly be made up of unconditioned air. As duct leakage increases, the percentage of conditioned air in the attic will also modestly increase in the absence of wind effects. The infiltration rate of unconditioned air related to duct leakage is then minimized if leakage causes some of the "conditioned air" in the attic to be recaptured. The reason for this, as mentioned earlier, may relate to how the duct leakage transports air from the attic to the conditioned space.

- In the case of the return leak, the occupied space is under positive pressure. This pressure pushes air from the conditioned space into the attic through the leaky suspended T-bar ceiling. This air, being cooler and denser than the attic air will tend to pool at the floor of the attic. The return leak draws attic air from a location that is about four feet above the ceiling and about 2.5 feet below the roof deck, well away from where the conditioned space air is welling up into the attic space thereby having a smaller percentage of conditioned air that can be recaptured.
- In the case of the supply leak, the occupied space is under negative pressure. The supply air that spills into the attic, being cooler and denser than the attic air tends to fall (from its discharge location about 3 feet above the attic floor) toward the floor of the attic. From that location on the floor of the attic, significant portions of that spilled supply air is drawn into the conditioned space.

Wind direction also appears to have some impact on the infiltration rate. Looking at the four cases of 30% return leak (Table 6-6), for example, the infiltration rate is substantially higher for the case with wind from the NNW. Examination of Table 6-7 (which has the infiltration test results sorted by wind direction) also suggests some wind direction dependence. The cause of this possible wind-direction dependence is not known.

Table 6-7. Air Infiltration Rate for Vented Attic Space (sorted by wind direction)

Test Configuration	Description	Average wind speed (mph)	Avg. wind direction	Air Changes per Hour
11	30% Return leak	7.6	NNW	1.71
15	30% Supply, 30% Return leak	6.7	NNW	1.54
10	15% Return leak	10.8	NNW	1.24
12	15% Supply leak	6.9	NW	1.08
14	15% Supply, 15% Return leak	9.8	N	1.26
13	30% Supply leak	5.5	N	1.26
13	30% Supply leak	2.2	N	0.83
15	30% Supply, 30% Return leak	2.6	E	0.68
11	30% Return leak	7.3	ESE	1.55
11	30% Return leak	7.4	ESE	1.51
13	30% Supply leak	8.5	ESE	1.21
13	30% Supply leak	3.7	ESE	1.05
11	30% Return leak	7.2	SE	1.59
13	30% Supply leak	9.7	SE	1.42
12	15% Supply leak	10.4	SE	1.14
	AVERAGE (all)			1.31

Natural Infiltration

Natural infiltration, which is air exchange between indoors and outdoors that is driven by the natural forces of wind and temperature difference (no HVAC fans operating), was measured with vented attic (Table 6-8). Four different tests were performed with wind that varied from 5.8 to 10.4 mph. In each case, the duct leaks were sealed (Test Configuration 9). There is relatively little relationship between wind speed and infiltration rate. Natural infiltration rates average 0.50 ach, and range from 0.45 to 0.59 ach. In previous research, a relationship between building airtightness (ACH50) and natural infiltration has been established; dividing ACH50 by 38 yields an approximation of natural infiltration. In this case, the building ACH50 is 27.8, so the predicted natural infiltration rate would be 0.70. We conclude that the natural infiltration rate is lower, for this configuration of building (nearly all leaks at the top), than the "divide by 40" method would indicate. An explanation for the difference between measured and expected (based on the "divide by 40" rule) is that the leakage of this building is predominantly at the top of the building. In fact, 90.2% of the total leakage is in the ceiling plane [(8224 – 805) / 8224, see Tables 6-3 and 6-4]. With so much of the leakage concentrated in one portion of the envelope, there is a lack of "complimentary" holes for air to flow in one side and out the other, much like a coke bottle without the cap.

Table 6-8. Natural Infiltration Rate (AH OFF) with Attic Vents Open

Test Configuration	Description	Average wind speed (mph)	Avg. wind direction	Air Changes per Hour
9	0% duct leak	10.4	NNW	0.59
9	0% duct leak	6.4	ESE	0.48
9	0% duct leak	7	ESE	0.45
9	0% duct leak	5.8	SE	0.50
Average				0.50

Infiltration with Attic Vents Sealed

When the attic vents are sealed, building ventilation rates drop precipitously, from an average of 1.31 ach for all tests with vented attic to 0.15 ach for all tests with unvented attic. Overall, infiltration is 8 times less. Furthermore, infiltration is no longer a function of duct leakage. Air leakage into or out of the ductwork makes almost no difference in the building ventilation rate because all of the air leakage and air exchange between zones is occurring inside the primary air boundary of the building. Note, for example, that the infiltration rate for Test Configuration 1 (no duct leaks) is essentially the same (0.14 ach) as for the other tests.

For the unvented attic, the building ACH50 is 5.1, so the predicted natural infiltration rate would be 0.13, or very nearly identical to the average measured infiltration of 0.15 ach.

Table 6-9. Air Change Rate When Attic Vents are Closed

Test Configuration	Description	Average wind speed (mph)	Avg. wind direction	Air Changes per Hour
5	30% Supply leak	6.7	NNW	0.24
1	0% duct leak	4.9	NNW	0.14
1	0% duct leak; NATURAL	3.4	NW	0.11
3	30% Return leak	3.2	N	0.12
7	30% Supply, 30% Return leak	6.2	NNE	0.19
7	30% Supply, 30% Return leak	5	NNE	0.14
7	30% Supply, 30% Return leak	3	ENE	0.15
	AVERAGE			0.15

6.3. Experimental Results

6.3.1. Three Types of Analysis

Analysis consisted of examining cooling energy use, creation of 24 hour AC energy demand profiles, and profiles of indoor and attic RH levels for the various experimental configurations.

Energy Use. Plots of cooling energy versus delta-temperature (outdoors minus indoors) with corresponding correlation coefficients have been developed. For each experiment, 30 to 45 days of data was obtained. After screening for problems related to weather (several hurricanes), sensor problems, and power outages, the average number of days of “clean” data was 21 per experiment. In order to obtain a wider range of delta-temperature (out minus in), we performed “flip-flop” testing, with most experiments run during representative periods of fall, winter, spring, and summer. Using this approach, we were able to obtain a reasonably wide range of daily delta-T values and therefore have enough data variation so that the coefficient of determination (r^2) for the best-fit line is reasonably high (average $r^2 = 0.92$).

Most of the normalization of the energy use to weather was implemented through the temperature differential discussed above. Some additional normalization to solar radiation levels and outdoor dew point temperatures were also implemented.

Demand and Temperature Profiles. In addition to the cooling energy versus delta-temperature analysis (described above), plots of 24-hour profiles of cooling energy (MBtu/h) and zone temperatures were developed. These profiles are typically a composite from 3 or more days of data. Cooling energy for each configuration has been normalized (between experiments) to the weather variables of temperature, solar radiation, and dew point temperature. In some cases, it was not possible to obtain comparability for all three variables.

RH Profiles. 24-hour profiles of indoor RH have been created for representative test configurations. The plots of RH show significant changes in indoor RH as a result of the amount of duct leakage, and even more as a result of whether the attic space is vented or not.

Appendix B contains plots of energy use, demand profiles, and temperature/RH profiles.

6.3.2. Energy Impacts of Duct Leakage

The experiments were divided into 16 configurations, with various levels of duct leakage and unvented and vented attic spaces. (Note that the space above the ceiling is more correctly referred to as a ceiling space, not an attic. However, for convenience of discussion and to minimize plot title lengths, the words “attic” and “ceiling space” will be used interchangeably.) Configurations 1 – 8 had an unvented attic. Configurations 9 – 16 had a vented attic.

Cooling energy use for the sixteen test configurations is summarized in Table 6-10. More accurately, this is the daily cooling energy (both sensible and latent; MBtu/h) delivered by the air handler into the supply plenum. The daily cooling energy use is calculated based on the real-time measured mass-flow rate of the supply air stream, the delta-temperature from return to supply, and the measured AC condensate (positive displacement pump output). From 13 to 43 days of “clean” data has been collected for each experiment. Best-fit regression equations were then developed. Cooling energy use (QC) was calculated at dT = 5^{o}F (outdoor temperature minus indoor temperature, or 81^{o}F outdoor temperature).

Table 6-10. Weather-Normalized Energy Use (assuming outdoor temperature is 5^{o}F warmer than indoors)

					Best-Fit Equation: QC = Constant + Coeff x dT						
Test #	**Attic Status**	**Attic Condition**	**RL**	**SL**	**Constant**	**Coeff**	**r^2**	**Cooling Energy (QC) for dT=5^{o}F (MBtu/d)**	**% Increase vs. Tests #1 & #9**	**% Increase vs. Test #1**	**% Increase Tests #9 vs. #1, #10 vs. #2, etc.**
1	unvented	hot/dry	0	0	235.2	25.52	0.7491	362.8	---	---	---
2	unvented	hot/dry	15%	0	243.5	29.07	0.8483	388.9	7.2%	7.2%	---
3	unvented	hot/dry	30%	0	282.2	25.17	0.9522	408.1	12.5%	12.5%	---
4	unvented	hot/dry	0	15%	320.6	24.86	0.8738	444.9	22.6%	22.6%	---
5	unvented	hot/dry	0	30%	339.7	29.43	0.8286	486.9	34.2%	34.2%	---
6	unvented	hot/dry	15%	15%	317.4	24.76	0.8874	441.2	21.6%	21.6%	---
7	unvented	hot/dry	30%	30%	328.7	33.00	0.9379	493.7	36.1%	36.1%	---
8	unvented	hot/dry	30%*	30%*	316.5	28.29	0.9293	457.9	26.2%	26.2%	---
AVG							0.8833	435.6	22.9%	22.9%	
9	vented	hot/humid	0	0	252.4	27.66	0.9592	390.7	---	7.7%	7.7%
10	vented	hot/humid	15%	0	257.1	34.82	0.9629	431.2	10.4%	18.9%	10.9%
11	vented	hot/humid	30%	0	284.0	34.64	0.984	457.2	17.0%	26.0%	12.0%
12	vented	hot/humid	0	15%	320.5	30.23	0.9159	471.6	20.7%	30.0%	6.0%
13	vented	hot/humid	0	30%	357.3	36.39	0.9868	539.2	38.0%	48.6%	10.7%
14	vented	hot/humid	15%	15%	316.8	38.25	0.9749	508.1	30.1%	40.1%	15.2%
15	vented	hot/humid	30%	30%	336.3	46.70	0.9184	569.8	45.9%	57.1%	15.4%
16	vented	hot/humid	30%*	30%*	338.1	41.77	0.9779	546.9	40.0%	50.8%	19.4%
AVG							0.9600	489.3	28.9%	39.9%	12.2%

* For Test numbers 8 and 16, RL and SL are located about 8 ft apart.
RL= return leak, SL = supply leak

Plots of best-fit regression analysis, from which the data of Table 6-10 was obtained, may be found in Appendix B (Figures B-1 through B-13).

In the following discussion, cooling energy has been calculated (based on the best-fit regression analysis) for an outdoor temperature that is 5°F warmer than indoors. A typical summer day in central Florida has an average outdoor temperature of about 82°F, or seven degrees warmer than indoors. However, in order to reflect cooling energy over the extended 8-month cooling season (March 15 – November 15), the seasonal energy savings are based on an average daily outdoor temperature of 80°F, five degrees warmer than indoors.

Energy Analysis Results from Unvented Attic

Test configuration 1 (0% RL, 0% SL). Cooling energy was found to be 362.8 MBtu/day.

Test configuration 2 (15% RL, 0% SL). Cooling energy was found to be 389.9 MBtu/day. A 15% return leak from an unvented attic (insulation at the ceiling) produces a 7.2% increase in cooling energy use compared to no duct leakage.

Test configuration 3 (30% RL, 0% SL). Cooling energy was found to be 408.1 MBtu/day. A 30% return leak from an unvented attic (insulation at the ceiling) produces a 12.5% increase in cooling energy use compared to no duct leakage.

The energy impacts of the 15% and 30% return leaks, with unvented attic, can be considered modest. There are two reasons why the increase in energy use is not larger. The first reason is related to the relatively high mass roof that significantly slows the transport of heat into the attic space. The roof is constructed of metal decking with an average of 2.5 inches of lightweight concrete on top covered with a light membrane finished with a black tar coat. The second reason is due to the lack of venting that allows the attic dew point temperature to be only slightly higher than the indoor dew point temperature (58.4°F in the attic versus 55.8°F in the room). The attic rarely gets hotter than outdoors (rarely above 93°F; see Figures B-14 through B-21), and the attic dew point temperature is much lower than outdoors. When the return leak is drawing air from the attic space, it depressurizes the attic space and pressurizes the occupied space. This pressure differential drives airflow through the ceiling. Given the relatively tight characteristics of the building envelope and the very leaky characteristic of the suspended T-bar ceiling (about 5 CFM50 per square foot), most of the pressure-driven airflow goes through the path of least resistance, namely the suspended T-bar ceiling. The energy consequences, therefore, are diminished.

Test configuration 4 (0% RL, 15% SL). Cooling energy was found to be 444.9 MBtu/day. A 15% supply leak into an unvented attic (insulation at the ceiling) produces a 22.6% increase in cooling energy use compared to no duct leakage.

Test configuration 5 (0% RL, 30% SL). Cooling energy was found to be 486.9 MBtu/day. A 30% supply leak into an unvented attic (insulation at the ceiling) produces a 34.2% increase in cooling energy use compared to no duct leakage.

We can conclude that supply leaks (into the unvented attic) produce approximately 3 times as much cooling energy waste compared return leaks of equal size, when the attic is unvented, the insulation is on the ceiling, and a massive roof resists the entry of solar-induced heat flux.

Test configuration 6 (15% RL, 15% SL). Cooling energy was found to be 441.2 MBtu/day. Equal 15% return and 15% supply leaks from/into an unvented attic (insulation at the ceiling) produce a 21.6% increase in cooling energy use compared to no duct leakage.

Test configuration 7 (30% RL, 30% SL). Cooling energy was found to be 493.7 MBtu/day. Equal 30% return and 30% supply leaks from/into an unvented attic (insulation at the ceiling) produces a 36.1% increase in cooling energy use compared to no duct leakage.

Comparing test configurations 6 and 7 to configurations 4 and 5, the addition of return leaks of equal-size to the existing supply leaks causes essentially no increase in cooling energy use compared to supply leaks alone.

Test configuration 8 (30% RL, 30% SL). The return and supply leak locations are much closer, allowing the return to capture ("regain") a portion of the cooling energy lost to the attic space. Cooling energy was found to be 457.9 MBtu/day. Equal 30% return leak and 30% supply leak that are in closer proximity (insulation at the ceiling and an unvented attic) produce a 26.2% increase in cooling energy use compared to no duct leakage. The energy penalty is 27% less than for test configuration 7 where the supply and return leaks are widely separated. We can conclude that 27% of the total cooling energy penalty that occurs with Test Configuration 7 (same leaks but separated) is recaptured by placing the return leak in the general vicinity of the supply leak.

Energy Analysis Results from Vented Attic

To change the experiments from the unvented attic to the vented attic, 23 attic vents were opened. They are located about three feet above the attic floor (ceiling plane) on all four sides of the building. Each vent has dimensions of 8" high by 16" wide (a single CMU was left out during construction to create each opening). Louvers are positioned on the exterior of the building to provide a rain shield, but they create relatively little resistance to airflow. Total gross vent area is 20.9 square feet, or 1 square foot of vent per 94 square feet of floor area. Insect screening is positioned in each vent to prevent entry of insects. Assuming a net free area fraction of 74% for the screening (based on measurements), the net attic vent opening is 15.5 square feet. This is equivalent to 1 square foot of vent opening per 127 square feet of floor area.

Test configuration 9 (0% RL, 0% SL). Cooling energy was found to be 390.7 MBtu/day. This is a 7.7% increase compared to no duct leaks and unvented attic.

Test configuration 10 (15% RL, 0% SL). Cooling energy was found to be 431.2 MBtu/day. A 15% return leak from a vented attic (insulation at the ceiling) produces a 10.4% increase in cooling energy use compared to no duct leakage and a vented attic.

Test configuration 11 (30% RL, 0% SL). Cooling energy was found to be 457.2 MBtu/day. A 30% return leak from a vented attic (insulation at the ceiling) produces a 17.0% increase in cooling energy use compared to no duct leakage and a vented attic.

The energy impacts of the 15% and 30% return leaks, with vented attic, are more substantial (compared to the unvented attic). Energy use for the 15% and 30% return leaks are 10.9% and 12.0% greater, respectively, when the attic is vented. The attic drybulb temperature is about 3^oF cooler with the vented attic (83^oF versus 86^oF). The increase in energy use with the vented attic is due to the higher level of water vapor in the attic air when vented. The attic dew point temperature is about 20^oF higher when vented (72.7^oF versus 52.5^oF). Total enthalpy of the attic air (taking into account both sensible and latent heat) is much higher for the vented attic, 38.9 Btu/lb for the vented attic versus 30.5 Btu/lb for the unvented attic. Given that the indoor enthalpy is about 26.8 Btu/lb, the enthalpy differential between indoors and attic air increases dramatically when vented (the enthalpy differential is three times greater with the vented attic).

Test configuration 12 (0% RL, 15% SL). Cooling energy was found to be 471.6 MBtu/day. A 15% supply leak into a vented attic (insulation at the ceiling) produces a 20.7% increase in cooling energy use compared to no duct leakage and a vented attic.

Test configuration 13 (0% RL, 30% SL). Cooling energy was found to be 539.2 MBtu/day. A 30% supply leak into a vented attic (insulation at the ceiling) produces a 38.0% increase in cooling energy use compared to no duct leakage and a vented attic.

We can conclude that supply leaks (into the vented attic) produce about 2.1 times as much cooling energy waste compared to return leaks of equal size, when the attic is vented, the insulation is on the ceiling, and a massive roof resists the entry of solar-induced heat flux.

We also conclude that energy use for the 15% and 30% supply leaks are 6.0% and 10.7% greater, respectively, when the attic is vented compared to unvented. The attic drybulb temperature is about 2.5^oF cooler with the vented attic (82^oF versus 84.5^oF). In spite of the higher drybulb temperature in the unvented attic, energy use with the vented attic is much higher due to the higher level of water vapor in the attic air. The attic dew point temperature is about 20^oF higher when vented (72.5^oF versus 52.5^oF). Total enthalpy of the attic air (taking into account both sensible and latent heat) is much higher for the vented attic, 38.6 Btu/lb versus 29.5 Btu/lb. Given that the indoor enthalpy is about 26.8 Btu/lb, the enthalpy differential between indoors and the attic increases dramatically when vented.

Note that the supply leaks depressurize the occupied space, thus causing unconditioned attic air to be drawn through the ceiling grid into the occupied space.

Test configuration 14 (15% RL, 15% SL). Cooling energy was found to be 508.1 MBtu/day. Equal 15% return and 15% supply leaks into a vented attic (insulation at the ceiling) produce a 30.1% increase in cooling energy use compared to no duct leakage and a vented attic.

Test configuration 15 (30% RL, 30% SL). Cooling energy was found to be 569.8 MBtu/day. Equal 30% return and 30% supply leaks into a vented attic (insulation at the ceiling) produces a 45.9% increase in cooling energy use compared to no duct leakage and a vented attic.

Comparing test configurations 14 and 15 to configurations 12 and 13, the addition of return leaks of equal-size to the existing supply leaks causes a modest increase in cooling energy use compared to supply leaks alone. For the unvented attic, there was essentially no increase from Test Configuration 5 to Test Configuration 7. For the vented attic, the increase from Test Configuration 13 to Test Configuration 15 was 5.7%. The reason for the greater energy penalty for the vented attic may occur because of wind blowing (moving) through the attic and disrupting the settling of cool supply air onto the attic floor.

Test configuration 16 (30% RL, 30% SL). The return and supply leak locations are much closer, allowing the return to capture ("regain") a portion of the cooling energy lost to the attic space. Cooling energy was found to be 546.9 MBtu/day. Equal 30% return and 30% supply leaks that are in closer proximity (insulation at the ceiling and a vented attic) produce a 40.0% increase in cooling energy use compared to no duct leakage and a vented attic. The energy penalty is 13% less than for test configuration 15 where the supply and return leaks are widely separated. We conclude that only 13% of the lost cooling energy that occurs with Test Configuration 15 (same leaks but further separated) is recaptured by placing the return leak in the general vicinity of the supply leak. The reader will recall that the "regain" for test configuration 8 was 27%. Clearly, the ability of lost energy from duct leakage to be recaptured ("regained") is substantially reduced by the venting of the attic space.

Unvented versus Vented Attic Overall Energy Impact

Referring to Table 6-10 (far right column), venting of the attic creates a 12.2% increase in cooling energy use, on average, for the eight different duct leak configurations. In general, attic venting creates the greatest increase in cooling energy use for larger duct leaks than smaller duct leaks, and for supply leaks than for return leaks. The greatest increase in cooling energy that results from attic venting occurs, however, in the case of 30% RL and 30% SL, with the leaks close together. When the attic is unvented, there is substantial regain of lost cooling energy. When the attic is vented, half or more of that regain disappears.

6.3.3. Time of Day (Peak) Energy Demand Impacts of Duct Leakage

Groups of days were selected from each test configuration from which to produce 24-hour profiles of cooling energy use. These days are not the hottest days that occur, and in fact are only slightly warmer than the average summer day.

Table 6-11 summarizes the indoor and outdoor conditions for the days used to create the 24-hour composites. The object of selecting the days from which to create the profiles was to match weather conditions as much as practicable. The most important criteria was delta-temperature (out – in). The daily temperature difference between outdoors and indoors ranges from 6.3 to 6.6^{o}F. The daily average solar radiation varied more widely; from 192 W/m^2 to 312 W/m^2.

Outdoor dew point temperature fell in the range of 70.3°F to 74.2°F. Wind also varied from 3.7 to 6.9 mph.

Plots of peak cooling energy (24-hour profiles) are found in Appendix B, one plot for each of the 16 test configurations. Table 6-12 summarizes the cooling energy that occurred during the period of 2 – 5 PM EST (3 – 6 PM EDT) for each test configuration.

Table 6-11. Julian Days and Weather Conditions for Days Used in Creating Energy, Temperature, and Relative Humidity 24-hour Profiles (Figures B-14 through B-35 in Appendix B)

Test Configuration (Julian days)	dT (°F)	T indoor (°F)	T outdoor (°F)	T attic (°F)	Solar (W/m²)	Wind (mph)
Test 1 (153,211,215,274-6)	6.5	75.0	81.5	85.6	242	6.7
Test 2 (180-182)	6.4	74.8	81.2	87.5	312	4.3
Test 3 (190-2,194,198)	6.4	75.0	81.4	85.4	287	4.3
Test 4 (164-166)	6.6	74.8	81.4	86.1	276	4.9
Test 5 (161,256-257)	6.6	74.9	81.4	81.3	216	4.3
Test 6 (170-173)	6.4	74.9	81.3	85.8	274	5.1
Test 7 (204-206,208)	6.4	74.8	81.2	84.7	304	4.1
Test 8 (265-268)	6.4	75.2	81.6	78.4	201	5.7
*Mean**	*6.5*	*74.9*	*81.4*	*84.4*	*264*	*4.9*
Test 9 (217,221,232,239)	6.5	74.9	81.4	85.6	283	4.2
Test 10 (191-193)	6.5	75.2	81.7	83.9	210	6.5
Test 11 (241-244)	6.5	75.0	81.5	84.5	241	4.1
Test 12 (220-223,225)	6.4	75.0	81.4	84.4	249	3.9
Test 13 (224, 256-259)	6.4	74.9	81.3	81.7	192	6.9
Test 14 (284,293,204-205)	6.3	74.9	81.2	84.0	222	4.9
Test 15 (262,193-196)	6.4	75.1	81.5	83.0	277	5.5
Test 16 (208-209,212-213)	6.3	75.0	81.3	81.4	230	3.7
Mean	*6.4*	*75.0*	*81.4*	*83.6*	*238*	*5.0*

Table 6-12. Indoor and Outdoor Conditions for Groups of 3 to 5 days (that were used to create composite 24-hour cooling energy use profiles)

Test	Delta-T (ºF)	T out (ºF)	T attic (ºF)	T out dewpt (ºF)	T attic dewpt (ºF)	T room dewpt. (ºF)	RH room (%)	Solar (W/m^2)	Wind (mph)	Peak 2-5pm (MBtu/h)
1	6.5	81.5	85.6	71.5	60.6	56.0	51.8	241.6	6.7	27.91
2	6.4	81.2	87.5	71.1	54.2	54.8	49.8	311.6	4.3	30.62
3	6.4	81.4	85.4	70.5	53.9	55.3	50.4	286.9	4.3	31.35
4	6.6	81.4	86.1	71.7	53.3	54.7	49.6	275.6	4.9	34.20
5	6.6	81.4	81.3	70.5	51.4	53.3	47.0	215.8	4.3	35.76
6	6.4	81.3	85.8	71.8	53.5	55.3	50.5	274.3	5.1	34.92
7	6.4	81.2	84.7	70.3	50.8	53.6	47.6	303.9	4.1	39.41
8	6.4	81.6	78.4	71.2	55.7	56.6	52.4	201.3	5.7	34.18
AVG	**6.5**	**81.4**	**84.4**	**71.1**	**54.2**	**55.0**	**49.9**	**263.9**	**4.8**	**33.54**
9	6.5	81.4	85.6	71.8	71.7	57.1	54.0	282.9	4.2	29.84
10	6.5	81.7	83.9	74.2	75.3	60.6	60.1	209.9	6.5	31.14
11	6.5	81.5	84.5	72.3	70.7	59.6	58.9	240.6	4.1	36.70
12	6.4	81.4	84.4	72.8	71.7	60.0	59.0	249.3	3.9	35.64
13	6.4	81.3	81.7	73.8	73.6	62.0	64.1	191.6	6.9	39.99
14	6.3	81.2	84.0	71.9	70.8	59.2	58.3	221.6	4.9	36.78
15	6.4	81.5	83.0	71.7	70.1	59.8	59.1	277.4	5.5	43.01
16	6.3	81.3	81.4	71.5	68.3	58.8	57.2	230.2	3.7	43.99
AVG	**6.4**	**81.4**	**83.6**	**72.5**	**71.5**	**59.6**	**58.8**	**237.9**	**5.0**	**37.14**

Table 6-13. Summary of Average (peak) Cooling Load for 2 - 5 PM Period for 16 Experiments

Test #	Attic Status	Attic Condition	RL	SL	Peak Cooling Load (MBtu/h)	% Increase vs. Test #1	% Increase vs. Tests #1 & #9
1	unvented	hot/dry	0	0	27.91	---	---
2	unvented	hot/dry	15%	0	30.62	9.7%	9.7%
3	unvented	hot/dry	30%	0	31.35	12.3%	12.3%
4	unvented	hot/dry	0	15%	34.2	22.5%	22.5%
5	unvented	hot/dry	0	30%	35.76	28.1%	28.1%
6	unvented	hot/dry	15%	15%	34.92	25.1%	25.1%
7	unvented	hot/dry	30%	30%	39.41	41.2%	41.2%
8	unvented	hot/dry	30%*	30%*	34.18	22.5%	22.5%
AVG					**33.54**	**20.2%**	**20.2%**
9	vented	hot/humid	0	0	29.84	6.9%	--
10	vented	hot/humid	15%	0	31.14	11.6%	4.7%
11	vented	hot/humid	30%	0	36.7	31.5%	24.6%
12	vented	hot/humid	0	15%	35.64	27.7%	20.8%
13	vented	hot/humid	0	30%	39.99	43.3%	36.4%
14	vented	hot/humid	15	15	36.78	31.8%	24.9%
15	vented	hot/humid	30	30	43.01	54.1%	47.2%
16	vented	hot/humid	30*	30*	43.99	57.6%	50.7%
AVG					**37.14**	**33.1%**	**29.9%**

* For Test numbers 8 and 16, RL and SL are located about 8 ft apart.
RL= return leak, SL = supply leak
Configurations compared to Test #1 (no duct leakage, unvented) and Test #9 (no duct leakage, vented)

Note that while considerable effort was taken to select days with comparable weather (temperature, solar, dew point temperature), there are variations, as can be seen in Table 6-11, between Test Configurations. As a consequence, the time of day energy use patterns cannot be considered as fully normalized to weather as was the case for total daily cooling energy. Furthermore, the peak period of 2-5 PM is influenced both by the daily average weather conditions and by the weather that occurs during and immediately before the 2-5 PM period. (In other words, some of the building cooling load response occurs with a significant delay [sometimes 6 to 8 hours] and some occurs with little delay.) Therefore, the reader can expect that the pattern of peak energy use will deviate somewhat from expectations.

<u>Unvented Attic Peak Cooling Impacts (2 – 5 PM EST)</u>

The reported peak cooling is the average cooling energy delivered by the AC system for the three hour period of 2 – 5 PM for the sample of days that form the composite.

Test configuration 1 (0% RL, 0% SL). Peak cooling energy was found to be 27.9 MBtu/hour.

Test configuration 2 (15% RL, 0% SL). Peak cooling energy was found to be 30.6 MBtu/hour, or 9.7% greater than the peak for Test Configuration 1.

Test configuration 3 (30% RL, 0% SL). Peak cooling energy was found to be 31.4 MBtu/hour, or 12.3% greater than the peak for Test Configuration 1.

Test configuration 4 (0% RL, 15% SL). Peak cooling energy was found to be 34.2 MBtu/hour, or 22.5% greater than the peak for Test Configuration 1.

Test configuration 5 (0% RL, 30% SL). Peak cooling energy was found to be 35.8 MBtu/hour, or 28.1% greater than the peak for Test Configuration 1.

We can conclude that supply leaks (into the unvented attic) produce approximately 2.3 times as much increase in peak cooling energy compared return leaks of equal size, when the attic is unvented, the insulation is on the ceiling, and a massive roof resists the entry of solar-induced heat flux.

Test configuration 6 (15% RL, 15% SL). Peak cooling energy was found to be 34.9 MBtu/hour, or 25.1% greater than the peak for Test Configuration 1.

Test configuration 7 (30% RL, 30% SL). Peak cooling energy was found to be 39.4 MBtu/hour, or 41.2% greater than the peak for Test Configuration 1.

Comparing Test Configurations 6 and 7 to Test Configurations 4 and 5, the addition of return leaks of equal-size to the existing supply leaks causes relatively little increase in peak cooling energy use compared to supply leaks alone, except for Test Configuration 7, where it appears that higher than normal solar radiation inflates the peak period cooling.

Test configuration 8 (30% RL, 30% SL). The return and supply leak locations are much closer, allowing the return to capture (“regain”) a portion of the cooling energy lost to the attic space. Peak cooling energy was found to be 34.2 MBtu/hour, or 22.5% greater than the peak for Test Configuration 1.

The peak demand reduction that occurs when the 30% RL and 30% SL are located about 8 feet apart appears to be large, showing an almost 50% peak demand reduction compared to Test Configuration 7. This appears, however, to be considerably overstated. The primary factor would seem to be solar radiation, which averages 304 W/m^2 for Test 7 but only 201 W/m^2 for Test 8.

Vented Attic Peak Cooling Impacts (2 – 5 PM EST)

As before, 23 attic vents were opened to change the experiments from the unvented attic to the vented attic. As can be seen in Table 6-12, the dew point temperature in the attic space increased dramatically, from about 54^{o}F to about 72^{o}F as a result of the venting. This higher level of latent heat causes substantial increases in peak period cool energy use.

Test configuration 9 (0% RL, 0% SL). Peak cooling energy was found to be 29.8 MBtu/hour. This is a 6.9% increase compared to no duct leaks and unvented attic.

Test configuration 10 (15% RL, 0% SL). Peak cooling energy was found to be 31.1 MBtu/hour, or 4.7% greater than the peak for Test Configuration 9.

Test configuration 11 (30% RL, 0% SL). Peak cooling energy was found to be 36.7 MBtu/hour, or 24.6% greater than the peak for Test Configuration 9.

Test configuration 12 (0% RL, 15% SL). Peak cooling energy was found to be 35.6 MBtu/hour, or 20.8% greater than the peak for Test Configuration 9.

Test configuration 13 (0% RL, 30% SL). Peak cooling energy was found to be 40.0 MBtu/hour, or 36.4% greater than the peak for Test Configuration 9.

We can conclude that supply leaks (into the vented attic) produce about 2.0 times as much Peak cooling energy waste compared return leaks of equal size, when the attic is vented, the insulation is on the ceiling, and a massive roof resists the entry of solar-induced heat flux.

We also conclude that energy use for the 15% and 30% supply leaks are 6.0% and 10.7% greater, respectively, when the attic is vented. The attic drybulb temperature (from Table 6-12) is about 0.8^{o}F cooler with the vented attic (83.6^{o}F versus 84.4^{o}F). In spite of the higher drybulb temperature in the unvented attic, energy use with the vented attic is much higher due to the higher level of water vapor in the attic air. The attic dew point temperature is about 20^{o}F higher when vented (72.7^{o}F versus 52.5^{o}F). Total enthalpy of the attic air (taking into account both sensible and latent heat) is much higher for the vented attic, 38.6 Btu/lb versus 29.5 Btu/lb. Given that the indoor enthalpy is about 26.8 Btu/lb, the enthalpy differential between indoors and the attic increases dramatically when vented.

Note that the supply leaks depressurize the occupied space, thus causing unconditioned attic air to be drawn through the ceiling grid into the occupied space.

Test configuration 14 (15% RL, 15% SL). Peak cooling energy was found to be 36.8 MBtu/hour. Equal 15% return and 15% supply leaks into a vented attic (insulation at the ceiling) produce a 24.9% increase in Peak cooling energy use compared to no duct leakage and a vented attic.

Test configuration 15 (30% RL, 30% SL). Peak cooling energy was found to be 43.0 MBtu/hour. Equal 30% return and 30% supply leaks into a vented attic (insulation at the ceiling) produces a 47.2% increase in Peak cooling energy use compared to no duct leakage and a vented attic.

Comparing test configurations 14 and 15 to configurations 12 and 13, the addition return leaks of equal-size to the existing supply leaks causes a modest increase in Peak cooling energy use compared to supply leaks alone. For the unvented attic, there was essentially no increase from Test Configuration 5 to Test Configuration 7. For the vented attic, the increase from Test Configuration 13 to Test Configuration 15 was 5.7%. The reason for the greater energy penalty for the vented attic may occur because of wind blowing (moving) through the attic and disrupting the settling of cool supply air onto the attic floor.

Test configuration 16 (30% RL, 30% SL). The return and supply leak locations are much closer, allowing the return to capture ("regain") a portion of the Peak cooling energy lost to the attic space. Peak cooling energy was found to be 44.0 MBtu/hour. Equal 30% return and 30% supply leaks that are in closer proximity (insulation at the ceiling and a vented attic) produce a 50.7% increase in Peak cooling energy use compared to no duct leakage and a vented attic. The peak cooling penalty is 7% greater than for test configuration 15 where the supply and return leaks are widely separated.

6.3.4. Temperature and Relative Humidity Impacts of Duct Leakage and Attic Venting

The conditioned space temperature was controlled by means of a thermostat. As long as the 5-ton AC system had sufficient cooling capacity, temperature would remain within a tight range. The thermostat was actually set to 77^{o}F, but produced almost exactly 75.0^{o}F in the building. Over the 2.5-year period of the experiments, temperatures (for given experimental periods) varied only from 74.8^{o}F to 75.2^{o}F, and the AC system had sufficient capacity to maintain temperatures throughout. During the hottest weather periods of some test configurations with the largest supply leaks, the AC system ran continuously for extended portions of the day, but the indoor temperature did not rise above the set-point temperature.

For the following discussion, refer to Table 6-11 for summary data and in Figure 6-3.

Attic drybulb temperature was affected by outdoor temperature and solar radiation. It was also affected, in some measure, by attic venting and by duct leakage. Venting appears to reduce the attic temperature by about 2^{o}F, taking other factors such as solar radiation and duct leakage levels into account.

The plots in Figure 6-3 below show daily average air temperature at three different heights in the attic near the intake of the return leak. The lowest height was 2.5 inches above R-19 insulation, middle height was 4 feet and 2 inches above insulation, and highest point was 7 feet above insulation and 1 foot below the roof deck. The average outdoor and indoor conditions during the same time period shown here can be found in Table 6-12. All duct test configurations have the same pattern of decreasing temperatures with decreasing height from the attic roof with the exception of tests 8 and 16. Tests 8 and 16 had the supply leak in the near vicinity of the return leakage. The directional nature of the supply leak had more influence on the highest temperature measurement. With the supply leak nearby it is logical for test 16 to have the lowest temperatures of the group. Next it can be seen that having only a 30% supply leak creates the next coolest temperatures in the vented attic. The highest temperatures occur at all heights when there are no duct leaks.

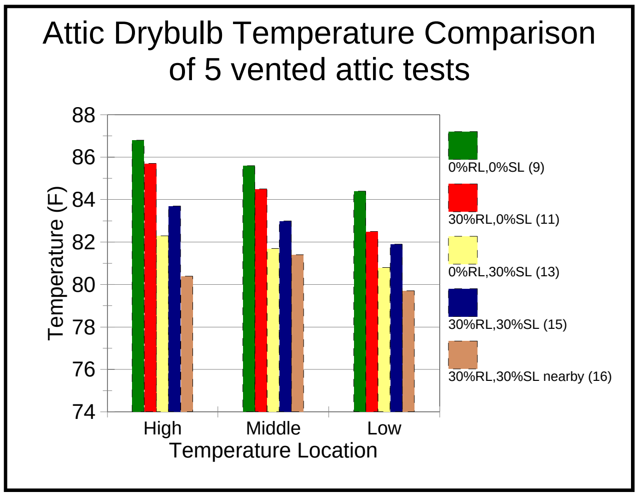

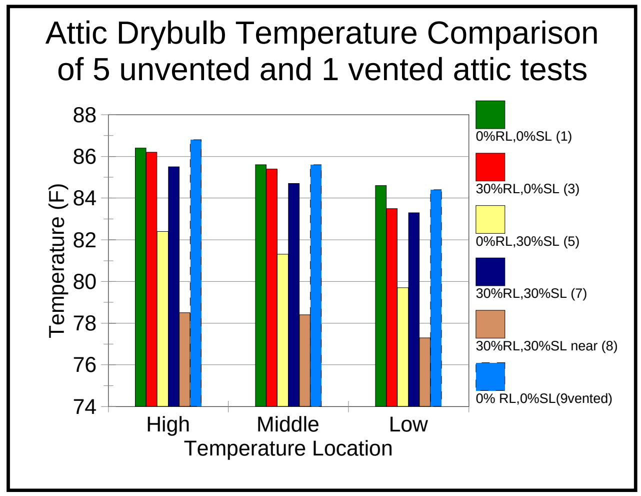

Figure 6-3. Comparing Attic Temperatures for Tests with Vented and Unvented Attics

Attic dew point temperature was slightly impacted by duct leakage. In the absence of duct leakage, the unvented attic (Test 1) had a dew point temperature that was about 5°F higher than the room dew point temperature. However, for all cases where the unvented attic had duct leakage (Tests 2 – 8), the attic dew point temperature was approximately equal to or lower than the room dew point temperature. There appears to be very little if any effect of duct leakage upon the dew point temperature of the vented attic. The largest supply leak tests showed about a 1°F drop in attic dew point compared to outdoors when wind speeds were moderately low, but otherwise no significant difference was noted.

Attic dew point temperatures increased dramatically when the attic was vented. The average attic dew point temperature increased from 54.2°F to 71.5°F when the vents were opened, average across Tests 9 – 16. Figure B-35 shows indoor and attic dew point temperatures for various unvented and vented attic spaces.

Indoor RH is impacted by duct leakage.

- For the unvented attic, the pattern is that duct leaks produce lower indoor RH and the tests with larger supply leaks produced the lowest indoor RH. This is because the added sensible load (and lost AC capacity) caused longer AC run-times that then removed additional amounts of water vapor from the building. Figures B-30 and B-31 show indoor and attic RH for the unvented attic.
- For the vented attic, the pattern is that no duct leaks (Test 9) produced the lowest indoor RH (54%). Note, however, that this is higher than the 52% RH experienced for Test 1. The introduction of return leaks and supply leaks, for most test configurations, produced about 58% to 60% indoor RH. The most extreme case (Test 13 with 64% RH) appeared to have high RH, in part, because the winds were stronger, the outdoor dew point temperatures were higher (73.8^{o}F), and solar radiation was lower (yielding some reduction in AC operation time). Figures B-32 and B-33 show indoor and attic RH for the vented attic.

Indoor RH is impacted by attic venting.

- For all 8 unvented attic test configurations, the average room RH was 50%.
- For all vented attic test configurations, the average room RH was 59%.

Even in the absence of duct leaks, venting of the attic (with a leaky ceiling plane) yields a significant increase in indoor RH (Figure B-34; comparison of Test 1 versus Test 9). In part, this increase occurred because of 3% return leaks (and approximately the same level of supply leaks). The remainder occurs because of air transport between the attic and occupied space, and because of moisture diffusion through the ceiling tiles.

6.4. Summary of Findings

Whole building testing at FSEC's Building Science Laboratory (BSL) systematically evaluated the airtightness, infiltration, relative humidity, energy, and peak demand impacts of duct leakage – during the cooling season – with various attic and ceiling space configurations. The two primary independent variables were the amount of attic venting and the amount of duct leakage. Data were collected with the building and ductwork in 16 different configurations. Configurations 1 through 8 were with an unvented attic (hot and dry attic conditions). Configurations 9 through 16 were with a vented attic (hot and humid attic conditions). Duct leak age rates of 0, 15 and 30% were imposed on both the return and supply sides of the air distribution system. Test data were collected over several hundred days during 2004, 2005, and 2006.

The building was found, by means of blower door testing, to be moderately airtight in the unvented attic configuration, with an ACH50 of 5.2. The pressure drop of 0.9 Pa across the ceiling and 49.1 Pa across the roof deck indicates that the roof deck is the primary air boundary. The building in the vented attic configuration was found to be very leaky, with an ACH50 of 29. The pressure drop of 39 Pa across the ceiling and 11 Pa across the roof deck indicates that the ceiling is the primary air boundary when the attic is vented.

Tracer gas decay testing found that the vented attic contributes substantially to the building infiltration rate. With no attic venting, the average infiltration rate was about 0.15 ach with or without duct leakage. With the attic vented and no duct leakage, the average infiltration rate was about 0.5 ach. With the attic vented and 15% duct leaks, the average infiltration rate was about 1.2 ach. With the attic vented and 30% duct leaks, the average infiltration rate was about 1.5 ach. The strength of the wind affected the vented attic infiltration rates significantly.

Attic dry bulb temperature averaged about 1^{o}F warmer for the unvented configuration. Attic humidity levels were dramatically impacted by attic venting. Attic dew point temperature (absolute humidity) averaged 54^{o}F when unvented and 72^{o}F when vented, with some variation based on duct leakage amount. Indoor dew point temperature increased substantially as a result of attic venting, from about 55^{o}F to about 60^{o}F. Indoor RH increased from 50% to 59%, on average, as a result of opening the attic vents.

Cooling energy use increased as a result of attic venting and as a result of duct leakage. Attic venting increased cooling energy use by an average of 12% for a range of duct leak configurations. Duct leakage increased cooling energy use by 20% to 35% for various duct leaks for the unvented attic. Duct leakage increased cooling energy use by 20% to 50% for various duct leaks for the vented attic.

Peak cooling demand increased by 10% to 40% for the unvented attic, for various duct leak configurations, and by 12% to 58% for the vented attic, for various duct leak configurations.

6.5. References

American Society of Heating, Refrigerating, and Air Conditioning Engineers, ASHRAE Standard 152-2004, “Method of Test for Determining the Design and Seasonal Efficiencies of Residential Thermal Distribution Systems”, January 2004.

Brennan, Terry, James B. Cummings, Joseph Lstiburek. “Unplanned Air Flows & Moisture Problems”. *ASHRAE Journal*, November, 2002.

Cummings, J.B., C.R. Withers, N. Moyer, P. Fairey, and B. McKendry. 1996. "Uncontrolled Air Flow in Non-Residential Buildings; Final Report", FSEC-CR-878-96, Florida Solar Energy Center, Cocoa, FL, April, 1996.

Cummings, J.B., C.R. Withers, N. Moyer, P. Fairey, and B. McKendry. "Field Measurement of Uncontrolled Air Flow and Depressurization in Restaurants". *ASHRAE Transactions*, 1996, Vol.102, Part 1, p.859.

Cummings, J.B., C.R. Withers, P. Fairey, B. McKendry, and N.A. Moyer, 1995, “Indoor Air Quality Impacts of Uncontrolled Air Flow and Depressurization in Eight Commercial Buildings in Central Florida”. Proceedings of the Eighth Annual Indoor Air Pollution Conference. Tulsa, OK, September 1995.

Cummings, J.B. and C.R. Withers. 1997. "Identifying Air Flow Failure Modes in Small Commercial Buildings: Tools and Methodologies for Building Commissioning Diagnostics". Proceedings of the Fifth National Conference on Building Commissioning. Huntington Beach, CA. April 1997.

Cummings, J.B. and C.R. Withers. "Building Cavities Used as Ducts: Air Leakage Characteristics and Impacts in Light Commercial Buildings". *ASHRAE Transactions*, 1998, Vol.104, Part 2, p.743 -752.

Cummings, J.B., C.R. Withers, and Don Shirey. 1997. "Controlling Ventilation and Space Depressurization in Restaurants in Hot and Humid Climates". Proceedings of the 18th Annual AIVC Conference, Volume 1, pp.153 - 161, Athens, Greece. September 1997.

Cummings, James. B. and Charles R. Withers, "Best Practice for the Location of Air and Thermal Boundaries in Small Commercial Buildings", Proceedings of 12th Annual Symposium on Improving Building Systems in Hot and Humid Climates, San Antonio, TX, May 2000.

Cummings, James B., Don B. Shirey, Charles Withers, Richard Raustad, and Neil Moyer. "Evaluating the Impacts of Uncontrolled Air Flow and HVAC Performance Problems on Florida's Commercial and Institutional Buildings", Final Report, FSEC-CR-1210-00. October, 2000.

Cummings, J., D. Shirey, and C. Withers. "Evaluating the Impacts of Uncontrolled Air Flow and HVAC Performance Problems on Florida's Commercial and Institutional Buildings.", FSEC-CR-1210-00, December 2000. Submitted to Florida Energy Office.

Delp W.W., Matson N. E., Tschudy E., Modera M.P. and Diamond R.C. "Field Investigation of Duct System Performance in California Light Commercial Buildings" ASHRAE Transactions, V104 Pt2 1998.

Delp W.W., Matson N. E., Tschudy E., Modera M.P. "Field Investigation of Duct System Performance in California Light Commercial Buildings (Round II)" Proc. ACEEE Summer Study 1998.

Persily, Andrew K., "Myths About Building Envelopes", ASHRAE Journal, March 1999, pp. 39 - 47.

Withers, C.R., J.B. Cummings, N. Moyer, P. Fairey, and B. McKendry. "Energy Savings from Repair of Uncontrolled Air Flow in 18 Small Commercial Buildings". *ASHRAE Transactions,* 1996, Vol. 102, Part 2, pp. 549-561.

Withers, C.R. and J.B. Cummings. "Ventilation, Humidity, and Energy Impacts of Uncontrolled Airflow in a Light Commercial Building." *ASHRAE Transactions,* 1998, Vol. 104, Part 2, pp. 733 - 742.

Withers, Charles R. and James B. Cummings, "Building Envelope Air Leakage Failure in Small Commercial Buildings Related to the Use of Suspended Tile Ceilings", Proceedings of 12th

Annual Symposium on Improving Building Systems in Hot and Humid Climates, San Antonio, TX, May 2000.

7. Whole Building Simulation Analysis

The whole building simulation analyses focuses on evaluating the impacts of various levels of uncontrolled air flows on building energy consumption. The levels of uncontrolled air flow will be dictated by variations in air distribution system leakage (supply and return), building shell airtightness, mechanical ventilation/exhaust air flow rates, and weather (primarily wind and temperature) that were observed in earlier field testing/monitoring in Florida and in New York. The range of parametric values will be established using information collected from the NY field-testing (Section 2) and previous field-testing in Florida (Cummings et al 1996).

7.1. Overview

In order to simulate uncontrolled airflow impact on a whole building performance, an air distribution system model is needed to simulate airflows and pressures, and interaction with the building envelope, HVAC system, and outdoors. The model used in this analysis was developed as a module in EnergyPlus. The model had been validated against measured airflow and temperature data from FSEC and ORNL. EnergyPlus was also validated in this project against FSEC measured data, by comparing AC energy use. Then a parametric study was performed to understand how to control uncontrolled airflows and associated energy impact. Recommendations and conclusions were made based on simulation results.

7.2. Model Development

DOE's EnergyPlus building energy simulation model was used as the simulation tool for whole building simulation analysis. The AirflowNetwork model in EnergyPlus was developed in work supported by the US DOE and NYSERDA. The model provides the ability to simulate the performance of an air distribution system, including supply and return leaks, and calculate multizone airflows driven by outdoor wind and forced air during HVAC system operation. The pressure and airflow model described here was developed based on AIRNET (Walton, 1989). This detailed model can be used to simulate thermal conduction and air leakage losses for air distribution systems in residential or light commercial buildings. This model replaces the obsolete models for COMIS (1990) and Air Distribution System (ADS). The main difference is that the AirflowNetwork model adopts the COMIS model approach of introducing envelope leakage at a specific surface and modulate window and door openings at specified input and current outdoor conditions in multizone airflow calculations. In contrast, the ADS model lumped all envelope leakage together. In addition, the model calculates multizone airflows driven by wind when the HVAC system turns off. This capability is equivalent to the COMIS model. The multizone airflow calculations are now performed at the system time step instead of at the zone time step. This enhancement will allow future development of hybrid ventilation system models. In general, the model provides combined capabilities of both COMIS and ADS. The detailed description of the model can be found in EnergyPlus Input Output Reference and Engineering Reference manuals.

7.3. Model Validation

There were two steps to perform model validation. The first step was to validate duct performance with given supply air flow rates and surrounding conditions. The outlet air temperature and flow rates at each duct component were compared to the measured data, including supply and return leaks. The purpose was to ensure the duct model works properly. The second step was to validate whole building performance to compare zone conditions and HVAC system energy use. The second step validated not only the duct model, but also whole building performance by utilizing many of EnergyPlus' state-of-the-art capabilities, including the use of existing models for moisture adsorption/desorption from interior building materials and AC equipment models that properly account for moisture removal under part-load operating conditions, which significantly impact resulting energy consumption and indoor humidity levels.

7.3.1. Duct Model Validation

The duct model assumes steady-state system operation without thermal capacity impact for both ducted airflows and the ductwork itself. The model description can be found in both EnergyPlus Input Output and Engineering References. After generating an EnergyPlus input file for a whole building including duct system characteristics, model validation was performed against measured data which was obtained from the Building Science Lab building described in Section 6. The supply air conditions at the discharge of the cooling coil were used as prescribed conditions and surrounding attic zone conditions were used as boundary conditions in the duct model validation. Given those boundary conditions, supply airflow rates and temperatures were modeled. Table 7-1 provides comparison (percent difference) between simulation results and measured data, for both average and maximum difference. The averaged percent airflow difference between simulation and measurement was obtained from 16 measured points, including ducts, supply registers, and return grills. The average percent temperature difference between simulation and measurement were obtained from 17 measured points, including coils, ducts, supply registers and return grills.

Table 7-1. Duct Model Validation Differences BetweenMeasured and Simulated Data

Case	Description	Airflow		Temperature	
		Avg (%)	Max (%)	Avg (%)	Max (%)
1	No leak	1.45	-4.12	1.95	3.82
2	30% Return leak	1.55	-3.00	1.76	3.08
3	30% Supply leak	2.79	-6.16	1.75	8.09
4	30% Supply and return leaks	3.03	-5.34	2.48	9.41

7.3.2. Model Limitations and Assumptions

Although EnergyPlus is a sophisticated building simulation tool, the current program has its limitations, compared to reality. Therefore, simplified assumptions or approaches were used in whole building validation. Main limitations and associated assumptions or approaches are described below:

- ***Fan Operation***. The present AirflowNetwork model only allows a constant volume fan, which operates continuously based on a given schedule, regardless of coil operation. The BSL building operates in auto-mode fan mode (fan cycles ON only when the compressor is active). In order to match reality, it was assumed that fan operates 30 minutes per hour between 1 AM and 6 AM and 45 minutes between 10 PM and 12 AM midnight. The fan runs continuously for the remainder of the day (i.e., 6 AM to 10 PM).

- ***Moisture Simulation***. EnergyPlus has two models to simulate moisture performance: Moisture Transfer Function (MTF) and Effective Moisture Penetration Depth (EMPD). The MTF model simulates heat and vapor transfer in a surface by assuming linear moisture properties within a certain range. Due to moisture non-linearities, it is difficult to use the MTF model for annual simulation without careful consideration of the moisture capacitance coefficients. The EMPD model only considers moisture adsorption/desorption at the interior surfaces. Neither model is able to provide complete simulation of moisture transfer in a wall assembly. Nevertheless, the EMPD model was used in the present study to include moisture adsorption and desorption at interior surfaces. The predicted indoor moisture (RH) level will deviate substantially from the measured values if the EMPD model is not used.

- ***Leaky Ceiling***. The acoustic ceilings are very leaky, with average measured leakage of 5 CFM50/ft^2. The current AirflowNetwork model has a component to deal with a small crack for a horizontal surface and may not be applicable to the very leaky ceiling. The main restriction is one-way flow. In reality, two-way flows occurs between the attic and office zones.

- ***Internal Air Circulation***. Since the air barrier in the BSL building is roof (when the attic space is not vented) and the thermal barrier is at the ceiling, the internal air circulation is expected to occur due to temperature difference between office zone and attic zone. The model is unable to calculate internal air circulation correctly.

Since model capabilities may not cover all realities of the building, differences between prediction and measurement are expected.

7.3.3. Whole Building Validation

Detailed instrumentation at the Building Science Lab building (described in Section 6) was used to obtain measured data, which was used as the basis for model validation. The measured data included internal sensible and latent loads, indoor and attic temperatures and RH, cooling system energy use, airflows, temperatures, and RH, and weather data (horizontal solar radiation, dry bulb temperature, relative humidity, wind speed and wind direction). Since EnergyPlus uses only direct normal and diffuse solar radiation, a weather data preprocessor was used to calculate direct normal and diffuse from measured horizontal solar radiation.

Due to model limitations, supply fan energy use was not compared. The building uses “auto” mode to control supply fan operation, simultaneous operation with a cooling coil, while the fan operation in simulations was scheduled based on input, because a constant volume fan was assumed. Therefore, indoor temperature, relative humidity, and cooling coil energy use were used as comparison between measurement and prediction for the whole building validation.

Validation data was collected in the BSL building for four test configurations: 1) no duct leakage, 2) 15% return leak, 3) 15% supply leak, and 4) 15% supply and 15% return leaks. The measurements were obtained between 6/10/2004 and 8/10/2004. Measured indoor conditions and cooling energy use were used to validate simulation results for the whole building performance. The building was divided into two zones (Office zone and Attic zone) in the model inputs, with the building air barrier located at the roof and the thermal barrier (R-19 fiberglass batts) located on top of the acoustic tile ceiling.

Validation No Duct Leaks. Modeled temperatures and relative humidity in the office zone and cooling energy use generally agree well with the measured data (Figures 7-1 through 7-3). Figures 7-1 and 7-2 show measured and predicted temperatures and RH in the office and attic zones with no supply and return leaks on 8/1-3/2004. Figure 7-3 shows measured and predicted cooling energy use for the same period. Since the model does not have the capability to simulate (predict) interzone airflows (due to the model limitations, mentioned above), it was found that addition of 200 CFM of airflow between the office and attic zones yielded good prediction.

Validation 15% Return Leakage. Modeled temperatures and relative humidity in the office zone and cooling energy use generally agree well with the measured data (Figures 7-4 through 7-6). Figures 7-4 and 7-5 show measured and predicted temperatures and RH in the office and attic zones with 15% return leakage on 7/2-4/2004. Figure 7-6 shows measured and predicted cooling energy use for the same period. Since a return leak is moving air across the ceiling (due to unbalanced air flow), no additional interzone flow was introduced.

Validation 15% Supply Leakage. Modeled temperatures and relative humidity in the office zone and cooling energy use generally agree well with the measured data (Figures 7-7 through 7-9). Figures 7-7 and 7-8 show measured and predicted temperatures and RH in the office and attic zones with 15% supply leakage on 6/11-13/2004. Figure 7-9 shows measured and predicted cooling energy use for the same period. Since there is a supply leak, no additional interzone flow was introduced.

Validation 15% Return and 15% Supply Leakage. Modeled temperatures and relative humidity in the office zone and cooling energy use generally agree well with the measured data (Figures 7-10 through 7-12). Figures 7-10 and 7-11 show measured and predicted temperatures and RH in the office and attic zones with 15% return and 15% supply leakage on 6/23-25/2004. Figure 7-12 shows measured and predicted cooling energy use for the same period. Since there are both return and supply leaks, no additional interzone flow was introduced.

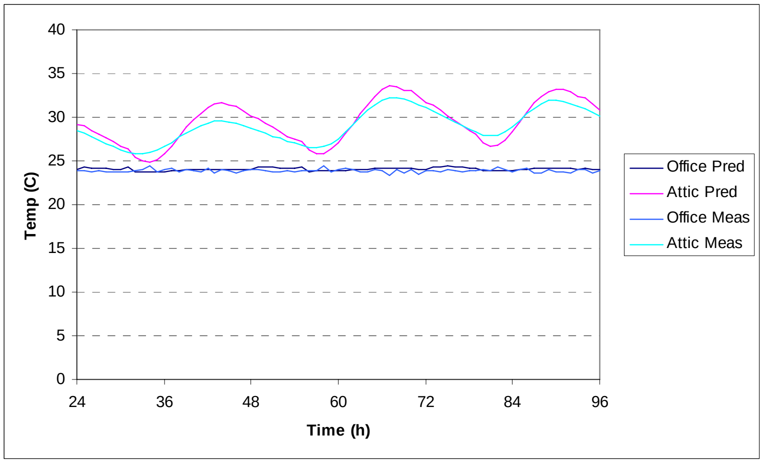

Figure 7-1. Predicted and Measured Zone Temperatures in the BSL Building (no duct leakage)

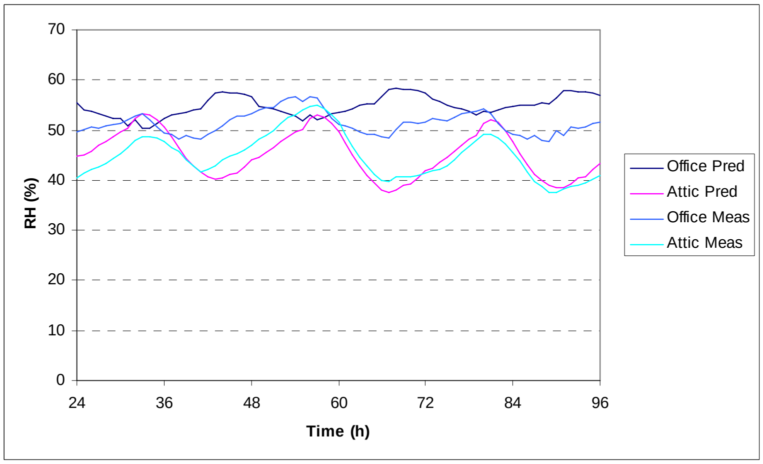

Figure 7-2. Predicted and Measured Zone Relative Humidity in the BSL Building (no duct leakage)

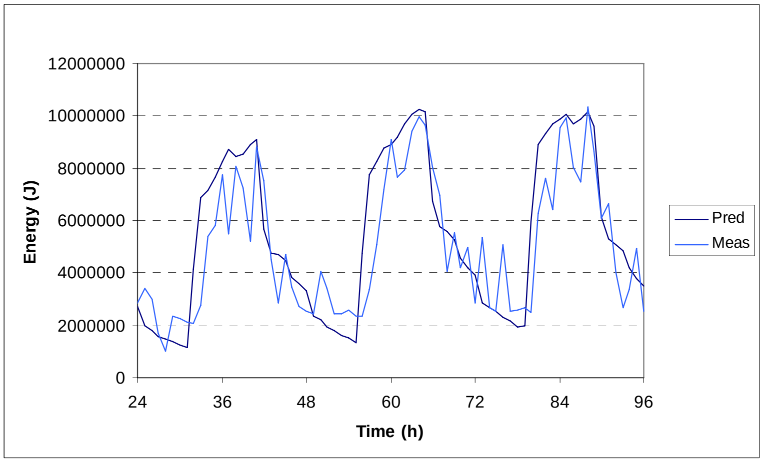

Figure 7-3. Predicted and Measured Delivered Cooling Energy in the BSL Building (no duct leakage)

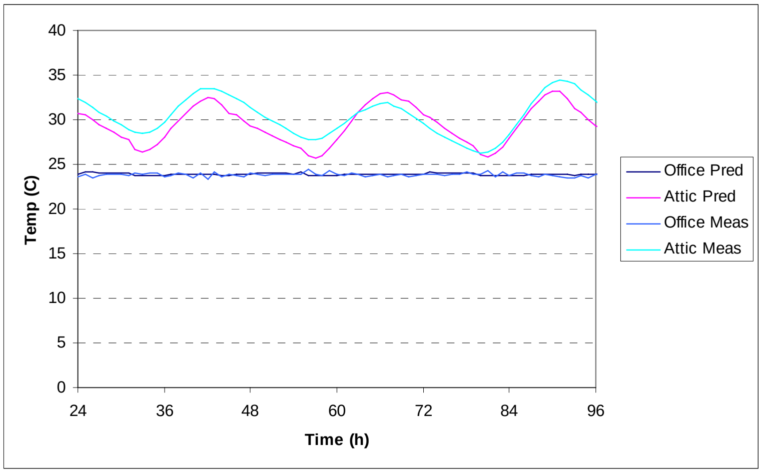

Figure 7-4. Predicted and Measured Zone Temperatures in the BSL Building (15% return leak)

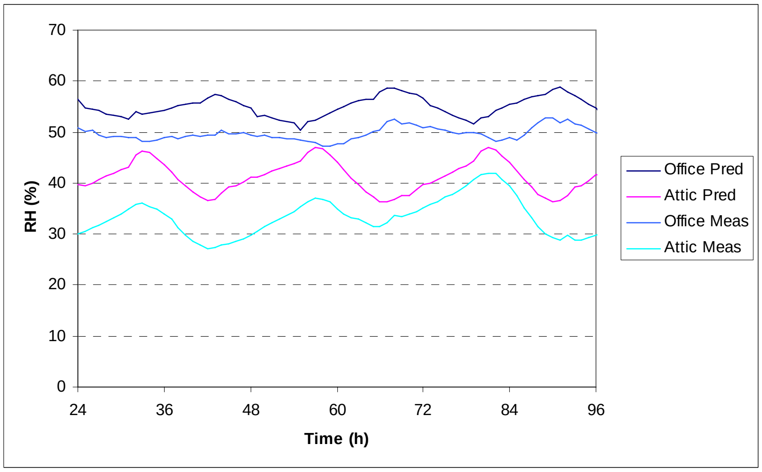

Figure 7-5. Predicted and Measured Zone Relative Humidity in the BSL Building (15% return leak)

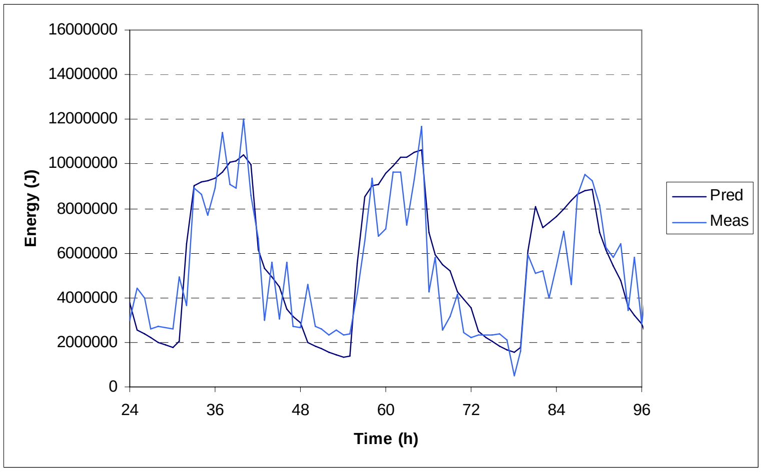

Figure 7-6. Predicted and Measured Delivered Cooling Energy in the BSL Building (15% return leak)

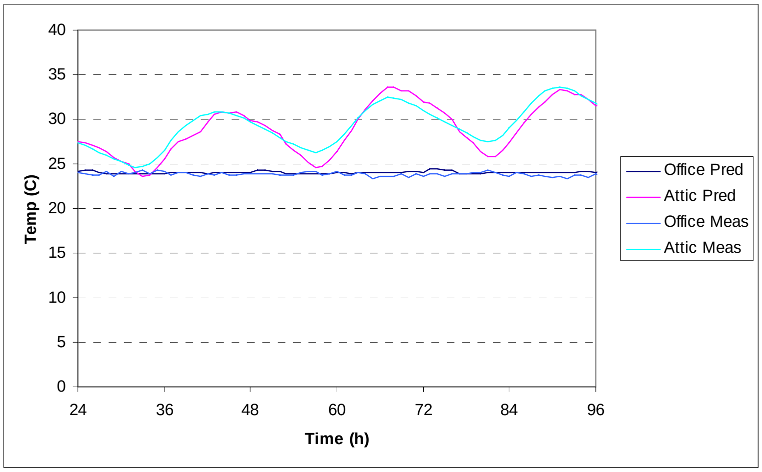

Figure 7-7. Predicted and Measured Zone Temperatures in the BSL Building (15% supply leak)

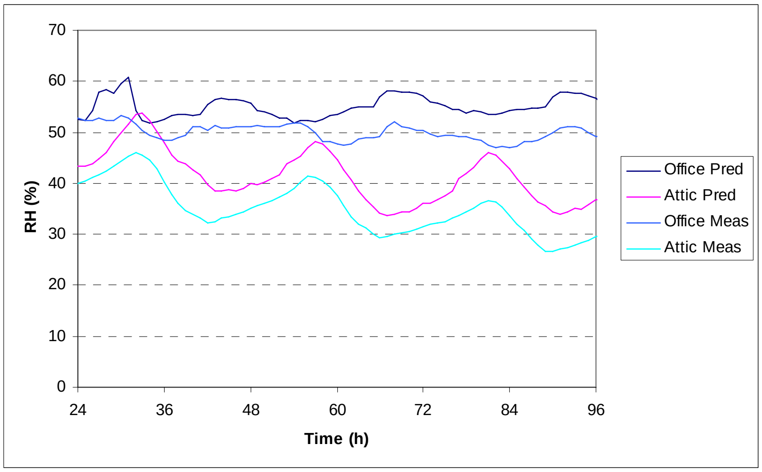

Figure 7-8. Predicted and Measured Zone Relative Humidity in the BSL Building (15% supply leak)

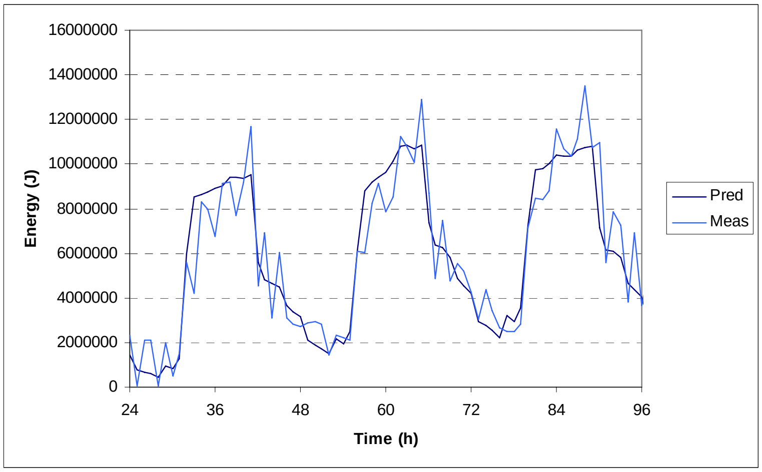

Figure 7-9. Predicted and measured delivered cooling energy in the BSL building (15% supply leak)

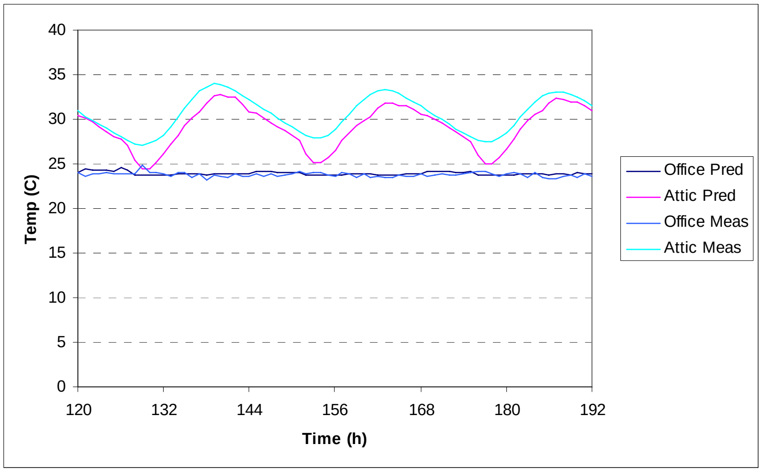

Figure 7-10. Predicted and Measured Zone Temperatures in the BSL Building (15% return and supply leaks)

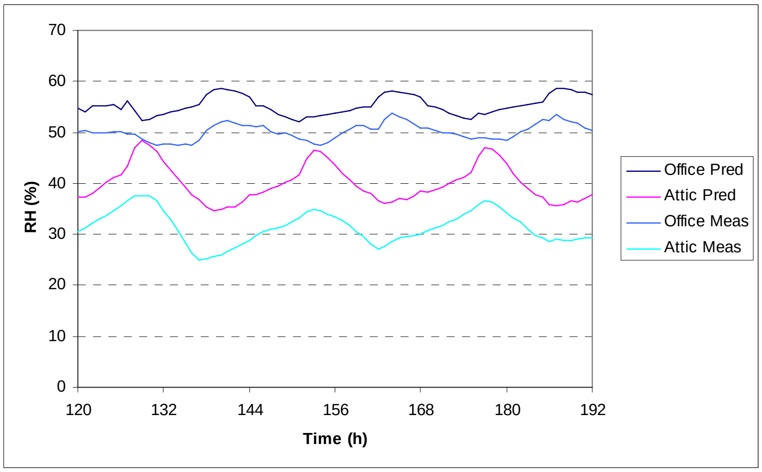

Figure 7-11. Predicted and Measured Zone Relative Humidity in the BSL Building (15% return and supply leaks)

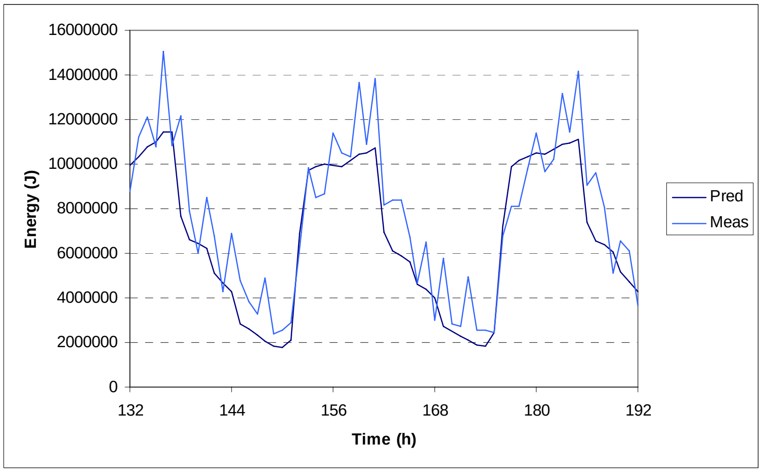

Figure 7-12. Predicted and Measured Delivered Cooling Energy in the BSL Building (15% return and supply leaks)

Table 7-2 presents absolute and percent differences between measured and modeled AC energy use. There appears to be a systematic error in the modeling results, with the model over-predicting cooling energy use for no duct leaks with a trend toward underpredicting AC energy use with supply leaks and balanced duct leaks. Due to limitations, the model overpredicts by about 10% with no duct leaks and underpredicts by about 12% for 15% return and 15% supply leaks.

Table 7-2. Measured Versus Modeled AC Energy Use for Four Duct Leak Configurations (unvented attic)

Case	Description	Period (day)	AC Energy Use (kWh)			
			Measured	Predicted	Difference	% Difference
1	No leak	3	101.25	111.30	10.05	9.9
2	15% Return	3	107.29	113.29	5.99	5.6
3	15% Supply	3	121.22	120.10	-1.12	-0.9
4	15% Return & Supply	2.5	130.66	115.50	-15.16	-11.6

7.4. Parametric Study

7.4.1. Building Characteristics

Although the BSL building is used as a prototypical small office, some building characteristics had to be changed to make the building close to real building. The BSL is used for a lab. Two thermal zones are assumed in simulations: office zone and attic zone. The description of the small office building, as modeled, is listed in Table 7-3.

Table 7-3. Building Description (as modeled)

Characteristics		
Physical characteristics		
	Floor area (ft^2)	2000
	Number of stories	1
Operating conditions		
	Heating setpoint	22 ^{o}C / 71.6 ^{o}F
	Cooling setpoint	24 ^{o}C / 75.2 ^{o}F
	Operation schedule	7AM – 7 PM
HVAC System		
	4 ton AC with COP=3.0	
	Gas Furnace with efficiency=0.8 and 20000 W capacity	
Outdoor air		150 cfm
	Number of People	10
Internal gains	Lights	2000 W
	Equipment	2000 W

TMY2 weather data for four cities in the southern region of the US were used in simulations: Tampa, Miami, New Orleans, and Houston. The four locations mainly represent hot, humid climates.

7.4.2. Parametric Analysis List

The main parameters include envelope leakage and duct leaks in the present study. The envelope leakage consists of three different leakage levels for office wall, attic wall, ceiling and roof: minimum, medium, and maximum. The exterior wall and roof leakage level was varied from 0.1 $CFM50/ft^2$ to 0.3 $CFM50/ft^2$, with the medium level at 0.2 $CFM50/ft^2$. The acoustic ceiling tile leakage level was varied from 3.5 $CFM50/ft^2$ to 6.5 $CFM50/ft^2$, with the medium level at 5 $CFM50/ft^2$. The envelope leakage range is based on field-testing in Florida.

Table 7-4 lists surface leakage values used in the parametric study analysis. No medium roof leakage values are applied, in order to reduce the number of simulations. Annual simulations were run with a total of 18 different envelope leakage cases. Table 7-5 summarizes the envelope leakage levels associated with each case number.

Table 7-4. Envelope Leakage Values ($CFM50/ft^2$) Used in the Annual Simulations

Surface Type	Minimum	Medium	Maximum
Exterior Wall	0.1	0.2	0.3
Attic / Roof	0.1	NA	0.3
Ceiling	3.5	5	6.5

Table 7-5. Cases and Associated Envelope Leaks

Case	Exterior Wall	Attic / Roof	Ceiling
1	Medium	Min	Min
2	Min	Min	Min
3	Max	Min	Min
4	Medium	Min	Medium
5	Min	Min	Medium
6	Max	Min	Medium
7	Medium	Min	Max
8	Min	Min	Max
9	Max	Min	Max
10	Medium	Max	Min
11	Min	Max	Min
12	Max	Max	Min
13	Medium	Max	Medium
14	Min	Max	Medium
15	Max	Max	Medium
16	Medium	Max	Max
17	Min	Max	Max
18	Max	Max	Max

Four different duct leak scenarios are used in the present study, listed in Table 7-6. It is assumed that all return and supply leaks occur in the attic zone. By adding four different types of duct leakage and four locations, the total number of annual simulations is 288.

Table 7-6. Duct System Leakage Values

Scenario	Description	Return leaks (%)	Supply leak (%)
No Leak	No leaks	0	0
S5R10	Dominated return leak	10	5
S10R5	Dominated supply leak	5	10
S10R10	Balance leaks	10	10

It should be noted that the outdoor airflow rate is determined by 15 cfm/person and not used as a parameter. In addition, no exhaust airflow rate is used because the current AirflowNetwork model is unable to simulate an air distribution system and a zone exhaust fan at the same time.

7.5. Simulation Results

7.5.1. Energy and RH Simulation Results

The simulation results reported in the present study are HVAC system energy use and indoor relative humidity during occupied periods. HVAC energy includes both the air conditioning system energy use (kWh) and the gas furnace heating system energy input (also expressed in kWh). Internal loads remain the same in all the cases. Good RH control is defined as RH≤ 60% (ASHRAE Standard 55), which in most cases will prevent mold growth. If indoor relative humidity is above 60%, it may yield indoor quality problems. ASHRAE Standard 160 (Proposed new standard currently under public review) recommends indoor design humidity with air-conditioning of 50%. Therefore, this analysis has examined the number of hours per year that the indoor RH exceeds 60% and the number of hours per year that the RH falls in the range of 50% to 60%. As it turns out, there are no hours when indoor RH exceeds 60%, according to the simulation results. Keep in mind that the building that is being modeled does not have venting of the attic space (ceiling space). Consequently, the roof deck is the primary air boundary of the building, and the uncontrolled airflows produced by the duct leakage are unable, therefore, to transport significant amounts of water vapor into the conditioned space. The resulting indoor RH would be dramatically different if the attic space were vented.

Figure 7-13 through 7-16 plot annual HVAC energy use in four locations with different envelope and duct leak configurations. The "no leak" legend represents ducts without leaks. The "S5R10" legend represents 5% supply leak and 10% return leak with respect to the total supply airflow. The "S10R5" and "S10R10" legends represent 10% supply leak and 5% return leak, and 10% supply leak and 10% return leak, respectively. The case numbers presented in figures are defined in Table 7-5.

Some energy conclusions can be drawn. In general, any duct leakage can cause more energy use. However, return leaks have less impact upon energy use than supply leaks for this type of building with unvented attic. The annual energy use for S10R5 and S10R10 (the same amount of supply leakage but different return leakage) are similar. In addition, the maximum building envelope leakage yields the largest impact on annual energy use (Cases 12, 15, and 18), because more infiltration is introduced through the envelope. The minimum building envelope leakage yields the lowest annual energy use (Cases 2, 5, and 8).

Figures 7-17 through 7-20 are frequency plots showing the number of hours with indoor relative humidity between 50 and 60% during occupied time. Since none of any cases has indoor relative humidity above 60% in all four climate locations, it is important to see the number of hours with RH between 50 and 60%, in order to determine which scenarios have the best humidity control. The largest numbers of hours occur in the cases with the maximum envelope leaks (Cases 12, 15, and 18), because more infiltration is brought into conditioned spaces. These cases also show the largest annual energy use. The lowest numbers of hours happen in the cases with the minimum envelope leaks, corresponding to the lowest annual energy use. Therefore, reducing envelope leaks can not only have better indoor humidity control, but also decrease annual energy use.

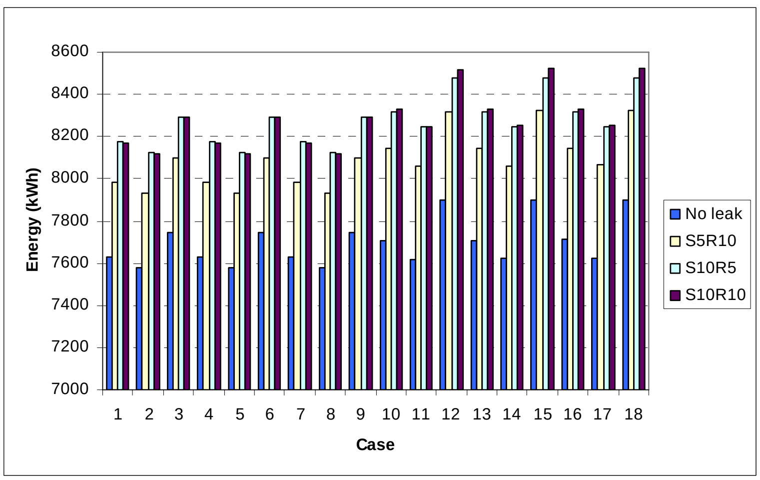

Figure 7-13. Annual HVAC System Energy Use in Tampa

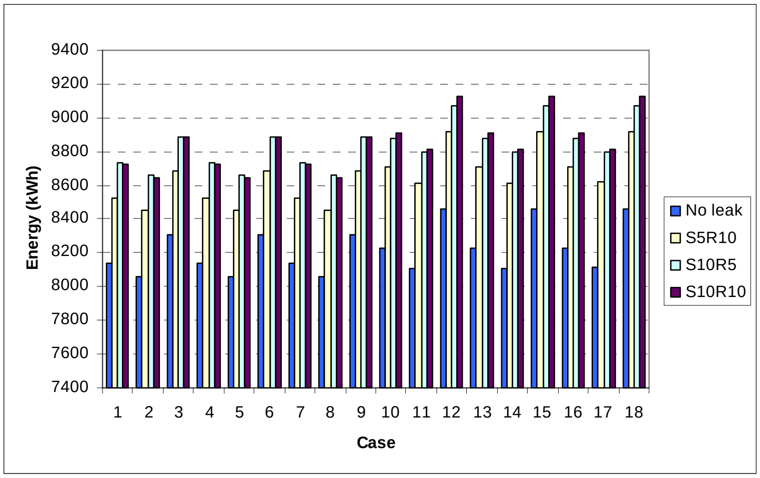

Figure 7-14. Annual HVAC System Energy Use in Miami

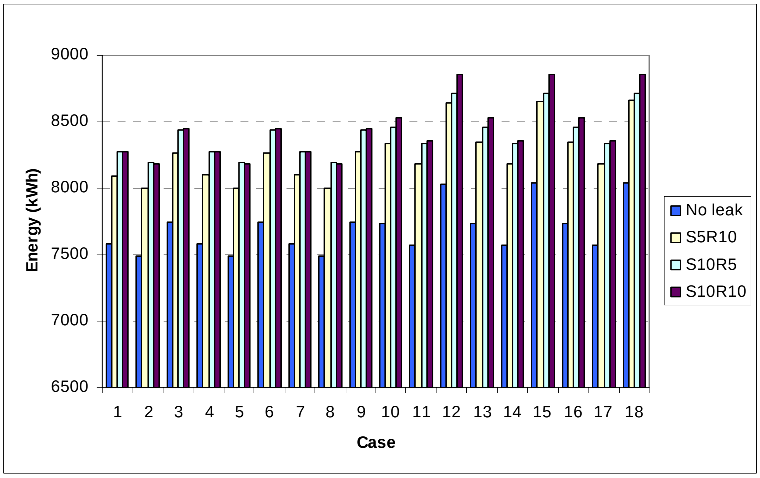

Figure 7-15. Annual HVAC System Energy Use in Houston

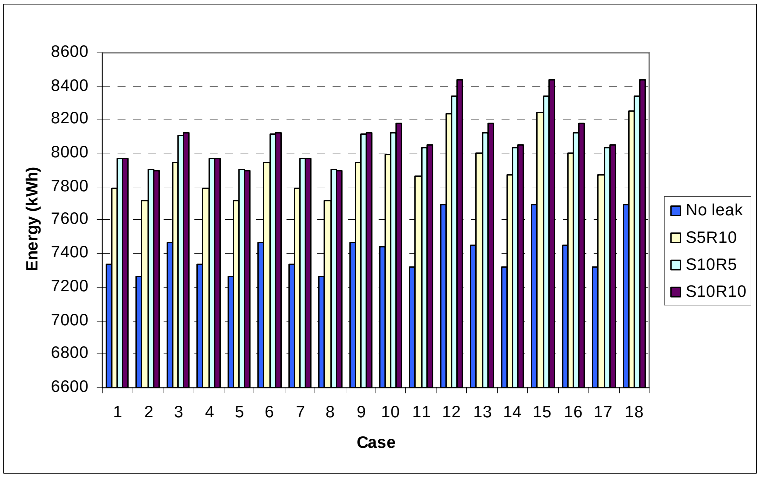

Figure 7-16. Annual HVAC System Energy Use in New Orleans

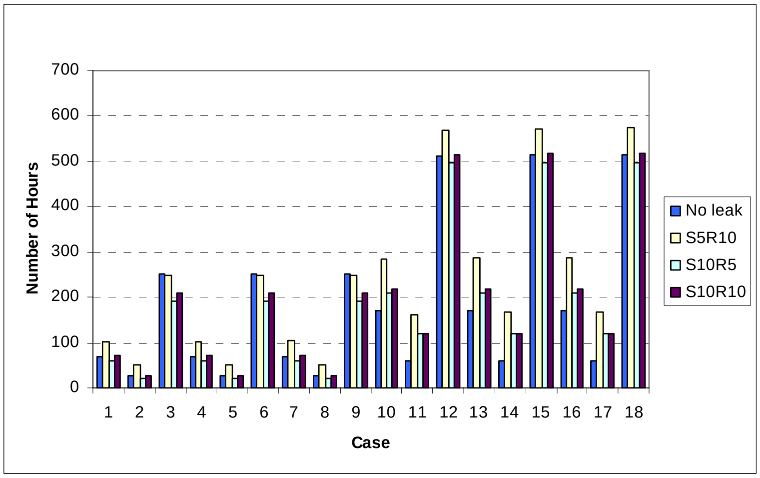

Figure 7-17. Number of Hours with Indoor RH between 50 and 60% in Tampa

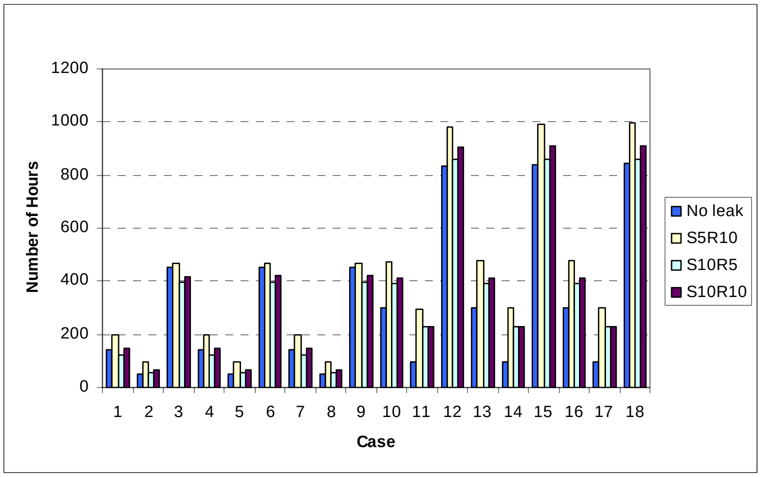

Figure 7-18. Number of Hours with Indoor RH between 50 and 60% in Miami

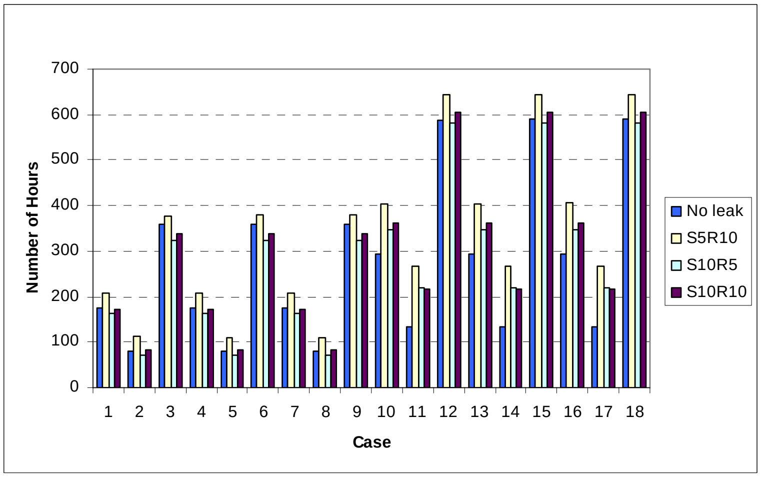

Figure 7-19. Number of Hours with Indoor RH between 50 and 60% in Houston

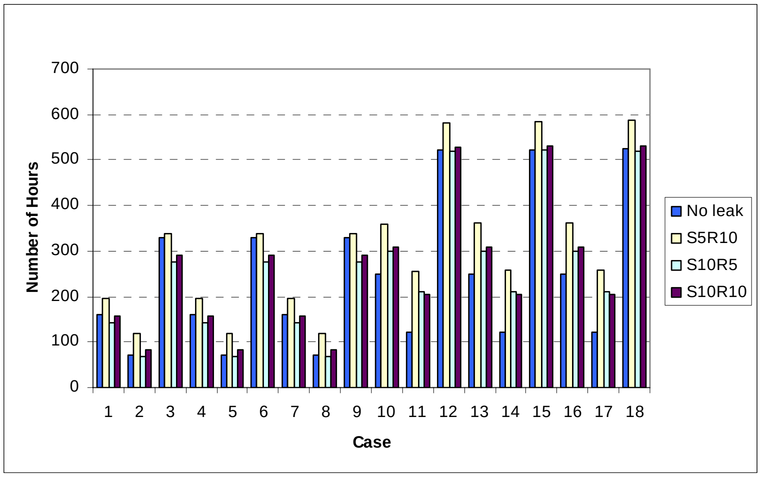

Figure 7-20. Number of Hours with Indoor RH between 50 and 60% in New Orleans

7.5.2. Summary of Simulated Energy and RH

Table 7-7 presents annual HVAC system energy use and the numbers of hours with indoor relative humidity between 50 and 60% for all 18 cases (for the average building envelope leakage). Miami has the highest annual HVAC energy use while New Orleans has the lowest. Miami also has the highest number of hours with indoor relative humidity above 50% while Tampa has the lowest.

Table 7-7. Annual HVAC Energy Use and RH

Location	HVAC Energy Use (kWh)				Number of Hours (with RH between 50% to 60%)			
	No leak	S5R10	S10R5	S10R10	No leak	S5R10	S10R5	S10R10
Tampa	7696	8091	8273	8279	182	237	183	194
Miami	8218	8652	8838	8850	314	421	342	364
Houston	7692	8259	8404	8443	272	336	284	296
New Orleans	7421	7927	8080	8109	242	310	253	263
Average	7757	8232	8399	8420	253	326	266	279

Notes: Number of occupied hours between 50% and 60%. Results are for the average building envelope tightness.

Annual HVAC energy use varies with different levels of envelope and duct leakage. With the unvented attic, the addition of 10% supply and 10% return leakage yields approximately 8.5% increase in combined cooling and heating energy use. The energy penalties would be much higher with the vented attic space, as was observed in the monitored data from the Building Science Lab building (see Table 6-10 in Section 6 of this report).

The simulation results show that RH is well controlled in the modeled building. In none of the cases does the indoor RH level exceed 60% during occupied hours. In fact, for the worst case (Miami with S5R10), indoor RH exceeds 50% for an average 1.6 hours per day (occupied hours). It was also true for the monitored data (from the Building Science Lab experiments) that indoor RH did not exceed 60% with the unvented attic. As long as the building envelope is tight, the standard AC system with “auto” fan control can achieve good RH control (even with duct leakage). While the duct leakage does, in fact, transport a modest amount of water vapor into the conditioned space (when the attic space is unvented and the insulation is at the ceiling level), it also transports large amounts of sensible heat from the attic space into the conditioned space which causes the AC system to run longer and remove, in effect, essentially all of the additional moisture that has been introduced.

7.6. Conclusions and Recommendations

The following conclusions can be drawn:

- Supply leaks have more HVAC energy use than return leaks.
- Good RH control can be maintained as long as the envelope is tight in hot, humid climates. The tight envelope also reduces uncontrolled airflows caused by unbalanced return and supply leaks.
- Ceiling leakage has little impact on indoor humidity levels.
- Envelope leaks also have an impact on energy use. A tighter building envelope yields lower HVAC energy use.

The following recommendations are given:

- It is a good practice to keep ducts tight so that uncontrolled airflow can be dramatically reduced.
- Do not vent the attic space unless the ceiling plane is quite airtight (not a suspended T-bar ceiling).
- Locate the thermal and air barriers at the same place. Otherwise, an unwanted internal air circulation may occur between conditioned (such as the office zone) and unconditioned space (such as attic zone).

Future studies

- The above conclusions and recommendations in the present study are based simulation results from the prototypical commercial building, mainly based on the FSEC BSL building. Since there are so many variations of small commercial buildings, it is recommended that more building types will be simulated to provide general conclusions and guidance.

The EnergyPlus will be enhanced in FY07 to be able to simulate a supply fan cycling ON only when the compressor is active using the AirflowNetwork model. Future simulations will provide more accurate results.

7.7. References

Walton, G. N. 1989, "AIRNET – A Computer Program for Building Airflow Network Modeling," NISTIR 89-4072, National Institute of Standards and Technology, Gaithersburg, Maryland

EnergyPlus (Version 1.3), 2006, Input Output Reference

EnergyPlus (Version 1.3), 2006, Engineering Reference

COMIS, 1990, "COMIS Fundamentals," Edited by H. E. Feustel and A. Rayner-Hooson, LBL-28560, Lawrence Berkeley National Laboratory, Berkeley, California

ASHRAE Standard 55, 2004, Thermal Environmental Conditions for Human Occupancy, ANSI/ASHRAE Standard 55-2004

ASHRAE Standard 160 (Proposed new standard for public review), 2006, Design Criteria for Moisture Control in Buildings, BSR/ASHRAE Standard 160P

8. UAF Training Developed for New York

The findings from this study pointed to the need to train engineers, contractors and other building practitioners on the need to address uncontrolled airflows in small commercial buildings. Our team – which included the Florida Solar Energy Center, Camroden Associates, CDH Energy, and Syracuse University – developed a one-day training course to meet this need in New York State. The basis for the training course was the workshop series on uncontrolled airflows and good design practice in commercial buildings[2] that FSEC has provided for several years in Florida.

The agenda for the one-day workshop is given in Table 8-1. The workshop was aimed at introducing the concepts uncontrolled air flows to New York building practitioners. Many photos and issues from the New York test sites (Sections 2 and 3 and Appendix A) were incorporated into the training materials. The issues of duct leakage, mechanically-induced pressure differences, and unbalanced air flows were all introduced and explored. The focus of the training was on helping designers understand and address these issues in new construction. Remediation approaches and impacts in existing buildings were also addressed. Northern UAF issues related to heating energy use and ice dams were a key focus.

Table 8-1. Agenda for One-Day UAF Workshop

Title: **Designing Buildings That Work: Solving the Uncontrolled Air Flow Problem**

7:30-8:00	Registration	
8:00 – 8:10	Welcome and Introduction	Henderson/Brennan
8:10 – 8:40	Your experience with buildings – class discussion	Brennan
8:40 – 9:20	Location of bulk water, air, thermal, and vapor barriers	Brennan
9:20 – 9:30	BREAK	
9:30 – 10:05	Location of bulk water, air, thermal, and vapor barriers	Brennan
10:05 – 10:55	Introduction to building air flows	Withers
10:55 – 11:05	BREAK	
11:05 – 11:30	The problem of the leaky building envelope	Withers
11:30 – 12:15	The nature and impacts of duct leakage	Withers
12:15 – 1:15	LUNCH	
1:15 – 1:55	Energy consequences of duct system failures	Henderson
1:55 – 2:45	Nature and impacts of unbalanced return air	Cummings
2:45 – 2:55	BREAK	
2:55 – 3:55	Nature and impacts of unbalanced exhaust air	Cummings
3:55 – 4:30	Overview: controlling air flows in buildings	Brennan

[2] FSEC current series of workshops on “Designing and Maintaining Failure-Proof Buildings” is described at http://www.fsec.ucf.edu/en/education/cont_ed/bldgs.htm

The workshop was held in Albany and Syracuse on April 20 and 21. Lisa Cleckner and Susan Pale from the Syracuse Center of Excellence handled workshop logistics. The workshop speakers included: Jim Cummings and Chuck Withers from FSEC, Terry Brennan from Camroden Associates, Bob Carver from NYSERDA, and Hugh Henderson from CDH Energy. In total, 60 participants took part in the two workshops. Participants included, engineers, architects, energy consultants, code officials, and contractors.

Table 8-2. Locations, Date and Attendance for One-day UAF Workshop

Date	Venue	Attendance
Thursday April 20, 2006	Syracuse Genesee Grand Hotel	15
Friday April 21, 2006	Albany Nanotechnology Center	45

9. Conclusions and Recommendations

This multi-faceted study evaluated several aspects of uncontrolled air flows in commercial buildings in both Northern and Southern climates. Field data were collected from 25 small commercial buildings in New York State to understand baseline conditions for Northern buildings.

Laboratory wall assembly testing was completed at Syracuse University to understand the impact of typical air leakage pathways on heat and moisture transport in wall assemblies in both Northern and Southern building applications. The experimental data from the laboratory tests were used to verify heat and moisture (HAM) simulation models that could be used evaluate a wider array of building applications and situations.

Whole building testing at FSEC's Building Science Laboratory (BSL) systematically evaluated the energy and IAQ impacts of duct leakage with various attic and ceiling configurations. This systematic test carefully controlled all aspects of building performance to quantify the impact of duct leakage and unbalanced flow. The newest features of the EnergyPlus building simulation tool were used to model the combined impacts of duct leakage, ceiling leakage, unbalanced flows, and air conditioner performance. The experimental data provided the basis to validate the simulation model so it could be used to study the impact of duct leakage over a wide range of climates and applications.

The main conclusions from this program are summarized below. Recommendations for future research are given in the subsequent section.

9.1. Summary and Conclusions

9.1.1. Field Testing

The field test results from the 25 small commercial buildings in New York identified some differences and some similarities compared to the Florida (Cummings et al 1996) and California (Delp et al 1998) field studies. A summary of the findings are listed below:

- The sample of 25 buildings in this study were larger on average than the 69 Florida buildings (median floor area of 9,204 ft^2 in NY compared to 5,030 ft^2 in Florida). However, the range of building types included in the sample were generally in line with the distribution of building types identified in the 1999 CBECS study for the Northeast region.
- The average ACH50 for NY buildings was 11.4 air changes per hour, compared to 16.7 air changes per hour in the Florida study. The lower ACH50 for the NY buildings appears to have been due to the smaller number of buildings without an air barrier at the ceiling or roof (16% in NY compared to 42% in Florida).

- The exponent determined from the blower door tests at 17 buildings averaged 0.65, which is in line with the FSEC study (with average of 0.61) as well as other industry experience.
- The average building in this study was depressurized by about 1.1 Pa, which is very similar to the FSEC findings for Florida Buildings. Only 7 of the tested buildings operated at positive pressure (one of these buildings was positive because it had a broken exhaust fan).
- The normalized fan power (Watts per cfm) was determined for several air handlers ranging from 2.5 to 55 tons. The average fan power was 0.59 W/cfm, which is in line with findings from other field studies (Proctor and Parker 2000). The data did not show any variation in normalized fan power as function of unit size or airflow.
- Duct leakage measurements were taken on 14 different systems from 8 different NY buildings. The average and median duct leakage (ELA-25) normalized for air conditioner tonnage was 12.8 and 7 in^2 per ton. The average values from the Florida and California field studies were 12.1 and 17.1, respectively. The NY buildings showed a wide degree of variation in duct leakage rates, similar to what had been observed in the other field studies.

At three of the tested buildings we identified and implemented improvements to reduce energy use and or improve comfort. The impact of these improvements was quantified by continuously monitoring building energy use and analyzing monthly utility bills.

A major lesson from all the tested buildings was to confirm the importance of designing and implementing an effective air barrier for the building. At a few of these buildings that were relatively new, seemingly-minor decisions made during construction had a significant impact on building energy use. For instance, installing gypsum board (or some other air barrier) above the t-bar ceiling at Sites 1, 2, 21 and 22 during construction would have created an effective air barrier at the ceiling for a modest cost. Once construction was complete and the building is occupied – with the ceiling tiles and electrical/mechanical systems in place – it is prohibitively disruptive and expensive to install an air barrier.

A somewhat surprising finding from the three mitigated buildings in this section was significant energy savings that can be provided by relatively minor, low-cost improvements. At Sites 1 and 2, replacing and/or repositioning fiberglass batts in the ceiling had significant energy impacts. The annual heating energy savings from fixing major voids in the building envelope were 44% at Site 1 and 37% at Site 2. We found missing or fallen fiberglass batts in two of 25 sites, or 8% of the buildings in this New York sample.

At Site 17 we used spray foam as a low-cost way to seal air leaks in a poorly-insulated attic floor. We also carefully sealed the elevator shaft in this historic, 3-story building. These modest, low-cost improvements resulted in annual heating energy savings of about 25%.

9.1.2. Wall Assembly Testing and Simulations

Another element of the program evaluated the impact of air leakage on the performance of various wall assemblies. Performance issues include understanding the impact of leakage on the thermal performance of the wall assembly as well as durability and IAQ issues related to condensation risk and mold formation inside the wall.

Two different wall assemblies were selected based on the field experiences in NY and Florida. Care was taken to construct the wall assemblies to be representative of normal construction practices, including workmanship related to window installation and sealing. The wall assemblies were tested in the Full-Scale Coupled Indoor/Outdoor Environmental Simulator (C-I/O-ES) at Syracuse University. Indoor and outdoor environmental conditions were imposed on the wall to represent climatic conditions typical of Northern and Southern small commercial buildings. The laboratory measurements focused on understanding the impact of air leakage on temperature and humidity conditions inside the wall assembly.

The following conclusions can be drawn from the laboratory test results:

- Detail elements can contribute significantly to thermal bridging. Steel studs especially those in exposed areas such as the window sill or plate can significantly affect the temperature profile of the construction.
- Change in airflow (reversal of air flow direction) from the exterior to the interior of side (from cold to warm side) can have a significant localized temperature effects within the assembly
- Although, the effect of airflows does not significantly affect the surface temperature of the steel studs, this effect is pronounced and highly affects the conditions within the assembly and more specifically the relative humidity within the insulation cavity. This in actuality becomes counter positive. As warm moisture laden air flows through the wall cold surfaces can cause the flowing air to be cooled. If cooled significantly below the dew point then condensation can take place.
- The thermal mass effect in the masonry wall appears to be very small. The sensors indicate that the appearance of steady state is reached relatively soon.

The simulation model LATENITE was used to predict the impact of air leakage on temperature and humidity conditions inside the wall assembly for a wide array of climatic conditions. The following conclusions were drawn from these simulation efforts:

- The significance of air leakage from wall assemblies and whole building is different. More leakage from the whole buildings does not necessarily mean more leakage from the wall assemblies per unit area. Larger buildings can have larger volume-to-surface area ratio meaning that smaller whole building leakage rate does not necessarily tell what air leakage the building envelope is exposed to.
- For steel frame structure, more condensation will occur at the place where the thermal bridge exists when the indoor air temperature is lower.
- Moisture accumulation in the wall assemblies has been simulated for several severe situations. For example, in the steel frame wall, the moisture tends to accumulate closer

to the interior side of wall assemblies when the air leakage flow comes from outside in the summer. In the winter, the moisture intends to accumulate closer to the exterior side of wall assemblies. Too much cooling can cause severe moisture condensation problems on the interior side of the walls in hot and humid climates, especially when a vapor barrier is located on the cold side of the wall assembly

- The steel frame wall had a polyethylene vapor retarder and the wall was not very leaky. However, the air pressure differences across the wall resulted in significant effects inside the wall cavity.
- Under hot and humid summer conditions, walls with an impermeable interior surface such as vinyl wall paper but otherwise leakage can lead excessive moisture accumulation behind the interior surface material, resulting favorable conditions for mold growth.

9.1.3. Whole Building Testing and Simulations

Whole building testing at FSEC's Building Science Laboratory (BSL) systematically evaluated the airtightness, infiltration, relative humidity, energy, and peak demand impacts of duct leakage – during the cooling season – with various attic and ceiling space configurations. The two primary independent variables were the amount of attic venting and the amount of duct leakage. Data were collected with the building and ductwork in 16 different configurations. Configurations 1 through 8 were with an unvented attic (hot and dry attic conditions). Configurations 9 through 16 were with a vented attic (hot and humid attic conditions). Duct leaks ranged from 0% to 15% to 30% on both return and supply sides of the air distribution system. Test data were collected over several hundred days during 2004, 2005, and 2006.

The building was found, by means of blower door testing, to be moderately airtight with the unvented attic, with an ACH50 of 5.2. The pressure drop of 0.9 Pa across the ceiling and 49.1 Pa across the roof deck indicates that the roof deck is the primary air boundary. The building was found to be very leaky with the vented attic, with an ACH50 of 29. The pressure drop of 39 Pa across the ceiling and 11 Pa across the roof deck indicates that the ceiling is the primary air boundary when the attic is vented.

Tracer gas decay testing found that the vented attic contributes substantially to the building infiltration rate. With no attic venting, the average infiltration rate was about 0.15 ach with or without duct leakage. With the attic vented and no duct leakage, the average infiltration rate was about 0.5 ach. With the attic vented and 15% duct leaks, the average infiltration rate was about 1.2 ach. With the attic vented and 30% duct leaks, the average infiltration rate was about 1.5 ach. The strength of the wind affected the vented attic infiltration rates significantly.

Attic dry bulb temperature averaged about 1^{o}F warmer when unvented. Attic humidity levels were dramatically impacted by attic venting. Attic dew point temperature (absolute humidity) averaged 54^{o}F when unvented and 72^{o}F when vented, with some variation based on duct leakage amount. Indoor dew point temperature increased substantially as a result of attic venting, from about 55^{o}F to about 60^{o}F. Indoor RH increased from 50% to 59%, on average, as a result of opening the attic vents.

Cooling energy use increased as a result of attic venting and as a result of duct leakage. Attic venting increased cooling energy use by an average of 12% for a range of duct leak configurations. Duct leakage increased cooling energy use by 20% to 35% for various duct leaks for the unvented attic. Duct leakage increased cooling energy use by 20% to 50% for various duct leaks for the vented attic.

Peak cooling demand increased by 10% to 40% for the unvented attic, for various duct leak configurations, and by 12% to 58% for the vented attic, for various duct leak configurations.

The AirflowNetwork model was recently incorporated into Version 1.3 of EnergyPlus as part of this project. These new feature provides the means to simulate the impacts of duct leakage, unbalanced air flows, and attic space interactions in an air conditioned building. An EnergyPlus model of the BSL was developed to simulate the performance of duct leakage under the various tested scenarios. The simulation model compared reasonably well with the experimental data, properly predicting space and attic humidity levels as well as air conditioner energy use. The model was then used to simulate the impacts of various levels of supply and return duct leakage for vented and unvented attics in a prototypical 2,000 ft^2 office building located in several different climates (Tampa, Miami, Houston, New Orleans). The simulation results confirmed many of the findings from the laboratory test:

- Both supply and return duct leaks increase air conditioner energy use,
- Supply leaks have are greater impact on HVAC energy use than return leaks,
- Good RH control is maintained as long as the envelope is tight in hot, humid climates; a tight envelope reduces the impact of unbalanced return and supply leaks.
- Leaks in the building envelope also have an impact on air conditioner energy use. A tighter building envelope yields lower HVAC energy use.

9.2. Recommendations for Future Work

A common theme from the field study portion of the project is the need create an effective air barrier at a modest cost with minimal disruption to the building occupants. Weatherization and insulation contractors need better information, approaches and diagnostic tools to identify and address air barrier problems.

New commercially-available materials – such as small polyurethane spray foam kits (with 200-500 board feet of foam) – offer the potential to cost effectively address these issues. Developing practical and cost effective ways to use these new materials can provide significant energy savings in existing buildings.

There also be potential to use lower cost diagnostic tools, such as infrared thermometers, to diagnose and identify problem areas in buildings instead of more expensive tools such as infrared cameras. Developing low cost means to quickly diagnose and identify opportunities to improve building performance will be of great use to building practitioners.

Both the wall assembly and whole testing efforts were complemented by efforts to develop and validate computer simulation approaches. In both cases these models can be used in future work to understand the impact of uncontrolled air flows in other building applications. The LATENITE model can be used to quantify the impact of air leakage on the durability, IAQ risks, and energy performance of wall assemblies in wide array of applications. Similarly, the newly developed AiflowNetwork features of EnergyPlus will provide the means to evaluate the impacts of duct leakage and unbalanced flows in a wide array of commercial and residential building applications.

Summary of Field Test Results (FSEC-Style Table)

Site	CBECS Category	Building	Description	Location	Year Built	Renovated	Age	Use	Stand Alone	Construction Type	Exterior Finish
1	office	Office Building	Human Service Agency	Utica, NY	1987		17	1	Yes	Frame/Masonry	Brick
2	office	Office Building	Accounting Office	Cazenovia, NY	1980	1996	8	1	No	Frame	cedar siding
3	restaurant	Restaurant	Chinese Take-Out Restaurant	Cazenovia, NY	1992		12	7	No	Frame	sedar siding
4	office	Office Building	Admin Office for Medical Testing	New Hartford, NY	1932	1960	44	1	Yes	Masonry	Stucco/Cinder Block
5	office	Office Building/Training Ctr	Engineering Offices & Training Center	Syracuse, NY	1974		30	2	Yes	Masonry	Brick
6	food	Supermarket	Supermarket	Hauppauge, NY	2002		2	4	No	Masonry	Stucco/Cinder Block
7	restaurant	Fast Food Restaurant	Fast Food Restaurant	Herkimer, NY	2002		2	7	Yes	Frame/Masonry	Block
8	worship	Church	Church	Rome, NY	1991		13	8	Yes	Frame/Masonry	Brick
9	restaurant	Fast Food Restaurant	Fast Food Restaurant	Lockport, NY	2002		2	7	Yes	Frame/Masonry	Block
10	office	Office Building	Department of Public Works	Ithaca, NY	1960	2000	4	2	Yes	Metal & Masonry	EFIS
11	office	Office Section Only	Airport Administration	Ithaca, NY	1995		9.0	1	No	Masonry	Brick
12	office	Office Building (2 story)	Manufacturing Office	Cazenovia, NY	1998		6	2	Yes	Metal	Aluminum Composite
13	public	Fire Department	Fire Department	Cazenovia, NY	1989		15	10	Yes	Masonry	Brick
14	public	Office Building	Public Safety (911 dispatch center)	Ithaca, NY	2004			2	Yes	Frame/Masonry	Brick
15	office	Office Building (2 story)	Coop Ext Office (General)	Ithaca, NY	1980	2001	3	2	No	Masonry	Stucco/EFIS
16	office	Office Building	Coop Ext Office (Agriculture)	Ithaca, NY	1980	2001	3	1	No	Masonry	Stucco/EFIS
17	assembly	Social Club (3 story)	Social Club	Syracuse, NY	1853	1893	111	7/8	Yes	Masonry	Brick
18a		Office	HVAC Offices	Syracuse, NY	1940	1986	18	1	No	Masonry	Brick
18c	warehouse	Warehouse	Carpet Warehouse	Syracuse, NY	1986		18	10	No	Masonry	Stucco/Cinder Block
19	office	Office Building	Teacher's Union Office	New Hartford, NY	1985		19	2	Yes	Frame/Masonry	Brick
20	assembly	Movie Theater	16 Theaters and an IMAX	Rochester, NY	1996		8	8	Yes	Masonry	Stucco/Cinder Block
21	service	Retail / Auto Service	Retail Auto Repair	Clinton, NY	1985		19	3	Yes	Frame	Metal Siding
22	retail	Retail Garage	Farm Equipment Sales & Repair	Clinton, NY	1996		8	3	Yes	Pole Barn	Metal Siding
23	retail	Retail	Big Box Retail	Oneonta, NY	2005			4	Yes	Masonry	Stucco/Cinder Block
24	nursing	Nursing Home (2 story)	Nursing Home	Waterville, NY	1970		34	5	Yes	Masonry	Brick
25	office	Office & Apartment	Office & Apartment	Cazenovia, NY	1900	1997	7	1	Yes	Frame	Vinyl Siding
Average					1976		17.2				
Median											

FSEC Average			***21.3***				
Standards							

Summary of Field Test Results (FSEC-Style Table)

Site	Insulation	Structural Wall	# Stories	Slab / Crawl	Roof Girder	Current Building Converted From	# AHUs	Heating Input (MBtuh)	Cooling (tons)	Tons/1000 ft^2	Gas Use (MBtu/ft^2-year)	Electricity Use (kWh/ft^2-year)
1	OSB/Fiberglass Batt	Wood Frame	1	Slab	Wood	No	2	320	10	1.98	56.5	7.8
2	Fiberglass Batt	Wood Frame	1	Slab	Wood	Previous Commercial	1	75	2.5	1.73	74.3	4.0
3	Fiberglass Batt	Wood Frame	1	Slab	Wood	Previous Commercial	1				616.0	26.5
4	Fiberglass Batt	Wood Frame	1	Slab	Steel	Previous Commercial	4		20	2.87	34.7	26.2
5	Rigid Insulation	Concrete Block	1	Slab	Steel	No	2		80	4.49	26.4	29.7
6	KOR/Fiberglass Batt	Metal Frame	1	Slab	Steel	No	7	1,836	81.5	1.43	41.0	39.3
7	Fiberglass Batt	Wood Frame	1	Slab	Wood	No	4	373	24	7.27	431.2	116.1
8	Fiberglass Batt	Wood Frame	2	Slab	Wood	No	8	825	28	3.25	58.5	2.4
9	Fiberglass Batt	Wood Frame	1	Slab	Wood	No	5	466	27	8.18	486.0	105.1
10	EFIS/Fiberglass Batt	Steel Frame	2	Slab	Steel	No	4	1,960	37	2.57	83.1	6.5
11		Concrete Block	1	Slab	Steel	No	2	178	8	2.43		
12	Fiberglass Batt	Steel Stud	2	Slab	Steel	No	10					
13	Rigid Insulation	Concrete Block	2	Slab	Steel	No	2	175	9.5	0.97	37.5	2.8
14	Fiberglass Batt	Studded	1	Slab	Wood	No	3	411	45	3.57	104.9	12.8
15	EFIS	Concrete Block	2	Slab	Wood	Previous Commercial	16		27.5	2.65	38.8	8.9
16	EFIS	Concrete Block	1	Slab	Steel	Previous Commercial	2		7	2.86	50.2	10.4
17	none	Brick	3	Basement	Wood	Previous Residential	10				61.4	4.2
18a	Fiberglass Batt	Wood Frame	1	Slab	Wood	Previous Commercial	2		9	1.49		
18c	Rigid Insulation	Concrete Block	1	Slab	Steel	Previous Commercial	1					
19	Fiberglass Batt	Wood Frame	1	Basement	Wood	Previous Commercial	4	400	10	0.73	29.0	3.4
20	EFIS/Fiberglass Batt	Metal Frame	2	Slab	Steel	No	35	7,160	541.5	5.63		
21	Fiberglass Batt	Wood Frame	1	Slab	Wood	Previous Commercial	1	150	5	1.50	70.9	6.1
22	Fiberglass Batt	Pole Barn	1	Slab	Wood	No	2					
23	EFIS	Concrete Block	1	Slab	Steel	No	20		293	2.22		
24	none	Concrete Block	2	Slab	Steel	No	19		37	0.42	93.8	7.2
25	Fiberglass Batt	Wood Frame	2	Basement	Wood	No	1		3	0.90		
Average							6.5	1,102	62.2	2.8	133.0	23.3
Median												
FSEC Average Standards							***3.13***		***16.1***	***3.38***		

Summary of Field Test Results (FSEC-Style Table)

Site	AHU Location	Duct Location	Supply (cfm)	Return (cfm)	Duct Type	Building Cavity Duct	Full Occupancy	Building Floor Area (ft^2)	Occupied Volume (ft^3)	Thermal Volume (ft^3)	Air Volume (ft^3)
1	Mechanical Room	Unconditioned Space	1952	2227	Metal/Flexduct	Ceiling Space	25	5,040	40,320	47,880	40,320
2	Mechanical Closet	Unconditioned Space	1048	820	Metal	None	10	1,443	12,386	13,829	12,386
3	Unit Heater	None	-	-	None	None	15	1,034	9,991	9,991	9,991
4	Attic	Unconditioned Space	4910	4332	Metal/Flexduct	None	50	6,974	65,670	73,806	115,067
5	Occupied Space	Conditioned Space	2971	-	Metal/Flexduct	Ceiling Space	170	17,819	257,389	287,760	287,760
6	Roof Top	Conditioned Space	29900	-	Metal	None	150	57,000	808,940	990,000	990,000
7	Roof Top	Conditioned Space	3610	-	Metal/Flexduct	None	100	3,300	27,591	38,002	38,002
8	Mechanical Room	Conditioned Space	11679	8274	Metal	None	75	8,607	98,056	119,301	119,301
9	Roof Top	Conditioned Space	5235	4173	Metal/Flexduct	None	100	3,300	27,591	38,002	38,002
10	Roof Top	Conditioned Space	11008	3538	Metal/Flexduct	Ceiling Space	50	14,400	121,423	170,869	170,869
11	Garage Area	Conditioned Space	1508	1249	Metal/Flexduct	None	25	3,289	30,968	40,833	40,833
12	Ceiling Space & Roof	Conditioned Space	10957	2037	Metal/Flexduct	Ceiling Space	60	12,700	100,568	137,169	137,169
13	Mech Rm & Ceiling Plenum	Conditioned Space	1893	1580	Metal/Flexduct	Ceiling Space	25	9,800	121,434	131,919	131,919
14	Mechanical Room	Conditioned Space	3253	857	Metal/Flexduct	Ceiling Space	30	12,600	125,042	153,996	153,996
15	Roof, Closet, wall	Conditioned Space	4211	2527	Metal/Flexduct	mixed	80	10,391	113,834	151,274	151,274
16	Exterior Shed	Conditioned Space	1931	1338	Metal/Flexduct	None	11	2,451	31,666	39,161	39,161
17	Basement	Conditioned Space		-	Metal	Basement	200	14,694	134,618	134,618	134,618
18a	Closet & Roof	Conditioned Space	3305	-	Metal	None	20	6,021	66,217	66,217	66,217
18c	Unit Heaters	None	-	-	None	None	30	10,700	307,808	307,808	307,808
19	Basement	Conditioned Space	4503	2857	Metal	None	40	13,720	133,198	133,198	133,198
20	Roof Top	Conditioned Space	-	-	Metal	None	800	96,214	2,472,106	2,472,106	2,472,106
21	Adjacent To Building	Semi-conditioned Space	1631	1587	Metal/Flexduct	None	10	3,332	29,433	29,433	29,433
22	In Space	Conditioned Space	1146	942	Metal/Flexduct	None	10	3,994	39,940	39,940	39,940
23	Roof Top	Conditioned Space	117050		Drop Box	None	150	132,000	3,168,000	3,168,000	3,168,000
24	Roof Top	Conditioned Space			Metal/Flexduct	None	200	88,000	704,000	704,000	704,000
25	Window	None			none	None	6	3,323	24,930	24,930	24,930
Average							101	20,852	348,966	366,309	367,550
Median								9,204	99,312	125,610	125,610

FSEC Average						***26.2***	***5,030***	***52,125***	***61,455***	***63,489***
Standards										

Summary of Field Test Results (FSEC-Style Table)

Site	Roof Slope	Ceiling Material	Air and Thermal Barrier Configuration	CFM50	ACH50	ELA (sq-in @ 4 Pa)	Surface Area (ft^2)	Occupied Space Surface Area (ft^2)	ELA/100 ft^2 Envelope Area (sq-in @ 4 Pa)	Power Law Coefficient, K	Power Law Exponent, n	Coefficient. of Determination (R^2) for $Q=KP^n$
1	Sloped	T-Bar Ceiling Tiles	7	20,988	31.2	1,567	8,118	12,672	19.3	2,659.2	0.528	0.998
2	Sloped	T-Bar Ceiling Tiles	7	6,807	33.0	447	2,842	4,285	15.7	706.2	0.579	0.978
3	Sloped	Gypsum Board	8	4,169	25.0	290	2,305	3,338	12.6	473.3	0.556	0.999
4	Sloped	T-Bar Ceiling Tiles	6	7,394	6.8	403	12,531	17,614	3.2	574.6	0.653	0.987
5	Flat	T-Bar Ceiling Tiles/Exposed	2	16,902	3.9	808	27,386	43,977	3.0	1,074.5	0.704	0.990
6	Flat	T-Bar Ceiling Tiles/Exposed	1	27,232	2.0	1,695	71,747	123,857	2.4	2,604.3	0.600	estimated
7	Flat	T-Bar Ceiling Tiles	2	6,332	13.8	375	6,033	8,360	6.2	560.0	0.620	estimated
8	Sloped	T-Bar Ceiling Tiles/Tiles Glued to Gypsum	8	12,467	7.6	602	11,820	20,672	5.1	804.9	0.700	0.971
9	Flat	T-Bar Ceiling Tiles	2	6,969	15.2	434	6,033	8,360	7.2	666.5	0.600	estimated
10	Flat	T-Bar Ceiling Tiles	2	13,090	6.5	412	19,695	28,025	2.1	435.2	0.870	0.9998
11	Flat	T-Bar Ceiling Tiles	2	3,934	7.6	210	6,838	9,269	3.1	296.9	0.661	avg
12	Flat	T-Bar Ceiling Tiles	2	5,687	3.4	454	14,341	18,129	3.2	800.5	0.501	0.992
13	Sloped	T-Bar Ceiling Tiles & Gypsum	8	8,188	4.0	311	15,149	23,025	2.1	364.5	0.795	0.999
14	Flat	T-Bar Ceiling Tiles (gypsum in garage)	8	9,279	4.5	495	20,168	30,924	2.5	697.9	0.661	0.988
15	Flat	T-Bar Ceiling Tiles/Metal Roof Decking	2	14,088	7.4	833	19,378	22,966	4.3	654.2	0.603	0.998
16	Flat	T-Bar Ceiling Tiles	2	1,819	3.4	68	5,767	7,342	1.2	79.0	0.802	0.992
17	Sloped	Plaster Walls	8	32,068	14.3	1,898	11,956	15,378	15.9	2,836.0	0.620	estimated
18a	Sloped	T-Bare Ceiling Titles	2	8,680	7.9	498	10,144	14,772	4.9	732.4	0.632	0.997
18c	Flat	Exposed	1	24,628	4.8	2,040	22,741	32,751	9.0	3,664.6	0.487	0.169
19	Sloped	T-Bar Ceiling Tiles	8	3,676	1.7	222	10,760	17,620	2.1	336.1	0.612	0.996
20	Flat	T-Bar Ceiling Tiles	2	33,955	0.8	2,721	163,565	258,115	1.7	4,802.0	0.500	estimated
21	Sloped	T-Bar Ceiling Tiles	7	18,929	38.6	1,120	5,523	8,855	20.3	1,674.0	0.620	estimated
22	Sloped	T-Bar Ceiling Tiles	7	11,907	17.9	705	6,674	10,668	10.6	1,053.0	0.620	estimated
23	Flat	Exposed	1									
24	Flat	T-Bar Ceiling Tiles	2	68,772	5.9	4,281	114,850	202,849	3.7	6,577.0	0.600	estimated
25	Sloped	T-Bar Ceiling Tiles/Gypsum	8	7,094	17.1	347	5,194	9,153	6.7	466.0	0.696	0.996
Average				15,002	11.4	929	24,062	38,119	6.7	1,423.7	0.633	0.941
Median				9,279	7.4	495	11,820	17,614	4.3	706.2	0.620	
FSEC Average				***9,131***	***16.7***		***7,828***			***857.6***	***0.610***	
Standards												

Summary of Field Test Results (FSEC-Style Table)

Infiltration: Normal Building Operation (ACH)	(cfm)	Nominal Leakage Rate (ACH50/20)	Infiltration AHUs Off (ACH)	OA+MA (cfm)	Total Return Duct Leakage	Exhaust (cfm)	Exhaust per Flr Area (cfm/ft^2)	Building Pressure with HVAC On (Pa)	Ductwork ELA (in^2 @ 25 Pa)	Supply Duct Area (ft^2)	Return Duct Area (ft^2)	ELA/100 ft^2 Duct Area (in^2 @ 25 Pa)	Supply CFM per ft^2 Duct Area (cfm/ft^2)	Leakage per 100 ft^2 Duct Area (cfm @ 25 Pa)	SMACNA Leakage Class cfm per 100 ft^2 (cfm @ 1-in water)
0.42	282	1.56		0	n/a	0	0.0		74.0						
0.44	91	1.65		0	491	62	0.0	-2.0	122.0	503.0	380.0	13.8	2.1	122	445
		1.25		0	n/a	3,094	3.0	-41.0							
0.18		0.34		0	1,372	180	0.0	-2.0				9.6	2.4	85	340
0.44	1875	0.20		~0	n/a	0		-1.3	107.0	2,941		3.6	1.0	32	112
		0.10		7,775	no data	3,947	-0.1	2.1							
		0.69		848	1,430	2,319	0.4	-4.8	149.0	458.0	81.0	32.5	7.9	244	1,321
0.24	394	0.38		no data	no data	0		4.7	212.0	837.0	705.0	21.7	5.2	223	553
		0.76		1,681	510	2,595	0.3	-2.0	52.4	559.0	236.0	9.4	9.4	58	436
		0.32		6,325	n/a	2,958	-0.2	6.0				6.0	3.6	53	205
0.25		0.38		no data	no data	0		-1.2							
0.23	384	0.17		406	n/a	854	0.0	-1.0							
		0.20		no data	no data	no data		-4.0				4.6	1.6	40	157
		0.22		no data	no data	no data		-3.9	92.0	1,946.0	913.0	3.2	2.3	29	86
		0.37		234	no data	no data		0.1							
0.36	190	0.17		150	no data	no data		1.1							
0.80		0.71		no data	no data	no data		-0.2							
		0.39		3,305	no data	no data		0.1							
		0.24		no data	no data	no data									
		0.08		no data	no data	278		-0.1							
		0.04		no data	no data	10,115		-3.0							
		1.93		0	no data	17	0.0	-2.0							
		0.89		0	no data	70	0.0	0.1							
						10,589	0.1	-2.0							
1.40	16427	0.29		4,759	no data	16,556	0.1	-2.5							
		0.85					0.0								
0.5		0.6		1,699	951	3,831.0		-2.4				11.6	3.9	98.3	406.2
						278.0		-1.2							
1.25			***0.43***	***697***	***418***	***1,149***		***-1.12***							
															SMACNA Std. = 48

Field Test Site 1 - Small Office Building, Utica, NY

Building from the Front (west)

Building from the Rear (east)

Figure A1-1. Photos of Building

CHARACTERISTICS

Building Description

The 5,040 sq ft facility is a one-story office building with two identical tenant spaces (both spaces are now used by one organization). Each space has separate gas and electric utilities. The building entrance to both spaces is through a vestibule at the south side. Each zone is conditioned by its own air handling unit. The air handlers are forced-air, gas-fired furnaces with A-coils for cooling. Figure A1-2 presents the building floor plan. The facility was built in 1987.

Construction Details

Walls are constructed of brick veneer, OSB sheathing, wood 2x4 studs and gypsum board interior covering. There is an air gap between the brick and OSB sheathing. The walls are insulated with 4” fiberglass insulation.

The roof is constructed of plywood decking on wooden roof trusses. Roofing material is asphalt shingles. Insulation is provided by 9½” paper-backed fiberglass batts that are stapled to the bottom chord of the trusses.

There is a T-bar (drop) ceiling approximately 18 inches below the attic insulation. This 18 inch space is used as the return plenum for the HVAC system. Figure A1-3 shows the details of the ceiling plenum.

The attic is vented with ridge venting, gable-end vents, and a vented cupola. The cupola is above the west section. Figure A1-4 illustrates typical wall and roof sections.

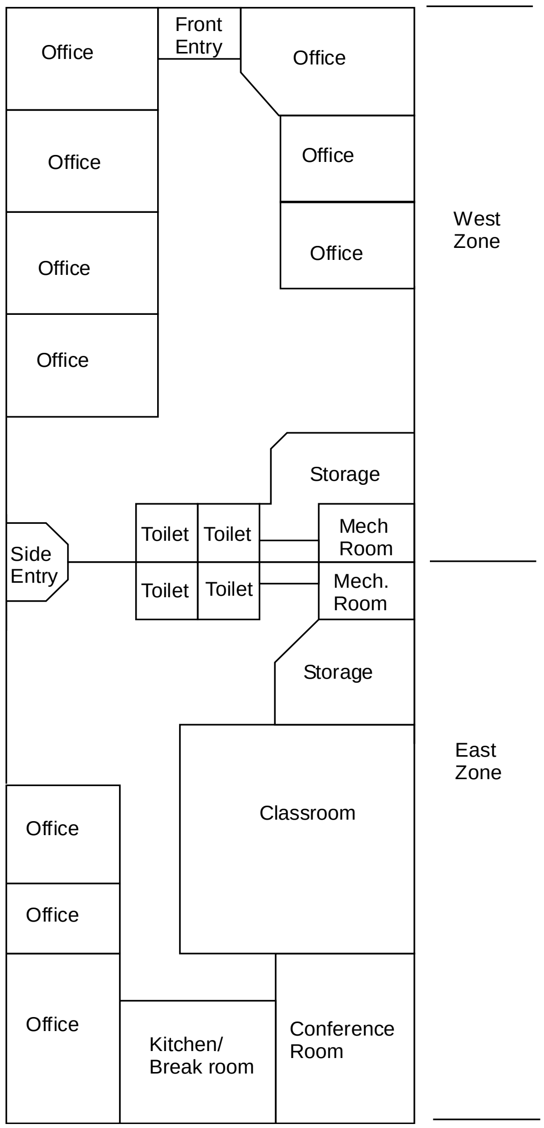

Figure A1-2. Building Floor Plan

Typical supply diffuser

← *Return duct in ceiling plenum*

← *Ceiling plenum with some falling insulation*

Figure A1-3. Photos of Ceiling Plenum Details

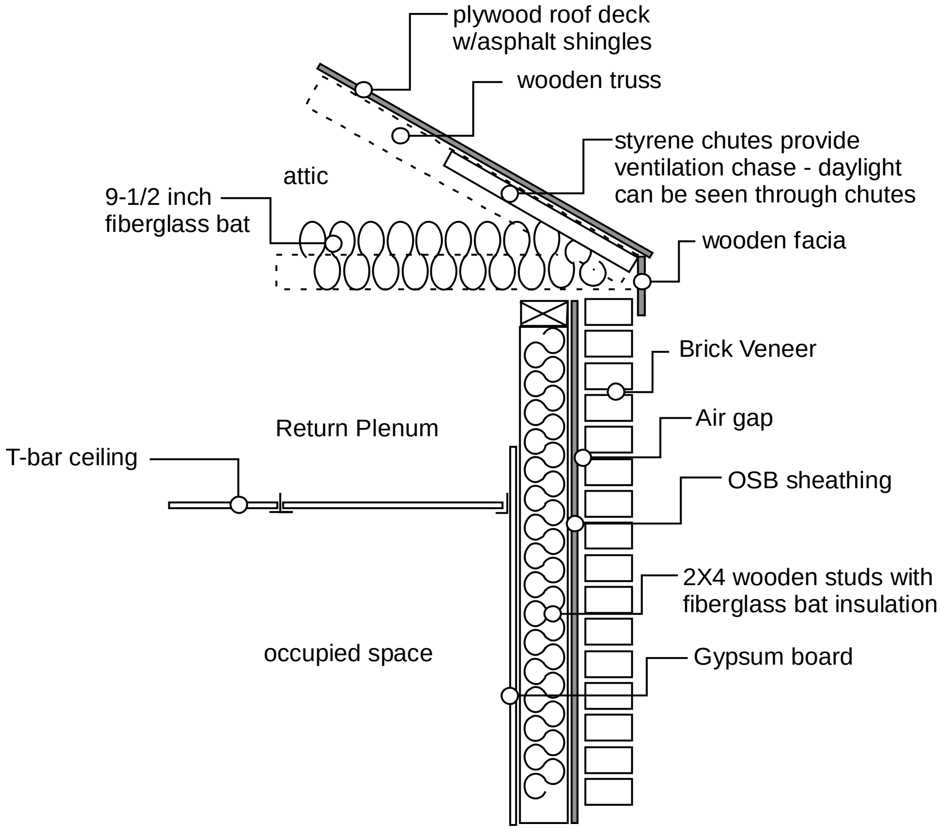

Typical section through wall and roof at Red Cross building in Utica. Gypsum board does not extend much above the T-bar ceiling or across the bottom chord of the roof truss. This leaves fiberglass insulating bat stapled to the truss chord and the T-bar ceiling to provide an air barrier between the occupied space and the ventilated attic. The problem is compounded because this space is a return air plenum.

Figure A1-4. Roof and Wall Sections

An inspection of the attic revealed that many of the fiberglass batts had fallen from between the roof trusses. Figure A1-5 shows the locations of the fallen fiberglass batts. The batts had fallen in November 2003 when a worker had gone into the attic to remove a squirrel and its nest. In the process several batts has been dislodged. Leaving large opening between the ceiling plenum and attic. In total a about 60 linear feet of fiberglass batts had been knocked down, mostly in the front part of the building.

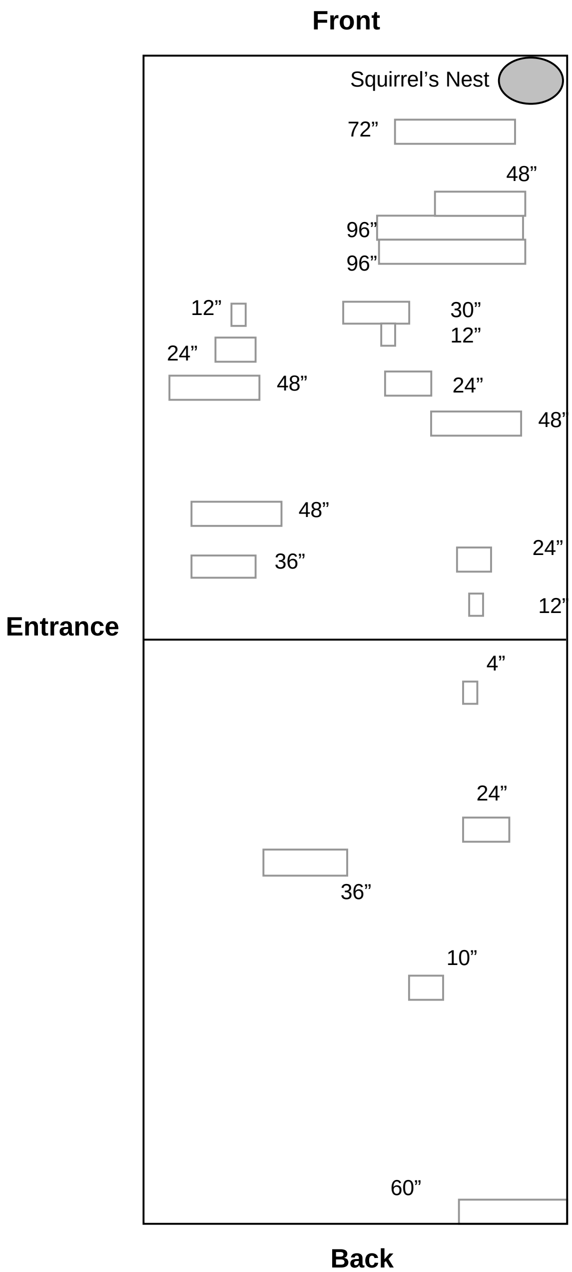

Total Length of Fallen Batts:

Front Area: 52.5 ft
Rear Area: 11.2 ft

Figure A1-5. Location of Fallen Fiberglass Batts (in March 2004)

HVAC System

Each area of the building is heated by a conventional gas-fired furnaces located in a mechanical room. Cooling is also provided by an A-coil on top of the furnace. There are no special provisions to provide ventilation in this residential style system. Supply ductwork is rectangular sheet metal ducting located above the drop ceiling. Each supply diffuser has a flex-duct takeoff. A short sheet metal return duct (8 ft) pulls air from the ceiling plenum (see Figure A1-3).

Each system as a separate setback thermostat.

Furnace, Ductwork & A-coil - East

Figure A1-6. Photos of HVAC System

Table A1-1. HVAC Equipment Installed at Site (each side)

Gas Furnace:	Luxaire 160 MBtu/h input
Air Conditioner – outdoor section:	Luxaire HASE-F060SA 5 ton AC
Air Conditioner – indoor coil:	Luxaire GTUA061AA2 5 ton A-coil w/ orifice

MEASUREMENTS

The test data below was taken on March 5 and March 30, 2004. Blower door, pressure mapping and supply air flow measurements were taken on March 5. Duct Blaster data was collected on March 30. Dan Gott, Terry Brennan, and Mike Clarkin were present both days. Hugh Henderson participated in Testing on March 30.

<u>Building Envelope Airtightness</u>

The leakage characteristics of the enclosure were assessed using fan pressurization methods. Two blower doors were used to depressurize the building to several pressure differences. The test was conducted with all interior doors open (including the glass doors connecting the east and west spaces) and all exterior doors and windows closed. The blower door at the front entry was set at the highest flow (5,400 cfm). The other blower door fan was installed at the rear entrance in the kitchen. Its speed was varied so that the pressure varied from 8 to 16 Pa.

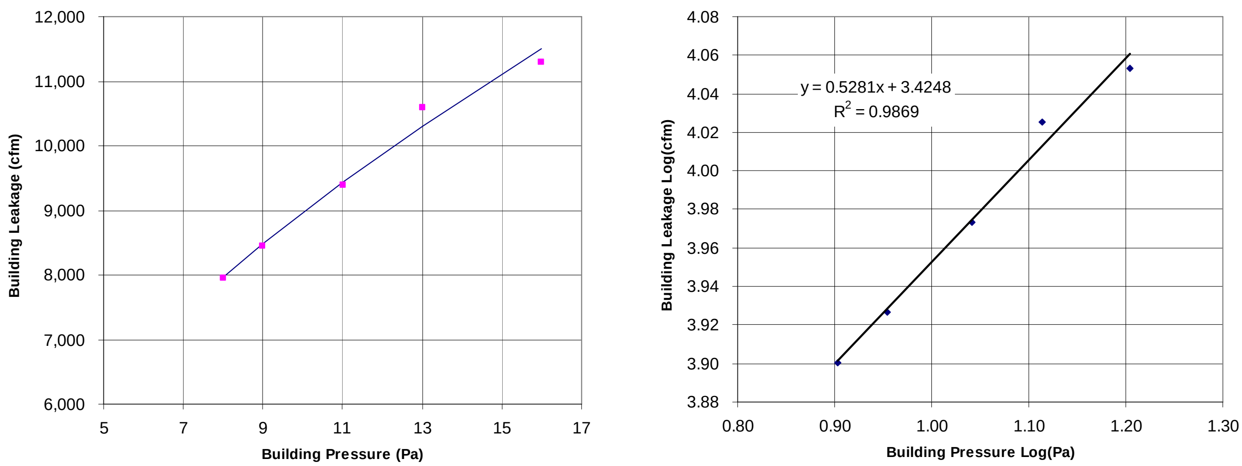

Figure A1-7. Variation of Building Leakage with Pressure: cfm = K(ΔP)^n

Table A1-2. Blower Door Test Data , Resulting Best-Fit Model Coefficients, and ELA

Test Results:

Flow Coefficient (K)	2659.2			
Exponent (n)	0.528			
Leakage area (LBL ELA @ 4 Pa)	1567	sq in	12.36	ELA / 100 sq ft
Airflow @ 50 Pa	20988.0	cfm	31.2	ACH @ 50

Test Data:

	Nominal Building Pressure (Pa)	Fan Pressure (Pa)	Nominal Flow (cfm)	Ring
1	8		7,950	O
2	9		8,450	O
3	11		9,400	O
4	13		10,600	O
5	16		11,300	O
6				
7				
8				
9				
10				

Notes: ELA is leakage area (in square inches) at reference pressure of 4 Pa.
ELA per 100 sq ft is based on total building envelope surface area (ceiling, walls and floor).

Pressure Mapping

The air pressure relationships in the building were determined using a digital micromanometer (DG2). During this test all interior doors were closed (except for the glass doors connecting zones, which remained open). The pressure difference across the building enclosure was 16 pascals (Pa). Figure A1-8 shows the pressure difference across the drop ceiling and the pressure difference across the fiberglass batt ceiling insulation. The arrows on figure indicate the direction of air flow (and decreasing pressure). The pressure difference split evenly – 8 Pa across each layer. This indicates that the leakage area through the fiberglass insulation layer is about equal to the leakage area through the drop ceiling. In the east wing the total pressure difference between the interior space and the attic was 16 Pa, virtually the same as that across the building shell. This implies that the leakage area between the outside and the attic space is very large compared to the leakage area through the fiberglass and the ceiling tile (i.e. the attic is wide open to ambient).

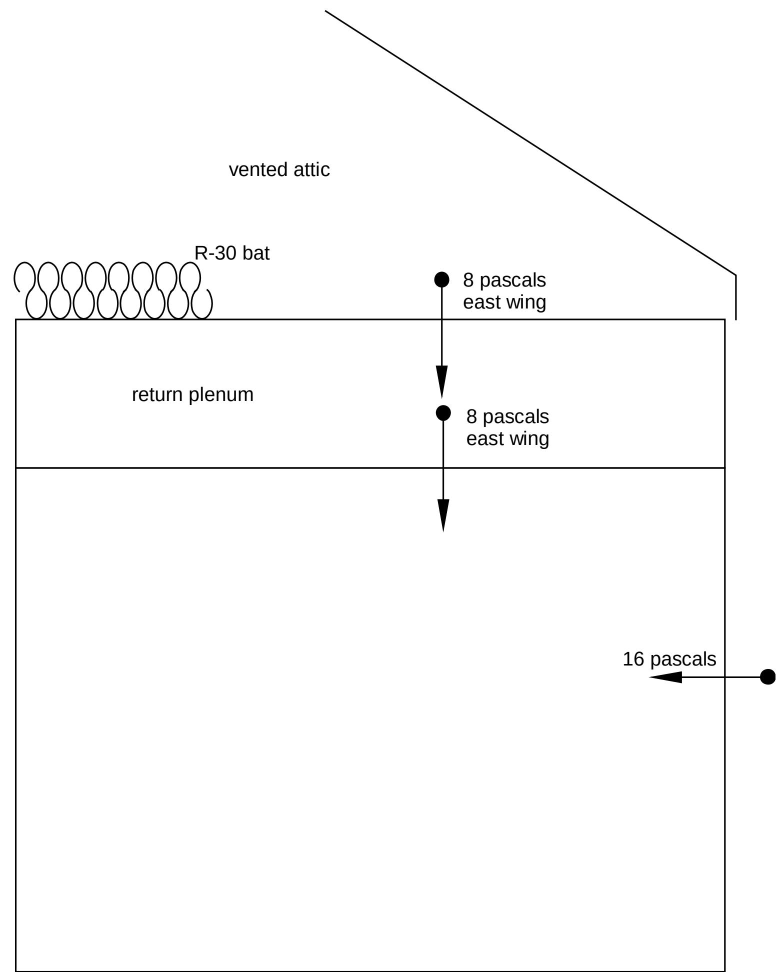

Figure A1-8. Pressure Drop Across Ceiling Elements During 16 Pa Depressurization Test

With the building depressurized, additional measurements were made to provide information on leakage between offices and corridors with doors closed. We also measured the impact of air handler operation on the room pressure differences.

During these tests all office doors were closed. The corridors were depressurized by approximately 20 Pa during two of the tests (AHU on and AHU off). Pressure relationships between enclosed spaces such as offices and the open core areas were measured. The graphics in Figure A1-9 show the pressure differences induced across the doorways to the corridors with the corridors depressurized. Operation of the AHU fans had very little impact (typically less than 1 Pa). Pressure drops across the doorways range between 5 and 13 Pa. The pressure difference between the rooms and corridor are less than half of the overall pressure difference to ambient. Therefore the room-to-outdoor leakage area is probably smaller than the leakage area between the rooms and the corridors.

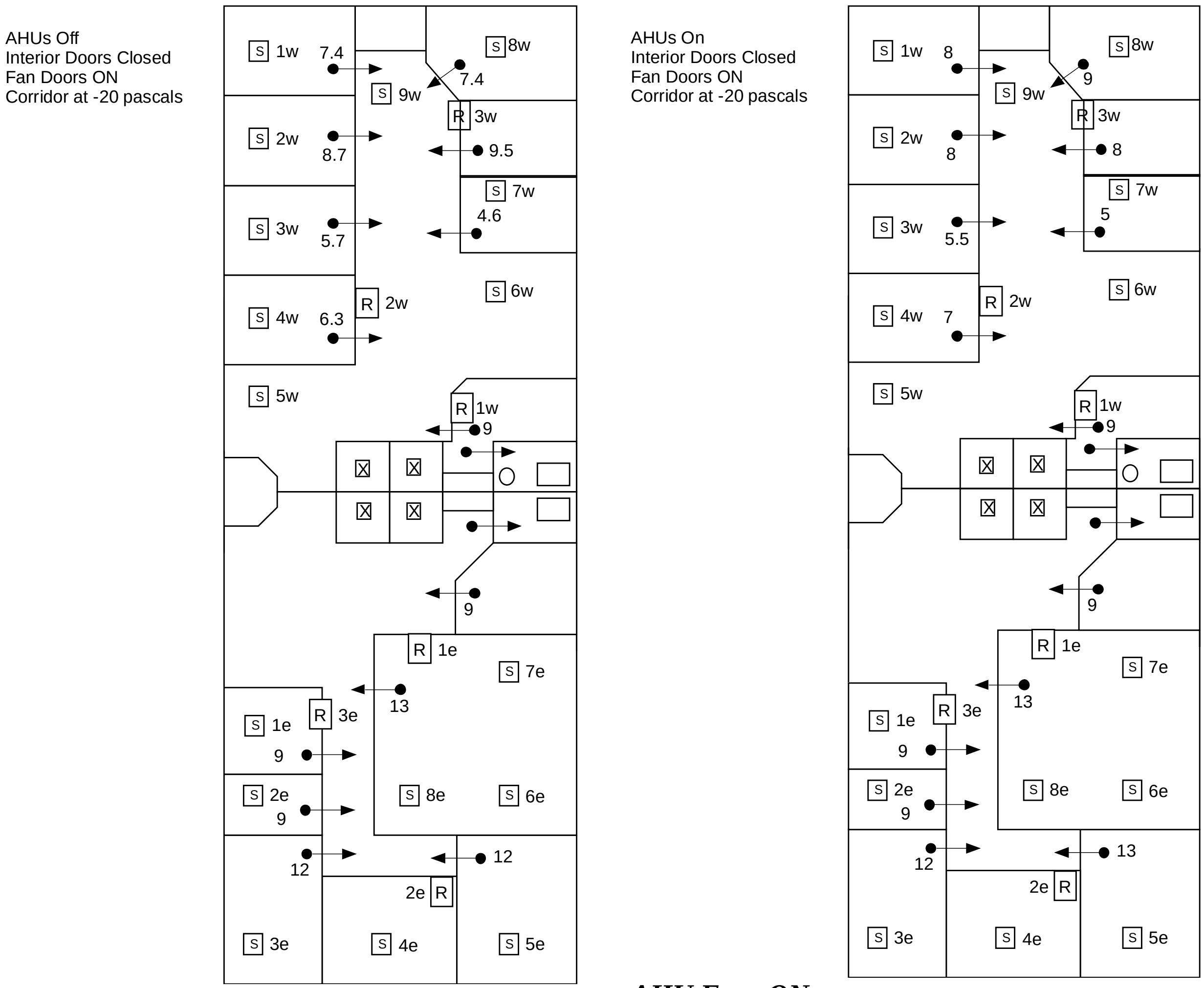

AHU Fans OFF

AHU Fans ON

Figure A1-9. Pressure Differences Between Rooms with Corridors Depressurized to Approx 20 Pa

Figure A1-10 shows the pressure differences induced by operation of the two air handler fans. Less than two pascals pressure difference is produced across any doorway by fan operation. The rooms with the greatest pressure differences would be expected the have the most supply air flow (see Table A1-3). The graph in Figure A1-10 confirms the correlation between the supply air flow and room pressure difference.

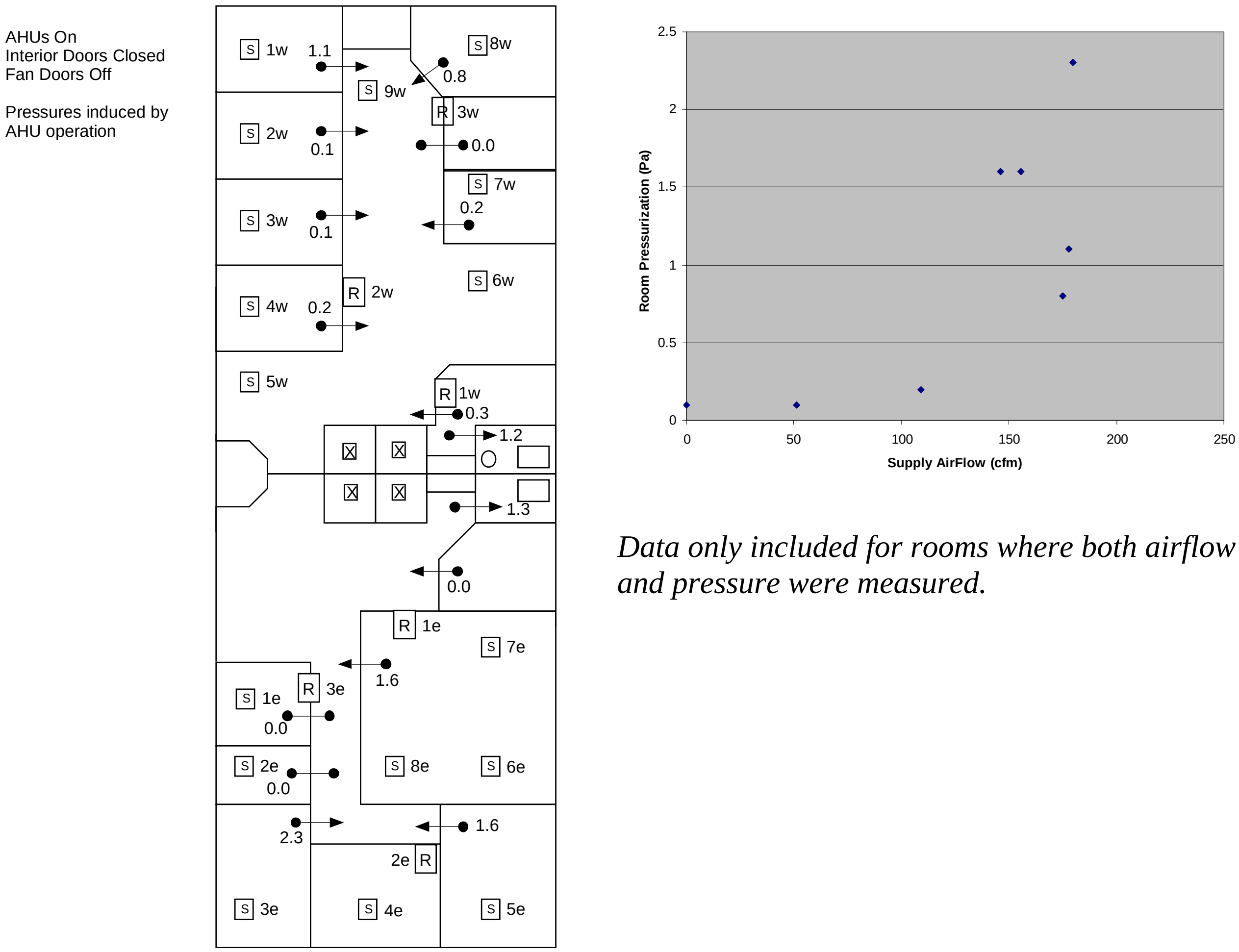

Data only included for rooms where both airflow and pressure were measured.

Figure A1-10. Pressure Differences Induced by AHU Fan Operation

HVAC Airflow Measurements

The airflow from each supply diffuser was measured using three different flow hoods (Shortridge, Alnor, and TSI). Table A1-3 presents the measurement results. The schematic in the table illustrates the locations of each supply and return diffuser.

The calibration was checked on Camroden's Alnor flowhood just before going to the field. CDH's Shortridge flowhood was also recently calibrated. Figure A1-11 compares the Alnor, TSI and Shortridge flowhoods. The Shortridge was selected as the reference and showed good agreement with the Alnor. The TSI reads were around 10-15% lower then these other two hoods[1]. The correlation between the TSI and Shortridge hoods in Figure A1-11 is used to correct the total flow for the east area taken with the TSI hood. This correction is applied in Table A1-3.

There was no measurable airflow entering the returns in the east wing. However, the returns in the West wing ceiling were measured at 140 cfm.

[1] The TSI hood uses a simpler airflow measuring apparatus that is considered to be less accurate than the Shortridge flowhood.

Table A1-3. Supply Airflow Measurements

West Area

Register ID	TSI	Shortridge	Alnor
1w	166	178	176
2w		51	
3w (no diffuser)			
4w	100	109	
5w	190	214	
6w		160	156
7w (closed)			
8w	168	175	163
Total		**887**	

East Area

Register ID	TSI	Shortridge	Alnor
1e (closed)			
2e (closed)			
3e	160	180	
4e	187	205	
5e	130	146	
6e	94	103	
7e	178	210	
8e	142	154	
9e	30		
10e	0		
Total	**921**		
Adjusted with Correlation		**1065**	

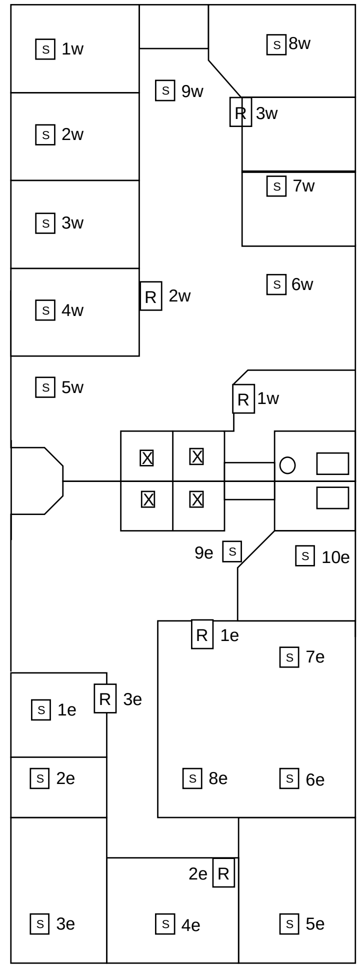

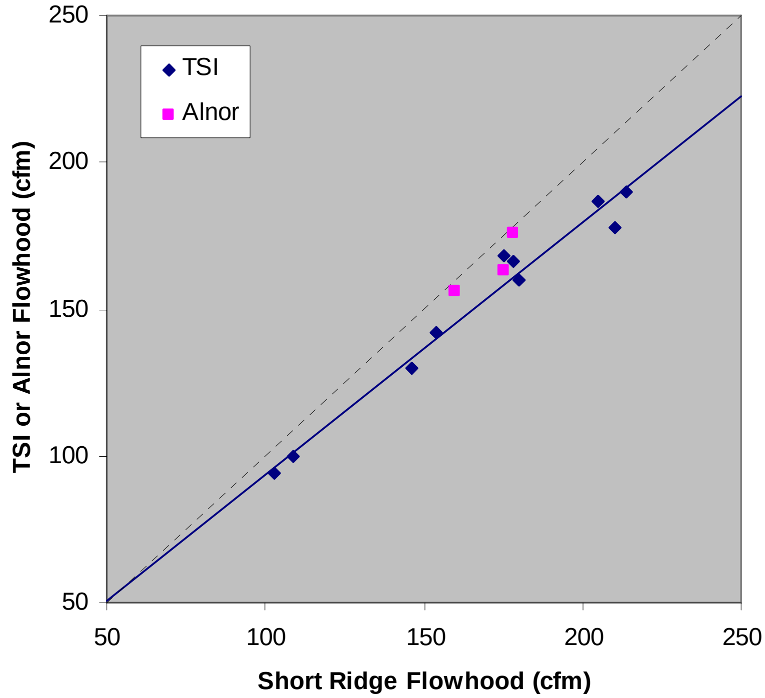

Figure A1-11. Comparison of Flowhood Readings

Table A1-4. Pitot Tube Readings In AC Return Duct

West Return Duct: 11.5" x 22"

	1	2	3
1	854	834	482
2	892	446	257
3	834	576	364

Avg: 615 fpm
Flow: 1,081 cfm

East Return Duct: 11.5" x 22"

	1	2	3
1	576	772	604
2	681	751	656
3	576	681	576

Avg: 652 fpm
Flow: 1,146 cfm

Table A1-5. Comparison of Supply and Return Airflow Measurements

	Flowhood / Supply Airflow (cfm)	**Pitot Tube / Return Airflow (cfm)**	**Supply/Return Ratio (-)**
West/Front AHU	887	1081	0.82
East/Rear AHU	1065	1146	0.93

Duct Leakage Measurements

A Duct Blaster was used to measure leakage rates on the duct work connected to the west and east air handling systems. The supply ductwork is in the plenum space between the drop ceiling and the insulation layer at the bottom chord of the truss. The return portion of the system consists of rectangular galvanized steel duct that opens directly into the return plenum near the mechanical room. In theory the return duct depressurizes the plenum space and draws air from return grilles located in the drop ceiling in the West Wing and in the lower portion of wall cavities open at the top in the East Wing.

The Duct Blaster fan was connected to depressurize the system at the return entrance in the plenum (see Figure A1-12 and Figure A1-13). Plastic wrap was used to cover each supply grill in the system. Duct tape was used to seal the access panel for the filter at the furnace return. Then the duct blaster was used to test the entire duct system (return, furnace cabinet, and supply). The seals at the supply grills and furnace filter with tested with a smoke puffer to confirm there was no leakage at those points.

Duct Blaster fitting on Return Duct in Plenum

Covered Diffuser

Duct Blaster Fan

Figure A1-12. Photos of Duct Blaster Setup and Testing

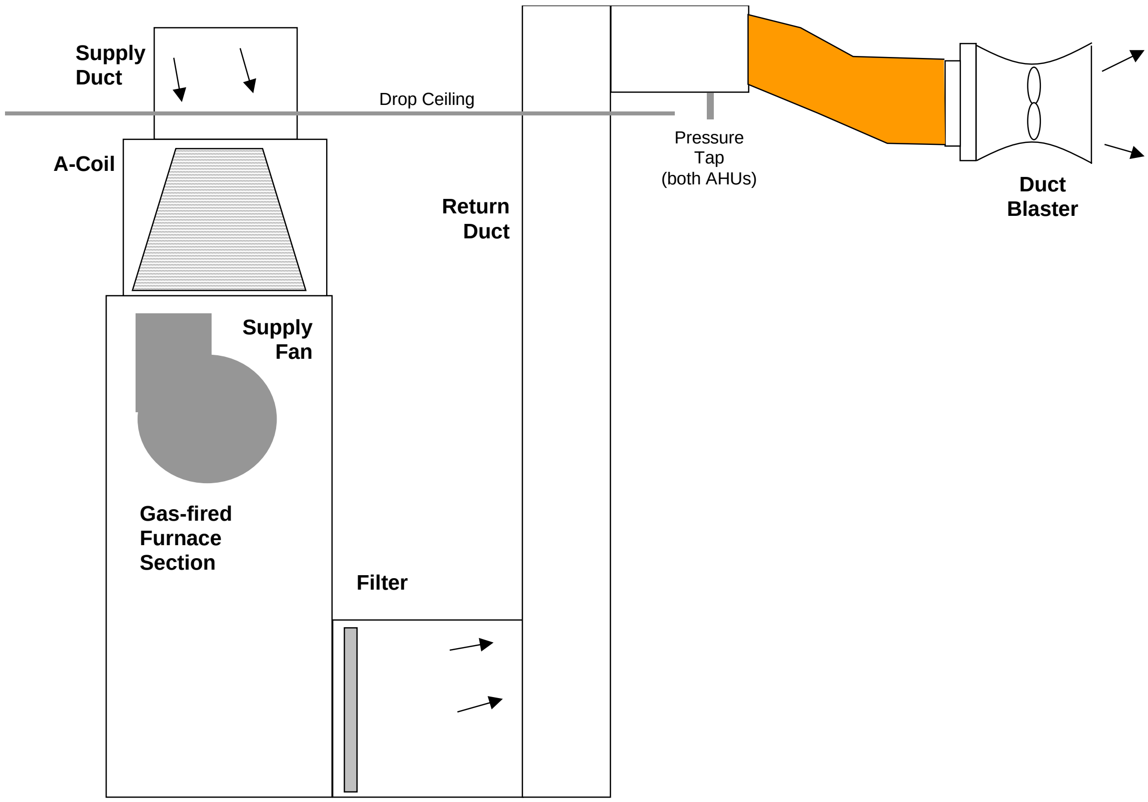

Figure A1-13. Schematic of Duct Blaster Setup

The leakage rate for the return duct alone was completed by wrapping the air filter in plastic, inserting it, and repeating the depressurization tests. The filter was pulled against its stops created a reasonably tight seal (as confirmed by using the smoke puffer).

Figure A1-14 shows the resulting measured data fit to a power function (raw data in Table A1-6). Table A1-7 shows the resulting coefficients, exponents, and regression statistics. Table A1-8 summarizes the resulting duct leakage rates and ELA at a reference pressure of 25 Pa. The total leakage of the supply ducts, AHU cabinet, and return ducts at 25 Pa is about 30% of the total flow rate. As would be expected, the leakage area for the return duct alone accounted for 30-40% of the total leakage of the system.

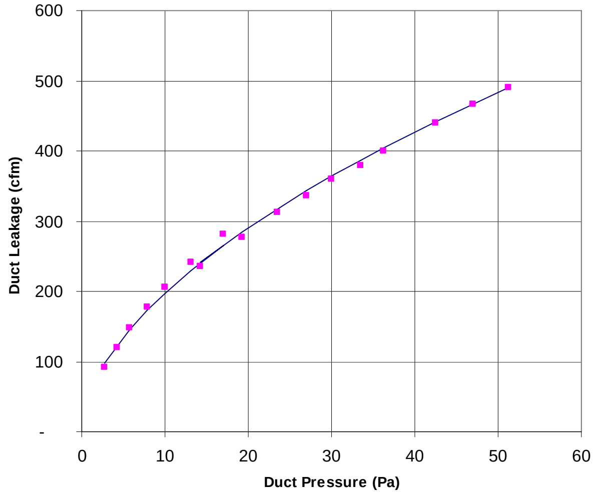

West Area – Total Ductwork

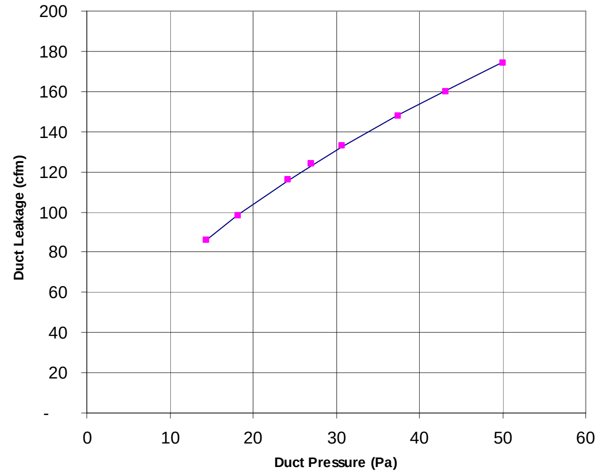

West Area – Return Ductwork

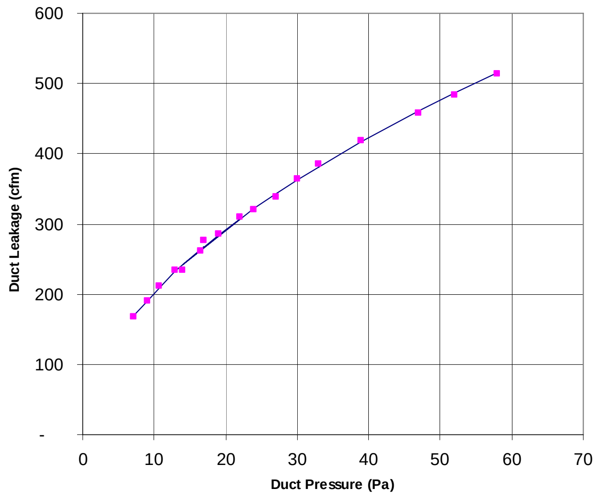

East Area – Total Ductwork

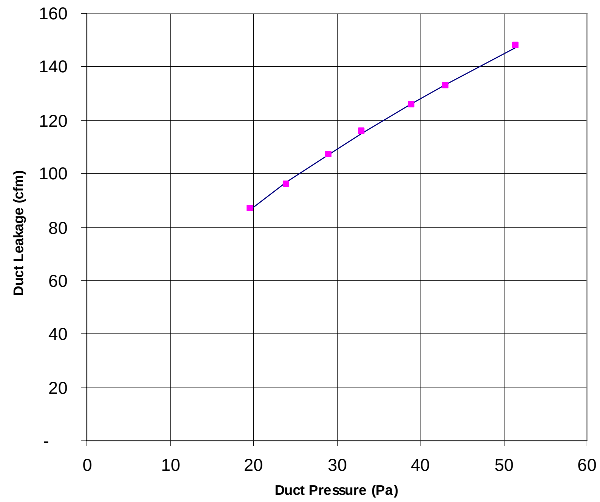

East Area – Return Ductwork

Figure A1-14. Duct-Blaster Tests on Total Ductwork (Supply, Unit, & Return) and Return Duct Only

Table A1-6. Raw Data from Duct-Blaster Tests

West Area – Total Ductwork

	Nominal Building Pressure (Pa)	Fan Pressure (Pa)	Nominal Flow (cfm)	Ring
1	51.3		490	1
2	47		467	1
3	42.5		440	1
4	36.2		400	1
5	33.5		380	1
6	30		360	1
7	27		336	1
8	23.5		313	1
9	19.2		277	1
10	14.3		236	1
11	17		281	2
12	13.1		241	2
13	10		206	2
14	7.9		178	2
15	5.8		148	2
16	4.2		120	2
17	2.8		92	2

West Area – Return Ductwork

	Nominal Building Pressure (Pa)	Fan Pressure (Pa)	Nominal Flow (cfm)	Ring
1	50		174	2
2	43.2		160	2
3	37.4		148	2
4	30.7		133	2
5	27		124	2
6	24.2		116	2
7	18.2		98	2
8	14.4		86	2
9				
10				
11				
12				
13				
14				
15				
16				
17				

East Area – Total Ductwork

	Nominal Building Pressure (Pa)	Fan Pressure (Pa)	Nominal Flow (cfm)	Ring
1	58		514	1
2	52		483	1
3	47		458	1
4	39		419	1
5	33		386	1
6	30		364	1
7	27		338	1
8	24		320	1
9	14		235	1
10	22		310	1
11	19		285	1
12	16.5		261	1
13	17		276	2
14	13		235	2
15	10.7		211	2
16	9		190	2
17	7.2		168	2

East Area – Return Ductwork

	Nominal Building Pressure (Pa)	Fan Pressure (Pa)	Nominal Flow (cfm)	Ring
1	51.5		148	2
2	43		133	2
3	39		126	2
4	33		116	2
5	29		107	2
6	24		96	2
7	19.6		87	2
8				
9				
10				
11				
12				
13				
14				
15				
16				
17				

Table A1-7. Coefficients, Exponents and Regression Statistics from Duct-Blaster Tests

	Total Ductwork			Return Only		
	K	n	R^2	K	n	R^2
West / Front	54.8	0.557	99.63%	19.0	0.566	99.97%
East / Rear	59.1	0.533	99.85%	16.7	0.552	99.92%

Notes: cfm = $K(Pa)^n$ / R^2 indicates fit of linear log-log regression

Table A1-8. Comparison of Supply and Return Airflow Measurements

	Flowhood / Supply Airflow (cfm)	Pitot-tube Traverse / Return Airflow (cfm)	Total Leakage (cfm @ 25)	Return Leakage (cfm @ 25)	Total ELA (sq in @ 25)	Return ELA (sq in @ 25)
West / Front	887	1080	329	118	37	13
East / Rear	1065	1150	329	99	37	11

Notes: Leakage and ELA at reference pressure of 25 Pa

Space Conditions

Figure A1-15 shows the average temperature profiles based on temperature readings taken with a HOBO datalogger. The thick line shows the average for each hour while the shaded region corresponds to one standard deviation about the average. The dotted lines correspond to the minimum and maximum for each hour. Sensors were placed in the Classroom at the east end of the building and the Common area at the west end and in west room 8. The temperature profile show that the thermostat sets back temperatures from 10 pm to 6 am each day. There is no apparent difference in the setback schedule used for the weekend. The east classroom overheats substantially during weekdays, but not on weekends. This overheating may be due to the high proportion of east supply air that enters that space (see Table A1-3). In contrast West Room 8 gets very little heating from the systems.

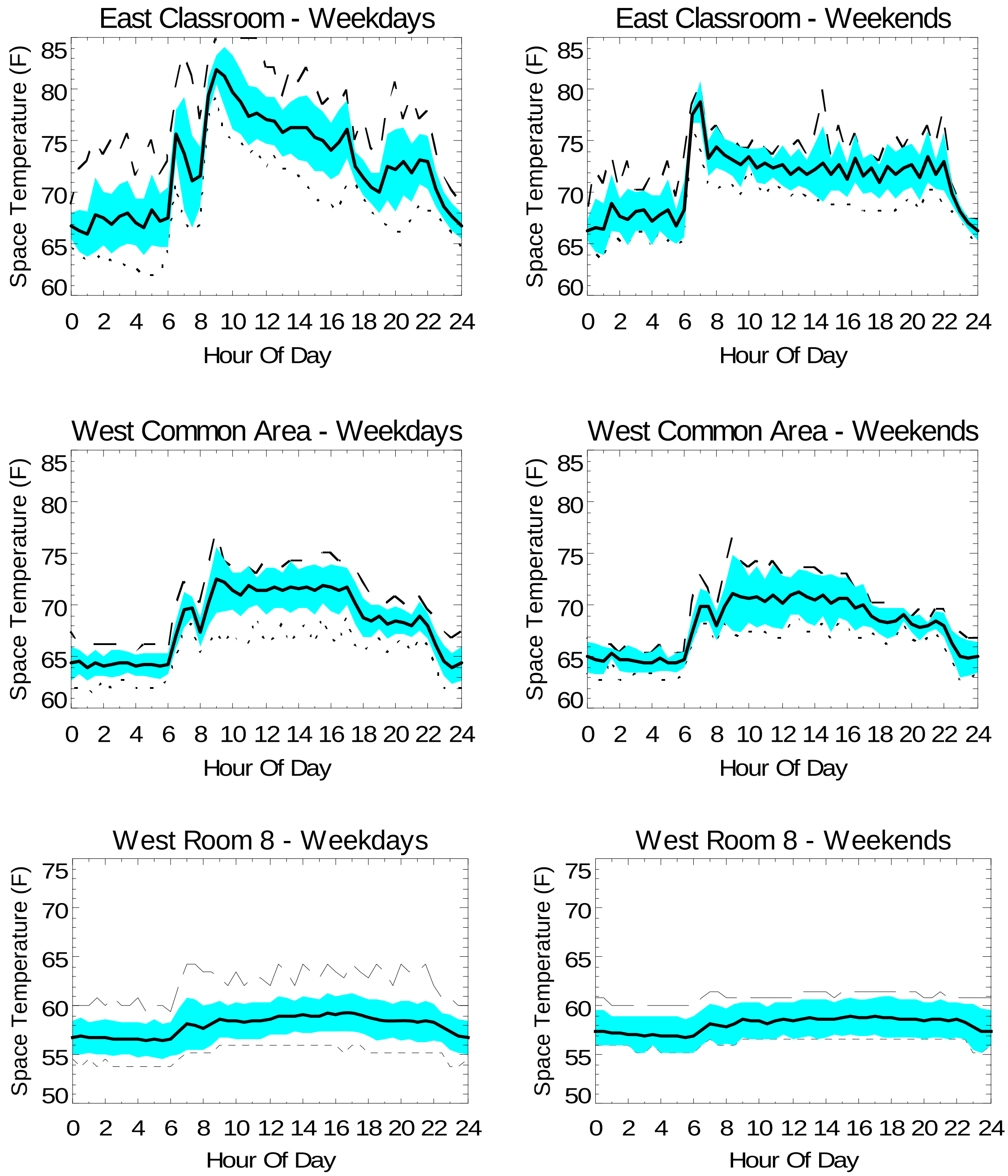

Figure A1-15. Measured Space Temperature Profiles (March 7 to March 29)

Figure A1-16 shows the CO_2 concentration in various locations in the building. The CO_2 concentration provides an indication of occupancy. The next section uses the CO_2 as a tracer gas to estimate the infiltration rate into the building. The data from the classroom, where large classes are frequently held on nights and weekends, shows the most promise for an evaluation of tracer gas decay.

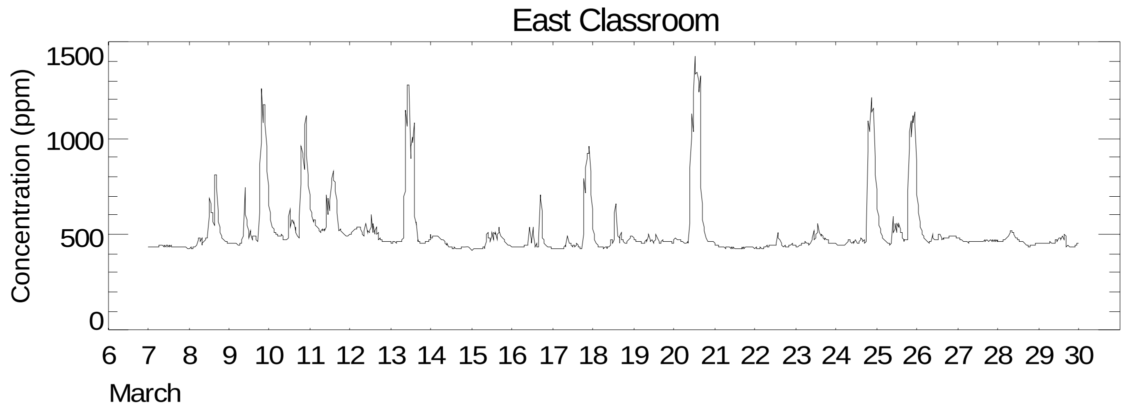

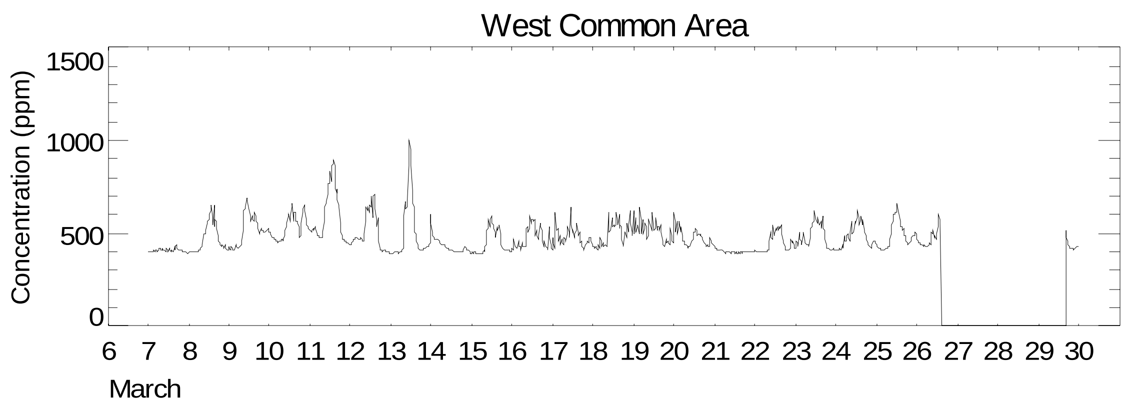

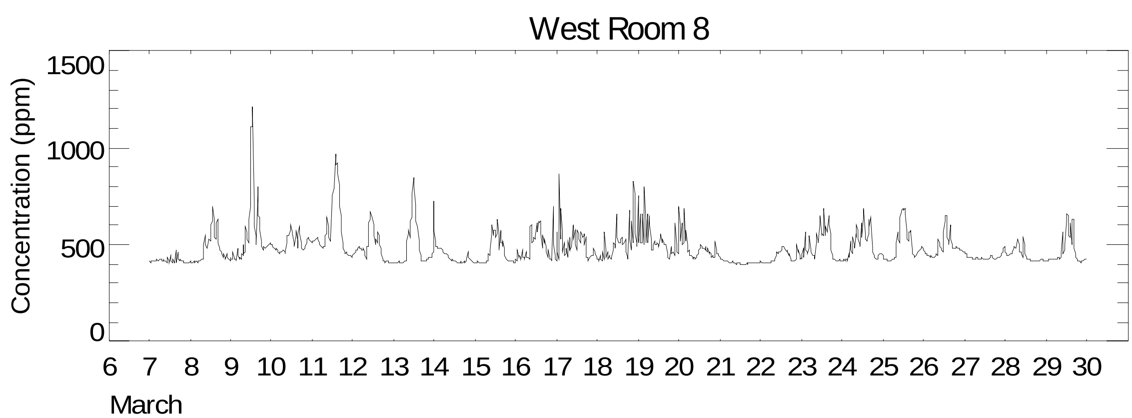

Figure A1-16. Measured CO_2 Concentration in Various Spaces (March 7 to March 29)

Infiltration Estimate from CO_2 Decay

Figure A1-17 and Figure A1-18 show the resulting decay trends using CO_2 levels immediately after high occupancy periods for the East Classroom. The calculated air change rate (ACH) is shown on each plot.

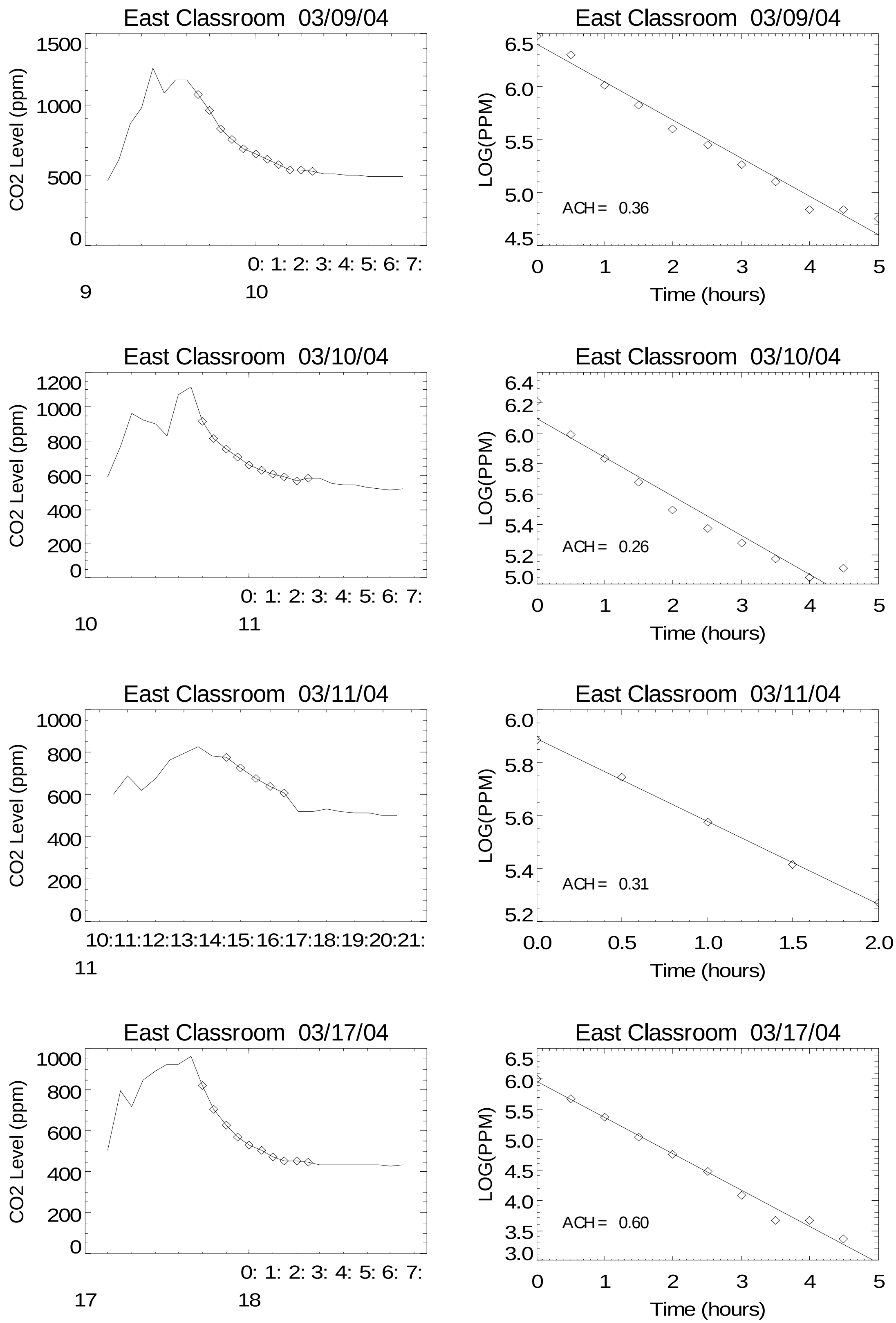

Figure A1-17. Tracer Gas Decay Using CO_2 for Various Periods (March 9-17)

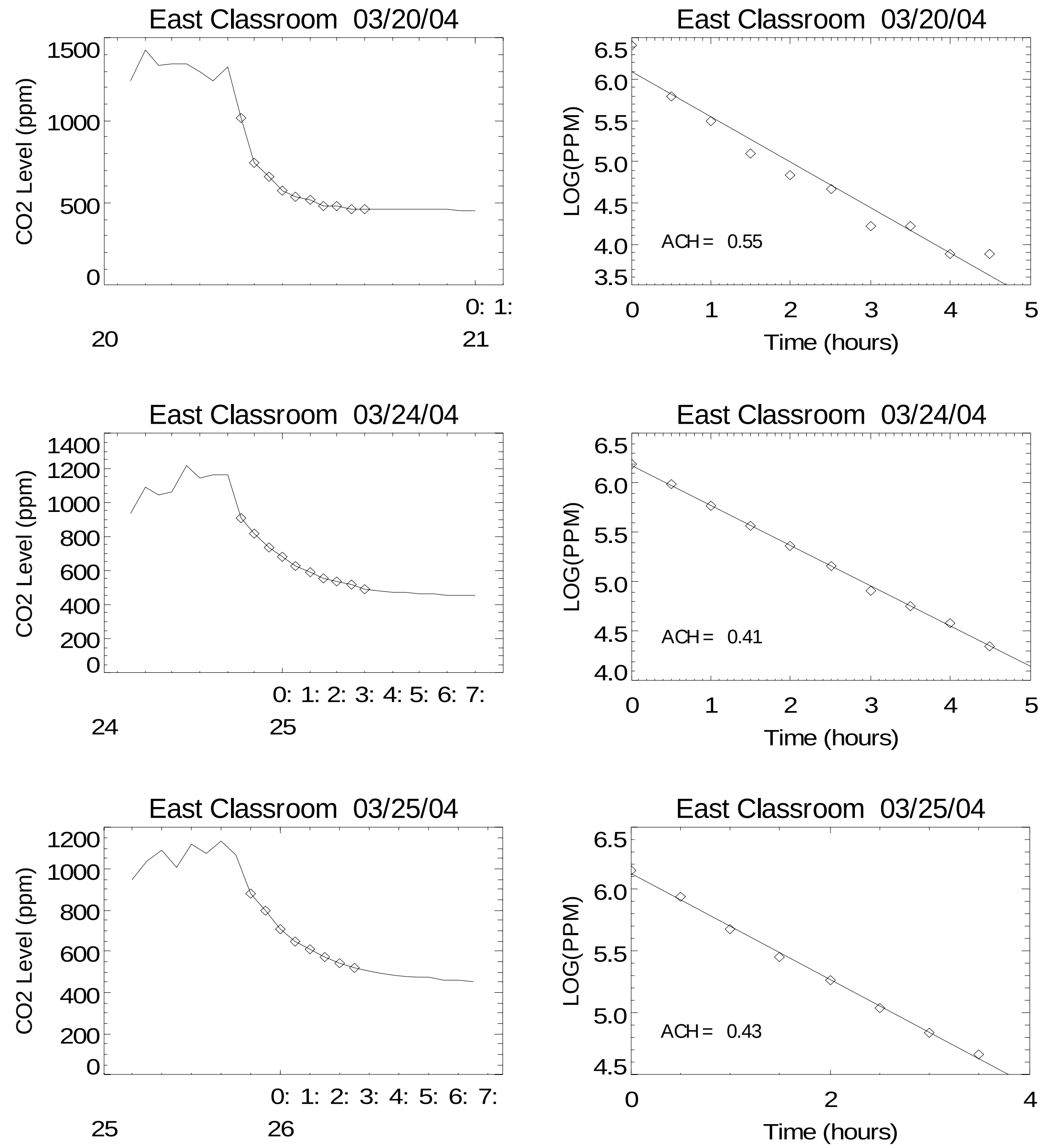

Figure A1-18. Tracer Gas Decay Using CO_2 for Various Periods (March 20-25)

Table A1-9 summarizes the results of the tracer gas decay tests in the plots above. The table also includes the ambient temperature recorded during each decay period listed in the table. Figure A1-19 compares the ACH and ambient temperature. With the exception of the data for March 9 and 10, the estimated ACH shows a highly linear trend with ambient temperature, as might be expected (it appears that the ambient temperature sensor was not yet located outdoors for March 9 and 10).

Table A1-9. Summary of Tracer Gas Decay Tests

Start Time	End Time	AHU Mode	ACH	Ambient Temp. (F)
09-Mar 09:30 PM	10-Mar 02:30 AM	Night Setback	0.36	~~30.3~~
10-Mar 10:00 PM	11-Mar 02:30 AM	Night Setback	0.26	~~30.1~~
11-Mar 02:30 PM	11-Mar 04:30 PM	Occupied	0.31	59.9
17-Mar 10:00 PM	18-Mar 02:30 AM	Night Setback	0.60	27.9
20-Mar 03:30 PM	20-Mar 08:00 PM	Day Setting	0.55	36.1
24-Mar 10:30 PM	25-Mar 03:00 AM	Night Setback	0.41	46.0
25-Mar 10:30 PM	26-Mar 02:30 AM	Night Setback	0.43	46.5

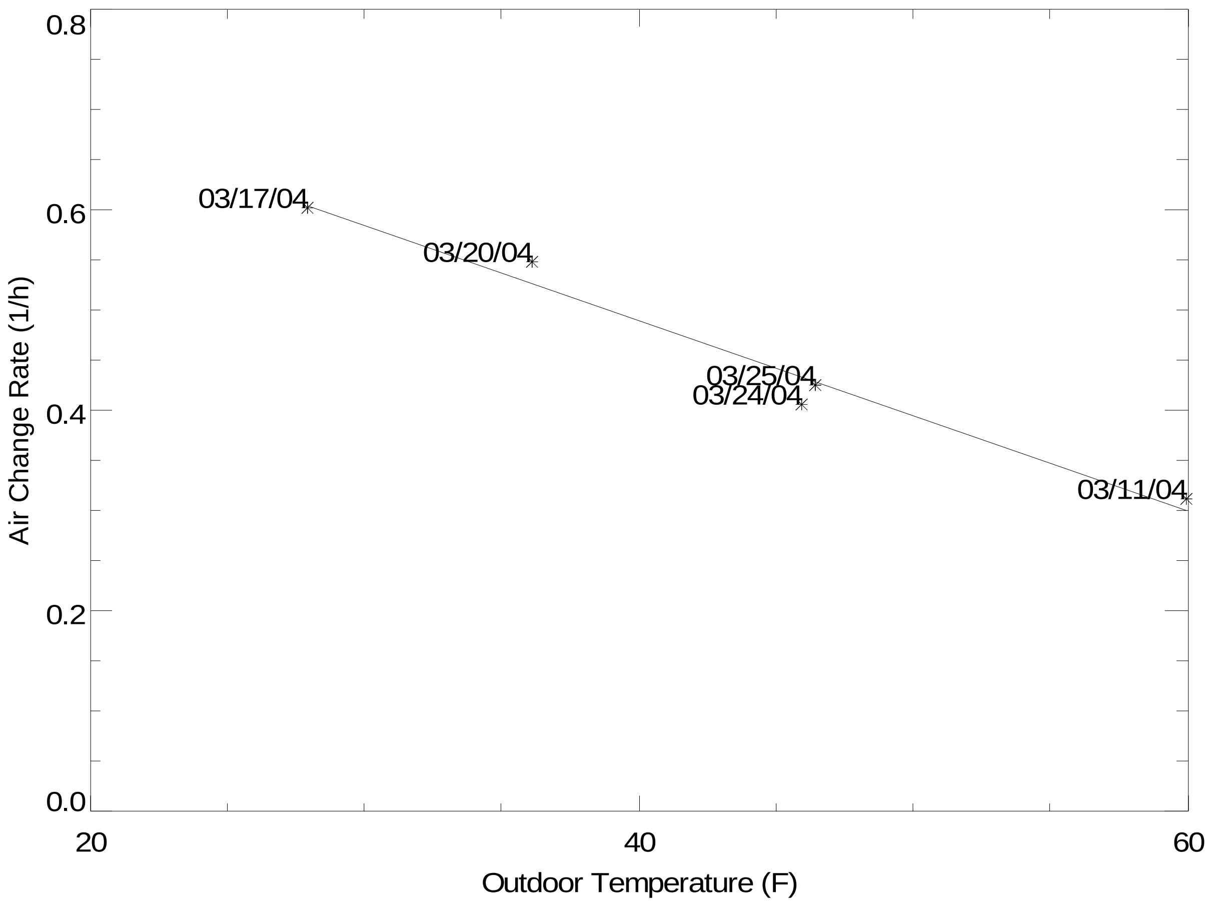

Figure A1-19. Variation of Air Change Rate (ACH) with Ambient Temperature

In comparison to the ACH values above, the nominal leakage rate (defined as ACH_{50} divided by 20) from the blower door test above is 1.56 ACH.

Utility Bills

Gas use is primarily for space heating. Water heating gas use is about 2 therms per month (or 6-7 MBtu/day, equivalent to 2 kWh/day) in the summer. This low usage rate implies little to no water use. The tables and graphs below show that gas use at the facility is up 50% in the most recent heating season. The load lines show that gas use at 20°F has nearly doubled.

The overall energy use index for the building is summarized below.

	Heating Energy Use Index (MBtu/ft^2-year)	Electric Use Index (kWh/ft^2-year)
2002-2003 Season	30.1	7.9
2003-2004 Season	47.7	7.6

Season is from March to March

Table A1-10. Summary of Gas Bills

		East /Rear Area			West / Front Area		
	Days in Period	(therms)	Cost	$/therm	(therms)	Cost	$/therm
4/5/2002	29	100	$ 105.51	1.06	56	$ 68.30	1.22
5/8/2002	33	51	$ 66.01	1.29	34	$ 51.00	1.50
6/7/2002	30	18	$ 36.42	2.02	13	$ 32.13	2.47
7/9/2002	32	0	$ 21.86	-	2	$ 23.03	11.52
8/7/2002	29	0	$ 21.86	-	3	$ 23.54	7.85
9/9/2002	33	0	$ 21.86	-	5	$ 25.00	5.00
10/7/2002	28	0	$ 21.86	-	5	$ 25.32	5.06
11/5/2002	29	41	$ 55.41	1.35	58	$ 69.69	1.20
12/6/2002	31	98	$ 112.66	1.15	114	$ 127.61	1.12
1/8/2003	33	131	$ 144.65	1.10	169	$ 180.60	1.07
2/6/2003	29	139	$ 155.66	1.12	194	$ 209.00	1.08
3/7/2003	29	139	$ 169.65	1.22	169	$ 201.78	1.19
4/7/2003	31	95	$ 146.37	1.54	127	$ 188.64	1.49
5/6/2003	29	44	$ 74.11	1.68	43	$ 72.91	1.70
6/6/2003	31	17	$ 41.47	2.44	14	$ 37.82	2.70
7/8/2003	32	0	$ 21.76	-	2	$ 23.44	11.72
8/7/2003	30	0	$ 21.76	-	2	$ 23.21	11.61
9/9/2003	33	0	$ 21.83	-	2	$ 23.15	11.58
10/7/2003	28	8	$ 29.52	3.69	15	$ 36.93	2.46
11/4/2003	28	26	$ 48.89	1.88	36	$ 59.57	1.65
12/4/2003	30	86	$ 110.94	1.29	123	$ 149.61	1.22
1/6/2004	33	164	$ 199.52	1.22	262	$ 306.22	1.17
2/4/2004	29	344	$ 392.83	1.14	484	$ 529.67	1.09
3/5/2004	30	229	$ 278.90	1.22	303	$ 358.91	1.18
2002-2003	365	717	$ 933.41	1.30	822	$ 1,037.00	1.26
2003-2004	364	1013	$ 1,387.90	1.37	1413	$ 1,810.08	1.28

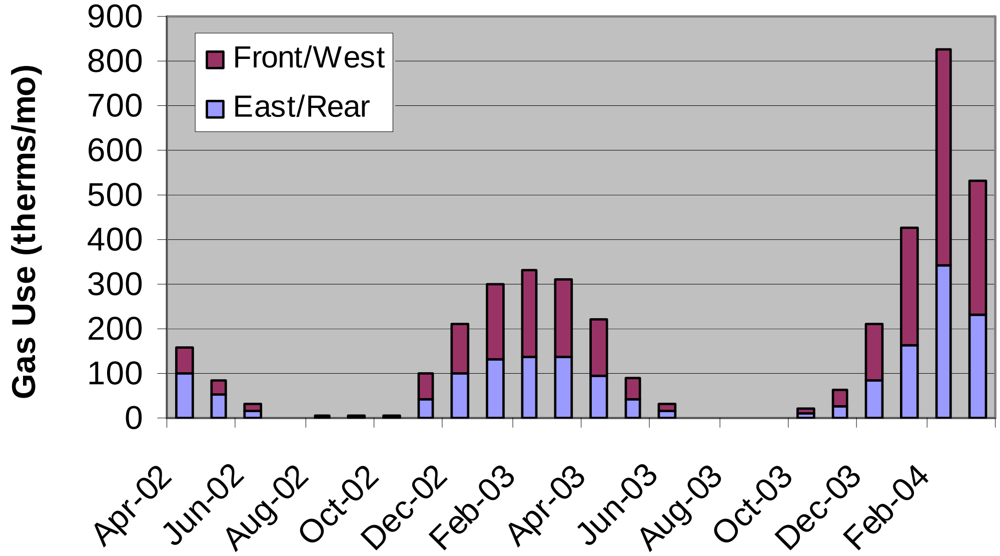

Figure A1-20. Monthly Gas Use Trends

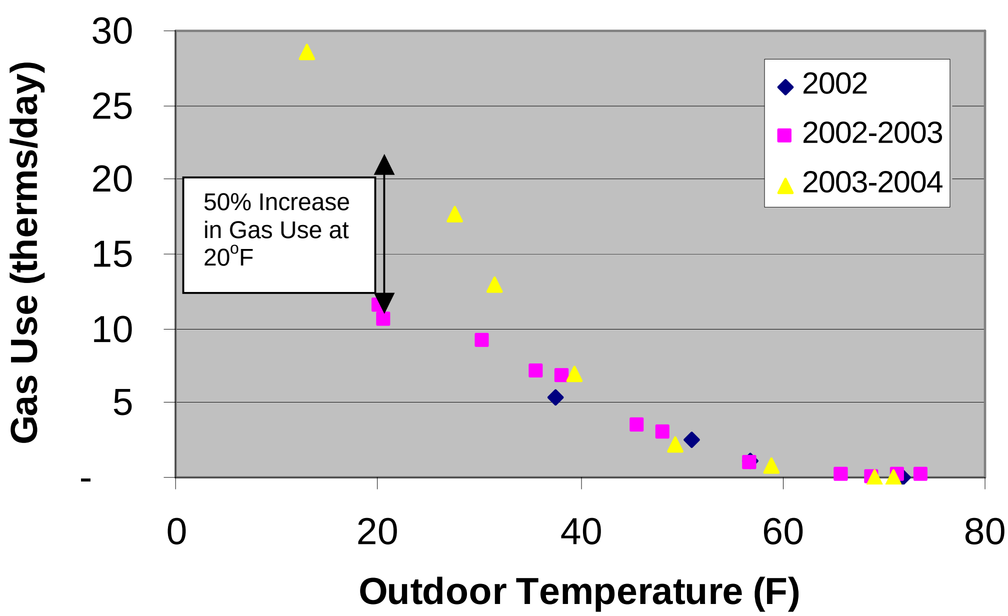

Figure A1-21. Variation of Gas Use With Ambient Temperature

Table A1-11. Summary of Electric Bills

	Days in Period	East /Rear Area kWh	East /Rear Area Cost	East /Rear Area $/kWh	West / Front Area kWh	West / Front Area Cost	West / Front Area $/kWh
4/5/2002	29	1,243	$ 180.76	0.15	2,377	$ 371.80	0.16
5/8/2002	33	1,368	$ 202.27	0.15	1,987	$ 345.02	0.17
6/7/2002	30	1,129	$ 167.45	0.15	1,666	$ 299.32	0.18
7/9/2002	32	1,689	$ 246.20	0.15	2,113	$ 355.71	0.17
8/7/2002	29	1,596	$ 241.62	0.15	2,125	$ 365.05	0.17
9/9/2002	33	1,725	$ 261.57	0.15	2,197	$ 373.55	0.17
10/7/2002	28	1,367	$ 214.33	0.16	1,567	$ 306.66	0.20
11/5/2002	29	1,140	$ 178.99	0.16	1,464	$ 275.49	0.19
12/6/2002	31	1,330	$ 203.82	0.15	1,824	$ 293.75	0.16
1/8/2003	33	1,413	$ 207.30	0.15	2,239	$ 340.71	0.15
2/6/2003	29	1,370	$ 201.21	0.15	2,362	$ 357.14	0.15
3/7/2003	29	355	$ 70.77	0.20	2,192	$ 359.46	0.16
4/7/2003	31	2,136	$ 314.77	0.15	1,948	$ 331.32	0.17
5/6/2003	29	1,100	$ 174.72	0.16	1,090	$ 261.85	0.24
6/6/2003	31	1,242	$ 189.23	0.15	2,044	$ 340.26	0.17
7/8/2003	32	1,350	$ 201.94	0.15	1,885	$ 332.04	0.18
8/7/2003	30	1,329	$ 198.85	0.15	2,030	$ 340.43	0.17
9/9/2003	33	1,493	$ 227.17	0.15	2,085	$ 364.18	0.17
10/7/2003	28	1,173	$ 184.02	0.16	1,443	$ 290.72	0.20
11/4/2003	28	1,035	$ 167.22	0.16	1,616	$ 313.51	0.19
12/4/2003	30	1,177	$ 183.19	0.16	1,974	$ 334.50	0.17
1/6/2004	33	1,201	$ 190.01	0.16	2,120	$ 364.02	0.17
2/4/2004	29	1,225	$ 201.89	0.16	2,397	$ 419.59	0.18
3/5/2004	30	1,214	$ 200.83	0.17	2,190	$ 368.43	0.17
2002-2003	365	15,725	$ 2,376.29	0.15	24,113	$ 4,043.66	0.17
2003-2004	364	15,675	$ 2,433.84	0.16	22,822	$ 4,060.85	0.18

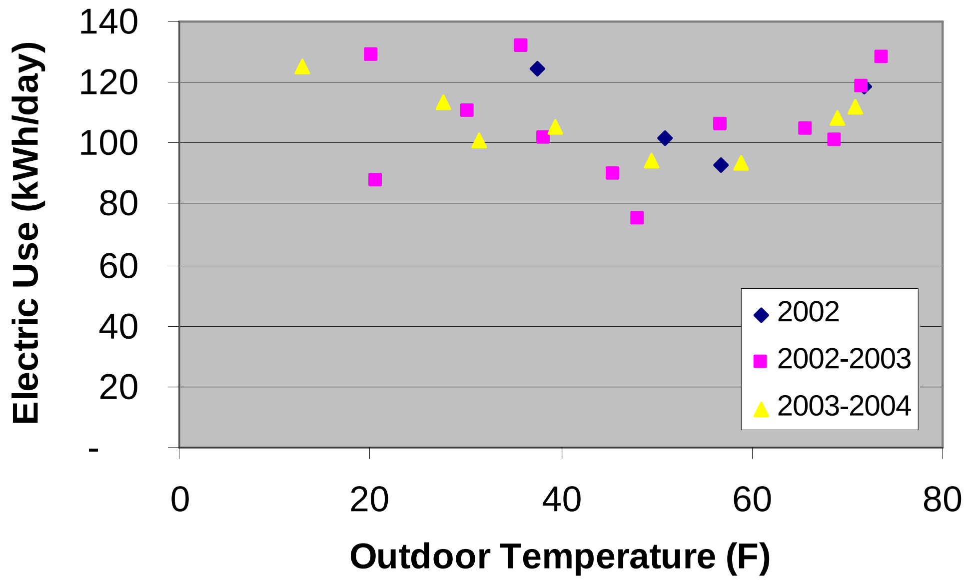

Figure A1-22. Variation of Electric Use With Ambient Temperature

REMEDIATION IMPACT

CDH had sent a letter to the site on January 20, 2005 reporting the problem with the fallen fiberglass batts. While we were never able to repeat the leakage test at the building (because the organization had sublet part of the space to another tenant) additional review of the utility bills revealed the large impact of putting the batts back into place.

The site appeared to have fixed the fallen insulation about the time CDH sent the letter in January 2005. The heating load line is much different from December 2003 to January 2005 when the batts were down. When the batts were put back in place, the heating load line resumed the trend that we had seen before December 2003.

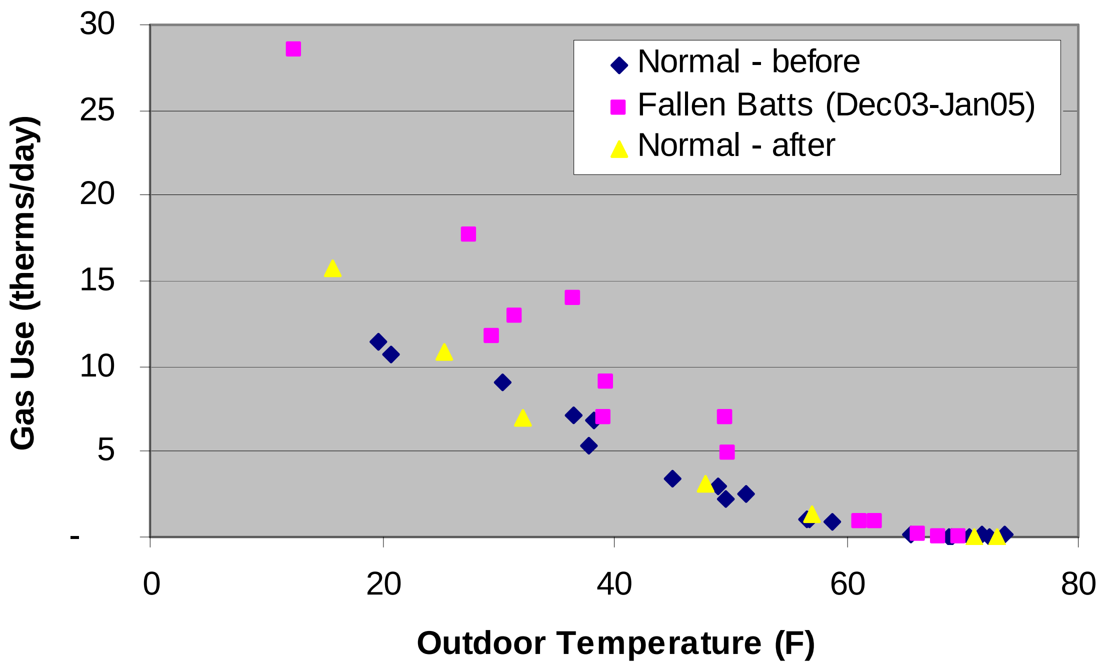

Figure A1-23. Impact of Fallen Fiberglass Batts on Heating Load Line

Table A1-12 summarizes the impact of the fallen fiberglass batts on the annual gas use per square foot of floor area. Gas use for the year was higher by 70-80% when the batts were down. The energy use impact was considerably greater on the front (or west) section of the building, where nearly 80% of the fallen batts were located. With the batts in place the gas use intensity was 32 MBtu per square foot per year, which is more inline with expectations for this type of building.

Table A1-12. Summary of Impact Fiberglass Batts on Annual Gas Use Index

	Gas Use Index (MBtu/ft^2-yr)		
	East	West	Total
Jul-02 - Jun-03	28.0	35.9	32.0
Jul-03 - Jun-04	46.0	63.8	54.9
Jul-04 - Jun-05	25.9	51.7	38.8
Insul Down	47.1	65.9	56.5

The insulation breach had no perceptible impact on cooling energy use as shown in Figure A1-24 below. Electric use in the warmer months was not as strongly affected by the large ceiling leak.

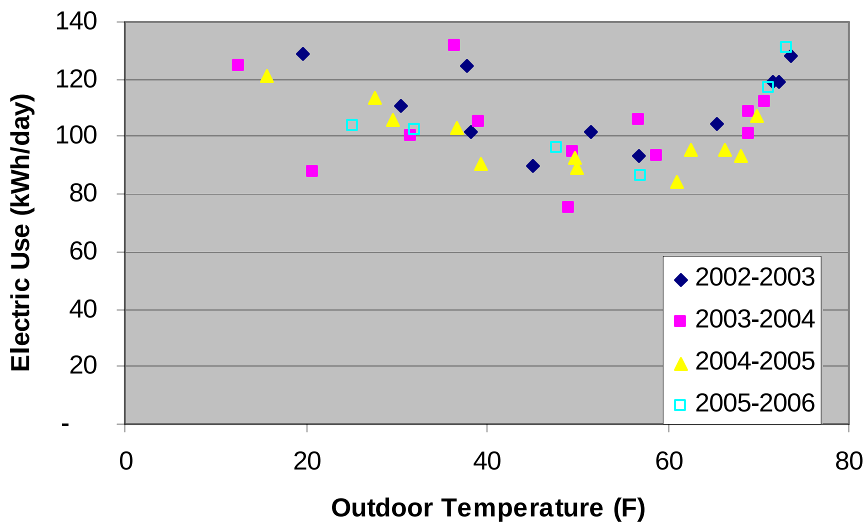

Figure A1-24. Variation of Electric Use for Different Periods

Table A1-13. Monthly Gas Use Showing the Period When the Fberglass Batts Were Down

		East /Rear Area			West / Front Area		
	Days in Month	Gas Use (therms)	Cost ($)	$/therm	Gas Use (therms)	Cost ($)	$/therm
4/5/2002	29	100	$ 105.51	$ 1.06	56	$ 68.30	$ 1.22
5/8/2002	33	51	$ 66.01	$ 1.29	34	$ 51.00	$ 1.50
6/7/2002	30	18	$ 36.42	$ 2.02	13	$ 32.13	$ 2.47
7/9/2002	32	-	$ 21.86	$ -	2	$ 23.03	$ 11.52
8/7/2002	29	-	$ 21.86	$ -	3	$ 23.54	$ 7.85
9/9/2002	33	-	$ 21.86	$ -	5	$ 25.00	$ 5.00
10/7/2002	28	-	$ 21.86	$ -	5	$ 25.32	$ 5.06
11/5/2002	29	41	$ 55.41	$ 1.35	58	$ 69.69	$ 1.20
12/6/2002	31	98	$ 112.66	$ 1.15	114	$ 127.61	$ 1.12
1/8/2003	33	131	$ 144.65	$ 1.10	169	$ 180.60	$ 1.07
2/6/2003	29	139	$ 155.66	$ 1.12	194	$ 209.00	$ 1.08
3/7/2003	29	139	$ 169.65	$ 1.22	169	$ 201.78	$ 1.19
4/7/2003	31	95	$ 146.37	$ 1.54	127	$ 188.64	$ 1.49
5/6/2003	29	44	$ 74.11	$ 1.68	43	$ 72.91	$ 1.70
6/6/2003	31	17	$ 41.47	$ 2.44	14	$ 37.82	$ 2.70
7/8/2003	32	-	$ 21.76	$ -	2	$ 23.44	$ 11.72
8/7/2003	30	-	$ 21.76	$ -	2	$ 23.21	$ 11.61
9/9/2003	33	-	$ 21.83	$ -	2	$ 23.15	$ 11.58
10/7/2003	28	8	$ 29.52	$ 3.69	15	$ 36.93	$ 2.46
11/4/2003	28	26	$ 48.89	$ 1.88	36	$ 59.57	$ 1.65
12/4/2003	30	86	$ 110.94	$ 1.29	123	$ 149.61	$ 1.22
1/6/2004	33	164	$ 199.52	$ 1.22	262	$ 306.22	$ 1.17
2/4/2004	29	344	$ 392.83	$ 1.14	484	$ 529.67	$ 1.09
3/5/2004	30	229	$ 278.90	$ 1.22	303	$ 358.91	$ 1.18
4/6/2004	32	204	$ 237.55	$ 1.16	241	$ 276.84	$ 1.15
5/5/2004	29	86	$ 115.26	$ 1.34	117	$ 149.25	$ 1.28
6/4/2004	30	10	$ 32.78	$ 3.28	17	$ 41.05	$ 2.41
7/7/2004	33	1	$ 22.72	$ 22.72	2	$ 23.60	$ 11.80
8/4/2004	28	-	$ 21.86	$ -	1	$ 22.75	$ 22.75
9/7/2004	34	-	$ 21.86	$ -	1	$ 22.73	$ 22.73
10/4/2004	27	7	$ 28.33	$ 4.05	17	$ 38.86	$ 2.29
11/2/2004	29	52	$ 77.01	$ 1.48	89	$ 116.91	$ 1.31
12/6/2004	34	93	$ 143.88	$ 1.55	214	$ 303.84	$ 1.42
1/5/2005	30	145	$ 200.43	$ 1.38	205	$ 274.76	$ 1.34
2/4/2005	30	182	$ 241.25	$ 1.33	291	$ 374.56	$ 1.29
3/5/2005	29	85	$ 124.72	$ 1.47	230	$ 301.96	$ 1.31
4/5/2005	31	56	$ 90.03	$ 1.61	162	$ 220.50	$ 1.36
5/4/2005	29	24	$ 52.68	$ 2.20	68	$ 110.57	$ 1.63
6/6/2005	33	12	$ 36.39	$ 3.03	30	$ 59.27	$ 1.98
7/7/2005	31	-	$ 21.99	$ -	1	$ 22.85	$ 22.85
8/5/2005	29	-	$ 21.99	$ -	-	$ 21.99	$ -
9/6/2005	32	-	$ 22.32	$ -	1	$ 23.39	$ 23.39
10/4/2005	28	-	$ 22.32	$ -	2	$ 24.92	$ 12.46
10/18/2005	14	-	$ 10.27	$ -	64	$ 137.52	$ 2.15
Jul-02 - Jun-03	**364**	**704**	**$ 987**	**$ 1.40**	**903**	**$ 1,185**	**$ 1.31**
Jul-03 - Jun-04	**364**	**1,157**	**$ 1,512**	**$ 1.31**	**1,604**	**$ 1,978**	**$ 1.23**
Jul-04 - Jun-05	**367**	**657**	**$ 1,061**	**$ 1.62**	**1,310**	**$ 1,870**	**$ 1.43**
Insul Down	**364**	**1,183**	**$ 1,540**	**$ 1.30**	**1,657**	**$ 2,036**	**$ 1.23**

Field Test Sites 2 & 3 - Small Office Building/Restaurant, Cazenovia NY

Restaurant Entrance in Front (Site 3, north)

Offices in Rear (Site 2, south)

Figure A2-1. Photos of Building

CHARACTERISTICS

Building Description

The 2,477 sq ft facility is a one-story building with offices in the rear (Site 2) and a small take-out restaurant (Site 3) in the front portion. The office and restaurant are separated by a firewall that goes through the attic. Figure A2-1 shows the entrance to the restaurant in the front of the building and the entrance to the offices in the rear. Each section is conditioned by its own air-handling unit and each has separate gas and electric utilities. The restaurant has a natural gas unit heater and the office section has a residential style forced air system. The restaurant has a small through-wall air conditioner and the office section of the building is cooled by an A-coil on top of the furnace. The facility was built in 1980s and in 1992 the restaurant was added on. In 1996, the office section of the building was renovated and new HVAC equipment and ductwork were installed. Figure A2-2 presents the building floor plan.

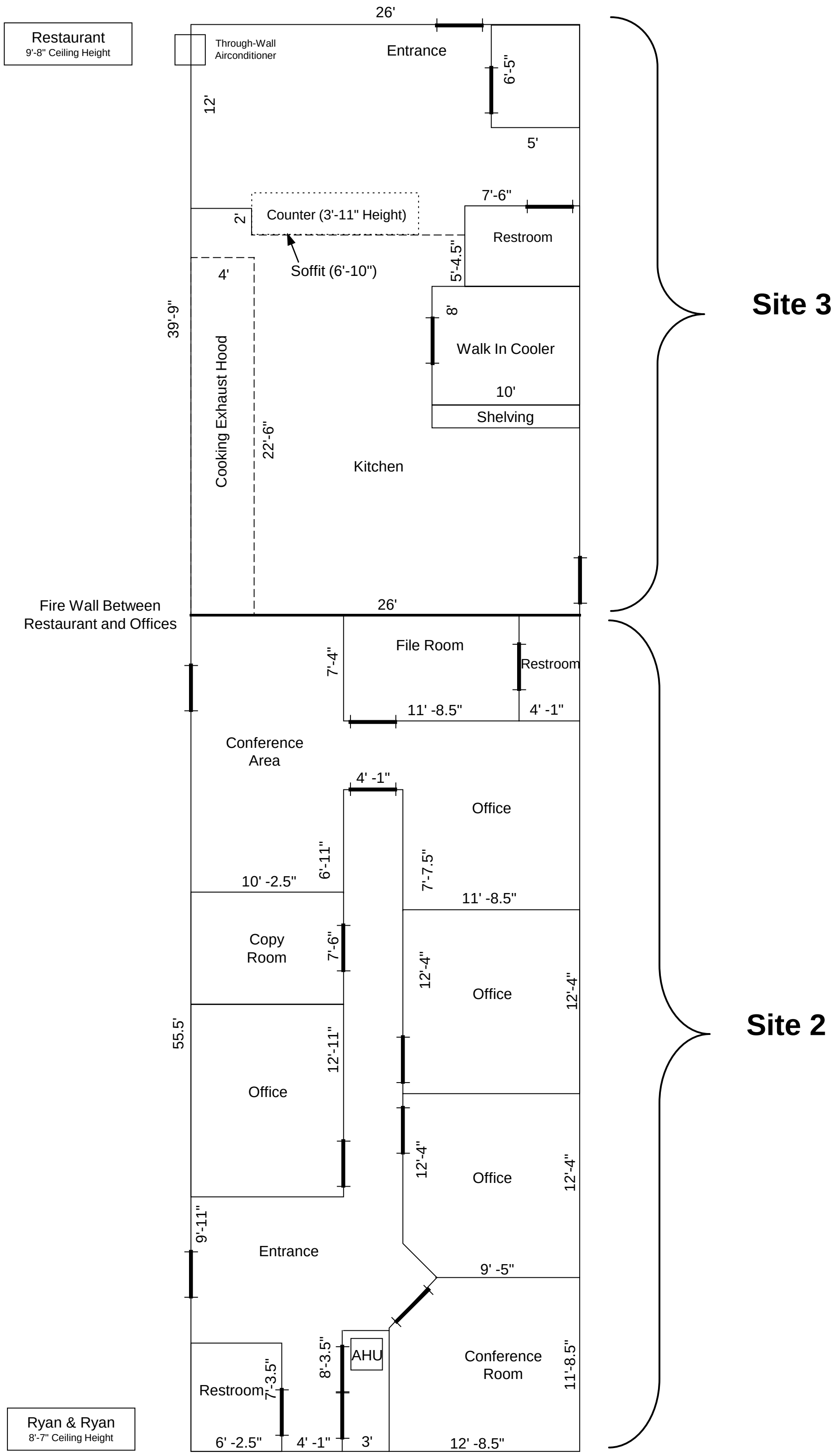

Figure A2-2. Facility Floor Plan, Showing the Office (Site 2) and the Restaurant (Site 3)

Construction Details

Exterior walls are constructed of wood clapboard siding, ½-in plywood sheathing, wood 2x4 studs and gypsum board interior covering. The walls are insulated with R-13 unfaced fiberglass insulation with 5-mil poly vapor barrier between the framed wall and gypsum board.

The roof is constructed of plywood decking on wooden roof trusses. Roofing material is asphalt shingles. Ceiling insulation is provided by 6-in paper-backed fiberglass batts that are stapled to the sides of the trusses.

There is a T-bar (drop) ceiling approximately 12 inches below the attic insulation in the office area.

The attic is vented with ridge venting and vented soffits. Figure A2-3, Figure A2-4, and Figure A2-5 illustrate the wall and roof sections for the restaurant and the office section of the building.

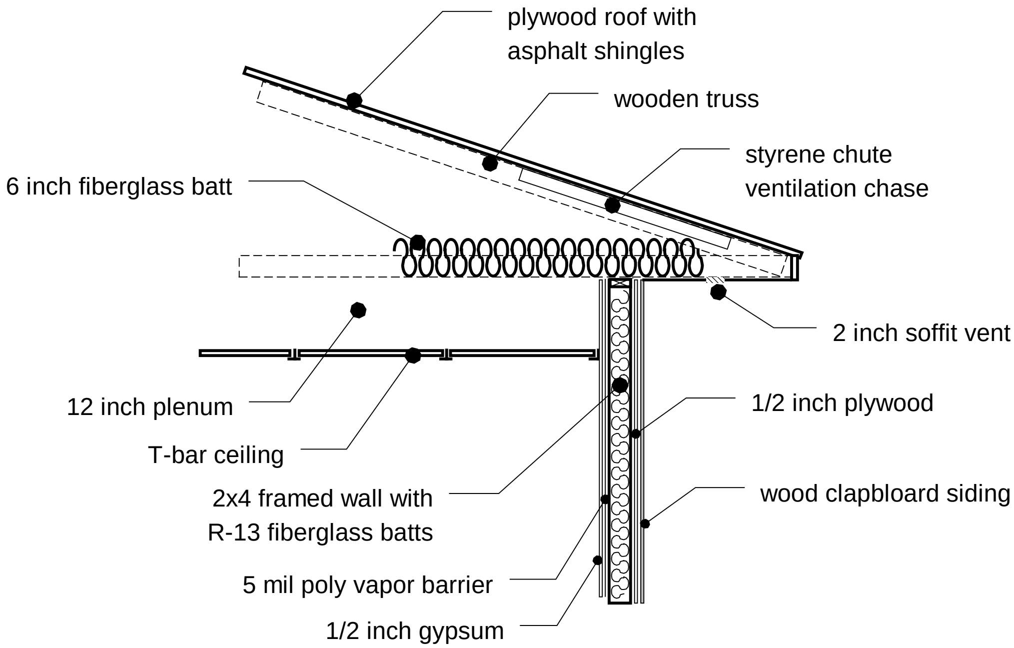

Figure A2-3. Roof and Wall Sections along the Length of the Office Section of the Building

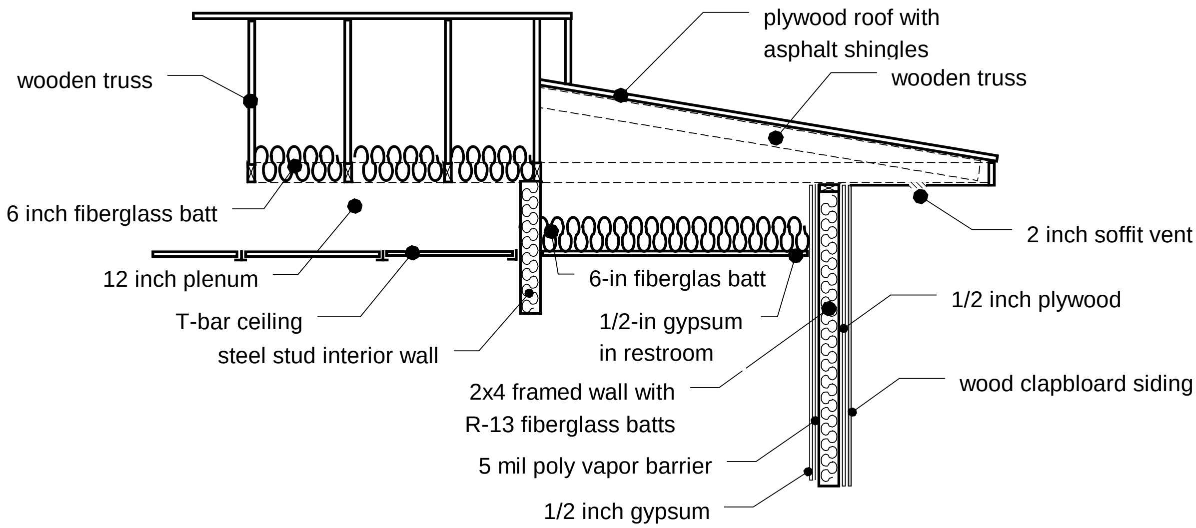

South End of Building

Roof Section at South End of Building

Figure A2-4. Roof and Wall Section for South End of Building (Site 2, office section)

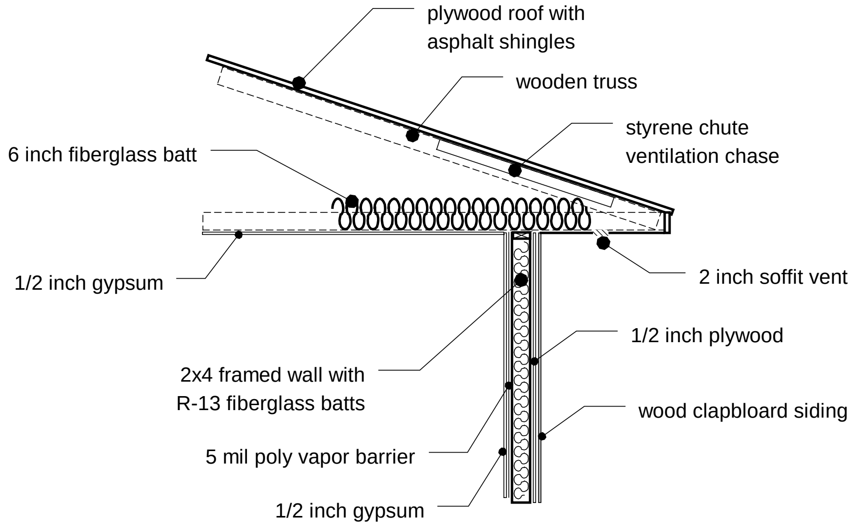

Roof and Wall Sections along the Length of the Building in the Restaurant

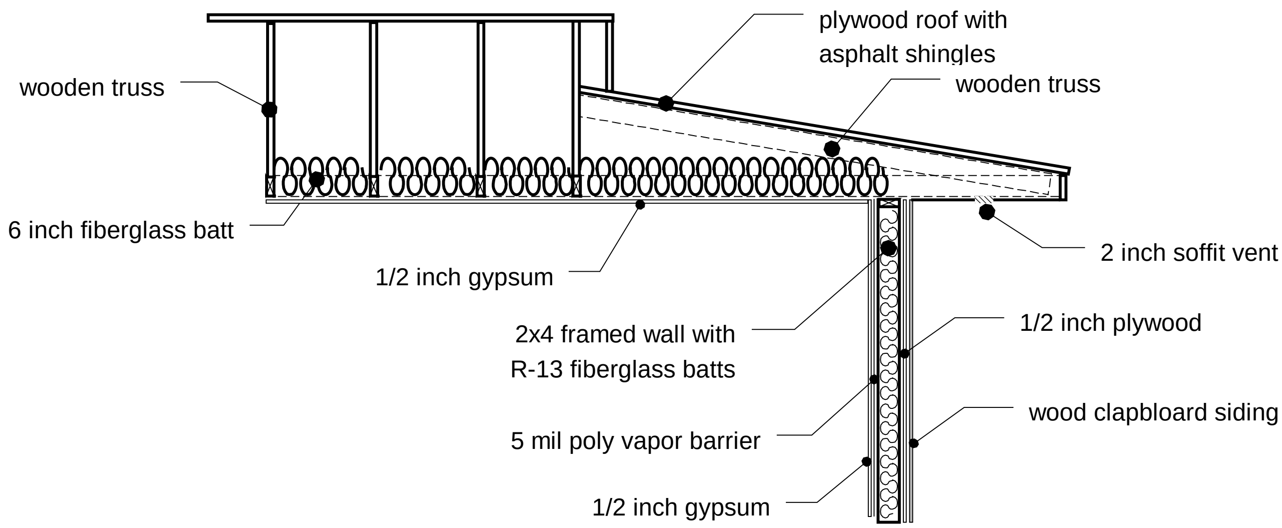

Roof and Wall Sections At the North End of the Building (restaurant)

Figure A2-5. Roof and Wall Sections for the Restaurant (Site 3)

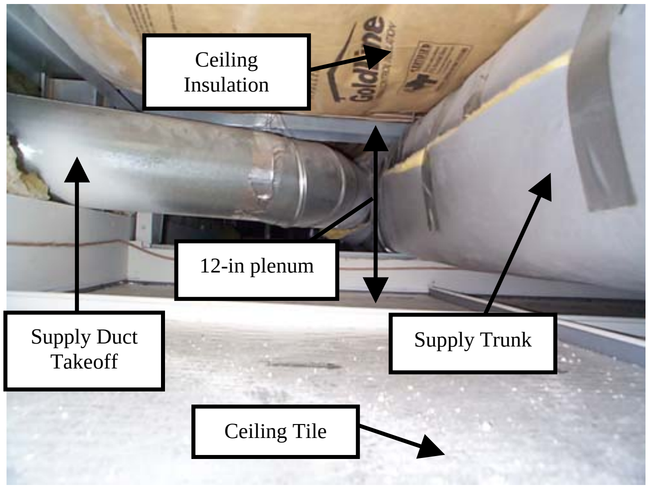

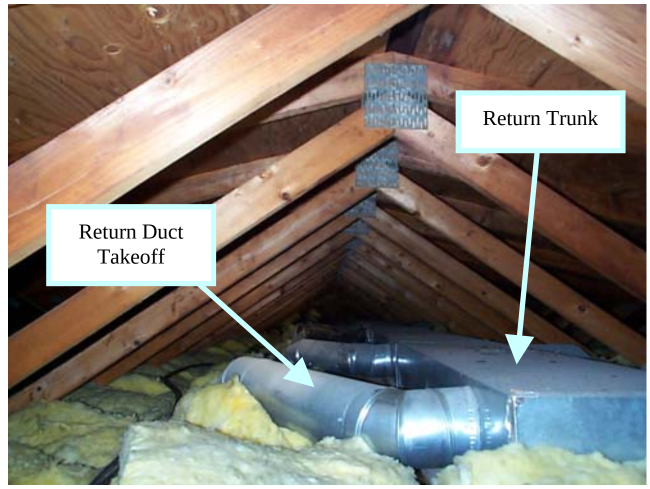

Figure A2-6. Office Section: Ceiling Plenum with Supply Ductwork and Attic with Return Ductwork

The firewall shown in Figure A2-7 prevents airflow interaction through the attic between the restaurant and office section of the building. With the restaurant pressurized 50 Pa, there was no detectable pressure change between the office section and outdoors or between the office section attic and conditioned space.

Figure A2-7. Firewall in Attic Between the Restaurant (Site 3) and Office (Site 2) Sections

HVAC System

A conventional gas-fired furnace with an A-coil cooling section heats and cools the office area of the building. There are no special provisions to provide ventilation. The supply and return ductwork is all sheet metal with a rectangular supply trunk and 6-in diameter takeoffs that lead to supply and return diffusers. The insulated supply trunk is located between the drop ceiling and insulation whereas the un-insulated return trunk and takeoffs are located above the ceiling insulation. The heating and cooling is setback weeknights from 5:00 pm to 8:00 am and on weekends.

The restaurant uses a single natural gas unit heater with no ductwork and a small through-wall air conditioner cools the takeout area during the summer. A large cooking exhaust hood depressurizes the restaurant causing fresh air to be pulled through a ventilation window and a hole cut in the ceiling to reduce the depressurization. The restaurant does not set back heating.

Table A2-1 lists the installed HVAC equipment for both the office section and the restaurant.

Table A2-1. HVAC Equipment Installed at Site

	Equipment	**Cooling Section**	**Heating Capacity (input MBtu/h)**	**Cooling Capacity (tons)**	**Measured Supply Fan Power (kW)**
Office Section	Acroaire GNJ075N12A1	Acroaire AF030GB1	75	2.5 ton	0.41
Restaurant	Unit Heater	Room A/C			
	Exhaust Fan Dayton 3C717 24-1/2 in. 1/2 hp				1.68

MEASUREMENTS

The test data below was taken in April and May 2004. Supply airflow measurements were taken on April 28 for the office section of the building. Blower door, pressure mapping, and duct leakage measurements were taken on April 29 for the office section. The duct leakage was tested a second time on May 11, 2004. On May 15, the Chinese restaurant was blower door tested. Test personnel were Hugh Henderson and Dan Gott.

Building Envelope Airtightness

The leakage characteristics of the enclosure were assessed using fan depressurization methods. The first test for the office section used the blower door to depressurize the building to several pressure differences between 14 to 35 Pa. The test was conducted with all interior doors open and all exterior doors and windows closed. The closet doors enclosing the AHU were closed and the furnace and water heater exhaust was sealed to prevent outside air from infiltrating. Figure A2-8 shows the office section leakage variation with building pressure.

Table A2-2 shows the results of the blower door test including model coefficients, effective leakage area (ELA), and air-changes-per-hour (ACH). The ELA is calculated using the Lawrence Berkeley Laboratory method, which calculates the leakage area at 4 Pa. The office section of the building has an effective leakage area of approximately 10.4 sq in per 100 sq ft of the total envelope and floor area. Another building leakage characteristic is the ACH at 50 pascals (ACH_{50}). The office section of the building has an ACH_{50} of 33.0. This result implies that at 50 Pa, the air in the office section of the building is displaced 33 times each hour.

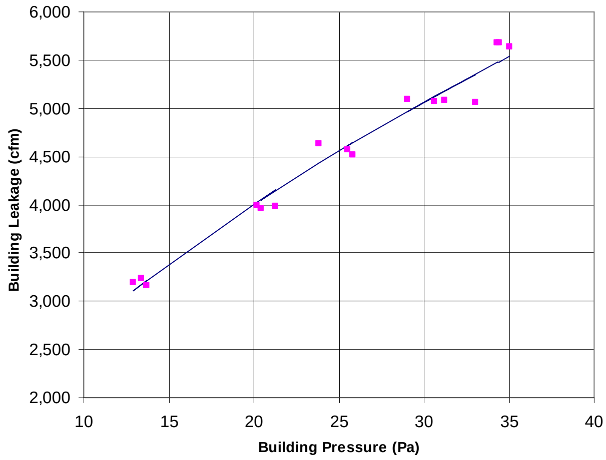

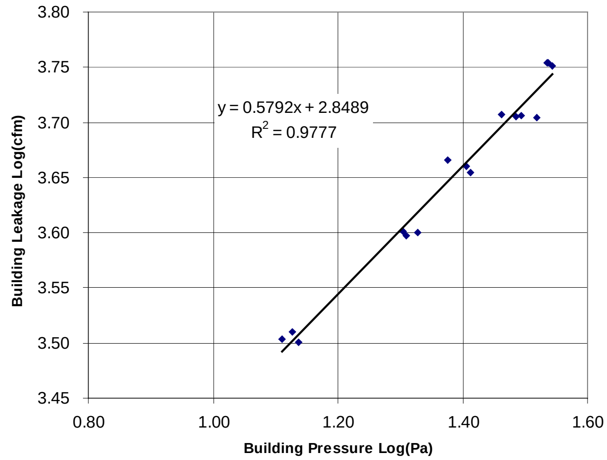

Figure A2-8. Office Section Variation of Building Leakage with Pressure: cfm = $K(\Delta P)^n$

Table A2-2. Office Section Blower Door Test Data, Resulting Best-Fit Model Coefficients, and ELA

Test Results:

Flow Coefficient (K)	706.2		1443	sq ft. floor area
Exponent (n)	0.579			
Leakage area (LBL ELA @ 4 Pa)	447	sq in	10.42	ELA / 100 sq ft
Airflow @ 50 Pa	6,807	cfm	33.0	ACH @ 50

Test Data:

	Nominal Building Pressure (Pa)	Nominal Flow (cfm)	Ring
1	35.0	5,641	none
2	34.4	5,680	none
3	34.3	5,675	none
4	29.0	5,096	none
5	31.2	5,082	none
6	33.0	5,060	none
7	30.6	5,069	none
8	25.5	4,575	none
9	25.8	4,515	none
10	23.8	4,631	none
11	20.4	3,959	none
12	21.3	3,986	none
13	20.2	3,993	none
14	13.4	3,238	none
15	12.9	3,190	none
16	13.7	3,168	none

Notes: ELA is leakage area (in square inches) at reference pressure of 4 Pa.
ELA per 100 sq ft is based on total building envelope surface area (ceiling, walls and floor).

Most of the building leakage that occurs in office section of the building comes from the closet enclosing the furnace and water heater. There is no drop ceiling in the closet allowing considerable infiltration. There was also significant amount of airflow coming through the drop ceiling where there was a ceiling tile missing near the closet. Figure A2-9 shows leakage problem areas allowing large amounts of infiltration from the space to the ceiling plenum.

No Ceiling in Closet Enclosing AHU and Water Heater

Missing Ceiling Tile Near Closet

Figure A2-9. Problem Areas in Office Section of the Building

To quantify the effect of adding a ceiling to the closet, we opened the closet doors and performed another depressurization test. The difference between the leakage tests with the closet doors open and closet doors closed should show the effect of adding a ceiling however the results were very similar. With the closet doors open, the ELA was essentially the same; 10.42 sq in. with closet doors closed and 10.39 sq-in with the closet doors open, but the ACH_{50} increased from 33.0 to 37.7 with the door. The leakage area results with the closet doors open and closed are essentially the same within the test uncertainty. We determined that the test results were similar because we did not actually eliminate the leakage through the closet ceiling; we just inserted an additional resistance (the closet doors) between the leak and the interior space.

We pressurized the Chinese restaurant because there were multiple pilot lights that would need to be shut off to prevent a back draft situation. The blower door was used to pressurize the restaurant to several pressure differences between 5 to 58 Pa. The test was conducted with all exterior doors and windows closed. The main exhaust fan and bathroom fans were blocked off as was the ventilation intake hole (see Figure A2-11). Figure A2-8 shows the restaurant leakage variation with building pressure.

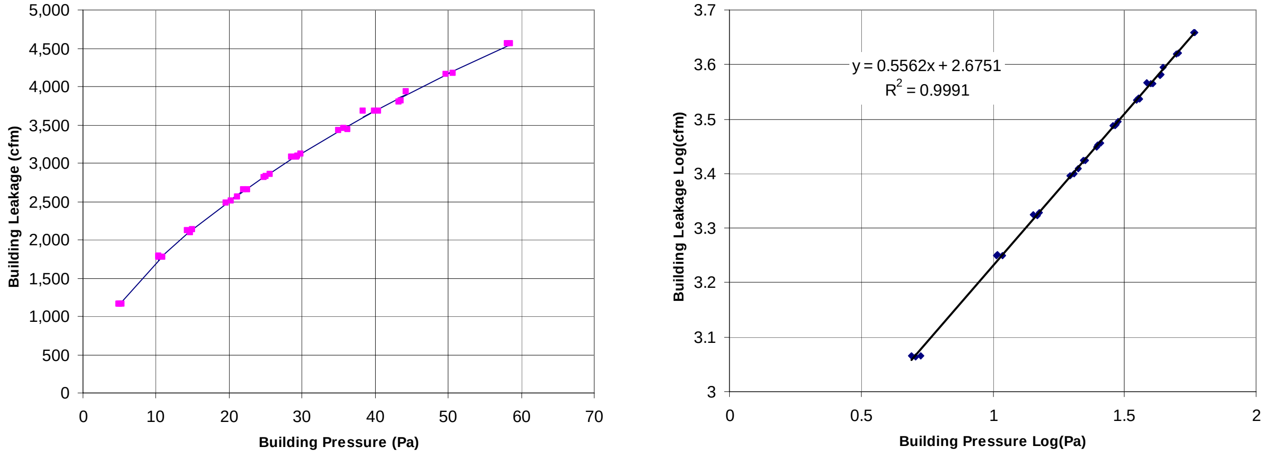

Figure A2-10. Restaurant -- Variation of Building Leakage with Pressure: cfm = K(ΔP)^n

Table A2-3 shows the results of the blower door test including model coefficients, ELA, and ACH. The restaurant has a leakage area of approximately 8.7 sq in per 100 sq ft and an ACH_{50} of 25.0.

Table A2-3. Restaurant -- Blower Door Test Data, Resulting Best-Fit Model Coefficients, and ELA

Test Results:

Flow Coefficient (K)	473.3	1033.5	sq ft. floor area
Exponent (n)	0.556		
Leakage area (LBL ELA @ 4 Pa)	290 sq in	8.69	ELA / 100 sq ft
Airflow @ 50 Pa	4169.4 cfm	25.0	ACH @ 50

Test Data:

	Nominal Building Pressure (Pa)	Nominal Flow (cfm)	Ring
1	58.1	4,566	none
2	58.5	4,565	none
3	49.7	4,164	none
4	50.7	4,174	none
5	43.5	3,812	none
6	43.3	3,795	none
7	44.3	3,935	none
8	38.3	3,684	none
9	40.4	3,676	none
10	39.9	3,677	none
11	35.0	3,433	none
12	36.2	3,442	none
13	35.7	3,460	none
14	29.8	3,126	none
15	28.6	3,081	none
16	29.2	3,080	none
17	29.4	3,091	none
18	25.6	2,859	none
19	24.8	2,813	none
20	25.1	2,832	none
21	20.3	2,511	none
22	19.6	2,484	none
23	21.1	2,566	none
24	22.5	2,652	A
25	22.0	2,655	A
26	15.0	2,128	A
27	14.7	2,099	A
28	14.3	2,116	A
29	10.4	1,781	A
30	10.3	1,774	A
31	10.9	1,775	A
32	4.9	1,161	A
33	5.1	1,160	A
34	5.3	1,162	A

Notes: ELA is leakage area (in square inches) at reference pressure of 4 Pa.
ELA per 100 sq ft is based on total building envelope surface area (ceiling, walls and floor).

There is a hole cut in the ceiling (likely cut for additional ventilation) near the side door shown in Figure A2-11. Even with this hole cut in the ceiling and the ventilation window open, the building still gets depressurized to 40.7 Pa with the cooking exhaust hood fan on and with exterior doors closed. This hole was approximately 168 sq-in. and accounts for approximately 42% of the total leakage area. At normal winter operating conditions, (all exterior doors closed and exhaust fans on) the hole allows approximately 1557 cfm of ventilation air enter the restaurant (as measured with a flow hood). With the restaurant depressurized, to 58 Pa, we could detect no pressure impacts in the office side of the building.

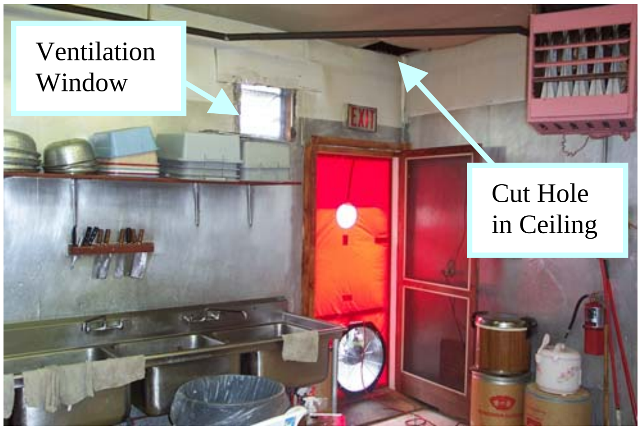

Hole in Ceiling Near Side Door

Close up of Cut Hole in Ceiling

Figure A2-11. Source of Leakage (Ventilation Air) in Chinese Restaurant

<u>Pressure Mapping (blower door testing)</u>

The air pressure relationships in the building were determined using a digital micro-manometer (DG 700) with the blower door operating. All interior doors were closed. The pressure difference across the office section of the building envelope was 20 Pa and a second test on the restaurant had a pressure difference of 50 Pa. Pressure relationships between enclosed spaces such as offices and the open core areas were measured. The graphics in Figure A2-12 show the pressure differences induced across the doorways to the corridor. For the office section of the building, pressure drops across the doorways range between 1 and 10 Pa with the corridor depressurized 20 Pa. When the Chinese restaurant is pressurized 50 Pa, the pressure drops across the two interior room were 11.4 Pa and 30.0 Pa.

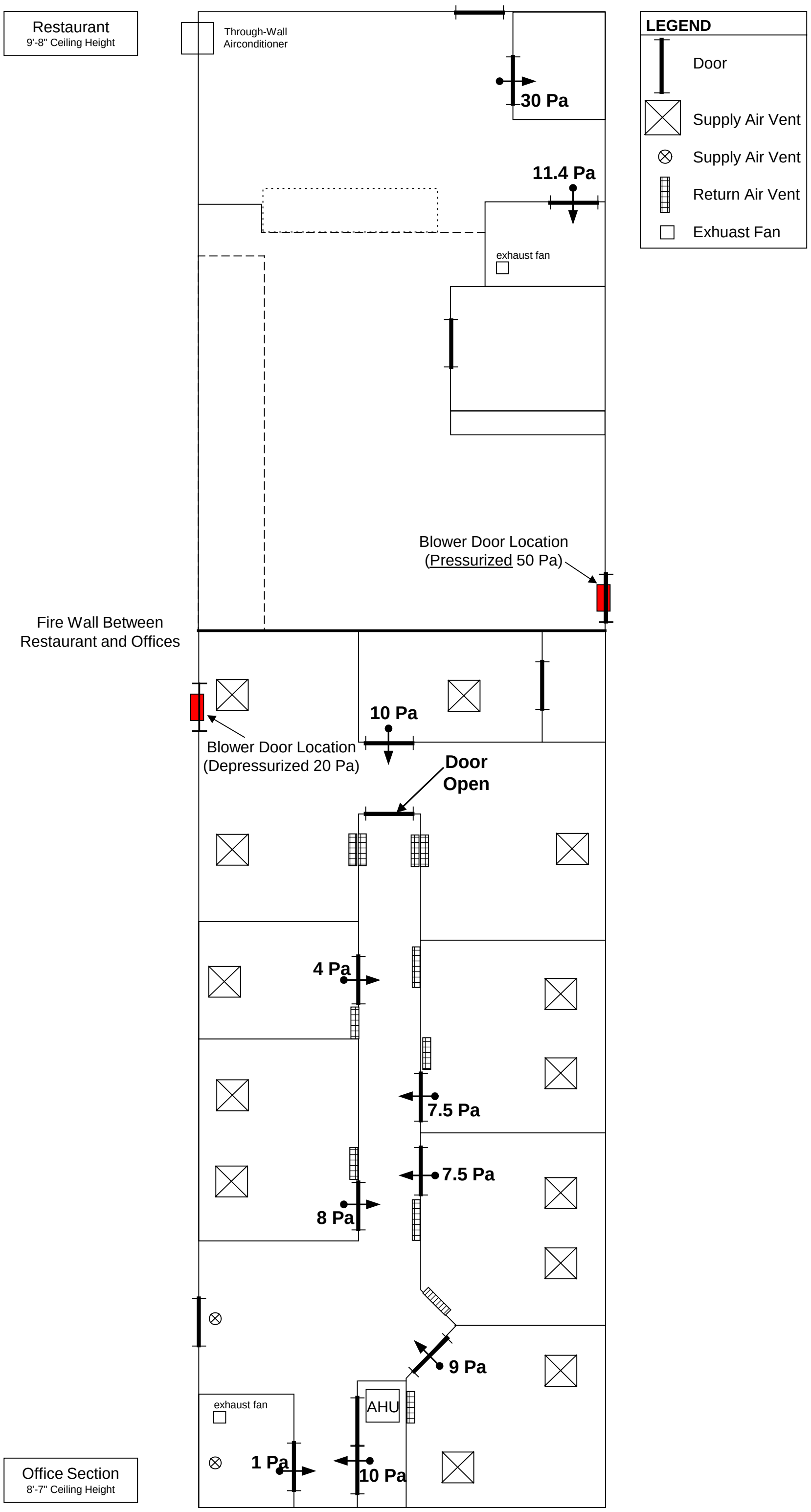

Chinese Restaurant Pressurized 50 Pa – Fans Off
Office Depressurized 20 Pa - AHU Fans Off

Figure A2-12. Room-to-Corridor Pressures

HVAC Airflow Measurements

The airflow for the furnace in the office section was measured using an equal area velocity traverse as shown in Table A2-4. The airflow from each supply diffuser was measured using a Shortridge flow hood. Table A2-5 compares the supply and return airflow for the office section of the building. Table A2-6 presents each diffuser airflow measurement and the schematic illustrates the locations of each supply and return diffusers and the respective airflow.

Table A2-4. Office Section Airflow Measured at AHU Main Supply Duct

Point	Velocity (fpm)
1	780
2	515
3	830
4	150
5	325
6	645
7	600
8	620
9	975
Average	604
Duct Area (ft^2)	1.71
Airflow (cfm)	1,035

Traverse Point Locations and Supply Duct Size

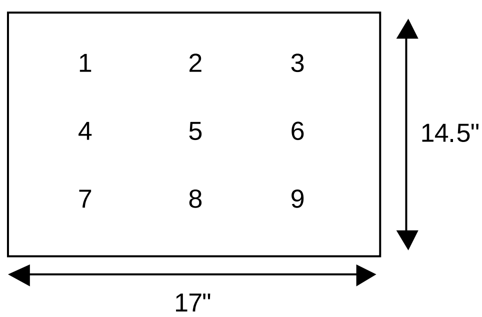

Table A2-5. Comparison of Supply and Return Airflow Measurements

	Equal Area Traverse Supply Airflow (cfm)	Flowhood Supply Airflow (cfm)	Flowhood Return Airflow (cfm)	Supply /Return Ratio	Normalized Fan Power (Watt/cfm)	Supply / Return Static Pressure (Pa)
Office Section AHU	1,035	1,048	820	1.3	0.40	25.5 / -57.5

Table A2-6. Airflow for Supply and Return Diffusers and Cooking Exhaust Hood

Cooking Exhaust Hood Airflow

Configuration	Airflow (cfm)
Exterior Doors Closed	3094
Side Door Open	5000

Office Section Diffuser Airflow

Label	Supply (cfm)
S1	77
S2	70
S3	78
S4	76
S5	77
S6	44
S7	113
S8	131
S9	0
S10	42
S11	57
S12	68
S13	73
S14	68
S15	74
Total	1048

Label	Return (cfm)
R1	50
R2	39
R3	43
R4	88
R5	105
R6	96
R7	112
R8	62
R9	101
R10	56
R11	68
Total	820

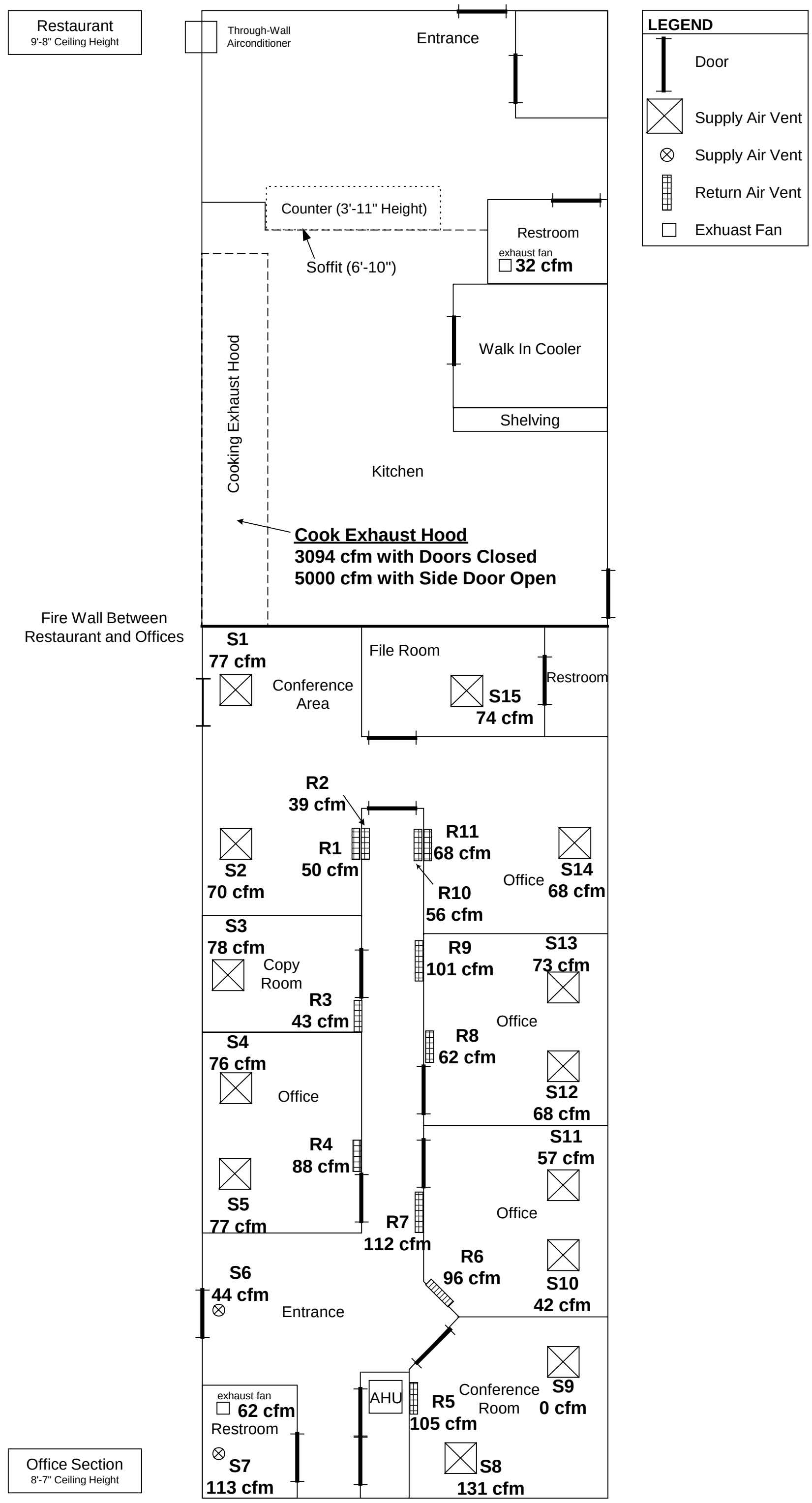

The Chinese restaurant cooking hood has a 24-½ inch Dayton upblast exhaust fan. The airflow through the exhaust fan was determined by adding the flow through the blower door and the flow through the hole cut in the ceiling (Figure A2-11). This method assumes that all the air entering the restaurant is coming through the hole cut in the ceiling and the blower door. Table A2-7 shows how we calculated the exhaust fan flow at 2 Pa and 40.7 Pa. Figure A2-13 shows how the measured exhaust hood flow compares to the Dayton 24-1/2 inch upblast fan curves [Model: 3C717].

Table A2-7. Cooking Exhaust Fan Flow

	Measured Flow at 2 Pa	**Measure Flow at 40.7 Pa**
Blower Door	5,027	1,537
Flow Hood (hole cut in ceiling)	0	1,557
Total	***5,027***	***3,094***

The difference in measure flow and the flow predicted by the fan curve is likely due to other leaks through the building envelope that were not measured. The measured exhaust fan flow at 40.7 Pa is likely much lower than the actual flow given the difference in slope between the measured curve and the Dayton fan curves.

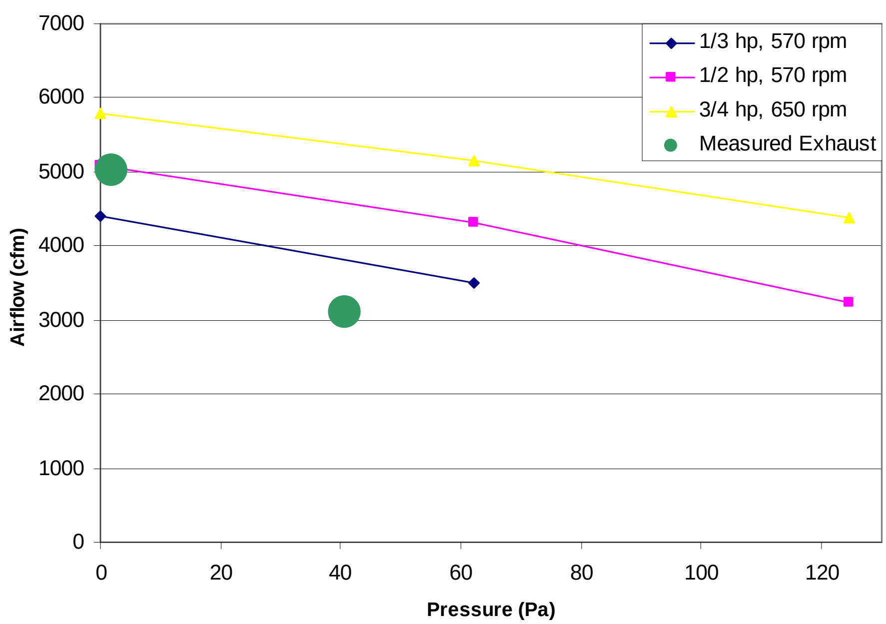

Figure A2-13. Measured Exhaust Fan Flow Compared to Dayton Upblast Fan Curves

Pressure Mapping (AHU Fans ON)

The air pressure relationships in the office section of the building were determined with the furnace fan on. The floor plan in Figure A2-15 shows the pressure differences induced across the doorways with the interior doors closed. At standard pressure with the office section furnace fan on, the maximum pressure drop across all the doorways was 1 Pa.

Figure A2-14 shows that the room pressure increases linearly with net airflow imbalance (supply – return) into the rooms of the office section of the building. The pressure differences and diffuser airflows are labeled in the floor plan in Figure A2-15.

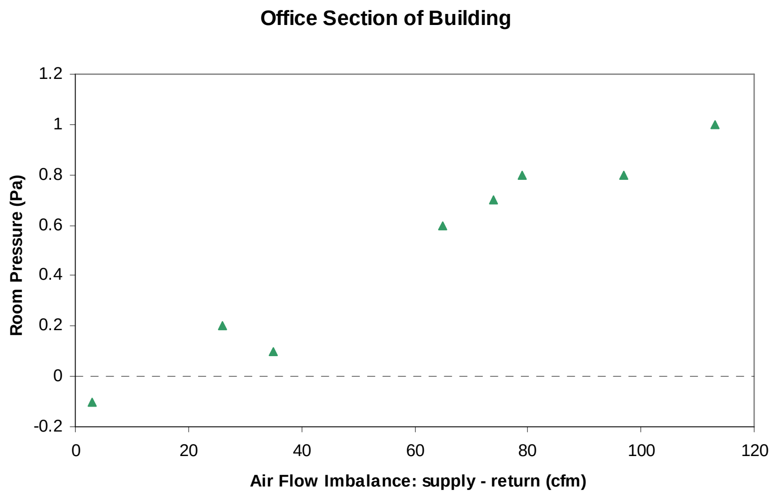

Figure A2-14. Pressure Differences Induced by AHU Fan Operation

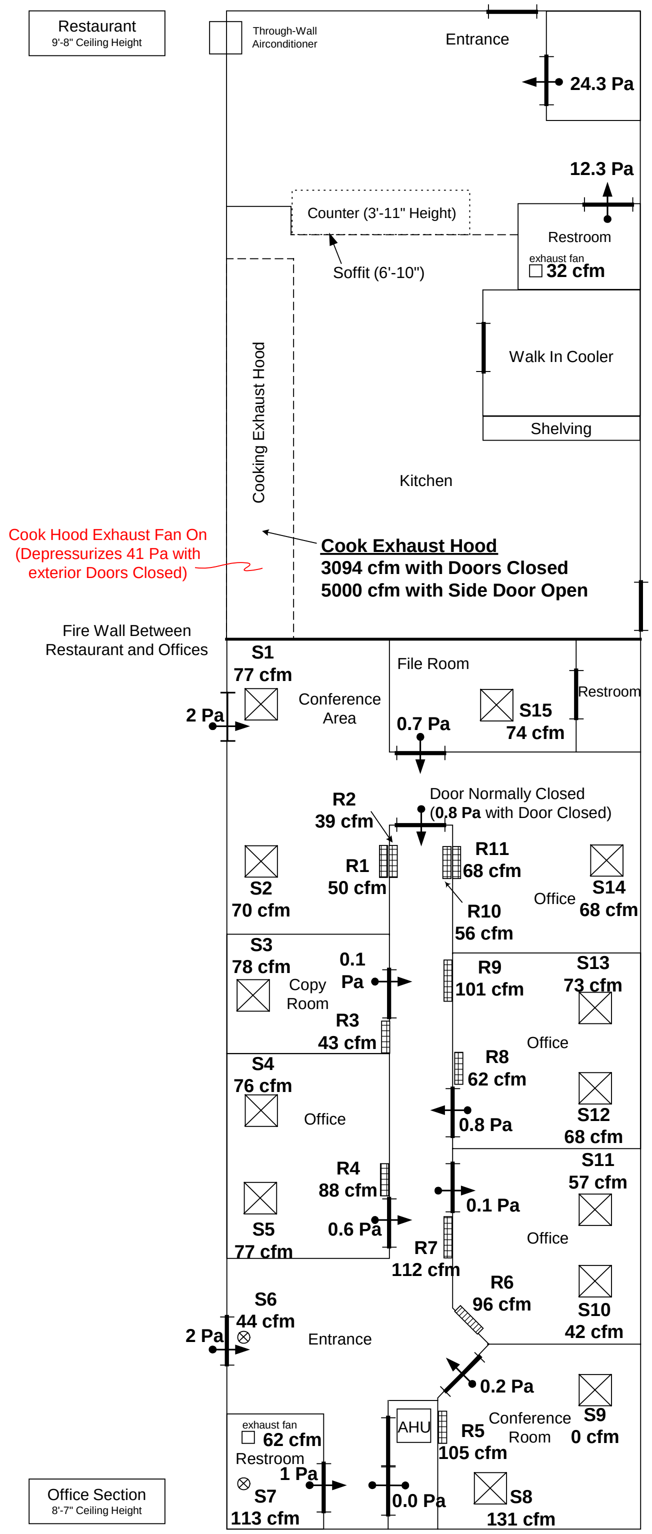

Chinese Restaurant – Cooking Exhaust Fan On
Offices at Standard Pressure - AHU Fans On

Figure A2-15. Pressure Differences between Rooms and Corridors

The air pressure relationships in the restaurant portion of the building were determined with the cooking exhaust hood on. The only heating equipment in the restaurant is a unit heater that does not use supply or return ducts to create potential airflow imbalances. The floor plan in Figure A2-15 shows the pressure differences induced across the doorways with the interior doors closed. For the restaurant with the exhaust fan operating, the pressure drops across the two small interior rooms were 12.3 Pa and 24.3 Pa.

We measured the static pressure of the restaurant with the cooking exhaust hood fan running with all exterior doors closed, one door open, and with one full screen door. We tested the building with a door open and with a screen door because these are typical operating configurations for this Chinese restaurant in the summer.

Table A2-8. Building Pressure with Exhaust Hood Fan Running

Configuration	Building Pressure (Pa)
Side Door Closed Front Door Closed Side Ventilation Window Open	-40.0
Side Screen Door Front Door Closed Side Ventilation Window Open	-5.0
Side Door Open Front Door Closed Side Ventilation Window Open	-2.0

Duct Leakage Measurements

A Duct Blaster was used to depressurize the office area ductwork to measure leakage rates. The Duct Blaster fan was connected to depressurize the entire system (return, furnace cabinet, and supply) using supply diffuser S1 (labeled diffusers are Figure A2-15). Plastic wrap was used to cover each supply and return grill in the system. The air filter was removed and the filter access panel was also sealed. The furnace filter access panel and the seals at the supply and return grills were tested with a smoke puffer to confirm there was no leakage with the system depressurized.

We also tested the leakage rate for the supply duct alone by wrapping the air filter in plastic, inserting it, and repeating the depressurization tests. There was very little difference in the pressure and airflow measurements giving reason to suspect an error in the test method. We moved the Duct Blaster system to supply diffuser S5 and the test had similar results. We realized that these duct airtightness test results are not accurate because the duct system cannot be uniformly depressurized using a single supply diffuser due the limited airflow through the relatively small 6-in. takeoffs.

To properly test the ductwork in the office section of the building, we cut a 10-in. diameter hole in the supply duct above the furnace as shown by the schematic in Figure A2-16. Figure A2-17 shows photos of the Duct Blaster set up to depressurize the ductwork from the supply side. Depressurizing the ductwork with the fan in this location produces relatively uniform pressures across the supply ductwork solving the problem of limited flow through the single 6-in supply takeoff.

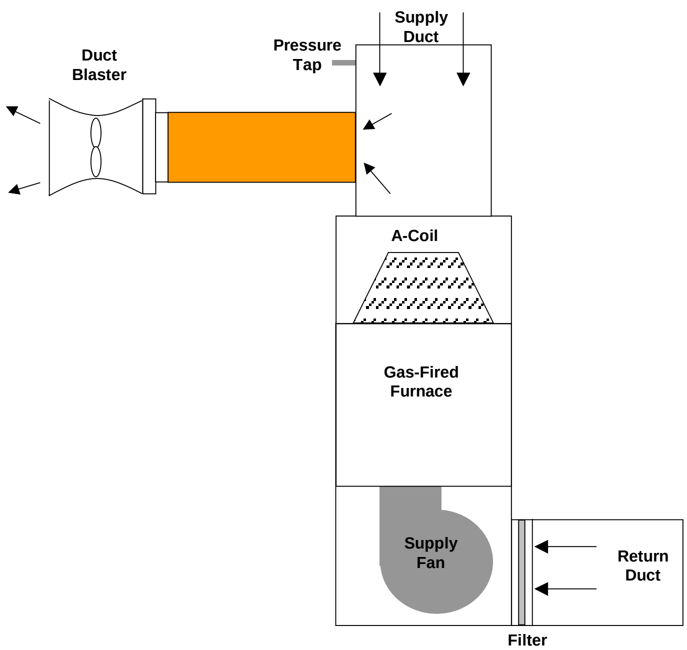

Figure A2-16. Duct Blaster Setup for Testing Supply Ductwork and Furnace Cabinet

Figure A2-17. Duct Blaster Setup for Duct Leakage Test

Plastic wrap was used to cover each supply grill in the system. With the AHU filter removed, duct tape was used to seal the access panel for the filter at the furnace return. Then the duct blaster was used to test the entire duct system (return, furnace cabinet, and supply). The seals at the supply and return grills and furnace filter access panel were tested with a smoke puffer to confirm there was no leakage at those points.

To measure the leakage rate in the supply ductwork and furnace cabinet alone, we wrapped the air filter in plastic wrap, inserted it, sealed the filter perimeter with tape, and repeated the depressurization test. In addition to being taped at the edges, the filter was pulled against its stops creating a reasonably tight seal (confirmed by using the smoke puffer).

Then we tested the return ductwork alone by cutting a hole and moving the Duct Blaster to the return side near the furnace. With the filter still wrapped in plastic, we tested for leaks again, and depressurized the ductwork to test for leakage in the return side.

Figure A2-18 shows the diffuser pressure mapping with the entire system depressurized 17 Pa and a second pressure map with only the return side depressurized 20 Pa. Figure A2-19 shows the resulting measured data fit to a power function (raw data in Table A2-9). Table A2-10 shows the resulting coefficients, exponents, and regression statistics. Table A2-11 summarizes the resulting duct leakage rates and ELA at a reference pressure of 25 Pa.

The sum of the leakage for the supply ductwork and furnace cabinet plus the return ductwork should produce equivalent results as the leakage test for the entire system; however the test for the entire system yielded lower leakage rates than the sum of the two tests on supply and return. This discrepancy is due to a large pressure drop across the furnace. The Duct Blaster was set up to depressurize the entire system from the supply side of the furnace. As a diagnostic check on the degree of pressurization, the pressure at the diffusers was measured by puncturing the plastic covering with a very small probe. The diffuser pressure map for the entire system shown in Figure A2-18 illustrates the pressure drop by noting that while the supply ductwork was approximately -7 Pa, the return ductwork was only –2 Pa. For this reason we will use the two separate tests (supply alone and return alone) to determine the leakage for the entire duct system.

The supply ductwork and furnace cabinet account for 54% of the effective leakage area and the return ductwork alone accounts for 46% of the ELA.

Entire System Depressurized 17 Pa at AHU *Return Ductwork Depressurized 20 Pa at AHU*

Figure A2-18. Diffuser Pressure Mapping with Ductwork Depressurized for Leakage Testing

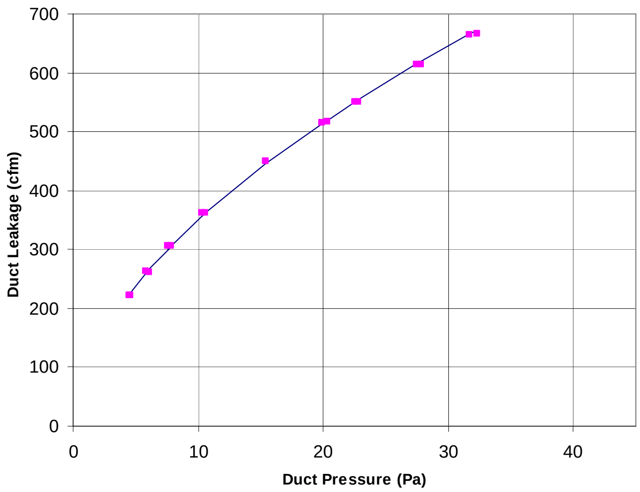

Supply Ductwork & Furnace Cabinet

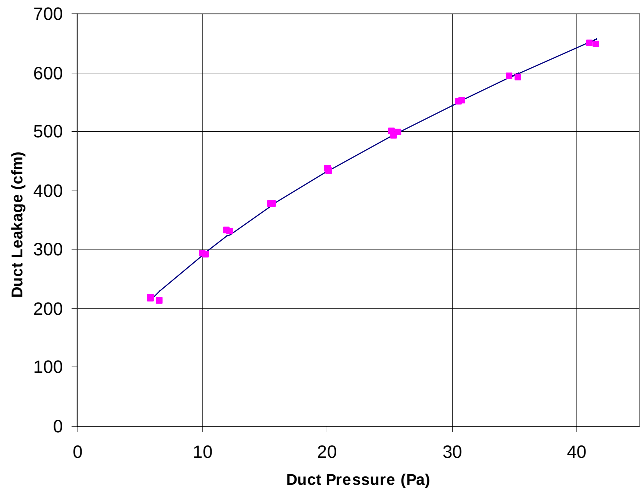

Return Ductwork

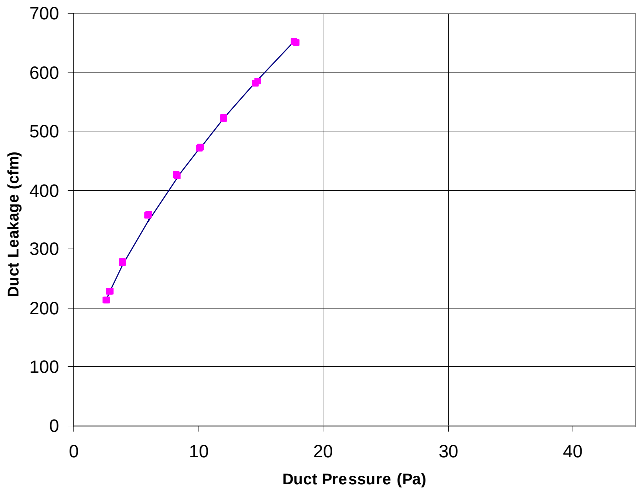

Entire Duct System (Supply, Return, and Furnace)

Figure A2-19. Duct-Blaster Tests on Supply Only, Return Only, and the Entire Duct System

Table A2-9. Raw Data from Duct-Blaster Tests

Supply Ductwork & Furnace Cabinet

Test Results:

Flow Coefficient (K)	97.3	
Exponent (n)	0.557	
Leakage area (LBL ELA @ 25 Pa)	66	sq in
Airflow @ 25 Pa	583.5	cfm

Test Data:

	Nominal Duct Pressure (Pa)	Nominal Flow (cfm)	Ring
1	32.3	666	1
2	31.7	664	1
3	27.8	615	1
4	27.5	615	1
5	22.8	551	1
6	22.5	551	1
7	20.3	517	1
8	19.9	516	1
9	15.4	450	1
10	15.4	450	1
11	10.6	362	1
12	10.3	362	1
13	7.6	306	1
14	7.8	306	1
15	6.1	262	1
16	5.8	263	1
17	4.5	223	1
18	4.6	222	1

Return Ductwork

Test Results:

Flow Coefficient (K)	77.7	
Exponent (n)	0.573	
Leakage area (LBL ELA @ 25 Pa)	56	sq in
Airflow @ 25 Pa	491.0	cfm

Test Data:

	Nominal Duct Pressure (Pa)	Nominal Flow (cfm)	Ring
1	41.0	650	1
2	41.6	647	1
3	34.6	593	1
4	35.3	591	1
5	30.6	550	1
6	30.8	552	1
7	25.4	493	1
8	25.7	499	1
9	25.2	501	1
10	20.1	437	1
11	20.2	434	1
12	15.7	378	1
13	15.5	377	1
14	12.2	331	1
15	12.0	333	1
16	10.0	293	1
17	10.3	292	1
18	6.6	213	1
19	5.9	219	1
20	5.9	217	1

Entire Duct System

Test Results:

Flow Coefficient (K)	122.0	
Exponent (n)	0.584	
Leakage area (LBL ELA @ 25 Pa)	91	sq in
Airflow @ 25 Pa	799.4	cfm

Test Data:

	Nominal Duct Pressure (Pa)	Nominal Flow (cfm)	Ring
1	17.7	652	1
2	17.9	650	1
3	14.8	585	1
4	14.6	581	1
5	12.1	523	1
6	12.1	521	1
7	10.1	470	1
8	10.2	472	1
9	8.4	423	1
10	8.3	425	1
11	6.0	357	1
12	6.1	358	1
13	4.0	278	1
14	4.0	276	1
15	3.0	228	1
16	2.9	228	1
17	2.7	212	1
18	2.6	212	1

Table A2-10. Coefficients, Exponents and Regression Statistics from Duct-Blaster Tests

	Supply Ductwork & Furnace Cabinet			Return Ductwork Only			Entire System (Supply, Return, Furnace)		
	K	n	R^2	K	n	R^2	K	n	R^2
Office Section	97.3	0.557	99.91%	77.7	0.573	99.68%	122.0	0.584	99.89%

Notes: cfm = $K(Pa)^n$ / R^2 indicates fit of linear log-log regression

Note that the duct leakage rate for the entire system in Table A2-11 was measured by testing the whole system at one time. A more accurate measure of the entire ductwork leakage is the sum of the two individual tests for supply and return (1,075 cfm @ 25 Pa, 122 sq-in ELA @ 25 Pa). Summing the individual tests for the supply and return gives more accurate results because the pressure throughout the ductwork was much more uniform for these individual tests.

Table A2-11. Comparison of Supply and Return Airflow Measurements

	Traverse / Supply Airflow (cfm)	Flowhood / Supply Airflow (cfm)	Flowhood / Return Airflow (cfm)	Supply Leakage (cfm @ 25)	Return Leakage (cfm @ 25)	Supply ELA (sq in @ 25)	Return ELA (sq in @ 25)
Office Section	1,035	1,048	820	583	491	66	56

Notes: Leakage and ELA at reference pressure of 25 Pa

The effective leakage area compared to the total duct surface area is shown in Table A2-12. For every 100 sq-ft of duct surface area, there is approximately 13.8 sq-in of duct leakage at 25 Pa. The Sheet Metal and Air Conditioning Contractors' National Association (SMACNA) classifies duct leakiness using duct leakage per 100 sq ft of duct area at a pressure of 1-in w.g. The SMACNA leakage class for the office section duct system is 445.

Table A2-12. Duct Leakage per 100 Square Foot of Duct Area

	Duct Area (sq ft)	ELA (sq in @ 25)	ELA/100 sq ft Duct Area (sq in @ 25)	Leakage (cfm @ 25 Pa)	Leakage per 100 sq ft Duct Area (cfm @ 25 Pa)	SMACNA Leakage Class cfm per 100 sq ft (cfm @ 1-in water)
Supply & AHU Cabinet	503	66	13.2	583	116	417
Return Ductwork	380	56	14.7	491	129	483
Total	882	122	13.8	1,075	122	445

Space Conditions

Figure A2-20 shows the average temperature profiles for the office section of the building based on temperature readings taken with a HOBO datalogger. The thick line shows the average for each hour while the shaded region corresponds to one standard deviation about the average. The dotted lines correspond to the minimum and maximum for each hour. A sensor was placed in the office next to the conference room on the south side. The temperature profiles show that the temperature is setback weeknights (5:00 pm – 8:00 am) and on weekends.

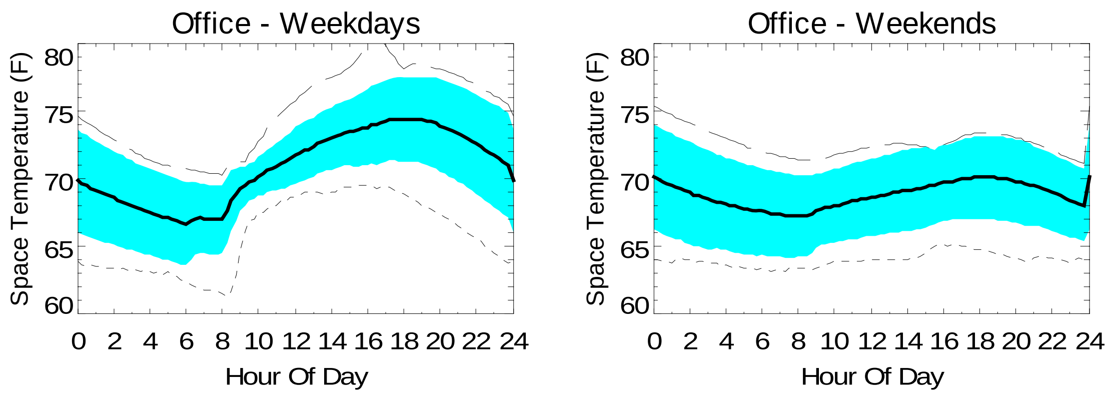

Figure A2-20. Measured Space Temperature Profile (April 30 to May 25)

Figure A2-21 shows the CO_2 concentration in the office next to the conference room on the south side and the corridor. On May 24, we released bottled CO_2 (tracer gas) into the office section of the building until concentrations reached 3,500 PPM as shown by the large spike in concentration. For this test, we also logged data with a second CO_2 sensor located in the corridor shown by the lower chart in Figure A2-21. The concentration of CO_2 released by people provides an indication of occupancy as shown by the variation CO_2 levels between April 30 and May 23. The next section uses the CO_2 as a tracer gas to estimate the infiltration rate into the building.

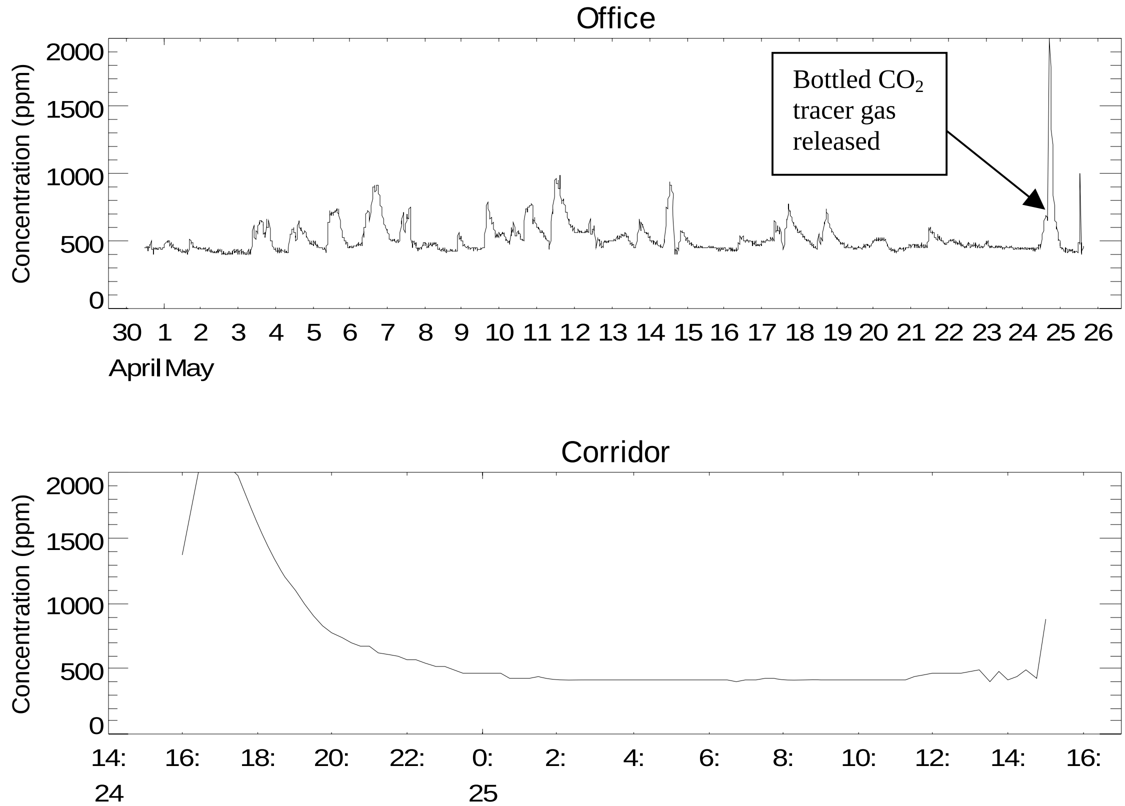

Figure A2-21. Measured CO_2 Concentration (April 30 to May 25)

Infiltration Estimate from CO_2 Decay

Figure A2-22 and Figure A2-23 show the resulting decay trends using CO_2 levels immediately after high occupancy periods and after releasing bottled CO_2 tracer gas. The predicted air change rate (ACH) is shown on each plot. The decay trend on May 24, 2004 shows the decay after bottled CO_2 tracer gas was released into the building.

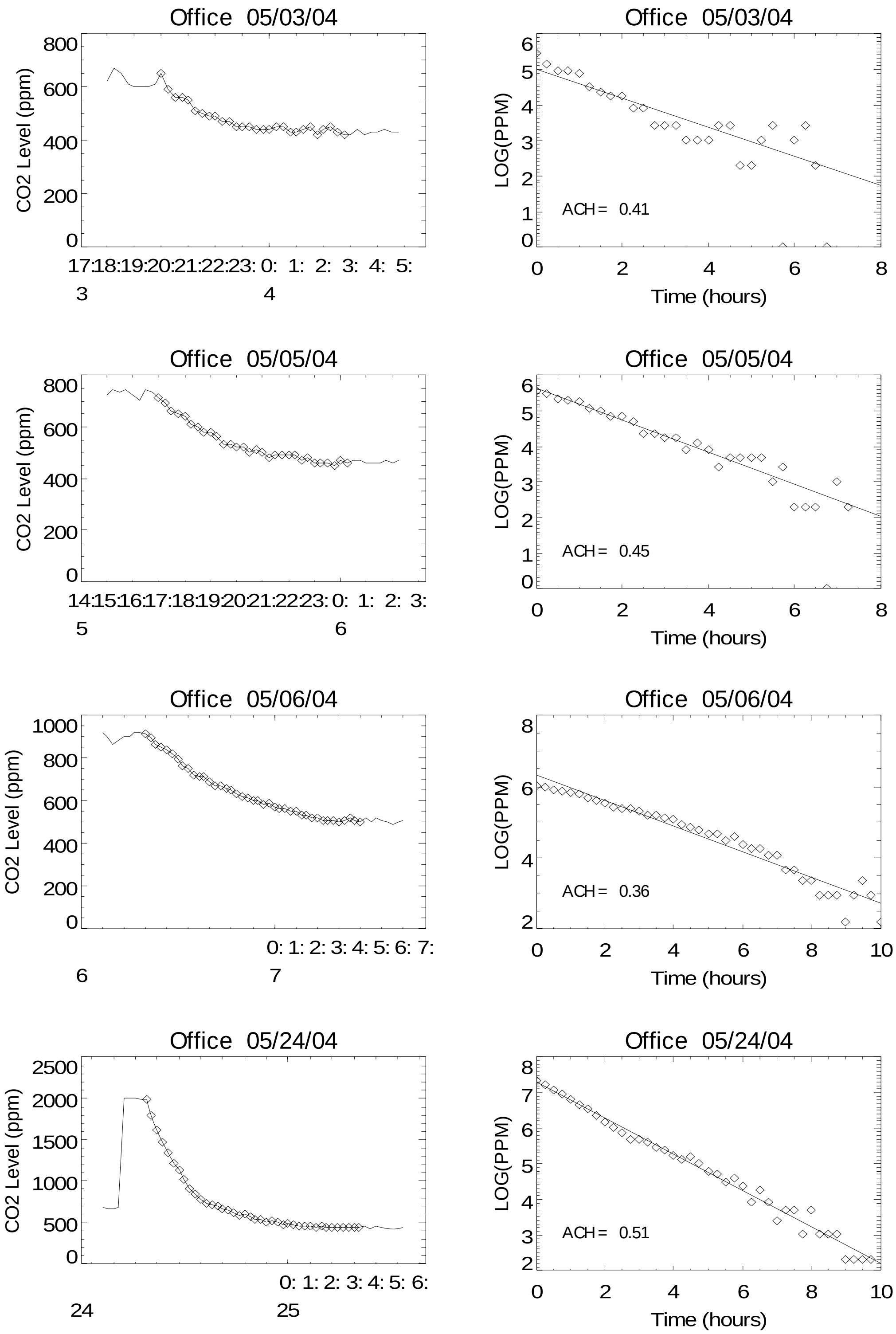

Figure A2-22. Tracer Gas Decay Using CO_2 for Various Periods

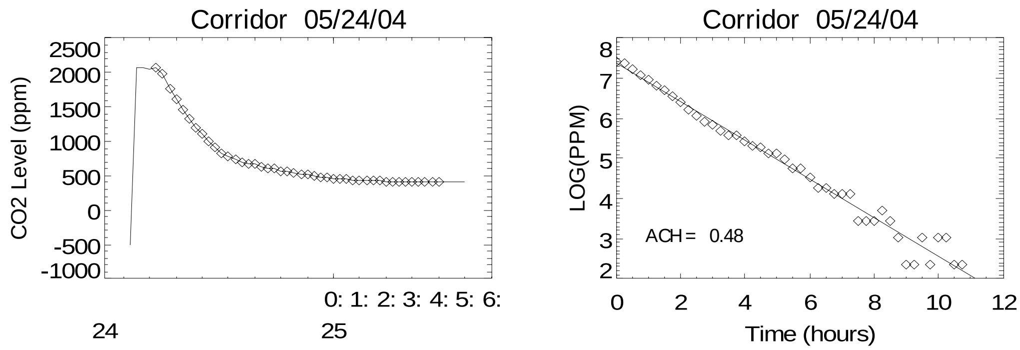

Figure A2-23. Tracer Gas Decay Using CO_2 for Various Periods

Table A2-13 summarizes the results of the tracer gas decay tests in the plots above. The table also includes the ambient temperature recorded during each decay period listed in the table. Using the CO_2 decays after occupancy, the office section of the building has an ACH between 0.36 and 0.45. During these times, the supply fan operated intermittently. During these tests, based on the decay after the bottled CO_2 was released on May 24, the office section of the building has an ACH of approximately 0.5. The test on May 24 (ACH = 0.5) is more reliable because the furnace fan was forced to run throughout the test to ensure that the tracer gas was thoroughly mixed and dispersed throughout the office section of the building.

Table A2-13. Summary of Tracer Gas Decay Tests for the Office Section of the Building

Office

Start Time	End Time	ACH	Flow (cfm)	Ambient Temp. (F)
03-May 08:00 PM	04-May 02:45 AM	0.41	84	40.5
05-May 05:00 PM	06-May 12:15 AM	0.45	93	46.5
06-May 06:00 PM	07-May 04:00 AM	0.36	75	59.5
24-May 05:30 PM	25-May 03:15 AM	0.51	106	---

Corridor

Start Time	End Time	ACH		Ambient Temp. (F)
24-May 05:15 PM	25-May 04:00 AM	0.48	99	---

Note: Flow determined with office section volume of 12,386 ft^3

The effective ventilation rate is about 100 cfm. In contrast, the measured difference between the supply and return was 228. This implies that about half of the return leaks are pulling in ambient air. The balance is pulled from the space.

The return leakage predicted from the Duct Blaster tests implies the return leakage was nearly 500 cfm at 25 Pa. This implies that the nominal return pressure of 25 Pa was much to high for this system.

In comparison to the ACH values above, the nominal leakage rate (ACH_{50} divided by 20) from the blower door test above is 1.65 ACH.

Utility Bills

Gas use is primarily used for space heating in the office section of the building and cooking is the primary use of gas in the restaurant. The overall energy index for the building is summarized in Table A2-14. The available electric and gas utility bill data is shown below in Table A2-15 and Table A2-16.

Table A2-14. Overall Energy Use Index

	Office Section of the Building		Restaurant	
	Heating Energy Use Index (MBtu/ft^2-year)	Electric Use Index (kWh/ft^2-year)	Heating Energy Use Index (MBtu/ft^2-year)	Electric Use Index (kWh/ft^2-year)
2001-2002 Season	66.4	4.17	601	26.4
2002-2003 Season	82.2	3.67	631	26.6

Season is from November to October

Table A2-15. Summary of Electric Bills

	Office Section of Building				
	Days in Month	Energy (kWh)	Cost ($)	$/kWh	Elec. Use per Sq-Ft (kWh/ft^2)
11/16/2001	29	409	$ 78.49	0.19	0.28
12/18/2001	32	468	$ 86.29	0.18	0.32
1/18/2002	31	550	$ 95.64	0.17	0.38
2/19/2002	32	625	$ 100.92	0.16	0.43
3/19/2002	28	659	$ 101.35	0.15	0.46
4/18/2002	30	737	$ 111.96	0.15	0.51
5/21/2002	33	443	$ 77.29	0.17	0.31
6/19/2002	29	373	$ 67.56	0.18	0.26
7/19/2002	30	480	$ 82.46	0.17	0.33
8/20/2002	32	535	$ 92.32	0.17	0.37
9/19/2002	30	382	$ 72.21	0.19	0.26
10/18/2002	29	355	$ 68.89	0.19	0.25
11/18/2002	31	349	$ 67.23	0.19	0.24
12/16/2002	28	410	$ 81.26	0.20	0.28
1/21/2003	36	548	$ 102.42	0.19	0.38
2/19/2003	29	564	$ 100.94	0.18	0.39
3/20/2003	29	657	$ 118.80	0.18	0.46
4/17/2003	28	758	$ 132.38	0.17	0.53
5/20/2003	33	385	$ 78.38	0.20	0.27
6/19/2003	30	322	$ 67.87	0.21	0.22
7/21/2003	32	362	$ 72.97	0.20	0.25
8/18/2003	28	362	$ 72.83	0.20	0.25
9/19/2003	32	323	$ 68.63	0.21	0.22
10/20/2003	31	286	$ 63.71	0.22	0.20
2001 - 2002	365	6,016	$ 1,035.38	0.17	4.17
2002 - 2003	367	5,326	$ 1,027.42	0.19	3.69

	Restaurant				
	Days in Month	Energy (kWh)	Cost ($)	$/kWh	Elec. Use per Sq-Ft (kWh/ft^2)
11/16/2001	29	1893	$ 293.17	0.15	1.83
12/18/2001	32	2076	$ 308.98	0.15	2.01
1/18/2002	31	1813	$ 270.21	0.15	1.75
2/19/2002	32	1856	$ 266.06	0.14	1.80
3/19/2002	28	1596	$ 237.68	0.15	1.54
4/18/2002	30	1985	$ 278.66	0.14	1.92
5/21/2002	33	2426	$ 321.46	0.13	2.35
6/19/2002	29	2403	$ 315.76	0.13	2.33
7/19/2002	30	2876	$ 372.63	0.13	2.78
8/20/2002	32	3153	$ 410.65	0.13	3.05
9/19/2002	30	2767	$ 374.42	0.14	2.68
10/18/2002	29	2465	$ 349.52	0.14	2.39
11/18/2002	31	2216	$ 321.34	0.15	2.14
12/17/2002	29	1816	$ 273.16	0.15	1.76
1/21/2003	35	2283	$ 311.04	0.14	2.21
2/19/2003	29	1927	$ 274.93	0.14	1.86
3/20/2003	29	2061	$ 302.54	0.15	1.99
4/17/2003	28	2017	$ 290.93	0.14	1.95
5/20/2003	33	2582	$ 359.90	0.14	2.50
6/19/2003	30	2515	$ 340.33	0.14	2.43
7/21/2003	32	3144	$ 398.38	0.13	3.04
8/18/2003	28	2845	$ 374.60	0.13	2.75
9/19/2003	32	2451	$ 340.71	0.14	2.37
10/20/2003	31	1793	$ 284.27	0.16	1.73
2001 - 2002	365	27,309	$ 3,799.20	0.14	26.42
2002 - 2003	367	27,650	$ 3,872.13	0.14	26.75

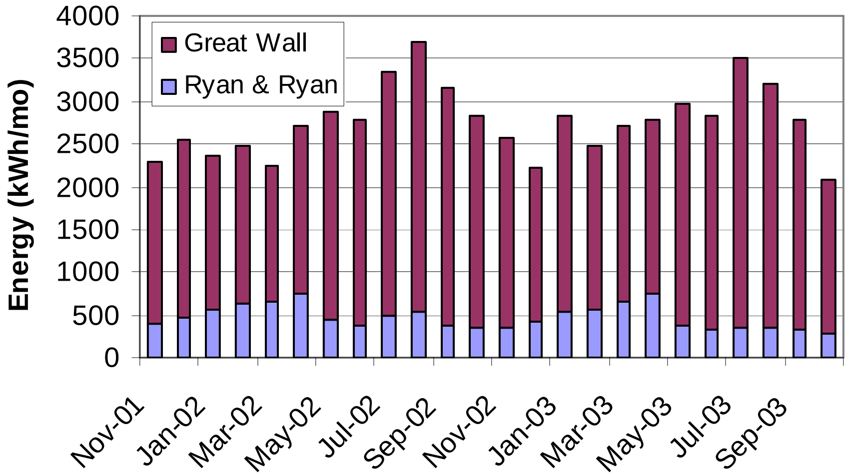

Figure A2-24. Monthly Electricity Use Trends

Table A2-16. Summary of Gas Bills

	Office Section of Building				
	Days in Month	Gas Use (therms)	Cost ($)	$/therm	Gas Use per Sq-Ft (MBtu/ft^2)
11/16/2001	29	77	$ 83.26	1.08	5.3
12/18/2001	32	111	$ 123.57	1.11	7.7
1/18/2002	31	215	$ 208.80	0.97	14.9
2/19/2002	32	196	$ 192.61	0.98	13.6
3/19/2002	28	138	$ 137.63	1.00	9.6
4/18/2002	30	86	$ 89.22	1.04	6.0
5/21/2002	33	94	$ 98.14	1.04	6.5
6/19/2002	29	14	$ 32.31	2.31	1.0
7/19/2002	30	3	$ 22.77	7.59	0.2
8/20/2002	32	2	$ 22.08	11.04	0.1
9/19/2002	30	3	$ 22.60	7.53	0.2
10/18/2002	29	19	$ 36.39	1.92	1.3
11/18/2002	31	115	$ 119.09	1.04	8.0
12/16/2002	28	157	$ 158.72	1.01	10.9
1/21/2003	36	295	$ 296.50	1.01	20.4
2/19/2003	29	255	$ 260.65	1.02	17.7
3/20/2003	29	173	$ 226.07	1.31	12.0
4/17/2003	28	93	$ 133.06	1.43	6.4
5/20/2003	33	52	$ 81.45	1.57	3.6
6/19/2003	30	13	$ 35.03	2.69	0.9
7/21/2003	32	3	$ 23.27	7.76	0.2
8/18/2003	28	3	$ 22.92	7.64	0.2
9/19/2003	32	3	$ 23.16	7.72	0.2
10/20/2003	31	31	$ 51.80	1.67	2.1
2001 - 2002	365	958	$ 1,069.38	1.12	66.4
2002 - 2003	367	1,193	$ 1,431.72	1.20	82.7

	Restaurant				
	Days in Month	Gas Use (therms)	Cost ($)	$/therm	Gas Use per Sq-Ft (MBtu/ft^2)
11/16/2001	29	522	$ 412.32	0.79	50.5
12/18/2001	32	558	$ 484.30	0.87	54.0
1/18/2002	31	530	$ 446.50	0.84	51.3
2/19/2002	32	567	$ 472.19	0.83	54.9
3/19/2002	28	515	$ 421.82	0.82	49.8
4/18/2002	30	577	$ 462.20	0.80	55.8
5/21/2002	33	604	$ 479.61	0.79	58.4
6/19/2002	29	455	$ 393.75	0.87	44.0
7/19/2002	30	445	$ 382.85	0.86	43.1
8/20/2002	32	483	$ 381.61	0.79	46.7
9/19/2002	30	469	$ 375.31	0.80	45.4
10/18/2002	29	482	$ 404.32	0.84	46.6
11/18/2002	31	528	$ 448.64	0.85	51.1
12/17/2002	29	570	$ 504.90	0.89	55.2
1/21/2003	35	689	$ 609.37	0.89	66.6
2/19/2003	29	615	$ 569.82	0.93	59.5
3/20/2003	29	574	$ 674.05	1.17	55.5
4/17/2003	28	477	$ 577.49	1.21	46.2
5/20/2003	33	568	$ 656.98	1.16	55.0
6/19/2003	30	522	$ 592.82	1.14	50.5
7/21/2003	32	507	$ 529.57	1.04	49.1
8/18/2003	28	449	$ 422.94	0.94	43.4
9/19/2003	32	531	$ 508.06	0.96	51.4
10/20/2003	31	531	$ 530.72	1.00	51.4
2001 - 2002	365	6,207	$ 5,116.78	0.82	600.6
2002 - 2003	367	6,561	$ 6,625.36	1.01	634.8

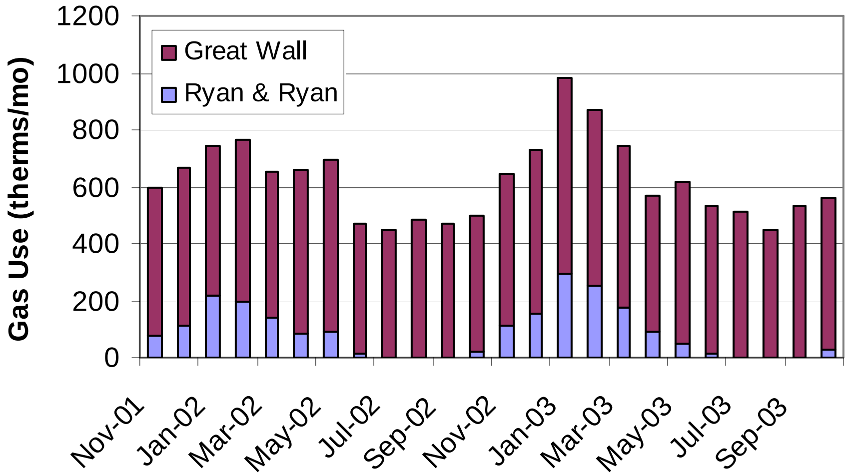

Figure A2-25. Monthly Gas Use Trends

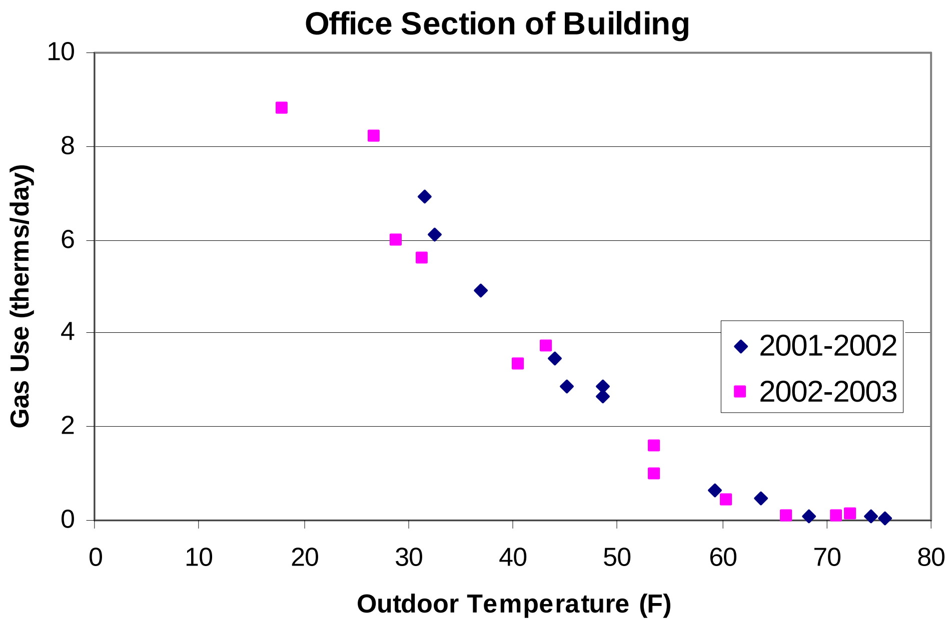

Figure A2-26. Variation of Gas Use with Ambient Temperature (office section)

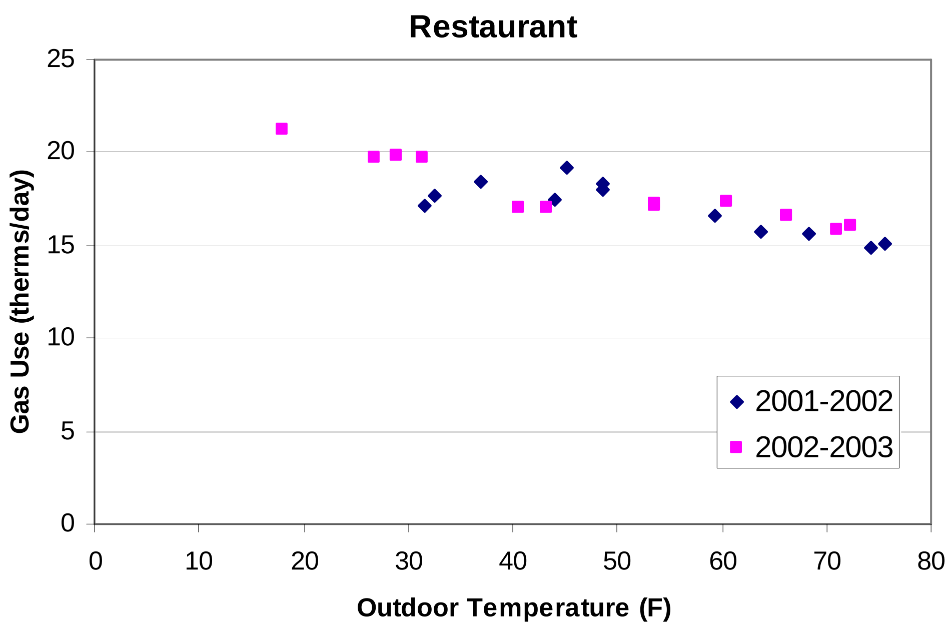

Figure A2-27. Variation of Gas Use with Ambient Temperature (restaurant)

An accounting firm uses the office section. The months of increased electric use circled in Figure A2-28 occur during the tax season (March and April).

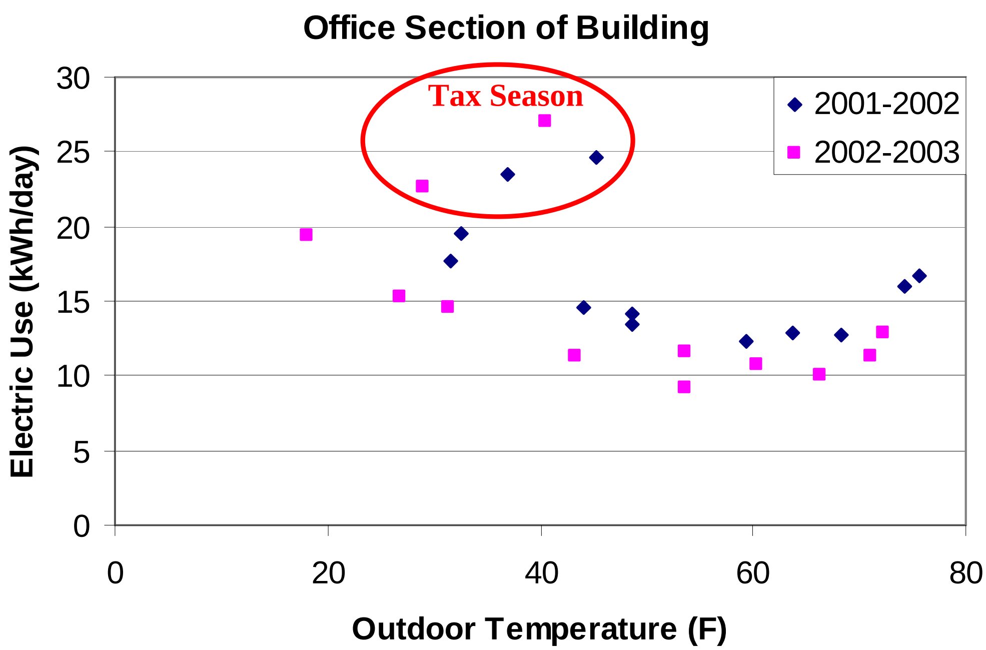

Figure A2-28. Variation of Electric Use with Ambient Temperature (office section)

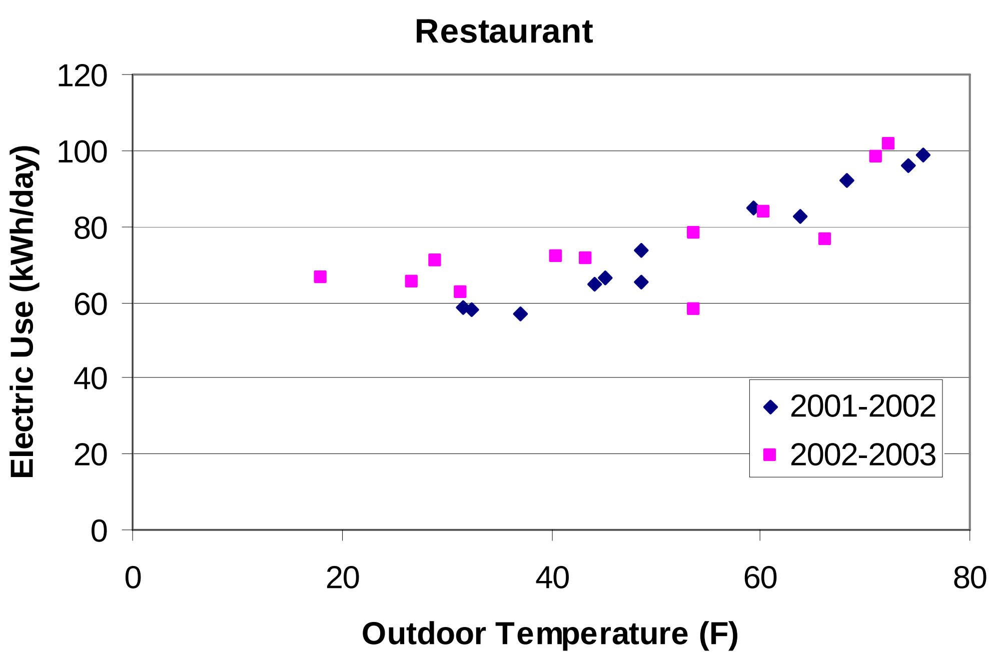

Figure A2-29. Variation of Electric Use with Ambient Temperature (restaurant)

Thermal Imaging of Building Envelope

Using a thermal imaging camera, several voids in the wall insulation (standard R-18 6-inch fiberglass batts) were observed. Correcting these voids requires removal of the gypsum board or the exterior sheathing, and was beyond the scope of this project. Some examples of wall voids are shown in Figure A2-30.

Wall Void Behind Electrical Service Entrance

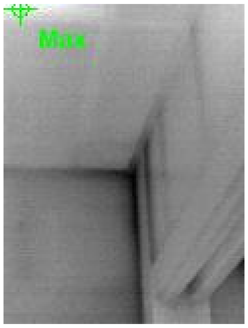

Wall Void on Northeast Corner

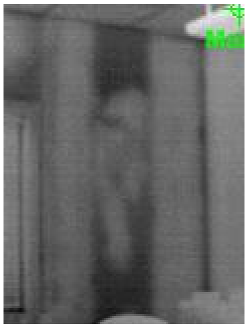

Inside View

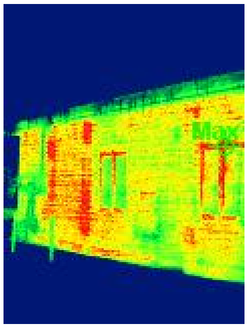

Outside View

Wall Void In Eastern Office

Figure A2-30. Wall Voids Discovered Using Thermal Imaging Camera

REMEDIATION

The office (site 2) was selected for remediation because it had has a very high leakage rate through the ceiling as well as leaky, uninsulated return ducts located in the attic space. After discussing various options (including eliminating the return duct) with the building owner, we decided to: replace fiberglass batts and fill obvious voids in the ceiling insulation, and 2) apply spray foam to the return duct in the attic to seal and insulate it. The major remediation dates are summarized below.

February 12, 2006	Owner starts to replace some fiberglass batts
February 19, 2006	CDH staff completes process of reposition batts and filling voids.
March 11, 2006	CDH staff applies sprayfoam insulation to return duct; fixes some additional voids.

<u>Envelope Sealing</u>

The first step in addressing the leakage issue with the building was to evaluate and repair the ceiling batts, and seal any major envelope leaks. The 12-inches of fiberglass batts that were installed during the building remodeling (in 1996) have fallen through the framing trusses, leaving large areas of the drop ceiling exposed directly to the attic space (Figure A2-31). The fiberglass batts act as both the thermal and air barrier in this building, with no sheathing on the underside of the trusses. The batts were originally installed with a friction fit, and no support underneath.

Figure A2-31. Hole in Fiberglass Insulation (Thermal and Air Barrier) – Viewed from Below

These large leaks allow conditioned air to escape into the attic space, warming the attic in the winter and causing large ice dams to form (Figure A2-32). The leakage also results in additional heating and cooling energy consumption, required to condition the infiltration that occurs to make up the air losses to the attic.

Figure A2-32. Ice Dams Formed from Leakage to the Attic

It was decided that a low cost way to mitigate these envelope leaks was to remove the drop ceiling tiles, identify and replace any batts which had fallen down, and support the batts from underneath with furring strips, attached to the underside of the truss.

On February 12, 2006 after a site survey with the building owner and discussions of the work to follow, the building owner replaced some of the batts himself. CDH Energy returned on February 19, and replaced and supported more batts, as well as sealed the perimeter of the building (by adhering the ceiling batts to the wall framing) with expandable foam.

Figure A2-33. Furring Strip Installed to Support Batts

Duct Insulation and Air Sealing

The un-insulated return ductwork in the attic also contributes to the ice dam issue by transferring heat from the space to the attic. These duct losses are magnified by the decrease in attic temperature that occurred when the envelope was sealed. To mitigate these losses, the decision was made to spray the return ductwork with expandable foam. This foam coating will seal leaks in the ductwork, and provide some insulation from the unconditioned attic.

Figure A2-34 displays a section of the ductwork before and after the foam was applied. The typical foam depth was between ½-inch and 1-inch thick, resulting in an applied insulation level of R2.5-R5. The transitions between the sheet metal return plenum and flexible duct takeoffs was coated, overlapping slightly onto the flexible duct.


Existing Return Ductwork


Return Ductwork with Insulation

Figure A2-34. Return Ductwork in Attic Space

During this work, a few additional gaps were identified in the fiberglass insulation and these were closed in the same manner as the previous fix (supporting the batts from below using furring strips).

Additional Monitoring of Remediation Impacts

A Campbell CR10 datalogger was installed to characterize the heating load and remediation impacts by measuring the furnace runtime, and to determine impact of return duct leakage on the heating load. The schematic below shows the location of measured points.

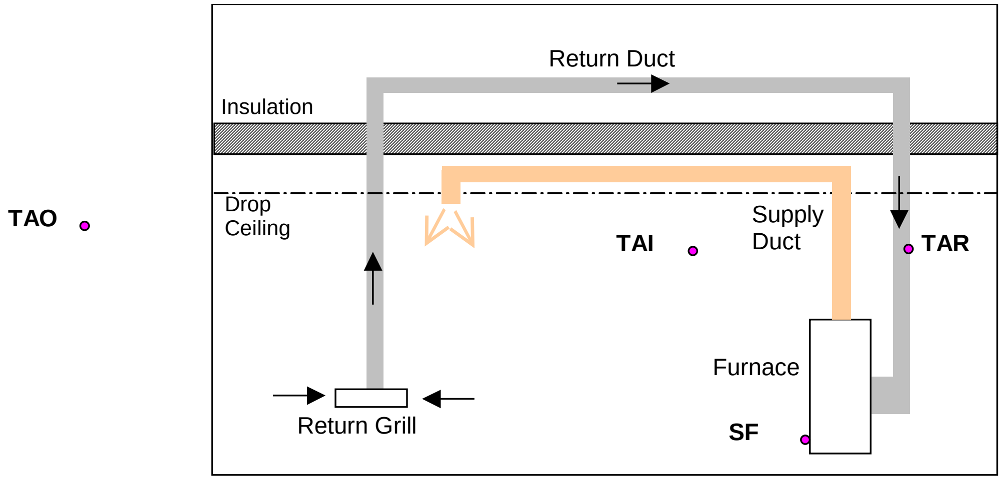

TAR – Return Air Temperature Entering Furnace
TAI – Indoor Temperature (F)
SF – Furnace Runtime (F)
TAO – Ambient Temperature (F) (from Syracuse Airport)

Figure A2-35. Monitored Data Point Locations for Remediation

Figure A2-36 displays the furnace operation and space temperature patterns observed on a shade plot. On the shade plot the day of year is shown on the x-axis and the hour of the day is shown on the y-axis. Each day consists of a vertical stripe containing 96 15-minute data records. Periods of higher furnace runtime, or higher space temperature, are shown with a darker shade of gray.

The space temperature plot (and to a lesser extent the furnace runtime plot) displays the thermostat setup and setback that occurs each weekday. Several changes in the thermostat schedule were observed, with a two-stage setup occurring at the start of monitoring, then switching to a single setup period halfway through January. Typically the building was brought to the comfort setting of 70°F at 8:30 AM each weekday. Near the beginning of March, a much lower setback temperature was used, and the building stayed warmer into the night (as evening occupancy persisted during this period).

In October and November, we see two setup periods in the morning during weekdays. Compared to the previous data, the space temperature during the setback period was much lower for this time frame than what was observed in the winter and spring. There is also very little furnace runtime during the setback period, indicating a more aggressive setback strategy.

Table A2-17 displays the observed thermostat setpoints. Typically these setpoints apply to the entire period with some periods of manual override occurring.

Table A2-17. Observed Thermostat Setpoints

Period	Typical Setpoints
January 7 – January 19, 2006	Weekday: 6:30 AM 68°F, 8:30 AM 71°F, 5:00 PM 62°F Weekend: 62°F
January 20 – February 28, 2006	Weekday: , 8:30 AM 70°F, 5:00 PM 62°F (55°F February 27) Weekend: 62°F
March 1 – March 9, 2006	Weekday: 6:30 AM 65°F, 8:30 AM 70°F, 5:00 PM 55°F Weekend: 55°F
March 9 – March 31, 2006 (Much manual override in this period)	Weekday: 6:30 AM 65°F, 8:30 AM 70°F, 5:00 PM 55°F or 62°F Weekend: 55°F or 62°F
April 1 – April 16, 2006 (Much manual override in this period)	Weekday: 8:30 AM 70°F, 5:00 PM 62°F (some 55°F) Weekend: 62°F
October 12 – November 8, 2006 (Very little manual override in this period)	Weekday: 6:00 AM 62°F, 8:30 AM 67°F, 5:00 PM 55°F Weekend: 8:30 AM 62°F, 5:00 PM 55°F

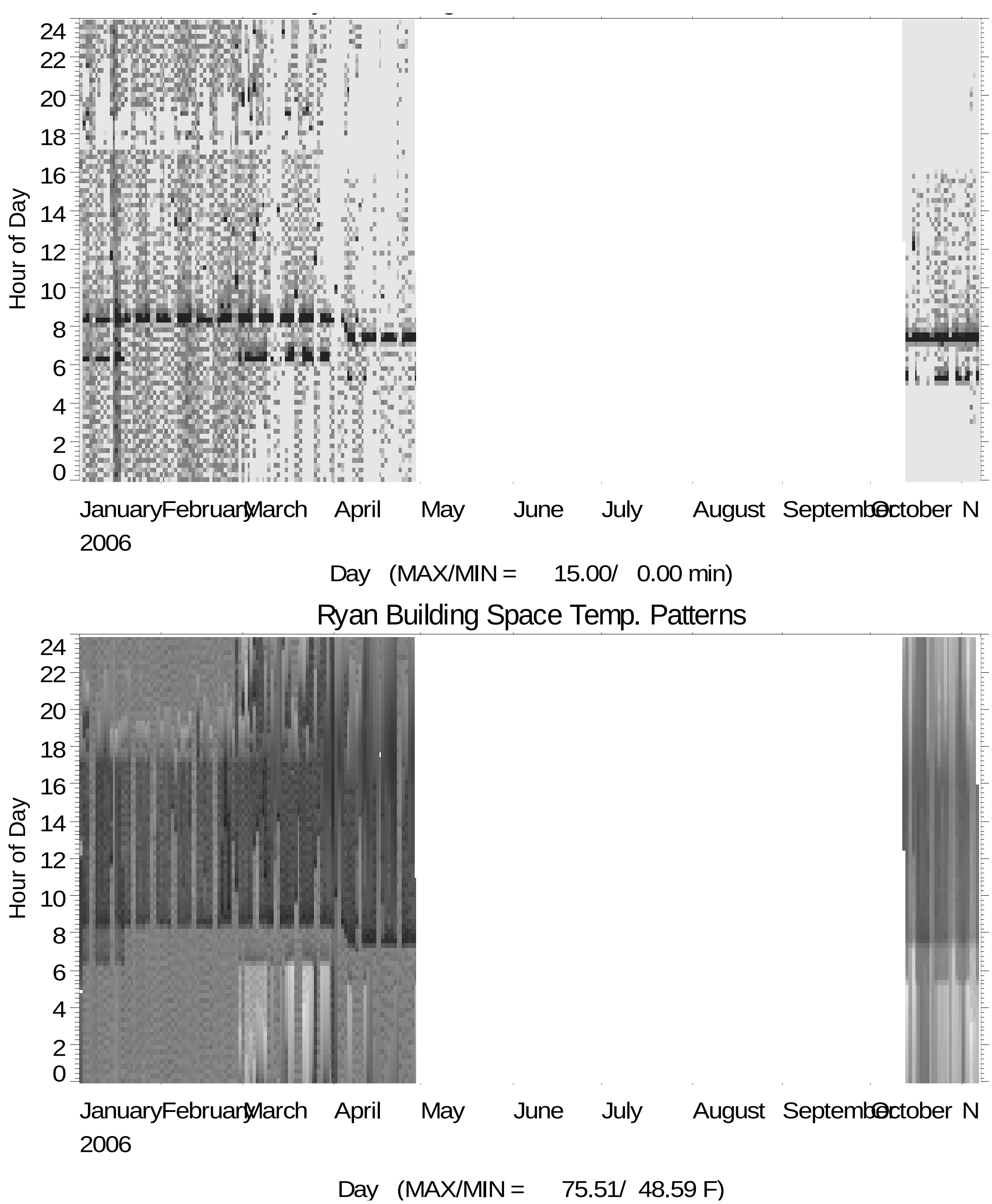

Figure A2-36. Furnace Runtime And Space Temperature Patterns

The measured runtime of the furnace was compared to the gas meter readings for the building to determine the typical fuel input for the furnace. A heating value of 1,020 Btu/cu ft was used to convert the meter readings to energy input. The gas meter is read to the nearest 100 cu ft, which results in a typical error of ±0.02 therm/h. The fuel input to the furnace averaged 0.712 therm/h or 71.2 MBtu/h. This agrees well with the nominal size of the furnace (75 MBtu/h input).

Table A2-18. Comparing Measured Furnace Runtime to Gas Meter Readings

Start Date	End Date	Start Meter Reading (cu ft)	End Meter Reading (cu ft)	Furnace Runtime (hours)	Gas Use (therms)	Furnace Input (Therm/h)
Jan 6, 2006	Jan 18, 2006	9,528	9,593	93.1	66.3	0.712
Jan 18, 2006	Feb 17, 2006	9,593	9,732	199.5	141.8	0.711
Feb 17, 2006	Feb 27, 2006	9,732	9,785	77.4	54.1	0.698
Feb 27, 2006	Mar 8, 2006	9,785	9,826	60.7	41.8	0.689
Mar 8, 2006	Apr 17, 2006	9,826	9,919	129.3	94.6	0.731
Totals/Average				***560.0***	***398.5***	***0.712 (0.69 – 0.73)***

Using the calculated fuel input and the measured daily runtime of the furnace, the current thermal load line for the building was calculated, and compared to the historic building load line. Compared to the 2002-2003 load line, currently the building is using approximately 285 therm/year less (24% less) than the building did in 2002-2003. This may be due to the use of a more aggressive thermostat setback now.

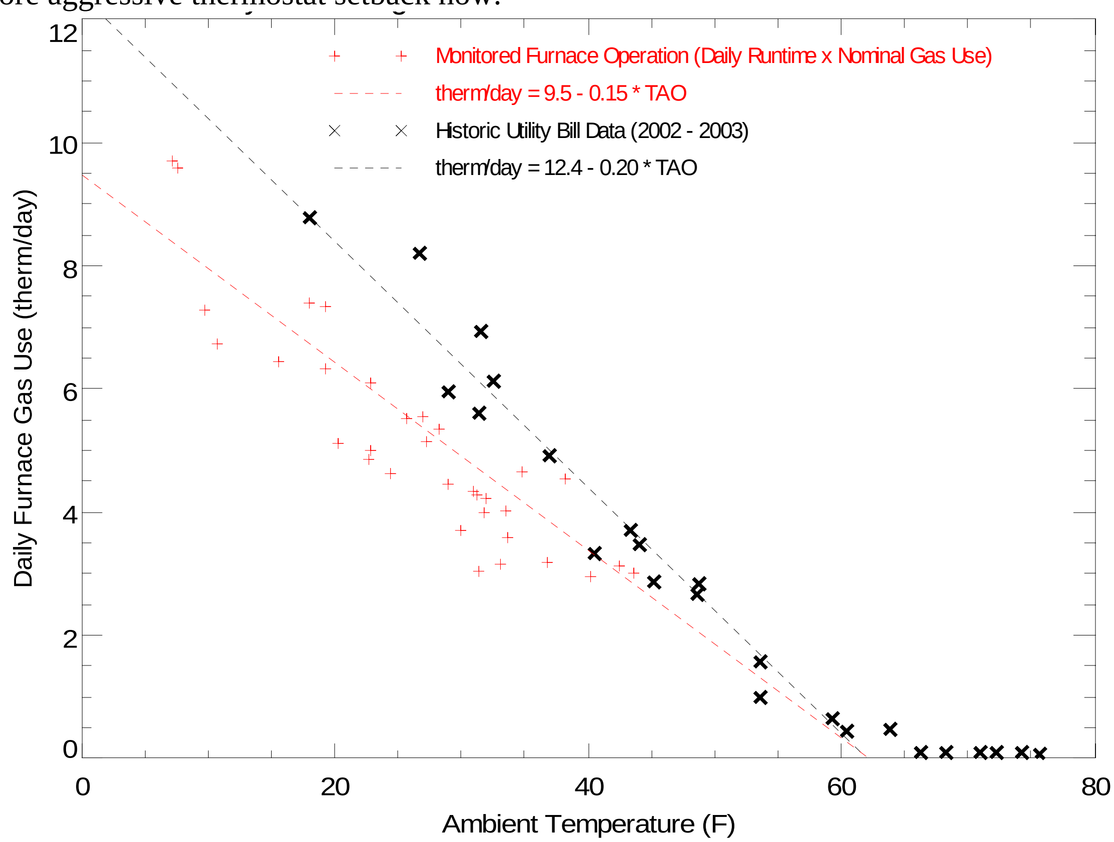

Figure A2-37. Comparing Monitored Gas Use (Based On Furnace Runtime) and Historic Utility Bill Data

Figure A2-38 shows the data collected for the base period. The return temperature is consistently lower than the space temperature, indicating a combination of thermal conduction loss from the return duct, as well as air leakage into the depressurized duct.

The return temperature typically ranged from 5-8°F lower than the space temperature, with some periods as low as 15°F lower than the space.

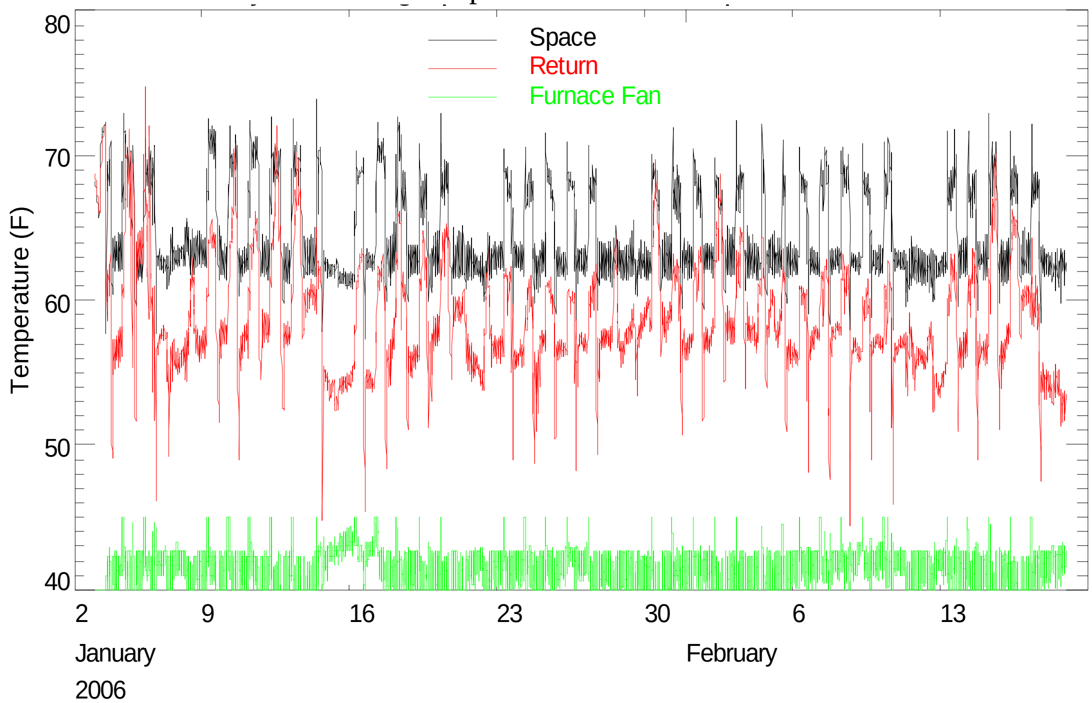

Figure A2-38. Space and Return Conditions For Base Building

Figure A2-39 shows transition period from the comfort setpoint to the setback temperature, the furnace fan remained off for an extended period of time. During this time the return temperature approaches ambient, rather than approaching the space temperature. The return temperature sensor is located in the un-insulated plenum inside the conditioned space. The deviation from the space temperature indicates that air is continuing to move while the fan is off, and that losses are continuing to occur. If the air were stagnant in the return plenum, the return temperature should approach the space temperature.

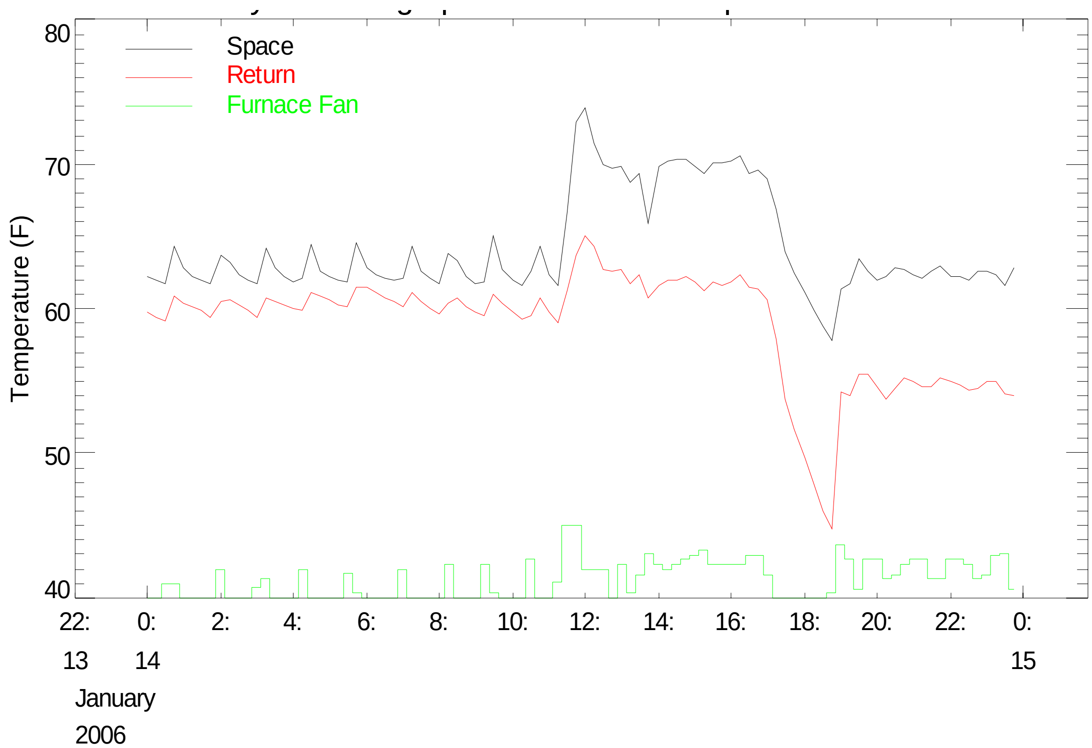

Figure A2-39. Space and Return Conditions For Base Building Typical Day with Setback

This remediation had a multifaceted impact on the building. With less leakage to the attic, the building uses less energy to maintain the space at the heating setpoint, providing energy and cost savings to the owners. The potential for ice damming has decreased, as the tighter building envelope lowers temperatures in attic. However, the decrease in attic temperatures caused an increase in the return duct losses, as shown in Figure A2-40. The temperature drop across the return ductwork system increased by an average of 1.3°F after the envelope was sealed on February 19 – confirming that the colder attic temperature.

When the return duct was insulated on March 11 the return duct temperature drop (TAR-TAI) decreased to just slightly below the original levels observed in the base period. Figure A2-41 shows that return duct temperature drop decreased by an average of 1.7ºF when the duct was insulated.

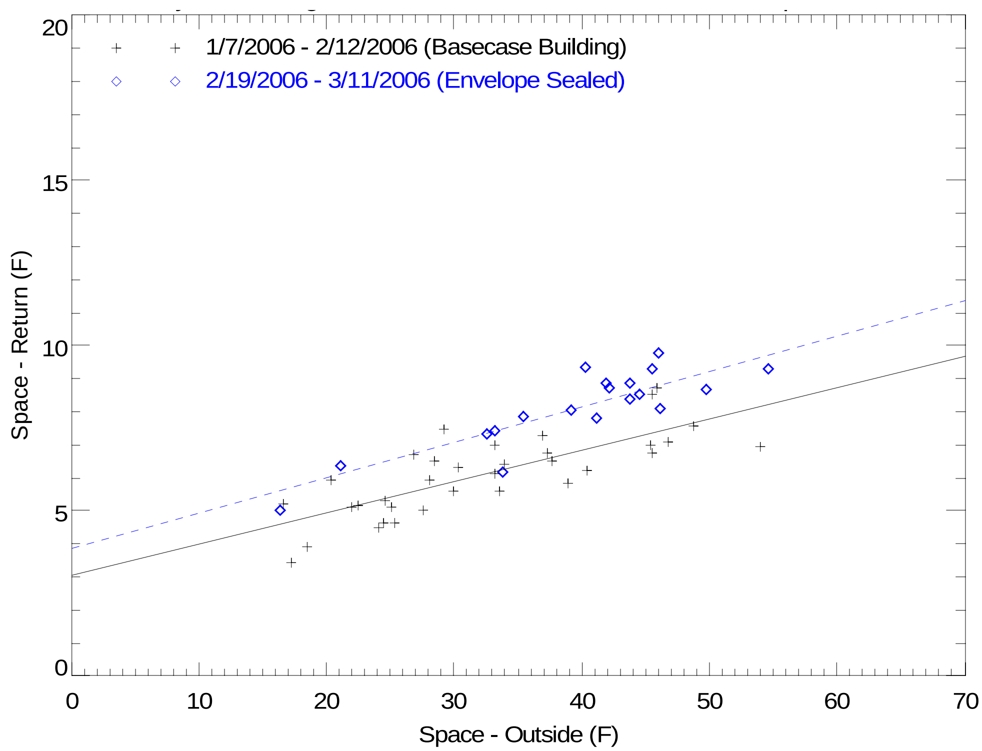

Figure A2-40. Change in Return Duct Temperature Drop: Tightening Envelope

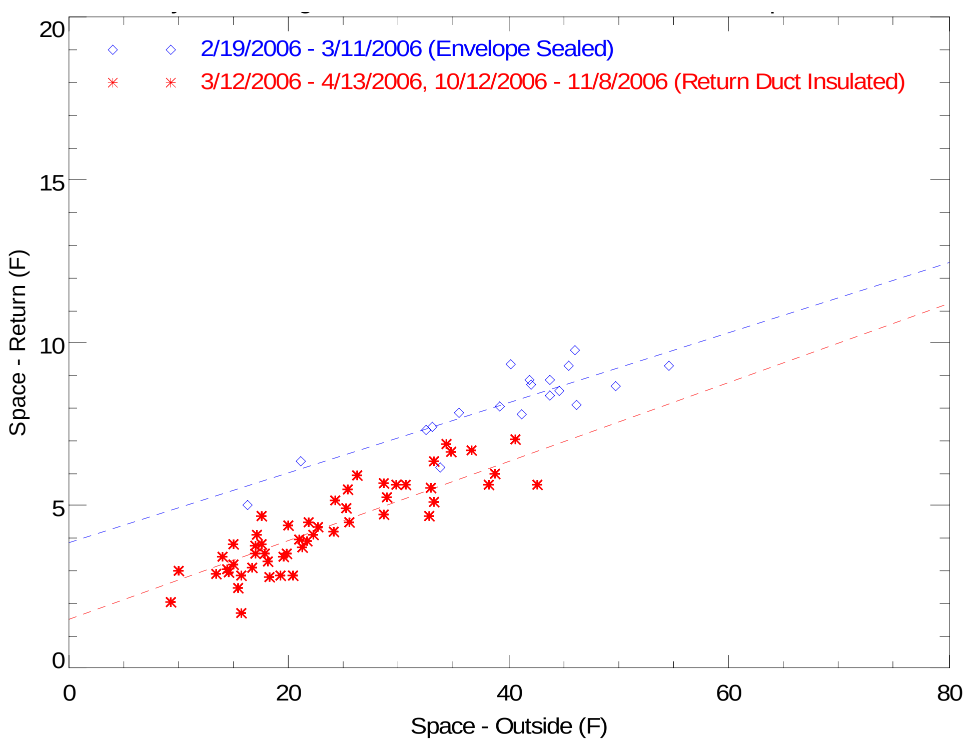

Figure A2-41. Change in Return Duct Temperature Drop: Duct Insulation

Using the trends above and the typical meteorological year data for Syracuse, NY an estimate for the total amount of losses through the return ductwork was calculated. The losses were calculated by multiplying the temperature drop in the duct by the measured furnace airflow, and then multiplying by the daily furnace runtime fraction. This represents the lower bound of the duct losses. The upper bound assumes that losses occur continuously, without considering furnace runtime. The actual level of losses is somewhere between these two extremes, because the temperature data imply that some air continues to move through the ductwork when the furnace is off, yet the air flow level is greatly decreased.

Table A2-19 and Table A2-20 display bin calculations using daily relations for the temperature drop in the return duct and the daily furnace runtime fraction. In Table A2-20 the daily runtime fraction is set to 1.0 to simulate constant losses from the ductwork. The annual impact of duct losses on the basecase building under these two scenarios ranged from 98 to 453 therms/year. Assuming that off-cycle losses are on the order of 25% of continuous fan operation, the annual duct losses for the base building would be about 190 therm/year.

Table A2-19. Duct Loss Calculation – Basecase Building with Furnace RTF (lower bound of losses)

[1]	[2]	[3]	[4]	[5]	[6] = 3.03 + 0.095*[5]	[7] = [6]*1.08 * 1,035 SCFM / 1000	[8] = (1.17 + 0.738 * [5])/100	[9] = [4]*[7]*[8]*24
Syracuse TMY2 Bin Data								
Bin Low	Bin High	Bin Med	Number of Days	Average Space Outdoor Temp Diff	Temp Drop Through Duct	Steady State Losses	Daily Furnace RTF	Acutal Losses
(F)	(F)	(F)	(days)	(F)	(F)	(MBtu/h)	(-)	(MBtu)
-25	-20	-22.0	0	-	-	-	-	-
-20	-15	-17.0	0	-	-	-	-	-
-15	-10	-12.0	0	-	-	-	-	-
-10	-5	-7.0	0	-	-	-	-	-
-5	0	-2.0	0	-	-	-	-	-
0	5	2.0	3	58	8.5	9.5	0.44	300.6
5	10	7.0	4	56	8.3	9.3	0.42	378.7
10	15	12.0	5	51	7.9	8.8	0.39	407.8
15	20	17.0	14	45	7.3	8.2	0.34	938.4
20	25	22.0	21	41	6.9	7.7	0.31	1,219.9
25	30	27.0	22	35	6.4	7.1	0.27	1,007.8
30	35	32.0	39	30	5.9	6.6	0.23	1,427.3
35	40	37.0	29	24	5.3	5.9	0.19	776.6
40	45	42.0	32	20	4.9	5.5	0.16	671.4
45	50	47.0	28	14	4.4	4.9	0.11	375.3
50	55	52.0	23	10	4.0	4.5	0.09	209.3
55	60	57.0	32	5	3.5	3.9	0.05	145.9
60	65	62.0	37	0	-	-	-	-
65	70	67.0	34	-4	-	-	-	-
70	75	72.0	25	-9	-	-	-	-
75	80	77.0	14	-14	-	-	-	-
80	85	82.0	3	-17	-	-	-	-
85	90	87.0	0	-	-	-	-	-

No days in temperature bin

Assumes no losses untill 10 F below space temperature

Total MBtu	**7,859.0**
therms @ 80% EFF	**98.2**

Table A2-20. Duct Loss Calculation – Basecase Building without Furnace RTF (upper bound of losses)

[1]	[2]	[3]	[4]	[5]	[6] = 3.03 + 0.095*[5]	[7] = [6]*1.08 * 1,035 SCFM / 1000	[8] = 1 (continuous)	[9] = [4]*[7]*[8]*24
Syracuse TMY2 Bin Data								
Bin Low	Bin High	Bin Med	Number of Days	Average Space Outdoor Temp Diff	Temp Drop Through Duct	Steady State Losses	Daily Furnace RTF	Acutal Losses
(F)	(F)	(F)	(days)	(F)	(F)	(MBtu/h)	(-)	(MBtu)
-25	-20	-22.0	0	-	-	-	-	-
-20	-15	-17.0	0	-	-	-	-	-
-15	-10	-12.0	0	-	-	-	-	-
-10	-5	-7.0	0	-	-	-	-	-
-5	0	-2.0	0	-	-	-	-	-
0	5	2.0	3	58	8.5	9.5	1.00	686.6
5	10	7.0	4	56	8.3	9.3	1.00	895.1
10	15	12.0	5	51	7.9	8.8	1.00	1,055.3
15	20	17.0	14	45	7.3	8.2	1.00	2,741.4
20	25	22.0	21	41	6.9	7.7	1.00	3,898.5
25	30	27.0	22	35	6.4	7.1	1.00	3,748.6
30	35	32.0	39	30	5.9	6.6	1.00	6,149.5
35	40	37.0	29	24	5.3	5.9	1.00	4,130.4
40	45	42.0	32	20	4.9	5.5	1.00	4,232.3
45	50	47.0	28	14	4.4	4.9	1.00	3,276.2
50	55	52.0	23	10	4.0	4.5	1.00	2,457.3
55	60	57.0	32	5	3.5	3.9	1.00	3,012.1
60	65	62.0	37	0	-	-	-	-
65	70	67.0	34	-4	-	-	-	-
70	75	72.0	25	-9	-	-	-	-
75	80	77.0	14	-14	-	-	-	-
80	85	82.0	3	-17	-	-	-	-
85	90	87.0	0	-	-	-	-	-

No days in temperature bin

Assumes no losses untill 10 F below space temperature

Total MBtu	**36,283.3**
therms @ 80% EFF	**453.5**

Net Energy Impact of Remediation

The net impact of the building remediation is observed in the change in furnace operation (and hence energy consumption). Due to the number of drastic thermostat setpoint changes observed during monitoring, direct comparison of the different periods was not possible. Therefore energy use data from before and after the remediation steps was compared to the daily indoor to outdoor ambient temperature.

Figure A2-42 displays the daily furnace runtime to the average indoor-outdoor temperature difference. The percentage on the plot legend indicates the average reduction in furnace runtime from each stage of the remediation efforts.

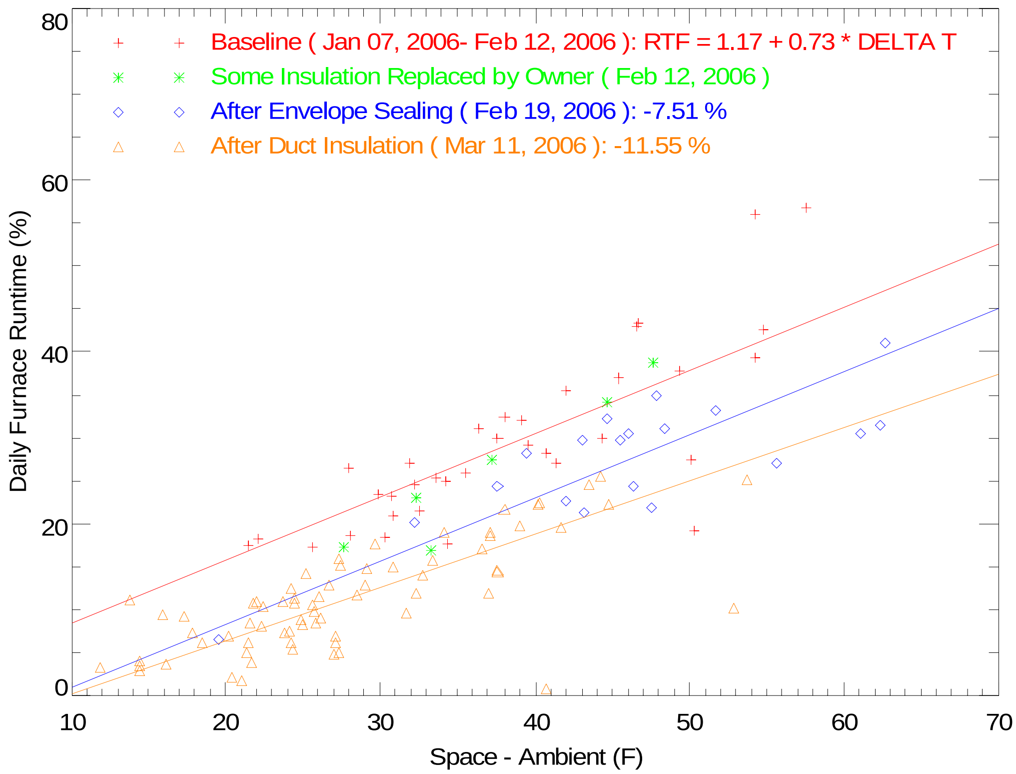

Figure A2-42. Impact of Remediation Efforts on Daily Furnace Runtime

By using the TMY2 data for Syracuse and a consistent space temperature/thermostat schedule, the annual impact of the remediation could be determined. The space temperature was set to be 70°F from 8:00 AM to 5:00 PM on weekdays, and 65°F for all other hours. Repalcing the insulation reduced furnace runtime (and gas consumption) by 37%. Adding the duct insulation (and further sealing of the envelope) reduced the furnace runtime by an additional 13%.

Table A2-21. Annual Impact of Remediation Efforts

	Hours	Gas Input @ 0.712 Therm/h (therms)	Savings (therms)	Savings (%)
Basecase Heating Hours	1203	856.7	N/A	N/A
Sealed Envelope Heating Hours	754	536.9	319.8	37%
Sealed Envelope + Duct Insulation Heating Hours	606	431.5	425.3	50%

Annual energy savings from the remediation totals 425 therm/year, and at a typical cost of natural gas of $1.50/therm, provides a cost savings of $638/year.

Impact of Remediation on Building Airtightness

The blower door tests were repeated in November 2006 after remediation was complete to assess the impact on building leakage. The test was repeated with the same conditions (AHU closet closed, exhaust fans sealed). Then the supply and return grills were covered and the test was repeated (to estimate the ducts leakage). Table A2-22 compares these newest test results to the original tests. Figure A2-43 and Table A2-23 show the test results the envelope with ducts, while Figure A2-44 and Table A2-24 show the results with the duct blocked off. The remediation efforts reduced the leakage area by 57 sq in (13%). The exponent changed from 0.58 to 0.65, confirming that many large holes had been fixed.

Table A2-22. Summary of Blower Door Test Results – Before and After Remediation

			Building Envelope			Ducts
	Flow Coeff. K	Exp. n	ELA@4 (sq in)	ELA / 100 sq ft (sq in/sq ft)	ACH_{50}	ELA@25 (sq in)
Before Remediation (Fig A2-8, Table A2-2)	706	0.579	447	10.42	33.0	
After Remediation	560	0.647	389	9.08	34.1	509
After Remediation (ducts sealed)	553	0.637		8.84	32.3	487
			57			23

The second blower door test was conducted with the supply and return grills sealed with duct mask. and was conducted to estimate the duct leakage to outdoors, This test provided an indication of the duct leakage to outdoors. The ELA at 25 Pascals is also shown in Table A2-22 to provide an indication of the duct leakage. The duct to outdoors in this case was 23 sq in, compared to a total duct leakage of 56 sq in determined for the return ducts before the remediation.

Table A2-23. Blower Door Test Data, Resulting Best-Fit Model Coefficients, and ELA - After Building Improvements

Test Results:

Flow Coefficient (K)	560.4	
Exponent (n)	0.647	
Leakage area (LBL ELA @ 4 Pa)	389 sq in	9.08 ELA / 100 sq ft
Airflow @ 50 Pa	7036.1 cfm	34.1 ACH @ 50

Test Data:

	Nominal Building Pressure (Pa)	Nominal Flow (cfm)	Ring
1	36	5,802	none
2	35.7	5,784	none
3	30	5,121	none
4	30.2	5,220	none
5	29.6	5,108	none
6	25.5	4,562	none
7	25.7	4,598	none
8	25.3	4,330	none
9	19.6	3,863	none
10	22.1	3,841	none
11	22.1	3,844	none
12	35.1	5,594	none
13	24.2	4,540	none
14	20.1	3,907	none
15	19.8	3,867	none
16	14.8	3,198	none
17	14.9	3,229	none
18	14.7	3,230	none
19	10.3	2,577	none
20	10.1	2,549	none
21	9.6	2,476	none

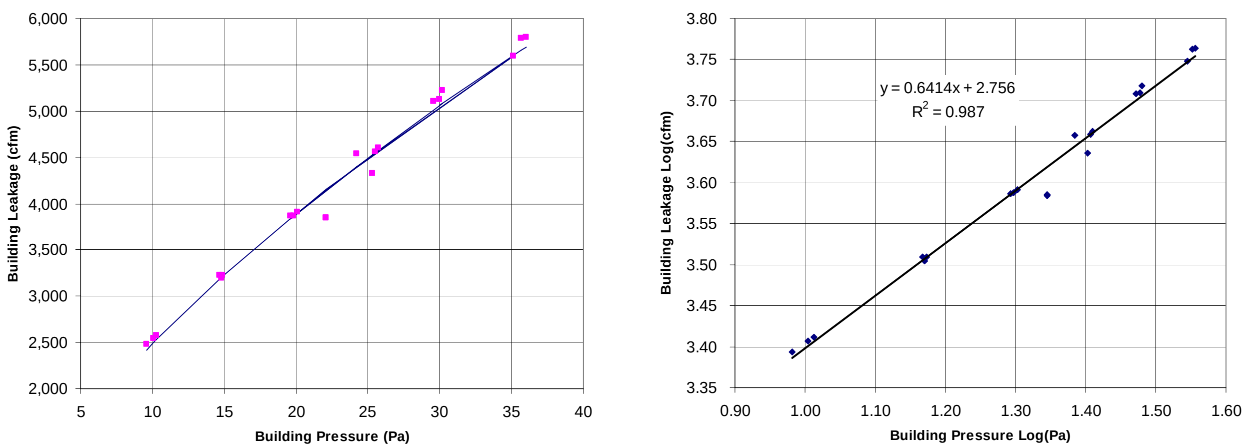

Figure A2-43. Office Section Variation of Building Leakage with Pressure: cfm = K(ΔP)^n

Table A2-24. Blower Door Test Data, Resulting Best-Fit Model Coefficients, and ELA - After Building Improvements and with Ducts Sealed

Test Results:

Flow Coefficient (K)	553.2		
Exponent (n)	0.637		
Leakage area (LBL ELA @ 4 Pa)	379 sq in	8.84	ELA / 100 sq ft
Airflow @ 50 Pa	6675.2 cfm	32.3	ACH @ 50

Test Data:

	Nominal Building Pressure (Pa)	Nominal Flow (cfm)	Ring
1	37.7	5,555	none
2	40.3	5,553	none
3	39.2	5,480	none
4	32.4	4,962	none
5	34.1	5,245	none
6	31.7	5,212	none
7	27.4	4,649	none
8	27.1	4,571	none
9	26.8	4,529	none
10	21.2	3,970	none
11	20.5	3,925	none
12	21.7	3,948	none
13	14.8	3,165	none
14	14.1	3,138	none
15	15.1	3,156	none
16	11.4	2,606	none
17	11.8	2,534	none
18	12.4	2,520	none

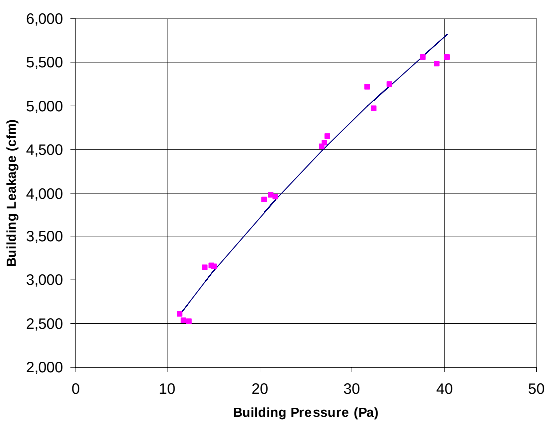

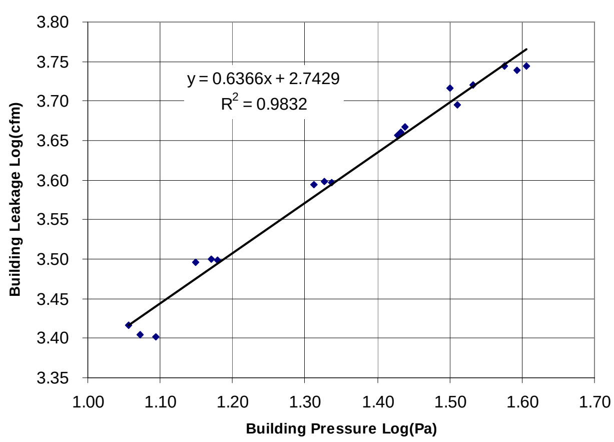

Figure A2-44. Office Section Variation of Building Leakage with Pressure: cfm = $K(\Delta P)^n$

Field Test Site 4 - Office Building, New Hartford, NY


Building from Street Side (West)


Entrance at Back of Building (East)


Side Building from Back (North)

Figure A4-1. Photos of Building

CHARACTERISTICS

Building Description

The 7,500 sq ft facility is a one-story building that was converted to office space in the 1960s. The structure was originally built as open, high-bay manufacturing building in 1932. Figure A4-1 shows the front of the building and the main entrance at the rear of the building. The building is set up with four air-handling units (AHU) that serve the space. The air handlers are forced-air, gas-fired units with a 5-ton cooling section. Fresh air is provided by a duct through the roof. There are also two small through-the-wall air conditioners in the IT department and computer room. Figure A4-2 presents the building floor plan.

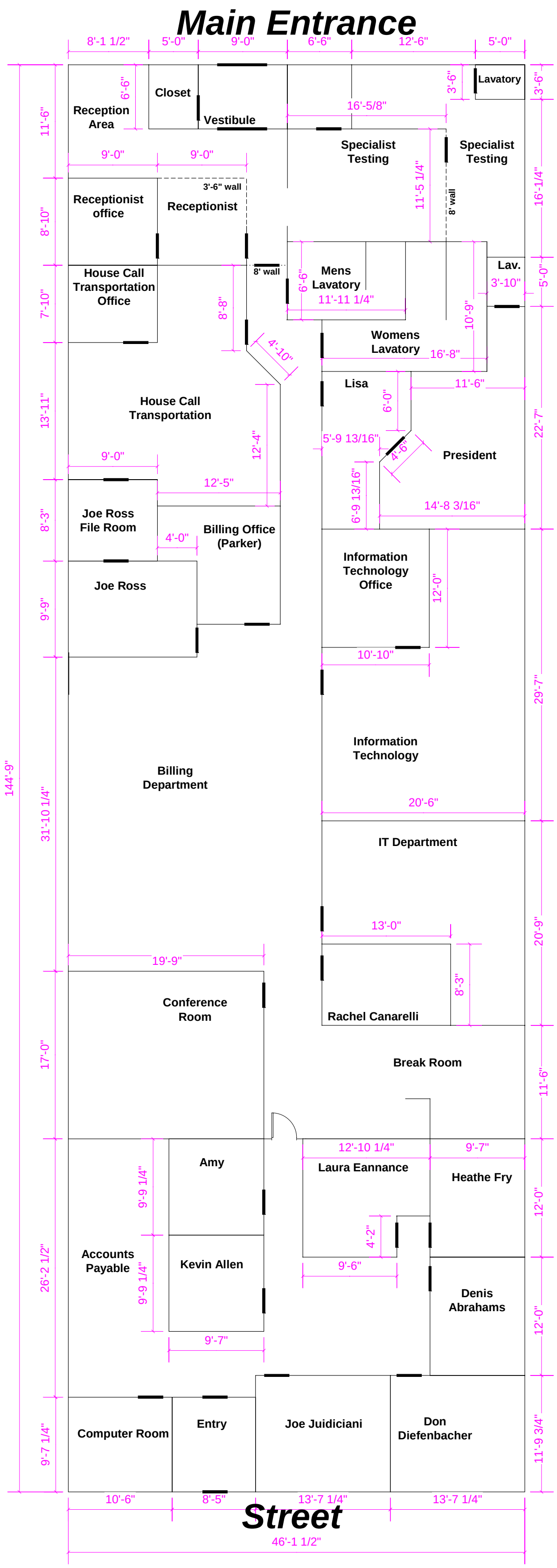

Figure A4-2. Building Floor Plan

Construction Details

Exterior walls are 8-in concrete block with 2x4 framed interior walls finished with ½-in gypsum board. The 2x4 stud walls are insulated with fiberglass. The 4-inch gap between the block and framed wall is also insulated with unfaced fiberglass insulation. The exterior side of the block wall is coated with stucco (that may be on top of additional foam insulation).

The roof is constructed of 1x6 tongue-and-groove wood plank on steel roof trusses. The roofing is asphalt shingles. Ceiling insulation is provided by 3.5 inches of rock wool, which sits on top of ½ inch fiberboard fastened to a frame of 2x4 cross members. The 2x4 ceiling frame is suspended by wire from the steel trusses. The fiberboard originally served as the ceiling. Now there is a T-bar (drop) ceiling approximately 14 inches below the fiberboard. The fiberboard has numerous large penetrations for ductwork, electrical, and plumbing connections.

The attic has two large roof vents that are normally closed. Figure A4-3 illustrates typical wall and roof sections. Figure A4-4 shows pictures of the roof decking, vents, ceiling insulation, ceiling plenum, and typical diffuser installation. Figure A4-5 and Figure A4-6 show detailed views of the ceiling and wall construction.

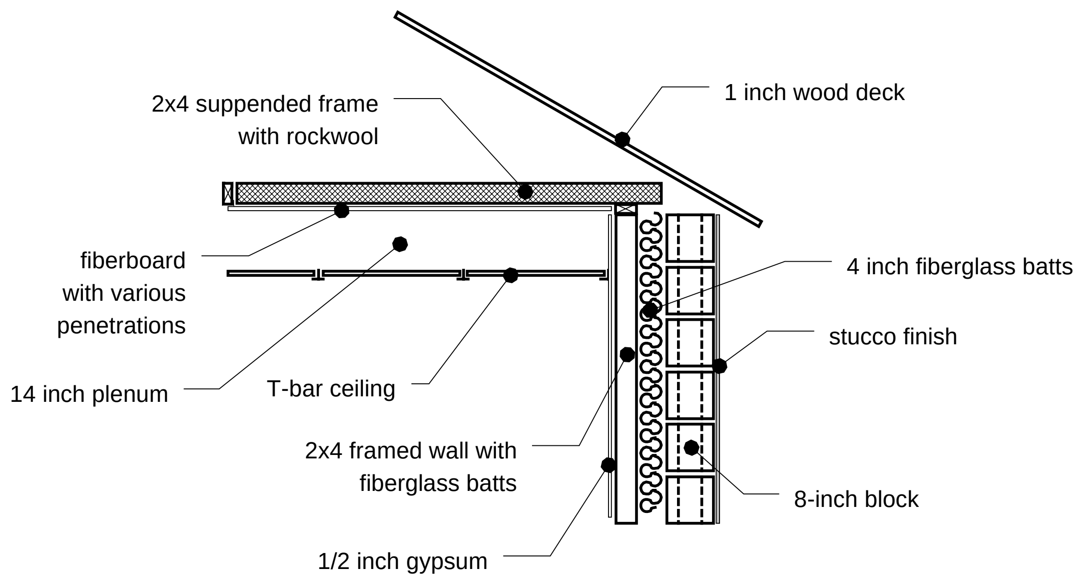

Figure A4-3. Roof and Wall Sections

Attic Vent through Roof Decking (Closed)

Rock Wool Ceiling Insulation

Ceiling Plenum

Typical Diffuser Installation

Figure A4-4. Photos of the Attic and Ceiling

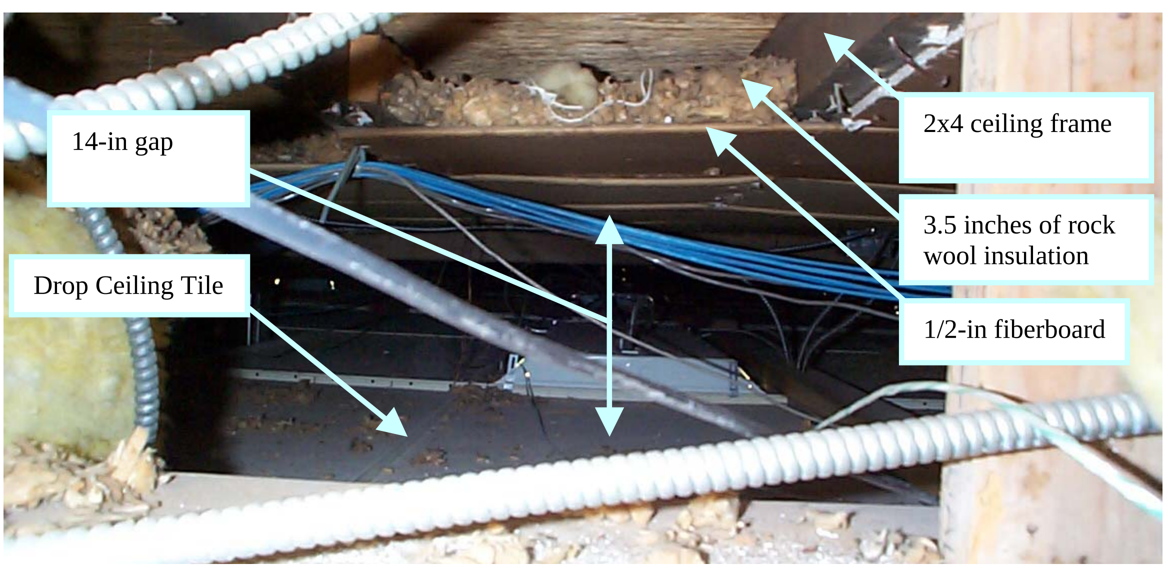

Figure A4-5. Ceiling Plenum and Insulation

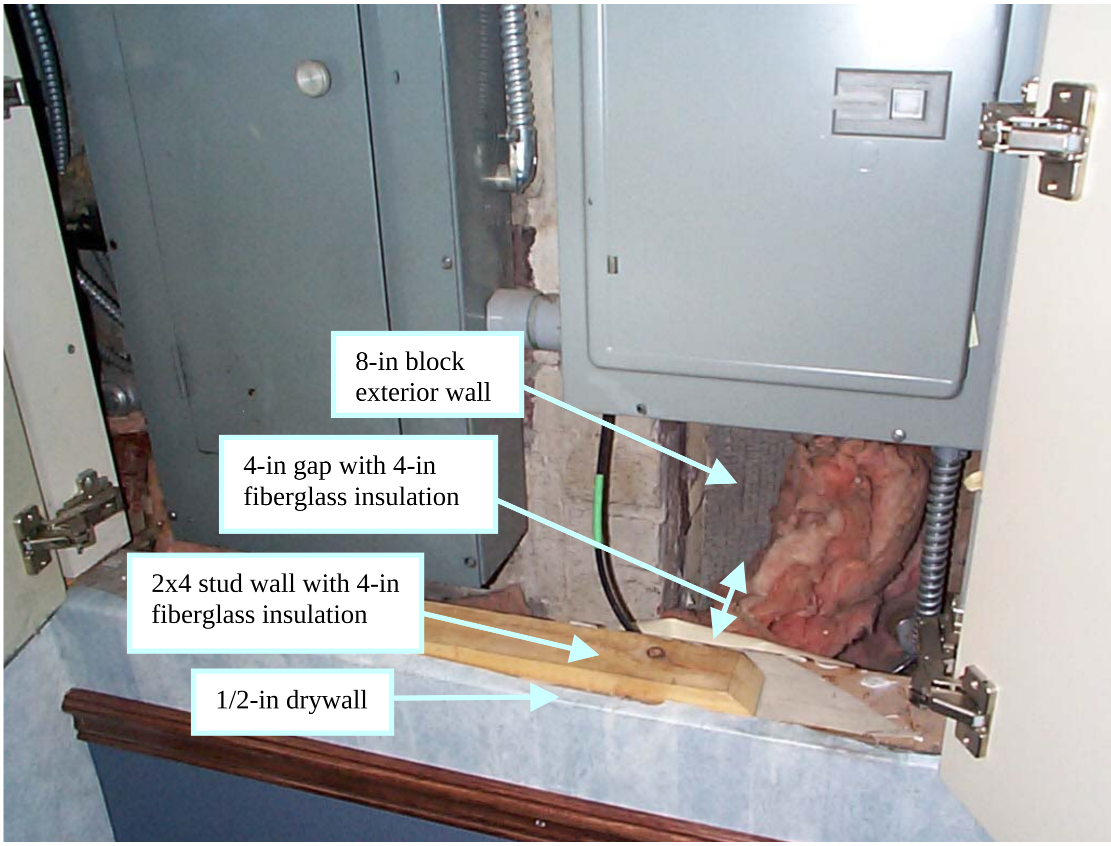

Figure A4-6. Wall Section

HVAC System

The building is conditioned by four separate air handling units (AHUs) mounted in the attic. Three of the systems (AHU #2, #3 and #4) have 1960s vintage AHUs with a supply fan and a DX A-coil. Heat is provided by a gas-fired duct heater mounted downstream of the air handler fan. AHU#1 is the opposite configuration. This system has a newer horizontal furnace with an integral supply fan. A DX coil is mounted down stream of the furnace fan. Each system has a 5 ton condensing unit located on a platform on the North side of the roof (see Figure A4-1). Figure A4-7 shows the four AHUs in the attic. Table A4-1 lists the HVAC equipment that serves the building. Note that the air-handling units are labeled in order as AHU #1 (closest to the street) through AHU #4 (at the rear of the building).

Each AHU has a fresh air duct that rises from the return duct vertically through the roof to a gooseneck (see Figure A4-1). The ventilation intake to each AHU was closed. Insulated supply and return ducts are located in the attic above the ceiling insulation. The supply ductwork for each system is includes a rectangular sheet metal duct with circular flexduct takeoffs. The return duct system includes several ceiling diffusers as well as five large ducted returns in the perimeter walls. Figure A4-8 displays the zones within the building and the corresponding AHU that serves each zone. Many of the AHU zones are intermingled.

AHU #1 (Front)

AHU #2

AHU #3

AHU #4 (Rear)

Figure A4-7. Four Air-Handling Units (AHUs) Located in Attic

Table A4-1. Summary HVAC Equipment Installed at Site

	Brand	**Heating Capacity MBtu/h**	**Cooling Capacity (tons)**	**Measured Supply Fan Power (kW)**
AHU #1			5	0.60
AHU #2	Peerless		5	0.32
AHU #3	Peerless		5	0.65
AHU #4	Peerless		5	0.53

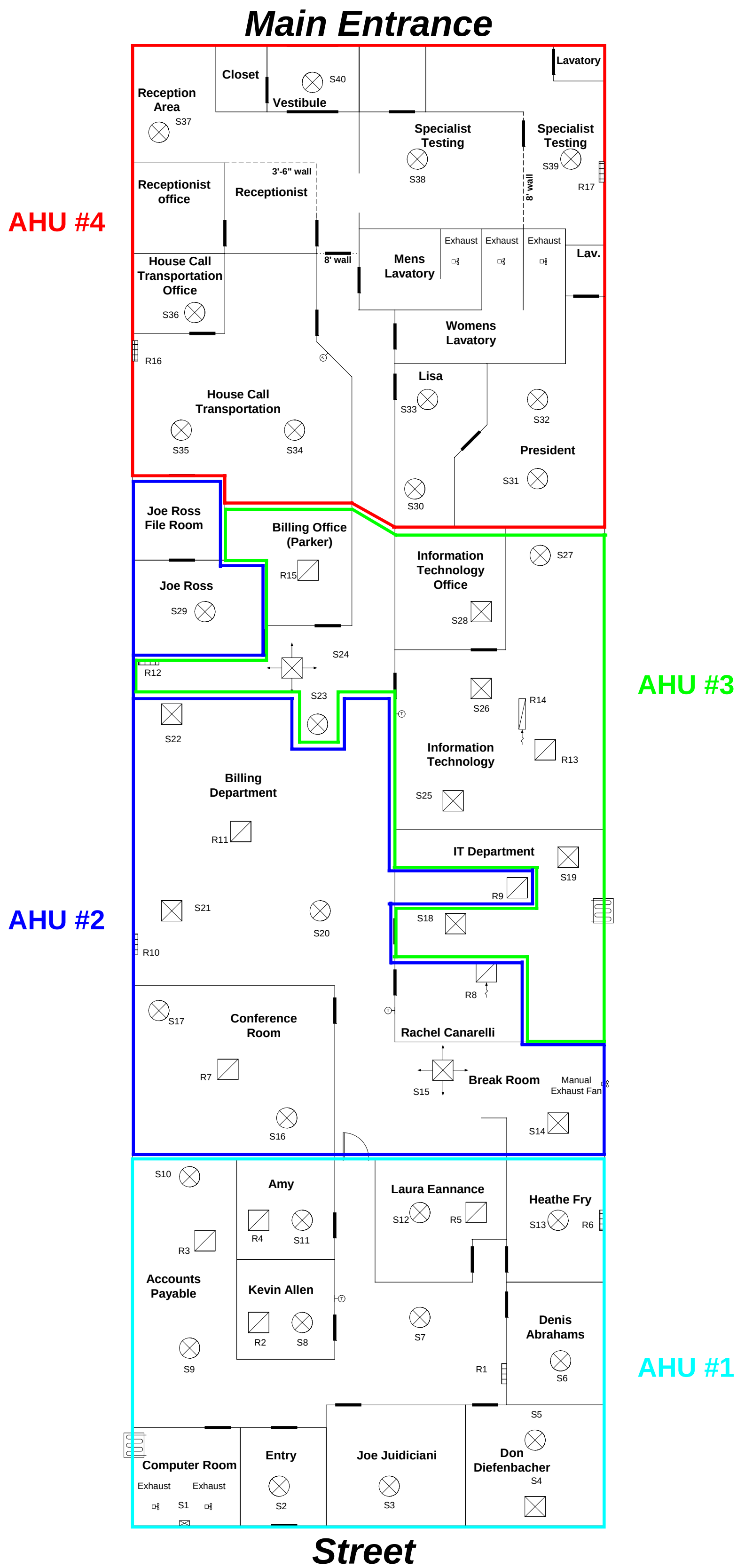

Figure A4-8. AHU Zones within Building

The building also used two room air conditioners, in the IT Department and the computer room. The building also has two inline fans to move air from one part of the building to another. These fans were apparently installed in to eliminate hot spots. Figure A4-9 shows one of these inline fans. The fan is controlled by a ceiling-mounted thermostat in the return side space. The fan pulls air from the space when it gets warm, inducing the flow of cooler air into the space.

Figure A4-9. One of Two Thermostat Controlled Inline Duct Fans

Each AHU is controlled by standard "Honeywell round" thermostat without setback controls (locations in Figure A4-8). The staff does not manually setback (or setup) thermostats on nights or weekends. All four supply fans operate in the constant fan mode continuously.

MEASUREMENTS

The test data below was taken on May 5 and May 15, 2004. Supply air flow measurements and duct leakage for AHU #4 were taken on May 5. Duct leakage measurements for AHU #2, blower door testing, and pressure mapping was completed on May 15. Test personnel were Dan Gott, Hugh Henderson, and Mike Clarkin for both days. Terry Brennan also participated in testing on May 5.

Building Envelope Airtightness

The leakage characteristics of the building enclosure were assessed using fan depressurization methods. Two blower doors were installed side-by-side in the main entrance doors to depressurize the building (Figure A4-10). All exterior doors and windows were closed. At this site, the test was conducted with all interior doors closed since about 25% of the rooms (eight doors) were locked and no key was available. Different pressures were maintained by changing the speed on one blower door and keeping the other fan constant. Fan flow measurements were recorded on both blower doors. The building pressure was varied from 56.6 Pa to 14.0 Pa. We repeated the test with most interior doors open (about 75% of the doors open; excluding the 8 locked doors) and found that door position had no impact on the pressure in the building. This tends to confirm that the test with doors closed was valid.

Figure A4-10. Two Blower Doors Setup for Depressurization (Main Entrance)

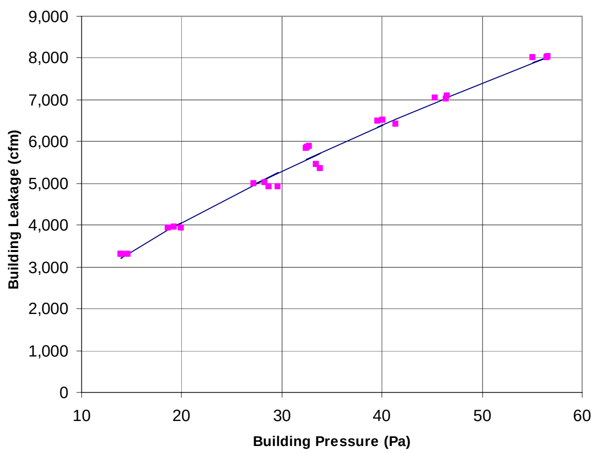

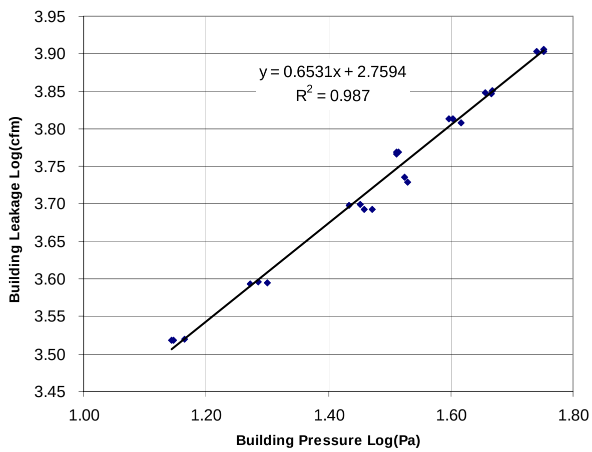

Figure A4-11. Variation of Building Leakage with Pressure: cfm = K(ΔP)^n

Table A4-2. Blower Door Test Data, Resulting Best-Fit Model Coefficients, and ELA

Test Results:

Flow Coefficient (K)	574.6	6,974	sq ft, floor area
Exponent (n)	0.653		
Leakage area (LBL ELA @ 4 Pa)	403 sq in	2.29	ELA / 100 sq ft
Airflow @ 50 Pa	7394.3 cfm	6.8	ACH @ 50

Test Data:

	Nominal Building Pressure (Pa)	Fan Pressure (Pa)	Nominal Flow (cfm)	Ring
1	56.6		8,042	none
2	55.1		8,012	none
3	56.5		8,011	none
4	46.4		7,026	none
5	46.5		7,095	none
6	45.3		7,042	none
7	41.4		6,423	none
8	39.6		6,498	none
9	40.1		6,506	none
10	32.4		5,845	none
11	32.5		5,874	none
12	32.7		5,877	none
13	33.8		5,355	none
14	33.4		5,446	none
15	27.2		4,986	none
16	29.6		4,927	none
17	28.7		4,932	none
18	28.3		5,007	none
19	18.7		3,922	none
20	20.0		3,929	none
21	19.3		3,948	none
22	14.6		3,305	none
23	13.9		3,301	none
24	14.0		3,303	none
25				none

Notes: ELA is leakage area (in square inches) at reference pressure of 4 Pa.
ELA per 100 sq ft is based on total building envelope surface area (ceiling, exterior walls and floor).

Pressure Mapping (Blower Door Testing)

Pressure readings in the building were taken using a digital micromanometer (DG 700) with the blower doors operating. All interior doors were closed. The pressure difference across the building envelope was 56 Pa. Figure A4-12 shows the pressure difference between the interior space and the attic. The pressure difference between the interior space and the attic was 5.5 Pa. This implies that the leakage area from the space to attic space is large and that the attic is closely coupled to the conditioned space. While the ceiling serves as the thermal barrier, the roof deck of the building is the air barrier.

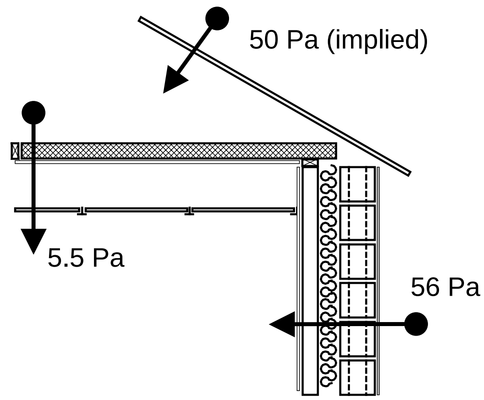

Figure A4-12. Pressure Drop across Ceiling Elements during 56 Pa Depressurization Test

Pressure measurements were also taken between various offices and corridors with doors closed. Figure A4-13 shows the pressure differences induced across the office doorways with the corridor depressurized. With the building depressurized to 56 Pa, pressures across the doorways ranged from 0.4 and 5.2 Pa. The pressure difference between the rooms and corridor are much less than the overall pressure difference to ambient.

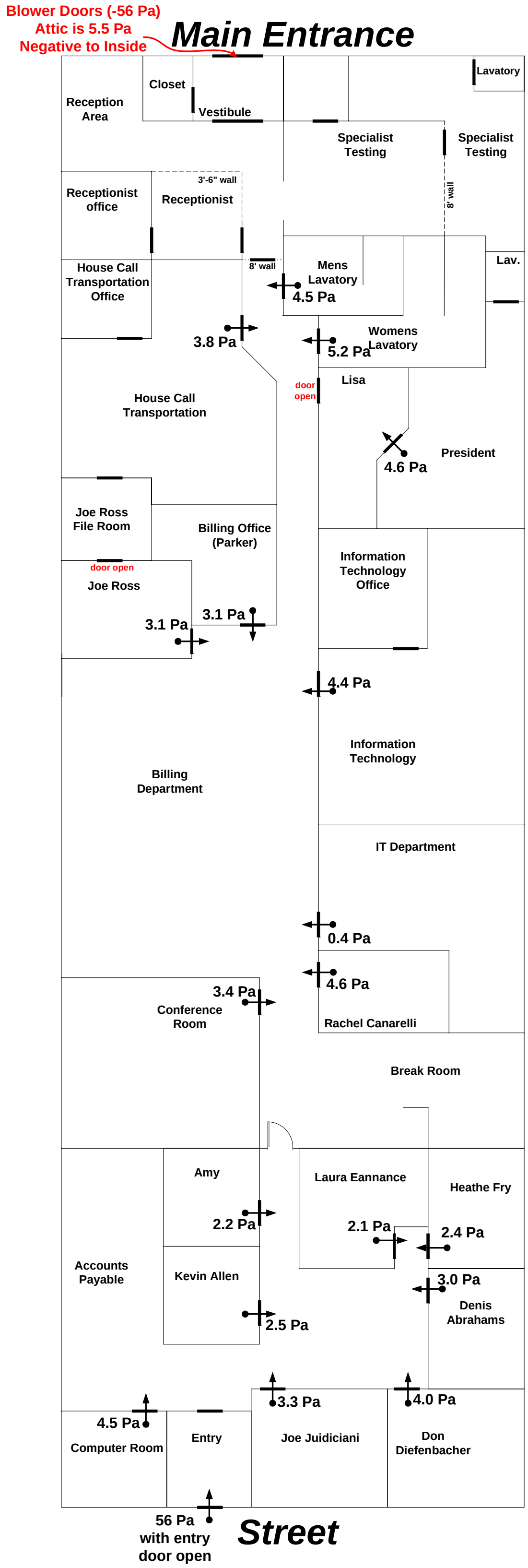

Corridors Depressurized 56 Pa

Figure A4-13. Room-to-Corridor Pressures with Building Depressurized to 56 Pa

HVAC Airflow Measurements

The airflow from each supply diffuser was measured using a TSI flow hood[1]. Table A4-3 presents the measurement results. The schematic in the table illustrates the location of each supply and return diffuser. One supply diffuser (S16) on AHU2 was found to be disconnected in the attic (see Figure A4-17). The opening in the main supply duct was discharging 791 cfm into the attic. With the S16 supply trunk connected, the supply air flow was 121 cfm. The readings in Table A4-3 were taken with S16 trunk off. Therefore, to predict the change in supply diffuser flow for the other diffusers with the duct trunk connected, we can use the change in supply and return static pressures with the duct trunk on and off. The flows were corrected with the equation below:

$$\frac{Q_2}{Q_1} = \sqrt{\frac{P_2}{P_1}}$$

The supply pressure changed from 17 to 26.4 Pa, so the predicted increase in the supply airflow on the AHU2 diffusers is 25%. The modest change in the return pressure is estimated to reduce the return airflow on AHU2 diffusers by 1.63%. The corrected flows for the AHU2 diffusers with the S16 trunk connected are listed in the second column in Table A4-3.

Table A4-4 lists the total supply and return airflows for each AHU. When the AHU2 flows were corrected as described above, the values are more inline with the other systems.

[1] The readings from the TSI flowhood were corrected using the correlation developed in the Site 1 report.

Table A4-3. Supply and Return Airflow Measurements

Label	Supply (cfm)	AHU #2 Duct Connected (cfm)
S1	91	
S2	137	
S3	268	
S4	200	
S5	37	
S6	103	
S7	86	
S8	83	
S9	20	
S10	86	
S11	24	
S12	120	
S13	117	
S14	140	174
S15	-	-
S16	-	121
S17	166	206
S18	177	
S19	29	
S20	208	259
S21	126	157
S22	59	73
S23	347	
S24	-	
S25	143	
S26	-	
S27	223	
S28	161	
S29	223	277
S30	35	
S31	154	
S32	not measured	
S33	-	
S34	205	
S35	217	
S36	151	
S37	219	
S38	202	
S39	302	
S40	51	
Total	4,910	5,257

Connected with inline fan (R8 → S15)

Connected with inline fan (R14 → S24)

Label	Return (cfm)	AHU #2 Duct Connected (cfm)
R1	234	
R2	87	
R3	268	
R4	98	
R5	100	
R6	427	
R7	194	191
R8	-	-
R9	143	141
R10	393	387
R11	279	275
R12	336	
R13	141	
R14	-	
R15	302	
R16	1,114	
R17	217	
Total	4,333	4,316

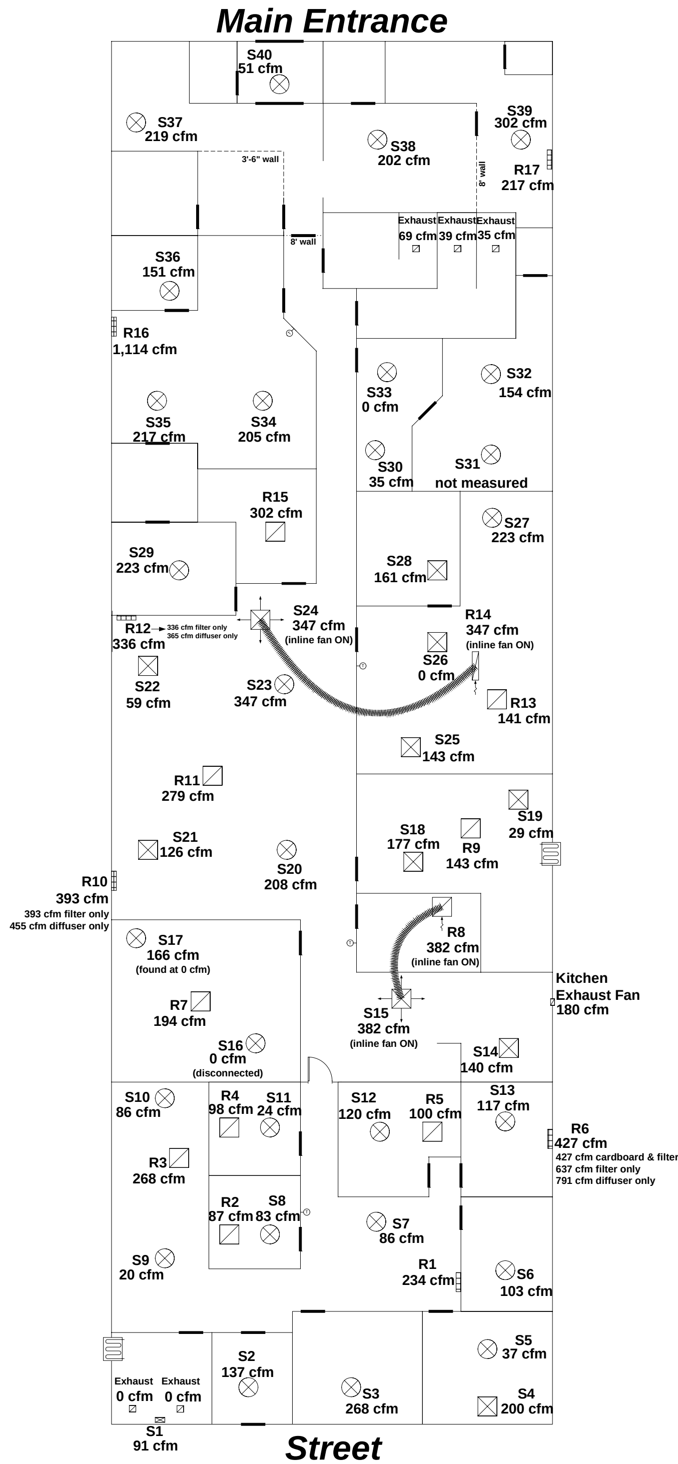

Table A4-4. Comparison of Supply and Return Airflow Measurements

	Flowhood Supply Airflow (cfm)	Flowhood Return Airflow (cfm)	Supply/ Return Ratio	Supply & Return Static (Pa)	Normalized Fan Power (Watt/cfm)
AHU #1	1,372	1,213	1.13		0.44
AHU #2	1,268[1]	993	1.28	26.4 & -12.4	0.25
duct disconnected	(920)	(1,009)	(0.91)	(17 & -12.4)	(0.35)
AHU #3	1,081	779	1.39		0.60
AHU #4	1,537	1,331	1.15	16 & -45	0.34

Note: 1- The S16 supply duct on AHU#2 was disconnected (see the duct leakage section below). The measured flow for all the supplies on AHU #2 was 950 cfm. Connecting the duct provides 121 cfm at diffuser S16, increases the supply diffuser flows at the other diffusers by 25%, and decreases return diffuser flows by 1.63%.

The total supply air flow is 5,258 cfm or about 0.7 cfm per sq-ft of floor area.

Pressure Mapping (AHU Fans On)

The air pressure relationships in the building were also determined with the AHU fans on. The graphics in Figure A4-15 show the pressure differences induced across the doorways with the AHU fans on and the office doors closed. Operation of the four AHU fans created pressures up to 6.2 Pa in some rooms.

The rooms with the greatest pressure differences tended to be those with the largest net airflow imbalance (net airflow imbalance = supply airflow – return airflow). Figure A4-14 shows the net airflow into the rooms is somewhat correlated to the pressurization relative to the corridors.

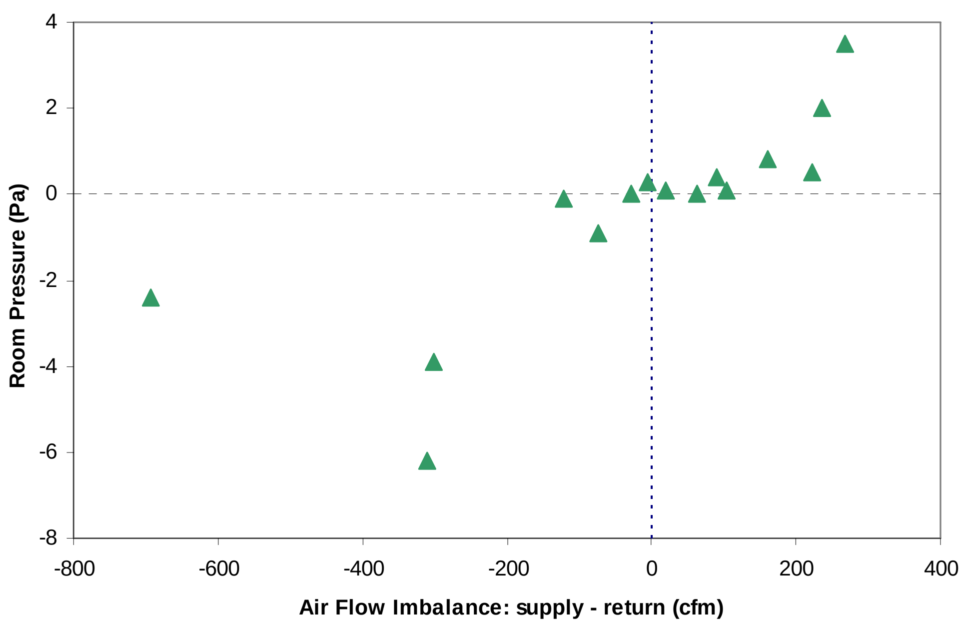

Figure A4-14. Pressure Differences Induced by AHU Fan Operation

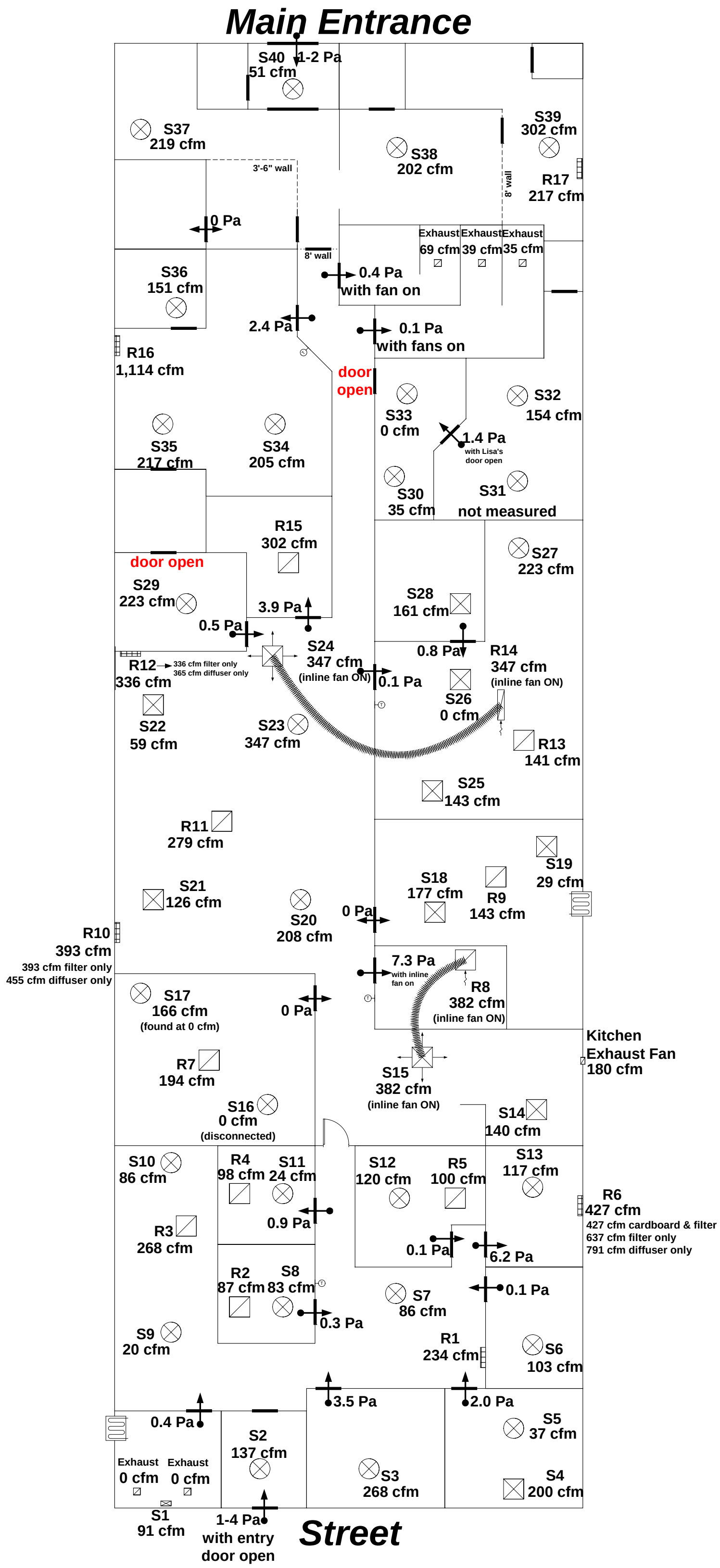

Figure A4-15. Pressure Differences between Rooms with AHU Fans On

Duct Leakage Measurements

A Duct Blaster was used to depressurize the ductwork to measure leakage rates. The Duct Blaster fan was connected to the AHU cabinet, as shown in Figure A4-16, to depressurize the entire duct system (AHU cabinet, supply duct, return duct). Plastic wrap was used to cover each supply and return grill in the system. The air filters were removed from the unit. In all tests, the seals at the supply/return grills were tested with a smoke puffer to confirm there was no leakage with the system depressurized.

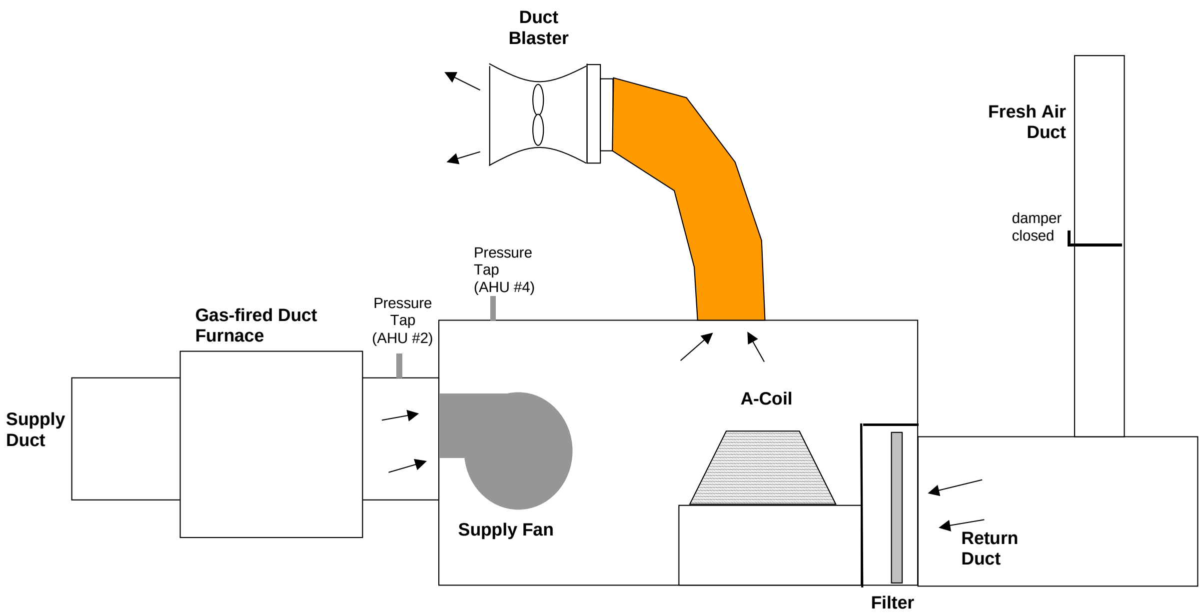

Figure A4-16. Duct Blaster Setup for Testing AHUs #4 and #2

AHU #4 (May 5)

The static pressure in the ductwork was measured at different locations for the two AHUs. For the testing of AHU #4 on May 5, the pressure tap was located at the top the AHU cabinet[2]. The results for AHU #4 are included in the tables and figures below. Since the recorded pressure was in the AHU cabinet, the actual pressures in the ductwork were lower in the supply and return trunks. Therefore the calculated leakage estimates normalized to 25 Pa tend to under predict the actual leakage rates. As a diagnostic check on the degree of pressurization, the pressure at each diffuser was measured by puncturing the plastic covering at each diffuser with a very small probe. Figure A4-18 shows the resulting pressures measured at each diffuser with the system depressurized to 15 Pa at the AHU cabinet. The pressures at the return grills were much closer to the AHU pressure than the supply grills.

[2] We later realized that this location was improper and used different pressure tap locations corresponding to each portion of the duct system for subsequent tests on AHU #2.

AHU #2 (May 15)
To test for duct leakage for AHU #2 on May 15, we located the static pressure probe in the supply duct past the supply fan but before the duct furnace (see Figure A4-16) and took several other pressure readings to confirm the validity of this location.

AHU #2 also had one main supply duct totally disconnected in the attic as shown in Figure A4-17. The flow though this open supply trunk was measured at 791 cfm (700 cfm uncorrected) with the TSI flow hood. The supply duct was reconnected for the duct leakage tests.

Figure A4-17. Photo Showing Disconnected Supply Duct on AHU #2 (Reconnected for Duct Testing)

Several pressure measurements were taken at various points for AHU #2 with the system depressurized. The pressure measured in the supply duct (-13 Pa) was very similar to the return side of the system (-13.5 Pa). The pressure nearest the Duct Blaster in the AHU cabinet was slightly larger (-16.5 Pa) than the duct static because of pressure losses through the supply fan (supply side) and DX coil (return side). Figure A4-18 shows the resulting pressures measured at each diffuser with the AHU #2 cabinet and duct system depressurized. The pressures at the supply diffuser are generally about 2 Pa higher than the return grills. This additional 2 Pa pressure drop in the supply duct is probably attributable to the duct heater on that side of the system. The uniformity of the pressures at most diffusers imply that leaks are uniformly spread around the system (with the exception of S22, where the smaller pressure implied more leakage).

The duct leakage test was repeated with the return duct blocked off. Several filters were blocked off with plastic and placed back into the AHU filter track. With the return ductwork sealed off, the AHU cabinet could be depressurized to –29 Pa. The quality of the seal was confirmed by measuring the return pressure. The pressure in the return duct was only –4 Pa, implying very little leakage past the filters.

AHU #4 Duct System Depressurized 15 Pa	
Diffuser Label	Pressure at Diffusers (Pa)
S30	0.0
S31	-2.5
S32	-3.8
S33	0.0
S34	-4.6
S35	-5.1
S36	-4.8
S37	-5.3
S38	-4.5
S39	-4.5
S40	-3.3
R16	-10.9
R17	-11.3

AHU #2 Duct System Depressurized 16.5 Pa	
Diffuser Label	Pressure at Diffusers (Pa)
S14	-8.6
S16	-8.3
S17	-9.0
S20	-9.5
S21	-8.8
S22	-5.3
S29	0.0
R7	-10.9
R9	-10.5
R11	-11.6

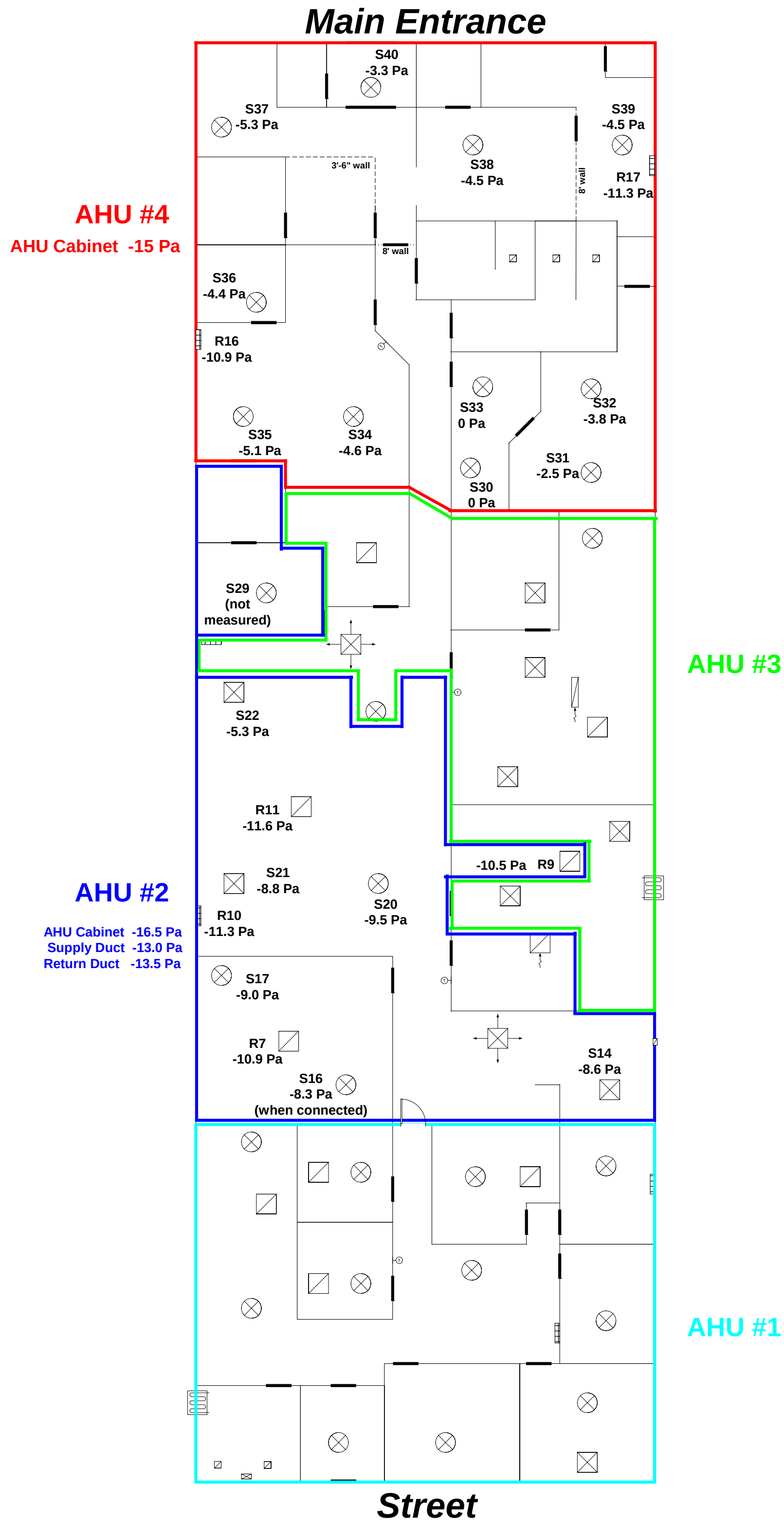

Figure A4-18. Diffuser Pressure Mapping with AHUs Depressurized

Figure A4-19 shows the resulting measured data from all these duct leakage tests fit to a power function (raw data in Table A4-5). Table A4-6 shows the resulting coefficients, exponents, and regression statistics. Table A4-7 summarizes the resulting duct leakage rates and ELA at a reference pressure of 25 Pa. The testing results for AHU #2 are most valid since the recorded pressure was more representative of the supply and return duct pressures. The measured diffuser pressures also confirm that the supply and return side of the system were pressurized to similar levels. The test with the return duct blocked off was also more valid for AHU #2 since a more positive seal was achieved.

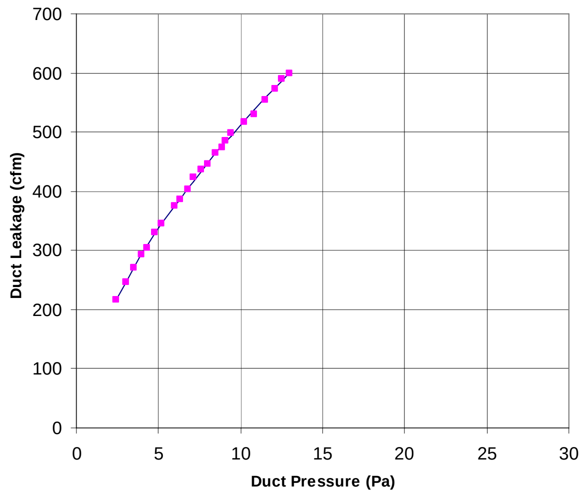

AHU #2 – Total Ductwork System

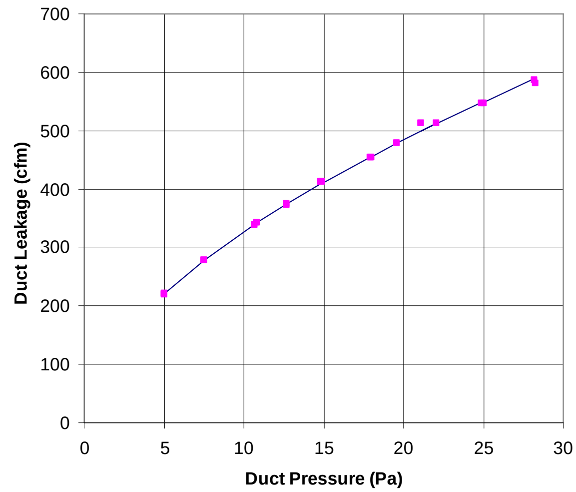

AHU #2 – Supply Ductwork & AHU Cabinet Only

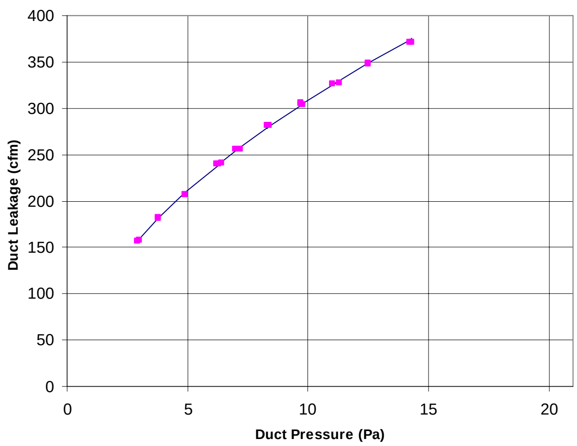

AHU #4 – Total Ductwork System

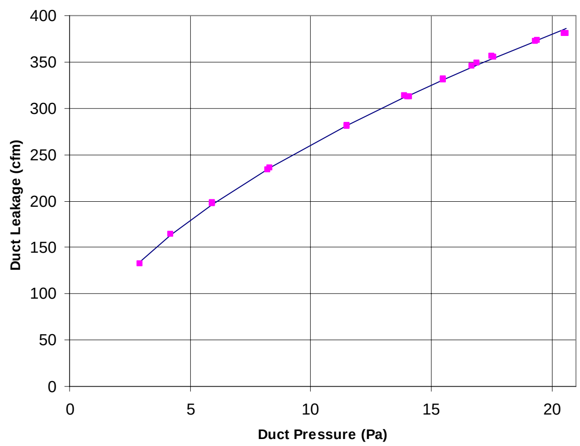

AHU #4 – Supply Ductwork & AHU Cabinet Only

Figure A4-19. Duct-Blaster Tests on Total Ductwork and Supply Duct & AHU Cabinet

The test of the ductwork on AHU #4 did not result in equal pressurization on both sides of the system (as shown by the diffuser pressures in Figure A4-18). Corresponding pressures were not taken in the supply and return ductwork (as was done for AHU #2). However, if we assume a 3.5 Pa drop, the measured pressures and flows for AHU #2 were similar to AHU #4. The test results for AHU #4 with the return side blocked off imply a positive seal was not achieved.

Table A4-5. Raw Data from Duct-Blaster Tests

AHU #2 – Total Ductwork System

Test Results:

Flow Coefficient (K)	127.0	
Exponent (n)	0.606	
Leakage area (LBL ELA @ 25 Pa)	101	sq in
Airflow @ 25 Pa	892.9	cfm

Test Data:

	Nominal Duct Pressure (Pa)	Nominal Flow (cfm)	Ring
1	13.0	600	1
2	12.5	590	1
3	12.1	574	1
4	11.5	555	1
5	10.8	530	1
6	10.2	518	1
7	9.4	499	1
8	9.1	485	1
9	8.9	475	1
10	8.5	465	1
11	8.0	447	1
12	7.6	436	1
13	7.1	424	1
14	6.8	403	1
15	6.3	387	1
16	6.0	375	1
17	5.2	345	1
18	4.8	331	1
19	4.3	305	1
20	4.0	294	1
21	3.5	270	1
22	3.0	247	1
23	2.4	216	1

AHU #2 – Supply Ductwork & AHU Cabinet Only

Test Results:

Flow Coefficient (K)	88.8	
Exponent (n)	0.566	
Leakage area (LBL ELA @ 25 Pa)	62	sq in
Airflow @ 25 Pa	549.5	cfm

Test Data:

	Nominal Duct Pressure (Pa)	Nominal Flow (cfm)	Ring
1	28.2	586	1
2	28.3	581	1
3	25.0	547	1
4	24.9	547	1
5	21.1	512	1
6	22.1	513	1
7	19.6	478	1
8	19.6	479	1
9	17.9	455	1
10	18.0	454	1
11	14.8	413	1
12	14.9	412	1
13	12.7	374	1
14	12.7	373	1
15	10.7	339	1
16	10.8	342	1
17	7.5	278	1
18	7.5	279	1
19	5.0	219	1
20	5.0	221	1

AHU #4 – Total Ductwork System

Test Results:

Flow Coefficient (K)	87.4	
Exponent (n)	0.548	
Leakage area (LBL ELA @ 25 Pa)	58	sq in
Airflow @ 25 Pa	509.5	cfm

Test Data:

	Nominal Duct Pressure (Pa)	Fan Pressure (Pa)	Nomial Flow (cfm)	Ring
1	14.3	80.4	371	1
2	14.2	80.2	371	1
3	12.5	70.4	348	1
4	12.5	70.9	349	1
5	11.0	62.2	327	1
6	11.3	62.3	327	1
7	9.8	54.0	304	1
8	9.7	54.6	306	1
9	9.7	54.4	305	1
10	8.4	46.1	281	1
11	8.3	46.4	282	1
12	8.4	46.1	281	1
13	7.2	38.3	256	1
14	7.0	38.2	256	1
15	6.2	33.5	240	1
16	6.3	33.6	240	1
17	6.4	34.0	241	1
18	4.9	25.0	207	1
19	4.9	24.9	207	1
20	3.8	19.1	181	1
21	3.8	19.4	183	1
22	2.9	14.3	157	1
23	3.0	14.6	158	1

AHU #4 – Supply Ductwork & AHU Cabinet Only

Test Results:

Flow Coefficient (K)	75.5	
Exponent (n)	0.539	
Leakage area (LBL ELA @ 25 Pa)	49	sq in
Airflow @ 25 Pa	428.0	cfm

Test Data:

	Nominal Duct Pressure (Pa)	Fan Pressure (Pa)	Nomial Flow (cfm)	Ring
1	20.6	84.7	381	1
2	20.5	84.5	381	1
3	19.4	81.4	374	1
4	19.3	80.8	372	1
5	17.5	73.8	356	1
6	17.6	73.7	356	1
7	16.7	69.5	345	1
8	16.9	70.7	348	1
9	15.5	63.9	331	1
10	15.5	64.3	332	1
11	15.5	63.9	331	1
12	13.9	57.4	314	1
13	14.0	56.9	312	1
14	14.1	56.9	313	1
15	11.5	46.1	281	1
16	11.5	45.8	280	1
17	8.2	31.7	233	1
18	8.3	32.5	236	1
19	5.9	22.7	197	1
20	5.9	22.6	197	1
21	5.9	23.0	199	1
22	4.2	15.8	165	1
23	2.9	10.2	132	1

Table A4-6. Coefficients, Exponents and Regression Statistics from Duct-Blaster Tests

	Total Ductwork			Supply & AHU Cabinet		
	K	n	R^2	K	n	R^2
AHU #2	127.0	0.606	99.95%	88.8	0.566	99.93%
AHU #4	87.4	0.548	99.93%	75.5	0.539	99.96%

Notes: cfm = $K(Pa)^n$ / R^2 indicates fit of linear log-log regression

Table A4-7. Comparison of Supply and Return Airflow Measurements

	Total Supply Diffuser Airflow (cfm)	Total Return Diffuser Airflow (cfm)	Total Leakage (cfm @ 25)	Supply & AHU Leakage (cfm @ 25)	Total ELA (sq in @ 25)	Supply & AHU ELA (sq in @ 25)
AHU #2	1,268	993	893	550	101	62
AHU #4	1,537	1,331	848	~~712~~	96	~~81~~

Notes: Leakage and ELA at reference pressure of 25 Pa

The effective leakage area compared to the total duct surface area for AHU #2 is shown in Table A4-8. For every 100 sq-ft of duct surface area, there is approximately 9.6 sq-in of duct leakage at 25 Pa. The Sheet Metal and Air Conditioning Contractors' National Association (SMACNA) classifies duct leakiness using duct leakage per 100 sq ft of duct area at a pressure of 1-in w.g. The SMACNA leakage class for the AHU #2 duct system 340.

Table A4-8. AHU #2 Duct Leakage per 100 Square Foot of Duct Area

	Duct Area (sq ft)	ELA (sq in @ 25)	ELA/100 sq ft Duct Area (sq in @ 25)	Leakage (cfm @ 25 Pa)	Supply CFM per Duct Area (cfm/ sq-ft)	Leakage per 100 sq ft Duct Area (cfm @ 25 Pa)	SMACNA Leakage Class cfm per 100 sq ft (cfm @ 1-in water)
Entire System	1,056	101	9.6	893	n/a	85	340
Supply & AHU Cabinet	518	62	12.0	550	2.45	106	390

If we assume the 3.5 Pa pressure drop from AHU cabinet to supply and return duct measured for AHU #2 also applies to AHU #4, then we can correct the leakage flow and ELA to the duct pressure. Increasing the nominal pressure by 3.5 Pa increases the nominal leakage from 848 to 911 cfm, or 8%. The ELA increases from 96 to 97 sq in, or less than 1%.

<u>Space Conditions</u>

Figure A4-20 shows the average temperature profiles based on temperature readings taken with a HOBO datalogger. The thick line shows the average for each hour while the shaded region corresponds to one standard deviation about the average. The dotted lines correspond to the minimum and maximum for each hour. Sensors were placed in the lobby/reception area, billing department, and the back area of the building. The temperature profiles show that the temperature is maintained throughout the nights and weekends.

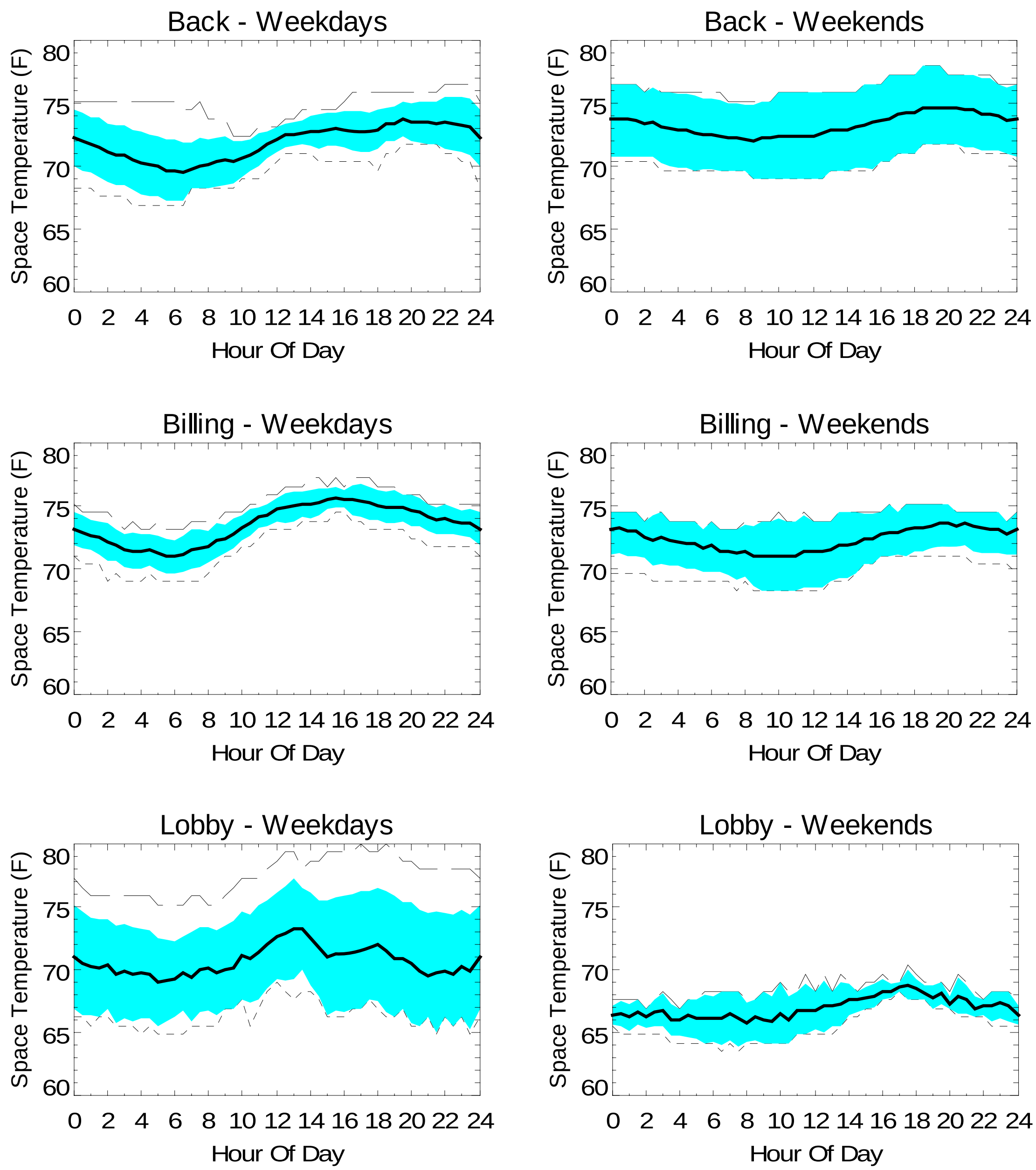

Figure A4-20. Measured Space Temperature Profiles (April 30 to May 15)

Figure A4-21 shows the CO_2 concentration in various locations in the building. The CO_2 concentration provides an indication of occupancy. The next section uses the CO_2 as a tracer gas to estimate the infiltration/ventilation rate into the building.

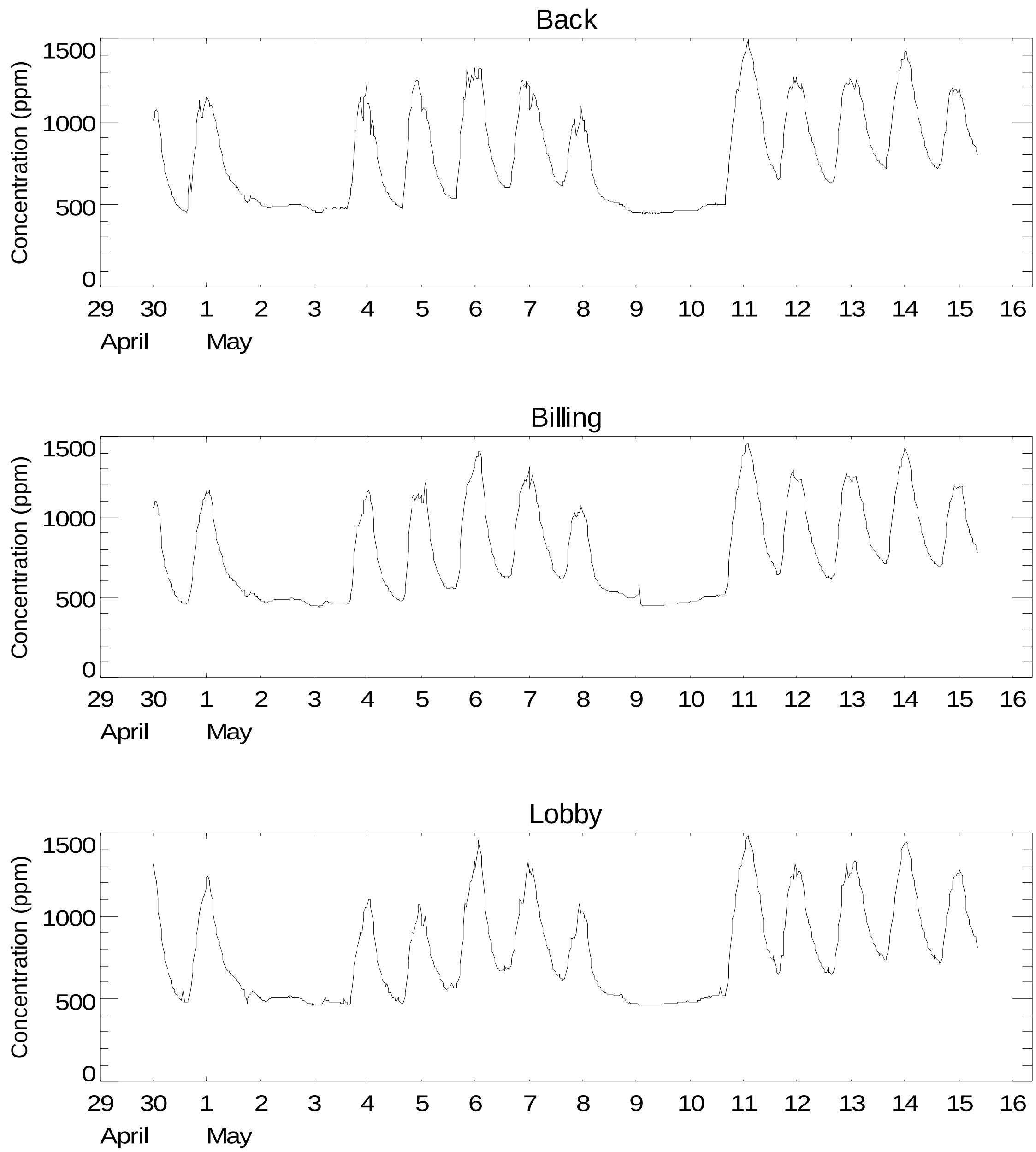

Figure A4-21. Measured CO_2 Concentration in Various Spaces (April 30 to May 15)

Infiltration Estimate from CO_2 Decay

Figure A4-22, Figure A4-23, and Figure A4-24 show the resulting decay trends using CO_2 levels immediately after high occupancy periods for the back area of the building, billing department, and lobby. The predicted air change rate (ACH) is shown on each plot.

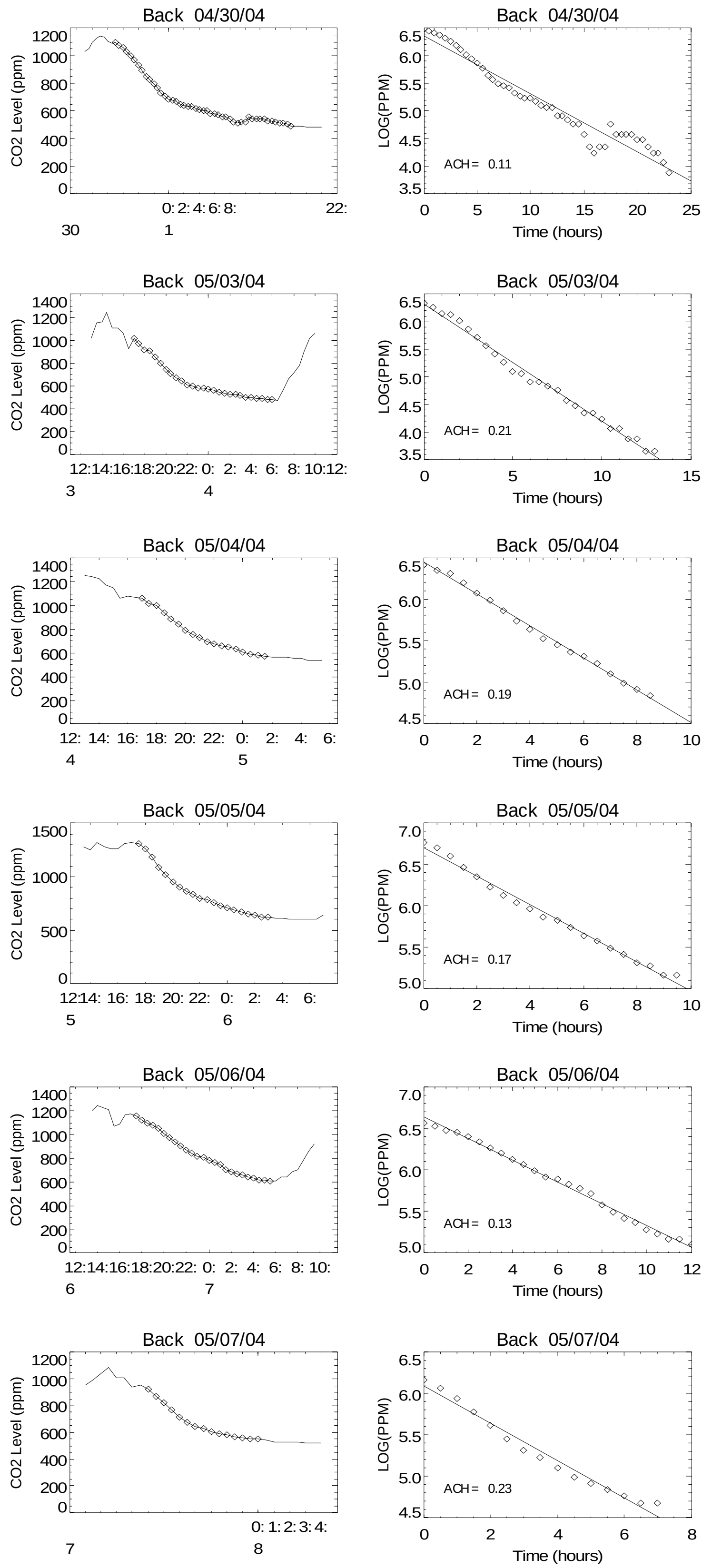

Figure A4-22. Back Area of Bldg Tracer Gas Decay Using CO_2 for Various Periods

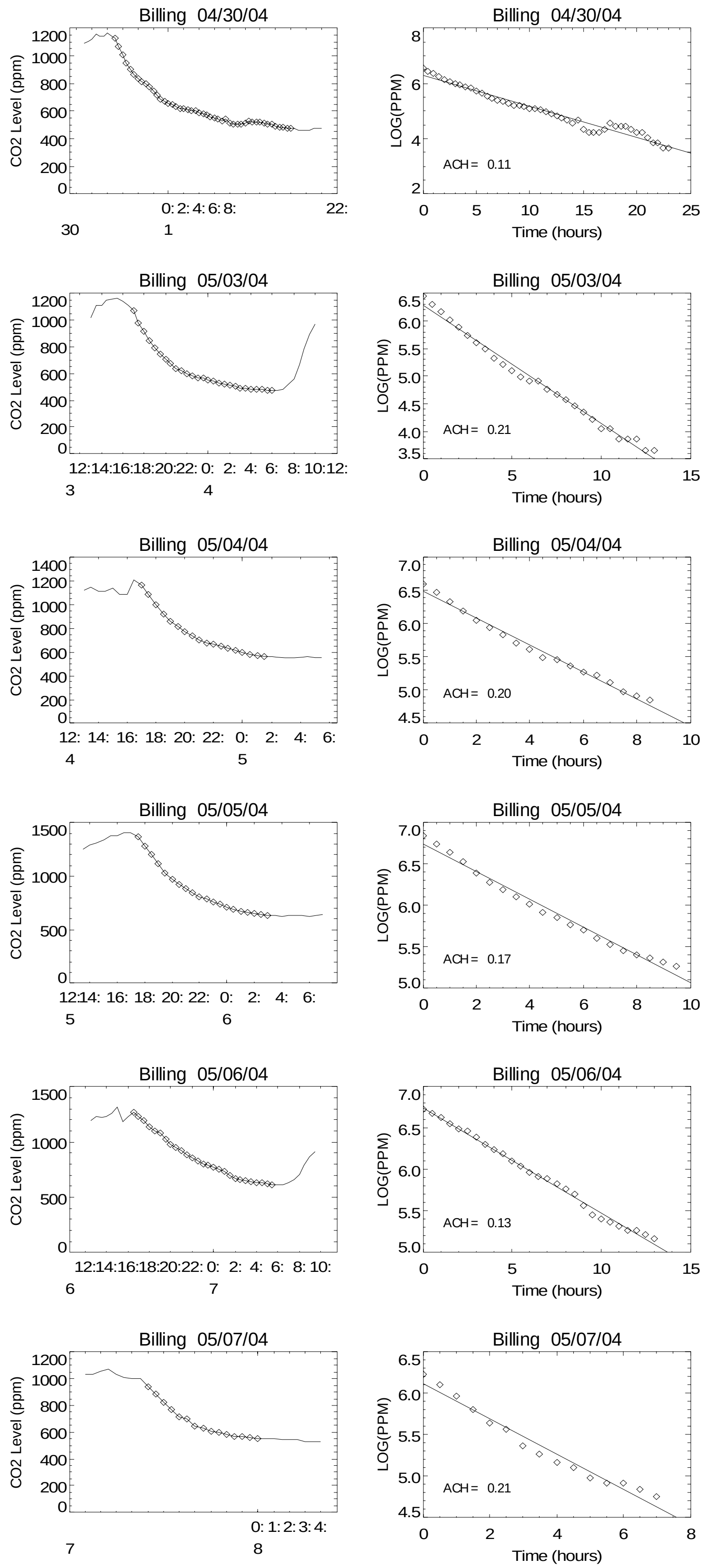

Figure A4-23. Billing Dept. Tracer Gas Decay Using CO_2 for Various Periods

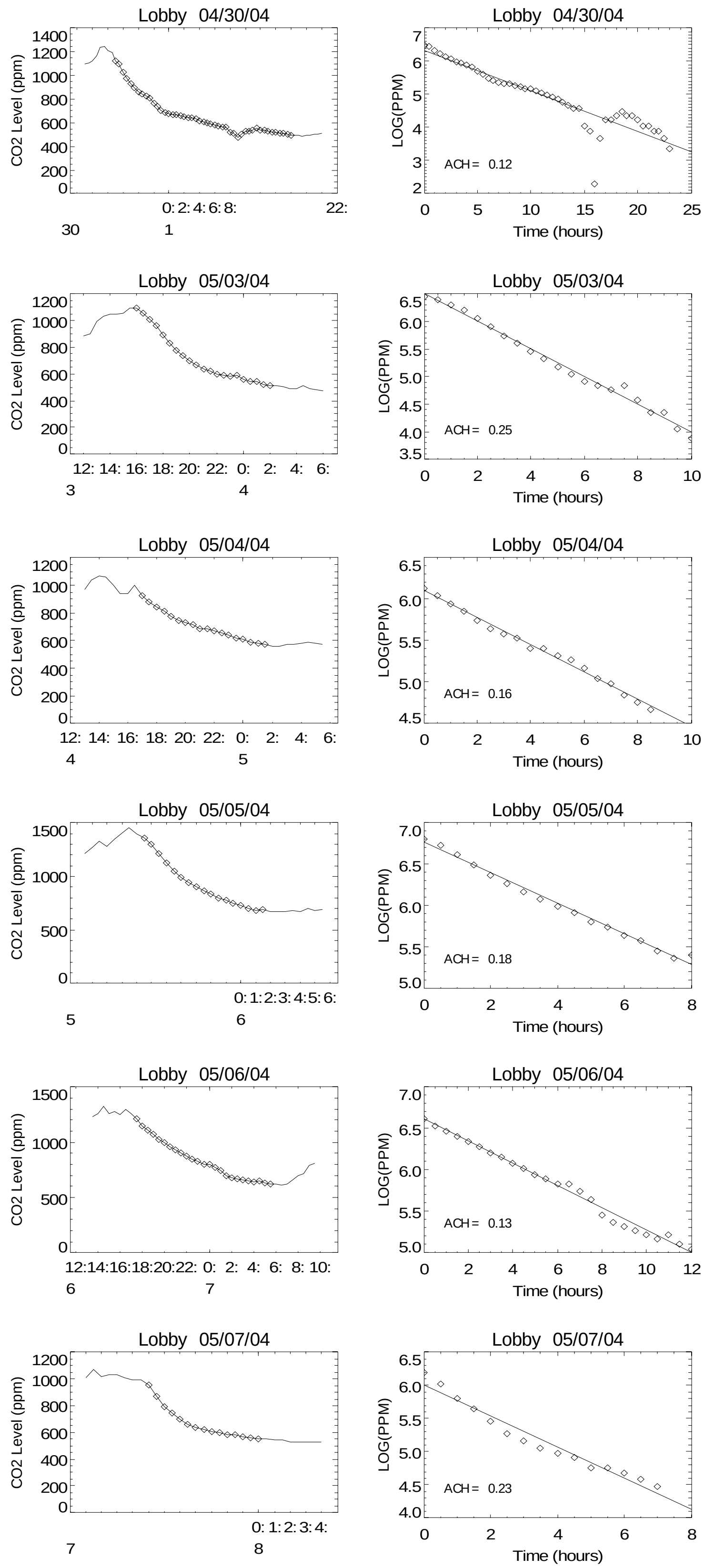

Figure A4-24. Lobby Tracer Gas Decay Using CO_2 for Various Periods

Table A4-9 summarizes the results of the tracer gas decay tests in the plots above. The table also includes the ambient temperature recorded during each decay period listed in the table. Figure A4-25 compares the ACH and ambient temperature. The estimated ACH shows a slight correlation with ambient temperature, implying stack effect plays a role.

Table A4-9. Summary of Tracer Gas Decay Tests

Back

Start Time	End Time	ACH	Flow (cfm)	Ambient Temp. (F)
30-Apr 05:00 PM	01-May 04:00 PM	0.11	115	73.9
03-May 05:00 PM	04-May 06:00 AM	0.21	232	46.9
04-May 05:00 PM	05-May 01:30 AM	0.19	212	46.2
05-May 05:30 PM	06-May 03:00 AM	0.17	189	47.9
06-May 05:30 PM	07-May 05:30 AM	0.13	143	62.5
07-May 05:00 PM	08-May 12:00 AM	0.23	247	58.3

Billing

Start Time	End Time	ACH	Flow (cfm)	Ambient Temp. (F)
30-Apr 05:00 PM	01-May 04:00 PM	0.11	123	73.9
03-May 05:00 PM	04-May 06:00 AM	0.21	234	46.9
04-May 05:00 PM	05-May 01:30 AM	0.20	222	46.2
05-May 05:30 PM	06-May 03:00 AM	0.17	184	47.9
06-May 04:30 PM	07-May 05:30 AM	0.13	139	63.2
07-May 05:00 PM	08-May 12:00 AM	0.21	233	58.3

Lobby

Start Time	End Time	ACH	Flow (cfm)	Ambient Temp. (F)
30-Apr 05:00 PM	01-May 04:00 PM	0.12	134	73.9
03-May 04:00 PM	04-May 02:00 AM	0.25	276	48.9
04-May 05:00 PM	05-May 01:30 AM	0.16	180	46.2
05-May 05:30 PM	06-May 01:30 AM	0.18	202	49.0
06-May 05:30 PM	07-May 05:30 AM	0.13	147	62.5
07-May 05:00 PM	08-May 12:00 AM	0.23	256	58.3

Note: Flow determined with building volume of 65,670 ft^3

In comparison to the ACH values above, the nominal leakage rate (defined as ACH_{50} divided by 20) from the blower door test above is 0.34 ACH.

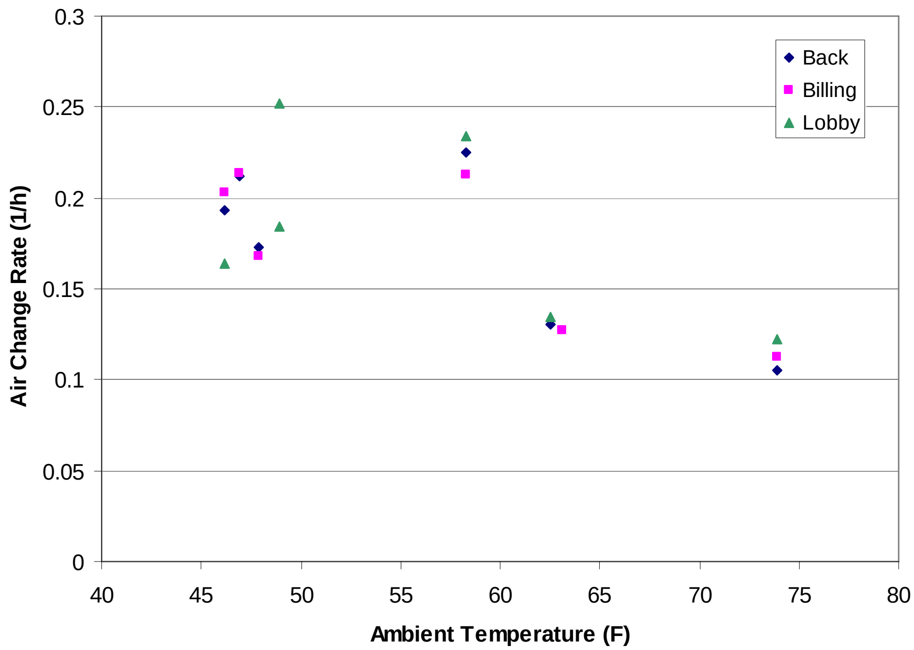

Figure A4-25. Variation of Air Change Rate (ACH) with Ambient Temperature

Utility Bills

Gas use is primarily used for space heating. The tables and graphs below show the gas and electric use trends for the facility. The overall energy use index for the building is summarized below.

	Heating Energy Use Index (MBtu/ft^2-year)	Electric Use Index (kWh/ft^2-year)
2002-2003 Season	40.5	25.7
2003-2004 Season	28.9	26.6

Season is from May to April

Table A4-10. Summary of Electric Bills

	Office Building Electric Utility Data				
	Days in Month	Energy (kWh)	Cost ($)	$/kWh	Elec. Use per Sq-Ft (kWh/sq ft)
5/16/2002	30	13,414	$ 1,695.25	0.13	1.79
6/17/2002	32	15,477	$ 1,833.58	0.12	2.06
7/17/2002	30	17,631	$ 2,078.80	0.12	2.35
8/16/2002	30	18,412	$ 2,245.21	0.12	2.45
9/17/2002	32	17,885	$ 2,194.40	0.12	2.38
10/16/2002	29	13,553	$ 1,796.41	0.13	1.81
11/14/2002	29	12,619	$ 1,666.08	0.13	1.68
12/16/2002	32	16,292	$ 1,918.20	0.12	2.17
1/16/2003	31	16,697	$ 1,860.99	0.11	2.23
2/14/2003	29	18,170	$ 2,045.89	0.11	2.42
3/17/2003	31	17,295	$ 2,089.94	0.12	2.31
4/15/2003	29	14,860	$ 1,874.74	0.13	1.98
5/15/2003	30	14,747	$ 1,890.82	0.13	1.97
6/17/2003	33	16,731	$ 2,002.18	0.12	2.23
7/17/2003	30	18,058	$ 2,110.28	0.12	2.41
8/15/2003	29	18,363	$ 2,129.73	0.12	2.45
9/17/2003	33	19,774	$ 2,314.52	0.12	2.64
10/16/2003	29	14,238	$ 1,818.20	0.13	1.90
11/14/2003	29	14,302	$ 1,794.63	0.13	1.91
12/16/2003	32	16,962	$ 1,974.72	0.12	2.26
1/16/2004	31	17,819	$ 2,193.46	0.12	2.38
2/17/2004	32	18,826	$ 2,388.88	0.13	2.51
3/17/2004	29	15,575	$ 1,978.67	0.13	2.08
4/19/2004	33	16,669	$ 2,153.90	0.13	2.22
2002-2003	364	192,305	$ 23,299.49	0.12	25.64
2003-2004	370	202,064	$ 24,749.99	0.12	26.94

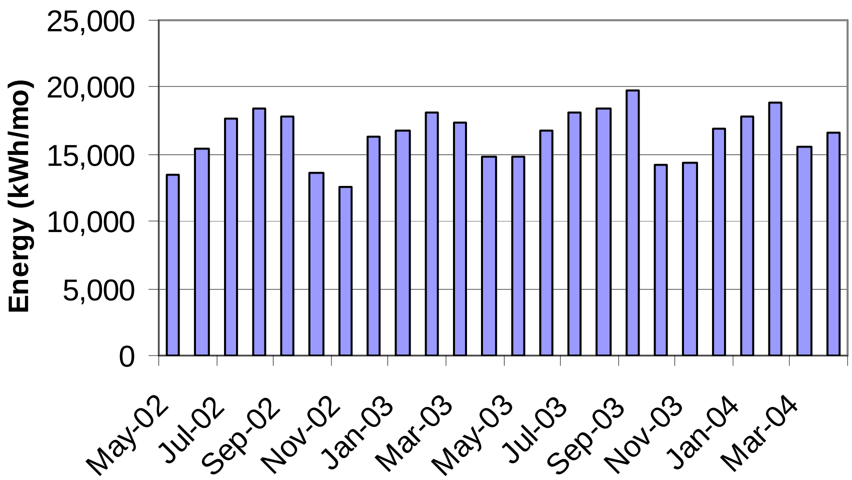

Figure A4-26. Monthly Electricity Use Trends

Table A4-11. Summary of Gas Bills

	Office Building Gas Utility Data [Meter (1) 4831353107]				
	Days in Month	Gas Use (therms)	Cost ($)	$/therm	Gas Use per Sq-Ft (therm/sq ft)
5/16/2002	30	26	$ 41.58	1.60	0.003
6/17/2002	32	2	$ 22.19	11.10	0.000
7/17/2002	30	-	$ 21.05	-	-
8/16/2002	30	-	$ 21.05	-	-
9/17/2002	32	-	$ 21.05	-	-
10/16/2002	29	2	$ 22.13	11.07	0.000
11/14/2002	29	50	$ 62.66	1.25	0.007
12/16/2002	32	216	$ 211.19	0.98	0.029
1/16/2003	31	158	$ 167.30	1.06	0.021
---	---	---	---	---	
---	---	---	---	---	
4/15/2003	89	211	$ 292.21	1.38	0.028
5/15/2003	30	21	$ 44.84	2.14	0.003
6/17/2003	33	5	$ 25.79	5.16	0.001
7/17/2003	30	-	$ 20.96	-	-
8/15/2003	29	-	$ 20.96	-	-
9/17/2003	33	-	$ 21.08	-	-
10/16/2003	29	6	$ 26.42	4.40	0.001
11/14/2003	29	25	$ 45.63	1.83	0.003
12/16/2003	32	77	$ 97.92	1.27	0.010
1/16/2004	31	96	$ 121.80	1.27	0.013
2/12/2004	27	144	$ 174.53	1.21	0.019
3/17/2004	34	68	$ 92.04	1.35	0.009
4/19/2004	33	42	$ 63.27	1.51	0.006
2002-2003	364	665	$ 882.41	1.33	0.089
2003-2004	370	484	$ 755.24	1.56	0.065

	Office Building Gas Utility Data [Meter (2) 4811353101]				
	Days in Month	Gas Use (therms)	Cost ($)	$/therm	Gas Use per Sq-Ft (therm/sq ft)
5/16/2002	30	132	$ 128.92	0.98	0.018
6/17/2002	32	29	$ 44.74	1.54	0.004
7/17/2002	30	19	$ 36.47	1.92	0.003
8/16/2002	30	19	$ 35.48	1.87	0.003
9/17/2002	32	20	$ 36.09	1.80	0.003
10/16/2002	29	32	$ 47.45	1.48	0.004
11/14/2002	29	194	$ 184.95	0.95	0.026
12/16/2002	32	352	$ 325.16	0.92	0.047
1/16/2003	31	432	$ 402.60	0.93	0.058
2/14/2003	29	320	$ 319.87	1.00	0.043
3/17/2003	31	644	$ 713.60	1.11	0.086
4/15/2003	29	169	$ 228.19	1.35	0.023
5/15/2003	30	114	$ 154.69	1.36	0.015
6/17/2003	33	72	$ 103.09	1.43	0.010
7/17/2003	30	13	$ 33.95	2.61	0.002
8/14/2003	28	13	$ 32.54	2.50	0.002
9/16/2003	33	18	$ 37.49	2.08	0.002
10/15/2003	29	31	$ 51.99	1.68	0.004
11/13/2003	29	76	$ 97.34	1.28	0.010
12/15/2003	32	218	$ 240.10	1.10	0.029
1/15/2004	31	337	$ 369.09	1.10	0.045
2/13/2004	29	366	$ 404.73	1.11	0.049
3/15/2004	31	282	$ 318.25	1.13	0.038
4/15/2004	31	155	$ 179.02	1.15	0.021
2002-2003	364	2,362	$ 2,503.52	1.06	0.315
2003-2004	366	1,695	$ 2,022.28	1.19	0.226

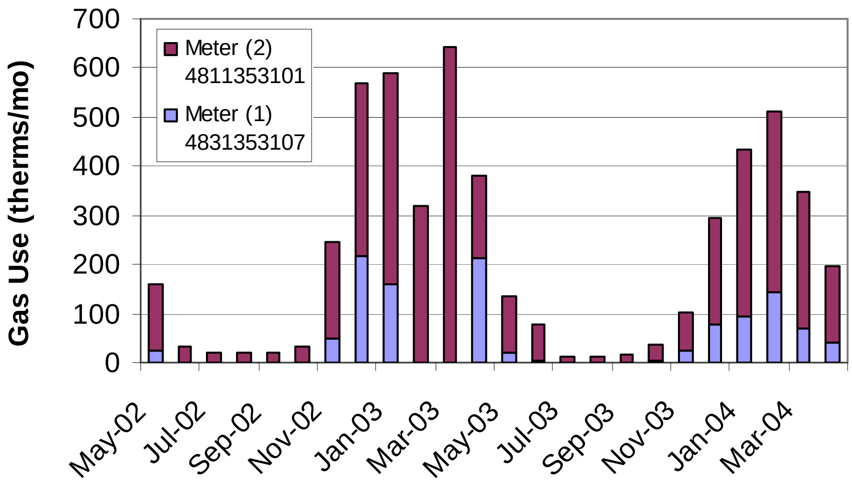

Figure A4-27. Monthly Gas Use Trends

Figure A4-28 shows the gas use variation with ambient temperature. There are two natural gas meters in parallel that measure the gas use for the building. The heating load appears to have decreased in the most recent season (2003-2004).

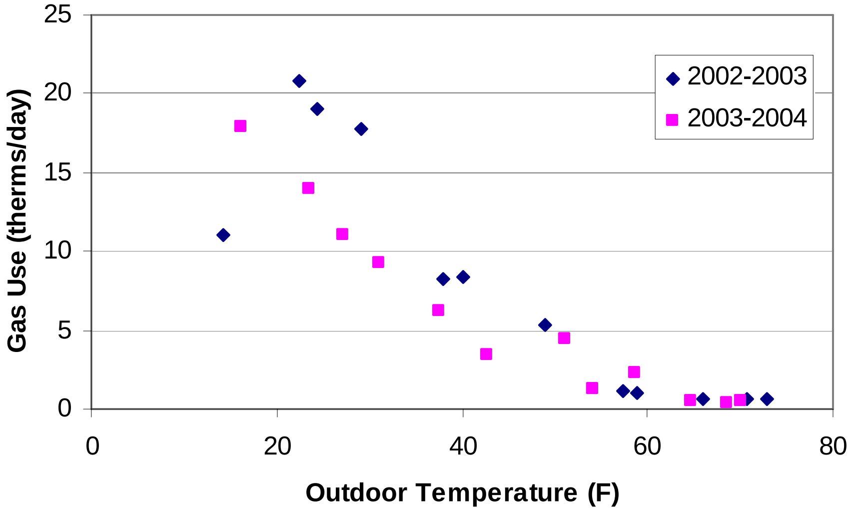

Figure A4-28. Variation of Gas Use with Ambient Temperature

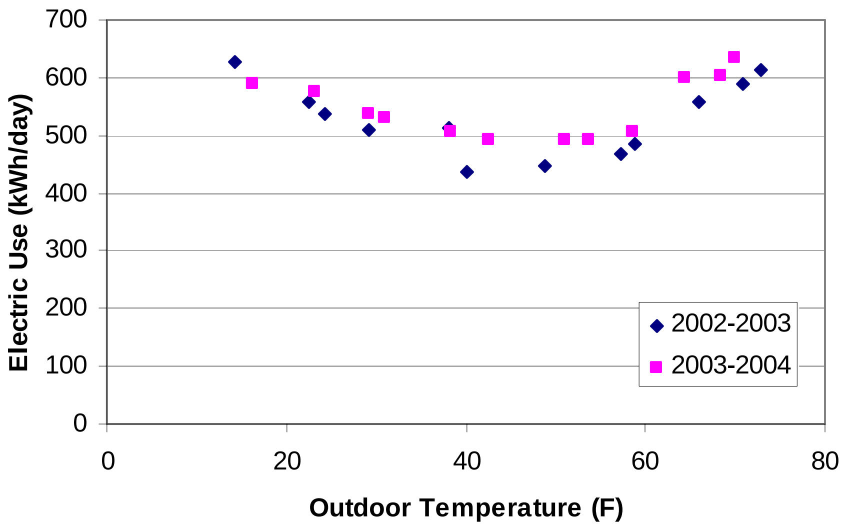

Figure A4-29. Variation of Electric Use with Ambient Temperature

Field Test Site 5 - Office Building/Training Center, Syracuse, NY

Front of Building and Main Entrance (East)


Rear of Building (West)

Figure A5-1. Photos of Building

CHARACTERISTICS

Building Description

The 18,000 sq ft facility is a one-story office/training center that was built in 1974. An attached garage (approximately 1,200 sq. ft.) is separated from the main building by block walls that extend from the floor to the roof. The garage is not included in this report since we did not have access to the garage and it is relatively sealed from the remainder of the building. The facility has an 6,700 sq-ft high-bay lab training area, 5 classrooms (one classroom can be split into two rooms), 6 offices with doors, several cubicles, a high bay TV studio, 3 lavatories, and 8 other miscellaneous rooms. Figure A5-1 shows the front and rear of the building. The training area is served by a constant volume air-handler and the remaining portion of the building is served by a variable-air-volume (VAV) system. The constant volume system has a 25-ton cooling section and the VAV system is an electric unit with a 55-ton cooling section. The VAV system is only used for cooling the office and classroom portions of the building. Electric baseboard heat at the perimeter of the facility is the only source of heating for the classrooms and offices. The constant volume unit has a relatively new gas fired duct heater.

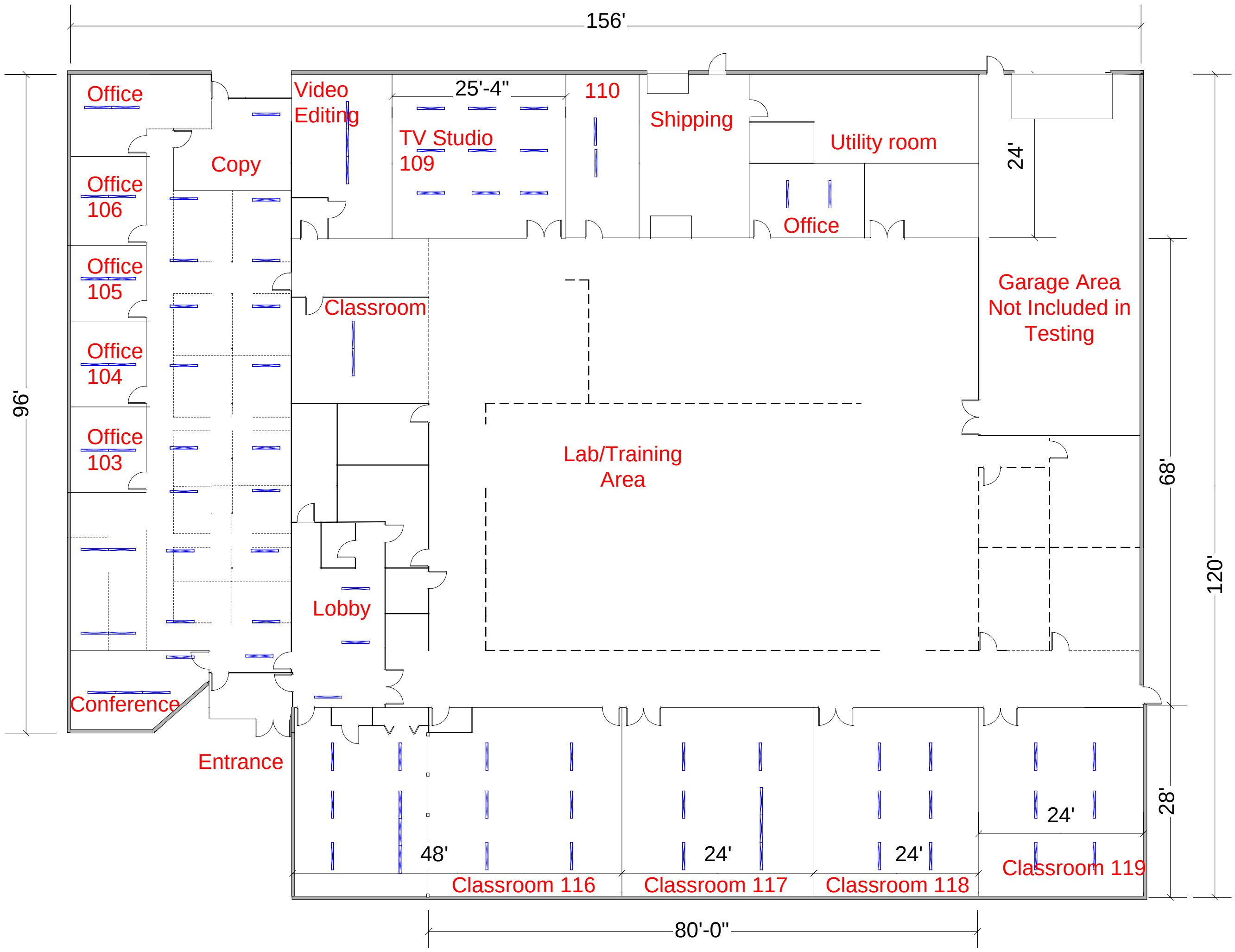

Figure A5-2. Building Floor Plan

Construction Details

Exterior walls are 6-in concrete block with 1-in rigid insulation and brick veneer exterior finish. The interior is finished with ½-in gypsum board. For soundproofing, the interior walls of the classrooms and TV studio are sand-filled concrete block with two layers of gypsum board.

The roof construction in the high bay training area consists of foam board, poured gypsum roof deck, rigid insulation, and built-up roofing. Areas with drop ceilings have an interior layer of gypsum board mounted under the foam board. The T-bar (drop) ceiling is typically 34-47 inches below the roof.

Figure A5-3 illustrates typical wall and roof sections for the high bay areas. Figure A5-4 shows the details of the roof and exterior wall construction for the classrooms and offices. Figure A5-5 shows pictures of the ceiling in the lab area and the ceiling plenum in the classrooms and office area.

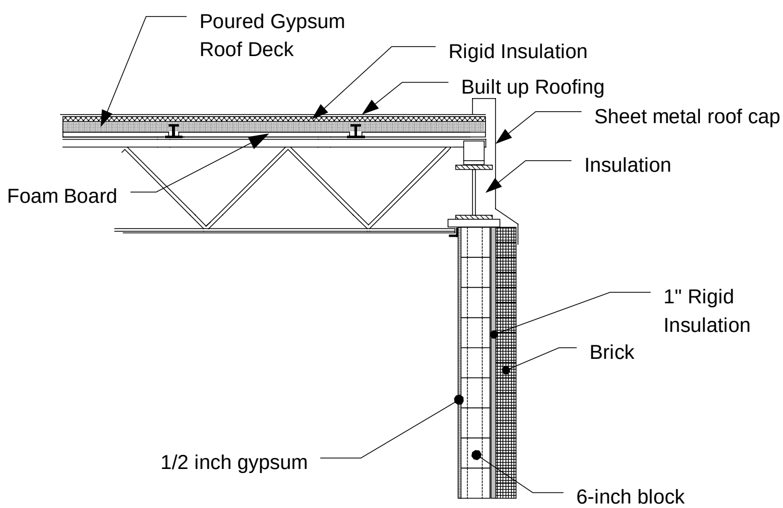

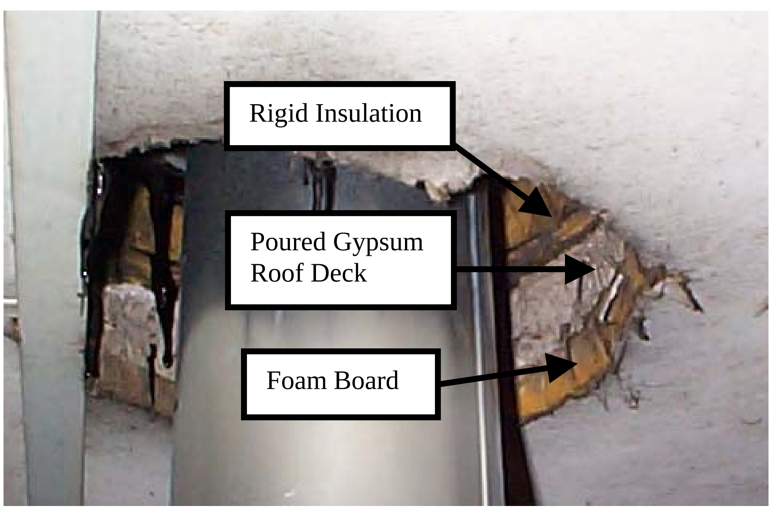

Roof Section for High Bay Areas

Figure A5-3. High Bay Area Roof and Wall Construction

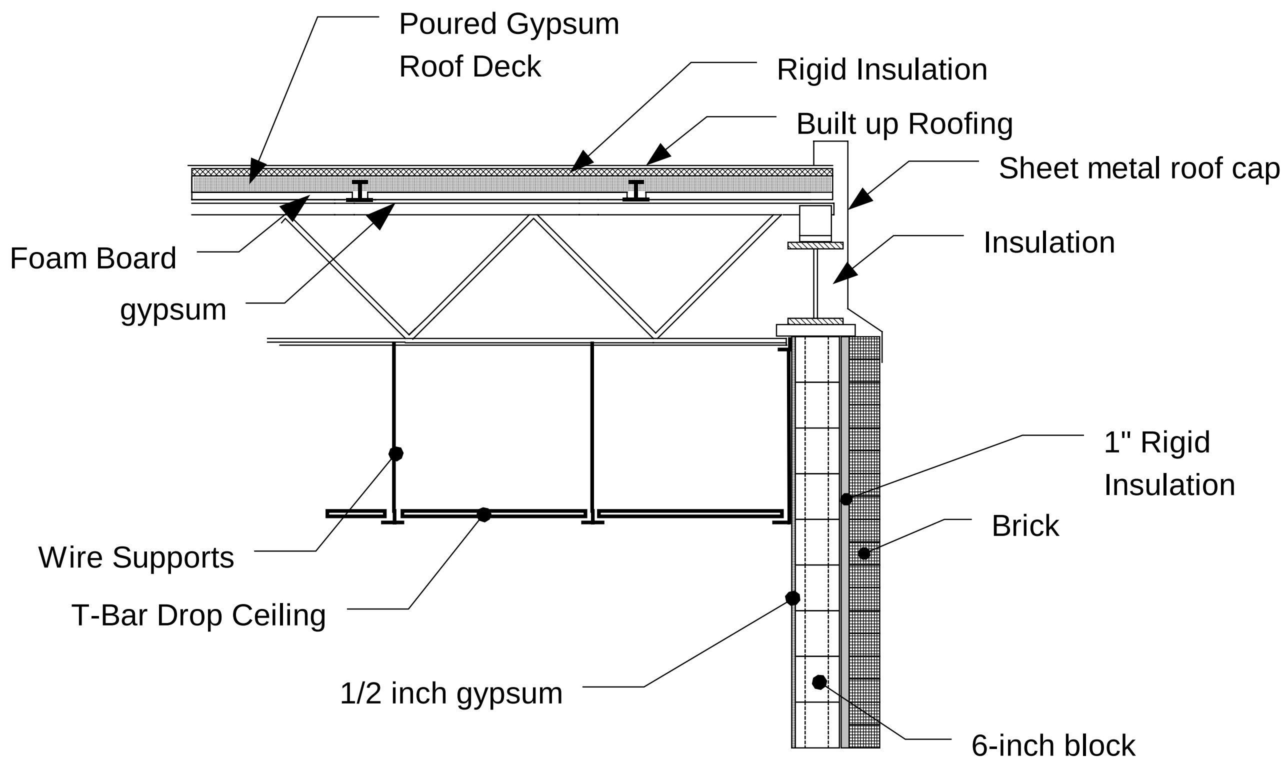

Figure A5-4. Classroom and Office Roof/Wall Construction with Drop Ceiling

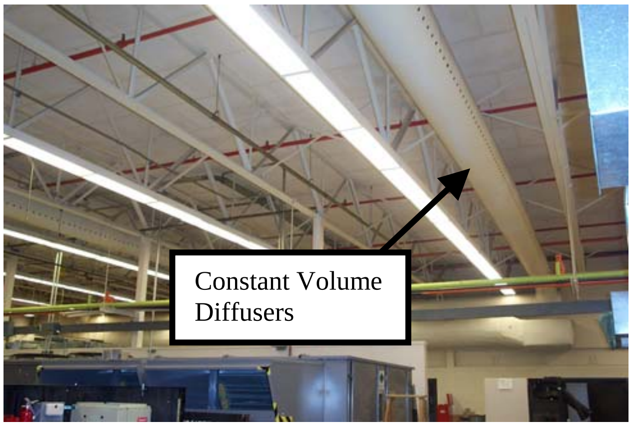

Ceiling in Lab/Training Area

Ceiling Plenum in Classrooms and Offices

Figure A5-5. Lab Area Ceiling and Ceiling Plenum for Classrooms/Offices

HVAC System

Figure A5-6 shows the location of the main supply and return ductwork for the variable air volume (VAV) and constant volume systems. Figure A5-7 shows pictures of the AHUs. The lab/training area is conditioned with a constant volume system with a cooling section and a gas-fired Sterling duct heater mounted downstream of the air handler supply fan[1]. The constant volume system uses three runs of perforated ducts to distribute supply air throughout the lab area (Figure A5-6). The classrooms and offices are heated with electric baseboard at the perimeter of the building and cooled by a VAV unit with linear supply diffusers. The VAV system has a separate return fan that pulls air from the ceiling plenum in the classrooms and offices. The constant volume unit has one large return grill located in the lab area. Fresh air is provided to both air-handlers through an outdoor air intake located at the rear of the building. There are outdoor air dampers and return dampers for both systems. The VAV system also has a return bypass damper that is set up in case of air contamination due to a fire or other contaminants (see Figure A5-16). To exhaust the contaminated air, the return dampers close and the bypass dampers open to the outdoors, venting the contaminated air. In addition the return bypass dampers, there are fire dampers in the roof of the training area. The dampers do not close completely. There are two condensing units totaling 55 tons for the VAV system and a single relatively new 25-ton condensing unit for the constant volume system located at the rear of the building near the shipping dock (Figure A5-8). Table A5-1 lists the data for the constant volume unit and the variable air volume unit.

[1] The gas heater was added in the last couple of years.

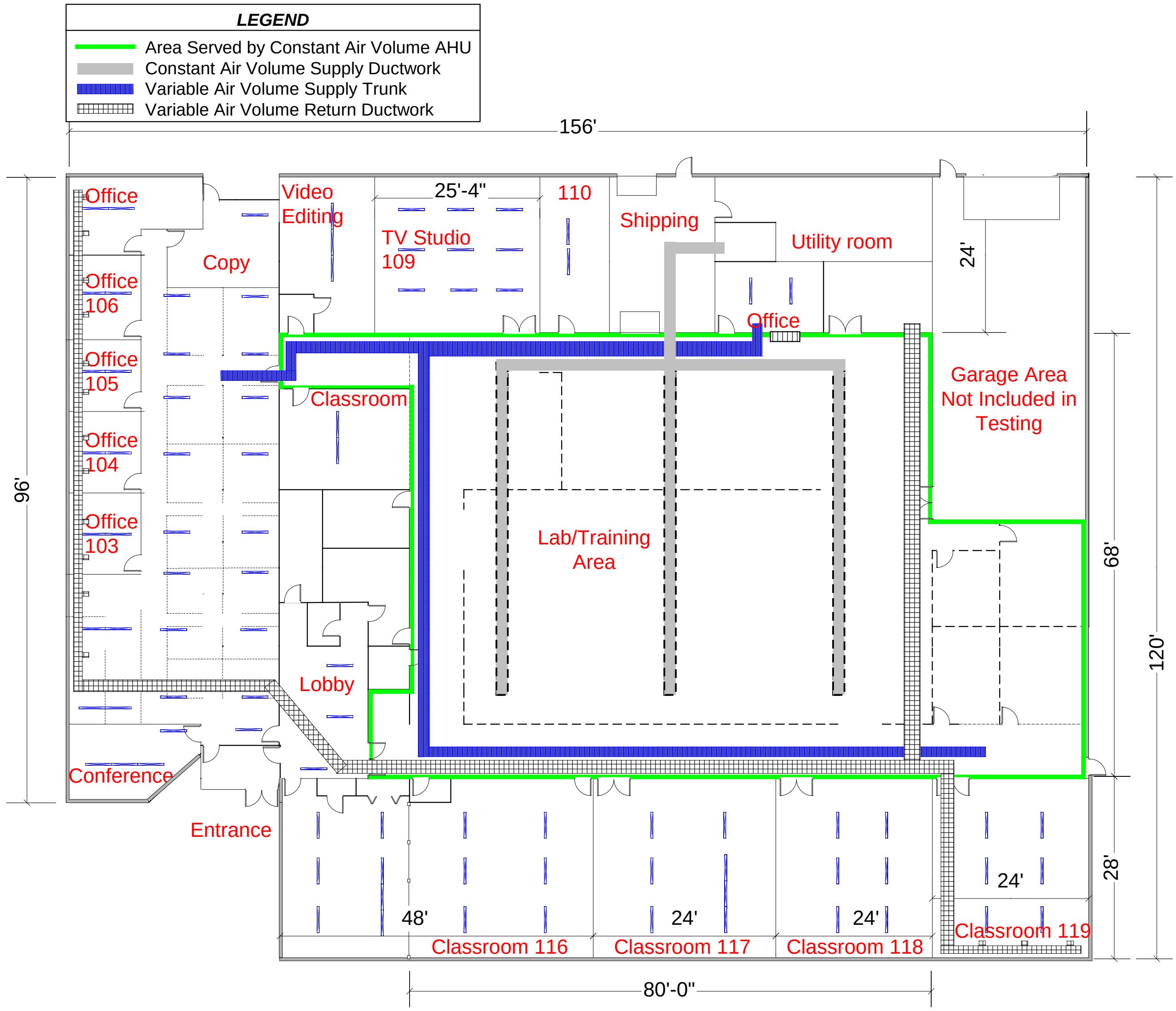

Figure A5-6. Constant Volume and VAV System Ductwork.


Constant Volume System


Sterling Duct Heater for Constant Volume Unit


Variable Air Volume System

Figure A5-7. Constant Volume and VAV Air-Handling Units

Figure A5-8. Constant Volume and VAV Condensing Units

Table A5-1. Summary HVAC Equipment Installed at Site

	Carrier AHU	Carrier Condenser	Cooling Capacity (tons)	Measured Fan Power (kW)
Constant Volume Units	40RR024	38AKS028	25	4.2
VAV Unit	39E28	(1) 38AD024 (1) 38AD028	Total = 55 tons	Supply Fan = 6.2 Return Fan = 2.6

The VAV system has insulated supply and un-insulated return ducts that run through the lab area (with the elevated ceiling) and into the plenum above the drop ceiling of the offices, TV studio, and classrooms. The supply ductwork is circular sheet metal varying in diameter from 6 – 30 inches typically with 1.5 inches of insulation. The VAV system has linear diffusers with a bladder style diffuser that is powered by duct static pressure. The diffusers have a bimetal thermostat to regulate the temperature in each space (Figure A5-9. VAV System Linear Diffusers). One bimetal thermostat typically controls two or three linear diffusers in series. The linear diffusers have a tab near the diffuser box to prevent leakage into the ceiling plenum.

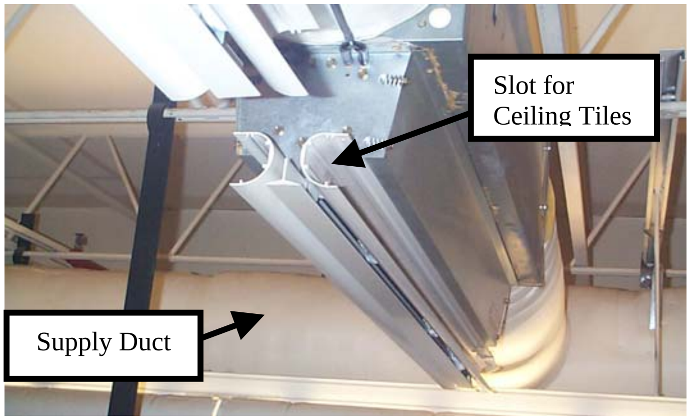

Linear Diffuser with No Drop Ceiling

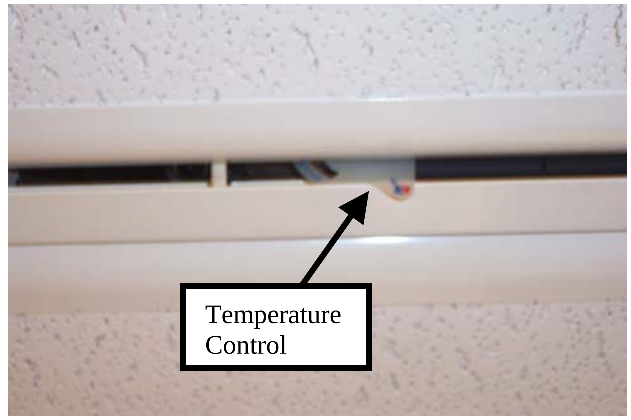

Linear Diffuser Temperature Control

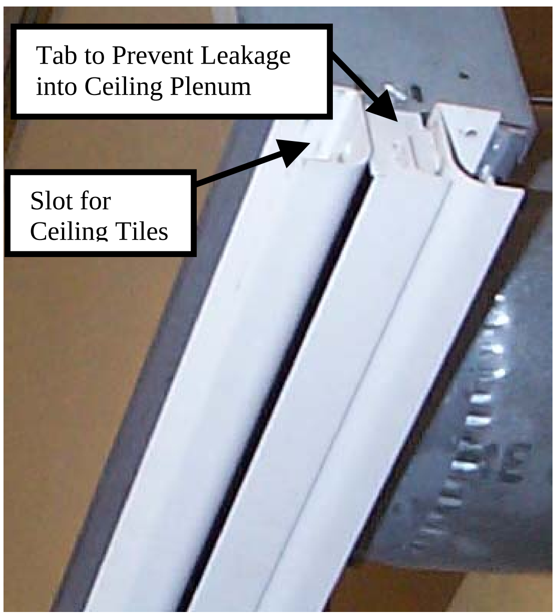

Linear Diffuser with Tab Preventing Leakage to Ceiling Plenum

Figure A5-9. VAV System Linear Diffusers

There are return ducts that lead to each of the classrooms and open up into the individual ceiling plenums to pull air from the rooms. The return duct that leads to the office section of the building continue within the office ceiling plenum along the perimeter of the building as illustrated in Figure A5-6. There are short rectangular duct takeoffs approximately every 25 ft along the east side of the building (Figure A5-10). Figure A5-11 shows the two types of return ductwork that pulls air from the classrooms. The lower picture in Figure A5-11 shows a typical return plenum in classrooms 116, 117 and 118 with the return duct simply protruding through the wall. The return for classroom 119 enters the ceiling plenum with rectangular duct takeoffs like the office section.

Figure A5-10. Return Ductwork in Ceiling Plenum over Offices

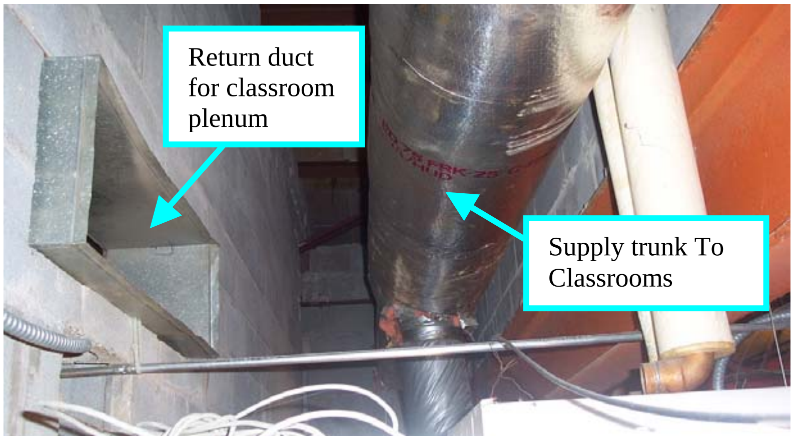

Return for Ceiling Plenum (Classrooms 116, 117, 118)

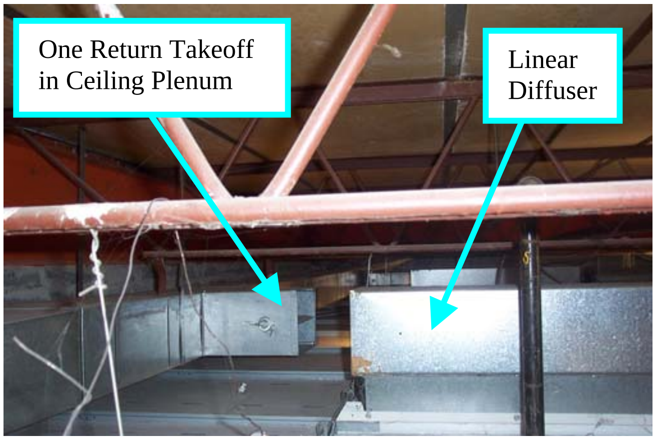

Return Ductwork Inside Ceiling Plenum (Classroom 119)

Figure A5-11. Returns for Classroom Ceiling Plenums

The training center has two barometric dampers to prevent the building from over-pressurizing. One barometric damper is connected to an exhaust system used when training students on gas furnaces. The second barometric damper is located in the classroom near the TV studio. This second damper has been sealed off by the facility personnel due to the noise it creates on windy days (Figure A5-12).

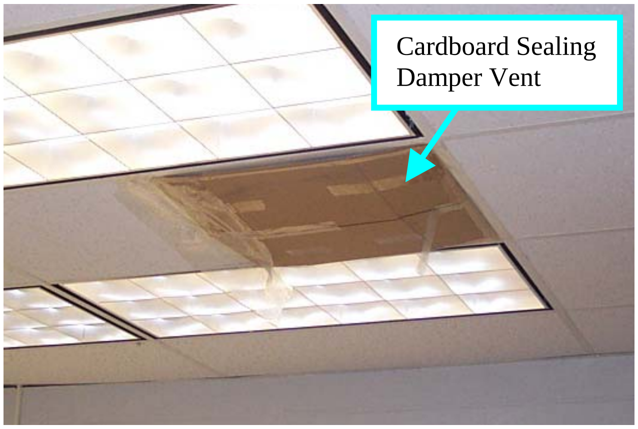

Barometric Damper Sealed Off


Flex Duct Takeoff to Damper Vent through Roof

Figure A5-12. Barometric Damper (Normally Sealed) in Classroom near TV Studio

The facility does not setback heating or cooling on the VAV or constant volume unit. There is a single standard thermostat in the lab/training area for the constant volume unit. The linear diffusers in classrooms and offices have individual thermostats for sets of two or three diffusers in series.

MEASUREMENTS

Blower door testing, pressure mapping, and duct leakage measurements were taken on June 4, 2004. CO_2, temperature, and relative humidity sensors were deployed throughout the building and set to record CO_2 levels and typical air conditions. We seeded the building with CO_2 tracer gas the night of June 4 to determine the air change rate for the facility. In addition to the large CO_2 decay the night of June 4, we continued recording data for two weeks to monitor typical air quality. Test personnel were Dan Gott, Kenneth Larchar, Hugh Henderson, and Mike Clarkin. Dan Gott collected temperature and CO_2 sensors on June 18, 2004.

Building Envelope Airtightness

The leakage characteristics of the building enclosure were assessed using fan depressurization methods. A blower door was set up in the rear of the building (shipping room) to depressurize the building. To seal the building, the lab exhaust system, restroom exhausts, barometric dampers, and the outdoor air intake for the AHUs were sealed. This test was performed twice. Initially, all interior doors were open (excluding closets and lavatories), and all exterior doors and windows were closed. One unseen exhaust fan was left on by accident for the first test. The second test was performed with the exhaust fan turned off. A noticeable difference is evident. With the exhaust fan off, the blower door depressurization actually induced reverse flow through the exhaust fan. With the fan on, the leakage area was effectively blocked (and possibly reversed). Blower door flow measurements were recorded for both setups. Figure A5-13 and Table A5-2 show the leakage variation with building pressure for test 1 with the exhaust fan on.

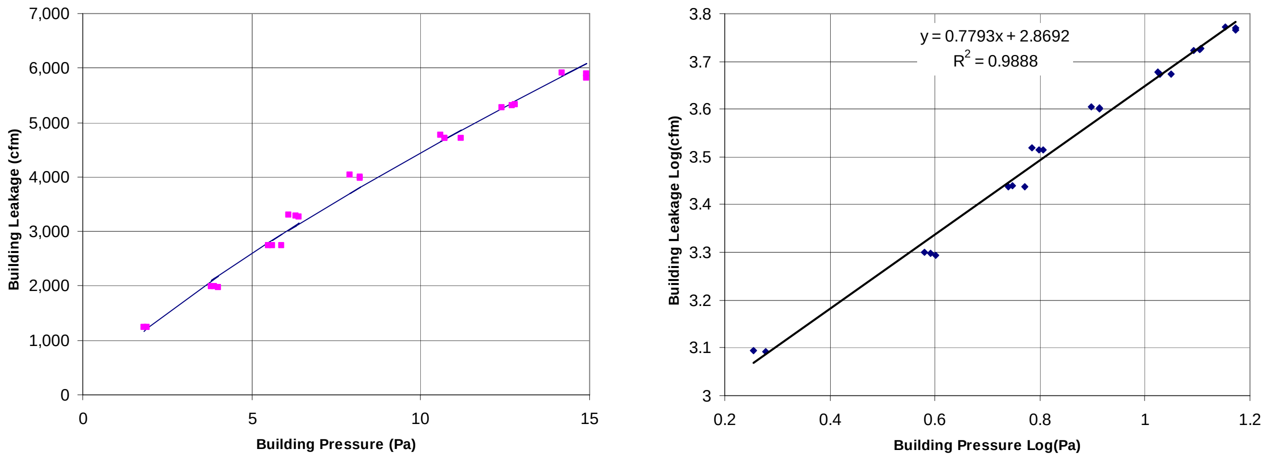

Figure A5-13. Variation of Building Leakage with Pressure: cfm = K(ΔP)^n (Exhaust Fan On)

Table A5-2 shows the results of the first blower door test including model coefficients, effective leakage area (ELA), and air-changes-per-hour (ACH). The ELA is calculated using the Lawrence Berkeley Laboratory method, which specifies the leakage area at 4 Pa. This building has an effective leakage area of approximately 1.4 sq in per 100 sq ft. Another building leakage characteristic is the ACH at 50 pascals (ACH_{50}). The building has an ACH_{50} of 3.6. This result implies that at 50 Pa, the air in the building is displaced 3.6 times each hour.

Table A5-2. Blower Door Test Data, Resulting Best-Fit Model Coefficients, and ELA (Exhaust Fan On)

Flow Coefficient (K)	739.9	17,819	sq ft, floor area
Exponent (n)	0.779		
Leakage area (LBL ELA @ 4 Pa)	617.6 sq in	1.40	ELA / 100 sq ft
Airflow @ 50 Pa	15601.4 cfm	3.64	ACH @ 50

Test Data:

Nominal Building Pressure (Pa)	Nominal Flow (cfm)	Ring
14.9	5,819	none
14.2	5,920	none
14.9	5,886	none
12.7	5,306	none
12.8	5,323	none
12.4	5,280	none
10.7	4,719	none
10.6	4,765	none
11.2	4,713	none
10.7	4,710	none
8.2	4,005	none
7.9	4,034	none
8.2	3,982	none
6.1	3,303	none
6.3	3,275	none
6.4	3,274	none
5.6	2,746	none
5.9	2,745	none
5.5	2,736	none
3.8	1,995	none
3.9	1,986	none
4.0	1,969	none
1.9	1,236	none
1.8	1,240	none

Notes: ELA is leakage area (in square inches) at reference pressure of 4 Pa.
ELA per 100 sq ft is based on total building envelope surface area (ceiling, exterior walls and floor).

Figure A5-14 and Table A5-3 show the leakage variation with building pressure for the second test with the exhaust fan off. Backwards flow through the exhaust fan was apparently induced for this case.

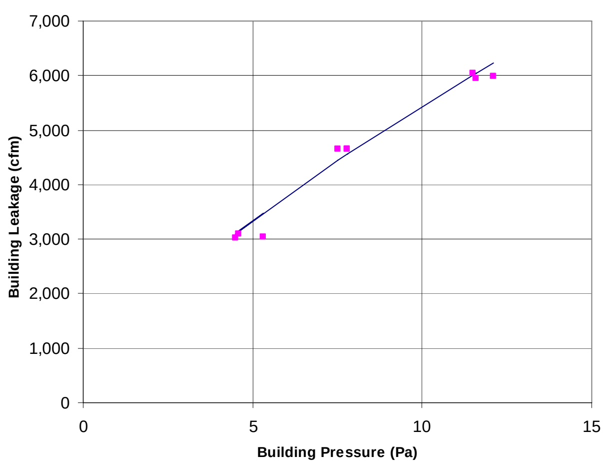

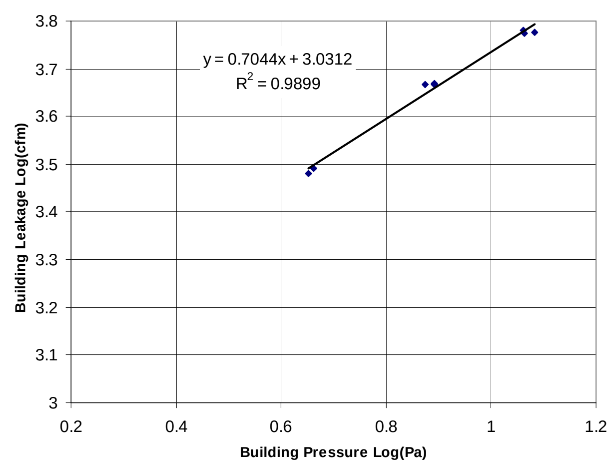

Figure A5-14. Variation of Building Leakage with Pressure: cfm = $K(\Delta P)^n$ (Exhaust Fan Off)

Table A5-3 shows the results of the blower door test 2 with the exhaust fan off. This test resulted in a leakage area of approximately 1.8 sq in per 100 sq ft and an ACH_{50} of 3.9.

Table A5-3. Blower Door Test Data, Resulting Best-Fit Model Coefficients, and ELA (Exhaust Fan Off)

Test Results:

Flow Coefficient (K)	1074.5		17,819	sq ft, floor area
Exponent (n)	0.704			
Leakage area (LBL ELA @ 4 Pa)	808.3	sq in	1.84	ELA / 100 sq ft
Airflow @ 50 Pa	16902.1	cfm	3.94	ACH @ 50

Test Data:

Nominal Building Pressure (Pa)	Nominal Flow (cfm)	Ring
12.1	5,988	none
11.5	6,043	none
11.6	5,957	none
7.8	4,648	none
7.8	4,660	none
7.5	4,656	none
4.5	3,027	none
5.3	3,038	none
4.6	3,098	none

Notes: ELA is leakage area (in square inches) at reference pressure of 4 Pa.
ELA per 100 sq ft is based on total building envelope surface area (ceiling, exterior walls and floor).

Table A5-4. Blower Door Test Summary

Test No.	Test Description	Flow Coeff. K	Exp. n	ELA (sq in)	ELA / 100 sq ft (sq in)	ACH_{50}
1	Men's Exhaust On	740	0.779	618	1.40	3.6
2	Men's Exhaust Off	1,074	0.704	808	1.84	3.9

The total building leakage area for test 1 with the exhaust fan on is 618 in^2 and for test 2 with the exhaust fan off the total leakage area is 808 in^2. The test with the fan operating skewed the results.

Pressure Mapping (Blower Door Testing)

Pressure readings in the building were taken using a digital micromanometer (DG 700) with the blower door operating. The pressure difference across the building envelope was 15 Pa. The arrows on the figure indicate the direction of airflow (and decreasing pressure). Figure A5-15 shows the pressure differences induced across the office and classroom doorways under these circumstances. With the building depressurized to 15 Pa, pressures across the doorways ranged from 0.1 to 0.3 Pa. The relatively small pressure difference between building spaces is considerably less than the overall pressure difference to ambient. This indicates that interior room-room resistance is much smaller than room-exterior resistance (i.e. the building envelope is tight). The garage area is effectively decoupled from the main building.

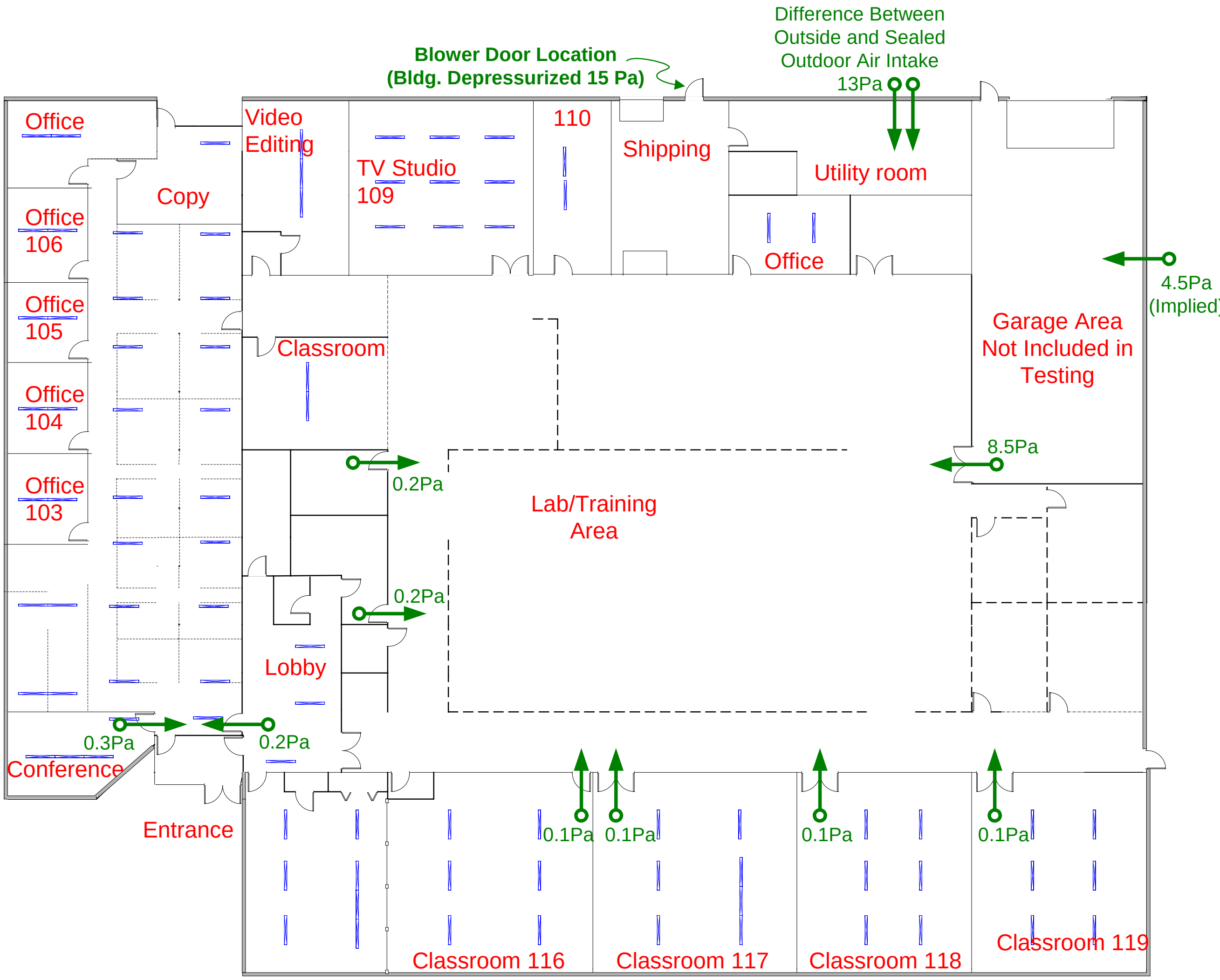

Figure A5-15. Room-to-Room Pressures with Building Depressurized to 15 Pa

HVAC Airflow and Pressure Measurements

The airflow for the VAV system was measured at the unit using the equal area method. Twenty data points were taken resulting in an average velocity of 92 fpm and airflow of 2,971 cfm. If we assume a max airflow of 275 cfm per ton (or 15,125 cfm total supply), the system was at 20% of full flow. The supply and return fan power at this operating condition was 8.8 kW, or 3 Watts per delivered cfm.

Figure A5-16 displays the static pressures throughout the VAV air-handler and the return fan. The positive pressures measured between the VAV unit and the return fan implies no fresh air is being brought into the space. The pressures in square brackets in the Figure A5-16 were taken with the outdoor air intake sealed with Duct Mask plastic wrap. Blocking off the air intake only had a small impact.

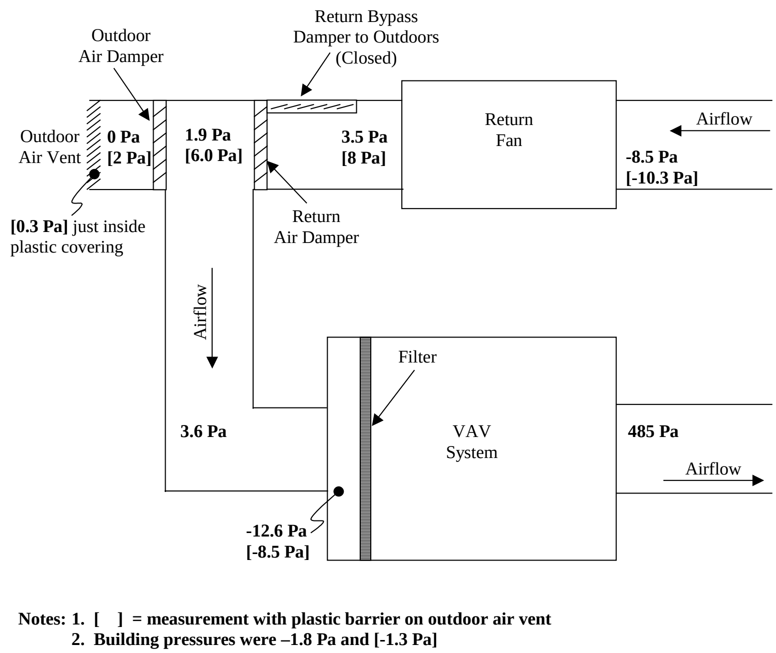

Figure A5-16. VAV System Static Pressures with Respect to Building

Static pressure measurements were also taken at various locations for the constant volume air handler as illustrated in Figure A5-17.

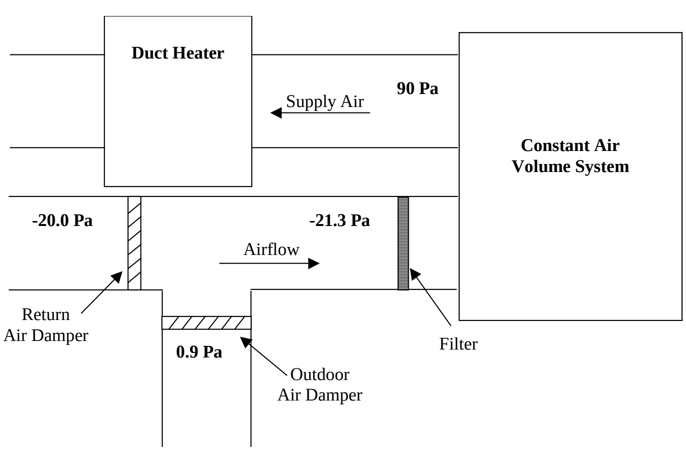

Figure A5-17. Constant Volume System with Static Pressures with Respect to Building

<u>Pressure Mapping (AHU Fans On)</u>

Figure A5-18 displays the pressure readings obtained under normal building conditions. AHUs were running and all exterior doors were closed. Respective interior doors were only closed when measurements were being taken. Interior building pressures ranged from 0.0 Pa to 7.0 Pa. The lavatories have the greatest pressure differences caused by the exhaust fans. The otherwise small range of pressures is an indication that there is little airflow imbalance between interior spaces. With the air-handlers operating normally, the building was depressurized between 1.0 and 1.5 Pa with respect to outdoors.

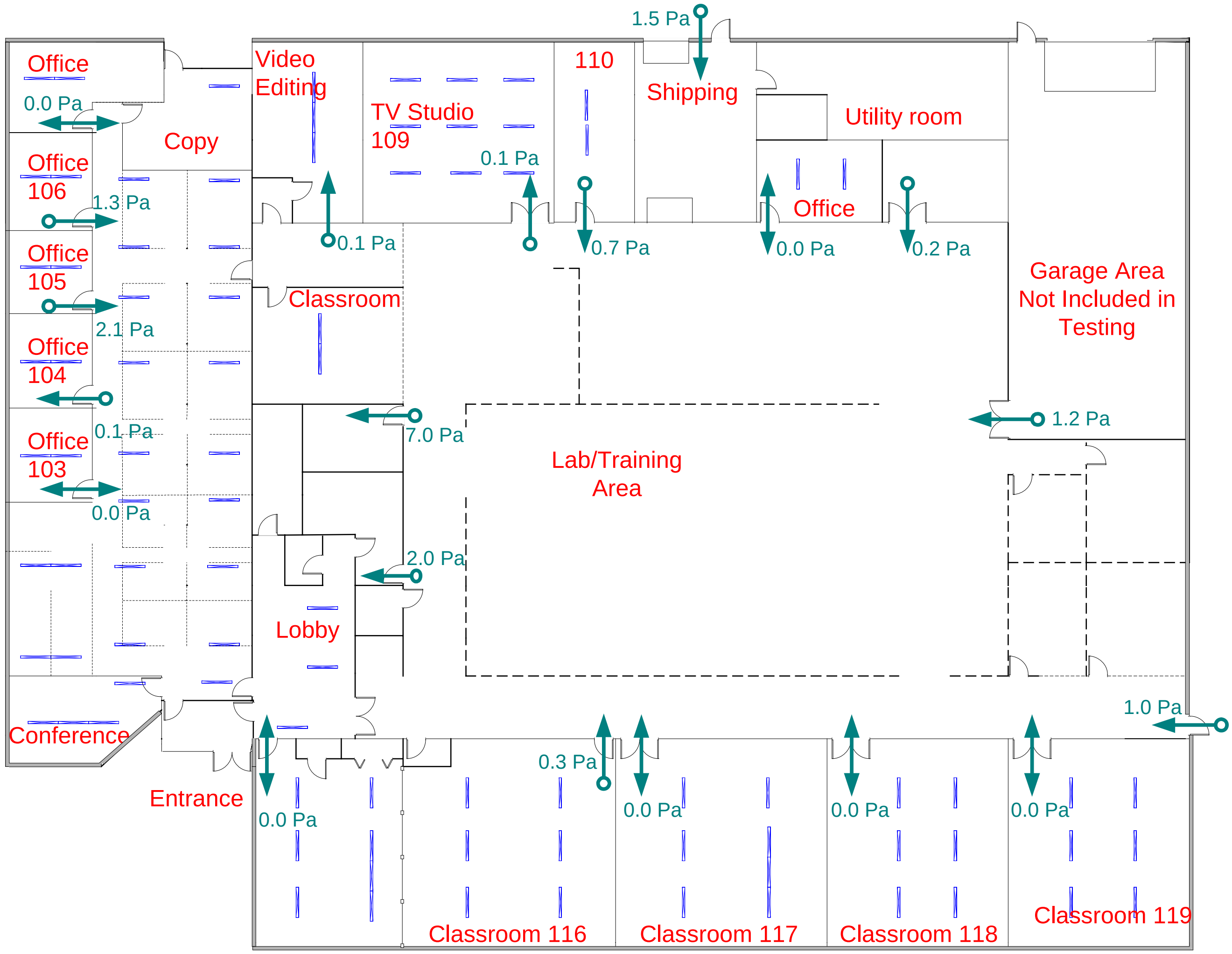

Figure A5-18. Pressure Differences between Rooms with AHU Fans On

Duct Leakage Measurements

The high positioning of the supply ductwork (approx.16 ft.) for the constant volume AHU prohibited duct leakage testing on that unit.

A Duct Blaster was used to depressurize the VAV system supply ductwork to measure leakage rates. Figure A5-19 shows how the Duct Blaster fan was connected to depressurize the AHU cabinet and supply ductwork. The static duct pressure tap was connected in the supply duct. Plastic wrap was used to cover each supply diffuser in the system. The return air and fresh air intake were isolated by sealing off their path into the AHU.

Due to the design and positioning of the diffusers, completely sealing the linear diffusers was not feasible. With the exception of the nine open diffusers in the TV studio, all diffusers were positioned flush with the drop ceilings. Figure A5-9 includes a picture of one diffuser in the TV studio standing alone. Figure A5-9 shows that this design allows a small amount of air to escape through the tabbed openings on the end. Under normal operating conditions, air leakage into the plenum space is insignificant.

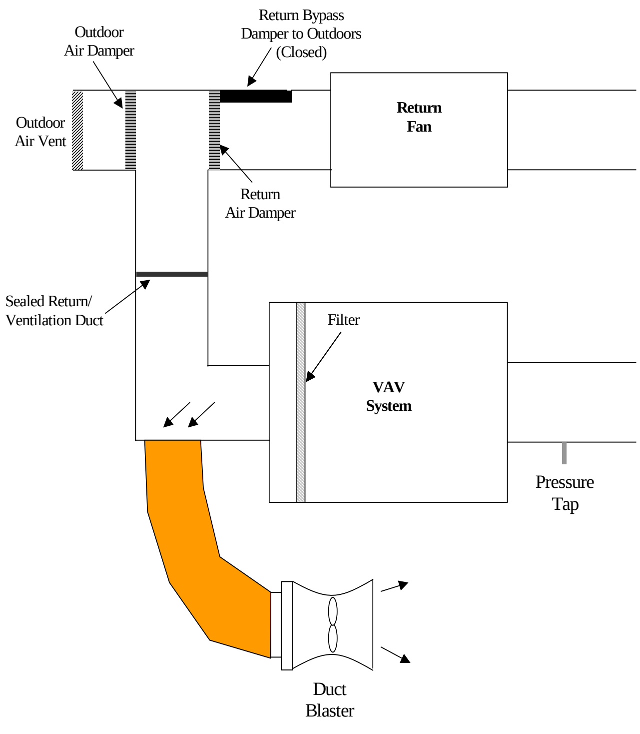

Duct blaster connected to VAV System for depressurization

Figure A5-19. Duct Blaster Set Up for Testing

Figure A5-20 shows the resulting measured data from the duct leakage test fit to a power function (raw data in Table A5-5).

Table A5-6 shows the resulting coefficients, exponents, and regression statistics. Table A5-7 summarizes the resulting duct leakage rates and ELA at a reference pressure of 25 Pa.

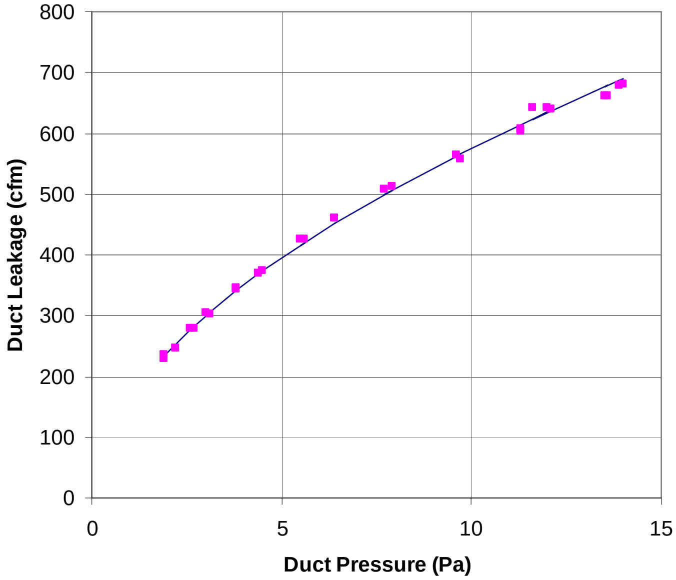

Figure A5-20. Duct-Blaster Tests on VAV System Supply Ductwork and Cabinet

Table A5-5. Raw Data from Duct-Blaster Tests

Test Results:

Flow Coefficient (K)	165.1
Exponent (n)	0.542
Leakage area (LBL ELA @ 25 Pa)	107 sq in
Airflow @ 25 Pa	946.0 cfm

Test Data:

	Nominal Duct Pressure (Pa)	Nominal Flow (cfm)	Ring
1	14.0	682	1
2	13.9	680	1
3	13.5	661	1
4	13.6	662	1
5	11.6	642	1
6	12.0	642	1
7	12.1	640	1
8	11.3	607	1
9	11.3	603	1
10	9.7	558	1
11	9.6	565	1
12	7.7	509	1
13	7.9	512	1
14	6.4	461	1
15	6.4	461	1
16	5.5	425	1
17	5.6	427	1
18	4.4	370	1
19	4.5	375	1
20	3.8	343	1
21	3.8	347	1
22	3.0	305	1
23	3.1	302	1
24	2.6	279	1
25	2.7	279	1
26	2.2	247	1
27	2.2	246	1
28	1.9	230	1
29	1.9	235	1

Table A5-6. Coefficients, Exponents and Regression Statistics from Duct-Blaster Tests

	Supply & AHU Cabinet		
	K	n	R^2
VAV System	165.1	0.542	99.79%

Notes: cfm = $K(Pa)^n$ / R^2 indicates fit of linear log-log regression

Table A5-7. Comparison of Supply and Return Airflow Measurements

	Total Supply Diffuser Airflow (cfm)	Total Leakage (cfm @ 25)	Supply & AHU ELA (sq in @ 25)
VAV System	2,971	946	107

Notes: Leakage and ELA at reference pressure of 25 Pa

The effective leakage area compared to the total duct surface area is shown in Table A5-8. For every 100 sq-ft of duct surface area, there is approximately 3.6 sq-in of duct leakage at 25 Pa. The Sheet Metal and Air Conditioning Contractors' National Association (SMACNA) classifies duct leakiness using duct leakage per 100 sq ft of duct area at a pressure of 1-in w.g. The SMACNA leakage class for the VAV duct system is 112.

Table A5-8. Duct Leakage Characteristics

	Duct Area (sq ft)	ELA (sq in @ 25)	ELA/100 sq ft Duct Area (sq in @ 25)	Leakage (cfm @ 25 Pa)	Supply CFM per Duct Area (cfm/ sq-ft)	Leakage per 100 sq ft Duct Area (cfm @ 25 Pa)	SMACNA Leakage Class cfm per 100 sq ft (cfm @ 1-in water)
Supply & AHU Cabinet	2,941	107	3.6	946	1.01	32	112

A sample of static pressures were taken at various linear diffusers with the supply ducts depressurized 14 Pa at the VAV air-handler. The results are shown below in Table A5-9. The modest pressures measured at the diffusers imply that the bladder is in each diffuser to restrict the flow.

Table A5-9. Static Pressure at Linear Diffuser with Ducts Depressurized 14 Pa

Diffuser Location	Pressure (Pa)
Office 103	-0.2
Sm. Isolated classroom	-0.4
Classroom #117	-1.4
Middle diffuser in Lobby	-2.9

Space Conditions

Figure A5-21 shows the average temperature profiles based on temperature readings taken with a HOBO data logger from June 4 to June 18, 2004. The thick line shows the average for each hour while the shaded region corresponds to one standard deviation about the average. The dotted lines correspond to the minimum and maximum for each hour. Sensors were placed in the training area, classroom 118, and the office area (across from office 104). The temperature profiles show that the temperature is maintained throughout the nights and weekends.

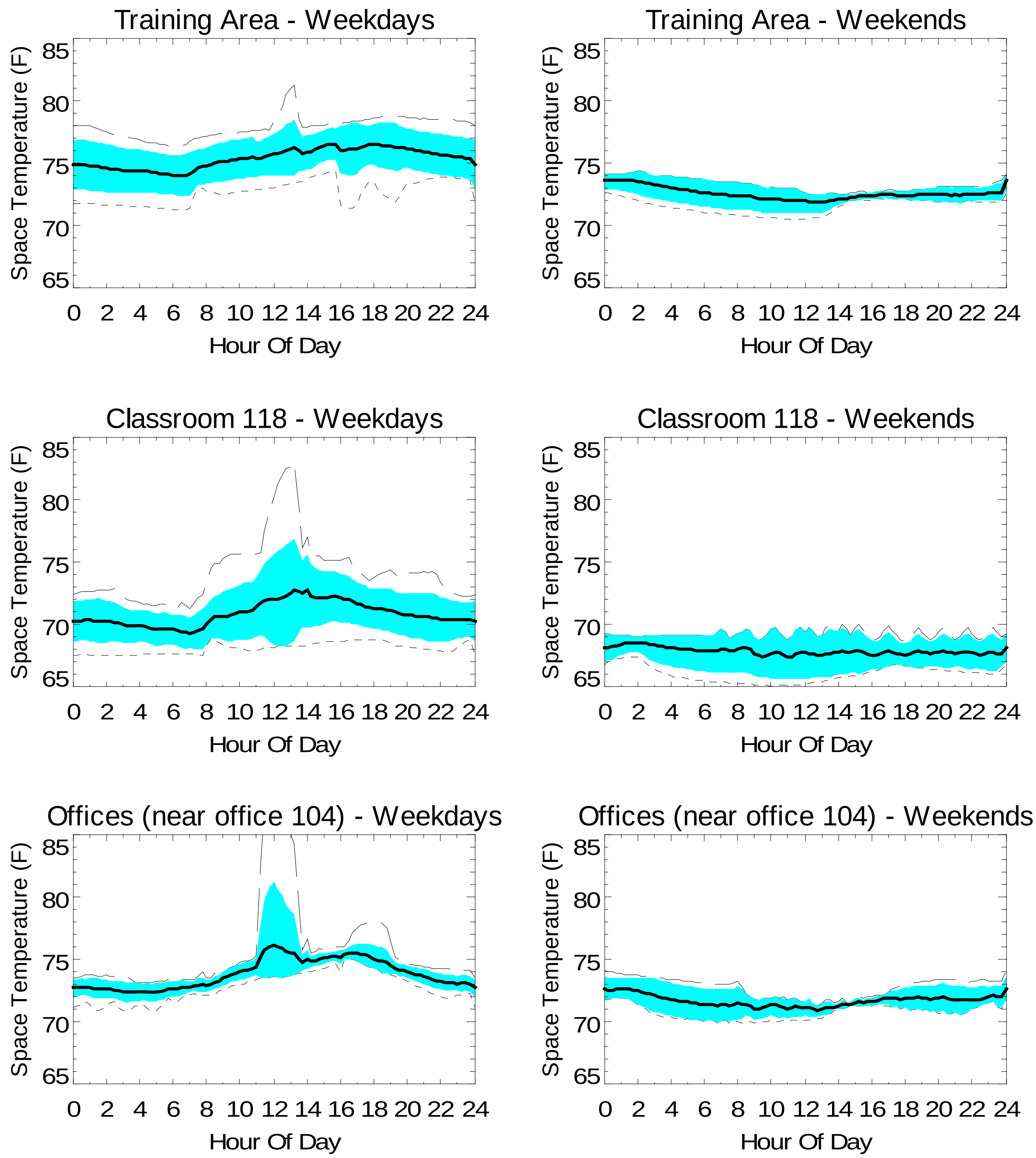

Figure A5-21. Measured Space Temperature Profiles (June 4 to June 18, 2004)

Figure A5-22 shows the CO_2 concentration in various locations in the building. The CO_2 concentration provides an indication of occupancy. The next section uses the CO_2 as a tracer gas to estimate the infiltration/ventilation rate into the building.

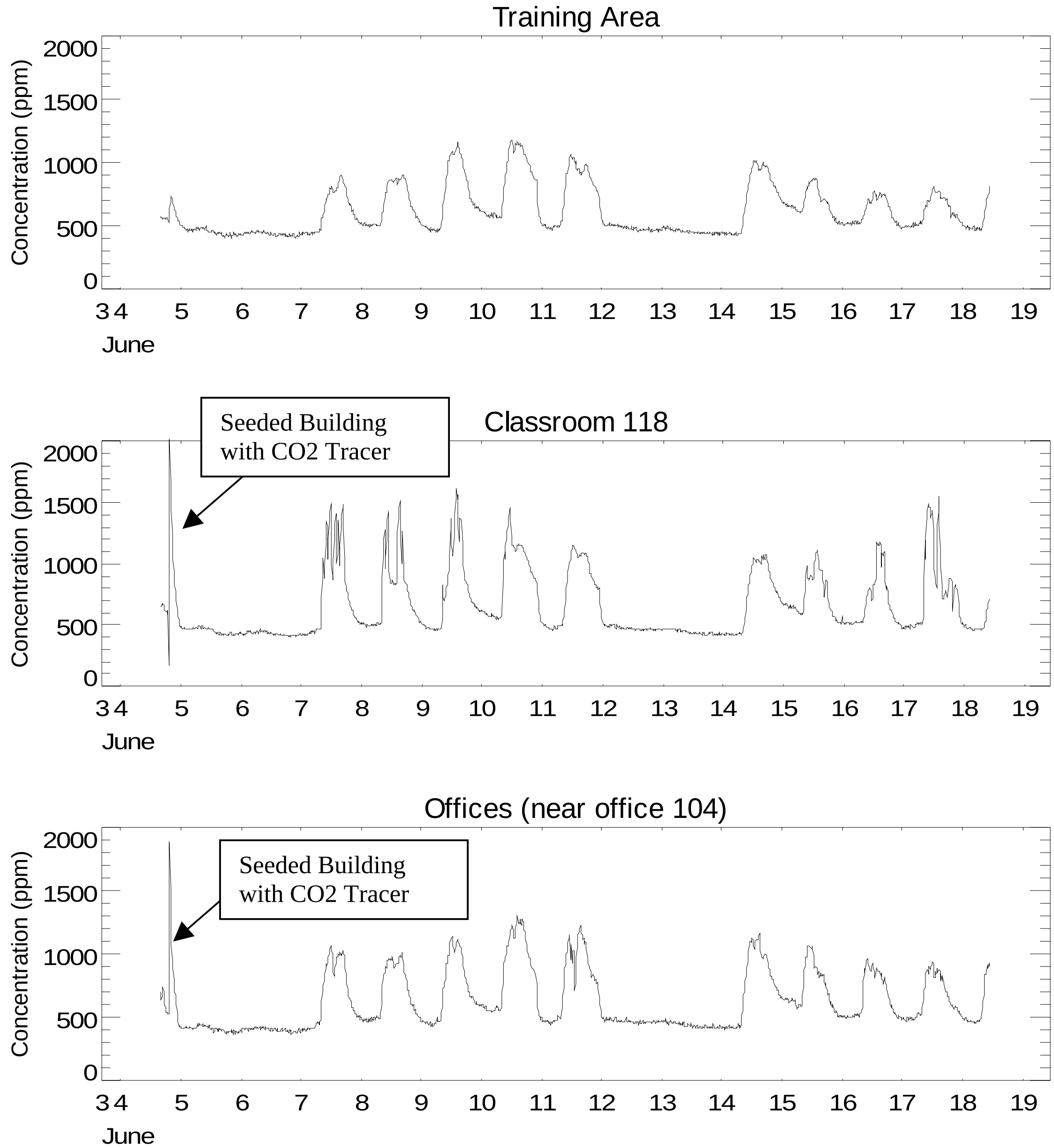

Figure A5-22. Measured CO_2 Concentration in Various Spaces (June 4 to June 18, 2004)

The following plots show the relative humidity for this building. The building did not exceed 60% relative humidity in the monitored areas for the entire monitoring period. Figure A5-26 displays the conditions inside the building compared with the ASHRAE comfort zone for cooling shown by the shaded region on the plot.

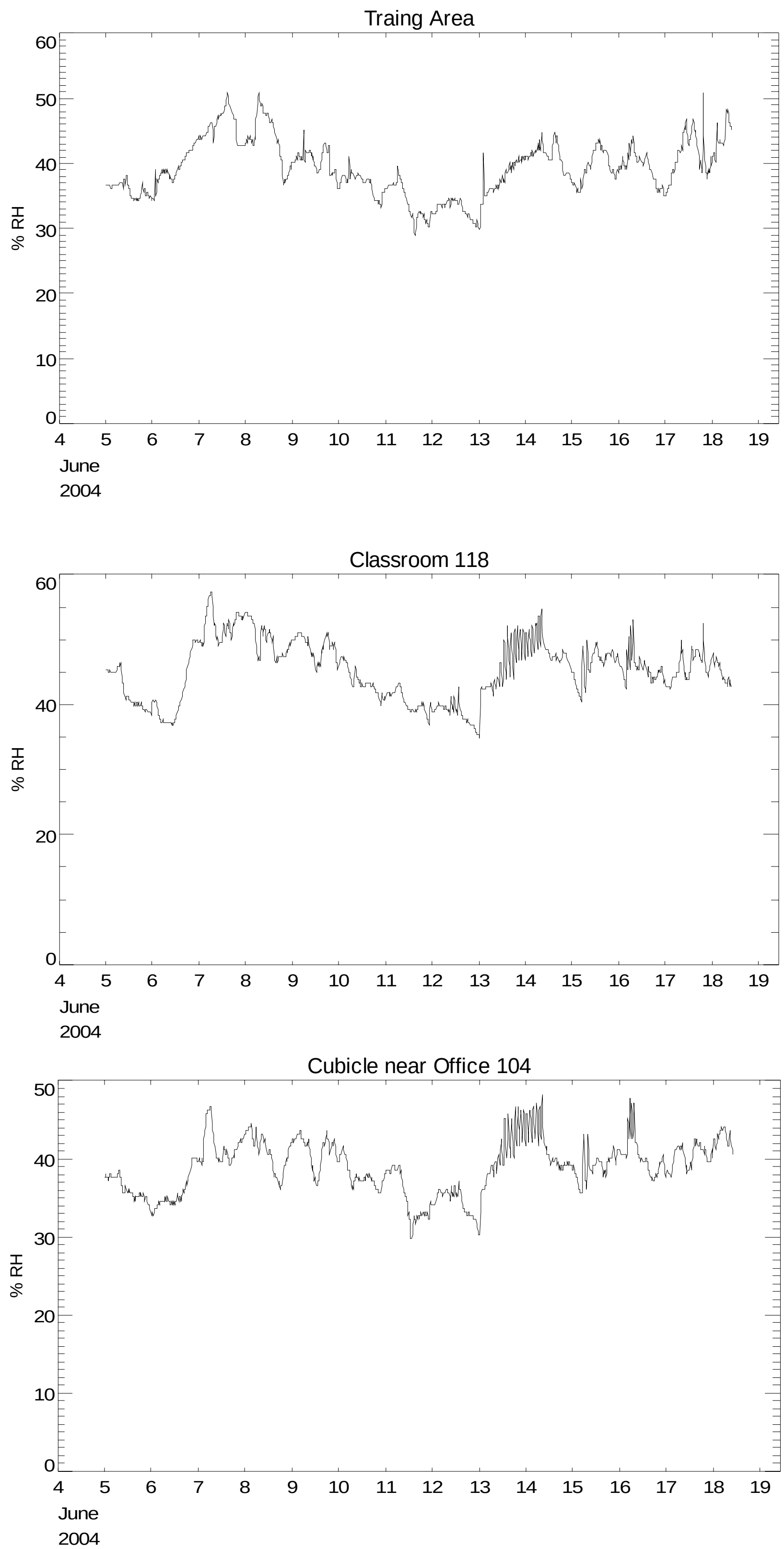

Figure A5-23. Measured Relative Humidity

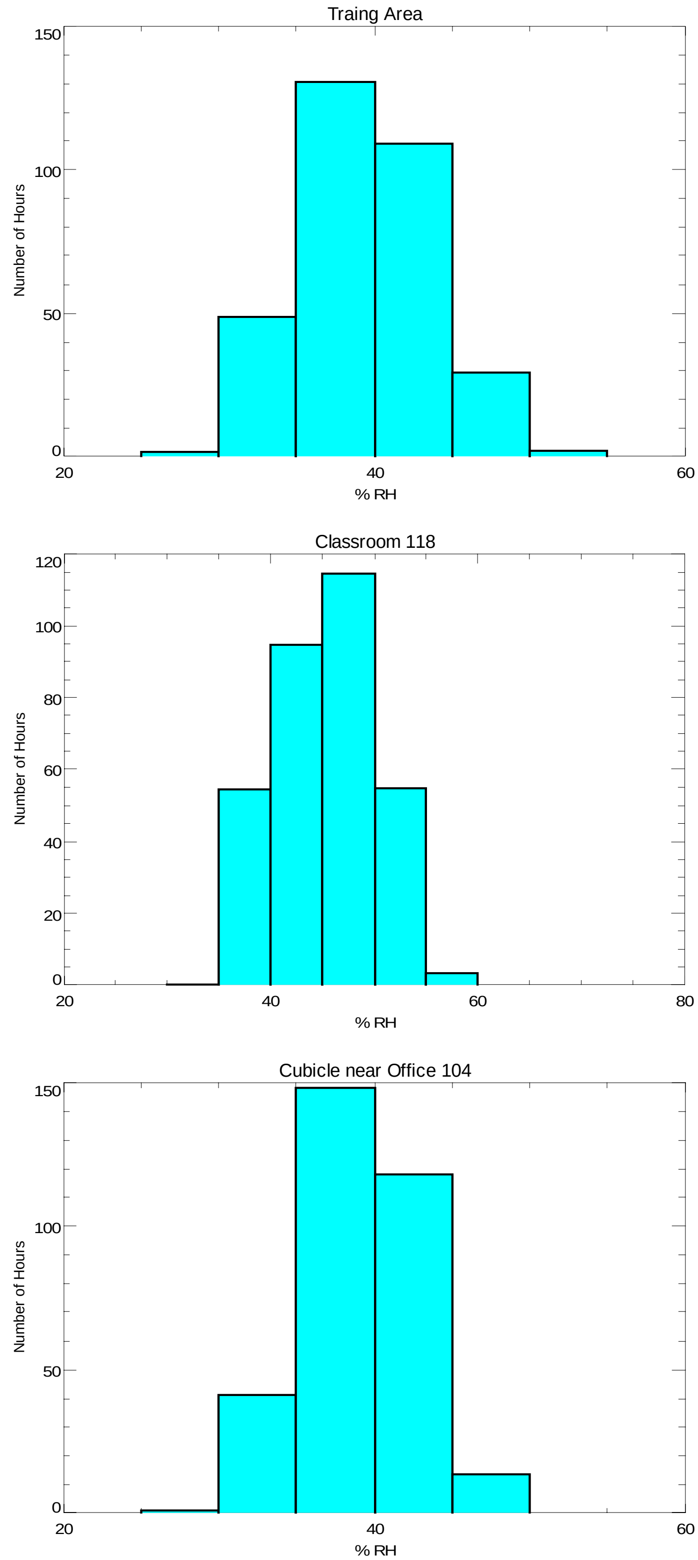

Figure A5-24. Duration of Relative Humidity Levels

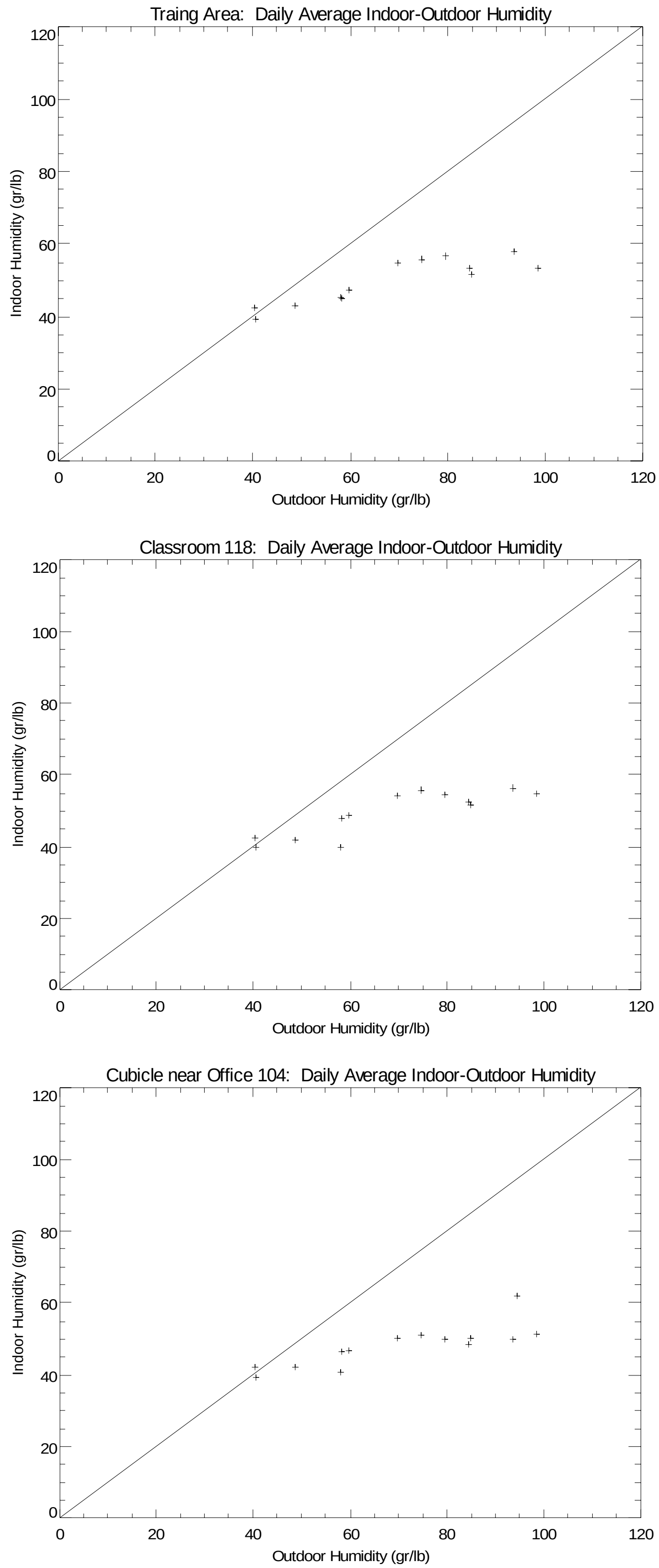

Figure A5-25. Indoor Humidity Variation with Outdoor Humidity

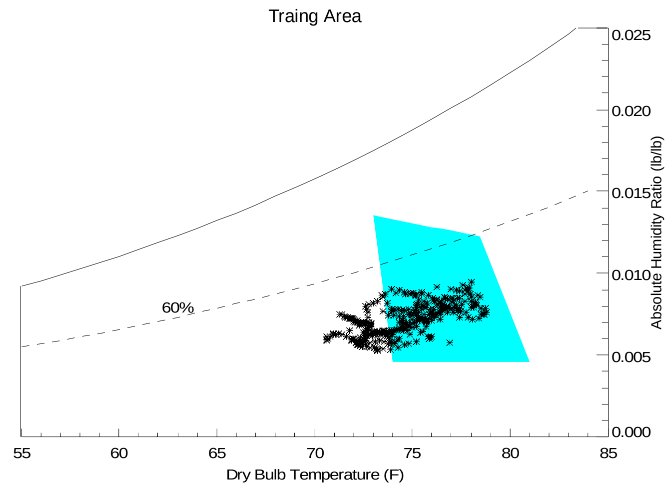

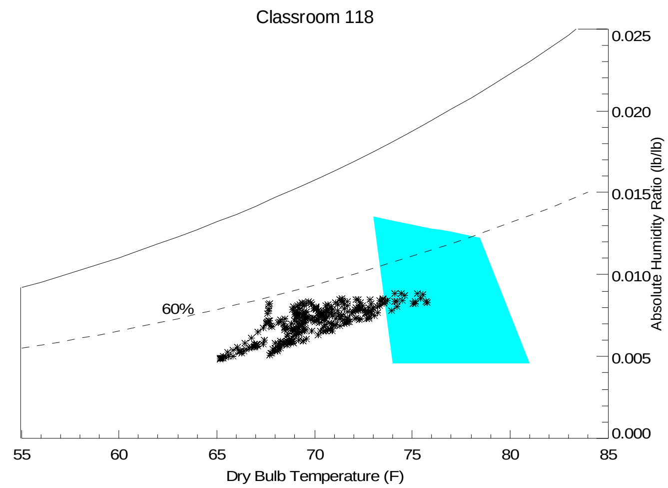

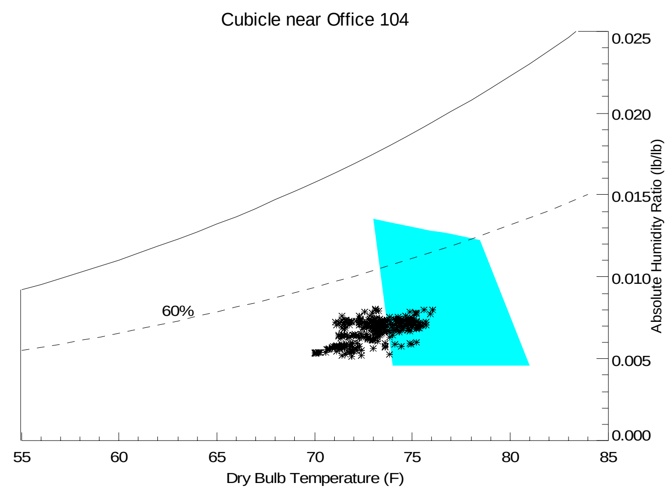

Figure A5-26. Indoor Air Quality Comparison with ASHRAE Comfort Zone for Cooling

Infiltration Estimate from CO_2 Decay

Figure A5-27, Figure A5-28, and Figure A5-29 show the resulting decay trends using CO_2 levels immediately after high occupancy periods for the lab/training, classroom, and office space areas of the building. The predicted air change rate (ACH) is shown on each plot.

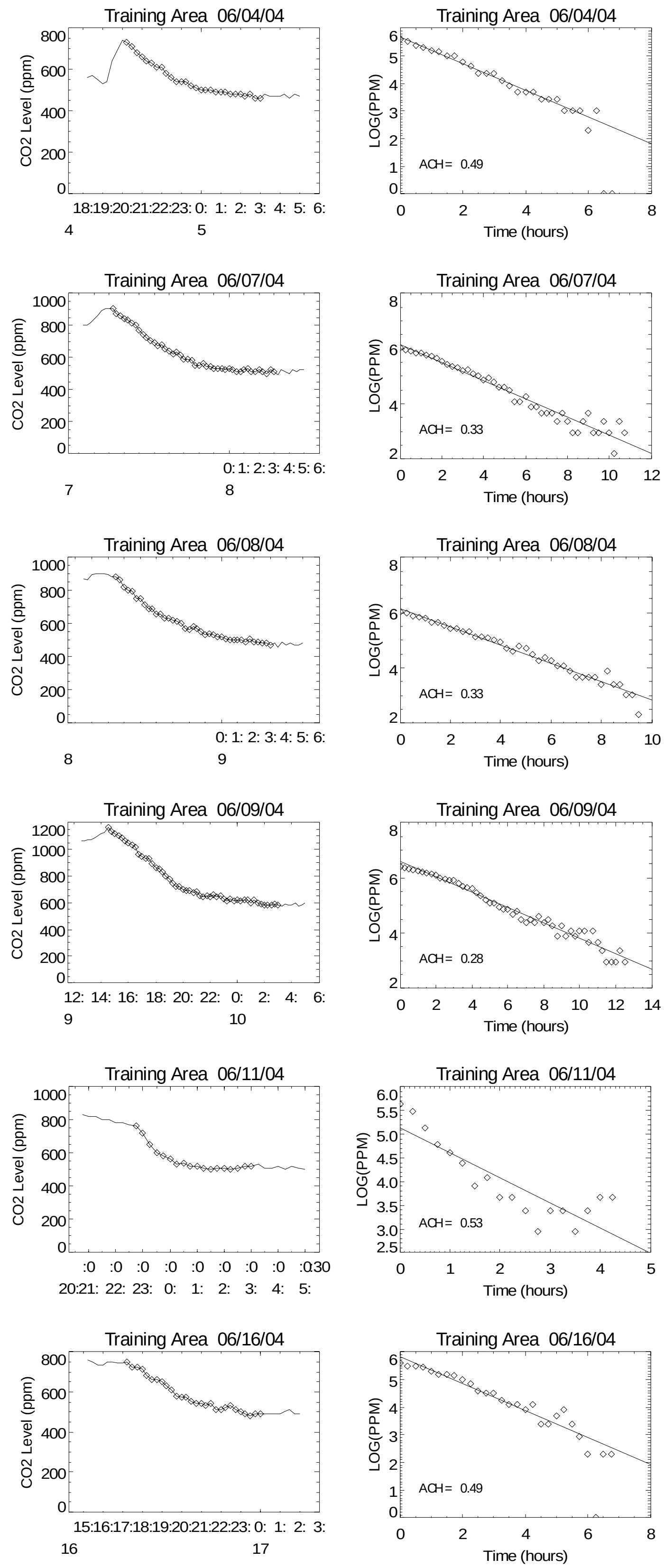

Figure A5-27. Lab/Training Area: Tracer Gas Decay Using CO_2

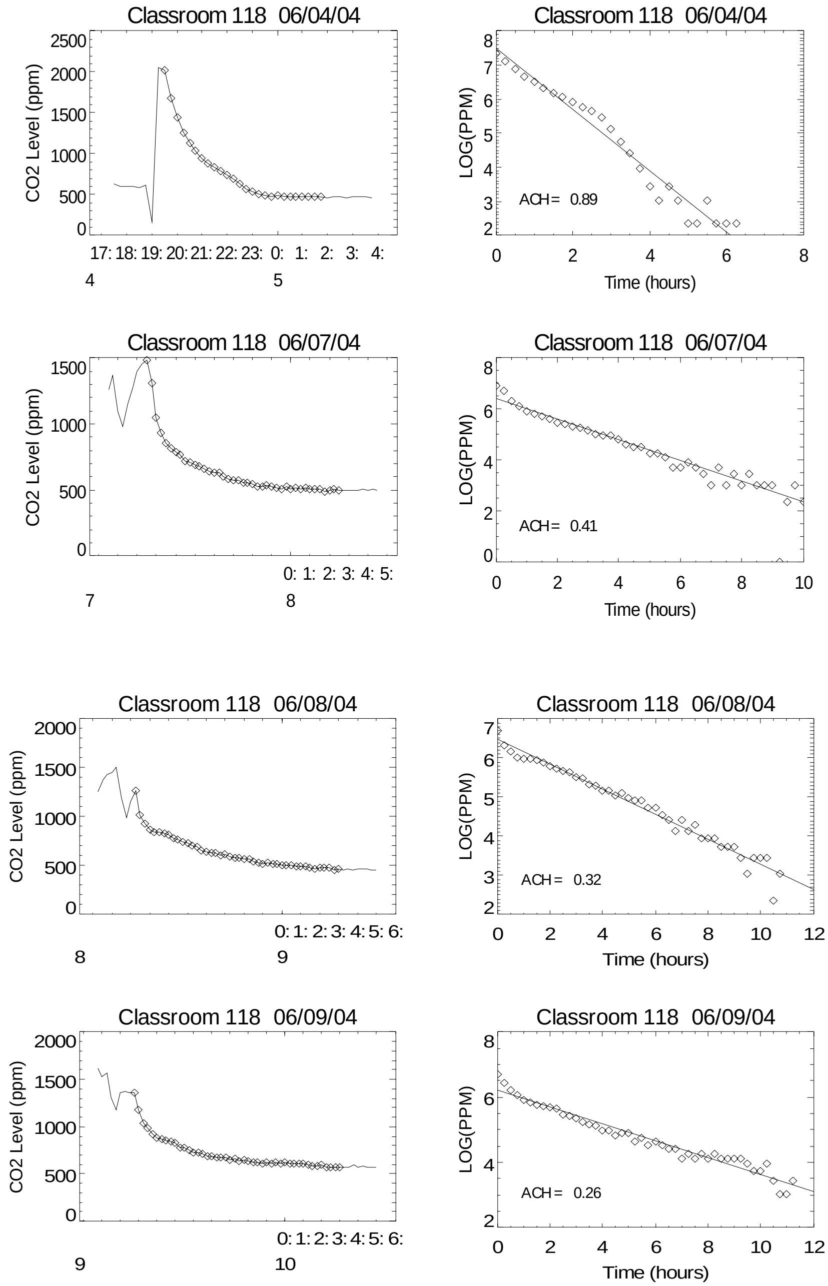

Figure A5-28. Classroom 118: Tracer Gas Decay Using CO_2

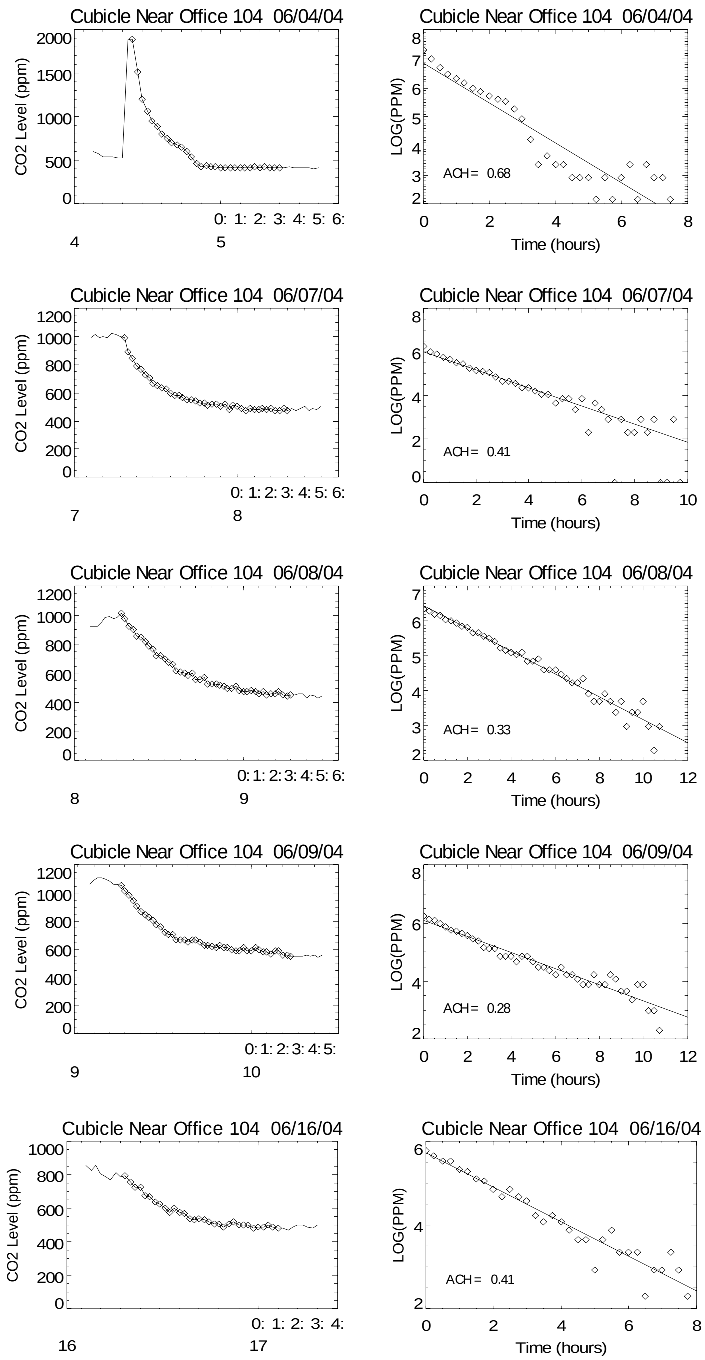

Figure A5-29. Cubical near Office 104: Tracer Gas Decay Using CO_2

Table A5-10 summarizes the results of the tracer gas decay tests in the plots above. The table also includes the calculated infiltration flow rate (cfm) based on the volume of the building.

Table A5-10. Summary of Tracer Gas Decay Tests

Lab/Training Area

Start Time	End Time	ACH	Flow (cfm)
04-Jun 08:15 PM	05-Jun 03:00 AM	0.49	2,291
07-Jun 04:15 PM	08-Jun 03:00 AM	0.33	1,543
08-Jun 05:30 PM	09-Jun 03:00 AM	0.33	1,543
09-Jun 02:30 PM	10-Jun 03:00 AM	0.28	1,309
11-Jun 10:45 PM	12-Jun 03:00 AM	0.53	2,478
17-Jun 05:15 PM	18-Jun 12:00 AM	0.49	2,291

Classroom 118

Start Time	End Time	ACH	Flow (cfm)
04-Jun 07:30 PM	05-Jun 01:45 AM	0.89	4,160
07-Jun 04:30 PM	08-Jun 02:30 AM	0.41	1,917
08-Jun 03:15 PM	09-Jun 03:00 AM	0.32	1,496
09-Jun 01:45 PM	10-Jun 03:00 AM	0.27	1,262
16-Jun 04:15 PM	17-Jun 01:00 AM	0.45	2,104

Office Space

Start Time	End Time	ACH	Flow (cfm)
04-Jun 07:30 PM	05-Jun 03:00 AM	0.68	3,179
07-Jun 05:15 PM	08-Jun 03:00 AM	0.41	1,917
08-Jun 04:15 PM	09-Jun 03:00 AM	0.33	1,543
09-Jun 03:45 PM	10-Jun 02:30 AM	0.28	1,309
10-Jun 09:45 PM	11-Jun 03:00 AM	0.53	2,478
16-Jun 05:15 PM	17-Jun 01:00 AM	0.41	1,917

Note: Flow determined with building volume of
280,480 ft^3

In comparison to the ACH values above, the nominal leakage rate (defined as ACH_{50} divided by 20) from the blower door test above is 0.2 ACH.

Utility Bills

Electricity is primarily used for space heating and air conditioning. The constant volume system heats using a relatively new gas-fired duct heater. Before the installation of this duct heater, the only source of heat in the facility was electric baseboard. The tables and graphs below show the gas and electric use trends for the facility. The overall energy use index for the building is summarized below.

	Heating Energy Use Index (MBtu/ft^2-year)	Electric Use Index (kWh/ft^2-year)
2003-2004 Season	26.4	29.7

Note: Season is from 6/03 to 5/04 for gas data and from 1/03 to 5/04 for electric data

Table A5-11. Summary of Gas Bills

	Days in Month	Gas Use (therms)	Cost ($)	$/therm	Gas Use per Sq-Ft (therm/sq ft)
6/19/2003	27	40	64.43	1.61	0.002
7/24/2003	35	12	32.21	2.68	0.001
8/20/2003	27	15	33.40	2.23	0.001
9/23/2003	34	22	41.16	1.87	0.001
10/22/2003	29	223	240.61	1.08	0.012
11/20/2003	29	550	532.20	0.97	0.031
12/22/2003	32	1,062	986.50	0.93	0.059
1/23/2004	32	1,499	1455.42	0.97	0.083
2/23/2004	31	712	726.06	1.02	0.040
3/23/2004	29	133	372.86	2.80	0.007
4/23/2004	31	355	374.00	1.05	0.020
5/21/2004	28	109	137.85	1.26	0.006
2003-2004	364	4,732	$ 4,997	1.06	0.263

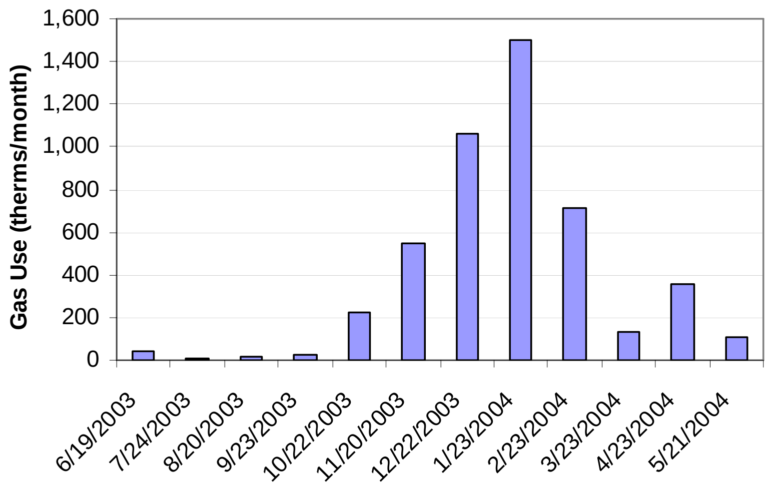

Figure A5-30. Monthly Gas Use Trend

Table A5-12. Summary of Electric Bills

	Days in Month	Energy (kWh)	Cost ($)	$/kWh	Elec. Use per Sq-Ft (kWh/sq ft)
1/23/2003	35	62,000	6,718.47	0.11	3.44
2/21/2003	29	56,240	6,980.04	0.12	3.12
3/24/2003	31	49,760	7,108.75	0.14	2.76
4/22/2003	29	36,080	4,819.77	0.13	2.00
5/23/2003	31	34,240	4,611.55	0.13	1.90
6/23/2003	31	33,120	4,226.21	0.13	1.84
7/24/2003	31	34,000	4,702.24	0.14	1.89
8/20/2003	27	28,400	3,967.18	0.14	1.58
9/23/2003	34	34,880	4,425.70	0.13	1.94
10/22/2003	29	36,800	5,739.43	0.16	2.04
11/20/2003	29	54,800	6,784.10	0.12	3.04
12/22/2003	32	67,360	7,869.44	0.12	3.74
1/23/2004	32	66,560	8,233.48	0.12	3.70
2/23/2004	31	52,560	6,852.84	0.13	2.92
3/23/2004	29	45,680	5,716.28	0.13	2.54
4/23/2004	31	39,600	5,310.54	0.13	2.20
5/21/2004	28	27,840	4,097.02	0.15	1.55
2003-2004	519	759,920	$ 98,163	0.13	42.22

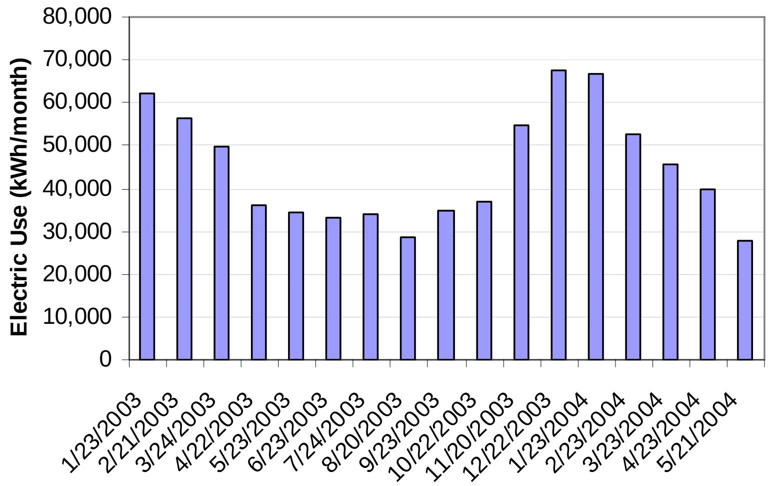

Figure A5-31. Monthly Electric Use Trend

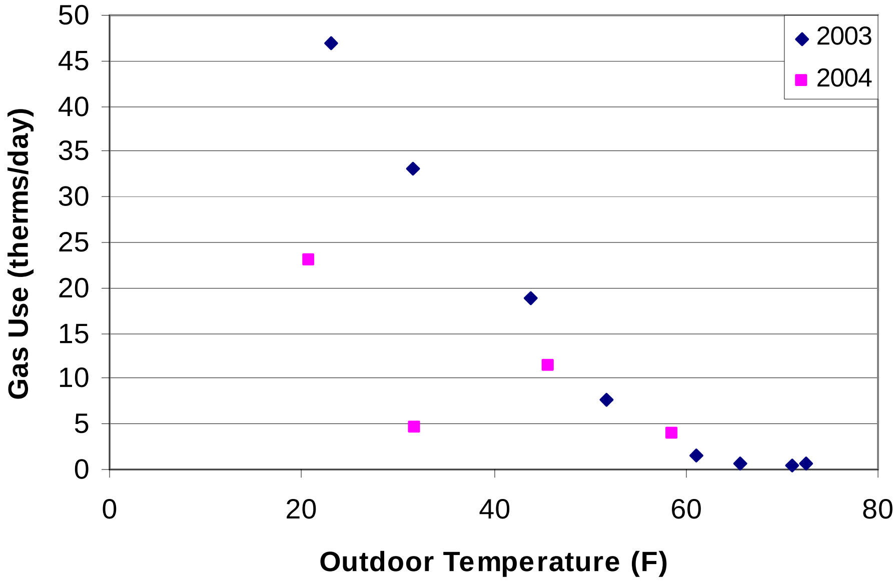

Figure A5-32. Variation of Gas Use with Ambient Temperature

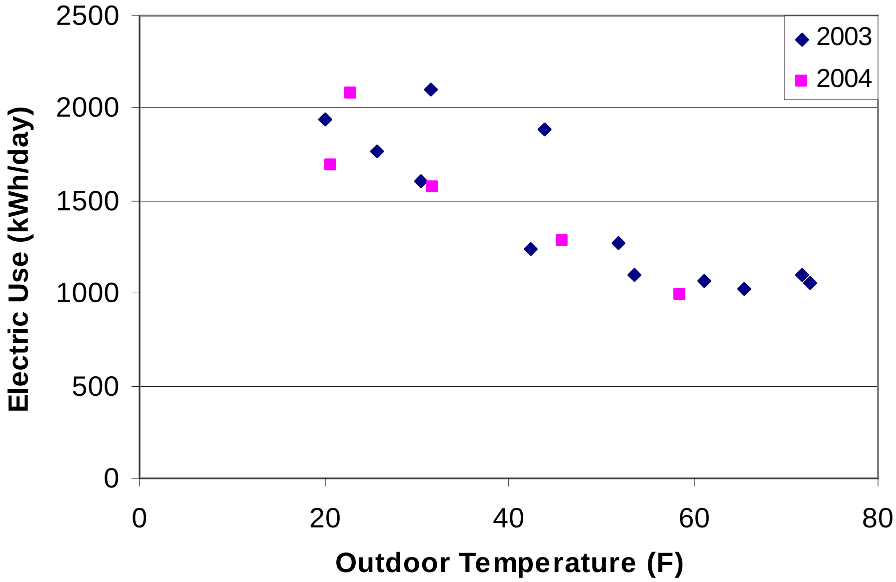

Figure A5-33. Variation of Electric Use with Ambient Temperature

Field Test Site 6 – Supermarket on Long Island, Hauppauge, NY

Front of Building (Southwest)

Figure A6-1. Photos of Building

CHARACTERISTICS

Building Description

The 57,000 sq ft facility is a one-story supermarket that was completely gutted to the block walls, expanded, and rebuilt in 2002. Figure A6-1 shows the front of the building. The store is heated and cooled with one large Munters unit and six smaller Carrier roof top units (RTU). The Munters unit serves the sales area (approx. 68% of store) and the Carrier RTUs serve individual spaces in the store such as the pharmacy. All roof top units are forced-air, gas-fired units with direct expansion (DX) cooling coils. All seven units provide ventilation to the store. In addition to the ventilation provided by the seven RTUs, a stand-alone ventilation fan (MAU-1) provides 1494 cfm of fresh are to the deli exhaust hood to reduce depressurization when the 4200 cfm deli exhaust fan is operating. There are eight roof exhaust fans. Figure A6-2 presents the building floor plan

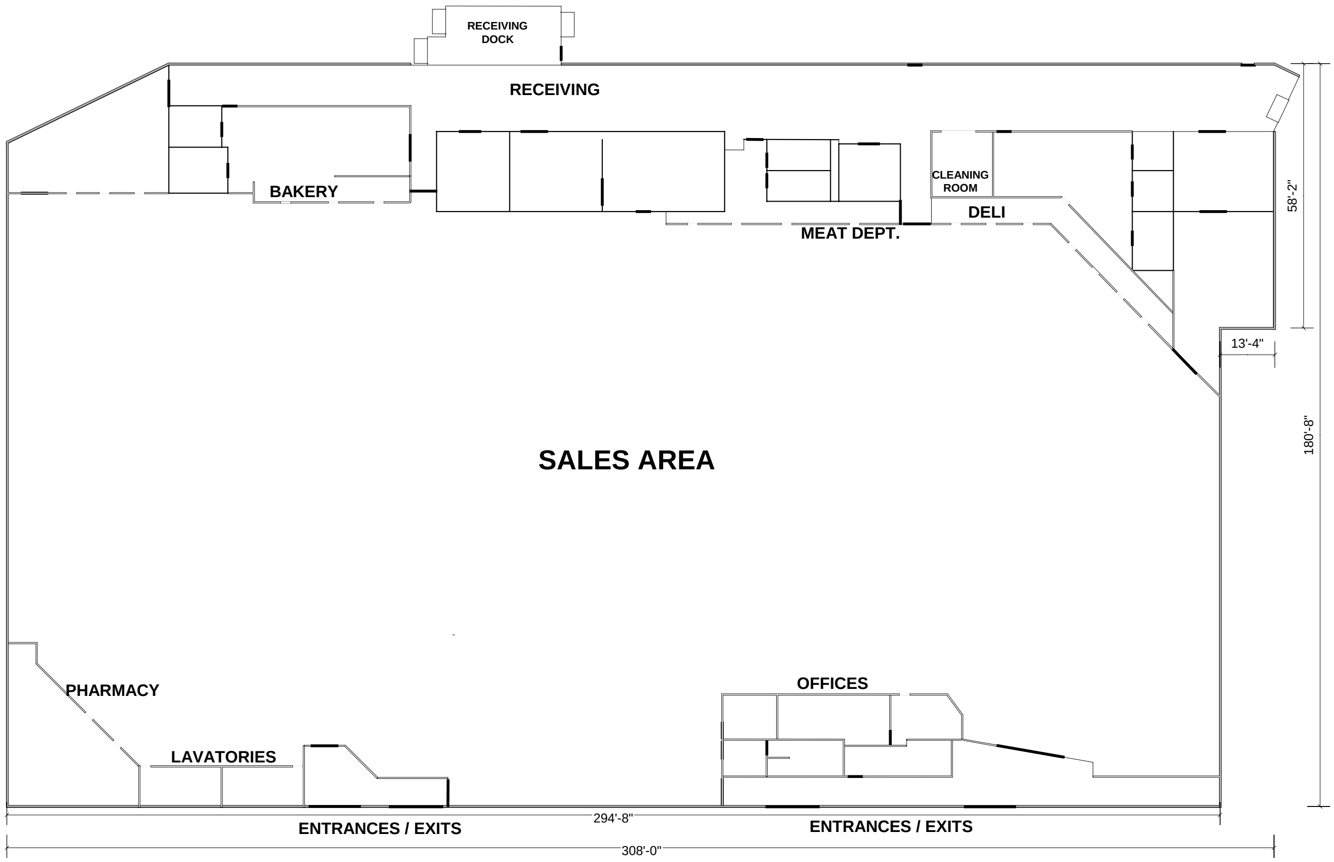

Figure A6-2. Building Floor Plan

Construction Details

The exterior walls on the front of the building are constructed of 8-in concrete block with KOR-Fill insulation, 4-in air space, 4-in brick veneer on the exterior and 3-in furring strips on the interior with 5/8” gypsum board. The upper 6.5 ft of the front exterior walls are 6-in metal stud walls with 6-in fiberglass batt insulation, 3-5/8” air gap, 5/8” dense glass with a synthetic stucco exterior finish. The exterior walls on the sides and rear of the building are constructed of 12-in concrete block with ICON insulation and 1-5/8” metal stud walls on the interior with 5/8” gypsum board.

The store has a flat roof constructed of sheet metal roof decking with 4-in rigid roof insulation and a 4-ply built-up roof. Most of the store has a suspended T-bar (drop) ceiling (approximately 4’-4” below the metal roof deck in the sales area). The store does not have a drop ceiling in the receiving area or in the in the sales area from the deli forward.

Figure A6-3 illustrates typical wall and roof sections for the front of the building and Figure A6-4 shows the sections for the sides and rear of the building.

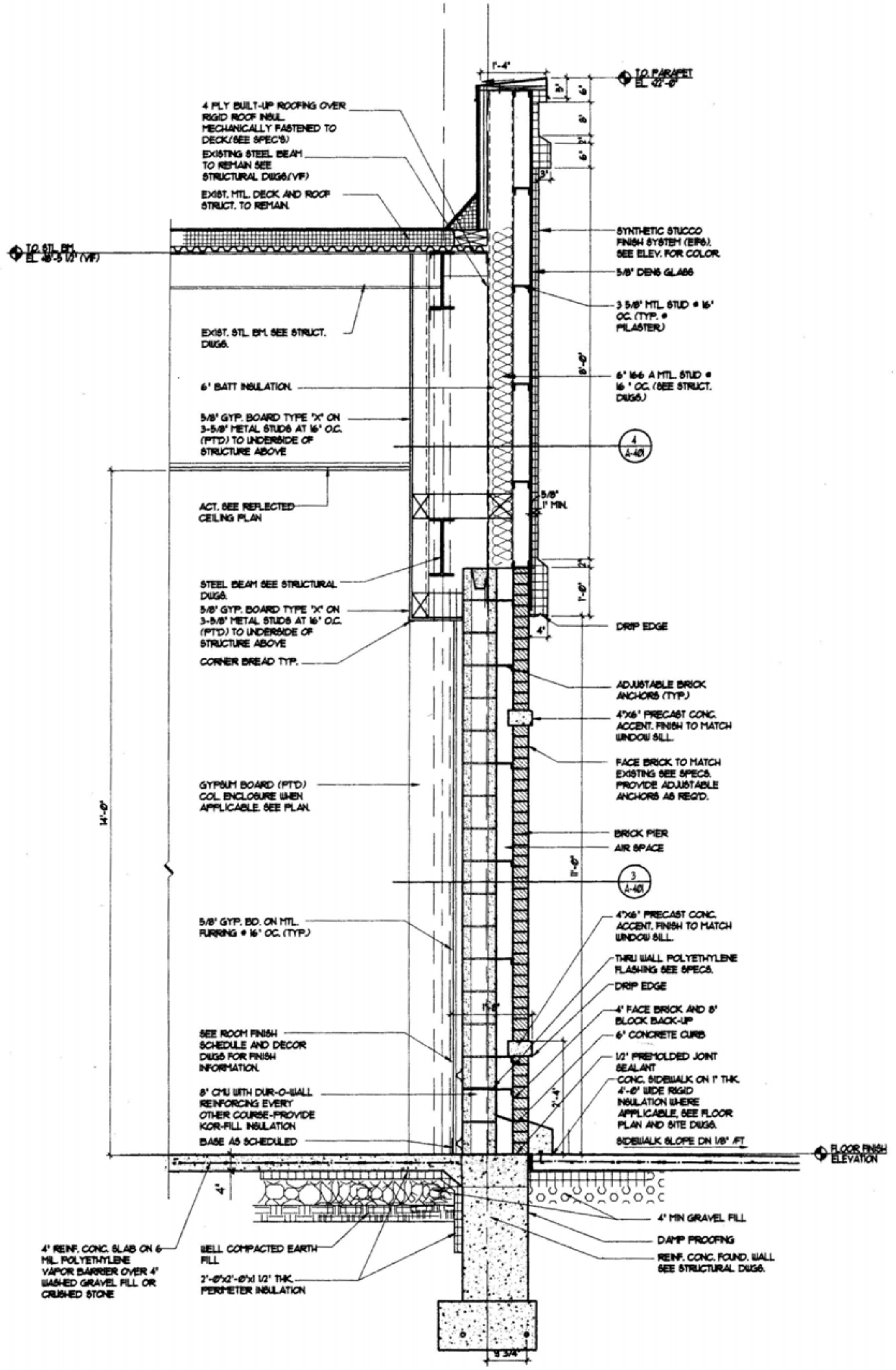

Figure A6-3. Roof and Wall Sections for the Front of the Building

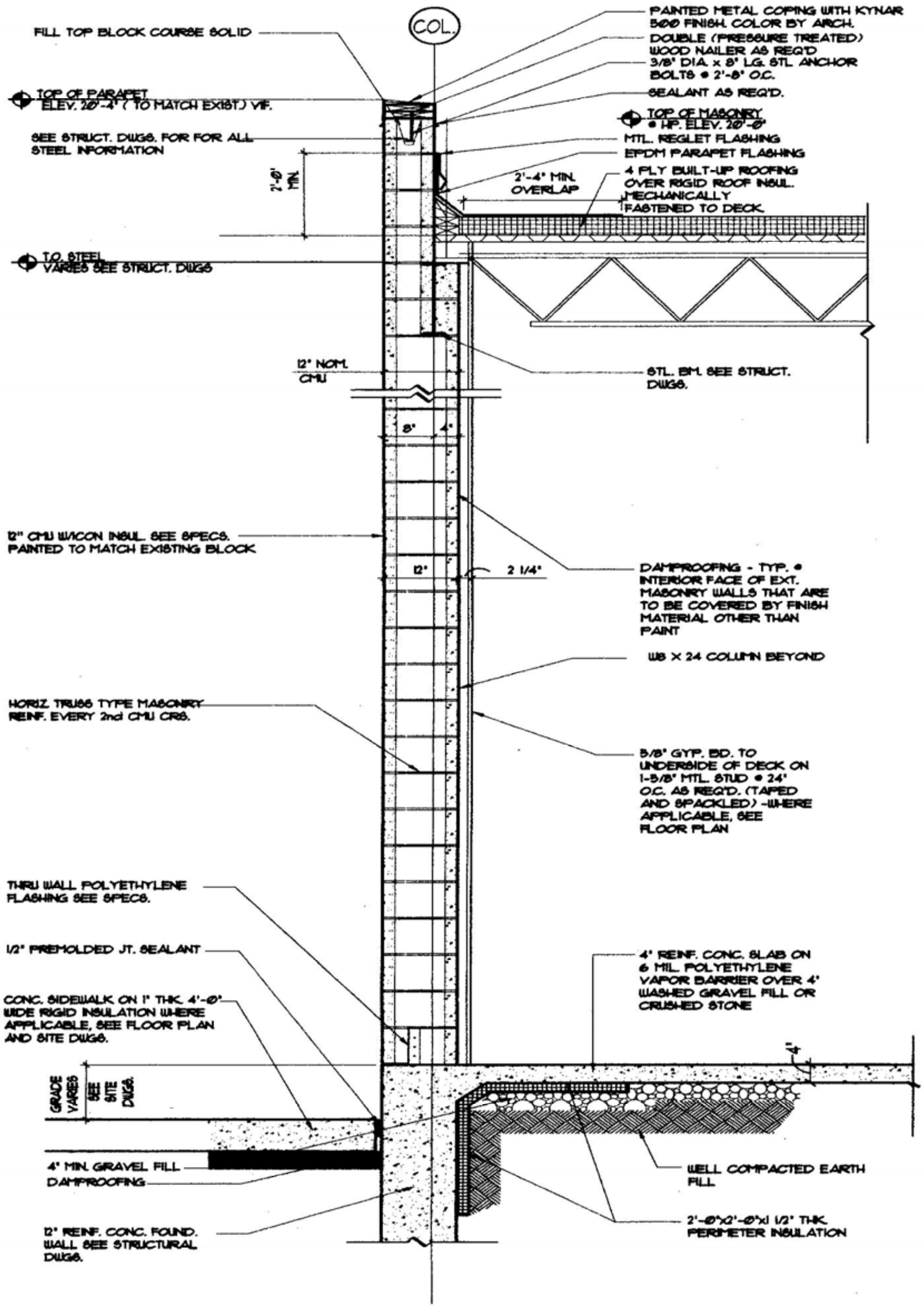

1 Typical Wall Section
SCALE:3/4" = 1'-0"

Figure A6-4. Roof and Wall Sections for the Sides and Rear of the Building

HVAC System

One Munters unit and six roof top units condition the building. Figure A6-5 shows the Munters unit, the two models of Carrier RTUs, and the make-up-air unit (MAU). Figure A6-6 shows the typical down blast and up blast exhaust fans. Figure A6-7 illustrates the locations of the HVAC equipment along with the ductwork that shows the various departments of the store served by this equipment. Table A6-1 lists the HVAC equipment that serves the building, Table A6-2 lists the roof exhaust fans, and Table A6-3 summarizes the equipment sizing.

All seven of the RTUs and the MAU provide ventilation; however we were on site (July 9, 2004) and only four of the seven units and the MAU were operating (Munters unit, RTU-2, 3, 4). The ventilation dampers on RTU-4 were completely closed. Seven of the eight roof exhaust fans were operating except for HEF-1, which had a broken fan belt.

The supply and return ductwork is located in the ceiling plenum.

The Danfoss control system controls the RTUs. The exhaust fans are manually operated.

RTU-1

RTU-2, 3, 5, 6, 7

RTU-4

MAU-1

Figure A6-5. Roof Top Units and Make-up-Air Unit

Typical Down Blast Fan

Typical Up Blast Fan

Figure A6-6. Roof Exhaust Fans

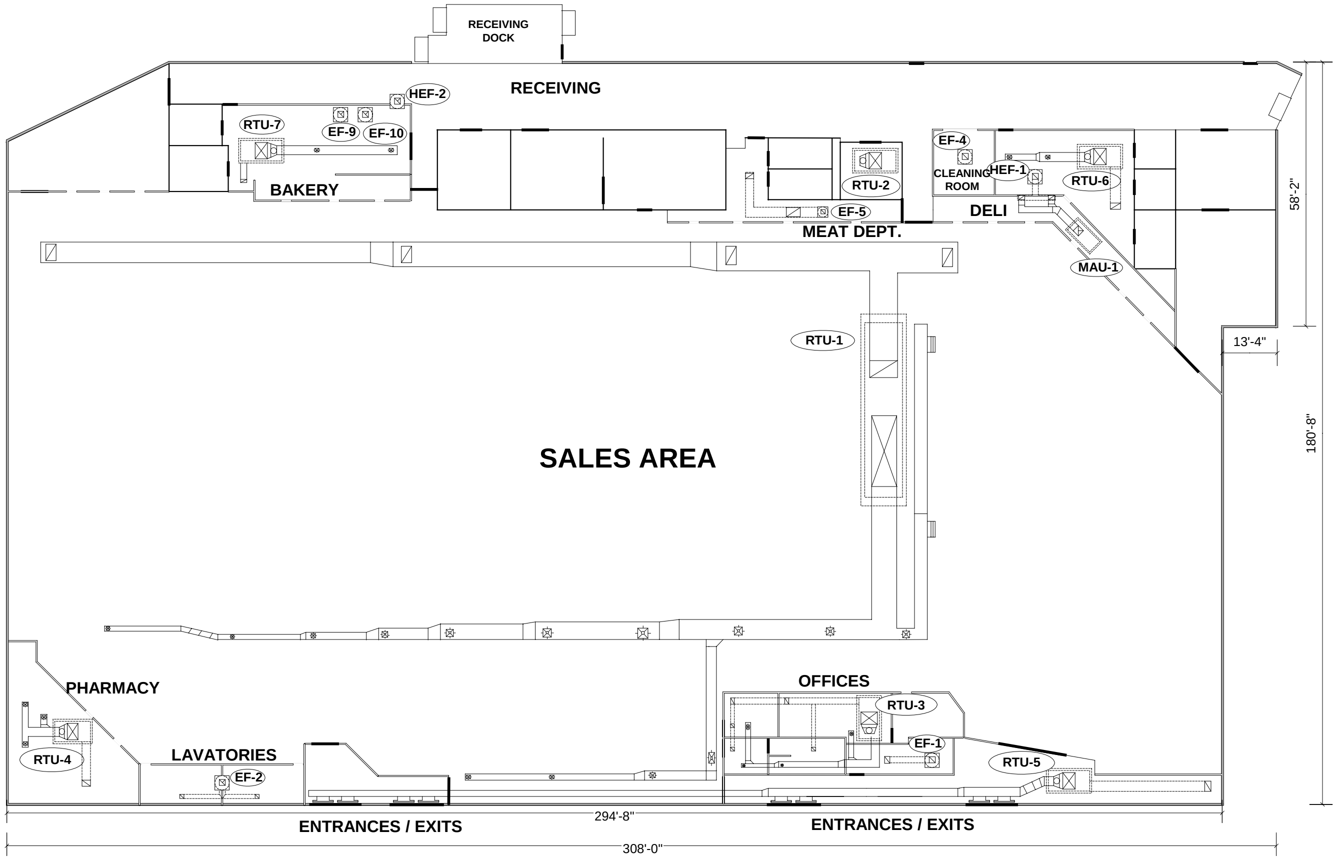

Figure A6-7. RTU, MAU, and Exhaust Fan Layout with Ductwork

Table A6-1. HVAC Equipment Installed at Site (Design Data)

	RTU-1 Sales Area	**RTU-2 Mezzanine**	**RTU-3 Front Office**	**RTU-4 Pharmacy**	**RTU-5 Entrance Vestibule**	**RTU-6 Deli**	**RTU-7 Bakery**	**MAU-1 Deli**
Manufacturer	Munters	Carrier	Carrier	Carrier	Carrier	Carrier	Carrier	
Model	S30ND45GG	48HJF006 -M-641CA	48HJF004 -M-641CA	48GP-024060311	48HJF009 -M-641CA	48HJF004 -M-641CA	48HJF004 -M-641CA	
Cooling (tons)	57	5	3	2	8.5	3	3	
Dehumid. (lb/h)	263							
Supply (cfm)	20,000	2,000	900	600	4,000	1,200	1,200	
Ventilation (cfm)	5,500	600	200	80	900	100	100	1,494
Fresh Air Fraction (design)	28%	30%	22%	13%	23%	8%	8%	
Gas Heating (Mbtuh output)	1,208	120	92	48.4	184	92	92	
Efficiency	75.5%	80%	80%	80.7%	82%	80%	80%	
Econimizer (yes/no)	yes	no	no	yes	no	no	no	n/a

Table A6-2. Roof Exhaust Fans Installed at Site

Exhaust Fan	Fan Type	Rated Airflow (cfm)
EF-1	Down Blast	900
EF-2	Down Blast	400
EF-4	Down Blast	300
EF-5	Down Blast	600
EF-9	Up Blast	750
EF-10	Up Blast	750
HEF-1	Up Blast	4200
HEF-2	Up Blast	700
Total		**8,600**

Table A6-3. Summary of HVAC Equipment Sizing

	Design Totals	Normalized
Cooling (tons)	81.5	699 ft^2/ton
SupplyAirflow (cfm)	29,900	0.52 cfm/ft^2
Ventilation Airflow (cfm)	8,974	0.16 cfm/ft^2
Exhaust Airflow (cfm)	8,600	0.15 cfm/ft^2
Gas Heating (Mbtuh output)	1,836	

MEASUREMENTS

The test data below was taken on June 9-10, 2004. Ventilation airflow measurements and building pressure mapping was completed on June 9. On June 10, standard operating static pressures were measured in the supply, return, and ventilation sections of the RTUs. Roof exhaust fan airflow measurements were also taken on June 10. Test personnel were Dan Gott and Kenneth Larchar for both days.

Pressure Mapping (AHU Fans On)

The air pressure relationships in the building were determined with the following HVAC equipment operating: RTU-1 through 4, MAU-1, and exhaust fans EF-1, 2, 4, 5, 9, 10. The graphics in Figure A6-8 show the pressure differences induced between the sales area and receiving area and across the building envelope with the AHU fans on and the interior doors closed. The building was pressurized approximately 2.3 Pa. HEF-1 was powered on, but the fan belt was broken. The building pressure would likely be negative or near zero if HEF-1 (4200 cfm exhaust fan) was operating properly. The effect of airflow imbalance on building pressure will be investigated in the section on HVAC ventilation and exhaust flow measurements.

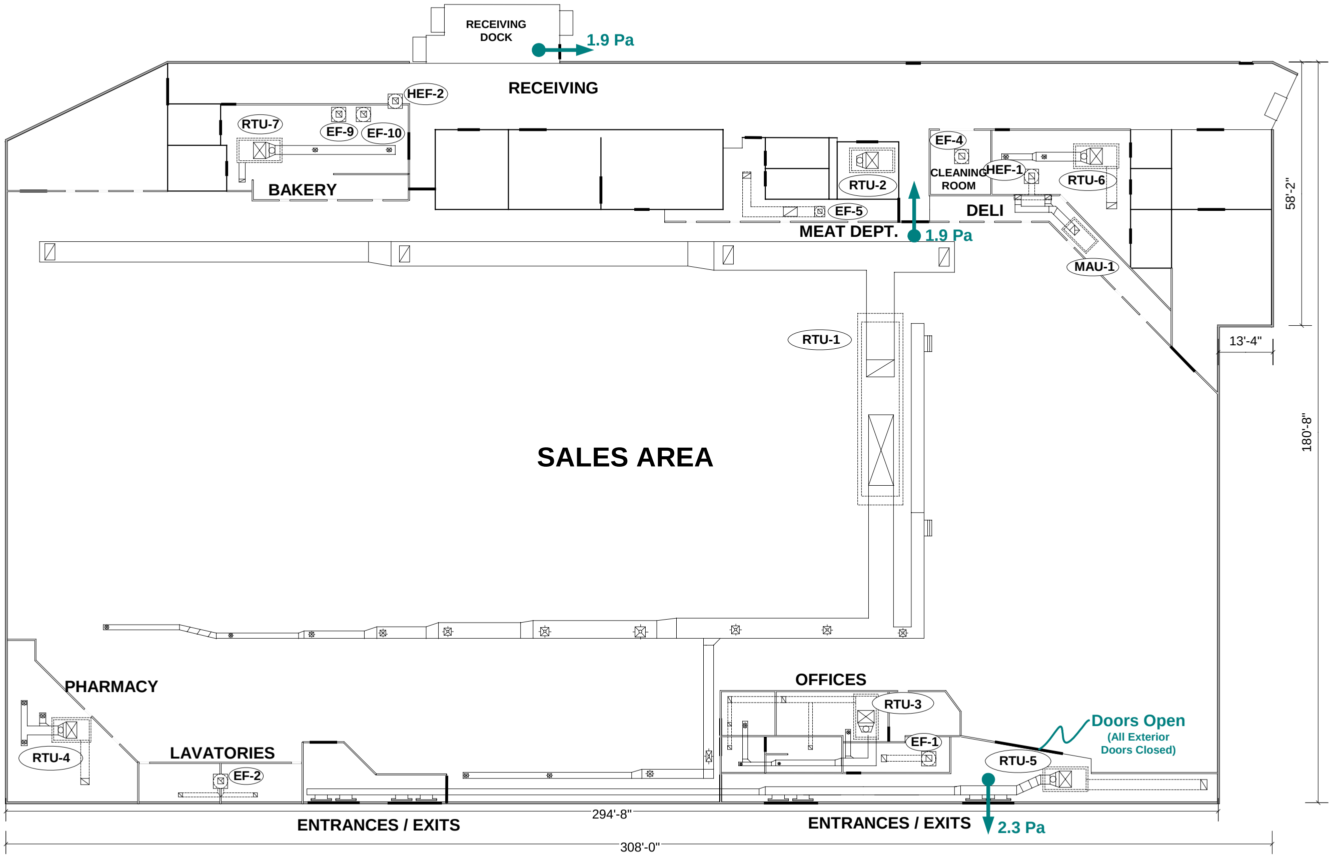

Figure A6-8. Pressure Differences between Rooms with AHU Fans On

HVAC Ventilation and Exhaust Measurements

Ventilation airflow was measured for the RTUs operating while on site July 9, 2004 (Munters Unit, RTU-2, RTU-3). RTU-4 was operating, but the ventilation dampers were closed. We did not measure the ventilation airflow on MAU-1 due to time constraints. The 2002 site plans specify a design ventilation of 1,494 cfm for MAU-1 which will be used for the analysis. The airflow was measured for seven of the nine exhaust fans. Eight of the nine exhaust fans were operating, but airflow was not measured on HEF-1 because the fan belt was broken.

The ventilation airflow for the Munters unit was measured using an equal area velocity traverse. We used cardboard to create a short duct around the ventilation intake to help straighten the airflow and create a finite space for the velocity measurements. Figure A6-9 shows the temporary cardboard duct attached to the ventilation intake.

Ventilation measurements were taken previously at this site on September 17, 2003. Two sets of measurements were taken on the same day (Table A6-4). The second set of readings (Test 2) used a longer "time constant" on the TSI hot wire anemometer in order to damp out the wind-induced fluctuations that were observed for the first set of readings (Test 1). The two sets of flow readings imply the fresh airflow was 8,800 to 9,600 scfm, which is significantly higher than the flow of 5,500 scfm specified on the drawings.

Table A6-5 shows the Munters unit ventilation measurements for two tests taken on July 9, 2004: one with the desiccant unit not running and one with the desiccant unit operating. The desiccant unit has a process fan which pulls additional fresh air into the unit. The flow increases approximately 11% (5,100 scfm to 5,800 scfm) when the desiccant is operating. The Munters ventilation flow is now within 7% of the flow specified on the drawings (5,500 scfm).

Figure A6-9. Munters Unit Ventilation Intake with Cardboard Duct to Direct Airflow

Table A6-4. Munters Unit Ventilation Airflow (September 17, 2003)

Ventilation Airflow	
Opening width	33 inches
Opening height	73 inches

Sep-03
Test 1
Time Const. = 1

	4.5"	12.5"	20.5"	28.5"
5.5"	850	730	680	480
13.5"	780	515	390	350
21.5"	575	500	420	300
29.5"	815	490	410	470
37.5"	900	490	410	420
45.5"	870	480	440	390
53.5"	825	600	420	460
61.5"	940	580	430	440
69.5"	900	825	530	520

Average	572.9	SFPM
Area	16.7	ft^2
Air Flow	**9584**	**SCFM**

Sep-03
Test 2
Time Const. = 5

	4.5"	12.5"	20.5"	28.5"
5.5"	540	640	600	480
13.5"	350	490	440	350
21.5"	650	540	420	380
29.5"	900	440	385	300
37.5"	880	490	440	370
45.5"	650	530	480	320
53.5"	820	470	430	400
61.5"	820	560	480	440
69.5"	690	760	520	440

Average	524.9	SFPM
Area	16.7	ft^2
Air Flow	**8780**	**SCFM**

Table A6-5. Munters Unit Ventilation Airflow (June 9, 2004)

Ventilation Airflow	
Opening width	33 inches
Opening height	73 inches

June-04
Test 1
Dessicant OFF

	4.5"	12.5"	20.5"	28.5"
5.5"	347	321	300	83
13.5"	390	330	290	134
21.5"	340	327	346	120
29.5"	360	307	305	174
37.5"	445	415	360	123
45.5"	353	324	341	120
53.5"	387	338	310	113
61.5"	387	398	480	147
69.5"	480	397	380	250

Average	306.2	SFPM
Area	16.7	ft^2
Air Flow	**5122**	**SCFM**

June-04
Test 2
Dessicant ON

	4.5"	12.5"	20.5"	28.5"
5.5"	375	346	330	162
13.5"	400	365	360	175
21.5"	468	380	324	146
29.5"	400	336	380	218
37.5"	500	520	336	146
45.5"	406	426	384	162
53.5"	440	333	353	180
61.5"	465	439	397	280
69.5"	515	210	420	327

Average	344.6	SFPM
Area	16.7	ft^2
Air Flow	**5764**	**SCFM**

Only two of the six Carrier RTUs (RTU-2 and RTU-3) were operating on June 10, 2004. The standard operating static pressures for these two Carrier units were measured in the ventilation hood, return section, and at the inlet side of the supply fan (Table A6-6).

Table A6-6. Standard Operating Static Pressures for RTUs (June 10, 2004)

Roof Top Unit	**Ventilation Static Press.**	**Return Static Pressure [before filter]**	**Supply Fan Intake Static Pressure [after filter]**
	(Pa)	**(Pa)**	**(Pa)**
RTU-2	-30.1	-98.5	-215
RTU-3	-12.8	-89.8	-176.5

The ventilation air provided by the Carrier RTUs was measured using a Duct Blaster fan connected to the ventilation hood on the RTU. The flow through the Duct Blaster fan at the standard operating static pressure in the ventilation hood is the amount of fresh air provide by that unit. Figure A6-10 shows how the Duct Blaster was used to measure RTU ventilation. Table A6-7 shows the results for the ventilation airflow tests on RTU-2 and RTU-3.

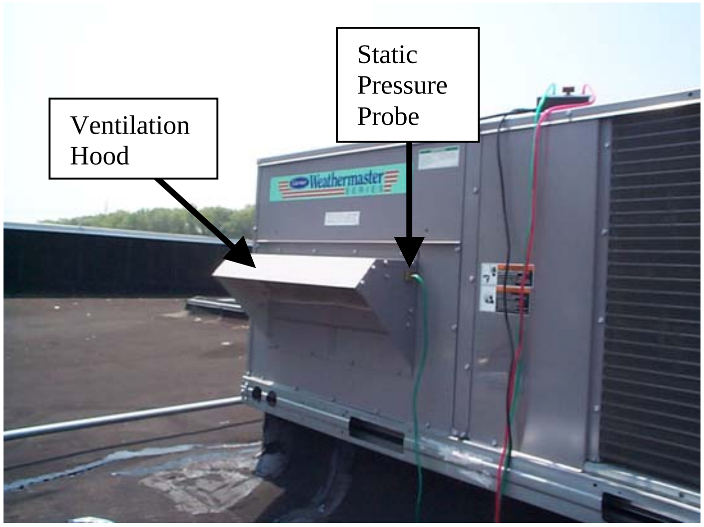

Standard Operating Static Pressure Measured in the Ventilation Hood just beyond the Ventilation Filter

Static Pressure Probe in Same Location With Duct Blaster Connected

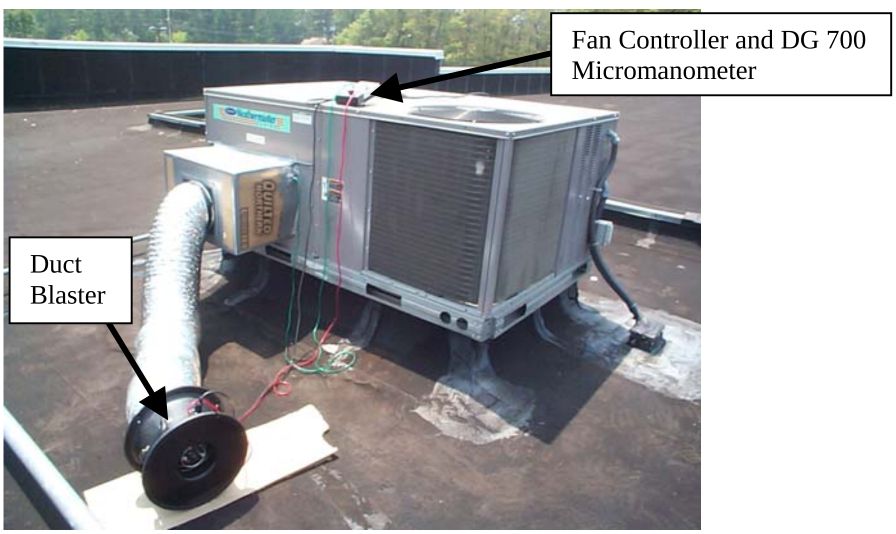

Duct Blaster Set Up to Measure RTU Ventilation

Figure A6-10. Duct Blaster Set Up to Measure Ventilation Airflow

Table A6-7. Roof Top Unit Ventilation Airflow Data

RTU-2

	Test Date (6/9/04)	Next Day (6/10/04)
Static Pressure in Ventilation Hood (Pa)	26.85	30.1
Airflow @ Average Ventilation Static (cfm)	238	
R-Squared	0.989	

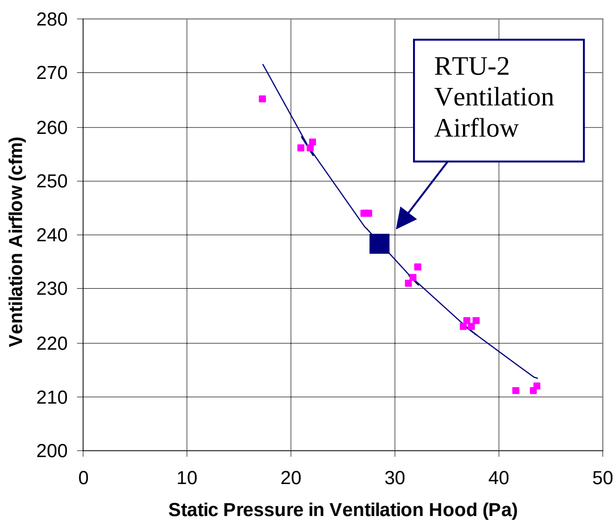

Test Data:

Nominal Ventilation Static (Pa)	Nominal Flow (cfm)	Ring
43.7	212	2
43.4	211	2
41.7	211	2
37.0	224	2
37.4	223	2
37.9	224	2
36.6	223	2
31.8	232	2
31.4	231	2
32.3	234	2
27.5	244	2
27.3	244	2
27.1	244	2
21.0	256	2
21.9	256	2
22.1	257	2
17.3	265	2

RTU- 3

	Test Date (6/9/04)	Next Day (6/10/04)
Static Pressure in Ventilation Hood (Pa)	14	12.8
Airflow @ Average Ventilation Static (cfm)	278	
R-Squared	0.898	

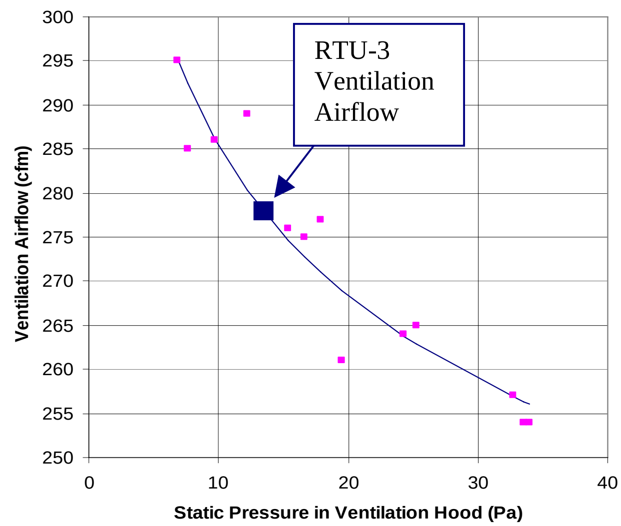

Test Data:

Nominal Ventilation Static (Pa)	Nominal Flow (cfm)	Ring
34.0	254	2
33.5	254	2
32.7	257	2
25.3	265	2
24.3	264	2
19.5	261	2
17.9	277	2
16.6	275	2
15.4	276	2
12.2	289	2
9.7	286	2
7.6	285	2
6.8	295	2

RTU-4 was operating while we were on site however; the ventilation dampers were closed as shown in Figure A6-11. The other five Carrier roof top units have a manually adjustable plate to change ventilation intake size (not electrically controlled dampers like RTU-4).

Figure A6-11. RTU-4 with Operating with Ventilation Dampers Closed

The airflow for each operating exhaust fan was measured using a capture tent. The tent was set up to measure the airflow through a fan when the static pressure inside the tent is zero Pa with respect to outdoors (Figure A6-12). There are three holes in the capture tent for various diameter fans. All the exhaust fans were tested using a Duct Blaster fan because all the airflows were less than the maximum Duct Blaster fan flow (approx. 1,500 cfm at 0 Pa). The Blower Door fan was only used to seal the tent hole sized for that fan. The third hole in the tent was sealed using the flexible duct transition piece[1] that came with the Duct Blaster. After sealing the hole in the

[1] The transition piece (from the flexible extension duct) is normally mounted to a duct or diffuser and then the flexible duct is connected between the duct transition piece and the Duct Blaster.

transition piece with Duct Mask plastic wrap, the transition piece was inserted into the tent (lower right picture in Figure A6-12).

To prevent the exhaust fan flow from backing up into the store, we started the Duct blaster fan and slowly zipped up the capture tent while adjusting the fan flow. Static pressure was measured inside the tent with respect to outdoors. When the exhaust flow was less than 800 cfm[2], the Duct Blaster flow conditioner was used and the velocity pressure was measured across the Duct Blaster fan using the pressure traverse that comes with the Duct Blaster. Several data points were taken at positive and negative static pressures in the tent to create a flow curve used to determine the exhaust fan flow at 0 Pa.

Table A6-8, Table A6-9, and Table A6-10 show the raw data and results for each exhaust fan that was tested.

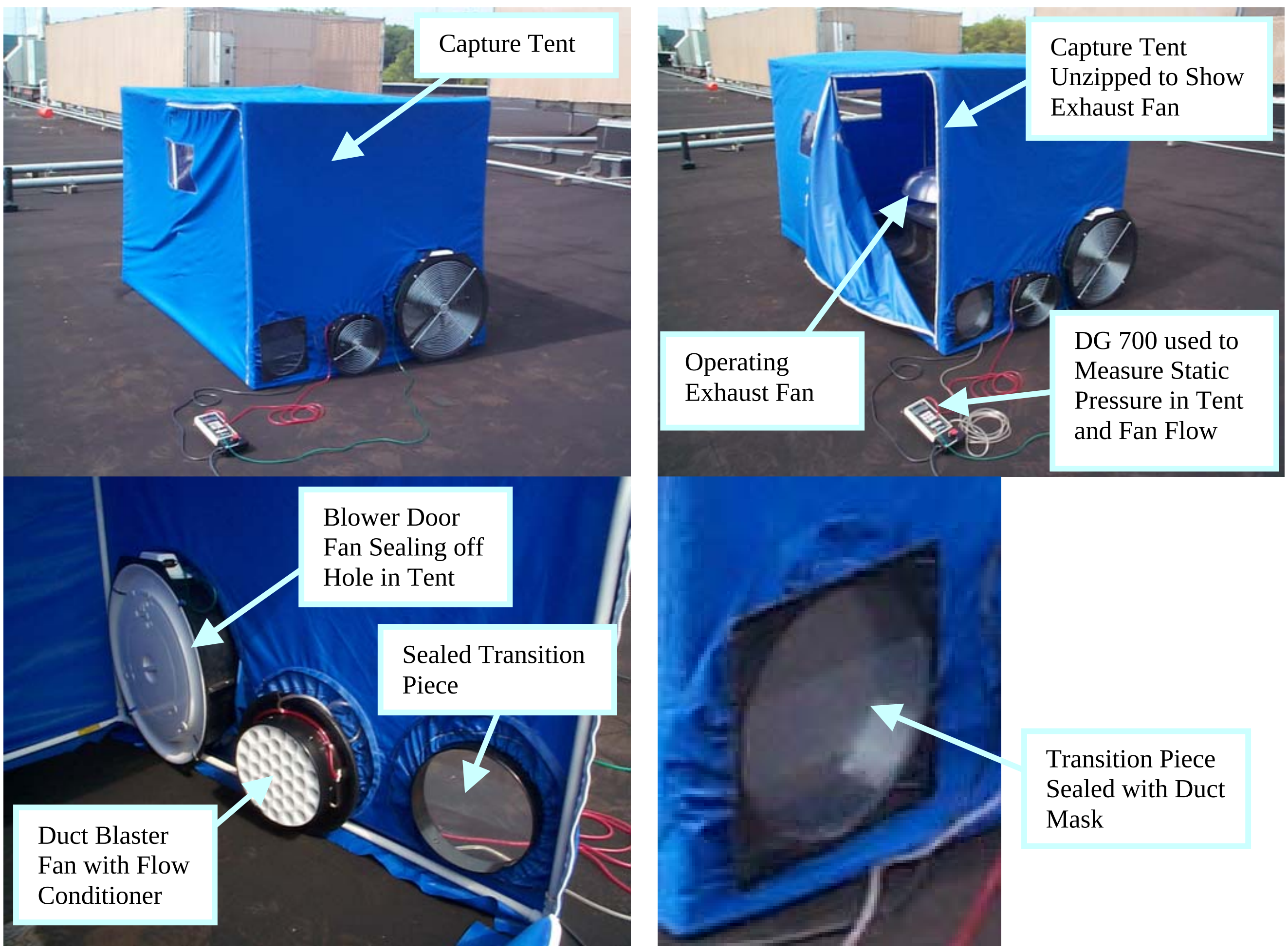

Figure A6-12. Capture Tent Set Up to Measure Exhaust Fan Flow

[2] One of the orifice rings 1-3 must be used with the flow conditioner which limits the Duct Blaster airflow to approximately 800 cfm at 0 Pa with ring 1.

Table A6-8. EF-1 and EF-2 Exhaust Fan Flow Data

EF-1

Test Results:

Slope	-6.5
Intercept	619.8
R-Squared	0.99
Airflow @ 0 Pa in tent	619.8 cfm

Test Data:

Nominal Duct Pressure (Pa)	Nominal Flow (cfm)	Ring
-12.9	704	1
-12.5	702	1
-12.6	701	1
-7.0	658	1
-4.6	654	1
-4.8	653	1
2.4	620	1
1.8	615	1
1.4	612	1
4.6	578	1
5.5	576	1
6.2	576	1
10.0	563	1
8.0	559	1
10.4	557	1
14.1	529	1
13.8	526	1
14.3	525	1

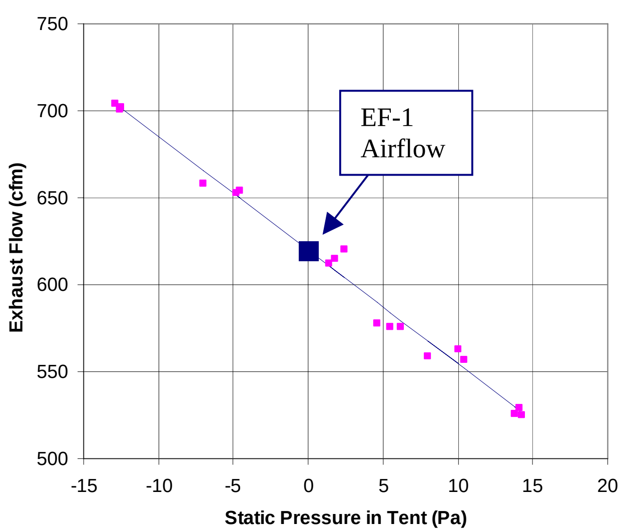

EF-2

Test Results:

Slope	-15.9
Intercept	755.8
R-Squared	0.93
Airflow	755.8 cfm

Test Data:

Nominal Duct Pressure (Pa)	Nominal Flow (cfm)	Ring
15.7	544	1
15.4	538	1
13.4	565	1
12.7	564	1
11.8	590	1
11.2	591	1
10.7	589	1
5.1	625	1
5.0	623	1
4.0	619	1
1.9	655	1
1.6	654	1
1.1	654	1
-2.8	860	open
-3.5	867	open
-3.7	870	open
-3.9	877	open
-8.1	922	open
-8.2	921	open
-9.6	924	open
-16.8	1014	open
-16.9	1011	open
-17.9	1017	open

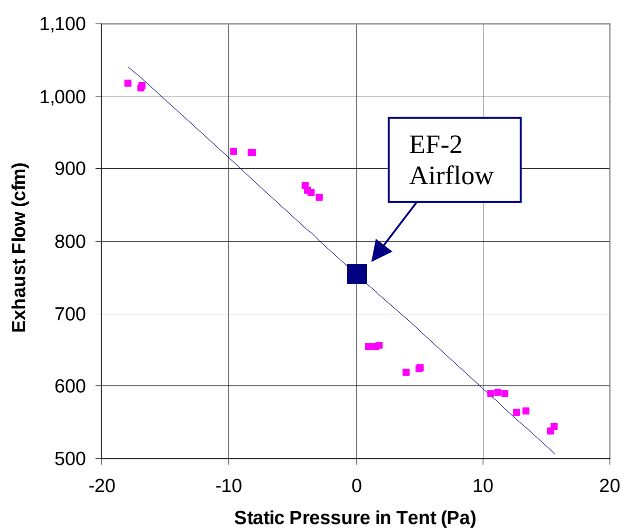

Table A6-9. EF-4 and EF-5 Exhaust Fan Flow Data

EF-4

Test Results:

Slope	-2.9
Intercept	390.3
R-Squared	0.99
Airflow	390.3 cfm

Test Data:

Nominal Duct Pressure (Pa)	Nominal Flow (cfm)	Ring
13.8	354	1
13.6	352	1
13.5	353	1
6.4	370	1
5.6	371	1
5.1	370	1
-4.7	409	1
-5.6	404	1
-5.7	407	1
-11.1	423	1
-11.9	425	1
-12.3	426	1

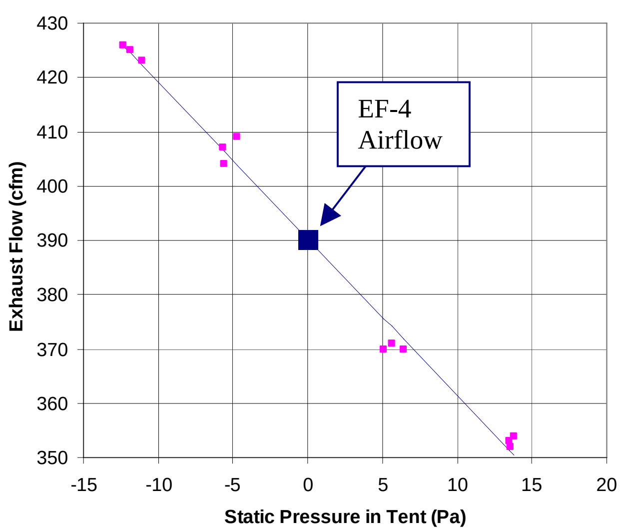

EF-5

Test Results:

Slope	-12.9
Intercept	812.3
R-Squared	0.92
Airflow	812.3 cfm

Test Data:

Nominal Duct Pressure (Pa)	Nominal Flow (cfm)	Ring
22.5	594	1
22.1	591	1
22.0	592	1
13.7	629	1
13.5	634	1
13.5	628	1
8.8	669	1
7.7	663	1
7.6	709	1
7.3	710	1
7.1	701	1
7.0	662	1
6.6	666	open
6.3	667	open
6.2	662	open
0.3	802	open
-0.5	842	open
-1.1	848	open
-1.3	843	open
-6.0	910	open
-6.5	913	open
-6.7	909	open
-13.7	1,028	open
-14.3	1,031	open
-15.1	1,023	open

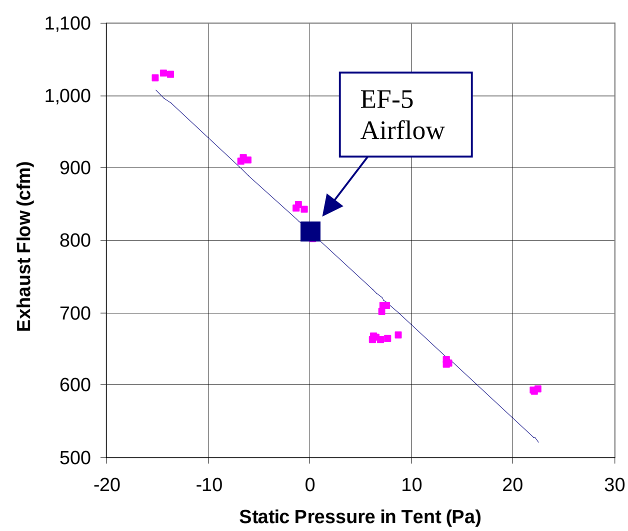

Table A6-10. EF-9 and EF-10 Exhaust Fan Flow Data

EF-9

Test Results:

Slope	-20.1
Intercept	627.1
R-Squared	0.99
Airflow	627.1 cfm

Test Data:

Nominal Duct Pressure (Pa)	Nominal Flow (cfm)	Ring
4.8	518	open
4.4	519	open
4.4	524	open
2.2	593	open
1.6	593	open
1.3	599	open
0.2	640	open
-0.2	644	open
-0.9	652	open
-7.0	786	open
-7.1	784	open
-7.4	790	open
-12.5	864	open
-12.6	869	open
-12.8	867	open

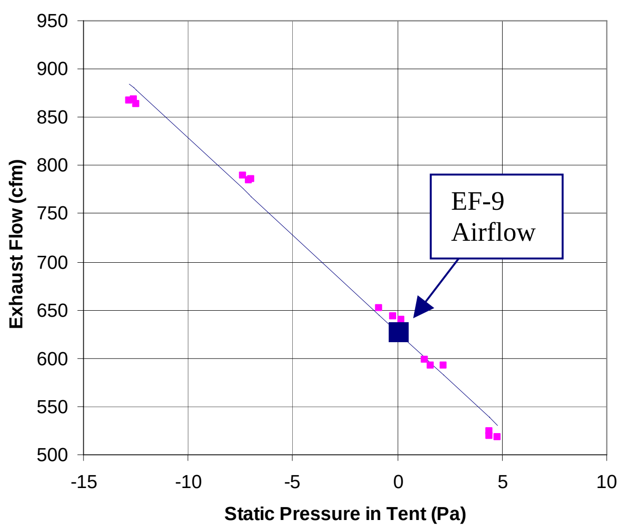

EF-10

Test Results:

Slope	-15.9
Intercept	741.5
R-Squared	0.97
Airflow	741.5 cfm

Test Data:

Nominal Duct Pressure (Pa)	Nominal Flow (cfm)	Ring
10.3	559	open
10.0	564	open
9.9	556	open
3.7	673	open
2.9	691	open
2.0	695	open
1.2	728	open
1.0	722	open
1.0	723	open
0.9	746	open
0.7	751	open
0.5	729	open
-3.5	836	open
-3.7	835	open
-4.0	841	open
-4.5	842	open
-15.6	974	open
-16.2	964	open
-16.4	973	open

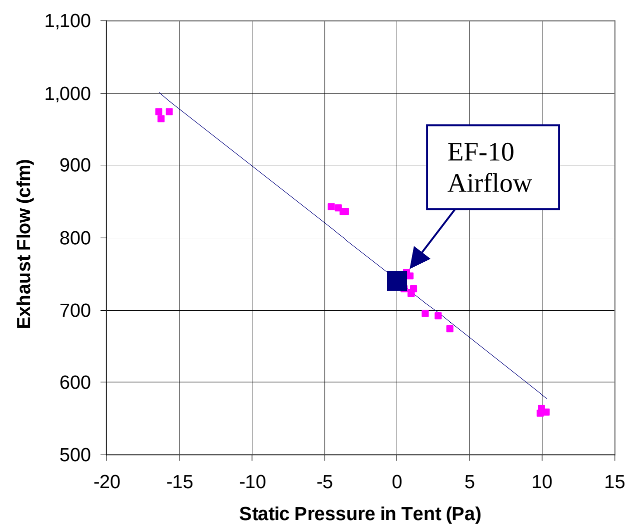

Table A6-11 and Table A6-12 show the roof top unit ventilation flows and exhaust fan flows. Table A6-13 shows the design totals for the HVAC equipment.

Table A6-11. HVAC Equipment Installed at Site

	RTU-1 Sales Area	RTU-2 Mezzanine	RTU-3 Front Office	RTU-4 Pharmacy	RTU-5 Entrance Vestibule	RTU-6 Deli	RTU-7 Bakery	MAU-1 Deli
Manufacturer	Munters	Carrier	Carrier	Carrier	Carrier	Carrier	Carrier	
Model	S30ND45GG	48HJF006 -M-641CA	48HJF004 -M-641CA	48GP-024060311	48HJF009 -M-641CA	48HJF004 -M-641CA	48HJF004 -M-641CA	
Cooling (tons)	57	5	3	2	8.5	3	3	
Supply (cfm)	20,000	2,000	900	600	4,000	1,200	1,200	
Design Ventilation (cfm)	5,500	600	200	80	900	100	100	1,494
Measured Ventilation Airflow (cfm)	5,764**	238	278	0 (dampers closed)	not running during test	not running during test	not running during test	
Design Fresh Air Fraction	28%	30%	22%	13%	23%	8%	8%	
Measured Fresh Air Fraction	29%	12%	31%	0%				

** The ventilation airflow for RTU-1 is 5,122 cfm (measured) with the dessicant wheel operating.

Table A6-12. Roof Exhaust Fans Installed at Site

Exhaust Fan	Fan Type	Rated Airflow (cfm)	Measured Airflow (cfm)
EF-1	Down Blast	900	620
EF-2	Down Blast	400	756
EF-4	Down Blast	300	390
EF-5	Down Blast	600	812
EF-9	Up Blast	750	627
EF-10	Up Blast	750	741
HEF-1	Up Blast	4200	belt broken
HEF-2	Up Blast	700	not running
Total		**8,600**	**3,947**

Table A6-13. Summary of HVAC Equipment Sizing

	Design		Measured	
	Totals	Normalized	Totals	Normalized
Ventilation Airflow (cfm)	8,974	0.16 cfm/ft^2	7,775*	0.14 cfm/ft^2
Exhaust Airflow (cfm)	8,600	0.15 cfm/ft^2	3,947**	0.07 cfm/ft^2

* This total includes the design flow for MAU-1 (1,494 cfm), which was not measured.

** The meausred total exhaust flow with HEF-1 operating properly would be 8147 cfm (0.14 cfm/ft^2)

On June 9, the ventilation airflow for the entire store was 7,775 cfm (measured RTU-1, 2, 3, and design flow for MAU-1) and the total store exhaust fan flow was measure at 3,947 cfm (all operating fans except HEF-1, which had a broken belt). The store was pressurized approximately 2 Pa with an airflow imbalance of 3,828 cfm more airflow entering the building envelope. If exhaust fan HEF-1 was operating properly, the airflow imbalance would be 372 cfm more airflow. We can assume the building pressurization would be close to zero if exhaust fan HEF-1 was operating.

Building Airtightness

The building was too large to complete a blower door test. However, we were able to use the measured flow imbalance and building pressure to infer a leakage rate by fitting this single data point to the flow-exponent function with an assumed exponent of 0.60 – 0.65. The resulting ACH_{50} was 2.0, assuming the range of measured pressures and exponents. This implies the building was very tight.

Flow Imbalance:	3,828 cfm
Pressure:	1.9-2.3 Pa
Assumed Exponent (n):	0.60-0.65
Resulting cfm_{50}:	24,200-32,000 cfm
Resulting ACH_{50}:	1.8-2.4 1/h
Assumed Flow Equation:	$Q = 2604.3 \cdot \Delta p^{0.6}$

Utility Gas and Electricity Use

The tables and graphs below show the gas and electric use trends for the facility. The overall energy use index for the building is summarized below.

	Heating Energy Use Index (MBtu/ft^2-year)	Electricity Use Index (kWh/ft^2-year)
Annual	~41[1]	39.3

Note: 1 - Gas use for the period Aug-02 to Jul-03. Does not include gas use by smaller RTUs.

Table A6-14. Summary of Electric Usage

Month	Days In Month	Facility Energy (kWh)	Facility Demand (kW)	Electric Use per Sq-Ft (kWh/Sq Ft)
Aug-02	31	240,531	482	4.2
Sep-02	30	225,633	444	4.0
Oct-02	31	193,280	421	3.4
Nov-02	30	166,070	311	2.9
Dec-02	31	164,049	301	2.9
Jan-03	31	167,021	277	2.9
Feb-03	28	152,590	287	2.7
Mar-03	31	172,612	311	3.0
Apr-03	30	164,330	346	2.9
May-03	31	187,225	344	3.3
Jun-03	30	205,056	445	3.6
Jul-03	31	248,544	464	4.4
Aug-03	31	232,883	438	4.1
Sep-03	30	196,926	407	3.5
Oct-03	31	175,318	336	3.1
Nov-03	30	170,234	369	3.0
Dec-03	31	164,973	299	2.9
Jan-04	31	162,478	274	2.9
Feb-04	29	152,802	261	2.7
Mar-04	31	182,107	329	3.2
Apr-04	30	182,211	323	3.2
12 Month*	***366***	***2,242,876***	***464***	**39.3**

**The 12 month totals and averages are for the period beginning April 1, 2003 and ending March 31,2004

Table A6-15. Monthly RTU-1 Component Energy Consumption

	Electricity Use					Gas Use			
Month	Supply Fan Energy (kWh)	Dessicant Process Fan Energy (kWh)	Dessicant Regen Fan Energy (kWh)	Condensing Section Energy (kWh)	Total RTU-1 Energy (kWh)	Dehumid. Gas Use (therms)	Space Heating Gas Use (therms)	Total RTU-1 Gas Use (therms)	Percent Data Collected (%)
Aug-02	3,132	947	829	4,273	9,181	710.4	0.0	710	40%
Sep-02	7,812	1,987	1,742	10,758	22,299	1,741.3	0.0	1,741	100%
Oct-02	8,028	807	704	2,953	12,492	706.7	721.2	1,428	100%
Nov-02	7,780	155	136	0	8,072	138.6	2,526.8	2,665	100%
Dec-02	8,071	39	35	0	8,145	55.6	3,784.1	3,840	100%
Jan-03	8,062	0	0	0	8,062	0.0	4,794.3	4,794	100%
Feb-03	7,182	0	0	0	7,182	0.0	4,122.0	4,122	99%
Mar-03	7,816	37	32	0	7,884	31.2	2,992.7	3,024	100%
Apr-03	7,754	0	0	114	7,868	0.0	2,346.1	2,346	100%
May-03	8,049	60	53	181	8,342	43.1	1,516.2	1,559	100%
Jun-03	7,810	645	565	2,089	11,109	414.1	474.3	888	100%
Jul-03	8,064	2,211	1,938	18,585	30,797	1,092.6	8.3	1,101	100%
Aug-03	7,948	3,129	2,742	20,616	34,436	2,129.4	0.0	2,129	100%
Sep-03	7,670	1,514	1,328	9,078	19,589	905.0	27.2	932	100%
Oct-03	8,072	353	310	459	9,194	199.1	514.4	714	100%
Nov-03	7,771	308	270	483	8,832	218.7	1,389.0	1,608	100%
Dec-03	8,072	91	80	0	8,244	88.3	2,710.9	2,799	100%
Jan-04	8,072	0	0	0	8,072	0.0	4,188.0	4,188	100%
Feb-04	7,552	0	0	0	7,552	0.0	3,068.8	3,069	100%
Mar-04	8,072	0	0	0	8,072	0.0	2,470.1	2,470	100%
Apr-04	7,795	6	5	0	7,806	11.5	2,340.4	2,352	100%
12-Month	***94,907***	***8,311***	***7,284***	***51,605***	***162,107***	***5,090***	***18,713***	***23,804***	
	37%	***3%***	***3%***	***20%***	***64%***	***10%***	***39%***	***49%***	

August 2002 to July 2003	23,286.0	therms
	40.9	MBtu/y-ft^2

Field Test Site 7 – Fast Food Restaurant, Herkimer, NY

Figure A7-1. Photo of Building (Southwest)

CHARACTERISTICS

Building Description

The 3,300 sq ft facility is a one-story fast food restaurant that was built in 2002. The facility is divided into two spaces - the customer dinning space in the front half of the building and the kitchen/food preparation space in the back half. Included are two restrooms, a small closet, and one manager's office. Figure A7-1 shows the front of the building. Four unitary rooftop units (two for each space) provide heating and cooling with natural gas furnaces for heat and DX compressors for cooling. Conditioned air is delivered to the store via ductwork installed above the suspended ceiling and ceiling diffusers. Two exhaust fans for the fryer and grill run continuously while the restaurant is open. A single down blast exhaust fan serves the restrooms. The building floor plan is shown in Figure A7-2.

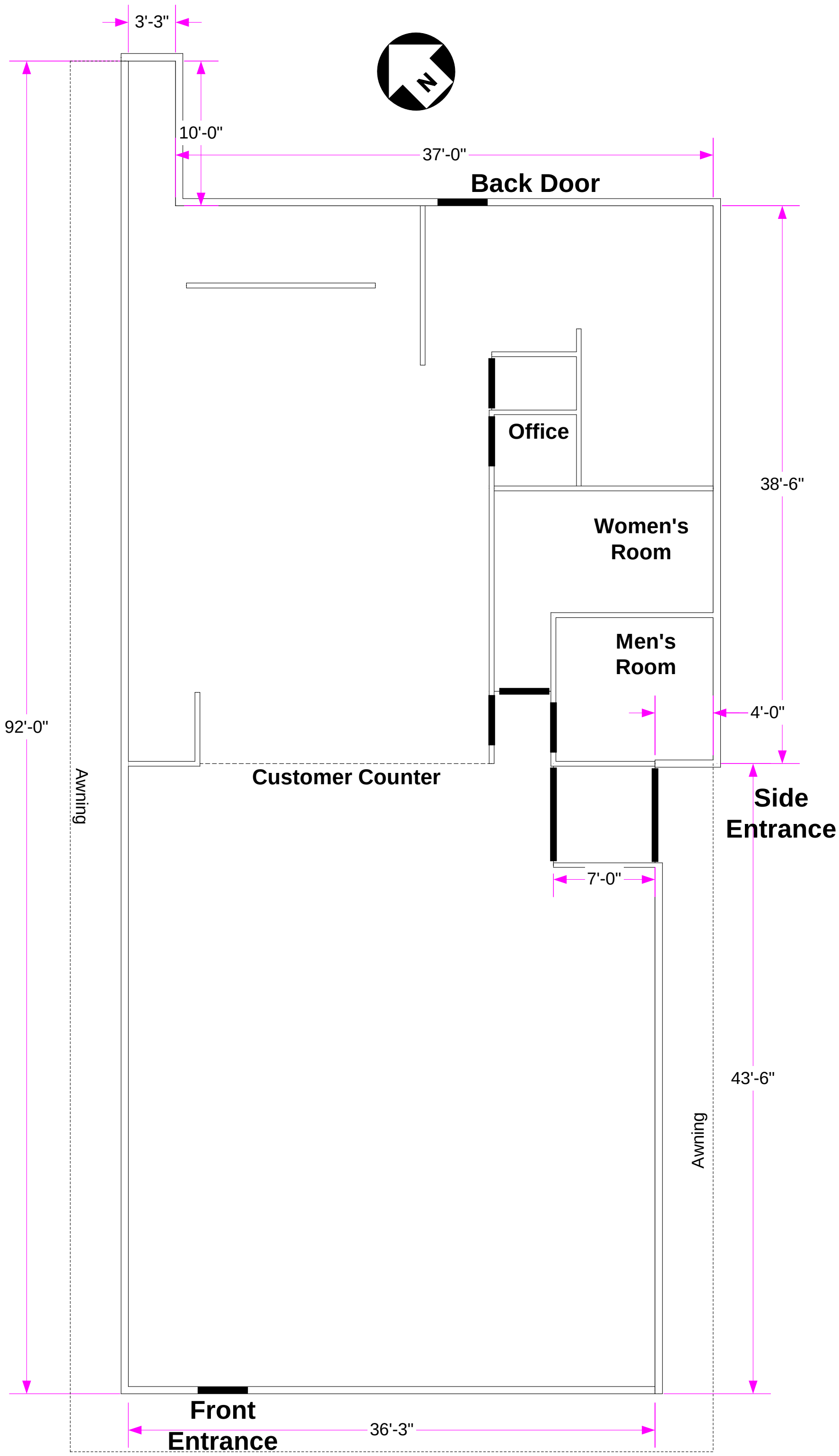

Figure A7-2. Building Floor Plan

Construction Details

Exterior walls are framed with wood 2x4 studs, insulated with 3.5 inches of fiberglass batt insulation between studs, covered with ½-inch plywood and finished with 4x6x12-inch decorative concrete block on the exterior. Interior walls are finished with ½-inch sheetrock and ¼-inch plastic paneling.

The building frame is completely constructed of wood, illustrated by Figure A7-3 and Figure A7-4. The roof joists and wall-roof framing are all constructed with wood instead of the more common steel fabrication in commercial buildings.

The roof construction consists of ½-inch plywood and approximately 3 inches of foam insulation finished with built-up roofing. The entire store has a suspended (drop) ceiling 40 inches below the plywood roof deck. This 40-inch plenum space is used for standard wiring, gas lines, and ductwork.

Figure A7-3 shows the details of the wall, ceiling, and roof construction. Figure A7-4 gives a picture of the ceiling plenum. Figure A7-5 illustrates typical wall and roof sections for exterior walls with the awning and Figure A7-6 illustrates wall without the awning.

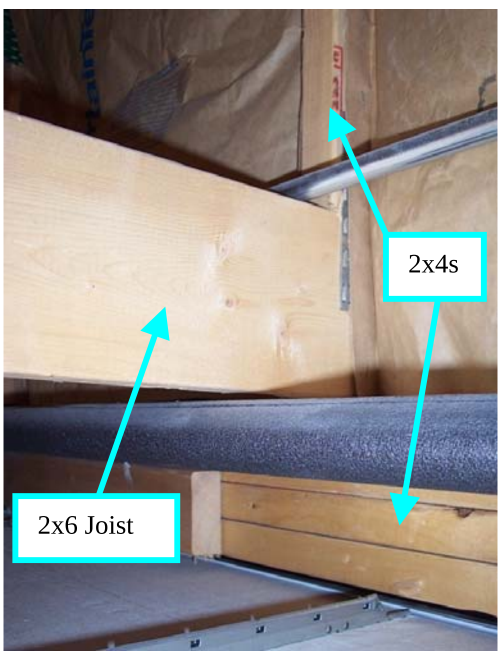

Wall and Ceiling Joist Construction

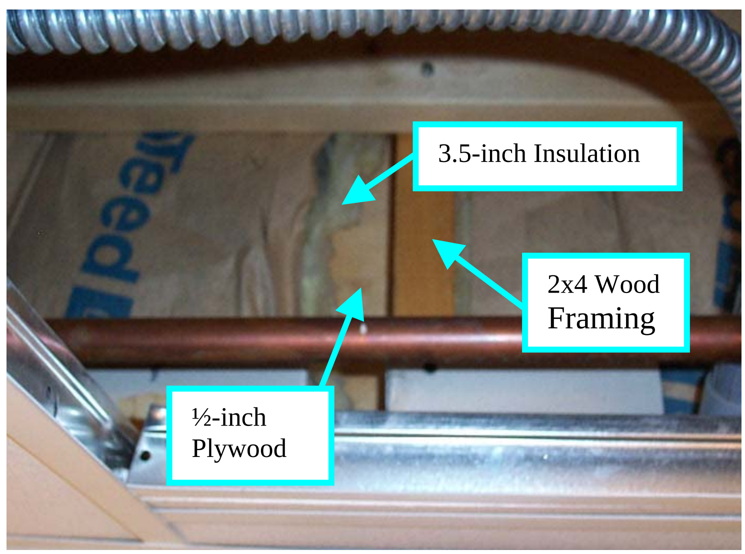

Wall Construction

Figure A7-3. Wall/Roof Construction

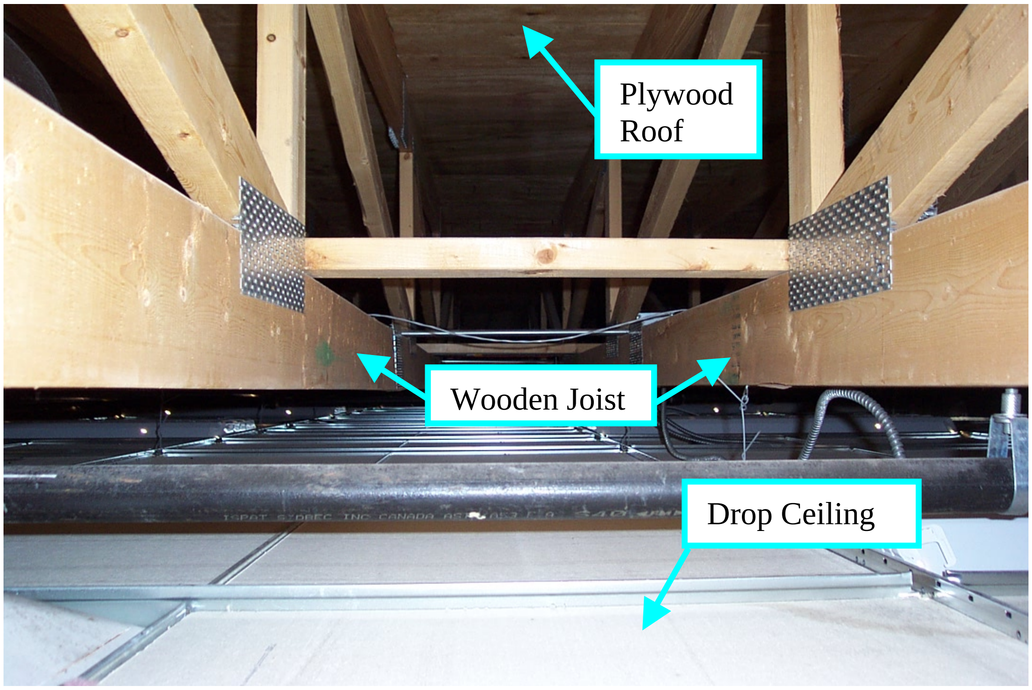

Figure A7-4. Ceiling Plenum

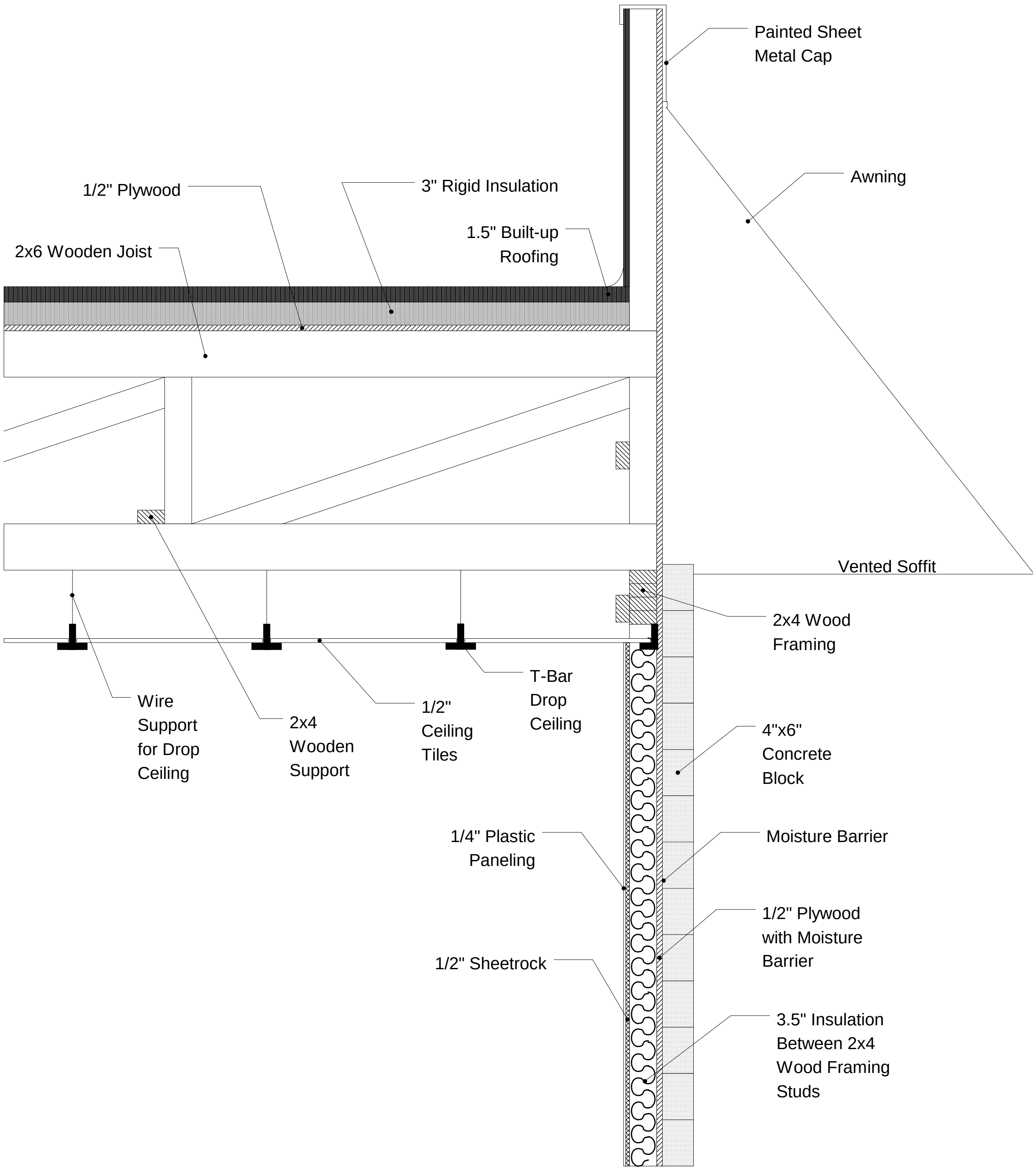

Figure A7-5. Roof, Ceiling and Wall Construction <u>with</u> Awning

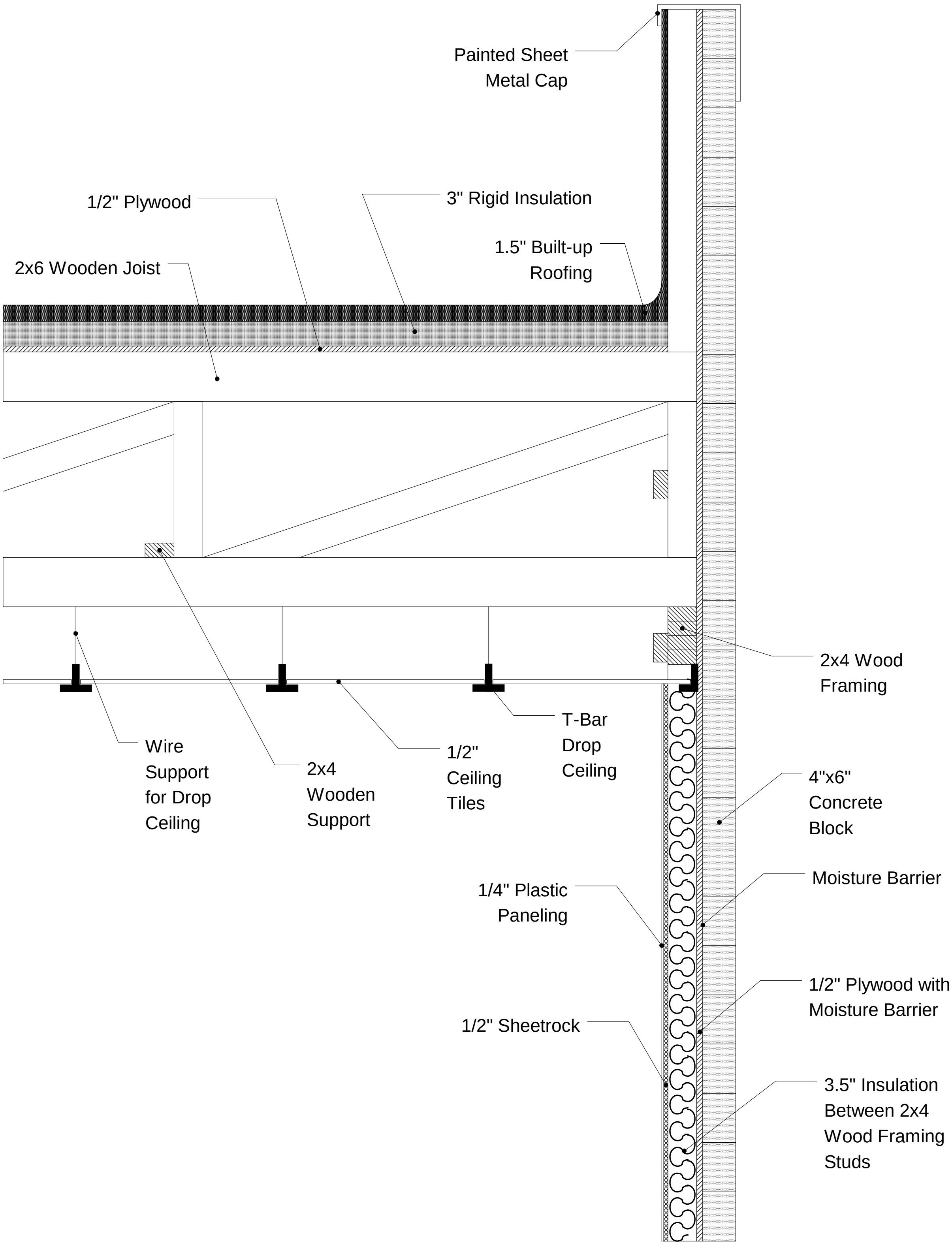

Figure A7-6. Roof, Ceiling and Wall Construction <u>without</u> Awning

HVAC System

Table A7-1 lists the HVAC equipment that serves the building.

Table A7-1. HVAC Equipment Installed at Site (Design Data)

	RTU-1 Back Grill Area	RTU-2 Kitchen	RTU-3 Dining & Counter	RTU-4 Front Dining
Manufacturer	Carrier	Carrier	Carrier	Carrier
Model	48HJE007--541HQ	48HJE007--541HQ	48HJE007--541HQ	48HJE007--541HQ
Cooling (tons)	6	6	6	6
Supply (cfm)	2,100	2,100	2,100	2,100
Gas Heating (MBtuh output)	93.15	93.15	93.15	93.15
Efficiency	81%	81%	81%	81%

Figure A7-7 provides pictures of the RTUs. Each unit is setup with a Honeywell Economizer. RTU-2 and RTU-4 had economizer dampers that were completely closed. The economizer for RTU-2 was disconnected and the economizer for RTU 4 was not working properly. Each unit has a six-ton cooling capacity.

Typical Rooftop Unit

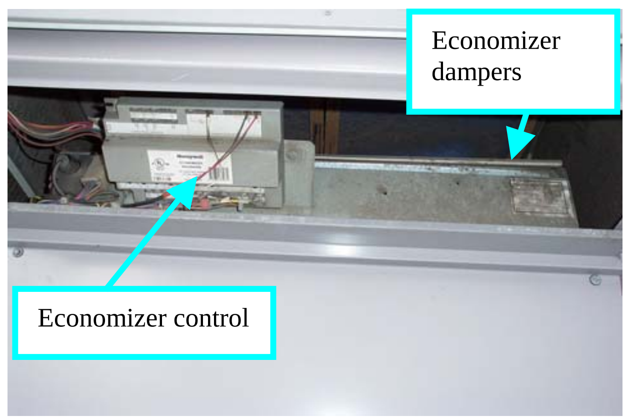

RTU Economizer

Figure A7-7. Roof Top Units

Rectangular sheet metal duct is used for supply air. Each 10”x12” supply trunk is about 24 feet long. Takeoffs, measuring 8”x10” range between 2-16 feet long. All ductwork is wrapped with 1 inch of insulation. Diffusers are standard 2-foot square four-cone ceiling diffusers (displayed in Figure A7-9). Figure A7-8 shows the approximate layout of the supply and return ductwork for RTU-3 and RTU-4 along with the corresponding zones served.

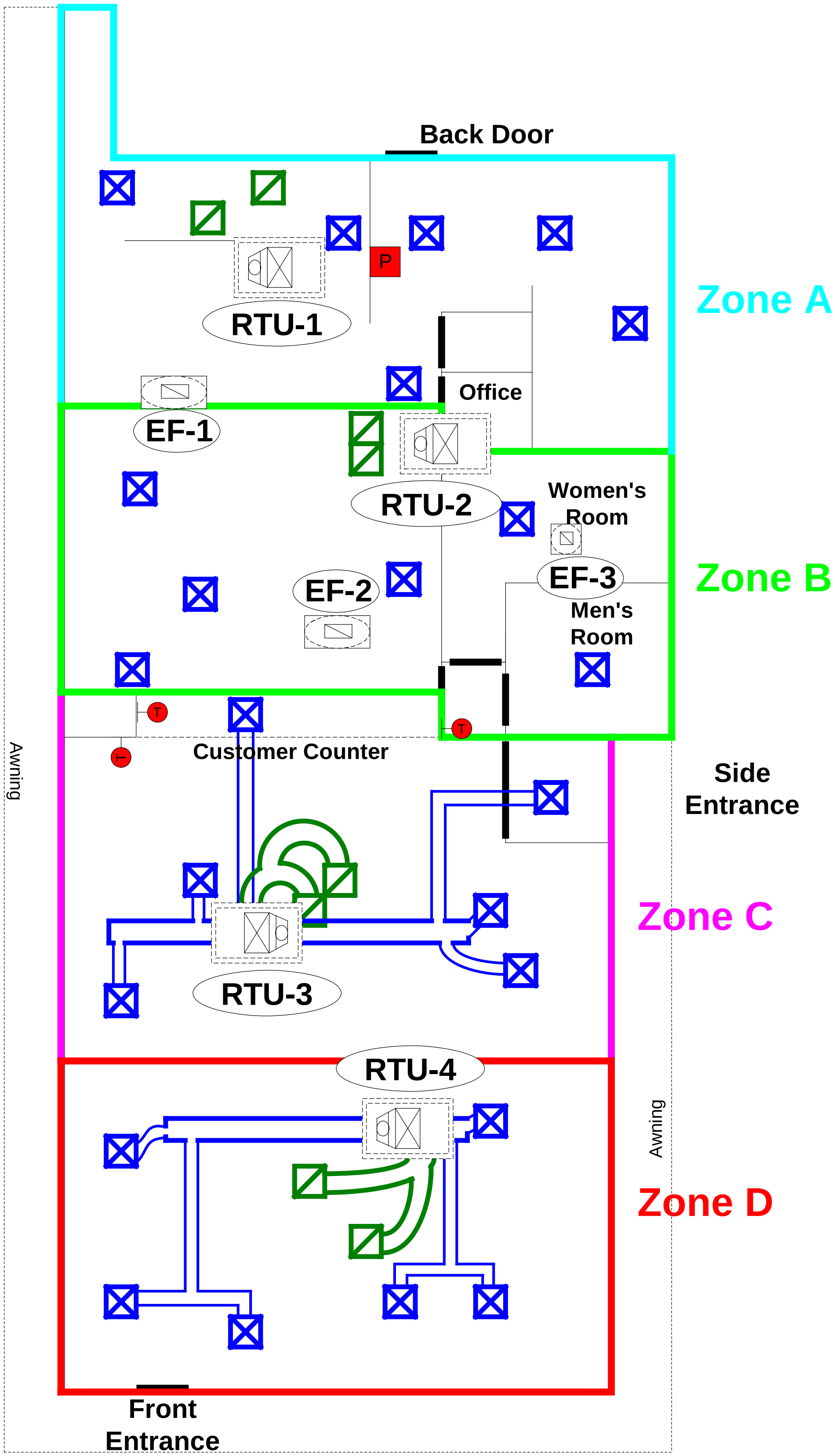

Figure A7-8. Supply and Return Duct System with Corresponding Zones

Figure A7-9. Four Cone Diffuser in Drop Ceiling

The return ductwork for each roof top unit consisted of two return grates - one return grate with a 12-inch return duct and a second grate with an 8-inch and 12-inch return duct. In the ceiling plenum, the three circular return ducts join to carry the return air to the rooftop unit. Figure A7-10 displays the drop ceiling return grates and circular duct connections.

Return Grate with Single 12-inch Return Duct

Return with 8 and 12-inch Return Ducts

Figure A7-10. Return Duct Connection in Drop Ceiling

Figure A7-11 shows the two large roof exhaust fans (EF-1 & EF-2) utilized in conjunction with kitchen grills and broilers. Table A7-2 lists the model numbers and areas served by the exhaust fans.

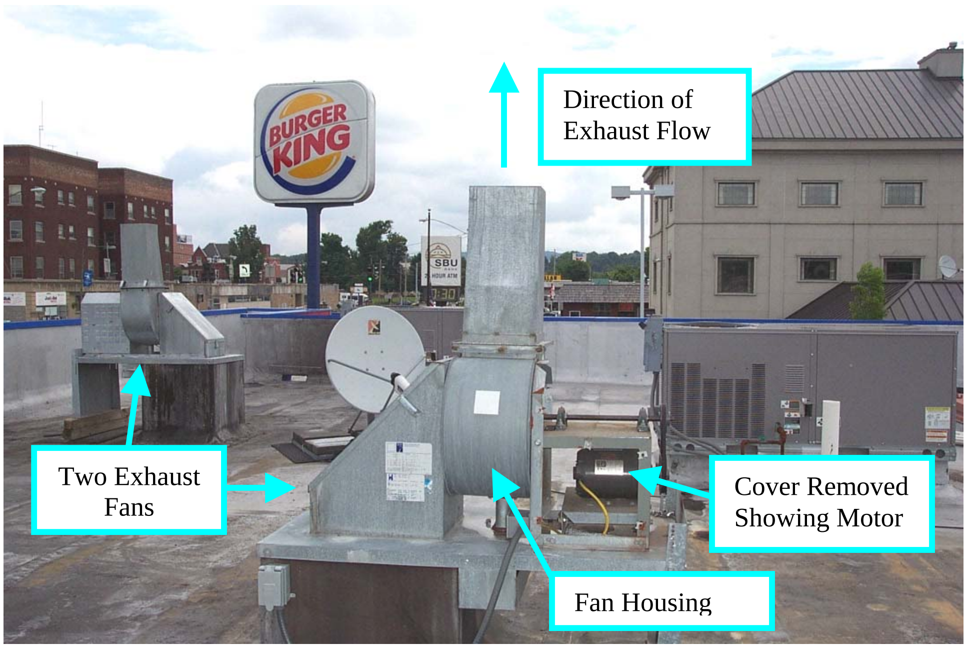

Figure A7-11. Grill and Fryer Exhaust Fans

Table A7-2. Exhaust Fan Summary

Exhaust Fans:	EF-1 Back Grill	EF-2 Kitchen	EF-3 Restrooms
Manufacturer	Penn Power	Penn Power	Penn Power
Model	D10DPBK	D10DPHT(BK)	DX105R

The facility has a Profile Systems controller to remotely control the HVAC equipment, exhaust fans, and exterior lighting. Off site monitoring personnel can change setpoints, setbacks, and exterior lighting usage via centralized network. There are three temperature sensors along the center of the store (see Figure A7-8 for sensor location). All three of the sensors are positioned within the same zone (on opposite sides of the customer counter) and relatively close together.

Typical Temperature Sensor

Profile Systems Controller

Figure A7-12. Air Monitoring Controls

MEASUREMENTS

Power readings, pressure mapping, and ventilation and exhaust flow measurements were taken on July 15, 2004. CO_2, temperature, and relative humidity sensors were deployed in two locations to record space conditions for the facility. On July 21, 2004, supply and return duct leakage measurements were taken and sensor data was downloaded. Sensors were redeployed to continue recording data for until August 17. Test personnel for July 15, 2004 were Dan Gott, Kenneth Larchar, and Hugh Henderson. Dan Gott and Kenneth Larchar completed testing on July 21, 2004. Dan Gott collected temperature/RH and CO_2 sensors on August 17, 2004.

Building Envelope Airtightness

Due to the nature of the business, we were not able to assess building leakage rates using fan depressurization methods. However, the leakage characteristics of the building envelope were inferred from the air flow imbalance and the operating pressure of the building. This single operating point is used with an assumed exponent of 0.6 to 0.65 to find the flow coefficient.

The resulting ACH_{50} was 13-15, assuming the range of measured pressures and exponents. This implies the building was very tight.

Flow Imbalance:	1,471 cfm (exhaust)
Pressure:	-4.5 Pa
Assumed Exponent (n):	0.60-0.65
Resulting cfm_{50}:	6,040-6,800 cfm

Resulting ACH_{50}: 13-15 1/h

Assumed Flow Equation: $Q = 560 \cdot \Delta p^{0.63}$

Pressure Mapping

Pressure readings in the building were taken using a digital micromanometer (DG 700) under normal operating conditions. With the RTUs and exhaust fans operating and all exterior doors closed, the building was depressurized approximately 3 – 5 Pa. Figure A7-13 shows the pressure differences across the main doorways and restrooms in the building. The arrows on the figure indicate the direction of airflow (and decreasing pressure).

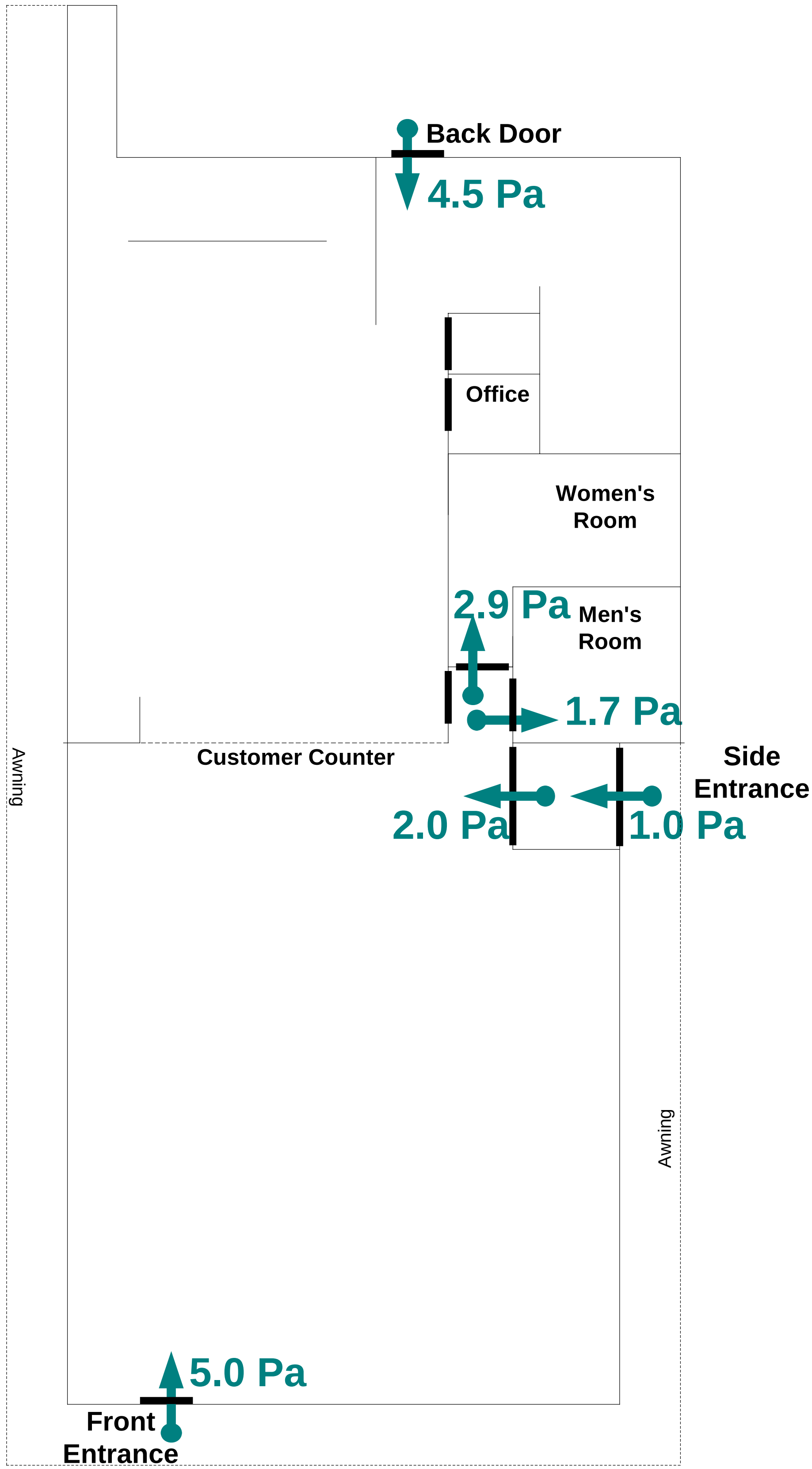

Figure A7-13. Pressure Differences under Normal Operating Conditions

HVAC Airflow Measurements

The ventilation air provided by the RTUs was measured using a Duct Blaster fan connected to the ventilation hood on the RTU. The flow through the Duct Blaster fan at the standard operating static pressure in the ventilation hood is the amount of fresh air provide by that unit. Ventilation airflow was only measured on RTU-1 and RTU-3 since the economizer dampers on RTU-2 and RTU-4 were closed. Figure A7-14 shows how the Duct Blaster was set up to measure RTU ventilation however the photos are from a different site (site 6) with almost identical roof top units. The same setup was used to test the roof tops at this restaurant. Table A7-3 shows the results for the ventilation airflow tests on RTU-1 and RTU-3.

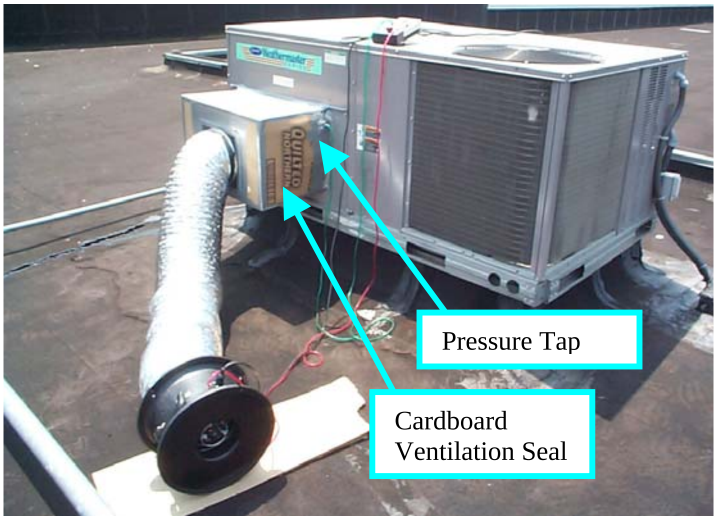

Figure A7-14. Duct Blaster Set Up to Measure Ventilation Airflow

Table A7-3. Roof Top Unit Ventilation Airflow Data

RTU-1

	Test Date (7/15/04)
Static Pressure in Ventilation Hood (Pa)	8.9
Airflow @ Average Ventilation Static (cfm)	444
R-Squared	0.867

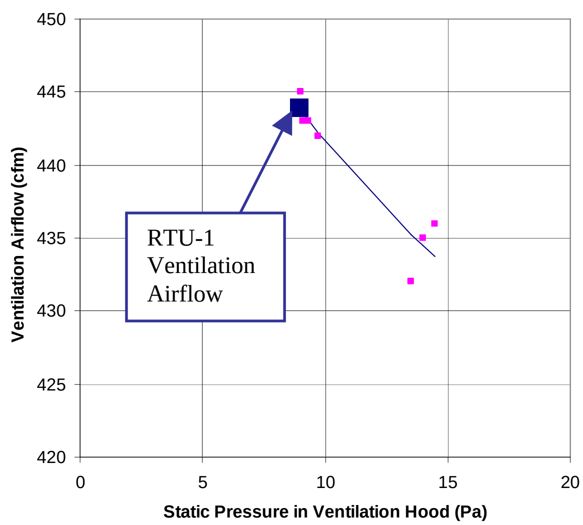

Test Data:

Nominal Ventilation Static (Pa)	Nominal Flow (cfm)	Ring
9.0	445	2
9.1	443	2
9.3	443	2
9.7	442	2
13.5	432	2
14.0	435	2
14.5	436	2

RTU-3

	Test Date (7/15/04)
Static Pressure in Ventilation Hood (Pa)	5.5
Airflow @ Average Ventilation Static (cfm)	403
R-Squared	0.879

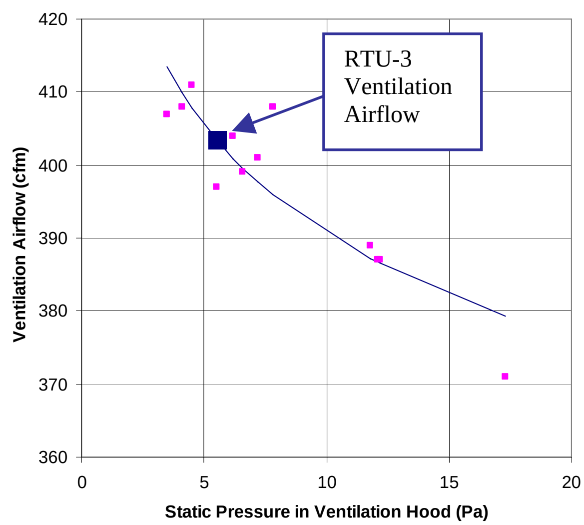

Test Data:

Nominal Ventilation Static (Pa)	Nominal Flow (cfm)	Ring
17.3	371	2
12.2	387	2
12.1	387	2
11.8	389	2
7.8	408	2
7.2	401	2
6.6	399	2
6.2	404	2
5.5	397	2
4.5	411	2
4.1	408	2
3.5	407	2

The airflow for the restroom exhaust fan (EF-3) was measured using a capture tent. The tent was set up to measure the airflow through a fan when the static pressure inside the tent is zero Pa with respect to outdoors (Figure A7-15). The photos in Figure A7-15 were taken at site 6 however the same setup was used to measure exhaust flow at this restaurant. There are three holes in the capture tent for various diameter fans. The exhaust fan was tested using a Duct Blaster fan because the airflow was less than the maximum Duct Blaster fan flow (approx. 1,500 cfm at 0 Pa). The Blower Door fan was only used to seal the tent hole sized for that fan. The third hole in the tent was sealed using the flexible duct transition piece[1] that came with the Duct Blaster. After sealing the hole in the transition piece with Duct Mask plastic wrap, the transition piece was inserted into the tent (lower right picture in Figure A7-15).

To prevent the exhaust fan flow from backing up into the store, we started the Duct blaster fan and slowly zipped up the capture tent while adjusting the fan flow. Static pressure was measured inside the tent with respect to outdoors. The Duct Blaster flow conditioner was used (since the exhaust flow was less than 800 cfm[2]) and the velocity pressure was measured across the Duct Blaster fan using the pressure traverse that comes with the Duct Blaster. Several data points were taken at positive and negative static pressures in the tent to create a flow curve used to determine the exhaust fan flow at 0 Pa. Table A7-4 shows the raw data and results for the restroom exhaust fan (EF-3).

[1] The transition piece (from the flexible extension duct) is normally mounted to a duct or diffuser and then the flexible duct is connected between the duct transition piece and the Duct Blaster.
[2] One of the orifice rings 1-3 must be used with the flow conditioner which limits the Duct Blaster airflow to approximately 800 cfm at 0 Pa with ring 1.

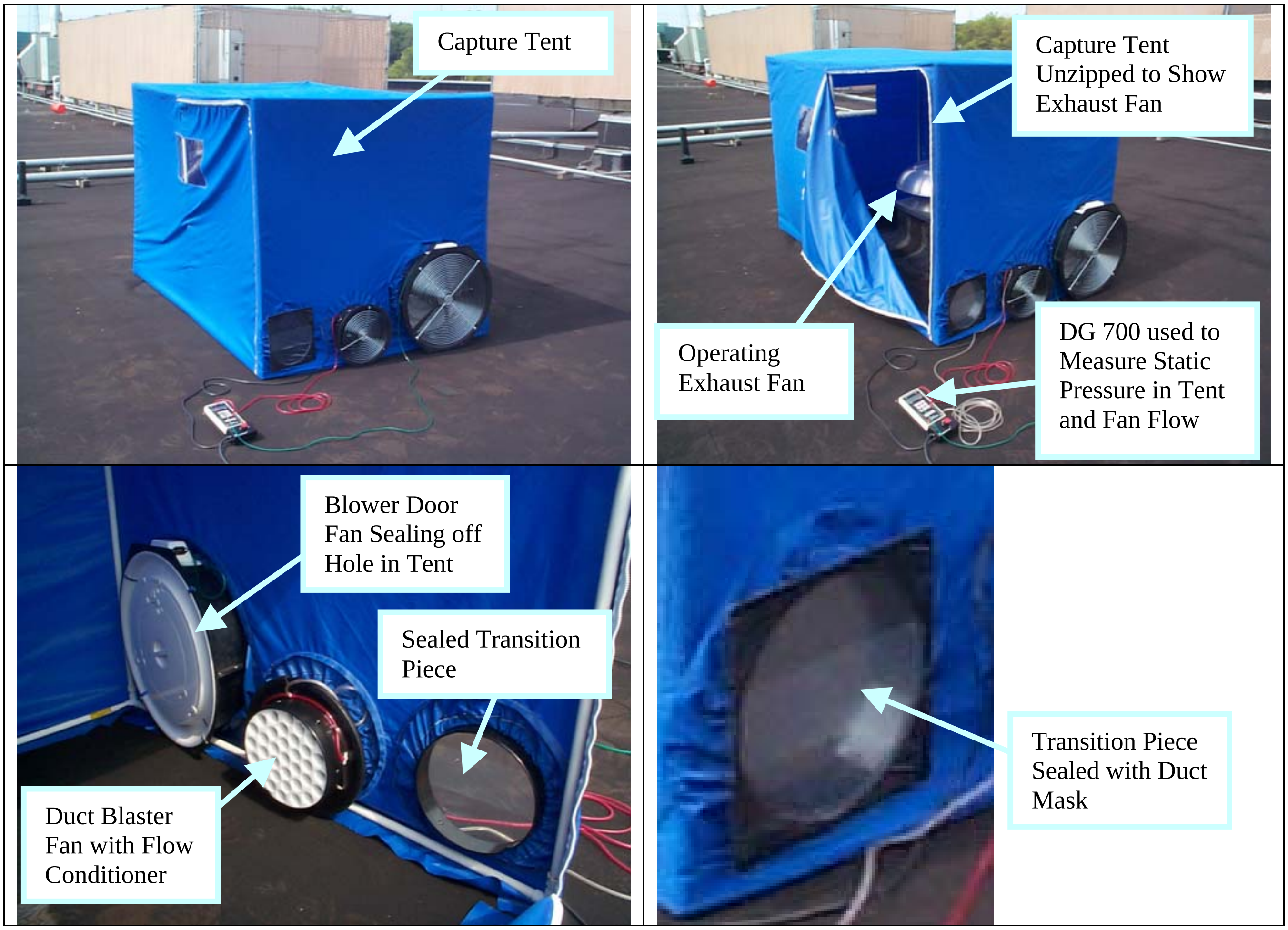

Figure A7-15. Capture Tent Set Up to Measure Exhaust Fan Flow (Photos from Site 6 – Supermarket)

Table A7-4. EF-3 Exhaust Fan Flow Data

EF-3

Test Results:

Slope	-5.5	
Intercept	303.9	
R-Squared	0.98	
Outdoor Air Pressure	0.0	Pascal
Airflow	303.9	cfm

Test Data:

Nominal Duct Pressure (Pa)	Nominal Flow (cfm)	Ring
-8.4	350	1
-8.0	350	1
-8.4	352	1
-5.2	337	1
-5.6	336	1
-5.4	337	1
0.1	296	1
-0.3	295	1
0.4	296	1
5.8	270	1
6.4	272	1
6.4	270	1
6.6	273	1
6.6	270	1

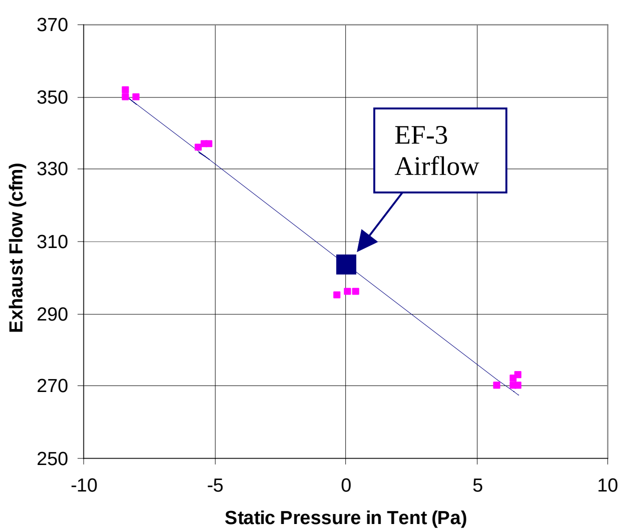

Since the capture tent would not fit over EF-1 or EF-2, we used a TSI hot wire anemometer to measure the exhaust flow by applying the equal area method (12 data points) for each fan. EF-1 has a measured airflow of 1,112 cfm (2,120 fpm average) and EF-2 has a measured airflow of 903 cfm (1,720 fpm average). Table A7-5 and Table A7-6 show the airflows and power usage for the exhaust fans and roof top units. Table A7-7 shows a summary of the HVAC equipment sizing normalized to floor area.

Table A7-5. Measured Data for Exhaust Fans Installed at Site

Exhaust fans	EF-1 Back Grill	EF-2 Kitchen	EF-3 Restrooms	Total
Exhaust Temperature (°F)	169	106	68	
Airflow (cfm)	903	1,112	304	2,319
Power (kW)	0.44	0.57		
Normalized Power (W/cfm)	0.49	0.51		

Table A7-6. Measured Data for RTUs

	Design Values	Measured Values					
	Supply Airflow (cfm)	Diffuser Supply (cfm)	Diffuser Return (cfm)	Ventilation Airflow (cfm)	Fresh Air Fraction	Supply Fan Power (kW)	Normalized Supply Fan Power (W/cfm)
RTU-1 Back Grill Area	2,100			444	21%*	1.14**	
RTU-2 Kitchen	2,100			0 (dampers closed)	0%	1.23**	
RTU-3 Dining & Counter	2,100	1,942	1286	403	21%	1.13	0.58
RTU-4 Front Dinning	2,100	1,668	1540	0 (dampers closed)	0%	1.05	0.63
Totals	8,400			848		1.14	

* This fresh air fraction is based on the design supply airflow.
** These power reading were taken previously in 2002

Table A7-7. Summary of HVAC Equipment Sizing

	Area Used for Normalization	Design		Measured	
		Totals	Normalized	Totals	Normalized
SupplyAirflow (cfm)	Dining Area	4,200	2.55 cfm/ft^2	3,610	2.19 cfm/ft^2
Ventilation Airflow (cfm)	Entire Building	----	----	848	0.26 cfm/ft^2
Exhaust Airflow (cfm)	Entire Building	----	----	2,319	0.70 cfm/ft^2

The supply and return airflow for the dining area (RTU-3 & RTU-4) was measured at the diffusers using a Shortridge flow hood. Positioning and various obstructions prohibited testing of the diffusers in the kitchen area (RTU-1 & RTU-2). Figure A7-16 illustrates the location of the supply and return diffusers and the corresponding airflow measurements. Table A7-8 displays the static pressures in the various sections of the four units during standard operation.

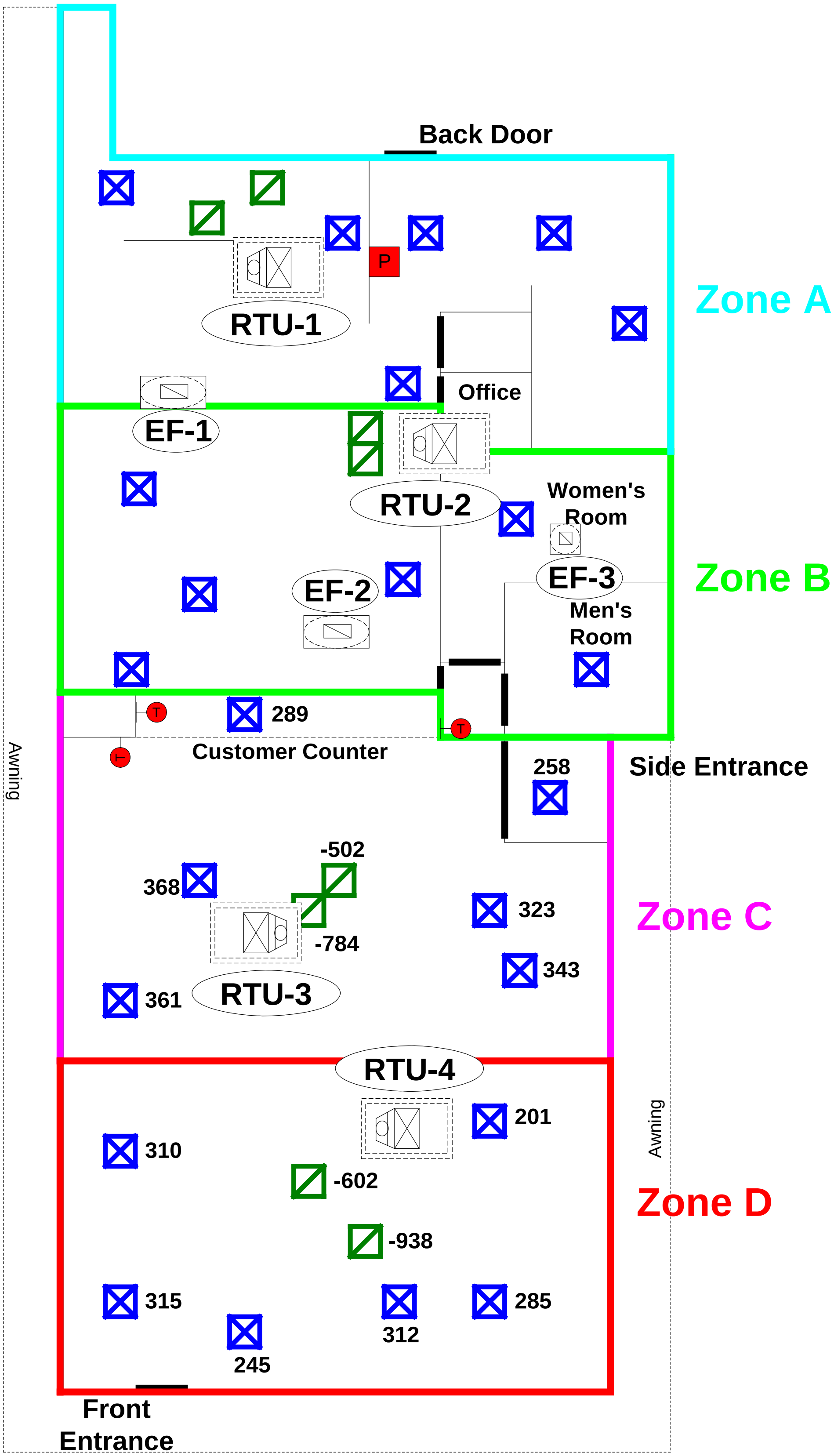

Figure A7-16. Diffusers Airflow Measurements

Table A7-8. Static Pressures in RTUs (Standard Operation on July 21, 2004)

	Ventilation (Pa)	Return (Pa)	Supply (Pa)	Inlet to Supply Fan (Pa)
RTU-1	**-9.5**	**-127.4**	**94.5**	**-252**
RTU-2	**0.3 (dampers closed)**	**-129.0**	**86.5**	**-243**
RTU-3	**-3.7**	**-111.0**	**163.9**	**-260**
RTU-4	**0.5 (dampers closed)**	**-139.4**	**200.0**	**-278**

Duct Leakage Measurements

A Duct Blaster was used to measure leakage rates for the supply and return ductwork of RTUs 3&4. In order to maintain comfort within the restaurant, all units were kept running except the one being tested. Plastic wrap was used to cover each supply and return diffuser for the roof top unit being tested. To isolate the supply side from the return side, we sealed off the supply fan (See Figure A7-17). A sufficient seal was verified by measuring the static pressure in the return side with the supply ductwork depressurized. When the supply side was depressurized approximately 28 Pa, the return side was depressurized less than 5 Pa verifying a relatively tight seal. The Duct Blaster was connected to the RTU by removing an exterior panel in the supply section as shown in Figure A7-18. The static pressure tap was located in the supply section of the RTU as shown in Figure A7-18. Static pressure and airflow measurements were taken with ductwork depressurized from 5 – 30 Pa. The return ductwork was tested in a similar manner by moving the Duct Blaster to the return section. The seal at the supply fan was tested again. A tight seal was verified by depressurizing the return section by 26 Pa and measuring the static pressure in the supply section (depressurized by only 4 Pa).

Unblocked Supply Side

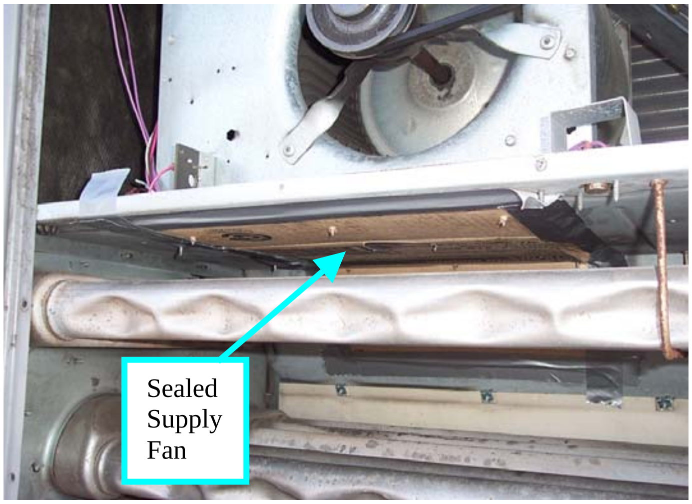

Blocked Supply Side

Figure A7-17. Sealing Supply from Return

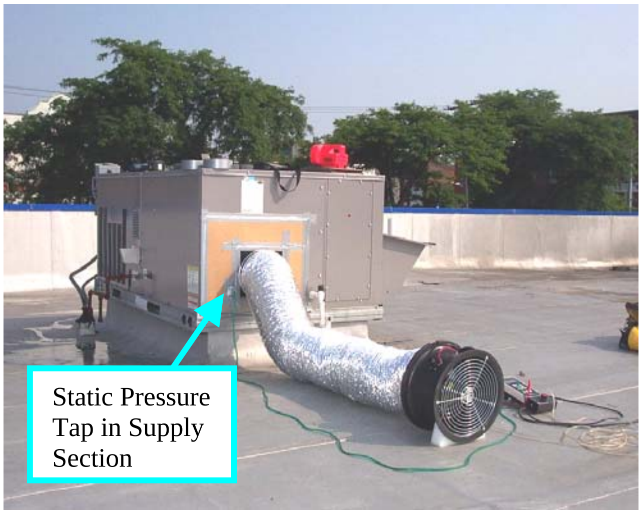

Supply Side

Return Side

Figure A7-18. Photos of Duct Blaster Setup and Testing

While supply and return ducts were depressurized, static pressures were taken at all corresponding supply and return diffusers. Figure A7-19 shows the resulting pressures measured at each diffuser with the ductwork for RTU-3 and RTU-4 depressurized. The uniformity of the pressures at the diffusers implies that leaks are uniformly spread around the systems. Table A7-9 summarizes the results.

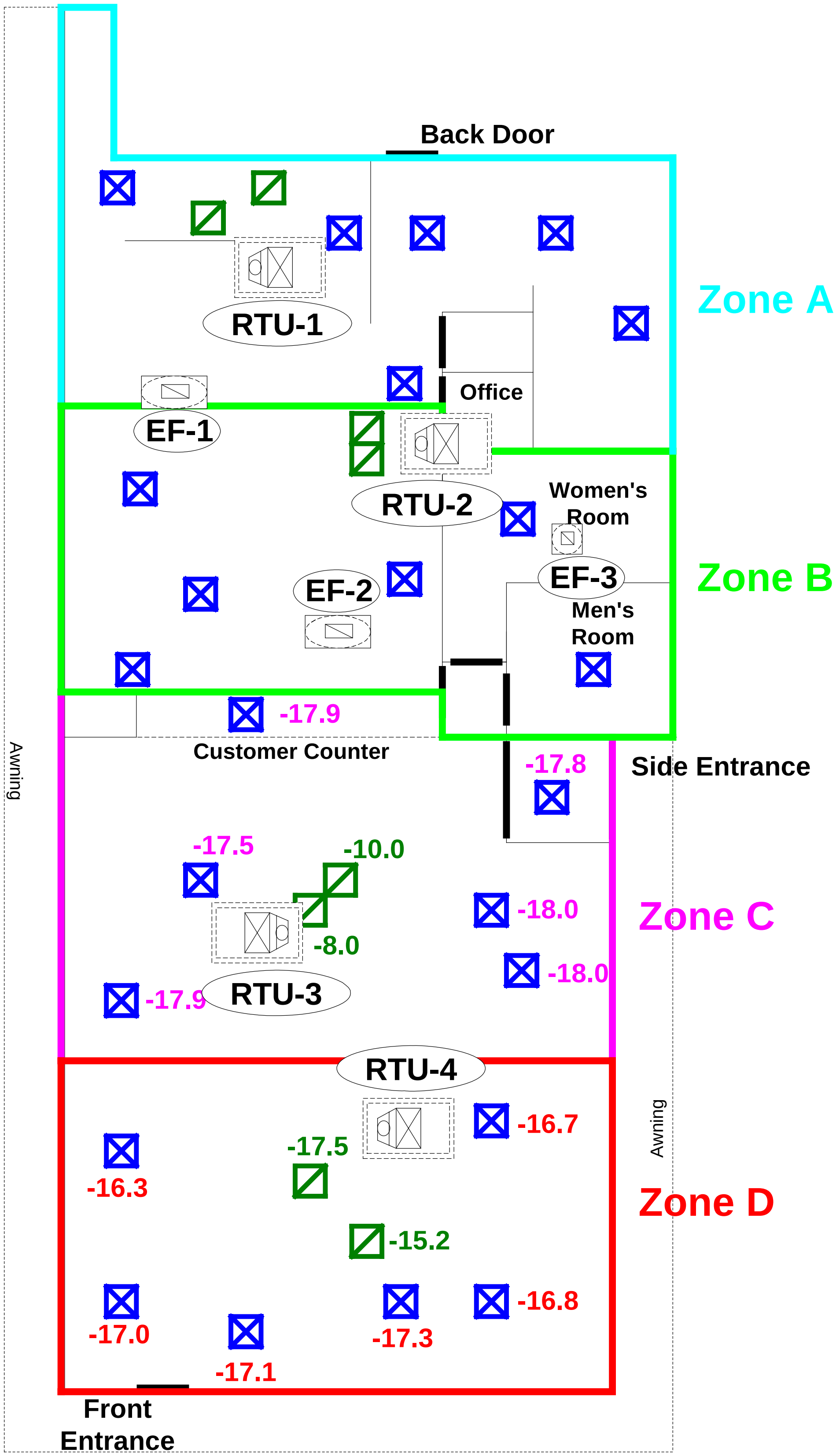

Figure A7-19. Supply/Return Pressure Mapping while System Depressurized

Table A7-9. Static Pressures at Diffusers with Ducts Depressurized Using Duct Blaster

	Corresponding Zone	Duct Depressurization (Pa)	Average Diffuser/Return Pressure (Pa)
RTU-3 Supply	C	-29.7	-18.2
RTU-3 Return	C	-20.0	-9.0
RTU-4 Supply	D	-26.5	-16.9
RTU-4 Return	D	-24.0	-16.4

Figure A7-20 shows the resulting measured data from the duct leakage tests fit to a power function (raw data in Table A7-10). Table A7-11 shows the resulting coefficients, exponents, and regression statistics. Table A7-12 summarizes the resulting duct leakage rates and ELA at a reference pressure of 25 Pa.

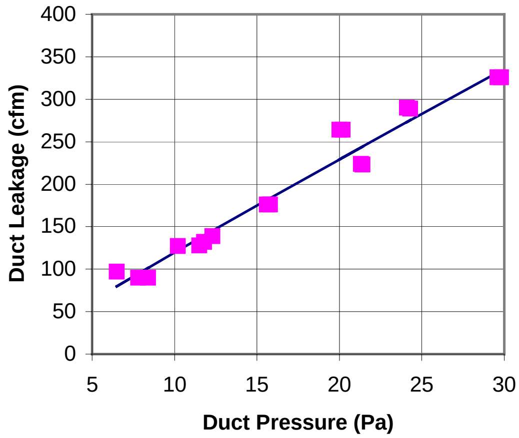

RTU-3 Supply Ductwork

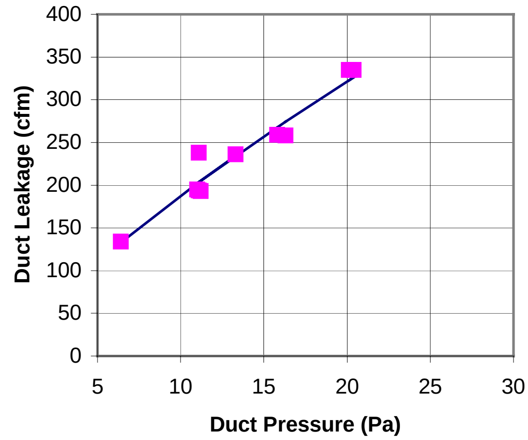

RTU-3 Return Ductwork

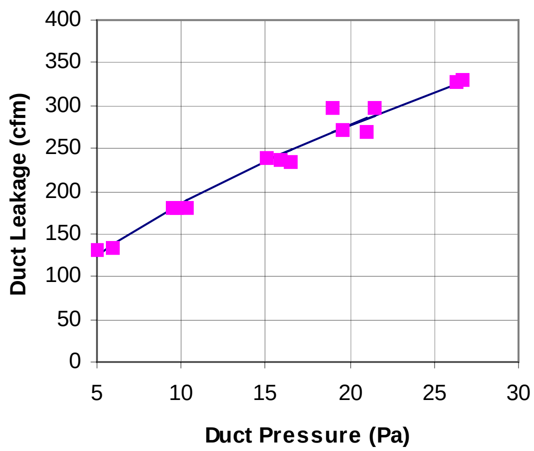

RTU-4 Supply Ductwork

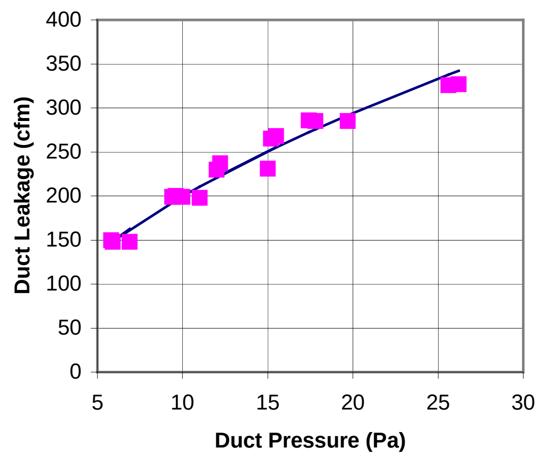

RTU-4 Return Ductwork

Figure A7-20. Duct-Blaster Tests on Supply and Return Ductwork

Table A7-10. Raw Data from Duct-Blaster Tests

RTU-3 Supply Ductwork

Nominal Duct Pressure (Pa)	Nominal Flow (cfm)	Ring
29.8	326	2
29.6	326	2
24.1	290	2
24.3	289	2
20.2	264	2
20.0	264	2
21.4	223	2
21.3	224	2
15.6	176	2
15.8	176	2
12.3	139	2
11.8	132	2
11.5	128	2
10.2	127	2
6.5	97	2
7.8	90	2
8.4	90	2

RTU-3 Return Ductwork

Nominal Duct Pressure (Pa)	Nominal Flow (cfm)	Ring
20.1	335	2
20.4	335	2
16.3	258	2
15.8	259	2
11.1	238	2
13.3	236	2
11.2	193	2
11.0	195	2
11.1	194	2
6.4	134	2

RTU-4 Supply Ductwork

Nominal Duct Pressure (Pa)	Nominal Flow (cfm)	Ring
26.7	330	2
26.3	328	2
19.0	297	2
21.5	298	2
19.6	271	2
21.0	270	2
15.1	239	2
16.5	234	2
15.9	236	2
10.3	181	2
9.5	181	2
9.7	181	2
6.0	134	2
5.0	132	2

RTU-4 Return Ductwork

Nominal Duct Pressure (Pa)	Nominal Flow (cfm)	Ring
26.2	327	2
25.6	326	2
19.7	285	2
17.8	285	2
17.4	286	2
15.2	265	2
15.5	268	2
12.0	230	2
12.2	237	2
15.0	231	2
11.0	198	2
9.4	199	2
9.6	200	2
10.0	199	2
5.9	148	2
6.9	148	2
5.8	150	2

Table A7-11. Coefficients, Exponents and Regression Statistics from Duct-Blaster Tests

	K	n	R^2
RTU-3 Supply	13.7	0.940	96.1%
RTU-3 Return	31.5	0.775	94.4%
RTU-4 Supply	49.2	0.577	98.0%
RTU-4 Return	55.2	0.559	96.5%

Notes: cfm = $K(Pa)^n$ / R^2 indicates fit of linear log-log regression

Table A7-12. Comparison of Supply and Return Airflow Measurements

	Diffuser Airflow (cfm)	Leakage (cfm @ 25)	Ductwork & AHU Cabinet (sq in @ 25)
RTU-3 Supply	1,942	283	32
RTU-3 Return	1,286	382	43
RTU-4 Supply	1,668	315	36
RTU-4 Return	1,540	333	38

Notes: Leakage and ELA at reference pressure of 25 Pa

The effective leakage area compared to the total duct surface area is shown in Table A7-13. On the supply side, there is 14 – 16 sq-in of duct leakage for every 100 sq-ft of duct surface. The leakage area for the return systems was nearly triple that of the supply systems (40 – 46 sq-in per 100 sq ft duct area). The Sheet Metal and Air Conditioning Contractors' National Association (SMACNA) classifies duct leakiness using duct leakage per 100 sq ft of duct area at a pressure of 1-in w.g. The SMACNA leakage class for the two systems varied between 518 and 2,415.

Table A7-13. Duct Leakage per 100 Square Foot of Duct Area

	Duct Area (sq ft)	ELA (sq in @ 25)	ELA/100 sq ft Duct Area (sq in @ 25)	Leakage (cfm @ 25 Pa)	Supply CFM per Duct Area (cfm/sq ft)	Leakage per 100 sq ft Duct Area (cfm @ 25 Pa)	SMACNA Leakage Class cfm per 100 sq ft (cfm @ 1-in water)
RTU-3 Supply	229	32	14	283	8.5	123	1,072
RTU-3 Return	94	43	46	382	n/a	406	2,415
RTU-4 Supply	229	36	16	315	7.3	138	518
RTU-4 Return	94	38	40	333	n/a	355	1,280

Table A7-14 shows the airflow balance for RTU-3 and RTU-4. Three airflow balance estimates are calculated as follows:

Gross Airflow Balance:

$$\Delta_{gross} = \text{Supply Diffuser cfm} - \text{Return Diffuser cfm} - \text{Ventilation cfm}$$

Net Airflow Balance Using CFM_{25}:

$$\begin{aligned}\Delta_{N25} = {} & (\text{Supply Diffuser cfm} + \text{Supply Leakage @ 25 Pa}) \\ & - (\text{Return Diffuser cfm} + \text{Return Leakage @ 25 Pa}) \\ & - \text{Ventilation cfm}\end{aligned}$$

Net Airflow Balance Using Average "Actual Static" in Ductwork:

$$\Delta_{Ncorrected} = (\text{Supply Diffuser cfm} + \text{Supply Leakage @ Actual Static}) - (\text{Return Diffuser cfm} + \text{Return Leakage @ Actual Static}) - \text{Ventilation cfm}$$

The last estimate for the RTU airflow balance ($\Delta_{Ncorrected}$) uses our best estimate for average "actual static" pressure in the ductwork during normal operation, which is one half of the plenum pressure as suggested in ASHRAE Standard 152P section B.2. For this ductwork, the net airflow estimate resulting in the smallest error is Δ_{N25}. The net airflow balance estimate with the value closest to zero gives the most accurate results for airflow combined with duct leakage. Figure A7-21 shows a diagram of the roof top units including the supply, return, and ventilation airflows as well as the duct leakage for the best estimate in this case which uses the CFM_{25} for duct leakage.

Table A7-14. Airflow Balance for Roof Top Units

	RTU-3	RTU-4
Diffuser Supply (cfm)	1,942	1,668
Diffuser Return (cfm)	1,286	1,540
Ventilation (cfm)	403	0
Supply Leakage - cfm25	283	315
- actual static	863	701
Return Leakage - cfm25	382	333
- actual static	709	591
Δgross	253	128
ΔN25	153	110
ΔNcorrected	407	238

Note: "actual static" is 1/2 the static pressure measure at the unit.

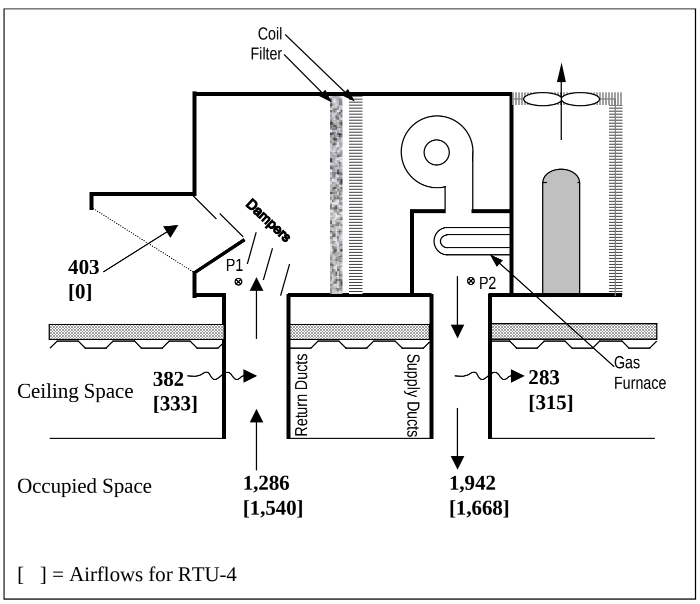

Figure A7-21. Airflow Balance for RTU-3 and RTU-4

Space Conditions

Figure A7-22 shows the average temperature profiles based on temperature readings taken with a HOBO data logger from July 15 to August 17, 2004. The thick line shows the average for each hour while the shaded region corresponds to one standard deviation about the average. The dotted lines correspond to the minimum and maximum for each hour. Sensors were placed in the customer dinning area and on the wall near the order counter.

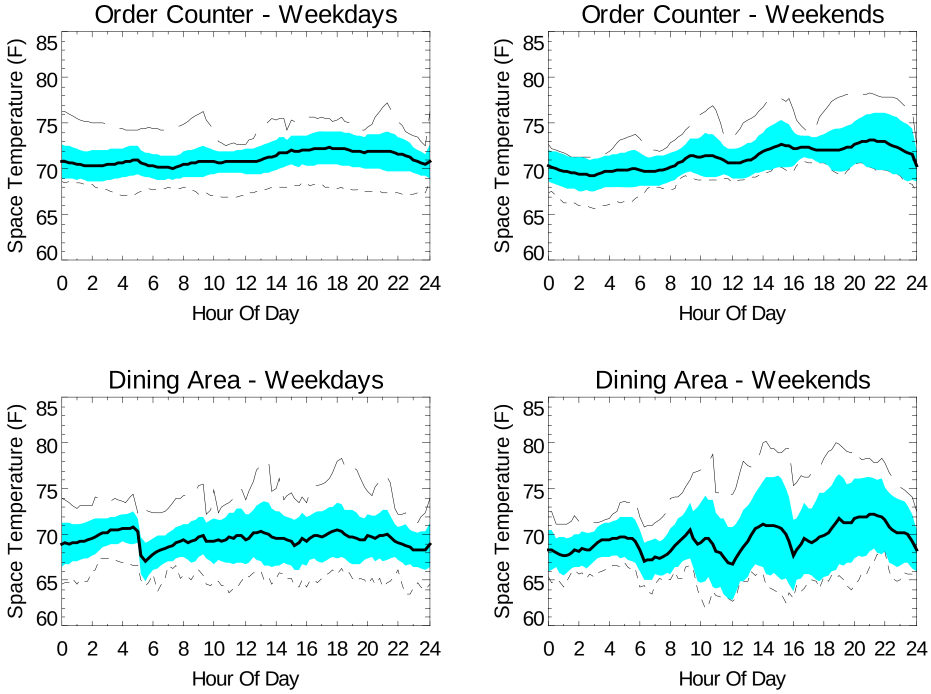

Figure A7-22. Measured Space Temperature Profiles

Figure A7-23 shows the CO_2 concentration in the area near the order counter. The CO_2 concentration provides an indication of occupancy. The next section uses the CO_2 as a tracer gas to estimate the infiltration/ventilation rate into the building.

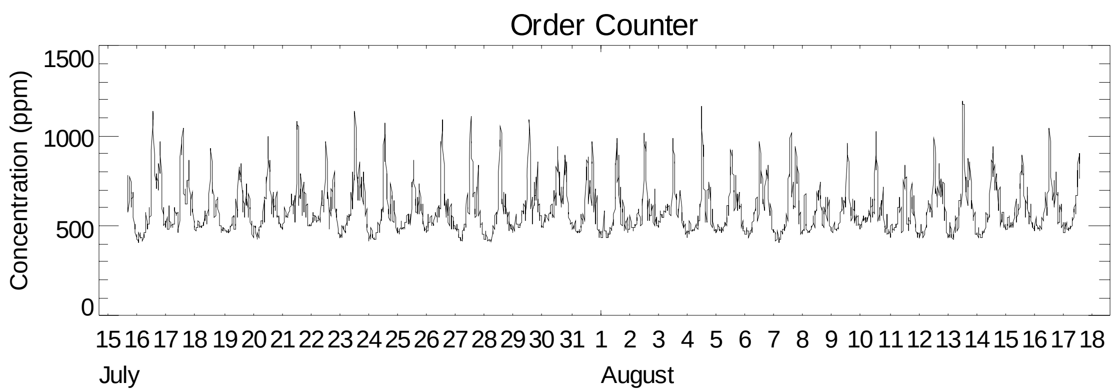

Figure A7-23. Measured CO_2 Concentration

The following plots show the relative humidity for this building. The relative humidity inside the store exceeded 60 percent for 30% of the time that the sensors were in place at the order counter and 49% of the time in the dining area. Figure A7-27 displays the conditions inside the building compared with the ASHRAE comfort zone for cooling shown by the shaded region on the plot.

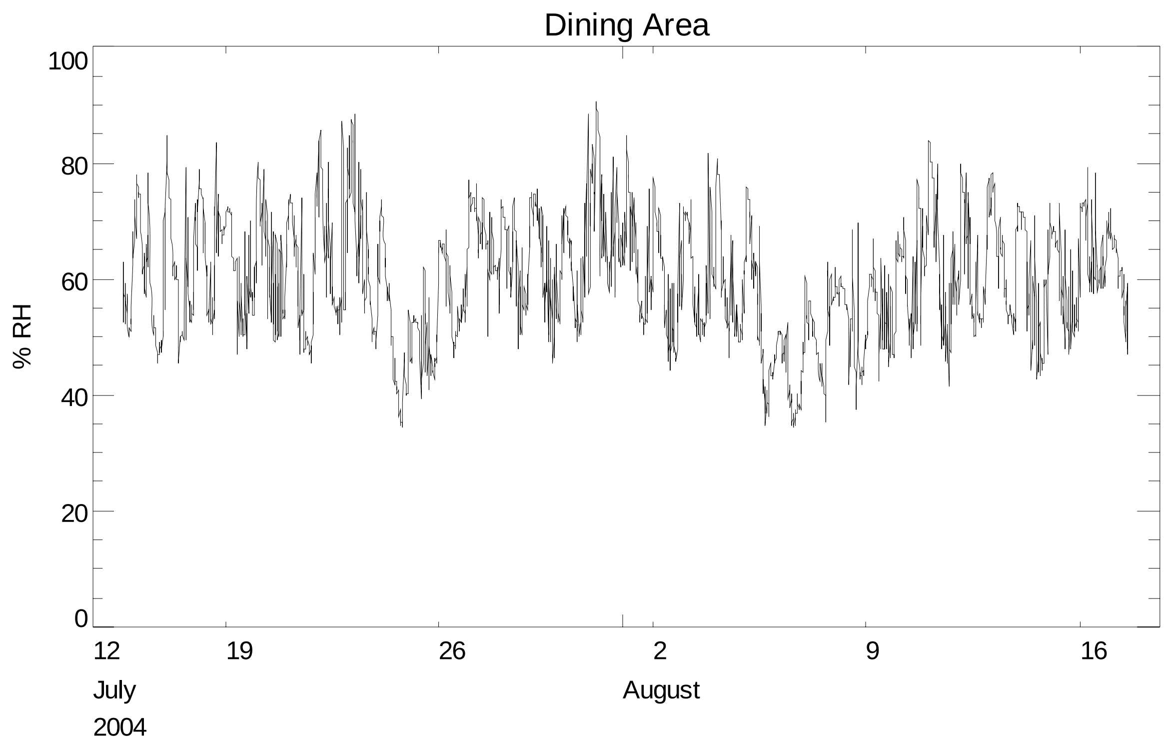

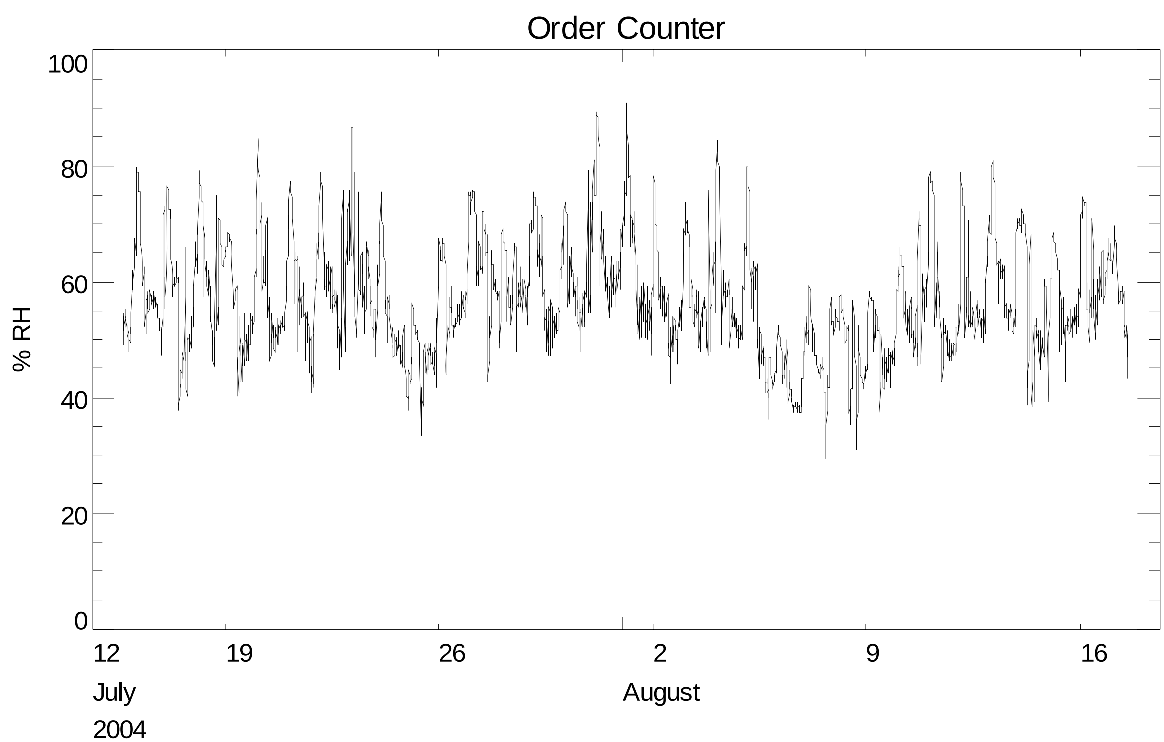

Figure A7-24. Measured Relative Humidity

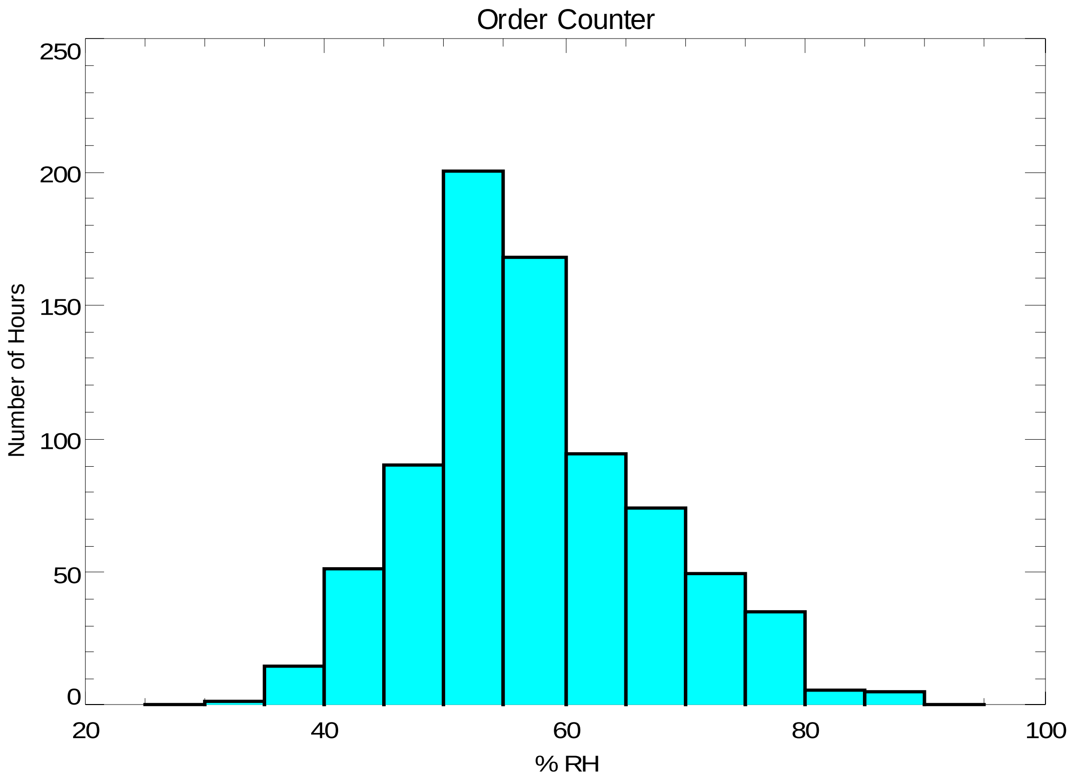

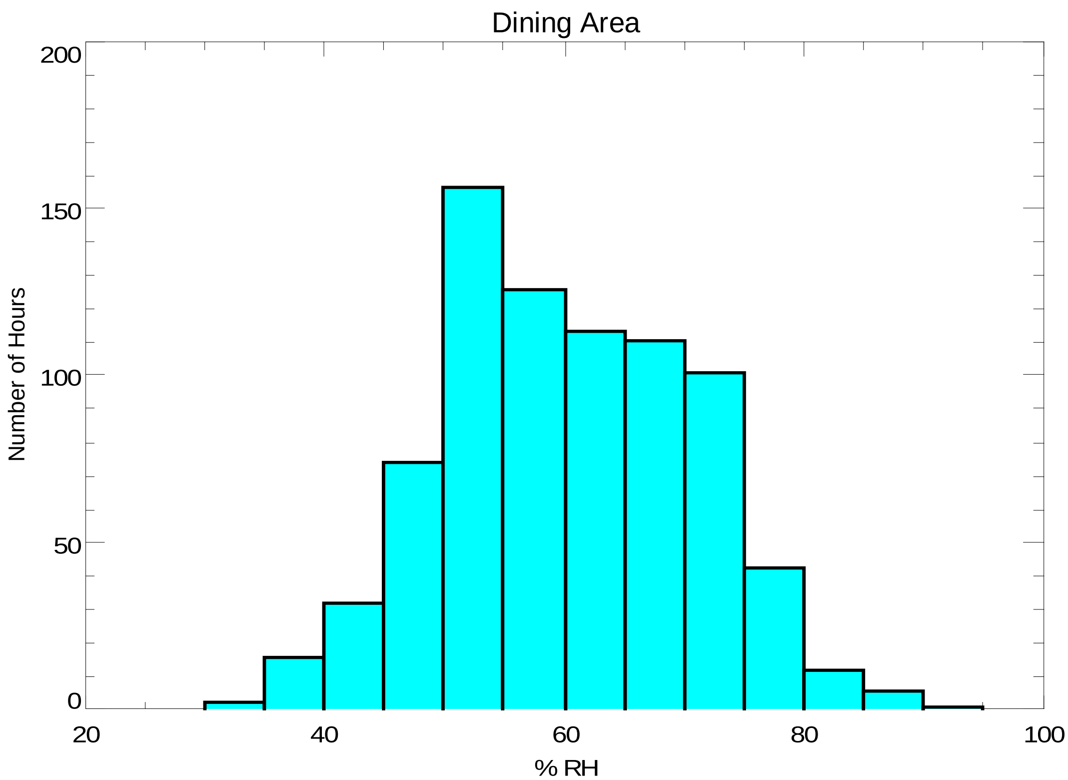

Figure A7-25. Duration of Relative Humidity Levels

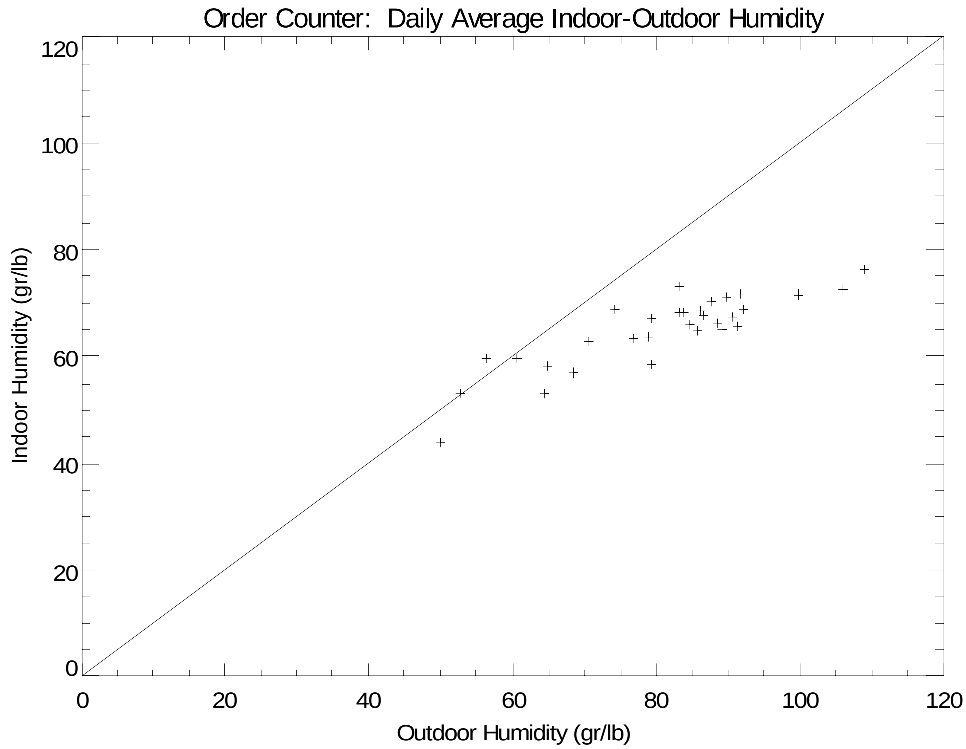

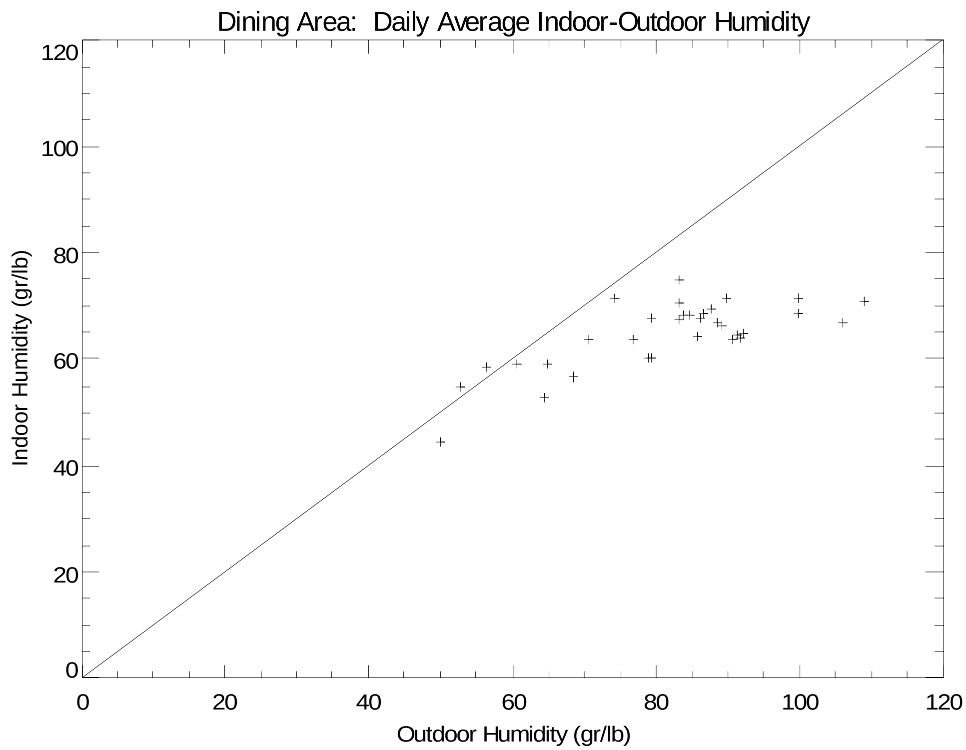

Figure A7-26. Indoor Humidity Variation with Outdoor Humidity

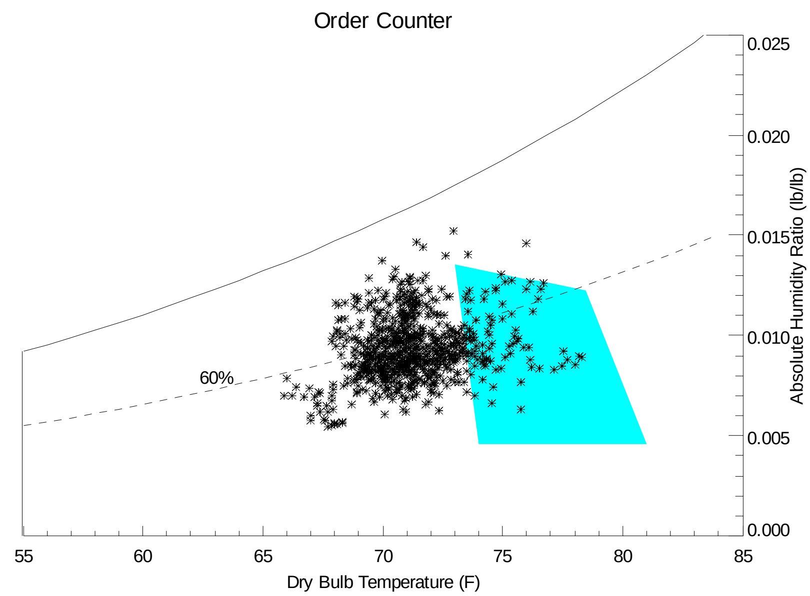

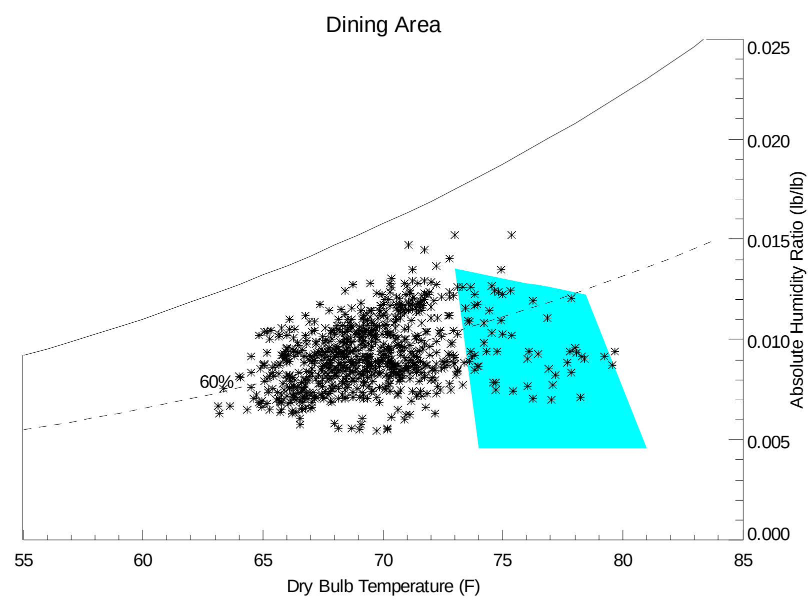

Figure A7-27. Indoor Air Quality Comparison with ASHRAE Comfort Zone for Cooling

Utility Bills

Electricity is primarily used for food preparation and air conditioning. Natural gas is used for heating and cooking. The tables and graphs below show the gas and electric use trends for the facility. The baseline gas use for cooking is 31.6 therm/day. The overall energy use index for the building is summarized below.

	Utility Gas Use		Utility Electric Use	
	Cooking Gas Use ($MBtu/ft^2$-year)	Heating Index ($MBtu/ft^2$-year)	Baseline Elec. Use (kWh/ft^2-year)	Cooling Index (kWh/ft^2-year)
2003-2004 Season	350	81.7	106.7	9.34

Note: Season is from June 2003 to May 2004

Table A7-15. Summary of Gas Bills

	Days in Month	Gas Use (therms)	Cost ($)	$/therm	Gas Use per Sq-Ft (therm/sq ft)
1/3/03	29	1,639	1,435	0.88	0.497
2/3/03	31	1,596	1,500	0.94	0.484
3/3/03	29	1,172	1,458	1.24	0.355
4/3/03	29	1,152	1,252	1.09	0.349
5/3/03	33	1,102	1,244	1.13	0.334
6/3/03	29	915	986	1.08	0.277
7/3/03	31	984	945	0.96	0.298
8/3/03	33	1,039	885	0.85	0.315
9/3/03	28	889	868	0.98	0.269
10/2/03	29	994	791	0.80	0.301
11/2/03	33	1,443	1,251	0.87	0.437
12/2/03	31	1,664	1,330	0.80	0.504
1/4/04	31	1,722	1,498	0.87	0.522
2/4/04	29	1,330	1,196	0.90	0.403
3/4/04	30	1,185	1,082	0.91	0.359
4/4/04	32	1,114	1,017	0.91	0.338
5/4/04	29	952	889	0.93	0.288
12-mo. Total	365	14,231	$ 12,737	0.90	4.312

Note: 12-month Total is from June 2003 to May 2004

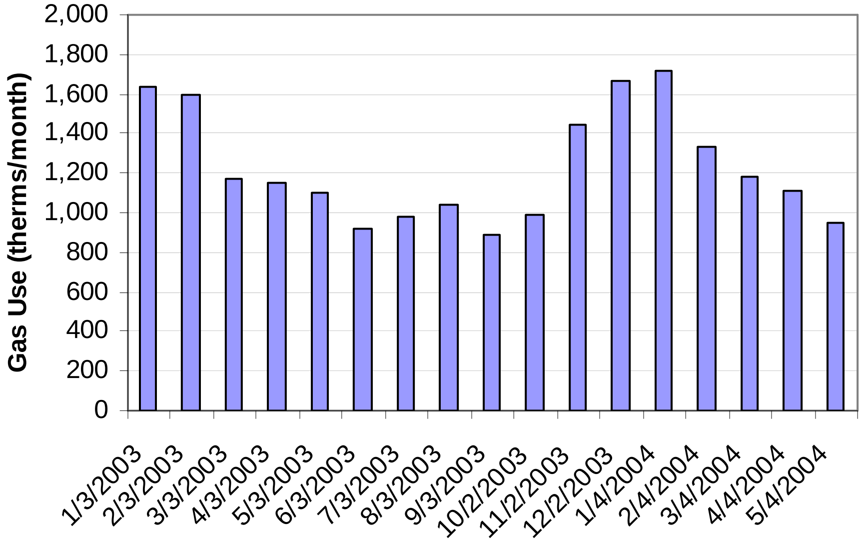

Figure A7-28. Monthly Gas Use Trend

Table A7-16. Summary of Electric Bills

	Days in Month	Demand (kW)	Energy (kWh)	Cost ($)	$/kWh	Elec. Use per Sq-Ft (kWh/sq ft)
1/3/03	30	64.8	27,920	2,930	0.10	8.46
2/3/03	31	64.8	29,760	3,329	0.11	9.02
3/3/03	29	69.6	27,360	3,095	0.11	8.29
4/3/03	29	69.6	27,680	3,050	0.11	8.39
5/3/03	33	----	32,960	3,454	0.10	9.99
6/3/03	29	77.6	31,040	3,299	0.11	9.41
7/3/03	31	75.2	34,560	3,595	0.10	10.47
8/3/03	33	80	38,640	4,141	0.11	11.71
9/3/03	28	77.6	31,360	3,426	0.11	9.50
10/2/03	29	78.4	31,360	3,646	0.12	9.50
11/2/03	33	72.8	34,080	3,880	0.11	10.33
12/2/03	31	67.2	30,800	3,107	0.10	9.33
1/4/04	31	64.8	30,960	3,718	0.12	9.38
2/4/04	29	66.4	28,160	3,353	0.12	8.53
3/4/04	30	71.2	28,800	3,514	0.12	8.73
4/4/04	32	80.8	32,320	3,667	0.11	9.79
5/4/04	29	76.8	30,960	3,451	0.11	9.38
12-mo. Total	365	81	383,040	$42,797	0.11	116.07

Note: 12-month Total is from June 2003 to May 2004

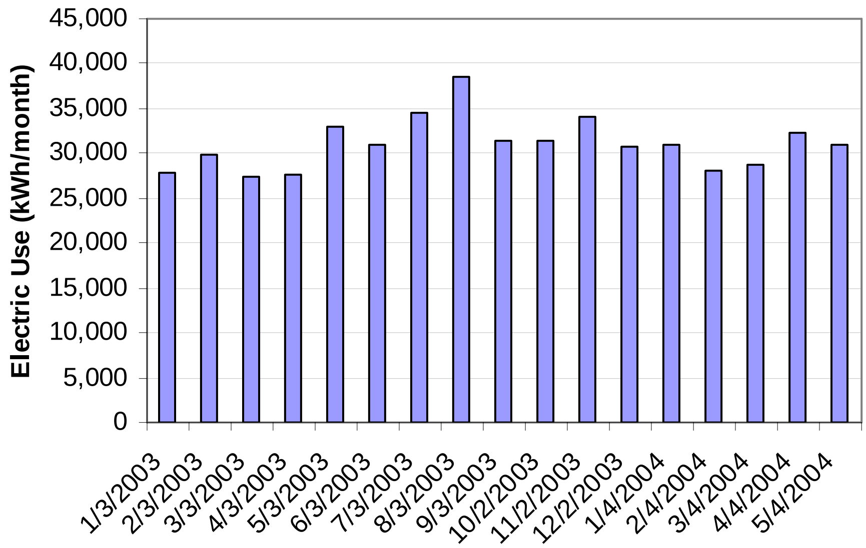

Figure A7-29. Monthly Electric Use Trend

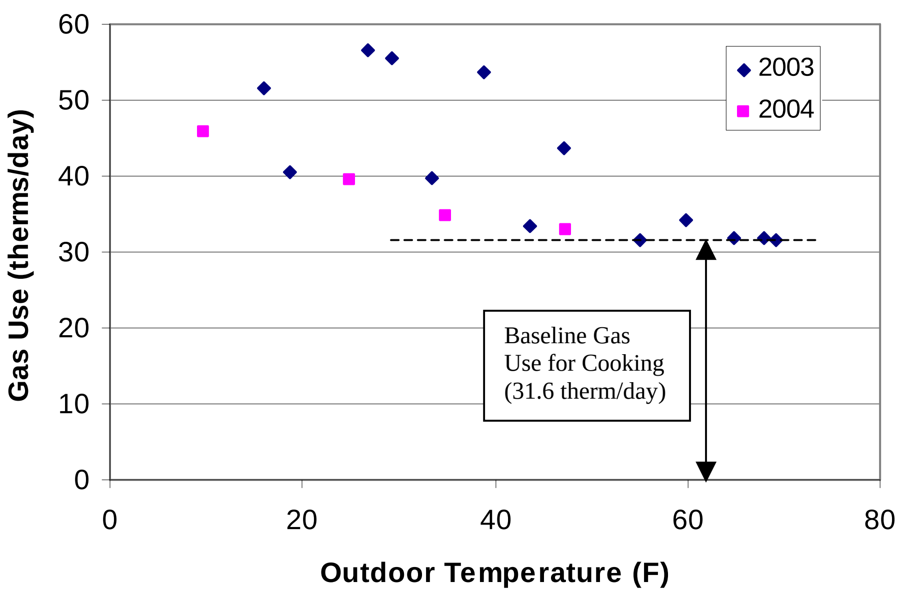

Figure A7-30. Variation of Gas Use with Ambient Temperature

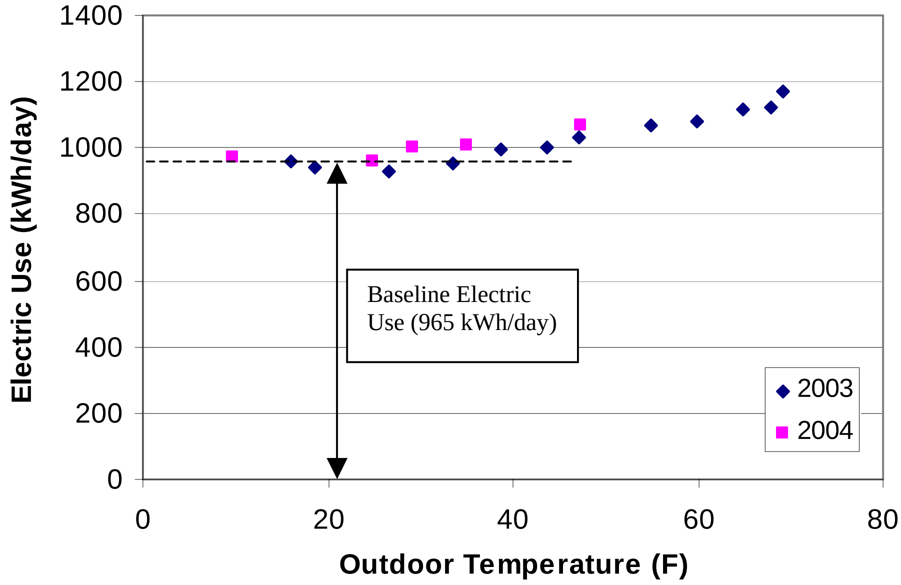

Figure A7-31. Variation of Electric Use with Ambient Temperature

Field Test Site 8 - Church, Rome, NY

Main Entrance at Rear of Building (East)

Side of Building (North)

Figure A8-1. Photos of Building

CHARACTERISTICS

Building Description

The 8,600 sq ft facility is a two-story church that was built in 1990. Figure A8-1 shows the east and north side of the building (building is symmetrical). The building uses eight furnaces to heat and cool the space. The furnaces are forced-air, gas-fired units with an A-coil cooling section. Four outdoor air vents provide ventilation air to each furnace. Each furnace powers a ventilation damper for economizer mode. Figure A8-2 presents the building floor plan.

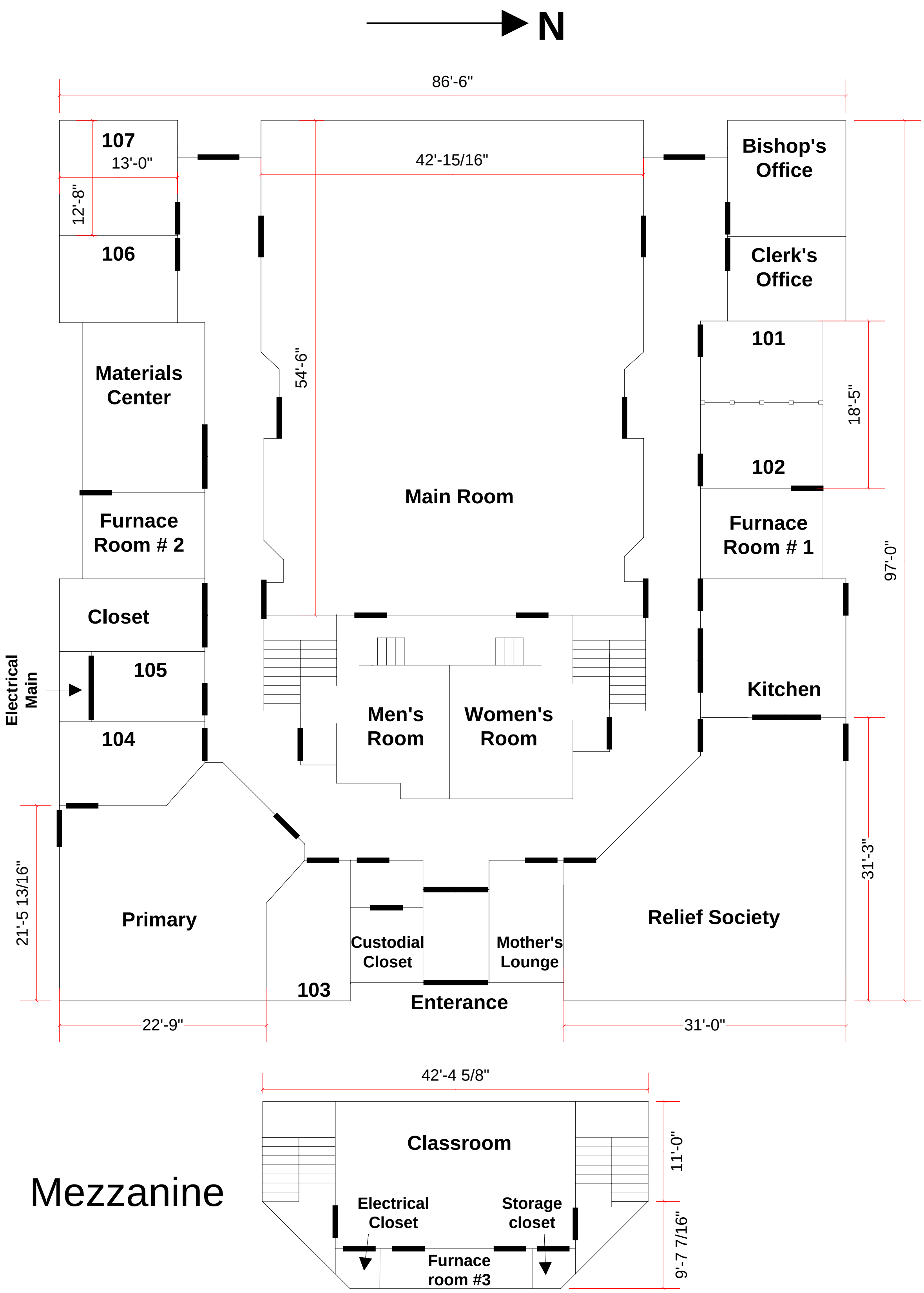

Figure A8-2. Building Floor Plan

Construction Details

Exterior walls are constructed of brick veneer, plywood sheathing, wood 2x6 studs, and gypsum board interior covering. There may be rigid foam insulation or an air gap between the brick and plywood sheathing. The walls are insulated with 6” fiberglass insulation.

The pitched roof is constructed of plywood decking on wooden cathedral style roof beams. Roofing material is asphalt shingles. Insulation is provided by 9½” paper-backed fiberglass batts that are stapled to the roof beams. The interior side of the roof construction is finished with ½-in gypsum board that is taped and spackled. The attic type space between the plywood decking and the gypsum board is vented with vented soffit.

There is a T-bar (drop) ceiling in the rooms around the perimeter of the church. The ceiling in the hallway around the church consists of ceiling tiles glued to the bottom of two sheets of ¾-in plywood. The two sheets of ¾-in plywood provide a walking surface in the ceiling plenum for duct system maintenance, etc. The ceilings in the main room (Chapel) and the upstairs classroom are cathedral ceilings with ceiling tiles glued to sheetrock. There is a ceiling plenum above the drop ceiling and the hallway ceiling around the perimeter of the building. The plenum area is a large space that increases in height from the edge of the building and follows the angle of the pitched roof until it ends at the inner wall of the hallway. There is no ceiling plenum above the upstairs classroom and the main room since these rooms have cathedral style ceilings.

Figure A8-3 illustrates typical wall and roof sections. Figure A8-4 shows pictures of the ceiling plenum and typical diffuser installation. Figure A8-5 shows the attic type space above the cathedral ceiling in the upstairs classroom. The picture on the right in Figure A8-5 shows a wall finished with gypsum board that is the east wall of the main room (Chapel).

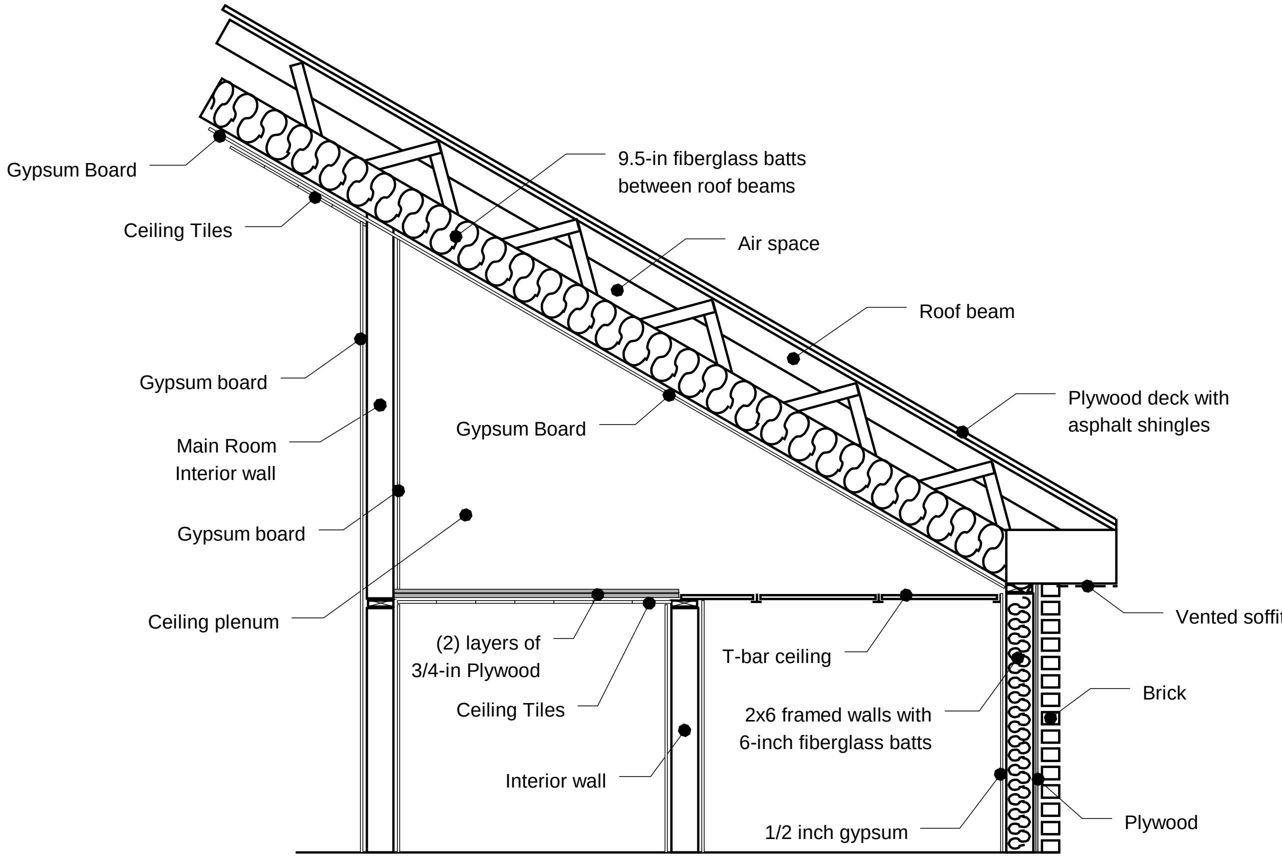

Figure A8-3. Roof and Wall Sections

Ceiling Plenum

Typical Diffuser Installation

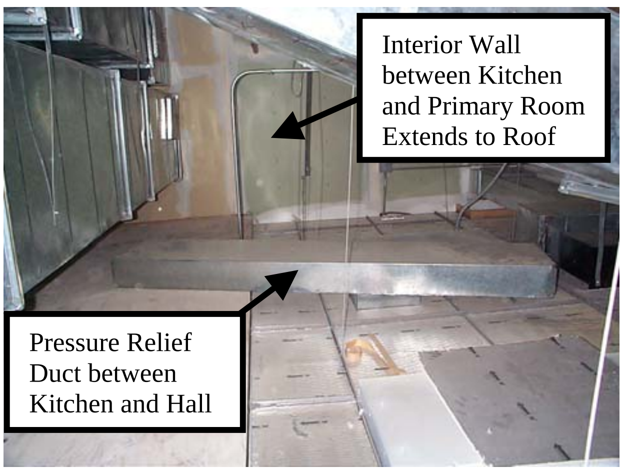

Ceiling Plenum Above Kitchen

Ceiling Plenum Interior Wall

Figure A8-4. Ceiling Plenum

Figure A8-5. Attic Type Space between the Roof and Primary Air Barrier

HVAC System

Eight furnaces in three separate mechanical rooms condition the building. Seven of the eight furnaces have a cooling section with an A-coil on top of the furnace and condensing units outside, on the ground. There are three 3-ton condensing units, one 4-ton unit, three 5-ton units located on the ground outside near the mechanical rooms on the north and south side of the building. Figure A8-6 shows the two models of furnaces used to heat and cool the church. Table A8-1 lists the HVAC equipment that serves the building.

Each furnace has a fresh air duct that pulls air from outdoor air vents on the sides of the building and the gable end above the main entrance. There are dampers in each of the ventilation ducts that are controlled by an economizer on each unit. Insulated supply and return ducts are located in the ceiling plenum (see location of plenum in Figure A8-3). The supply and return ductwork is rectangular sheet metal ducts with 1-in insulation on the inside of all ducts as shown in Figure A8-7. Most of the supply and return diffusers are located in the ceiling however there are a few supply and return grills in the walls. The main room and the upstairs classroom have both supply and return diffusers in the walls and the relief society has supply diffusers in the walls. Figure A8-8 displays the zones within the building and the corresponding AHU that serves each zone.

Lennox Furnace (F3)
Model: G20Q3/4E

Lennox Furnace (F6)
Model: G20Q4E

Figure A8-6. Two Models of Lennox Furnaces

Figure A8-7. Insulated Ductwork

Table A8-1. Summary HVAC Equipment Installed at Site

Furnace	Location	Brand	Model	Heating Capacity (MBtu/h)	Cooling Capacity (tons)
F-1	North Side	Lennox	G20Q3/4E-100-1	100	3
F-2	North Side	Lennox	G20Q3/4E-125-2	125	5
F-3	North Side	Lennox	G20Q3/4E-125-2	125	5
F-3	South Side	Lennox	G20Q3/4E-125-2	125	5
F-4	South Side	Lennox	G20Q3/4E-100-1	100	3
F-5	South Side	Lennox	G20Q3/4E-100-1	100	4
F-6	Upstairs	Lennox	G20Q4E-75-2	75	3
F-7	Upstairs	Lennox	G20Q4E-75-1	75	None

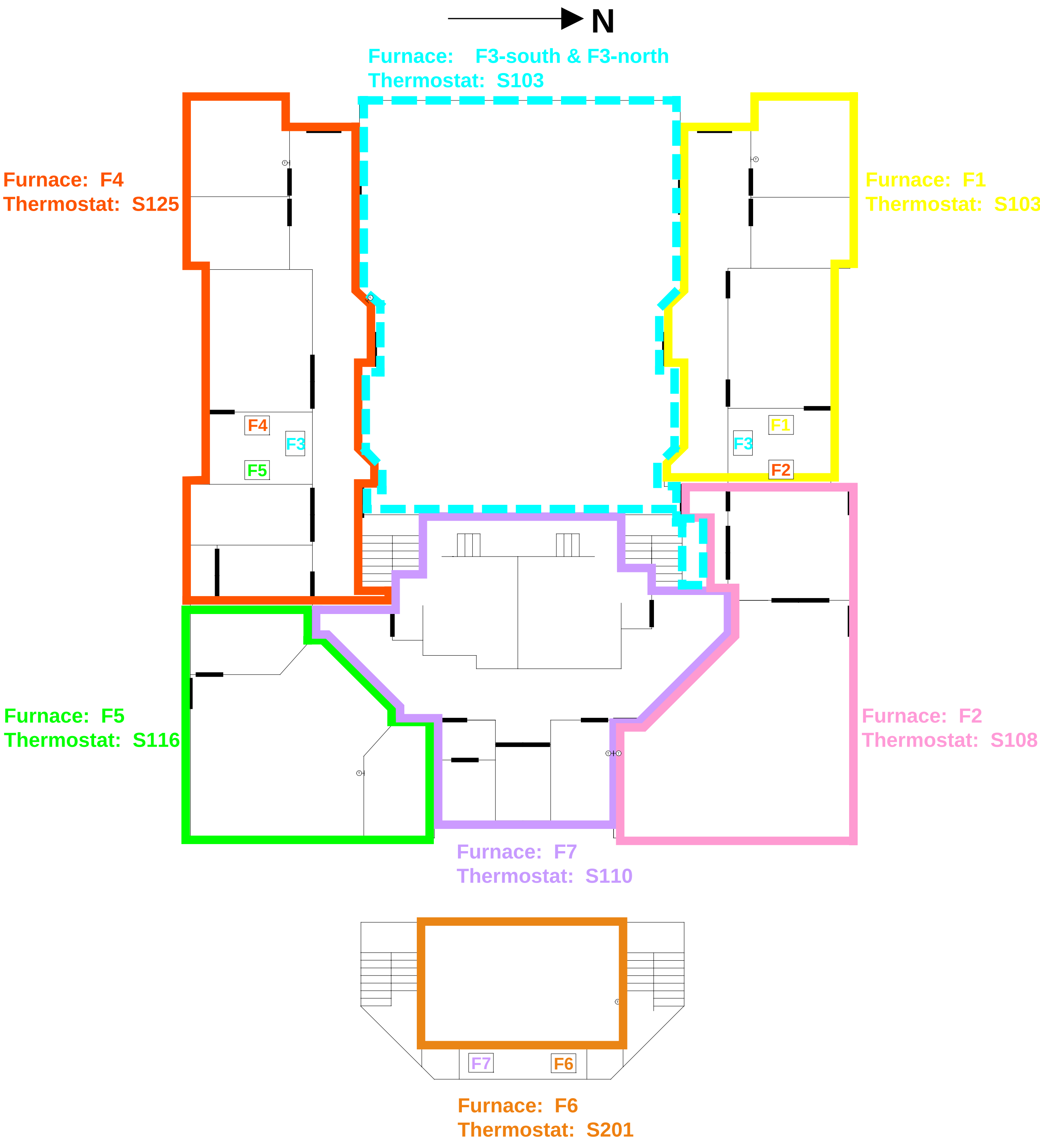

Figure A8-8. AHU Zones within Building

There are seven temperature sensors and corresponding controllers for the eight furnaces. A single temperature sensor and controller controls the two furnaces that serve the main room (F-3 north and F-3 south). The heating setpoint is 72°F (65°F in summer) and the cooling setpoint is 71°F (76°F in winter). There are occupied and unoccupied modes.

MEASUREMENTS

The test data below was taken on July 22 and August 2, 2004. Blower door testing and pressure mapping were completed on July 22. Supply and return airflow measurements at each diffuser and duct leakage measurements were taken on August 2. We also released CO_2 tracer gas into the building on August 2 to record the rate of decay to determine the infiltration rate. We collected the CO_2 and temperature/RH sensors on August 17. Test personnel were Dan Gott and Kenneth Larchar for all days.

Building Envelope Airtightness

The leakage characteristics of the building enclosure were assessed using both fan depressurization and fan pressurization methods. A single blower door was installed in the exterior door for the primary room on the southeast corner of the building. All exterior doors and windows were closed. The building was tested in the following configuration:

- All interior doors open
- All exhaust fans were sealed (restrooms and kitchen)
- All outdoor air ventilation intakes were sealed
- All furnace exhausts were sealed
- Fresh-air intakes for upstairs furnace room were sealed

The building pressure was varied from 20 Pa to 5 Pa. Figure A8-9 shows the various equipment that was sealed from the outdoors. Figure A8-10 shows the building leakage variation with building pressure.

Outdoor Air Vents (1 of 2)

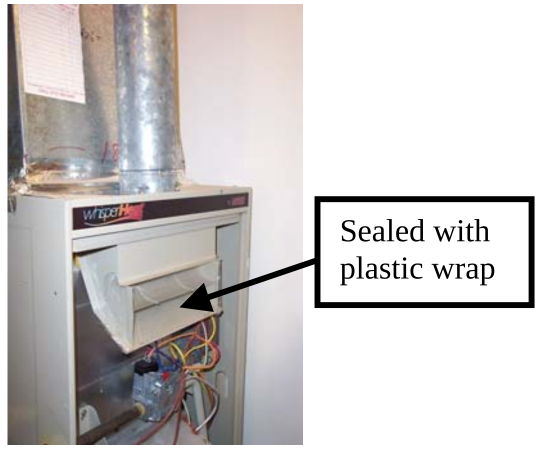

Furnace Exhaust Vent (1 of 8)

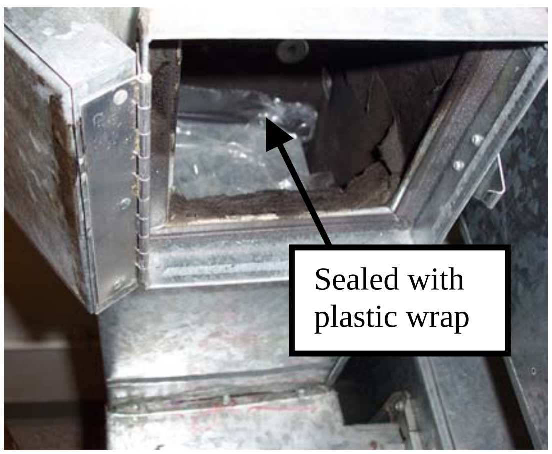

Ventilation Duct for Upstairs Furnaces (1 of 2)

Fresh Air Vent for Upstairs Furnaces (1 of 2)

Figure A8-9. Sealed Vents and Exhaust for Blower Door Test

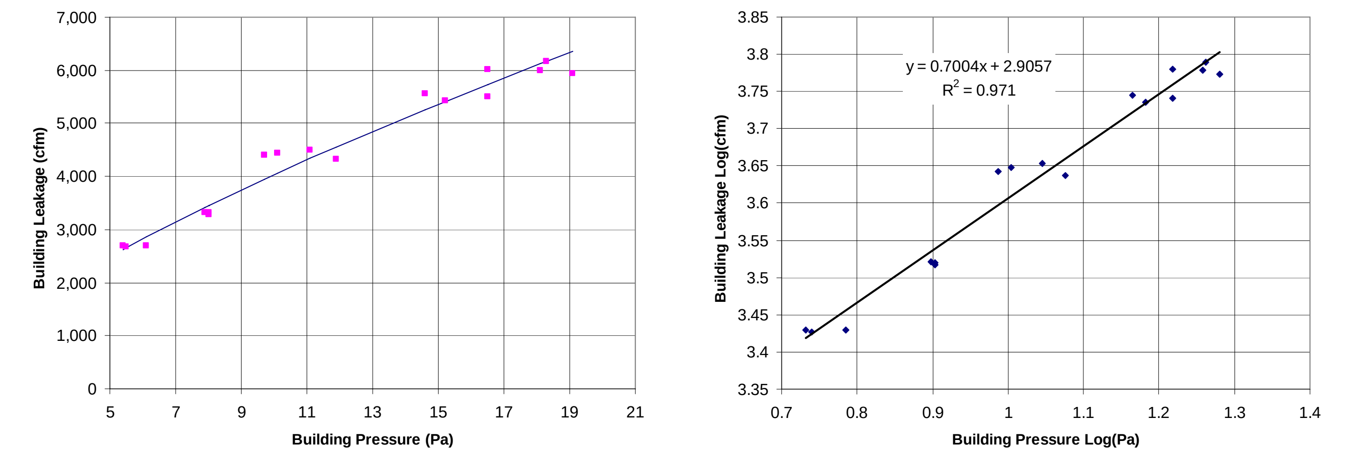

Pressurization Test – All Doors Open (Test 1)

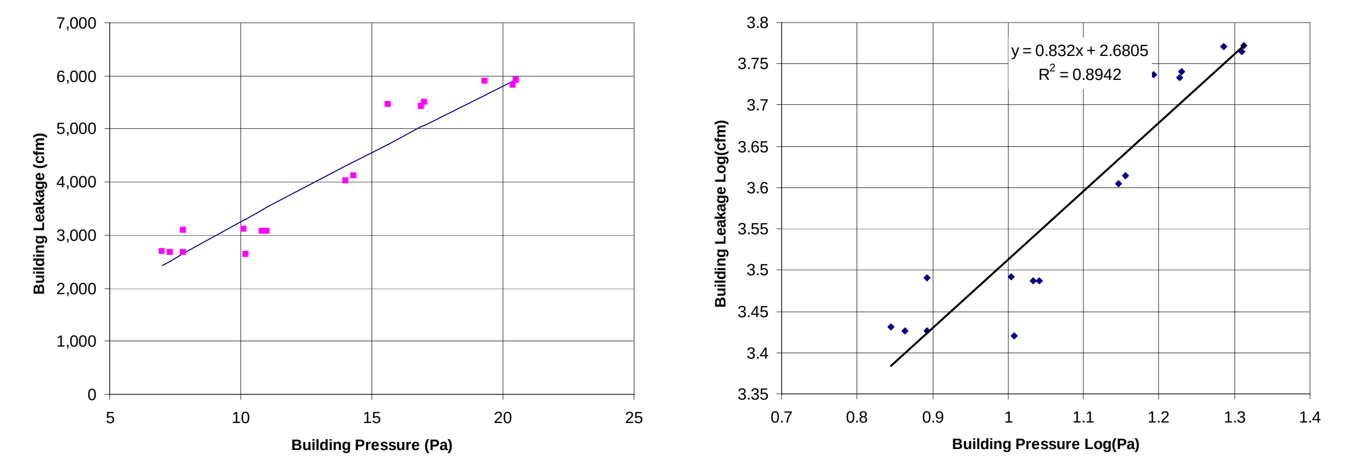

Depressurization Test – All Doors Open (Test 2)

Figure A8-10. Variation of Building Leakage with Pressure: $cfm = K(\Delta P)^n$

Table A8-2 shows the results of the blower door tests including model coefficients, effective leakage area (ELA), and air-changes-per-hour (ACH). The ELA is calculated using the Lawrence Berkeley Laboratory method, which calculates the leakage area at 4 Pa. The building has an effective leakage area of approximately 2.91 sq in per 100 sq ft of the total envelope area including floor area. Another building leakage characteristic is the ACH at 50 pascals (ACH_{50}). The building has an ACH_{50} of 7.6. This result implies that at 50 Pa, the air in the building is displaced 7.6 times each hour.

Table A8-2. Blower Door Test Data, Resulting Best-Fit Model Coefficients, and ELA

Pressurization – All Doors Open (Test 1)

Test Results:

Flow Coefficient (K)	804.9	8,607	sq ft, floor area
Exponent (n)	0.700		
Leakage area (LBL ELA @ 4 Pa)	602 sq in	2.91	ELA / 100 sq ft
Airflow @ 50 Pa	12,467.6 cfm	7.6	ACH @ 50

Test Data:

	Nominal Building Pressure (Pa)	Nominal Flow (cfm)	Ring
1	19.1	5,938	none
2	18.3	6,164	none
3	18.1	5,997	none
4	16.5	6,022	none
5	16.5	5,503	none
6	15.2	5,432	none
7	14.6	5,549	none
8	11.9	4,330	none
9	11.1	4,498	none
10	10.1	4,440	none
11	9.7	4,392	none
12	8.0	3,314	none
13	8.0	3,286	none
14	7.9	3,323	none
15	6.1	2,690	none
16	5.5	2,668	none
17	5.4	2,691	none

Depressurization – All Doors Open (Test 2)

Test Results:

Flow Coefficient (K)	479.2	8,607	sq ft, floor area
Exponent (n)	0.832		
Leakage area (LBL ELA @ 4 Pa)	430 sq in	2.08	ELA / 100 sq ft
Airflow @ 50 Pa	12,419.1 cfm	7.6	ACH @ 50

Test Data:

	Nominal Building Pressure (Pa)	Nominal Flow (cfm)	Ring
1	20.5	5,915	none
2	20.4	5,824	none
3	19.3	5,906	none
4	17.0	5,503	none
5	16.9	5,418	none
6	15.6	5,460	none
7	14.3	4,112	none
8	14.0	4,028	none
9	11.0	3,066	none
10	10.8	3,069	none
11	10.2	2,634	none
12	10.1	3,106	none
13	7.8	3,091	none
14	7.8	2,669	none
15	7.3	2,668	none
16	7.0	2,696	none

Notes: ELA is leakage area (in square inches) at reference pressure of 4 Pa.
ELA per 100 sq ft is based on total building envelope surface area (ceiling, exterior walls and floor).

We repeated the blower door tests with all interior doors closed. The building pressures varied from 28 Pa to 5 Pa. The results of the test with the interior doors closed are shown below

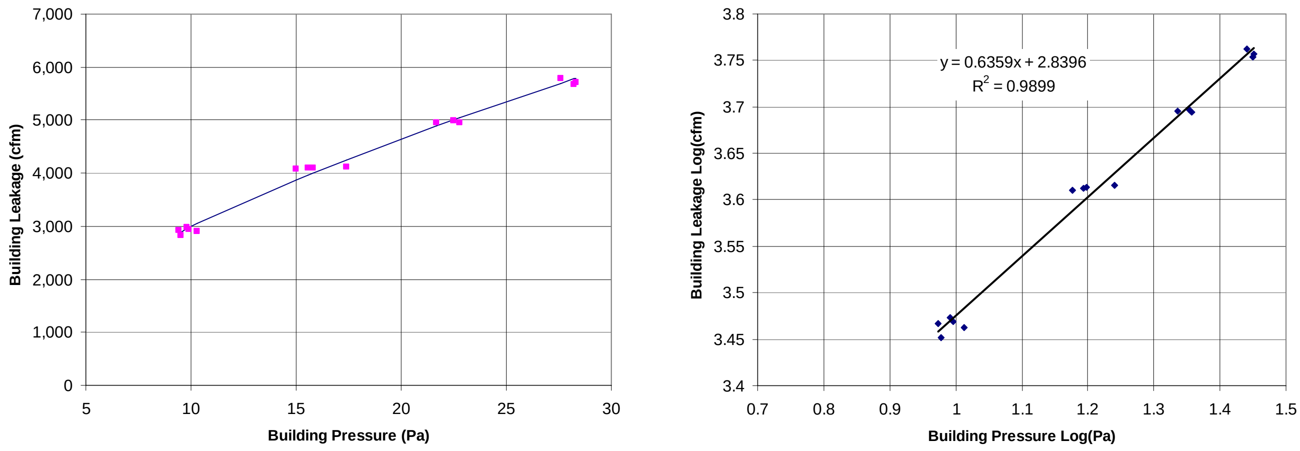

Depressurization Test – All Doors Closed (Test 3)

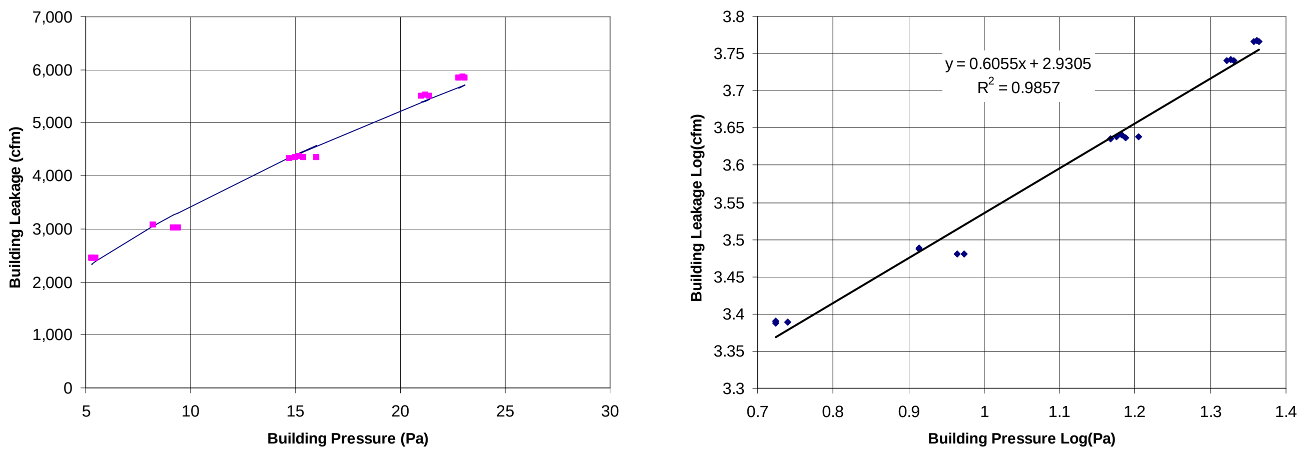

Depressurization Test – All Doors Closed (Test 4)

Figure A8-11. Variation of Building Leakage with Pressure: cfm = $K(\Delta P)^n$

Table A8-3. Blower Door Test Data, Resulting Best-Fit Model Coefficients, and ELA

Depressurization – All Doors Closed (Test 3)

Test Results:

Flow Coefficient (K)	691.1		8,607	sq ft, floor area
Exponent (n)	0.636			
Leakage area (LBL ELA @ 4 Pa)	473	sq in	2.29	ELA / 100 sq ft
Airflow @ 50 Pa	8,317.6	cfm	5.1	ACH @ 50

Test Data:

	Nominal Building Pressure (Pa)	Nominal Flow (cfm)	Ring
1	28.3	5,709	none
2	28.2	5,673	none
3	27.6	5,780	none
4	22.8	4,948	none
5	22.5	4,981	none
6	21.7	4,955	none
7	17.4	4,125	none
8	15.8	4,105	none
9	15.6	4,101	none
10	15.0	4,080	none
11	10.3	2,900	none
12	9.9	2,948	none
13	9.8	2,976	none
14	9.5	2,827	none
15	9.4	2,927	none

Depressurization – All Doors Closed (Test 4)

Test Results:

Flow Coefficient (K)	852.0		8,607	sq ft, floor area
Exponent (n)	0.605			
Leakage area (LBL ELA @ 4 Pa)	559	sq in	2.70	ELA / 100 sq ft
Airflow @ 50 Pa	9,102.2	cfm	5.6	ACH @ 50

Test Data:

	Nominal Building Pressure (Pa)	Nominal Flow (cfm)	Ring
1	23	5,856	none
2	22.8	5,842	none
3	23.1	5,836	none
4	21.0	5,498	none
5	21.2	5,522	none
6	21.4	5,510	none
7	15.2	4,370	none
8	15.4	4,335	none
9	15.0	4,345	none
10	16.0	4,347	none
11	14.7	4,325	none
12	9.4	3,025	none
13	9.2	3,025	none
14	8.2	3,077	none
15	8.2	3,076	none
16	5.5	2,451	none
17	5.3	2,438	none
18	5.3	2,453	none

Notes: ELA is leakage area (in square inches) at reference pressure of 4 Pa.
ELA per 100 sq ft is based on total building envelope surface area (ceiling, exterior walls and floor).

Table A8-4 shows a summary of the blower door tests including model coefficients, ELA per 100 sq-ft of envelope area including floor area, and ACH_{50}.

Table A8-4. Summary of Blower Door Test Results

Test No.	Test Description	Flow Coeff. K	Exp. n	ELA / 100 sq ft (sq in)	ACH_{50}
1	Pressurized Doors Open	805	0.700	2.91	7.6
2	Depressurized Doors Open	479	0.832	2.08	7.6
3	Depressurized Doors Closed	691	0.636	2.29	5.1
4	Depressurized Doors Closed	852	0.605	2.70	5.6

Pressure Mapping (Blower Door Testing)

Pressure readings in the building were taken using a digital micromanometer (DG 700) with the blower doors operating. The pressure difference across the building envelope was 29 Pa with all interior doors closed. Figure A8-12 shows the pressure difference between the interior spaces and outdoors with the building depressurized. The pressure difference between the interior space and the ceiling plenum was 7 Pa. This implies that the leakage area from the space to the ceiling plenum is large and that the plenum is closely coupled to the conditioned space. The gypsum board attached to the roof beams of the building is the primary air barrier and the insulation between the roof beams is the primary thermal barrier.

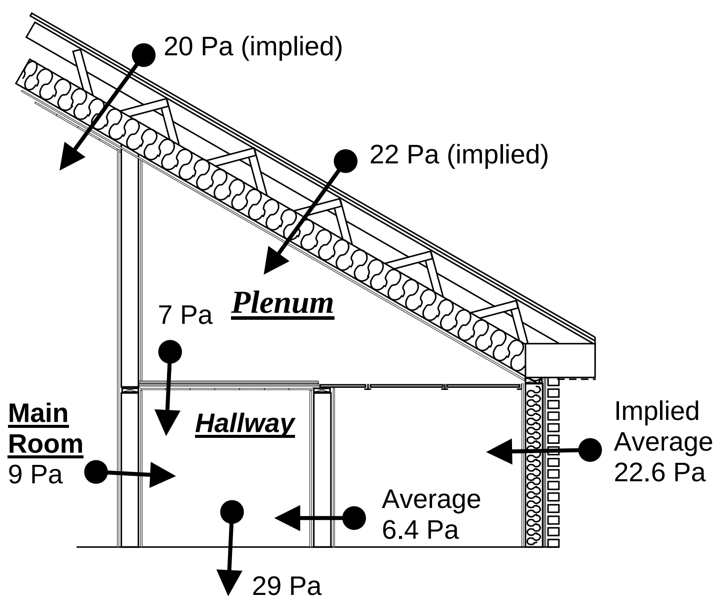

Figure A8-12. Pressure Drop across Ceiling Elements during 29 Pa Depressurization Test

Pressure measurements were also taken between all interior rooms and the hallway with doors closed. Figure A8-13 shows the pressure differences induced across the doorways with the corridor depressurized. With the building depressurized to 29 Pa, pressures across the doorways ranged from 3.2 and 9.1 Pa. The pressure difference between the rooms and corridor are much less than the overall pressure difference to ambient.

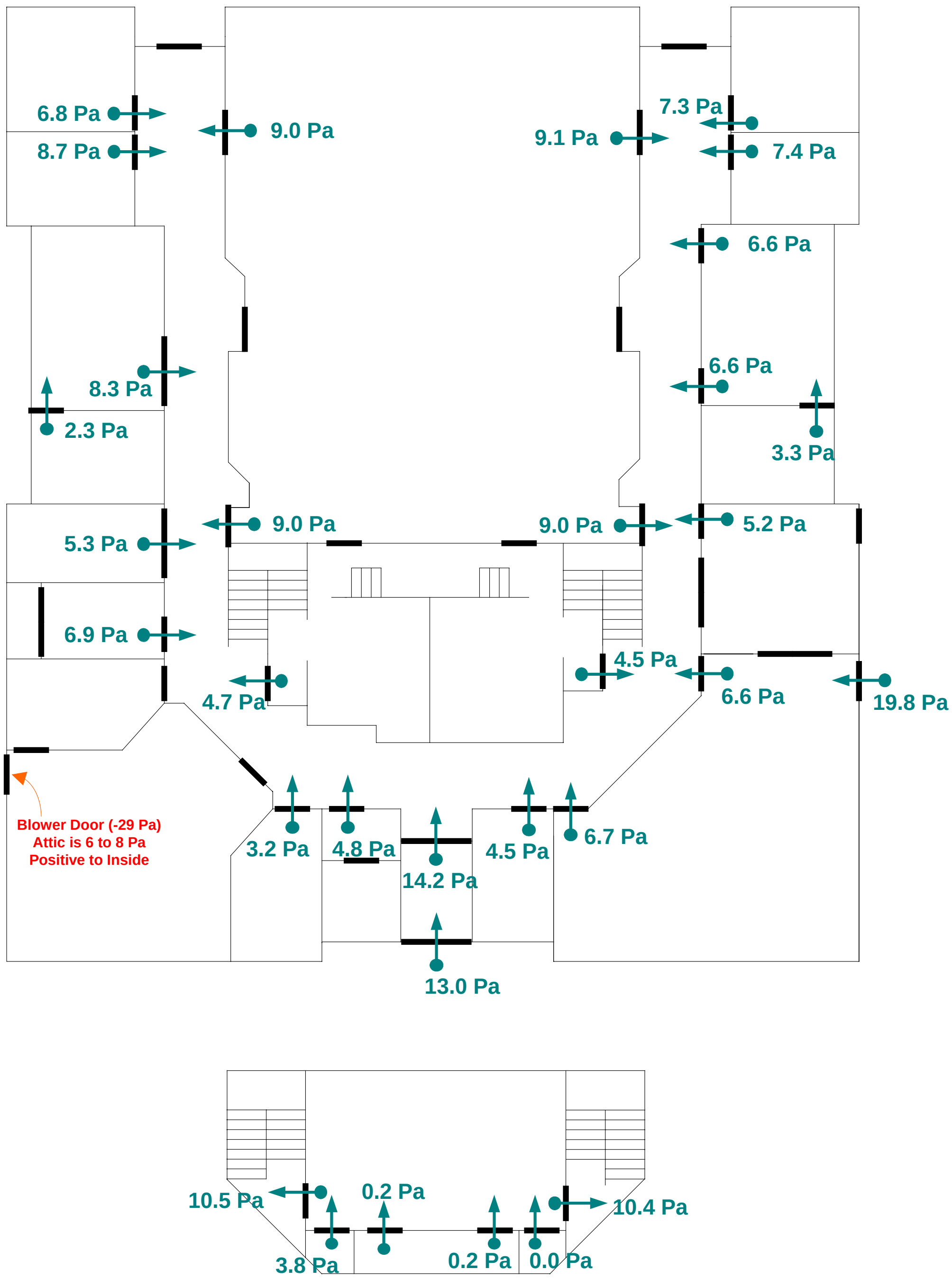

Figure A8-13. Room-to-Corridor Pressures with Building Depressurized to 29 Pa

HVAC Airflow Measurements

The airflow from each supply diffuser was measured using a Shortridge flow hood. The total supply air flow is 11,679 cfm or about 1.36 cfm per sq-ft of floor area.

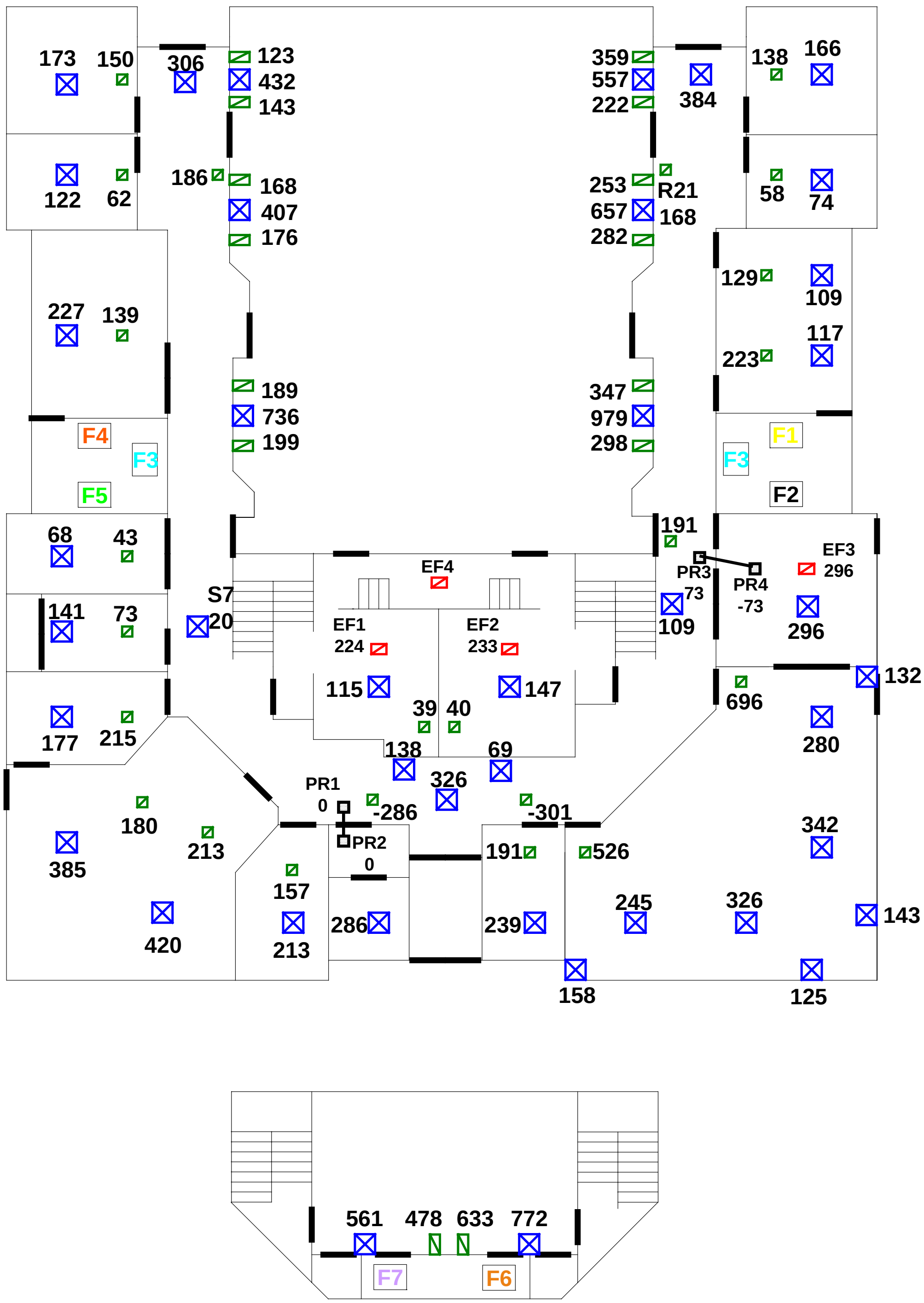

Figure A8-14. Supply and Return Airflow Measurements (cfm)

Table A8-5. Comparison of Supply and Return Airflow Measurements

Furnace	Location	Flowhood Supply Airflow (cfm)	Flowhood Return Airflow (cfm)	Supply / Return Ratio	Measured Supply Fan Power (kW)	Normalized Supply Fan Power (W/cfm)	Supply Static (Pa)	Return Static (Pa)
F-1	North Side	850	716	1.2				
F-2	North Side	2,047	1,413	1.4				
F-3	North Side	2,302	1,761	1.3				
F-3	South Side	1,575	998	1.6	0.66	0.42	21	-19.3
F-4	South Side	1,057	653	1.6	0.55	0.52		
F-5	South Side	1,195	765	1.6	0.58	0.49		
F-6	Upstairs	1,333	1,111	1.2	0.62	0.47	47	-30
F-7	Upstairs	1,320	857	1.5				

Pressure Mapping (AHU Fans ON)

The air pressure relationships in the building were also determined with the AHU fans on. The graphics in Figure A8-15 show the pressure differences induced across the doorways with the AHU fans on and the interior doors closed. Operation of the eight furnace fans created pressures up to 5.8 Pa however most pressures ranged from –3.0 to 1.6 Pa. Four of the five depressurized rooms actually have a positive net airflow (more supply airflow than return airflow). Three of the rooms with negative pressures were the rooms west of furnace room #1 (Bishop’s Office, Clerks Office, and Room 101/102). The operation of the furnaces depressurizes the furnace rooms creating negative pressures in the rooms next to the furnace rooms that are not separated by interior walls extending to the roof. The primary room is not depressurized because the east wall of furnace room #1 extends to the roof of the building. A similar result occurs on the south side of the building for the materials center caused by air being pulled into furnace room #2. The classroom upstairs is also depressurized due to the operation the furnaces in furnace room #3. Figure A8-16 shows the relation between room pressures and net airflow imbalance (net airflow imbalance = supply airflow – return airflow). The negative pressures are caused by air being pulled up through the drop ceiling into the plenum and into the furnace rooms. This does not have an adverse effect on the energy usage because the plenum space is below the primary air and thermal barrier.

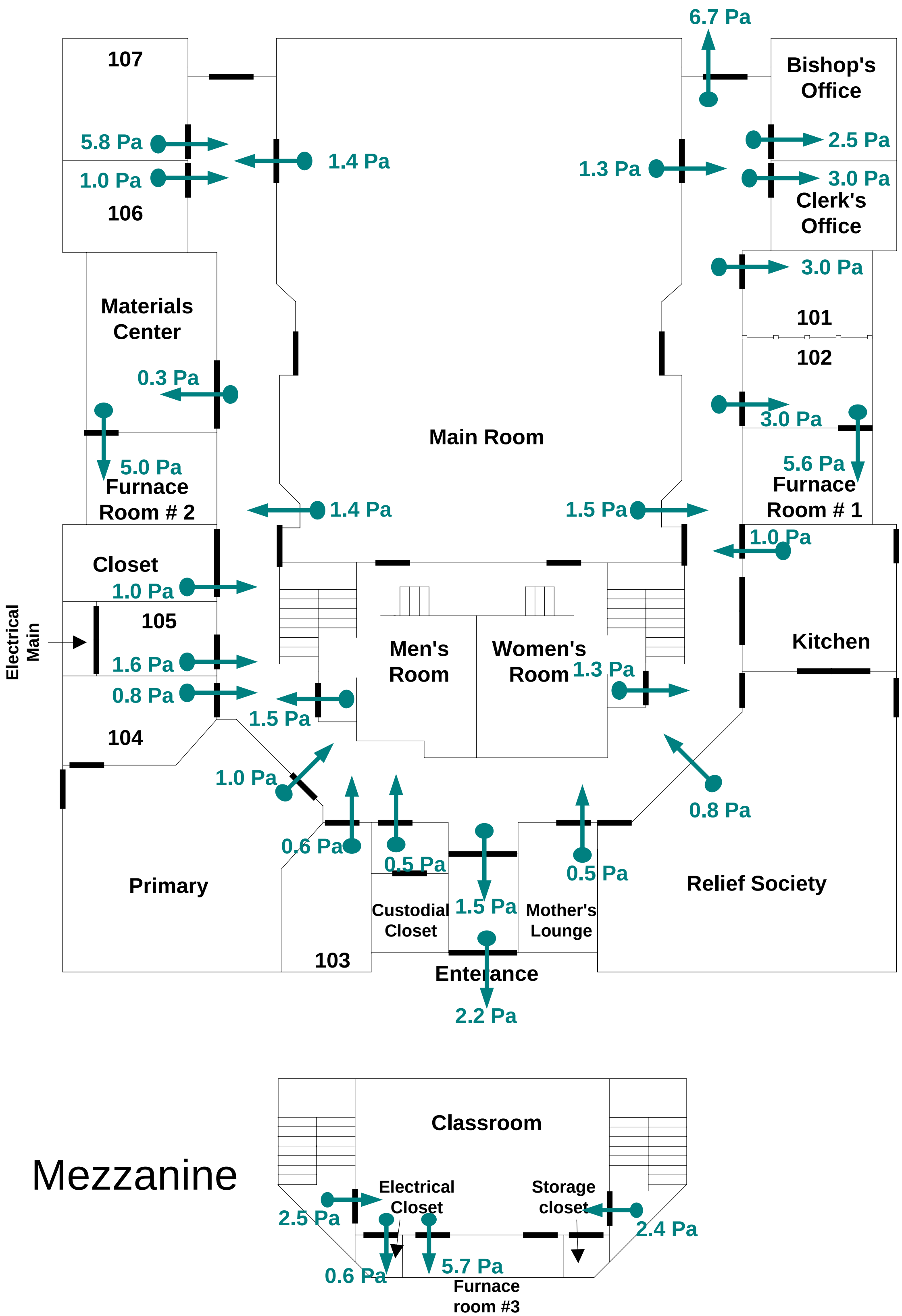

Figure A8-15. Pressure Differences between Rooms with AHU Fans ON

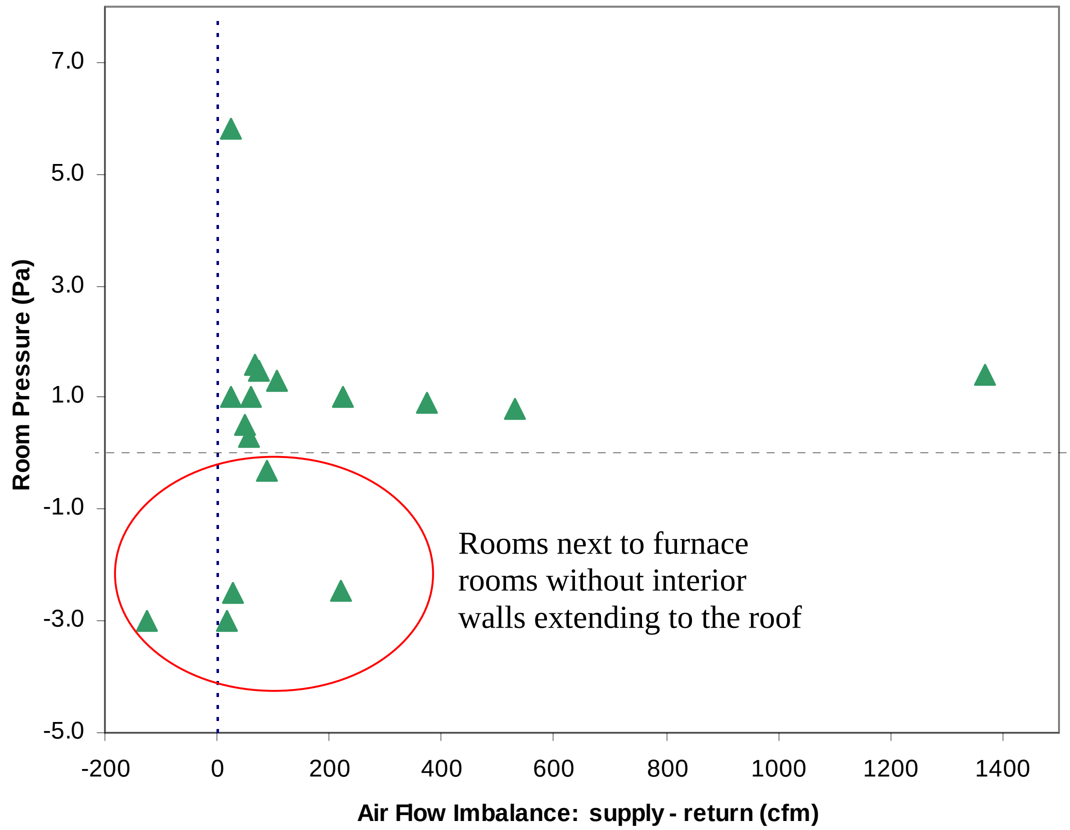

Figure A8-16. Pressure Differences Induced by AHU Fan Operation

Duct Leakage Measurements

A Duct Blaster was used to depressurize the ductwork to measure leakage rates. The supply and return ducts were tested for furnaces F3 (south) and F6 (upstairs). The Duct Blaster fan was connected to the supply fan section in the furnace cabinet, as shown in Figure A8-17. When testing the supply side, the furnace filter was wrapped in plastic, reinserted, and duct taped around the edges to ensure a good seal. For the return side, the filter was removed, the supply fan was sealed with plastic wrap on both sides, and the duct blaster was mounted to the furnace again. To verify a good seal separating the supply and return, we depressurized the ductwork being tested and measured the static pressure in the other duct system. In all four instances, the pressure on the opposite side of the seal was very small (-0.1 to -0.4 Pa) verifying a good seal. Plastic wrap was used to cover each supply and return grill in the system. In all tests, the seals at the supply and return grills were tested with a smoke puffer to confirm there was no leakage with the system depressurized.

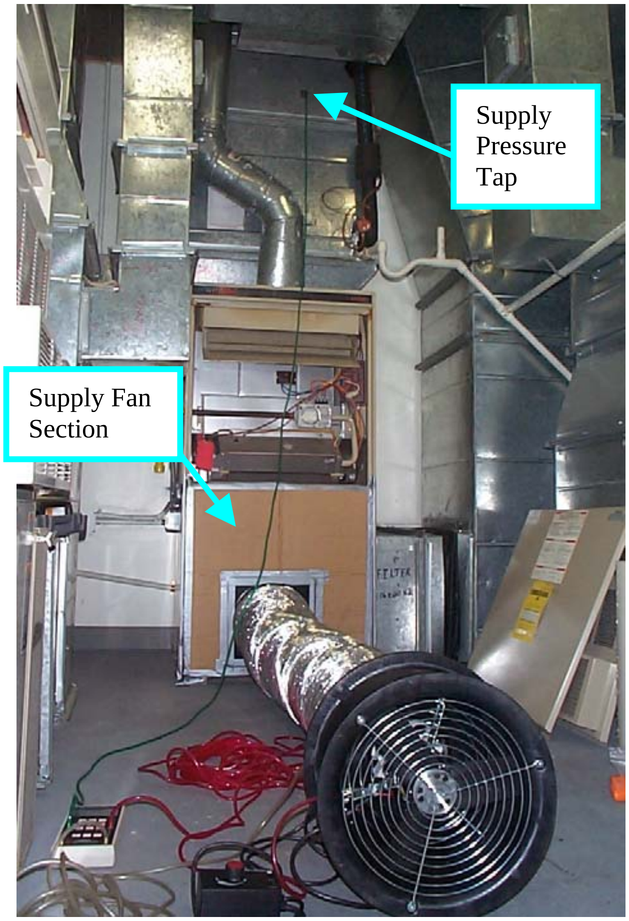

Duct Blaster connected to Furnace (F-3 south)

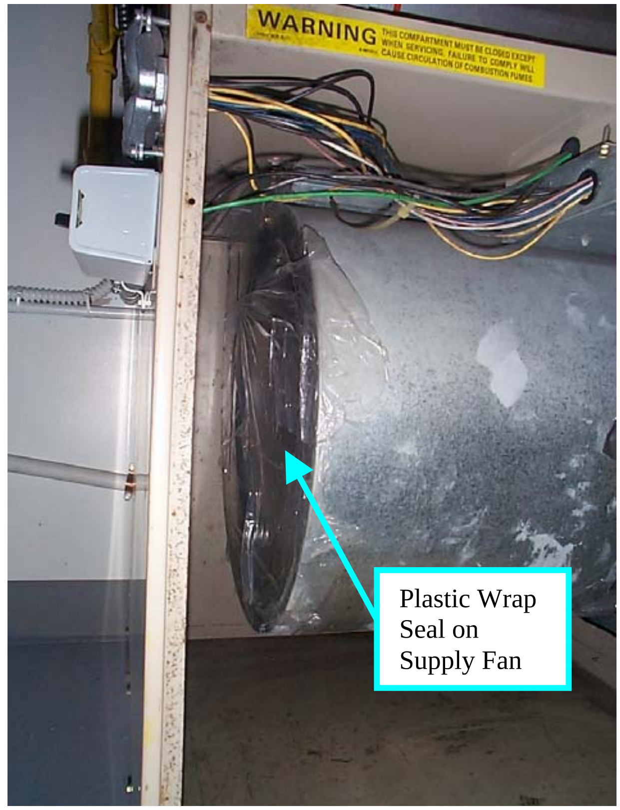

Supply Fan Sealed for Return Ductwork Test

Figure A8-17. Duct Blaster Set Up for Testing F3 & F6

As a diagnostic check on the degree of pressurization, the pressure at each supply diffuser and return grill was measured by puncturing the plastic covering at each diffuser with a very small probe. Table A8-6 shows the resulting pressures measured at each supply and return for F3 and F6 with the system depressurized. The uniformity of the pressures at most diffusers implies that leaks are uniformly spread around the system.

Table A8-6. Diffuser Pressure with Ductwork Depressurized

Furnace F3 Duct System	
Diffuser Label	**Pressure at Diffusers (Pa)**
S37	-43.5
S38	-42.4
S39	-42.9
R29	-13.5
R30	-13.5
R31	-13.7
R32	-13.7
R33	-13.1
R34	-11.6

*Note: Supply ductwork was depressurized 44.3 Pa and Return ductwork was depresurized 16.6 Pa

Furnace F6 Duct System	
Diffuser Label	**Pressure at Diffusers (Pa)**
S40	no data
S41	no data
R35	-73.6
R36	-73.2

*Note: Supply ductwork was depressurized 40 Pa and Return ductwork was depresurized 80.7 Pa

Figure A8-18 shows the resulting measured data from the duct leakage tests fit to a power function (raw data in Table A8-7). Figure A8-18 also shows our best estimate for duct leakage during normal operation, which uses one half of the plenum pressure as suggested in ASHRAE Standard 152P section B.2. Table A8-8 shows the resulting coefficients, exponents, and regression statistics. Table A8-9 summarizes the resulting duct leakage rates and ELA at a reference pressure of 25 Pa. After completing the duct leakage test for F-6 and reviewing the results, we realized that the economizer damper was not completely closed. To correct for this unsealed leakage we subtracted the area of the unsealed portion in the ventilation duct (15 in^2). The damper was open approximately 1.5 inches and the duct is 10 inches wide.

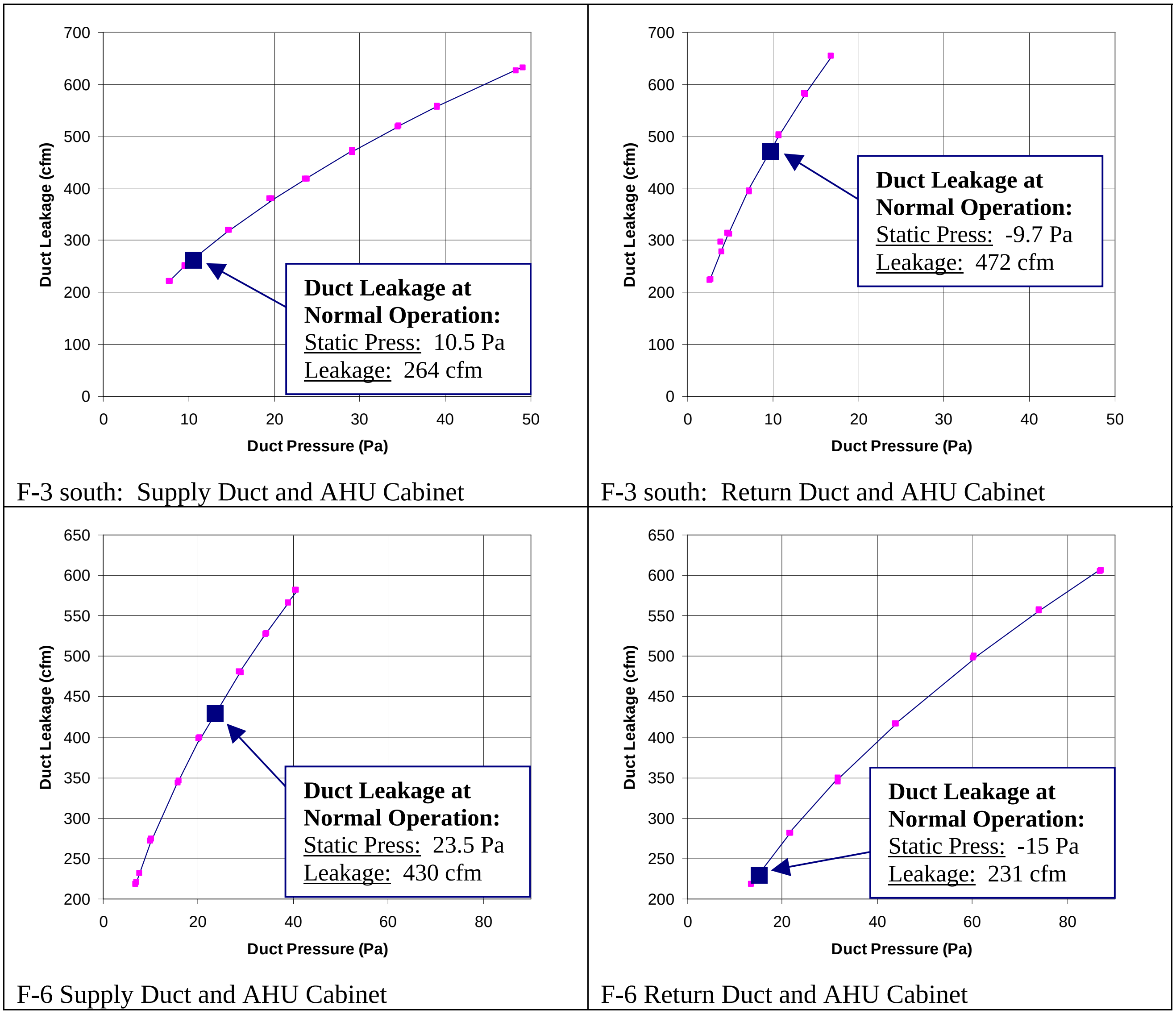

F-3 south: Supply Duct and AHU Cabinet

F-3 south: Return Duct and AHU Cabinet

F-6 Supply Duct and AHU Cabinet

F-6 Return Duct and AHU Cabinet

Figure A8-18. Duct-Blaster Tests on F-3 & F-6 Ductwork and AHU Cabinets

Table A8-7. Raw Data from Duct-Blaster Tests

F-3 south: Supply Duct and AHU Cabinet

Test Results:

Flow Coefficient (K)	69.2	
Exponent (n)	0.569	
Leakage area (LBL ELA @ 25 Pa)	49	sq in
Airflow @ 25 Pa	432.2	cfm

Test Data:

	Nominal Duct Pressure (Pa)	Nominal Flow (cfm)	Ring
1	49.1	631	A1
2	48.3	627	A1
3	39.1	556	A1
4	39.1	558	A1
5	34.6	520	A1
6	34.5	518	A1
7	29.1	470	A1
8	29.2	473	A1
9	23.6	419	A1
10	23.8	419	A1
11	19.5	380	A1
12	19.7	380	A1
13	14.6	320	A1
14	14.7	320	A1
15	9.6	251	A1
16	9.6	249	A1
17	7.7	221	A1
18	7.8	221	A1

F-3 south: Return Duct and AHU Cabinet

Test Results:

Flow Coefficient (K)	125.8	
Exponent (n)	0.584	
Leakage area (LBL ELA @ 25 Pa)	93	sq in
Airflow @ 25 Pa	823.0	cfm

Test Data:

	Nominal Duct Pressure (Pa)	Nominal Flow (cfm)	Ring
1	16.8	654	A1
2	16.8	654	A1
3	13.8	581	A1
4	13.7	583	A1
5	10.7	504	A1
6	10.7	501	A1
7	7.3	394	A1
8	7.3	395	A1
9	4.9	312	A1
10	4.7	314	A1
11	3.9	297	A1
12	4.0	278	A1
13	2.7	224	A1
14	2.8	225	A1

F-6 Supply Duct and AHU Cabinet

Test Results:

Flow Coefficient (K)	76.7	
Exponent (n)	0.546	
Leakage area (LBL ELA @ 25 Pa)	50	sq in
Airflow @ 25 Pa	445.0	cfm

Test Data:

	Nominal Duct Pressure (Pa)	Nominal Flow (cfm)	Ring
1	40.7	582	A1
2	40.4	582	A1
3	39.0	566	A1
4	38.9	566	A1
5	34.4	528	A1
6	34.3	527	A1
7	28.7	481	A1
8	29.0	480	A1
9	20.1	398	A1
10	20.4	399	A1
11	15.7	344	A1
12	16.0	346	A1
13	10.0	272	A1
14	10.2	274	A1
15	7.6	232	A1
16	6.8	218	A1
17	7.0	221	A1

F-6 Return Duct and AHU Cabinet

Test Results:

Flow Coefficient (K)	52.0	
Exponent (n)	0.551	
Ventilation area not sealed	15	sq in
Leakage area (LBL ELA @ 25 Pa)	~~35~~	~~sq in~~
Corrected (LBL ELA @ 25 Pa)	*20*	*sq in*
Airflow @ 25 Pa	305.9	cfm

Test Data:

	Nominal Duct Pressure (Pa)	Nominal Flow (cfm)	Ring
1	87.1	606	A1
2	86.8	605	A1
3	74.1	556	A1
4	74.0	557	A1
5	60.2	498	A1
6	60.3	501	A1
7	43.8	417	A1
8	43.9	417	A1
9	31.7	345	A1
10	31.8	350	A1
11	21.6	282	A1
12	21.7	282	A1
13	14.5	228	A1
14	14.6	227	A1
15	13.5	218	A1

Table A8-8. Coefficients, Exponents and Regression Statistics from Duct-Blaster Tests

	Supply & AHU Cabinet			Return Ductwork		
	K	n	R^2	K	n	R^2
F-3 south	69.2	0.569	99.98%	125.8	0.584	99.68%
F-6 upstairs	76.7	0.546	99.98%	52.0	0.551	99.99%

Notes: cfm = $K(Pa)^n$ / R^2 indicates fit of linear log-log regression

Table A8-9. Comparison of Supply and Return Airflow Measurements

	Total Supply Diffuser Airflow (cfm)	Total Return Diffuser Airflow (cfm)	Supply & Furnace Leakage (cfm @ 25)	Return Leakage (cfm @ 25)	Supply & Furnace ELA (sq in @ 25)	Return ELA (sq in @ 25)
F-3 south	1,575	998	432	823	49	93
F-6 upstairs	1,333	1,111	445	306	50	20

Notes: Leakage and ELA at reference pressure of 25 Pa

Table A8-10 lists the ductwork used to estimate the supply and return duct area for the AHUs. The effective leakage area compared to the total duct surface area for furnaces F-3 and F-6 is shown in Table A8-11 and Table A8-12. The Sheet Metal and Air Conditioning Contractors' National Association (SMACNA) classifies duct leakiness using duct leakage per 100 sq ft of duct area at a pressure of 1-in w.g.

Table A8-10. AHU Ductwork Size and Area

Furnace F-3

	Type/Size	Quantity	Supply Side Length (ft)	Return Side Length (ft)	Duct Area Supply Side (sq ft)	Duct Area Return Side (sq ft)
Supply Trunks	16" x 12"	1	14.9		69.6	
	16" x 18"	1	16.3		92.1	
	20" x 20"	1	20.9		139.4	
takeoffs	11" x 12"	3	27.0		310.5	
Return Trunks	12" x 14"	1		11.2		48.4
	16" x 18"	1		16.3		92.1
	16" x 26"	1		34.3		239.8
takeoffs	5" x 14"	6		14.5		275.5
AHU Cabinet	26" x 26" x 82"	1			59.2	
Total					***670.9***	***655.7***

Furnace F-6

	Type/Size	Quantity	Supply Side Length (ft)	Return Side Length (ft)	Duct Area Supply Side (sq ft)	Duct Area Return Side (sq ft)
Supply Trunks	18" x 19"	1	2.3		14.4	
	13" x 14"	1	21.0		94.5	
takeoffs	12" x 12"	2	1.5		12.0	
Return Trunks	18" x 23"	1		1.5		10.3
	16" x 16"	1		5.0		26.7
takeoffs	12" x 16"	2		1.3		11.7
AHU Cabinet	21" x 26" x 69"	1			45.0	
Total					***165.9***	***48.6***

Table A8-11. Duct Leakage per 100 Square Foot of Duct Area (F-3 South)

	Duct Area (sq ft)	ELA (sq in @ 25)	ELA/100 sq ft Duct Area (sq in @ 25)	Leakage (cfm @ 25 Pa)	Supply CFM per ft^2 (cfm/ sq-ft)	Leakage per 100 sq ft (cfm @ 25 Pa)	SMACNA Leakage Class (cfm @ 1-in water)
Supply & AHU Cabinet	671	49	7.3	432	2.35	64	238
Return	656	93	14.2	823	n/a	126	480
Total	***1,327***	***142***	***10.7***	***1,255***	***n/a***	***95***	**----**

Table A8-12. Duct Leakage per 100 Square Foot of Duct Area (F-6 Upstairs)

	Duct Area (sq ft)	ELA (sq in @ 25)	ELA/100 sq ft Duct Area (sq in @ 25)	Leakage (cfm @ 25 Pa)	Supply CFM per ft^2 (cfm/ sq-ft)	Leakage per 100 sq ft (cfm @ 25 Pa)	SMACNA Leakage Class (cfm @ 1-in water)
Supply & AHU Cabinet	166	50	30.4	445	8.03	268	942
Return	49	20	40.5	306	n/a	630	----
Total	***215***	***70***	***32.7***	***751***	***n/a***	***350***	**----**

Table A8-13 shows the airflow balance for F-3 south and F-6 upstairs. Three airflow balance estimates are calculated as follows:

Gross Airflow Balance:

$$\Delta_{gross} = \text{Supply Diffuser cfm} - \text{Return Diffuser cfm} - \text{Ventilation cfm}$$

Net Airflow Balance Using CFM_{25}:

$$\Delta_{N25} = (\text{Supply Diffuser cfm} + \text{Supply Leakage @ 25 Pa}) - (\text{Return Diffuser cfm} + \text{Return Leakage @ 25 Pa}) - \text{Ventilation cfm}$$

Net Airflow Balance Using Average "Actual Static" in Ductwork:

$$\Delta_{Ncorrected} = (\text{Supply Diffuser cfm} + \text{Supply Leakage @ Actual Static}) - (\text{Return Diffuser cfm} + \text{Return Leakage @ Actual Static}) - \text{Ventilation cfm}$$

The last estimate for the RTU airflow balance ($\Delta_{Ncorrected}$) uses our best estimate for average "actual static" pressure in the ductwork during normal operation, which is one half of the plenum pressure as suggested in ASHRAE Standard 152P section B.2. Table A8-13 uses an estimate for ventilation airflow based on the supply return ratio since we did not measure the outdoor airflow to these units. For this ductwork, the net airflow estimate resulting in the smallest error is $\Delta_{Ncorrected}$ for F-3 south and Δ_{N25} for F-6 upstairs. The net airflow balance estimate with the value closest to zero gives the most accurate results for airflow combined with duct leakage. Figure A8-19 shows a diagram of the furnaces including the supply, return, and ventilation airflows as well as the duct leakage for the best estimate.

Table A8-13. Airflow Balance for Furnaces

	F-3 south	F-6 upstairs
Diffuser Supply (cfm)	1,575	1,333
Diffuser Return (cfm)	998	1,111
Ventilation (cfm) - estimate	577	222
Supply Leakage - cfm25	432	445
- actual static	264	430
Return Leakage - cfm25	823	306
- actual static	472	231
Δgross	0	0
ΔN25	-391	139
ΔNcorrected	-208	199

1) Note: "actual static" is the static pressure measured in supply/return trunk.
2) Ventilation estimate base on supply/return ratio.

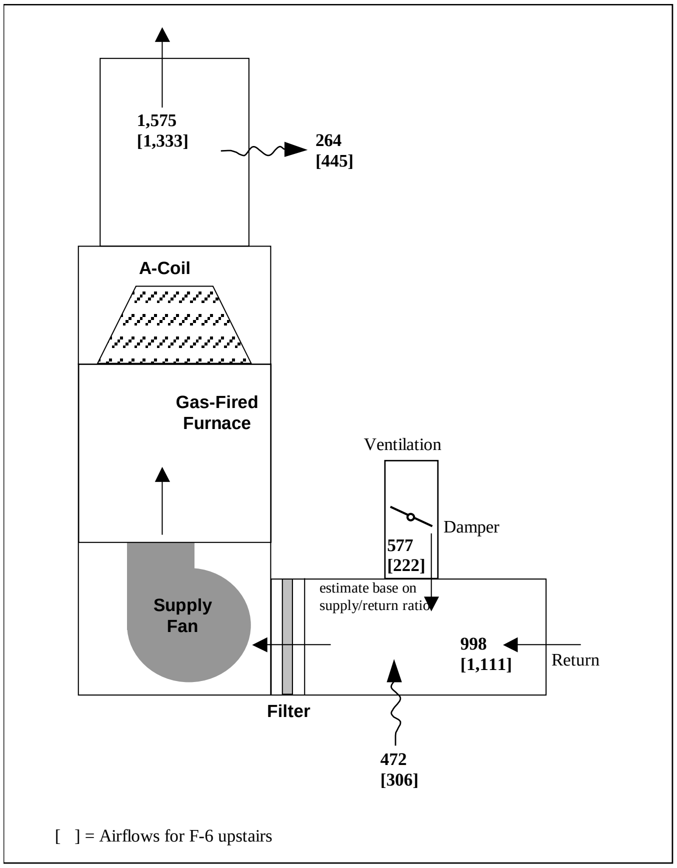

Figure A8-19. Airflow Balance for F-3 South and F-6 Upstairs

Space Conditions

Figure A8-20 shows the average temperature profiles based on temperature readings taken with a HOBO data logger from July 22 to August 17, 2004. The thick line shows the average for each hour while the shaded region corresponds to one standard deviation about the average. The dotted lines correspond to the minimum and maximum for each hour. Sensors were placed in the main room (Chapel), Relief Society Room, and in the Primary Room. The temperature profile plots on the left contain data from days when the building is occupied on Sundays. The profile plots on the right use data from Monday – Saturday.

Each of the seven digital temperature controllers have occupied and unoccupied modes each with temperature setback/setups. Table A8-14 shows how the setpoints for summer and winter. There is a 3-hour occupied override button on each of the thermostats for use during unscheduled events.

Table A8-14. Temperature Setpoints for Summer and Winter

	Summer		Winter	
	Occupied	Unoccupied	Occupied	Unoccupied
Heat	65	63	72	
Cool	71	76	76	

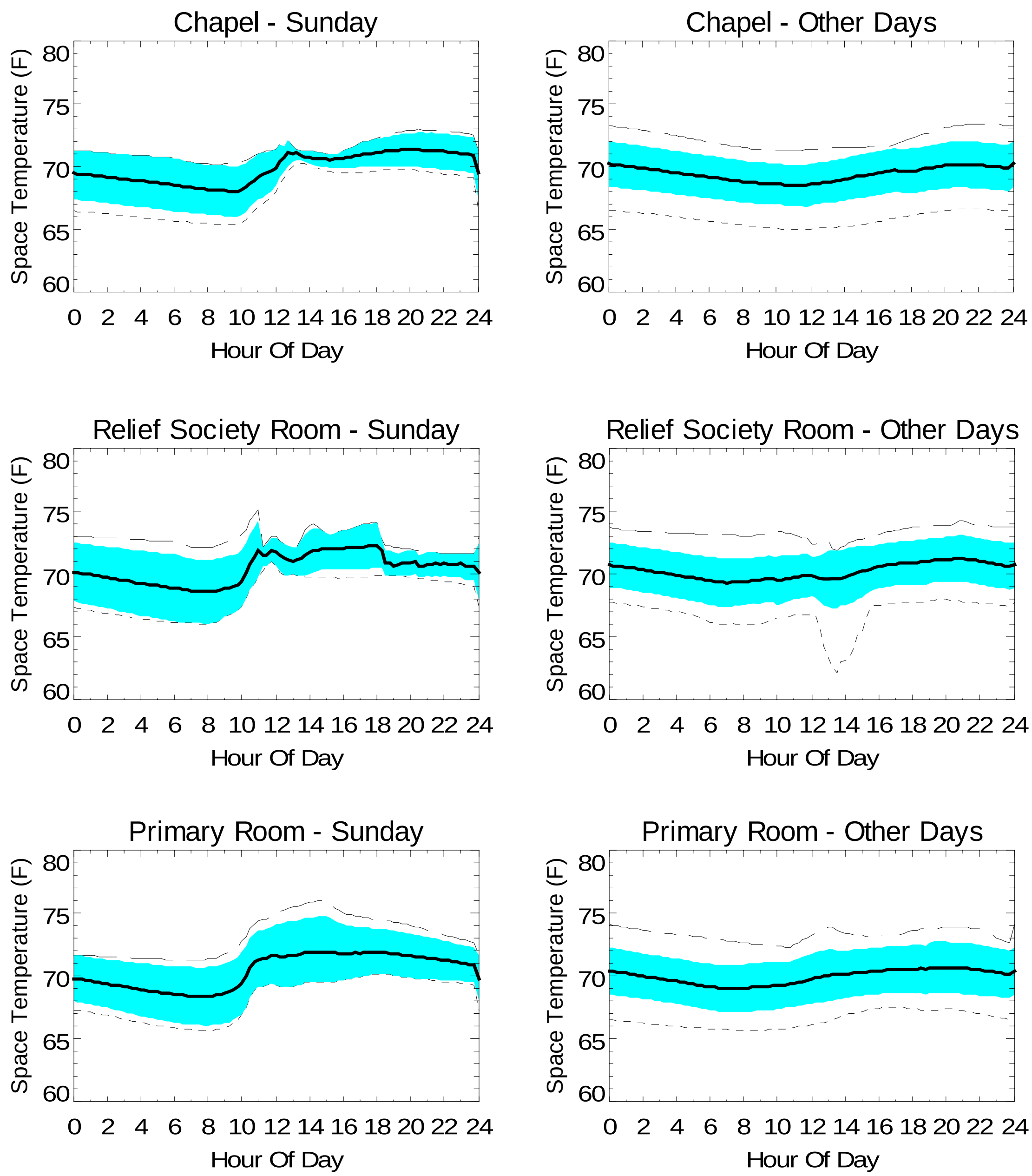

Figure A8-20. Measured Space Temperature Profiles

Figure A8-21 shows the CO_2 concentration in various locations in the building. The CO_2 concentration provides an indication of occupancy. The next section uses the CO_2 as a tracer gas to estimate the infiltration/ventilation rate into the building. Most of the large spikes in CO_2

occur on Sundays (July 25 and August 1, 8, 15). The large spike on August 2 is when we seeded the building with CO_2.

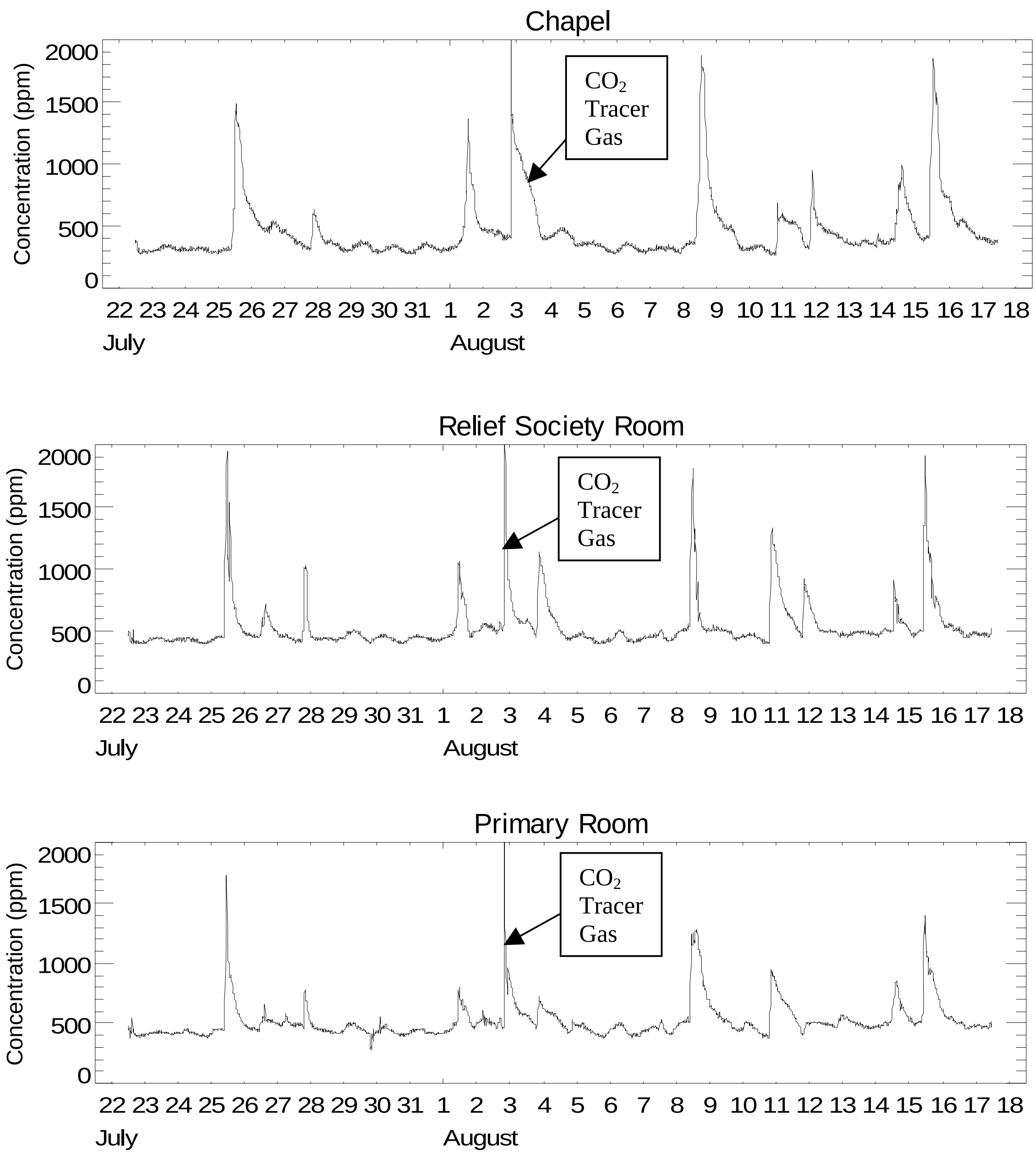

Figure A8-21. Measured CO_2 Concentration in Various Spaces

The following plots show the relative humidity for this building. The chapel was over 60 percent relative humidity for the entire monitoring period, the relief society 72% of the time, and the primary room 83% of the time. Figure A8-25 displays the conditions inside the building compared with the ASHRAE comfort zone for cooling shown by the shaded region on the plot.

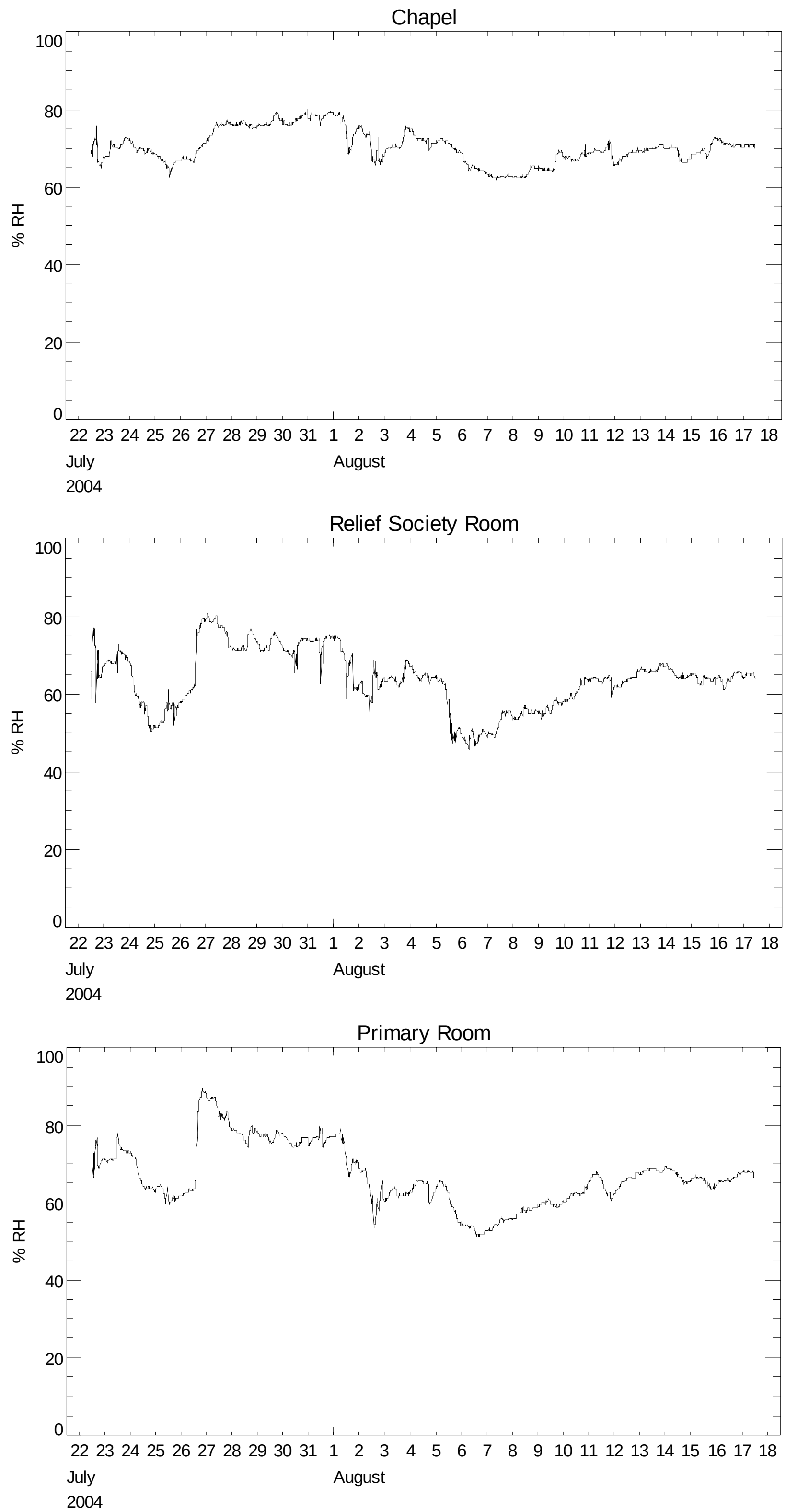

Figure A8-22. Measured Relative Humidity

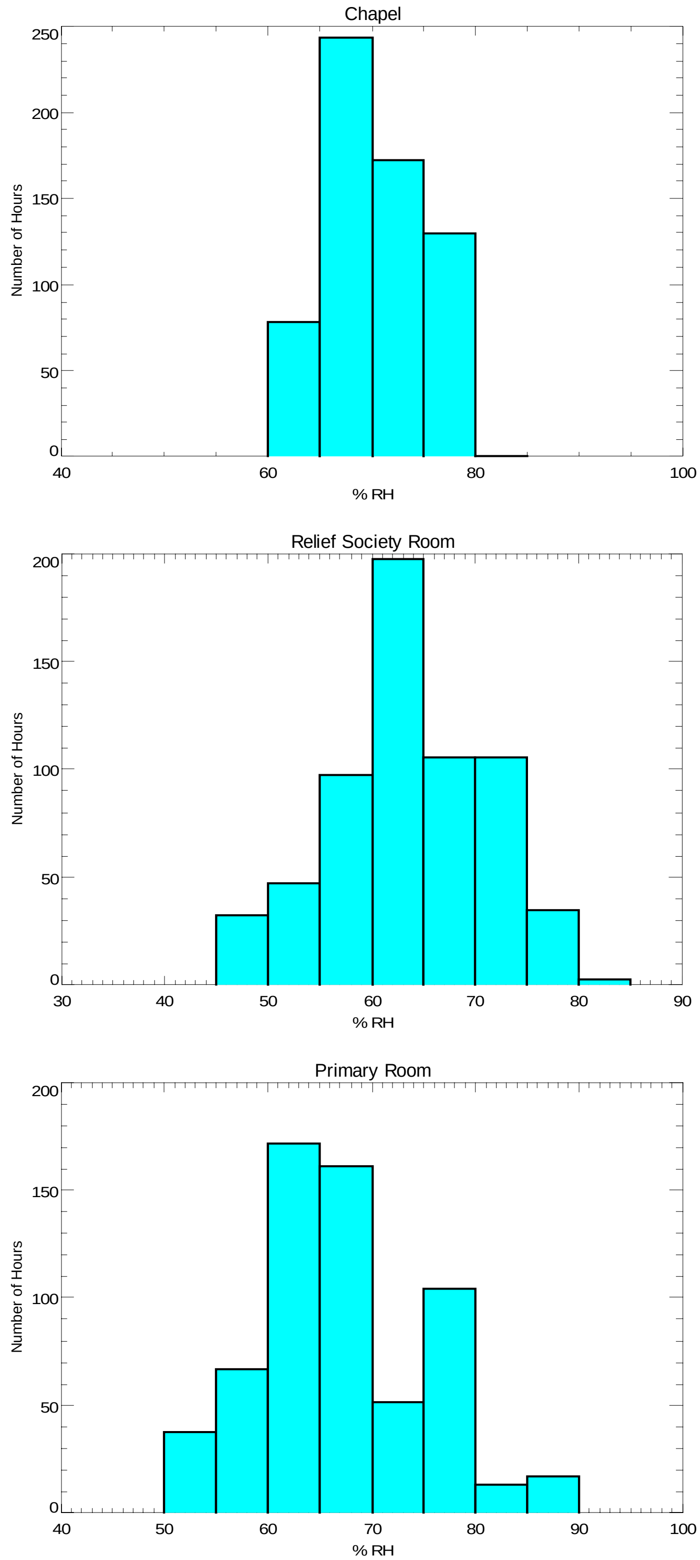

Figure A8-23. Duration of Relative Humidity Levels

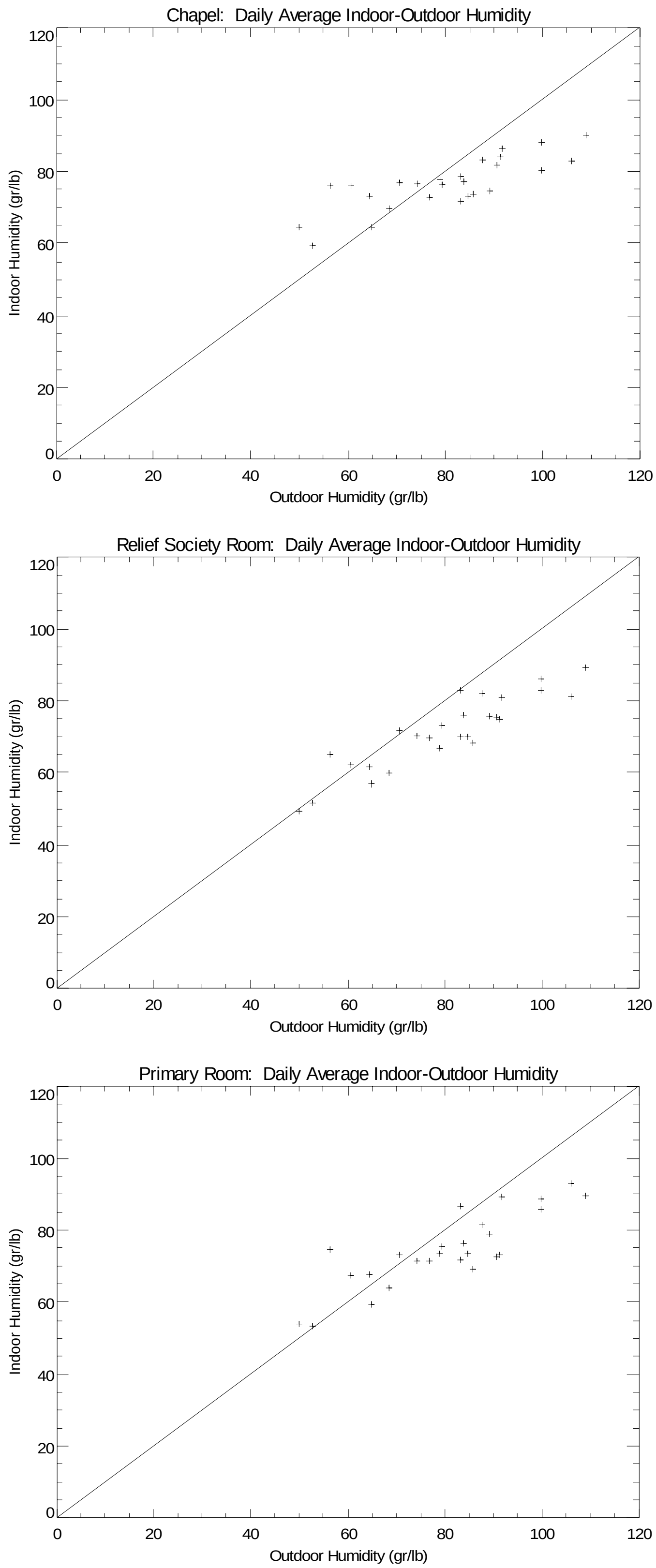

Figure A8-24. Indoor Humidity Variation with Outdoor Humidity

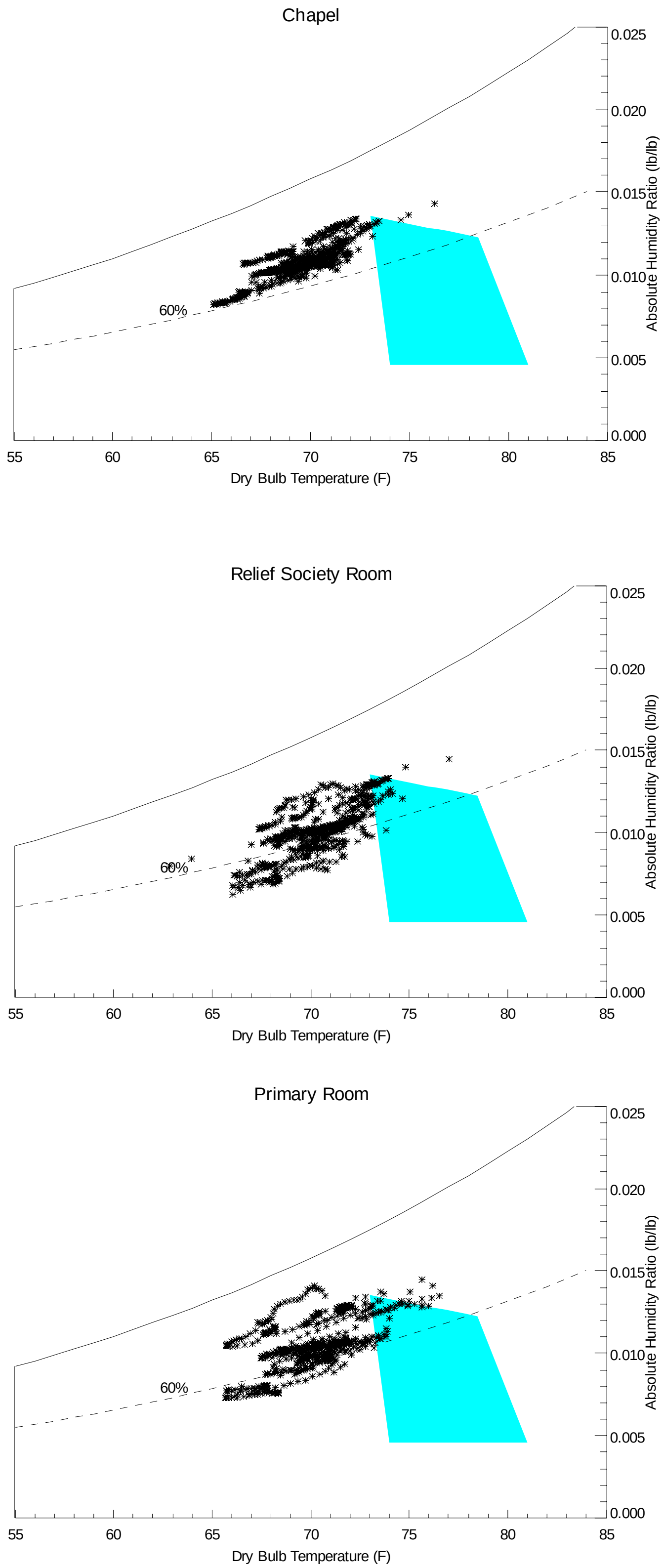

Figure A8-25. Indoor Air Quality Comparison with ASHRAE Comfort Zone for Cooling

Infiltration Estimate from CO_2 Decay

Figure A8-26, Figure A8-27, and Figure A8-28 show the resulting decay trends using CO_2 levels immediately after high occupancy periods for the Chapel, the Relief Society room, and the Primary room. The predicted air change rate (ACH) is shown on each plot. CO_2 tracer gas was used to seed the building on August 2, 2004.

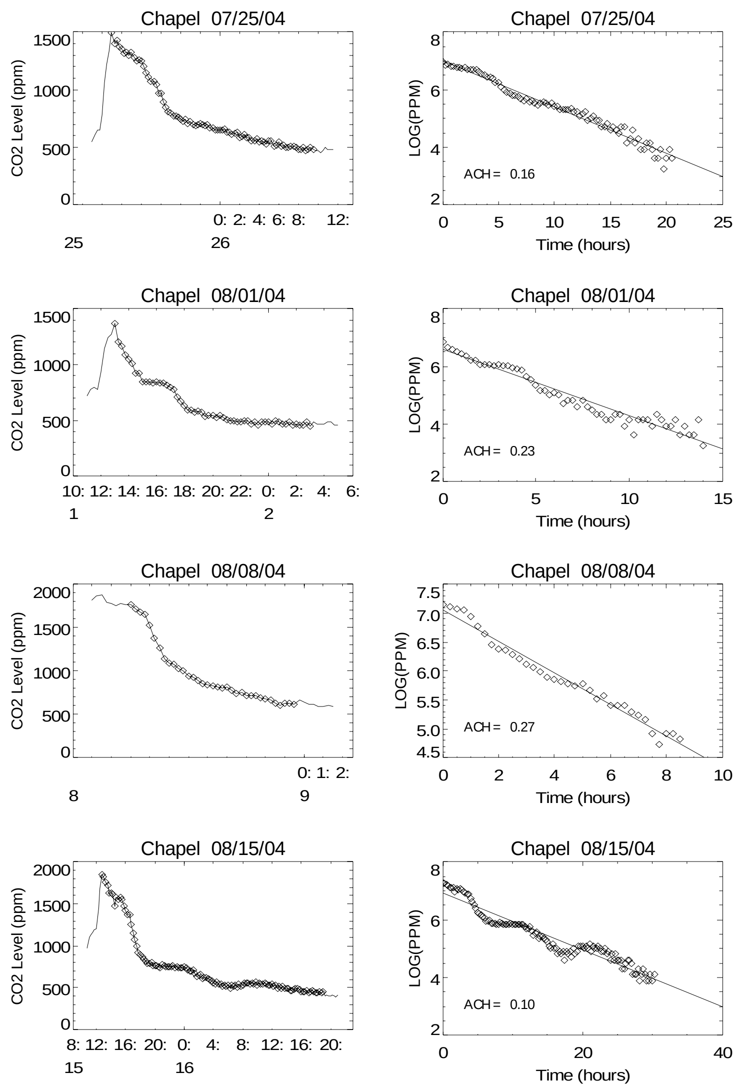

Figure A8-26. Main Room (Chapel): Tracer Gas Decay Using CO_2 for Various Periods

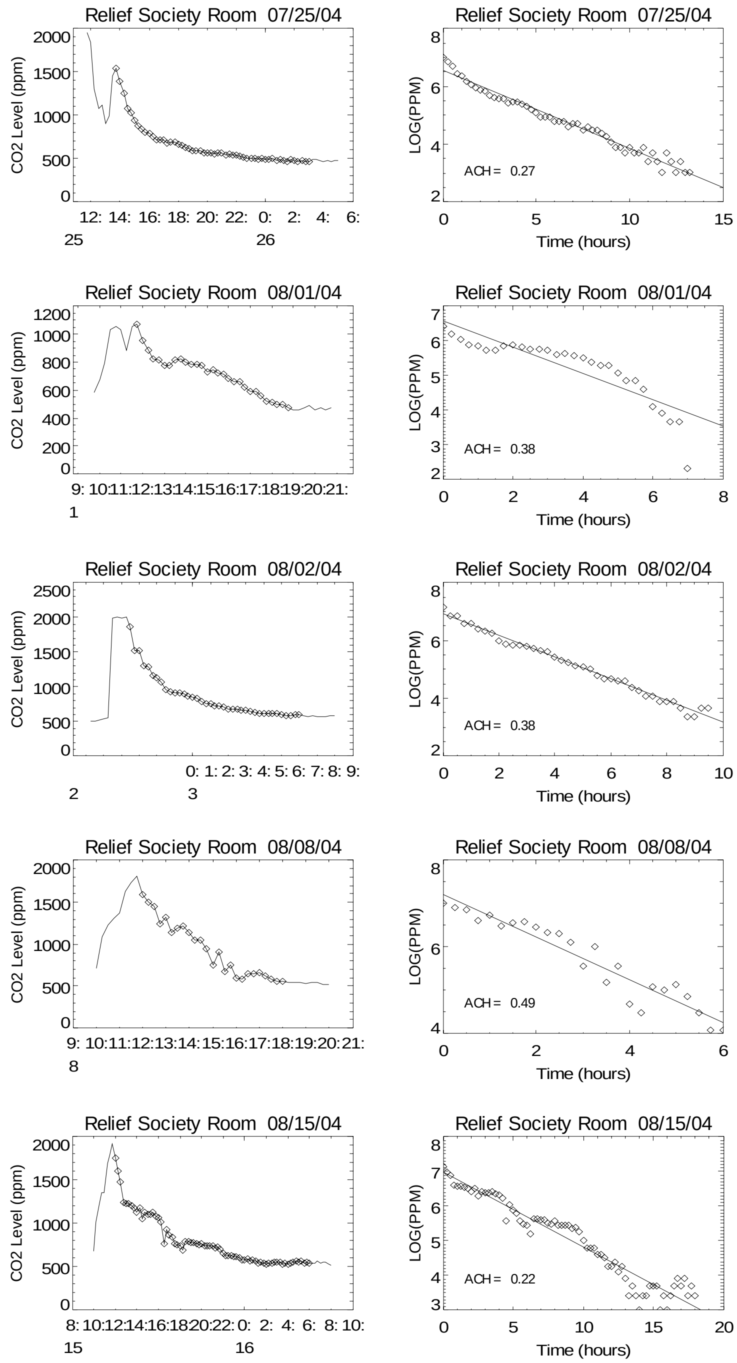

Figure A8-27. Relief Society: Tracer Gas Decay Using CO_2 for Various Periods

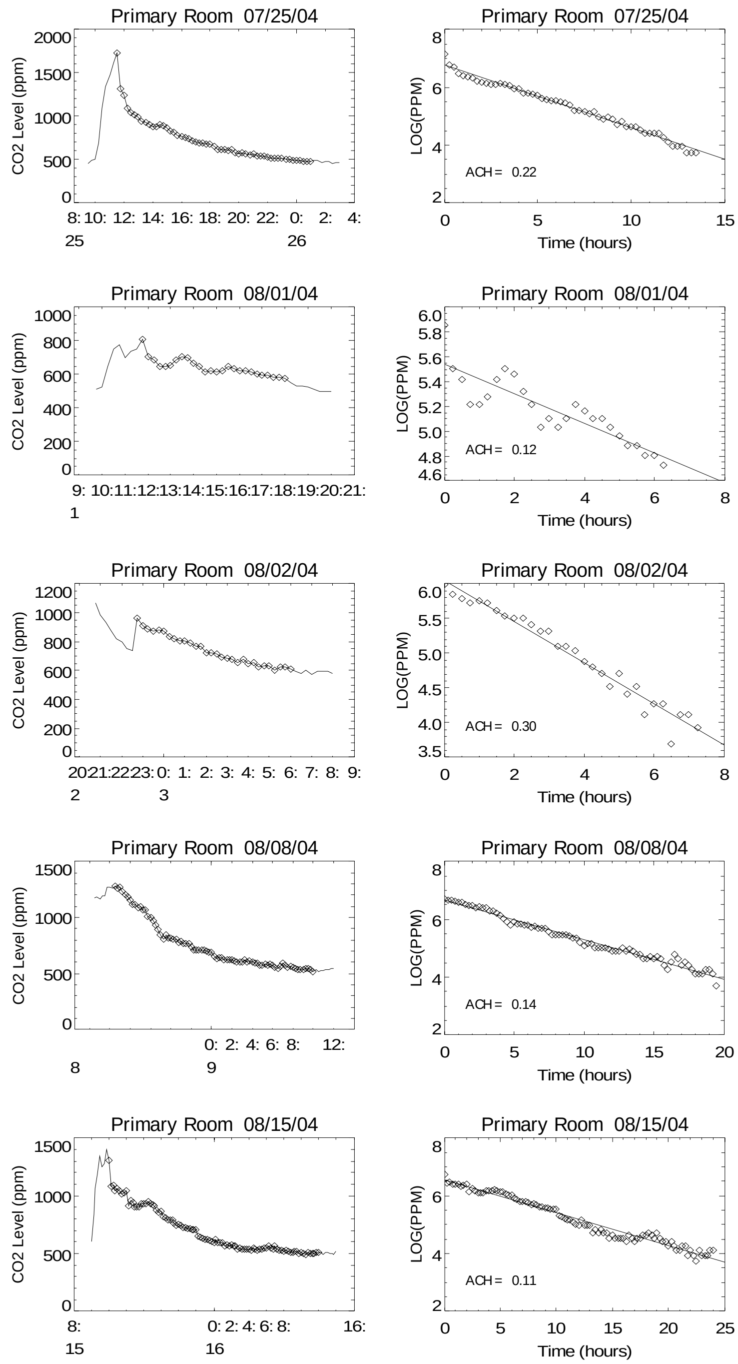

Figure A8-28. Primary Room: Tracer Gas Decay Using CO_2 for Various Periods

Table A8-15 summarizes the results of the tracer gas decay tests in the plots above. The table also includes the estimated infiltration airflow based on the building volume of 98,056 ft^3.

Table A8-15. Summary of Tracer Gas Decay Tests

Chapel

Start Time	End Time	ACH	Flow (cfm)
25-Jul 01:00 PM	26-Jul 09:30 AM	0.16	262
01-Aug 01:00 PM	02-Aug 03:00 AM	0.23	377
08-Aug 03:00 PM	08-Aug 11:30 PM	0.27	446
15-Aug 12:45 PM	16-Aug 07:00 PM	0.10	160

Relief Society

Start Time	End Time	ACH	Flow (cfm)
25-Jul 01:45 PM	26-Jul 03:00 AM	0.27	439
01-Aug 11:45 AM	01-Aug 06:45 PM	0.38	622
02-Aug 08:30 PM	03-Aug 06:00 AM	0.38	615
08-Aug 12:00 PM	08-Aug 06:00 PM	0.49	803
15-Aug 12:00 PM	16-Aug 06:00 AM	0.22	352

Primary

Start Time	End Time	ACH	Flow (cfm)
25-Jul 11:30 AM	26-Jul 01:00 AM	0.22	357
01-Aug 11:45 AM	01-Aug 06:00 PM	0.12	195
02-Aug 10:45 PM	03-Aug 06:00 AM	0.30	485
08-Aug 02:30 PM	09-Aug 10:00 AM	0.14	222
15-Aug 12:00 PM	16-Aug 12:00 PM	0.11	187

Note: Flow determined with building volume of: **98,056** ft^3

In comparison to the ACH values above, the nominal leakage rate (defined as ACH_{50} divided by 20) from the blower door test above is 0.38 ACH.

Utility Bills

Gas use is primarily used for space heating. The tables and graphs below show the gas and electric use trends for the facility. The overall energy use index for the building is summarized below.

	Heating Energy Use Index ($MBtu/ft^2$-year)	Electric Use Index (kWh/ft^2-year)
2002-2003 Season	55.4	2.52
2003-2004 Season	61.5	2.15

Season is from June 2002 to May 2003 and from June 2003 to May 2004

Table A8-16. Summary of Electric Bills

	Days in Month	Energy (kWh)	Cost ($)	$/kWh	Elec. Use per Sq-Ft (kWh/sq ft)
6/24/2002	33	1,600	164.95	0.10	0.18
7/26/2002	29	1,280	138.01	0.11	0.14
8/26/2002	31	2,400	258.93	0.11	0.27
9/25/2002	28	1,120	130.01	0.12	0.13
10/23/2002	33	1,280	147.62	0.12	0.14
11/22/2002	27	1,280	145.31	0.11	0.14
12/23/2002	32	2,720	287.83	0.11	0.31
1/27/2003	32	1,920	197.05	0.10	0.22
2/24/2003	33	3,360	334.93	0.10	0.38
3/26/2003	25	1,280	143.61	0.11	0.14
4/24/2003	33	2,880	299.12	0.10	0.32
5/27/2003	28	1,280	144.05	0.11	0.14
6/24/2003	34	1,760	185.72	0.11	0.20
7/28/2003	29	1,760	182.16	0.10	0.20
8/27/2003	34	1,440	151.24	0.11	0.16
9/25/2003	27	1,120	124.45	0.11	0.13
10/24/2003	31	1,600	175.06	0.11	0.18
11/24/2003	27	1,760	189.97	0.11	0.20
12/23/2003	34	1,600	172.68	0.11	0.18
1/27/2004	30	2,400	260.89	0.11	0.27
2/24/2004	33	1,760	200.26	0.11	0.20
3/25/2004	27	1,920	221.87	0.12	0.22
4/26/2004	35	1,120	136.98	0.12	0.13
5/25/2004	28	1,120	126.00	0.11	0.13
2002-2003	364	22,400	$ 2,391	0.11	2.52
2003-2004	369	19,360	$ 2,127	0.11	2.18

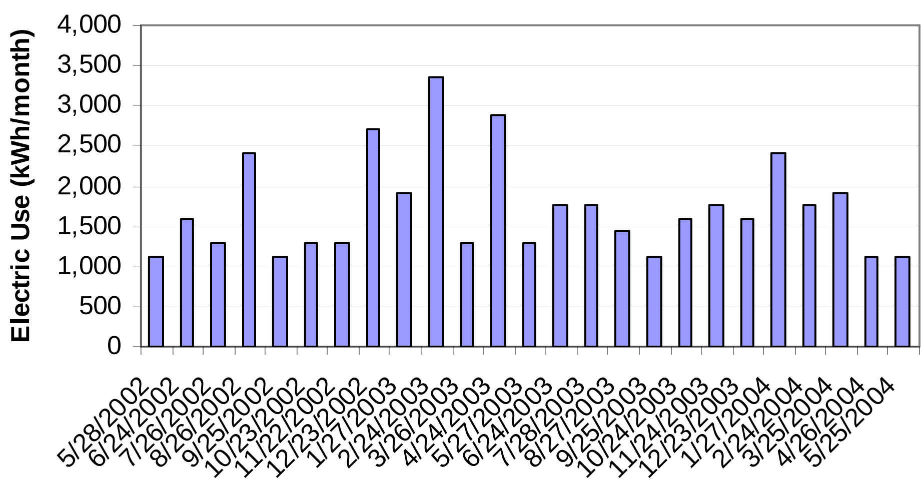

Figure A8-29. Monthly Electricity Use Trends

Table A8-17. Summary of Gas Bills

	Days in Month	Gas Use (therms)	Delivery Cost ($)	Delivery $/therm	Gas Use per Sq-Ft (therm/sq ft)
6/24/2002	31	92	35.78	0.39	0.010
7/26/2002	31	11	18.81	1.71	0.001
8/26/2002	29	11	18.81	1.71	0.001
9/25/2002	32	13	19.54	1.50	0.001
10/23/2002	29	170	41.03	0.24	0.019
11/22/2002	28	446	56.36	0.13	0.050
12/23/2002	31	733	73.38	0.10	0.082
1/27/2003	34	1,030	88.92	0.09	0.116
2/24/2003	31	930	78.47	0.08	0.104
3/26/2003	29	713	67.52	0.09	0.080
4/24/2003	29	504	56.32	0.11	0.057
5/27/2003	30	260	43.44	0.17	0.029
6/24/2003	32	87	33.77	0.39	0.010
7/28/2003	31	76	33.08	0.44	0.009
8/27/2003	32	12	17.96	1.50	0.001
9/25/2003	29	11	17.73	1.61	0.001
10/24/2003	29	239	41.86	0.18	0.027
11/24/2003	29	454	55.95	0.12	0.051
12/23/2003	32	829	78.15	0.09	0.093
1/27/2004	30	906	80.98	0.09	0.102
2/24/2004	33	1,355	101.99	0.08	0.152
3/25/2004	29	762	72.78	0.10	0.086
4/26/2004	33	562	64.10	0.11	0.063
5/25/2004	28	207	43.43	0.21	0.023
2002-2003	364	4,913	$ 598	0.12	0.552
2003-2004	367	5,500	$ 642	0.12	0.618

Note: The cost per therm ($/therm) only represents the delivery charges for the natural gas.

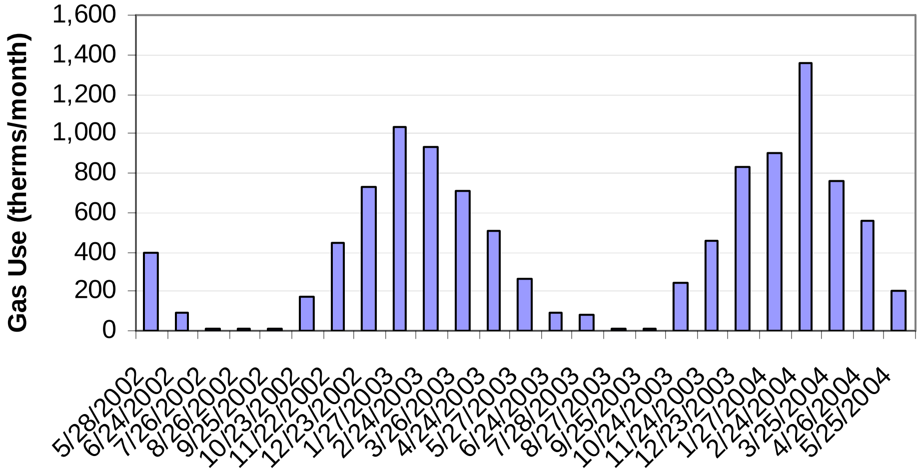

Figure A8-30. Monthly Gas Use Trends

Figure A8-31 shows the gas use variation with ambient temperature and Figure A8-32 shows the electricity use variation with ambient temperature. The variation in electricity use is likely due to large variation in occupancy.

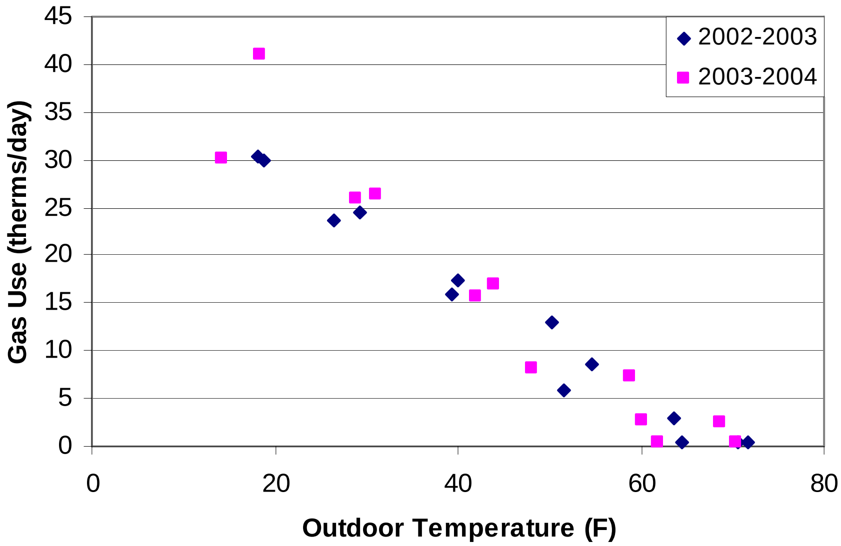

Figure A8-31. Variation of Gas Use with Ambient Temperature

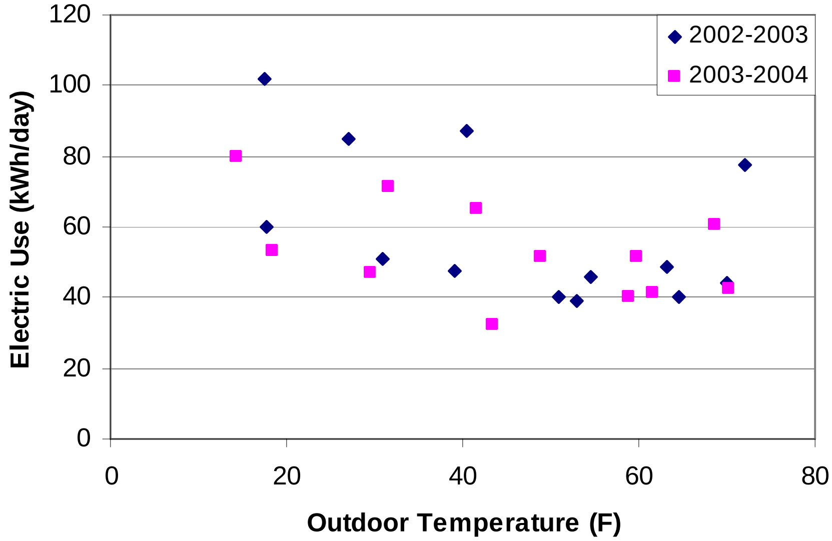

Figure A8-32. Variation of Electric Use with Ambient Temperature

Field Test Site 9 – Fast Food Restaurant, Lockport, NY

Figure A9-1. Photo of Building (Northeast)

CHARACTERISTICS

Building Description

The 3,300 sq ft facility is a one-story fast food restaurant that was built in 2002. The facility is partially divided into two spaces - the customer dinning space in the front half of the building and the kitchen/food preparation space in the back half. Included are two restrooms, a small locker room, and one manager's office. Figure A9-1 shows the front of the building. Five unitary rooftop units provide heating and cooling with natural gas furnaces for heat and DX compressors for cooling. Conditioned air is delivered to the store via ductwork installed above the suspended ceiling and ceiling diffusers. Two exhaust fans for the fryer and grill run continuously while the restaurant is open. A single down blast exhaust fan serves the restrooms. The building floor plan is shown in Figure A9-2.

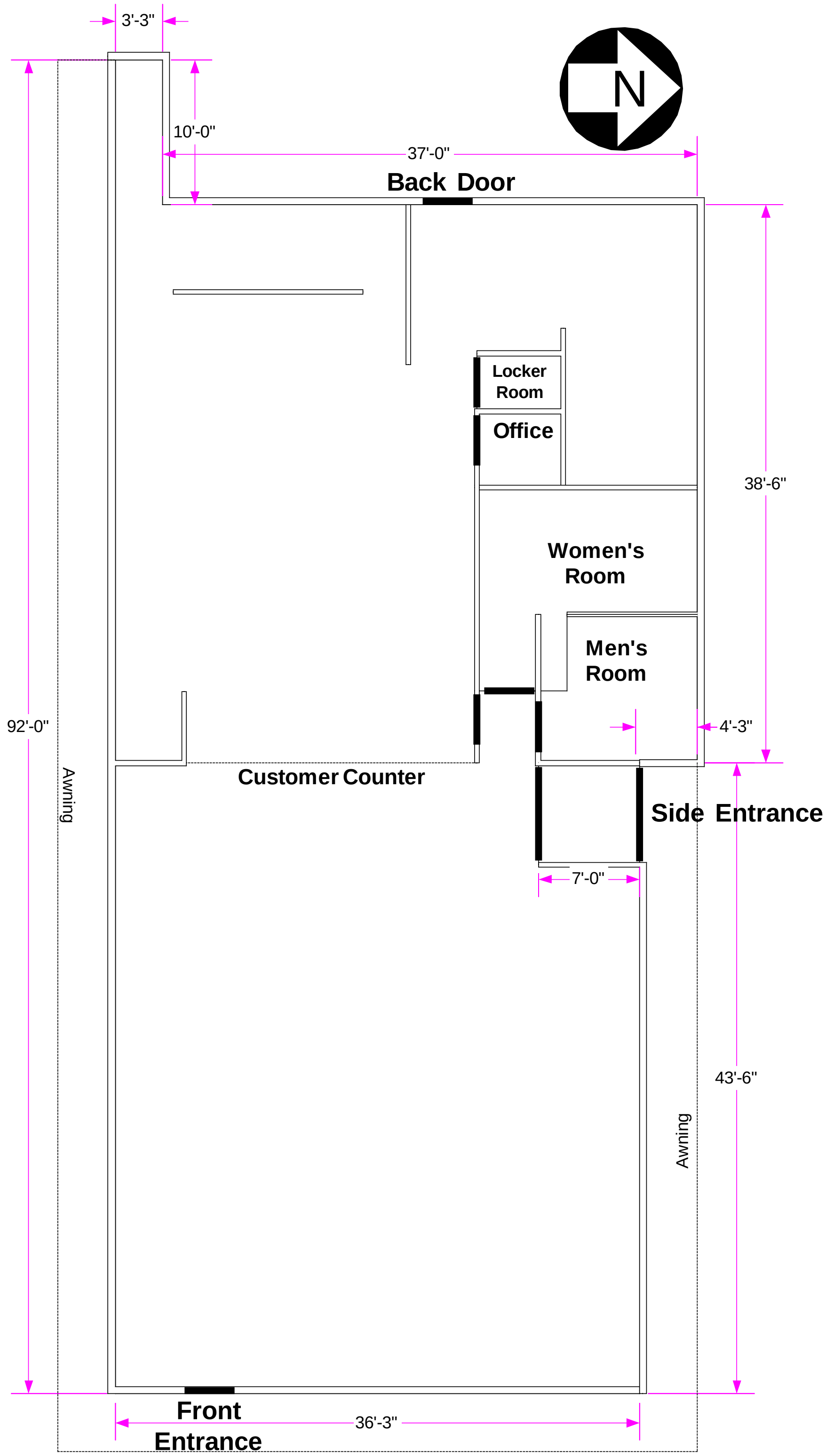

Figure A9-2. Building Floor Plan

Construction Details

Exterior walls are framed with wood 2x4 studs, insulated with 3.5 inches of fiberglass batt insulation between studs, covered with ½-inch plywood and finished with 4x6x12-inch decorative concrete block on the exterior. Interior walls are finished with ½-inch sheetrock and ¼-inch plastic paneling.

The building frame is completely constructed of wood, illustrated by Figure A9-3 and Figure A9-4. The roof joists and wall-roof framing are all constructed with wood instead of the more common steel fabrication in commercial buildings. Wood framed construction is common for this fast food chain.

The roof construction consists of ½-inch plywood and approximately 3 inches of foam insulation finished with built-up roofing. The entire store has a suspended (drop) ceiling 40 inches below the plywood roof deck. This 40-inch plenum space is used for standard wiring, gas lines, and ductwork.

A sheetrock wall in the ceiling plenum space separates the kitchen area from the dining area ceiling plenum. Presumably, this was constructed to prevent kitchen odors from circulating throughout the plenum space and entering the dinning area.

Figure A9-3 shows the details of the wall, ceiling, and roof construction. Figure A9-4 shows a picture of the ceiling plenum. Figure A9-5 illustrates typical wall and roof sections for exterior walls with the awning and Figure A9-6 illustrates wall sections without the awning.

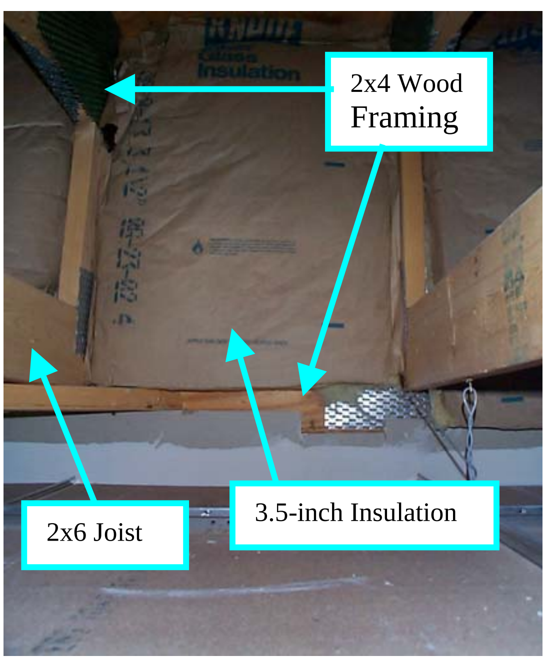

Wall and Ceiling Construction

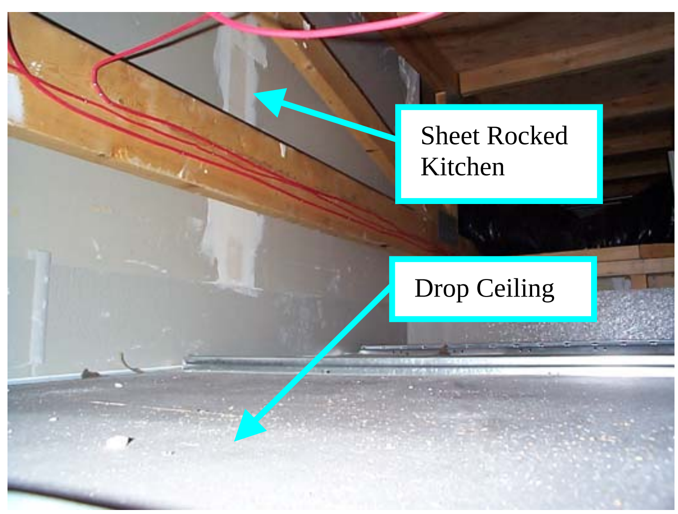

Sheet Rocked Wall in Kitchen Plenum

Figure A9-3. Wall/Roof Construction

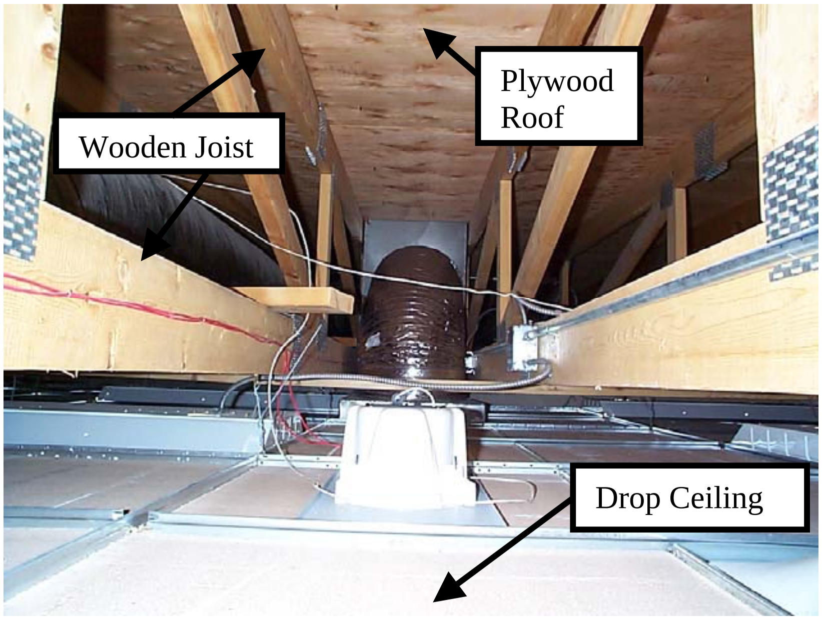

Figure A9-4. Ceiling Plenum

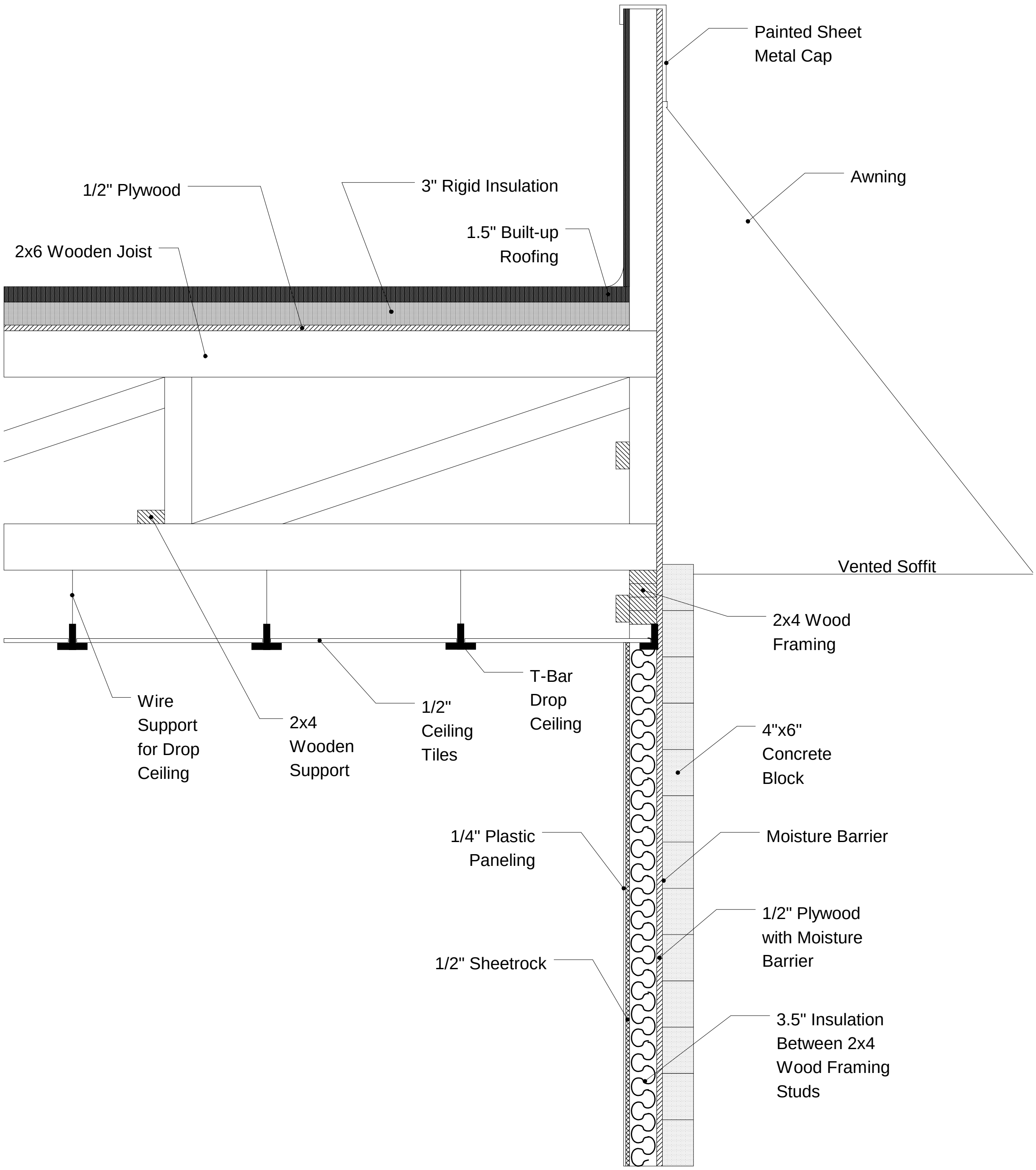

Figure A9-5. Roof, Ceiling and Wall Construction with Awning

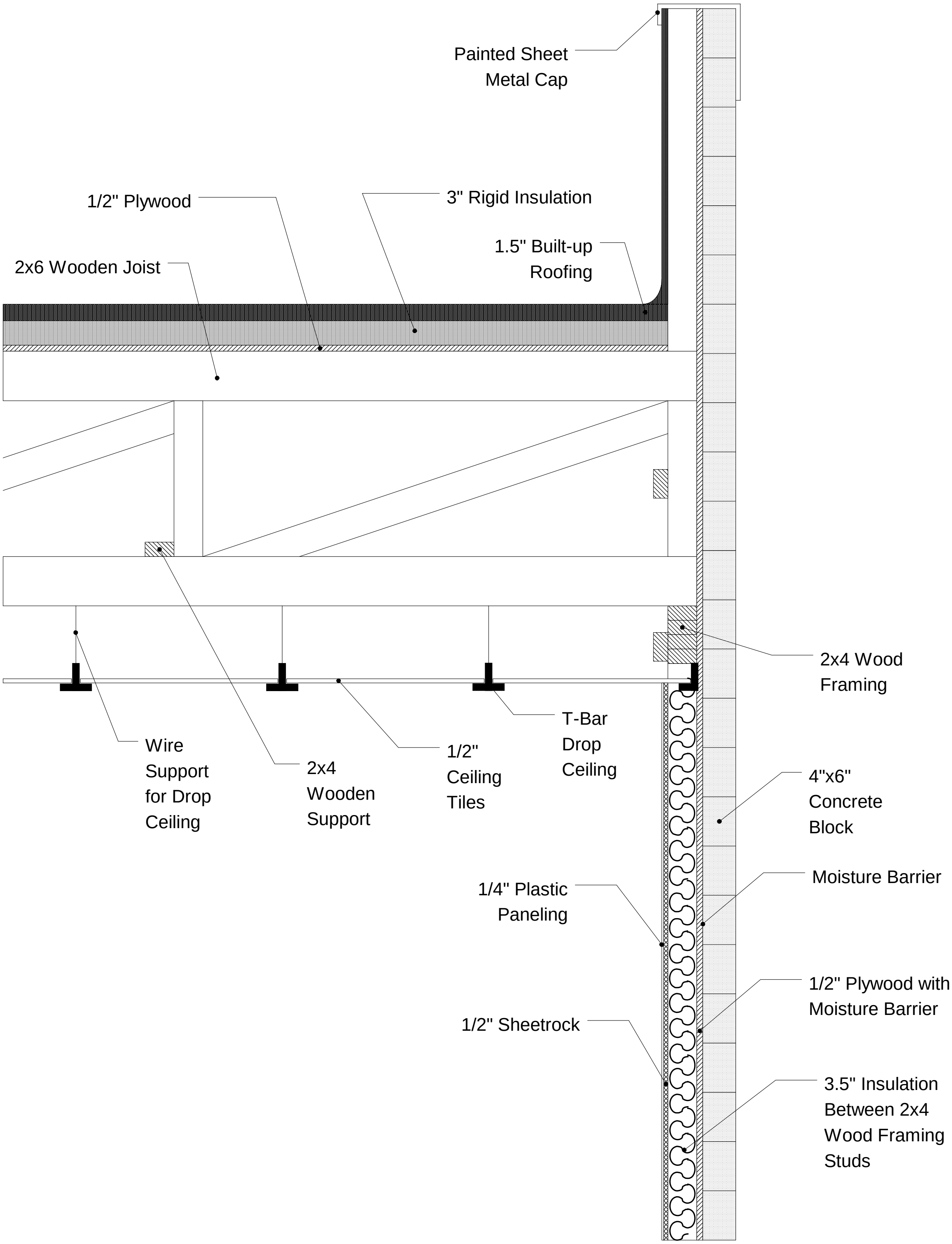

Figure A9-6. Roof, Ceiling and Wall Construction without Awning

HVAC System

Table A9-1 lists the HVAC equipment that serves the building.

Table A9-1. HVAC Equipment Installed at Site (Design Data)

	RTU-1 Front Dining	RTU-2 Mid-Dining	RTU-3 Counter	RTU-4 Kitchen	RTU-5 Rear
Manufacturer	Carrier	Carrier	Carrier	Carrier	Carrier
Model	48HJE006--541HQ	48HJE006--541HQ	48HJE006--541HQ	48HJE007--541HQ	48HJE007--541HQ
Cooling (tons)	5	5	5	6	6
Supply (cfm)	1,750	1,750	1,750	2,100	2,100
Gas Heating (MBtuh output)	93.15	93.15	93.15	93.15	93.15
Efficiency	81%	81%	81%	81%	81%

Figure A9-7 provides pictures of the RTUs. Each unit has a Honeywell Economizer. RTU-1, 2, and 3 have a 5-ton cooling capacity, while RTU-4 and RTU-5 have a 6-ton cooling capacity.

Typical Rooftop Unit

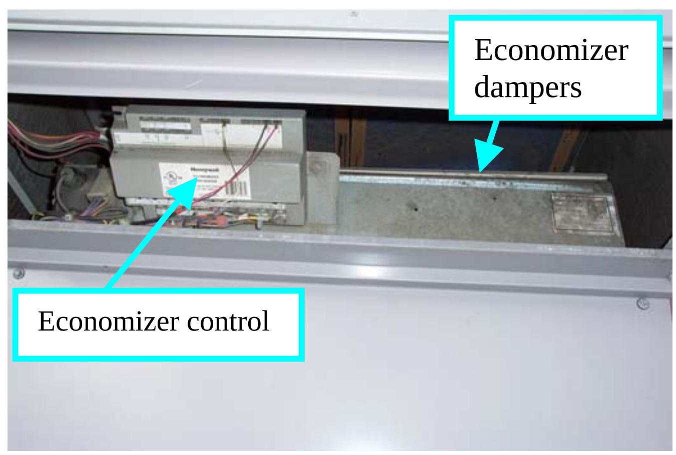

RTU Economizer

Figure A9-7. Roof Top Units

Rectangular sheet metal duct is used for supply trunks. Each 14"x16" supply trunk is about 10 feet long. Circular flexduct takeoffs, measuring 12 inches in diameter range from 2-12 feet long. Occasional 8-10 inch flexduct is used for longer lengths of 9-17 feet. All supply ductwork has 1-inch of insulation. Supply diffusers are standard 2-foot square three-cone ceiling diffusers (displayed in Figure A9-9). Figure A9-8 shows the approximate layout of the supply and return ductwork for RTU-1, 2, and 3 along with the corresponding zones served.

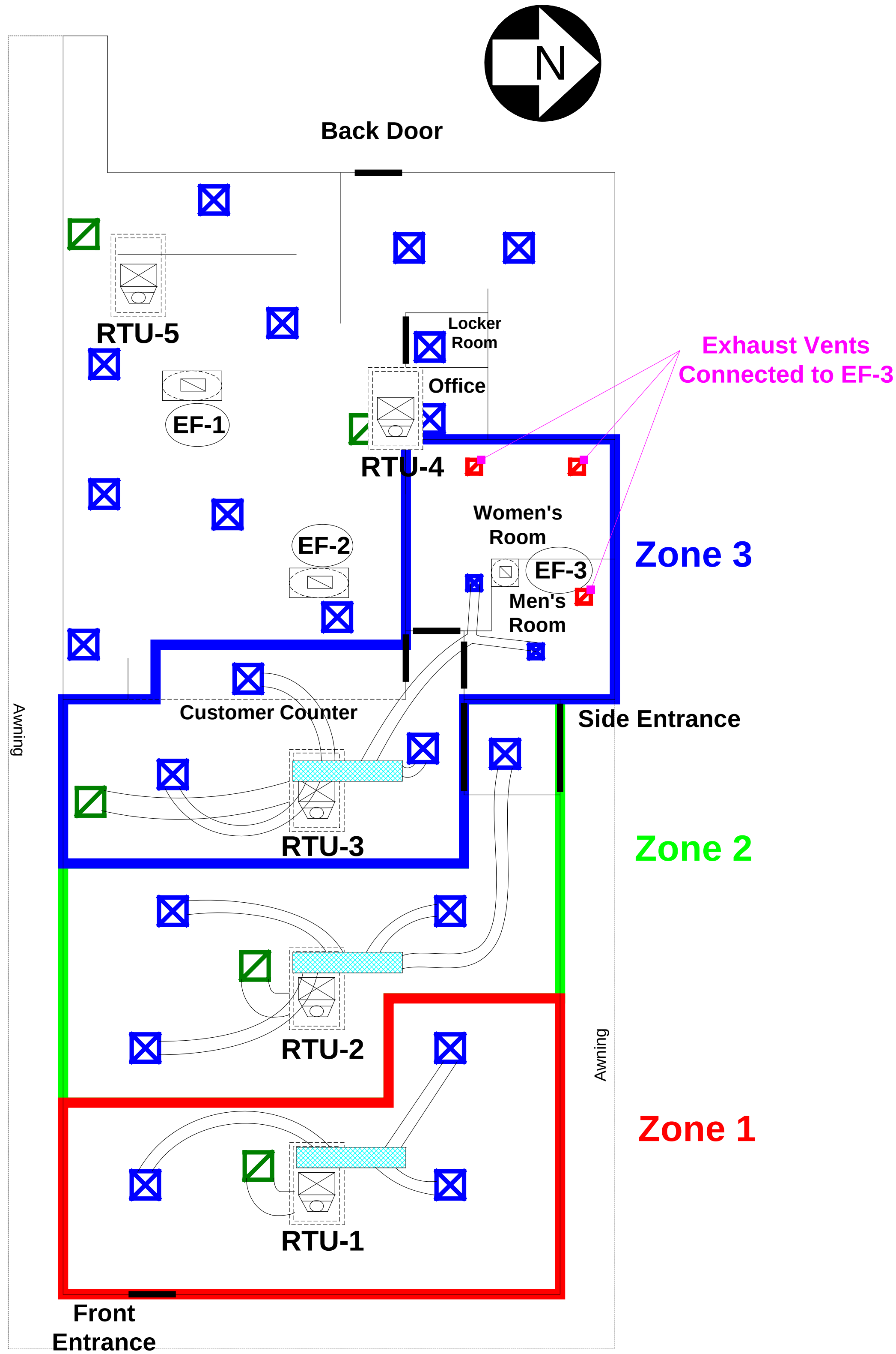

Figure A9-8. Supply and Return Duct System with Corresponding Zones

Figure A9-9. Three Cone Supply Diffuser in Drop Ceiling

The return ductwork for each roof top unit consists of a 2-foot square return grate (in the drop ceiling) with an 18 inch diameter flexduct attached just above the drop ceiling returning air to a rectangular 20”x24”x36” return trunk that connects to the RTU. Figure A9-10 displays the drop ceiling return grates and circular duct connections. Excluding the return for RTU-3, all returns are 2-3 feet offset from directly below the RTU itself, making the return ducts very short as illustrated in Figure A9-8 and Figure A9-10.

Return Grate with 18-inch Return Duct

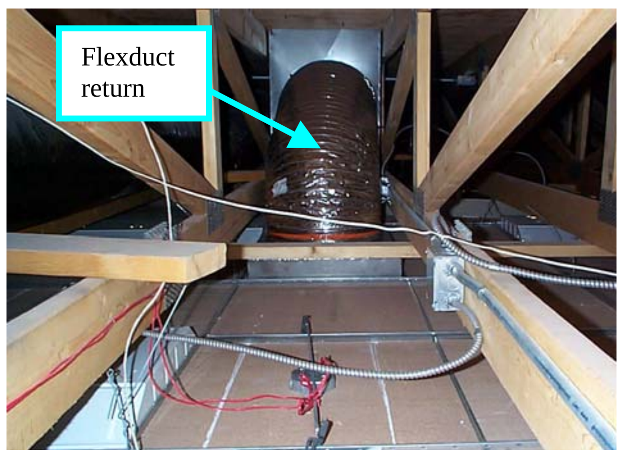

Return Duct and Return Trunk in Plenum

Figure A9-10. Return Duct Connections in Drop Ceiling Space

Figure A9-11 shows the two large roof exhaust fans (EF-1 & EF-2) utilized in conjunction with kitchen grill and fryer. Also pictured is the restroom exhaust fan (EF-3). Table A9-2 lists the model numbers and areas served by the exhaust fans.

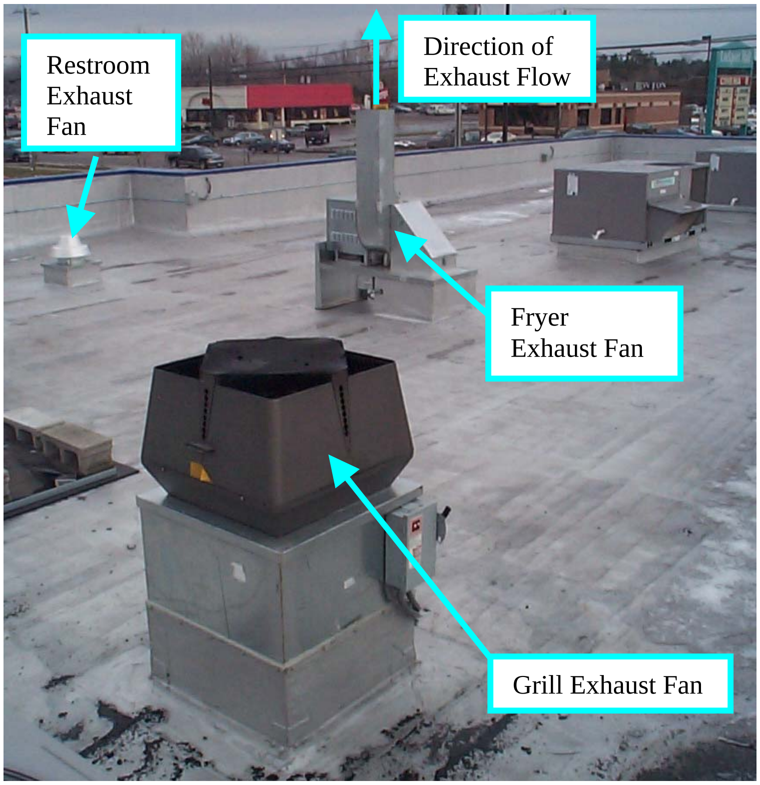

Figure A9-11. Grill and Fryer Exhaust Fans

Table A9-2. Exhaust Fans

	EF-1 Back Grill	**EF-2 Fryer**	**EF-3 Restrooms**
Manufacturer		Penn Ventilation	Dayton
Model		D10DPBK	4YC65

The facility has a Profile Systems controller to remotely control the HVAC equipment, exhaust fans, and exterior lighting. Off-site monitoring personnel can change setpoints, setbacks, and exterior lighting usage via centralized network. Only one sensor was located, to the right of the customer counter (labeled in Figure A9-8).

Figure A9-12. Typical Johnson Controls Temperature Sensor

MEASUREMENTS

All testing was completed the two days of August 11-12, 2004. Power readings, ventilation, and exhaust flow measurements were taken on August 11, 2004. On August 12, 2004, diffuser/return airflow, pressure mapping, and supply and return duct leakage measurements were taken. CO_2, temperature and relative humidity sensors were deployed the morning of August 11 in two locations to record space conditions for the facility and then collected again on August 12. Test personnel for both days were Dan Gott and Kenneth Larchar.

Building Envelope Airtightness

Due to the nature of the business, we were not able to assess building leakage rates using fan depressurization methods. However, the leakage characteristics of the building envelope were inferred from the air flow imbalance and the operating pressure of the building. This single operating point is used with an assumed exponent of 0.58 to 0.62 to find the flow coefficient.

The resulting ACH_{50} was 14-16, assuming the range of measured pressures and exponents. This implies the building was very tight.

Flow Imbalance:	1,010 cfm (exhaust)
Pressure:	-2.0 Pa
Assumed Exponent (n):	0.58-0.62
Resulting cfm_{50}:	6,500-7,400 cfm
Resulting ACH_{50}:	14-16 1/h
Assumed Flow Equation:	$Q = 666.5 \cdot \Delta p^{0.60}$

Pressure Mapping

Pressure readings in the building were taken using a digital micromanometer (DG 700) under normal operating conditions. With the RTUs and exhaust fans operating under normal conditions for August and all exterior doors closed, the building was depressurized by approximately 2.0 Pa. Figure A9-14 shows the pressure differences across the main doorways and restrooms in the building. The arrows on the figure indicate the direction of airflow (and decreasing pressure). The measurements on August 12, 2004 imply that the dining area is negative 0.8 Pa to the men's room. The positive pressure in the men's room (relative the dining area) is likely due to the airflow imbalance of 34 cfm (142 cfm of supply air and 108 cfm of exhaust air).

There is a ceiling vent to the plenum space between the double doors at the side entrance (Figure A9-13). This vent is installed to prevent depressurization of the entrance that may cause the doors to slam shut.

Figure A9-13. Vent to Plenum at Entrance

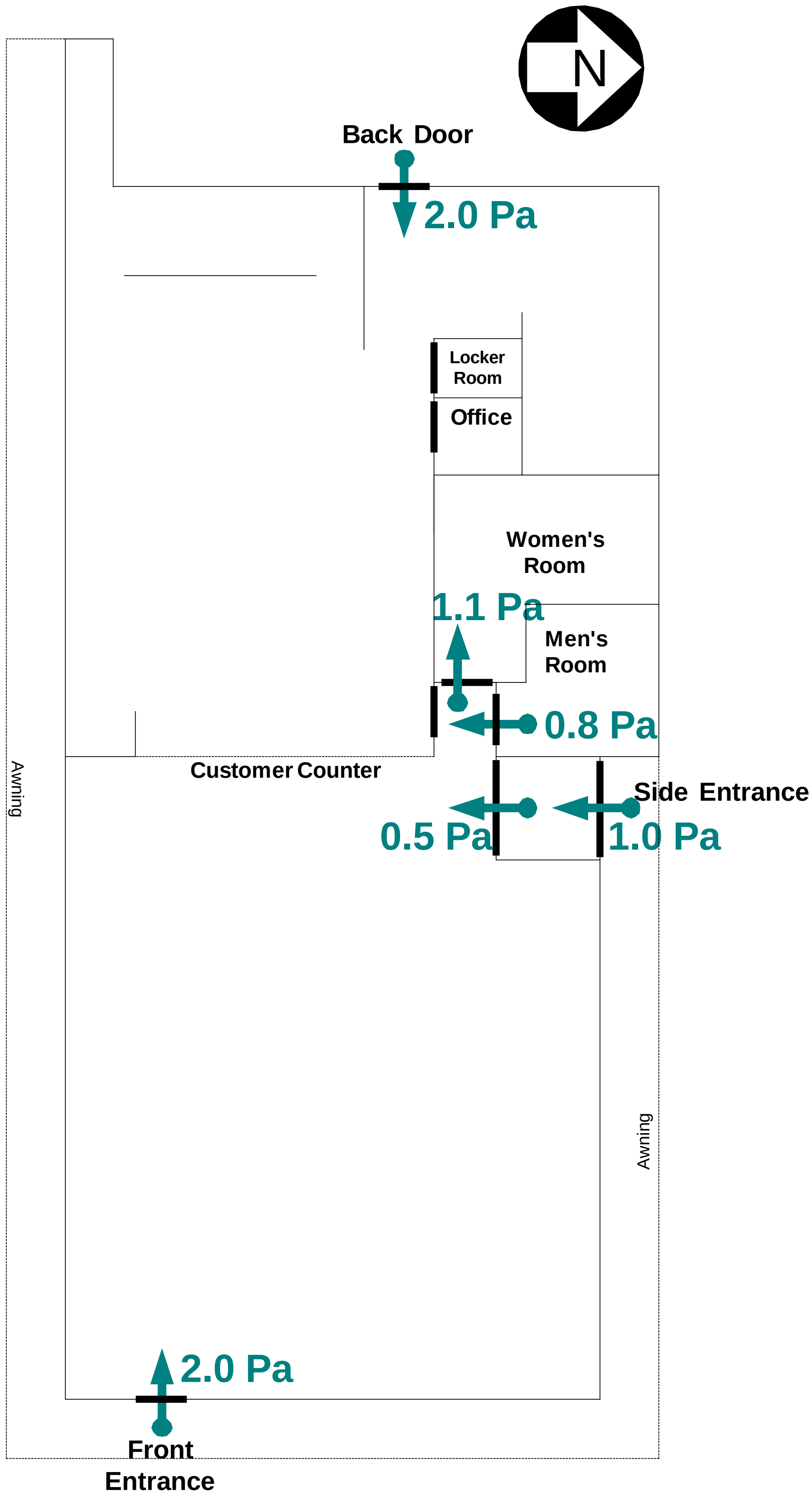

Figure A9-14. Pressure Differences under Normal Operating Conditions

HVAC Airflow Measurements

The ventilation air provided by the RTUs was measured using a Duct Blaster fan connected to the ventilation hood on the RTU. The flow through the Duct Blaster fan at the standard operating static pressure in the ventilation hood is the amount of fresh air provided by that unit. Figure A9-15 shows how the Duct Blaster was set up to measure RTU ventilation. Ventilation airflow was measured on all five of the RTUs. The economizer dampers on RTU-1 were in the closed position however, we still measured a minimal 52 cfm of ventilation flow. The ventilation airflow of RTU-1 (with the closed dampers) is an indication of the leakage through the economizer dampers. Table A9-3, Table A9-4, and Table A9-5 show the results for the ventilation airflow tests on all five units.

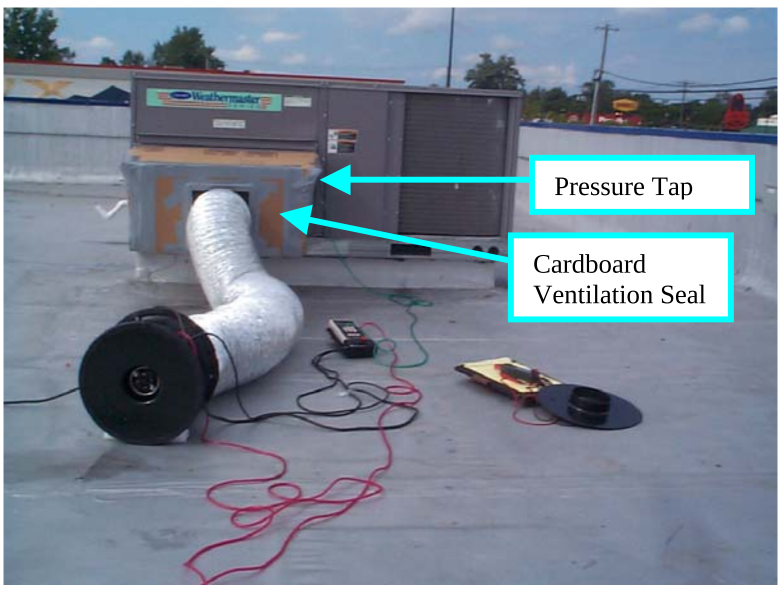

Figure A9-15. Duct Blaster Set Up to Measure Ventilation Airflow

Table A9-3. Roof Top Unit Ventilation Airflow Data

RTU-1

	Test Date 8/11/04
Static Pressure in Ventilation Hood (Pa)	-0.4
Airflow @ Average Ventilation Static (cfm)	52.1
R-Squared	0.969

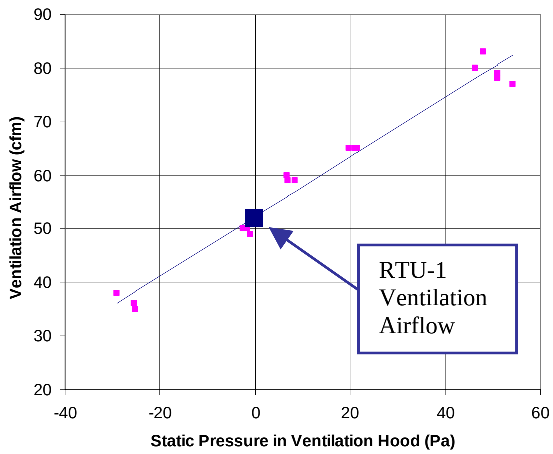

Test Data:

Nominal Ventilation Static (Pa)	Nominal Flow (cfm)	Ring
54.2	77	3
51.0	78	2
50.9	79	3
48.0	83	2
46.2	80	3
21.4	65	3
21.1	65	3
19.8	65	3
8.3	59	3
6.8	59	3
6.6	60	3
-1.1	49	3
-1.6	50	3
-2.6	50	3
-25.3	35	3
-25.4	36	3
-29.1	38	3

RTU-2

	Test Date 8/11/04
Static Pressure in Ventilation Hood (Pa)	-10.1
Airflow @ Average Ventilation Static (cfm)	438.7
R-Squared	0.696

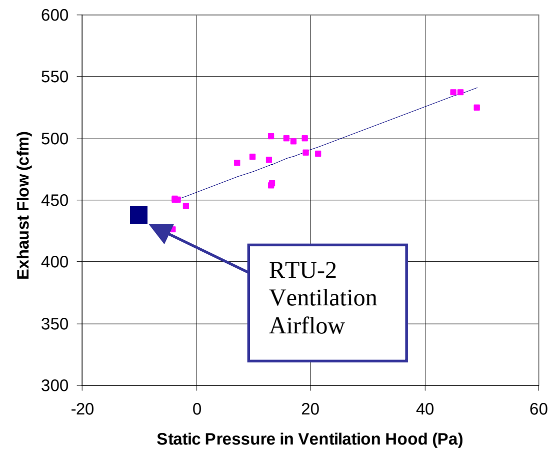

Test Data:

Nominal Ventilation Static (Pa)	Nominal Flow (cfm)	Ring
49.2	525	1
46.4	537	1
45.2	537	1
21.5	487	1
19.3	488	1
19.1	500	1
17.2	497	1
15.8	500	1
13.3	463	1
13.2	462	1
13.1	501	1
12.8	482	1
10.0	485	1
7.2	480	1
-1.7	445	1
-3.2	450	1
-3.6	450	1
-3.7	451	1
-4.0	426	1
-5.5	437	1
-9.2	434	1
-9.8	443	1
-13.3	455	1
-17.6	478	1
-24.0	446	1
-28.0	463	1

Table A9-4. Roof Top Unit Ventilation Airflow Data

RTU-3

	Test Date 8/11/04
Static Pressure in Ventilation Hood (Pa)	-2.6
Airflow @ Average Ventilation Static (cfm)	197.5
R-Squared	0.862

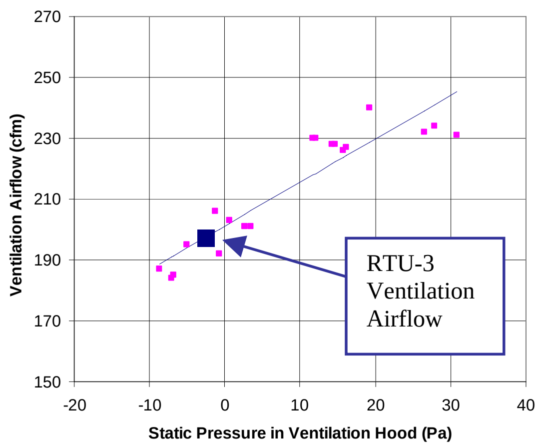

Test Data:

Nominal Ventilation Static (Pa)	Nominal Flow (cfm)	Ring
30.8	231	1
27.9	234	1
26.5	232	1
19.2	240	1
16.1	227	1
15.7	226	1
14.7	228	1
14.3	228	1
12.1	230	1
11.7	230	1
3.5	201	1
2.6	201	1
0.6	203	1
-0.7	192	1
-1.3	206	1
-5.0	195	1
-6.8	185	1
-7.1	184	1
-8.7	187	1
-9.8	203	1
-10.1	188	1
-16.4	175	1
-21.5	180	1

RTU-4

	Test Date 8/11/04
Static Pressure in Ventilation Hood (Pa)	-1.2
Airflow @ Average Ventilation Static (cfm)	218.1
R-Squared	0.943

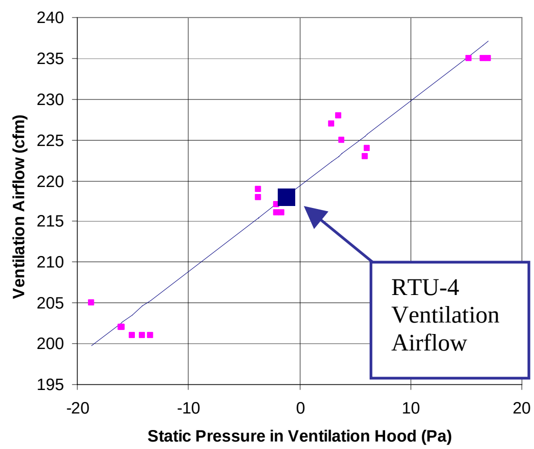

Test Data:

Nominal Ventilation Static (Pa)	Nominal Flow (cfm)	Ring
17.0	235	2
16.5	235	2
15.2	235	2
6.1	224	2
5.9	223	2
3.8	225	2
3.5	228	2
2.9	227	2
-1.6	216	2
-2.1	216	2
-2.1	217	2
-3.7	218	2
-3.7	219	2
-13.4	201	2
-14.1	201	2
-15.1	201	2
-16.0	202	2
-16.1	202	2
-18.7	205	2

Table A9-5. Roof Top Unit Ventilation Airflow Data

RTU-5

	Test Date 8/11/04
Static Pressure in Ventilation Hood (Pa)	-29.7
Airflow @ Average Ventilation Static (cfm)	678.2
R-Squared	0.509

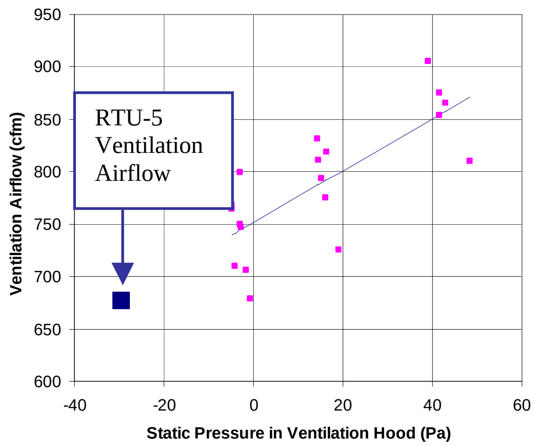

Test Data:

Nominal Ventilation Static (Pa)	Nominal Flow (cfm)	Ring
48.3	810	open
43.0	865	open
41.7	875	open
41.7	854	open
39.0	905	open
19.0	725	open
16.4	819	open
16.1	775	open
15.3	793	open
14.6	811	open
14.4	831	open
-0.6	679	open
-1.5	706	open
-2.8	747	open
-2.9	799	open
-2.9	750	open
-4.1	710	open
-4.7	768	open
-4.7	764	open
-6.0	842	open
-6.7	830	open
-7.8	750	open
-20.7	695	open
-21.3	694	open
-23.2	728	open

The airflow for the restroom exhaust fan (EF-3) and kitchen grill exhaust fan (EF-1) were measured using a capture tent. The tent was set up to measure the airflow through a fan when the static pressure inside the tent is zero pascals with respect to outdoors (Figure A9-16). There are three holes in the capture tent for various diameter fans. The exhaust fans were tested using a Duct Blaster fan because the airflow was less than the maximum Duct Blaster fan flow (approx. 1,500 cfm at 0 Pa). The Blower Door fan was only used to seal the tent hole sized for that fan. The third hole in the tent was sealed using the flexible duct transition piece[1] that came with the Duct Blaster. After sealing the hole in the transition piece with Duct Mask plastic wrap, the transition piece was inserted into the tent.

To prevent the restroom exhaust fan flows from backing up into the store, we started the Duct blaster fan and slowly zipped up the capture tent while adjusting the fan flow. Static pressure was measured inside the tent with respect to outdoors. The Duct Blaster flow conditioner was used (since the exhaust flow was less than 800 cfm[2]) and the velocity pressure was measured across the Duct Blaster fan using the pressure traverse that comes with the Duct Blaster. Several data points were taken at positive and negative static pressures in the tent to create a flow curve used to determine the exhaust fan flow at 0 Pa.

The kitchen grill exhaust fan (EF-1) was tested in a similar manor, but without the flow conditioner (since exhaust flow was greater than 800 cfm). We maintained negative pressures inside the capture tent to prevent exhaust from backing up into the store. The restroom exhaust air temperature was 70^{o}F and the grill exhaust temperature was 201^{o}F. Table A9-6 shows the raw data and results for both exhaust fans.

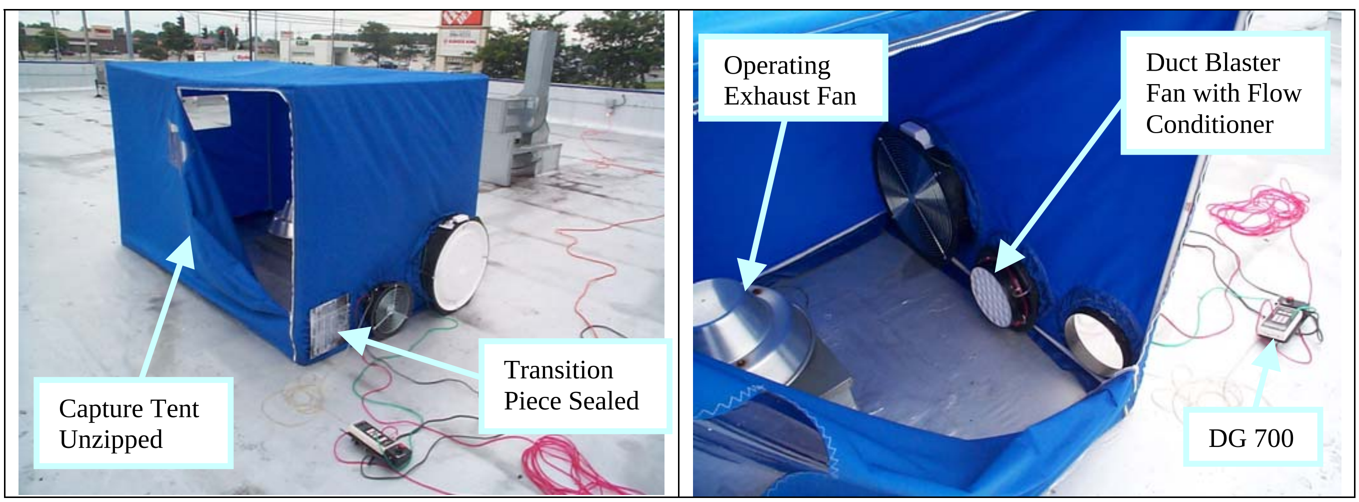

Figure A9-16. Capture Tent Set Up to Measure Exhaust Fan Flow

[1] The transition piece (from the flexible extension duct) is normally mounted to a duct or diffuser and then the flexible duct is connected between the duct transition piece and the Duct Blaster.
[2] One of the orifice rings 1-3 must be used with the flow conditioner which limits the Duct Blaster airflow to approximately 800 cfm at 0 Pa with ring 1.

Table A9-6. EF-3 Exhaust Fan Flow Data

EF-1

Test Results:

Slope	-5.6
Intercept	1080.4
R-Squared	0.91
Airflow	1080.4 cfm

Test Data:

Nominal Tent Pressure (Pa)	Nominal Flow (cfm)	Ring
-4.0	1092	open
-4.0	1097	open
-5.2	1108	open
-7.6	1142	open
-8.4	1134	open
-8.5	1116	open
-9.3	1147	open
-18.3	1190	open
-18.5	1175	open
-18.8	1183	open

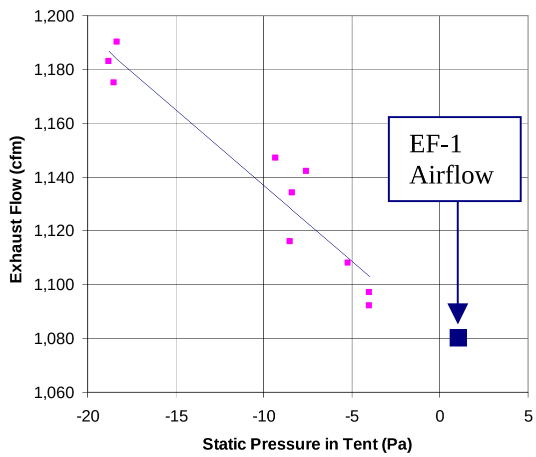

EF-3

Test Results:

Slope	-6.1
Intercept	325.5
R-Squared	0.91
Airflow	325.5 cfm

Test Data:

Nominal Tent Pressure (Pa)	Nominal Flow (cfm)	Ring
11.5	270	2
10.4	270	2
10.3	267	2
9.2	269	2
8.6	266	2
8.1	268	2
2.8	310	2
1.4	310	2
1.2	309	2
0.2	309	2
0.1	309	2
-0.4	309	2
-2.3	360	2
-3.0	357	2
-3.3	359	2
-4.1	358	2
-4.8	358	2
-6.1	358	2

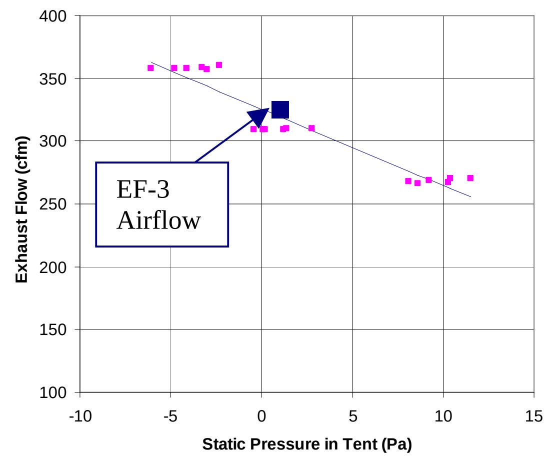

Since the capture tent would not fit over EF-2, we used a TSI hot wire anemometer to measure the exhaust flow by applying the equal area method (12 data points) for the fan. EF-2 has a measured airflow of 1,189 cfm (2,140 fpm average at 110°F).

To check the capture tent airflow results for EF-1, an equal area traverse was also used to determine the exhaust flow (thus measuring EF-1 two different ways). The results were less than

6% different (capture tent: 1,080 cfm, equal area method: 1,013 cfm). Table A9-7 and Table A9-8 show the airflows and power usage for the exhaust fans and roof top units. Table A9-9 shows a summary of the HVAC equipment sizing normalized to floor area.

Table A9-7. Measured Data for Exhaust Fans Installed at Site

	EF-1 Back Grill	EF-2 Fryer	EF-3 Restroom	Total
Exhaust Temperature (°F)	201	110	70	
Airflow (cfm)	1,080	1,189	325	2,595
Power (KW)	0.72*	0.92		
Power Factor	0.80*	0.74		
Normalized Power (W/cfm)	0.67*	0.77		

* Assumes a power factor of 0.8.

Table A9-8. Measured Data for RTUs

	Design Values	Measured Values					
	Supply Airflow (cfm)	Diffuser Supply (cfm)	Diffuser Return (cfm)	Ventilation Airflow (cfm)	Fresh Air Fraction	Supply Fan Power (kW)	Normalized Supply Fan Power (W/cfm)
RTU-1 Front Dining	1,750	1,652	1,443	52	3%	0.88**	0.53
RTU-2 Mid-Dining	1,750	1,884	1,226	439	23%	0.94**	0.50
RTU-3 Order Counter	1,750	1,699	1,504	197	12%	0.88**	0.52
RTU-4 Kitchen	2,100			218	10%*	1.00**	
RTU-5 Rear	2,100			678	32%*	1.06**	
Totals	9,450			1,585		0.95	

* Fresh air fraction is based on the design supply airflow.
** Supply fan power from December 2002.

Table A9-9. Summary of HVAC Equipment Sizing

	Area Used for Normalization	Design		Measured	
		Totals (cfm)	Normalized	Totals (cfm)	Normalized
SupplyAirflow (cfm)	Dining Area	5,250	2.69 cfm/ft^2	5,235	2.68 cfm/ft^2
Ventilation Airflow (cfm)	Entire Building	----	---- cfm/ft^2	1,681	0.51 cfm/ft^2
Exhaust Airflow (cfm)	Entire Building	----	---- cfm/ft^2	2,595	0.79 cfm/ft^2

The supply and return airflow for the dining area (RTU-1, 2, and 3) was measured at the diffusers using a Shortridge flow hood. Positioning and various obstructions prohibited testing of the diffusers in the kitchen area (RTU-4 & RTU-5). Figure A9-17 illustrates the location of the supply and return diffusers and the corresponding airflow measurements. Table A9-10 displays the static pressures in the various sections of the five units during standard operation.

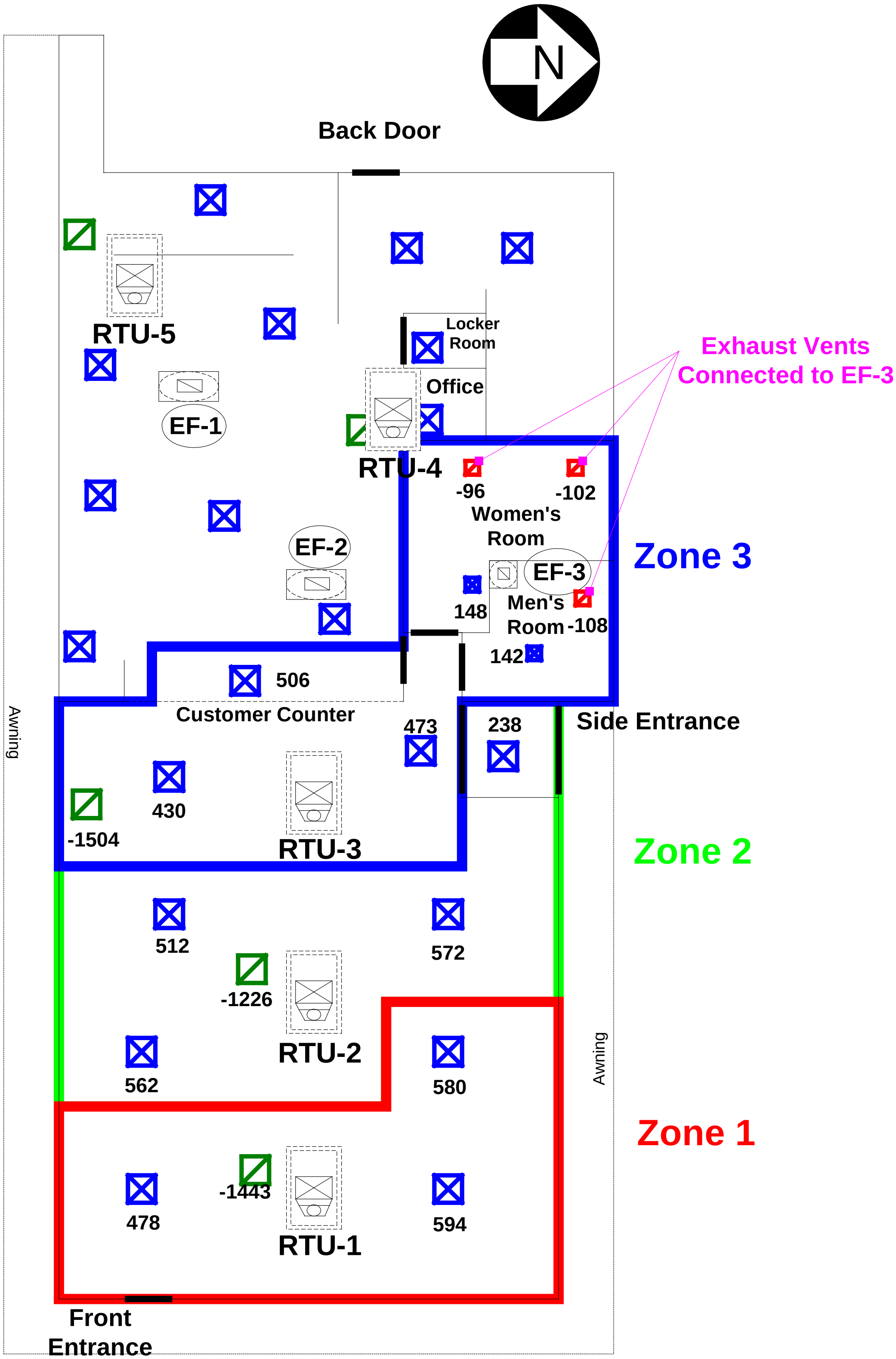

Figure A9-17. Diffusers Airflow Measurements

Table A9-10. Static Pressures in RTUs (Standard Operation on August 11, 2004)

	Ventilation (Pa)	Return (Pa)	Supply (Pa)	Inlet to Supply Fan (Pa)
RTU-1	-0.4 (dampers closed)	-137.5	85.3	-237.7
RTU-2	-10.13	-124.7	88.8	-219.0
RTU-3	-2.57	-130.3	57.2	-222.0
RTU-4	-1.20	-145.6	75.7	-255.7
RTU-5	-29.67	-140.6	95.0	-236.3

Duct Leakage Measurements

A Duct Blaster was used to measure leakage rates for the supply and return ductwork for the roof top units that serve the dining area (RTU-1, 2, and 3). In order to maintain comfort within the restaurant, all units were kept running except the one being tested. Plastic wrap was used to cover each supply and return diffuser for the roof top unit being tested. To isolate the supply side from the return side, we sealed off the supply fan (See Figure A9-18). To verify a good seal separating the supply and return, we depressurized the ductwork being tested and measured the static pressure in the other duct system. In all instances, the pressure on the opposite side of the seal was small. The pressure in the ductwork being tested averaged 89% greater than the ductwork not being tested.

To test the supply ductwork, the Duct Blaster was connected to the RTU by removing an exterior panel in the supply section as shown in Figure A9-19. The static pressure tap was located in the supply section. Several static pressure and airflow measurements were taken with ductwork depressurized from 9 – 104 Pa. The return ductwork was tested in a similar manner by moving the Duct Blaster to the return section (Figure A9-19). The seal at the supply fan was tested again.

Unblocked Supply Side

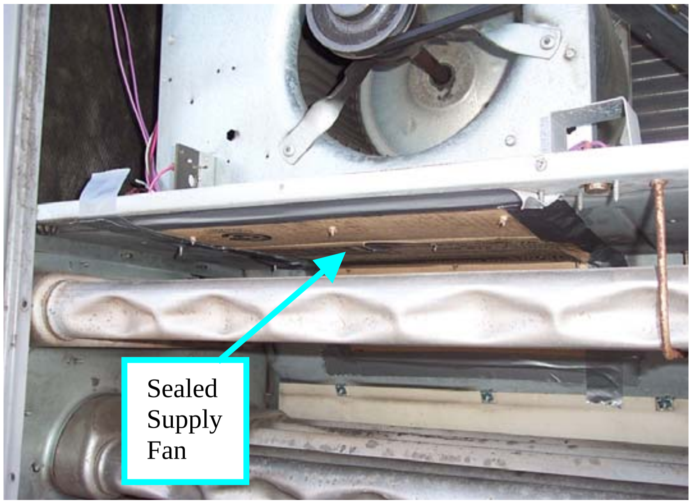

Blocked Supply Side

Figure A9-18. Sealed Supply Fan to Isolated Supply and Return Sections

Supply Side Return Side

Figure A9-19. Duct Blaster Set Up for Duct Leakage Testing

With the supply and return ductwork depressurized, static pressures were taken at all corresponding supply and return diffusers as a diagnostic check on the degree of pressurization. Figure A9-20 shows the resulting pressures measured at each diffuser with the ductwork for RTU-1, 2, and 3 depressurized. The uniformity of the pressures at the diffusers implies that leaks are uniformly spread around the systems. Table A9-11 summarizes the results of the diffuser static pressures.

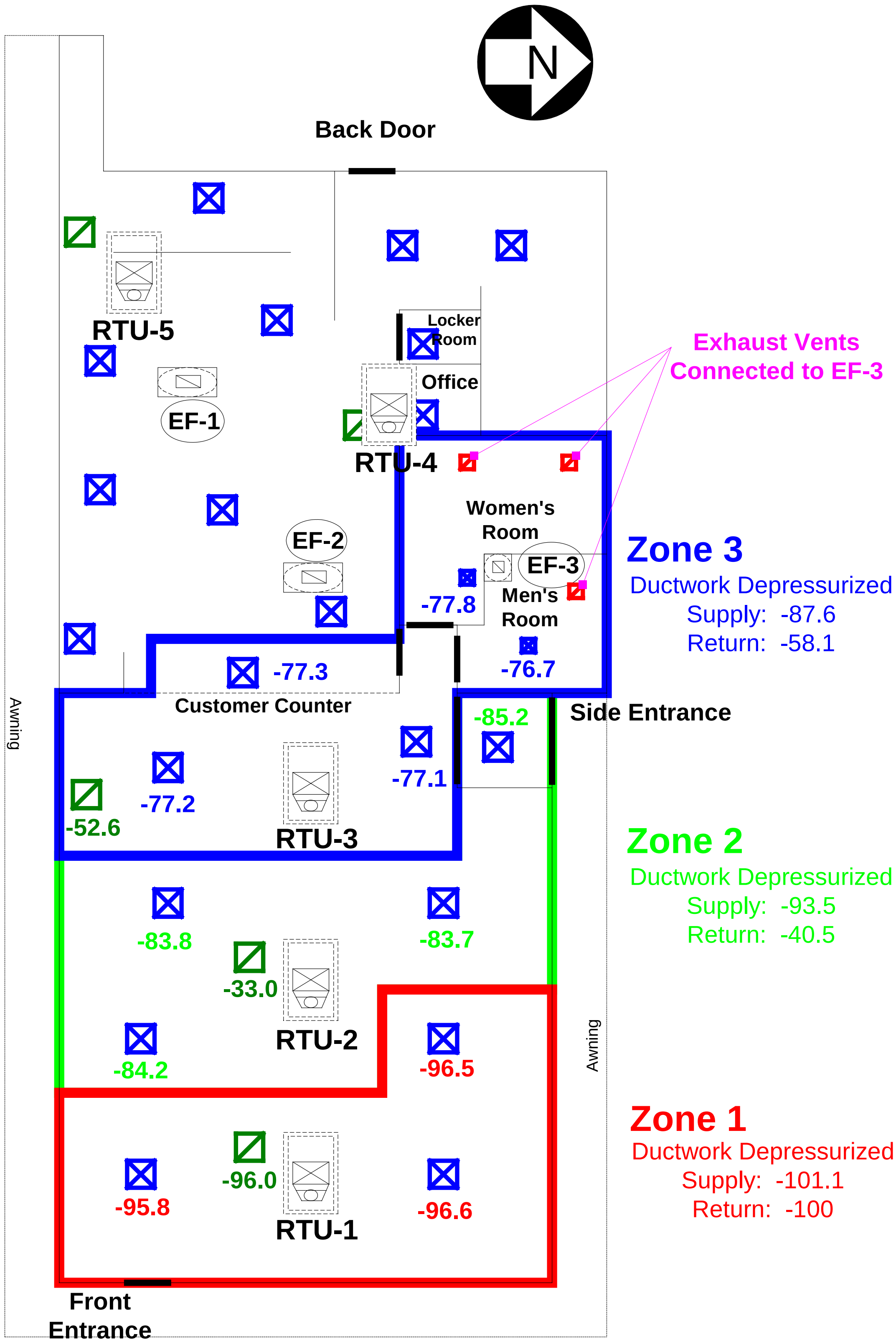

Figure A9-20. Supply and Return Pressure Mapping with Ductwork Depressurized

Table A9-11. Static Pressure at Linear Diffuser with Ducts Depressurized 14 Pa

	Corresponding Zone	Duct Depressurization (Pa)	Average Diffuser Pressure (Pa)	Pressure Drop (Pa)
RTU-1 Supply	1	-101.1	-96.3	4.8
RTU-1 Return	1	-100.0	-96.0	4.0
RTU-2 Supply	2	-93.5	-84.2	9.3
RTU-2 Return	2	-40.5	-33.0	7.5
RTU-3 Supply	3	-87.6	-77.2	10.4
RTU-3 Return	3	-58.1	-52.6	5.5

Figure A9-21 shows the resulting measured data from the duct leakage tests fit to a power function (raw data in Table A9-12 and Table A9-13). Figure A9-21 also shows our best estimate for duct leakage during normal operation, which uses one half of the plenum pressure as suggested in ASHRAE Standard 152P section B.2. Table A9-14 shows the resulting coefficients, exponents, and regression statistics. Table A9-15 summarizes the resulting duct leakage rates and ELA at a reference pressure of 25 Pa.

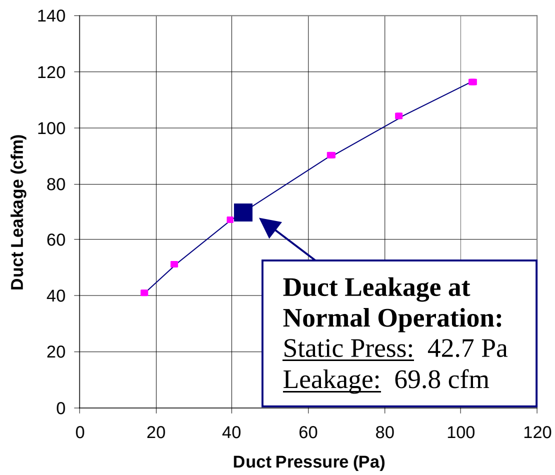

RTU-1 Supply Ductwork

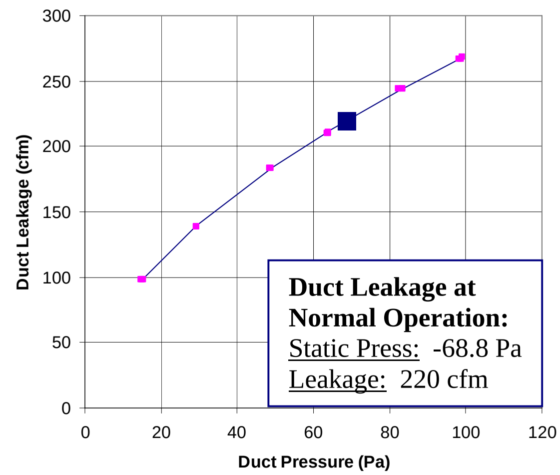

RTU-1 Return Ductwork

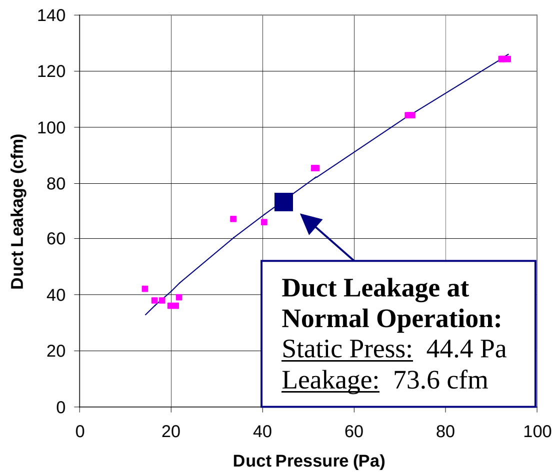

RTU-2 Supply Ductwork

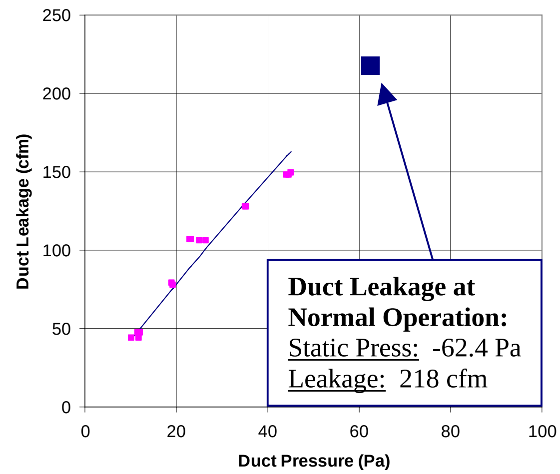

RTU-2 Return Ductwork

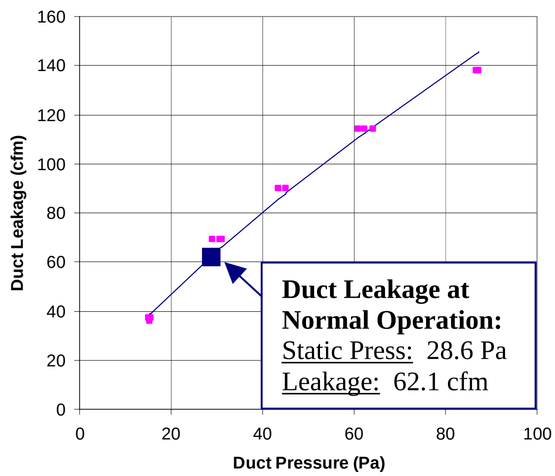

RTU-3 Supply Ductwork

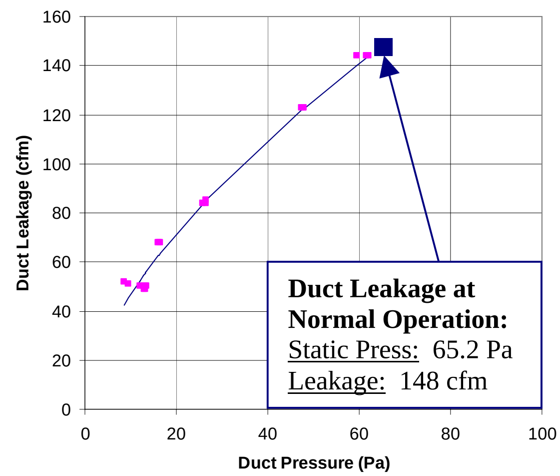

RTU-3 Return Ductwork

Figure A9-21. Duct Blaster Tests for Supply and Return Ductwork

Table A9-12. Raw Data from Duct Blaster Tests

RTU-1 Supply Ductwork

Flow Coefficient (K)	7.9	
Exponent (n)	0.580	
Leakage area (LBL ELA @ 25 Pa)	5.8	sq in
Airflow @ 25 Pa	51.2	cfm

Test Data:

	Nominal Duct Pressure (Pa)	Nominal Flow (cfm)	Ring
1	103.5	116	3
2	103.2	116	3
3	103.0	116	3
4	84.1	104	3
5	83.9	104	3
6	83.6	104	3
7	66.3	90	3
8	66.1	90	3
9	65.9	90	3
10	39.7	67	3
11	39.5	67	3
12	39.5	67	3
13	25.0	51	3
14	24.8	51	3
15	24.7	51	3
16	17.2	41	3
17	17.1	41	3
18	16.9	41	3

RTU-1 Return Ductwork

Test Results:

Flow Coefficient (K)	22.9	
Exponent (n)	0.535	
Leakage area (LBL ELA @ 25 Pa)	14.5	sq in
Airflow @ 25 Pa	128.1	cfm

Test Data:

	Nominal Duct Pressure (Pa)	Nominal Flow (cfm)	Ring
1	99.0	268	2
2	98.7	267	2
3	98.3	267	2
4	83.5	244	2
5	83.4	244	2
6	82.4	244	2
7	63.9	210	2
8	63.8	211	2
9	63.5	210	2
10	48.7	183	2
11	48.6	183	2
12	48.5	183	2
13	29.4	139	2
14	29.2	139	2
15	29.2	139	2
16	15.4	98	2
17	15.0	98	2
18	14.9	98	2

RTU-2 Supply Ductwork

Test Results:

Flow Coefficient (K)	4.8	
Exponent (n)	0.718	
Leakage area (LBL ELA @ 25 Pa)	5.5	sq in
Airflow @ 25 Pa	48.7	cfm

Test Data:

	Nominal Duct Pressure (Pa)	Nominal Flow (cfm)	Ring
1	93.8	124	3
2	92.6	124	3
1	92.4	124	3
2	72.7	104	3
3	72.4	104	3
4	71.9	104	3
5	51.8	85	3
6	51.6	85	3
7	51.4	85	3
8	51.3	85	3
9	40.4	66	3
10	33.8	67	3
11	21.9	39	3
12	21.2	36	3
13	19.9	36	3
14	18.1	38	3
15	16.5	38	3
16	14.4	42	3

RTU-2 Return Ductwork

Test Results:

Flow Coefficient (K)	5.3	
Exponent (n)	0.900	
Leakage area (LBL ELA @ 25 Pa)	10.9	sq in
Airflow @ 25 Pa	95.9	cfm

Test Data:

	Nominal Duct Pressure (Pa)	Nominal Flow (cfm)	Ring
1	45.1	149	3
2	44.6	148	3
3	44.1	148	3
4	35.3	128	3
5	35.1	128	3
6	26.6	106	3
7	25.1	106	3
8	23.3	107	3
9	23.0	107	3
10	19.2	78	3
11	19.1	79	3
12	12.1	47	3
13	12.0	47	3
14	11.9	47	3
15	11.9	44	3
16	11.7	47	3
17	10.3	44	3

Table A9-13. Raw Data from Duct Blaster Tests

RTU-3 Supply Ductwork

Test Results:

Flow Coefficient (K)	4.8	
Exponent (n)	0.763	
Leakage area (LBL ELA @ 25 Pa)	6.4	sq in
Airflow @ 25 Pa	56.1	cfm

Test Data:

	Nominal Duct Pressure (Pa)	Nominal Flow (cfm)	Ring
1	87.3	138	3
2	87.1	138	3
1	86.8	138	3
2	64.2	114	3
3	62.3	114	3
4	60.9	114	3
5	45.2	90	3
6	45.1	90	3
7	43.4	90	3
8	31.1	69	3
9	30.7	69	3
10	29.0	69	3
11	15.6	37	3
12	15.4	36	3
13	15.1	37	3

RTU-3 Return Ductwork

Test Results:

Flow Coefficient (K)	11.3	
Exponent (n)	0.616	
Leakage area (LBL ELA @ 25 Pa)	9.3	sq in
Airflow @ 25 Pa	82.1	cfm

Test Data:

	Nominal Duct Pressure (Pa)	Nominal Flow (cfm)	Ring
1	62.2	144	3
2	61.7	144	3
1	59.6	144	3
2	47.8	123	3
3	47.8	123	3
4	47.5	123	3
5	26.5	84	3
6	26.4	85	3
7	25.8	84	3
8	16.5	68	3
9	16.2	68	3
10	16.1	68	3
11	13.6	50	3
12	13.3	49	3
13	13.2	50	3
14	13.1	49	3
15	12.8	50	3
16	12.0	50	3
17	9.6	51	3
18	8.6	52	3

Table A9-14. Coefficients, Exponents and Regression Statistics from Duct Blaster Tests

	Supply & 1/2 AHU Cabinet			Return & 1/2 RTU Cabinet		
	K	n	R^2	K	n	R^2
RTU-1	7.9	0.580	99.99%	22.9	0.535	99.98%
RTU-2	4.8	0.718	96.05%	5.3	0.900	96.71%
RTU-3	4.8	0.763	98.89%	11.3	0.616	95.98%

Notes: $cfm = K(Pa)^n$ / R^2 indicates fit of linear log-log regression

Table A9-15. Comparison of Supply and Return Airflow Measurements

	Supply & 1/2 AHU Cabinet			Return & 1/2 RTU Cabinet		
	Total Supply Diffuser Airflow (cfm)	Leakage (cfm @ 25)	Supply & AHU ELA (sq in @ 25)	Total Return Airflow (cfm)	Leakage (cfm @ 25)	Return & AHU ELA (sq in @ 25)
RTU-1	1,652	51	5.8	1,443	128	14.5
RTU-2	1,884	49	5.5	1,226	96	10.9
RTU-3	1,699	56	6.4	1,504	82	9.3

Notes: Leakage and ELA at reference pressure of 25 Pa

Table A9-16 lists the ductwork used to estimate the supply and return duct area for the RTUs. The effective leakage area compared to the total duct surface area is shown in Table A9-17. On the supply side, there is 2.7 – 3.9 sq-in of duct leakage for every 100 sq-ft of duct surface. The leakage area for the return systems ranged from 8.4 – 23 sq-in per 100 sq ft duct area. The Sheet Metal and Air Conditioning Contractors' National Association (SMACNA) classifies duct leakiness using duct leakage per 100 sq ft of duct area at a pressure of 1-in w.g. The SMACNA leakage class for the three RTUs varied between 124 and 1,202.

Table A9-16. RTU Ductwork Size and Area

RTU-1

	Type/Size (in)	Length (ft)	Supply Side Duct Area (sq ft)	Return Side Duct Area (sq ft)
Supply Trunks	14" x 16"	10	50.0	
takeoffs	12" dia.	25	78.5	
AHU Cabinet	18" x 24"	3	21.0	
Return Trunk	20" x 24"	3		22.0
takeoffs	18" dia.	3		14.1
AHU Cabinet	18" x 36"	3		27.0
Total			***149.5***	***63.1***

RTU-2

	Type/Size (in)	Length (ft)	Supply Side Duct Area (sq ft)	Return Side Duct Area (sq ft)
Supply Trunks	14" x 16"	10	50.0	
takeoffs	12" dia.	31	97.4	
takeoffs	8" dia.	17	35.6	
AHU Cabinet	18" x 24"	3	21.0	
Return Trunk	20" x 24"	3		22.0
takeoffs	18" dia.	3		14.1
AHU Cabinet	18" x 36"	3		27.0
Total			***204.0***	***63.1***

RTU-3

	Type/Size (in)	Length (ft)	Supply Side Duct Area (sq ft)	Return Side Duct Area (sq ft)
Supply Trunks	14" x 16"	10	50.0	
takeoffs	12" dia.	35	110.0	
takeoffs	10" dia.	9	23.6	
AHU Cabinet	18" x 24"	3	21.0	
Return Trunk	20" x 24"	3		22.0
takeoffs	18" dia.	13		61.3
AHU Cabinet	18" x 36"	3		27.0
Total			***204.5***	***110.3***

Table A9-17. Duct Leakage Characteristics

	Duct Area (sq ft)	ELA (sq in @ 25)	ELA/100 sq ft Duct Area (sq in @ 25)	Leakage (cfm @ 25 Pa)	Supply CFM per ft^2 Duct Area (cfm/ sq-ft)	Leakage per 100 sq ft Duct Area (cfm @ 25 Pa)	SMACNA Leakage Class cfm per 100 sq ft (cfm @ 1-in water)
RTU-1 Supply	150	5.8	3.9	51	11.0	34	130
RTU-2 Supply	204	5.5	2.7	49	9.2	24	124
RTU-3 Supply	205	6.4	3.1	56	8.3	27	159
RTU-1 Return	63	14.5	23.0	128	n/a	203	694
RTU-2 Return	63	10.9	17.2	96	n/a	152	1,202
RTU-3 Return	110	9.3	8.4	82	n/a	74	307

Table A9-18 shows the airflow balance for RTU-1, RTU-2, and RTU-3. Three airflow balance estimates are calculated as follows:

Gross Airflow Balance:

$$\Delta_{gross} = \text{Supply Diffuser cfm} - \text{Return Diffuser cfm} - \text{Ventilation cfm}$$

Net Airflow Balance Using CFM_{25}:

$$\Delta_{N25} = (\text{Supply Diffuser cfm} + \text{Supply Leakage @ 25 Pa}) - (\text{Return Diffuser cfm} + \text{Return Leakage @ 25 Pa}) - \text{Ventilation cfm}$$

Net Airflow Balance Using Average "Actual Static" in Ductwork:

$$\Delta_{Ncorrected} = (\text{Supply Diffuser cfm} + \text{Supply Leakage @ Actual Static}) - (\text{Return Diffuser cfm} + \text{Return Leakage @ Actual Static}) - \text{Ventilation cfm}$$

The last estimate for the RTU airflow balance ($\Delta_{Ncorrected}$) uses our best estimate for average "actual static" pressure in the ductwork during normal operation, which is one half of the plenum pressure as suggested in ASHRAE Standard 152P section B.2. For this ductwork, the net airflow estimate resulting in the smallest error is $\Delta_{Ncorrected}$ for RTU-1 & 2. The corrected net airflow balance, Δ_{N25}, yields results with the least error for RTU-3. The net airflow balance estimate with the value closest to zero gives the most accurate results for airflow combined with duct leakage. Figure A9-22 shows a diagram of the roof top units including the supply, return, and ventilation airflows as well as the duct leakage for the best estimate in airflow balance.

Table A9-18. Airflow Balance for Roof Top Units

	RTU-1	RTU-2	RTU-3
Diffuser Supply (cfm)	1,652	1,884	1,699
Diffuser Return (cfm)	1,443	1,226	1,504
Ventilation (cfm)	52	439	197
Supply Leakage - cfm25	51	49	56
- actual static	70	74	62
Return Leakage - cfm25	128	96	82
- actual static	220	218	148
ΔGross	157	219	-2
ΔN25	80	172	-28
ΔNcorrected	7	75	-88

Note: "actual static" is 1/2 the static pressure measure at the unit.

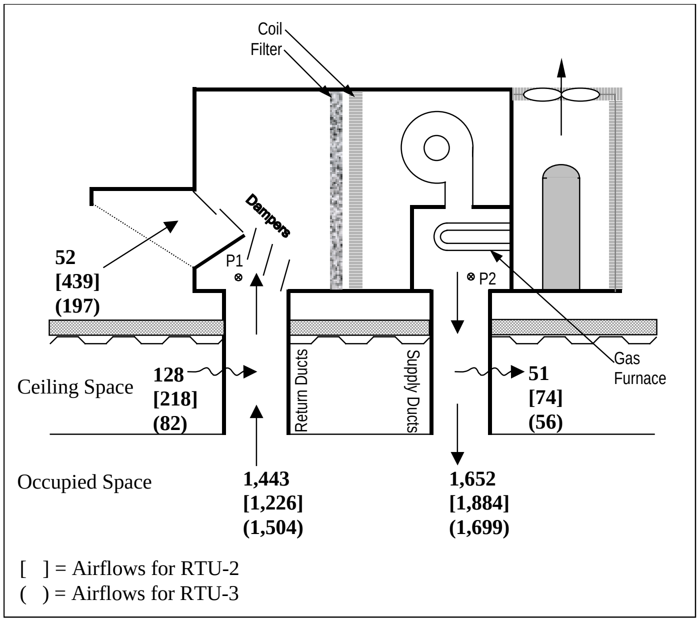

Figure A9-22. Airflow Balance for RTU-1, 2, & 3

Space Conditions

Figure A9-23 shows the average temperature profiles based on temperature readings taken during the two days of on site testing (August 11-12, 2004). Sensors were placed near the order counter and the employee locker room.

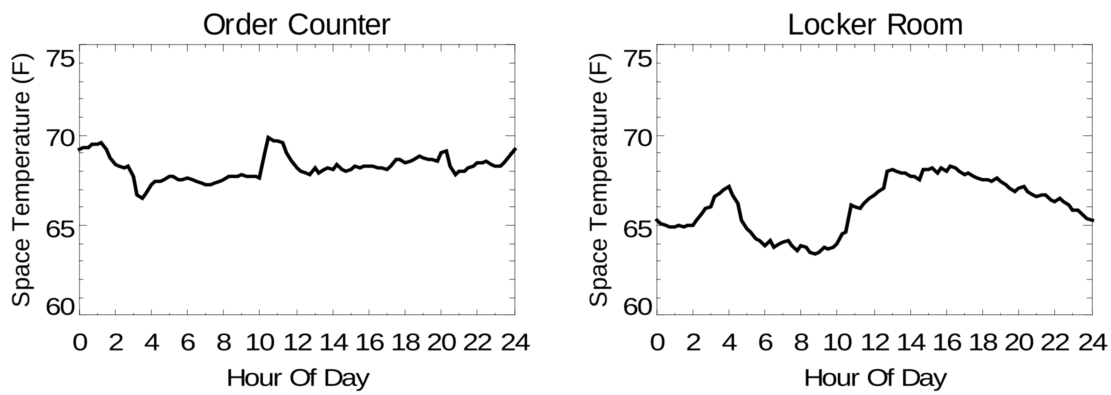

Figure A9-23. Measured Space Temperature Profiles

Figure A9-24 shows the CO_2 concentration in the area near the order counter. The CO_2 concentration provides an indication of occupancy. The next section uses the CO_2 as a tracer gas to estimate the infiltration/ventilation rate into the building.

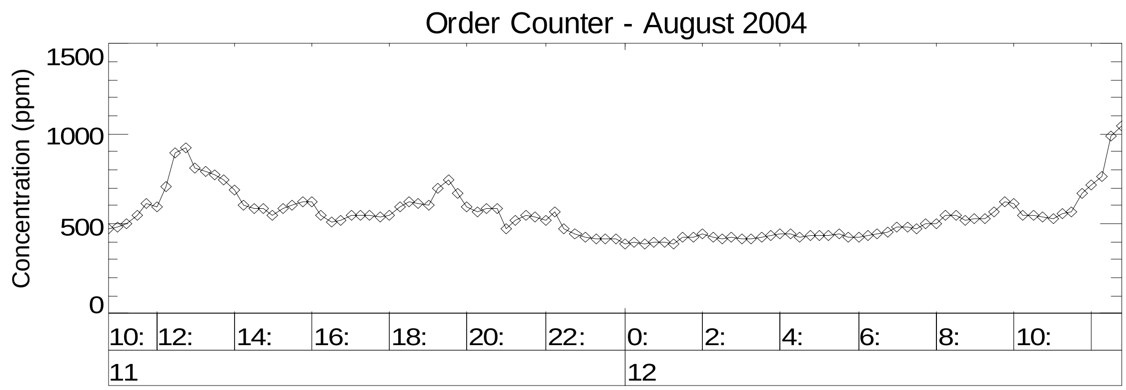

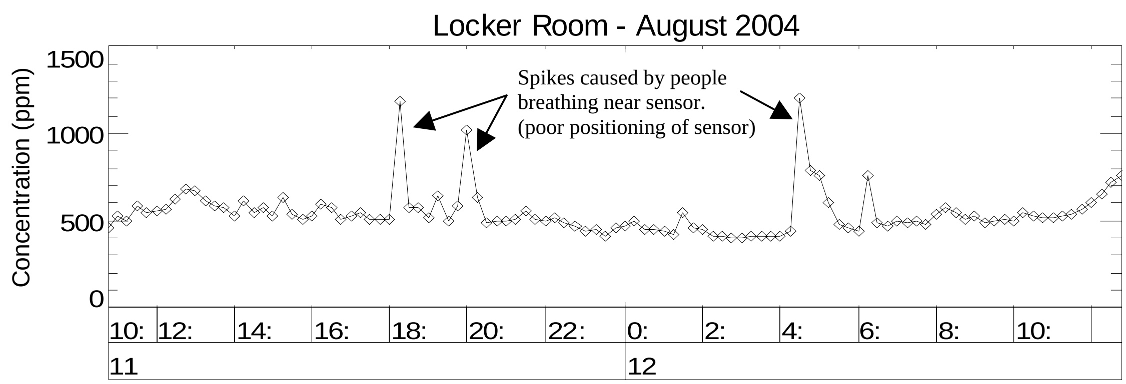

Figure A9-24. Measured CO_2 Concentration

Although there is only 32 hours of data (August 11-12, 2004), the following plots show the relative humidity for this building during the monitoring period. Figure A9-26 displays the conditions inside the building compared with the ASHRAE comfort zone for cooling shown by the shaded region on the plot.

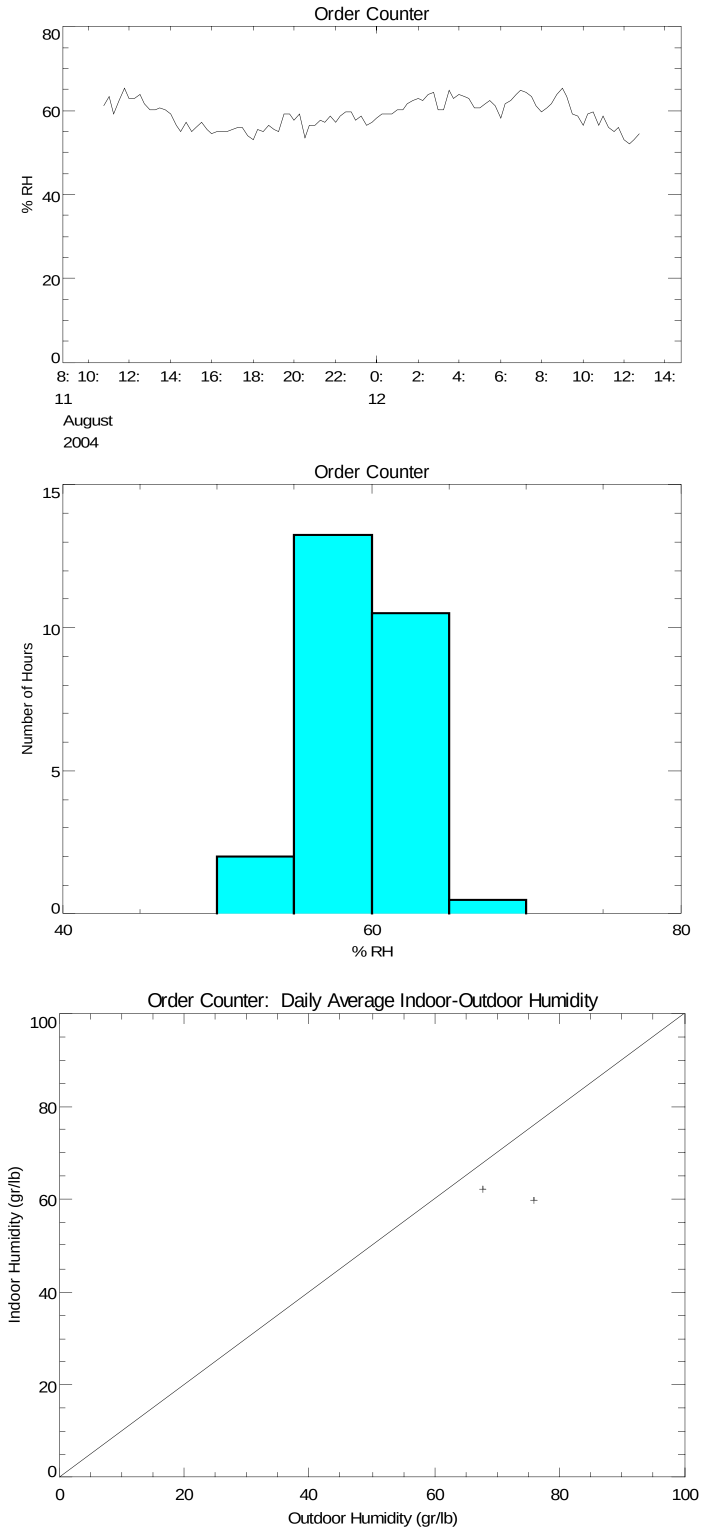

Figure A9-25. Humidity Conditions (August 11 – 12, 2004)

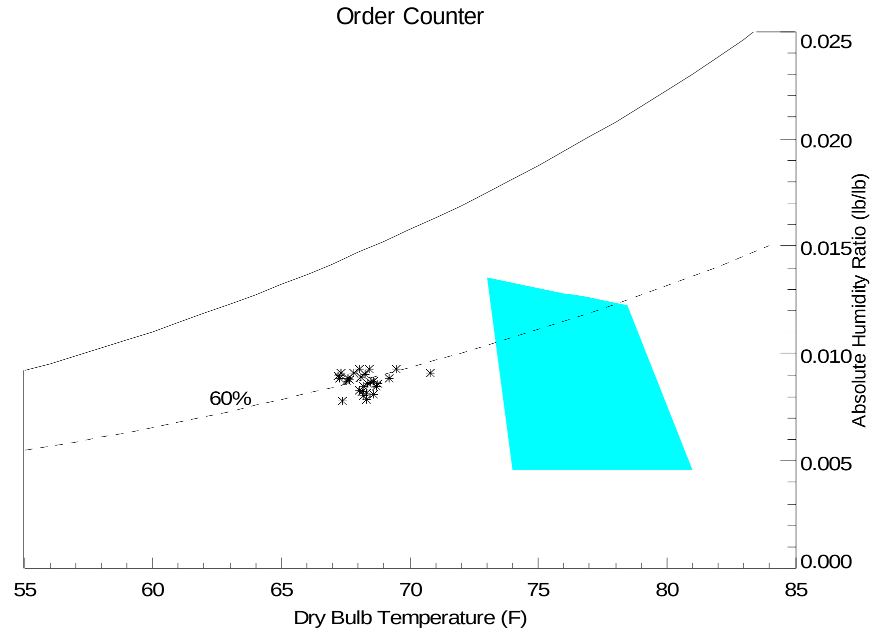

Figure A9-26. Indoor Air Quality Comparison with ASHRAE Comfort Zone for Cooling

Utility Bills

Electricity and gas use are both primarily used for food preparation. Natural gas is used to heat the facility and electricity is used for air conditioning. The tables and graphs below show the gas and electric use trends for the facility. The overall energy use index for the building is summarized below.

	Utility Gas Use		Utility Electric Use	
	Cooking Gas Use ($MBtu/ft^2$-year)	Heating Index ($MBtu/ft^2$-year)	Baseline Elec. Use (kWh/ft^2-year)	Cooling Index (kWh/ft^2-year)
2003-2004 Season	400	84.6	99.1	5.78

Note: Season is from August 2003 to July 2004

Table A9-19. Summary of Gas Bills

	Days in Month	Gas Use (therms)	Cost ($)	$/therm	Gas Use per Sq-Ft (therm/sq ft)
Aug-03	31	1,009	$ 946	0.94	0.306
Sep-03	30	1,046	$ 1,047	1.00	0.317
Oct-03	31	1,020	$ 1,010	0.99	0.309
Nov-03	30	1,348	$ 1,361	1.01	0.408
Dec-03	31	1,387	$ 1,434	1.03	0.420
Jan-04	31	1,881	$ 1,985	1.06	0.570
Feb-04	29	1,895	$ 1,928	1.02	0.574
Mar-04	31	1,635	$ 1,353	0.83	0.495
Apr-04	30	1,340	$ 1,276	0.95	0.406
May-04	31	1,165	$ 1,191	1.02	0.353
Jun-04	30	1,196	$ 1,214	1.02	0.362
Jul-04	31	1,122	$ 1,146	1.02	0.340
2003-2004	366	16,044	$ 15,889	0.99	4.862

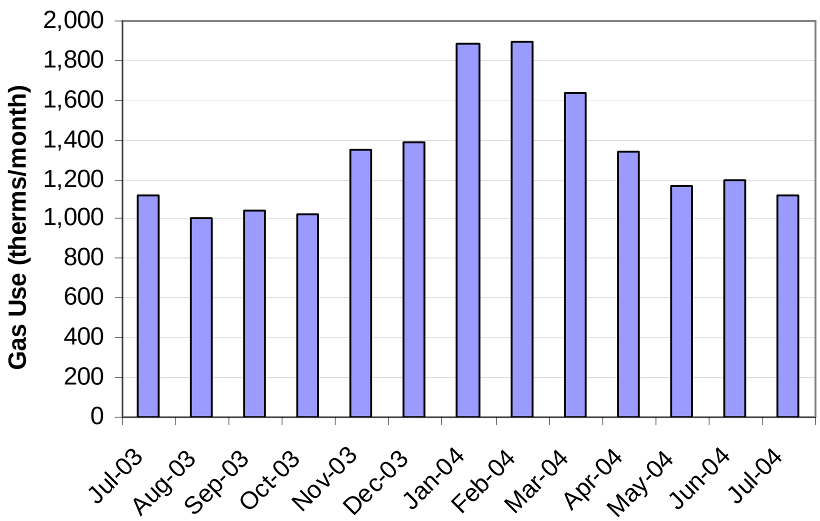

Figure A9-27. Monthly Gas Use Trend

Table A9-20. Summary of Electric Bills

	Days in Month	Demand (kW)	Energy (kWh)	Cost ($)	$/kWh	Elec. Use per Sq-Ft (kWh/sq ft)
Aug-03	31	66.4	33,200	$ 3,378	0.10	10.06
Sep-03	30	68.0	32,320	$ 3,320	0.10	9.79
Oct-03	31	61.6	27,120	$ 2,816	0.10	8.22
Nov-03	30	57.6	30,160	$ 3,011	0.10	9.14
Dec-03	31	57.6	27,360	$ 2,789	0.10	8.29
Jan-04	31	52.8	29,280	$ 2,922	0.10	8.87
Feb-04	29	48.8	25,920	$ 2,588	0.10	7.85
Mar-04	31	53.6	26,240	$ 2,648	0.10	7.95
Apr-04	30	56.8	25,920	$ 2,661	0.10	7.85
May-04	31	61.6	26,480	$ 2,749	0.10	8.02
Jun-04	30	60.8	31,520	$ 3,169	0.10	9.55
Jul-04	31	60.8	31,440	$ 3,149	0.10	9.53
2003-2004	366	68	346,960	$ 35,200	0.10	105.14

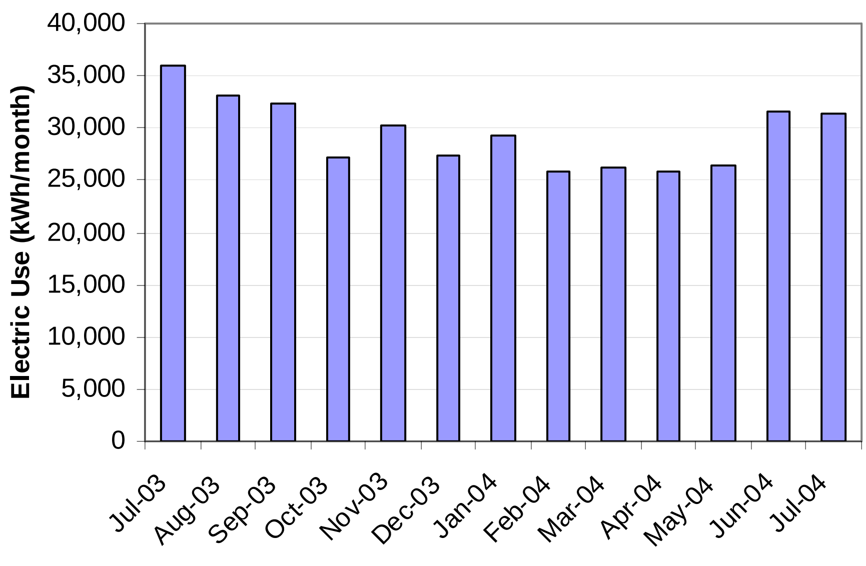

Figure A9-28. Monthly Electric Use Trend

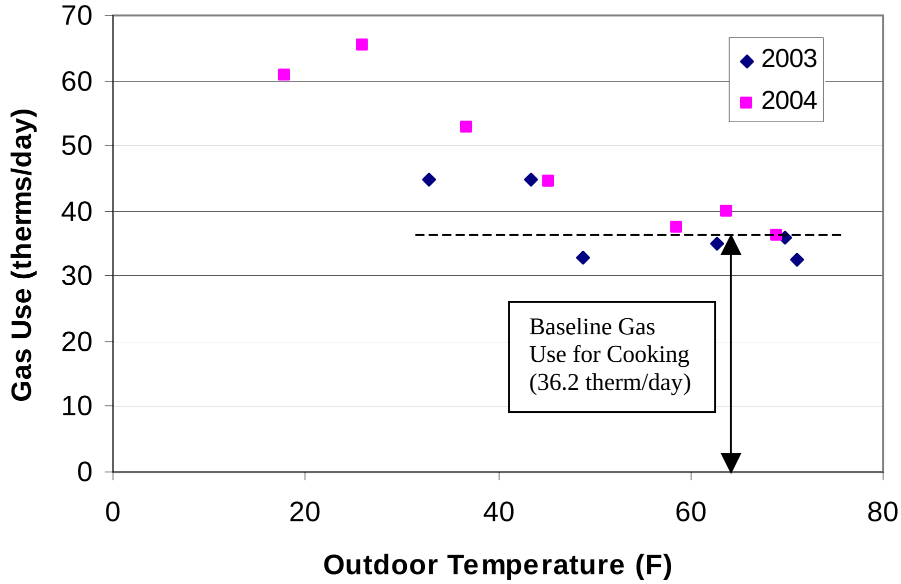

Figure A9-29. Variation of Gas Use with Ambient Temperature

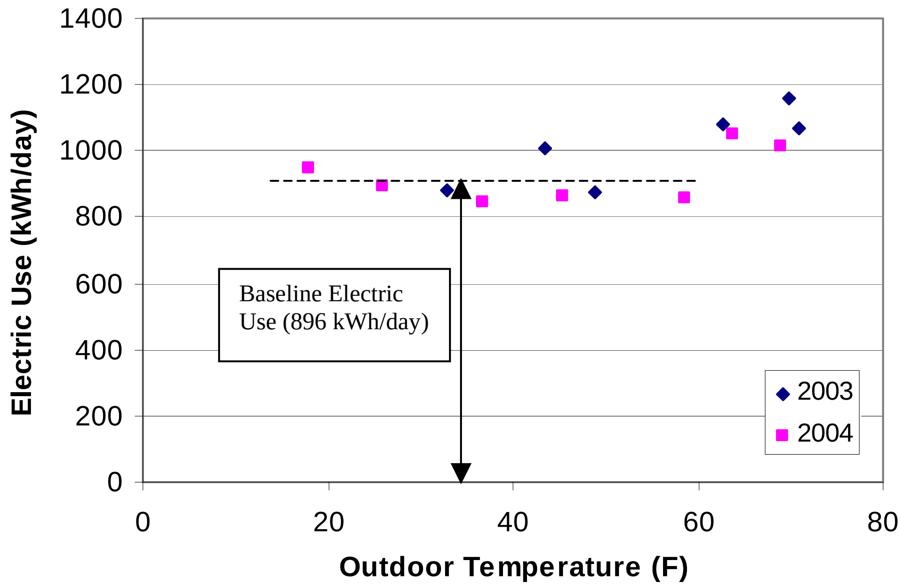

Figure A9-30. Variation of Electric Use with Ambient Temperature

Field Test Site 10 – Tompkins County DPW, Ithaca, NY

Figure A10-1. Photo of Building (Southwest)

CHARACTERISTICS

BUILDING DESCRIPTION

The Tompkins County DPW is a 55,000 sq-ft facility is a two-story building with large attached high-bay garages on the north and east sides of the building. The building also contains 14,400 sq-ft of office section, which is the subject of this report. The facility was originally built in the 1960's and was completely renovated and added onto in the year 2000. Figure A10-1 shows a photo of the building from the southwest corner. The building uses two natural gas hot water boilers to heat the building. The first floor has hot water perimeter heat and the second floor is heated with a roof top unit (RTU) containing a hot water coil in the supply trunk just inside the building. Three RTUs with DX coils cool the first floor and one RTU cools the second floor. A single heat recovery ventilator (HRV) provides tempered outdoor air the RTUs. The HRV has a hot water coil for supplemental heat to boost the ventilation air temperature if needed. Each RTU has a economizer, but the linkages were found to be disabled - allowing the HRV to supply most of the ventilation air. The floor plan for the building is shown in Figure A10-2 and Figure A10-3.

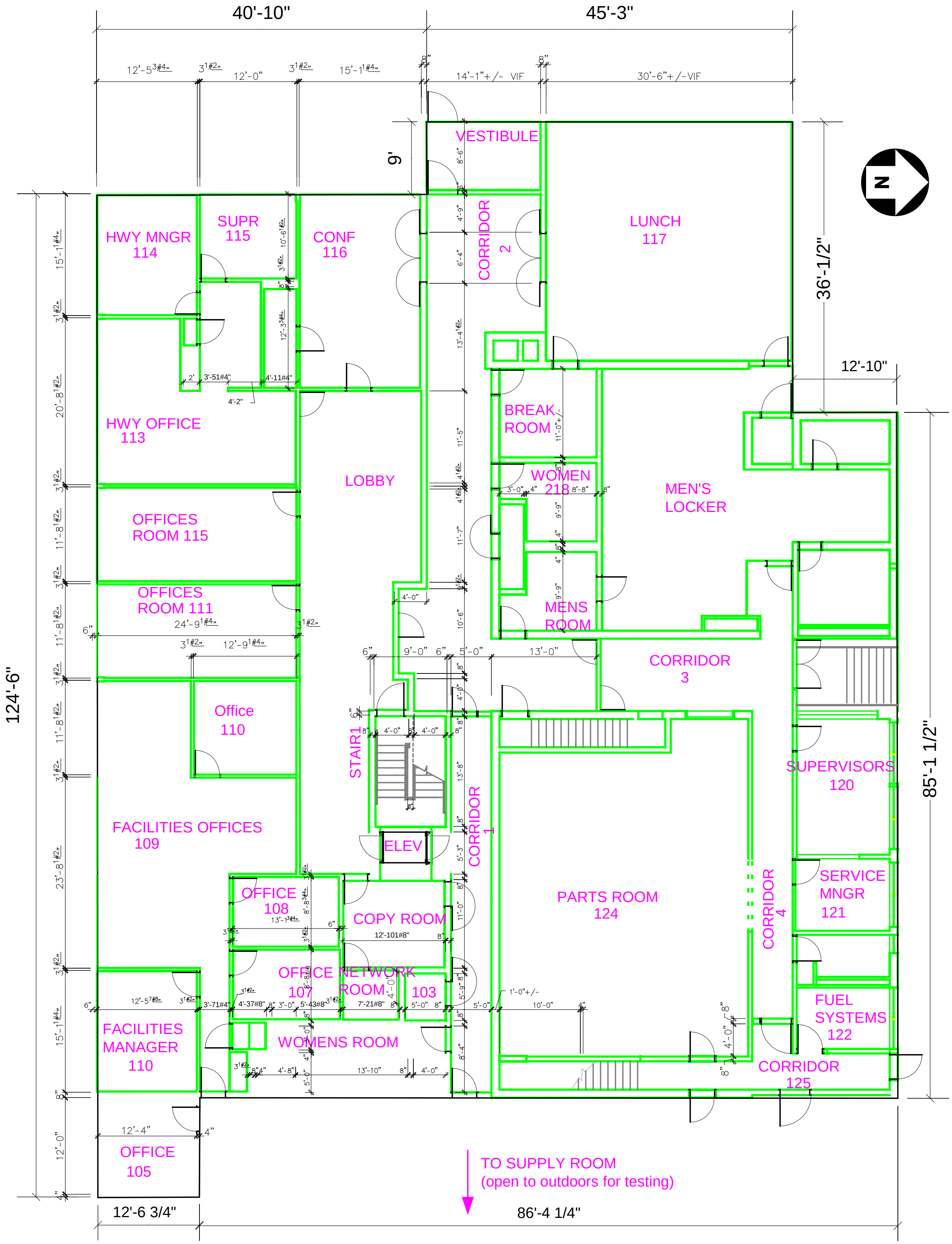

Figure A10-2. First Floor Building Plan – Office Area Only

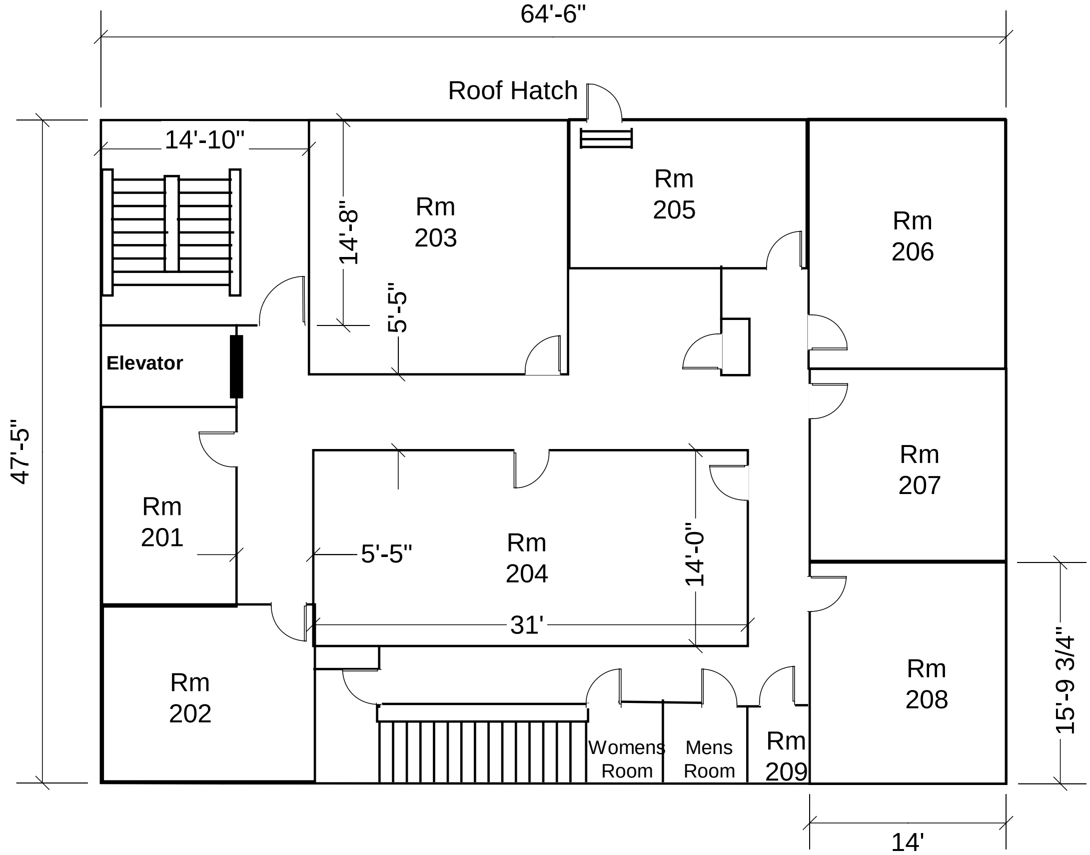

Figure A10-3. Second Floor Building Plan – Office Area Only

Construction Details

Two typical exterior walls construction types are shown in detail in Figure A10-4 and Figure A10-5. Exterior wall system 1 is a metal stud wall and exterior wall system 2 is an 8-in concrete block wall. Both wall systems use foam board insulation on the exterior with stucco exterior finish and gypsum board interior covering.

The building has a built-up roof with approximately 3 inches of rigid foam insulation and metal decking on the underside of the roof.

There is a T-bar (drop) ceiling on both floors of the building. The first floor uses the space between the ceiling and the roof (ceiling space) as a return plenum. The RTU for the second floor has ducted returns. The ductwork on both floors is insulated and located in the ceiling space.

Figure A10-4 illustrates typical wall and roof sections. Figure A10-6 shows pictures of the ceiling plenum and typical diffuser installation.

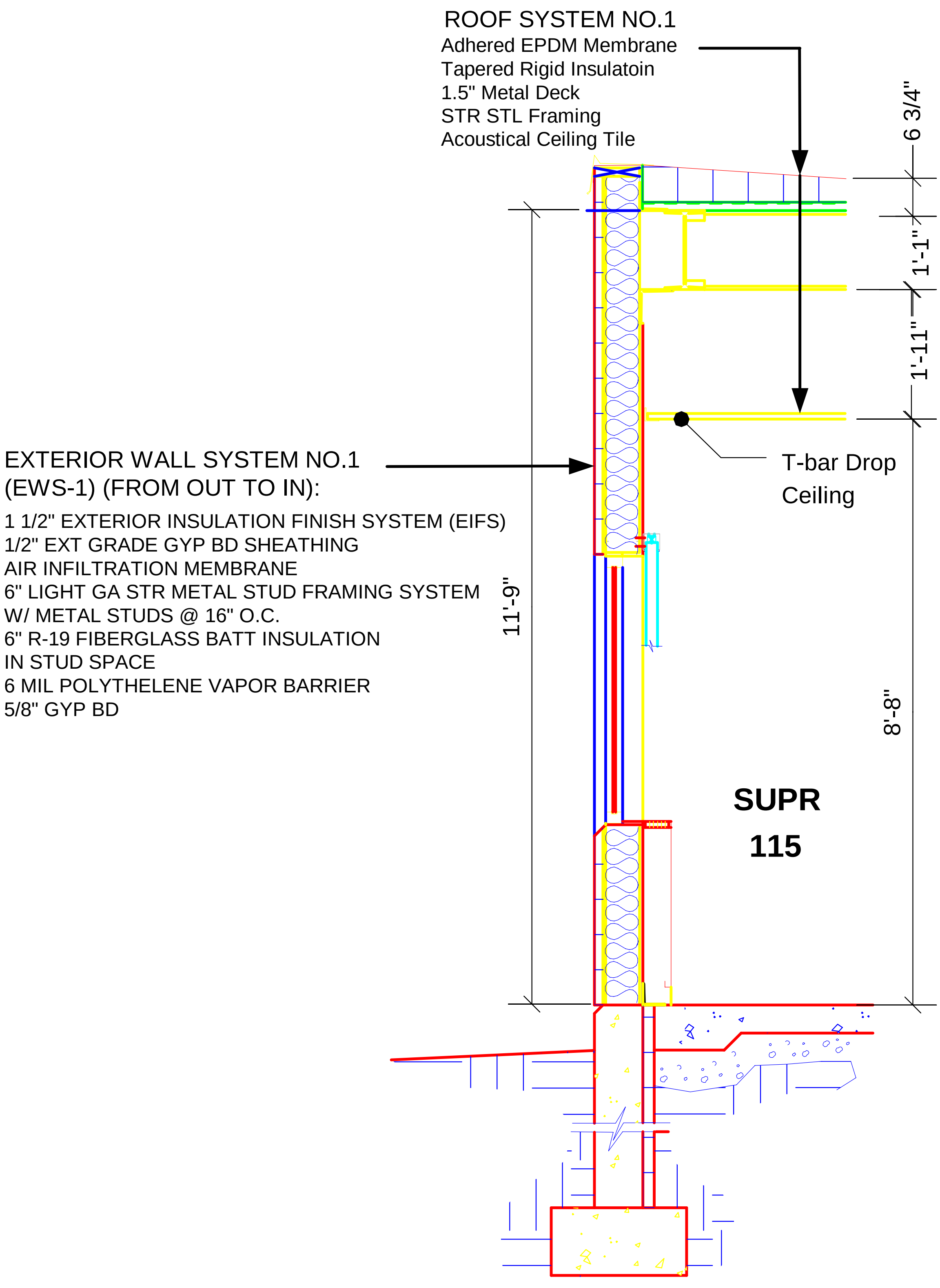

Figure A10-4. Exterior Wall and Roof Section for First Floor

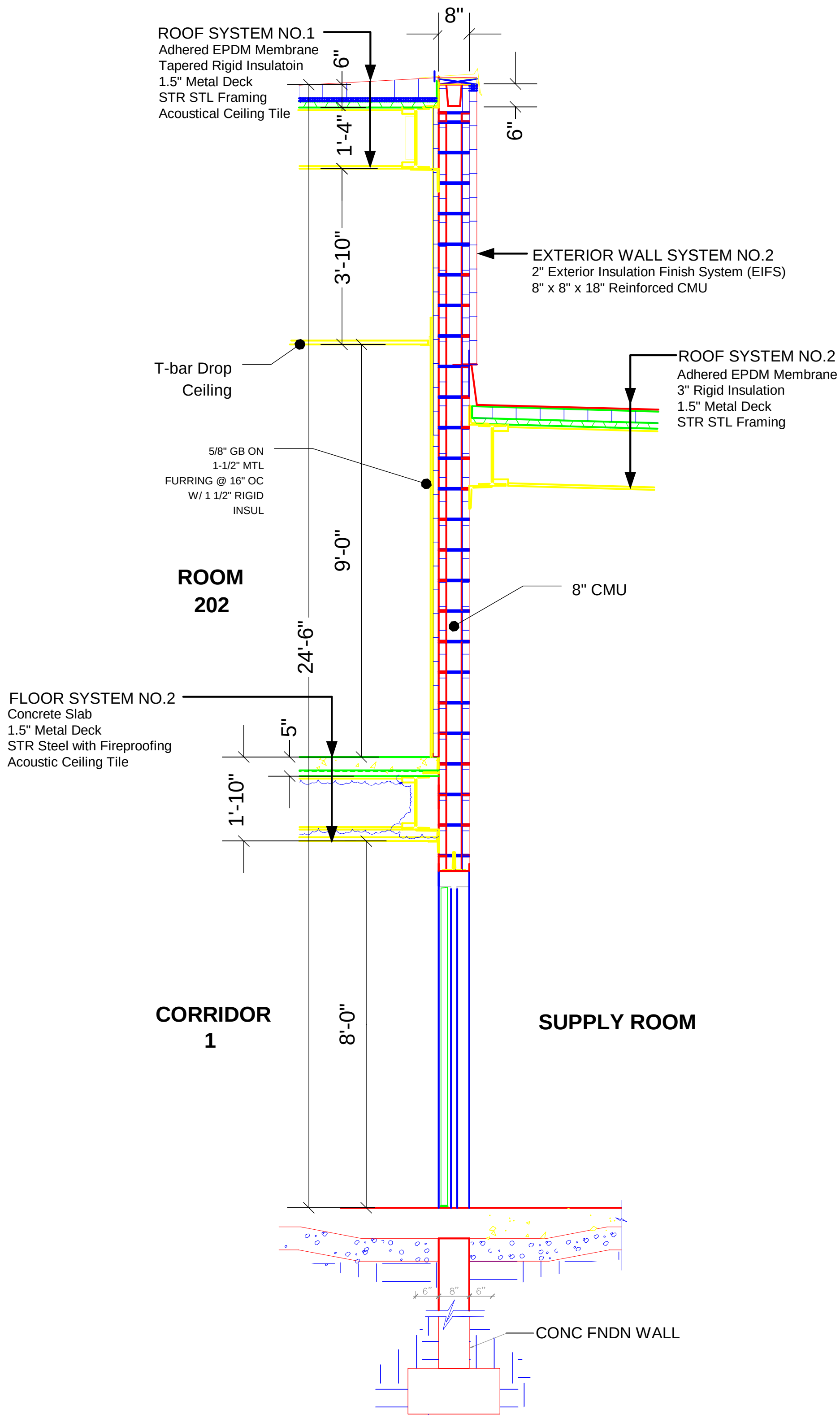

Figure A10-5. Floor, Wall, and Roof Section for Second Floor

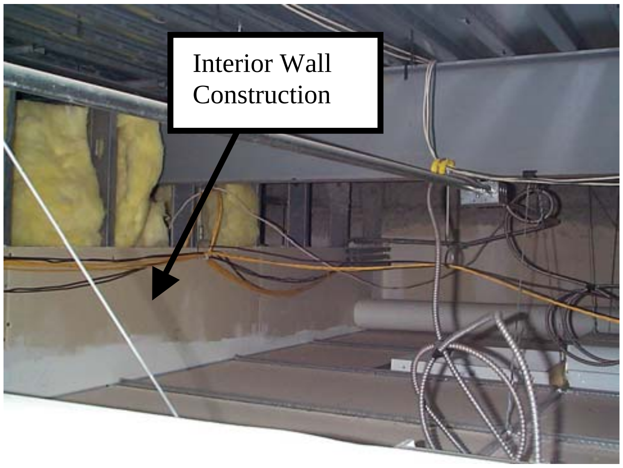

Ceiling Plenum

Plenum Transfer Duct Between Interior Walls

Typical Supply Diffuser Installation

Typical Return Grill to Ceiling Plenum

Figure A10-6. Ceiling Plenum (First Floor)

HVAC System

The building is heated using two hot water boilers. Hot water perimeter heat is used on the first floor and a single RTU with a hot water coil in the supply duct heats the second floor. There are four RTUs with DX coils that provide cooling. Three RTUs cool the first floor and a single RTU cools the second floor. This building has a heat recovery ventilator (HRV) to temper the outdoor air before entering the return section of the RTUs. The HRV recovers heat from several small exhaust fans throughout the building using a heat pipe heat exchanger. The RTU supply fans operate year round during occupied mode to provide ventilation to the space. The HRV has a supplemental hot water coil to temper the ventilation air during very low ambient temperature. Figure A10-7, Figure A10-8, and Figure A10-9 show RTUs, heat recovery ventilator (HRV), and the two boilers that serve the entire office section. Table A10-1 lists the HVAC equipment that serves the building.

The first floor has insulated supply ducts located in the ceiling return plenum. The second floor has insulated supply and return ducts that are located in the ceiling space. The supply and return ductwork is constructed using both rectangular and round insulated sheet metal ducts with flexduct takeoffs to the diffusers. The first floor has ceiling mounted supply diffusers and return grills. The second floor has ceiling mounted supply diffusers and both wall and ceiling mounted returns. Figure A10-10 and Figure A10-11 display the ductwork and the corresponding RTUs that serve each zone within the building.

RTU-1 (Cooling Only – First Floor)
Trane Model: TCD090D30ABC

RTU-2 (Cooling Only – First Floor)
Trane Model: TCD102C30AAB

RTU-3 (Cooling Only – First Floor)
Trane Model: TCD150C30ACA

RTU-4 (Cooling and Hot Water Coil for Heating – Second Floor)
Carrier Model: 50TJ-009-501

Figure A10-7. Roof Top Units

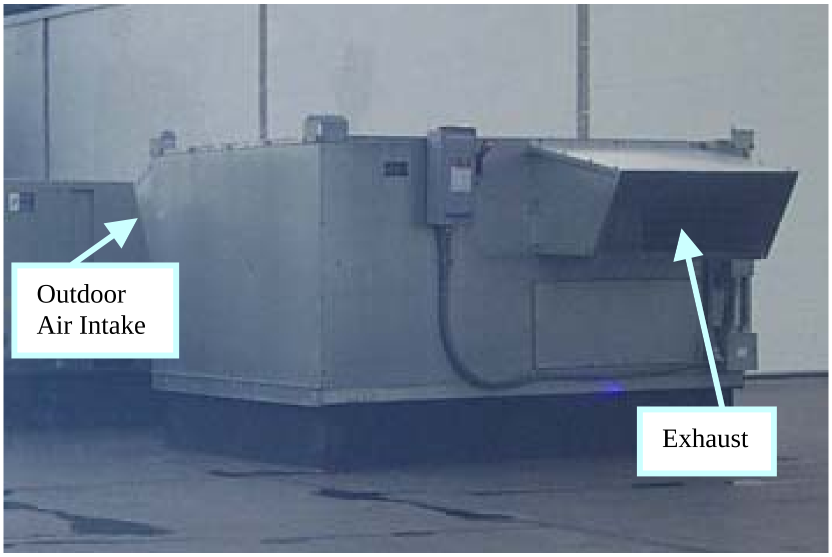

Figure A10-8. RenewAire Heat Recovery Unit

Figure A10-9. Hot Water Tube Boilers

Table A10-1. Summary HVAC Equipment Installed at Site

HVAC Equipment	Serves	Brand	Model	Heating Capacity (MBtu/h)	Cooling Capacity (tons)
RTU-1	First Floor	Trane	TCD090D30ABC	none	7.5
RTU-2	First Floor	Trane	TCD102C30AAB	none	8.5
RTU-3	First Floor	Trane	TCD150C30ACA	none	12.5
RTU-4	Second Floor	Carrier	50TJ-009-501	Hot Water Coil	8.5
HRV-1	All RTUs	RenewAire		HW Supp. Heat	none
Boilers (1&2)	Both Floors	Bryan	L-36	1,960	none

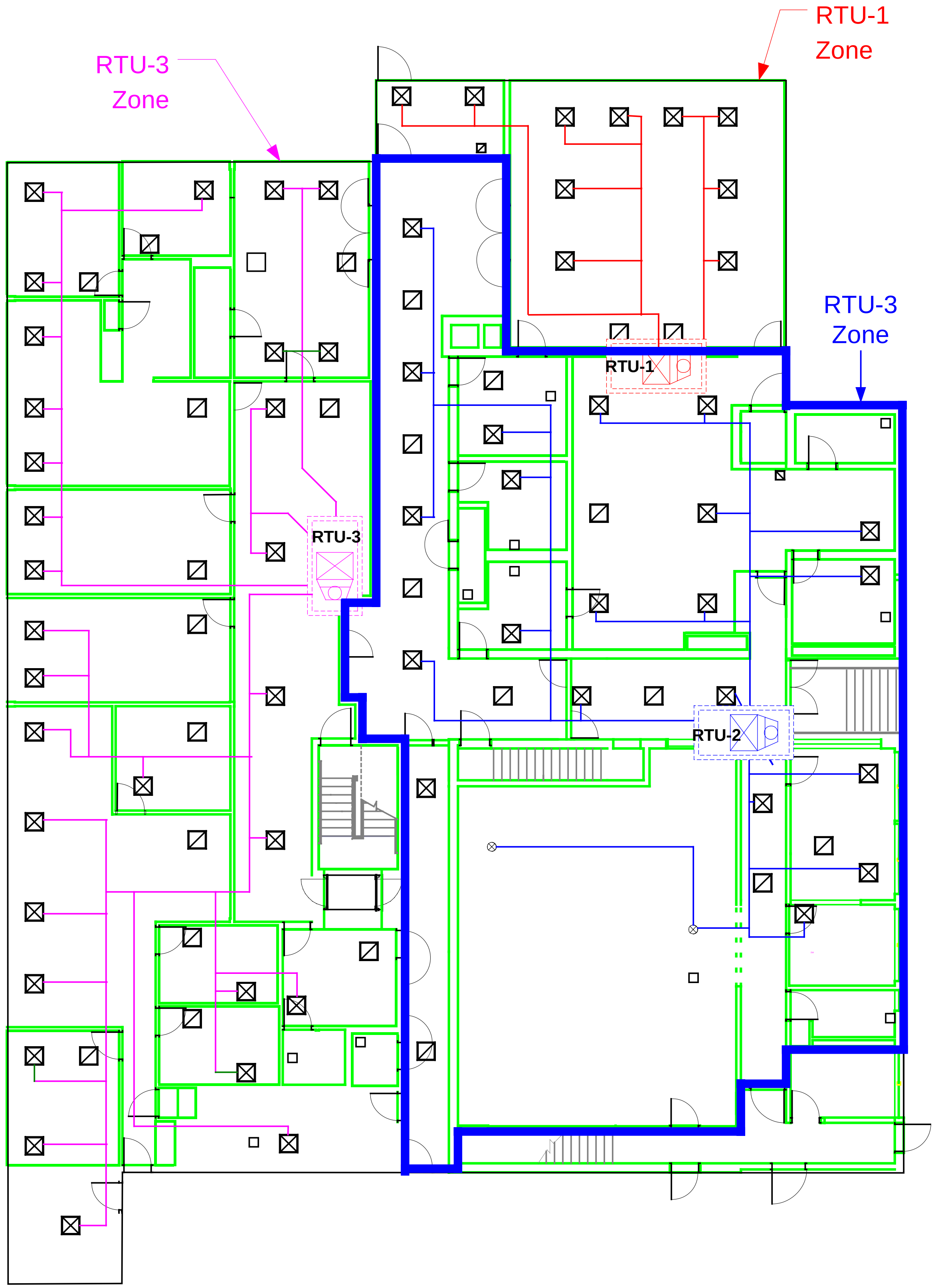

Figure A10-10. First Floor AHU Zones within Building

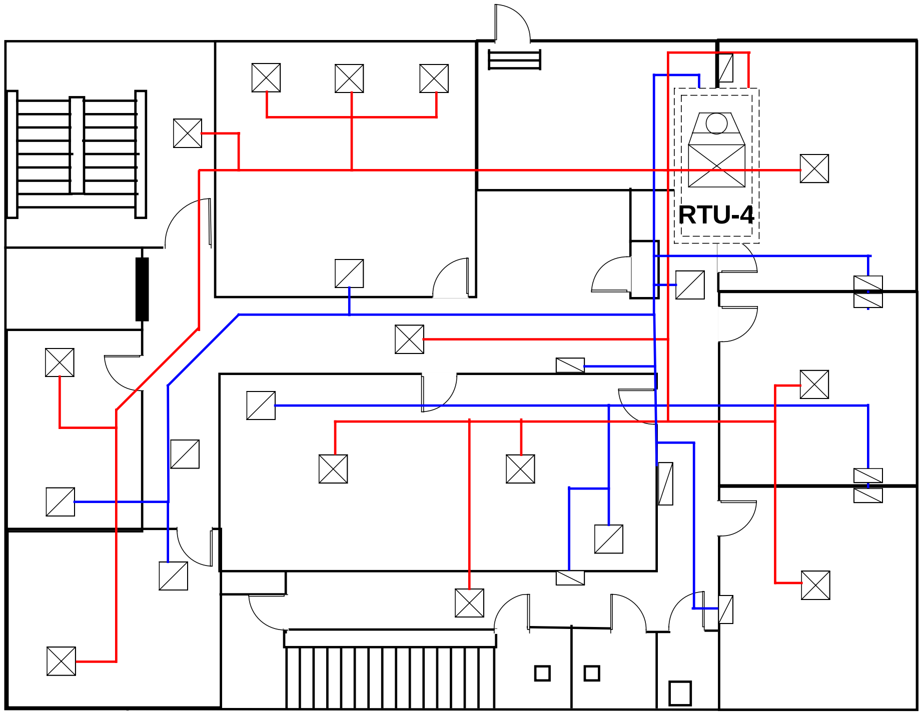

Figure A10-11. Second Floor Zone within Building (RTU-4)

A Johnson Controls Metasys controller controls the four RTUs, HRV, and boilers. There are several temperature sensors to monitor the temperature in each of the zones. Each temperature sensor controls a damper to increase or decrease the airflow through a section of duct that typically leads to several diffusers. The Metasys heating and cooling setpoints control the on/off operation of the RTUs and the boilers. The heating setpoint is 70°F and the cooling setpoint is 74°F (75°F upstairs). The boilers begin operating when the outdoor ambient temperature falls below 65°F.

MEASUREMENTS

The test data below was taken on September 16 - 17, 2004. Supply and return airflow measurements at each diffuser and duct leakage measurements were taken on September 16. Blower door testing and pressure mapping were completed on September 17. Dan Gott collected the CO_2 and temperature/RH sensors on October 12. Test personnel were Dan Gott and Adam Walburger for both days.

Building Envelope Airtightness

The leakage characteristics of the building enclosure were assessed using fan pressurization methods. A single blower door was installed in the doorway at the end of corridor 1 (labeled in Figure A10-13), which leads to the supply room that was open to the outdoors for testing. All exterior doors and windows were closed. The building was tested in the following configuration:

- All interior doors open
- All exhaust fans sealed inside building
- HRV-1 intake and exhaust were sealed
- Economizer dampers closed on RTUs

The building pressure was varied from 21.5 Pa to 6.8 Pa. Figure A10-12 shows the building leakage variation with building pressure.

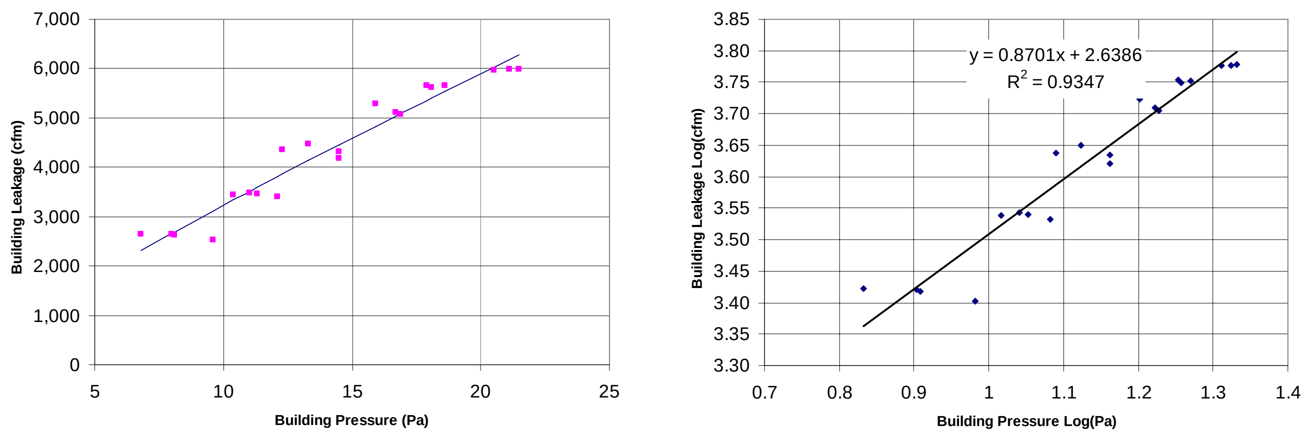

Depressurization Test – All Doors Open

Figure A10-12. Variation of Building Leakage with Pressure: cfm = K(ΔP)^n

Table A10-2 shows the results of the blower door tests including model coefficients, effective leakage area (ELA), and air-changes-per-hour (ACH). The ELA is calculated using the Lawrence Berkeley Laboratory method, which calculates the leakage area at 4 Pa. The building has an effective leakage area of approximately 1.47 sq in per 100 sq ft of the total envelope area including floor area. Another building leakage characteristic is the ACH at 50 pascals (ACH_{50}). The building has an ACH_{50} of 6.5.

Table A10-2. Blower Door Test Data, Resulting Best-Fit Model Coefficients, and ELA

Depressurization – All Interior Doors Open

Test Results:

Flow Coefficient (K)	435.2		13,899	sq ft, floor area
Exponent (n)	0.870			
Leakage area (LBL ELA @ 4 Pa)	411.9	sq in	1.47	ELA / 100 sq ft
Airflow @ 50 Pa	13,090	cfm	6.47	ACH @ 50

Test Data:

Nominal Building Pressure (Pa)	Nominal Flow (cfm)	Ring
21.5	5,995	none
21.1	5,984	none
20.5	5,976	none
18.6	5,660	none
18.1	5,620	none
17.9	5,667	none
16.9	5,070	none
16.7	5,115	none
15.9	5,290	none
14.5	4,314	none
14.5	4,180	none
13.3	4,468	none
12.3	4,346	none
12.1	3,406	none
11.3	3,465	none
11.0	3,485	none
10.4	3,449	none
9.6	2,522	none
8.1	2,618	none
8.0	2,638	none
6.8	2,641	none

Notes: ELA is leakage area (in square inches) at reference pressure of 4 Pa.
ELA per 100 sq ft is based on total building envelope surface area (ceiling, exterior walls and floor).

<u>Pressure Mapping (Blower Door Testing)</u>

Pressure readings in the building were taken using a digital micromanometer (DG 700) with the blower door operating. The pressure difference across the building envelope (inside to outside the building) was 20 Pa. The pressure difference between the interior space and the ceiling plenum was 0 Pa measured at several locations on the first and second floors throughout the building. This implies that the leakage area from the occupied space to the ceiling plenum is large and that the plenum is closely coupled to the conditioned space. The roof of the building is the primary air and thermal barrier.

Pressure measurements were taken between the main corridors and interior rooms with doors closed. Figure A10-13 and Figure A10-14 show the pressure differences induced across the doorways with the corridors depressurized. With the building depressurized to 20 Pa, pressures across the doorways ranged between 0.0 and 2.8 Pa. The pressure difference between the rooms and corridor are much less than the overall pressure difference to ambient. This implies that the room-to-room leakage is much greater than the leakage across the building envelope. The pressures measured across doorways were measured in reference to an interior space that had a free path back to the blower door (open interior doors).

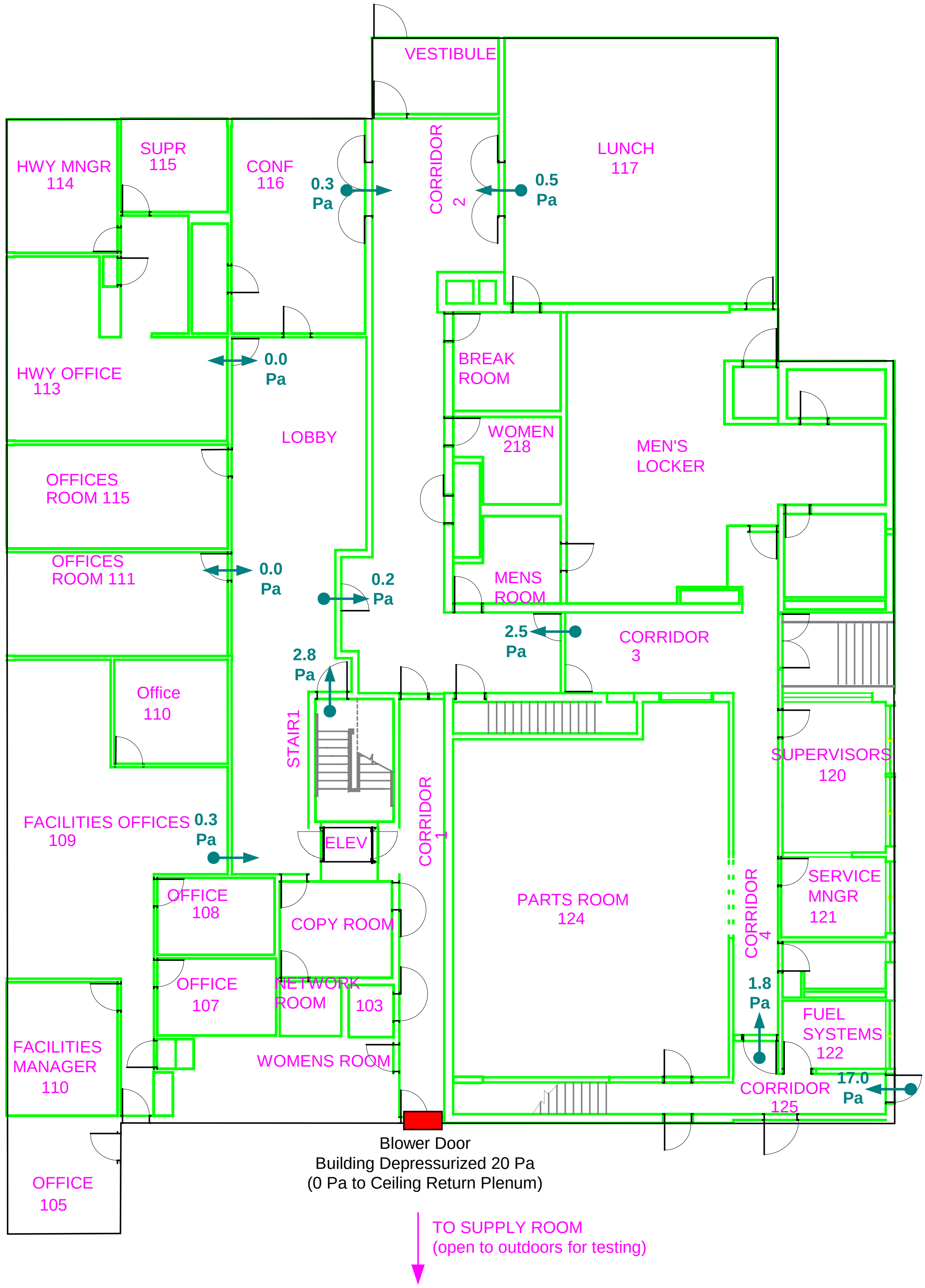

Figure A10-13. First Floor Room-to-Corridor Pressures with Building Depressurized to 20 Pa

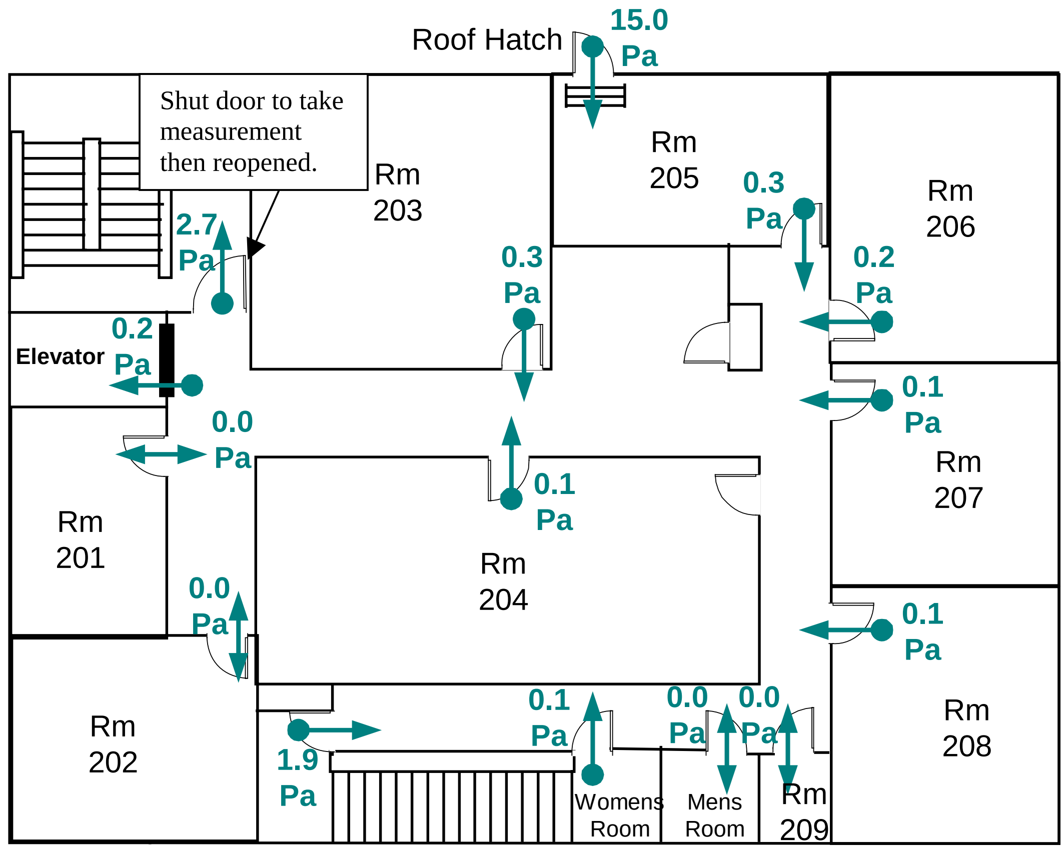

Figure A10-14. Second Floor Room-to-Corridor Pressures with Building Depressurized to 20 Pa

HVAC Airflow Measurements

The airflow from each supply diffuser was measured using a Shortridge flow hood. The total supply airflow is approximately 11,000 cfm[1] or 0.76 cfm per sq-ft of floor area. Figure A10-15 and Figure A10-16 display the airflow at each diffuser and exhaust on the first floor and second floor. The ductwork shows which RTU supplies air the to the diffusers. Table A10-4 and Table A10-5 show the measurements for the HRV ventilation supply airflow and exhaust airflow for September 16, 2004.

[1] One supply and three return diffuser airflows were not measured. The airflows for these diffusers were estimated using the average of the measured diffuser airflows in the corresponding system.

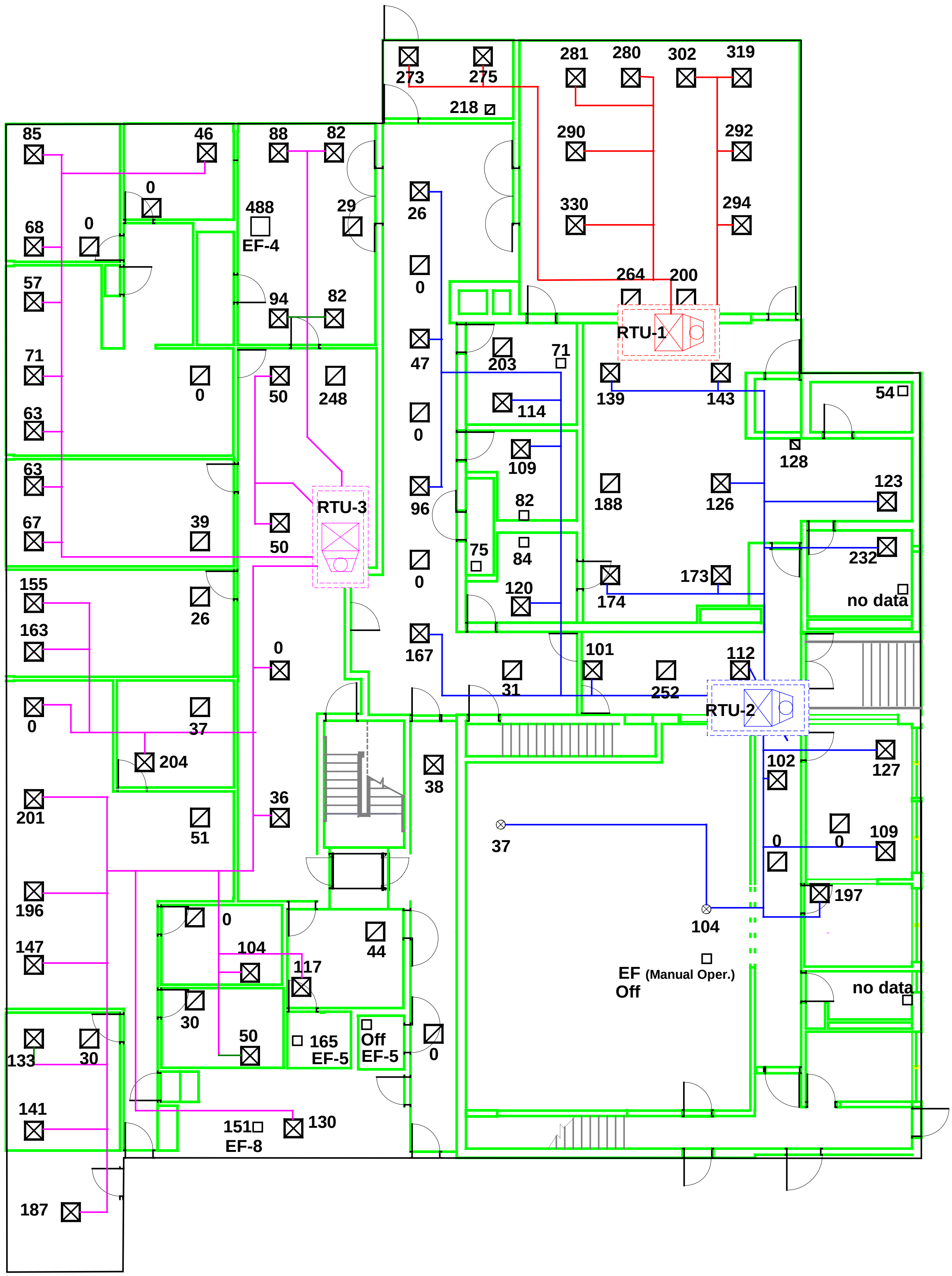

Figure A10-15. First Floor Supply and Return Airflow Measurements (cfm)

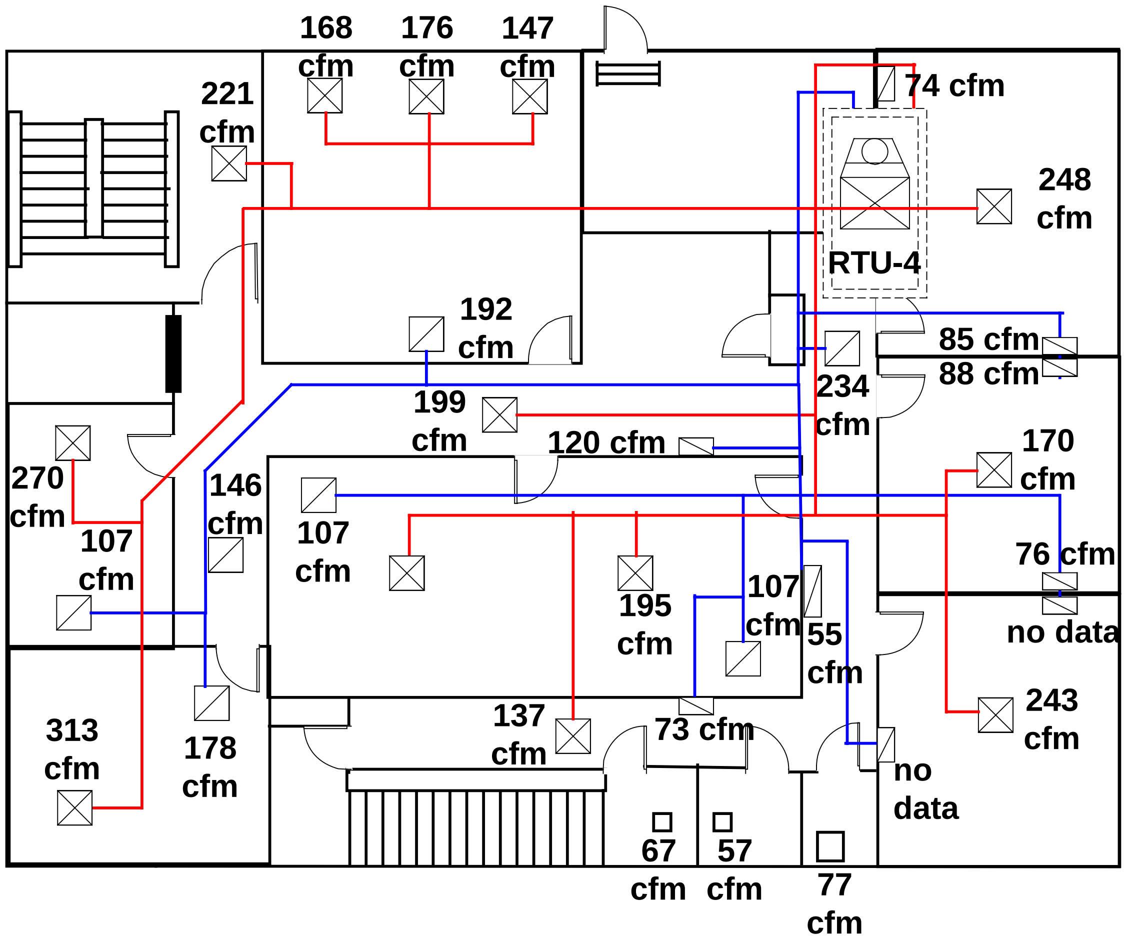

Figure A10-16. Second Floor Supply and Return Airflow Measurements (cfm)

Table A10-3. Comparison of Supply and Return Airflow Measurements

RTU	Serves	Flowhood Supply Airflow (cfm)	Flowhood Return Airflow (cfm)	Supply / Return Ratio	Return Type	Measured Supply Fan Power (kW)	Normalized Supply Fan Power (W/cfm)	Supply Static (Pa)	Return Static (Pa)
RTU-1	First Floor	2,936	464	6.3	Ceiling Space Plenum	0.99	0.34	95	-34
RTU-2	First Floor	2,716	735	3.7	Ceiling Space Plenum				
RTU-3	First Floor	2,930	534	5.5	Ceiling Space Plenum				
RTU-4	Second Floor	2,426	1,805	1.3	Ducted			114.7	-88
Total		***11,008***	***3,538***						

Table A10-4. Heat Recovery Ventilator Airflow (Ventilation Airflow)

HRV Ventilation Airflow		
Opening width	76	inches
Opening height	17	inches

Equal Area Velocity Traverse (fpm)

790	710	330	180	200	820	650	370	870
1040	1050	820	805	860	950	480	1030	960
310	350	310	210	320	280	320	320	450
			t-plate	t-plate				

Average	584.6	SFPM
Area	9.0	ft^2
Air Flow	**5245**	**SCFM**

Table A10-5. Heat Recovery Ventilator Airflow (Exhaust Airflow)

Exhaust Airflow		
Opening width	8.5	inches
Opening height	32	inches

Equal Area Velocity Traverse (fpm)

2300	700	400	690	2300
2030	440	360	400	1910
980	610	480	410	2500
fan		plate		fan

Average	1100.7	SFPM
Area	1.9	ft^2
Air Flow	**2079**	**SCFM**

There is some ventilation air provided by the RTUs even though the economizers are disabled and the HRV is the main supply of outdoor air. With a single blower door the maximum building depressurization was 21 Pa, however with the blower door and the RTUs operating the building reached maximum pressurization of 27 Pa. The building reached a greater pressure difference across the building envelope with the RTUs operating because the RTUs provide some ventilation air. To reach a particular building pressure using the blower door with the RTUs operating required less airflow through the blower door because the remaining airflow was provided by the RTUs. An estimate of the RTU ventilation airflow during normal building operation is the difference in airflow between the building pressurization tests (with RTUs on/off) at the typical building envelope pressure. The power law equations for the two flow curves (RTUs ON and RTUs OFF) are show below:

$$\text{RTUs ON}: \quad Q_{\text{on}} = K_{on} P_{env}^{n_{on}}$$
$$\text{RTUs OFF}: \quad Q_{\text{off}} = K_{off} P_{env}^{n_{off}}$$
$$\text{RTU Outdoor Air Flow}: \quad K_{off} P_{env}^{n_{off}} - K_{on} P_{env}^{n_{on}}$$
$$\text{RTU Outdoor Air Flow}: \quad 435.2 P_{env}^{0.870} - 80.4 P_{env}^{1.303}$$

where Q is the flow through the blower door fan, P_{env} is the pressure difference across the building envelope, and K and n are the coefficient and exponent for the power law equation. The pressure across the building envelope (P_{env}) varied between 1.8 Pa and 9.9 Pa due to wind pressure and airflow imbalance. Therefore, the total outdoor airflow from the RTUs using the average normal operating envelope pressure is approximately 1,080 cfm. Figure A10-17 shows the two blower door pressure-flow curves with the RTUs off and on.

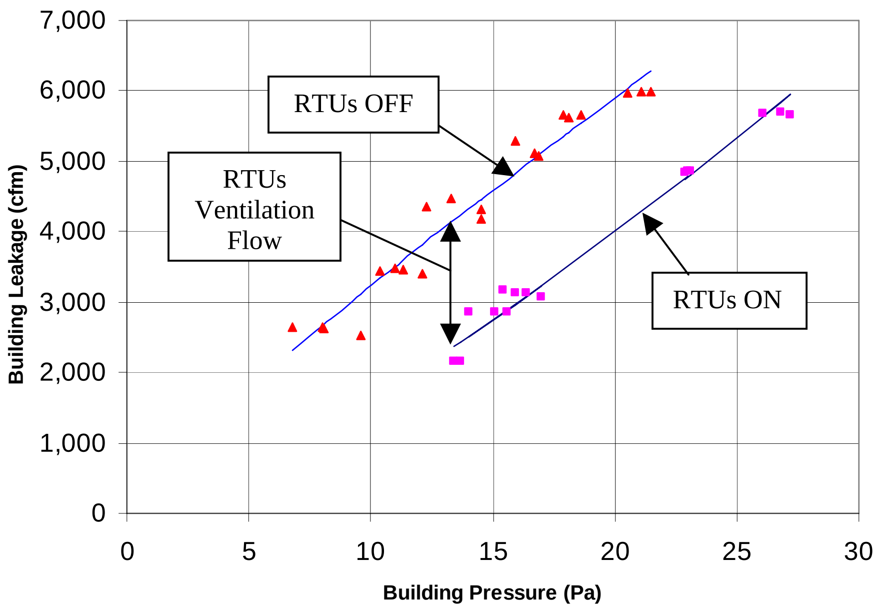

Figure A10-17. Airflow Variation with Building Pressure with RTUs Off and On.

The ventilation flow for the entire building includes the HRV Ventilation (5,245 cfm) and the RTU ventilation (1,080 cfm), which yields approximately 6,325 cfm. The building exhaust fans with design and measured airflows are shown in Table A10-6. The building airflow imbalance (ventilation cfm – exhaust cfm) is approximately 3,442 cfm (6,325 cfm – 2,883 cfm), which agrees with the positive building envelope pressures measured during normal operating conditions.

The total supply diffuser airflow is approximately 11,000 cfm, which means that 57.5% of the supply air is outdoor air. The ventilation rate is approximately 0.44 cfm/ft^2 floor area.

Table A10-6. Building Exhaust Fans

Exhaust Fan	Design Exhaust Flow (cfm)	Measured Exhaust Flow (cfm)
HRV	2,330	2,079
Locker Room 104	115	151
Equipment Room 103	115	off
Network Room	115	165
Conference Room 116	380	488
Janitor Closet 119	100	75
Total	***3,155***	***2,958***

Pressure Mapping (AHU Fans On)

The air pressure relationships in the building were also determined with the RTU and HRV fans on. The graphics in Figure A10-18 show the pressure differences induced across the doorways with the AHU fans on and the individual doorway closed. With the building in normal configuration, we would close an interior door and measure the pressure across the doorway. Operation of the four RTUs and the HRV created interior pressures differences up to 2.5 Pa. The building was pressurized with respect to outdoors between 1.8 Pa (2nd floor roof hatch) and 9.9 Pa (corridor near office 110). This pressure may vary if the manually operated exhaust fans were turned on or if the RTU economizers were used.

During the blower door depressurization tests with all the HVAC equipment turned off, employees working in the building began to smell combustion gas from the boiler room located below the cafeteria. We did not expect the boilers to be operating, but the outdoor temperature fell below 65°F causing a boiler to start. Even though the door to the boiler room was completely sealed and the ceiling of the boiler room is concrete, we could still smell the combustion gas with the building depressurized. A small hole (approximately 4-in diameter) in the ceiling of the boiler room was only covered by floor tile and allowing boiler combustion gas to be pulled into the cafeteria. Under typical operating conditions, this is not a problem because the boiler room operates at approximately 2.5 Pa depressurized from the surrounding rooms.

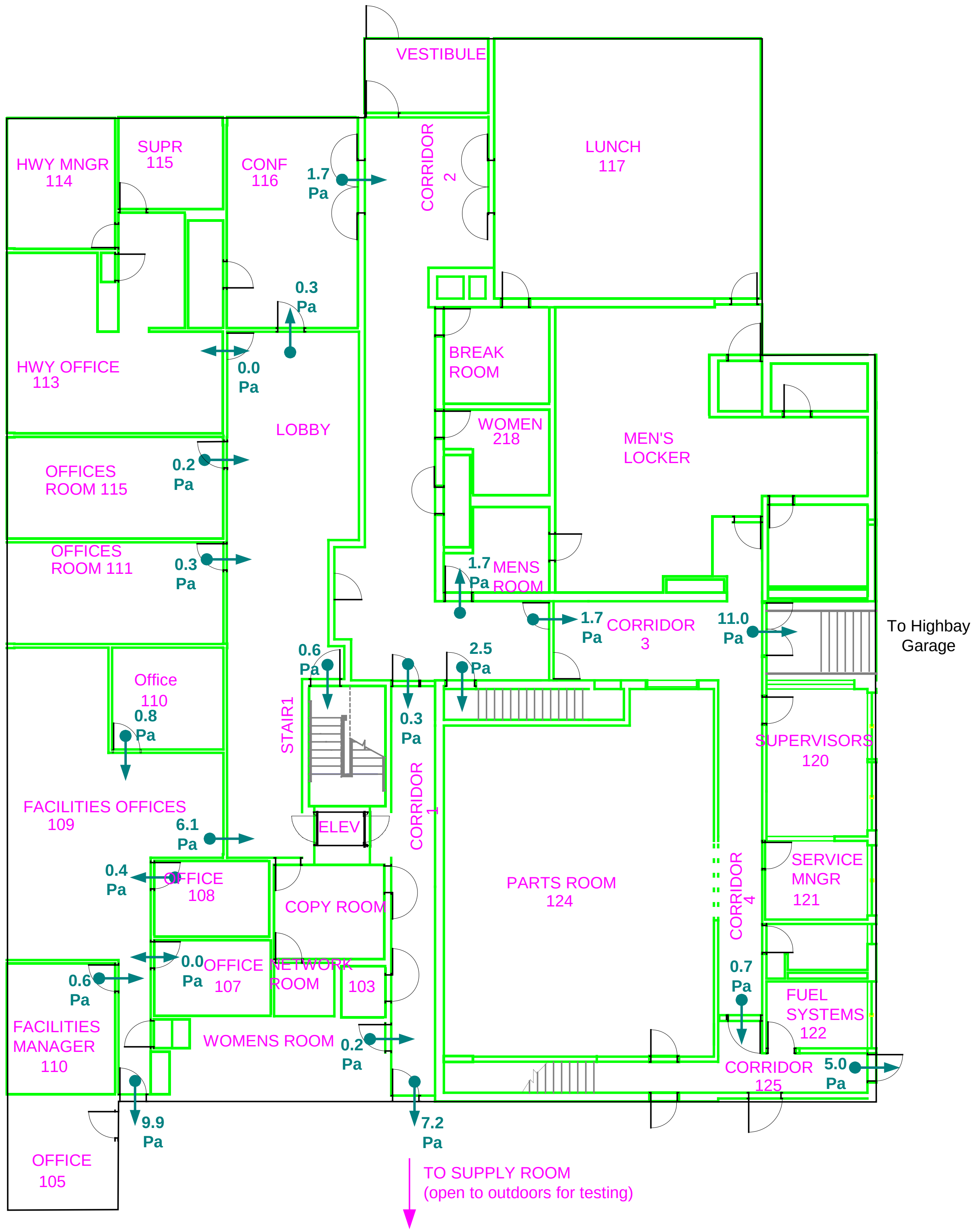

Figure A10-18. First Floor Pressure Differences between Rooms with AHU Fans On

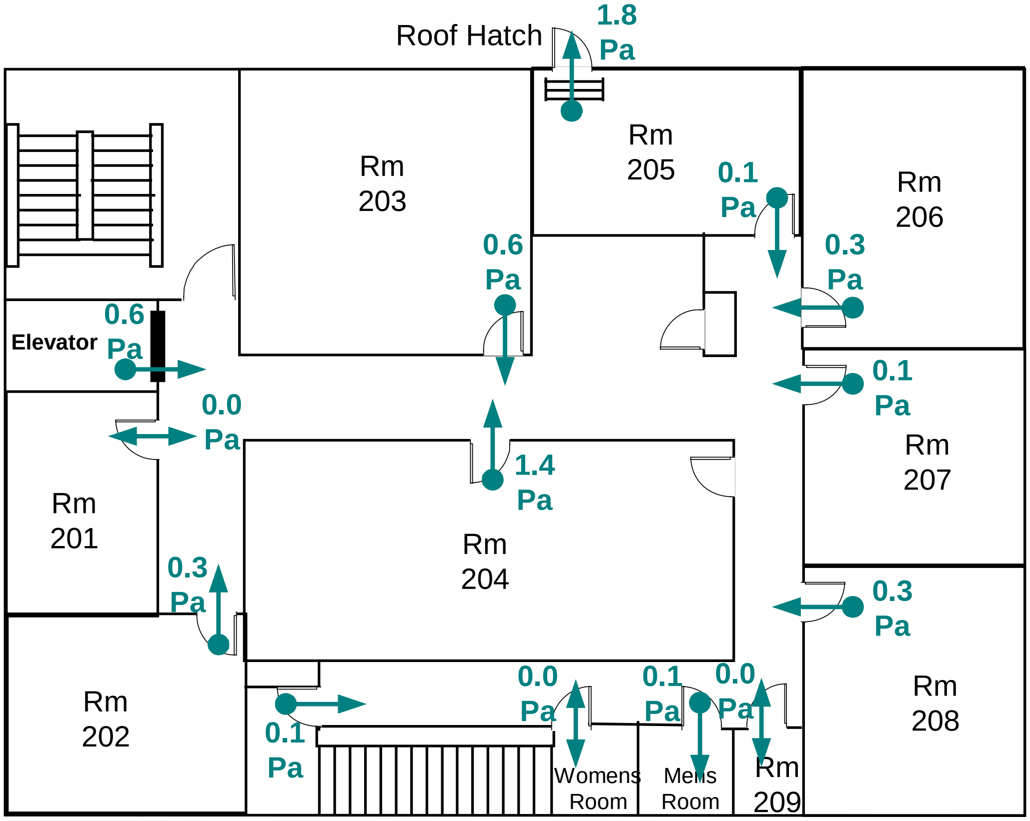

Figure A10-19. Second Floor Pressure Differences between Rooms with AHU Fans On

Duct Leakage Measurements

A Duct Blaster was used to depressurize the ductwork to measure leakage rates. The supply ducts were tested for RTU-1 (cafeteria and vestibule) and RTU-4 (2^{nd} Floor). The Duct Blaster fan was connected to the supply fan section in the RTU cabinet, as shown in Figure A10-20. Sealing the return side of the RTU and sealing the ventilation intake isolated the supply ductwork. The static pressure tap was located in the supply plenum. RTU-1, 2, and 3 have ceiling space return plenums so we did not test the return leakage on these systems. RTU-4 has ducted returns, however we did not test the return ductwork because we could not depressurize the system. We connect the Duct Blaster to the return side and sealed all of the return diffusers, but we could only depressurize the ductwork to 6 Pa. Possibly, there is a connection to the return ductwork from the HRV or some other opening to the return system.

Duct Blaster Connected to RTU-1

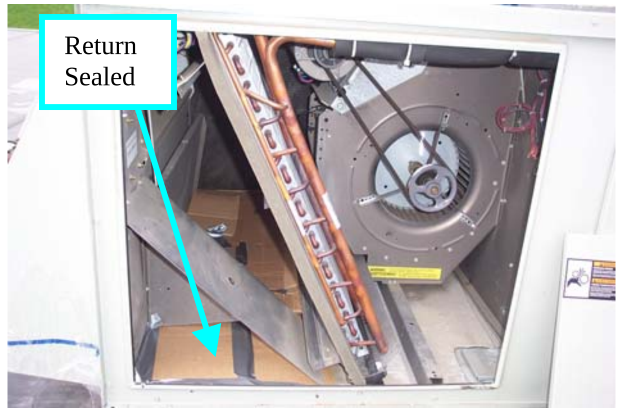

Return Sealed to Isolate Supply Ductwork

Ventilation Hood Sealed

Figure A10-20. Duct Blaster Setup for Roof Top Units

As a diagnostic check on the degree of pressurization, the pressure at each supply diffuser was measured by puncturing the plastic covering at each diffuser with a very small probe. Figure A10-21 shows the resulting pressures measured at each supply diffuser for RTU-1 and RTU-4 with the system depressurized. The uniformity of the pressures at most diffusers implies that leaks are uniformly spread around the system.

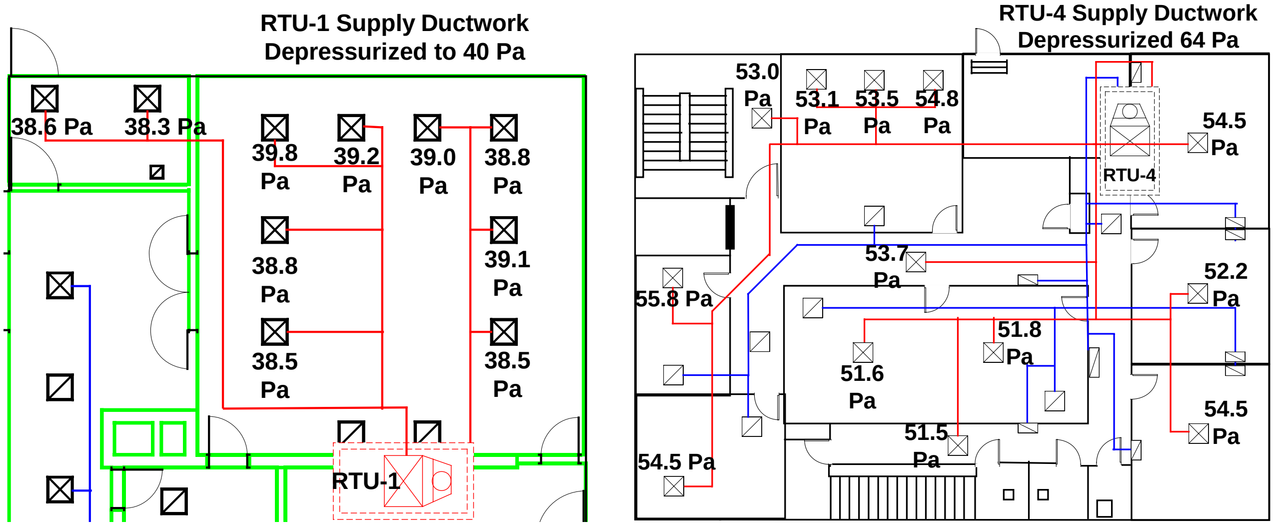

Figure A10-21. Diffuser Pressures with Ductwork Depressurized

Figure A10-22 shows the resulting measured data from the duct leakage tests fit to a power function (raw data in Table A10-7). Figure A10-22 also shows our best estimate for duct leakage during normal operation, which uses one half of the plenum pressure as suggested in ASHRAE Standard 152P section B.2. Table A10-8 shows the resulting coefficients, exponents, and regression statistics. Table A10-9 summarizes the resulting duct leakage rates and ELA at a reference pressure of 25 Pa. The duct leakage in this case has little effect on energy use because all the ductwork is located inside the primary air and thermal barrier.

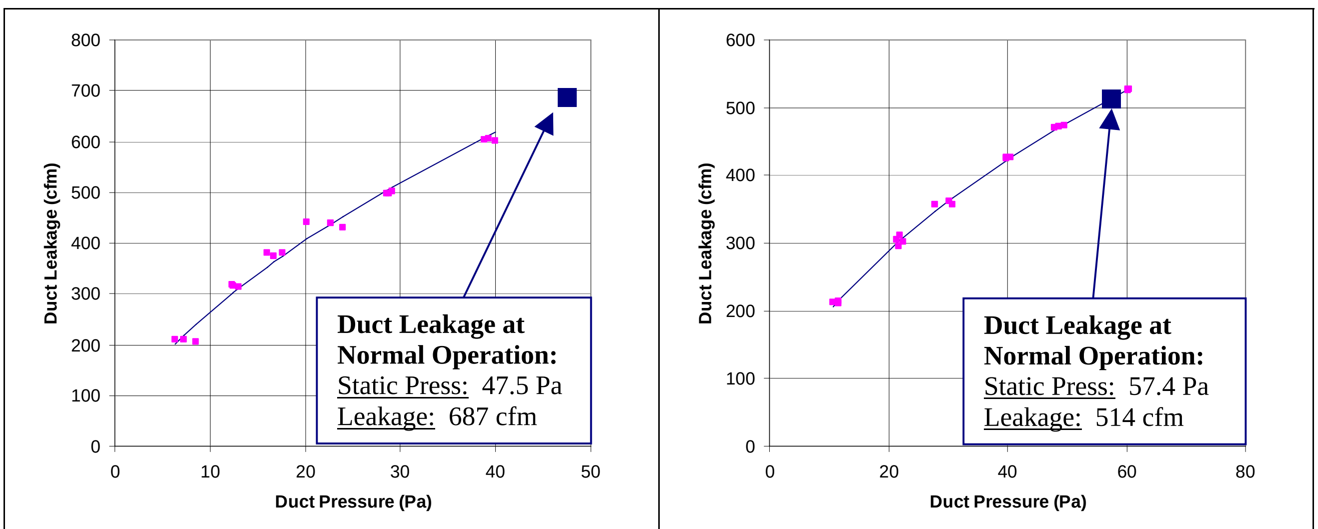

RTU-1 (Supply Ductwork) RTU-4 (Supply Ductwork)

Figure A10-22. Duct-Blaster Tests on RTU-1 & RTU-4 Ductwork

Table A10-7. Raw Data from Duct-Blaster Tests

RTU-1 (Supply Ductwork)

Test Results:

Flow Coefficient (K)	65.0	
Exponent (n)	0.611	
Leakage area (LBL ELA @ 25 Pa)	53	sq in
Airflow @ 25 Pa	464.3	cfm

Test Data:

	Nominal Duct Pressure (Pa)	Nominal Flow (cfm)	Ring
1	40.0	602	A1
2	39.3	605	A1
3	38.8	603	A1
4	29.1	501	A1
5	28.8	497	A1
6	28.6	498	A1
7	24.0	430	A1
8	22.7	439	A1
9	20.2	442	A1
10	17.6	380	A1
11	16.7	373	A1
12	16.0	381	A1
13	13.0	313	A1
14	12.4	315	A1
15	12.3	318	A1
16	8.5	206	A1
17	7.3	209	A1
18	6.3	209	A1

RTU-4 (Supply Ductwork)

Test Results:

Flow Coefficient (K)	57.0	
Exponent (n)	0.543	
Leakage area (LBL ELA @ 25 Pa)	37	sq in
Airflow @ 25 Pa	327.4	cfm

Test Data:

	Nominal Duct Pressure (Pa)	Nominal Flow (cfm)	Ring
1	60.4	527	A1
2	60.3	526	A1
3	60.2	527	A1
4	49.6	473	A1
5	48.6	472	A1
6	48.0	471	A1
7	40.6	427	A1
8	39.9	425	A1
9	39.8	427	A1
10	30.8	356	A1
11	30.2	361	A1
12	27.9	357	A1
13	22.4	301	A1
14	22.0	311	A1
15	21.8	295	A1
16	21.3	305	A1
17	11.6	214	A1
18	11.6	211	A1
19	10.6	213	A1

Table A10-8. Coefficients, Exponents and Regression Statistics from Duct-Blaster Tests

	Supply & AHU Cabinet		
	K	n	R^2
RTU-1	65.0	0.611	97.64%
RTU-4	57.0	0.543	99.65%

Notes: cfm = $K(Pa)^n$ / R^2 indicates fit of linear log-log regression

Table A10-9. Comparison of Supply Airflow Measurements

	Total Supply Diffuser Airflow (cfm)	Supply & AHU Cabinet Leakage (cfm @ 25)	Supply & AHU Cabinet ELA (sq in @ 25)
RTU-1	2,936	464	53
RTU-4	2,426	327	37

Notes: Leakage and ELA at reference pressure of 25 Pa

Table A10-10 lists the ductwork used to estimate the supply and return duct area for the RTUs. The effective leakage area compared to the duct surface area for RTU-1 and RTU-4 is shown in Table A10-11. The Sheet Metal and Air Conditioning Contractors' National Association (SMACNA) classifies duct leakiness using duct leakage per 100 sq ft of duct area at a pressure of 1-in w.g.

Table A10-10. RTU Ductwork Size and Area

RTU-1

	Type/Size	Supply Side Length (ft)	Duct Area Supply Side (sq ft)
Supply Trunks	30" x 20"	8.0	66.7
	26" x 10"	6.0	36.0
Supply Ducts	20" x 10"	19.6	97.9
	16" 10"	15.8	68.6
	16" x 8"	15.8	63.3
	10" x 8"	47.5	142.5
takeoffs	10" dia.	38.8	101.4
AHU Cabinet	approx. 4' x 4' x 4'		80.0
Total			***656.5***

RTU-4

	Type/Size	Supply Side Length (ft)	Duct Area Supply Side (sq ft)
Supply Trunks	30" x 16"	36.0	276.0
Supply Ducts	18" x 12"	22.5	112.5
	16" x 8"	39.1	156.5
	14"x 8"	40.1	147.0
	12" dia.	3.8	11.8
takeoffs	8" dia.	82.1	171.9
AHU Cabinet	approx. 4' x 4' x 2'		56.0
Total			***931.6***

Table A10-11. Duct Leakage per 100 Square Foot of Duct Area

		Duct Area (sq ft)	ELA (sq in @ 25)	ELA/100 sq ft Duct Area (sq in @ 25)	Leakage (cfm @ 25 Pa)	Supply CFM per ft^2 Duct Area (cfm/ sq-ft)	Leakage per 100 sq ft Duct Area (cfm @ 25 Pa)	SMACNA Leakage Class cfm per 100 sq ft (cfm @ 1-in water)
RTU-1	Supply & AHU Cabinet	656	53	8.0	464	4.47	71	288
RTU-4	Supply & AHU Cabinet	932	37	4.0	327	2.60	35	122

Figure A10-23 shows the airflow balance for RTU-1. The ventilation airflow for RTU-1 (270 cfm) was estimated as ¼ of the total ventilation airflow measured for all four RTUs (see section on HVAC Airflow Measurements). To check the duct leakage measurements using fan pressurization, we compared the supply airflow at the plenum for RTU-1 to the total supply airflow measured at the diffusers (Table A10-12). The difference in supply airflow at the unit and the airflow measured at the diffusers yields ductwork leakage of 1,201 cfm and the fan pressurization test estimates 687 cfm of leakage at operating pressure. The estimated average "actual static" pressure used to calculate the normal operating static pressure is one half of the pressure measured at the plenum (ASHRAE Standard 152P section B.2).

Table A10-12. RTU-1 Supply Ductwork Leakage

Supply Airflow		Supply Ductwork Leakage	
Airflow at Unit (cfm)	Airflow at Diffusers (cfm)	Flow at Unit minus Flow at Diffusers (cfm)	Fan Press. Method @ Est. Actual Static (cfm)
4,137	2,936	1,201	687

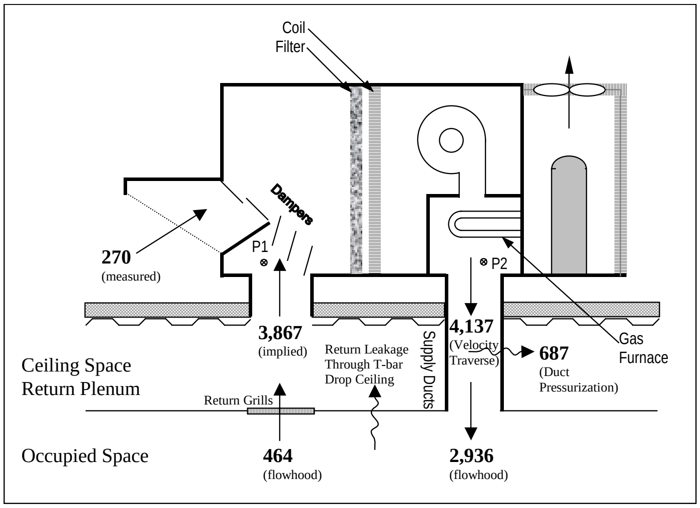

Figure A10-23. Airflow Balance for RTU-1

Space Conditions

Figure A10-24 shows the average temperature profiles based on temperature readings taken with a HOBO data logger from September 17 to October 12, 2004. The thick line shows the average for each hour while the shaded region corresponds to one standard deviation about the average. The dotted lines correspond to the minimum and maximum for each hour.

A Johnson Controls Metasys controller controls the four RTUs, HRV, and boilers. The controller uses several temperature sensors to monitor the temperature in each of the zones. Each temperature sensor controls a damper to increase or decrease the airflow through a section of duct that typically leads to several diffusers. The Metasys heating and cooling setpoints control the on/off operation of the RTUs and the boilers. The heating setpoint is 70°F and the cooling setpoint is 74°F (75°F upstairs). The boilers begin operating when the outdoor ambient temperature falls below 65°F.

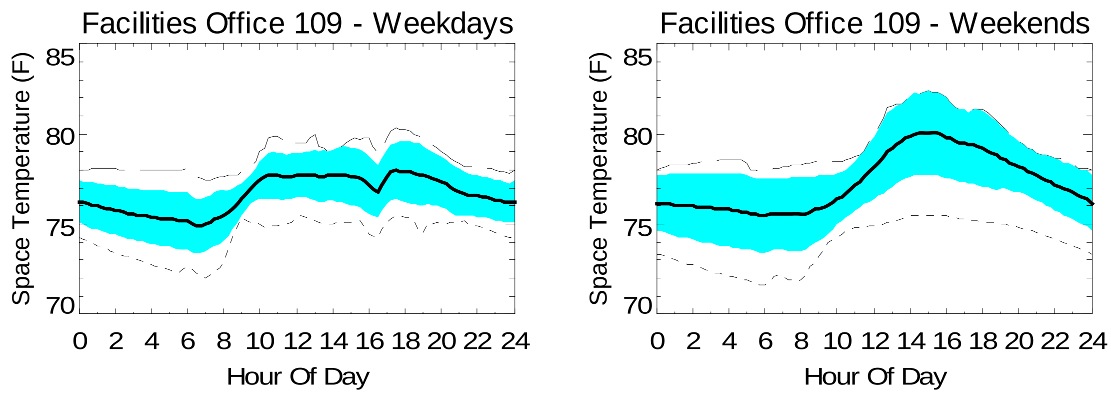

Figure A10-24. Measured Space Temperature Profiles

Figure A10-25 shows the CO_2 concentration in various locations in the building. The CO_2 concentration provides an indication of occupancy, however in the facilities office the CO_2 trend is driven by the HVAC equipment. The relatively low occupancy per square foot and high ventilation rates help maintain a very low CO_2 concentration. The CO_2 concentration typically stays below 774 ppm in the facilities office and below 576 ppm in office 202. The next section uses the CO_2 as a tracer gas to estimate the infiltration/ventilation rate into the building.

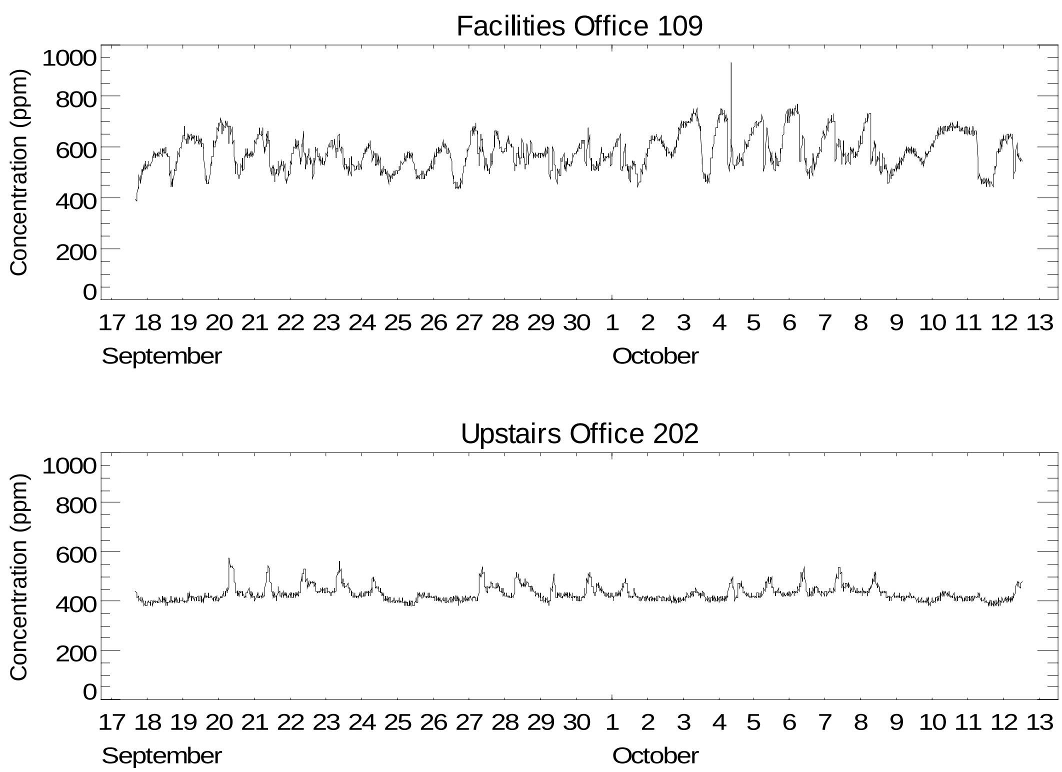

Figure A10-25. Measured CO_2 Concentration in Various Spaces

The following plots show the relative humidity for this building. The maximum relative humidity in the facilities office was 55.6% during the monitoring period. Figure A10-29 displays the conditions inside the building compared with the ASHRAE comfort zone for cooling shown by the shaded region on the plot.

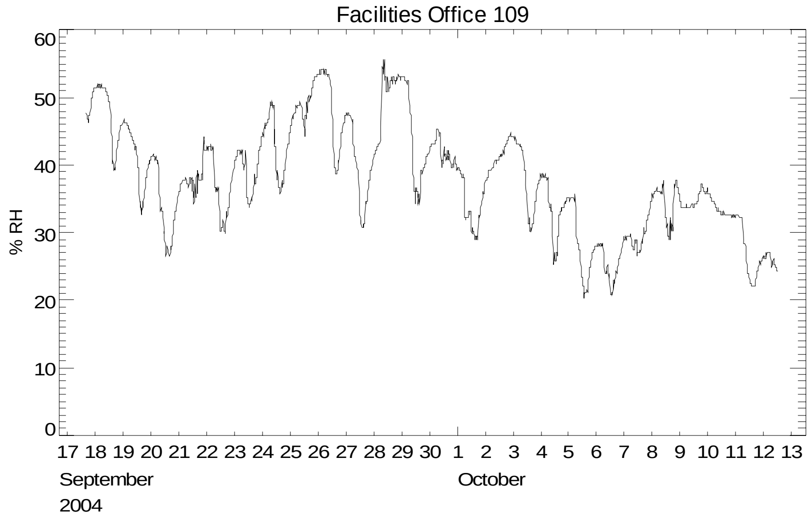

Figure A10-26. Measured Relative Humidity

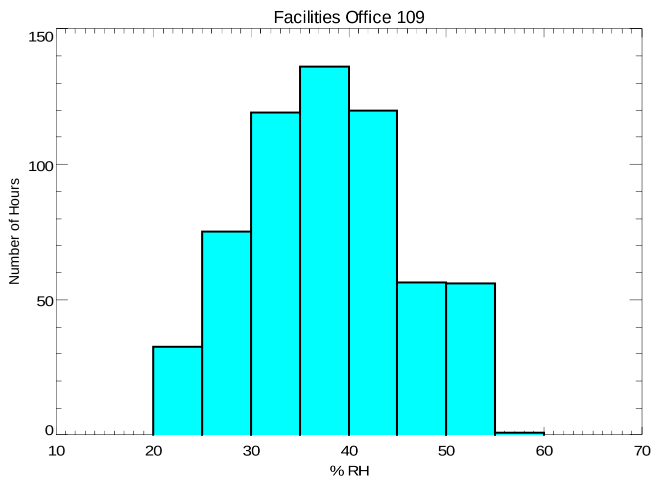

Figure A10-27. Duration of Relative Humidity Levels

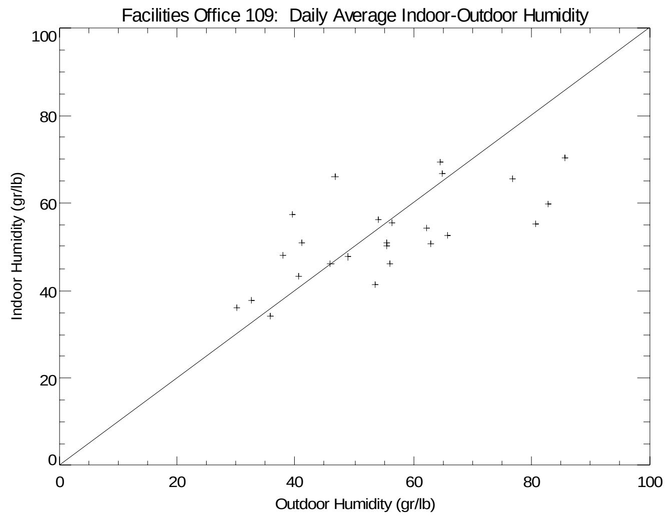

Figure A10-28. Indoor Humidity Variation with Outdoor Humidity

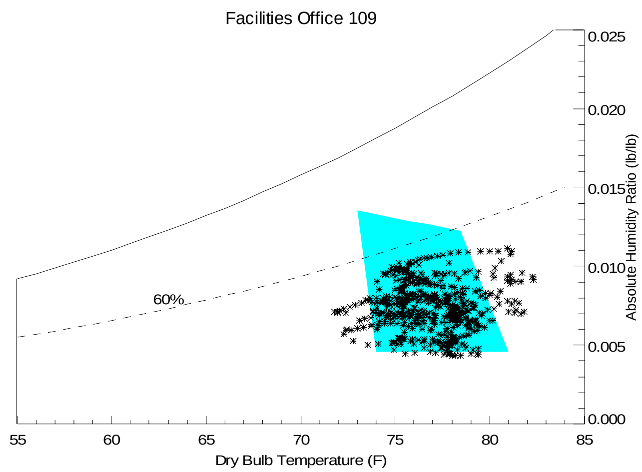

Figure A10-29. Indoor Air Quality Comparison with ASHRAE Comfort Zone for Cooling

Infiltration Estimate from CO_2 Decay

Figure A10-30 and Figure A10-31 show the resulting decay trends using CO_2 levels immediately after high occupancy periods for the facilities office 109 and upstairs office 202. The predicted air change rate (ACH) is shown on each plot.

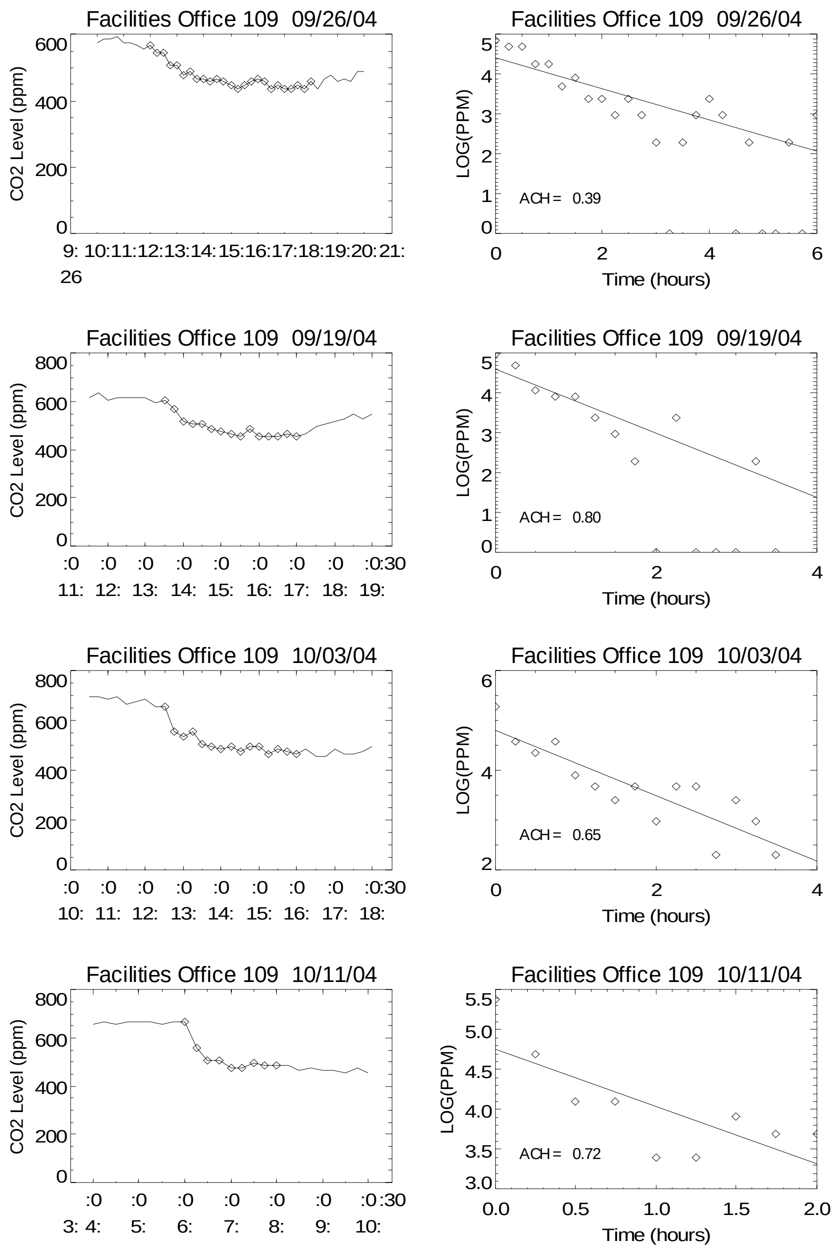

Figure A10-30. Facilities Office 102: Tracer Gas Decay Using CO_2 for Various Periods

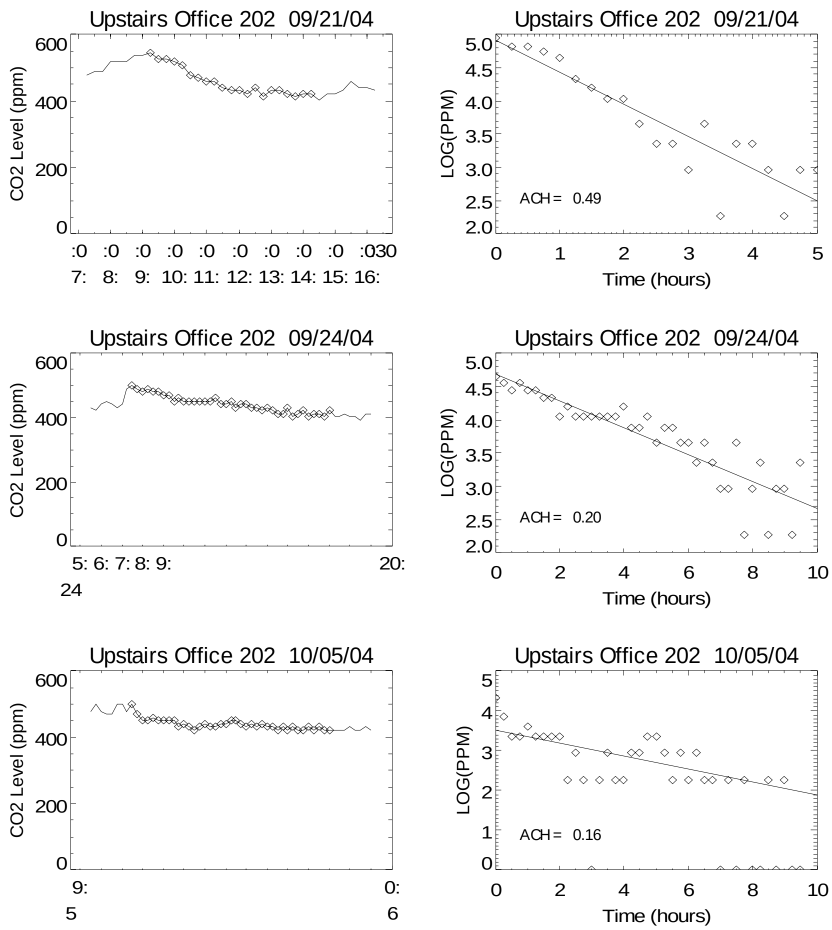

Figure A10-31. Relief Society: Tracer Gas Decay Using CO_2 for Various Periods

Table A10-13 summarizes the results of the tracer gas decay tests in the plots above. The table also includes the estimated infiltration airflow based on the building volume of 120,903 ft^3.

Table A10-13. Summary of Tracer Gas Decay Tests

Facilities Office 109

Start Time	End Time	ACH	Flow (cfm)
26-Sep 12:00 PM	26-Sep 06:00 PM	0.39	789
19-Sep 01:30 PM	19-Sep 05:00 PM	0.80	1,622
03-Oct 12:30 PM	03-Oct 04:00 PM	0.65	1,316
11-Oct 06:00 AM	11-Oct 08:00 AM	0.72	1,461

Upstairs Office 202

Start Time	End Time	ACH	Flow (cfm)
21-Sep 09:15 AM	21-Sep 02:15 PM	0.49	983
24-Sep 07:30 AM	24-Sep 05:00 PM	0.20	412
05-Oct 11:30 AM	05-Oct 09:00 PM	0.16	328

Note: Flow determined with building volume of: **121,423** ft^3

In comparison to the ACH values above, the nominal leakage rate (defined as ACH_{50} divided by 20) from the blower door test above is 0.32 ACH. The ACH values in Table A10-13 for the facilities office were calculated using CO_2 decays that were due to HVAC operation.

BUILDING ENERGY USE HISTORY

The building uses natural gas primarily for space heating, with a small amount consumption used for domestic hot water. Electricity consumption is primarily used for area and task lighting, with HVAC and plug loads being secondary electricity uses.

Table A10-14 displays the historic electricity billing data for the building. Annual electricity consumption averages near 360,000 kWh/year, with an electricity energy use index of 6.5 kWh/sq ft/year. The electricity use index is based on the total floor area of the building, which is 55,000 sq ft.

Table A10-14. Summary of Electric Bills

Billing End Date	Days in Month	Demand (kW)	Energy (kWh)	Cost ($)	$/kWh	Elec. Use per Sq-Ft (kWh/sq ft)
1/12/2001	31	70.8	36,360	3,448.61	0.095	0.66
2/12/2001	31	64.8	34,800	3,149.50	0.091	0.63
3/15/2001	31	64.8	35,520	3,016.20	0.085	0.65
4/12/2001	28	61.2	27,360	2,427.50	0.089	0.50
5/11/2001	29	54	21,000	2,036.05	0.097	0.38
6/12/2001	32	54	19,680	2,143.24	0.109	0.36
7/12/2001	30	60	21,600	2,500.73	0.116	0.39
8/10/2001	29	57.6	19,440	2,285.20	0.118	0.35
9/12/2001	33	54	21,700	2,346.37	0.108	0.39
10/9/2001	27	57	18,000	2,095.69	0.116	0.33
11/6/2001	28	66	23,700	2,635.75	0.111	0.43
12/11/2001	35	77	34,000	3,506.19	0.103	0.62
Total 2001	***364***	***77***	***313,160***	***31,591***	***0.101***	***5.7***

Billing End Date	Days in Month	Demand (kW)	Energy (kWh)	Cost ($)	$/kWh	Elec. Use per Sq-Ft (kWh/sq ft)
1/14/2002	34	82	40,400	3,940.03	0.098	0.73
2/12/2002	29	90	41,100	4,101.46	0.100	0.75
3/14/2002	30	80	41,000	3,797.39	0.093	0.75
4/15/2002	32	68	36,500	3,170.72	0.087	0.66
5/14/2002	29	88	32,100	3,037.57	0.095	0.58
6/13/2002	30	88	32,800	3,056.33	0.093	0.60
7/15/2002	32	92	31,400	3,025.21	0.096	0.57
8/13/2002	29	88	26,200	2,711.60	0.103	0.48
9/12/2002	30	81	24,500	2,637.19	0.108	0.45
10/10/2002	28	83	24,700	2,559.61	0.104	0.45
11/8/2002	29	87	29,200	2,875.98	0.098	0.53
12/11/2002	33	88	37,300	3,298.76	0.088	0.68
Total 2002	***365***	***92***	***397,200***	***38,212***	***0.096***	***7.2***

Billing End Date	Days in Month	Demand (kW)	Energy (kWh)	Cost ($)	$/kWh	Elec. Use per Sq-Ft (kWh/sq ft)
1/14/2003	34	82	43,700	3,748.38	0.086	0.79
2/12/2003	29	82	38,200	3,669.33	0.096	0.69
3/14/2003	30	82	37,900	3,655.80	0.096	0.69
4/14/2003	31	86	33,900	3,399.88	0.100	0.62
5/14/2003	30	94	29,500	3,185.44	0.108	0.54
6/13/2003	30	91	27,700	3,009.62	0.109	0.50
7/16/2003	33	102	26,800	3,048.91	0.114	0.49
8/15/2003	33	95	28,100	3,065.43	0.109	0.51
9/12/2003	25	93	21,400	2,540.78	0.119	0.39
10/10/2003	28	89	22,100	2,550.28	0.115	0.40
11/10/2003	31	91	28,500	3,048.38	0.107	0.52
12/12/2003	32	82	36,900	3,577.63	0.097	0.67
Total 2003	***366***	***102***	***374,700***	***38,500***	***0.103***	***6.8***

Billing End Date	Days in Month	Demand (kW)	Energy (kWh)	Cost ($)	$/kWh	Elec. Use per Sq-Ft (kWh/sq ft)
1/12/2004	33	86	41,700	3,934.49	0.094	0.76
2/12/2004	29	84	40,900	3,861.09	0.094	0.74
3/12/2004	29	85	35,900	3,511.70	0.098	0.65
4/14/2004	33	86	36,400	3,576.98	0.098	0.66
5/12/2004	28	85	25,600	2,772.81	0.108	0.47
6/14/2004	33	96	27,100	2,995.76	0.111	0.49
7/15/2004	31	93	26,200	2,904.81	0.111	0.48
8/12/2004	28	90	24,100	2,722.63	0.113	0.44
9/10/2004	29	88	24,100	1,391.41	0.058	0.44
10/8/2004	28	90	24,000	1,406.25	0.059	0.44
11/8/2004	31	88	28,000	1,215.66	0.043	0.51
12/13/2004	35	85	35,300	1,359.25	0.039	0.64
Total 2004	***367***	***96***	***369,300***	***31,653***	***0.086***	***6.7***

Billing End Date	Days in Month	Demand (kW)	Energy (kWh)	Cost ($)	$/kWh	Elec. Use per Sq-Ft (kWh/sq ft)
1/14/2005	32	88	41,200	1,273.17	0.031	0.75
2/11/2005	28	93	38,400	1,286.87	0.034	0.70
3/14/2005	31	95	42,600	1,447.82	0.034	0.77
4/13/2005	30	88	34,500	1,310.25	0.038	0.63
5/11/2005	28	87	23,600	1,122.90	0.048	0.43
6/13/2005	33	94	25,600	1,212.53	0.047	0.47
7/13/2005	30	101	23,500	1,171.14	0.050	0.43
8/12/2005	30	96	24,500	1,156.65	0.047	0.45
9/12/2005	31	91	19,900	1,018.73	0.051	0.36
10/11/2005	29	85	19,100	830.40	0.043	0.35
11/7/2005	27	72	18,600	575.93	0.031	0.34
12/6/2005	29	71	24,600	519.05	0.021	0.45
Total 2005	***358***	***101***	***336,100***	***12,925***	***0.038***	***6.1***

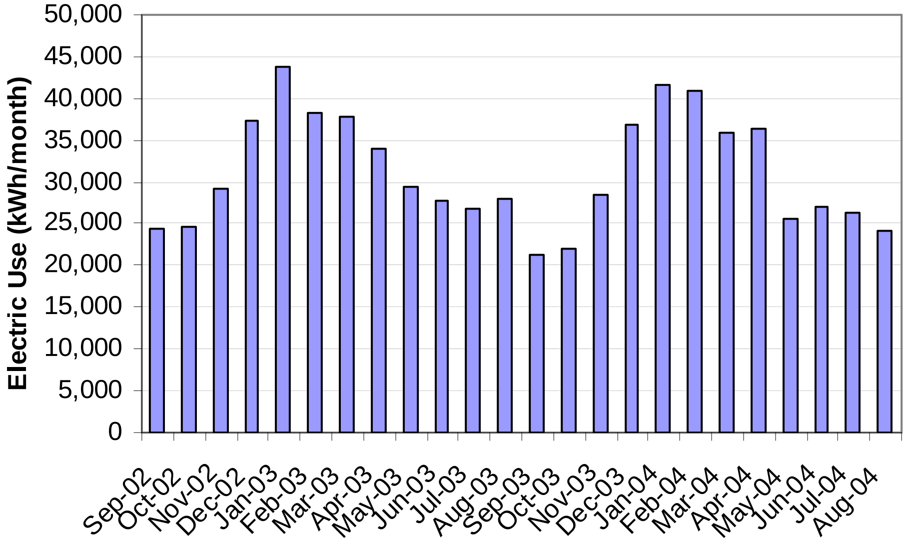

Figure A10-32. Monthly Electricity Use Trends (Last 24 Months)

Table A10-15. Summary of Gas Bills

	Days in Month	Gas Use (therms)	Cost ($)	$/therm	Gas Use per Sq-Ft (therm/sq ft)
1/12/2001	31	9407.3	10811.06	1.15	0.171
2/12/2001	31	8339.1	11911.65	1.43	0.152
3/15/2001	31	7769.2	8634.12	1.11	0.141
4/12/2001	28	5419.5	5568.52	1.03	0.099
5/11/2001	29	1685.2	1836.2	1.09	0.031
6/12/2001	32	93.2	123.31	1.32	0.002
7/13/2001	31	72.2	91.57	1.27	0.001
8/10/2001	28	51.5	67.27	1.31	0.001
9/11/2001	32	20.5	36.29	1.77	0.000
10/9/2001	28	72	80.85	1.12	0.001
11/5/2001	27	1049.2	816.75	0.78	0.019
12/11/2001	36	4734.1	3827.02	0.81	0.086
1/14/2002	13	2933.4	1334.7	0.46	0.053
2/12/2002	29	6947.5	5039.85	0.73	0.126
3/14/2002	30	6653.8	4451.3	0.67	0.121
4/15/2002	32	6514.9	5344.08	0.82	0.118
5/14/2002	29	4614.7	3814.18	0.83	0.084
6/13/2002	30	3141.2	2578.17	0.82	0.057
7/15/2002	32	498.3	489.54	0.98	0.009
8/13/2002	29	253.4	257.28	1.02	0.005
9/12/2002	30	70.9	81.64	1.15	0.001
10/10/2002	28	142	151.23	1.07	0.003
11/8/2002	29	4922.4	4169.66	0.85	0.089
12/11/2002	33	7313.9	6473.15	0.89	0.133
1/14/2003	34	9478.1	2318.44	0.24	0.172
2/12/2003	29	7847.8	7533.98	0.96	0.143
3/14/2003	30	12223.3	12487.18	1.02	0.222
4/14/2003	31	5136.7	7100.83	1.38	0.093
5/14/2003	30	3330.1	3284.39	0.99	0.061
6/13/2003	30	2368.9	2359	1.00	0.043
7/16/2003	33	1109.2	1175.05	1.06	0.020
8/13/2003	28	357.7	421.22	1.18	0.007
9/12/2003	30	276	311.9	1.13	0.005
10/10/2003	28	82.1	106.17	1.29	0.001
11/10/2003	31	6778.5	6111.62	0.90	0.123
12/12/2003	32	5714	5696.65	1.00	0.104
1/14/2004	33	8629.1	8528.05	0.99	0.157
2/12/2004	29	9105.7	8985.42	0.99	0.166
3/12/2004	29	6640.9	6578.99	0.99	0.121
4/14/2004	33	6249	6193.82	0.99	0.114
5/12/2004	28	2521.7	2557.43	1.01	0.046
6/14/2004	33	1821.1	1873.87	1.03	0.033
7/15/2004	31	1304.5	1371.44	1.05	0.024
8/12/2004	28	1028.4	1102.62	1.07	0.019
2001	***364***	***38713***	***43805***	***1.13***	***0.704***
2002	***344***	***44006***	***34185***	***0.78***	***0.800***
2003	***366***	***54702***	***48906***	***0.89***	***0.995***
2004	***244***	***37300***	***37192***	***1.00***	***0.678***

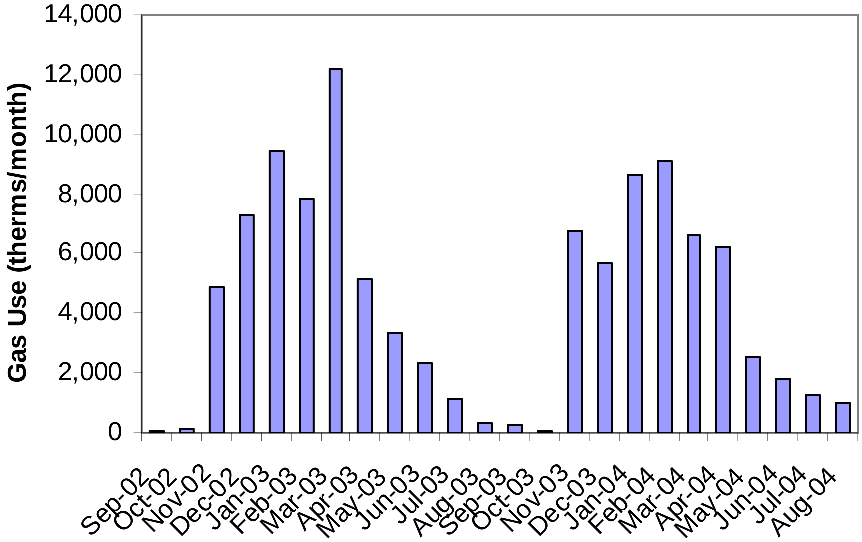

Figure A10-33. Monthly Gas Use Trends (Last 24 Months)

Figure A10-34 shows the gas use variation with ambient temperature and Figure A10-35 shows the electricity use variation with ambient temperature.

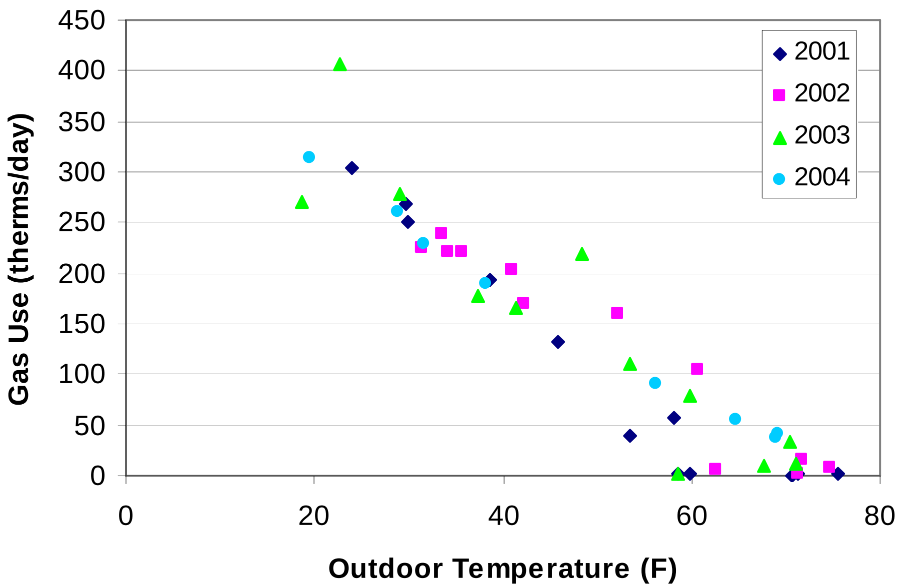

Figure A10-34. Variation of Gas Use with Ambient Temperature

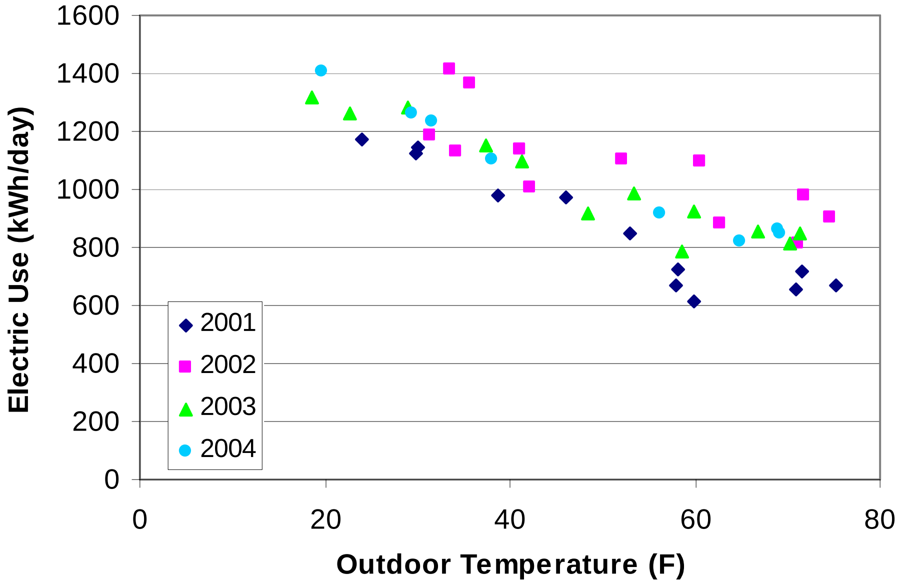

Figure A10-35. Variation of Electric Use with Ambient Temperature

Field Test Site 11 – Crash, Fire, Rescue Building, Ithaca, NY


South Corner of Building


Main Entrance (Southeast)


Back Side of Building (East Half)


Back Side of Building (North Corner)

Figure A11-1. Photos of Building

CHARACTERISTICS

Building Description

The 22,000 sq ft facility is a crash fire and rescue building that was built in 1995. Figure A11-1 shows all four sides of the building. The building has an office section and a high bay section. The office section has two horizontal furnaces that serve the training room and front conference room. The furnace the supplies the training room has a hot water coil for heating. A natural gas hot water boiler that supplies perimeter heaters heats the remainder of the office section. The horizontal furnaces are forced air furnaces with an A-coil evaporator. The individual offices are cooled by ductless split units. A single outdoor air vent provides ventilation to each of the furnaces. The high bay garages have radiant heaters around the perimeter of each bay and a roof top unit (RTU) supplies forced air heat to two of the bays. Figure A11-2 presents the building floor plan.

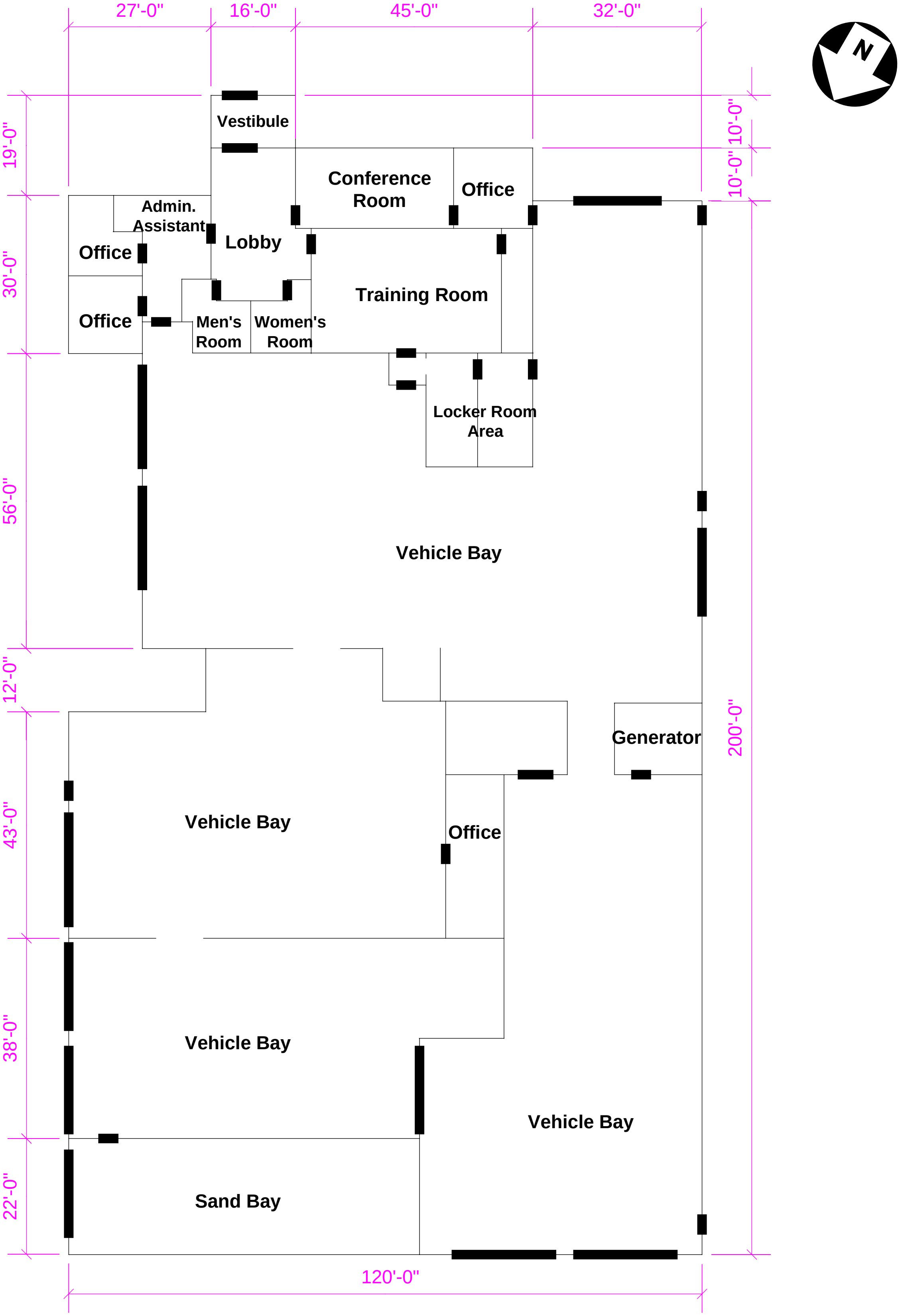

Figure A11-2. Building Floor Plan

Construction Details

Exterior walls are constructed of concrete block with brick veneer exterior finish. The interior finish for the office section of the building is either gypsum board, painted concrete block, or brick veneer that was previously exterior wall.

The building has a flat built-up roof with rigid foam insulation and metal decking on the underside of the roof. The training room in the office section has additional 6-in fiberglass batt insulation suspended between the metal roof deck and the ceiling tiles.

There is a T-bar (drop) ceiling in the office section of the building. The supply and return ducts for the office section are located in the ceiling space. The roof deck is the ceiling for the high bay areas.

Figure A11-3 illustrates the typical wall and roof construction for the office section and the high bay section. The major difference between the offices and the high bay garage wall construction is the gypsum board and T-bar drop ceiling interior finishing of the office section. Figure A11-4 shows pictures of the ceiling plenum in the training room and typical diffuser installation. The training room has an additional layer of fiberglass batt insulation suspended between the roof deck and the T-bar drop ceiling as shown in Figure A11-4

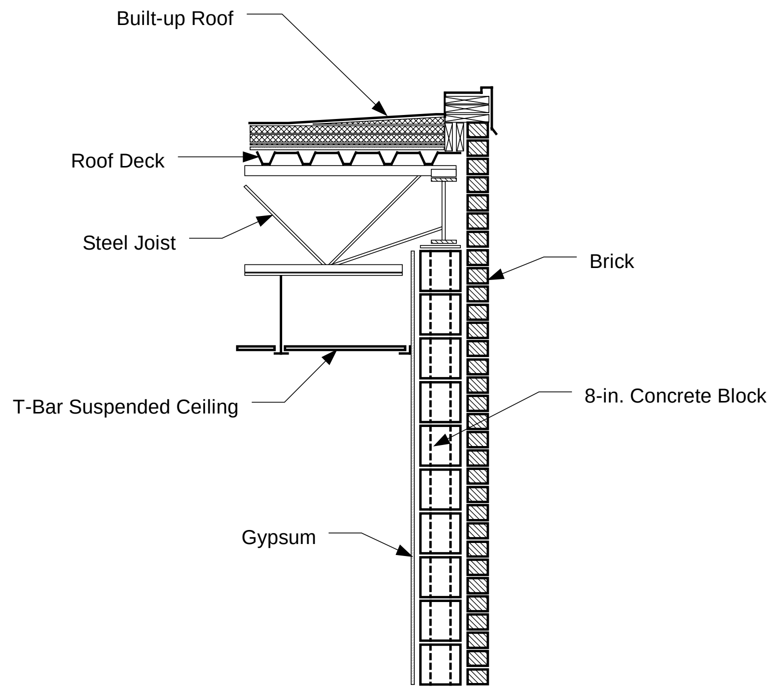

Office Section

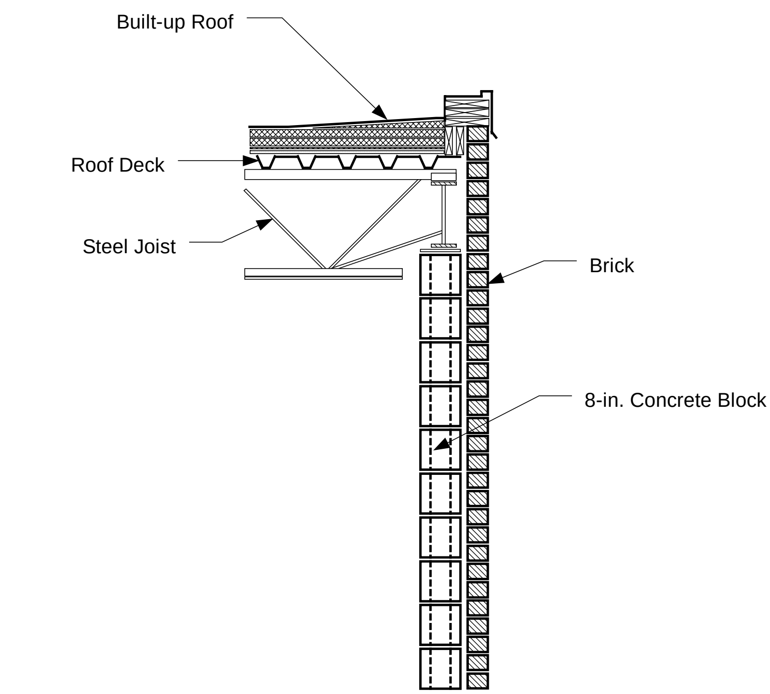

High Bay Section

Figure A11-3. Roof and Wall Sections

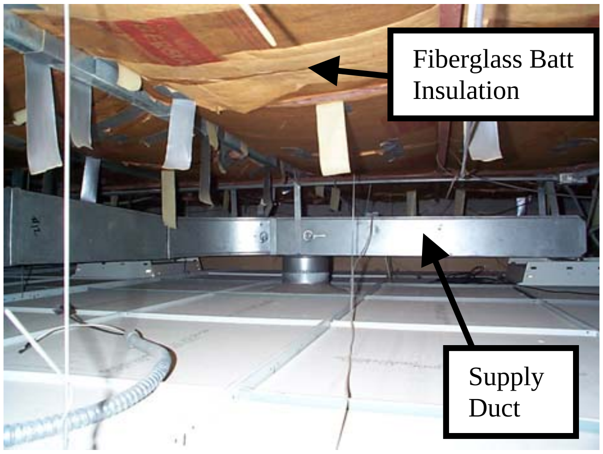

Ceiling Plenum in Training Room

Typical Supply Diffuser Installation

Figure A11-4. Ceiling Plenum in Office Section

HVAC System

The office section has two horizontal furnaces that serve the training room (unit 1) and front conference room (unit 2). The furnace that supplies the training room has a hot water coil for heating. A natural gas hot water boiler supplies the training room furnace and perimeter heaters in the remainder of the office section. The horizontal furnaces are forced air furnaces with an A-coil evaporator. Each furnace has a 2.5-ton condensing unit on the roof. The individual offices are cooled by 1-ton ductless split units. A single outdoor air vent provides ventilation to each of the furnaces. The high bay garages have radiant heaters around the perimeter of each bay and a roof top unit (RTU) supplies forced air heat to two of the bays. The RTU provides ventilation when the unit is operating. Figure A11-5, Figure A11-6, and Figure A11-7 shows the HVAC equipment that serves the building and Table A11-1 lists the HVAC equipment data.

Supply and return ducts are located in the ceiling space of the office section. The supply and return ductwork is rectangular sheet metal ducts. A portion of the ductwork for the two horizontal furnaces is insulated and a portion is un-insinuated. The furnaces and some insulated ductwork are located in the high bay section of the building, which is ultimately outdoors in the summer months because the overhead doors are nearly always open in the summer. The supply diffusers are located in the ceiling of the training room and front conference room and the returns are located in the walls.

RTU that serves the high bay garages has un-insulated ductwork that located a few feet below the roof deck in the conditioned space. A small portion of ductwork on top of the roof is insulated.

Sanyo Ductless Split Unit
Model: KS1211W / RS1211

Sanyo Condensing Units
Model: CL1211

Figure A11-5. Sanyo Ductless Split Systems

Trane Horizontal Furnaces (Units 1 & 2)

Trane Condensing Units for Furnaces
Model: TTX030C100A1

Unit 1 Hot Water Coil

H.B. Smith Hot Water Boiler for Office Section
Model: G100-W-10 HS1D

Figure A11-6. HVAC Equipment for Office Section of Building

 Trane Roof Top Unit for High Bay Garages Model: GRBA50GDJF0L7GQ102AOCEFJLPQRVY48	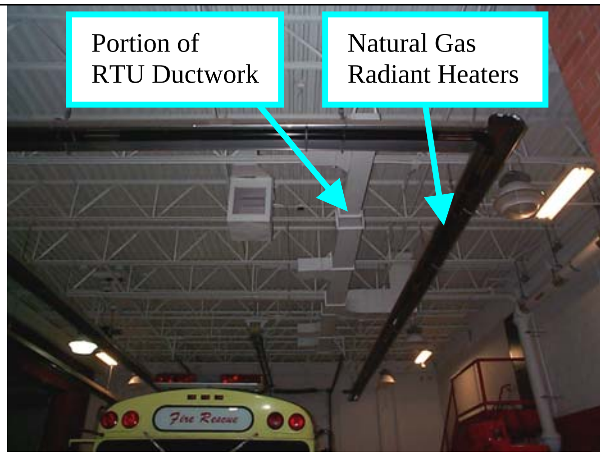 Radiant Heaters for High Bay Section

Figure A11-7. HVAC Equipment for High Bay Section of Building

Table A11-1. Summary HVAC Equipment Installed at Site

HVAC Equip	Serves	Brand	Model	Heating Capacity (MBtu/h)	Cooling Capacity (tons)
Ductless Split Units	Front Offices	Sanyo	KS1211W / RS1211 Condenser: CL1211		1
Unit 1	Training Room	Trane	Condenser: TTX030C100A1	Hot water Coil	2.5
Unit 2	Front Conf. Room	Trane	Condenser: TTX030C100A1	None	2.5
Hot Water Boiler	Office Section	H.B. Smith	G100-W-10 HS1D	178.2	n/a
RTU	High Bay Garages	Trane	GRBA50GDJF0L7GQ1 2AOCEFJLPQRVY48	400	None

There are 5 programmable thermostats: (2) for the horizontal furnaces and (3) for the three small ductless split units that cool the individual offices. Table A11-2 shows the setpoints for the HVAC equipment serving the office section and high bay areas.

Table A11-2. Temperature Setpoints for Summer and Winter

Location	Heating Setpoint (°F)	Cooling Setpoint (°F)
Office 1	70	78
Office 2	71	70
Admin. Office	70	73
Unit 1 (front conference room)	73	72
Unit 2 (Training Room)	70	78
RTU for High Bay Garages		
Radiant Heaters		

MEASUREMENTS

The test data below was taken on August 29, 2004. For this building, we focused on blower door testing and pressure mapping. Using the blower door to depressurize and pressurize the office section, we were able to determine duct leakage to the outdoors for the office section. Test personnel were Dan Gott, Adam Walburger, and Mike Clarkin. Dan Gott returned on November 10, 2004 to retrieve CO_2 and temperature/RH sensors.

Building Envelope Airtightness

Office Section Airtightness

The leakage characteristics of the building enclosure were assessed using both fan depressurization and fan pressurization methods. For the office section, a single blower door was installed in the south door of the front conference room and the overhead doors were open to the outdoors. All exterior doors and windows were closed. Doors leading to the high bay section were also closed. The building was tested in the following configuration:

- All interior doors open
- All exhaust fans were sealed
- All outdoor air ventilation intakes were sealed
- Tests were completed with AHUs on and AHUs off

The building pressure was varied from 80 Pa to 8 Pa. Figure A11-8 shows the exhaust fans that were sealed. The ventilation intake for the two furnaces was also sealed although it cannot be seen in the photo. Figure A11-9 and Figure A11-10 show the office section leakage variation with building pressure.

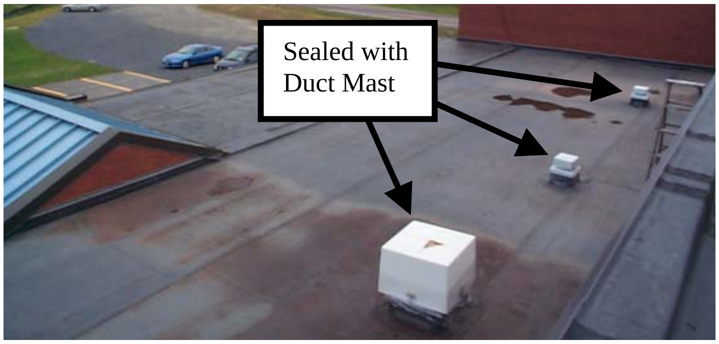

Figure A11-8. Sealed Exhaust Fans for Blower Door Test

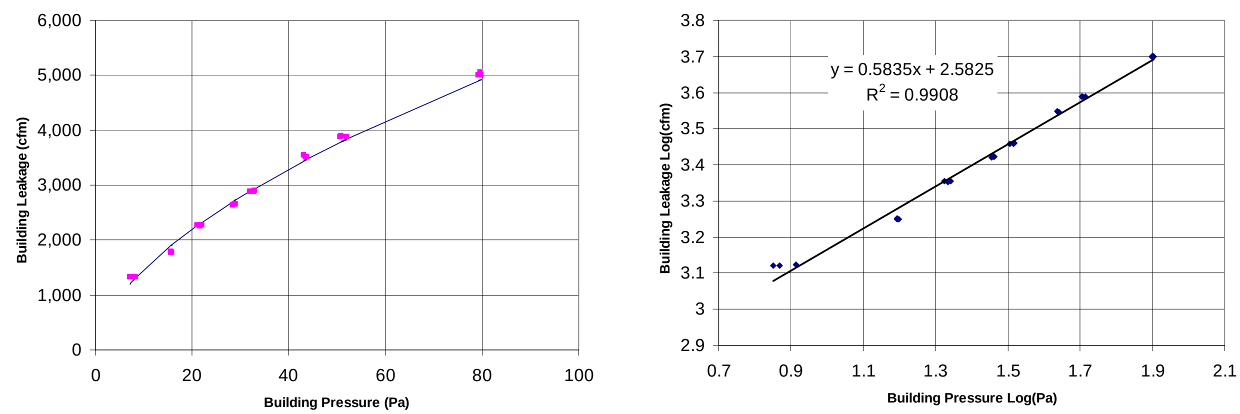

Depressurization Test – AHUs OFF (Test 1)

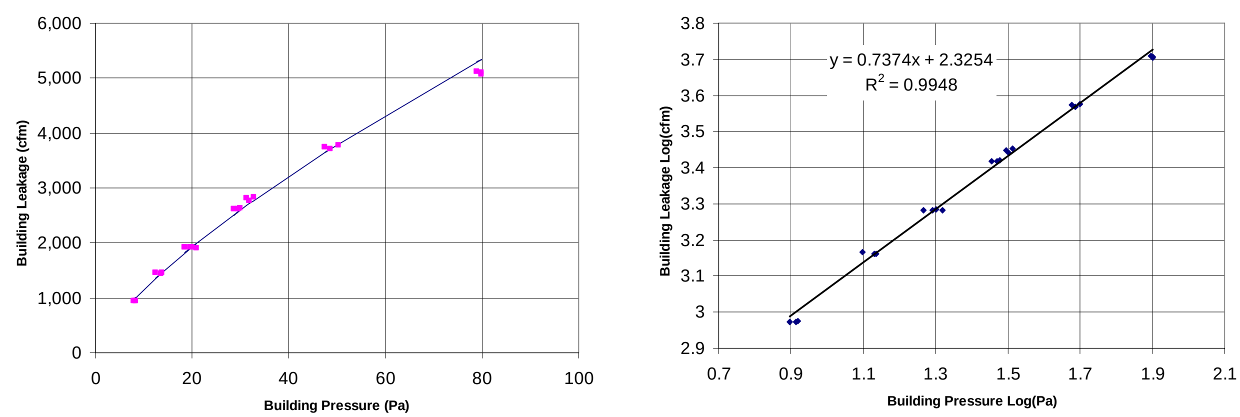

Pressurization Test – AHUs OFF (Test 2)

Figure A11-9. Office Section: Variation of Building Leakage with Pressure: cfm = K(ΔP)^n

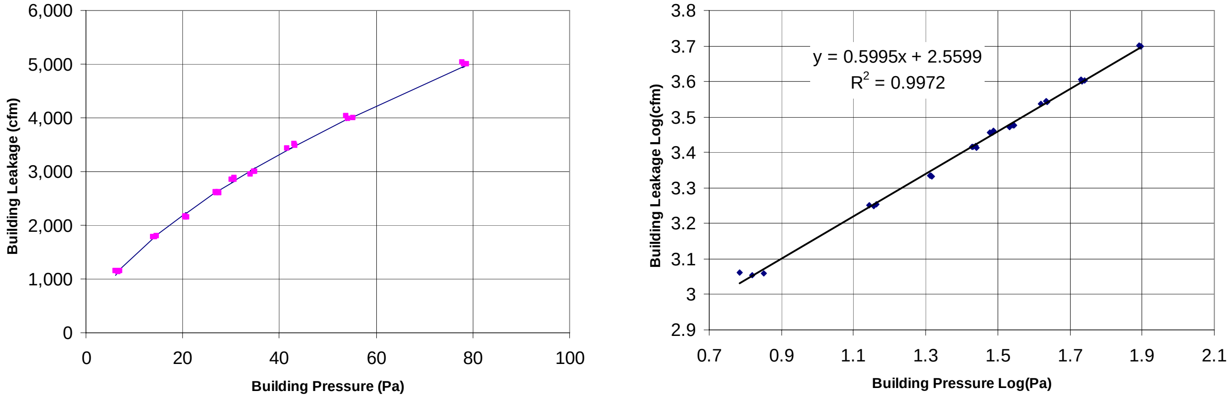

Depressurization Test – AHUs ON (Test 3)

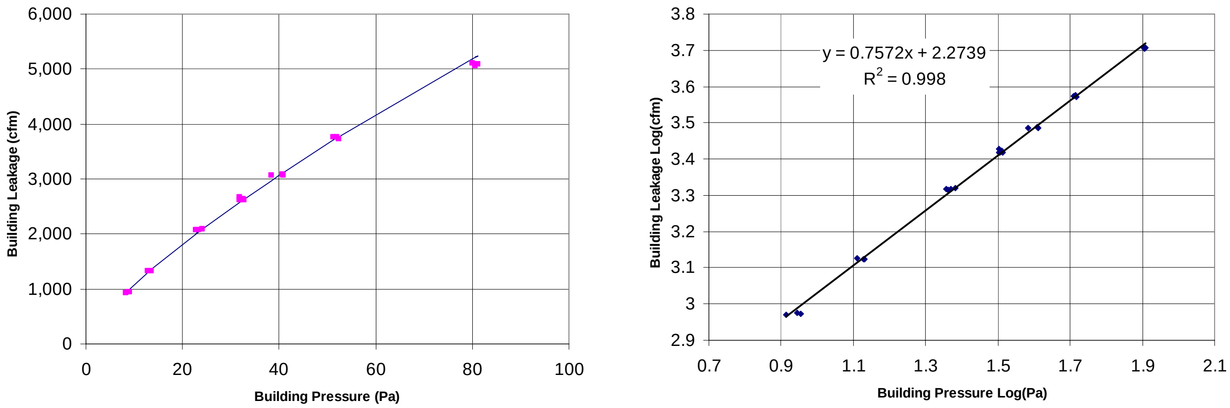

Pressurization Test – AHUs ON (Test 4)

Figure A11-10. Office Section: Variation of Building Leakage with Pressure: cfm = K(ΔP)^n

Table A11-3 and Table A11-4 show the results of the blower door tests including model coefficients, effective leakage area (ELA), and air-changes-per-hour (ACH). The ELA is calculated using the Lawrence Berkeley Laboratory method, which calculates the leakage area at 4 Pa. The office section of the building has an effective leakage area of approximately 2.15 sq in per 100 sq ft of the total envelope area including floor area. Another building leakage characteristic is the ACH at 50 pascals (ACH_{50}). The office section of the building has an ACH_{50} of 7.24.

Table A11-3. Office Section: Blower Door Test Data, Resulting Best-Fit Model Coefficients, and ELA

Depressurization Test – AHUs OFF (Test 1)

Test Results:

Flow Coefficient (K)	382.3	3,289 sq ft, floor area
Exponent (n)	0.584	
Leakage area (LBL ELA @ 4 Pa)	243.3 sq in	2.62 ELA / 100 sq ft
Airflow @ 50 Pa	3748.7 cfm	7.26 ACH @ 50

Test Data:

Nominal Building Pressure (Pa)	Nominal Flow (cfm)	Ring
79.7	5,048	none
79.3	5,002	none
79.9	4,998	none
50.9	3,887	none
51.9	3,882	none
50.7	3,871	none
43.2	3,543	none
43.5	3,507	none
43.7	3,515	none
32.0	2,879	none
33.0	2,893	none
32.8	2,879	none
28.5	2,638	none
29.0	2,649	none
28.8	2,648	none
22.0	2,270	none
21.1	2,263	none
21.6	2,258	none
15.6	1,781	none
15.8	1,772	none
15.6	1,783	none
8.2	1,327	none
7.4	1,320	none
7.1	1,320	none

Pressurization Test – AHUs OFF (Test 2)

Test Results:

Flow Coefficient (K)	211.5	3,289 sq ft, floor area
Exponent (n)	0.737	
Leakage area (LBL ELA @ 4 Pa)	166.6 sq in	1.80 ELA / 100 sq ft
Airflow @ 50 Pa	3786.6 cfm	7.34 ACH @ 50

Test Data:

Nominal Building Pressure (Pa)	Nominal Flow (cfm)	Ring
78.9	5,121	none
79.8	5,104	none
79.8	5,069	none
50.2	3,772	none
47.4	3,738	none
48.6	3,709	none
32.7	2,841	none
31.8	2,764	none
31.3	2,811	none
28.6	2,625	none
30.0	2,640	none
29.5	2,612	none
19.6	1,916	none
20.0	1,923	none
18.5	1,920	none
20.9	1,913	none
12.5	1,465	none
13.5	1,447	none
13.7	1,451	none
8.2	942	none
7.9	941	none
8.3	947	none

Notes: ELA is leakage area (in square inches) at reference pressure of 4 Pa.
ELA per 100 sq ft is based on total building envelope surface area (ceiling, exterior walls and floor).

Table A11-4. Office Section: Blower Door Test Data, Resulting Best-Fit Model Coefficients, and ELA

Depressurization Test – AHUs ON (Test 3)

Test Results:

Flow Coefficient (K)	363.0	3,289	sq ft, floor area
Exponent (n)	0.600		
Leakage area (LBL ELA @ 4 Pa)	236.1 sq in	2.55	ELA / 100 sq ft
Airflow @ 50 Pa	3788.7 cfm	7.34	ACH @ 50

Test Data:

Nominal Building Pressure (Pa)	Nominal Flow (cfm)	Ring
77.8	5,036	none
78.2	5,005	none
78.8	4,999	none
55.2	4,002	none
53.7	4,027	none
54.2	3,989	none
41.6	3,441	none
43.2	3,481	none
43.1	3,515	none
34.1	2,954	none
35.0	2,998	none
34.8	3,001	none
30.1	2,858	none
30.7	2,885	none
30.6	2,852	none
27.6	2,595	none
26.8	2,612	none
26.9	2,607	none
27.4	2,620	none
20.8	2,146	none
20.6	2,157	none
20.5	2,163	none
13.9	1,785	none
14.3	1,778	none
14.6	1,796	none
7.1	1,145	none
6.6	1,134	none
6.1	1,151	none

Pressurization Test – AHUs ON (Test 4)

Test Results:

Flow Coefficient (K)	187.9	3,289	sq ft, floor area
Exponent (n)	0.757		
Leakage area (LBL ELA @ 4 Pa)	152.1 sq in	1.64	ELA / 100 sq ft
Airflow @ 50 Pa	3633.2 cfm	7.04	ACH @ 50

Test Data:

Nominal Building Pressure (Pa)	Nominal Flow (cfm)	Ring
80.6	5,059	none
81.2	5,082	none
80.1	5,100	none
52.0	3,761	none
52.3	3,736	none
51.3	3,758	none
40.9	3,063	none
40.7	3,075	none
38.4	3,062	none
32.5	2,638	none
32.4	2,643	none
31.9	2,673	none
31.9	2,619	none
32.1	2,619	none
32.7	2,622	none
22.7	2,074	none
23.4	2,080	none
23.0	2,069	none
24.1	2,087	none
12.9	1,334	none
13.5	1,329	none
13.4	1,331	none
8.8	943	none
8.2	934	none
9.0	939	none

Notes: ELA is leakage area (in square inches) at reference pressure of 4 Pa.
ELA per 100 sq ft is based on total building envelope surface area (ceiling, exterior walls and floor).

We repeated test 1 (depressurize office section with AHUs off), but with the interior door open to the locker room area, which increase the office section floor area by 480 sq-ft. The locker rooms are attached to the office section however there is no heating, cooling, or exhaust in this space. The locker room has an effective leakage area of 1.72 sq-in per 100 sq-ft of floor area at 4 Pa and an ACH_{50} of 15.0. Table A11-5 shows a summary of the blower door tests including model coefficients, ELA per 100 sq-ft of envelope area including floor area, and ACH_{50}. Figure A11-11 shows the office section including locker room area leakage variation with building pressure.

Office Section Including Locker Area
Depressurization Test – AHUs OFF (Test 5)

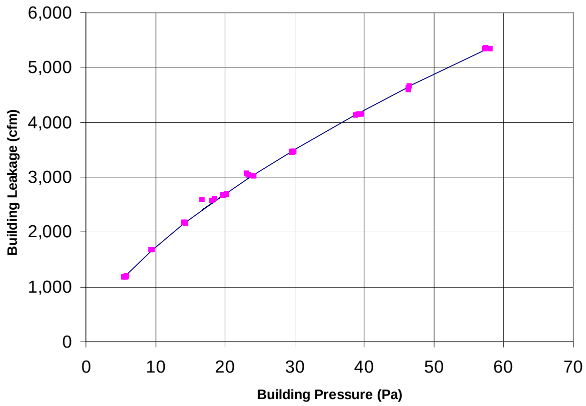

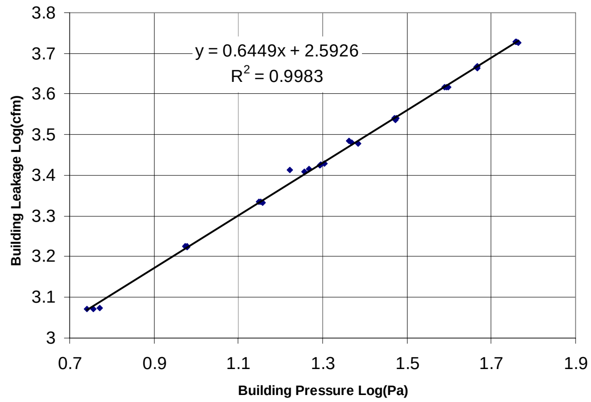

Test Results:

Flow Coefficient (K)	391.4	3,769 sq ft, floor area
Exponent (n)	0.645	
Leakage area (LBL ELA @ 4 Pa)	271.2 sq in	2.55 ELA / 100 sq ft
Airflow @ 50 Pa	4879.2 cfm	8.25 ACH @ 50

Test Data:

Nominal Building Pressure (Pa)	Nominal Flow (cfm)	Ring
57.4	5,355	none
58.1	5,331	none
57.3	5,341	none
46.4	4,599	none
46.3	4,622	none
46.5	4,658	none
39.6	4,136	none
39.2	4,146	none
38.8	4,132	none
29.7	3,445	none
29.6	3,470	none
29.9	3,470	none
23.1	3,059	none
24.2	3,013	none
23.4	3,026	none
16.7	2,586	none
18.5	2,600	none
18.1	2,570	none
19.7	2,665	none
19.8	2,676	none
20.2	2,680	none
14.2	2,166	none
14.1	2,169	none
14.4	2,156	none
9.4	1,680	none
9.5	1,680	none
9.5	1,674	none
5.9	1,186	none
5.5	1,180	none

Figure A11-11. Office Section with Locker Area: Variation of Building Leakage with Pressure

Table A11-5. Summary of Blower Door Test Results for Office Section

Test No.	Portion of Building	Test Description	Flow Coeff. K	Exp. n	ELA (sq-in @ 4 Pa)	ELA / 100 sq ft (sq in)	ACH_{50}
1	Office Section	Depressurized AHUs OFF	382	0.584	243	2.62	7.26
2	Office Section	Pressurized AHUs OFF	212	0.737	167	1.80	7.34
3	Office Section	Depressurized AHUs ON	363	0.600	236	2.55	7.34
4	Office Section	Pressurized AHUs ON	188	0.757	152	1.64	7.04
5	Office Section & Locker Area	Depressurized AHUs OFF	391	0.645	271	2.55	8.25

Entire Building Airtightness

Two blower doors were used to depressurize the entire building to test for envelope leakage. One blower door was installed in the person-door leading to the sand bay (which was open to the outdoors) and the second blower door was installed in the person-door on the southwest corner of the building. All exterior doors and windows were closed. Doors leading to the office section were open. The building was tested in the following configuration:

- All interior doors open
- All exhaust fans were sealed
- All outdoor air ventilation intakes were sealed
- RTU ventilation dampers were closed

The building pressure was varied from approximately 25 Pa to 11 Pa. Figure A11-12 shows the various equipment that was sealed for the blower door testing on the entire building. There are over twenty exhaust fans and passive vents that were sealed for this testing. Figure A11-13 shows the building leakage variation with building pressure. We also tested the high bay area separate from the office section. Test 8 shown in Figure A11-13 was completed with the doors closed that lead to the office section.

Figure A11-12. Sealed Exhaust Fans for Blower Door Test

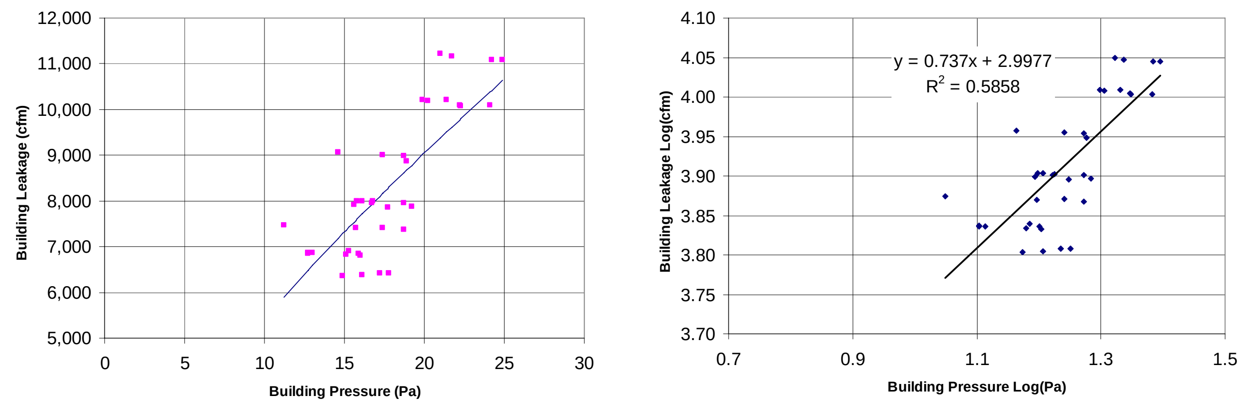

Depressurization (Test 6): Entire Building

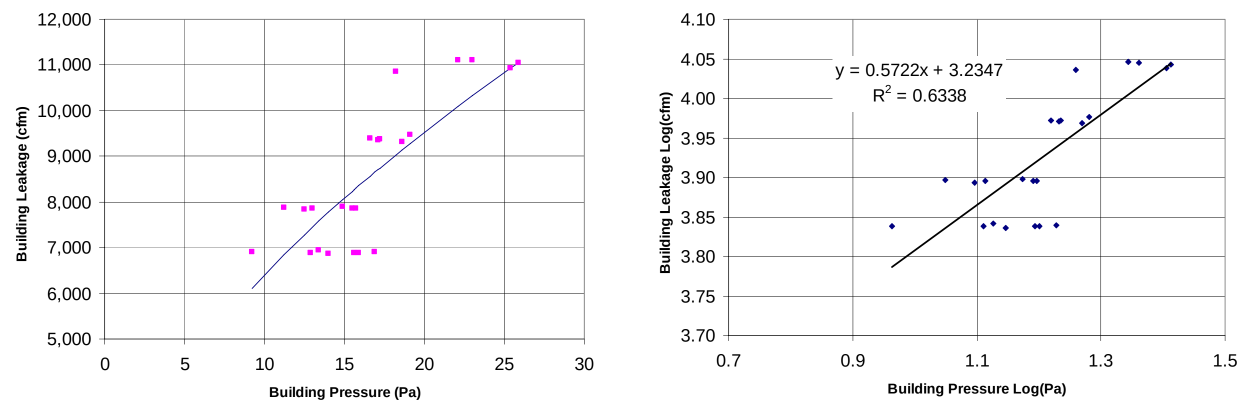

Depressurization (Test 7): Entire Building

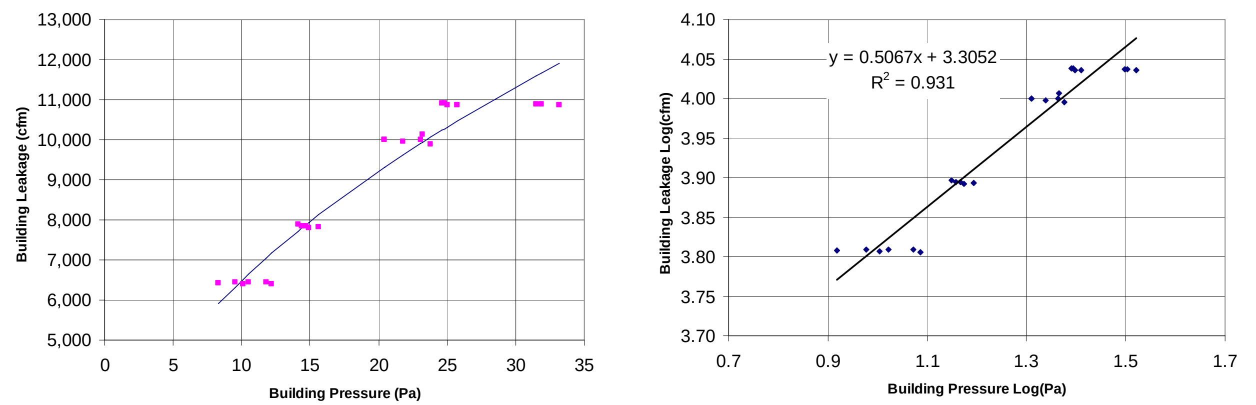

Depressurization (Test 8): High Bay Area Only

Figure A11-13. Variation of Building Leakage with Pressure: cfm = $K(\Delta P)^n$

Table A11-6 shows the results of the entire building blower door tests including model coefficients, effective leakage area (ELA), and air-changes-per-hour (ACH). Table A11-7 shows the results for the depressurization test on the high bay area only. The entire building has an effective leakage area of approximately 1.56 sq-in per 100 sq ft of the total envelope area including floor area. The entire building has an ACH_{50} of 2.49. This result implies that at 50 Pa, the air in the building is displaced 2.49 times each hour.

Table A11-6. Entire Building: Blower Door Test Data, Resulting Best-Fit Model Coefficients, and ELA

Depressurization (Test 6): Entire Building

Test Results:

Flow Coefficient (K)	994.8	22,247	sq ft, floor area
Exponent (n)	0.737		
Leakage area (LBL ELA @ 4 Pa)	783 sq in	1.31	ELA / 100 sq ft
Airflow @ 50 Pa	17,780 cfm	2.6	ACH @ 50

Test Data:

Nominal Building Pressure (Pa)	Nominal Flow (cfm)
24.9	11,077
24.2	11,084
24.1	10,090
22.3	10,082
22.2	10,097
21.7	11,157
21.4	10,210
21.0	11,214
20.2	10,185
19.9	10,210
19.2	7,887
18.9	8,874
18.7	8,996
18.7	7,965
18.7	7,371
17.8	6,420
17.7	7,868
17.4	9,015
17.4	7,421
17.2	6,427
16.8	7,985
16.7	7,956
16.1	7,999
16.1	6,383
16.0	6,807
15.9	6,853
15.8	7,999
15.7	7,410
15.6	7,916
15.3	6,910
15.1	6,819
14.9	6,358
14.6	9,057
13.0	6,860
12.7	6,865
12.7	6,857
11.2	7,476

Depressurization (Test 7): Entire Building

Test Results:

Flow Coefficient (K)	1716.6	22,247	sq ft, floor area
Exponent (n)	0.572		
Leakage area (LBL ELA @ 4 Pa)	1075 sq in	1.81	ELA / 100 sq ft
Airflow @ 50 Pa	16,100 cfm	2.4	ACH @ 50

Test Data:

Nominal Building Pressure (Pa)	Nominal Flow (cfm)
25.9	11,044
25.4	10,930
23.0	11,101
22.1	11,109
19.1	9,475
18.6	9,309
18.2	10,858
17.2	9,366
17.1	9,360
16.9	6,909
16.6	9,385
15.9	6,892
15.7	7,855
15.6	6,891
15.5	7,859
14.9	7,893
14.0	6,863
13.4	6,939
13.0	7,853
12.9	6,885
12.5	7,830
11.2	7,876
9.2	6,897

Notes: ELA is leakage area (in square inches) at reference pressure of 4 Pa.
ELA per 100 sq ft is based on total building envelope surface area (ceiling, exterior walls and floor).

Table A11-7. High Bay Section: Blower Door Test Data, Resulting Best-Fit Model Coefficients, and ELA

Depressurization (Test 8): High Bay Area Only

Test Results:

Flow Coefficient (K)	2019.3	18,959 sq ft, floor area
Exponent (n)	0.507	
Leakage area (LBL ELA @ 4 Pa)	1155 sq in	2.22 ELA / 100 sq ft
Airflow @ 50 Pa	14,660 cfm	2.2 ACH @ 50

Test Data:

Nominal Building Pressure (Pa)	Nominal Flow (cfm)
33.2	10,866
31.9	10,890
31.5	10,893
25.7	10,871
25.0	10,877
24.8	10,910
24.6	10,910
23.8	9,893
23.2	10,144
23.1	10,003
21.8	9,954
20.4	10,009
20.4	9,999
15.6	7,828
14.9	7,804
14.7	7,849
14.4	7,834
14.1	7,882
12.2	6,398
11.8	6,443
10.5	6,445
10.1	6,402
9.5	6,443
8.3	6,433

Notes: ELA is leakage area (in square inches) at reference pressure of 4 Pa.
ELA per 100 sq ft is based on total building envelope surface area (ceiling, exterior walls and floor).

Due to the large building volume, two blower doors (totaling approx. 11,000 cfm) could only depressurize the building approximately 10 pascals. The test data reached 25 Pa however this was caused by the addition of wind effects. The wind varied the building pressure between 5 and 15 Pa. By the time we had prepared the entire building for blower door testing, the wind speed reached 21 mph causing a large variation in the blower door measurement data. The variation in data is seen in Figure A11-13 and is represented by the low R-squared values of 0.6.

Figure A11-14 shows the wind speed throughout the day of testing on September 29, 2004.

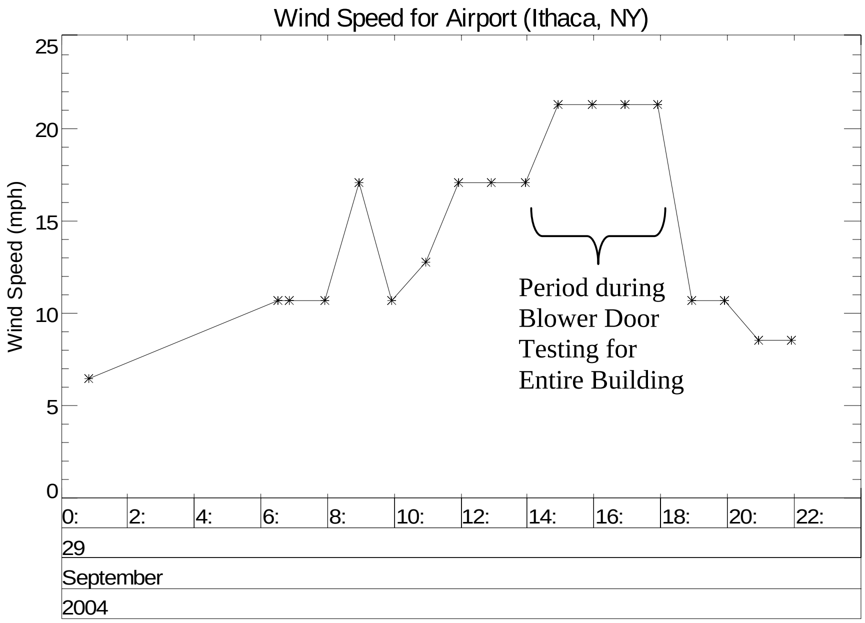

Figure A11-14. Wind Speed for Building for September 29, 2004

Pressure Mapping (Blower Door Testing)

Pressure readings in the building were taken using a digital micromanometer (DG 700) with the blower doors operating. The pressure difference across the building envelope was 56 Pa with all interior doors open.

Pressure measurements were taken between interior rooms with doors closed and the main corridors. Figure A11-15 shows the pressure differences induced across the doorways with the office section of the building depressurized. With the building depressurized to 56 Pa, pressures across the doorways ranged between 0.1 and 9.6 Pa. This implies that the room-to-room leakage is much great than the leakage across the building envelope. The pressures measured across doorways were measured in reference to an interior space that had a free path back to the blower door (open interior doors).

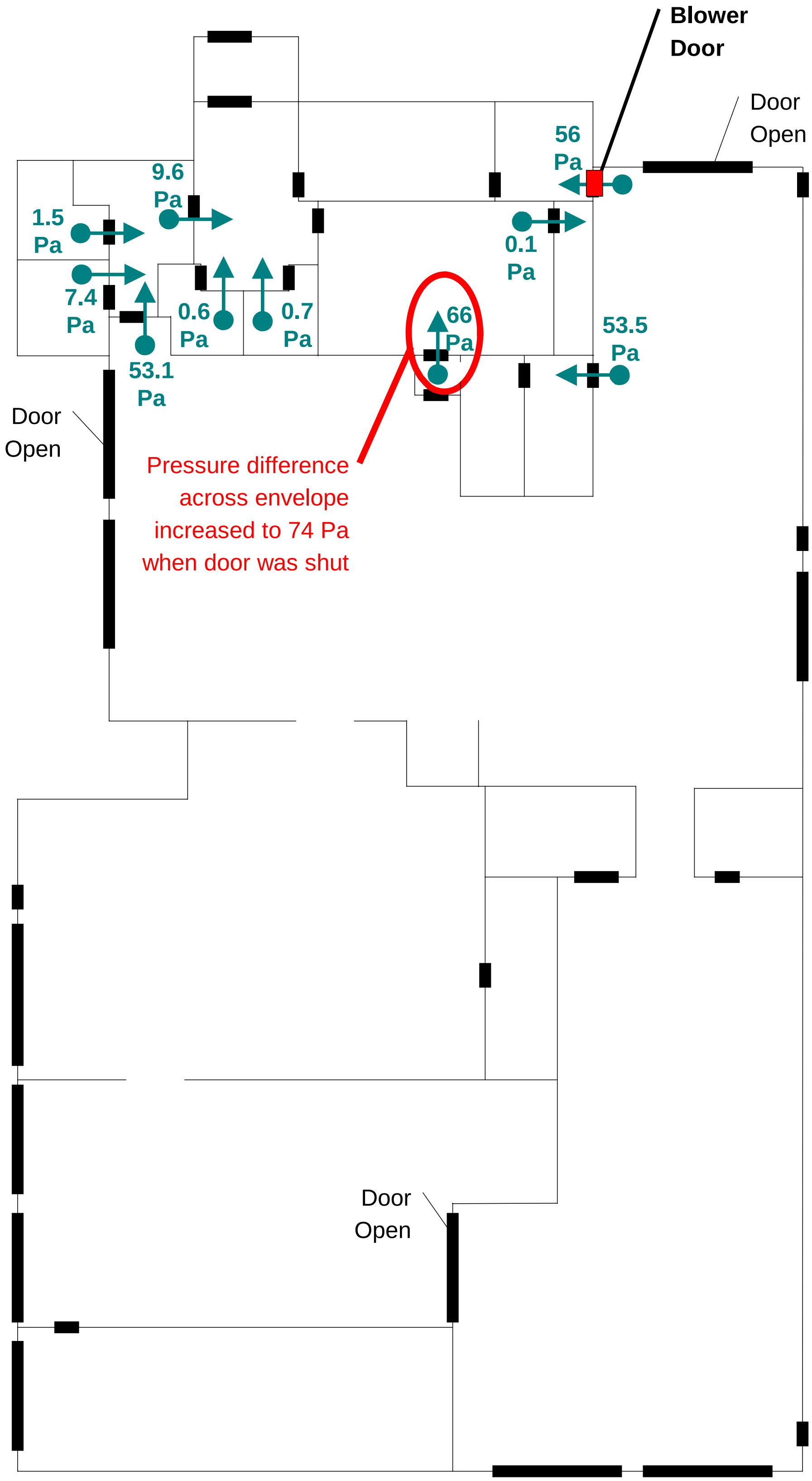

Figure A11-15. Room-to-Corridor Pressures with Building Depressurized to 56 Pa

HVAC Airflow Measurements

The airflow from each supply diffuser was measured using a Shortridge flow hood. The total supply airflow is 1,508 cfm or about 1.0 cfm per sq-ft of floor area served by units 1 and 2 (not the entire office section).

Figure A11-16. Supply and Return Airflow Measurements (cfm)

Table A11-8. Comparison of Supply and Return Airflow Measurements

Furnace	Serves	Flowhood Supply Airflow (cfm)	Flowhood Return Airflow (cfm)	Supply / Return Ratio	Return Type	Supply Static (Pa)	Return Static (Pa)
Unit 1	Training Room	842	792	1.1	Ducted	36.4	-12.7
Unit 2	Front Conf. Room	666	457	1.5	Ducted	64.5	-27.1
Total		***1,508***	***1,249***	***1.2***			

Pressure Mapping (AHU Fans On)

The air pressure relationships in the building were also determined with the building in normal operation with the office section units on. The graphics in Figure A11-17 show the pressure differences induced across the doorways with the AHU fans on and the individual doorway closed. There was no HVAC equipment operating in the high bay section of the building. With the building in normal configuration, we would close an interior door and measure the pressure across the doorway. Operation of the two horizontal furnaces combined with the wind effects created interior pressures differences up to 0.6 Pa. The building was depressurized by approximately 1.0 to 3.4 Pa with respect to outdoors. The envelope pressure for the high bay garage section will change with the operation of the RTU or exhaust fans.

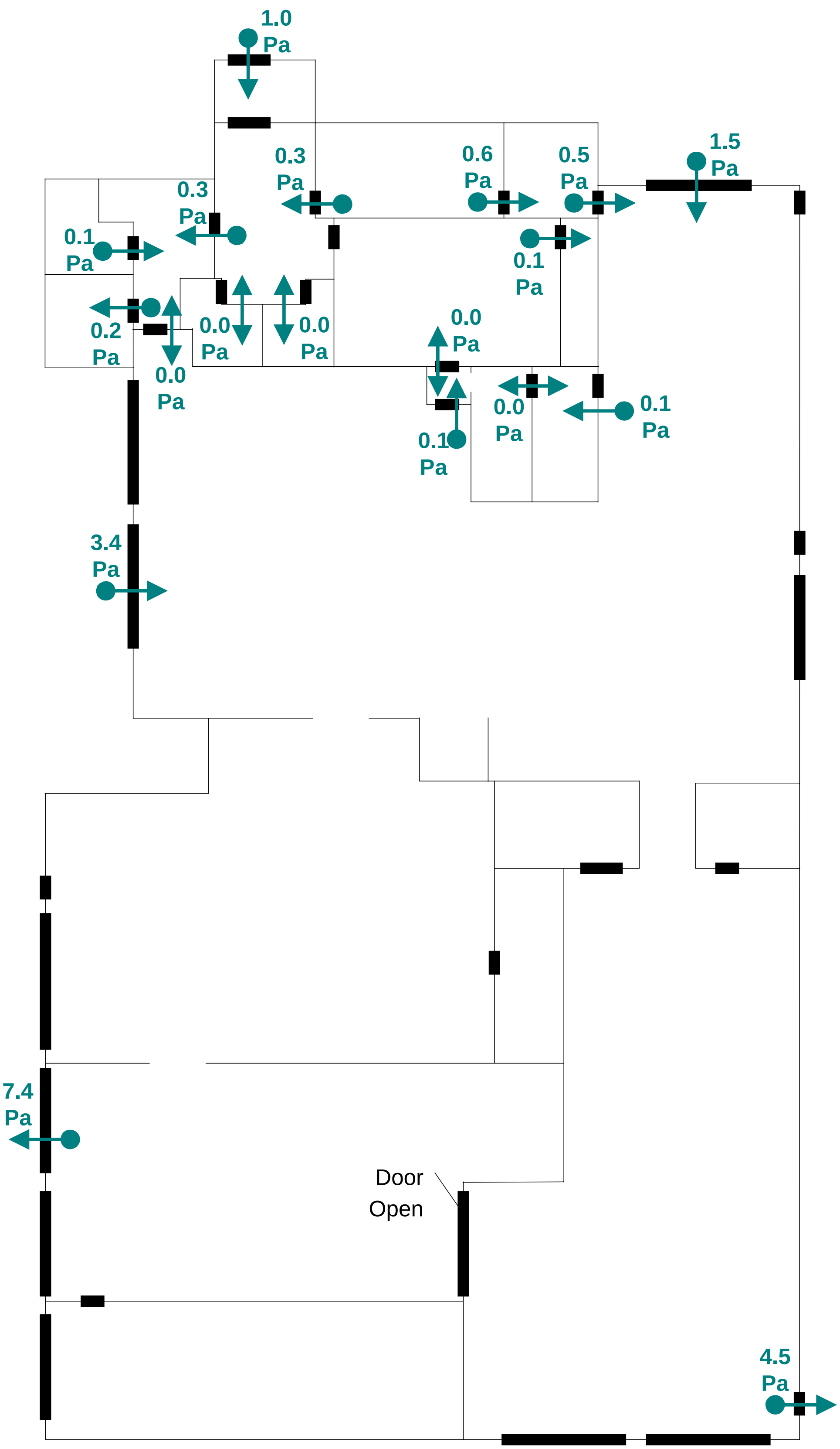

Figure A11-17. First Floor Pressure Differences between Rooms with AHU Fans On

Duct Leakage Measurements

A DeltaQ test was performed on the office section of the building to determine the duct leakage to the outdoors or high bay area in this case. The model for duct leakage is given by the following equation:

$$\Delta Q(\Delta P) = Q_s\left[\left(1+\frac{\Delta P}{\Delta P_s}\right)^{n_s} - \left(\frac{\Delta P}{\Delta P_s}\right)^{n_s}\right] - Q_r\left[\left(1-\frac{\Delta P}{\Delta P_r}\right)^{n_r} + \left(\frac{\Delta P}{\Delta P_r}\right)^{n_r}\right]$$

where:
ΔQ = difference between the supply and return leaks
Q_s = supply leak flow at operating conditions to outside
Q_r = return leak flow at operating conditions to outside
ΔP = pressure difference across envelope (in – out)
ΔP_s = pressure difference between supply and building (building as reference)
ΔP_r = pressure difference between building and return (return as reference, ΔP_r *is positive*)
n_s = supply leakage pressure exponent
n_r = return leakage pressure exponent

The DeltaQ test was developed for use with residential buildings. "The DeltaQ test combines a model of the house and duct system with the results of house pressurization tests with the air handler on an off to determine the duct leakage air flows to outside conditioned space at operating conditions" [LBNL-49749]. We used this same test method to determine duct leakage to the outdoors at operating pressure on small commercial buildings. The main difference for the DeltaQ test between residential and small commercial buildings is that there are usually several air handlers in commercial buildings whereas homes usually have only a single furnace. Having more than one air handler leads to the following results:

1. Test results include total duct leakage to outdoors for every air handler
2. Plenum pressures and exponents are fitted rather than measured values

The first result determines the net duct leakage to the outdoors rather than the leakage for individual AHUs, which is the result we are looking for since it is the net duct leakage that effects energy use. The second result is actually the preferred method of solving for the duct leakage to the outdoors. Walker, Dickerhoff, and Sherman [LBNL-49749] have determined that it is advantageous to let plenum pressures be determined by fitting the measurements using a multi-variant least squares technique. Walker, Dickerhoff, and Sherman have also determined that fitting to the measured data is typically more robust if the duct leakage pressure exponents are fixed at 0.6. If there is a disconnected duct or it is know that the leakage behaves like an orifice, then a pressure exponent of 0.5 is preferred.

Two horizontal furnaces and a portion of the ductwork are located in the high bay area, which is considered unconditioned space in the summer time because the overhead doors are usually left open. During the wintertime, the duct leakage to the high bay area would have little effect on energy use since the leaks are in the conditioned garage space. Figure A11-18 shows the DeltaQ test results for the office section of the building. The DeltaQ duct leakage (supply – return) at zero pascals is the leakage to the outdoors at operating pressure. The two horizontal furnaces pulls in 21.7 cfm of outdoor air into the office section.

All of the 21.7 cfm can be assigned to unit 2 because after testing we found that unit 1 had a metal mesh pre-filter upstream of the hot water coil that was completely plugged. We found the plugged pre-filter because the return plenum pressure was –330 Pa and the supply plenum was zero pascals static pressure. The operating static pressures are shown in Table A11-9.

Table A11-9. Plenum Pressures while Operating

Furnace	Filter Condition	Supply / Return Plenum (Pa)
Unit 1 (Training Room)	Plugged pre-filter	0 / -330
Unit 1 (Training Room)	No pre-filter, new furnace filter	36.4 / -127
Unit 2 (Front Conf. Room)	Used furnace filter	27.1 / 64.5

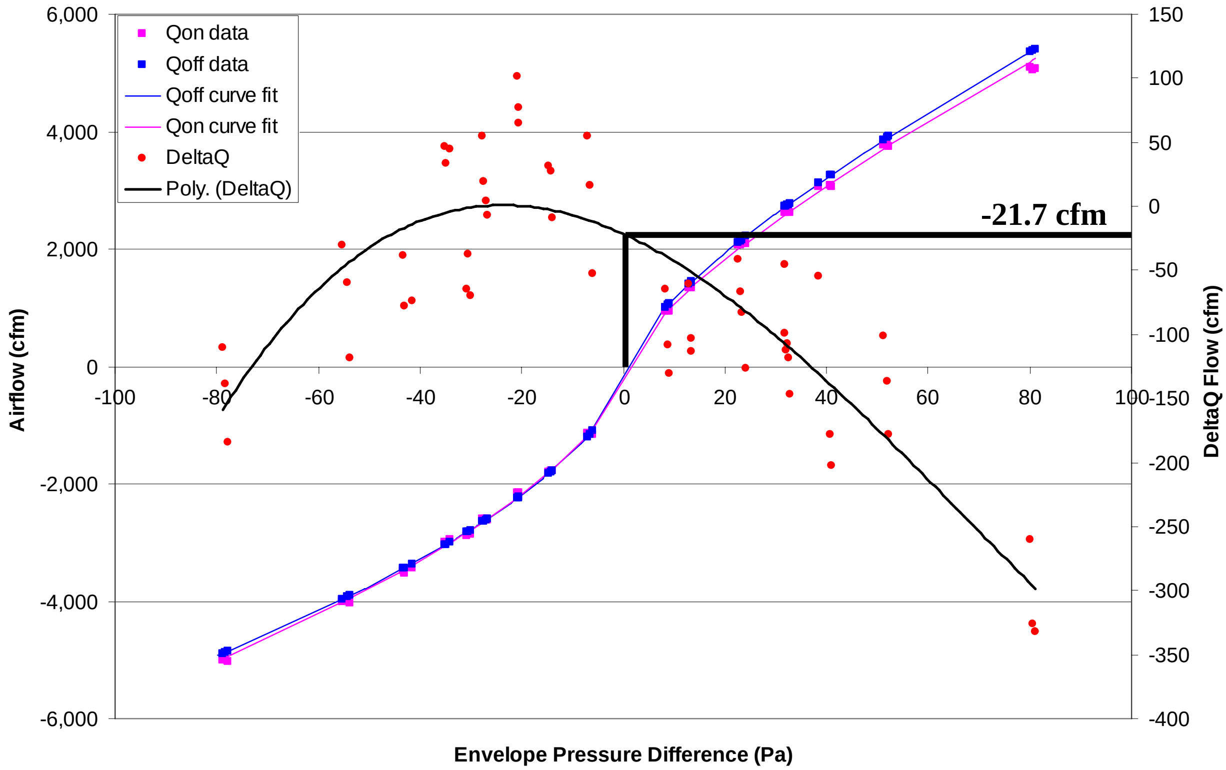

Figure A11-18. DeltaQ Test Results for Office Section of Building

Space Conditions

Figure A11-19 shows the average temperature profiles based on temperature readings taken with a HOBO data logger from September 17 to October 12, 2004. The thick line shows the average for each hour while the shaded region corresponds to one standard deviation about the average. The dotted lines correspond to the minimum and maximum for each hour. Sensors were placed in the training room and the administration assistant lobby area.

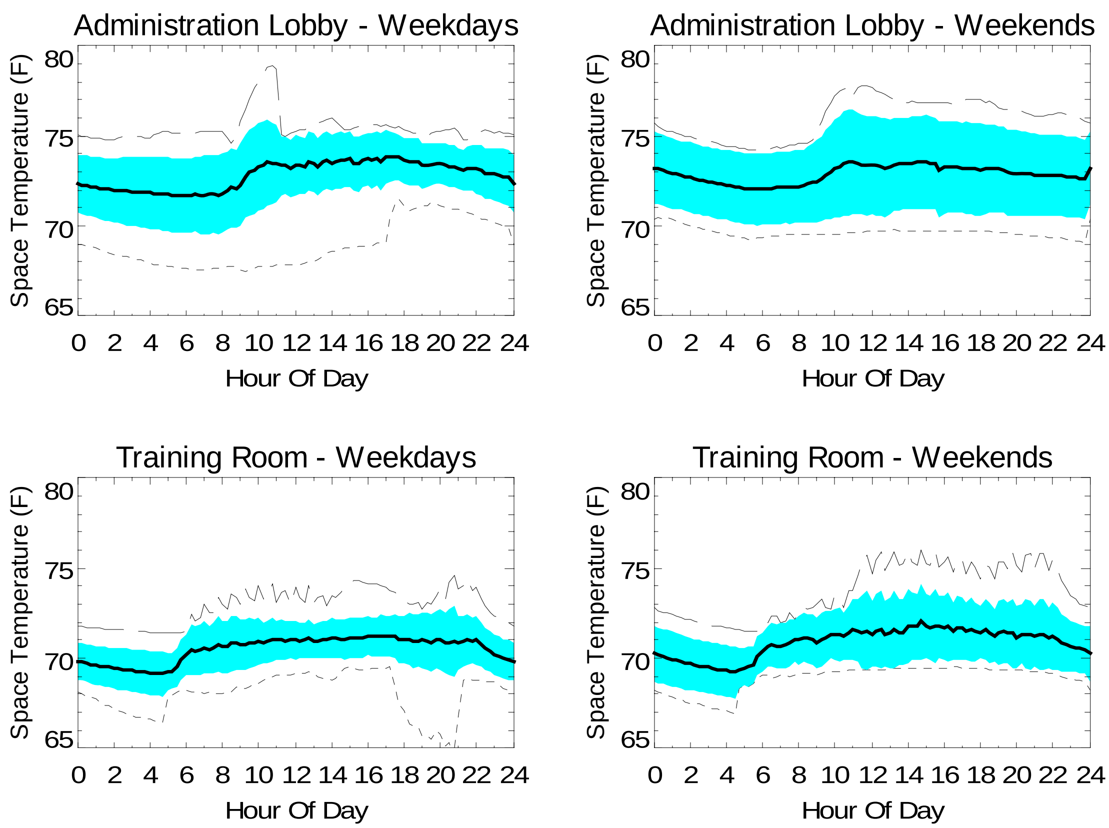

Figure A11-19. Measured Space Temperature Profiles

Figure A11-20 shows the CO_2 concentration in various locations in the building. The CO_2 concentration provides an indication of occupancy. The next section uses the CO_2 as a tracer gas to estimate the infiltration/ventilation rate into the building. On November 2, 2004, the training room maintained a CO_2 concentration over 1,500 PPM for 8 hours as shown in Figure A11-21.

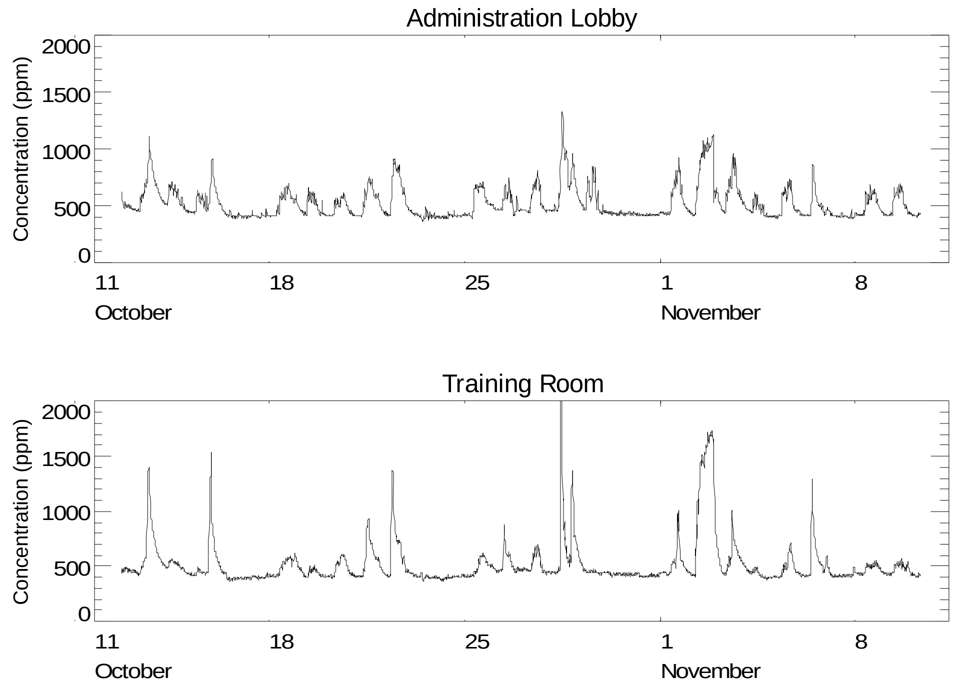

Figure A11-20. Measured CO_2 Concentration in Various Spaces

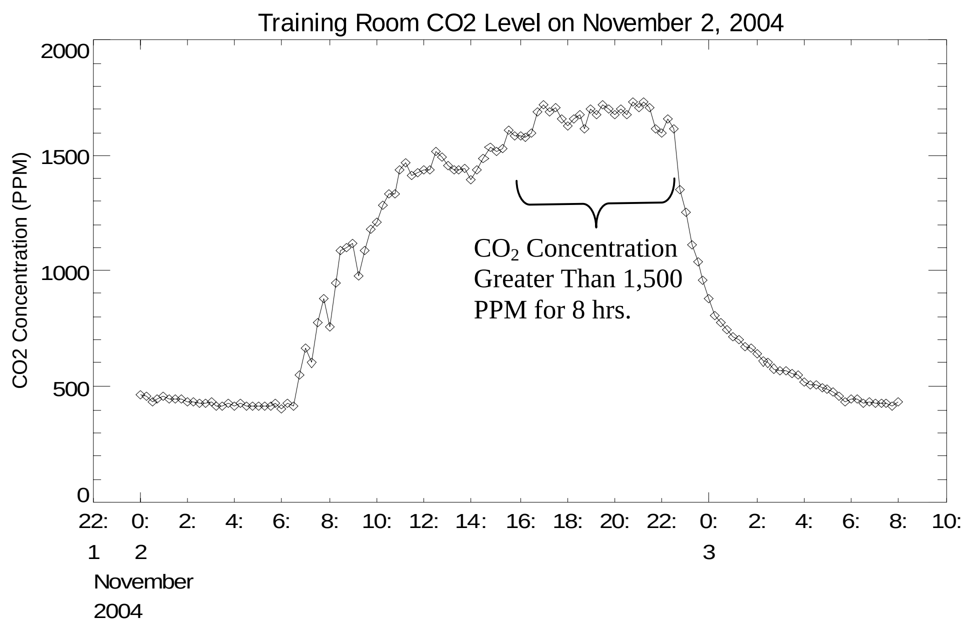

Figure A11-21. Training Room CO_2 on November 2, 2004

The following plots show the relative humidity for this building. The maximum relative humidity during the monitoring period was 63.3% in the training room. Figure A11-25 displays the conditions inside the building compared with the ASHRAE comfort zone for cooling shown by the shaded region on the plot.

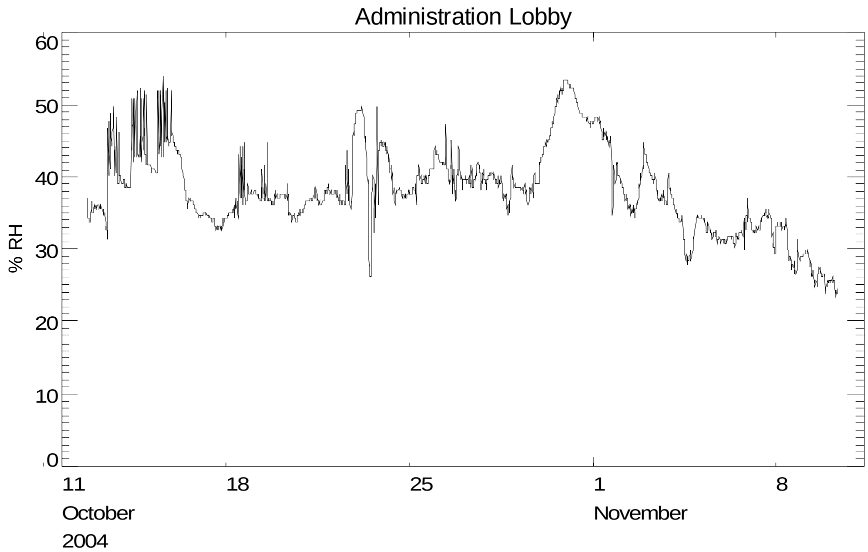

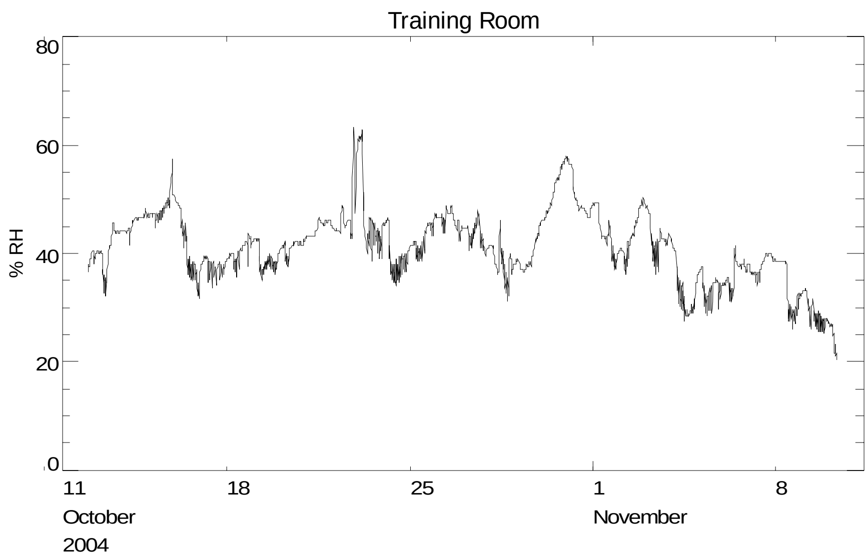

Figure A11-22. Measured Relative Humidity

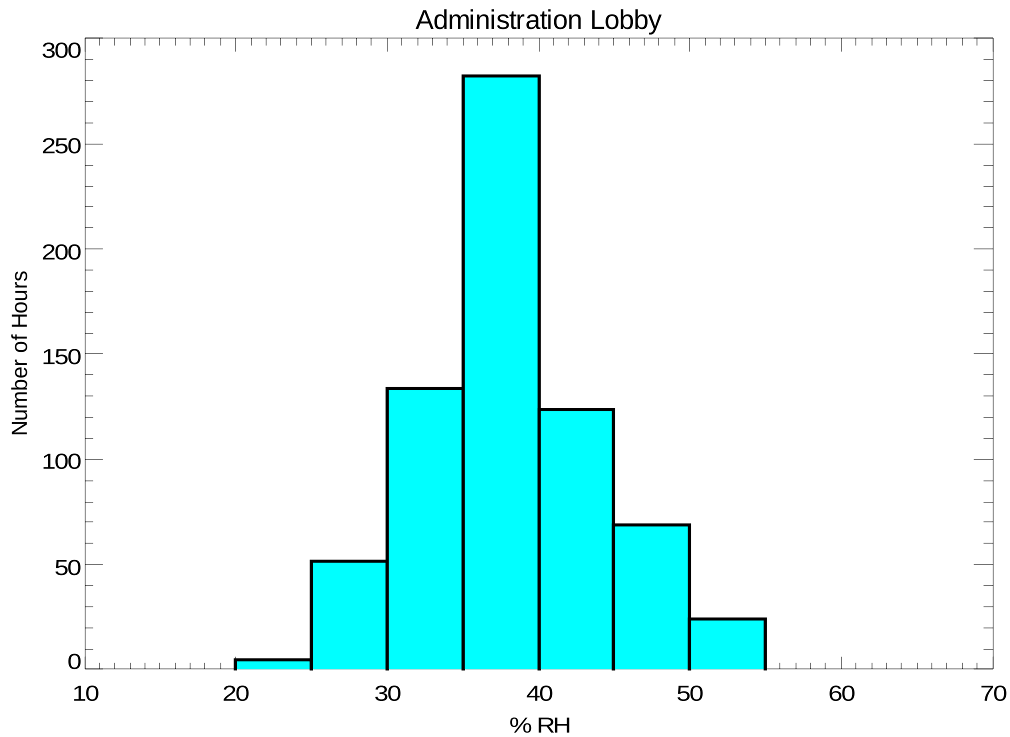

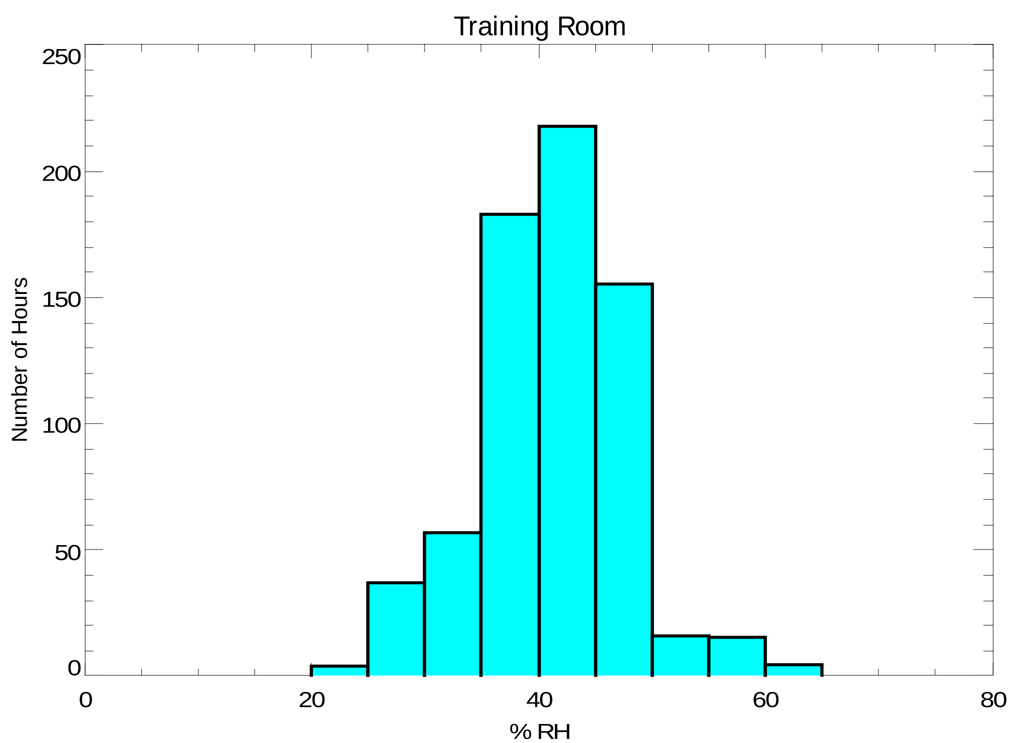

Figure A11-23. Duration of Relative Humidity Levels

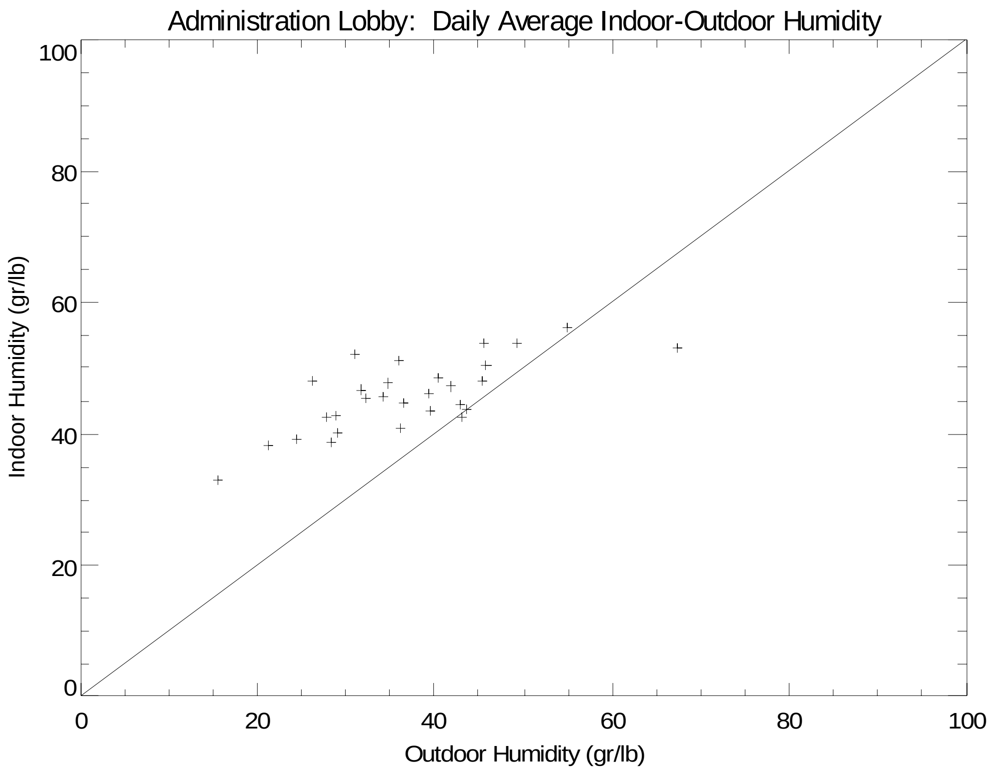

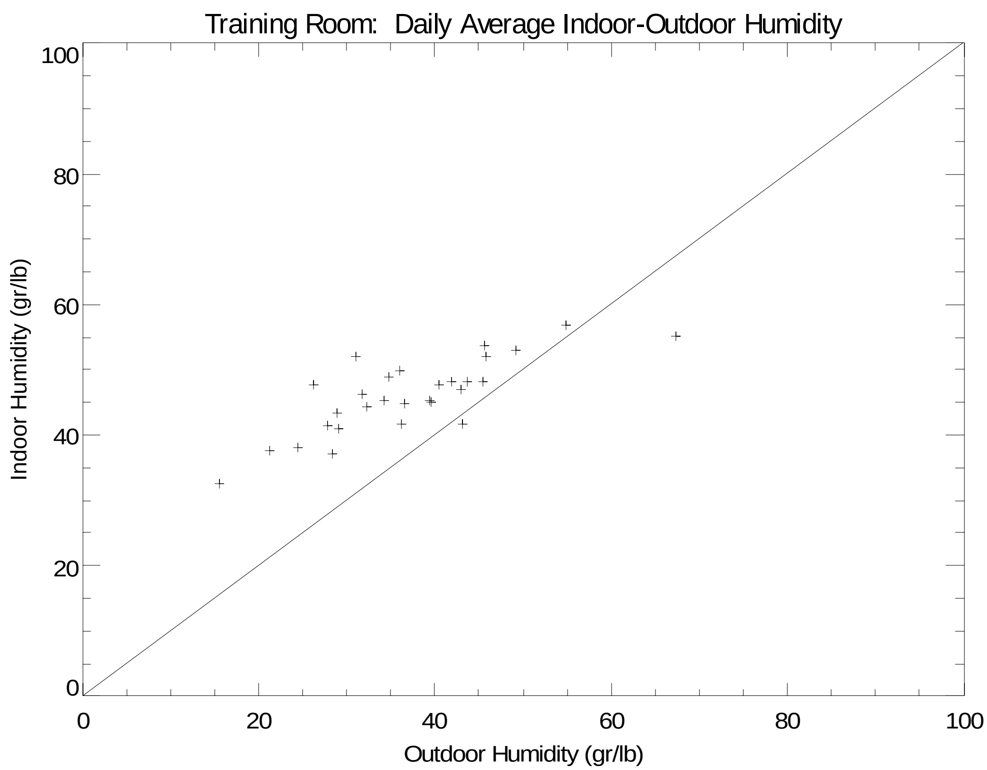

Figure A11-24. Indoor Humidity Variation with Outdoor Humidity

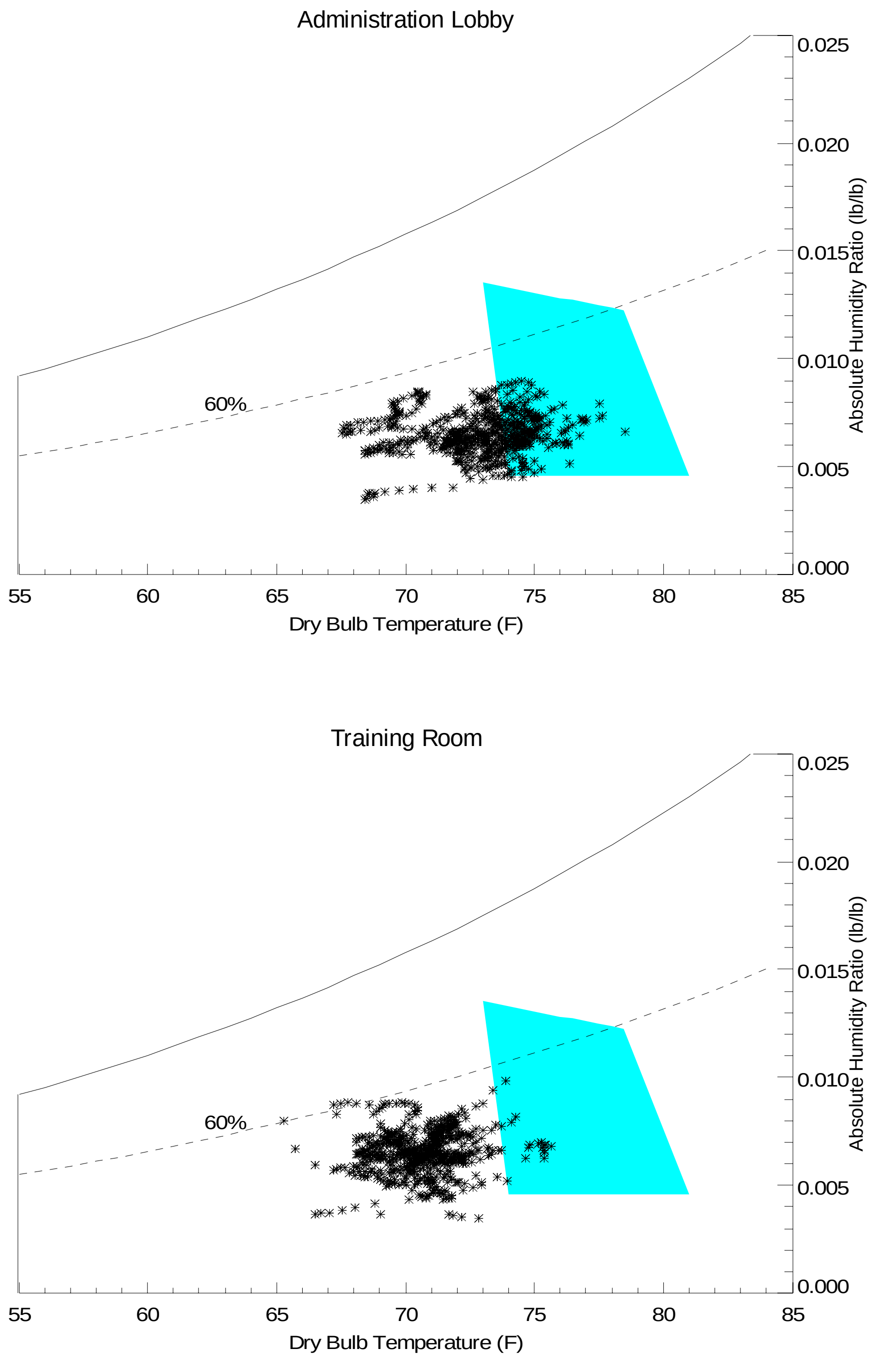

Figure A11-25. Indoor Air Quality Comparison with ASHRAE Comfort Zone for Cooling

Infiltration Estimate from CO_2 Decay

Figure A11-26 and Figure A11-27 show the resulting decay trends using CO_2 levels immediately after high occupancy periods for the facilities office 109 and upstairs office 202. The predicted air change rate (ACH) is shown on each plot.

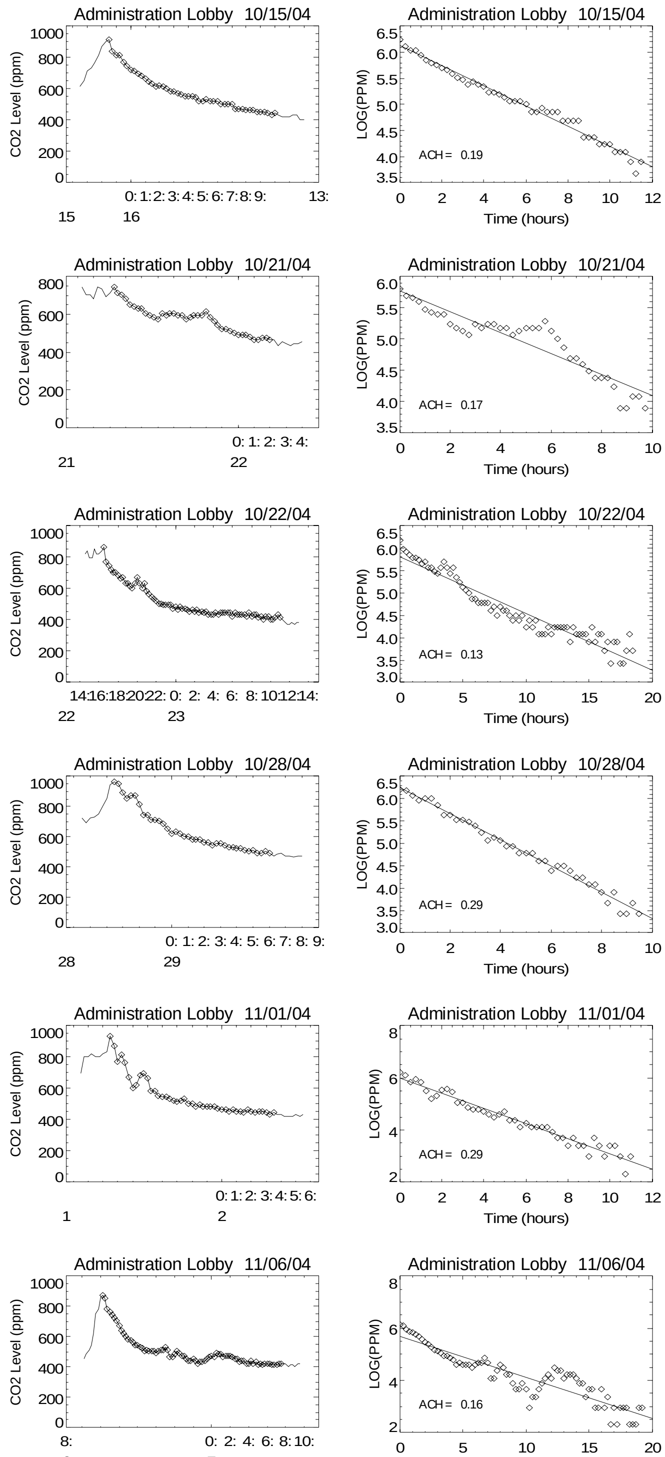

Figure A11-26. Administration Lobby: Tracer Gas Decay Using CO_2 for Various Periods

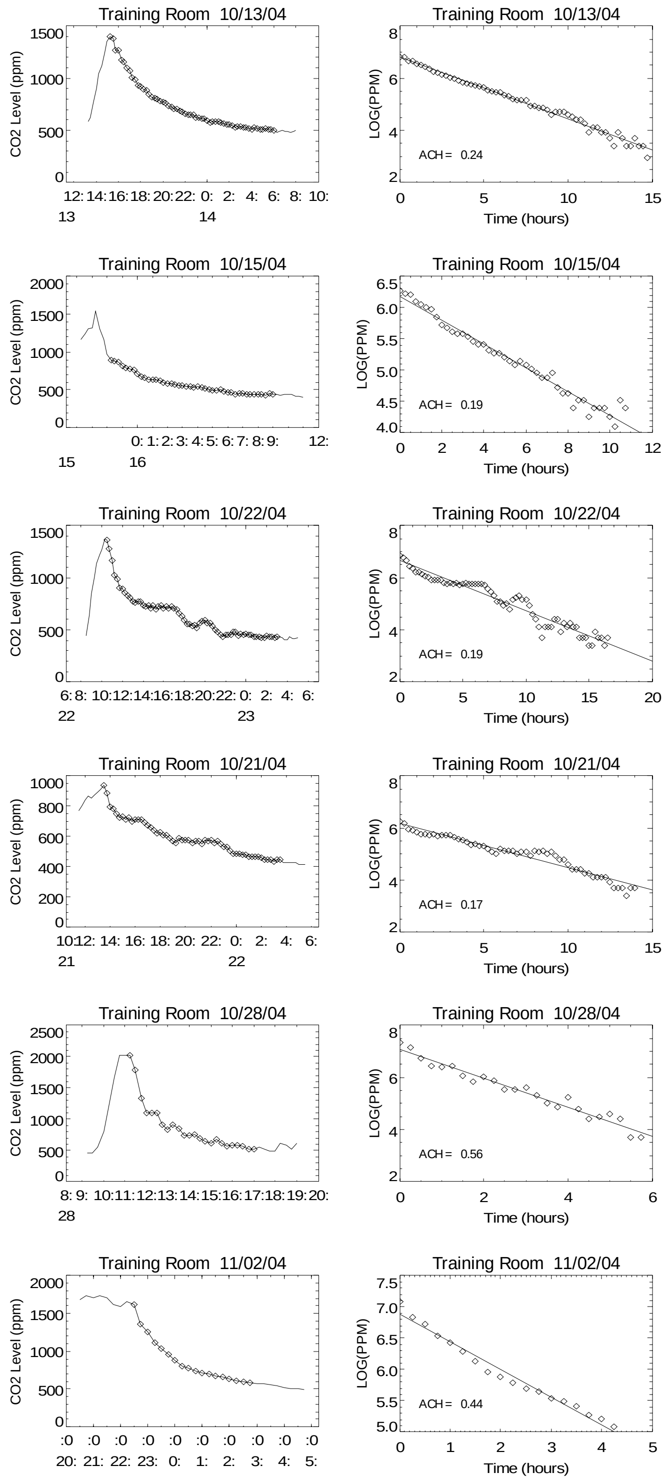

Figure A11-27. Training Room: Tracer Gas Decay Using CO_2 for Various Periods

Table A11-10 summarizes the results of the tracer gas decay tests in the plots above. The table also includes the estimated infiltration airflow based on the building volume of 120,903 ft^3.

Table A11-10. Summary of Tracer Gas Decay Tests

Administration Lobby

Start Time	End Time	ACH	Flow (cfm)
15-Oct 10:30 PM	16-Oct 10:00 AM	0.19	99
21-Oct 04:15 PM	22-Oct 02:00 AM	0.17	87
22-Oct 04:30 PM	23-Oct 11:00 AM	0.13	65
28-Oct 08:30 PM	29-Oct 06:00 AM	0.29	151
01-Nov 04:30 PM	02-Nov 03:30 AM	0.29	150
06-Nov 12:15 PM	07-Nov 07:30 AM	0.16	81

Training Room

Start Time	End Time	ACH	Flow (cfm)
13-Oct 03:15 PM	14-Oct 06:00 AM	0.24	123
15-Oct 10:15 PM	16-Oct 09:00 AM	0.19	98
22-Oct 10:30 AM	23-Oct 03:00 AM	0.19	100
21-Oct 01:30 PM	22-Oct 03:30 AM	0.17	88
28-Oct 11:15 AM	28-Oct 05:00 PM	0.56	287
02-Nov 10:30 PM	03-Nov 02:45 AM	0.44	227

Note: Flow determined with office section volume of: **30,968** ft^3

In comparison to the ACH values above, the nominal leakage rate (defined as ACH_{50} divided by 20) from the blower door test above is 0.32 ACH.

Utility Bills

Gas use is primarily used for space heating. The tables and graphs below show the gas and electric use trends for the facility. The overall energy use index for the building is summarized below.

	Heating Energy Use Index ($MBtu/ft^2$-year)	Electric Use Index (kWh/ft^2-year)
2002-2003 Season	62.2	8.1
2003-2004 Season	56.1	7.9

Season is from October to September

Table A11-11. Summary of Electric Bills

	Days in Month	Energy (kWh)	Demand (kW)	Cost ($)	$/kWh	Elec. Use per Sq-Ft (kWh/sq ft)
10/30/2002	28	12,880	45.6	1,414.87	0.110	0.58
12/3/2002	34	17,680	46.4	1,694.03	0.096	0.79
1/9/2003	37	20,800	33.4	1,820.24	0.088	0.93
2/3/2003	25	13,840	50.4	1,660.72	0.120	0.62
3/5/2003	30	16,160	49.6	1,848.77	0.114	0.73
4/3/2003	29	14,720	32.8	1,560.26	0.106	0.66
5/5/2003	32	15,520	43.2	1,732.70	0.112	0.70
6/4/2003	30	13,680	37.6	1,523.59	0.111	0.61
7/2/2003	28	13,200	45.6	1,560.74	0.118	0.59
8/4/2003	33	15,200	32	1,591.67	0.105	0.68
9/3/2003	30	13,280	42.4	1,536.83	0.116	0.60
10/2/2003	29	13,520	41.6	1,549.40	0.115	0.61
10/30/2003	28	13,440	32.8	1,454.66	0.108	0.60
12/3/2003	34	16,560	44.8	1,834.88	0.111	0.74
1/5/2004	33	17,440	36.8	1,818.24	0.104	0.78
2/3/2004	29	16,000	51.2	1,843.16	0.115	0.72
3/4/2004	30	16,240	37.6	1,727.80	0.106	0.73
4/2/2004	29	14,240	32.8	1,514.53	0.106	0.64
5/3/2004	31	13,440	33.6	1,456.98	0.108	0.60
6/2/2004	30	10,720	27.2	1,168.25	0.109	0.48
7/1/2004	29	10,800	31.2	1,215.38	0.113	0.49
8/3/2004	33	13,040	28	1,367.02	0.105	0.59
8/31/2004	28	10,800	61.6	1,503.95	0.139	0.49
9/29/2004	29	21,040	76.8	2,510.94	0.119	0.95
2002-2003	***365***	***180,480***	***50.4***	***$ 19,494***	***0.108***	***8.11***
2003-2004	***363***	***173,760***	***76.8***	***$ 19,416***	***0.112***	***7.81***

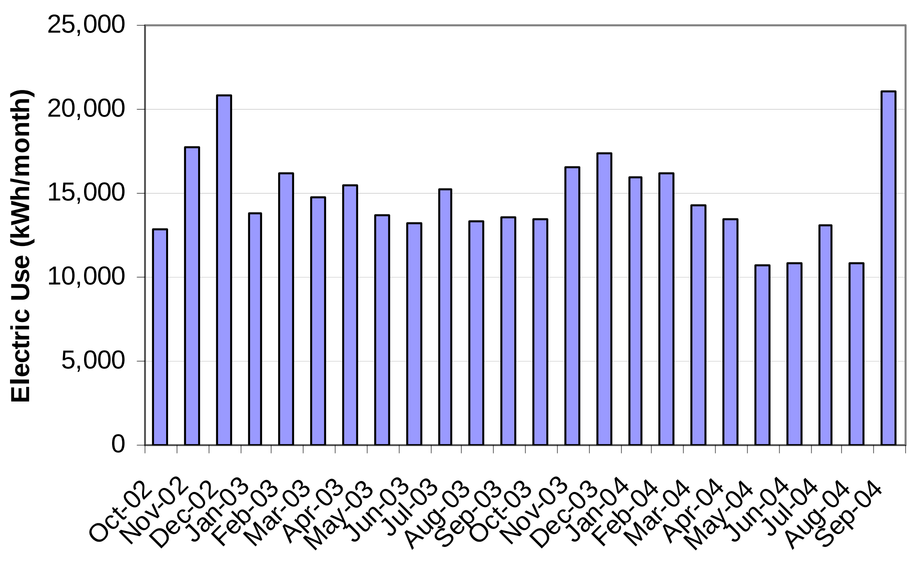

Figure A11-28. Monthly Electricity Use Trends

Table A11-12. Summary of Gas Bills

	Days in Month	Gas Use (therms)	Cost ($)	$/therm	Gas Use per Sq-Ft (therm/sq ft)
10/30/2002	33	846	829.29	0.98	0.038
12/3/2002	34	1,963	1838.82	0.94	0.088
1/3/2003	31	2,519	2026.83	0.80	0.113
2/3/2003	31	3,018	2511.00	0.83	0.136
3/5/2003	30	2,841	2657.93	0.94	0.128
4/3/2003	29	1,482	1826.86	1.23	0.067
5/5/2003	32	983	957.71	0.97	0.044
6/4/2003	30	171	203.11	1.19	0.008
7/2/2003	28	22	41.90	1.88	0.001
8/4/2003	33	2	18.83	9.42	0.000
9/3/2003	30	3	19.20	6.40	0.000
10/2/2003	29	174	191.80	1.10	0.008
11/4/2003	33	681	665.68	0.98	0.031
12/3/2003	29	1,218	1094.75	0.90	0.055
1/5/2004	33	2,240	2046.44	0.91	0.101
2/3/2004	29	3,547	3546.33	1.00	0.159
3/4/2004	30	2,229	2175.12	0.98	0.100
4/2/2004	29	1,427	1402.06	0.98	0.064
5/3/2004	31	881	926.92	1.05	0.040
6/2/2004	30	164	198.43	1.21	0.007
7/1/2004	29	15	33.49	2.20	0.001
8/3/2004	33	0	17.40	-	0.000
8/31/2004	28	0	17.40	-	0.000
9/29/2004	29	0	17.40	-	0.000
2002-2003	***370***	***14,025***	***$ 13,123***	***0.94***	***0.630***
2003-2004	***363***	***12,402***	***$ 12,141***	***0.98***	***0.557***

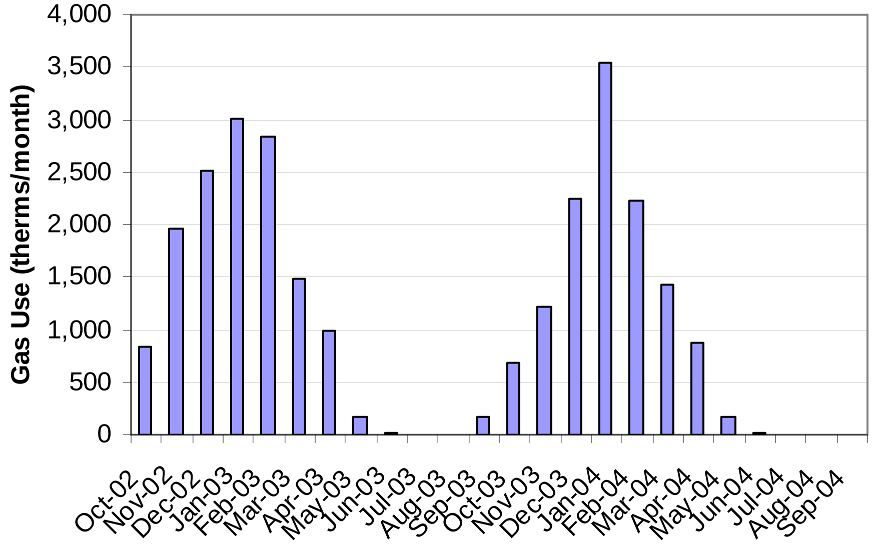

Figure A11-29. Monthly Gas Use Trends

Figure A11-30 shows the gas use variation with ambient temperature and Figure A11-31 shows the electricity use variation with ambient temperature.

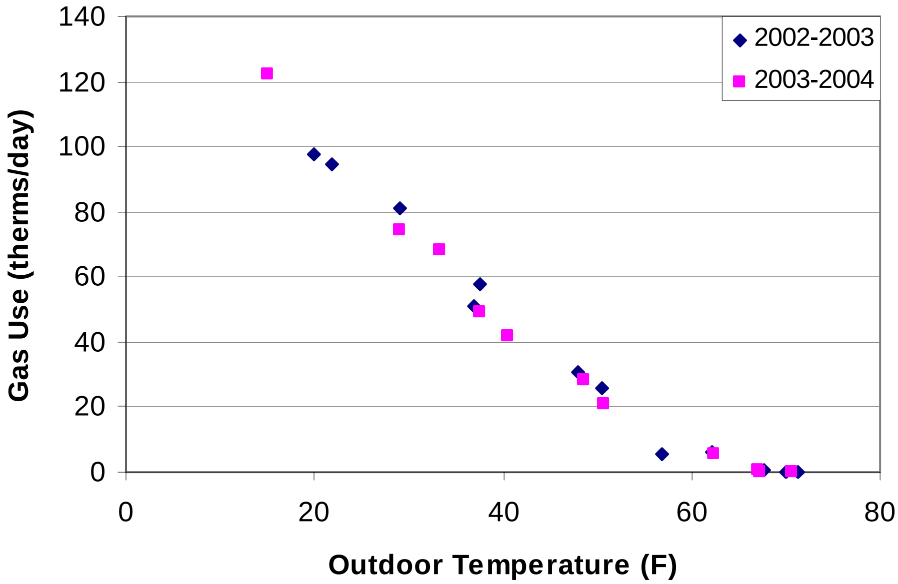

Figure A11-30. Variation of Gas Use with Ambient Temperature

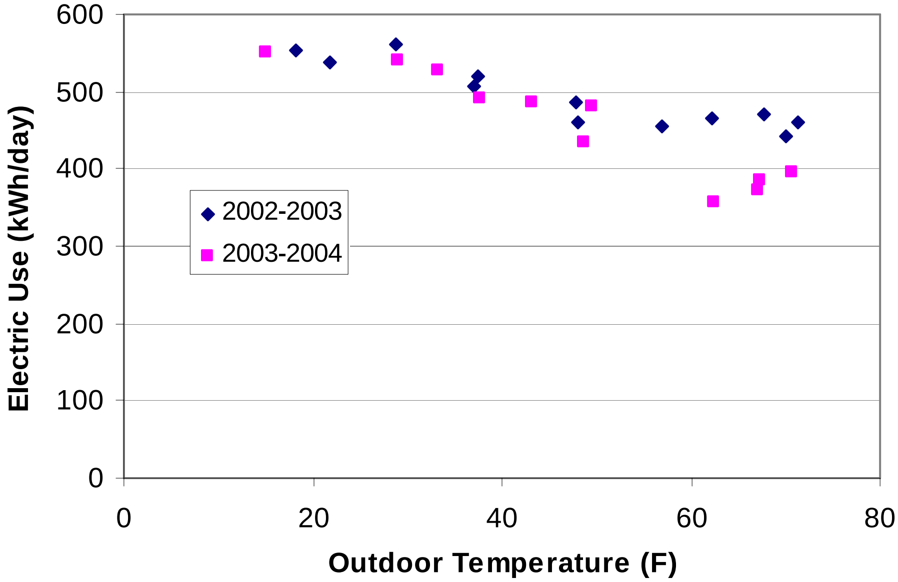

Figure A11-31. Variation of Electric Use with Ambient Temperature

Field Test Site 12 – Office Building, Cazenovia, NY

Main Entrance (South)

Rear of Building (Northeast)

Figure A12-1. Photo of Building (West)

CHARACTERISTICS

Building Description

The 77,000 sq-ft facility is a two-story office building with large attached manufacturing space on the north side of the building. This report focuses on the 12,700 sq-ft two story office space. The facility was originally built in the 1986 and the two-story office section tested in this report was built in 1998. Figure A12-1 shows photos of the main entrance and the rear of the building. Water source heat pumps (WSHP) located in the ceiling space provide heating and cooling for the two-story office section. The water loop temperature maintained using a natural gas boiler and cooling tower. The boiler does not run often because the facility uses the process water from die casting to heat the water loop. In addition, there is an Aaon energy recovery unit (ERV) with an enthalpy wheel that can provide 3-tons of cooling or heating to temper the ventilation air if needed. The Aaon unit has an economizer mode that disables the enthalpy wheel rotation when the outdoor temperature falls below 55°F and the space calls for cooling. A Novar controller centrally controls all the HVAC equipment for this building. Figure A12-2 presents the building floor plan.

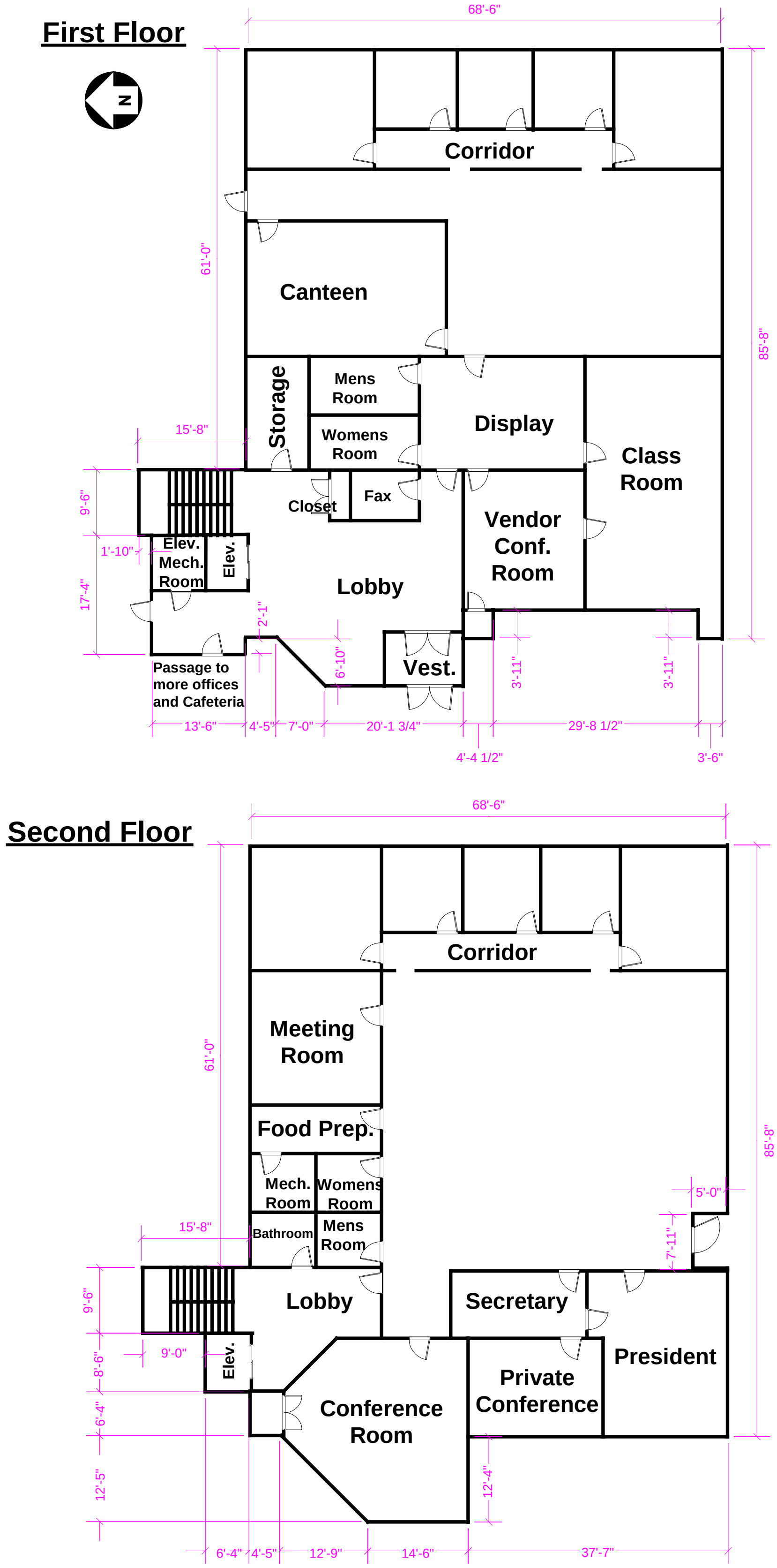

Figure A12-2. First Floor Building Plan

Construction Details

The wall and roof construction are detailed in Figure A12-3. The exterior walls are 6-in steel stud walls with R-19 fiberglass batt insulation. The steel stud walls are enclosed in 5/8-in gypsum board and the exterior is finished with an air infiltration barrier and aluminum composite exterior panels that are attached to 7/8-in steel channel. The interior is finished with 5/8-in gypsum board.

The building has a flat roof with a metal roof deck, vapor barrier, and 3 inches of polyisocyanurate insulation. The roof is finished with 0.060-in EPDM mechanically fastened membrane.

There is a T-bar (drop) ceiling on both floors of the building. Both floors use the space between the ceiling and the roof (ceiling space) as a return plenum. The water source heat pumps (WSHP) and the supply ductwork are located in the ceiling plenum. There is no return ductwork.

Figure A12-3 illustrates typical wall and roof sections. Figure A12-4 shows a picture of the ceiling plenum and typical diffuser installation.

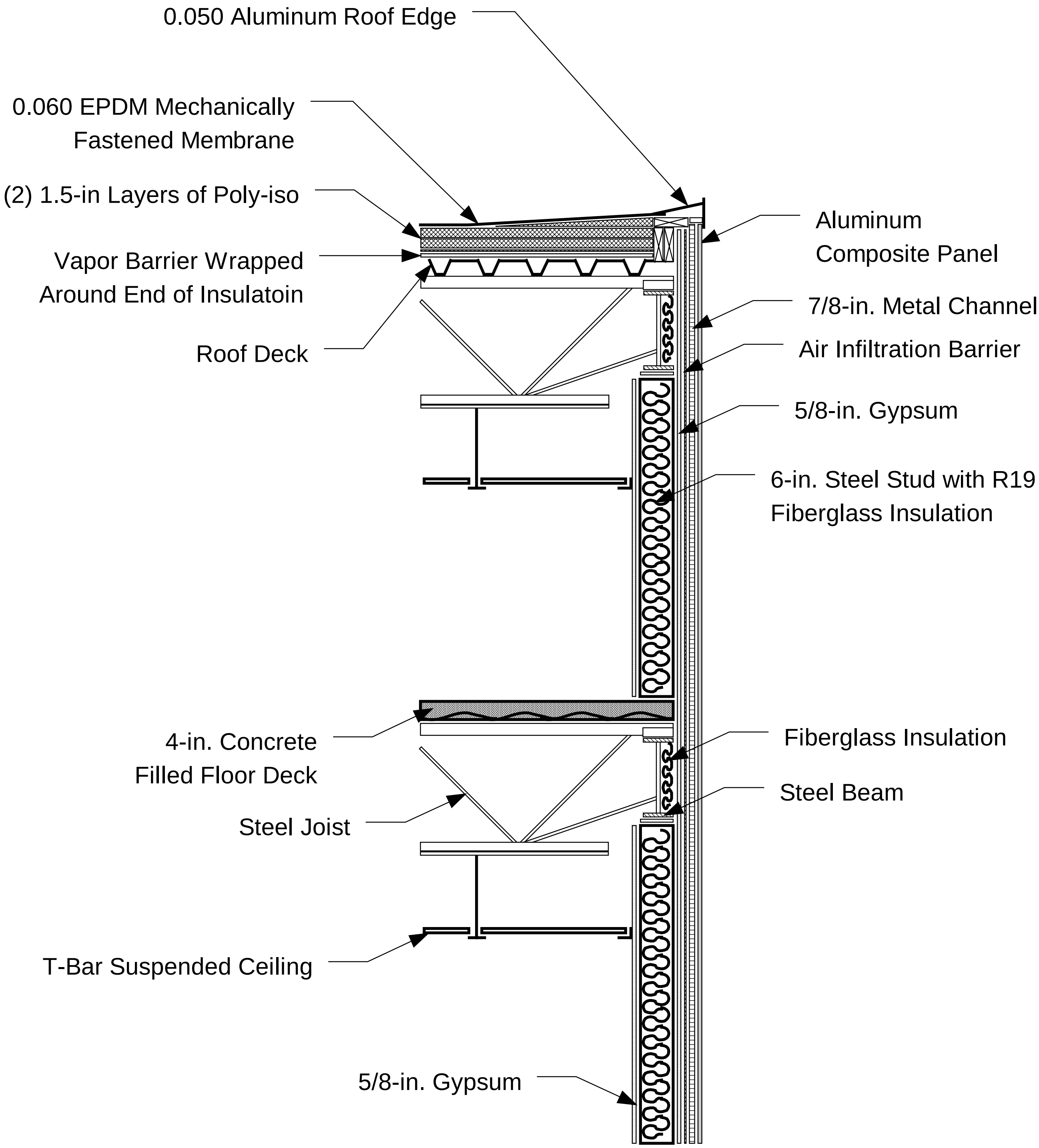

Figure A12-3. Exterior Wall and Roof Section for Two-Story Office Section

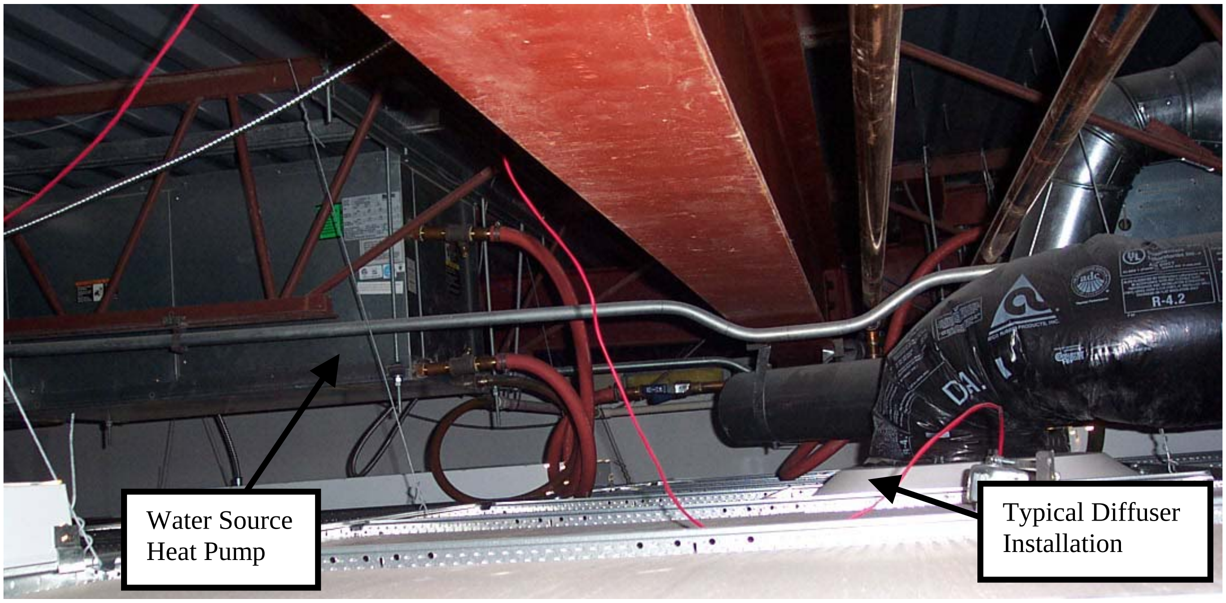

Figure A12-4. Ceiling Plenum

<u>HVAC System</u>

Water source heat pumps (WSHP) located in the ceiling space provide heating and cooling for the two-story office section. The water loop temperature maintained between approximately 55°F and 85°F using a natural gas boiler and cooling tower. The natural gas boilers do not run often because the water loop is heated with the rejected heat from a die casting manufacturing process. In addition, there is an Aaon energy recovery unit (ERV) with an enthalpy wheel. A Novar controller centrally controls all the HVAC equipment for this building.

The Aaon energy recovery ventilator (ERV) with a 3-ton cooling section and an enthalpy wheel is located on the roof. The ERV provides tempered outdoor air to the first and second floors through un-insulated ducts that empty near the return for each WSHP. The ERV pulls air from the second floor ceiling return plenum and is directed through an enthalpy wheel that exhanges heat and moisture with the incoming outdoor air. When the building calls for cooling and the outdoors temperature is below 55°F, the ERV runs in economizer mode (i.e., the wheel rotation stops) to provide free cooling. Figure A12-5, Figure A12-6, and Figure A12-7 show the energy recovery ventilator (ERV), WSHPs, and the boiler and cooling towers that maintain the water loop temperature for the WSHPs. Table A12-1 lists the HVAC equipment that serves the building.

The supply ducts located in the ceiling return plenum along with the WSHPs. There is no return ductwork. The supply ductwork is insulated metal trunks with flexduct to the diffusers. The two story office section has a ceiling return plenum however there are only 4 ceiling return grills on the first floor and one return grill on the second floor.

Figure A12-5. One of the WSHPs Serving Office Section

Figure A12-6. Aaon 3-ton Rooftop with Enthalpy Wheel Unit

Figure A12-7. Hot Water Boiler and Cooling Towers to Maintain Water Loop Temperature

Table A12-1. Summary HVAC Equipment Installed at Site

HVAC Equipment	Serves	Brand	Model	Heating Capacity (MBtu/h)	Cooling Capacity (tons)
WSHPs					
ERV	Both Floors	Aaon	RK-03-3-E0-212: W0000A00H0000B	38.6	3
Boiler	Both Floors	Lochinvar	CBN0985	797.85	n/a
Chiller #1	Entire Bldg.	Evapco			
Chiller #2	Entire Bldg.	Evapco			

A Novar controller centrally controls the WSHPs, boiler, and cooling towers. The water loop control points are 65°F and 84°F. Most of the WSHP supply fans run continuously although the WSHP that serves the president's section of the building is scheduled to turn off at the space heating setpoint. The heating setpoint is 70°F and the cooling setpoint is 72°F. The Novar system switches to unoccupied mode between 7:00 PM and 5:00 AM, which changes the heating setpoint reduces to 60°F and the cooling setpoint increases to 80°F.

MEASUREMENTS

The test data below was taken on October 19 and on November 2, 2004. Jim Cummings, Hugh Henderson, and Dan Gott were present on October 19 to perform blower door testing, pressure mapping, and supply and return airflow measurements. Dan Gott was on site November 2 to measure the return, exhaust, and supply airflows for the Aaon ERV and deploy three CO_2 and Temperature/RH sensors. Dan Gott was on site January 7 to seed the building with CO_2 tracer gas. Dan Gott collected the CO_2 and temperature/RH sensors on January 13, 2005.

Building Envelope Airtightness

The leakage characteristics of the building enclosure were assessed using fan pressurization methods. A single blower door was installed on the second floor in the south doorway (labeled in Figure A12-9). All exterior doors and windows were closed. The building was tested in the following configuration:

- All interior doors open
- Exhaust fans sealed from outdoors
- Aaon ERV intake and exhaust vent sealed at unit

The building pressure was varied from 11 Pa to 45 Pa. Figure A12-8 shows the building leakage variation with building pressure. The table in Figure A12-8 shows the results of the blower door tests including model coefficients, effective leakage area (ELA), and air-changes-per-hour (ACH). The ELA is calculated using the Lawrence Berkeley Laboratory method, which calculates the leakage area at 4 Pa. The building has an effective leakage area of approximately 2.51 sq in per 100 sq ft of the total envelope area including floor area. Another building leakage characteristic is the ACH at 50 pascals (ACH_{50}). The building has an ACH_{50} of 3.4.

Depressurization Test – Entire 2-Story Section

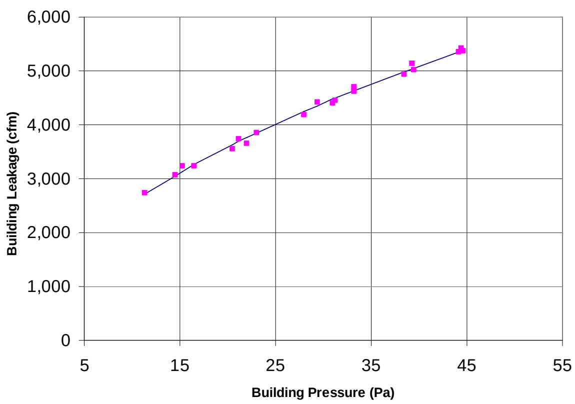

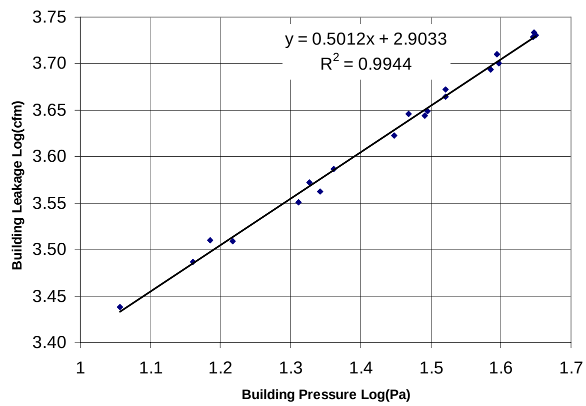

Test Results:

Flow Coefficient (K)	800.5	11,949 sq ft, floor area
Exponent (n)	0.501	
Leakage area (LBL ELA @ 4 Pa)	454.4 sq in	2.51 ELA / 100 sq ft
Airflow @ 50 Pa	5,687 cfm	3.39 ACH @ 50

Test Data:

Nominal Building Pressure (Pa)	Nominal Flow (cfm)	Ring
44.6	5,374	none
44.4	5,413	none
44.2	5,350	none
39.5	5,017	none
39.3	5,130	none
39.3	5,130	none
38.5	4,934	none
33.2	4,617	none
33.2	4,703	none
31.3	4,452	none
31.0	4,401	none
29.4	4,422	none
28.0	4,190	none
23.0	3,857	none
22.0	3,647	none
21.2	3,730	none
20.5	3,554	none
16.5	3,229	none
15.3	3,235	none
14.5	3,067	none
11.4	2,740	none

Notes: ELA is leakage area (in square inches) at reference pressure of 4 Pa.
ELA per 100 sq ft is based on total building envelope surface area (ceiling, exterior walls and floor).

Figure A12-8. Variation of Building Leakage with Pressure: $cfm = K(\Delta P)^n$

Pressure Mapping (Blower Door Testing)

Pressure readings in the building were taken using a digital micro-manometer (DG 700) with the blower door operating. The pressure difference across the building envelope was 45 Pa for the first floor pressure mapping and 50.6 Pa for the second floor. The ceiling space/return plenum was 1.1 Pa negative to the occupied space. This implies that the leakage area from the occupied space to the ceiling plenum is large and that the plenum is closely coupled to the conditioned space. The roof of the building is the primary air and thermal barrier.

Pressure measurements were taken between interior rooms with doors closed and the main corridors. Figure A12-9 shows the pressure differences induced across the doorways with the corridors depressurized. With the building depressurized to 45 Pa, pressures across the doorways ranged between 0.0 and 4.9 Pa. The pressure difference between the rooms and corridors are much less than the overall pressure difference to ambient. This implies that the room-to-room leakage is much great than the leakage across the building envelope. The pressures measured across doorways were measured in reference to an interior space that had a free path back to the blower door (open interior doors).

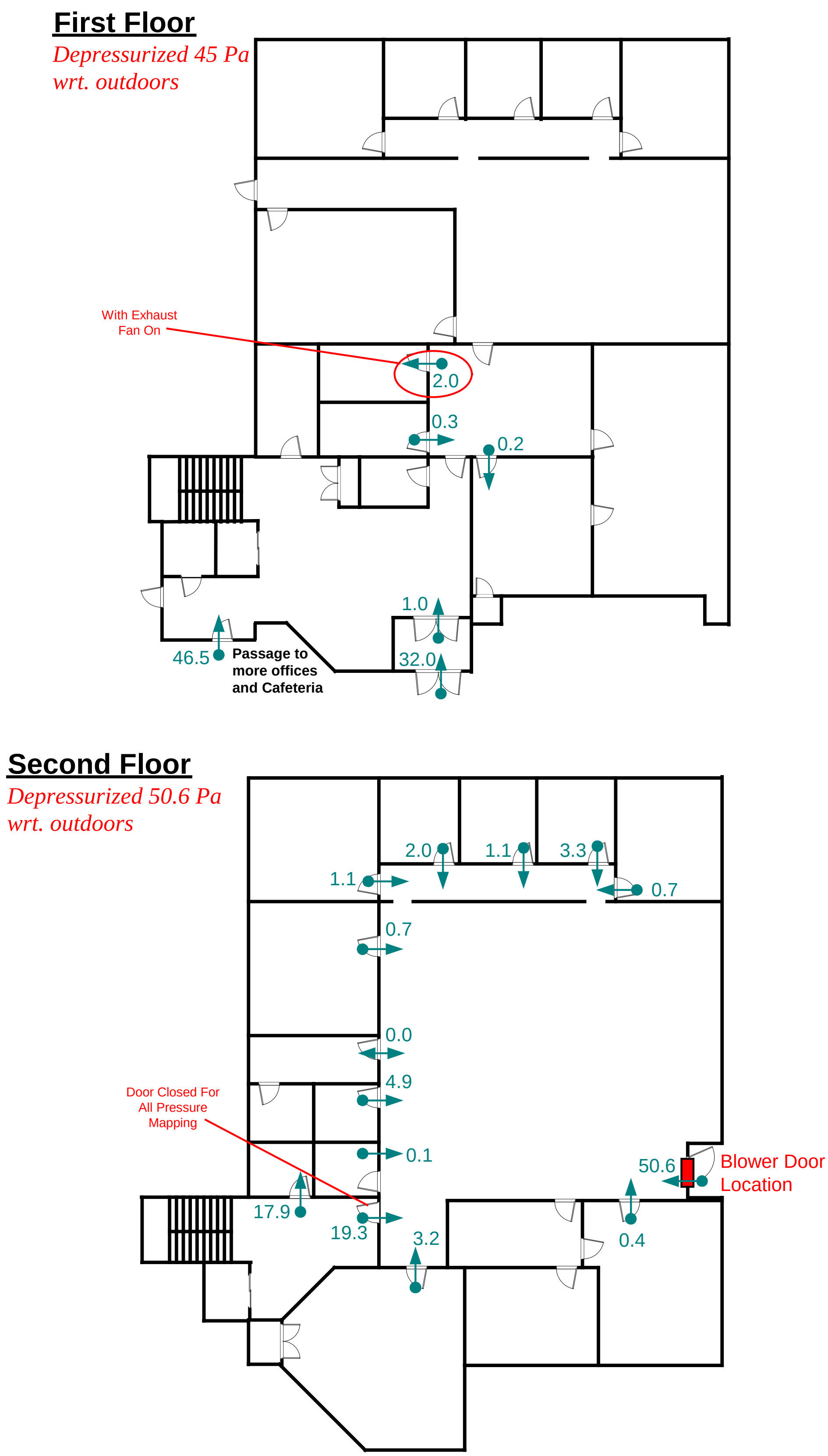

Figure A12-9. Room-to-Corridor Pressures with Building Depressurized (50 Pa)

HVAC Airflow Measurements

The airflow from each supply diffuser was measured using a Shortridge flow hood. The total supply airflow is approximately 11,000 cfm[1] or 0.87 cfm per sq-ft of floor area. Figure A12-10 displays the airflow at each diffuser and exhaust on the first floor and second floor. Table A12-2 summarizes the total supply and return airflow for the two-story office section.

[1] Four supply diffuser airflows and one return airflows were not measured. The airflows for these diffusers were estimated using the average of the measured diffuser airflows in the corresponding room/office space.

First Floor

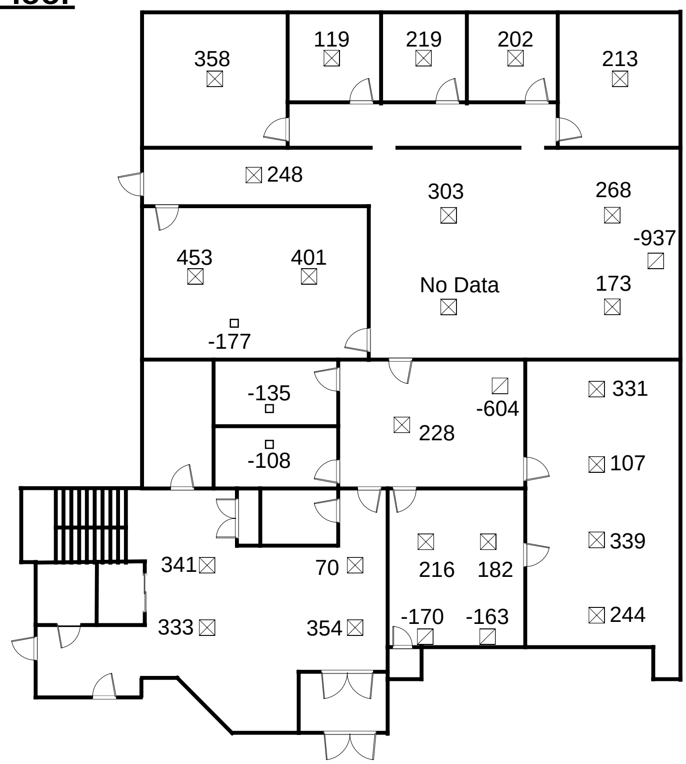

Second Floor

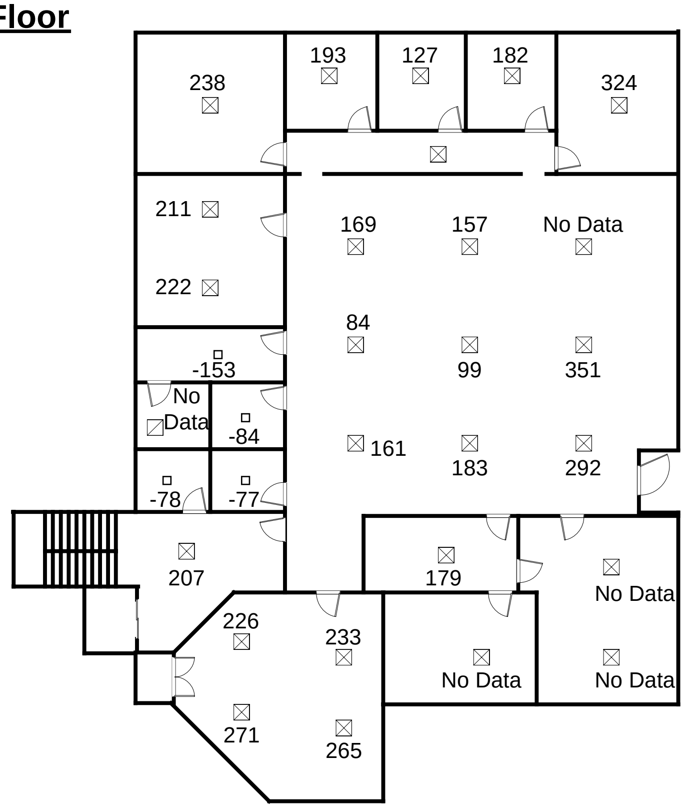

Figure A12-10. Supply and Return Airflow Measurements (cfm)

Table A12-2. Comparison of Supply and Return Airflow Measurements

HVAC Equip	Supply Airflow (cfm)	Return Airflow (cfm)	Method of Airflow Measurement	Measured Supply Fan Power (kW)	Normalized Supply Fan Power (W/cfm)
Sum of WSHPs	10,957	2,037	Flowhood at Diffusers		
Aaon ERV	1,236	1,962	Equal Area Traverse at Unit	0.9	0.6

Figure A12-11 shows a schematic of the Aaon ERV illustrating the airflow paths and measured static pressure for the various sections of the unit. Figure A12-12 shows pictures of the individual sections in the ERV unit. Table A12-3, Table A12-5, Table A12-4, and Table A12-6 show the airflow measurements for the Aaon ERV supply, return, exhaust, and ventilation measured on November 1, 2004. Table A12-7 lists the bathroom and food area exhaust fan airflows that total 812 cfm, however these fans do not run continuously (and were not on during the testing.

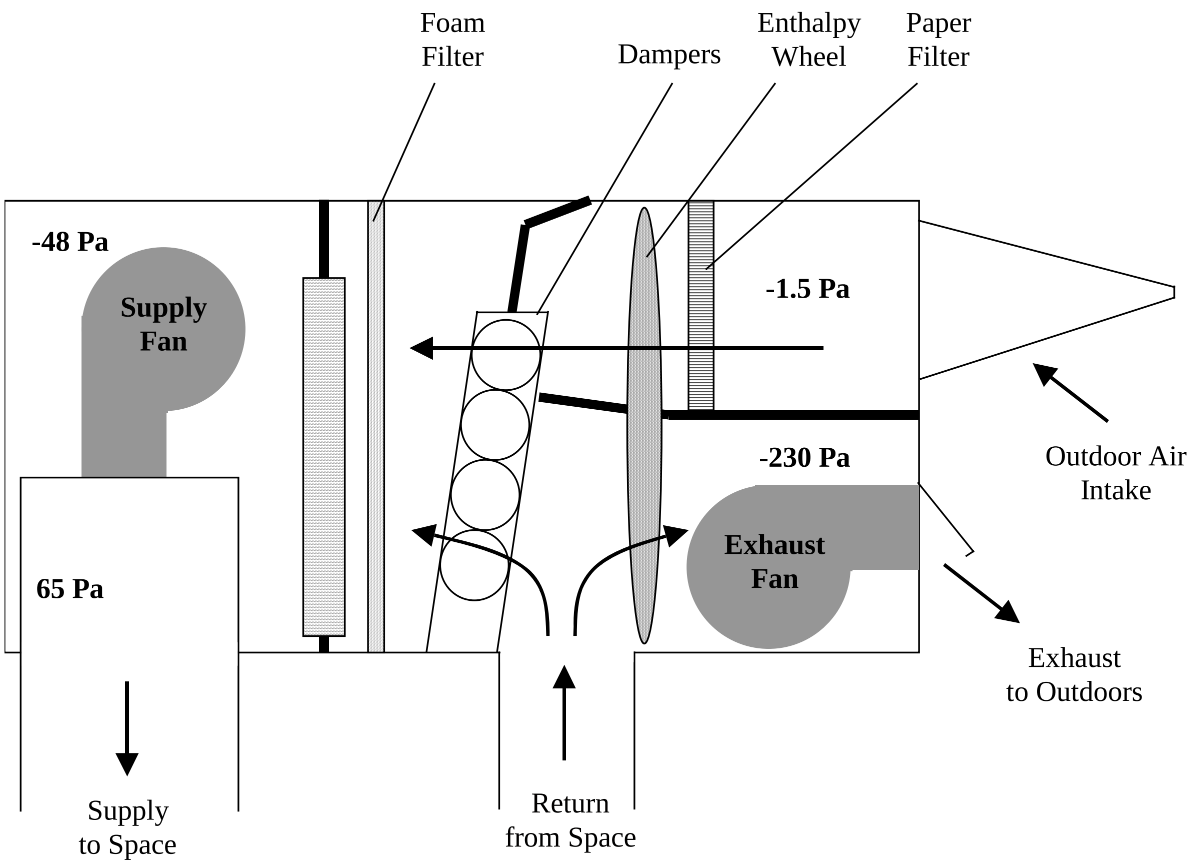

Figure A12-11. Aaon ERV Schematic with Measured Static Pressures

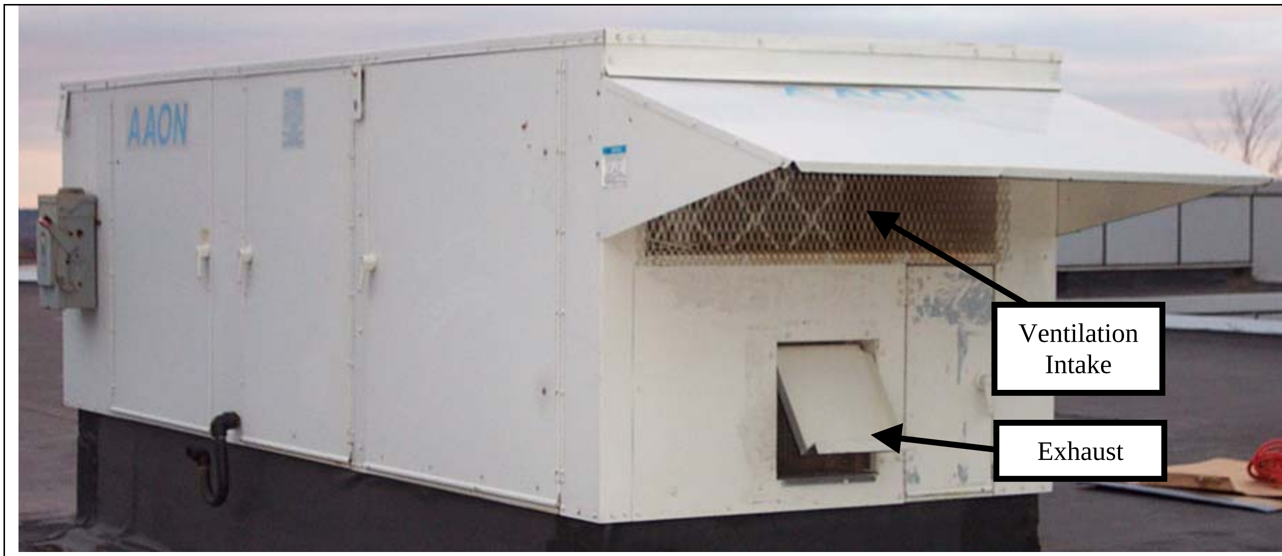

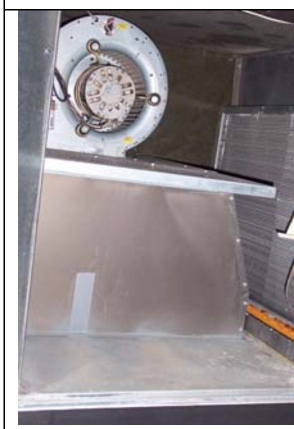
Supply Section


Return & Vent. Dampers


Enthalpy Wheel


Ventilation Section (top)
Exhaust Section (bottom)

Figure A12-12. Photos of Each Section in the Aaon ERV

Table A12-3 and Table A12-5 show the measured airflow for the ERV with the enthalpy wheel OFF (i.e., not spinning). Table A12-4 and Table A12-6 show the measured airflow for the ERV with the enthalpy wheel ON (i.e., spinning)

Table A12-3. Aaon ERV Supply and Return Airflow (Enthalpy Wheel Off)

ERV Return Airflow (from space)		
Opening width	36	inches
Opening height	14.25	inches

Equal Area Velocity Traverse (fpm)

565	545	540	495
565	525	555	525
565	560	600	570

Average	550.8	SFPM
Area	3.6	ft^2
Air Flow	**1,962**	**SCFM**

ERV Supply Airflow (to Space)		
Opening width	22.5	inches
Opening height	20.5	inches

Equal Area Velocity Traverse (fpm)

500	190	140	140
550	235	170	180
735	305	165	390
835	690	410	540

Average	385.9	SFPM
Area	3.2	ft^2
Air Flow	**1,236**	**SCFM**

Table A12-4. Aaon ERV Supply and Return Airflow (Enthalpy Wheel On)

ERV Return Airflow (from space)		
Opening width	36	inches
Opening height	14.25	inches

Equal Area Velocity Traverse (fpm)

635	590	660	665
570	565	560	535
570	585	565	570

Average	589.2	SFPM
Area	3.6	ft^2
Air Flow	**2,099**	**SCFM**

ERV Supply Airflow (to Space)		
Opening width	22.5	inches
Opening height	20.5	inches

Equal Area Velocity Traverse (fpm)

485	240	148	162
505	269	153	260
725	340	215	356
860	800	408	505

Average	401.9	SFPM
Area	3.2	ft^2
Air Flow	**1,287**	**SCFM**

Table A12-5. Aaon ERV Exhaust and Ventilation Airflow (Enthalpy Wheel Off)

Exhaust Airflow

	Test Date 11/1/04
Static Pressure in Ventilation Hood (Pa)	-216.0
Airflow @ Average Ventilation Static (cfm)	835.7
R-Squared	0.998

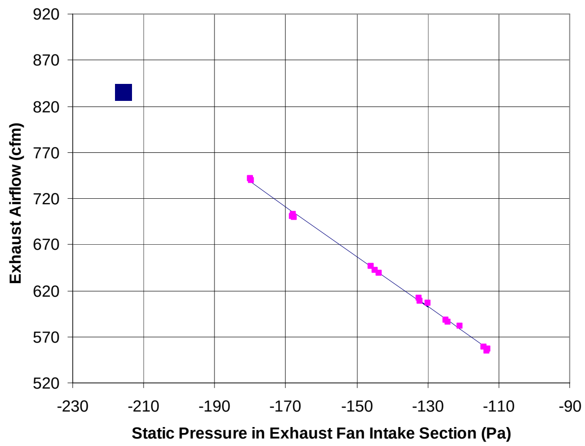

Test Data:

Nominal Ventilation Static (Pa)	Nominal Flow (cfm)	Ring
-180.0	742	1
-179.6	739	1
-180.0	742	1
-167.8	703	1
-167.7	699	1
-168.2	701	1
-143.7	639	1
-146.0	647	1
-144.7	642	1
-129.8	607	1
-132.3	609	1
-132.4	612	1
-125.0	588	1
-124.4	586	1
-120.8	582	1
-114.3	559	1
-113.3	555	1
-113.1	557	1

Ventilation Airflow

	Test Date 11/1/04
Static Pressure in Ventilation Hood (Pa)	-1.5
Airflow @ Average Ventilation Static (cfm)	442.5
R-Squared	0.967

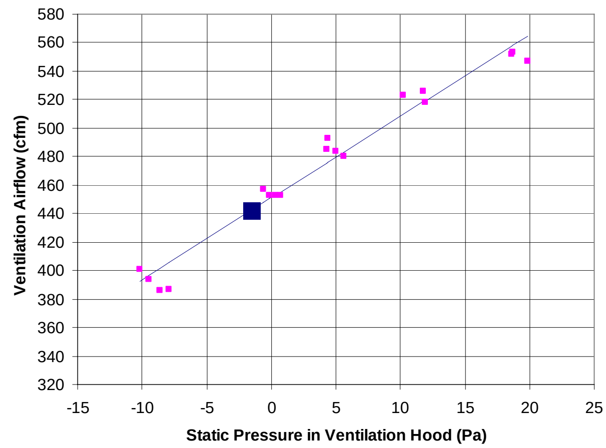

Test Data:

Nominal Ventilation Static (Pa)	Nominal Flow (cfm)	Ring
19.9	547	1
18.7	553	1
18.6	552	1
11.9	518	1
11.8	526	1
10.2	523	1
5.6	480	1
5.0	484	1
4.4	493	1
4.3	485	1
0.7	453	1
0.3	453	1
-0.1	453	1
-0.6	457	1
-7.9	387	1
-8.6	386	1
-9.5	394	1
-10.2	401	1

Table A12-6. Aaon ERV Exhaust and Ventilation Airflow (Enthalpy Wheel On)

Exhaust Airflow

	Test Date 11/1/04
Static Pressure in Ventilation Hood (Pa)	-216.0
Airflow @ Average Ventilation Static (cfm)	872.4
R-Squared	0.997

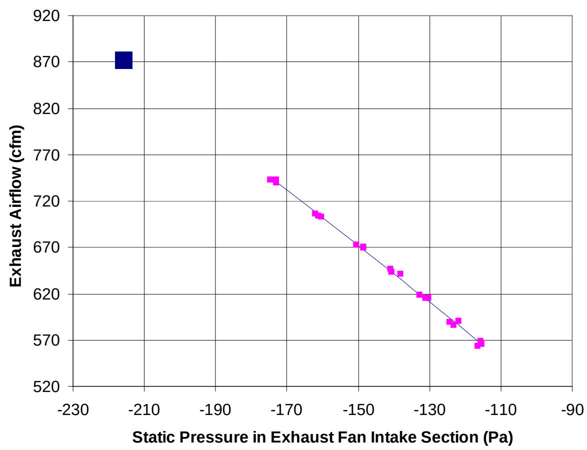

Test Data:

Nominal Ventilation Static (Pa)	Nominal Flow (cfm)	Ring
-174.6	743	1
-173.0	740	1
-172.8	743	1
-161.9	706	1
-161.0	704	1
-160.2	703	1
-150.5	672	1
-148.6	669	1
-148.5	670	1
-141.0	647	1
-140.7	643	1
-138.0	641	1
-132.6	618	1
-131.1	615	1
-130.2	615	1
-124.3	589	1
-123.1	586	1
-121.7	590	1
-116.3	563	1
-115.6	569	1
-115.3	565	1

Ventilation Airflow

	Test Date 11/1/04
Static Pressure in Ventilation Hood (Pa)	-1.8
Airflow @ Average Ventilation Static (cfm)	369.7
R-Squared	0.984

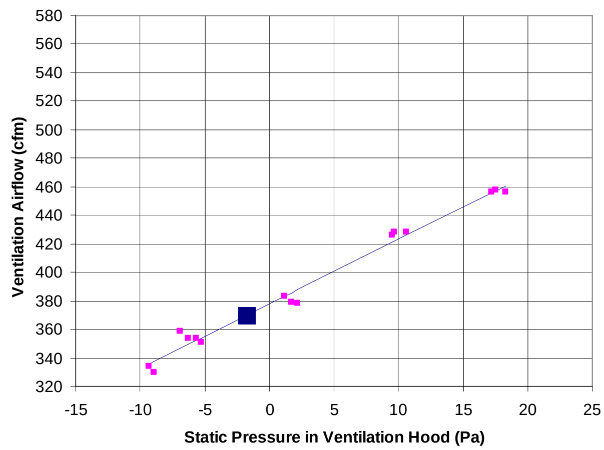

Test Data:

Nominal Ventilation Static (Pa)	Nominal Flow (cfm)	Ring
18.3	456	1
17.5	458	1
17.2	456	1
10.6	428	1
9.7	428	1
9.5	426	1
2.2	378	1
1.7	379	1
1.2	383	1
-5.3	351	1
-5.7	354	1
-6.3	354	1
-6.9	359	1
-8.9	330	1
-9.3	334	1

Table A12-7. Bathroom and Food Area Exhaust Fan Airflows

Location	Exhaust Airflow (cfm)
Canteen	177
Mens Rm	135
Womens Rm	108
Food Prep.	153
Womens Rm	84
Lobby Bathroom	78
Mens Rm	77
Total	***812***

Note: These fans do not run continuously.

Table A12-8 summarizes the measured airflows for the Aaon ERV unit. Figure A12-13 illustrates of the airflows and static pressure. The airflow was measured 1) with the unit in normal operation for ambient conditions (enthalpy wheel off) and 2) with the enthalpy wheel operating by overriding the controls to put the unit into the cooling mode. In theory, the airflows should balance. However, in practice, measurement errors in determining each airflow result in the “flow “imbalance” listed in the table.

Table A12-8. Measured Airflows for Aaon ERV Unit

	Supply (to space) (cfm)	Return (from space) (cfm)	Exhaust Outlet (cfm)	Ventilation Inlet (cfm)	Flow Imbalance (cfm)
Enthalpy Wheel Off	1,236	1,962	836	442	-333
Enthalpy Wheel On	1,287	2,099	872	370	-309

Note: Flow imbalance is from accumulation of measurment errors

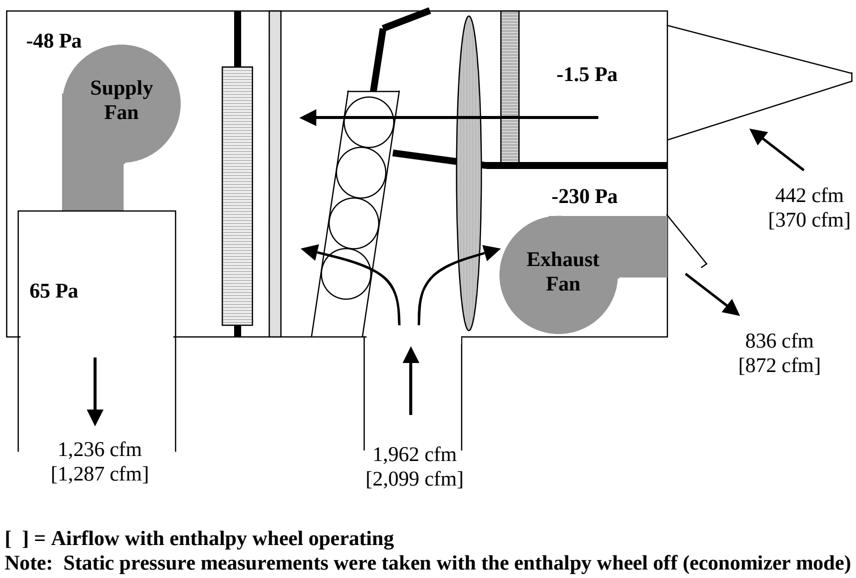

Figure A12-13. Aaon ERV Airflow

Figure A12-14 shows the expected airflows for this unit based on the manufacturer's published data. Because the unit had very short return and supply ductwork, the airflows were much higher than expected. The exhaust flow rate does match expectations since the pressure drop is solely due to the wheel (and not any duct work). Because air can easily enter the return duct, less airflow is induced through the fresh air section of the enthalpy wheel.

Summer Design Conditions

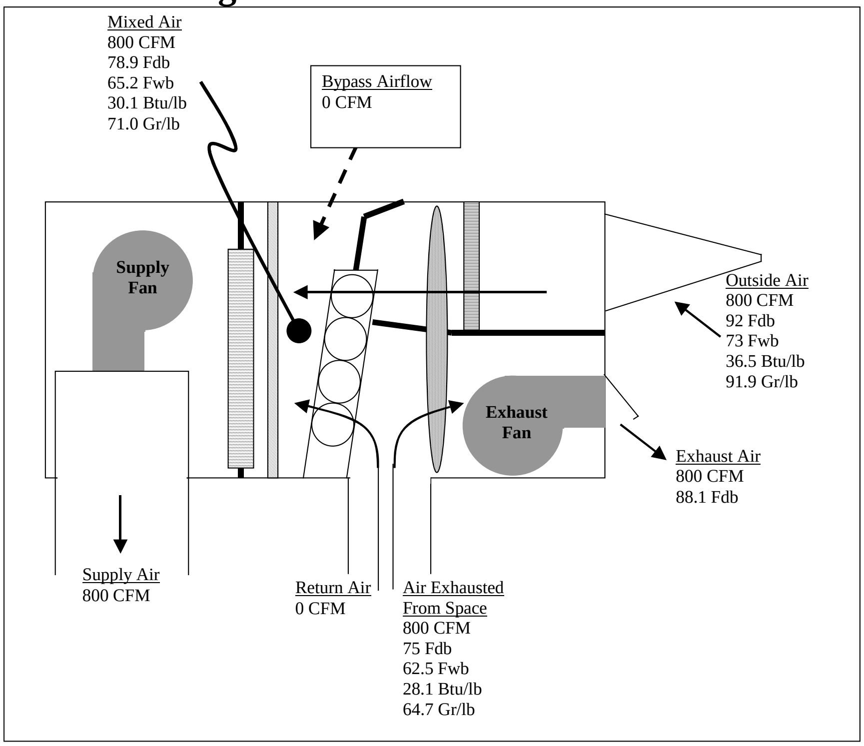

Winter Design Conditions

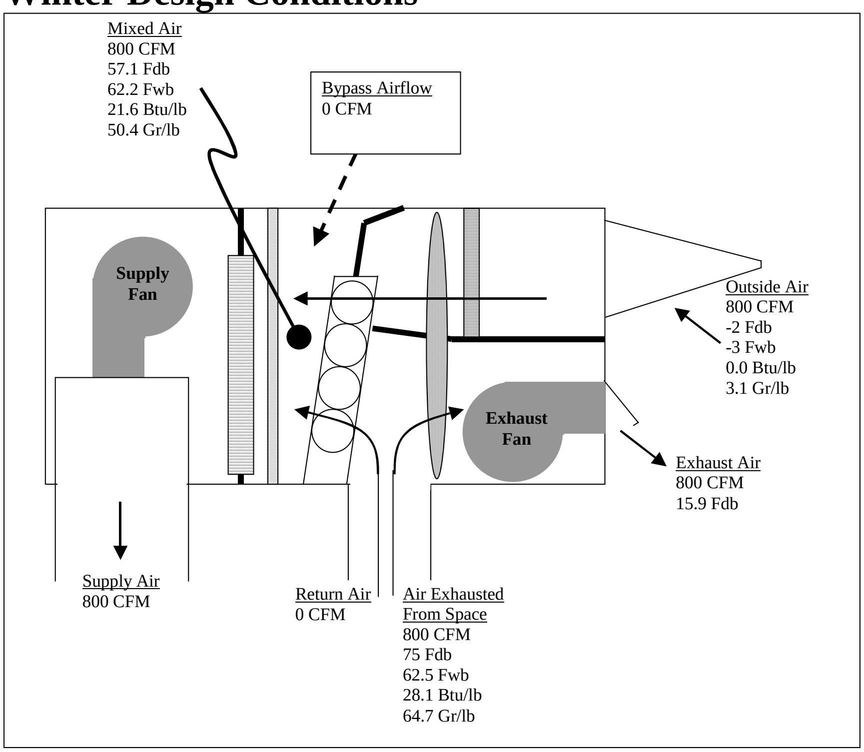

Figure A12-14. Published Performance Data for Aaon ERV

Pressure Mapping (AHU Fans On)

The air pressure relationships in the building were also determined with the WSHPs and ERV fans on. The graphics in Figure A12-15 show the pressure differences induced across the doorways with the fans on and the individual doorway closed. With the building in normal configuration, we would close an interior door and measure the pressure across the doorway. Operation of the all WSHPs and the ERV created interior pressures differences up to 4.3 Pa. The building was pressurized with respect to outdoors between 1.1 Pa and 6.0 Pa with an average around 3.7 Pa. This pressure may vary if the manually operated exhaust fans were turned on or if the ERV economizer dampers change position.

First Floor

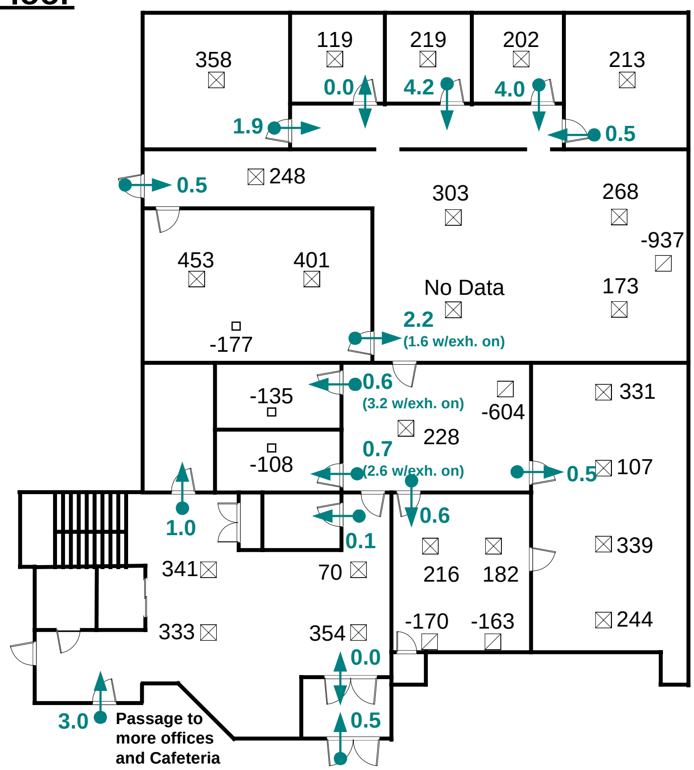

Second Floor

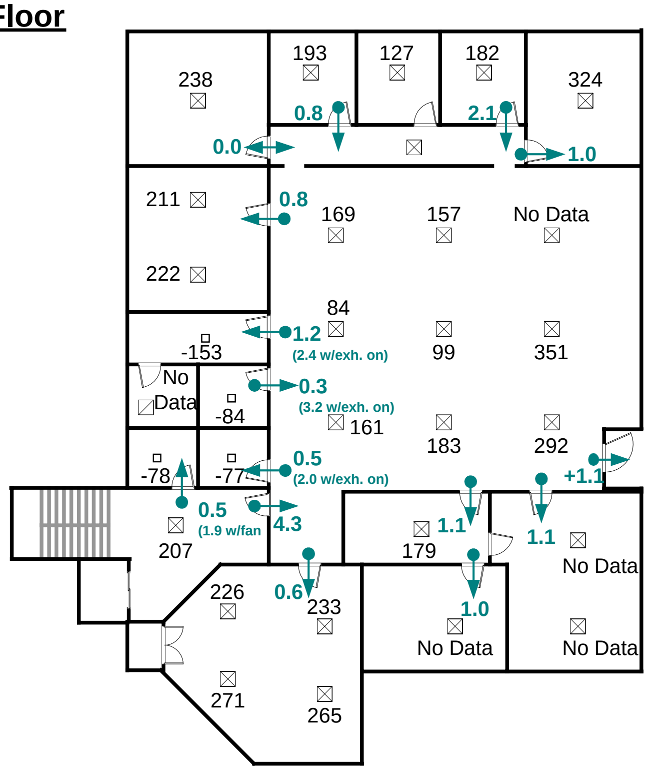

Figure A12-15. Pressure Difference between Rooms with WSHP and ERV Fans On

Duct Leakage Measurements

We did not test for duct leakage since all the ducts were in the building envelope. There were several WSHPs with separate small supply duct systems located inside the primary air and thermal barrier. The WSHPs are located in the ceiling space, which is also the ceiling return plenum.

Space Conditions

Figure A12-16 shows the average temperature profiles based on temperature readings taken with a HOBO data logger from November 2, 2004 to January 13, 2004. The thick line shows the average for each hour while the shaded region corresponds to one standard deviation about the average. The dotted lines correspond to the minimum and maximum for each hour. Sensors were placed in the central office area on the first floor, conference room on the first floor, second floor near the food prep area, and for the tracer gas decay test in the central office area on the second floor.

A Novar controller centrally controls the WSHPs, ERV, boiler, and cooling towers. The water loop control points are 65°F and 84°F. Most of the WSHP supply fans run continuously although the WSHP that serves the president's section of the building is scheduled to turn off at the space heating setpoint. The heating setpoint is 70°F and the cooling setpoint is 72°F. The Novar system switches to unoccupied mode between 7:00 PM and 5:00 AM, which changes the heating setpoint reduces to 60°F and the cooling setpoint increases to 80°F.

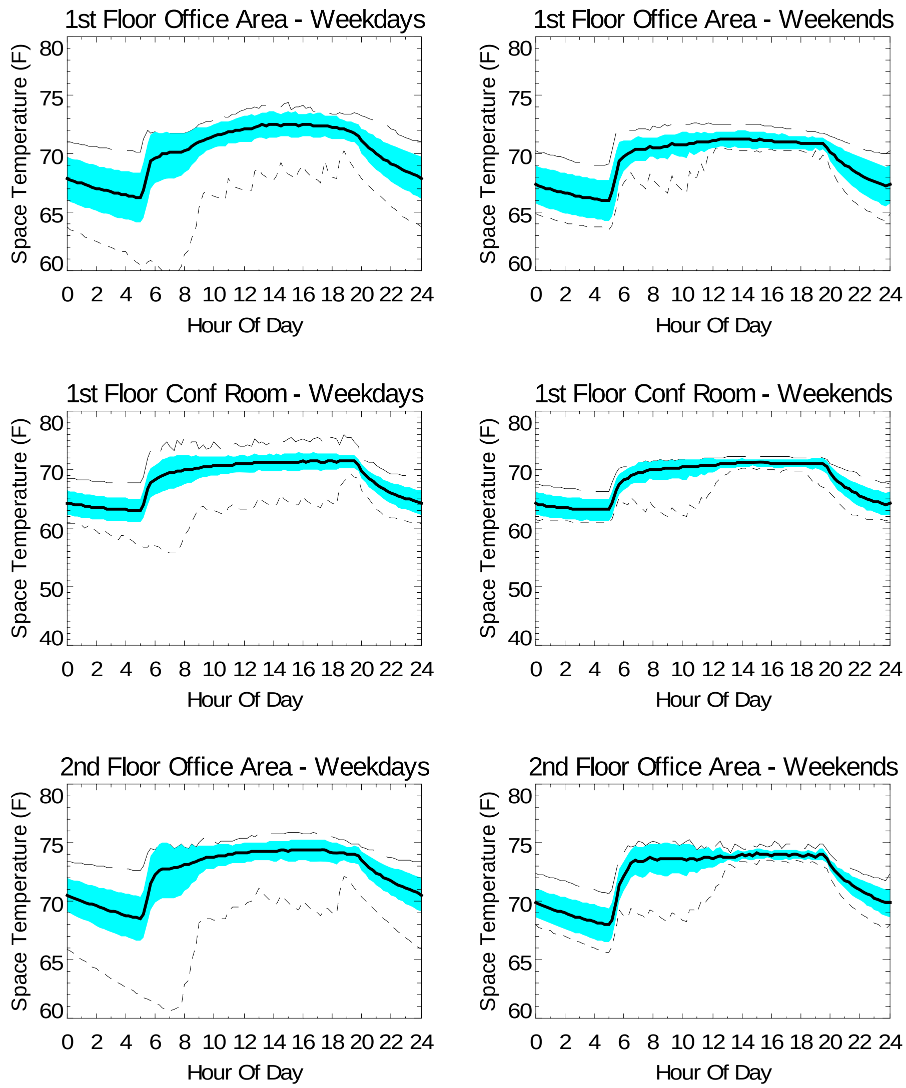

Figure A12-16. Measured Space Temperature Profiles

Figure A12-17 shows the CO_2 concentration in various locations in the building. The CO_2 concentration provides an indication of occupancy. The next section uses the CO_2 as a tracer gas to estimate the infiltration/ventilation rate of the building. The large spike on January 7 occurred when we seeded the building with CO_2.

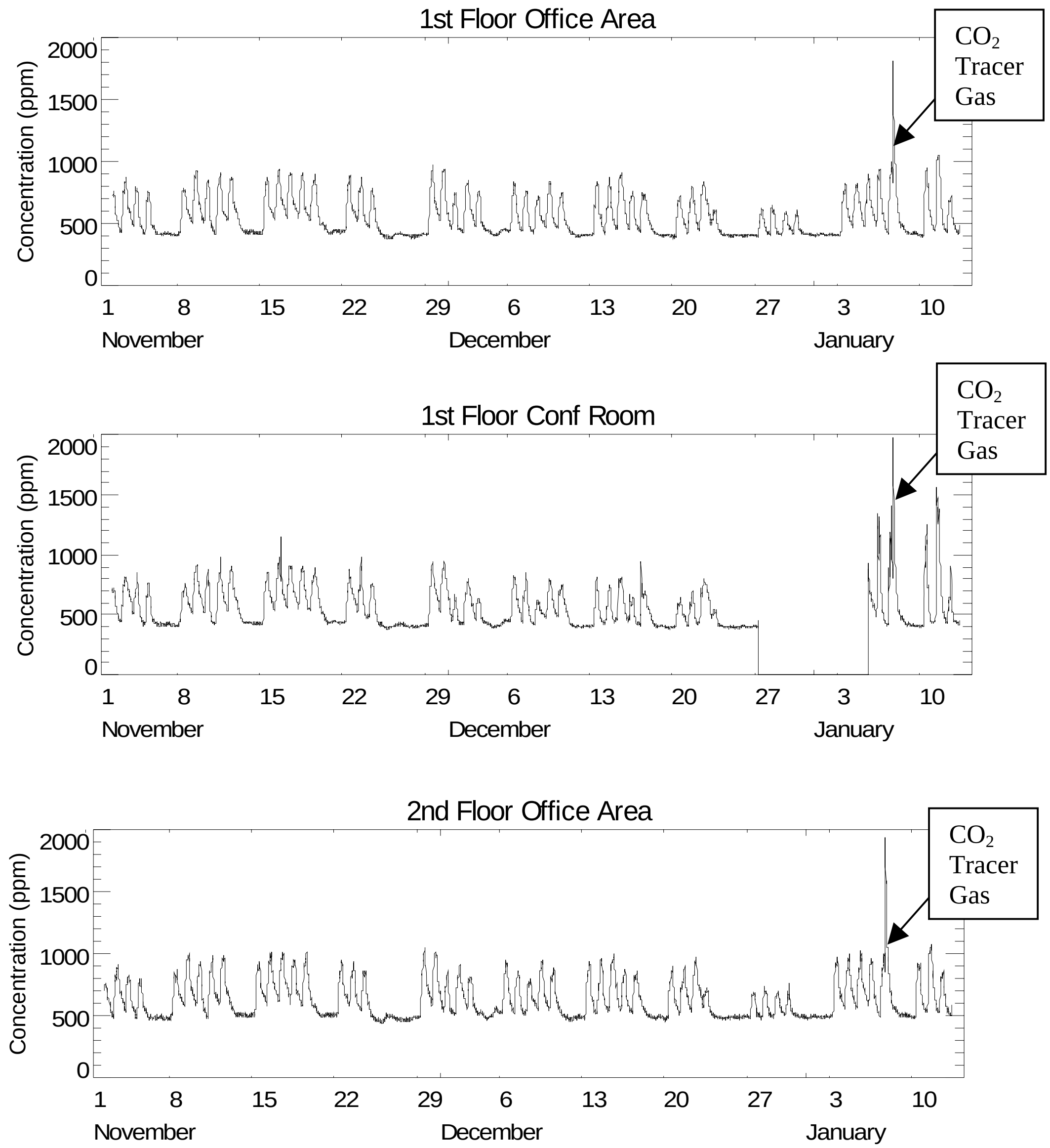

Figure A12-17. Measured CO_2 Concentration in Various Spaces

The following plots show the relative humidity for this building. The building did not exceed 55% relative humidity during the monitoring period from November 2004 to January 13, 2005. Figure A12-21 displays the conditions inside the building compared with the ASHRAE comfort zone for cooling shown by the shaded region on the plot.

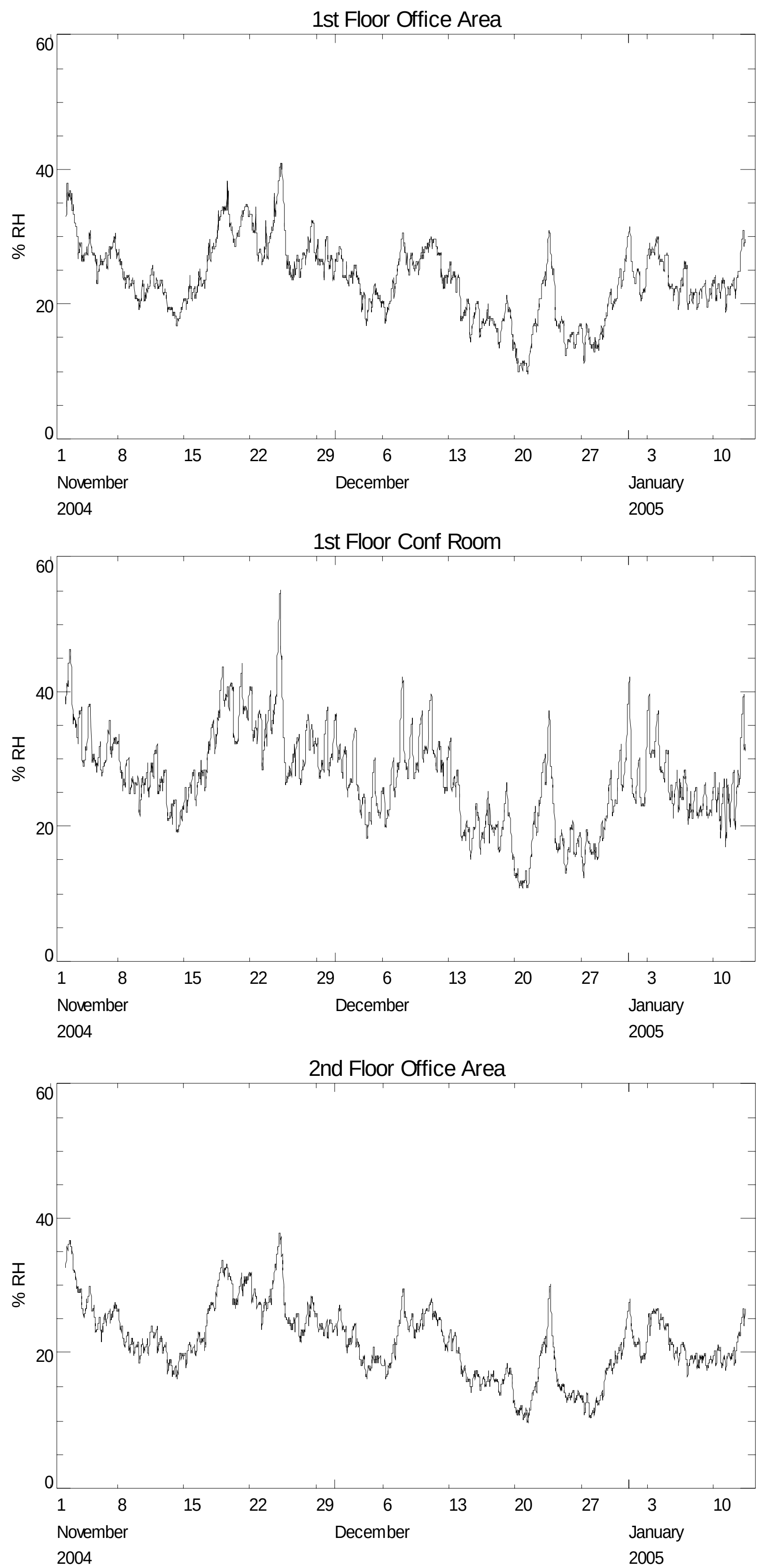

Figure A12-18. Measured Relative Humidity

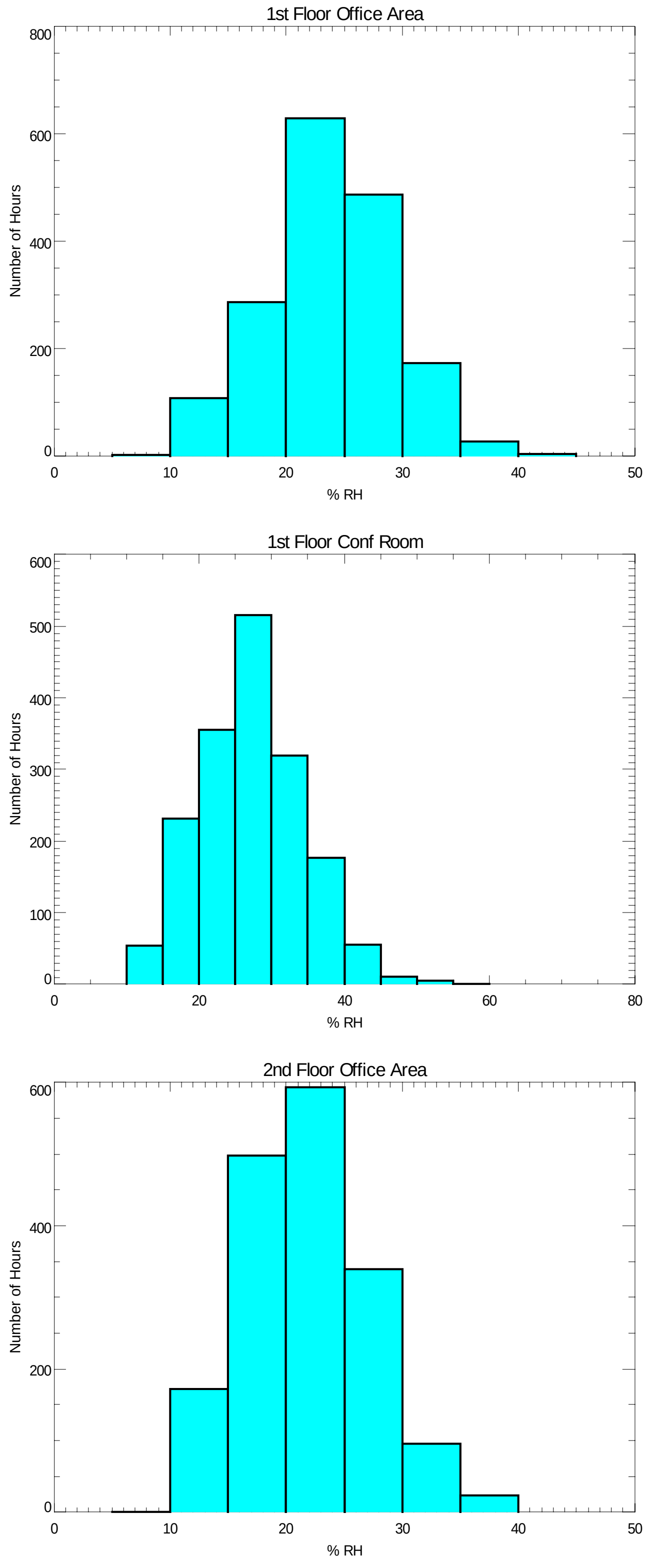

Figure A12-19. Duration of Relative Humidity Levels

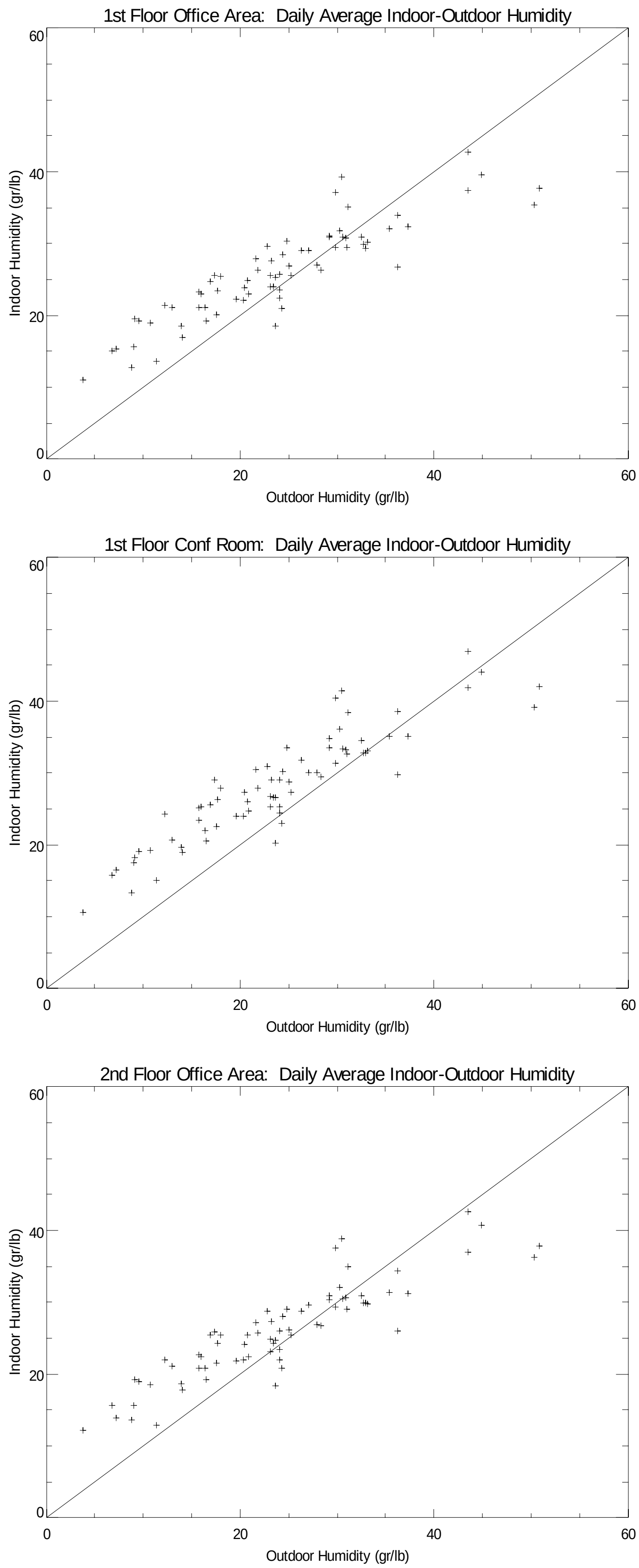

Figure A12-20. Indoor Humidity Variation with Outdoor Humidity

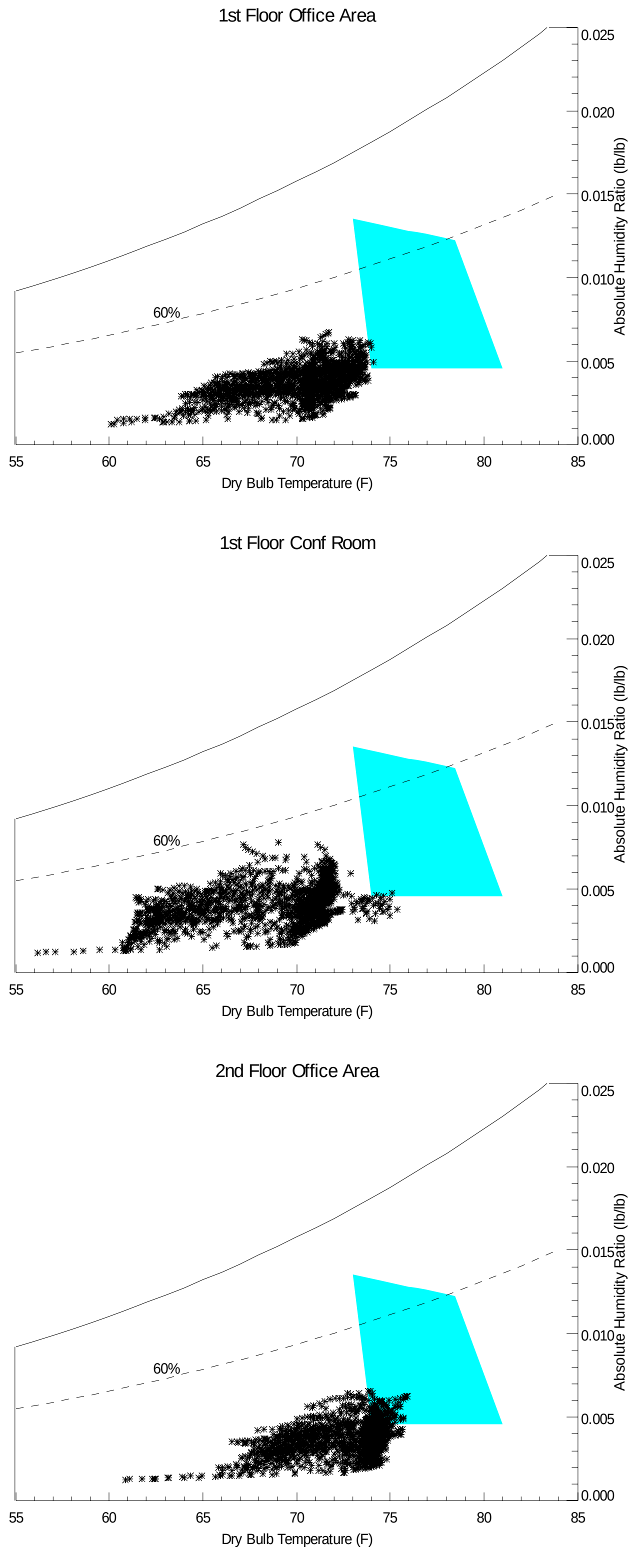

Figure A12-21. Indoor Air Quality Comparison with ASHRAE Comfort Zone for Cooling

Infiltration Estimate from CO_2 Decay

Figure A12-22 show the resulting tracer gas decay trends immediately after seeding the building with CO_2. The predicted air change rate (ACH) is shown on each plot.

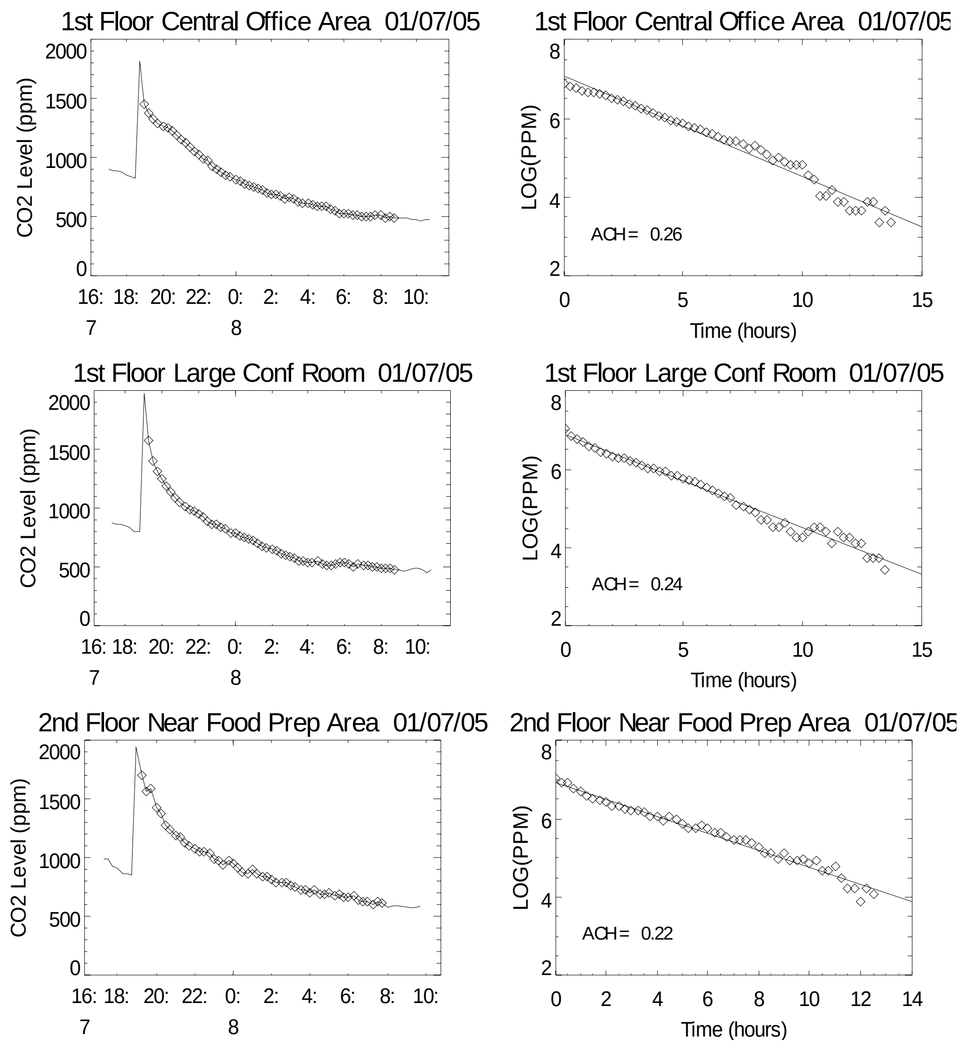

Figure A12-22. Tracer Gas Decay Using CO_2 for Various Periods

Table A12-9 summarizes the results of the tracer gas decay tests in the plots above. The table also includes the estimated mechanically induced infiltration airflow based on the building volume of 100,568 ft^3. The measured ventilation airflow for the Aaon ERV with the enthalpy wheel operating was measured to be 370 cfm. The estimated mechanically induced ventilation rate determined from the CO_2 tracer gas test is 384 cfm.

Table A12-9. Summary of Tracer Gas Decay Tests

	Start Time	End Time	ACH	Flow (cfm)
1st Floor Office Area	07-Jan 07:00 PM	08-Jan 08:45 AM	0.26	429
1st Floor Conference Room	07-Jan 07:15 PM	08-Jan 08:45 AM	0.24	400
2nd Floor Offices Near Food Prep Area	07-Jan 07:15 PM	08-Jan 07:45 AM	0.22	364
2nd Floor Offices in Central Area	07-Jan 07:15 PM	08-Jan 05:45 AM	0.20	343
Average			***0.23***	***384***

Note: Flow determined with building volume of: **100,568** ft^3

In comparison to the ACH values above, the nominal leakage rate (defined as ACH_{50} divided by 20) from the blower door test above is 0.17 ACH.

Utility Bills

The available energy use data is not representative of the energy used by the two-story office section described in this report. The two-story office section is only 17% of the entire facility. The remainder of the building is used for manufacturing and has different building construction type. So the utility data were not included here.

Field Test Site 13 – Fire Department, Cazenovia, NY

Front of Building (South)

Southeast Corner of Building

West Side of Building

Rear of Building (North)

Figure A13-1. Photos of Building

CHARACTERISTICS

Building Description

The 9,800 sq-ft facility is a two-story fire department comprised of mostly of high bay garage space with a small lobby, kitchen, storage rooms, and conference room on the first floor. The second floor (1,400 sq-ft) has three mechanical rooms, an office, and a lounge room. The facility was built in 1989. Figure A13-1 shows each side of the building with the main entrance of the building facing directly south. The building uses a natural gas boiler to supply hot water to perimeter heaters and the garages are heated using ceiling mounted natural gas radiant heaters. The front lobby, front office, and vestibule are cooled by one air handling unit (AHU). A second AHU cools the rear training room and upstairs lounge room. A packaged terminal air conditioner (PTAC) cools an upstairs office. Figure A13-2 presents the building floor plan.

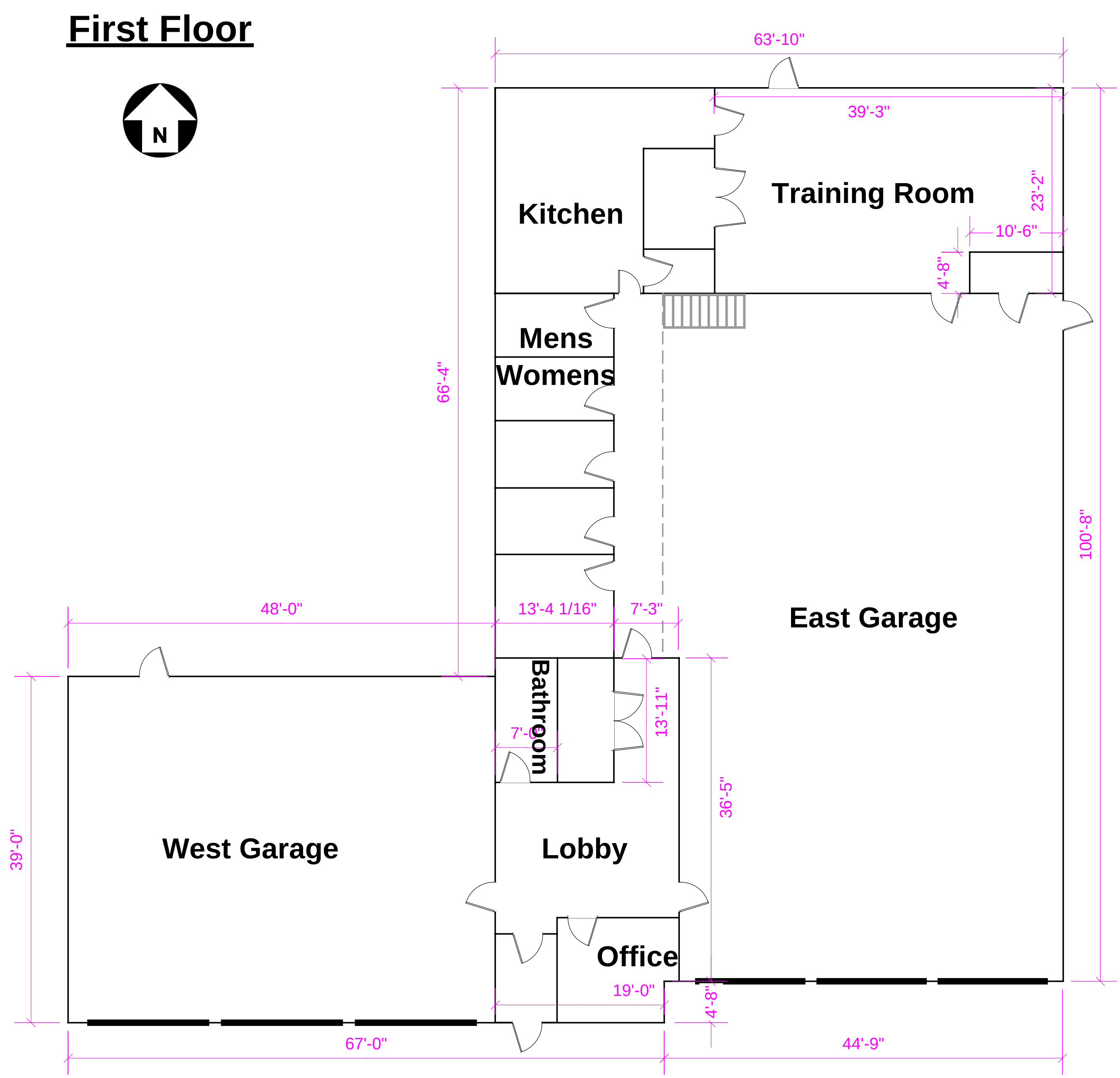

Figure A13-2. First Floor Building Plan

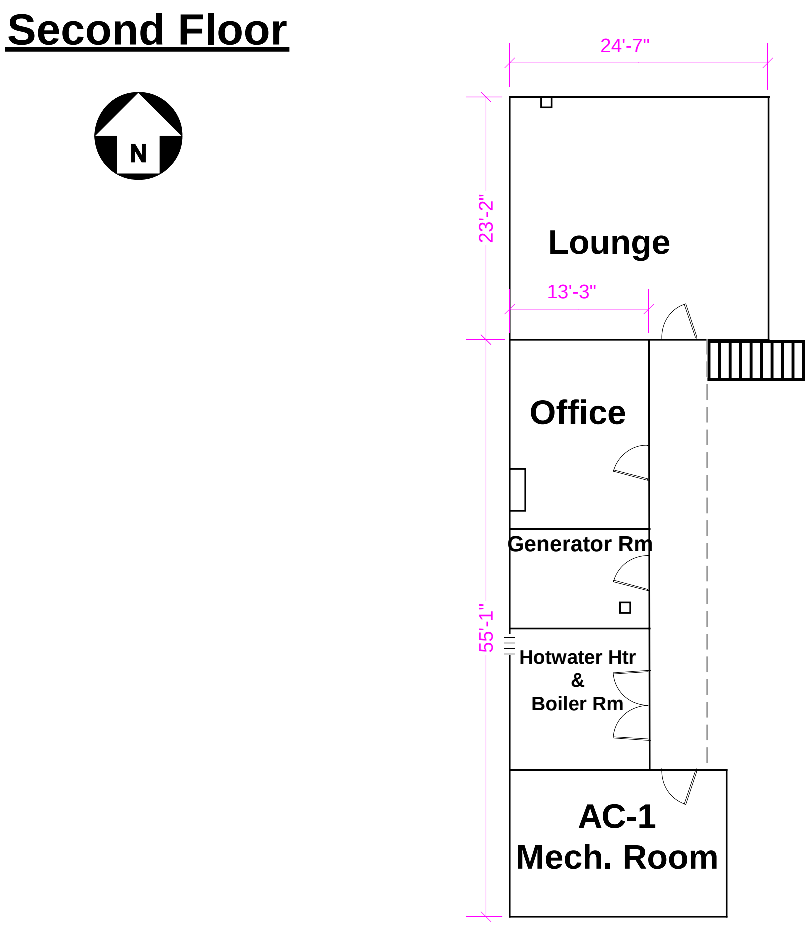

Figure A13-3. Second Floor Building Plan

Construction Details

The exterior walls are 8-in concrete block with 2-in rigid insulation and brick veneer exterior finish. The exterior block walls have a painted interior finish. The lobby and front office served by AC-1 and the training room served by AC-2 have a T-bar suspended ceiling. The exterior wall and roof construction is shown in Figure A13-4 for areas with a T-bar ceiling. The majority of the building has similar construction, but without a suspended ceiling. The training room uses the space above the T-bar ceiling as a return plenum. All the ductwork is insulated and located in the ceiling space.

The building has a pitched roof with 6-in paper faced fiberglass batt insulation located at the gypsum board primary air barrier. The roof is constructed with wooden trusses, plywood decking, and asphalt shingles. The attic is vented using perforated soffits and ridge venting.

Figure A13-5 shows pictures of the attic, ceiling plenum, and typical diffuser installation.

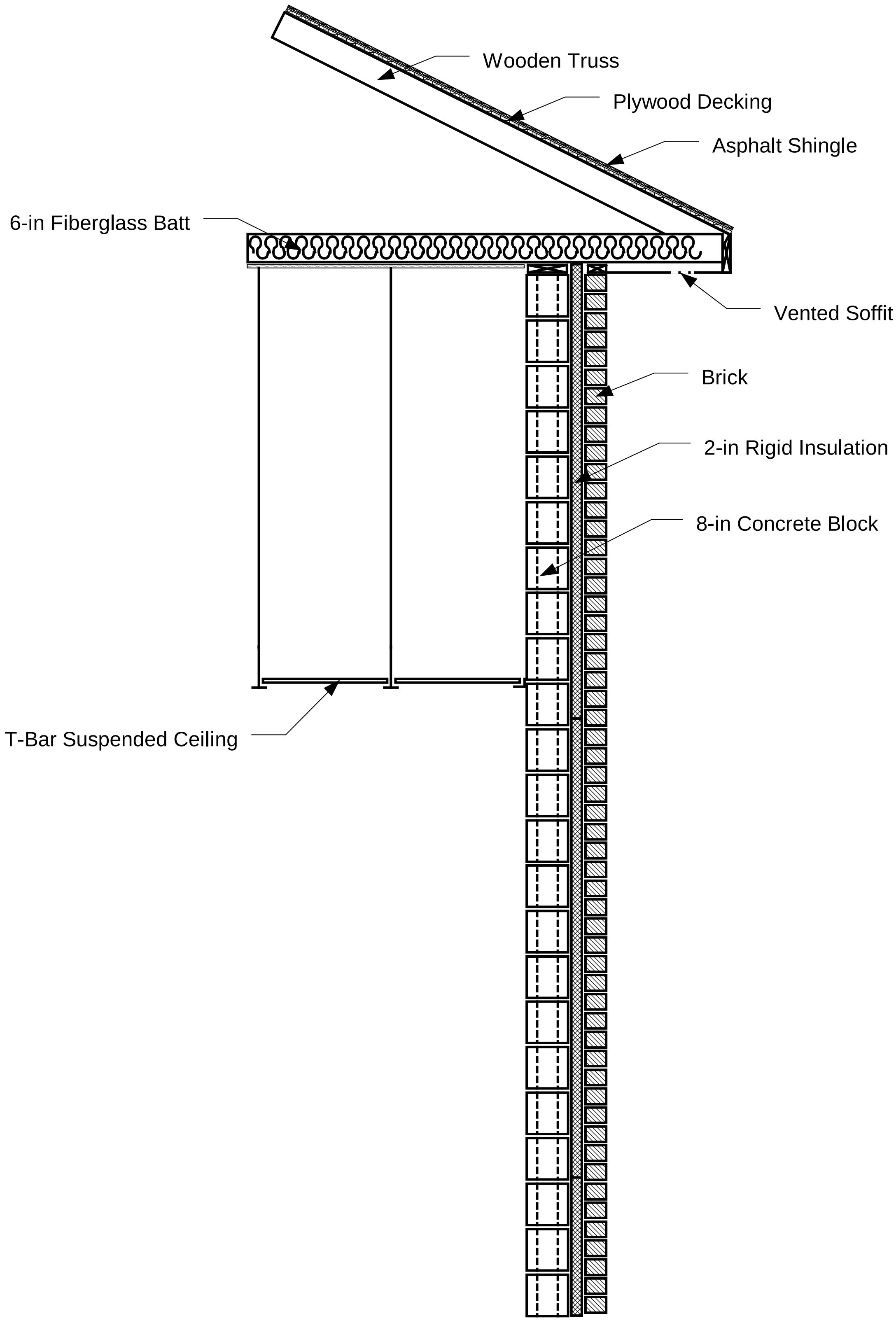

Figure A13-4. Floor, Wall, and Roof Section for Second Floor

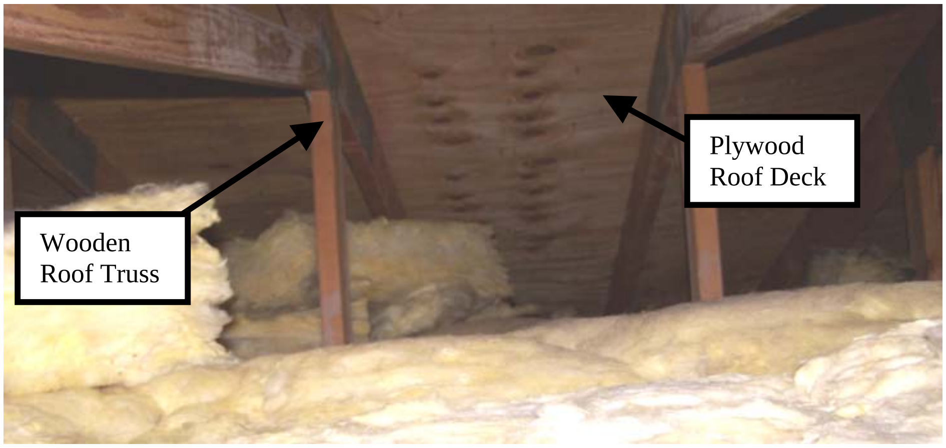

Attic

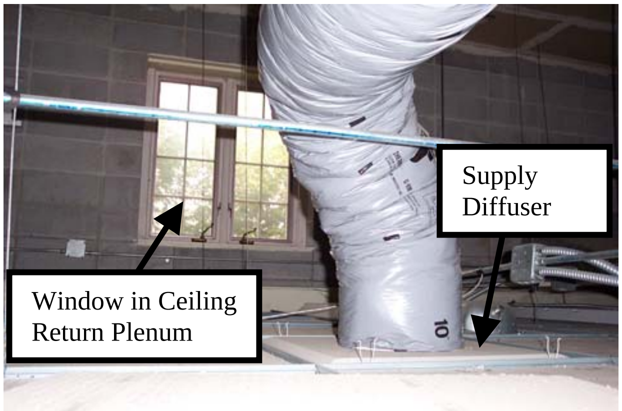

Typical Supply Diffuser Installation

Return Grill to Ceiling Plenum for AC-2

Figure A13-5. Attic and Ceiling Plenum

HVAC System

The building has hot water perimeter heat served by a single natural gas boiler. The high bay garages are have natural gas radiant heaters located at the ceiling. Two air handlers cool the lobby area, front office, training room, and lounge. AC-1 is a 2-ton horizontal air handler that cools the lobby, front office, and vestibule. AC-2 is a 7.5-ton air handler that serves the training room on the first floor and lounge located on the second floor. The upstairs office is cooled by a packaged terminal air conditioner (PTAC). Figure A13-6 - Figure A13-9 show the air handling equipment, boilers and perimeter heaters, and radiant heaters. Table A13- 1 lists the HVAC equipment that serves the building.

The ductwork for AC-1 and AC-2 is insulated rectangular steel ductwork with flexduct takeoffs. AC-2 is located in the ceiling space above the training room and uses the ceiling space as a return plenum. All of the supply and return diffusers are ceiling mounted. Figure A13-10 and Figure A13-11 display the zones and corresponding air handlers that served each zone within the building.

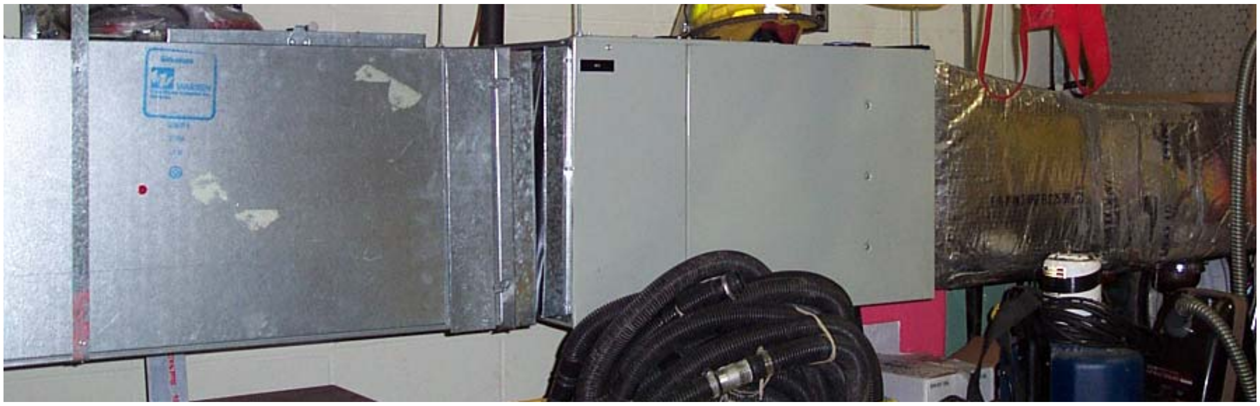

AC-1 (Cooling Only)
American Standard Inc Model: TWH030B140A0

AC-2 (Cooling Only)
Trane Climate Master, Unit Type: CCDB03AB0J, Basic Unit: H3A1R01L0AF

Figure A13-6. Air Handling Units Serving Building

CU-1 (Condenser)
Trane Model: TTB024C100A2

CU-2 (Condenser)
Trane Model: BTA0900300MB

Figure A13-7. Air Handling Units Serving Building

Boiler
Peerless Model: 85-175-WP-H

Hot Water Perimeter Heat

Figure A13-8. Hot Water Boiler and Perimeter Heat

Figure A13-9. Radiant Heaters for High Bay Garages

Table A13- 1. Summary HVAC Equipment Installed at Site

HVAC Equipment	Serves	Brand	Model	Heating Capacity (MBtu/h)	Cooling Capacity (tons)
AC-1	Lobby, Vestibule, Office	American Std. Inc.	*TWH030B140A0*	none	2
AC-2	Training Room, Lounge	Trane	*CCDB03AB0J*	none	7.5
AC-3 (PTAC)	Second Floor Office	Trane		none	
Boiler	First Floor	Peerless	*85-175-WP-H*	175	n/a

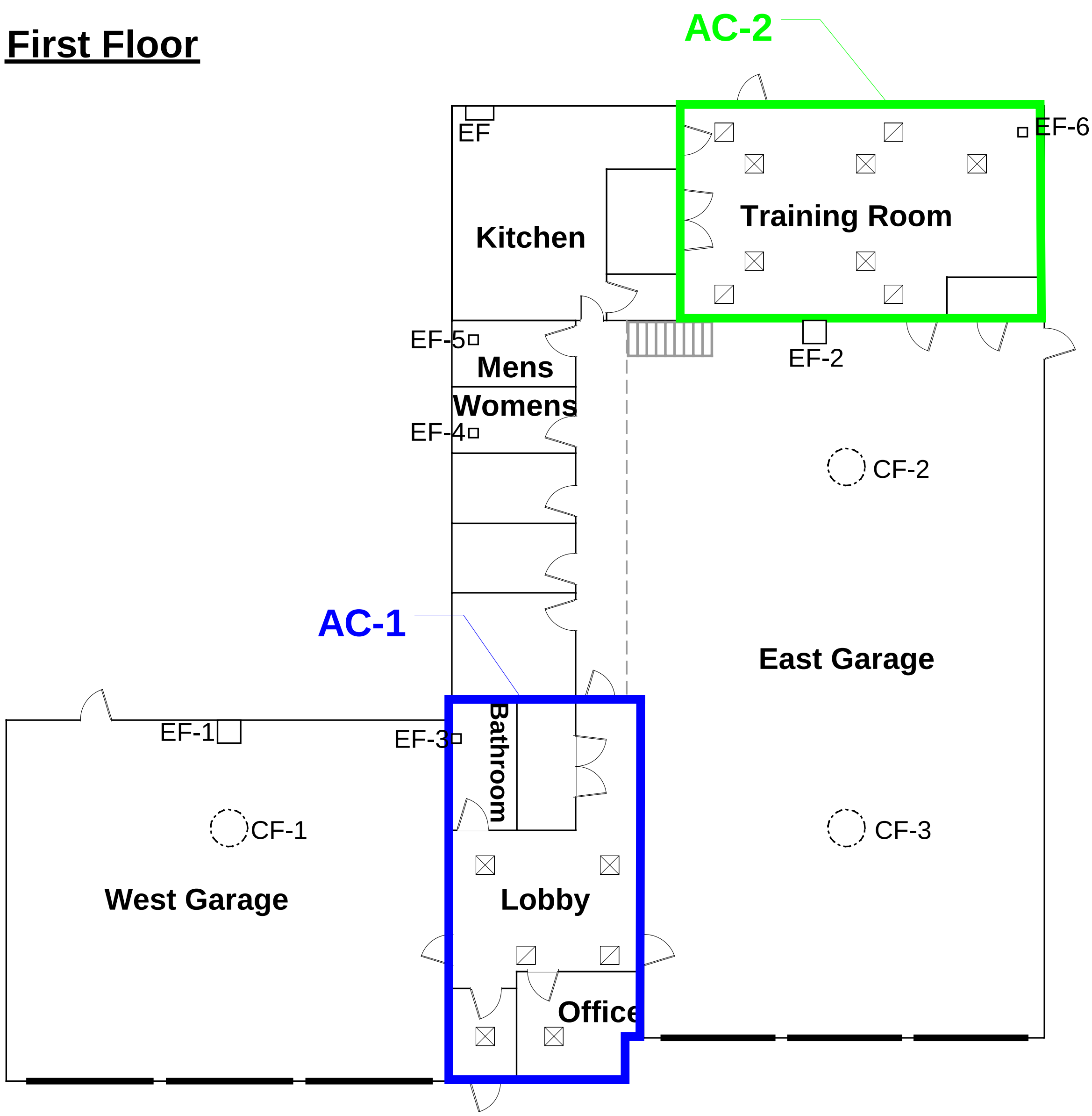

Figure A13-10. First Floor AHU Zones within Building

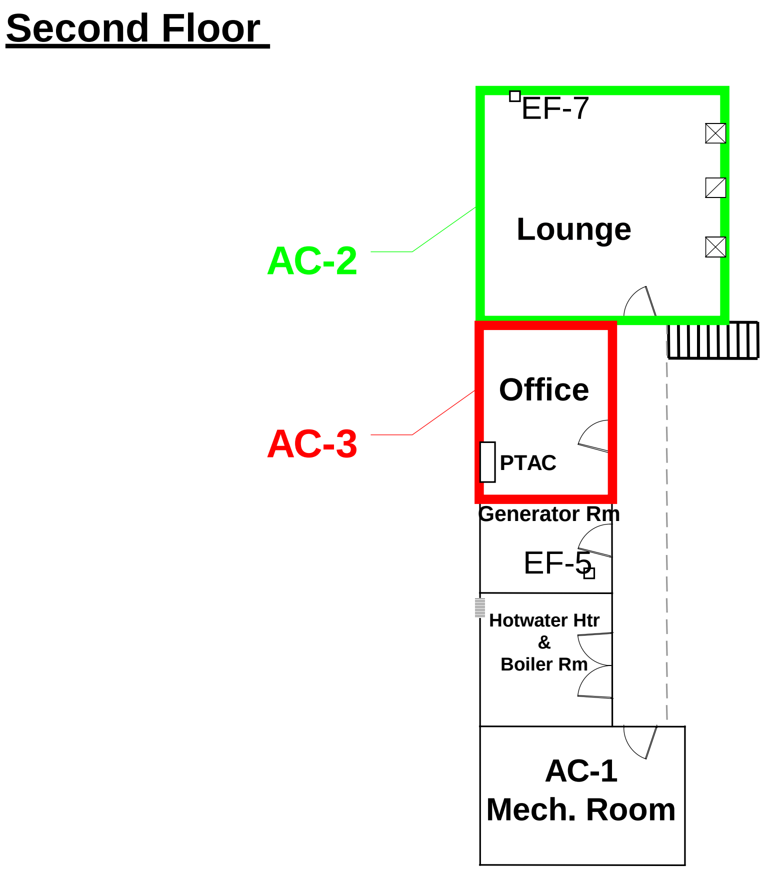

Figure A13-11. Second Floor AHU Zones within Building

The heating and cooling is controlled using standard thermostats. The heating setpoint for both AC-1 and AC-2 is 68°F. The thermostats do not allow for setback/setup and the facility personnel do not manually change the setpoint. The exhaust fans are manually controlled and used only a few times a year. The facility uses the kitchen exhaust fan less than ounce a year.

MEASUREMENTS

The test data below was taken on November 3 & 5, 2004. Blower door testing, pressure mapping, and duct leakage measurements were taken on November 3. Supply and return airflow measurements were taken at each diffuser and pressure mapping was completed with the large garage exhaust fans on. Test personnel were Mike Clarkin and Dan Gott on November 3 and Dan Gott on November 5. Dan Gott collected temperature/RH sensors on January 18, 2005.

Building Envelope Airtightness

The leakage characteristics of the building enclosure were assessed using fan pressurization methods. A single blower door was installed in the training room exit doorway at the north end of the building (labeled in Figure A13-13). All exterior doors and windows were closed. The building was tested in the following configuration:

- All interior doors open
- AHUs off
- All exhaust fans sealed
- Outdoor air intakes sealed

The building pressure was varied from 9 Pa to 33 Pa. Figure A13-12 shows the building leakage variation with building pressure.

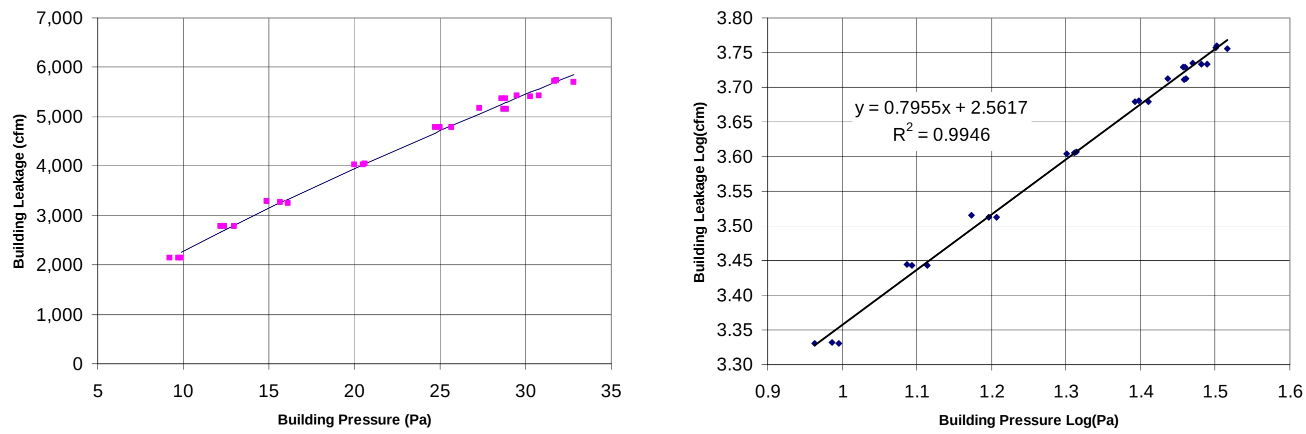

Depressurization Test – All Doors Open

Figure A13-12. Variation of Building Leakage with Pressure: cfm = K(ΔP)^n

Table A13- 2 shows the results of the blower door tests including model coefficients, effective leakage area (ELA), and air-changes-per-hour (ACH). The ELA is calculated using the Lawrence Berkeley Laboratory method, which calculates the leakage area at 4 Pa. The building has an effective leakage area of approximately 1.35 sq in per 100 sq ft of the total envelope area including floor area. Another building leakage characteristic is the ACH at 50 pascals (ACH_{50}). The building has an ACH_{50} of 4.0. This result implies that at 50 Pa, the air in the building is displaced 4 times each hour.

Table A13- 2. Blower Door Test Data, Resulting Best-Fit Model Coefficients, and ELA

Depressurization – All Interior Doors Open

Test Results:

Flow Coefficient (K)	364.5	7,876	sq ft, floor area
Exponent (n)	0.795		
Leakage area (LBL ELA @ 4 Pa)	311.1 sq in	1.35	ELA / 100 sq ft
Airflow @ 50 Pa	8,188 cfm	4.05	ACH @ 50

Test Data:

Nominal Building Pressure (Pa)	Nominal Flow (cfm)	Ring
32.8	5,693	none
31.8	5,743	none
31.7	5,709	none
30.8	5,416	none
30.3	5,405	none
29.5	5,429	none
28.9	5,154	none
28.8	5,368	none
28.7	5,145	none
28.6	5,360	none
27.3	5,166	none
25.7	4,777	none
25.0	4,792	none
24.7	4,779	none
20.6	4,045	none
20.5	4,033	none
20.0	4,016	none
16.1	3,250	none
15.7	3,259	none
14.9	3,279	none
13.0	2,774	A
12.4	2,778	A
12.2	2,783	A
9.9	2,138	A
9.7	2,147	A
9.2	2,144	A

Notes: ELA is leakage area (in square inches) at reference pressure of 4 Pa.
ELA per 100 sq ft is based on total building envelope surface area (ceiling, exterior walls and floor).

Pressure Mapping (Blower Door Testing)

Pressure readings in the building were taken using a digital micromanometer (DG 700) with the blower door operating. The pressure difference across the building envelope was 49 Pa. The lobby was 2 Pa negative to the plenum and the training room is 0.4 Pa negative the plenum. The attic was 12.2 Pa negative to the mechanical room for AC-1. This implies that the leakage area from the occupied space to the ceiling plenum is large and that the plenum is closely coupled to the conditioned space. The gypsum board mounted to the bottom chord of the roof trusses is the primary air barrier and the thermal barrier is fiberglass batt insulation located on top of the gypsum board.

Pressure measurements were taken between interior rooms with doors closed. Figure A13-13 and Figure A13-14 show the pressure differences induced across the doorways with the open portion of the building depressurized. With the building depressurized to 49 Pa, pressures across the doorways ranged between 0.0 and 27.5 Pa. The large pressure differences (20.5 – 27.5 Pa) between the depressurized open space and the lobby on the first floor and the three mechanical rooms implies that these spaces are well connected to the outdoors. The pressure mapping was completed with all the interior doors closed except the training room door leading to the east garage. The doors were left in the same configuration for all pressure measurements.

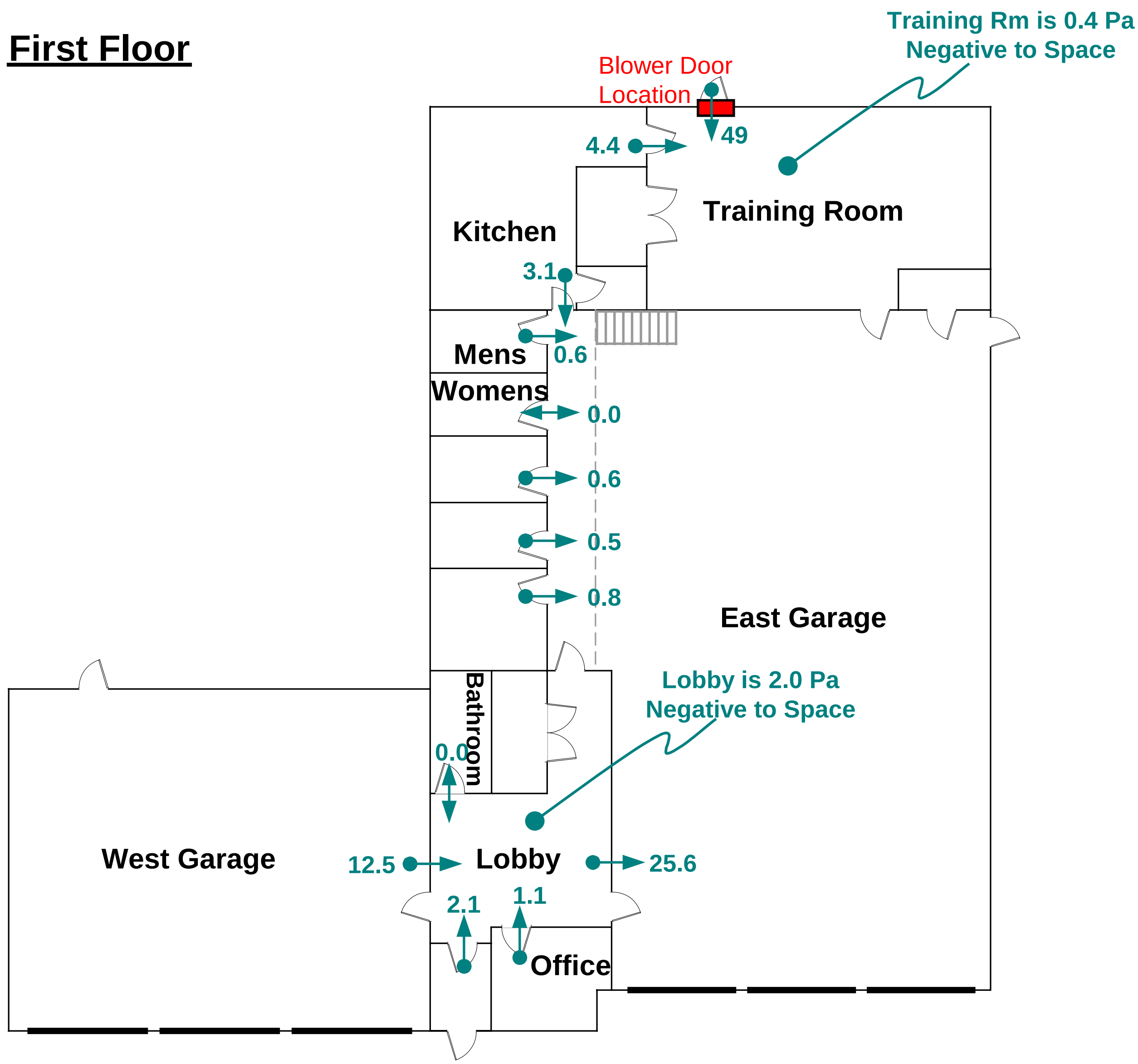

Figure A13-13. First Floor Room-to-Corridor Pressures with Building Depressurized to 49 Pa

Second Floor

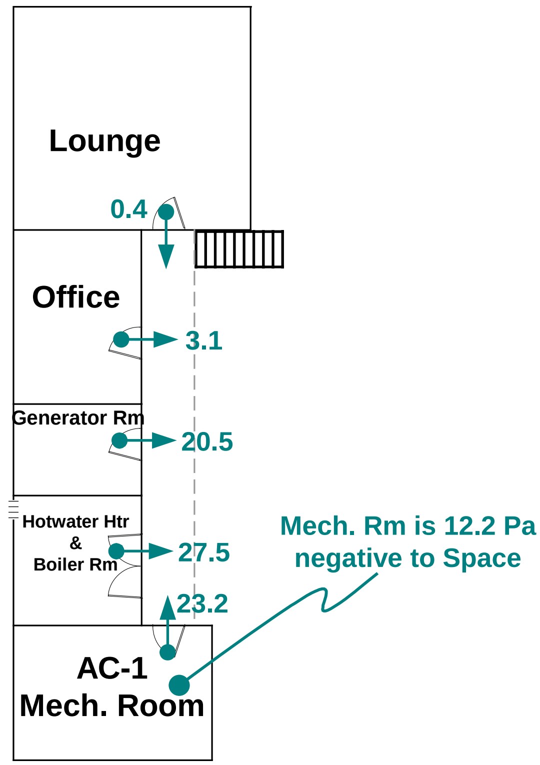

Figure A13-14. Second Floor Room-to-Corridor Pressures with Building Depressurized to 20 Pa

HVAC Airflow Measurements

The airflow from each supply diffuser was measured using a Shortridge flow hood. The total supply airflow is approximately 1,893 cfm or 0.82 cfm per sq-ft of floor area[1]. Figure A13-15 and Figure A13-16 display the airflow at each diffuser and exhaust on the first floor and second floor.

[1] Floor area served by AC-1 and AC-2 (2310 sq-ft).

First Floor

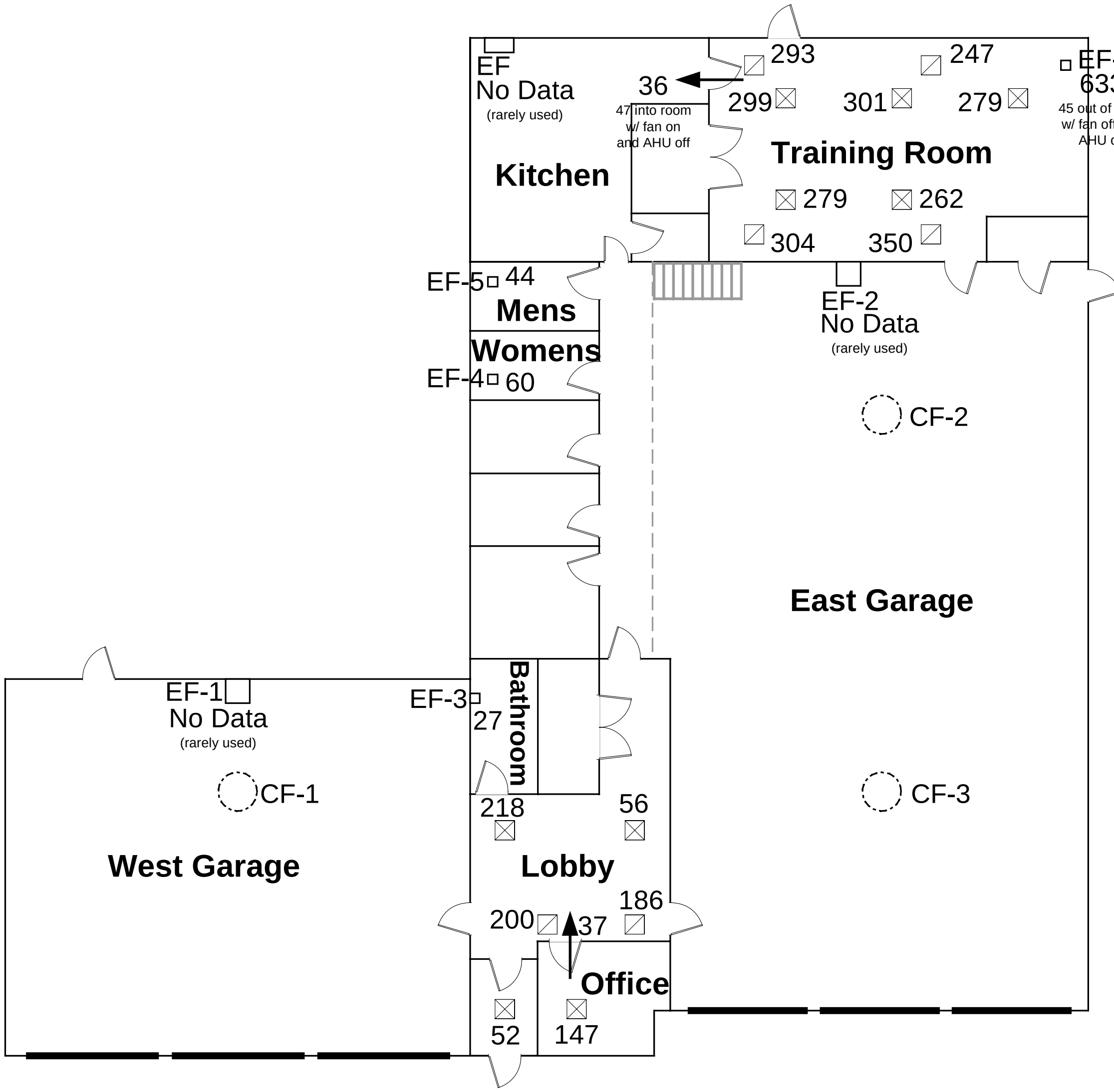

Figure A13-15. First Floor Supply and Return Airflow Measurements (cfm)

Second Floor

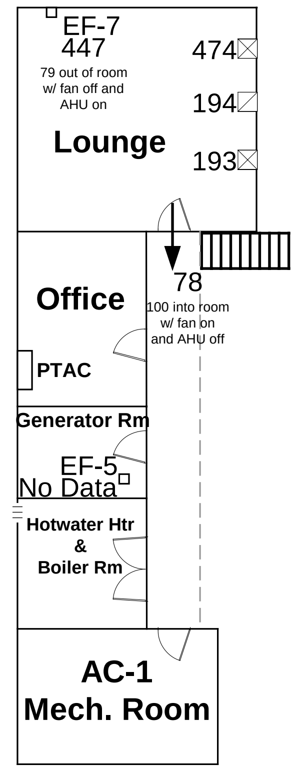

Figure A13-16. Second Floor Supply and Return Airflow Measurements (cfm)

Table A13- 3. Comparison of Supply and Return Airflow Measurements

AHU	Serves	Flowhood Supply Airflow (cfm)	Flowhood Return Airflow (cfm)	Supply / Return Ratio	Return Type	Measured Supply Fan Power (kW)	Normalized Supply Fan Power (W/cfm)	Supply Static (Pa)	Return Static (Pa)
AC-1	Lobby & Front Office	473	386	1.2	Ducted	0.36	0.76	32.5	-16.8
AC-2	Training Room & Lounge	1,420	1,194	1.2	Ceiling Plenum				
Total		***1,893***	***1,580***	***1.2***					

Pressure Mapping (AHU Fans On)

The air pressure relationships in the building were also determined with the air handling units on and with the east and west garage exhaust fans on. The graphics in Figure A13-17 and Figure A13-18 show the pressure differences induced across the doorways with the AHU fans on and the doorways closed. Operation of the AHUs created interior pressure differences up to 1.5 Pa. The building was pressurized with respect to outdoors between 0.4 Pa and 8.7 Pa with an average of approximately 4 Pa.

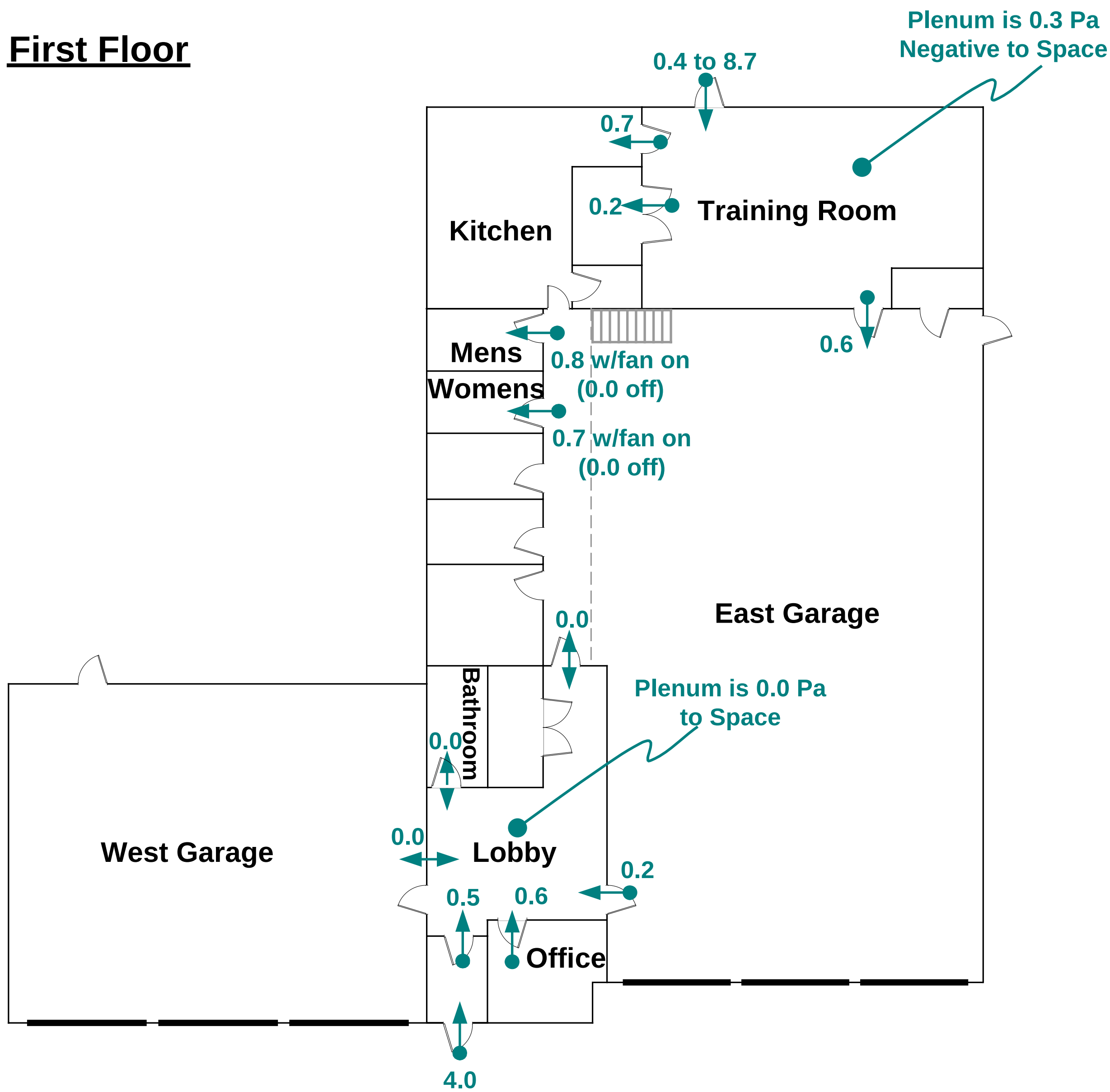

Figure A13-17. First Floor Pressure Differences between Rooms with AHU Fans On

Second Floor

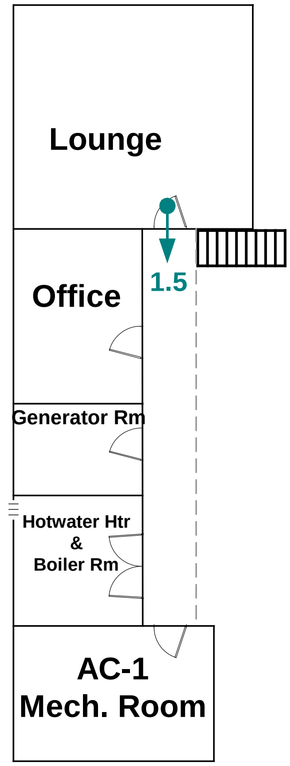

Figure A13-18. Second Floor Pressure Differences between Rooms with AHU Fans On

The air pressure relationships in the building were also determined with the large exhaust fans operating for the east and west garages. The graphics in Figure A13-19 through Figure A13-21 show the pressure differences induced across the doorways with the each exhaust fan operating separately. Operation of the AHUs created interior pressure differences up to 1.5 Pa. The building was pressurized with respect to outdoors between 0.4 Pa and 8.7 Pa with an average of approximately 4 Pa.

First Floor

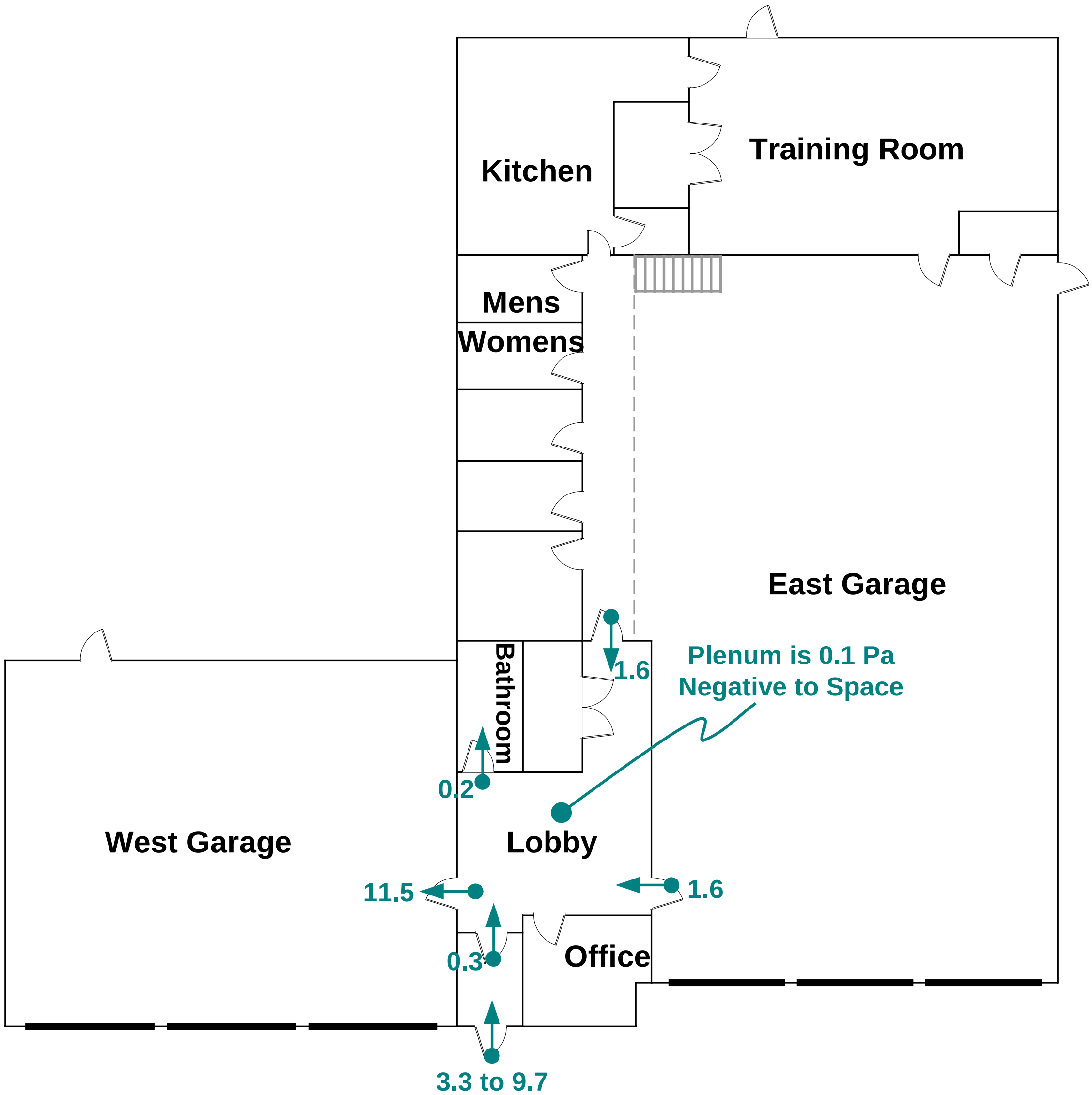

Figure A13-19. First Floor Pressure Differences between Rooms with West Garage Exhaust On (EF-1)

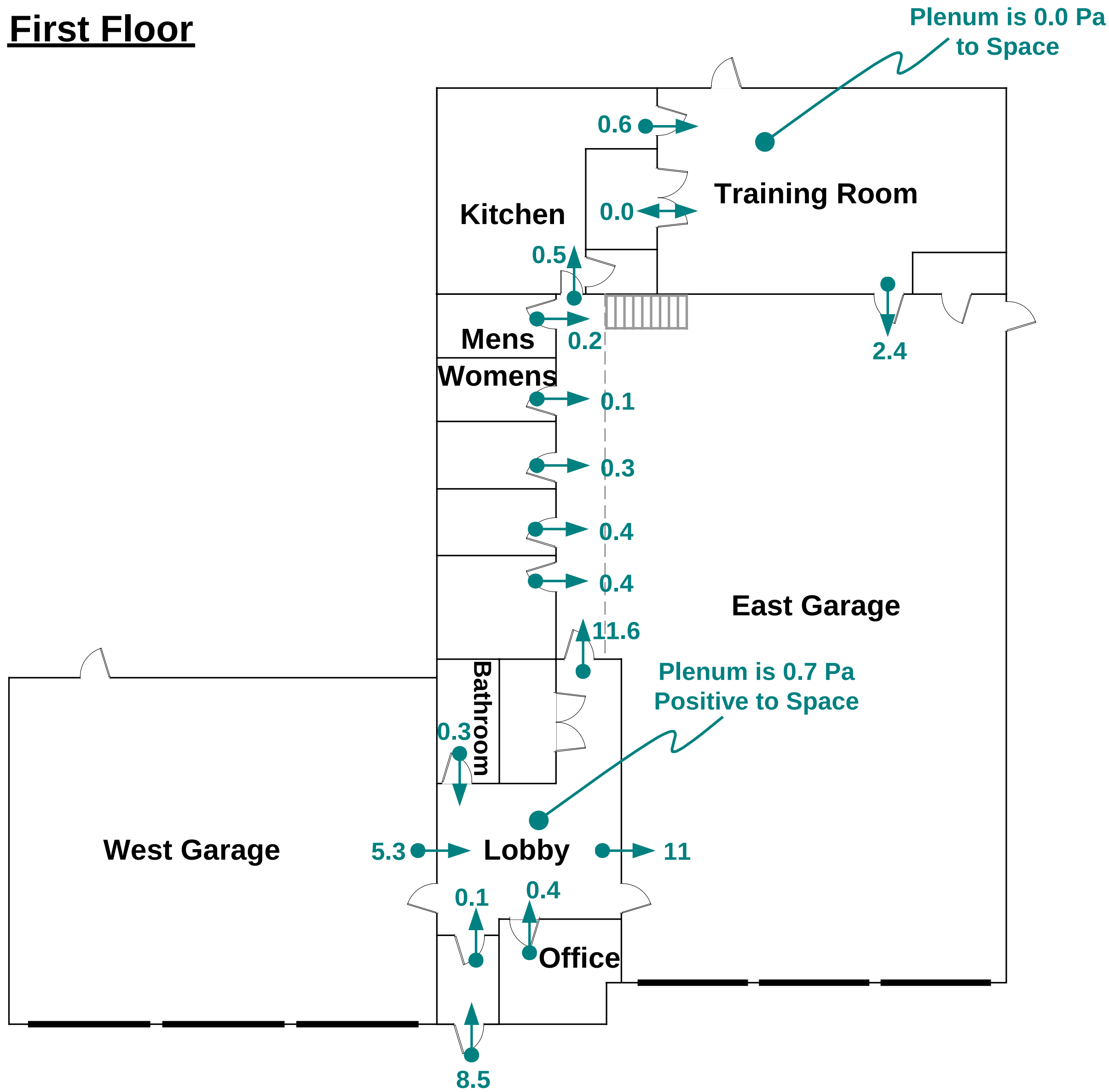

Figure A13-20. First Floor Pressure Differences between Rooms with <u>East Garage Exhaust On (EF-2)</u>

Second Floor

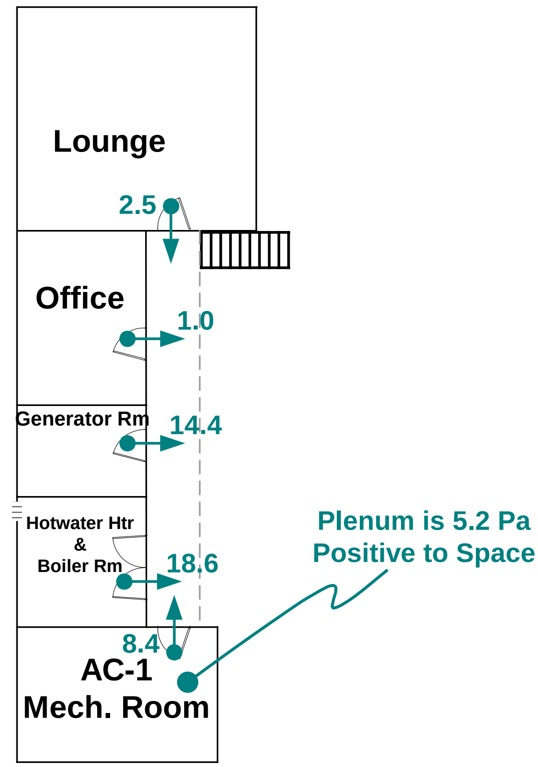

Figure A13-21. Second Floor Pressure Differences between Rooms with <u>East Garage Exhaust On (EF-2)</u>

Duct Leakage Measurements

A Duct Blaster was used to depressurize the ductwork to measure leakage rates. The air distribution system was tested for AC-1 (lobby, vestibule, front office). The Duct Blaster fan was connected to the return trunk using an access door. First, the furnace filter was removed and the entire system was tested for leakage. The static pressure tap was located in the return plenum. There was a 10 Pa pressure drop across the furnace when the return ductwork was depressurized 84 Pa. The return ductwork was also tested separately by creating a seal at the furnace filter. The filter was wrapped in duct mask, inserted, and sealed around the edges with duct tape. We verified that the return side was isolated from the supply side by depressurizing the return ductwork and measuring the static pressure on the supply side. With the return side depressurized by 123 Pa, the static pressure on the supply side measured only 0.8 Pa depressurized. The static pressure tap was located in the return plenum.

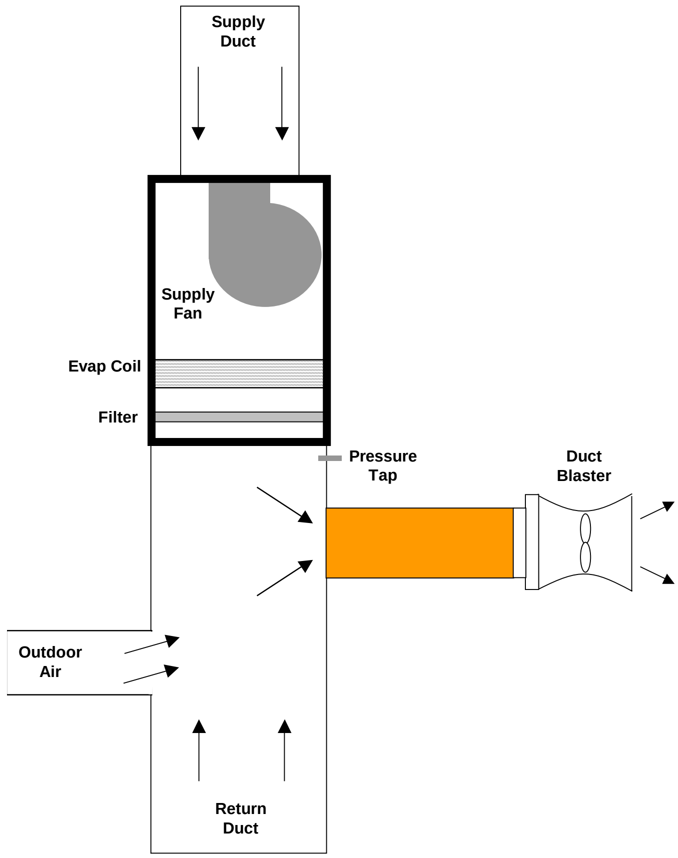

Figure A13-22. Duct Blaster Setup for Roof Top Units

As a diagnostic check on the degree of pressurization, the pressure at each supply diffuser was measured by puncturing the plastic covering at each diffuser with a very small probe. Figure A13-23 shows the resulting pressures measured at each supply diffuser for AC-1 with the system depressurized. The return ductwork was depressurized 84 Pa and the supply ductwork was depressurized 74 Pa (measured at the unit). The diffusers with large variation from the static pressure measure at the unit are connected to a relatively leaky duct.

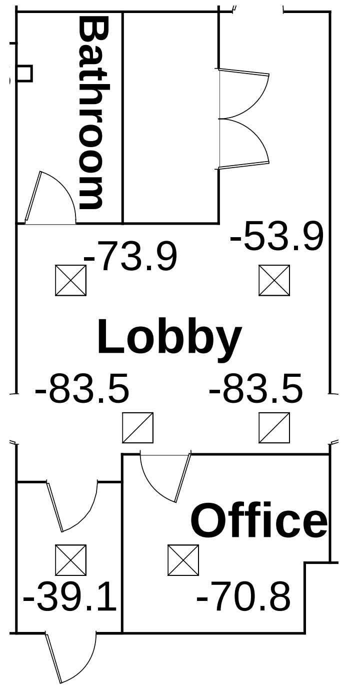

Figure A13-23. AC-1 Diffuser Pressures (Pa) with Ductwork Depressurized

Figure A13-24 shows the resulting measured data from the duct leakage tests fit to a power function (raw data in Table A13- 4). Figure A13-24 also shows our best estimate for duct leakage during normal operation, which uses one half of the plenum pressure as suggested in ASHRAE Standard 152P section B.2. Table A13- 5 shows the resulting coefficients, exponents, and regression statistics. Table A13- 6 summarizes the resulting duct leakage rates and ELA at a reference pressure of 25 Pa. As shown in Figure A13-24, the return duct leakage at normal operating static pressure (-8.4 Pa) for the AC-1 is estimated to be 64 cfm. Duct leakage for this building has little effect on energy use since all of the ductwork in this building is inside the primary air and thermal barrier. To verify the duct leakage measurements using fan pressurization we compared the supply airflow at the plenum for AC-1 to the total supply airflow measured at the diffusers. The difference in supply airflow at the unit and the airflow measured at the diffusers yield ductwork leakage of 1,201 cfm and the fan pressurization test estimates 1,049 cfm of leakage.

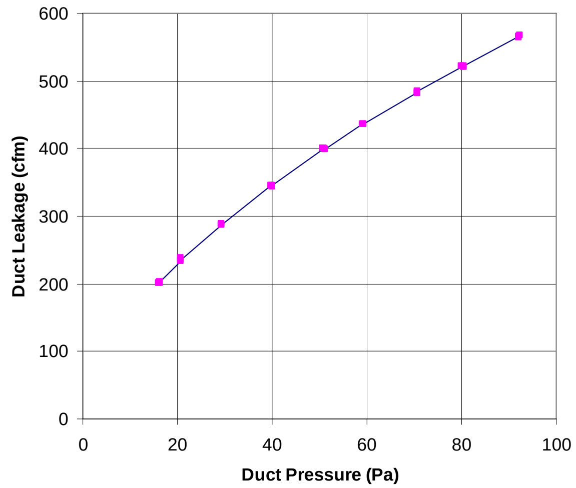

AC-1 (Entire Air Distribution System)

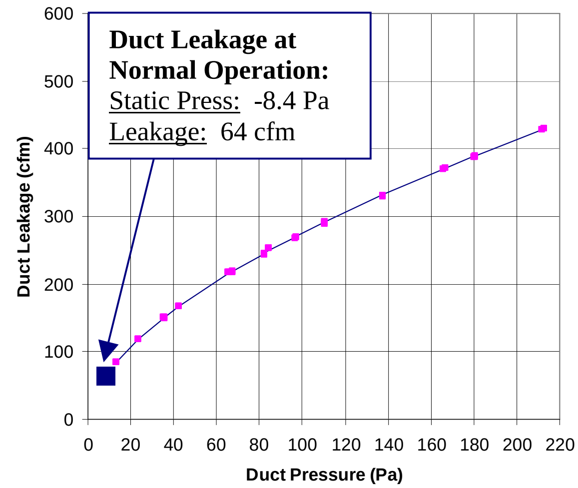

AC-1 (Return and Ventilation Ductwork)

Figure A13-24. Duct-Blaster Tests on AC-1 Ductwork

Table A13- 4. Raw Data from Duct-Blaster Tests

AC-1 (Entire Air Distribution System)

Test Results:

Flow Coefficient (K)	39.2	
Exponent (n)	0.590	
Leakage area (LBL ELA @ 25 Pa)	30	sq in
Airflow @ 25 Pa	262.1	cfm

Test Data:

	Nominal Duct Pressure (Pa)	Nominal Flow (cfm)	Ring
1	92.3	567	A1
2	92.1	566	A1
3	92.0	565	A1
4	80.5	522	A1
5	80.5	521	A1
6	80.0	522	A1
7	70.8	485	A1
8	70.6	483	A1
9	70.6	482	A1
10	59.3	437	A1
11	59.2	436	A1
12	59.1	436	A1
13	51.1	399	A1
14	51.0	400	A1
15	50.8	400	A1
16	40.0	345	A1
17	39.9	344	A1
18	39.8	346	A1
19	29.2	287	A1
20	29.2	287	A1
21	29.2	288	A1
22	20.7	239	A1
23	20.6	233	A1
24	20.6	235	A1
25	16.2	201	A1
26	16.2	202	A1
27	16.1	201	A1

AC-1 (Return and Ventilation Ductwork)

Test Results:

Flow Coefficient (K)	18.4	
Exponent (n)	0.587	
Leakage area (LBL ELA @ 25 Pa)	14	sq in
Airflow @ 25 Pa	122.0	cfm

Test Data:

	Nominal Duct Pressure (Pa)	Nominal Flow (cfm)	Ring
1	213.0	430	A1
2	213.0	429	A1
3	212.0	428	A1
4	180.7	390	A1
5	180.5	387	A1
6	180.0	387	A1
7	166.8	372	A1
8	166.0	370	A1
9	165.9	370	A1
10	137.5	331	A1
11	137.5	330	A1
12	137.4	331	A1
13	110.7	289	A1
14	110.5	292	A1
15	110.3	290	A1
16	97.0	269	A1
17	97.0	269	A1
18	96.7	268	A1
19	84.6	253	B2
20	84.6	253	B2
21	84.4	253	B2
22	82.4	245	A1
23	82.3	245	A1
24	82.2	244	A1
25	67.7	219	A1
26	67.7	217	A1
27	67.7	218	A1
28	65.8	218	B2
29	65.7	218	B2
30	65.6	217	B2
31	42.6	167	B2
32	42.5	167	B2
33	42.4	167	B2
34	35.6	151	B2
35	35.6	150	B2
36	35.5	151	B2
37	23.7	118	B2
38	23.6	118	B2
39	23.6	118	B2
40	13.4	84	B2
41	13.4	84	B2
42	13.4	84	B2

Table A13- 5. Coefficients, Exponents and Regression Statistics from Duct-Blaster Tests

	AC-1 Lobby & Office		
	K	**n**	**R^2**
Entire System & AHU Cabinet	39.2	0.590	99.98%
Return Ductwork	18.4	0.587	99.98%

Notes: cfm = $K(Pa)^n$ / R^2 indicates fit of linear log-log regressic

Table A13- 6. Supply and Return Airflow Measurements

	AC-1 (Lobby and Front Office)		
	Diffuser Airflow (cfm)	**Leakage (cfm @ 25)**	**ELA (sq in @ 25)**
Entire System & AHU Cabinet	n/a	262	29.7
Return Ductwork	386	122	13.8
Estimated Supply Ductwork	473	140	15.9

Notes: Leakage and ELA at reference pressure of 25 Pa

Table A13- 7 lists the ductwork used to estimate the supply and return duct area for AC-1. The effective leakage area compared to the duct surface area for AC-1 is shown in Table A13- 8. The Sheet Metal and Air Conditioning Contractors' National Association (SMACNA) classifies duct leakiness using duct leakage per 100 sq ft of duct area at a pressure of 1-in w.g.

Table A13- 7. RTU Ductwork Size and Area

	Type/Size	Length (ft)	Duct Area (sq ft)
Supply Trunks	11.75" x 16.5"	49.0	230.7
Supply Takeoffs	10" dia.	18.8	49.1
Return Trunks	20" x 25"	5.0	37.5
	11.75" x 16.5"	29.0	136.5
Return Takeoffs	10" dia.	6.5	17.0
Ventilation Duct	11.5" x 16"	34.0	155.8
AHU Cabinet	approx. 20" x 25"	3.0	22.5
Total			***649.2***

Table A13- 8. Duct Leakage per 100 Square Foot of Duct Area

	Duct Area (sq ft)	ELA (sq in @ 25)	ELA/100 sq ft Duct Area (sq in @ 25)	Leakage (cfm @ 25 Pa)	Supply CFM per ft^2 Duct Area (cfm/ sq-ft)	Leakage per 100 sq ft Duct Area (cfm @ 25 Pa)	SMACNA Leakage Class cfm per 100 sq ft (cfm @ 1-in water)
Entire System	649	30	4.6	262	n/a	40	157
Return and Ventilation Ducts	346.9	14	4.0	122	n/a	35	136
Estimated Supply and Cabinet	302.3	16	5.3	140	1.56	46	---

Table A13- 9 shows the airflow balance for AC-1. Three airflow balance estimates are calculated as follows:

Gross Airflow Balance:

$$\Delta_{gross} = \text{Supply Diffuser cfm} - \text{Return Diffuser cfm} - \text{Ventilation cfm}$$

Net Airflow Balance Using CFM_{25}:

$$\Delta_{N25} = (\text{Supply Diffuser cfm} + \text{Supply Leakage @ 25 Pa}) - (\text{Return Diffuser cfm} + \text{Return Leakage @ 25 Pa}) - \text{Ventilation cfm}$$

Net Airflow Balance Using Average "Actual Static" in Ductwork:

$$\Delta_{Ncorrected} = (\text{Supply Diffuser cfm} + \text{Supply Leakage @ Actual Static}) - (\text{Return Diffuser cfm} + \text{Return Leakage @ Actual Static}) - \text{Ventilation cfm}$$

The last estimate for the RTU airflow balance ($\Delta_{Ncorrected}$) uses our best estimate for average "actual static" pressure in the ductwork during normal operation, which is one half of the plenum pressure as suggested in ASHRAE Standard 152P section B.2. Table A13- 9 uses an estimate for ventilation airflow based on the supply return ratio since we did not measure the outdoor airflow to this unit. For this ductwork, the net airflow estimate resulting in the smallest error is Δ_{N25} for AC-1. The net airflow balance estimate with the value closest to zero gives the most accurate results for airflow combined with duct leakage. Figure A13-25 shows a diagram of the horizontal air handler including the supply, return, and ventilation airflows as well as the duct leakage for the best estimate in airflow balance.

Table A13- 9. Airflow Balance for Roof Top Units

	AC-1
Diffuser Supply (cfm)	473
Diffuser Return (cfm)	386
Ventilation (cfm) - estimate	87
Supply Leakage - cfm25	140
- actual static	109
Return Leakage - cfm25	122
- actual static	64
∆gross	0
∆N25	18
∆Ncorrected	44

1) Note: "actual static" is the static pressure measured in supply/return trunk.
2) Ventilation estimate base on supply/return ratio.

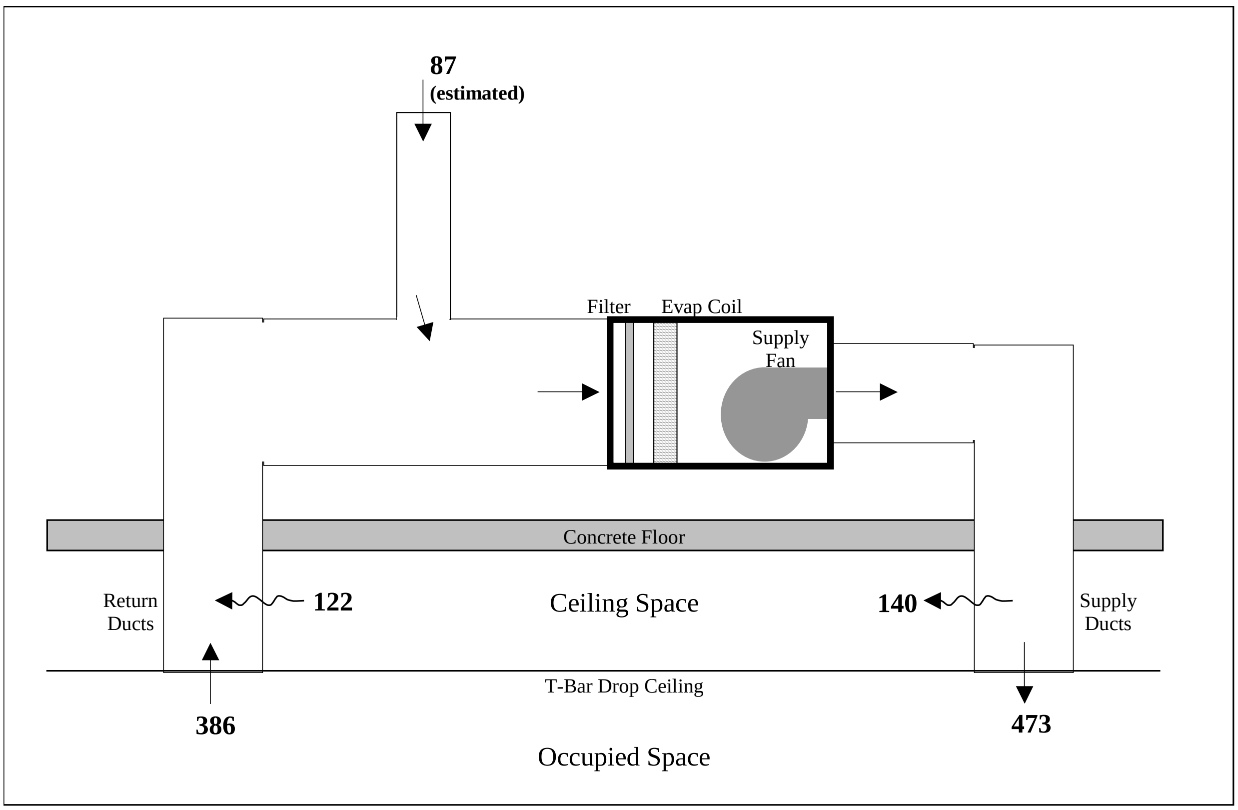

Figure A13-25. Airflow Balance for AC-1

Space Conditions

Figure A13-26 shows the average temperature profiles based on temperature readings taken with a HOBO data logger from November 5, 2004 to February 18, 2005. The thick line shows the average for each hour while the shaded region corresponds to one standard deviation about the average. The dotted lines correspond to the minimum and maximum for each hour. Sensors were placed in the lobby and training room.

The building uses standard on/off thermostats with no setback for the evening or weekends. The profile plots in Figure A13-26 confirm that there is no heating setback. The average room temperature during the monitoring period was 67.4°F for the Lobby and 64.7°F for the training room.

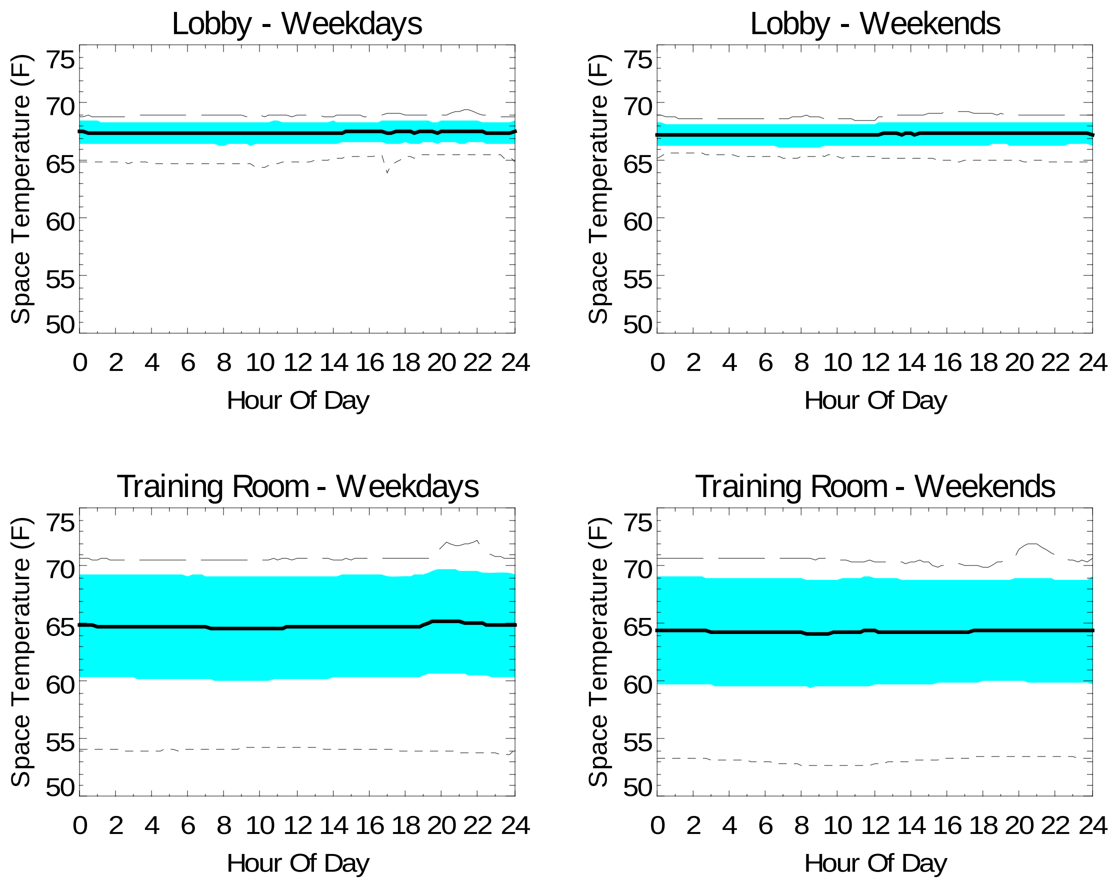

Figure A13-26. Measured Space Temperature Profiles

The following plots show the relative humidity for this building. The maximum relative humidity in the lobby and training room was 64.5% during the monitoring period. Figure A13-30 displays the conditions inside the building compared with the ASHRAE comfort zone for cooling shown by the shaded region on the plot.

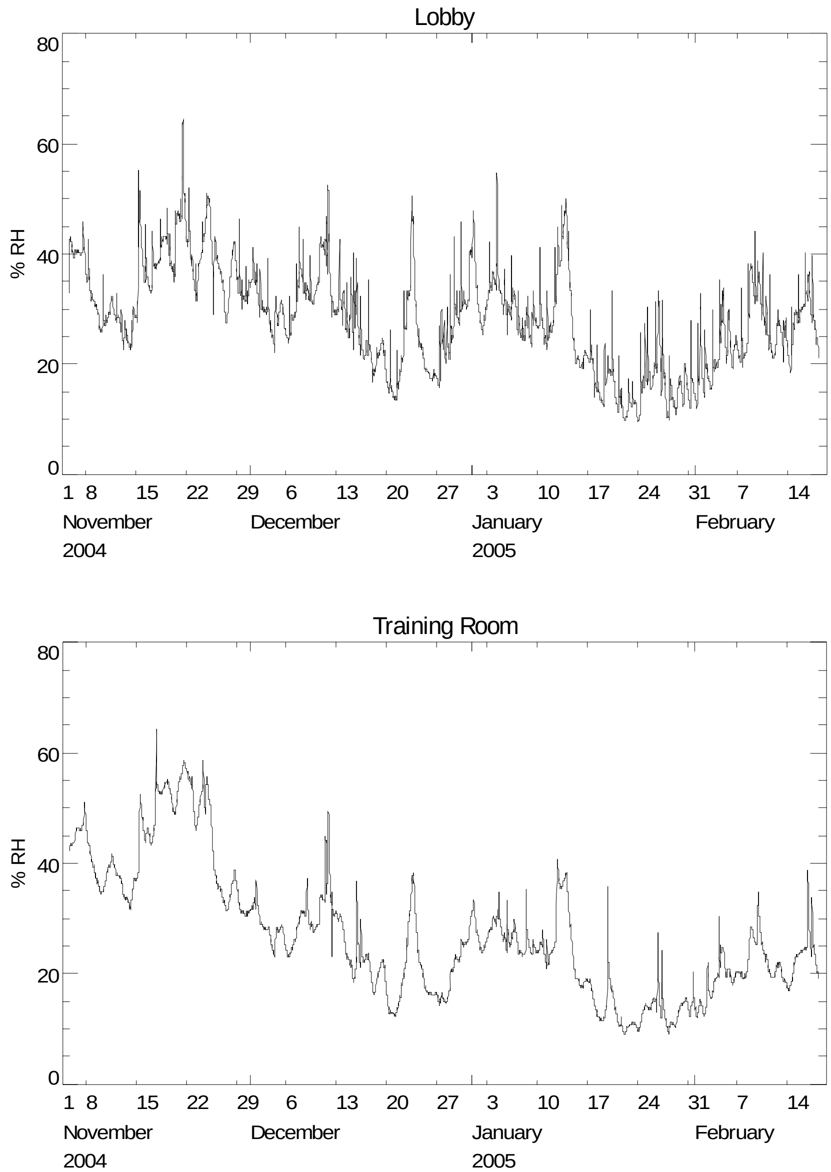

Figure A13-27. Measured Relative Humidity

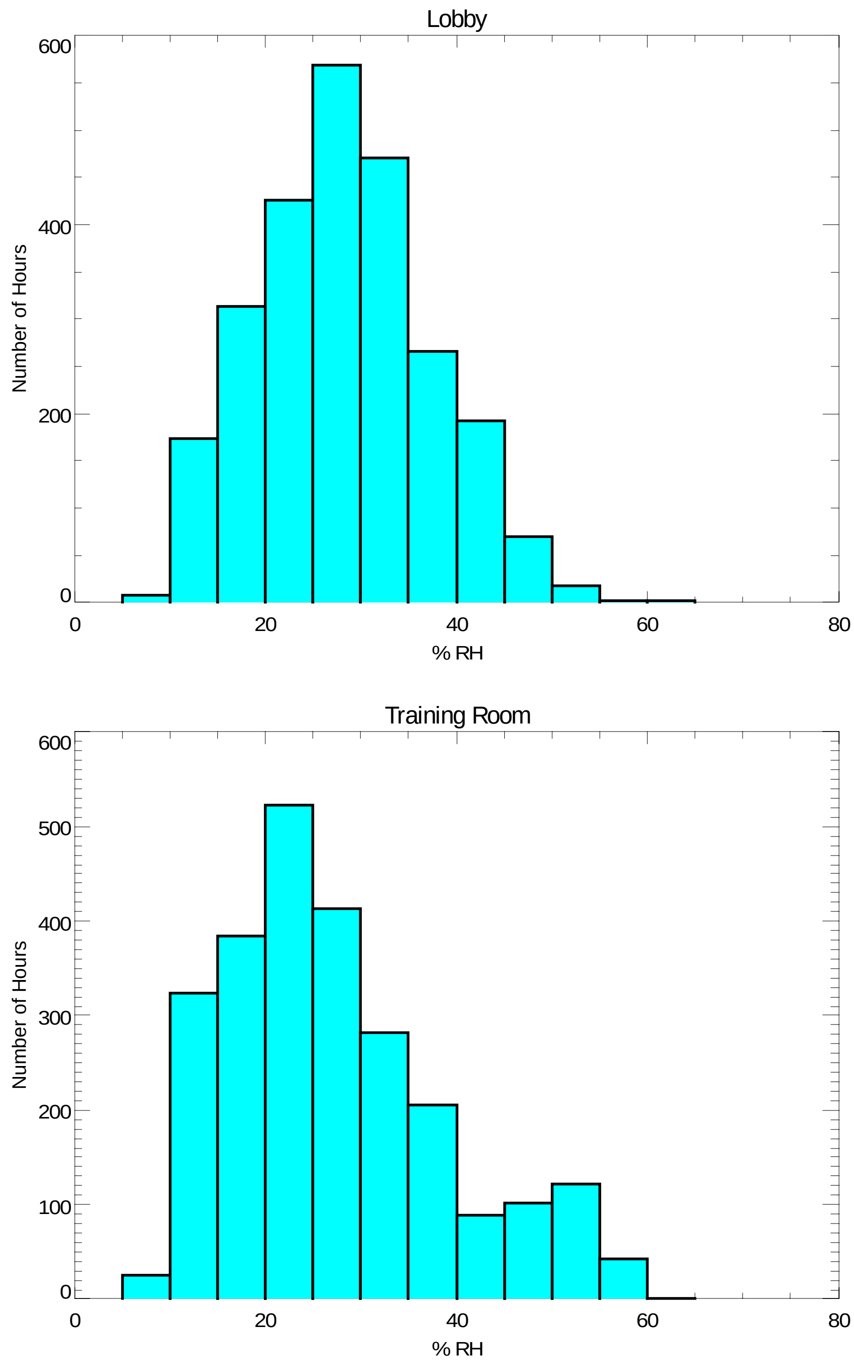

Figure A13-28. Duration of Relative Humidity Levels

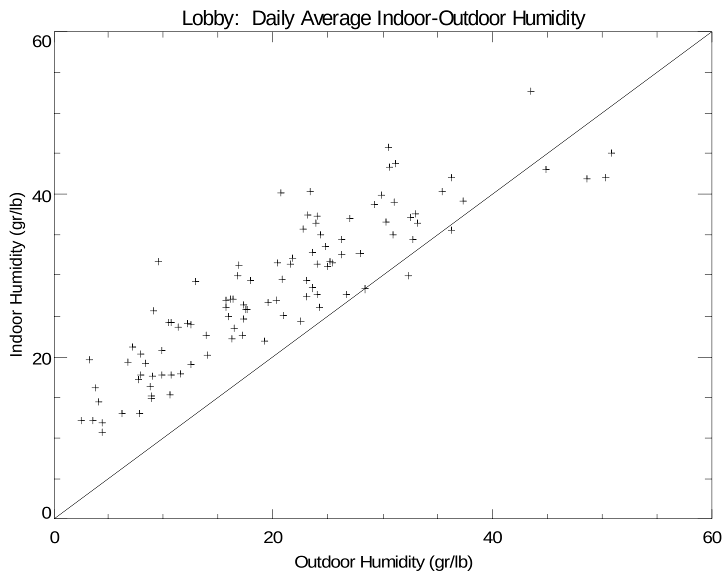

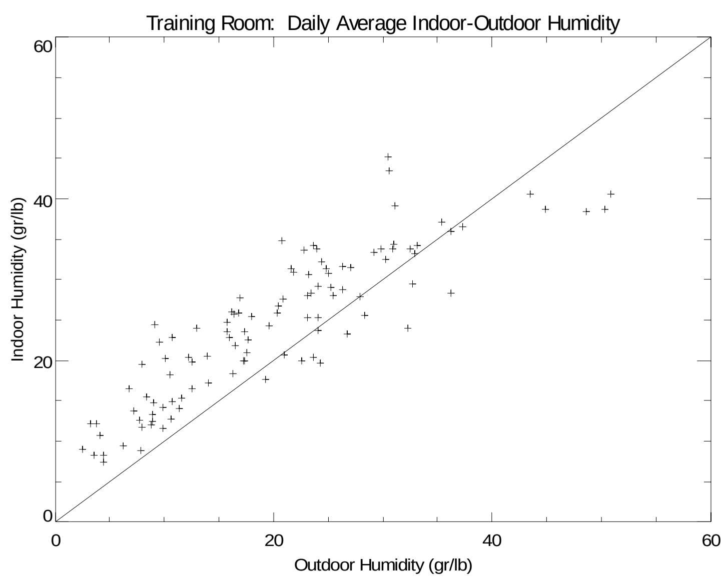

Figure A13-29. Indoor Humidity Variation with Outdoor Humidity

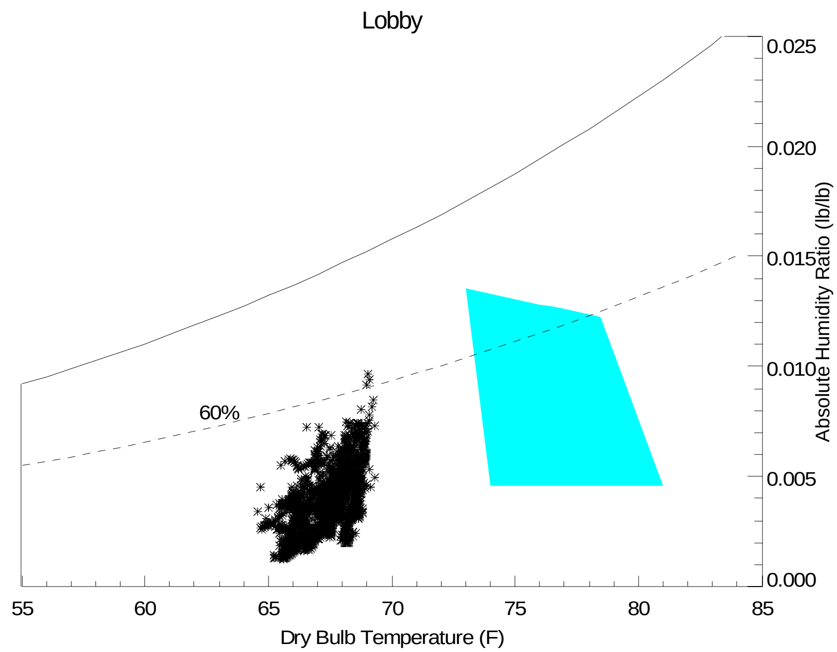

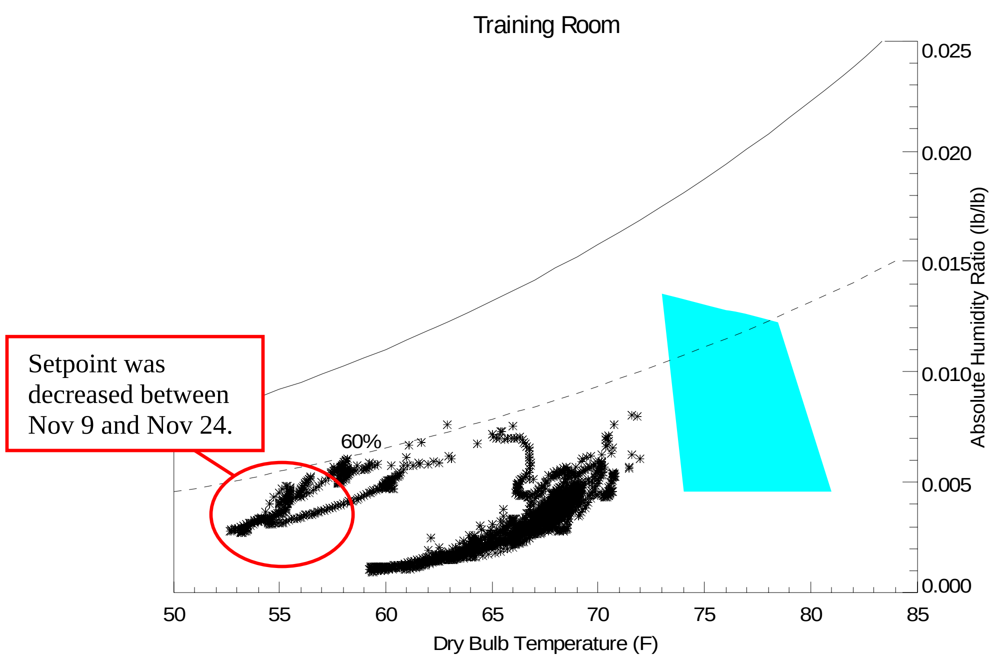

Figure A13-30. Indoor Air Quality Comparison with ASHRAE Comfort Zone for Cooling

Utility Bills

Gas use is primarily used for space heating. The tables and graphs below show the gas and electric use trends for the facility. The overall energy use index for the building is summarized below.

	Gas Use Index (MBtu/ft^2-year)	Electric Use Index (kWh/ft^2-year)
2004	37.5	2.8

Table A13- 10. Summary of Electric Bills

	Days in Month	Demand (kW)	Energy (kWh)	Cost ($)	$/kWh	Elec. Use per Sq-Ft (kWh/sq ft)
1/20/2004	34	21.6	2,960	498.68	0.17	0.30
2/20/2004	31	14.0	2,200	374.65	0.17	0.22
3/18/2004	27	11.6	1,880	321.71	0.17	0.19
4/20/2004	33	15.2	2,360	404.52	0.17	0.24
5/18/2004	28	16.4	1,880	349.77	0.19	0.19
6/17/2004	30	13.6	2,040	336.05	0.16	0.21
7/20/2004	33	18.8	2,360	405.81	0.17	0.24
8/19/2004	30	20.8	2,480	438.35	0.18	0.25
9/17/2004	29	18.8	2,360	420.46	0.18	0.24
10/18/2004	31	14.0	2,040	353.43	0.17	0.21
11/15/2004	28	24.4	2,080	449.91	0.22	0.21
12/16/2004	31	12.4	2,400	365.24	0.15	0.24
2004	365	24.4	27,040	$4,719	0.17	2.76

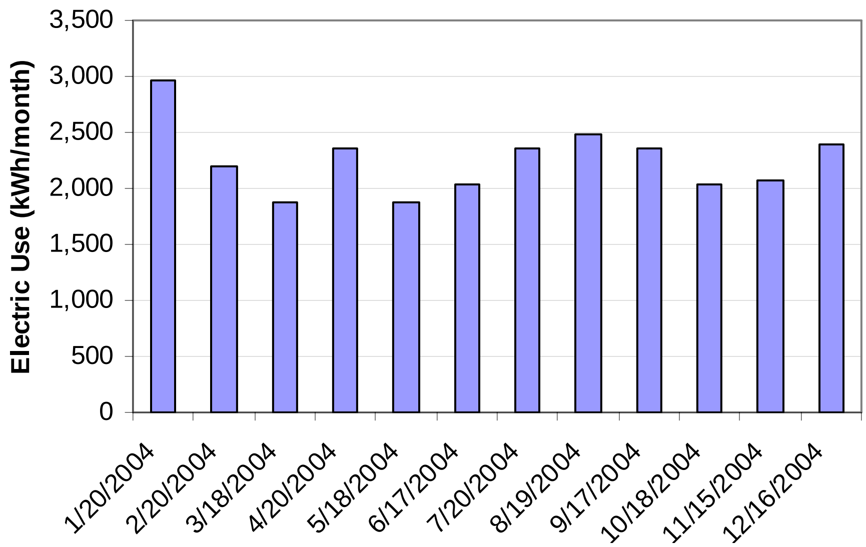

Figure A13-31. Monthly Electricity Use Trends

Table A13- 11. Summary of Gas Bills

	Days in Month	Gas Use (therms)	Cost ($)	$/therm	Gas Use per Sq-Ft (therm/sq ft)
1/20/2004	34	837	782.56	0.93	0.085
2/20/2004	31	808	772.77	0.96	0.082
3/18/2004	27	452	441.95	0.98	0.046
4/20/2004	33	453	434.21	0.96	0.046
5/18/2004	28	160	184.48	1.15	0.016
6/17/2004	30	50	70.97	1.42	0.005
7/20/2004	33	34	55.07	1.62	0.003
8/19/2004	30	32	53.73	1.68	0.003
9/17/2004	29	26	45.06	1.73	0.003
10/18/2004	31	92	106.42	1.16	0.009
11/16/2004	29	184	216.16	1.17	0.019
12/16/2004	30	543	622.65	1.15	0.055
2004	365	3,671	$3,786	1.03	0.375

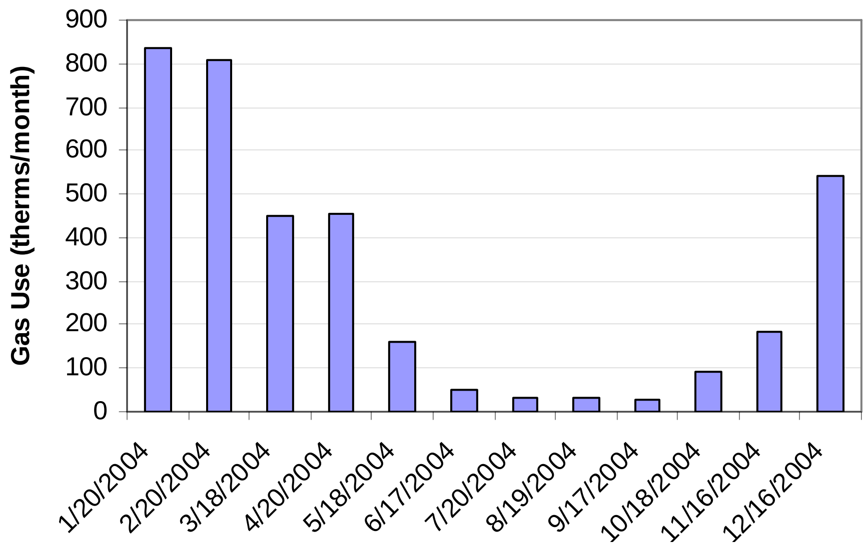

Figure A13-32. Monthly Gas Use Trends

Figure A13-33 shows the gas use variation with ambient temperature and Figure A13-34 shows the electricity use variation with ambient temperature.

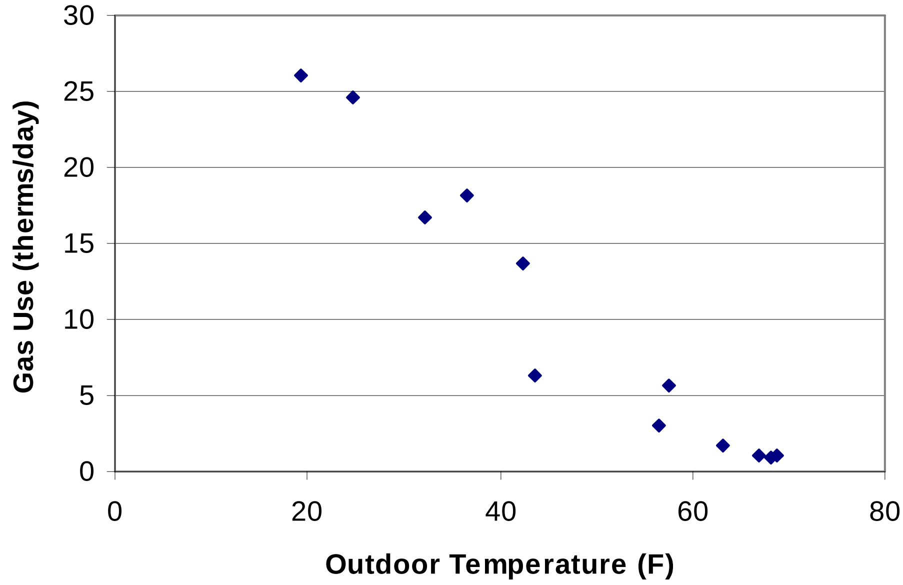

Figure A13-33. Variation of Gas Use with Ambient Temperature

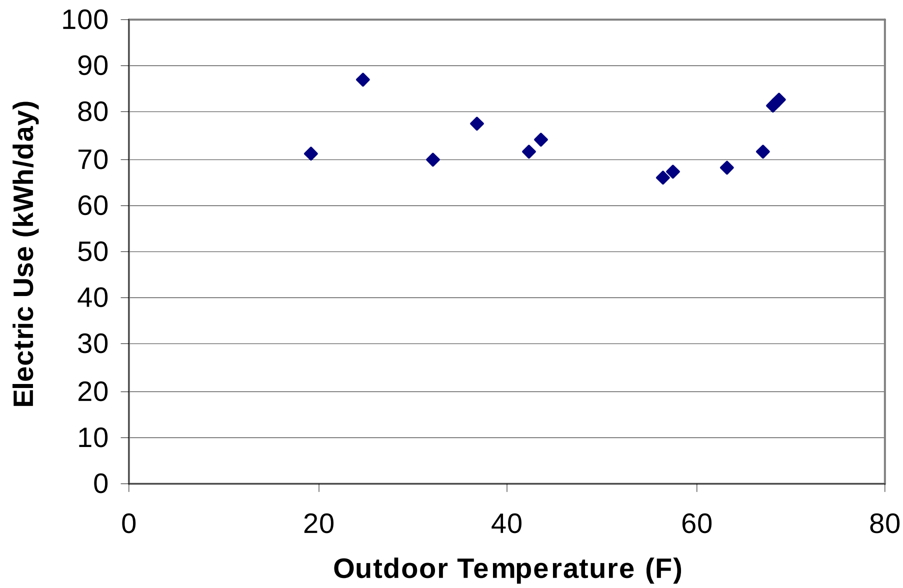

Figure A13-34. Variation of Electric Use with Ambient Temperature

Field Test Site 14 – Office Building (911 Dispatch Center), Ithaca, NY

Main Entrance (Southwest)

Rear of Building (Northeast)

Figure A14-1. Photos of Building

CHARACTERISTICS

Building Description

The 12,600 sq-ft facility is a single story office building, built in 2004, and designed specifically for an emergency response center. Figure A14-1 shows a photos of the building from the southwest and northeast corner. Two variable air volume (VAV) air handlers heat and cool the majority of the building. A third constant volume air handler heats and cools the network room. The garage is heated with radiant heaters and a natural gas unit heater. There are approximately six electric wall heater units in the vestibules and restrooms. Two boilers and a single chiller provide hot water and chilled water to the air handlers for heating and cooling. Figure A14-2 presents the building floor plan.

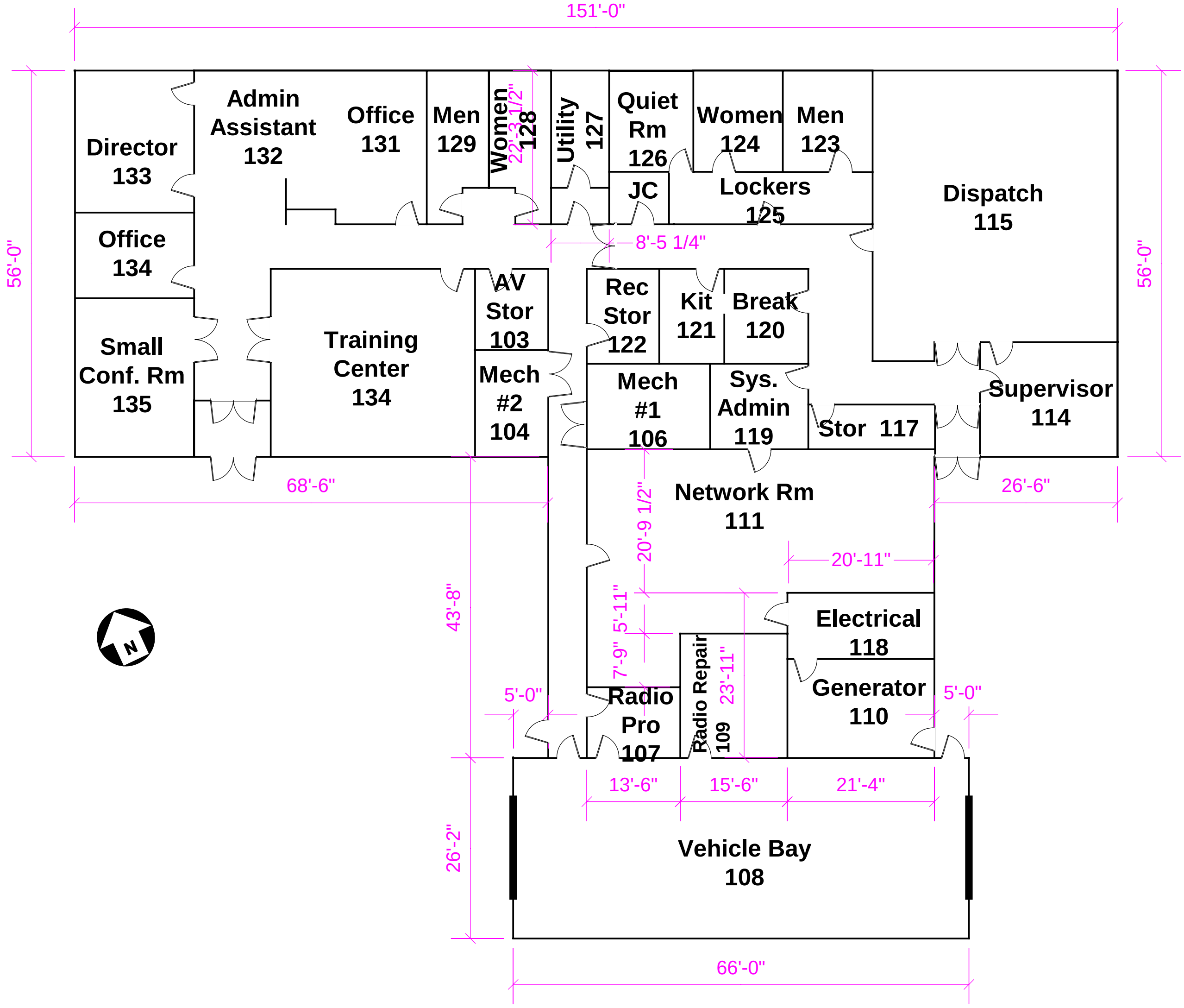

Figure A14-2. First Floor Building Plan

Construction Details

The exterior walls are 2 x 6 stud walls with fiberglass batt insulation and brick veneer exterior. The interior is finished with gypsum board. The building has a pitched roof with vented soffits and ridge venting. The roof is constructed with wooden trusses, plywood roof deck, and asphalt shingles.

There is a T-bar (drop) ceiling in the entire building excluding the garage. The supply and return ductwork is located in the ceiling space, which is inside the primary air and thermal barrier. The supply and return trunks are steel ducts with interior fiberglass insulation. Each difusser is served by an insulated flexduct takeoff.

Figure A14-3 illustrates typical wall and roof sections. Figure A14-4 shows pictures of the ceiling plenum and typical diffuser installation.

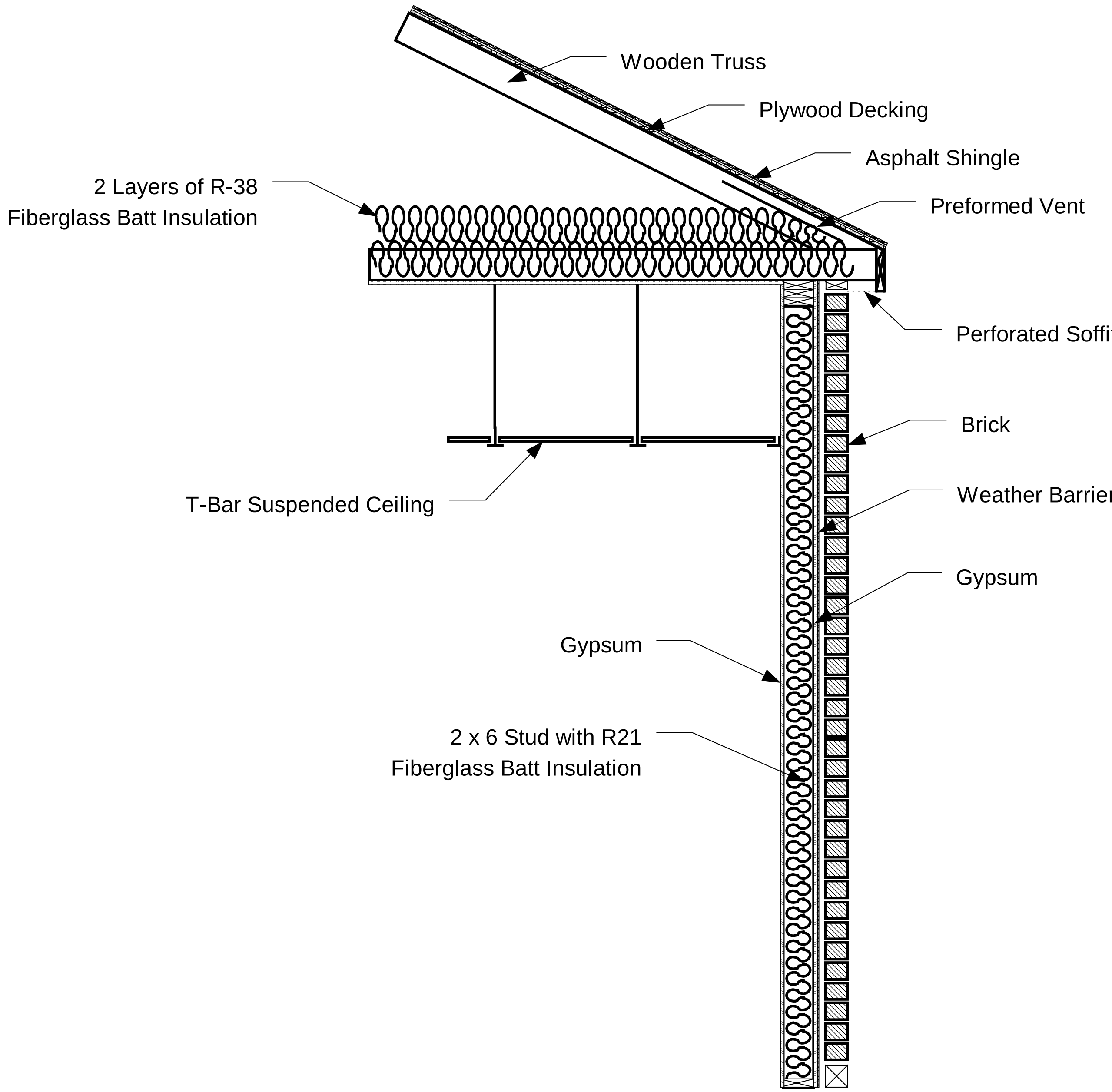

Figure A14-3. Exterior Wall and Roof Section

Ceiling Plenum

Linear Diffuser VAV Box

Typical Diffuser Installation

Typical Supply and Return Grill

Figure A14-4. Ceiling Plenum (First Floor)

<u>HVAC System</u>

The building has three air handlers that heat and cool using hot water supplied by two Raypak boilers and chilled water supplied by one York chiller. There are approximately 6 wall heater units in for the vestibules and restrooms. AHU-1 & AHU-2 are VAV units that serve the majority of the occupied space and AHU-3 is a constant volume unit dedicated to condition the network room. Figure A14-5 - Figure A14-8 show the various heating and cooling equipment for this building. Table A14-1 summarizes the HVAC equipment that serves the building.

VAV Unit (AHU-1 & AHU-2 are identical)
York Model: AP-105
Coil Model:
BA0060830.00x048G01HB016S032WH02R
Coil Model:
CA0061230.25x048G08CC020S035WH16R

Constant Volume Unit (AHU-3)
Canatal Model: 8CU10

Figure A14-5. Roof Top Units Serving Building

Wall Heater Unit (Used in Vestibules and Bathrooms)
Rittling Model: RFRWI-350

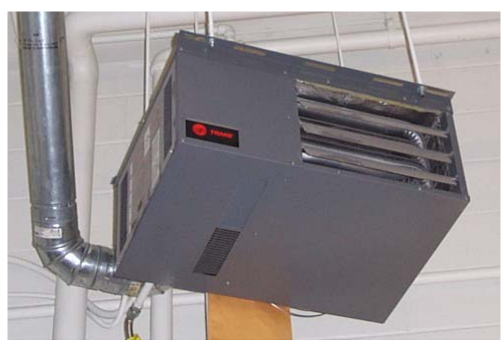

Unit Heater

Figure A14-6. Heater Unit for Vestibules and Restrooms and Unit Heater in the Garage

Boilers (B-1 & B-2)
Raypak Model: H3-0302

Figure A14-7. Copper Fin Tube Hot Water Boiler

Chiller (CH-1)
York Model/PIN:
YCAL0050EC46XCASDTXLTXBLXXXX45SX1XXXXXDXSAXXXXXX3BXXLXNHXXXXXX

Figure A14-8. York Chiller

Table A14-1. Summary HVAC Equipment Installed at Site

HVAC Equipment	Serves	Brand	Model	Heating Capacity (MBtu/h)	Cooling Capacity (tons)
AHU-1	East Wing	York	AP-105	130	15
AHU-2	West Wing	York	AP-105	130	15
AHU-3	Network Room	Canatal	8CU10	61.1	10
Reheat Units	Vestibules and Restrooms	Rittling	RFRWI-350	15	None
Unit Heaters	Garage	Trane			
Boilers 1	AHUs & Reheat Units	Raypak	H3-0302	252	N/A
Boilers 2	AHUs & Reheat Units	Raypak	H3-0302	252	N/A
Chiller	AHUs	York	See Figure A14-8	N/A	45.5

The air distribution system for AHU-1 & 2 has ducted returns and AHU-3 pulls return air from the space into the bottom of the unit. The supply and return ductwork is located in the ceiling space and is constructed of rectangular sheet metal ducts with flexduct takeoffs. The ductwork was extensively sealed at the joints and all penetrations through interior walls were also sealed as shown in Figure A14-9. Figure A14-10 and Figure A14-11 display the AHU zones and ductwork for the entire building.

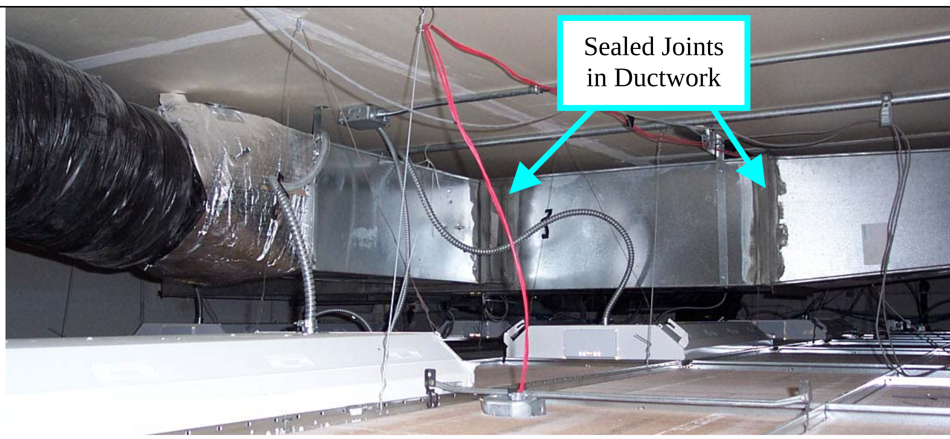

Sealed Ductwork

Sealed Penetration Through Wall

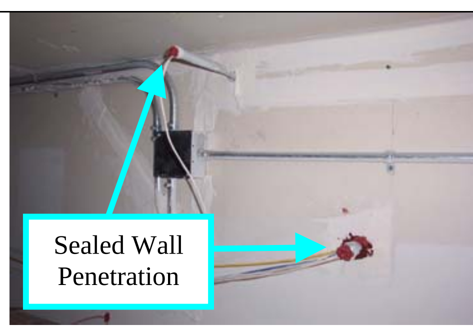

Sealed Interior Wall Penetrations

Figure A14-9. Sealed Ductwork Connections and Sealed Penetrations through Interior Walls

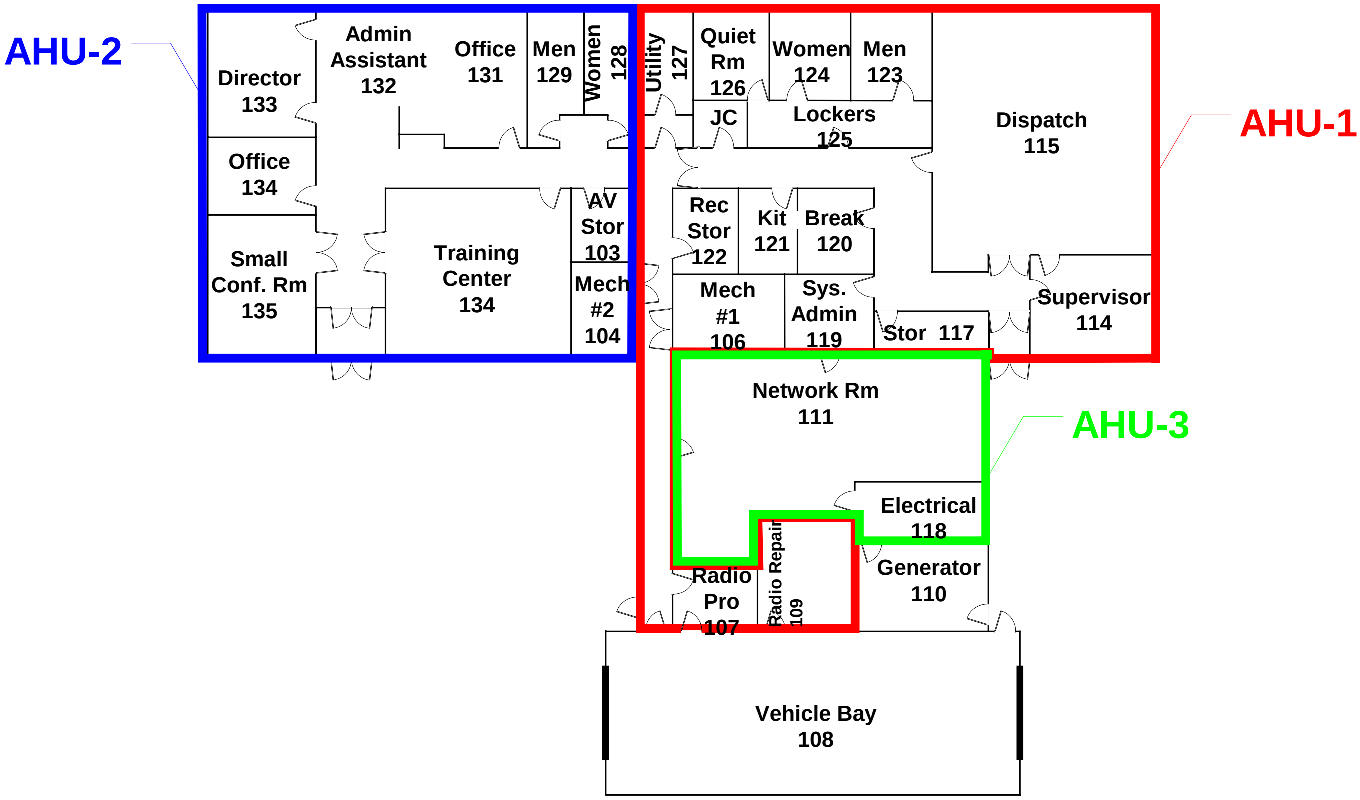

Figure A14-10. AHU Zones within Building

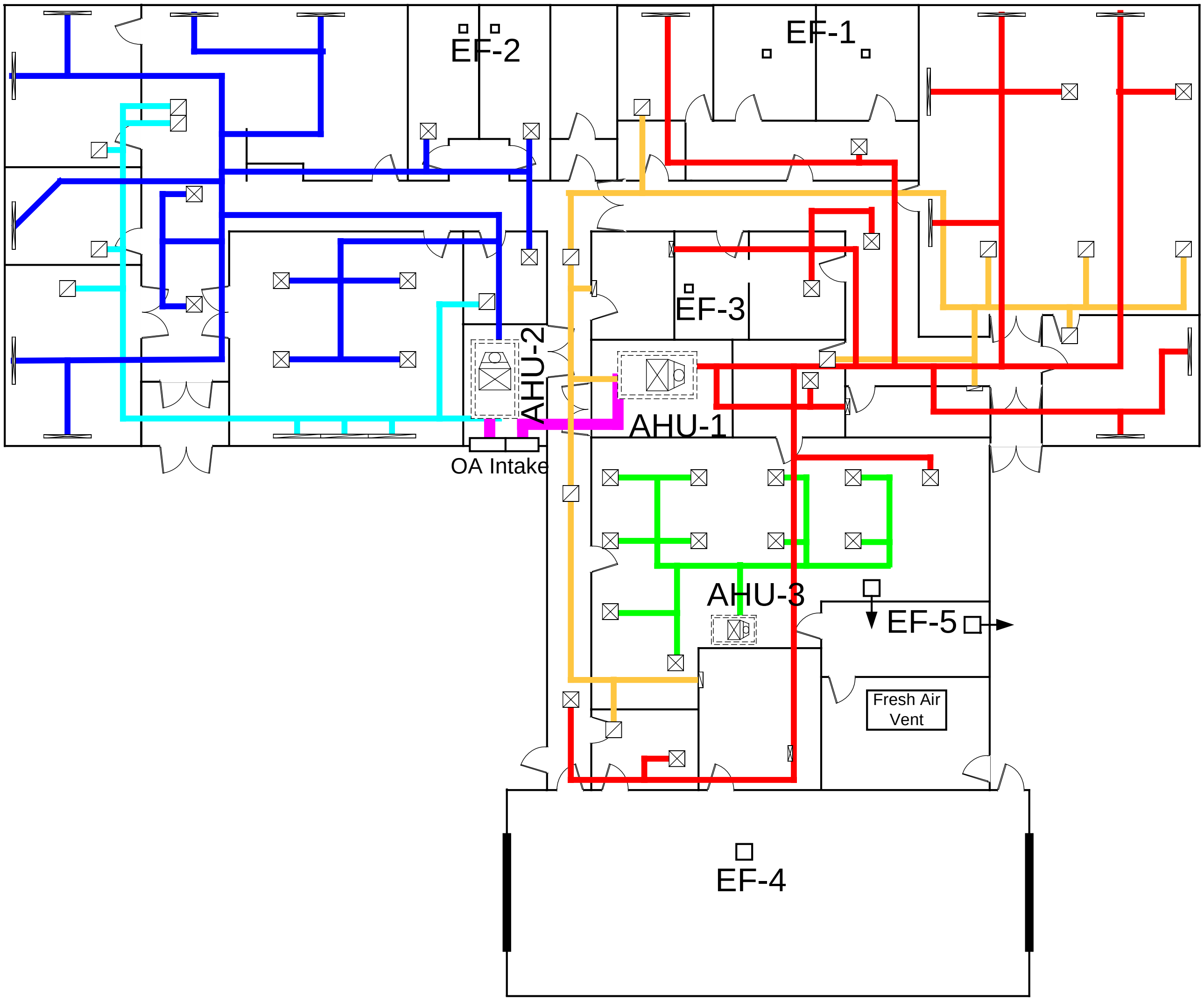

Figure A14-11. AHU Location and Corresponding Ductwork Serving Each Zone

A Johnson Controls Metasys system controls the HVAC equipment. The Metasys system is managed from an off site facilities building. There are several zone thermostats to control the VAV air distribution system. The heating setpoint is 70°F and the cooling setpoint is 74°F.

MEASUREMENTS

The test data below was taken on November 9 – 10, 2004. Blower door testing and pressure mapping was completed on November 9. Supply and return airflow measurements at each diffuser and duct leakage measurements were taken on November 10. Test personnel were Dan Gott and Mike Clarkin for both days. Dan Gott collected the CO_2 and temperature/RH sensors on January 15.

Building Envelope Airtightness

The leakage characteristics of the building enclosure were assessed using fan pressurization methods. A single blower door was installed in the west doorway closest to the garage (labeled in Figure A14-14). All exterior doors and windows were closed. The building was tested in the following configuration:

- All interior doors open
- All exhaust fans turned off and sealed inside building
- Outdoor Air intakes sealed
- Rooms 110, 118, & 127 were sealed from the conditioned space (these rooms were vented to outdoors)
- Bypass Dampers for AHU-1 and AHU-2 were closed

Rooms 110, 118, and 127 were sealed from the conditioned space rather than sealed to the outdoors since they contained operating mechanical equipment that could not be shutdown. Room 110 had a large (approx. 8-ft x 6-ft) fresh air vent located on the pitched roof for the generator. Room 118 is a vented electrical room. Room 127 is the boiler room with fresh air intake and gas hot water heater. The building pressure was varied from 30 Pa to 6 Pa, however the building was depressurized by 3.9 Pa without the blower door operating. The building leakage plots were adjusted for this natural building depressurization. For example, when the building is depressurized 30 Pa with the blower door operating, the airflow through the blower door only corresponds to depressurizing the building by an additional 26.1 Pa (26.1 + 3.9 = 30 Pa).

Figure A14-12 shows the building leakage variation with building pressure for the entire building and Figure A14-13 shows envelope leakage with the door closed that connects the 1,700 sq-ft garage to the offices. Figure A14-12 and Figure A14-13 also show the results of the blower door tests including model coefficients, effective leakage area (ELA), and air-changes-per-hour (ACH). The ELA is calculated using the Lawrence Berkeley Laboratory method, which calculates the leakage area at 4 Pa. The entire building has an effective leakage area of approximately 1.6 sq in per 100 sq ft of the total envelope area including floor area. Another building leakage characteristic is the ACH at 50 pascals (ACH_{50}). The building has an ACH_{50} of 4.5. This result implies that at 50 Pa, the air in the building is displaced 4.5 times each hour. Table A14-2 summarizes the flow coefficient, exponent, ELA, and ACH_{50} for the two blower door tests.

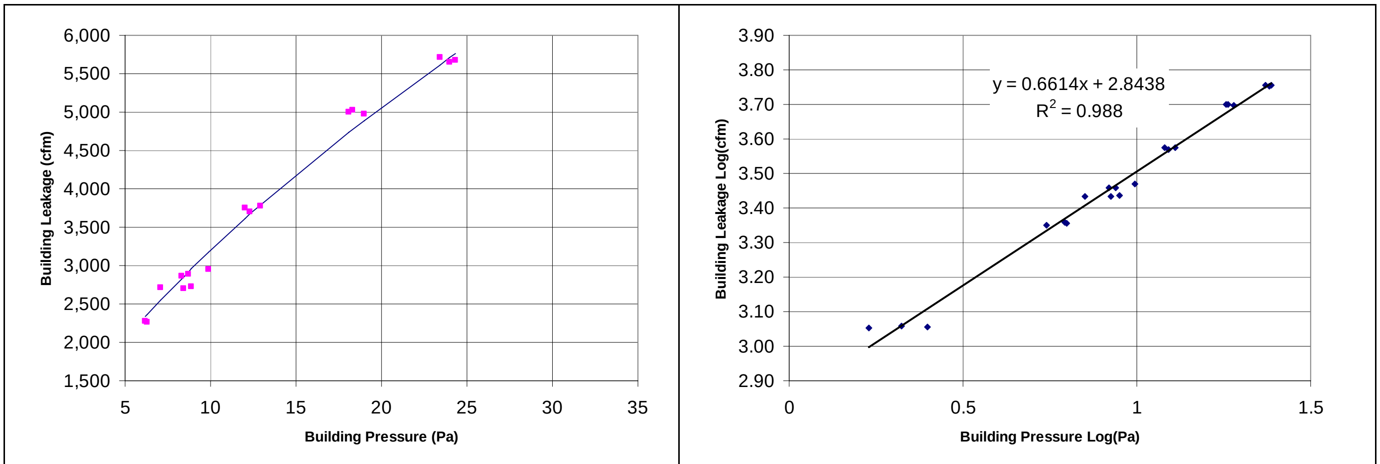

Test Results:

Flow Coefficient (K)	697.9	11,990 sq ft, floor area
Exponent (n)	0.661	
Leakage area (LBL ELA @ 4 Pa)	494.6 sq in	1.60 ELA / 100 sq ft
Airflow @ 50 Pa	9,279 cfm	4.45 ACH @ 50

Test Data:

Nominal Building Pressure (Pa)	Nominal Flow (cfm)	Ring
24.3	5,680	none
24.0	5,646	none
23.4	5,711	none
19.0	4,969	none
18.3	5,020	none
18.1	5,004	none
12.9	3,770	none
12.3	3,701	none
12.0	3,751	none
9.9	2,944	none
8.9	2,728	none
8.7	2,882	none
8.4	2,704	none
8.3	2,867	none
7.1	2,717	none
6.3	2,261	none
6.2	2,281	none
5.5	2,245	none
2.5	1,138	none
2.1	1,142	none
1.7	1,132	none

Notes: ELA is leakage area (in square inches) at reference pressure of 4 Pa.
ELA per 100 sq ft is based on total building envelope surface area (ceiling, exterior walls and floor).

Figure A14-12. Entire Building: Variation of Building Leakage with Pressure: cfm = K(ΔP)^n

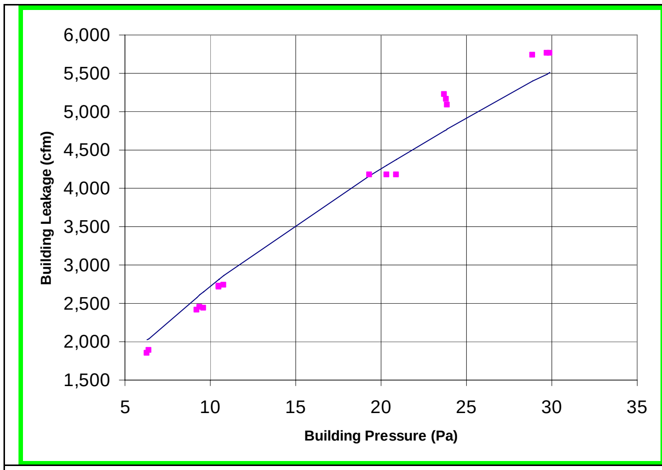

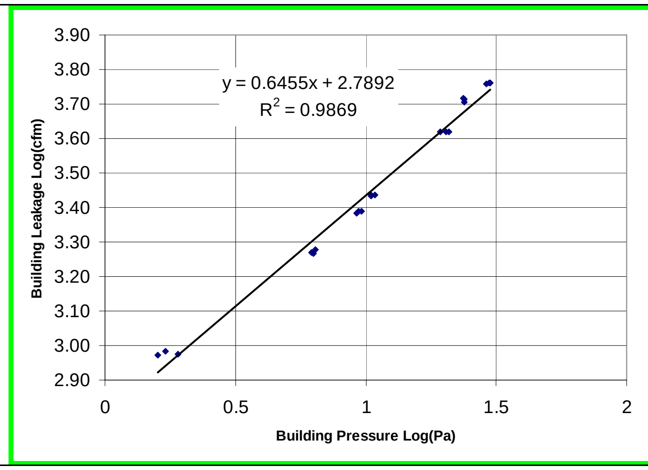

Test Results:

Flow Coefficient (K)	615.4	10,449 sq ft, floor area
Exponent (n)	0.645	
Leakage area (LBL ELA @ 4 Pa)	426.7 sq in	1.70 ELA / 100 sq ft
Airflow @ 50 Pa	7,688 cfm	4.74 ACH @ 50

Test Data:

Nominal Building Pressure (Pa)	Nominal Flow (cfm)	Ring
29.9	5,757	none
29.7	5,758	none
28.9	5,735	none
23.9	5,086	none
23.8	5,163	none
23.7	5,220	none
20.9	4,171	none
20.3	4,173	none
19.3	4,173	none
10.8	2,736	none
10.5	2,718	none
10.5	2,727	none
9.6	2,441	none
9.4	2,453	none
9.2	2,415	none
6.4	1,891	none
6.3	1,845	none
6.2	1,856	none
1.9	947	none
1.7	965	none
1.6	937	none

Notes: ELA is leakage area (in square inches) at reference pressure of 4 Pa.
ELA per 100 sq ft is based on total building envelope surface area (ceiling, exterior walls and floor).

Figure A14-13. Building Without Garage: Variation of Building Leakage with Pressure: cfm = $K(\Delta P)^n$

Table A14-2. Summary of Blower Doors Tests

	Flow Coeff. K	Exp. n	ELA	ELA / 100 sq ft (sq in)	ACH_{50}	CFM_{50}
Entire Bldg.	698	0.66	495	1.60	4.5	9,279
Bldg. w/out Garage	615	0.65	427	1.70	4.7	7,688

Pressure Mapping (Blower Door Testing)

Pressure readings in the building were taken using a digital micromanometer (DG 700) with the blower door operating. The pressure difference across the building envelope was 31 Pa. The gypsum board attached to the bottom chord of the trusses is the primary air barrier and the two layers of fiberglass batts laid on top of the gypsum is the primary thermal barrier.

Pressure measurements were taken between interior rooms with doors closed and the main corridors. Figure A14-14 shows the pressure differences induced across the doorways with the corridors depressurized and all interior doors closed. With the corridors depressurized to 31 Pa, pressures across the doorways ranged between 0.0 and 8.2 Pa. The pressure difference between the rooms and corridor are much less than the overall pressure difference to ambient. The relatively large pressure difference of 8.2 Pa that occurred in the locker room area (room 127) implies that this area has a large leak to the outdoors.

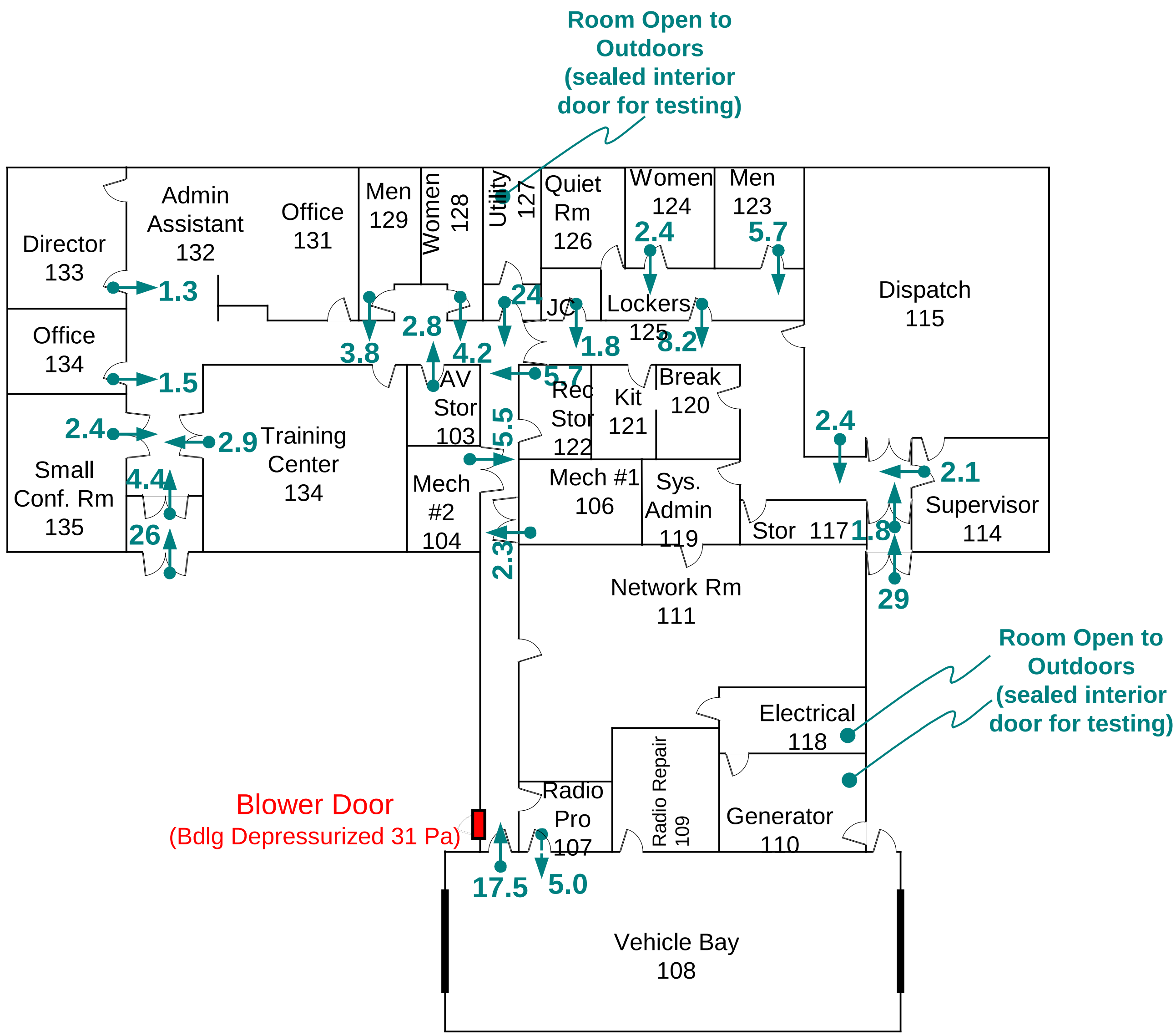

Figure A14-14. First Floor Room-to-Corridor Pressures with Building Depressurized

HVAC Airflow Measurements

The airflow from each supply diffuser was measured using a Shortridge flow hood. The air handler (AHU-2) that serves the west wing was not operating because of a control fault. The supply diffuser airflow for AHU-1 & AHU-2 is approximately 7,398 cfm[1]. Table A14-3 shows the normalized supply airflow for the building. The total supply and return airflow for AHU-1 was 3,250 cfm and 1,100 cfm giving a supply to return ratio of 2.95. The minimum design outdoor airflow of 1,400 cfm is a good estimate for this day of testing because the maximum outdoor temperature was approximately 46°F. Figure A14-15 displays the airflow at each diffuser and exhaust. The ductwork shows which AHU supplies air the to the diffusers.

Table A14-3. Normalized Supply Airflow

		Measured Values		Design Values	
Zone	Floor Area Served (sq-ft)	Diffuser Supply Airflow (cfm)	Normalized Supply Airflow (cfm/sq-ft)	Supply Airflow (cfm)	Normalized Supply Airflow (cfm/sq-ft)
AHU-1 (east wing)	5,250	3,253	0.62	3200	0.61
AHU-2 (west wing)	3,830	no data	no data	3200	0.84
AHU-3 (network room)	1,480	4,146	2.80	6000	4.05
Garage	1,727	0	n/a	0	n/a
Generator Room	313	0	n/a	0	n/a

[1] Four supply and two return diffuser airflows were not measured. The airflows for these diffusers were estimated using the average of the measured diffuser airflows in the corresponding system.

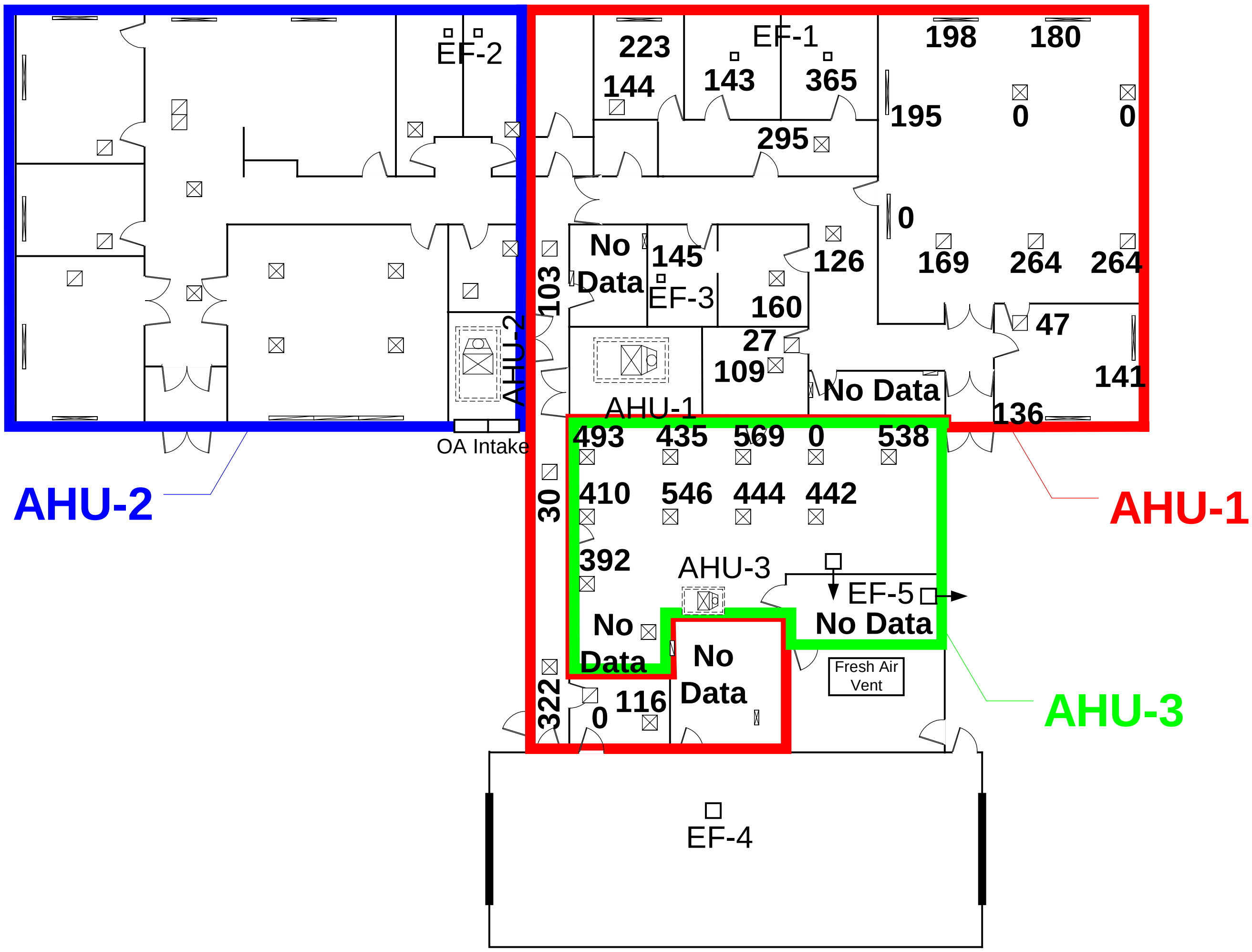

Figure A14-15. First Floor Supply and Return Airflow Measurements (cfm)

Table A14-4. Building Exhaust Fans

Exhaust Fan	Rooms Served	Design Exhaust Flow (cfm)	Measured Exhaust Flow (cfm)
EF-1	Showers	550	508
EF-2	Toilets	450	no data
EF-3	Kitchen	300	145
EF-4	Vehicle Bay	570	no data
EF-5	Electrical Rm	300	no data
Total		***2,170***	

Pressure Mapping (AHU Fans On)

The air pressure relationships in the building were also determined with AHU-1 and AHU-3 fans on. However, this is not normal operating condition, since AHU-2 was not operating because of a control fault. The graphics in Figure A14-16 show the pressure differences induced across the doorways with the AHU fans on, exhaust fans on that normally operate, and the interior doorways closed. Operation of 2 of 3 air handlers and the normally operating exhaust fans created interior pressures differences up to 33.1 Pa. The building was depressurized with respect to outdoors by 4.4 Pa. The rooms without exhaust fans are closely coupled to the conditioned space with pressures less than 3.4 Pa. The restrooms are normally depressurized 5.0 – 8.6 Pa. The electrical room is depressurized by 31.3 Pa with respect to the network room and the largest pressure difference of 33.1 Pa occurred between the electrical room and the generator room. The electrical room has an exhaust fan and the generator room is open to the outdoors.

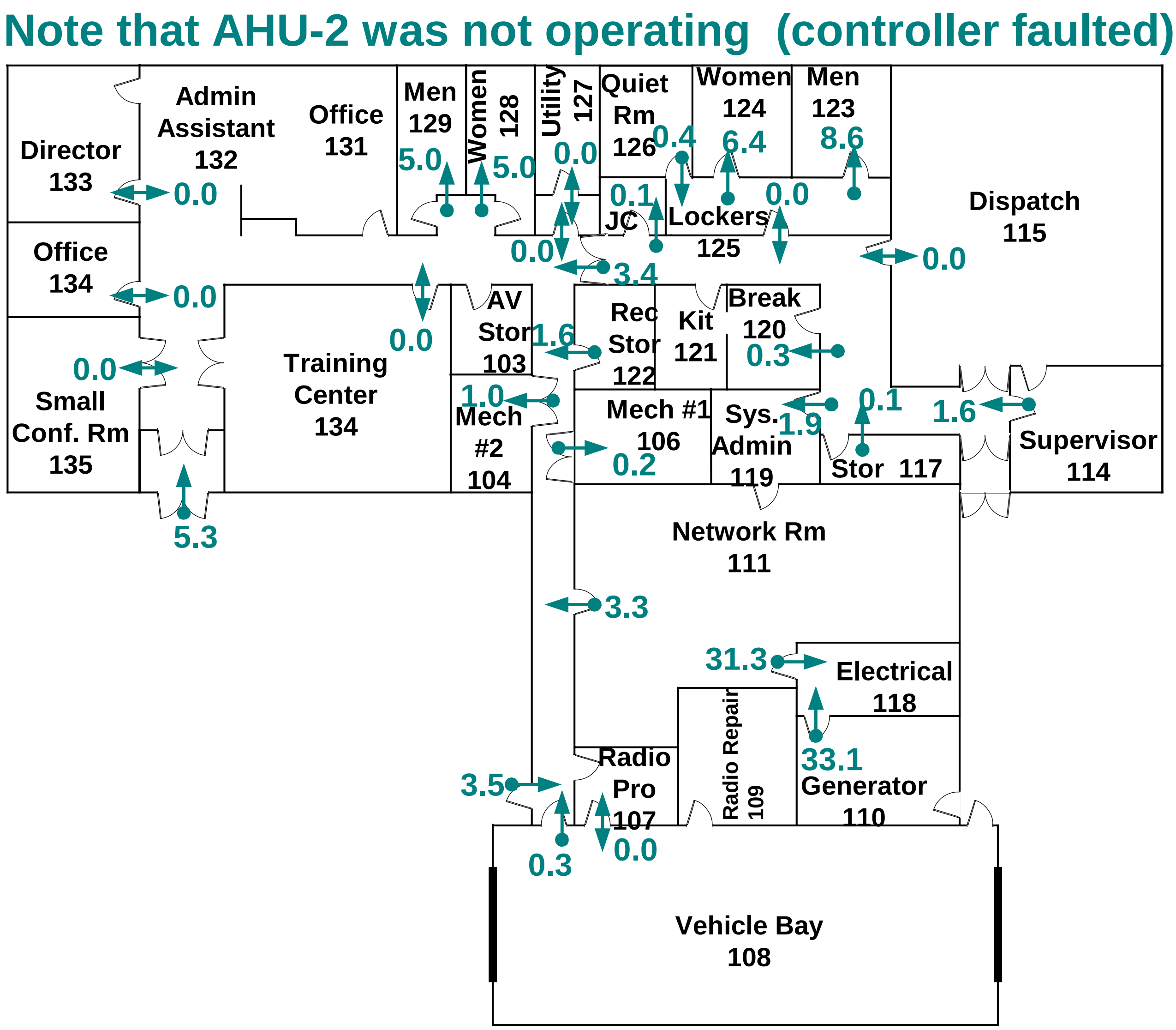

Figure A14-16. First Floor Pressure Differences between Rooms with AHU Fans On

Duct Leakage Measurements

A Duct Blaster was used to depressurize the supply and return ductwork for AHU-2 (west wing) to measure leakage rates. Each supply and return diffuser was sealed using duct mask. The Duct Blaster fan was first connected to the return section and then the supply fan section in the AHU cabinet. Figure A14-17 shows the Duct Blaster setup and the duct mask seal to isolate the return section and supply fan section in the AHU. The outdoor air intake for AHU-2 was also sealed with duct mask and the bypass dampers for the VAV system were closed. The static pressure tap was located in the supply or return plenum corresponding to the ductwork being tested.

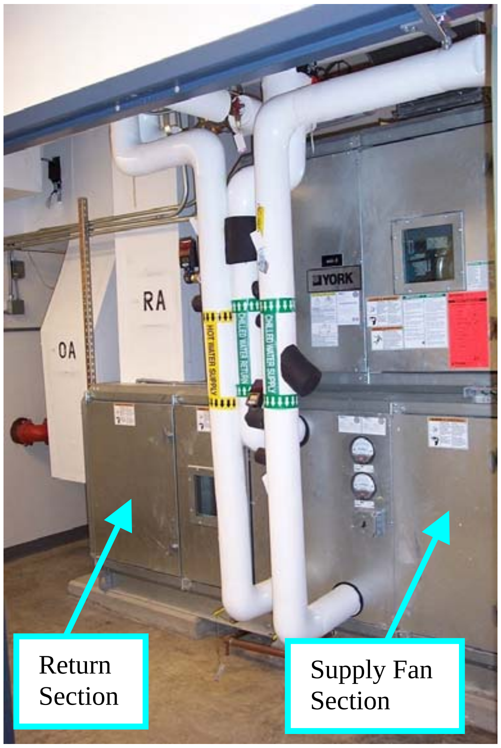

AHU-2

Duct Blaster Connected to Supply Section

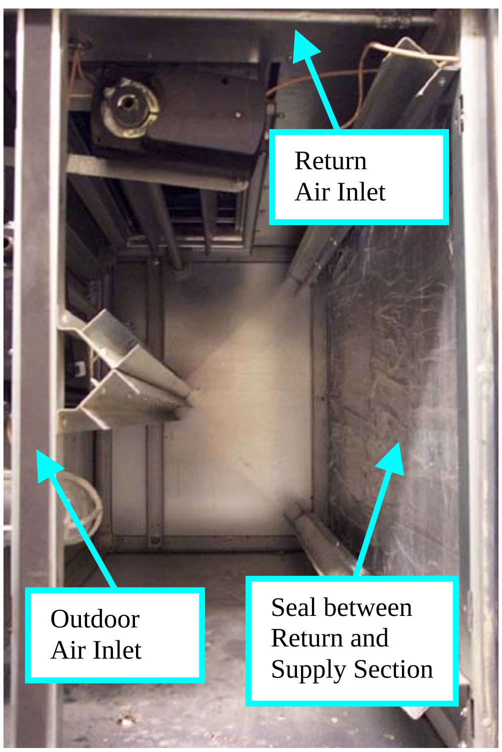

Seal Isolating Supply & Return Ductwork

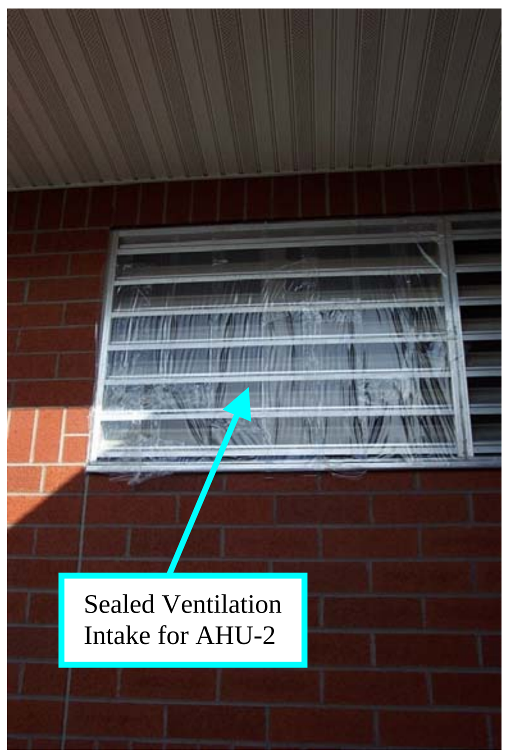

AHU-2 Ventilation Intake

Figure A14-17. Duct Blaster Setup for AHU-2 (West Wing)

As a diagnostic check on the degree of pressurization, the pressure at each supply diffuser was measured by puncturing the plastic covering at each diffuser with a very small probe. Figure A14-18 shows the resulting pressures measured at each supply and return diffuser for AHU-2 with the system depressurized.

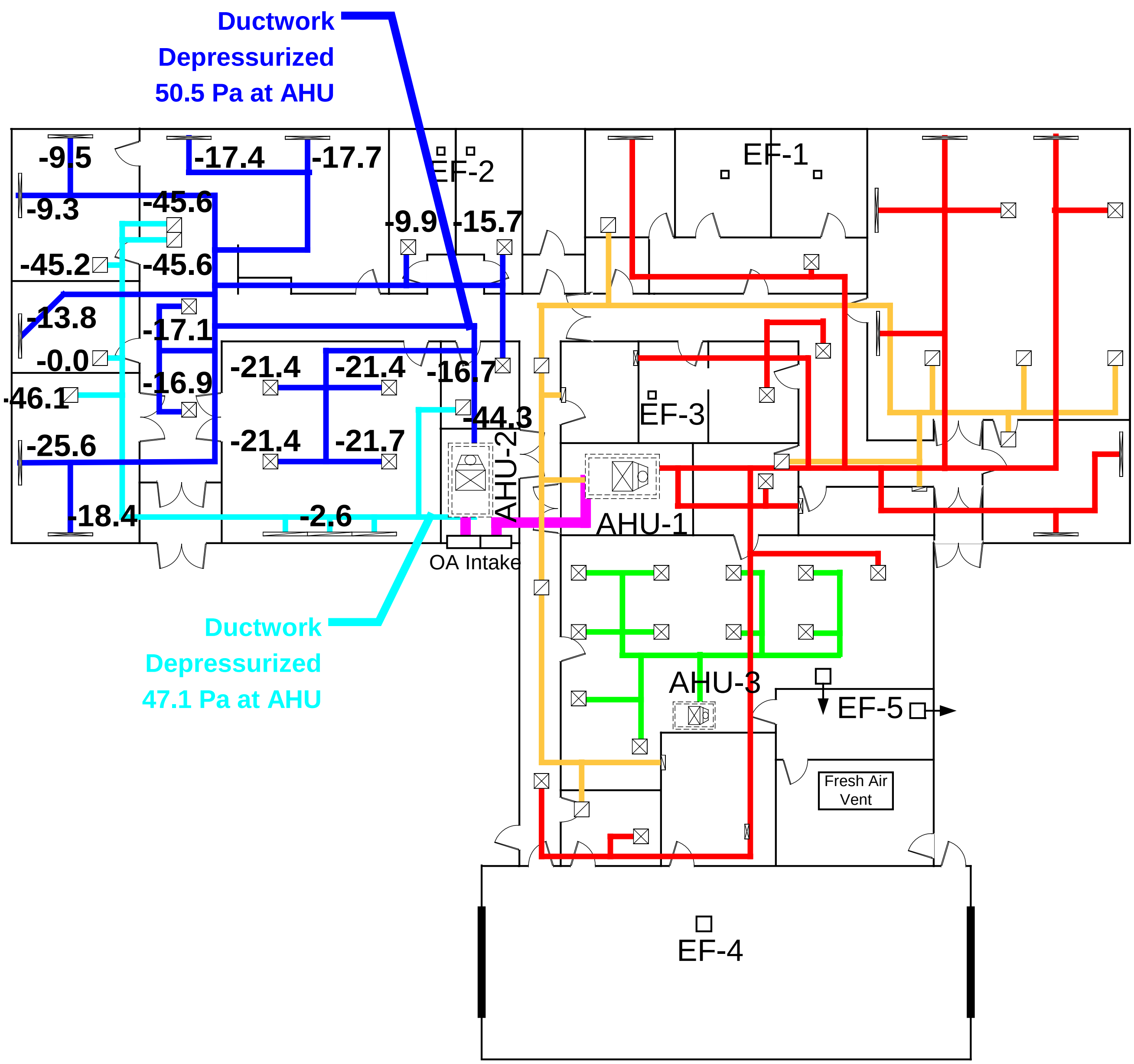

Figure A14-18. Diffuser Pressures with Ductwork Depressurized

Figure A14-19 shows the resulting measured data from the duct leakage tests fit to a power function (raw data in Table A14-5). Table A14-6 shows the resulting coefficients, exponents, and regression statistics. Table A14-7 summarizes the resulting duct leakage rates and ELA at a reference pressure of 25 Pa. Although AHU-2 was not operating, we did measure the static pressure for AHU-1, which is an identical air handler. The supply plenum static pressure for AHU-1 was 60 Pa and the return plenum static was 7 Pa. If the static pressure for AHU-1 and AHU-2 are similar, the estimated duct leakage during normal operation for AHU-2 is approximately 438 cfm for the supply ductwork and 143 cfm for the return ductwork. These estimates for duct leakage during normal operation use one half the static pressure measured in the supply/return plenums as suggested in ASHRAE Standard 152P section B.2. The leakage has little effect on energy use because all of the ductwork is located inside the primary air and thermal barrier.

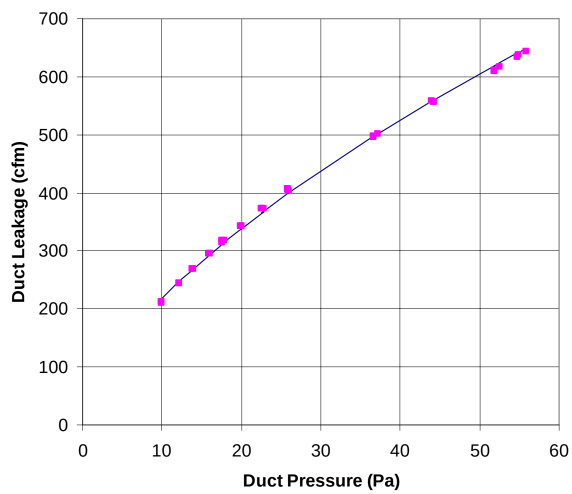

AHU-2 (Supply Ductwork and AHU Cabinet)

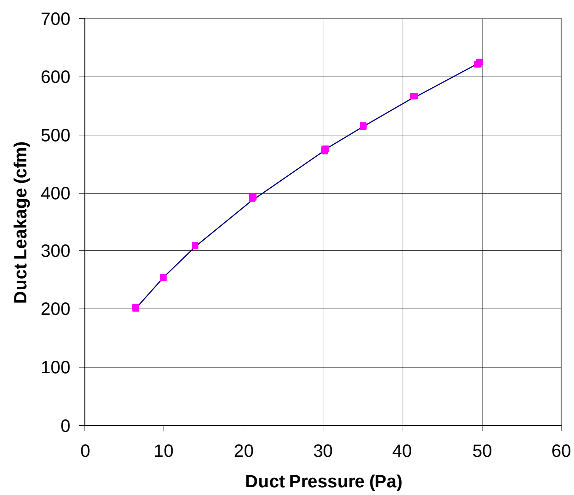

AHU-2 (Return, Vent, and Bypass Ductwork)

Figure A14-19. Duct-Blaster Tests on RTU-1 & RTU-4 Ductwork

Table A14-5. Raw Data from Duct-Blaster Tests

AHU-2 (Supply Ductwork and AHU Cabinet)

Test Results:

Flow Coefficient (K)	50.5	
Exponent (n)	0.635	
Leakage area (LBL ELA @ 25 Pa)	44	sq in
Airflow @ 25 Pa	389.7	cfm

Test Data:

	Nominal Duct Pressure (Pa)	Nominal Flow (cfm)	Ring
1	55.8	643	A1
2	54.9	637	A1
3	54.7	633	A1
4	52.5	617	A1
5	51.9	611	A1
6	51.9	610	A1
7	44.3	556	A1
8	44.3	557	A1
9	44.0	558	A1
10	37.2	502	A1
11	36.7	495	A1
12	36.7	497	A1
13	25.9	407	A1
14	26.0	403	A1
15	25.9	404	A1
16	22.6	372	A1
17	22.6	372	A1
18	22.8	372	A1
19	19.9	343	A1
20	20.0	343	A1
21	20.0	343	A1
22	17.6	315	A1
23	17.6	318	A1
24	17.8	318	A1
25	16.0	295	A1
26	15.9	296	A1
27	16.0	296	A1
28	13.9	269	A1
29	13.8	269	A1
30	13.8	268	A1
31	12.2	244	A1
32	12.2	245	A1
33	12.2	244	A1
34	10.0	211	A1
35	9.9	211	A1
36	9.9	210	A1

AHU-2 (Return, Vent, and Bypass Ductwork)

Test Results:

Flow Coefficient (K)	71.3	
Exponent (n)	0.555	
Leakage area (LBL ELA @ 25 Pa)	48	sq in
Airflow @ 25 Pa	425.9	cfm

Test Data:

	Nominal Duct Pressure (Pa)	Nominal Flow (cfm)	Ring
1	49.8	624	A1
2	49.7	621	A1
3	49.5	620	A1
4	41.5	566	A1
5	41.5	565	A1
6	41.6	565	A1
7	35.1	513	A1
8	35.1	515	A1
9	35.1	514	A1
10	30.3	475	A1
11	30.3	472	A1
12	30.4	474	A1
13	21.2	390	A1
14	21.2	392	A1
15	21.3	392	A1
16	13.9	308	A1
17	13.9	309	A1
18	14.0	309	A1
19	9.9	254	A1
20	9.9	253	A1
21	9.9	253	A1
22	6.5	202	A1
23	6.5	202	A1
24	6.5	201	A1

Table A14-6. Coefficients, Exponents and Regression Statistics from Duct-Blaster Tests

	AHU-2 Duct Leakage Coefficients		
	K	n	R^2
Supply & AHU Cabinet	50.5	0.635	99.84%
Return, Vent., & Bypass Ducts	71.3	0.555	99.99%

Notes: cfm = $K(Pa)^n$ / R^2 indicates fit of linear log-log regression

Table A14-7. Comparison of Supply and Return Duct Leakage

	Duct Leakage (cfm @ 25)	ELA (sq in @ 25)
Supply & AHU Cabinet	390	44
Return, Vent., & Bypass Ducts	426	48
Total	***816***	***92***

Notes: Leakage and ELA at reference pressure of 25 Pa

Table A14-8 lists the ductwork used to estimate the supply and return duct area for the AHU-2. The effective leakage area compared to the duct surface area for AHU-2 is shown in Table A14-9. The Sheet Metal and Air Conditioning Contractors' National Association (SMACNA) classifies duct leakiness using duct leakage per 100 sq ft of duct area at a pressure of 1-in w.g.

Table A14-8. AHU-2 Ductwork Size and Area

AHU-2 Supply

	Type/Size	Supply Side Length (ft)	Duct Area Supply Side (sq ft)
Supply Trunks	30" x 20"	18.5	154.2
Supply Ducts	28" x 14"	38.0	266.0
	22" x 14"	4.0	24.0
	14" x 10"	39.0	156.0
	10" x 8"	15.0	45.0
	16" x 10"	58.0	251.3
	12" x 10"	70.5	258.5
	10" x 10"	26.0	86.7
	8" x 8"	40.0	106.7
	6" x 6"	10.0	20.0
	26" x 14"	20.0	133.3
	14" x 12"	15.0	65.0
	12" x 12"	28.0	112.0
	14" x 14"	3.5	16.3
Diffuser Boxes	48" x 6" x 12"	7 diff boxes	77.0
AHU Cabinet	approx. 10' x 6' x 4.5'	only supply sec.	174.0
Total			***1,946***

AHU-2 Return

	Type/Size	Return Side Length (ft)	Duct Area Return Side (sq ft)
Return Trunks	30" x 20"	12.0	100.0
Return Ducts	26" x 12"	52.5	332.5
	20"x 12"	5.0	26.7
	20"x 10"	18.0	90.0
	6"x 6"	19.5	39.0
Takeoffs	10"x 12"	36.5	133.8
Diffuser Boxes	48" x 6" x 12"	3 diff boxes	33.0
Ventilation Trunk	30" x 20"	6.0	50.0
AHU Cabinet	approx. 10' x 6' x 4.5'	only return sec.	108.0
Total			***913***

Table A14-9. Duct Leakage per 100 Square Foot of Duct Area

	Duct Area (sq ft)	ELA (sq in @ 25)	ELA/100 sq ft Duct Area (sq in @ 25)	Leakage (cfm @ 25 Pa)	Supply CFM per ft^2 Duct Area (cfm/ sq-ft)	Leakage per 100 sq ft Duct Area (cfm @ 25 Pa)	SMACNA Leakage Class cfm per 100 sq ft (cfm @ 1-in water)
Supply & AHU Cabinet	1,946	44	2.3	390	2.31**	20	86
Return, Vent., & Bypass Ducts	913	48	5.3	426	n/a	47	167
Total	2,859	92	3.2	816		29	

**Note that the design supply fan airflow is used for this calculation.

Table A14-10 shows the airflow balance for AHU-2. This table is only a rough estimate:

1. The supply fan and return airflows are DESIGN values (not measured)
2. The ventilation airflow is the minimum design airflow. The minimum value is used because the maximum outdoor air temperature was 46°F.
3. The "actual" supply and return leakage are calculated using the static pressures from AHU-1 since AHU-2 was not operating. The operating static pressures should be similar for AHU-1 and AHU-2 because the units are identical.
4. The diffuser supply and diffuser return airflows are calculated by subtracting the duct leakage from the design airflows.

The supply and return duct leakage during normal operation is calculated using our best estimate for average "actual static" pressure in the ductwork, which is one half of the plenum pressure as suggested in ASHRAE Standard 152P section B.2. Figure A14-20 shows a diagram of the air-handling unit including the design airflows for supply, return, and ventilation. The duct leakage shown in Figure A14-20 was calculated using the static pressure measured from AHU-1, which is an identical unit to AHU-2. The static pressures were not measured on AHU-2 because the unit was not operating due to a controller fault.

Table A14-10. Rough Estimate for Airflow Balance on AHU-2

	AHU-2 (west wing)
Design Supply Fan Airflow (cfm)	4,500
Design Return Airflow (cfm)	3,100
Diffuser Supply (cfm)	4,062
Diffuser Return (cfm)	2,957
Ventilation (cfm) - design minimum	1,400
Supply Leakage - cfm25	390
- actual static	438
Return Leakage - cfm25	426
- actual static	143

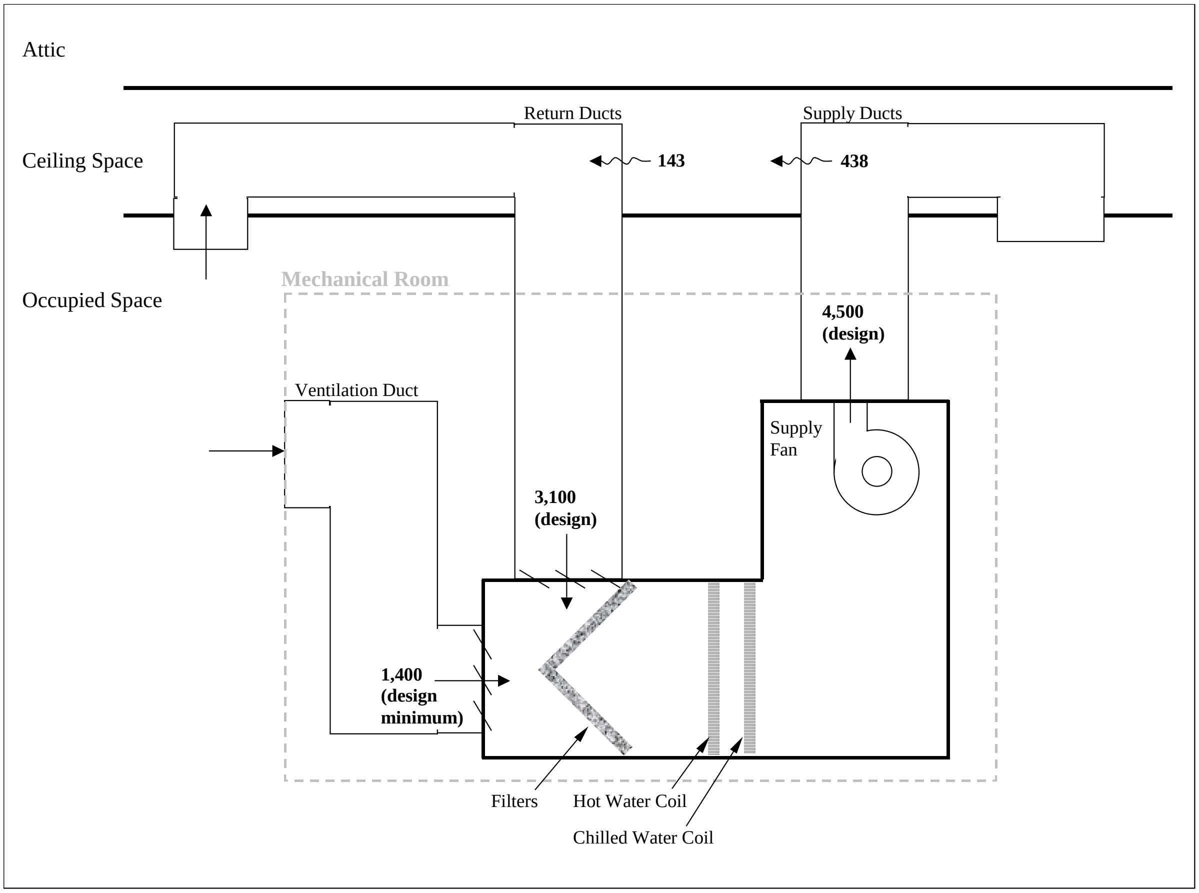

Figure A14-20. Airflow Balance for AHU-2

Space Conditions

Figure A14-21 shows the average temperature profiles based on temperature readings taken with a HOBO data logger from November 15, 2004 to January 15, 2005. The thick line shows the average for each hour while the shaded region corresponds to one standard deviation about the average. The dotted lines correspond to the minimum and maximum for each hour.

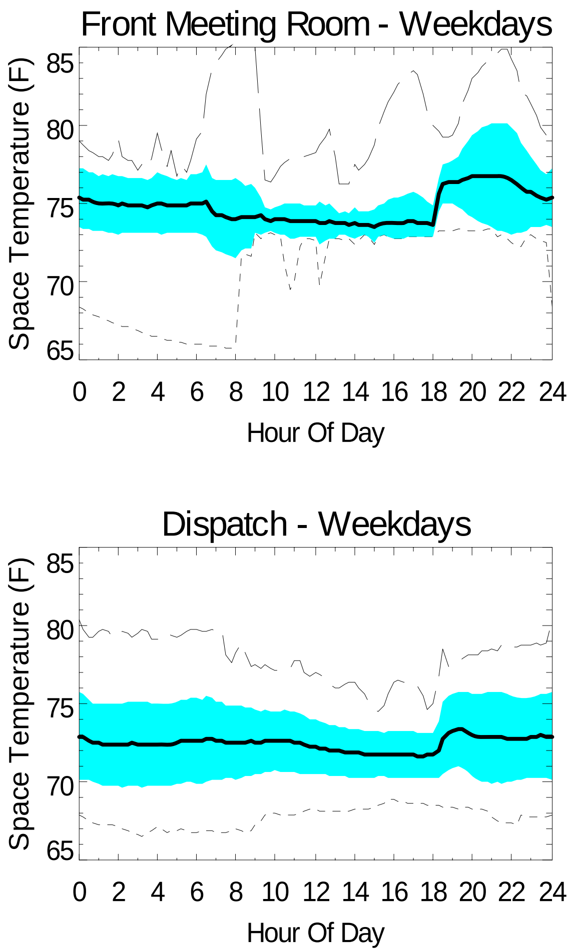

Figure A14-21. Measured Space Temperature Profiles

Figure A14-22 shows the CO_2 concentration in various locations in the building. The CO_2 concentration provides an indication of occupancy. The high ventilation rates help maintain a very low CO_2 concentration. The CO_2 concentration typically stays below 500 ppm in the Dispatch room. There was also a CO_2 sensor in the Conference room, however, the logger was either not set up correctly, or the information on the logger was damaged, thus the information on the data logger for that room was not useful.

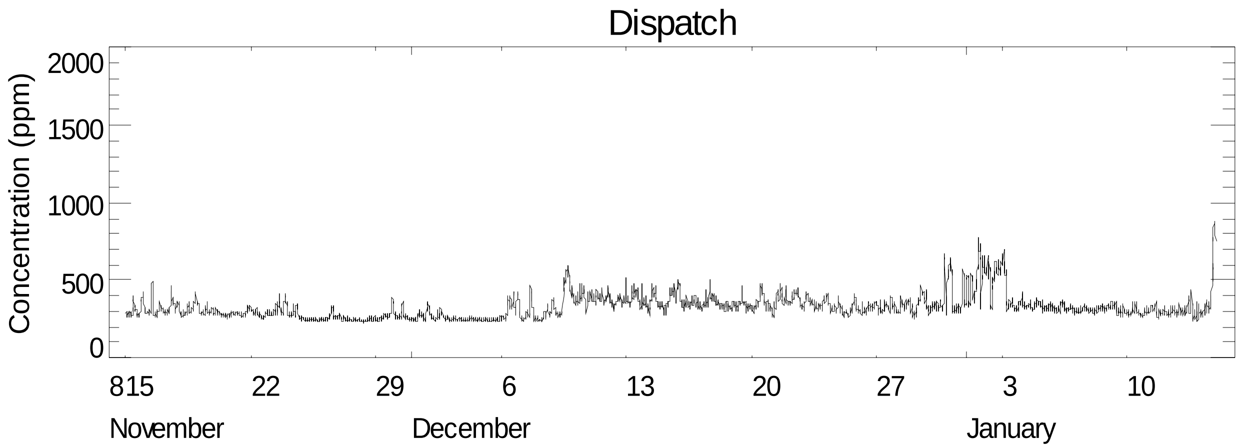

Figure A14-22. Measured CO_2 Concentration in Various Spaces

The following plots show the relative humidity for this building. Figure A14-26 displays the conditions inside the building compared with the ASHRAE comfort zone for cooling shown by the shaded region on the plot.

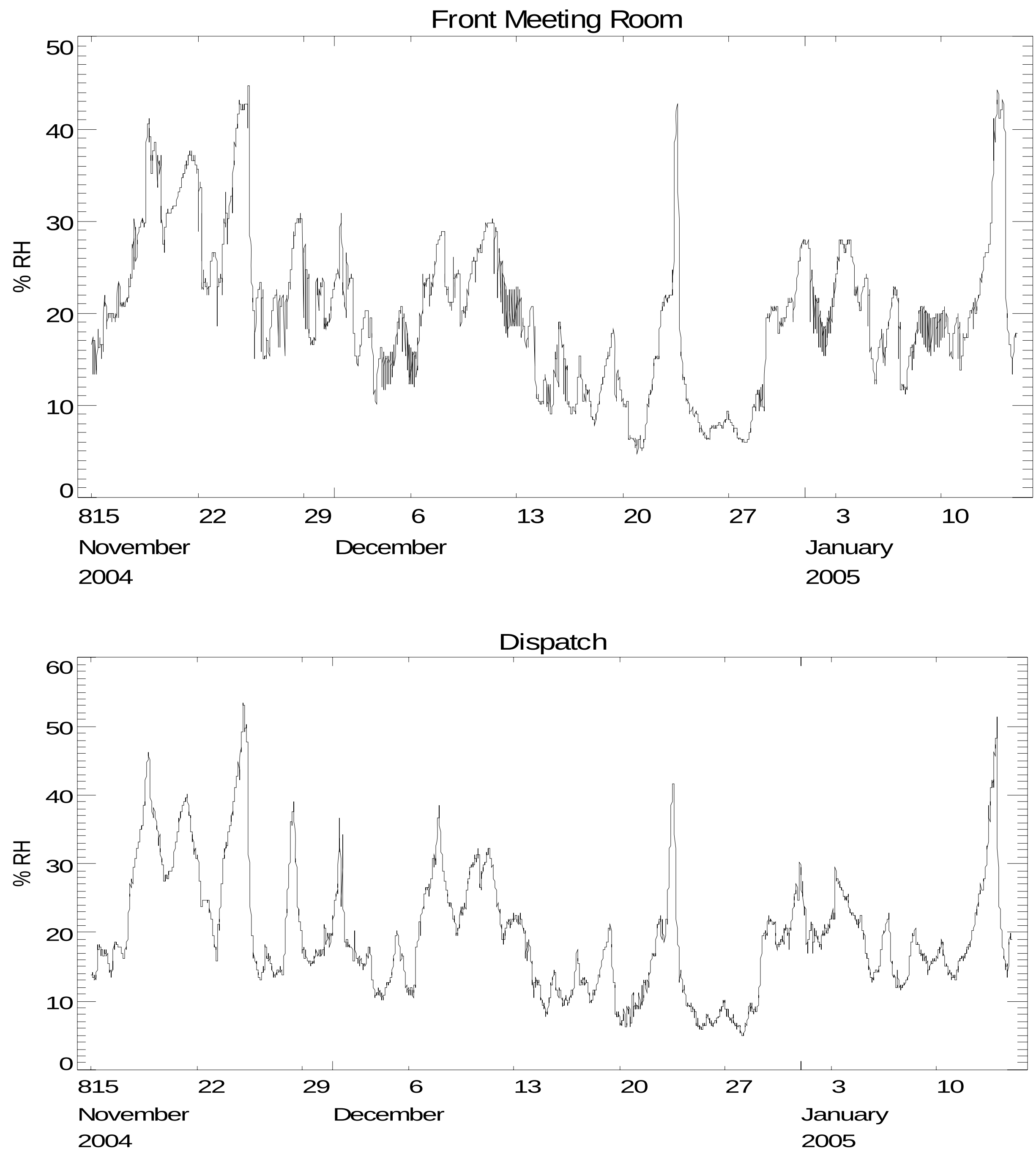

Figure A14-23. Measured Relative Humidity

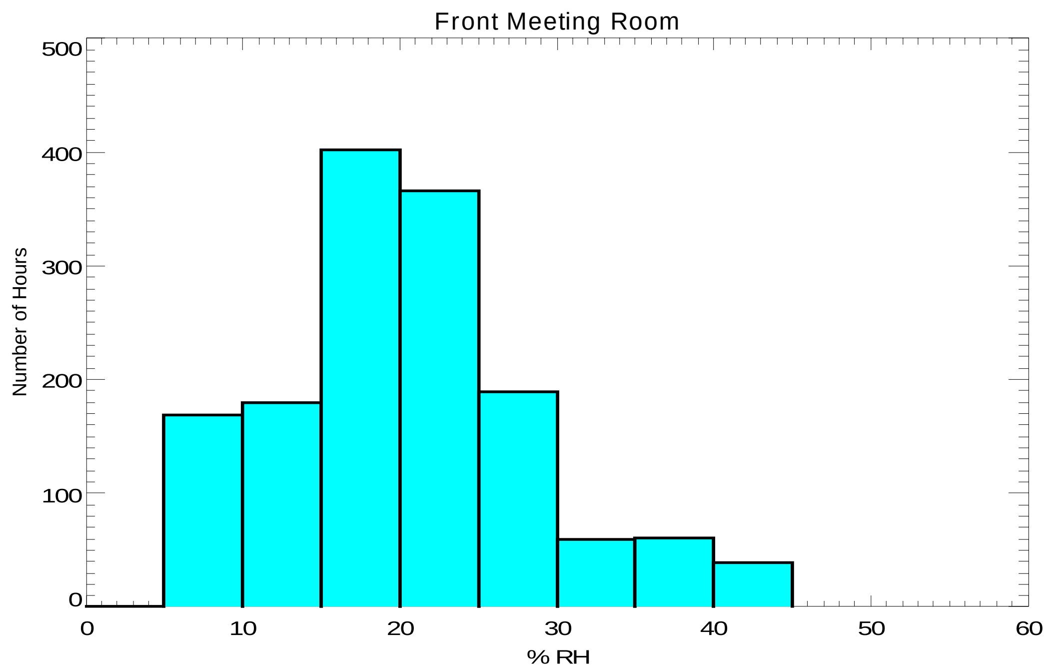

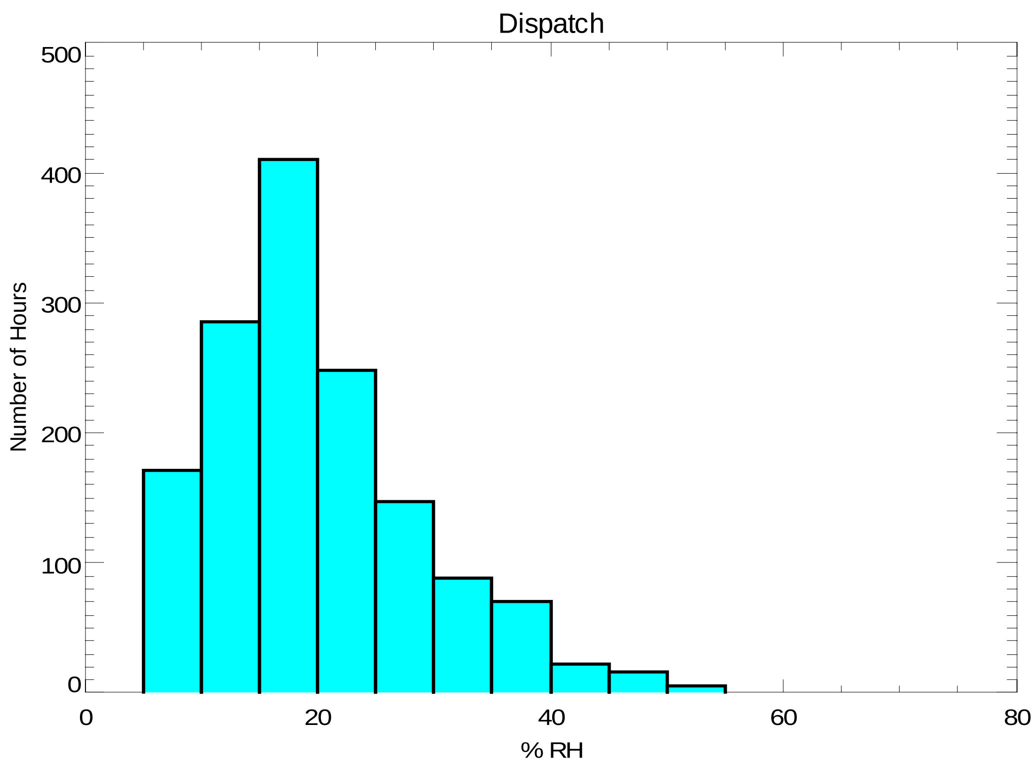

Figure A14-24. Duration of Relative Humidity Levels

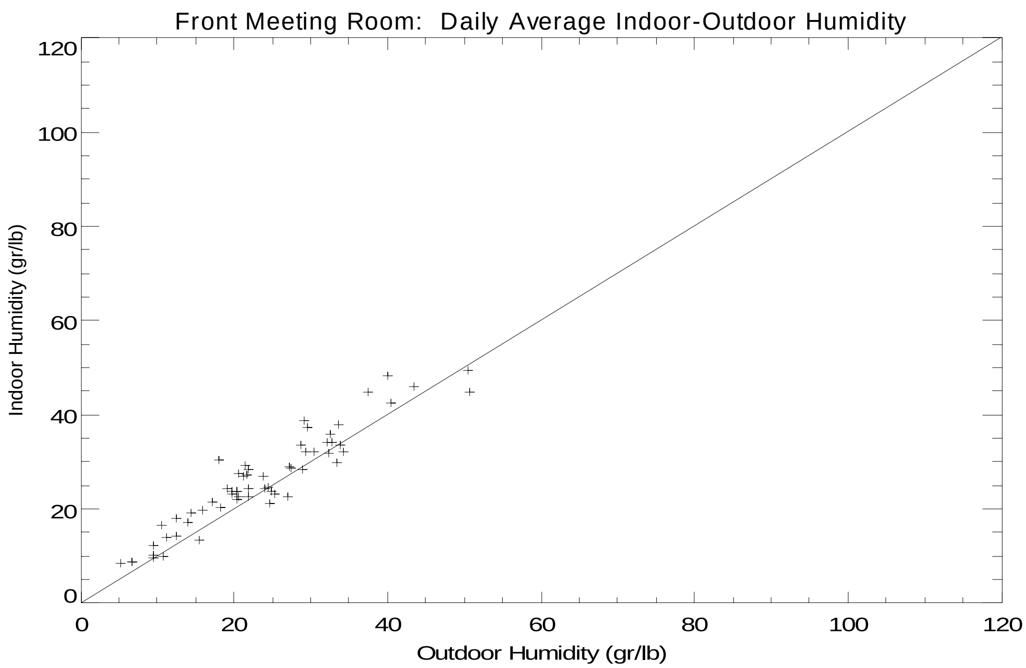

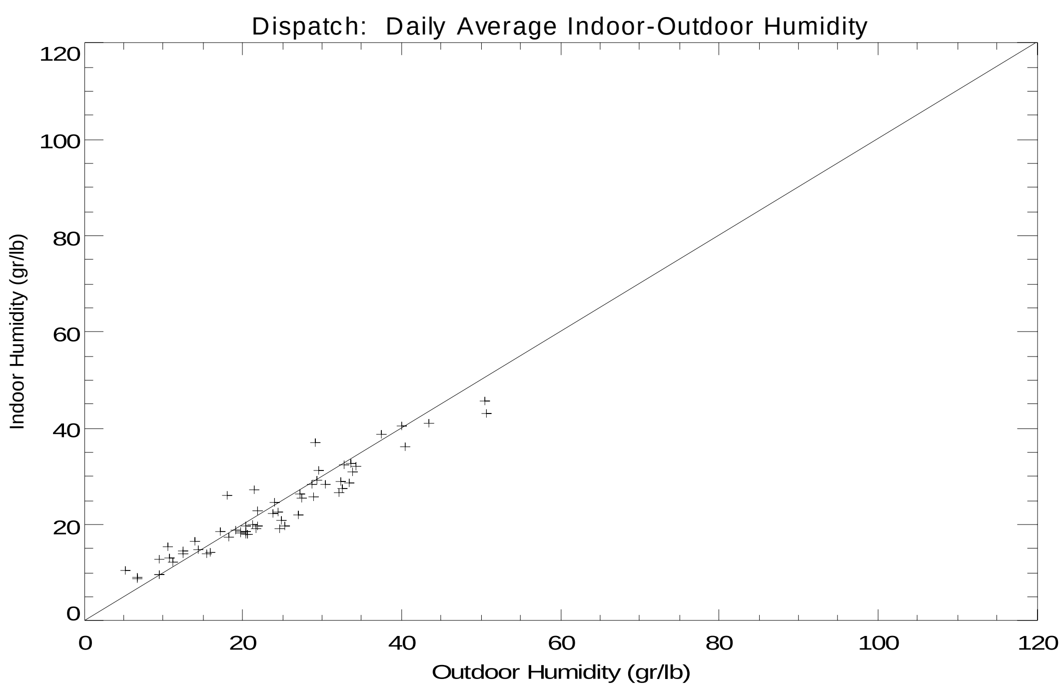

Figure A14-25. Indoor Humidity Variation with Outdoor Humidity

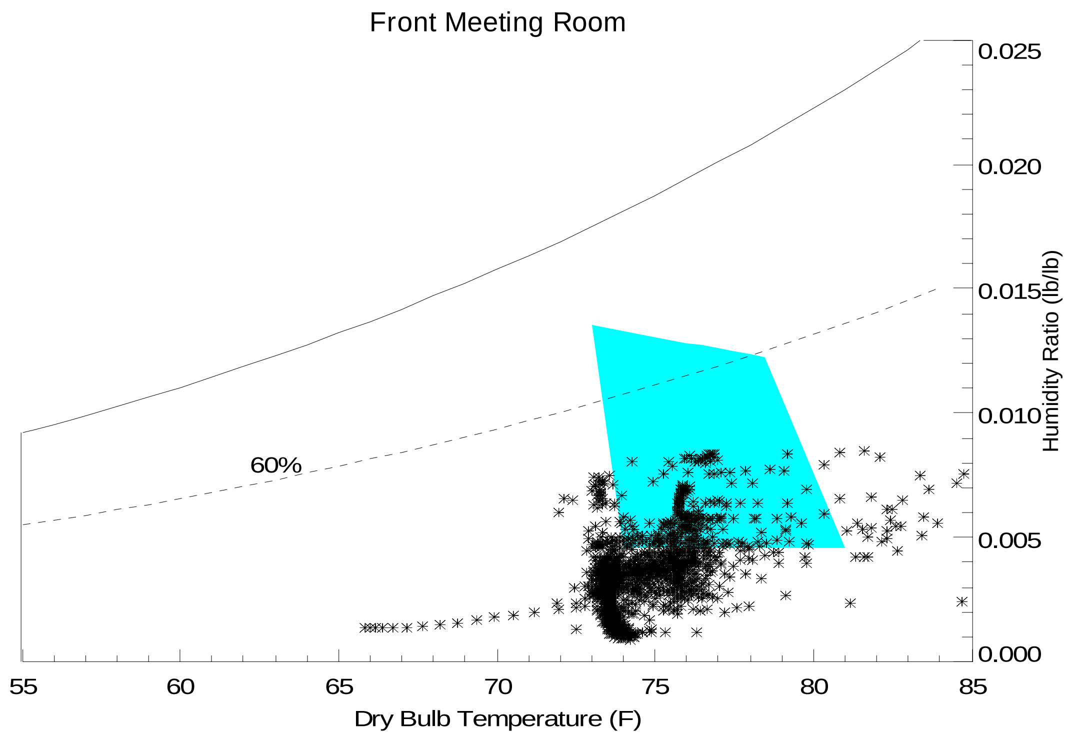

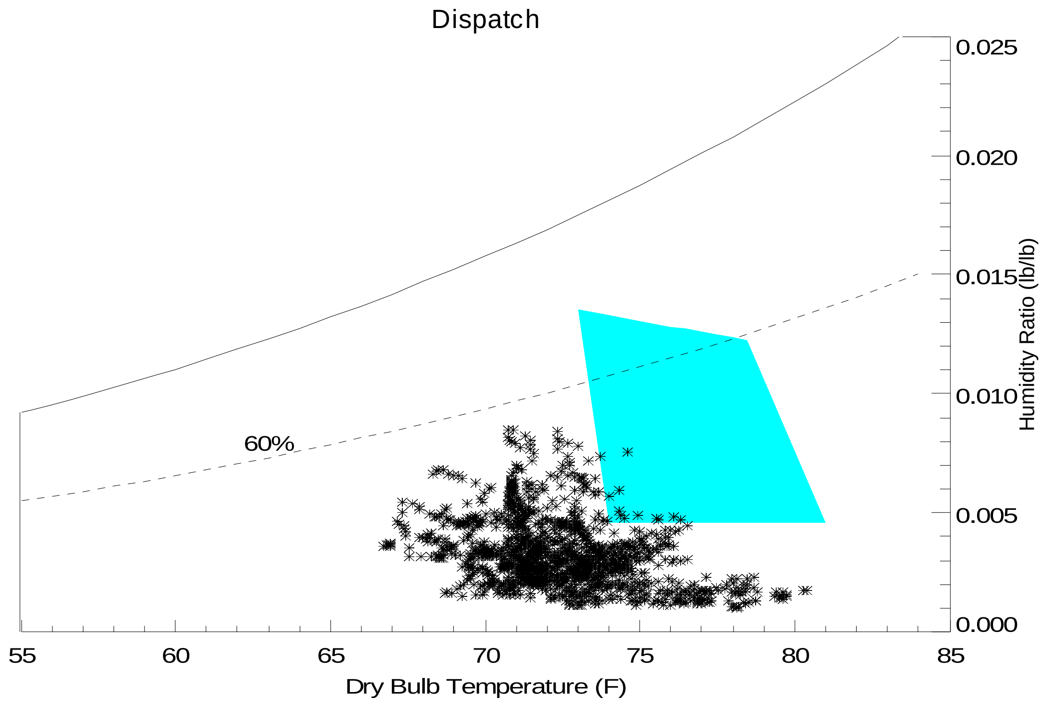

Figure A14-26. Indoor Air Quality Comparison with ASHRAE Comfort Zone for Cooling

Infiltration Estimate from CO_2 Decay

Figure A14-27 and Figure A14-28 show the resulting decay trends using CO_2 levels immediately after high occupancy periods for the facilities office 109 and upstairs office 202. The predicted air change rate (ACH) is shown on each plot.

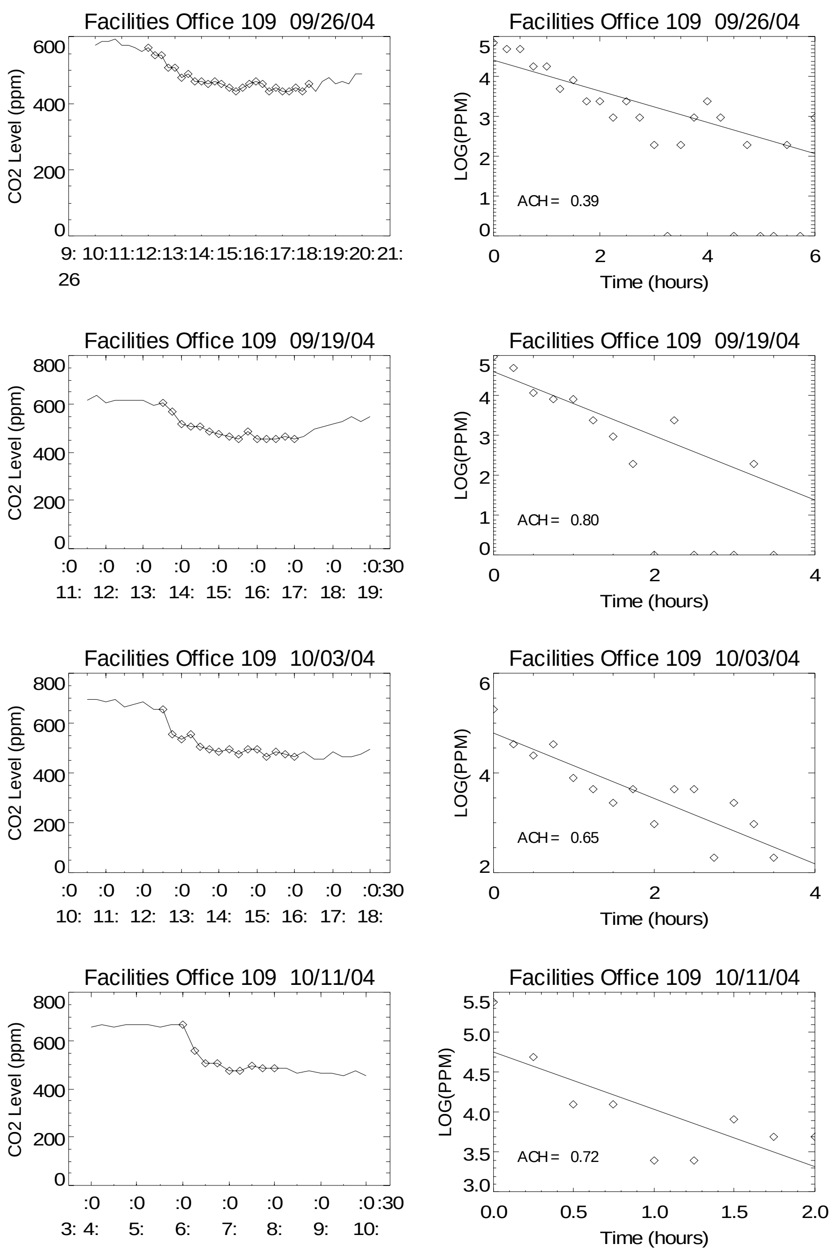

Figure A14-27. Facilities Office 102: Tracer Gas Decay Using CO_2 for Various Periods

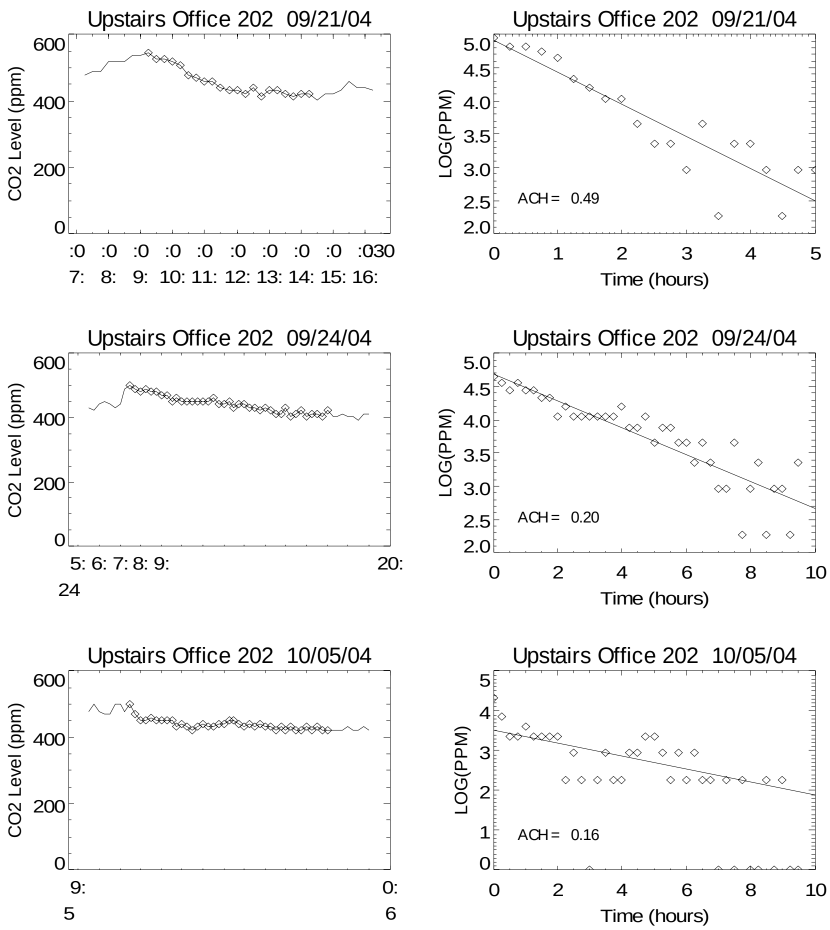

Figure A14-28. Relief Society: Tracer Gas Decay Using CO_2 for Various Periods

Table A14-11 summarizes the results of the tracer gas decay tests in the plots above. The table also includes the estimated infiltration airflow based on the building volume of 120,903 ft^3.

Table A14-11. Summary of Tracer Gas Decay Tests

Facilities Office 109

Start Time	End Time	ACH	Flow (cfm)
26-Sep 12:00 PM	26-Sep 06:00 PM	0.39	789
19-Sep 01:30 PM	19-Sep 05:00 PM	0.80	1,622
03-Oct 12:30 PM	03-Oct 04:00 PM	0.65	1,316
11-Oct 06:00 AM	11-Oct 08:00 AM	0.72	1,461

Upstairs Office 202

Start Time	End Time	ACH	Flow (cfm)
21-Sep 09:15 AM	21-Sep 02:15 PM	0.49	983
24-Sep 07:30 AM	24-Sep 05:00 PM	0.20	412
05-Oct 11:30 AM	05-Oct 09:00 PM	0.16	328

Note: Flow determined with building volume of: **121,423** ft^3

In comparison to the ACH values above, the nominal leakage rate (defined as ACH_{50} divided by 20) from the blower door test above is 0.32 ACH. The ACH values in Table A14-11 for the facilities office were calculated using CO_2 decays that were likely due to HVAC operation.

Utility Bills

Gas use is primarily used for space heating. The tables and graphs below show the gas and electric use trends for the facility. The following utility bill analysis may not be representative of the energy use during normal operation because the building was not fully occupied for these billing periods.

	Gas Use Index* ($MBtu/ft^2$-year)	Electric Use Index* (kWh/ft^2-year)
2004 (estimated)	104.9	12.8

* Note: This energy use index may not represent normal operation because the building was not fully occupied.

Table A14-12. Summary of Electric Bills

	Days in Month	Energy (kWh)	Demand (kW)	Cost ($)	$/kWh	Elec. Use per Sq-Ft (kWh/sq ft)
2/3/2004	29	6,600	20	841.48	0.127	0.52
3/4/2004	30	7,400	20	918.35	0.124	0.59
4/2/2004	29	8,800	----	1,264.92	0.144	0.70
5/3/2004	31	11,000	52	1,573.82	0.143	0.87
6/2/2004	30	21,000	----	2,600.09	0.124	1.67
7/1/2004	29	23,800	64	2,927.74	0.123	1.89
8/3/2004	33	27,600	60	3,248.62	0.118	2.19
8/31/2004	28	23,400	64	2,889.67	0.123	1.86
Jan-04 to Aug-04	***239***	***129,600***	***64.0***	***$ 16,265***	***0.125***	***10.29***
Estimated Annual	***365***	***161,174***	***64.0***	***$ 20,765***	***0.129***	***12.79***

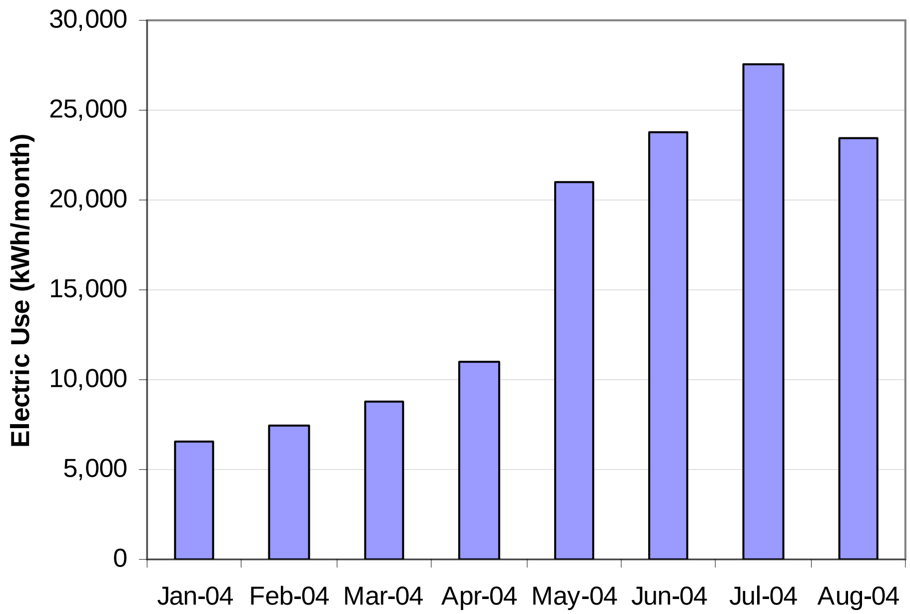

Figure A14-29. Monthly Electricity Use Trends (last 24 months)

Table A14-13. Summary of Gas Bills

	Days in Month	Gas Use (therms)	Cost ($)	$/therm	Gas Use per Sq-Ft (therm/sq ft)
2/3/2004	29	1,701	1699.16	1.00	0.135
3/4/2004	30	1,432	1432.37	1.00	0.114
4/2/2004	29	1,101	1103.61	1.00	0.087
5/3/2004	31	688	748.45	1.09	0.055
6/2/2004	30	761	839.96	1.10	0.060
7/1/2004	29	764	837.77	1.10	0.061
8/3/2004	33	701	766.42	1.09	0.056
8/31/2004	28	586	650.82	1.11	0.046
Jan-04 to Aug-04	***239***	***7,732***	***$ 8,079***	***1.04***	***0.614***
Estimated Annual	***365***	***13,218***	***13,659***	***1.03***	***1.049***

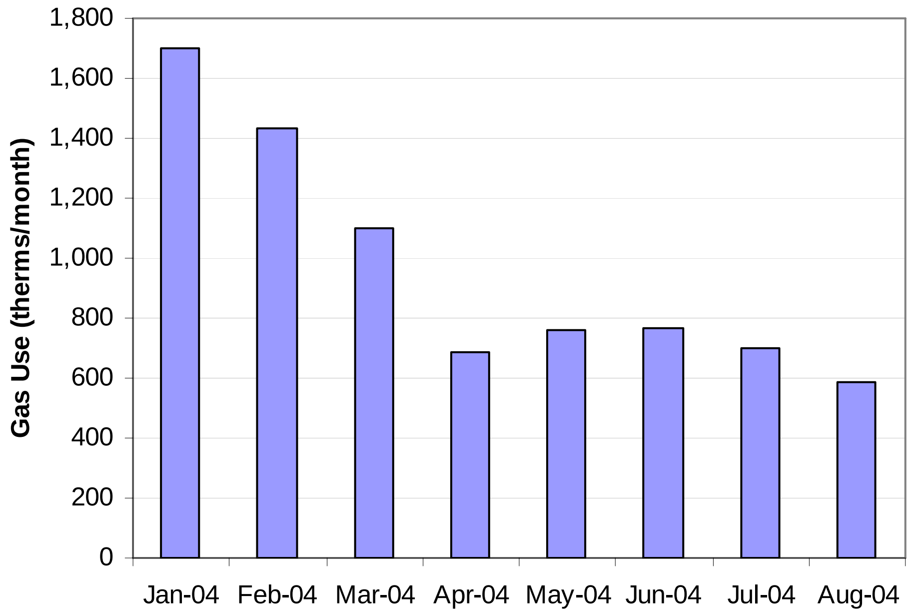

Figure A14-30. Monthly Gas Use Trends (last 24 months)

Figure A14-31 shows the gas use variation with ambient temperature and Figure A14-32 shows the electricity use variation with ambient temperature.

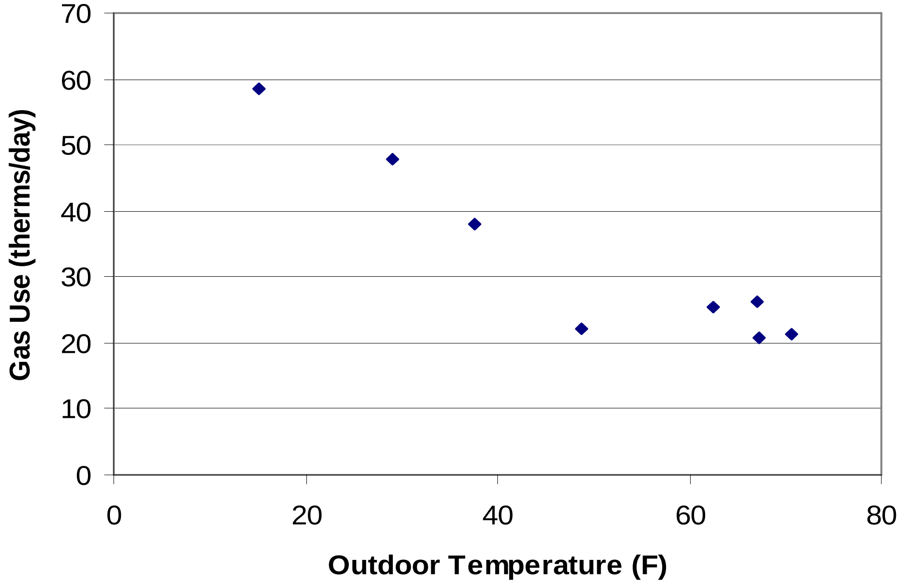

Figure A14-31. Variation of Gas Use with Ambient Temperature

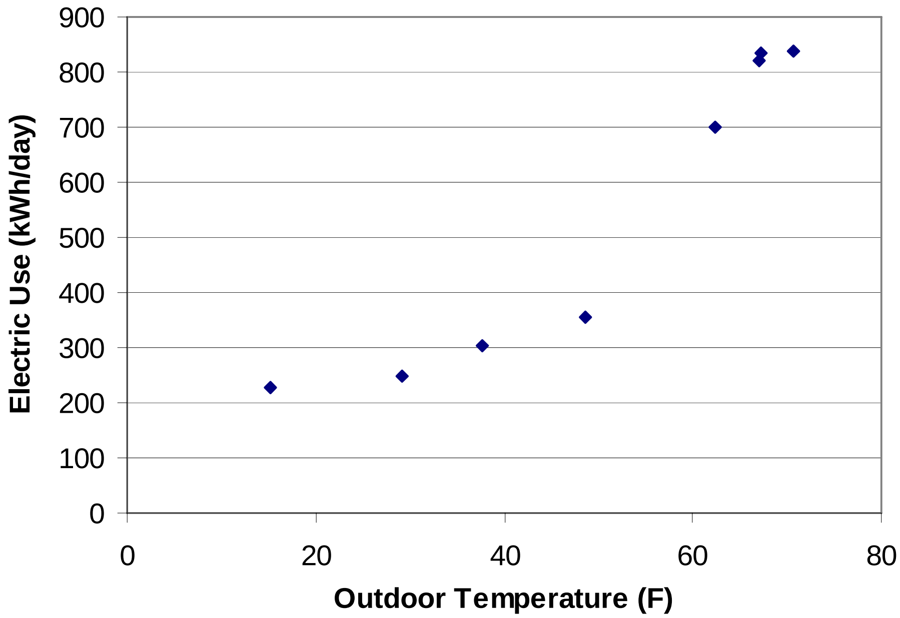

Figure A14-32. Variation of Electric Use with Ambient Temperature

Field Test Site 15/16 – Office Building, Ithaca, NY


Main Entrance (Site 15, south)


Rear of Ag. Building (Site 16, south)


West Side of Willow Building (Site 15)


Street Side of Willow Building (Site 15, north)


Front of Ag. Building (Site 16, north)


East Side of Ag. Building (Site 16)


Connection Hallway (north)

Figure A15-1. Photos of Buildings

CHARACTERISTICS

Building Description

The 12,800 sq-ft facility is a two-building complex that includes a two-story building located on Willow Ave. (Site 15) and a single story building on West Lincoln St. (the Ag Building, Site 16). The two buildings are now connected by a hallway. The first floor (7,350 sq-ft) of the Willow Building has conference rooms, a kitchen, a lobby with an information booth, a bathroom, and three mechanical rooms. The second floor (2,950 sq-ft) is comprised of office space, a meeting room, and a small kitchen. The Agriculture building (Site 16) is comprised of office space and a storage/mechanical room (2,500 sq-ft). The facility was originally two separate buildings that were renovated into offices in 1989. Each building has separate electrical and mechanical systems as well as separate electric and gas meters. The connecting hallway was added to join the two buildings in 2001. Mechanical work was done in 2004 to improve the ventilation system. New Exterior finish insulation (EFIS) was added to most of the building in 2004. The photos in Figure A15-1 show the building from various angles. The building entrance faces the parking lot to the south. Figure A15-2 and Figure A15-3 shows the building floor plan.

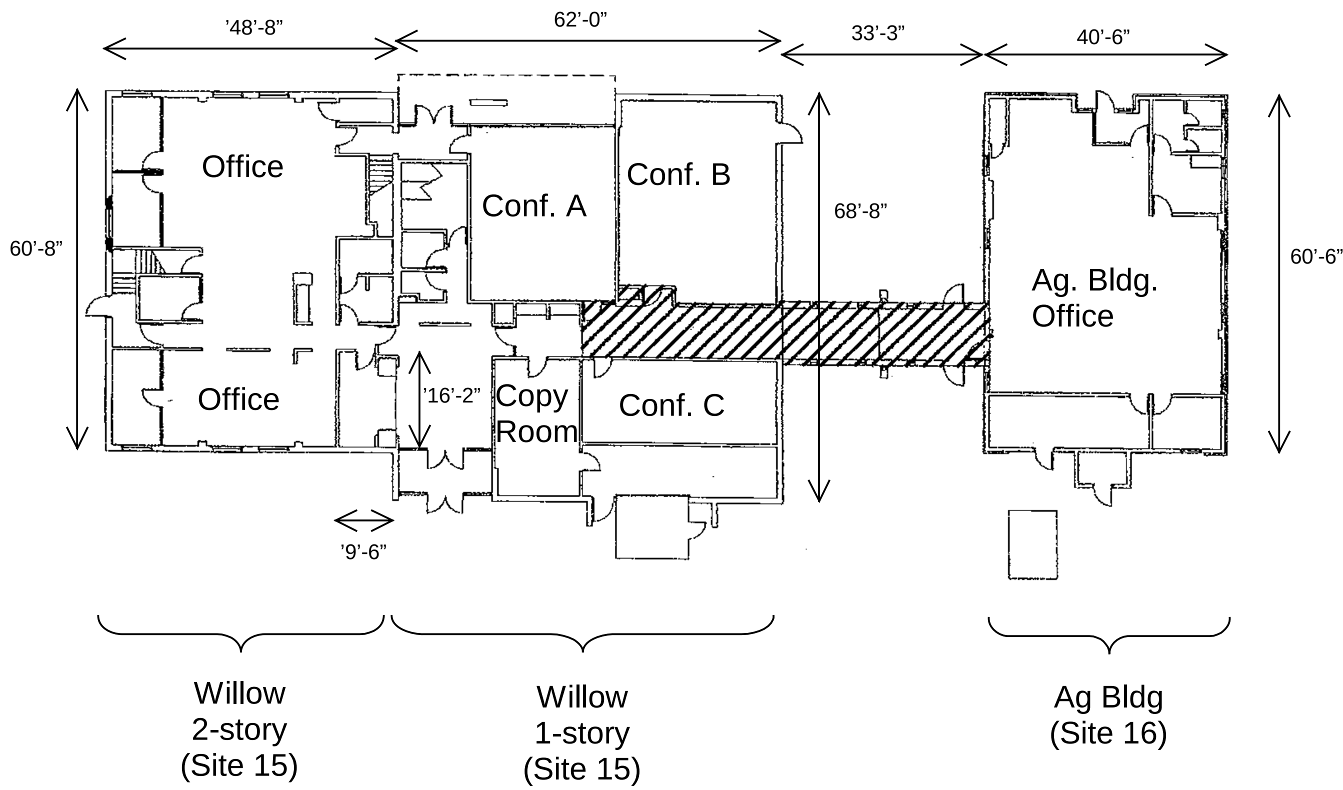

Figure A15-2. First Floor of Two Buildings

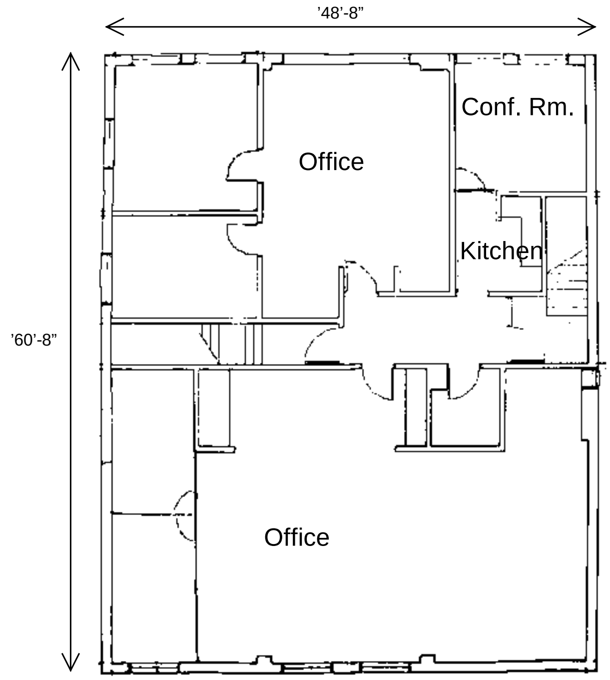

Figure A15-3. Second Floor of Building (Site 15)

Construction Details

Both buildings are concrete block construction with insulation at the roof deck. New exterior insulation (3 or 4 inch EPS foam) with a stucco coating (EFIS) was added to most of the building surfaces in 2004.

Rear of Ag Building (Site 16) where new EFIS begins/ends

Front of Ag Building where EFIS stops near meter

Additional roof insulation was added to the two-story portion of Willow (Site 15) when the roof was replaced, as shown Figure A15-4 and Figure A15-5. The exhaust fan details show that insulation was added on top of the roof deck, which causes the exhaust fan to sit relatively close to the roof.

The Ag building (Site 16) was constructed with insulated panels at the roof. The panels, shown in Figure A15-4, have gypsum board on the bottom and sit on top of the structural steel.

Exhaust fan “submerged” in New Roof & Insulation – Willows Second-story roof

Insulated Panels at Roof Deck in Ag Building

Figure A15-4. Photos Showing Roof and Ceiling Details

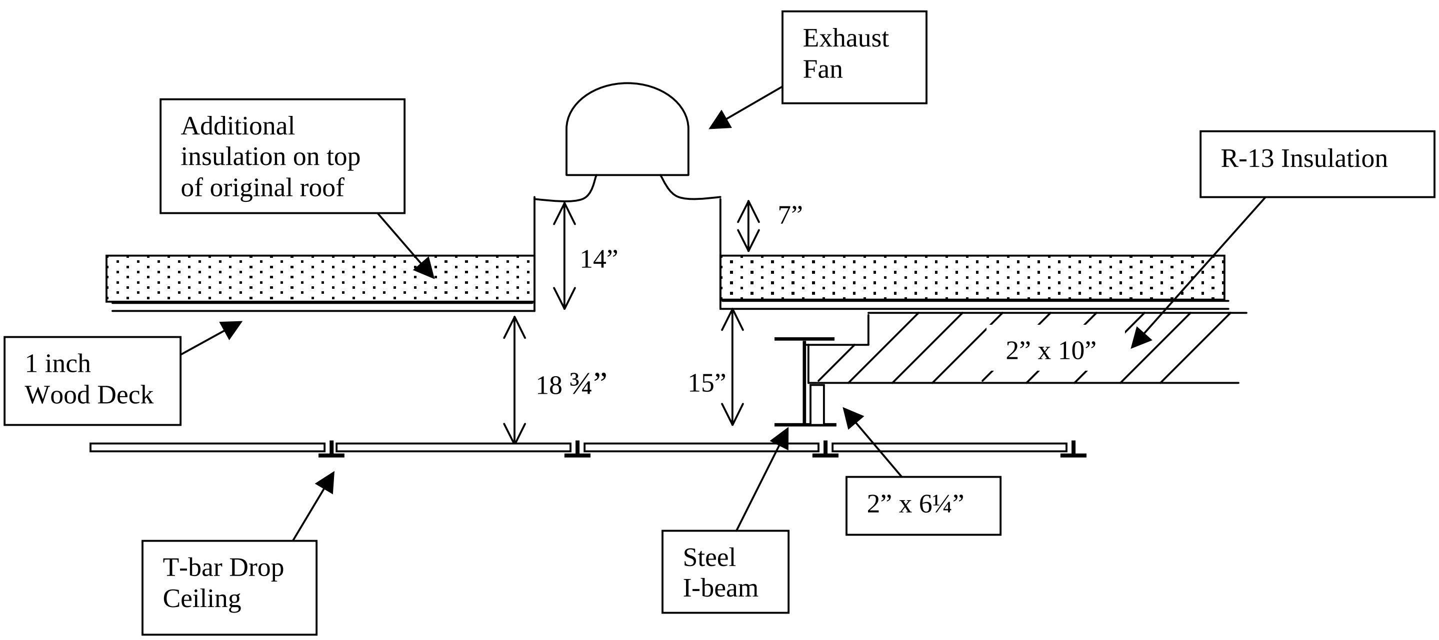

Figure A15-5. Second Floor Ceiling Construction Details (Site 15)

HVAC System

Figure A15-6 and Figure A15-7 show the locations of the HVAC equipment and supply/return grills in the building. Table A15-1 lists the equipment. Figure A15-9 shows pictures of various HVAC units for the building.

Table A15-1. Summary HVAC Equipment Installed at Site 15 & 16

Site	HVAC Equipment	Area	Manufacturer & Model	Heating Capacity (MBtu/h)	Cooling Capacity (tons)
15	AHU-1	Willow 1st flr west	Carrier Condensing units	-	3
	AHU-2	Right half of Section 1		-	3
	AHU-3	Info Booth, Section 2		-	3
	Ductless unit	Copy Room	Ductless split unit	-	~2
	RTU	Conf. Rooms, Sec. 2	York D3CG090N13025ECE	-	7½
	Console PTAC	Willow 1st & 2nd flrs	McQuay/SG K9L5W	hw	3/4
	Main Exhaust Fan	Willow 2nd Floor	Cheasa RDB165		
	Copyrm Exh Fan	Willow 2nd Floor			
16	Furnace/DX	Ag Building	Ducane AC10 B42-A		3½
	Furnace/DX	Ag Building	Ducane AC10 B42-A		3½

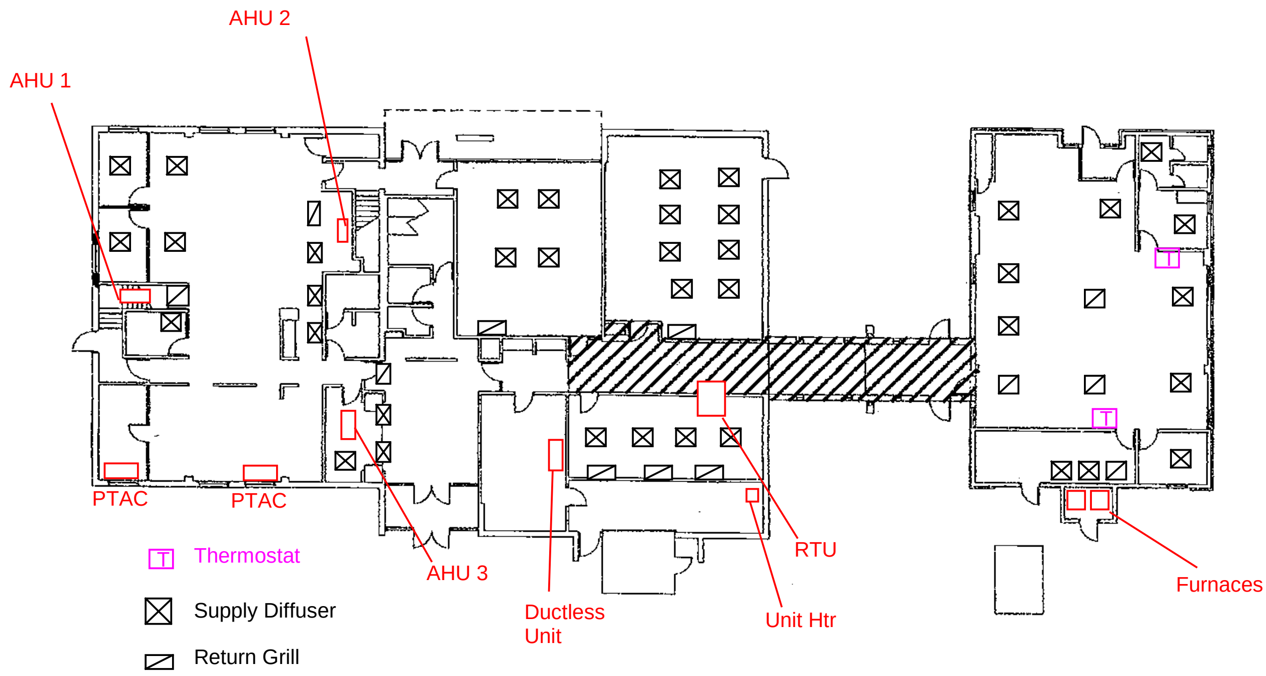

Figure A15-6. First Floor AHU Zones within Two Buildings

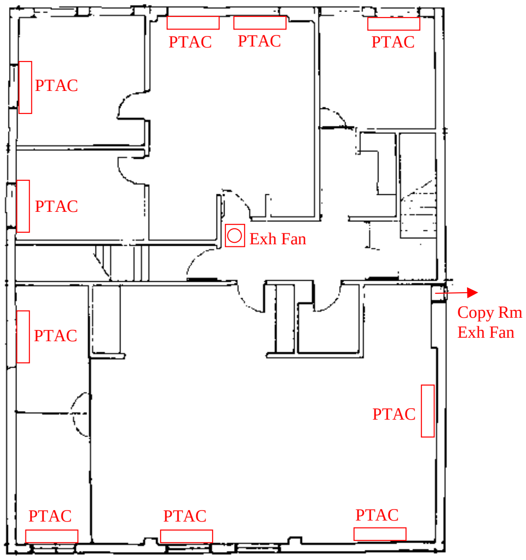

Figure A15-7. Second Floor PTAC Units

The HVAC system in the Willow Building (Site 15) includes 12 Packaged Terminal Air Conditioners (PTACs) in the 2-story section. The condenser section for each PTAC goes through the wall. Each PTAC is capable of pulling in fresh air. The PTACs include hot water coils and hot water baseboard around the perimeter of the building. Three additional residential style AHUs provide cooling and ventilation to the core areas of the first floor. The 3 condensing units corresponding to the AHUs are located on the single story roof of Willow (2 other condensing units have been abandoned in place).

The single-story section of Willow is cooled and heated by a York 7½ ton Roof Top Unit (RTU). The RTU includes a gas furnace section. The RTUs and AHUs are controlled by setback thermostats. The hot water baseboard heaters is provided by hot water from a natural gas boiler. The boiler has 5-6 hot water zones. Each PTAC has its own integral thermostat.

Two of the AHUs in Willow have a fresh air intake damper to provide ventilation. The damper in AHU1 was found to be closed and let in only 38 cfm of fresh air. The outdoor damper for AHU 2 was installed but not properly wired.

AHU 1 was slightly tilted so that it spilled condensate from its drain pan on the floor. The condensate floods the closet and a nearby office. For this reason, the AHU is only used for ventilation during the heating season and is turned off during the summer. This drainage problem could be fixed by changing the current drain location or leveling the unit.

York Roof Top Unit on top of Willow

Carrier Condensing Units Serving AHUs on top of Willow (3 operating, 2 abandoned)

Console PTAC with Front Cover Off

PTAC Exterior Grill

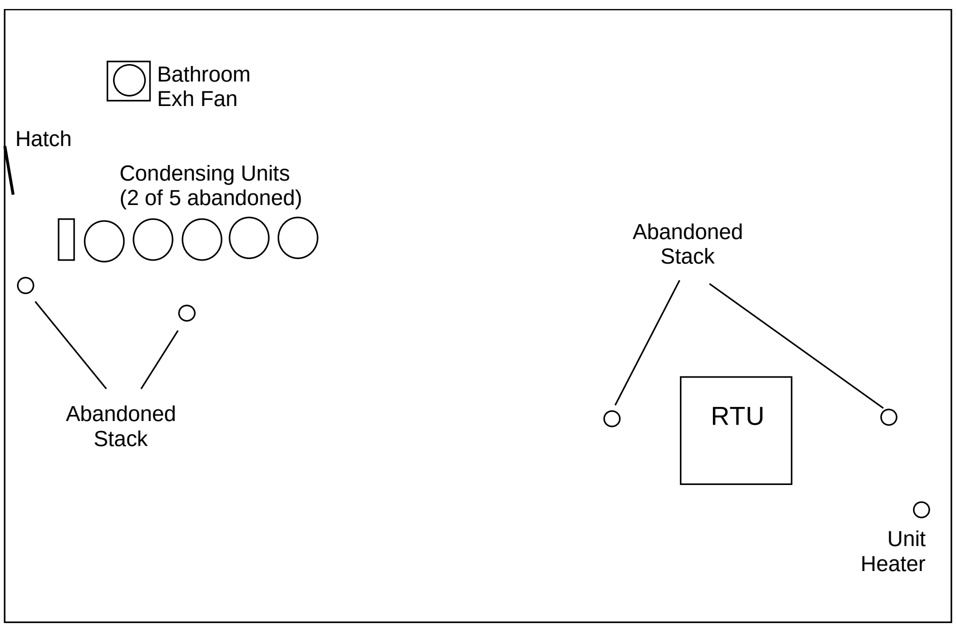

Single-Story Roof on Willow

Figure A15-8. HVAC Equipment in Willow Building (Site 15)

The agricultural building is conditioned by two furnaces with DX cooling coils. The furnaces are located in the furnace shed on the back of the building. The cooing coil is located downstream of furnace just inside the building (see Figure A15-9 and Figure A15-10). The Ducane condensing units are located outside beside the furnace shed.


"Furnace Shed" on back of Ag Building

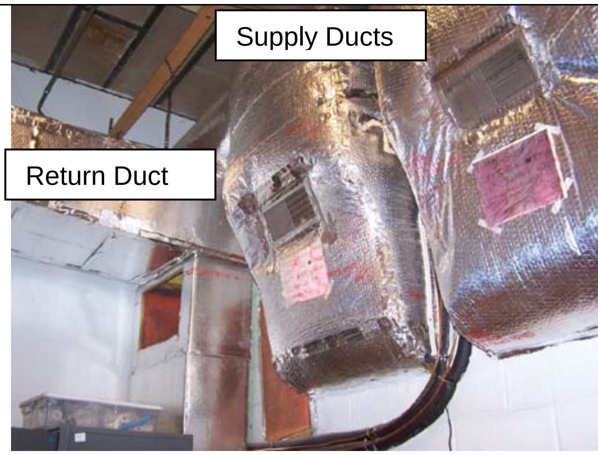

Supply Ducts and Cooling Coils


Furnace Flue Vents and Supply Air Ducts


Furnace on top of Return Air Plenum in Shed

Figure A15-9. HVAC Units in the Ag Building (Site 16)

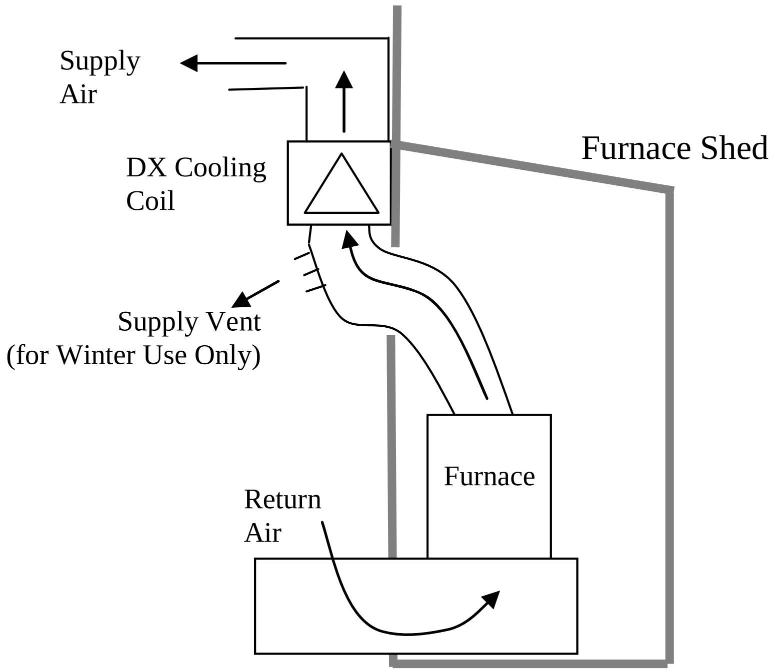

Figure A15-10. Furnace/Cooling Coil for Agriculture Building (Site 16)

MEASUREMENTS

The test data below was taken on May 24 and 25, 2005. Blower door testing and pressure mapping for the Willow Building (Site 15) were done on May 24. Blower door testing and pressure mapping for the Agriculture Building (Site 16), and a tracer gas test were done on May 25. Supply and return airflow testing measurements were taken throughout the two days. Test Personnel were John Carpenter, Mike Clarkin, and Hugh Henderson for both days of testing. Personnel from Performance Systems Contracting also participated. John Carpenter returned to the site May 26 to obtain the data for the tracer gas test. The CO_2 Sensors and the Temperature/RH sensors were retrieved on October 28, 2005.

Building Envelope Airtightness

The leakage characteristics of the building enclosure were assessed using fan pressurization methods. The building was too large to test as a whole; therefore, building was divided into 3 different sections for separate air tightness tests. Figure A15-11 shows the sections or areas pressurized for each test. The first section was the two story part of Willow, excluding the front desk and lobby area. The second section was comprised of the lobby and front desk, meeting rooms, the copy room, the storage room and the connection hallway. This division between sections 1 and 2 was selected to conform with a firewall that ran up into the ceiling plenum. The third section was the agriculture building.

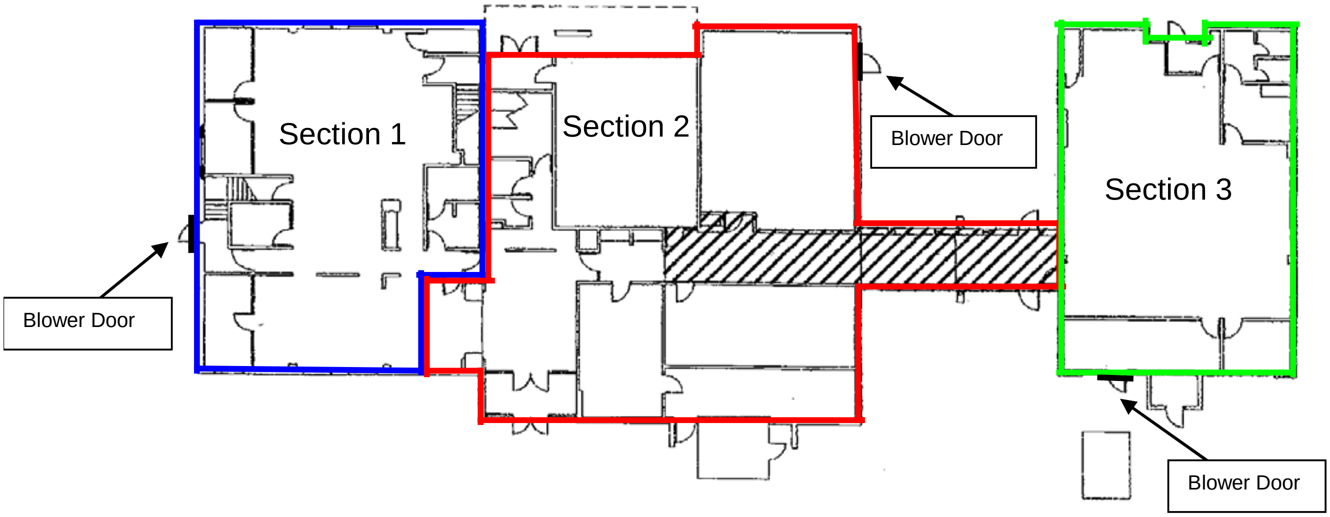

Figure A15-11. Building Sections Used for Blower Door Testing

A single blower door was installed and used for all tests. The blower door location used for each section is shown in the Figure above. All exterior doors and windows were closed. To the extent possible, the building sections were tested in the following configuration:

- All interior doors open
- AHUs off
- RTU off and ventilation intakes sealed
- All exhaust fans sealed
- Outdoor air intakes sealed

In section 1, the building pressure was varied from 14 Pa to 42 Pa. Figure A15-12 shows the building leakage variation with building pressure. Table A15-2 shows the results of the blower door tests in section 1 including model coefficients, effective leakage area (ELA), and air-changes-per-hour (ACH). The ELA is calculated using the Lawrence Berkeley Laboratory method, which calculates the leakage area at 4 Pa. The building has an effective leakage area of approximately 4.65 sq in per 100 sq ft of the total envelope area (including floor area). Another building leakage characteristic is the ACH at 50 Pascal's (ACH_{50}). The building has an ACH_{50} of 8.2.

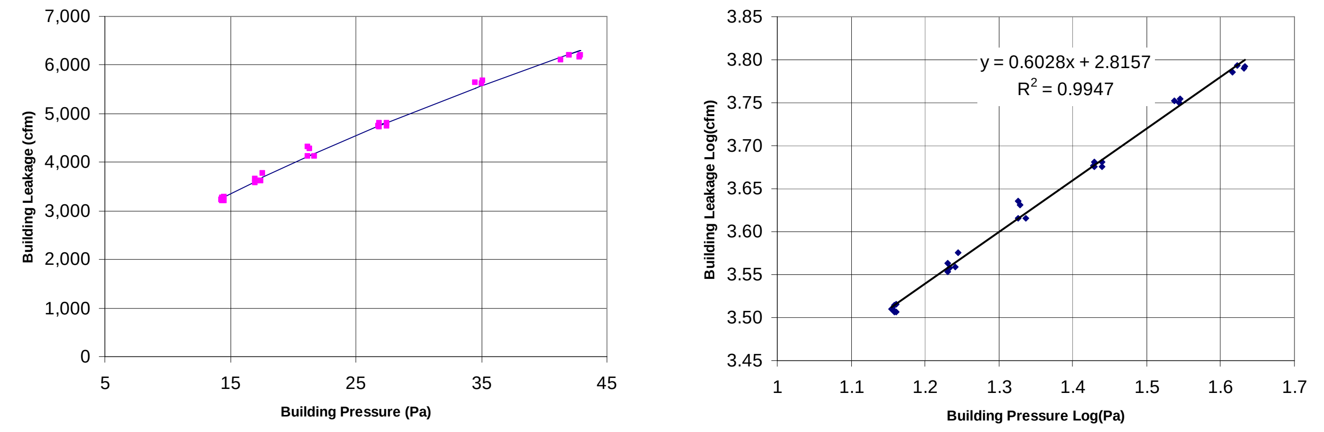

Depressurization Test – Section 1

Figure A15-12. Variation of Building Leakage with Pressure: cfm = K(ΔP)^n

Table A15-2. Blower Door Test Data, Resulting Best-Fit Model Coefficients, and ELA: Section 1

Test Results:

Flow Coefficient (K)	654.2	5,191	sq ft, floor area
Exponent (n)	0.603		
Leakage area (LBL ELA @ 4 Pa)	427 sq in	4.65	ELA / 100 sq ft
Airflow @ 50 Pa	6,915.1 cfm	8.2	ACH @ 50

Using Camroden BD

Test Data:

	Nominal Building Pressure (Pa)	Nominal Flow (cfm)	Ring
1	42.0	6,208	none
2	42.8	6,160	none
3	42.9	6,202	none
4	41.3	6,098	none
5	35.1	5,677	none
6	35.0	5,624	none
7	34.5	5,646	none
8	26.8	4,753	none
9	26.9	4,794	none
10	27.5	4,798	none
11	26.9	4,734	none
12	27.5	4,737	none
13	21.2	4,326	none
14	21.7	4,126	none
15	21.3	4,276	none
16	21.2	4,123	none
17	17.6	3,768	none
18	17.1	3,610	none
19	17.0	3,658	none
20	17.0	3,580	none
21	17.4	3,622	none
22	14.4	3,215	none
23	14.5	3,209	none
24	14.4	3,222	none
25	14.4	3,267	none
26	14.3	3,232	none
27	14.5	3,279	none

Notes: ELA is leakage area (in square inches) at reference pressure of 4 Pa.
ELA per 100 sq ft is based on total building envelope surface area (ceiling, exterior walls and floor).

In section 2, the building pressure was varied from 10 Pa to 30 Pa. Figure A15-13 shows the building leakage variation with building pressure.

Table A15-3 shows the results of the blower door tests in section 2 including model coefficients, effective leakage area (ELA), and air-changes-per-hour (ACH). Section 2 has an ELA of approximately 2.94 sq in per 100 sq ft of total envelope area. The ACH_{50} for the section was calculated to be 6.8.

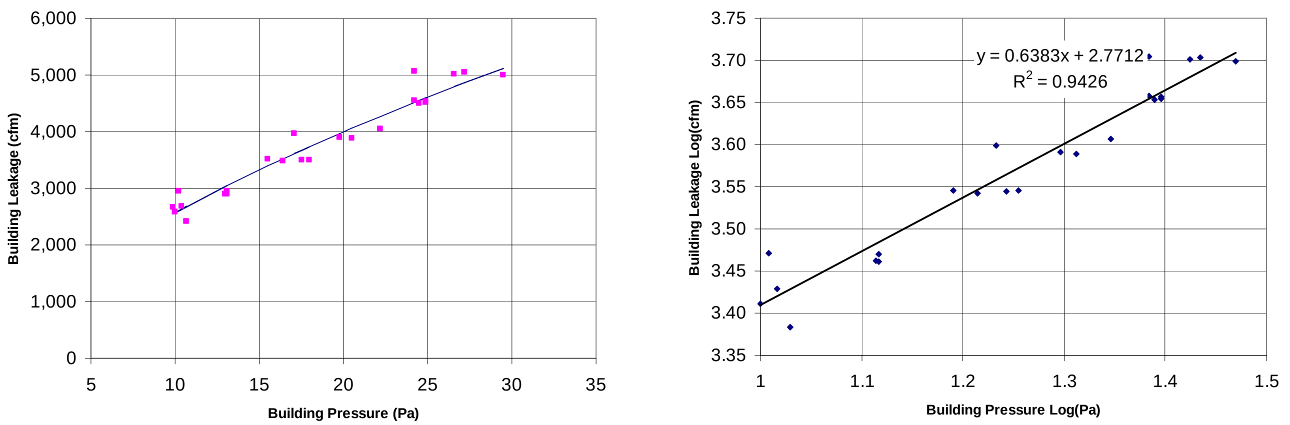

Depressurization Test – Section 2

Figure A15-13. Variation of Building Leakage with Pressure: cfm = K(ΔP)^n

Table A15-3. Blower Door Test Data, Resulting Best-Fit Model Coefficients, and ELA: Section 2

Test Results:

Flow Coefficient (K)	590.4	4,419 sq ft, floor area
Exponent (n)	0.638	
Leakage area (LBL ELA @ 4 Pa)	405 sq in	2.94 ELA / 100 sq ft
Airflow @ 50 Pa	7,172.8 cfm	6.8 ACH @ 50

Test Data:

	Nominal Building Pressure (Pa)	Nominal Flow (cfm)	Ring
1	26.6	5,020	none
2	29.5	5,004	none
3	27.2	5,047	none
4	24.2	5,069	none
5	24.2	4,551	none
6	24.5	4,498	none
7	24.9	4,531	none
8	24.9	4,518	none
9	22.2	4,045	none
10	20.5	3,885	none
11	19.8	3,904	none
12	17.1	3,972	none
13	17.5	3,507	none
14	18.0	3,508	none
15	16.4	3,489	none
16	15.5	3,514	none
17	13.1	2,948	none
18	13.0	2,898	none
19	10.2	2,955	none
20	13.1	2,894	none
21	10.0	2,580	none
22	10.7	2,419	none
23	9.9	2,672	none
24	10.4	2,687	none

Notes: ELA is leakage area (in square inches) at reference pressure of 4 Pa.
ELA per 100 sq ft is based on total building envelope surface area (ceiling, exterior walls and floor).

In section 3 (the Ag building, Site 16) the building pressure was varied from 8 Pa to 30 Pa. Figure A15-14 shows the building leakage variation with building pressure. Table A15-5 shows the results of the blower door tests in section 3, including model coefficients, effective leakage area (ELA), and air-changes-per-hour (ACH). Section 3 has an ELA of approximately 0.9 sq in per 100 sq ft of total envelope area. The ACH_{50} for the section was calculated to be 3.4.

Since this building was extremely airtight, the test was repeated with the air gap under the main door taped off. This gap under the 36 inch door was about ½ to ¾ inch or about 18-27 square inches. The test result for this test are given in Figure A15-15 and Table A15-6. The exponent increased slightly to 0.83 as would be expected (all the remaining leakage paths become very long, so the exponent approaches 1). The measured ELA for the building dropped by about 16 square inches, in reasonable agreement with the observed size of the gap under the door.

Table A15-4 summarizes the air tightness measurements made on each building

Table A15-4. Summary of Envelop Tightness Data for Each Building Section

		Flow Coeff. K	Exp. n	ELA (sq in)	ELA / 100 sq ft (sq in/sq ft)	ACH_{50}
Site 14	Section 1	654.2	0.603	427	4.65	8.2
	Section 2	590.4	0.638	405	2.94	6.8
	Sections 1 & 2 combined			833	3.63	7.4
Site 15	Section 3	79.0	0.802	68	0.93	3.4
	Section 3 (door sealed)	57.8	0.833	52	0.71	2.8

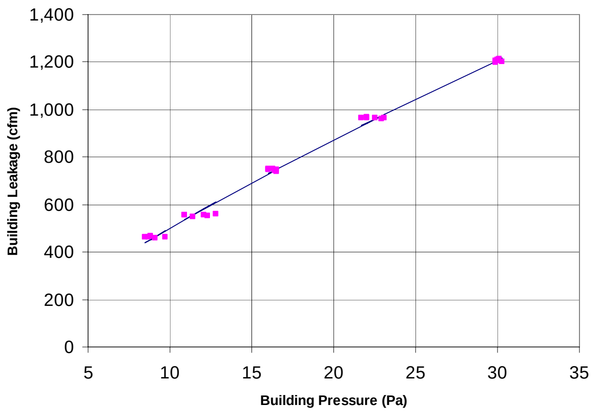

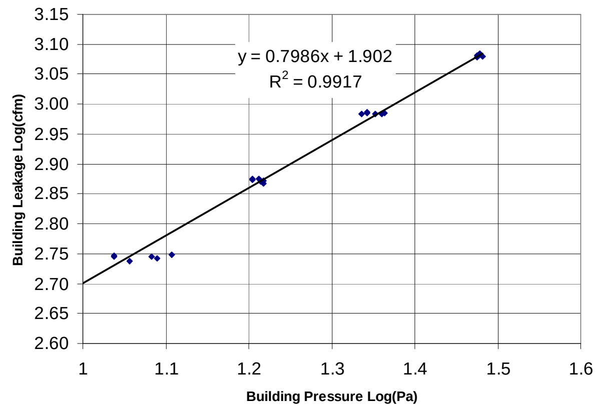

Depressurization Test – Section 3

Figure A15-14. Variation of Building Leakage with Pressure: cfm = $K(\Delta P)^n$

Table A15-5. Blower Door Test Data, Resulting Best-Fit Model Coefficients, and ELA: Section 3

Test Results:

Flow Coefficient (K)	79.0	2,249 sq ft, floor area
Exponent (n)	0.802	
Leakage area (LBL ELA @ 4 Pa)	68 sq in	0.93 ELA / 100 sq ft
Airflow @ 50 Pa	1,819.5 cfm	3.4 ACH @ 50

Test Data:

	Nominal Building Pressure (Pa)	Nominal Flow (cfm)	Ring
1	29.9	1,198	b
2	30.3	1,203	b
3	29.9	1,207	b
4	30.0	1,208	b
5	30.0	1,207	b
6	30.1	1,213	b
7	23.1	965	b
8	22.0	966	b
9	21.7	963	b
10	22.5	963	b
11	22.9	962	b
12	22.0	969	b
13	16.0	749	b
14	16.3	750	b
15	16.0	747	b
16	16.5	745	b
17	16.4	743	b
18	16.5	738	b
19	10.9	558	b
20	10.9	557	b
21	11.4	547	b
22	12.3	552	b
23	12.8	560	b
24	12.1	556	b
25	9.1	460	b
26	8.5	461	b
27	8.7	462	b
28	9.7	462	b
29	8.8	466	b
30	8.8	466	b

Notes: ELA is leakage area (in square inches) at reference pressure of 4 Pa.
ELA per 100 sq ft is based on total building envelope surface area (ceiling, exterior walls and floor).

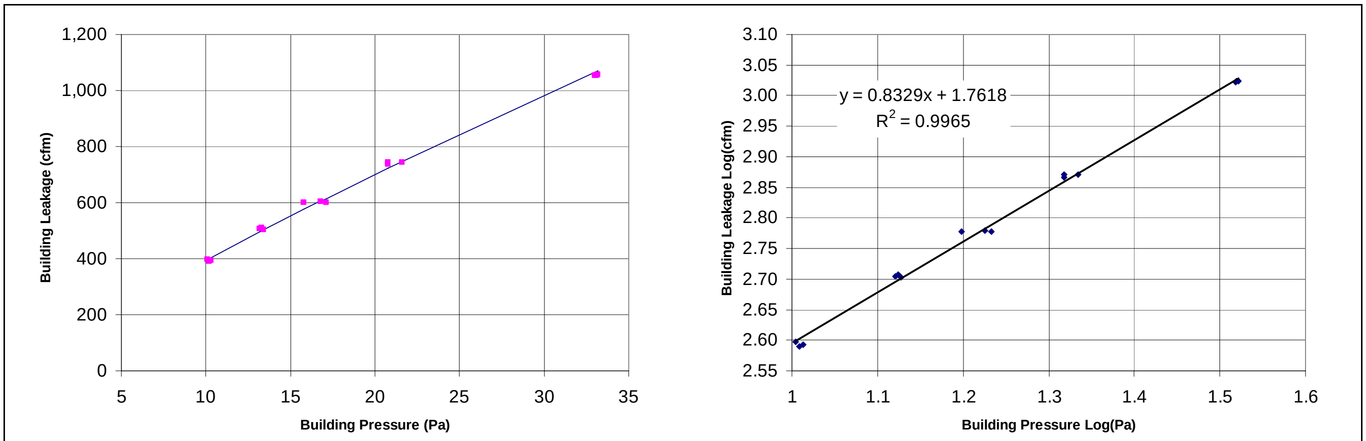

Depressurization Test – Section 3 (door sealed)

Figure A15-15. Variation of Building Leakage with Pressure: cfm = K(ΔP)^n

Table A15-6. Blower Door Test Data, Resulting Best-Fit Model Coefficients, and ELA: Section 3 (door)

Test Results:

Flow Coefficient (K)	57.8	2,249 sq ft, floor area
Exponent (n)	0.833	
Leakage area (LBL ELA @ 4 Pa)	52 sq in	0.71 ELA / 100 sq ft
Airflow @ 50 Pa	1,502.7 cfm	2.8 ACH @ 50

Test Data:

	Nominal Building Pressure (Pa)	Nominal Flow (cfm)	Ring
1	33.0	1,052	b
2	33.1	1,055	b
3	33.2	1,056	b
4	21.6	743	b
5	20.8	736	b
6	20.8	742	b
7	17.1	599	b
8	16.8	602	b
9	15.8	599	b
10	13.2	506	b
11	13.4	504	b
12	13.3	509	b
13	10.1	396	b
14	10.3	392	b
15	10.2	389	b

Notes: ELA is leakage area (in square inches) at reference pressure of 4 Pa.
ELA per 100 sq ft is based on total building envelope surface area (ceiling, exterior walls and floor).

Pressure Mapping (during blower door testing)

Pressure readings in the building were taken using a digital micromanometer (DG 700) with the blower door operating. Pressure measurements were taken between interior rooms with doors closed.

In building section 1, the pressure difference across the building envelope was 20 Pa with the blower door operating. The pressure differences for a number of different locations are shown in Figure A15-16. The pressure difference between the ceiling and the space was measured in a number of locations, and all of these readings were at or very close to zero. The smaller pressure differences between sections 1 and 2 imply that some of the measured leakage is actually zone-to-zone instead of to the building exterior.

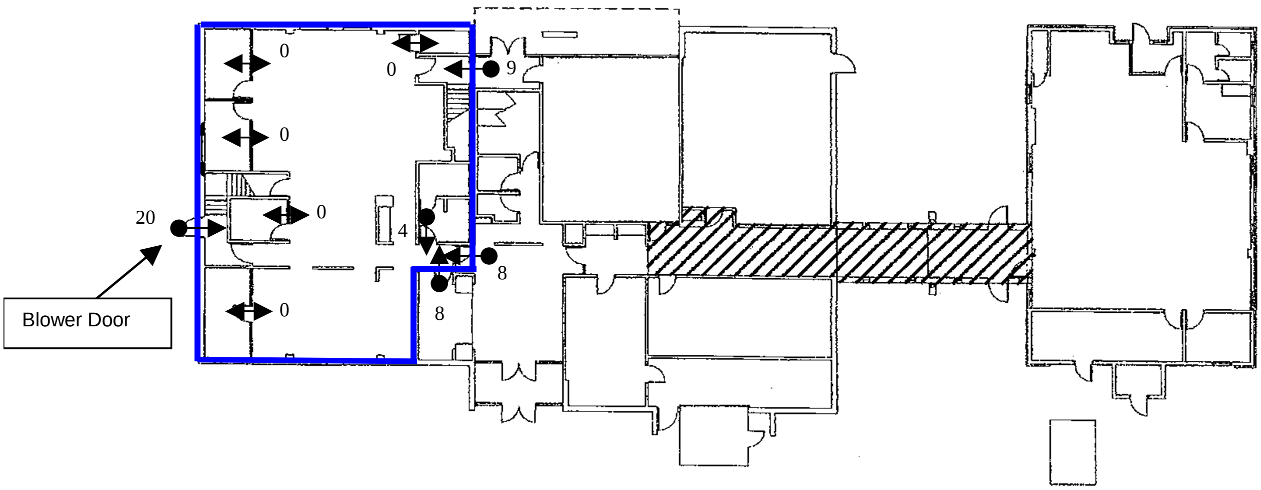

Figure A15-16. Section 1 Pressure Mapping with Building Depressurized to 20 Pa

Building section 2 was also pressure mapped at a building envelope pressure of 20 Pa. The pressure differences at various locations in this section of the building are shown in Figure A15-17. Measurements were taken of the pressure difference across the ceiling. Any pressure differences were very small (0-1 Pa). Again, some portion of the measured leakage was zone-to-zone leakage between sections 1 and 2. The pressures indicate that the storage room at the back of the building (next to the main entrance) was a major source of leakage, as would be expected given the garage door & greenhouse in that section. The pressures in the rest rooms imply that some of the zone-to-zone leakage was occurring in the walls behind the bathroom.

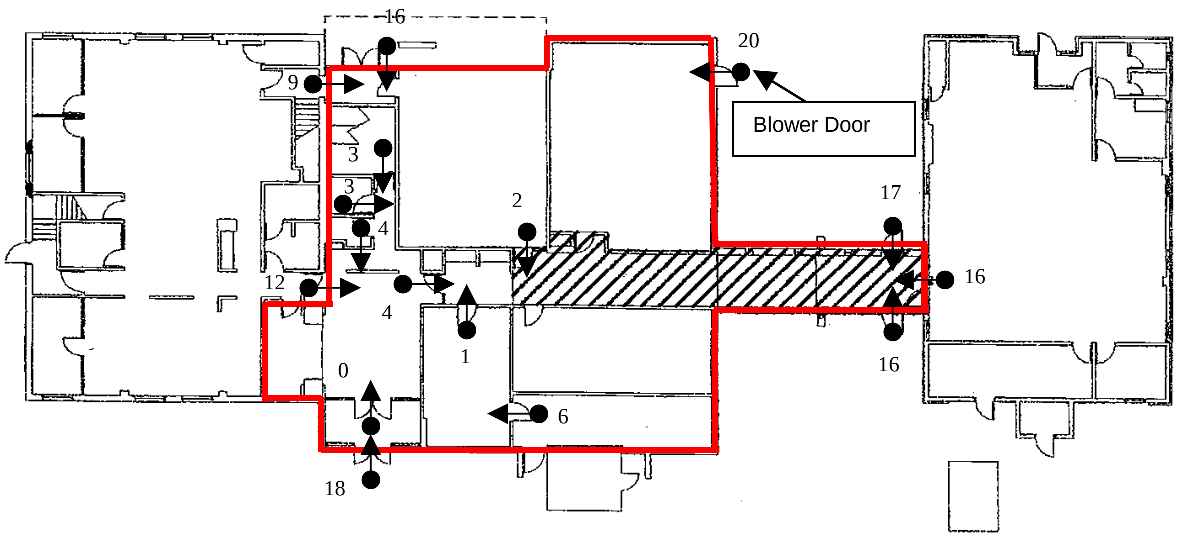

Figure A15-17. Section 2 Pressure Mapping with Building Depressurized to 20 Pa

Building section 3 was pressured to 80 Pa for the pressure mapping. Figure A15-18 shows the pressure differences for various locations for section 3. There was only a 20 Pa drop across the outside front door, implying that the front vestibule area accounted for some of leakage to outdoors. The furnace shed was half way between the building and outdoors, which implies that some of the leakage from the space is occurring through the ductwork. The ceiling has a small pressure difference of 1.3 Pa relative to the office, implying almost no leakage through the roof of the building.

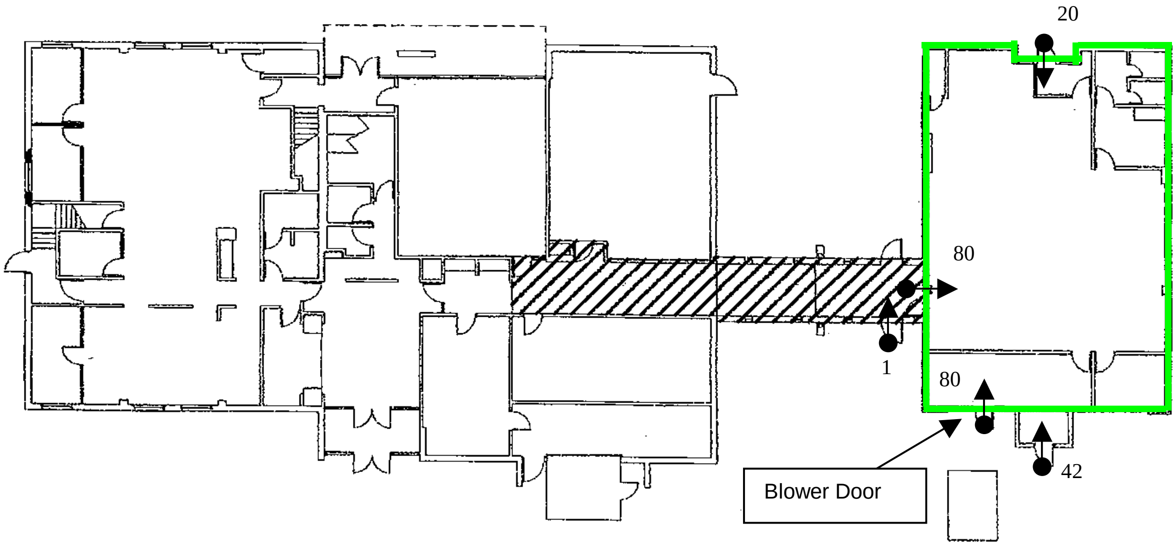

Figure A15-18. Section 3 Pressure Mapping with Building Depressurized to 80 Pa

HVAC Airflow Measurements

The airflow from each supply diffuser was measured using a Shortridge flow hood (compensated mode). The total supply airflow is approximately 6,142 cfm or 0.48 cfm per sq-ft of total floor area. This number is low for an office because the PTACs (which were not measured) would account for additional flow. Figure A15-19 and Figure A15-20 display the measured airflow at each diffuser and exhaust on the first floor and second floor.

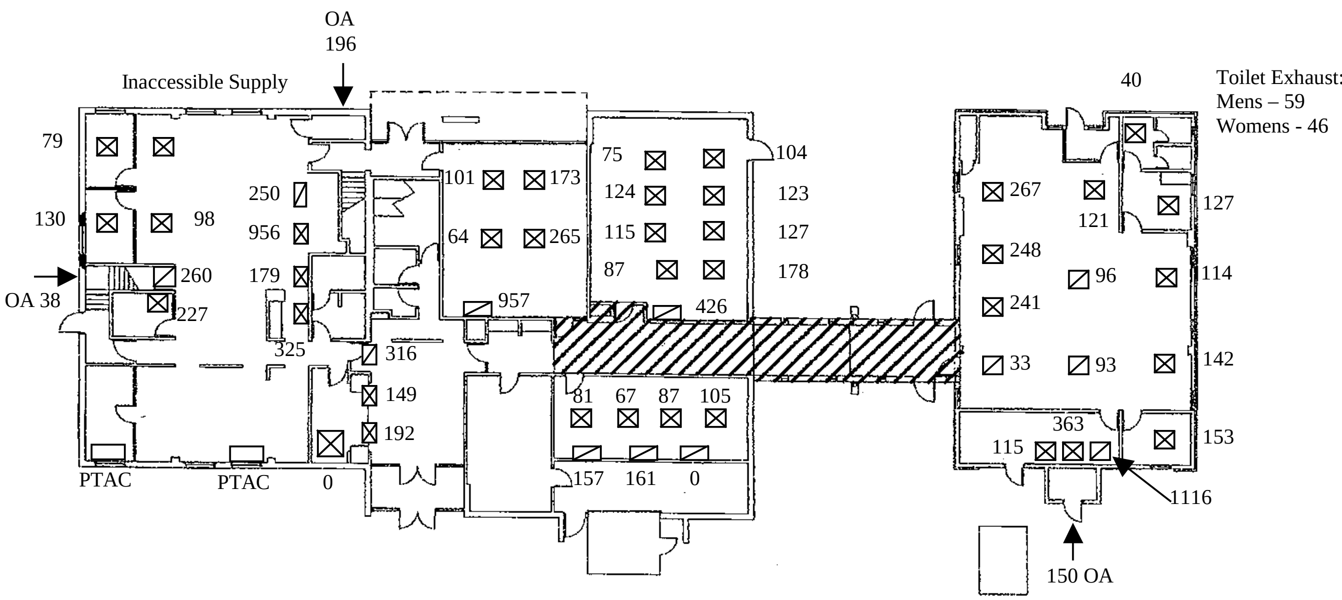

Figure A15-19. First Floor Supply and Return Airflow Measurements (cfm)

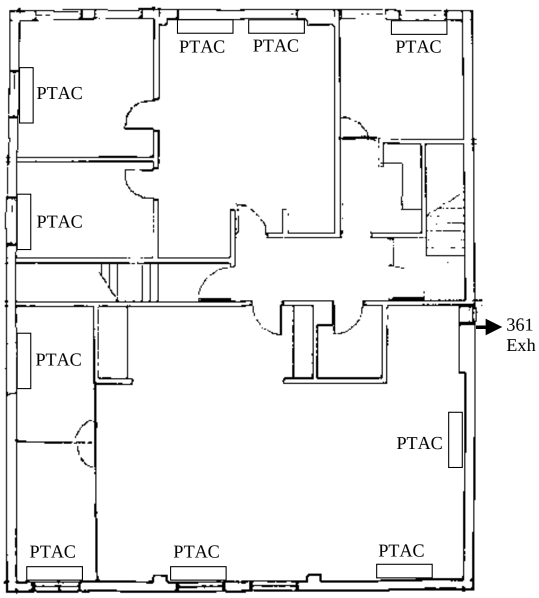

Figure A15-20. Second Floor Supply and Return Airflow Measurements (cfm)

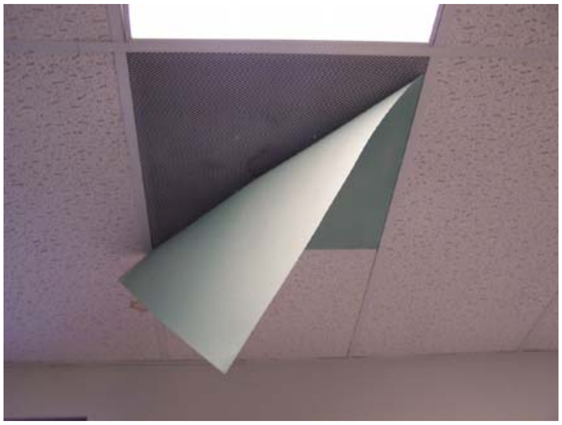

Measured flow – 248 cfm

Measured flow – 114 cfm

Figure A15-21. Blocked Supply Ducts in Ag Building

AHUs in Willow

Label	Measured (cfm)
AHU1-S1	79
AHU1-S2	130
AHU1-S3	98
AHU1-S4	227
AHU1-S5	na
AHU1-R	-260
AHU1-OA	-38
AHU2-S1	956
AHU2-S2	179
AHU2-S3	325
AHU2-R	-250
AHU2-OA	-196
AHU3-S1	192
AHU3-S2	149
AHU3-R	-316

RTU

Label	Measured (cfm)
RTU-S1	101
RTU-S2	173
RTU-S3	64
RTU-S4	265
RTU-R1	-957
RTU-S5	75
RTU-S7	124
RTU-S8	115
RTU-S9	87
RTU-S10	104
RTU-S11	123
RTU-S12	127
RTU-S13	178
RTU-R2	-426
RTU-S14	81
RTU-S15	67
RTU-S16	87
RTU-S17	105
RTU-R3	-157
RTU-R4	-161
RTU-R5	0

Ag Building

Label	Measured (cfm)	
AGE-S1	363	
AGE-S2	153	
AGE-S3	142	
AGE-S4	114	
AGE-S5	127	
AGE-S6	40	
AGE-S7	121	
AGW-S1	115	
AGW-S2	241	
AGW-S3	248	
AGW-S4	267	
AG-R1	1,116	manually cut hole
AG-R2	96	
AG-R3	93	
AG-R4	33	

All Measurments w/ Shortridge Hood (compensated)

Table A15-7 is a summary of the supply, return and ventilation airflows for the HVAC units in the building. There is generally more supply airflow than return in most of the systems. This generally indicates return leaks, which do not cause energy concerns since all the ducts are in the space but may cause problems with comfort. AHU-2 in the two-story section of Willow had the large amount of unaccounted for airflow. This was due to a large hole in one of the return ducts when the new ventilation duct has been recently added in 2004.

Table A15-7. Comparison of Supply, Return and Ventilation Airflow Measurements

HVAC Equip	Supply (cfm)	Return (cfm)	OA (cfm)	Diff = S-R-O (cfm)	Ratio = S/(R+O)	Notes
AHU-1	534	260	38		1.79	
AHU-2	1,460	250	196	1,014	3.27	large return leak
AHU-3	341	316	0	25	1.08	
RTU	1,876	1,701	-	175	1.10	OA not measured
AGE	1,060	1,338	150	593	1.30	combined returns
AGW	871					
Total	6,142	3,865	384	1,807		

Generally the supply air flow rates through the equipment were lower than expected. Most packaged cooling systems run at 400 cfm per ton. Table A15-8 shows that these system ran in the 200-300 cfm/ton range. The low air flows result in very cold supply air temperatures and explain the “sooting” that was observed on the supply diffusers in the conference rooms (i.e., The diffuser surfaces are below the dew point of the room air and therefore moisture condenses. Dust adheres and collects on these moist surfaces).

Table A15-8. Normalized Air Flow and Fan Power Measurements

	Size (tons)	Supply (cfm)	Fan Pwr (kW)	Pwr (Watt/cfm)	Supply (cfm/ton)
AHU-1	3	534	0.27	0.51	178
AHU-2	3	1460	0.29	0.20	487
AHU-3	3	341	0.23	0.67	114
RTU	7.5	1876	0.87	0.46	250
AGE	3.5	1060	0.46	0.43	303
AGW	3.5	871	0.43	0.49	249

Pressure Mapping (AHU Fans ON)

The air pressure relationships in the building were also determined with the air handling units and the roof top unit on. Figure A15-22 shows the pressure differences induced across the doorways with the AHU and RTU fans on and the doorways closed. Operation of the AHUs created interior pressure differences up to 1.5 Pa. The building was pressurized with respect to outdoors between 0 Pa and 1.7 Pa. These differences are very modest and were partially induced by the slightly windy outdoor conditions.

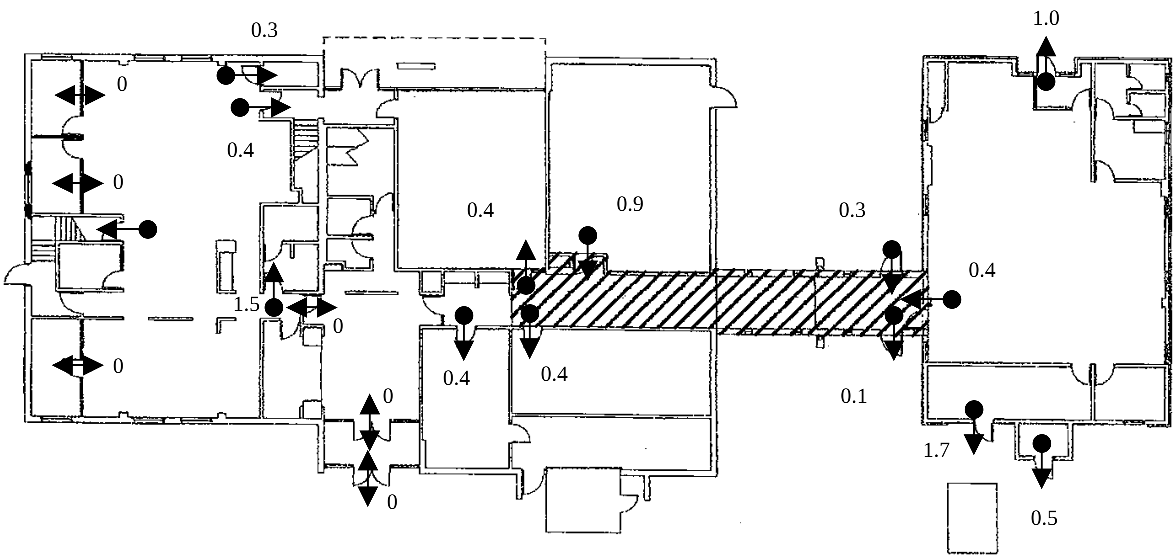

Figure A15-22. First Floor Pressure Differences between Rooms with AHU Fans ON

Duct Leakage Measurements

No Duct leakage test was performed at this site because all the duct leakage area is inside the building envelope.

Space Conditions

Figure A15-23 shows the average temperature profiles based on temperature readings taken with a HOBO data logger from May 26, 2005 to October 28, 2005. The thick line shows the average for each hour while the shaded region corresponds to one standard deviation about the average. The dotted lines correspond to the minimum and maximum for each hour. Sensors were placed in the agriculture building and the upstairs office.

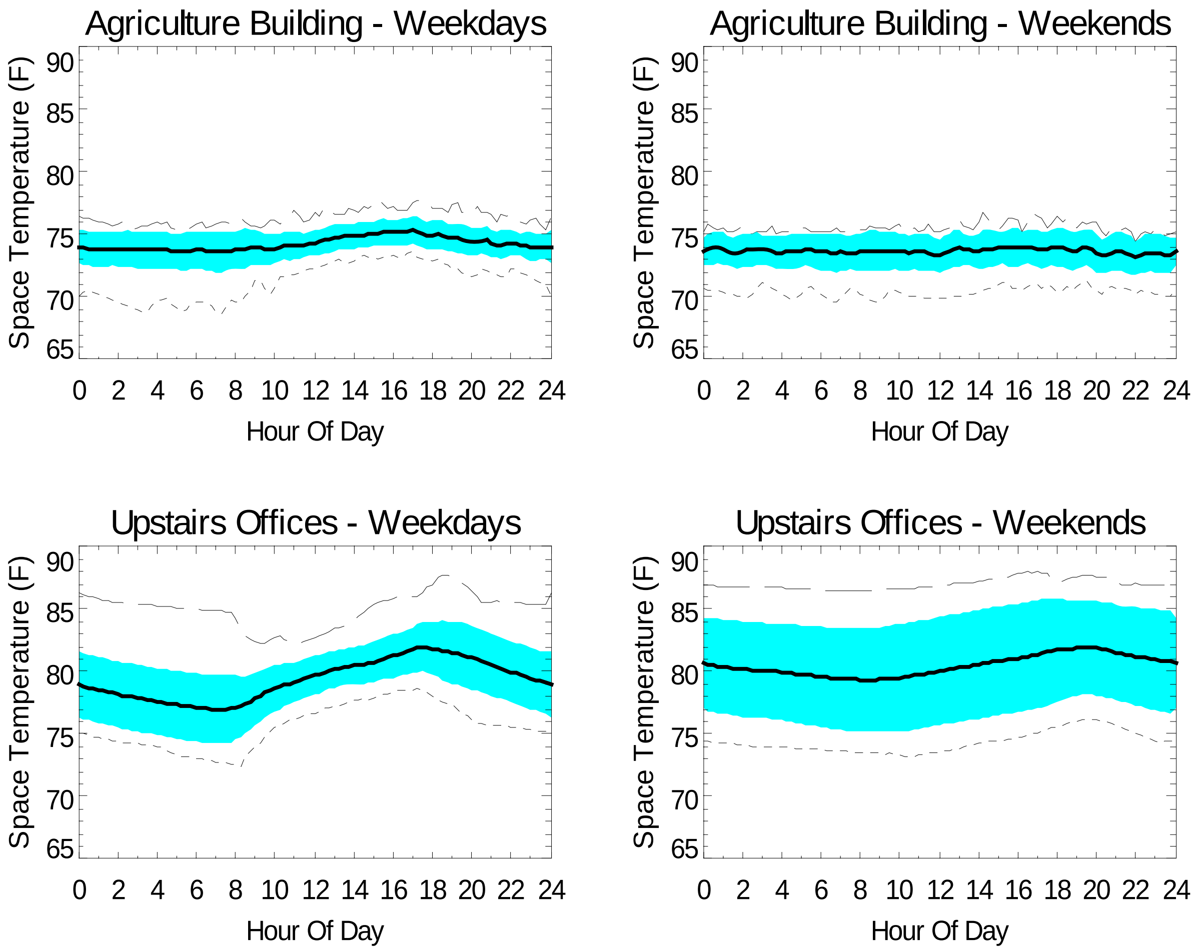

Figure A15-23. Measured Space Temperature Profiles

Figure A15-24 shows the CO_2 concentration in various locations in the building. The CO_2 concentration provides an indication of occupancy. The agricultural building has a good ventilation rate with evening low concentrations around 500 ppm and daytime high around 1000 ppm. The upstairs office has similar numbers with an evening low of 400 ppm and a daytime high of 800 ppm. The conference room also has an evening low of about 400 ppm, but the daytime high can be anywhere from 1000 ppm to over 1500 ppm. These high spikes in the CO_2 concentration are not necessarily a sign of poor ventilation rate, but rather an indication of the room usage. The room is used for only a few hours in any given day, but when it is in use, there are typically a large number of people in the room.

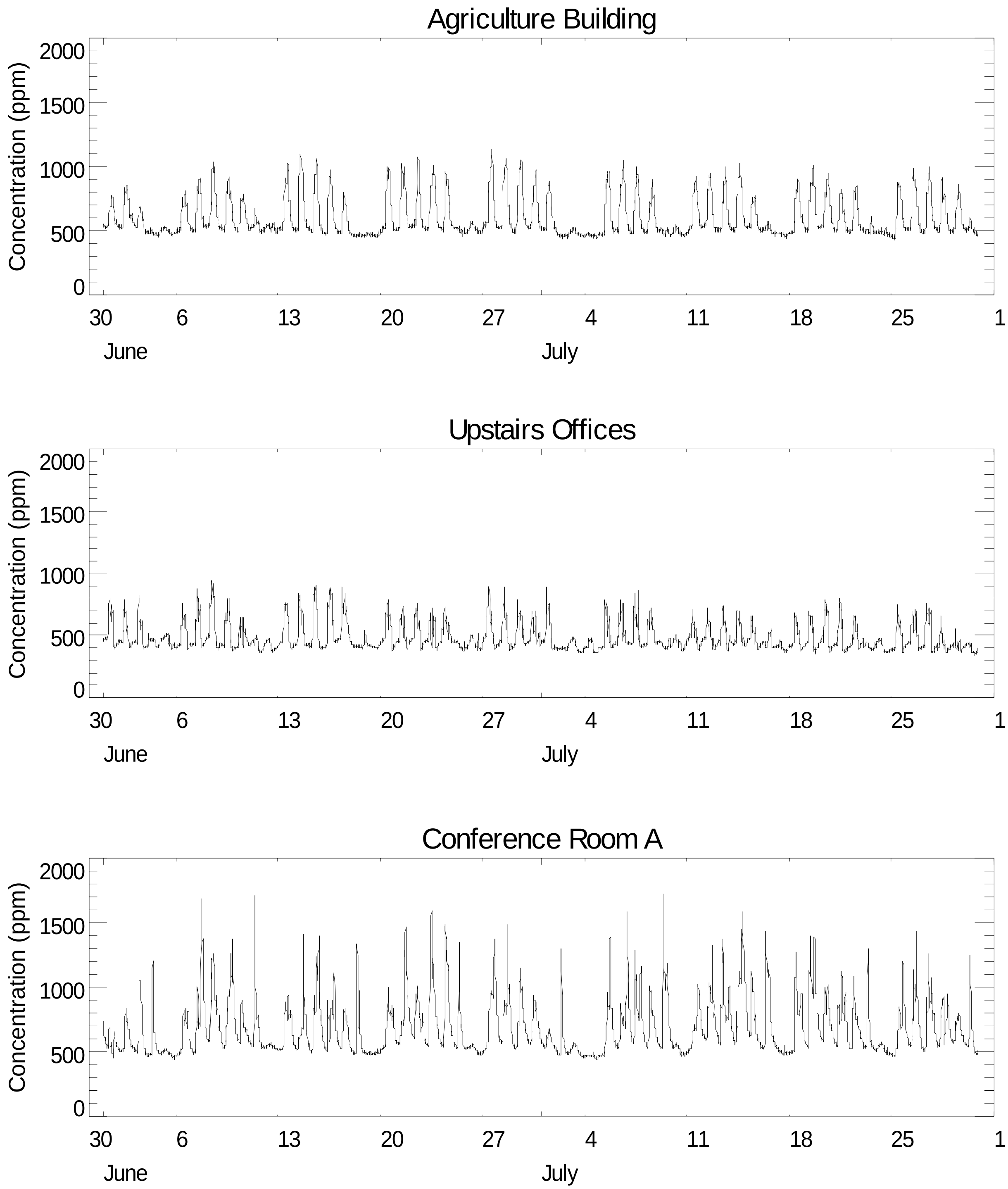

Figure A15-24. Measured CO_2 Concentration in Various Spaces

The following plots show the relative humidity for this building. Figure A15-28 displays the conditions inside the building compared with the ASHRAE comfort zone for cooling shown by the shaded region on the plot.

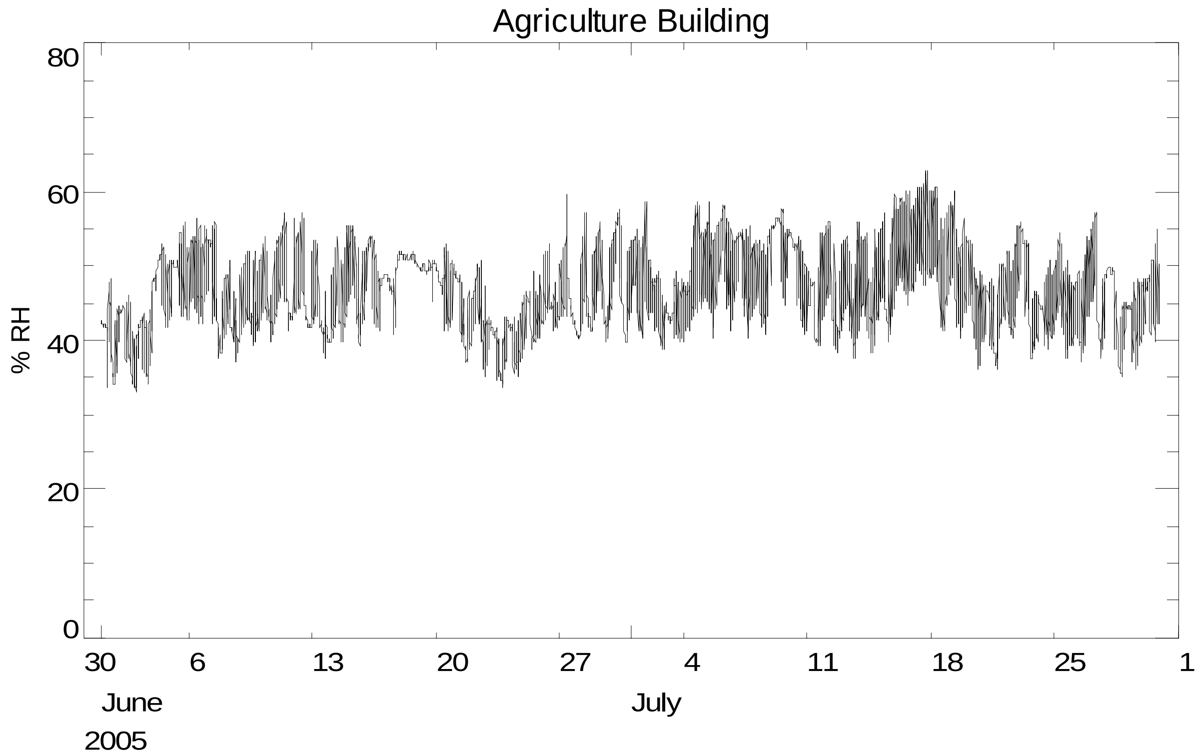

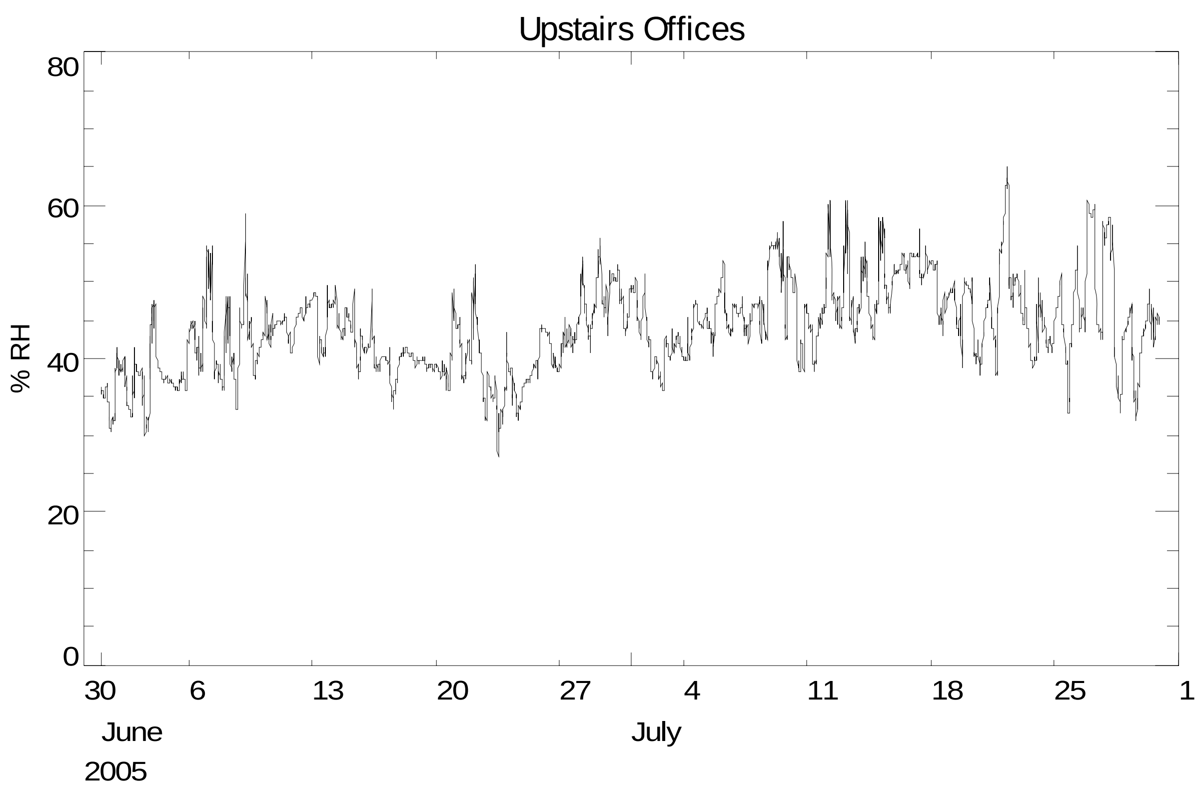

Figure A15-25. Measured Relative Humidity

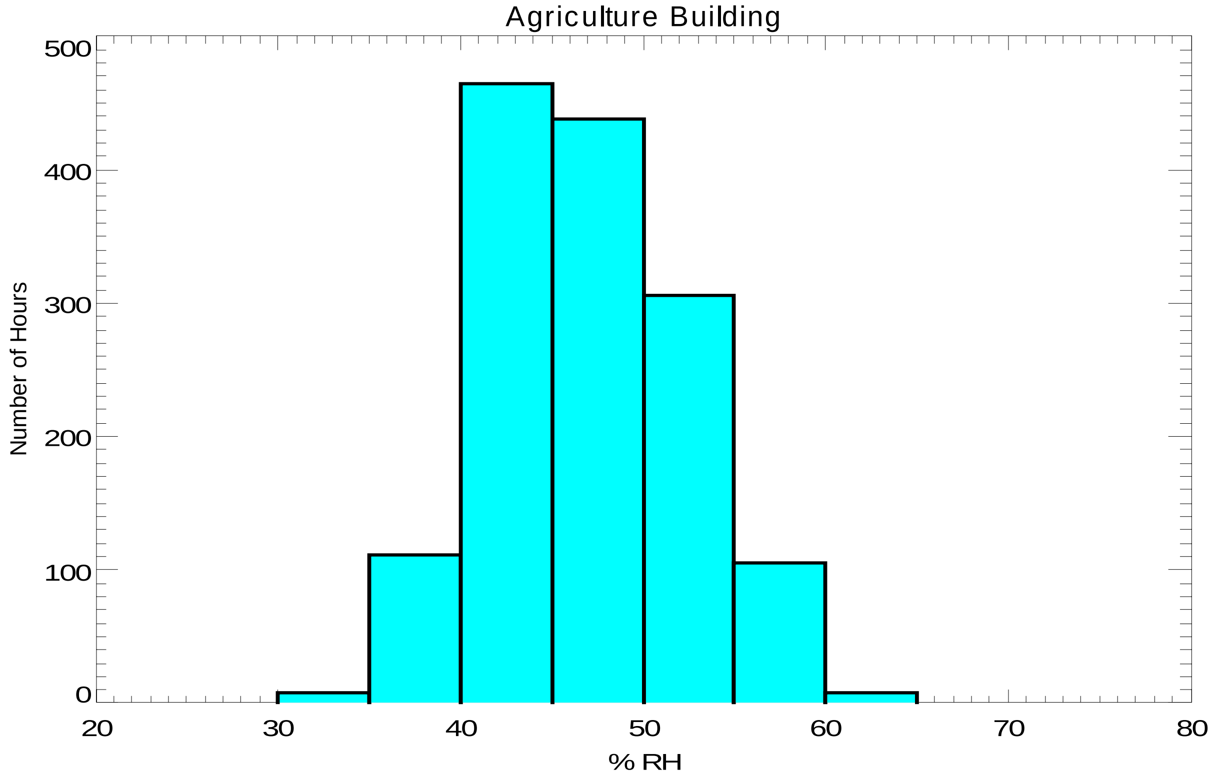

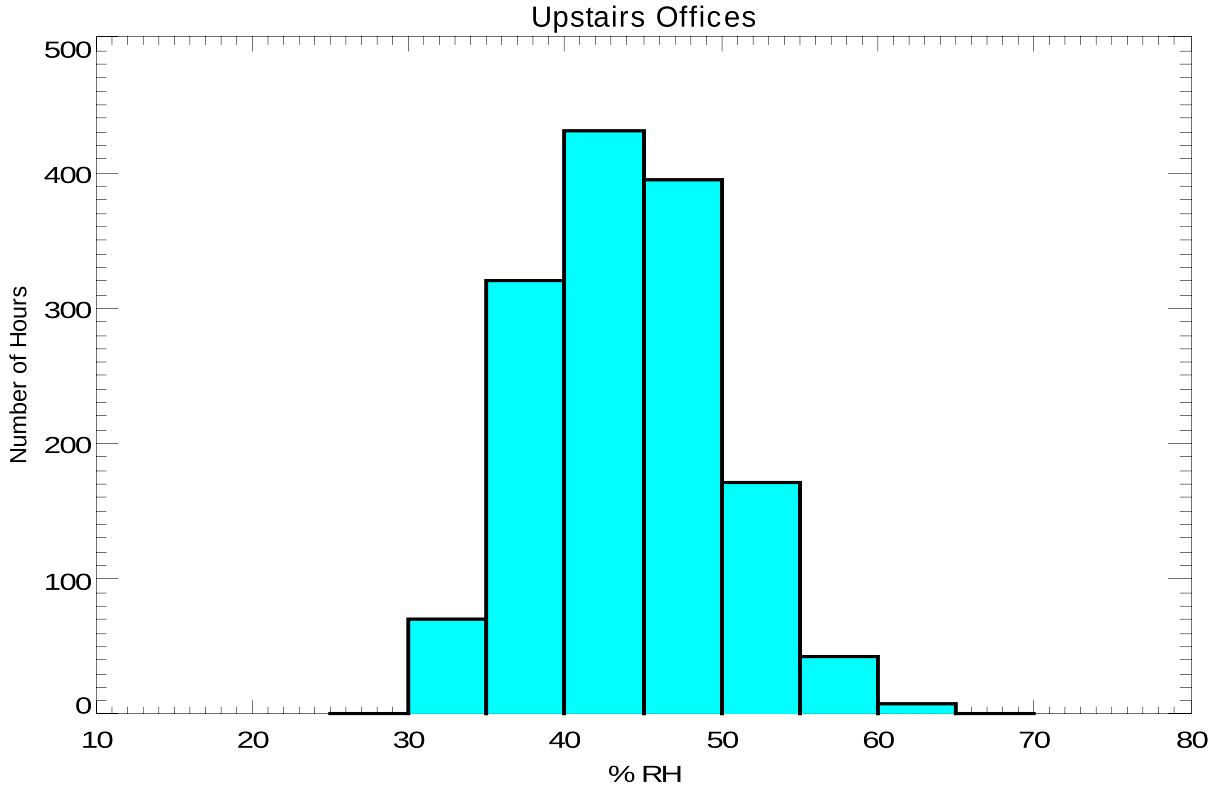

Figure A15-26. Duration of Relative Humidity Levels

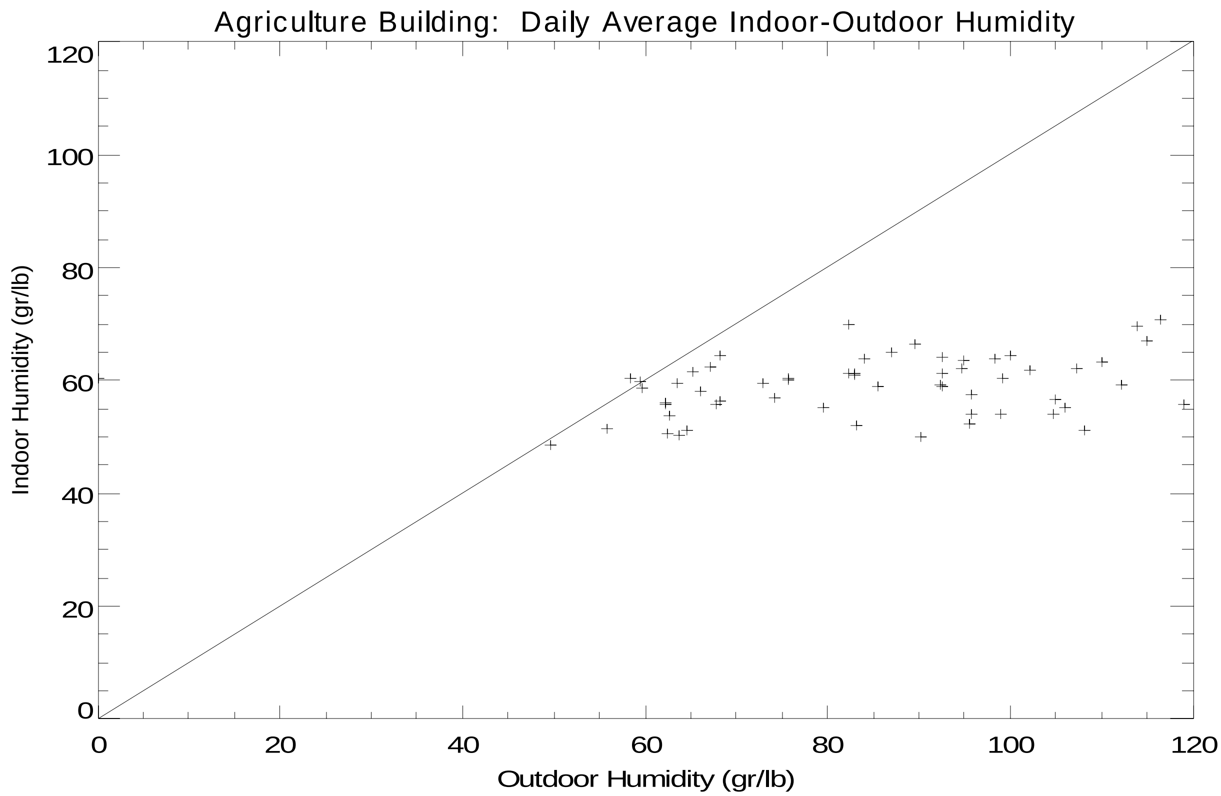

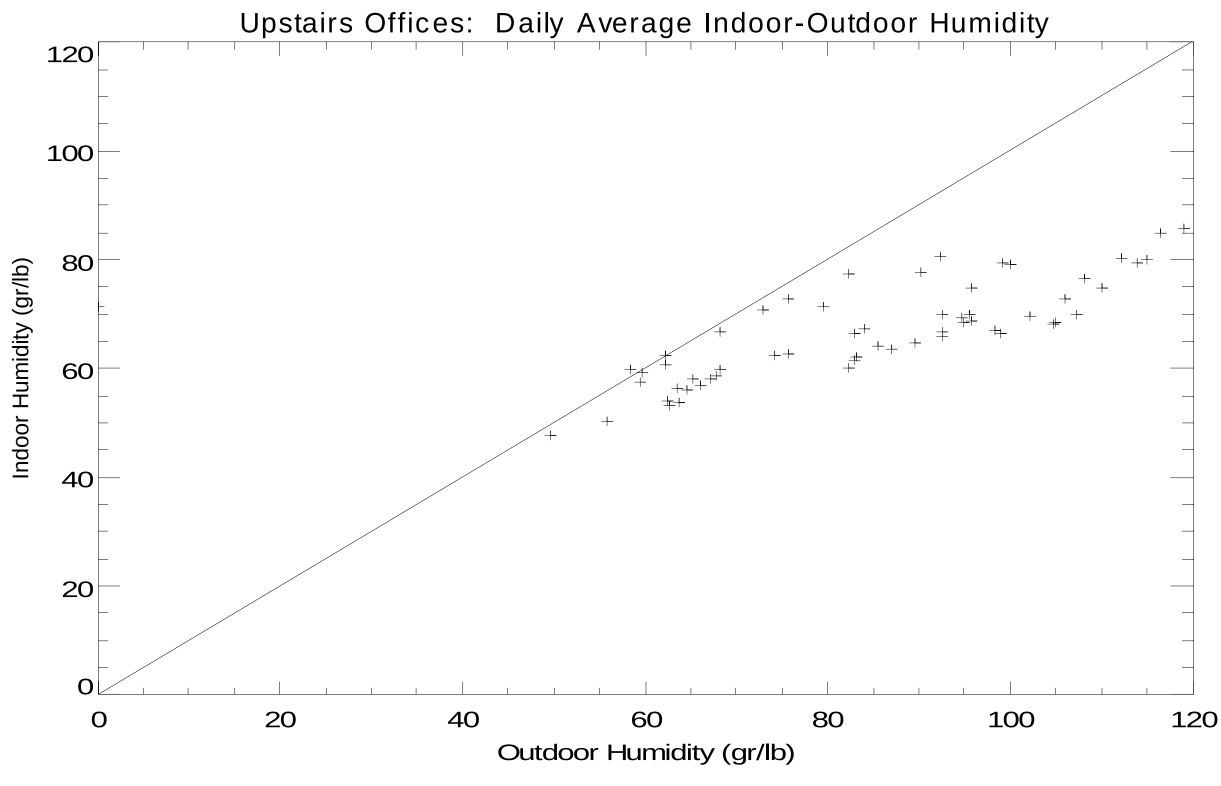

Figure A15-27. Indoor Humidity Variation with Outdoor Humidity

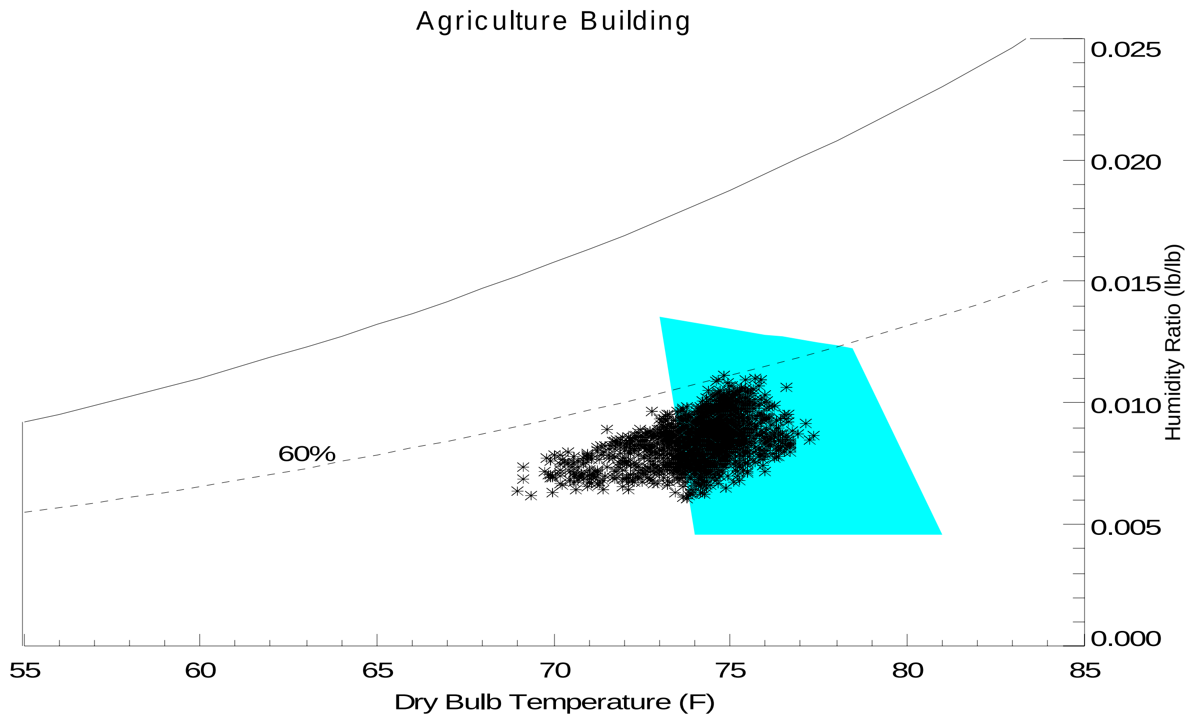

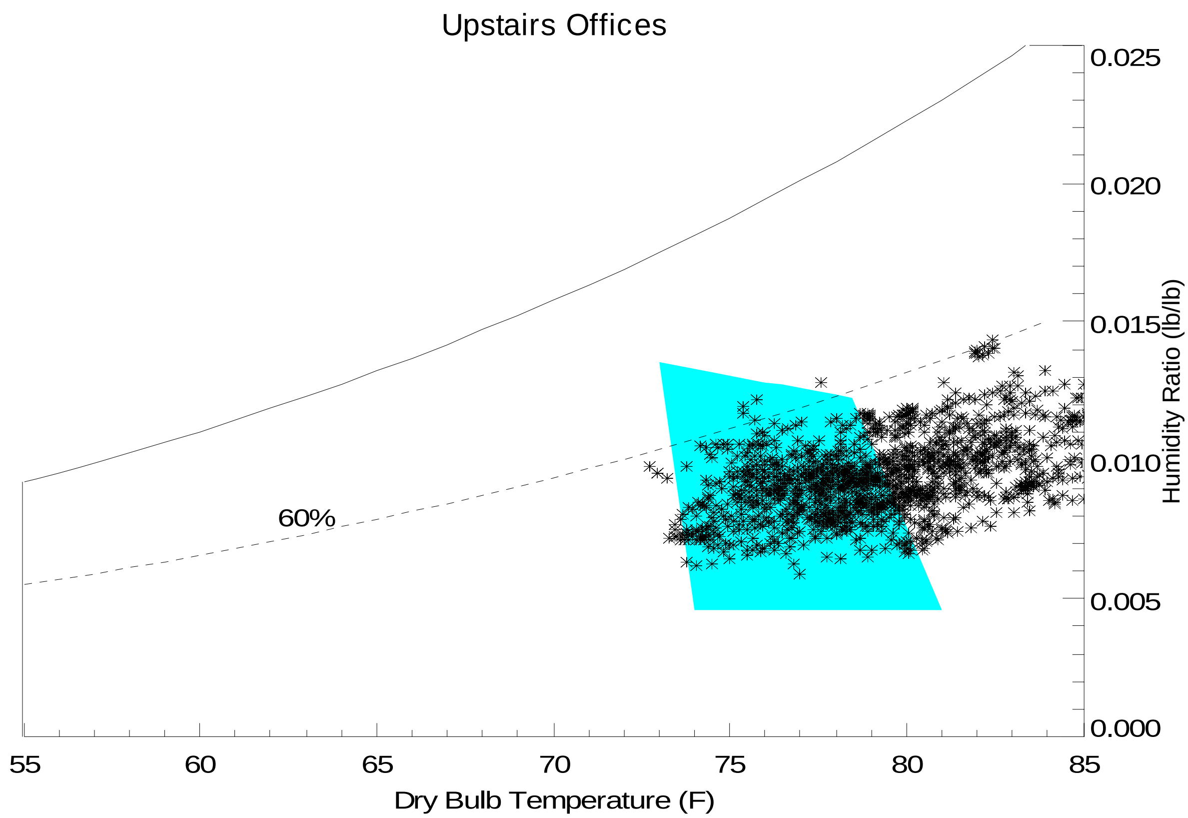

Figure A15-28. Indoor Air Quality Comparison with ASHRAE Comfort Zone for Cooling

Infiltration Estimate from CO_2 Decay

Figure A15-29 shows the resulting decay trend using CO_2 levels in the Ag Building immediately after CO_2 was injected to increase the space well above 2,000 ppm. The predicted air change rate (ACH) is determined by fitting the measured data to an exponential decay. The calculated air change rate is 0.36. The Ag Building has a net volume of 26,000 ft^3 to the drop ceiling. The gross building volume is 31,700 ft^3. Therefore the effective ventilation rate of the space is 156-190 cfm, depending on which volume is used. The air flow rate measured through the vented door in the furnace shed, with the HVAC system operating normally was 150 cfm. All this ventilation was strictly due to duct leakage in the furnace shed.

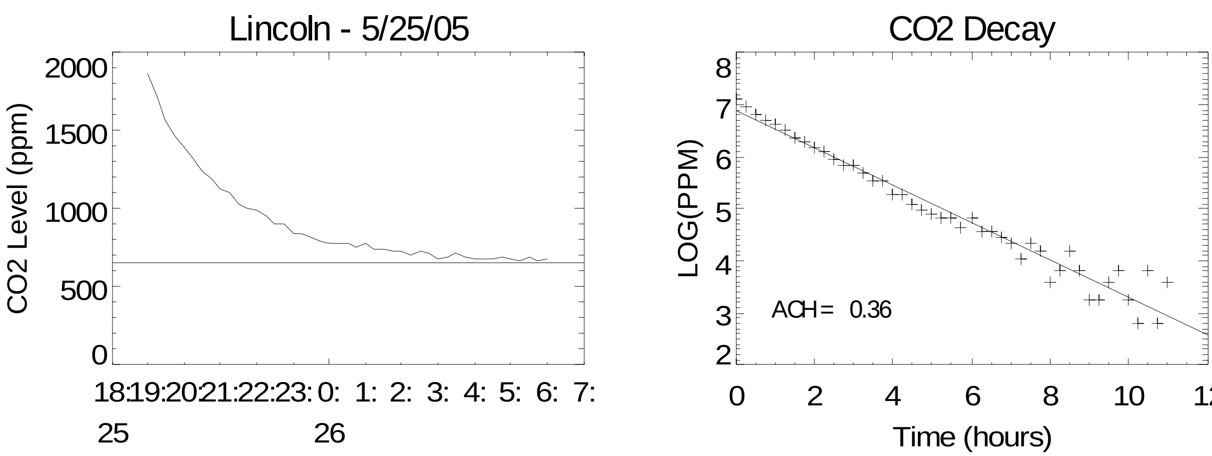

Figure A15-29. Measured Decay of CO_2 Concentration in Building for Tracer Gas Test on May 25

Utility Bills

Both gas and electricity are used for heating of the building. The tables and graphs below show the gas and electric use trends for the facility. The buildings utility bills are individually calculated for the two separate buildings. Gas and electric use are evaluated for each building in the pages that follow and summarized in Table A15-9 below.

Table A15-9. Summary of Gas and Electric Use Indexes

	Gas Use Index (MBtu/ft^2-year)	Electric Use Index (kWh/ft^2-year)	Peak (Watts/ft^2)
Willow	38.8	8.9	4.2
Lincoln	50.2	10.4	5.2
Total	41.0	9.2	4.4

Energy use is typical of a commercial office building. The temperature dependent portion of the electric load – or the portion attributable to cooling, is estimated to be about 20% or 25,000 kWh per year.

Table A15-10. Breakdown of Cooling and Base Electric Loads

	Willow (kWh)	Lincoln (kWh)	Total (kWh)	
Base Use	73,073	20,380	93,453	79%
Cooling	19,647	5,090	24,737	21%
Total	92,720	25,470	118,190	100%

Table A15-11. Summary of Electric Bills – Willow

	Cooperative Extension - Willow - Electric Utility Data			
	Days in Month	Energy (kWh)	Demand (kW)	Elec. Use per Sq-Ft (kWh/sq ft)
1/21/2004	35	7,362	25.3	0.71
2/18/2004	28	7,128	27.7	0.69
3/24/2004	35	8,658	24.6	0.83
4/19/2004	26	6,516	28	0.63
5/17/2004	28	7,416	36.5	0.71
6/17/2004	31	9,180	39.9	0.88
7/19/2004	32	9,378	40.8	0.90
8/17/2004	29	9,396	43.5	0.90
9/15/2004	29	8,622	38.5	0.83
10/14/2004	29	6,930	31.3	0.67
11/15/2004	32	6,714	24.8	0.65
12/15/2004	30	6,624	26.2	0.64
1/18/2005	34	6,480	22.5	0.62
2/16/2005	29	6,552	24.6	0.63
Most recent 12 Months	***364***	***92,466***	***43.5***	***8.90***
Annualized	***365***	***92,720***	***43.5***	***8.92***

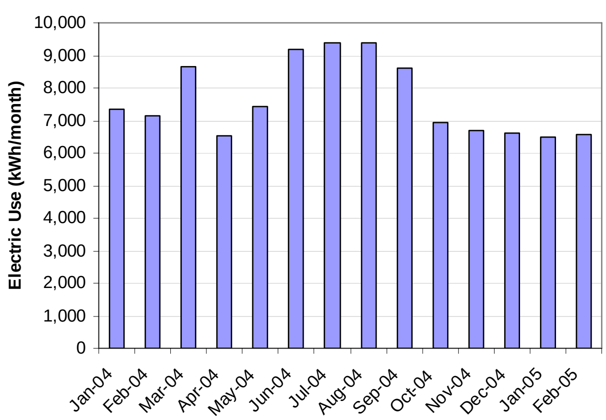

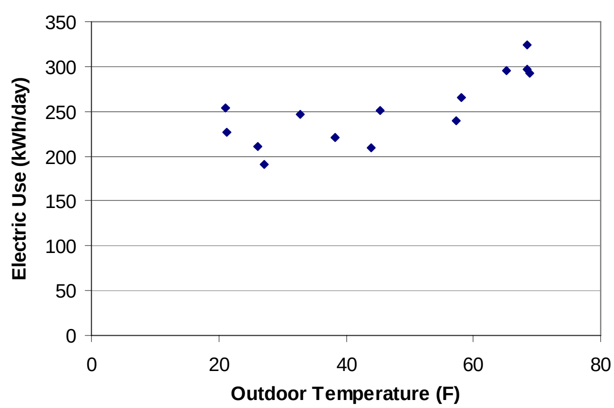

Figure A15-30. Monthly Electricity Use Trends – Willow

Table A15-12. Summary of Electric Bills – Lincoln

	Cooperative Extension - Lincoln - Electric Utility Data			
	Days in Month	Energy (kWh)	Demand (kW)	Elec. Use per Sq-Ft (kWh/sq ft)
1/7/2004	68	3,654	6.4	1.49
3/4/2004	57	3,924	6.6	1.60
5/4/2004	61	4,122	6.8	1.68
7/2/2004	59	4,770	12.7	1.95
9/1/2004	61	5,022	12	2.05
11/1/2004	61	4,122	9.7	1.68
1/4/2005	64	3,708	6.4	1.51
3/4/2005	59	3,726	6.4	1.52
Most recent 12 Months	***365***	***25,470***	***12.7***	***10.40***

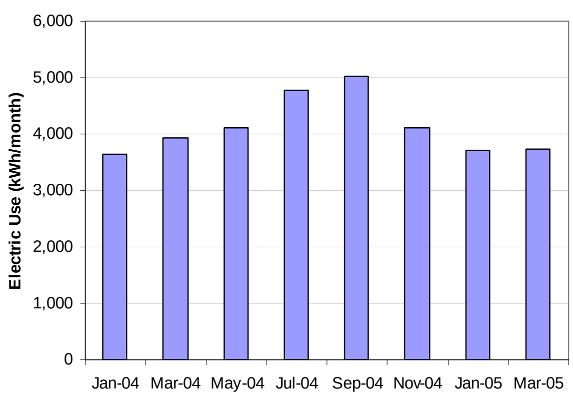

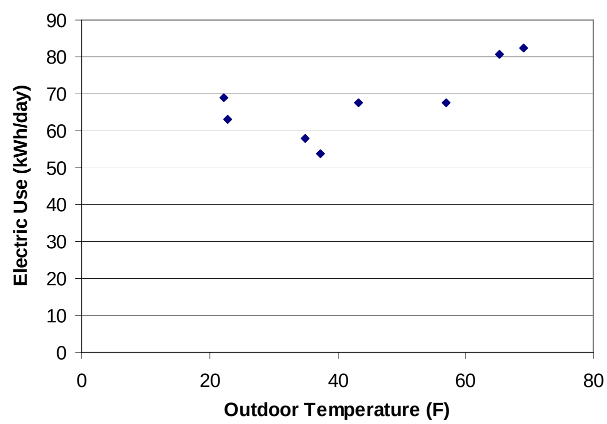

Figure A15-31. Monthly Electricity Use Trends – Lincoln

Table A15-13. Summary of Gas Bills – Willow

	Cooperative Extension - Willow - Gas Utility Data		
	Days in Month	Gas Use (therms)	Gas Use per Sq-Ft (therm/sq ft)
1/21/2004	35	884.5	0.085
2/18/2004	28	751.8	0.072
3/24/2004	35	917.4	0.088
4/19/2004	26	590.8	0.057
5/17/2004	28	218.1	0.021
6/17/2004	31	2.0	0.000
7/19/2004	32	1.0	0.000
8/17/2004	29	7.1	0.001
9/15/2004	29	1.0	0.000
10/14/2004	29	38.6	0.004
11/15/2004	32	315.3	0.030
12/15/2004	30	400.6	0.039
1/18/2005	34	801.9	0.077
2/16/2005	29	731.3	0.070
Most recent 12 Months	***364***	***4,025***	***0.387***
Annualized	***365***	***4,036***	***0.388***

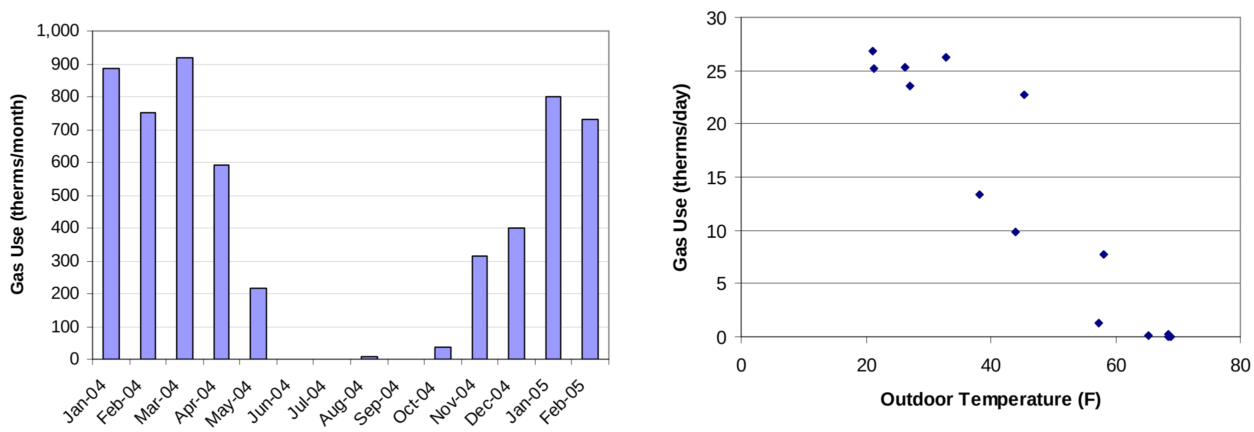

Figure A15-32. Monthly Gas Use Trends – Willow

Table A15-14. Summary of Gas Bills – Lincoln

	Cooperative Extenstion - Lincoln Gas Utility Data		
	Days in Month	Gas Use (therms)	Gas Use per Sq-Ft (therm/sq ft)
1/7/2004	68	508.5	0.208
3/4/2004	57	820.5	0.335
5/4/2004	61	178.9	0.073
7/2/2004	59	9.1	0.004
9/1/2004	61	1	0.000
11/1/2004	61	59.1	0.024
1/4/2005	64	432.1	0.176
3/4/2005	59	548.9	0.224
Most Recent 12 months	***365***	***1,229***	***0.502***

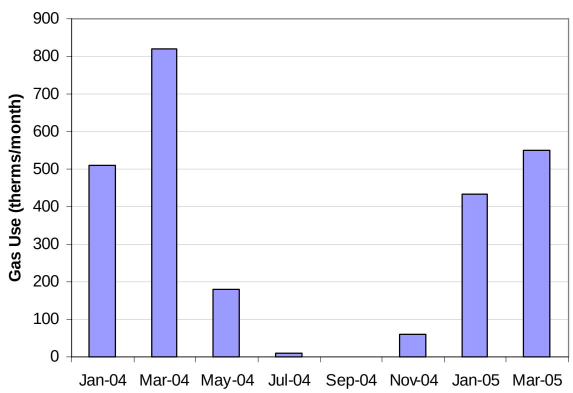

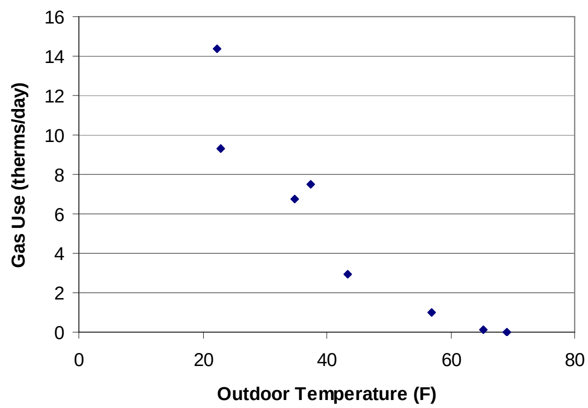

Figure A15-33. Monthly Gas Use Trends – Lincoln

<u>Summary and Recommendations</u>

Ag Building Ventilation. The Ag. Building envelope was very tight and the HVAC system provided no explicit ventilation. However, duct leakage in the furnace shed did effectively provide ventilation at a rate fairly appropriate for the occupant density, or about 13-15 cfm per person. This situation could potentially create a hazardous condition if combustion byproducts are not properly vented from the shed (due to a furnace HX or vent failure).

<u>Recommendation</u>: Add a ventilation duct from the return plenum to outdoors in the Furnace shed so ventilation air comes from outdoors.

RTU Airflow. The RTU airflow is low relative to the size of the unit. At least one of the return ducts in conf room C was totally blocked. The restrictive return ducts may be at least part of the reason for low air flow.

<u>Recommendation</u>: Add a large return opening from the return duct into the main hallway. Increase the uncut for each conference room door to ensure sufficient air flow and air balance. Or implement other means to

Block or Remove Abandoned Roof Vents. The roof of the one-story section of Willow has several roof penetrations that are no longer required. These four stacks were typically flue vents for duct furnaces or unit heaters that are no longer installed. At least one of these exhaust vents was totally open. In other cases they were blocked or sealed.

<u>Recommendation</u>: Seal or remove all unused vents in roof.

Commission AHU Ventilation. In 2004, ventilation was explicitly added to two of the AHUs on the first floor of Willow. Dampers and ducts were added to bring fresh air into the space. The controls were not fully installed and commissioned.

<u>Recommendation</u>: Commission and verify the outdoor damper controls to function properly. The outdoor damper should open during the occupied period. Controls could also be added to shut the damper when the ambient temperatures are very low (e.g., below zero) to prevent comfort problems. While this may not strictly meet the code, natural infiltration is likely to provide sufficient ventilation at these times.

Fix AHU-1 Drainpan. The AHU-1 is slightly tilted so that condensate spills from the unit before it goes down the condensate drain (it is also possible that the condensate drain is plugged). Currently this unit is not used in the summer because it floods a nearby office.

<u>Recommendation</u>: Either straighten the AHU or move the condensate drain to the other side of the drain pan so that condensate does not spill from the unit.

Reconnect the 2^nd^ Floor Exhaust Fan. The 2-story section of Willow has a large two-speed exhaust fan that is not longer wired. It appears that the electric breaker for the fan was changed to serve another electric circuit in 2003-2004. The fan had been manually operated to ventilate the second floor. A ceiling tile must be removed for the fain to operate. It appears that the fan was originally installed to operate continuously to induce ventilation flow through the PTACs. However the fan may be have been too loud so continuous operation was abandoned.

Recommendation: Re-wire the fan and add or reinstate the ability for two-speed or variable speed operation. Use the fan in the swing season (when ambient is 50-65°F) to provide "economizer cooling". Add a damper if automatic operation is desirable.

Field Test Site 17 – Organization/Meeting Hall, Syracuse, NY

Main Entrance (East)

Rear of Building (Southeast)

Front of Building (North)

Sun Porch (West)

Figure A17-1. Club - Syracuse, NY

CHARACTERISTICS

Building Description

The 18,000 sq-ft facility is a three-story house that was converted into meeting hall for a social organization in 1949 (Figure A17-1). The four-story building has three full floors plus a full attic and basement. The building was originally built in 1853 and was later remodeled in 1893. The building is heated by a steam boiler that serves nine steam coils and eleven radiators. Three of the nine steam coils use a fan for forced convection. The other coils depend on natural convection to distribute heat through the heating vents (incoming air is pulled from the basement). The building does not have central cooling, however some spaces are cooled by window air-conditioners. A kitchen exhaust hood is the only mechanical exhaust in building. The hood measures 11 feet by 3 feet and exhausts to the rear of the building.

The building has a working elevator, which serves the first, second, and third floors. The top of the elevator shaft (where the elevator mechanical systems are located) is in the attic and is enclosed in a stick-frame room with 1/4-inch fiberboard sheathing. The elevator shaft is subject to significant stack effect during the winter, and is a large source of building leakage. Figure A17-2 through Figure A17-4 display the floor plans for each story of the building.

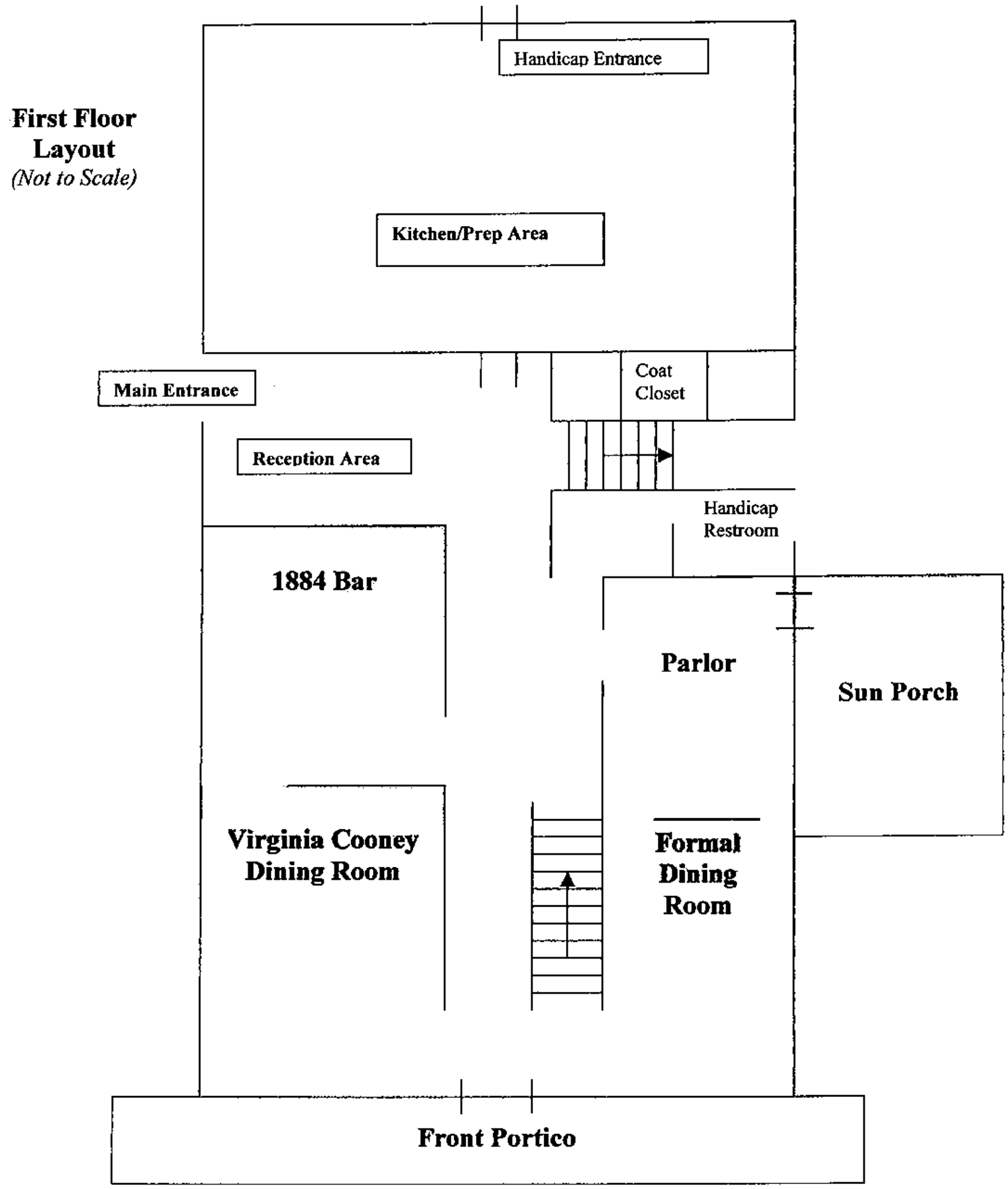

Figure A17-2. Floor Plan – First Floor

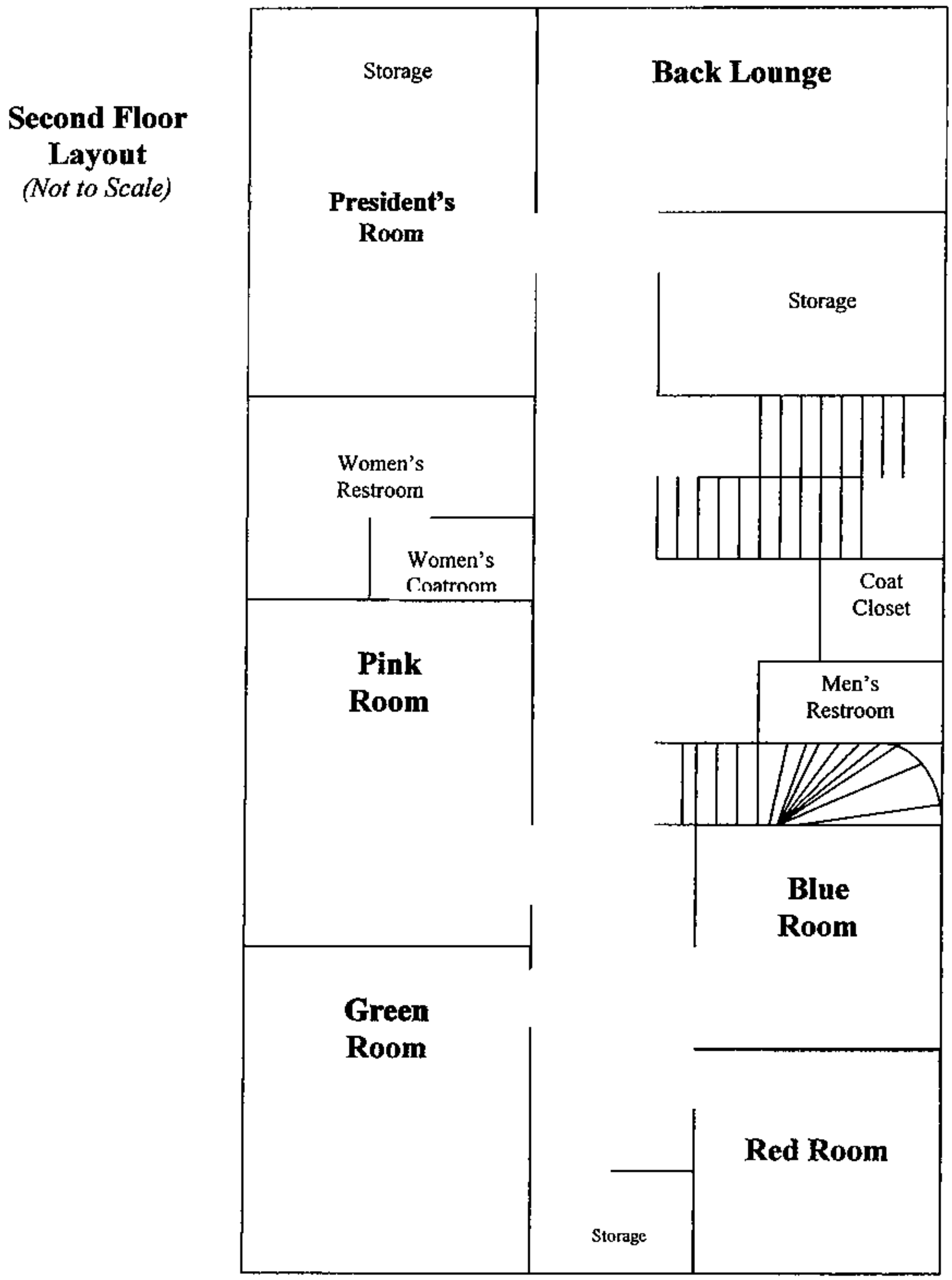

Figure A17-3. Floor Plan –Second Floor

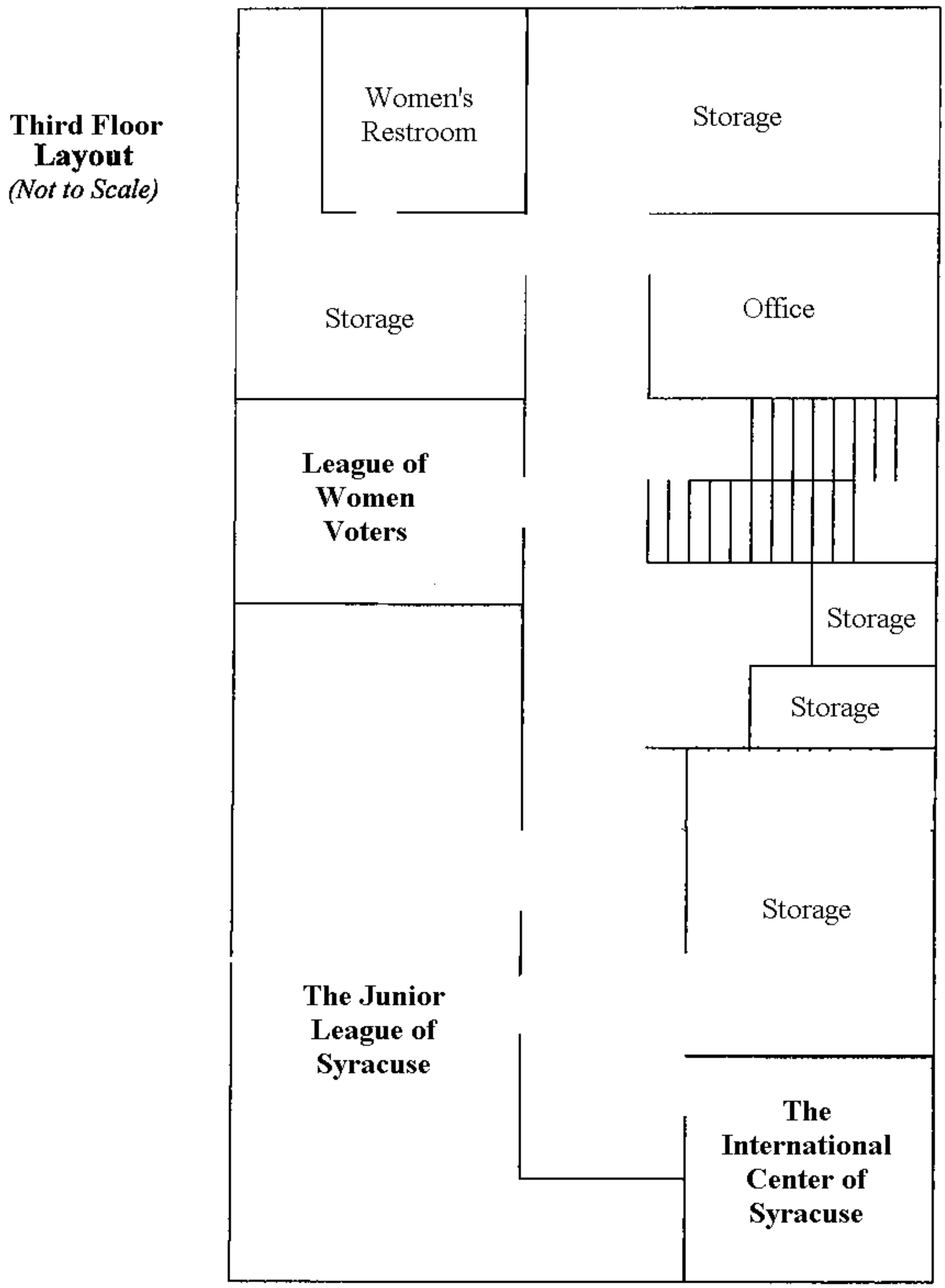

Figure A17-4. Building Floor Plan –Third Floor

Construction Details

The exterior walls are constructed of two layers of 3-inch brick separated by a 6-inches of rubble. The interior walls are wood frame construction covered by plaster and lathe. Some rockwool insulation has been installed above the third floor ceiling to form a thermal boundary between the occupied space and attic. The building has five chimneys running from the basement through the roof, connected to a total of ten fireplaces. The fireplaces are no longer in use and have been closed off with loose fiberglass insulation. The roof is wood frame construction with a mixture of built up roofing (tar and paper), and shingles.

Figure A17-5. Corinthian Club Roof – Built Up Roof and Shingled Roof Transition

HVAC System

The heating for the building is provided with a combination of steam convection coils located in the basement, and radiators located on the first and second floors. Heat from the steam coils are ducted to a number of rooms in the front (north) of the building. Only three of the steam coils use fans for forced convection, the other six coils depend on natural convection to induce a flow to the vents (airflow is induced from the basement). In addition to the heating coils, there are eighteen radiators placed in various rooms on the first and second floor. Figure A17-6 and Figure A17-7 show the locations of the supply vents, the radiators, the exhaust hood, the thermostats, and the fireplaces.

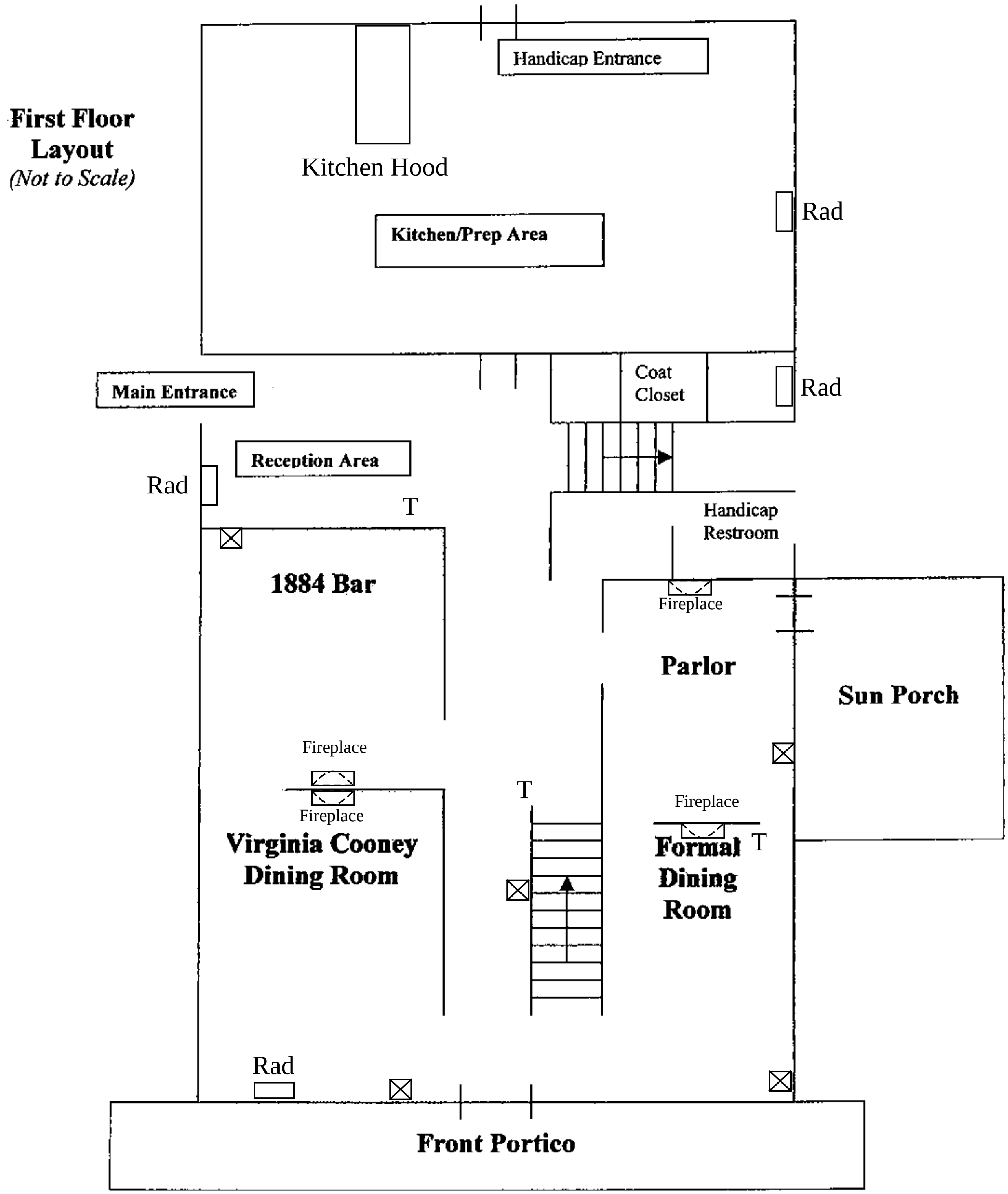

Figure A17-6. Vents, Radiators, Thermostats, and Fireplaces – First Floor

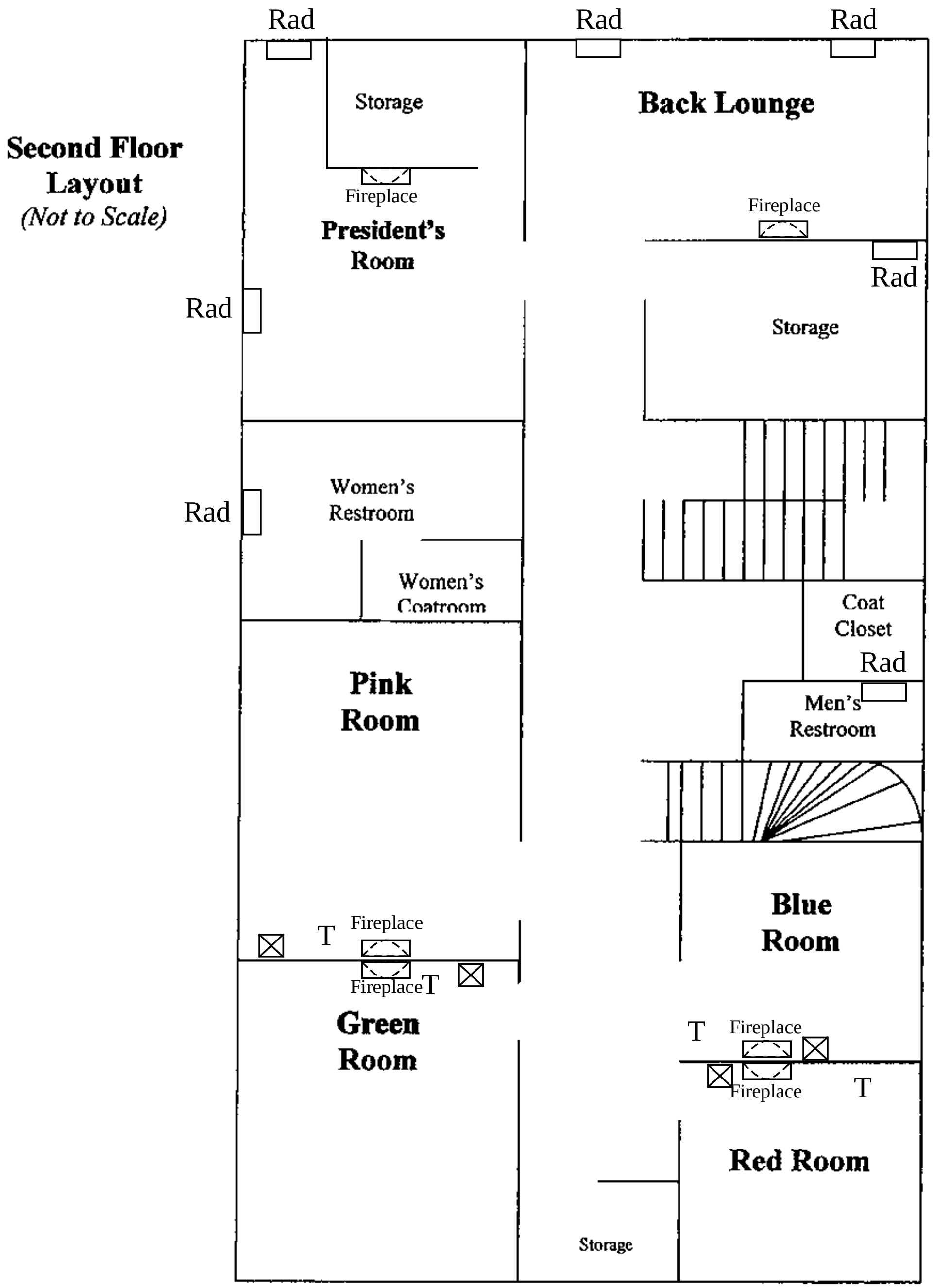

Figure A17-7. Vents, Radiators, Thermostats, and Fireplaces – Second Floor

The fans that control the airflow from the forced air heating coils originally had a set point temperature of 130°F and 110°F. The building personnel said that it was rare for the fans to come on. Considering this, the set point temperature was reduced to 100°F. This should help heat the building better during the winter. Additionally, for one of the induced flow heaters, the employees place a fan in the basement directing the air upward into the first floor to assist with heating.

Figure A17-8. Steam Convector Unit with Fan

Figure A17-9. Steam Coil without Fan (natural convection induces airflow from the basement)

Table A17-1. Summary HVAC Equipment Installed at Site

HVAC Equipment	Rooms Served	Brand/Model	Number of Units
AHU	Green, Blue, Cooney		3
Heating Coil	First and Second Floor		6
Steam Boiler	Entire Building		3 Stages (1.2 MMBtu/h total)
Radiator	Entire Building		18

There are a number of thermostats throughout the building control valves to the radiators. All are manually set and are changed by employees as they see fit depending on the time of year and current weather conditions.

MEASUREMENTS

Most of the test data below was taken on June 7, 2005. John Carpenter, Mike Clarkin, and Hugh Henderson performed the pressure mapping, the ventilation readings, and the supply airflow measurements on June 7. The building envelope tightness was measured by Mike Clarkin and John Carpenter on July 12, 2005. The CO_2 and Temperature/RH Sensors were placed in the building by John Carpenter on June 9, 2005. John Carpenter returned to the site and picked up the sensors on July 12, 2005.

Building Envelope Airtightness

The leakage characteristics of the building enclosure were assessed using fan pressurization methods. The building was depressurized using a door leading out to the sun porch.
A single blower door was installed and used for the testing. All exterior doors and windows were closed. The building was tested in the following configuration:

- All interior doors open
- Kitchen Exhaust Fans On (exhausting an additional 3655 cfm)
- Kitchen Exterior Door Closed

During the blower door test, the building was pressurized from 3.6 Pa to 7.2 Pa. Figure A17-10 shows the building leakage variation with building pressure and summarizes the leakage statistics including the model coefficients, effective leakage area (ELA), and air-changes-per-hour (ACH). The ELA is calculated using the Lawrence Berkeley Laboratory method, which calculates the leakage area at 4 Pa. The building has an effective leakage area of approximately 13 sq in per 100 sq ft of the total envelope area (including floor area). Another building leakage characteristic is the ACH at 50 Pascal's (ACH_{50}), which is this case was 8.5.

The regression analysis predicted a very low (and non-physical) exponent of 0.39. This unexpected result was most likely due to the narrow range of pressures used in the analysis. To correct for this error, we also found the best fit to the data while forcing the exponent to be 0.62. The resulting best fit equation with an exponent of 0.62 is show at the red dotted line on Figure A17-10. The leakage statistics determined by theses two methods are summarized in Table A17-2. The ELA remains about the same but the ACH 50, which is extrapolated well beyond the measured data range, increases from 8.5 to 14.3.

Table A17-2. Summary of Building Airitightness Data

	Flow Coeff. K	Exp. n	ELA (sq in)	ELA / 100 sq ft (sq in/sq ft)	Flow @ 50 Pa (cfm_{50})	ACH_{50}
Door & Exhaust Fan	4,126.6	0.391	2011	13.08	19,068	8.5
Door & Exhaust Fan (n=0.62)	2,836.0	0.620	1898	12.34	32,068	14.3

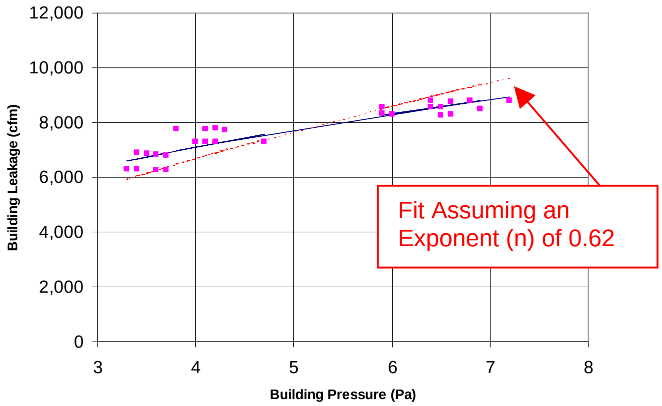

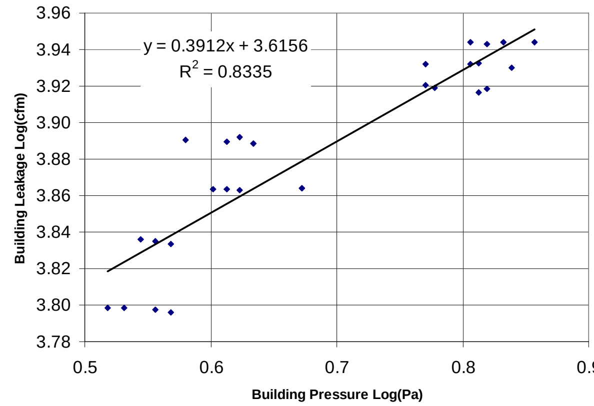

Test Results:

Flow Coefficient (K)	4126.6	
Exponent (n)	0.391	
Leakage area (LBL ELA @ 4 Pa)	2011.2 sq in	13.08 ELA / 100 sq ft
Airflow @ 50 Pa	19,068 cfm	8.50 ACH @ 50

Test Data:

Nominal Building Pressure (Pa)	Nominal Flow (cfm)	Ring
7.2	8,787	none
6.6	8,768	none
6.4	8,789	none
6.8	8,786	none
5.9	8,552	none
6.5	8,557	none
6.9	8,515	none
6.4	8,554	none
6.6	8,286	none
6.0	8,295	none
5.9	8,325	none
6.5	8,255	none
4.2	7,795	none
3.8	7,772	none
4.1	7,753	none
4.3	7,734	none
4.2	7,292	none
4.7	7,315	none
4.2	7,299	none
4.1	7,304	none
4.0	6,890	none
3.4	6,856	none
3.5	6,836	none
3.6	6,816	none
3.7	6,252	none
3.4	6,287	none
3.3	6,288	none
3.6	6,272	none

Figure A17-10. Blower Door Test Data, Resulting Best-Fit Model Coefficients, and ELA

Pressure Mapping (Building Depressurized with Blower Door)

Pressure readings in the building were taken using a digital micromanometer (DG 700) with the blower door operating to depressurize the building. Pressure measurements between adjacent spaces were taken between interior rooms with doors closed.

The building was depressurized to 4.5 Pa (referenced to outdoors) with the blower door operating. The pressure differences between adjacent spaces in the building with the building depressurized are shown in Figure A17-11 through Figure A17-13. Perimeter zones that displayed a high pressure difference across the doorway (greater than 1.0 Pa) are highlighted as being the zones with the most leakage.

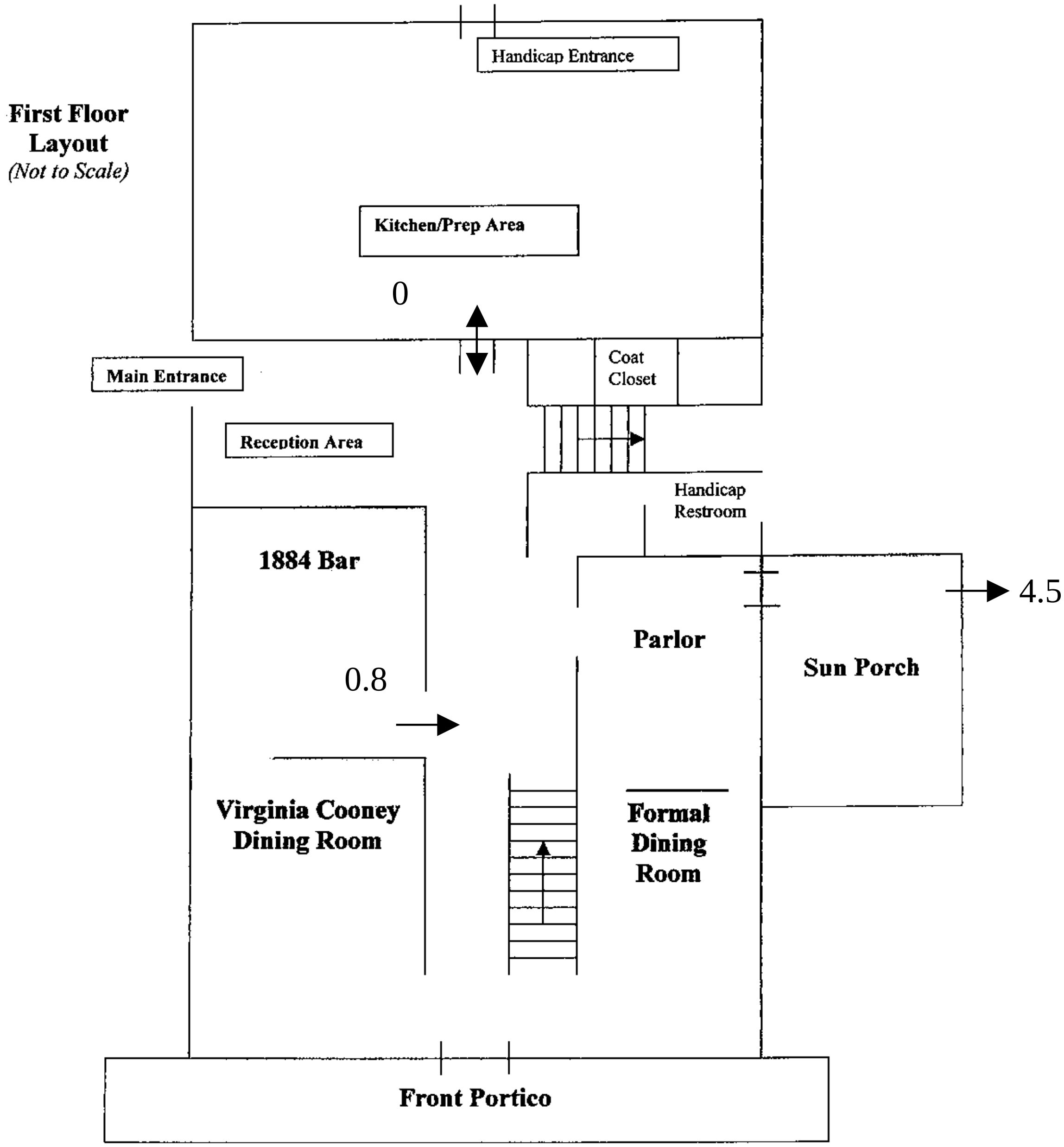

Figure A17-11. Pressure Mapping with Building Depressurized to 4.5 Pa – First Floor

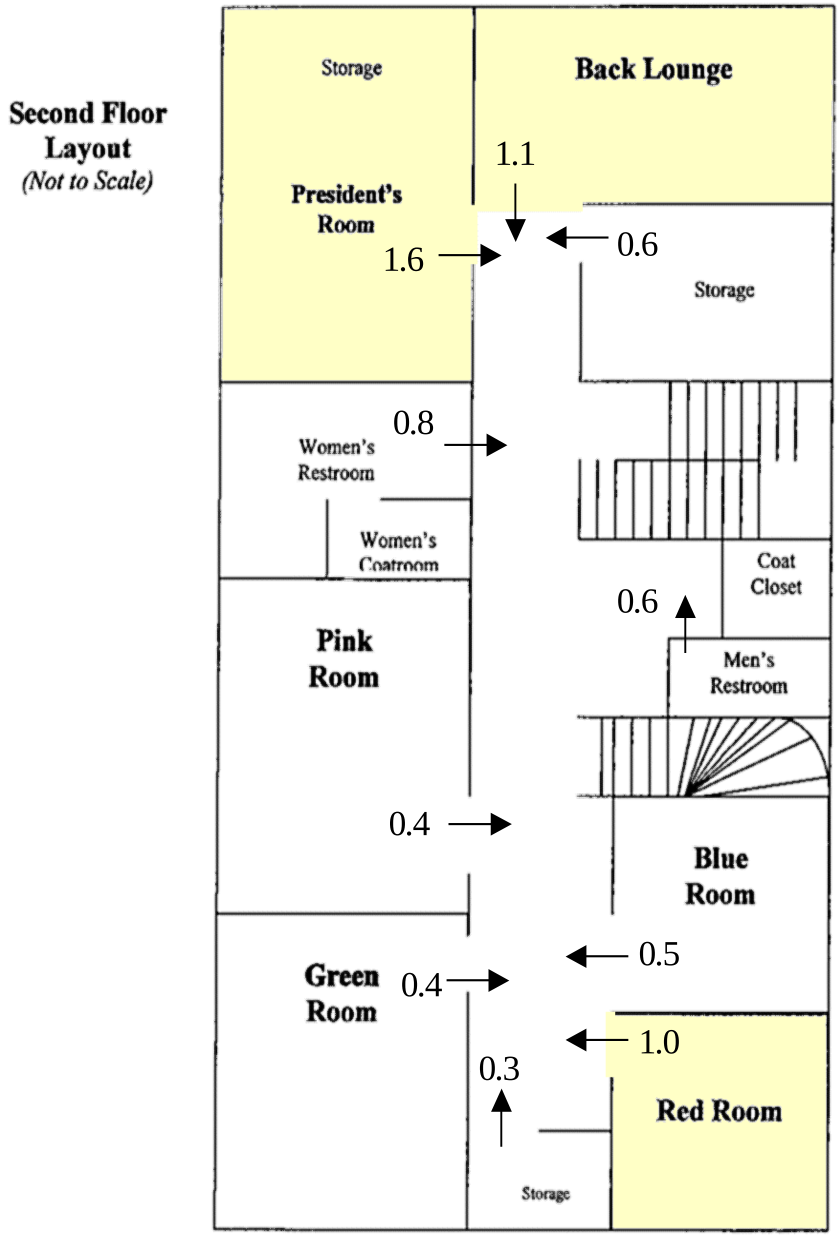

Figure A17-12. Pressure Mapping with Building Depressurized to 4.5 Pa – Second Floor

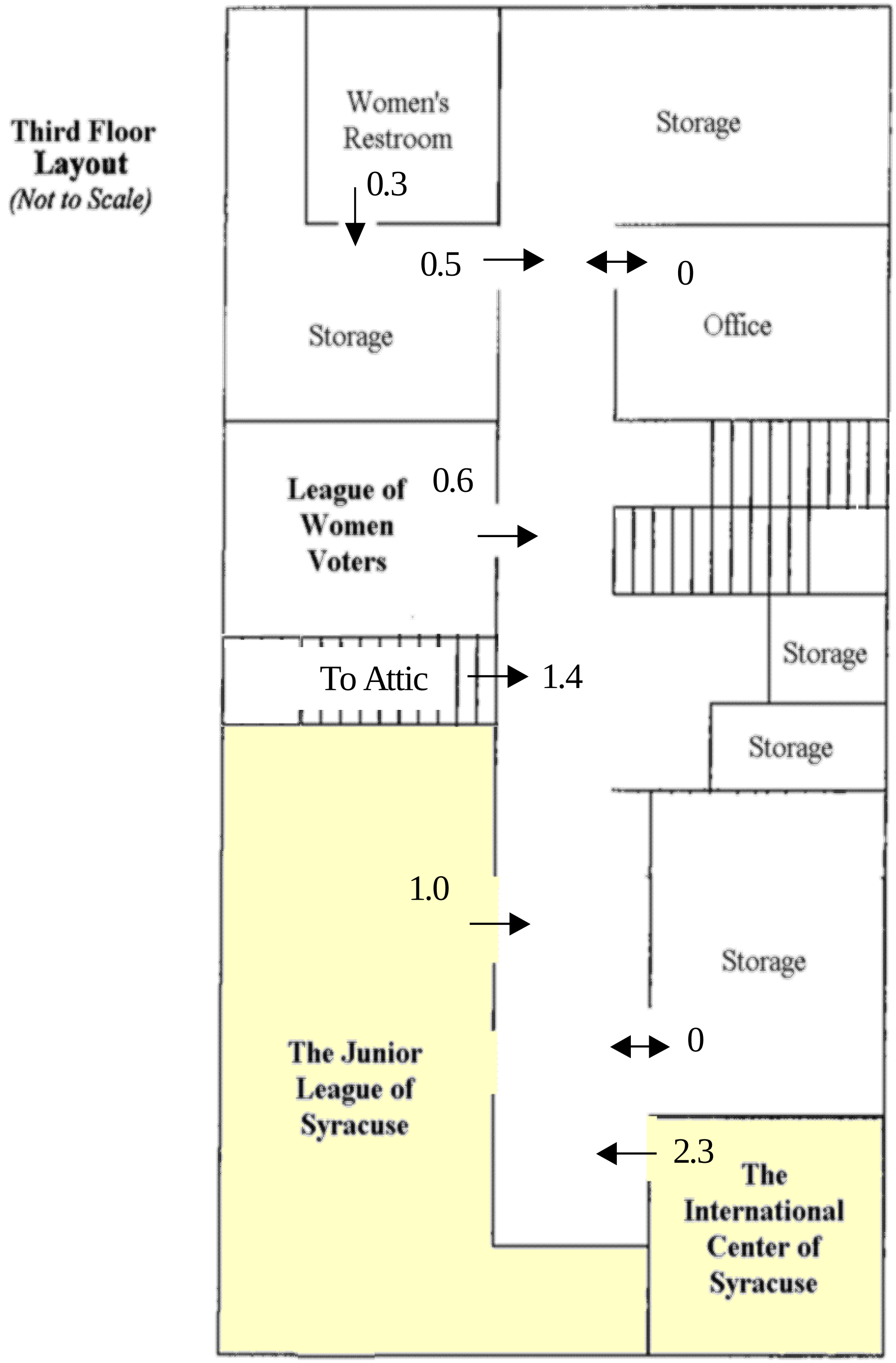

Figure A17-13. Pressure Mapping with Building Depressurized to 4.5 Pa – Third Floor

HVAC Airflow Measurements

Only three of the supply vents are served by the steam fan coils. Airflow from each supply vent was measured using a Shortridge flow hood. Two sets of airflow readings were taken with the supply fans on both high and low settings. Figure A17-14 and Figure A17-15 show the supply measurements for the first and second floor.

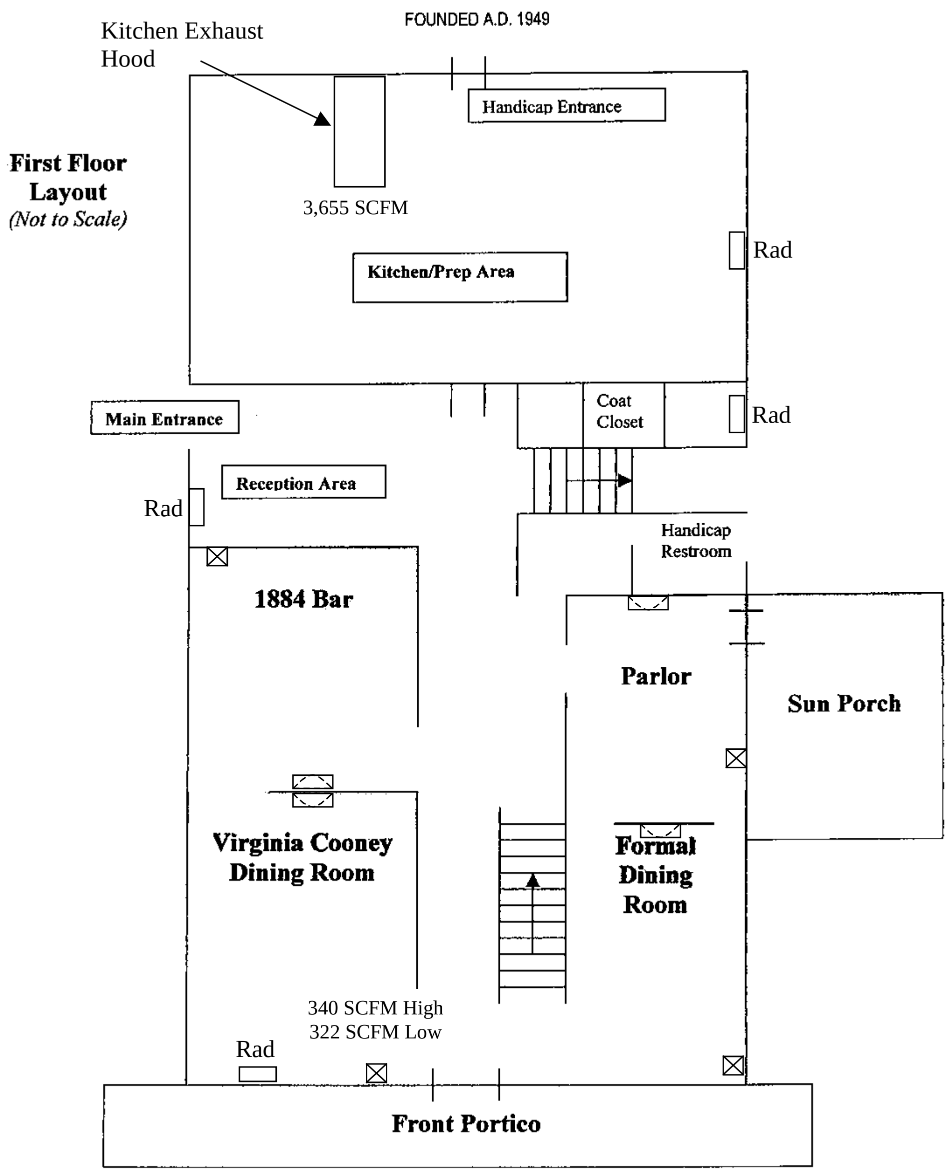

Figure A17-14. First Floor Supply/Exhaust Flow Rates

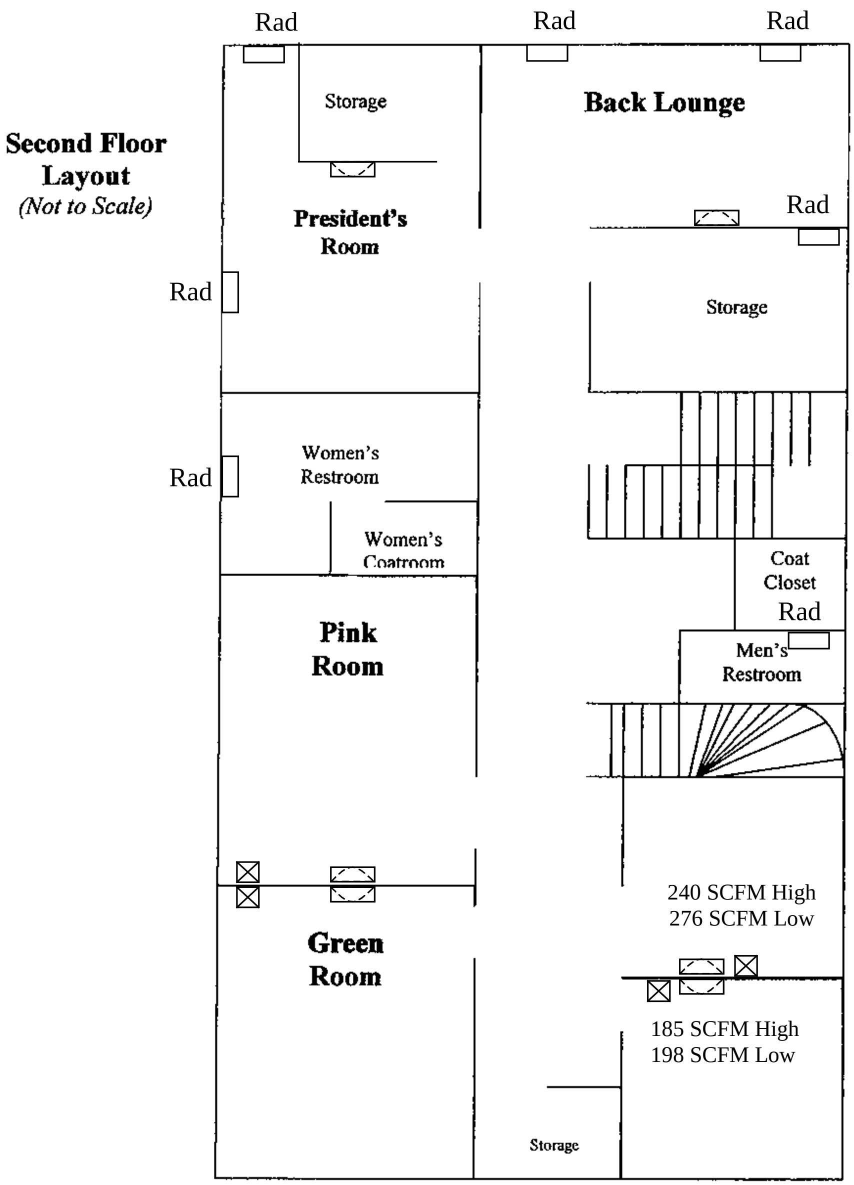

Figure A17-15. Second Floor Supply Flow Rates

All supply air for the steam fan coils is supplied directly from the basement, with no direct return ducting, nor air filtration in use. The total supply airflow was measured to be 814 SCFM.

The kitchen exhaust flow hood measures 34 sq ft (3 ft × 11 ft 4 in). The airflow rate of the hood was measured at 3,655 SCFM. The airflow was measured using a hot wire anemometer and an equal area traverse of 30 point of the exhaust hood face area. When the exhaust hood is on and all the doors in the kitchen are blocked closed, the kitchen is depressurized by 18 Pa with respect to the main hallway on the first floor. The depressurization normally causes the door leading to the hallway to remain open by about 6 inches, and reduces the depressurization to 8 Pa. With the back door open (typical during the summer periods) then the depressurization of the kitchen with respect to the remainder of the building is only 1-2 PA.

Pressure Mapping (AHU Fans On)

Only three rooms in the building have forced air vents in them: the Virginia Cooney Dining Room on the first floor, and the Red and Blue Rooms on the second floor. The Dining room is a very open room with a large entrance to the hallway that cannot be closed, therefore a pressure reading was impossible. Measuring the pressure difference between the Red and Blue Rooms to the hallway indicated that the room pressurization from the steam coil fan operation was 1.5 – 2.5 Pa. When the fans for the forced air heating coils are on, the basement decreases pressure by 0.5 Pa below its nominal pressure.

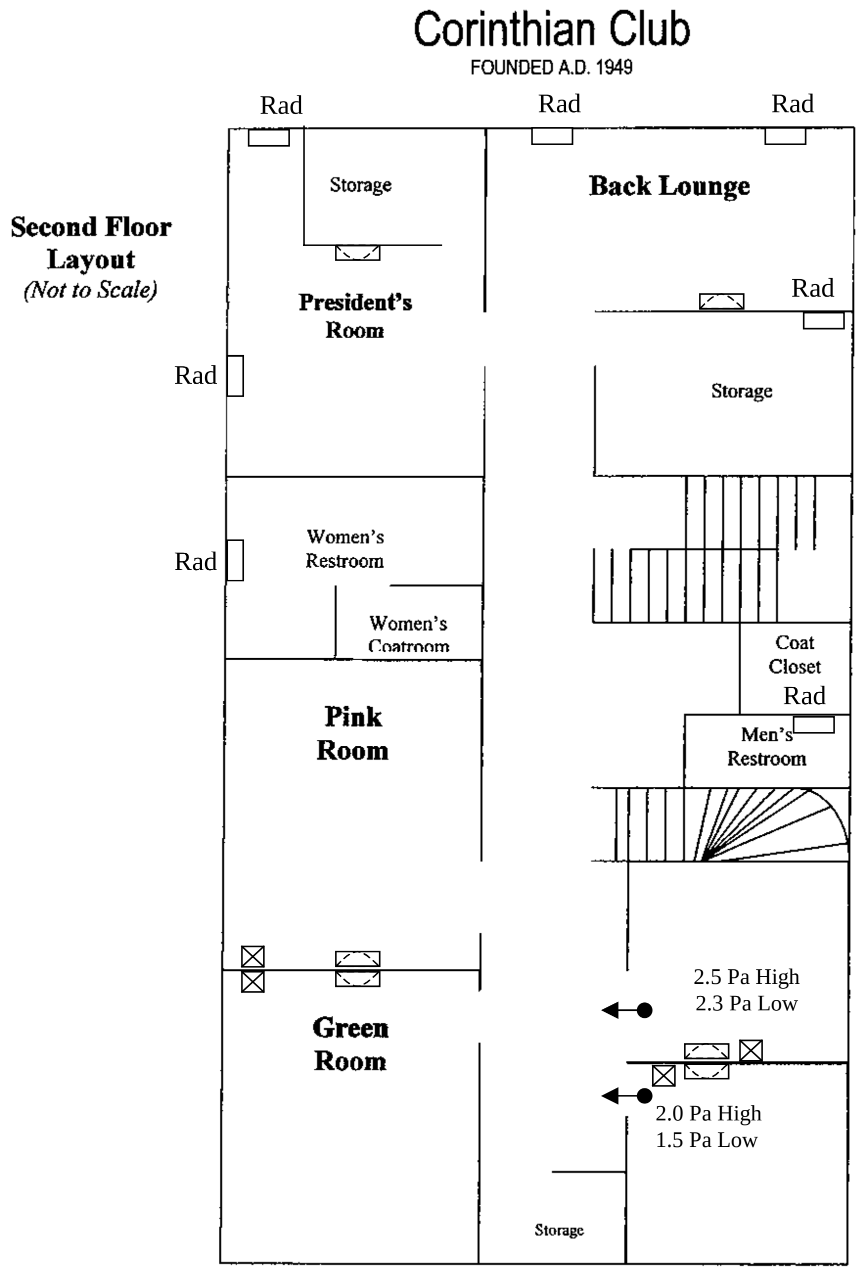

Figure A17-16. Pressure Mapping between Rooms with Steam Coil Fans Operation – Second Floor

Duct Leakage Measurements

No duct leakage test was performed. .

Space Conditions

After the blower door testing, space temperature and relative humidity levels for several sections of the building were recorded using HOBO data loggers. Space conditions were sampled on a 15-minute basis, compared to hourly ambient data from the Syracuse airport. Table A17-3 lists the monitored periods and spaces monitored.

Table A17-3. Space Conditions Monitoring Period Summary

Start Date	End Date	Monitored Spaces
June 10, 2005	July 11, 2005	Parlor (first floor) Second floor hallway Parlor CO_2 levels Second floor hallway CO_2 levels
January 7, 2006	February 8, 2006	Parlor (first floor) Second floor hallway Attic (unconditioned)
March 7, 2006	????	Parlor (first floor) Attic (unconditioned)

Figure A17-17 displays the space conditions data collected during the summer monitoring period (June 10 – July 11, 2005). Typically the upstairs areas of the building are 4-5°F warmer than the first floor. The space temperatures tend to converge as the ambient temperature approaches 60°F. The upstairs areas have a correspondingly lower relative humidity level, due to the elevated space temperatures. The humidity ratio (total moisture content in the air) for both spaces were very similar.

Figure A17-18 directly compares the daily average space conditions data collected during the summer monitoring period to daily average ambient conditions. A slight depression in space temperature occurs above 80°F ambient due to the use of window air conditioners. The moisture removal of the window air conditioners is observed as a drop in the space humidity ratio data with ambient conditions above 80 gr/lb. The window air conditioning units are providing a maximum grain depression of 30 gr/lb at peak ambient humidity levels.

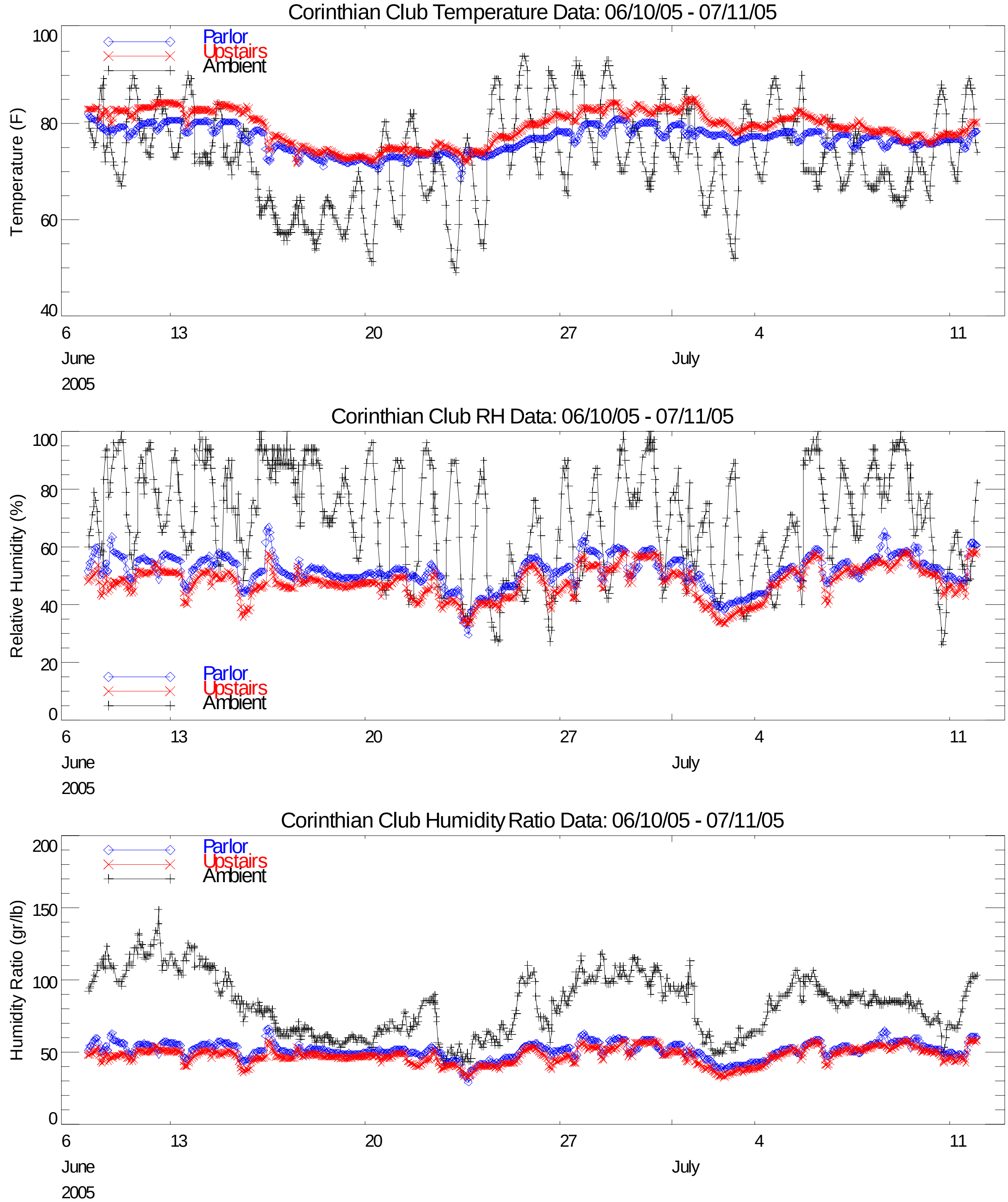

Figure A17-17. Space Conditions Data – Summer Monitoring Period

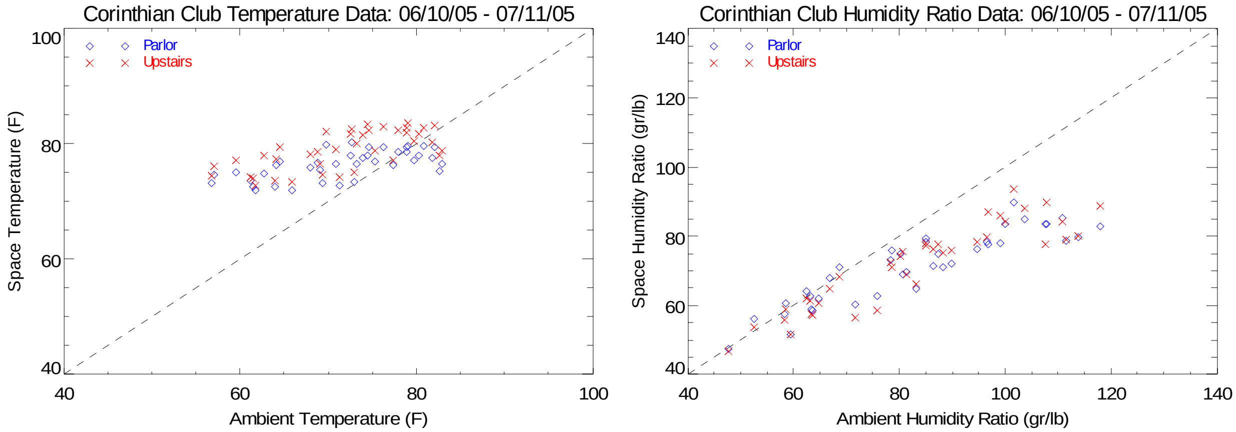

Figure A17-18. Daily Average Relations of Temperature and Humidity Ratio to Ambient Conditions – Summer Monitoring Period

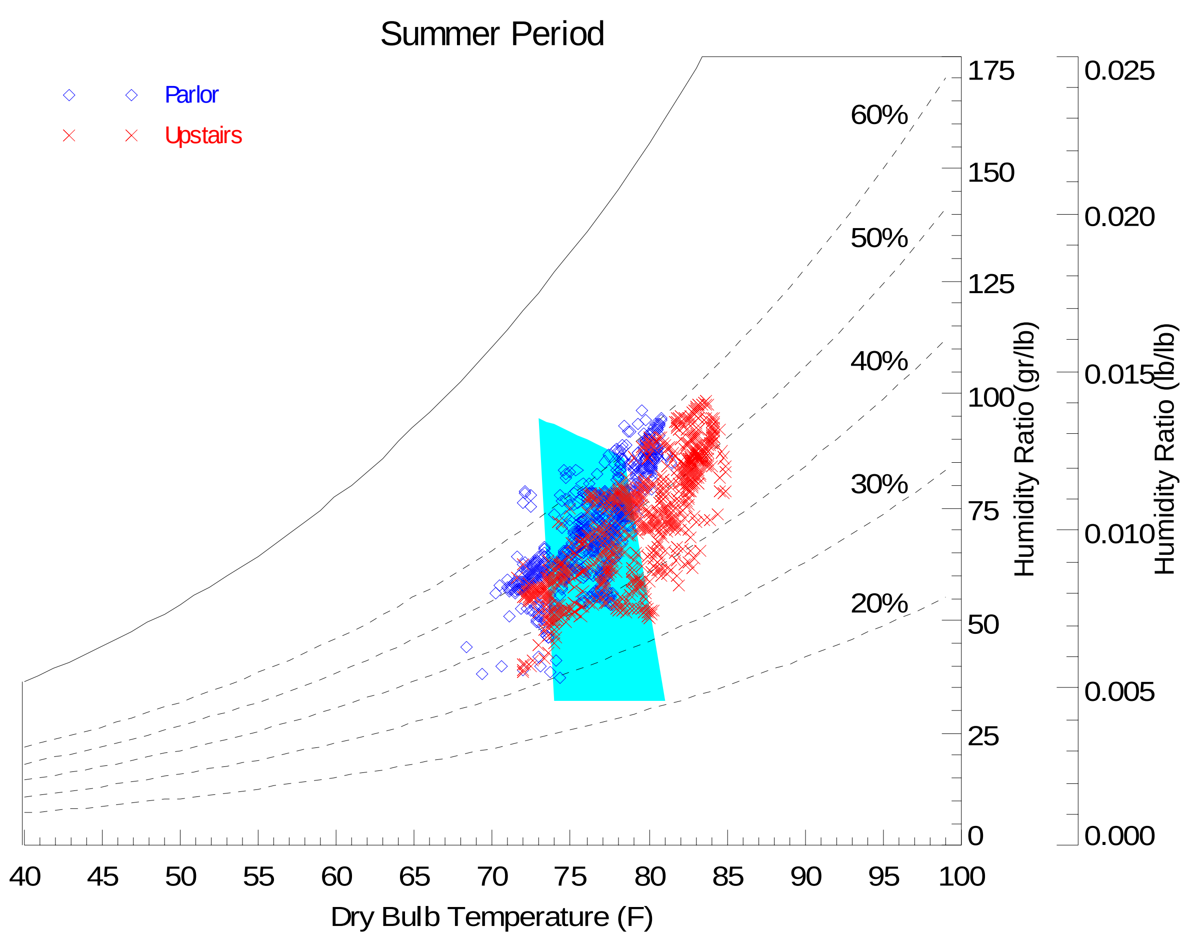

Figure A17-19. Space Conditions Psychrometric Chart – Summer Monitoring Period

Figure A17-20 displays the space conditions data collected during the winter monitoring periods (January 7 – March 23, 2005). During the winter period, the parlor and first floor areas of the building are 4-5°F warmer than the third floor, and have correspondingly different relative humidity levels, due to the difference in temperature. This temperature stratification agrees well with the comments from the building manager, who confirmed it is necessary to keep the first floor near 75°F in order to keep the upper floor adequately warm. The attic temperature was roughly halfway between the space temperatures and the ambient temperature.

The humidity ratio for the third floor and attic area are slightly elevated compare to the first floor humidity ratio. Often the space humidity ratio exceeds the ambient humidity ratio, especially during very dry conditions. This moisture generation in the space occurs due to steam system losses, and is most prevalent during periods of the highest boiler loading (coldest temperatures and correspondingly driest ambient humidity levels).

Figure A17-21 directly compares the daily average space conditions data collected during the winter monitoring period to daily average ambient conditions. The attic temperature data begins to trend more toward the space temperature and away from ambient temperature as ambient temperature decreases. A slight inflection point in the attic temperature data is observed near 35°F.

The corresponding daily humidity ratio data does not display the same trend as the temperature data. The attic humidity ratio is very close to the space humidity ratio, rather than between the space and ambient level observed in the temperature data. This may imply that the losses to the attic are more related to deficiencies in the thermal insulation barrier, rather than air leakage into the attic. Analyzing the moisture data during this period is harder than analyzing the temperature data, due to the relatively low levels of humidity observed both in the space and at ambient conditions.

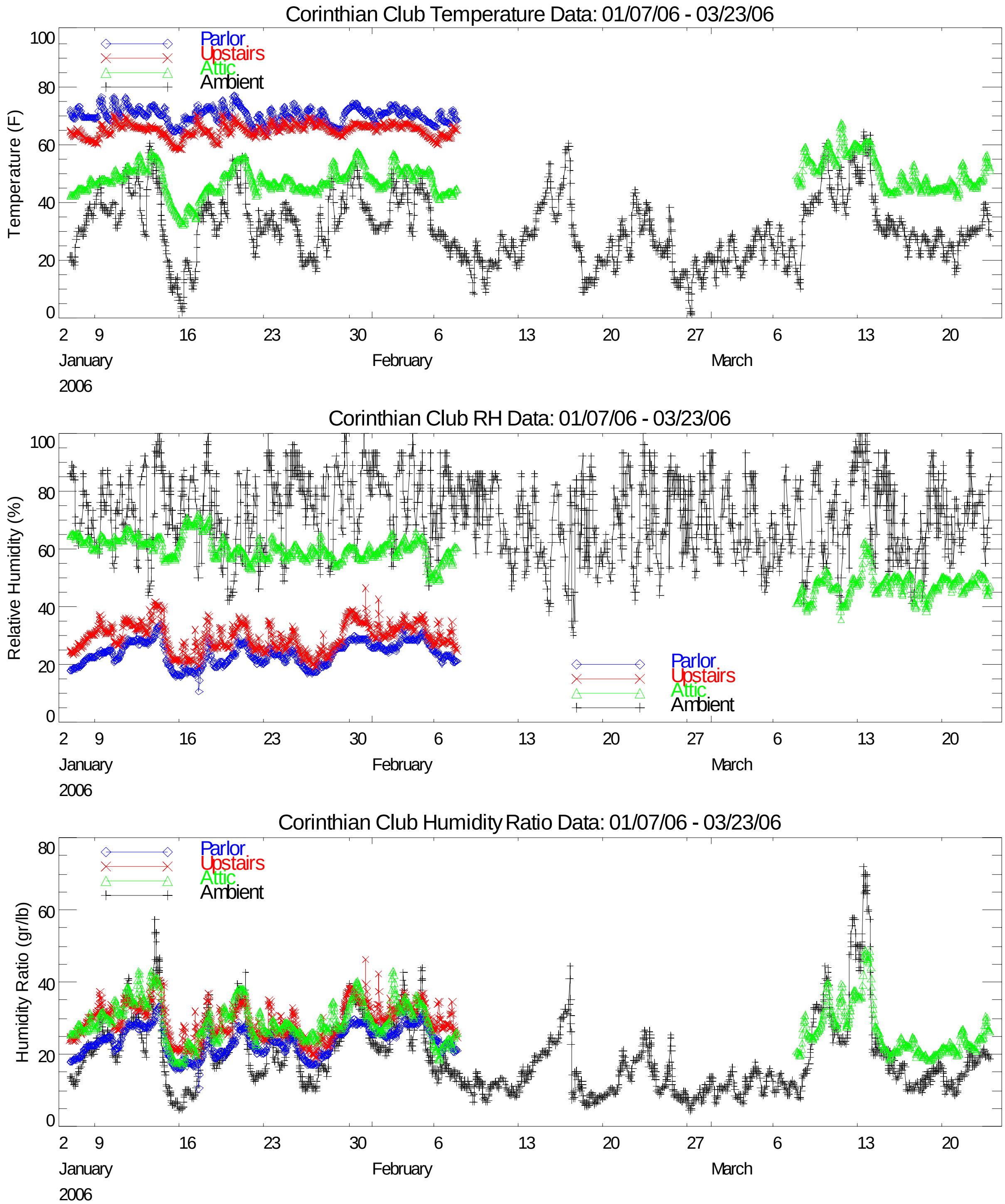

Figure A17-20. Space Conditions Data – Winter Monitoring Period

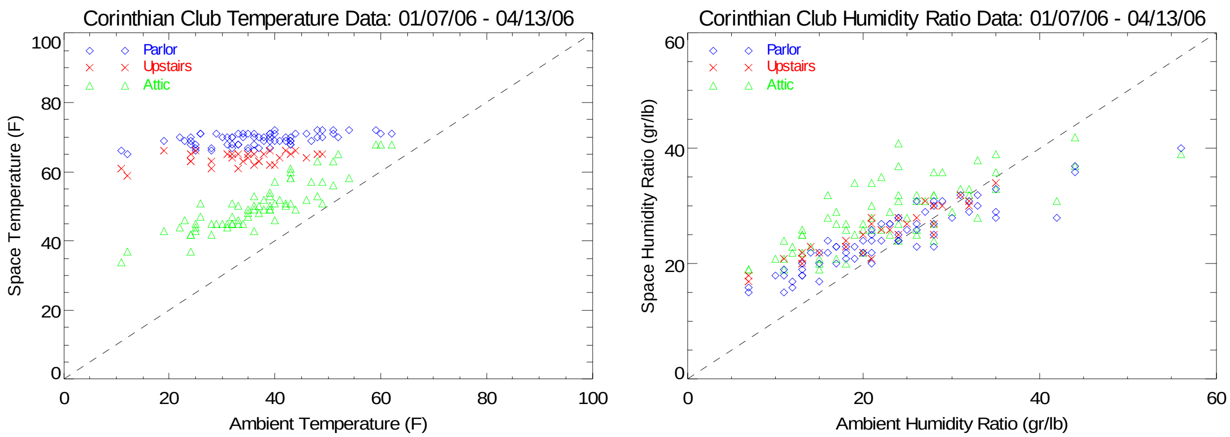

Figure A17-21. Daily Average Relations of Temperature and Humidity Ratio to Ambient Conditions – Summer Monitoring Period

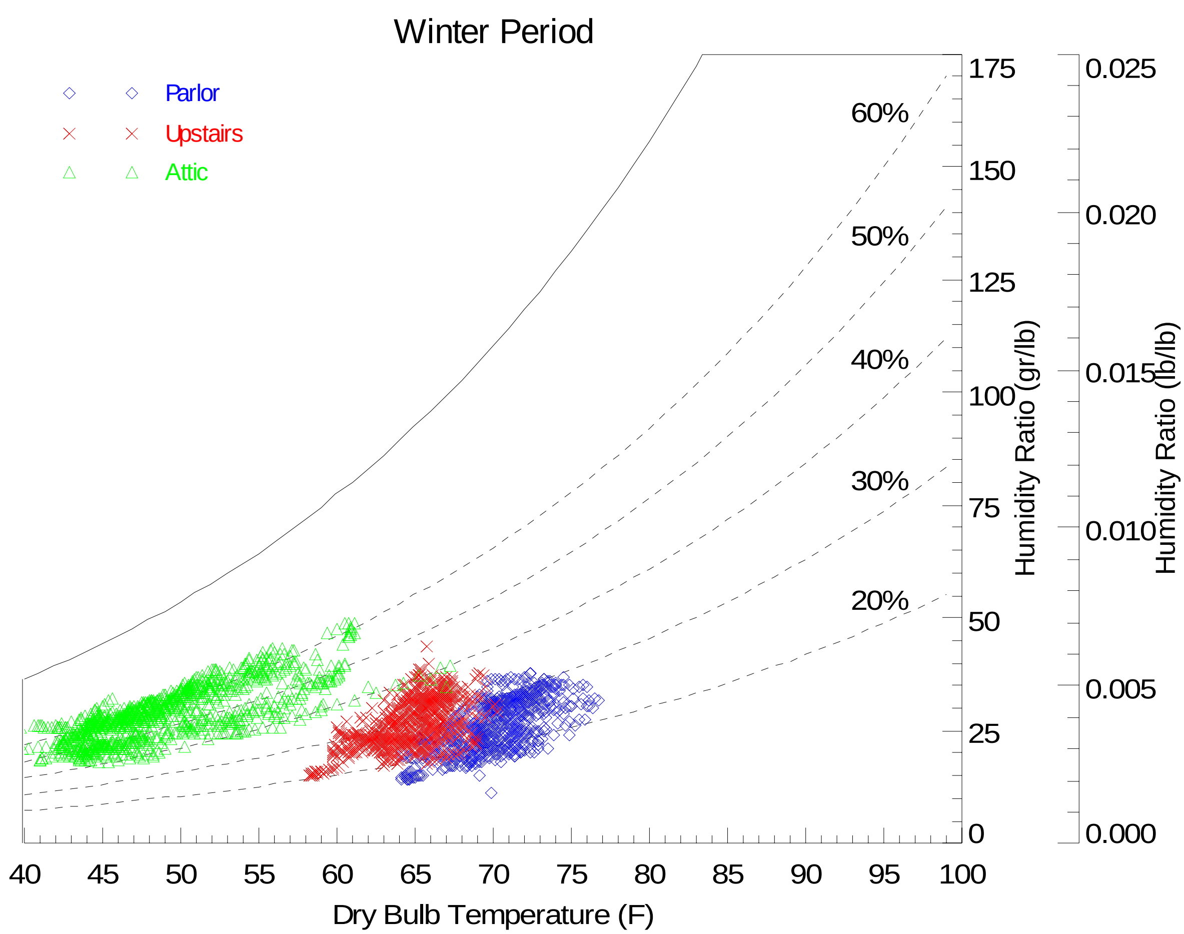

Figure A17-22. Space Conditions Psychrometric Chart – Winter Monitoring Period

During the summer monitoring period, CO2 data was collected in the parlor area and the second floor hallway. The CO_2 concentration provides an indication of occupancy. CO2 concentrations in each area reached a maximum of 1,500 PPM during periods of higher occupancy.

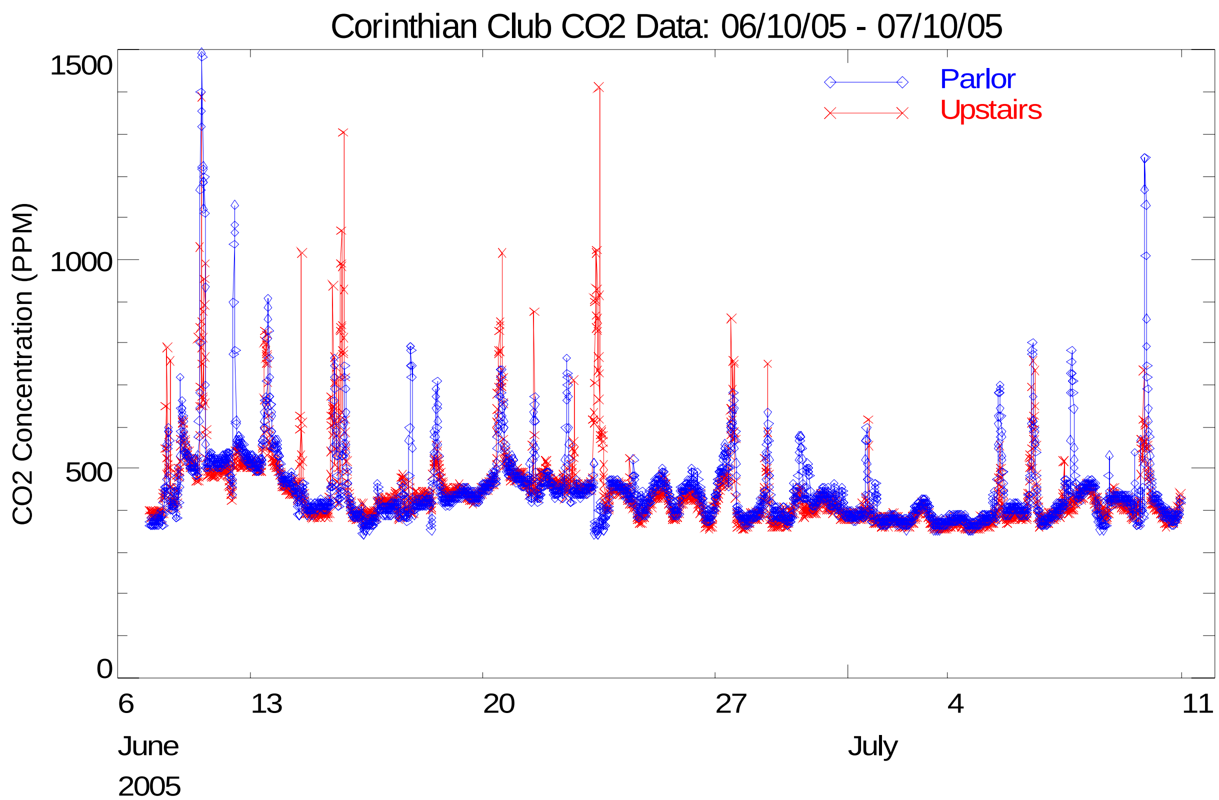

Figure A17-23. Measured CO_2 Concentration in Various Spaces

<u>Infiltration Estimate from CO_2 Decay</u>

Using the spikes in the CO2 data from periods of high occupancy, and the resulting decay, the normal air change rate (ACH) from infiltration during the summer period was determined. Three different decays were examined, using data from sensors installed on both floors. The decay results indicated that the building ACH is on the order of 0.7 - 0.8 ACH. Measurements of the building geometry indicate the building has an occupied volume of 119,375 cu. ft., and an effective ventilation rate of 1,492 SCFM.

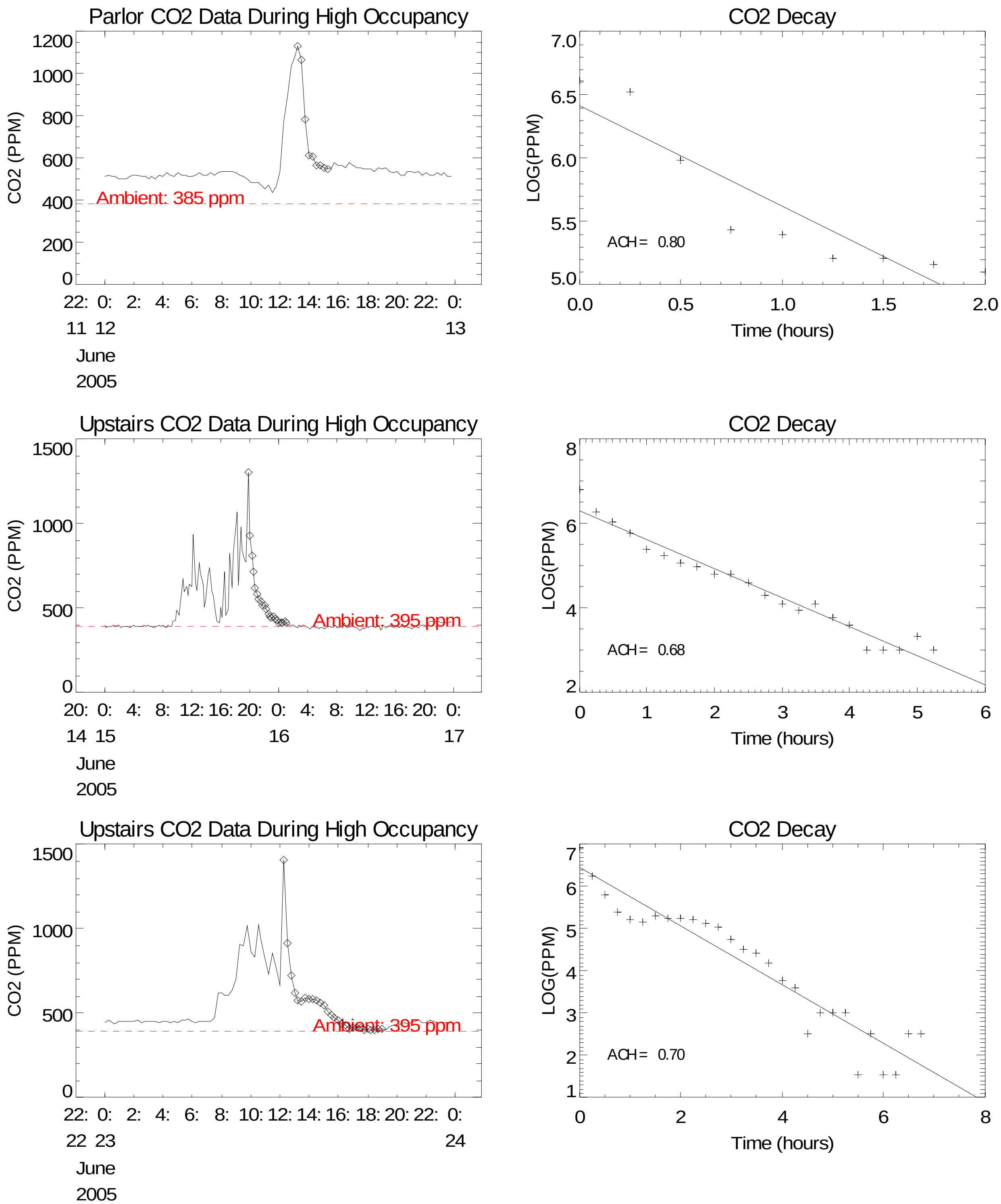

Figure A17-24. Measured Decay of CO_2 Concentration from Elevated Occupancy

Utility Bills

The gas use in the building is primarily used for space heating and cooking. Lunch is cooked every weekday with evening meals occurring about 3 days a week. The overall energy use is summarized below.

Table A17-4. Summarization of Energy Use per square foot per year

Heating Energy Use Index (MBtu/ft^2-year)	Electric Use Index (kWh/ft^2-year)
61.4	4.2

Table A17-5. Summary of Electric Bills

	Corinthian Club (Syracuse) - Electric Utility Data					
Billing End Date	Days in Month	Energy (kWh)	Demand (kW)	Cost ($)	$/kWh	Elec. Use per Sq-Ft (kWh/sq ft)
9/22/2004	29	5,523	30.9	875.09	$ 0.158	0.31
10/21/2004	29	5,598	25.2	840.61	$ 0.150	0.31
11/17/2004	27	5,216	30.7	864.17	$ 0.166	0.29
12/20/2004	33	7,143	27.5	988.77	$ 0.138	0.40
1/20/2005	31	7,494	28	1,028.77	$ 0.137	0.42
2/17/2005	28	6,846	26.5	999.56	$ 0.146	0.38
Total	***177***	***37,820***	***30.9***	***$ 5,597***	***$ 0.148***	***2.10***
Estimated Annual (2004)*	***366***	***75,417***		***$ 11,161***	***$ 0.148***	***4.19***

*Based on electricity use trend with ambient temperature.

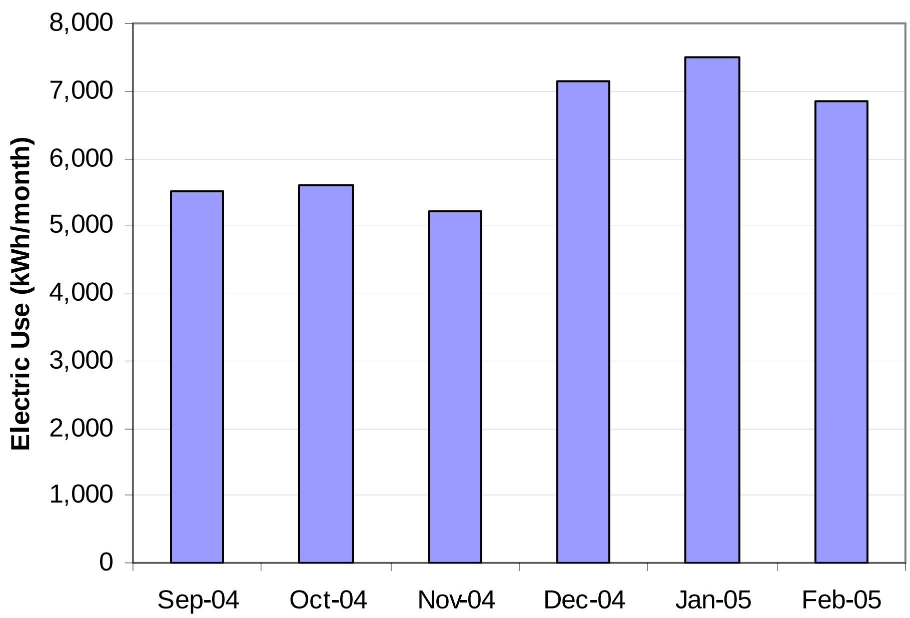

Figure A17-25. Monthly Electric Use Trend

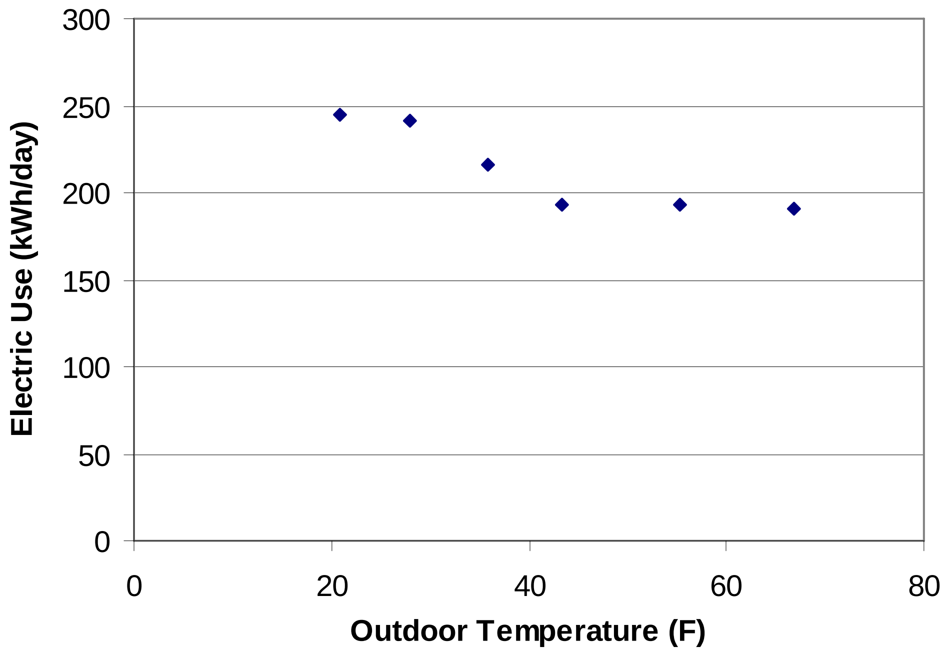

Figure A17-26. Variation of Electric Use with Ambient Temperature

Table A17-6. Summary of Gas Bills

	Corinthian Club (Syracuse) - Gas Utility Data				
Billing End Date	**Days in Month**	**Gas Use (therms)**	**Cost ($)**	**$/therm**	**Gas Use per Sq-Ft (therm/sq ft)**
9/22/2004	29	116	143.73	1.24	0.006
10/21/2004	29	378	397.20	1.05	0.021
11/17/2004	27	848	958.08	1.13	0.047
12/20/2004	33	1,566	1824.43	1.17	0.087
1/20/2005	31	1,945	2165.64	1.11	0.108
2/17/2005	28	2,024	2213.23	1.09	0.112
3/22/2005	33	2,146	2291.44	1.07	0.119
4/20/2005	29	760	902.58	1.19	0.042
Total	***239***	***9,783***	***$ 10,896***	***1.11***	***0.544***
Estimated Annual (2004)*	***366***	***11,047***	***$ 12,304***	***1.11***	***0.614***

*Based on gas use trend with ambient temperature.

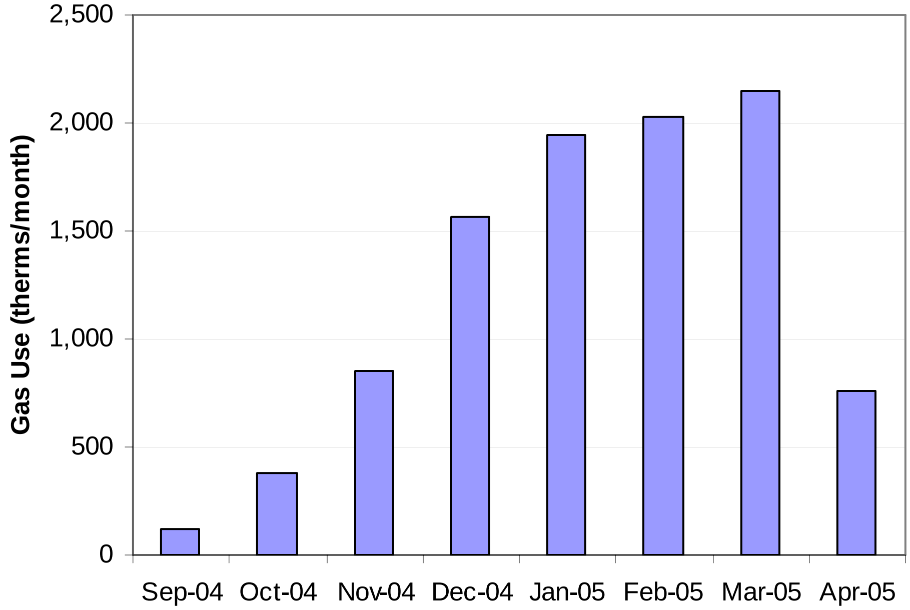

Figure A17-27. Monthly Gas Use Trends

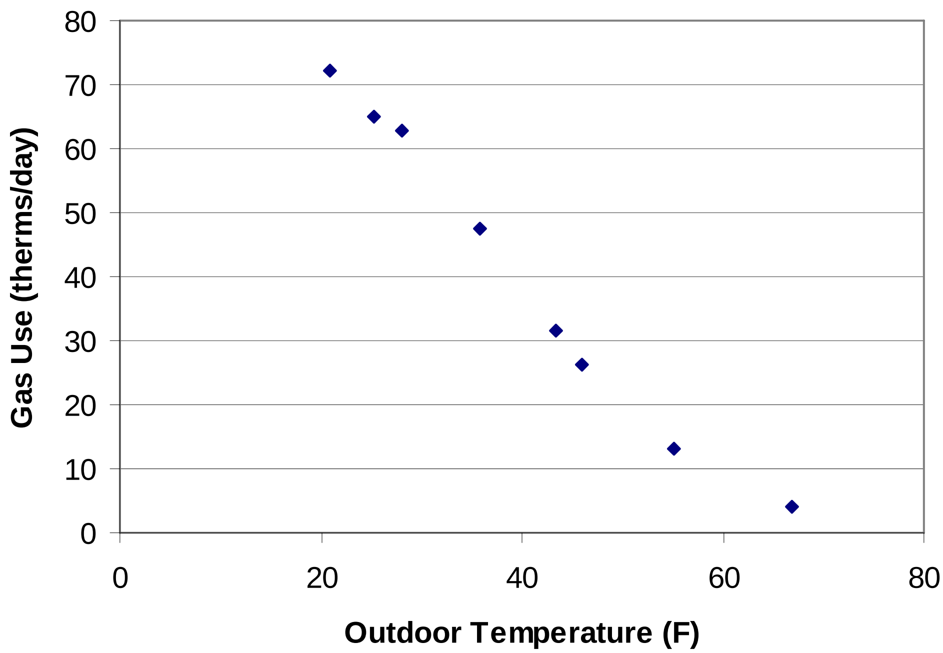

Figure A17-28. Variation of Gas Use with Ambient Temperature

REMEDIATION

On February 23, 2006 the attic was surveyed with a thermal imaging camera. Several large leakage areas were identified along the perimeter attic wall (where the attic floor deck meets the brick wall), around each of the five chimney penetrations, and around each of the roof support braces.

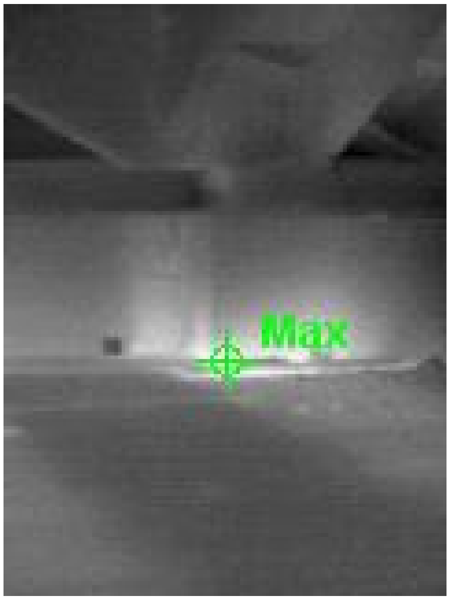

Leak along perimeter wall

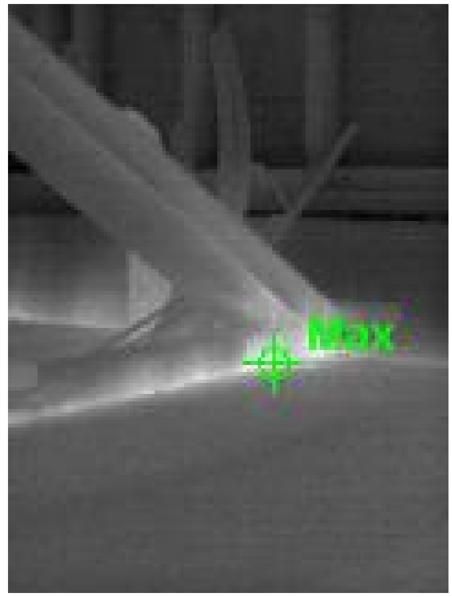

Leak along ceiling support brace

Figure A17-29. Thermal Imaging Camera Results

Based on the observations from the imaging camera, it was decided that a low cost way to mitigate these losses to the attic would be to spray expandable foam at the location of each leak. It was also determined that the small room housing the elevator winch (located in the attic) was an additional source of leakage. The elevator mechanical room is constructed out of exterior wood framing, sheathed with asbestos board with no insulation, and is not well sealed from the attic space (Figure A17-30). Calking and weather-stripping was added to this room to help seal the room from the attic and reduce the impact of stack effect moving conditioned air up the elevator shaft into the attic. On March 23, 2006 we returned to the building to perform these steps.

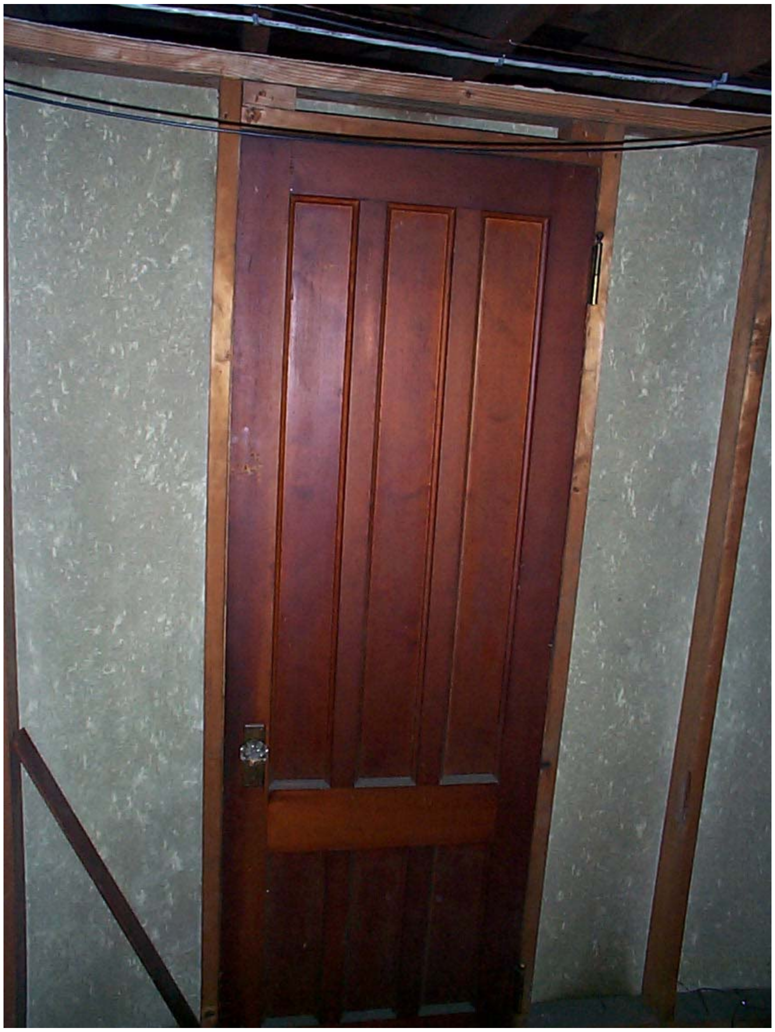

Figure A17-30. Exterior of Elevator Mechanical Room (Viewed from Attic)

Prior to spraying the expandable foam, areas of extreme leakage were identified using an infrared thermometer. The typical attic floor temperature away from a leak was near 41ºF, but areas where leaks occurred had a much higher surface temperature. Some areas were as high as 57ºF (Figure A17-31). Areas where leaks were identified were marked with marking paint.

The entire perimeter of the attic was sprayed with expandable foam. The foam was applied with the spray tip flush with the crack between floor deck and the wall, to ensure the foam expanded downward into the crack. In other areas, the foam was applied to both surfaces (the wall and the floor) to seal the surfaces together.

Attic Floor Temperature away from Leak

Attic Floor Temperature at Leak

Marking Leaks Areas before Spraying

Leakage Area Sealed with Foam

Figure A17-31. Diagnosing and Sealing Perimeter Leaks in the Attic

Figure A17-32 displays typical areas where leaks were identified and filled with foam.

Around Chimney Penetration

Entire Perimeter

Roof Bracing

Large Area Leak Around Drain Plumbing

Figure A17-32. Different Types of Leaks Sealed with Expandable Foam

The elevator mechanical room was sealed using clear silicone adhesive caulk, which was wet mopped into each seam in the asbestos board. The joints between the ceiling and wall, and floor and wall were also caulked. A closed cell foam rubber weather striping was applied to the mechanical room doorway. Figure A17-33 displays some photos of the work performed on the mechanical room.

 Caulking and Weather Striping	 Corner Joints and Butt Joints Caulked

Figure A17-33. Sealing the Elevator Mechanical Room

Boiler Monitoring

Boiler runtime variation with ambient temperature was monitored for a period of five weeks, spanning from March 8, 2006 to April 14, 2006. The boiler is a modular boiler with three sections, each with an input of 400 Mbtu/h for a total of 1.2 MMBtu/h. The three sections operate in unison providing only a single stage of heating capacity.

The runtime of the boiler was monitored using a current status switch on the 24 VAC control circuit for the natural gas valve (Figure A17-34).

Figure A17-34. Current Status Switch on 24 VAC Control Transformer for Boiler Natural Gas Train

The boiler runtime data was monitored for 15 days prior to the building remediation steps to establish a baseline for comparison.

Remediation Results

The impact of sealing the elevator shaft was determined immediately after the caulking was finished. Prior to caulking, the pressure difference between the attic space and the elevator shaft was measured, using a digital micromanometer. After the calking was completed, the pressure difference was measured again. Calking the elevator shaft raised the pressure difference from 1.2 PA (positive relative to the attic), to 2.5 PA.

Figure A17-35 displays the monitored boiler runtime data for before and after the remediation steps were performed. Multiplying the baseline boiler runtime trend (before building remediation) by the nominal boiler input (1.2 MMBtu/h) agrees well with the historic natural gas data. At 20°F ambient temperature, the historic gas consumption indicates a gas use of approximately 70 therm/day. The calculated baseline boiler gas use at this temperature based on 6 hours/day of runtime is 72 therm/day (6 hrs × 1.2 MMBtu/h × 10 therm/MMBtu).

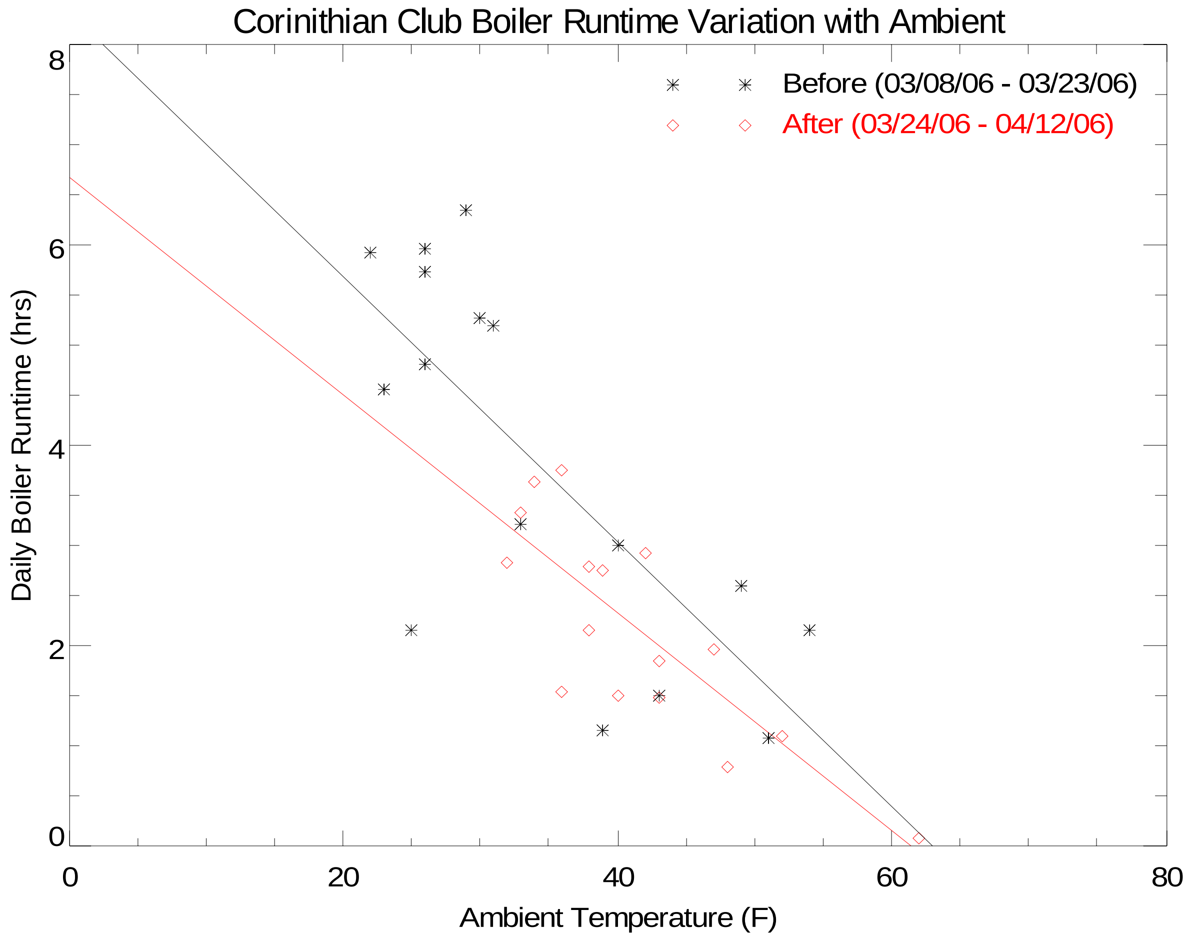

Figure A17-35. Boiler Runtime Variation with Ambient

The trendlines indicate that after the remediation, the boiler is operating 1.6 hours/day less at 0°F ambient. The impact is lower at milder conditions, and both trends converge at approximately the same point near 62°F.

Comparison of daily boiler runtime with the indoor to ambient temperature difference (which accounts for variations in thermostat set point) indicate similar results. The trends indicate that at a 70°F temperature difference to outdoors (approximately 0°F ambient), the boiler will operate 2.1 hours/day less after the remediation.

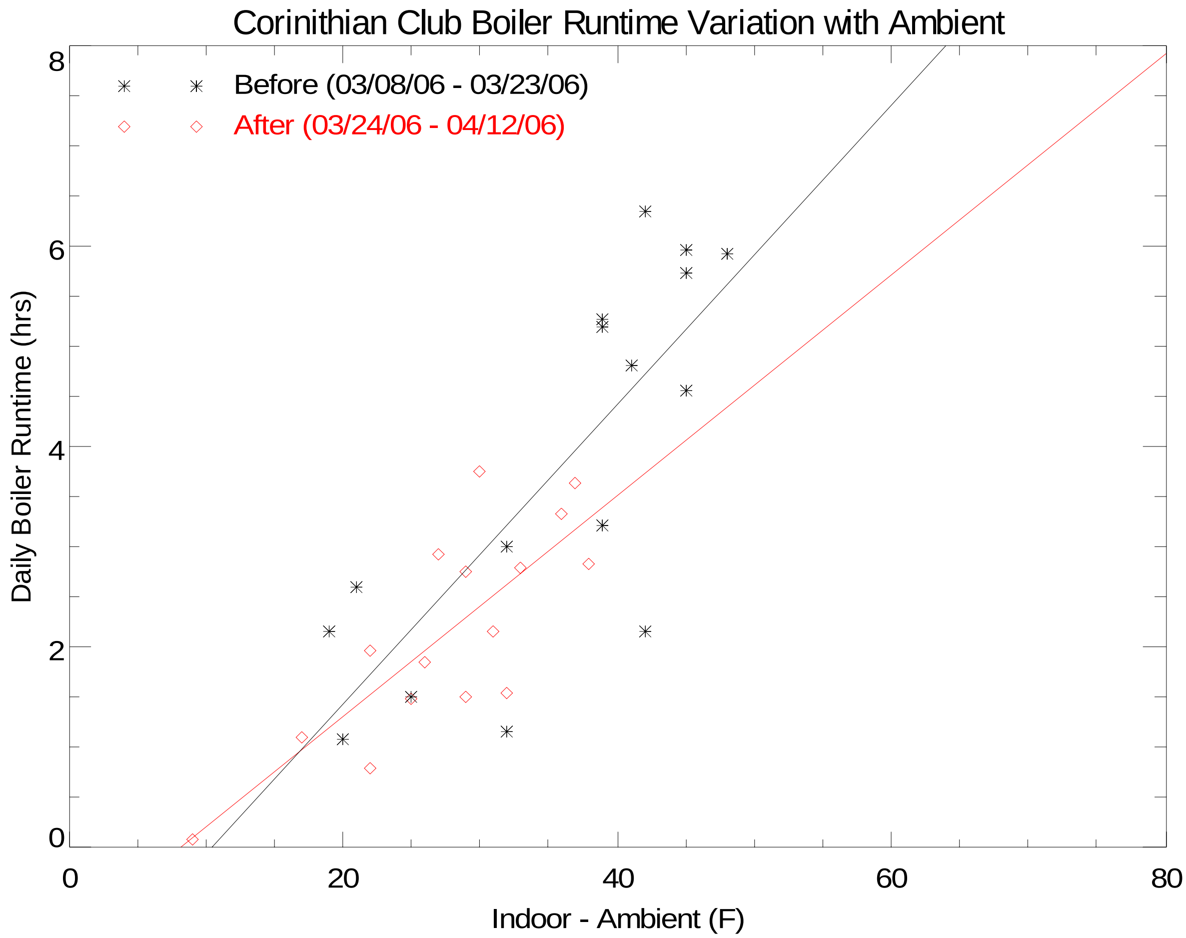

Figure A17-36. Boiler Runtime Variation with Indoor – Ambient Temperature Difference

Comparing space conditions before and after the remediation displayed inconclusive results.

Using the boiler runtime trends for the baseline and remediation periods, and bin data of the daily average temperature for Syracuse (from the Syracuse TMY2 file), the annual savings was calculated. Annually the boiler runtime was reduced by 199 hours, resulting in 2,389 therms of natural gas savings. At the previous cost of natural gas ($1.10/therm), the remediation work is saving approximately $2,600/year. With the recent increases in natural gas costs, the actual annual savings is like on the order of $3,600/year (estimated at $1.50/therm).

Table A17-7. Annual Savings Calculation from Remediation

[1]	[2]	[3]	[4]	[5] = [8.33 - 0.133*[3]] * [4]	[6] = [6.68 - 0.109*[3]] * [4]	[7] = [6] - [5]	[8] = -4.35 + 1.06*[6]
Syracuse TMY2 Bin Data							
Bin Low (F)	**Bin High (F)**	**Bin Med (F)**	**Number of Days (days)**	**Baseline Boiler Runtime (hours)**	**Remediated Boiler Runtime (hours)**	**Runtime Reduction (hours)**	**Boiler Gas Savings @ 1.2 MMBtu/h Input (therms)**
-25	-20	-22.0	0	-	-	-	-
-20	-15	-17.0	0	-	-	-	-
-15	-10	-12.0	0	-	-	-	-
-10	-5	-7.0	0	-	-	-	-
-5	0	-2.0	0	-	-	-	-
0	5	2.0	3	24.2	19.4	4.8	58
5	10	7.0	4	29.6	23.7	5.9	71
10	15	12.0	5	33.7	26.8	6.8	82
15	20	17.0	14	85.1	67.6	17.5	210
20	25	22.0	21	113.7	89.9	23.8	286
25	30	27.0	22	104.5	82.2	22.3	268
30	35	32.0	39	159.4	124.4	35.0	420
35	40	37.0	29	99.3	76.7	22.6	271
40	45	42.0	32	88.4	67.2	21.2	254
45	50	47.0	28	58.8	43.6	15.2	183
50	55	52.0	23	33.1	23.2	9.8	118
55	60	57.0	32	24.8	14.9	9.9	118
60	65	62.0	37	4.1	-	4.1	50
65	70	67.0	34	-	-	-	-
70	75	72.0	25	-	-	-	-
75	80	77.0	14	-	-	-	-
80	85	82.0	3	-	-	-	-
85	90	87.0	0	-	-	-	-
Totals				**858.6**	**659.6**	**199.1** **23%**	**2,389**

At the end of November 2006, the monthly gas bills were compared to weather data to develop gas use load lines for before and after the remediation (on March 24, 2006). Figure A17-37 shows this data from with linear regression models fit to the data with daily average temperatures over 60°F. The most recent months of October and November (shown as yellow diamonds) returned to the original trend. When we visited the site on November 29, 2006, we found the door to elevator room in the attic was not full closed. We theorize that door had been opened to service elevator during the summer. This anecdotal demonstrates the large impact that the stack can have in three story building. Its appears that efforts to seal the elevator room most-likely accounted for the large portion of the energy savings.

Table A17-8 uses the same bin data from Table A17-7 with the load lines based on gas use. The predicted savings from this analysis are very similar to savings predicted from the boiler runtime data. Annual gas savings are 2,711 therms (25%) compared the analysis above that predicted 2,389 therms (23%).

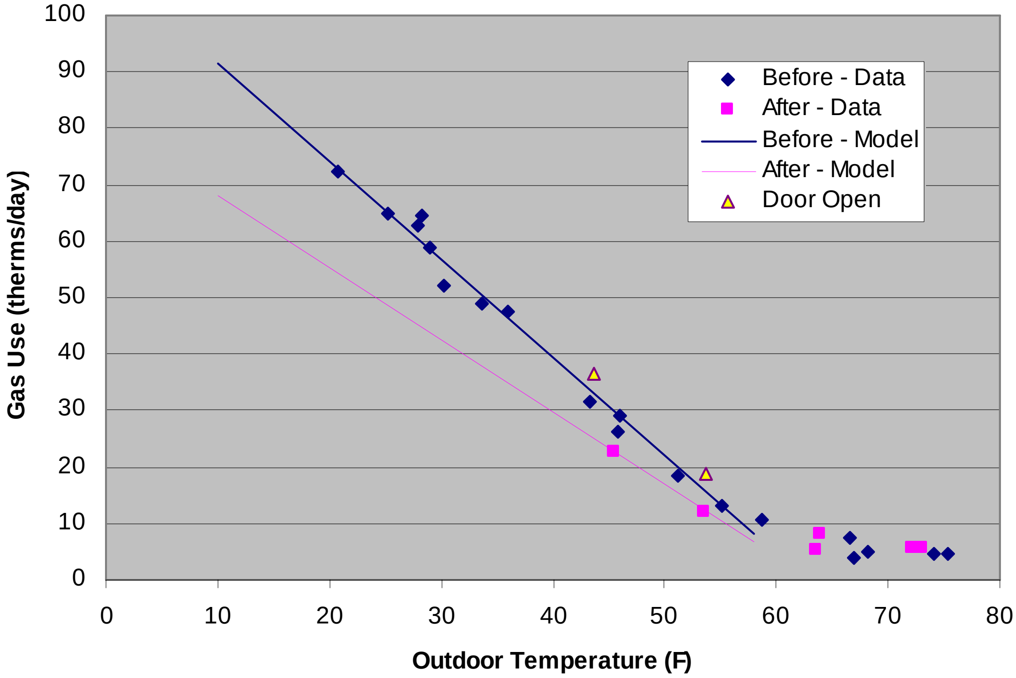

Figure A17-37. Monthly Gas Use vs. Ambient Temperature

Table A17-8. Annual Savings Calculation from Gas Bills

Temp	No of			After		Savings
Bin (F)	Days	therms/day	therms	therms/day	therms	therms
2.5	3	104.7	314.0	77.8	233.5	80.5
7.5	4	96.0	383.9	71.4	285.6	98.3
12.5	5	87.3	436.3	65.0	324.9	111.4
17.5	14	78.6	1,099.9	58.6	819.9	280.0
22.5	21	69.9	1,467.1	52.1	1,095.0	372.1
27.5	22	61.2	1,345.5	45.7	1,005.9	339.6
32.5	39	52.5	2,045.9	39.3	1,532.8	513.1
37.5	29	43.8	1,269.0	32.9	953.6	315.4
42.5	32	35.1	1,121.8	26.5	846.9	275.0
47.5	28	26.4	738.0	20.0	561.3	176.7
52.5	23	17.7	406.1	13.6	313.4	92.7
57.5	32	9.0	286.5	7.2	230.6	55.9
Totals:	***252***		***10,914***		***8,203***	***2,711***
						25%

On November 29, 2006, we repeated the blower door test to evaluate if the remediation had changed the building air tightness. The test was completed in the morning when the winds were very calm and the ambient temperature was about 45-50ºF. The blower door test was repeated with the kitchen exhaust fan running (exhausting 3655 cfm). For this test we were able to depressurize the building to -17 Pa (compared to -7.2 Pa for the previous test). The building pressure before testing was about –1.5 Pa. Table A17-9 compares air leakage statistics before and after the remediation (the "before" data is taken from Table A17-2). The leakage area decreased by about 800 square inches (about 5.5 square feet) due to the spraying foam to fill airgaps between the attic and the conditioned space. Both the leakage area and the air change rate at 50 Pa decreased by 40%.

Table A17-9. Impact of Remediation on Building Airtightness

	Flow Coeff. K	Exp. n	ELA (sq in)	ELA / 100 sq ft (sq in/sq ft)	Flow @ 50 Pa (cfm_{50})	ACH_{50}
Before	2,836.0	0.620	1898	12.34	32,068	14.3
After	1,608.4	0.637	1101	7.16	19,404	8.6
			58%			61%

After the remediation, the attic displayed temperatures higher than the previous trend, rather than closer to ambient. After the remediation, milder ambient temperatures and increases solar irradiation can cause the attic temperature to exceed the ambient temperature. Similar increases in humidity ratio were observed in the attic after remediation, as increased attic temperatures result in off-gassing of entrained moisture in building materials. The true impact of the remediation on attic space conditions will not be observed until next winter, when cold, dry ambient conditions occur.

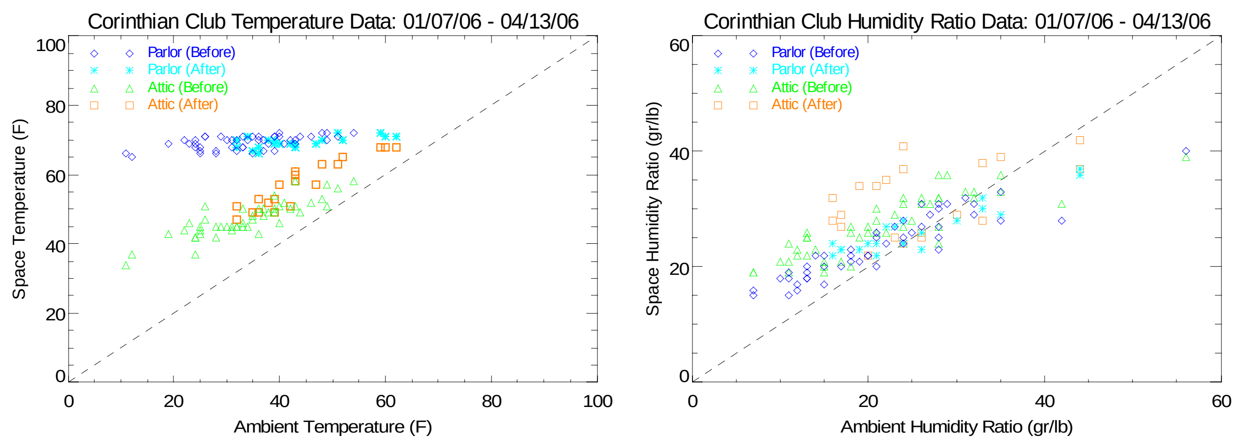

Figure A17-38. Comparing Space Conditions Before and After Remediation

Field Test Site 18 – Office/Metal Shop/Warehouse, Syracuse, NY

CHARACTERISTICS

Building Description

The 27,620 sq-ft facility contains an office, a sheet metal working shop, and a warehouse. The office is housed in the original building, which was built in 1940 and expanded in the 1950s to include the bay area. The sheet metal shop was built as an addition in 1963. The warehouse was added in 1986. The office (6,020 sq-ft) contains bathrooms, offices, a reception booth, and storage rooms. The metal shop (10,900 sq-ft) contains the bay area and the metal working area. The warehouse (10,700 sq-ft) is mostly used for storage space, but has a bathroom and a small office in it. The office, metal shop, and bay area are used by HVAC contractor for their regular business operations. The warehouse is rented out to a separate tenant, who uses the facility for a storage warehouse. The building entrance for the office area and bay faces the parking lot to the east. Figure A18-1 and Figure A18-2 shows the building floor plan.

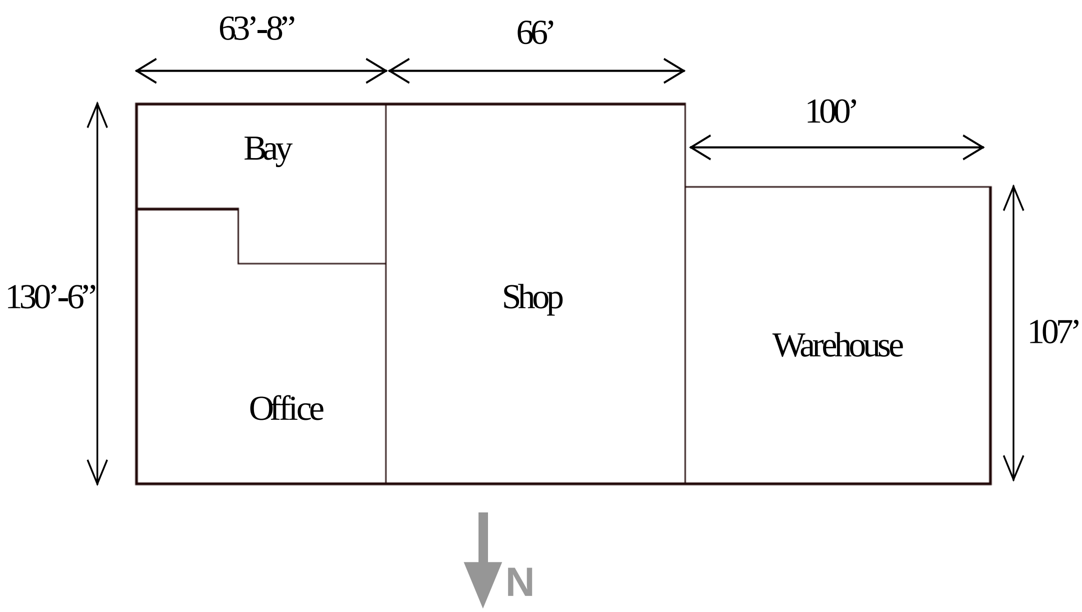

Figure A18-1. Floor Plan

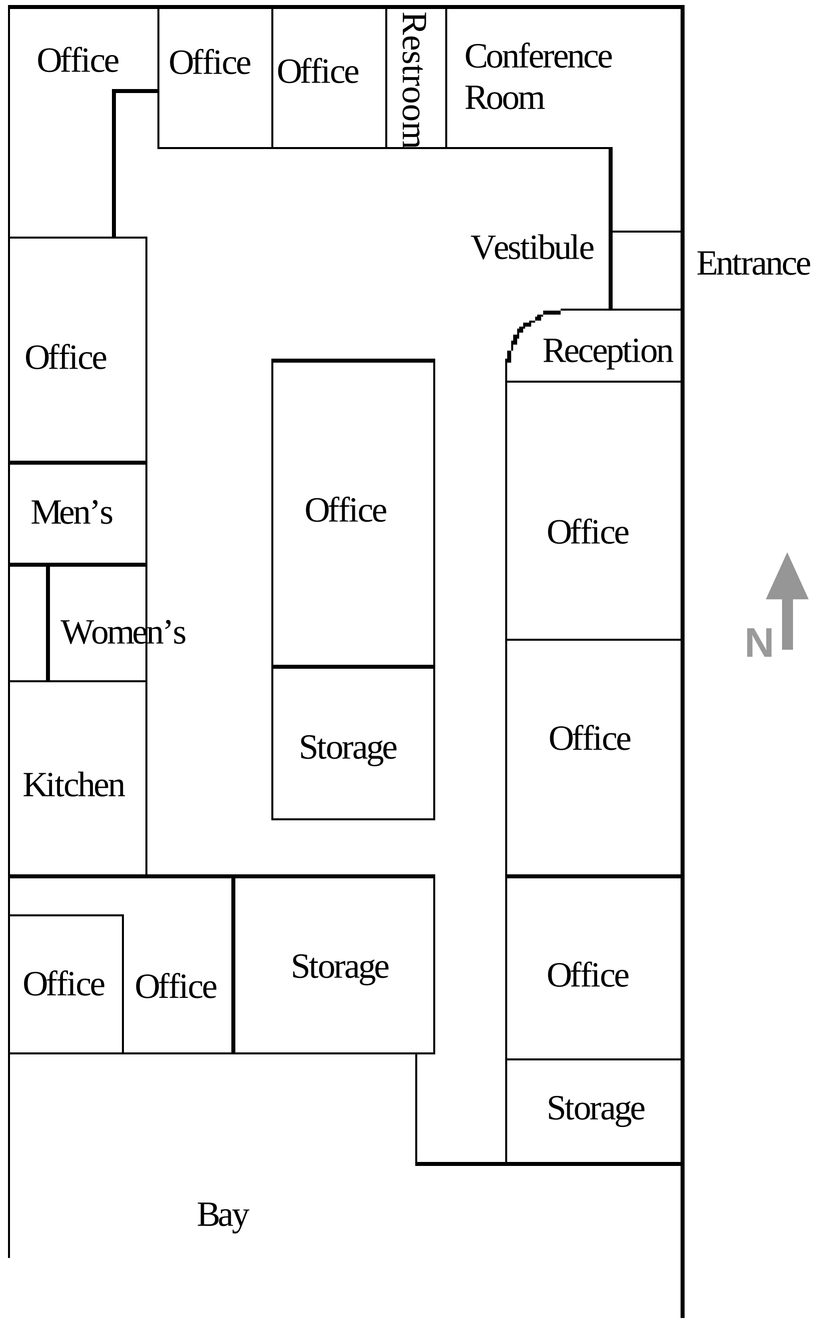

Figure A18-2. Office Floor Plan

Construction Details

The buildings are built with concrete block construction. The majority of the building does not appear to have any type of insulation at the wall, except in the office section of the building. The office building has an interior wood frame construction in addition to the concrete block construction. The wood frame is insulated and then covered with dry wall, shown in Figure A18-3.

The newer parts of the building (i.e., the warehouse) have a metal roof deck with insulation. The shop roof has several skylights in it. The office and bay roofs have wood frame construction with a roof deck and insulation.

Exterior Wall Construction

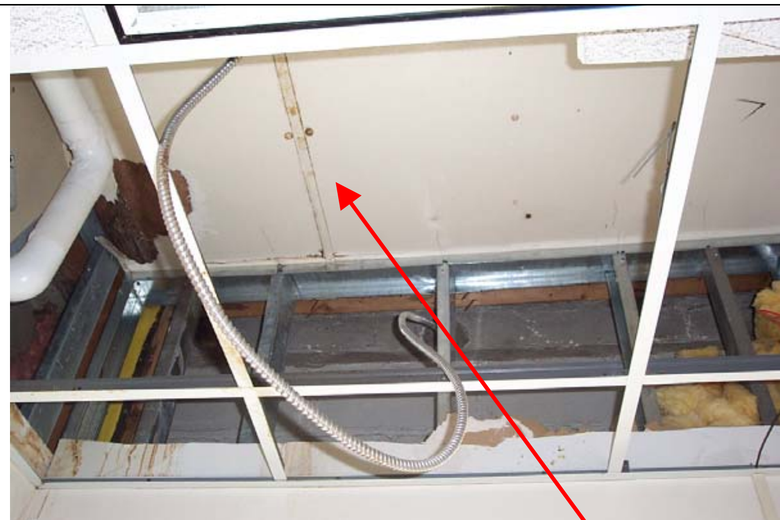

Metal studs on Exterior Walls In Office Area

Underside of Roof (Above Drop Ceiling) has Finished Panels

Figure A18-3. Wall construction

HVAC System

Figure A18-4 shows the locations of the HVAC equipment and supply/return grills in the building. Table A18-1 lists the equipment. Figure A18-4 shows pictures of various HVAC units for the building.

Table A18-1. Summary HVAC Equipment Installed at Site

HVAC Equipment	Area	Manufacturer & Model	Heating Capacity (MBtu/h)	Cooling Capacity (tons)
RTU	Office	Carrier 48HJE007-531	93.1	6
Split Unit	Office	Carrier 38TKB060500		3
Space Heaters	Warehouse/Bay/Shop			-

	
Split Unit Condenser	Roof Top Unit
	
Unit Heater in Shop Area	

Figure A18-4. HVAC Equipment

The office portion of the building uses two separate HVAC units. A Carrier Roof Top Unit (RTU) is used to heat and cool the north end the office space, which includes most of the offices and the conference room. The portion of the office space near the bay areas is heated and cooled with a Carrier Split System AC Unit. This area includes the storage space, a few offices and the hallway areas. The heating set points for both of these systems are 60°F during unoccupied times, and 69°F during occupied times. The cooling set points are 80°F during unoccupied times, and 74°F during occupied times. Occupied time is set for 7:30am to 5:30pm on weekdays.

The bay area, shop, and warehouse are all heated by ceiling mounted space heaters. The space heaters' settings are adjusted by personnel, as needed depending on the current weather conditions. In the winter, the warehouse is very cold during operating hours, reportedly because the building is extremely leaky and the loading bay doors are opened and closed often.

MEASUREMENTS

The test data below was taken on July 8 and July 12, 2005. Blower door testing and pressure mapping for the office was done on July 8. Blower door testing and pressure mapping for the bay, shop, and warehouse were done on July 12. Supply and return airflow testing measurements were taken on July 8. Test Personnel were John Carpenter and Mike Clarkin for both days of testing.

Building Envelope Airtightness

The leakage characteristics of the building enclosure were assessed using fan pressurization methods. The building was too large to test as a whole; therefore, the building was divided into 3 different sections for separate air tightness tests. Figure A18-5 shows the sections or areas pressurized for each test. The first section was comprised of the office area. The second section was comprised of the bay and the metal shop. The third section was the warehouse.

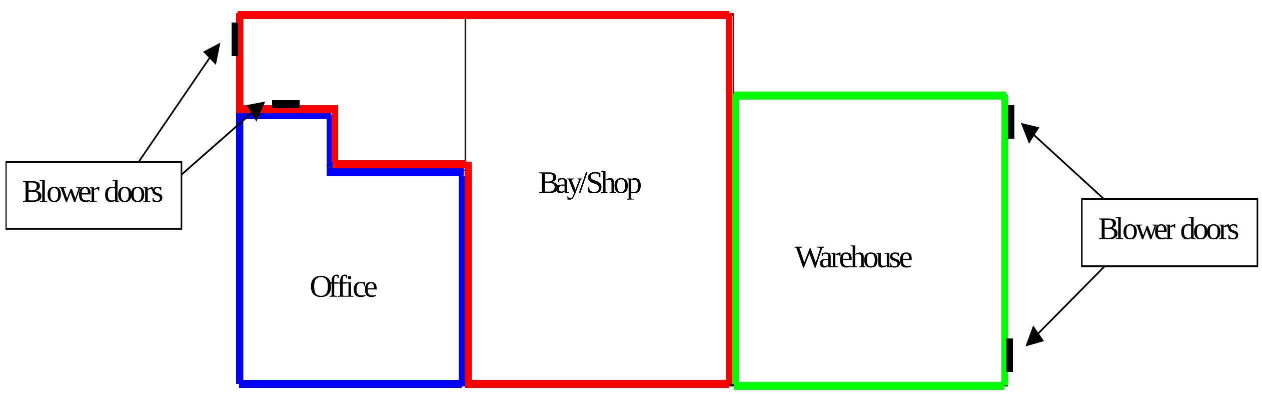

Figure A18-5. Building Sections Used for Blower Door Testing

A single blower door was installed and used for testing the office and the metal shop and bay. The warehouse required two blower doors in order to maintain depressurization. The blower door location used for each section is shown in the Figure above. All exterior doors and windows were closed. The garage doors in the bay area were open to outdoors when the office was tested. To the extent possible, the building sections were tested in the following configuration:

- All interior doors open
- RTU off and ventilation intakes sealed
- All exhaust fans sealed
- Split System AC Unit off and ventilation intakes sealed

In the office, the building pressure was varied from 7 Pa to 33 Pa. Figure A18-6 shows the building leakage variation with building pressure. Table A18-2 shows the results of the blower door tests in the office including model coefficients, effective leakage area (ELA), and air-changes-per-hour (ACH). The ELA is calculated using the Lawrence Berkeley Laboratory method, which calculates the leakage area at 4 Pa. The building has an effective leakage area of approximately 3.38 sq in per 100 sq ft of the total envelope area (including floor area). The building has an ACH at 50 Pascal's (ACH_{50}) of 7.87.

In the metal shop and bay area, the building pressure was varied from 1 Pa to 9 Pa with one blower door. The doors to the office were closed. Figure A18-7 shows the building leakage variation with building pressure. Table A18-3 shows the results of the blower door tests in the shop and bay area including model coefficients, effective leakage area (ELA), and air-changes-per-hour (ACH). The shop and bay has an ELA of approximately 3.48 sq in per 100 sq ft of total envelope area (this area includes the shop-to-office interior walls, which are technically not an exterior wall). The ACH_{50} for the section was calculated to be 3.31.

The warehouse, was large so two blower doors were used to depressurize the space. The building pressure was varied from 6 Pa to 11 Pa. Figure A18-8 shows the building leakage variation with building pressure. Table A18-4 shows the results of the blower door tests in the warehouse including model coefficients, effective leakage area (ELA), and air-changes-per-hour (ACH). The warehouse has an ELA of approximately 6.23 sq in per 100 sq ft of total envelope area. The ACH_{50} for the section was calculated to be 4.8.

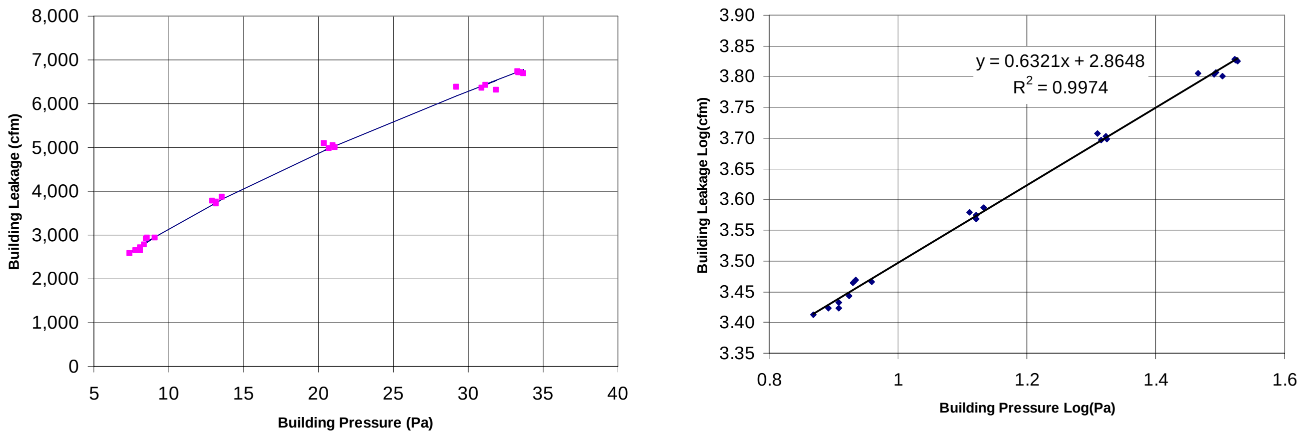

Depressurization Test – Office

Figure A18-6. Variation of Building Leakage with Pressure: cfm = $K(\Delta P)^n$

Table A18-2. Blower Door Test Data, Resulting Best-Fit Model Coefficients, and ELA: Office

Test Results:

Flow Coefficient (K)	732.4	5,297 sq ft, floor area
Exponent (n)	0.632	
Leakage area (LBL ELA @ 4 Pa)	498.5 sq in	3.38 ELA / 100 sq ft
Airflow @ 50 Pa	8,685 cfm	7.87 ACH @ 50

Test Data:

Nominal Building Pressure (Pa)	Nominal Flow (cfm)	Ring
33.5	6,708	none
33.3	6,730	none
33.4	6,719	none
33.7	6,691	none
31.2	6,417	none
30.9	6,355	none
31.9	6,321	none
29.2	6,377	none
20.4	5,097	none
20.7	4,972	none
21.0	5,047	none
21.1	4,999	none
13.6	3,856	none
13.2	3,749	none
13.2	3,702	none
12.9	3,788	none
8.4	2,779	none
8.6	2,942	none
8.5	2,915	none
9.1	2,930	none
7.4	2,588	none
8.1	2,705	none
8.1	2,651	none
7.8	2,650	none

Notes: ELA is leakage area (in square inches) at reference pressure of 4 Pa.
ELA per 100 sq ft is based on total building envelope surface area (ceiling, exterior walls and floor).

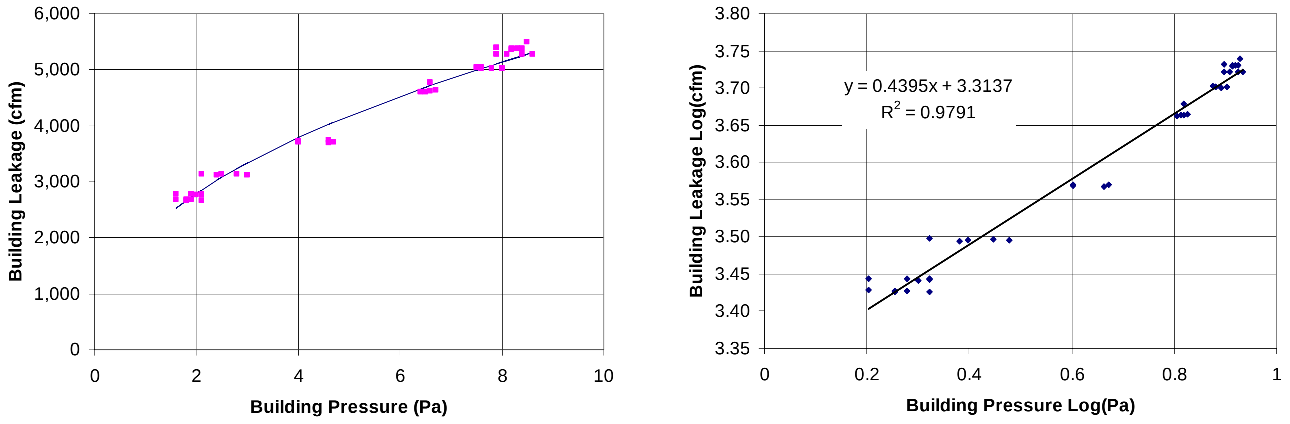

Depressurization Test – Metal Shop and Bay

Figure A18-7. Variation of Building Leakage with Pressure: cfm = $K(\Delta P)^n$

Table A18-3. Blower Door Test Data, Resulting Best-Fit Model Coefficients, and ELA: Shop

Test Results:

Flow Coefficient (K)	2059.4	10,037	sq ft, floor area
Exponent (n)	0.439		
Leakage area (LBL ELA @ 4 Pa)	1073.2 sq in	3.48	ELA / 100 sq ft
Airflow @ 50 Pa	11,493 cfm	3.31	ACH @ 50

Test Data:

Nominal Building Pressure (Pa)	Nominal Flow (cfm)	Ring
8.5	5,488	a
8.4	5,370	a
8.2	5,359	a
8.3	5,384	a
8.2	5,379	a
7.9	5,390	a
7.9	5,272	a
8.1	5,274	a
8.4	5,275	a
8.6	5,269	a
8.0	5,024	a
7.8	5,017	a
7.6	5,029	a
7.5	5,040	a
7.6	5,033	a
6.7	4,627	a
6.6	4,612	a
6.5	4,602	a
6.4	4,598	a
6.6	4,773	a
6.5	4,602	a
4.7	3,712	a
4.6	3,697	a
4.0	3,708	a
4.0	3,717	a
2.8	3,137	a
3.0	3,126	a
2.4	3,124	a
2.5	3,132	a
2.1	3,143	a
2.1	2,778	a
2.1	2,772	a
2.0	2,764	a
1.6	2,774	a
1.9	2,775	a
1.8	2,664	a
2.1	2,666	a
1.9	2,675	a
1.8	2,674	a
1.6	2,682	a

Notes: ELA is leakage area (in square inches) at reference pressure of 4 Pa.
ELA per 100 sq ft is based on total building envelope surface area (ceiling, exterior walls and floor).

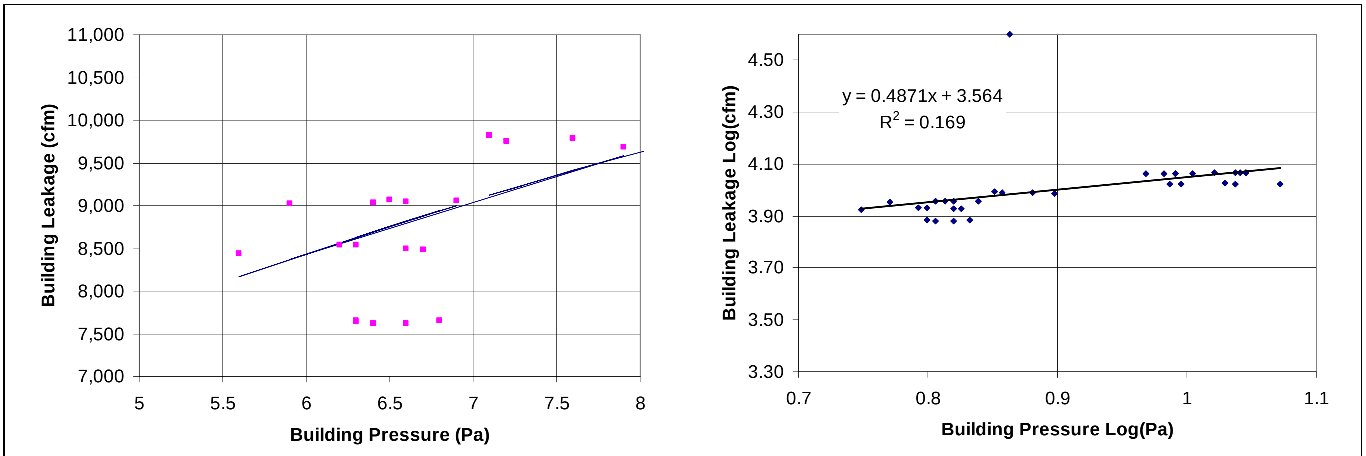

Depressurization Test – Warehouse

Figure A18-8. Variation of Building Leakage with Pressure: cfm = $K(\Delta P)^n$

Table A18-4. Blower Door Test Data, Resulting Best-Fit Model Coefficients, and ELA: Warehouse

Test Results:

Flow Coefficient (K)	3664.6	10,010 sq ft, floor area
Exponent (n)	0.487	
Leakage area (LBL ELA @ 4 Pa)	2040.0 sq in	6.23 ELA / 100 sq ft
Airflow @ 50 Pa	24,640 cfm	4.80 ACH @ 50

Test Data:

Nominal Building Pressure (Pa)	Nominal Flow (cfm)	Ring
10.9	11,711	none
10.5	11,704	none
11.0	11,696	none
11.1	11,712	none
11.1	11,702	none
10.1	11,541	none
9.8	11,614	none
9.3	11,575	none
9.6	11,556	none
9.8	11,553	none
10.7	10,621	none
9.7	10,535	none
9.9	10,571	none
11.8	10,562	none
10.9	10,558	none
7.6	9,786	none
7.2	9,758	none
7.3	39,707	none
7.1	9,824	none
7.9	9,687	none
5.9	9,023	none
6.5	9,065	none
6.6	9,040	none
6.9	9,060	none
6.4	9,038	none
6.2	8,534	none
5.6	8,434	none
6.6	8,492	none
6.3	8,538	none

Notes: ELA is leakage area (in square inches) at reference pressure of 4 Pa.
ELA per 100 sq ft is based on total building envelope surface area (ceiling, exterior walls and floor).

Table A18-5 summarizes the air tightness measurements made on each section of the building. The office was effectively isolated from the metal shop and bay area. The warehouse, which is a totally separate building, had a fair amount of leakage area, though the ACH50 is relatively small do to its high ceiling and large volume. Exponents for the shop and warehouse imply that the holes are relatively large, probably due to exhaust fans or other openings in mechanical equipment.

Table A18-5. Summary of Envelop Tightness Data for Each Building Section

	Flow Coeff. K	Exp. n	ELA (sq n)	ELA / 100 sq ft (sq in/sq ft)	ACH_{50}
Office	732.4	0.632	498	3.38	7.9
Metal Shop and Bay	2,059.4	0.439	1073	3.48	3.3
Warehouse	3,664.6	0.487	2040	6.23	4.8

Pressure Mapping (Blower Door Testing)

Pressure readings in the building were taken using a digital micromanometer (DG 700) with the blower door operating. Pressure measurements were taken between interior rooms with doors closed.

The pressure difference across the building envelope was 33 Pa with the blower door operating. The pressure differences for a number of different locations are shown in Figure A18-9. The pressure difference between the ceiling and the space was measured in a number of locations, and all of these readings were at zero, because the space above the ceiling tiles is used as a return plenum. All interior pressure readings are very low, less than 2 Pa.

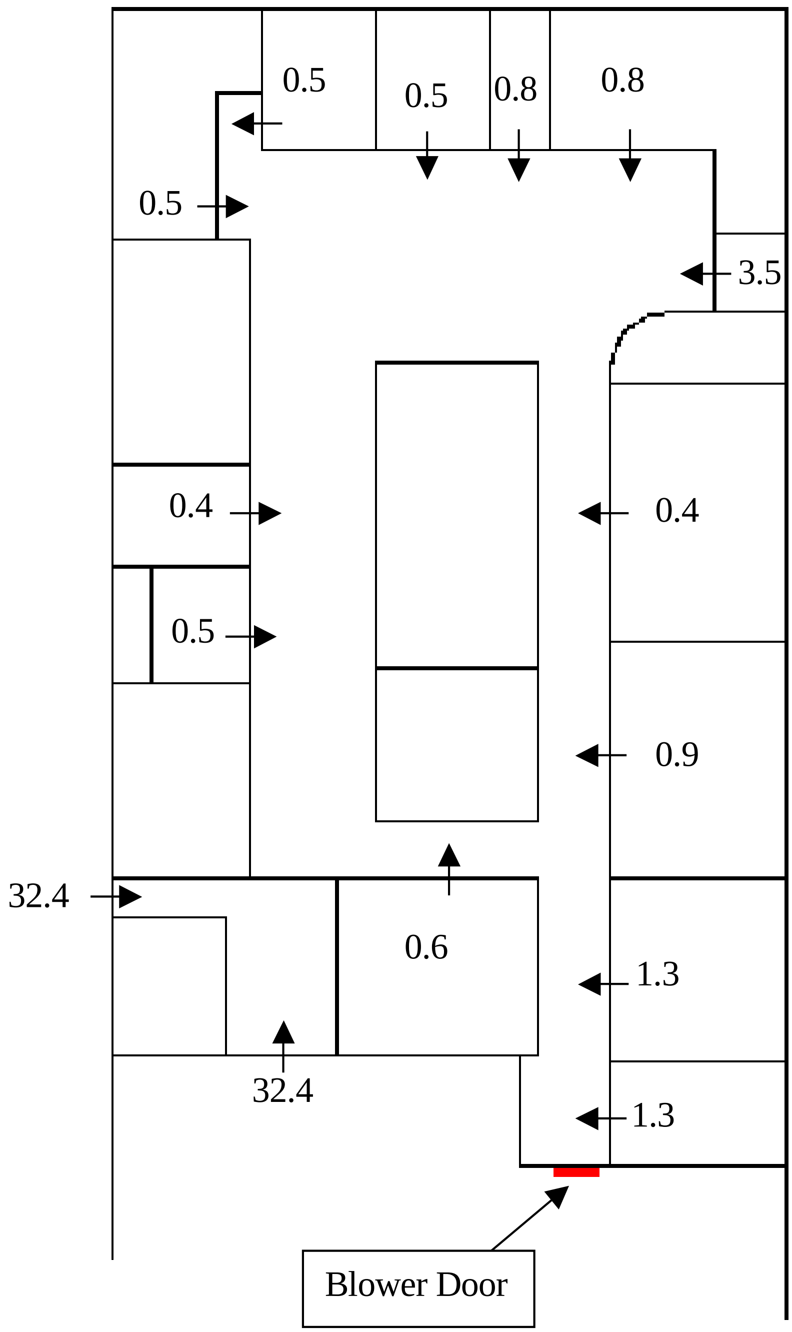

Figure A18-9. Pressure Mapping with Office Area Depressurized to 33 Pa

HVAC Airflow Measurements

The airflow from each supply and exhaust diffuser was measured using a Shortridge flow hood (compensated mode). The return airflow could not be measured because the ceiling plenum is used as a return. Figure A18-10 displays the measured airflow at each diffuser in the office. Total supply flow of the measured ductwork was 3305 cfm. This does not include the supply duct in one of the storage rooms; this duct was in such a place that it could not be measured. The total exhaust flow out of the building was measured to be 288 cfm. The return airflow could not be measured because the ceiling was the return plenum.

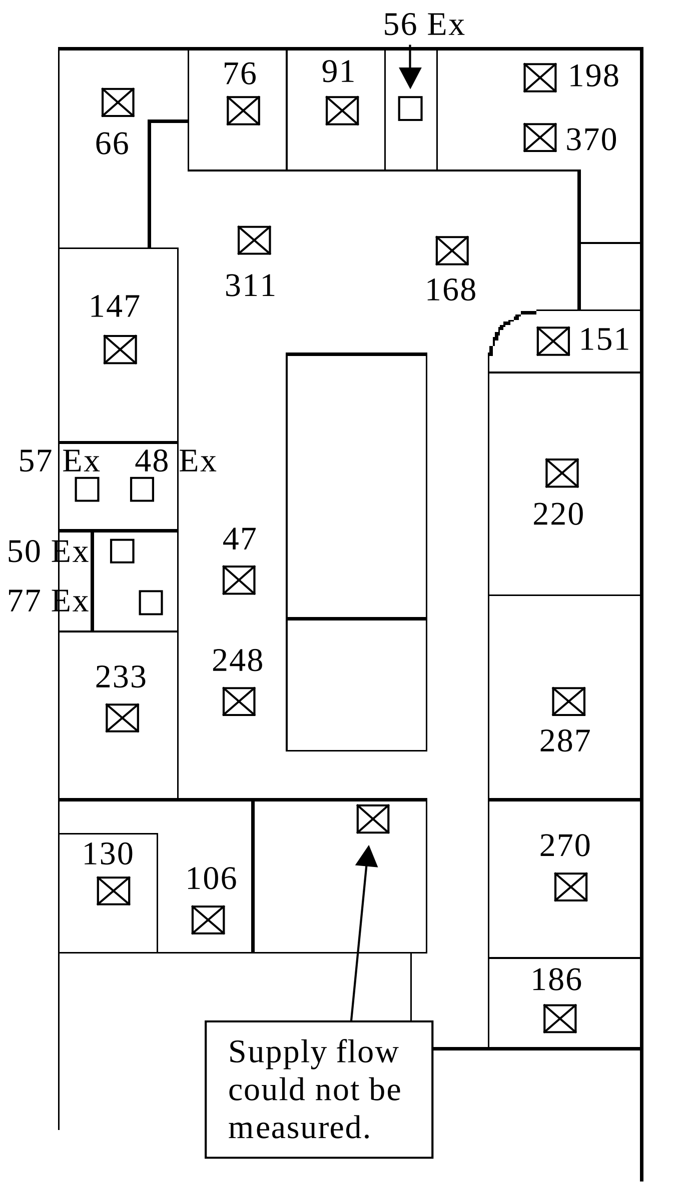

Return Grate Leading into Ceiling Plenum

Figure A18-10. Office Supply and Exhaust Airflow Measurements (cfm)

Pressure Mapping (AHU Fans On)

The air pressure relationships in the building were also determined with the split unit and the roof top unit on. Figure A18-11 shows the pressure differences induced across the doorways with the unit fans on and the doorways closed. Operation of the units created interior pressure differences up to 1.1 Pa. Only the office was pressure mapped because the other areas of the building did not have interior rooms.

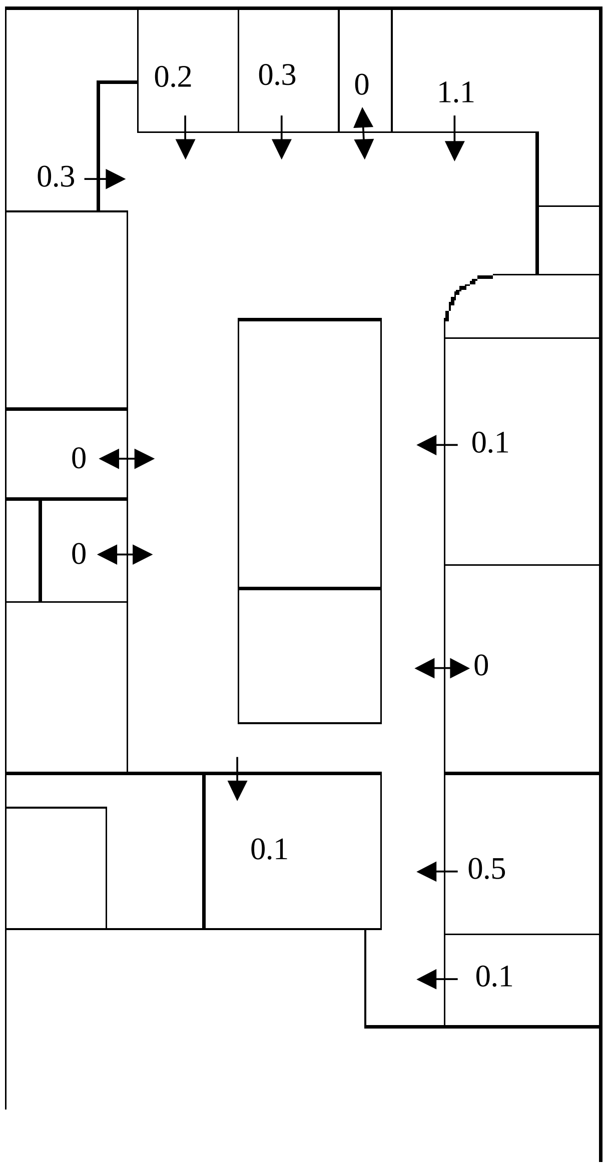

Figure A18-11. First Floor Pressure Differences between Rooms with AHU Fans On

Duct Leakage Measurements

No Duct leakage test was performed at this site because all the duct leakage area is inside the building envelope.

Space Conditions

The data for the space conditions is currently being collected and will be added to the report in a future revision.

Utility Bills

Utility Information was not available.

Field Test Site 19 – Office Building, New Hartford, NY

Main Entrance (North)

Figure A19-1. Photos of Building

CHARACTERISTICS

Building Description

The 14,500 sq-ft facility is a one story office building with a full basement that is located in New Hartford, New York. The first floor (7,250 sq-ft) contains conference rooms, a kitchen, a lobby with an information booth, two Men's bathrooms, two Women's bathrooms, and all the offices. The basement (7,250 sq-ft), which is mostly unused, contained all four packaged HVAC units and the ductwork. The facility was originally built for two tenants, but has been renovated for use by a single tenant. Each half of the building has separate electrical and mechanical systems as well as separate electric and gas meters. Figure A19-1 shows the building's main entrance from the front, which faces to the north. Figure A19-2 shows the building floor plan for the west half of the building, which contains mostly offices and the reception area. Figure A19-3 shows the building floor plan for the east half of the building, which contains mostly conference rooms and the computer area.

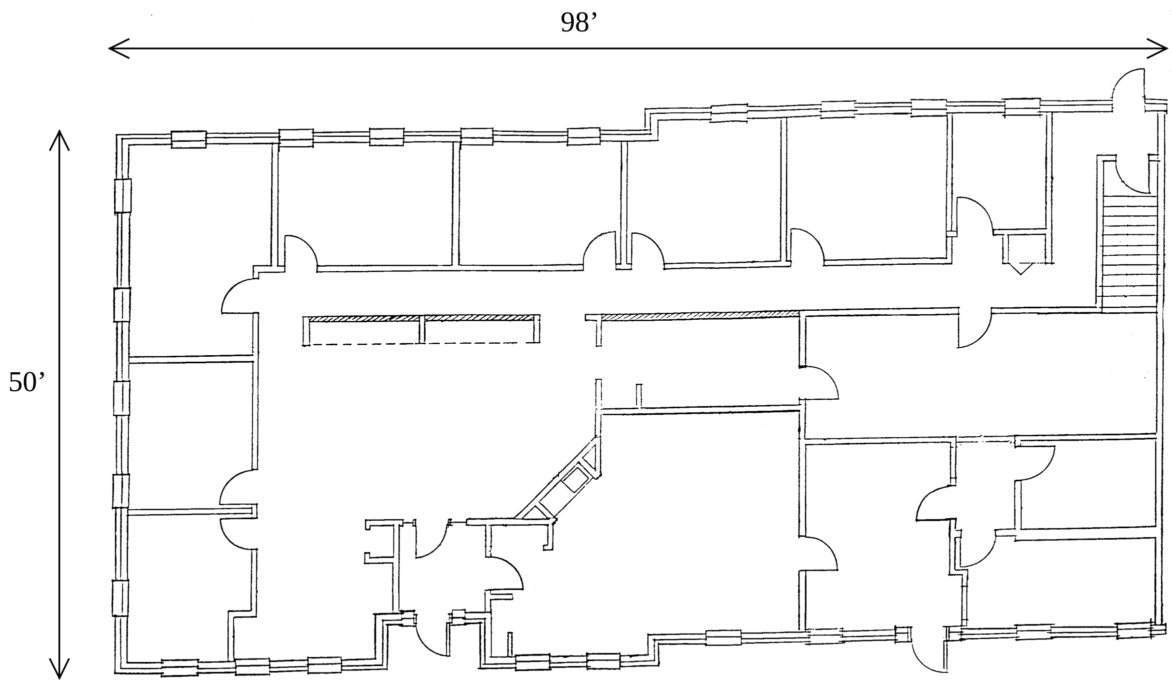

Figure A19-2. Western Half of Building (Office)

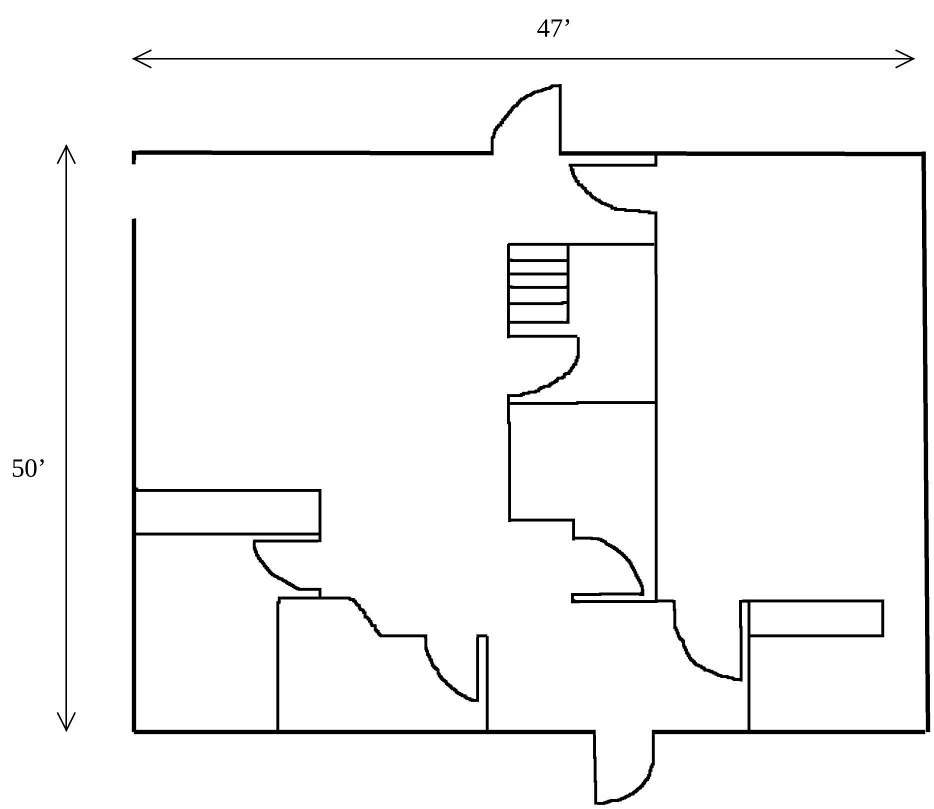

Figure A19-3. Eastern Half of the Building (Conference)

Construction Details

The exterior walls were frame construction with brick veneer. Inside wood frame walls include fiberglass insulation, a plastic vapor barrier, and dry wall. The interior walls are also constructed with a wood frame, insulation, and dry wall. The space has of a drop ceiling with gypsum board a few feet above it and fiberglass batt insulation installed above the gypsum. The attic is vented.

HVAC System

Table A19-1 lists the HVAC equipment. Figure A19-4 shows pictures of various HVAC units for the building.

Table A19-1. Summary HVAC Equipment Installed at Site

HVAC Equipment	Area	Manufacturer & Model	Heating Capacity (MBtu/h)	Cooling Capacity (tons)
Packaged AC / Gas Furnces	1st Floor and Basement	Lennox Conservator III	100 each 400 total	2.5 each 10 total

The HVAC system consisted of four Lennox Conservator III packaged split system air conditioners with gas furnaces. The heating capacity for each unit is 100,000 MBtu/hr for a total of 400,000 MBtu/hr in heating for the building. The cooling capacity is 2.5 tons per unit, which is a total of 10 tons of cooling for the building. The set points for the units are controlled by four thermostats, two in each half of the building. All ductwork is insulated.

There are two fresh air intakes for the units. Each intake serves two units. There is a vent in the exterior wall that leads directly into the basement, which appears to have previously been used for fresh air intake. It is currently a large opening which is a large air leak. This abandoned intake should be sealed in order to conserve heating and cooling energy.

One of the Packaged Units (Unit 2) is leaking condensate onto the floor in the basement and should be serviced in order to fix the problem.

Lennox Furnace and A-Coil Unit

Lennox Condensing Units

Outdoor Air Intake

Abandoned Outdoor Air Intake

Figure A19-4. HVAC Equipment in the Building

MEASUREMENTS

The test data below was taken on August 17, 2005. Blower door testing and pressure mapping was done on August 17. Supply and return airflow testing measurements were taken on August 17. Test Personnel were John Carpenter and Mike Clarkin.

Building Envelope Airtightness

The leakage characteristics of the building enclosure were assessed using fan pressurization methods. A single blower door was installed and used for all tests. All exterior doors were closed (and the windows of the building are not operable). The building was tested in a number of different configurations as listed in the table below. The basement doors separated the first flow from the basement of the building. The four AHUs were on for the first test but off for the last two. The fresh air intakes to the AHUs (including the unused one) were open for the first two tests but sealed for the last four.

Table A19-2. Different Test Configurations fopr Blower Door Testing

	Basement Doors	AHU	Fresh Air Intake
Test 1	Closed	On	Open
Test 2	Open	On	Open
Test 3	Closed	On	Sealed
Test 4	Open	On	Sealed
Test 5	Open	Off	Sealed
Test 6	Closed	Off	Sealed

For all tests, the building pressure was varied from a low of 5 Pa to 27-33 Pa with the interior doors open. Figure A19-5 through Figure A19-10 show the building leakage variation with building pressure and the blower door test statistics, including model coefficients, effective leakage area (ELA), and air-changes-per-hour (ACH). The volume of the building used in the calculations includes the basement (133,198 ft^3) and the envelope surface area includes the top 2.5 ft of the basement wall (17,620 ft^2).

The building has an effective leakage area of approximately 1.2-1.3 sq in per 100 sq ft of the total envelope area (including floor area). The ACH at 50 Pascal's (ACH_{50}) using the volume of both floors is 1.6-1.7. This building was very tight.

Test 1 and 2 are show the impact of having the door between the basement and the first floor open and closed for the case with the AHUs and the fresh air intakes for open. Tests 2 and 3 are a similar set of tests with the fresh air inlet sealed. Tests 6 and 5 repeat the series with the AHU fan off. Table A19-3 summarizes the results for all 6 of tests. The results show that opening and closing the door between the basement and the first floor had very little impact. Sealing the fresh air inlets did have noticeable impact; this change reduced the leakage area by 20-60 sq in. Sealing the fresh air inlets also allow the building to be depressurized by an additional 9 to 10 Pa. Operation of the AHU fans did not have a big impact once the fresh air intakes were sealed.

Table A19-3. Blower Door Test Summary

				Flow Coeff. K	Exp. n	ELA (sq in)	ELA / 100 sq ft (sq in/sq ft)	Flow @ 50 Pa cfm_{50}	ACH_{50}
1	Intake Open	AHU On	Closed	412.6	0.61	271.72	1.54	4,457	2.01
2			Open	336.1	0.68	244.32	1.39	4,800	2.16
3	Intake Closed	AHU ON	Closed	340.2	0.61	224.67	1.28	3,705	1.67
4			Open	336.1	0.61	222.28	1.26	3,676	1.66
6	Intake Closed	AHU OFF	Closed	369.7	0.58	233.82	1.33	3,563	1.61
5			Open	308.0	0.64	211.19	1.20	3,730	1.68

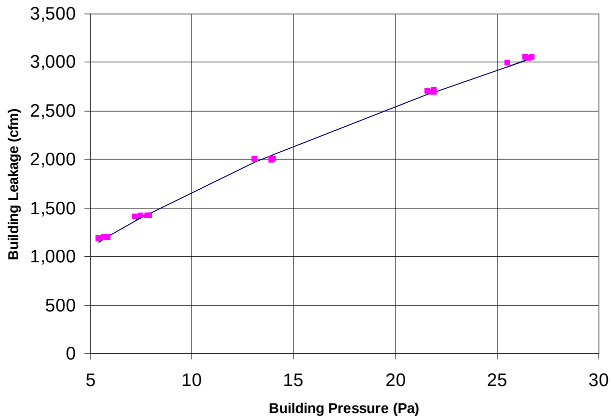

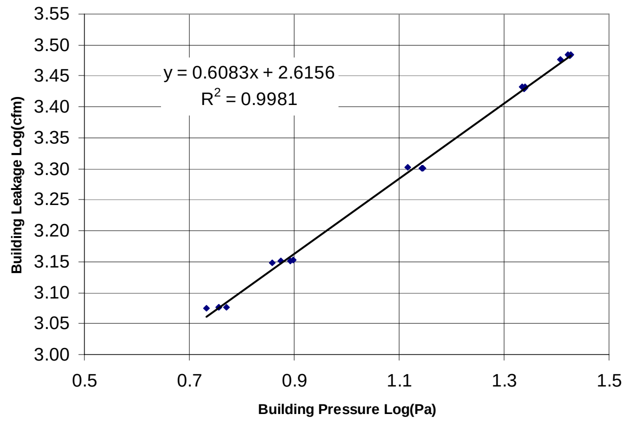

Depressurization Test 1

Test Results:

Flow Coefficient (K)	412.6	
Exponent (n)	0.608	
Leakage area (LBL ELA @ 4 Pa)	271.7 sq in	1.54 ELA / 100 sq ft
Airflow @ 50 Pa	4,457 cfm	2.01 ACH @ 50

Test Data:

Nominal Building Pressure (Pa)	Nominal Flow (cfm)	Ring
25.5	2,997	a
26.4	3,048	a
26.7	3,049	a
26.6	3,039	a
21.9	2,709	a
21.9	2,696	a
21.8	2,691	a
21.6	2,704	a
14.0	2,002	a
13.9	2,003	a
13.9	1,997	a
13.1	2,006	a
7.2	1,405	a
7.5	1,415	a
7.9	1,424	a
7.8	1,419	a
5.7	1,193	a
5.4	1,189	a
5.7	1,193	a
5.9	1,191	a
0.0	-	a
0.0	-	a
0.0	-	a
0.0	-	a
0.0	-	a
0.0	-	a
0.0	-	a
0.0	-	a
0.0	-	a

Notes: ELA is leakage area (in square inches) at reference pressure of 4 Pa.
ELA per 100 sq ft is based on total building envelope surface area (ceiling, exterior walls and floor).

Figure A19-5. Variation of Building Leakage with Pressure and Leakage Statistics – Test 1

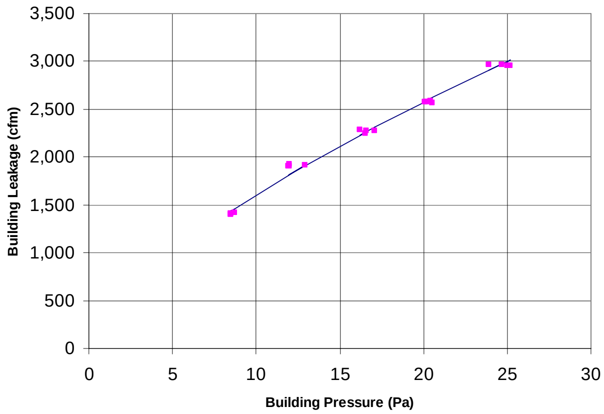

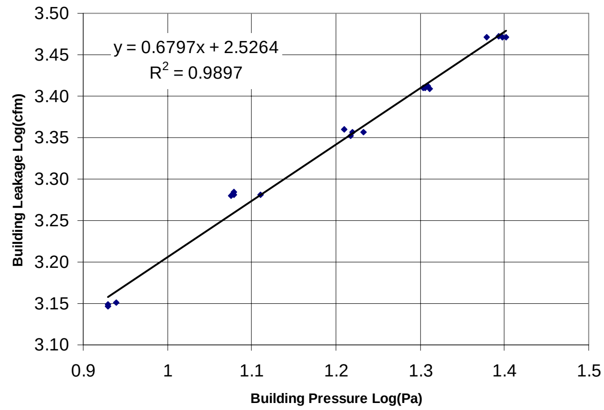

Depressurization Test 2

Test Results:

Flow Coefficient (K)	336.1	
Exponent (n)	0.680	
Leakage area (LBL ELA @ 4 Pa)	244.3 sq in	1.39 ELA / 100 sq ft
Airflow @ 50 Pa	4,800 cfm	2.16 ACH @ 50

Test Data:

Nominal Building Pressure (Pa)	Nominal Flow (cfm)	Ring
23.9	2,961	a
24.7	2,963	a
25.0	2,956	a
25.2	2,958	a
20.1	2,572	a
20.2	2,573	a
20.5	2,563	a
20.4	2,583	a
17.1	2,276	a
16.2	2,289	a
16.6	2,273	a
16.5	2,249	a
12.0	1,927	a
11.9	1,907	a
12.0	1,908	a
12.9	1,911	a
8.7	1,417	a
8.5	1,410	a
8.5	1,403	a
8.5	1,401	a

Notes: ELA is leakage area (in square inches) at reference pressure of 4 Pa.
ELA per 100 sq ft is based on total building envelope surface area (ceiling, exterior walls and floor).

Figure A19-6. Variation of Building Leakage with Pressure and Leakage Statistics – Test 2

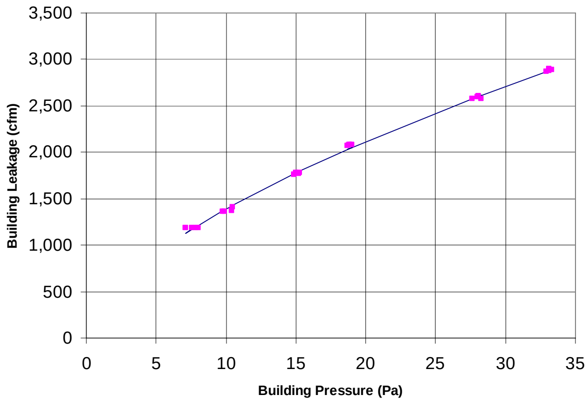

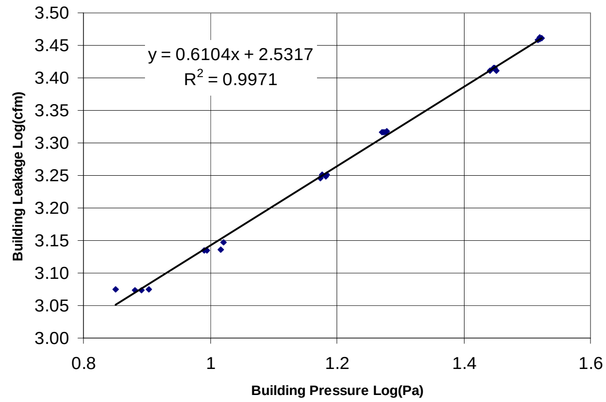

Depressurization Test 3

Test Results:

Flow Coefficient (K)	340.2	
Exponent (n)	0.610	
Leakage area (LBL ELA @ 4 Pa)	224.7 sq in	1.28 ELA / 100 sq ft
Airflow @ 50 Pa	3,705 cfm	1.67 ACH @ 50

Test Data:

Nominal Building Pressure (Pa)	Nominal Flow (cfm)	Ring
32.9	2,870	a
33.3	2,887	a
33.1	2,879	a
33.1	2,898	a
28.0	2,600	a
28.1	2,601	a
28.3	2,576	a
27.6	2,578	a
18.9	2,076	a
18.8	2,076	a
18.7	2,072	a
19.0	2,080	a
15.3	1,783	a
15.0	1,783	a
15.2	1,772	a
14.9	1,759	a
10.5	1,405	a
10.4	1,367	a
9.9	1,364	a
9.8	1,363	a
7.1	1,190	a
7.6	1,186	a
7.8	1,185	a
8.0	1,188	a

Notes: ELA is leakage area (in square inches) at reference pressure of 4 Pa.
ELA per 100 sq ft is based on total building envelope surface area (ceiling, exterior walls and floor).

Figure A19-7. Variation of Building Leakage with Pressure and Leakage Statistics – Test 3

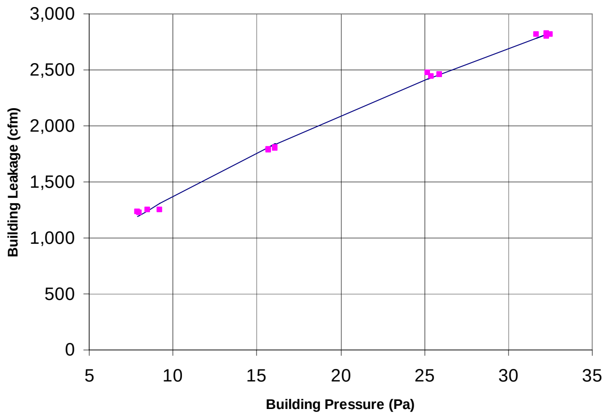

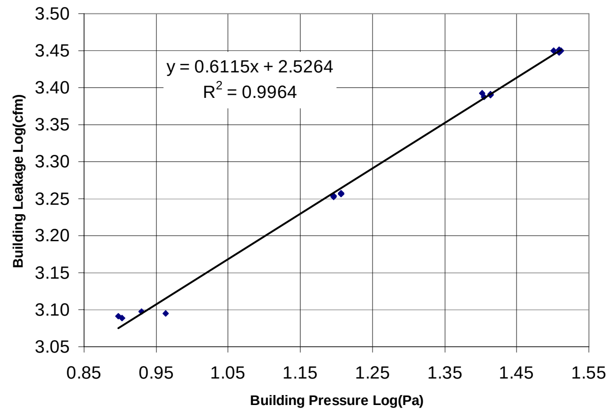

Depressurization Test 4

Test Results:

Flow Coefficient (K)	336.1	
Exponent (n)	0.611	
Leakage area (LBL ELA @ 4 Pa)	222.3 sq in	1.26 ELA / 100 sq ft
Airflow @ 50 Pa	3,676 cfm	1.66 ACH @ 50

Test Data:

Nominal Building Pressure (Pa)	Nominal Flow (cfm)	Ring
31.7	2,818	a
32.3	2,825	a
32.5	2,818	a
32.3	2,799	a
25.9	2,461	a
25.9	2,456	a
25.2	2,472	a
25.4	2,444	a
15.7	1,794	a
16.1	1,811	a
16.1	1,802	a
15.7	1,787	a
9.2	1,246	a
8.5	1,250	a
8.0	1,227	a
7.9	1,234	a

Notes: ELA is leakage area (in square inches) at reference pressure of 4 Pa.
ELA per 100 sq ft is based on total building envelope surface area (ceiling, exterior walls and floor).

Figure A19-8. Variation of Building Leakage with Pressure and Leakage Statistics – Test 4

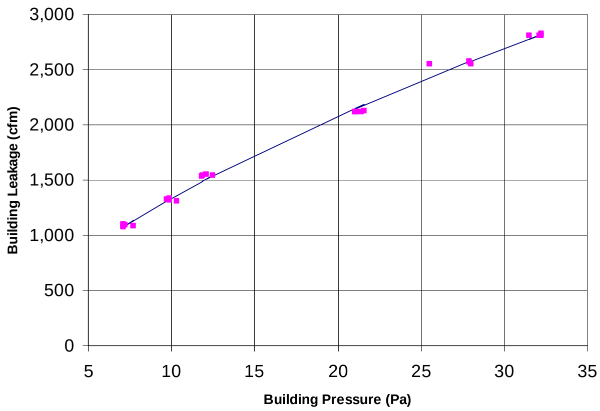

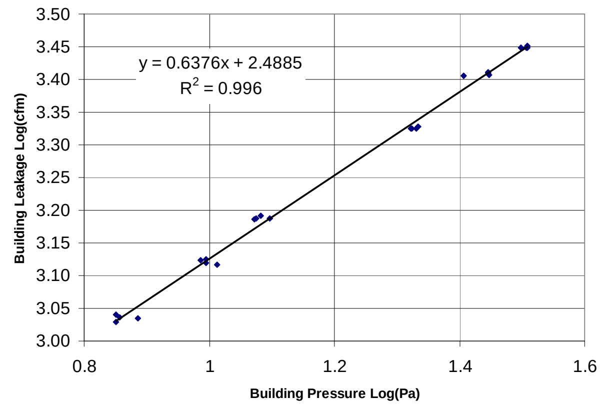

Depressurization Test 5

Test Results:

Flow Coefficient (K)	308.0	
Exponent (n)	0.638	
Leakage area (LBL ELA @ 4 Pa)	211.2 sq in	1.20 ELA / 100 sq ft
Airflow @ 50 Pa	3,730 cfm	1.68 ACH @ 50

Test Data:

Nominal Building Pressure (Pa)	Nominal Flow (cfm)	Ring
32.1	2,808	a
32.2	2,812	a
31.5	2,808	a
32.2	2,823	a
28.0	2,550	a
27.9	2,565	a
27.9	2,575	a
25.5	2,548	a
21.0	2,115	a
21.1	2,116	a
21.6	2,129	a
21.4	2,115	a
12.1	1,554	a
12.5	1,542	a
11.9	1,541	a
11.8	1,533	a
10.3	1,308	a
9.7	1,329	a
9.9	1,333	a
9.9	1,315	a
7.1	1,098	a
7.7	1,083	a
7.1	1,071	a
7.2	1,088	a

Notes: ELA is leakage area (in square inches) at reference pressure of 4 Pa.
ELA per 100 sq ft is based on total building envelope surface area (ceiling, exterior walls and floor).

Figure A19-9. Variation of Building Leakage with Pressure and Leakage Statistics – Test 5

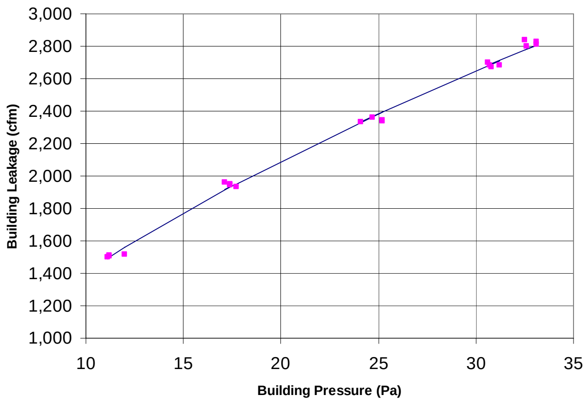

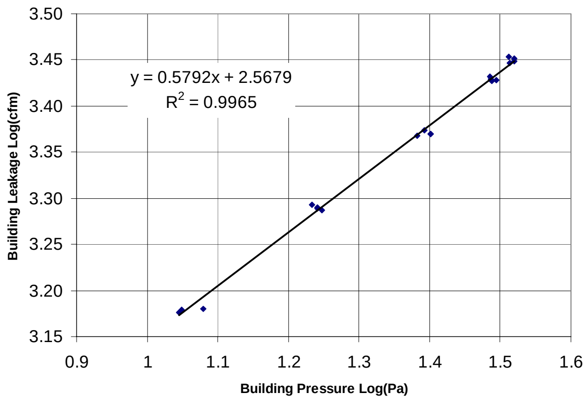

Depressurization Test 6

Test Results:

Flow Coefficient (K)	369.7	
Exponent (n)	0.579	
Leakage area (LBL ELA @ 4 Pa)	233.8 sq in	1.33 ELA / 100 sq ft
Airflow @ 50 Pa	3,563 cfm	1.61 ACH @ 50

Test Data:

Nominal Building Pressure (Pa)	Nominal Flow (cfm)	Ring
32.6	2,799	a
33.1	2,811	a
33.1	2,829	a
32.5	2,839	a
30.7	2,685	a
30.6	2,701	a
30.8	2,674	a
31.2	2,681	a
25.2	2,341	a
24.1	2,334	a
24.7	2,362	a
25.2	2,342	a
17.7	1,936	a
17.4	1,944	a
17.1	1,961	a
17.4	1,949	a
12.0	1,514	a
11.2	1,508	a
11.2	1,511	a
11.1	1,501	a
6.1	1,062	a
5.9	1,089	a
6.0	1,082	a
5.5	1,060	a

Notes: ELA is leakage area (in square inches) at reference pressure of 4 Pa.
ELA per 100 sq ft is based on total building envelope surface area (ceiling, exterior walls and floor).

Figure A19-10. Variation of Building Leakage with Pressure and Leakage Statistics – Test 6

Pressure Mapping (Blower Door Testing)

Pressure readings in the building were taken using a digital micromanometer (DG 700) with the blower door operating. Pressure measurements were taken between interior rooms with doors closed.

For the pressure mapping, the pressure difference across the building envelope was 35 Pa with the blower door operating. The pressure differences for a number of different locations are shown in Figure A19-11 and Figure A19-12. The pressure difference between the ceiling and the space was measured in both halves of the building. In the office area, the pressure difference was 3.6 Pa from ceiling to space. In the conference area, the pressure difference was only 0.3 Pa, with the exception of the pressure difference to the basement.

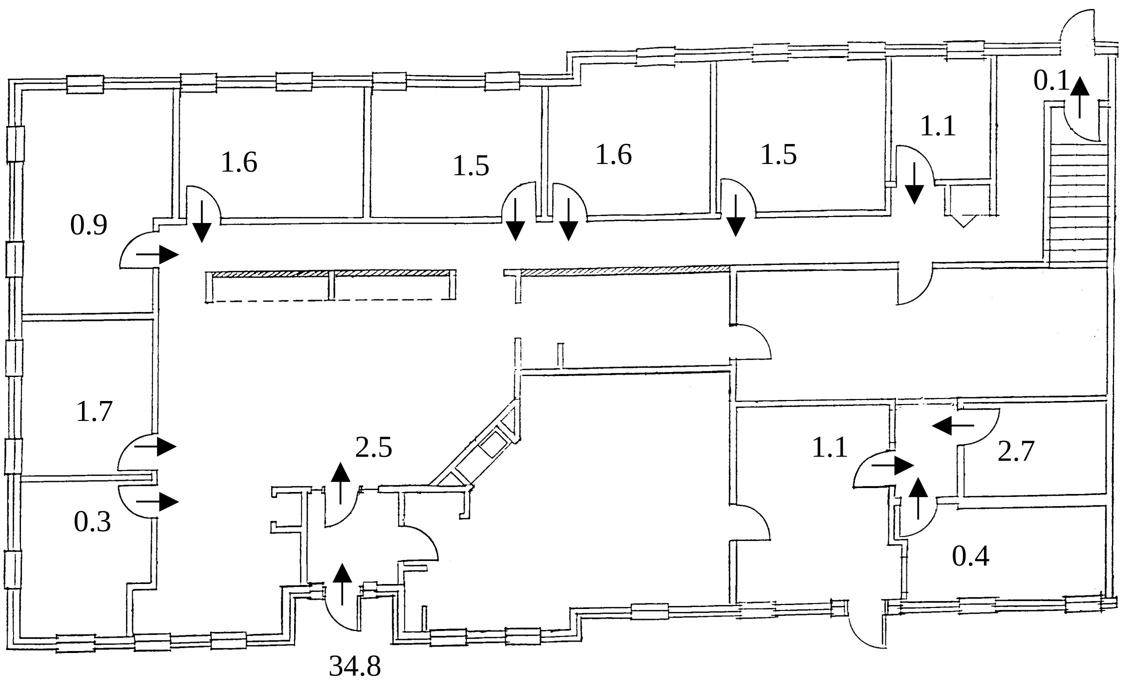

Figure A19-11. Pressure Mapping with Building Depressurized to 34 Pa

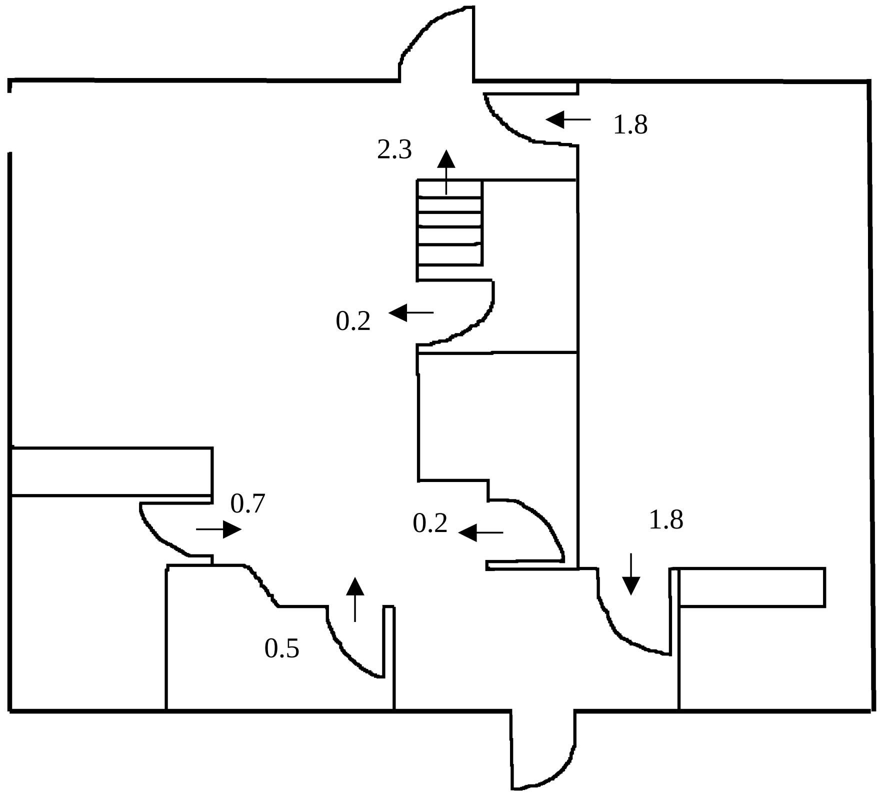

Figure A19-12. Pressure Mapping with Building Depressurized to 34 Pa

HVAC Airflow Measurements

The airflow from each supply diffuser was measured using a Shortridge flow hood (compensated mode). The total supply airflow is approximately 4,503 cfm, while the total return air is only 2,857 cfm. Figure A19-13 and Figure A19-14 display the measured airflow at each diffuser, return, and exhaust on the first floor. The basement supply and return ducts were not measured.

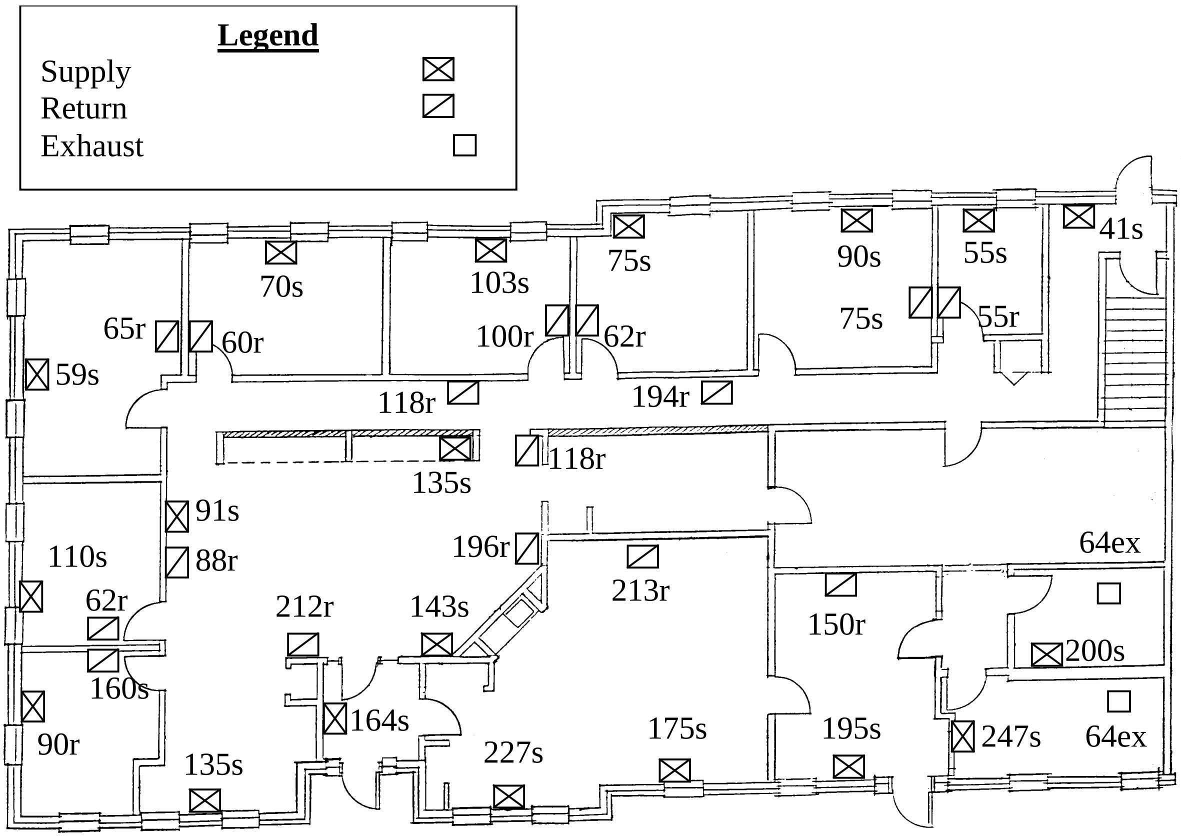

Figure A19-13. Supply and Return Airflow Measurements (cfm)

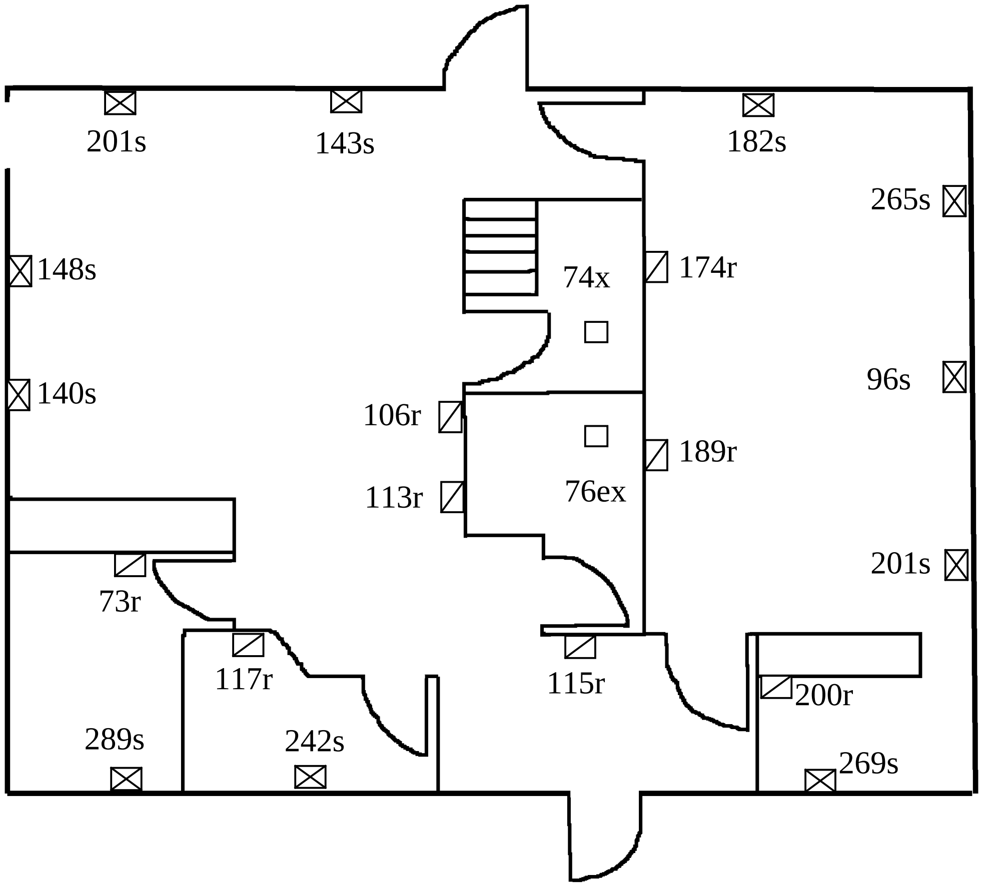

Figure A19-14. Supply and Return Airflow Measurements (cfm)

Table A19-4 is a summary of the supply, return and ventilation airflows for the HVAC units in the building. There is generally more supply airflow than return in most of the systems. This generally indicates return leaks, which do not cause energy concerns since all the ducts are in the space but may cause problems with comfort.

Table A19-4. Supply, Return and Ventilation Airflow Measurements

	Unit 1 - Airflow (cfm)	
	Supply	Return
	59	65
	70	60
	103	100
	75	62
	90	75
	55	55
	41	194
Total	**493**	**611**

	Unit 2 - Airflow (cfm)	
	Supply	Return
	160	90
	110	62
	135	118
	164	212
	143	196
	135	118
	227	213
	175	150
	195	-
	247	-
	200	-
Total	**1891**	**1159**

	Unit 3 - Airflow (cfm)	
	Supply	Return
	289	73
	242	117
	140	115
	148	113
	201	106
	143	-
Total	**1163**	**524**

	Unit 4 - Airflow (cfm)	
	Supply	Return
	269	189
	144	174
	96	200
	265	-
	182	-
Total	**956**	**563**

Exhaust Airflow (cfm)	
Bathroom	Airflow
Men's 1	64
Women's 1	64
Men's 2	74
Women's 2	76
Total	**278**

	Total Airflow (cfm)	
Unit #	Supply	Return
1	493	611
2	1891	1159
3	1163	524
4	956	563
Total	**4503**	**2857**

Three of the four units had good airflow for the cooling that they supply. In general, there should be about 400 cfm of airflow for every ton of cooling capacity to prevent condensing in the ductwork. The only unit, which did not come close to this amount, was unit 1. However, it is possible that the ductwork for Unit 2 was mislabeled and some of that supply vents should be for unit 1. Table A19-5 shows the ranges in which the units ran in cfm/ton.

Table A19-5. Normalized Air Flow Measurements

	Supply (tons)	Supply (cfm)	Supply (cfm/ton)
Unit 1	2.5	493	197.2
Unit 2	2.5	1891	756.4
Unit 3	2.5	1163	465.2
Unit 4	2.5	956	382.4

Pressure Mapping (AHU Fans On)

The air pressure relationships in the building were also determined with the air-handling units on. Figure A19-15 shows the pressure differences induced across the doorways with the AHUs on and the doorways closed. Operation of the AHUs created mostly small pressure differences of less than 1 Pa. The building, with the air handlers running, was not pressurize or depressurized with respect to outdoors. The pressure differences observed were 0.1 Pa or less, which were likely caused by fluctuations of the outside wind conditions.

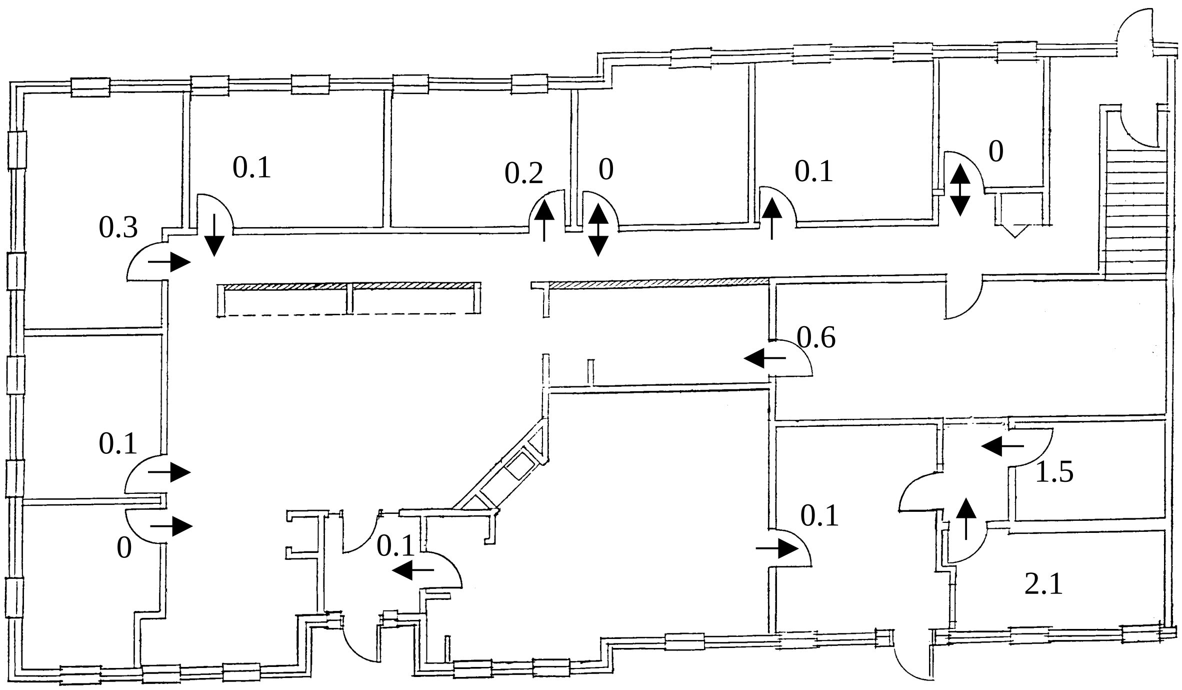

Figure A19-15. Pressure Differences between Rooms with AHU Fans On

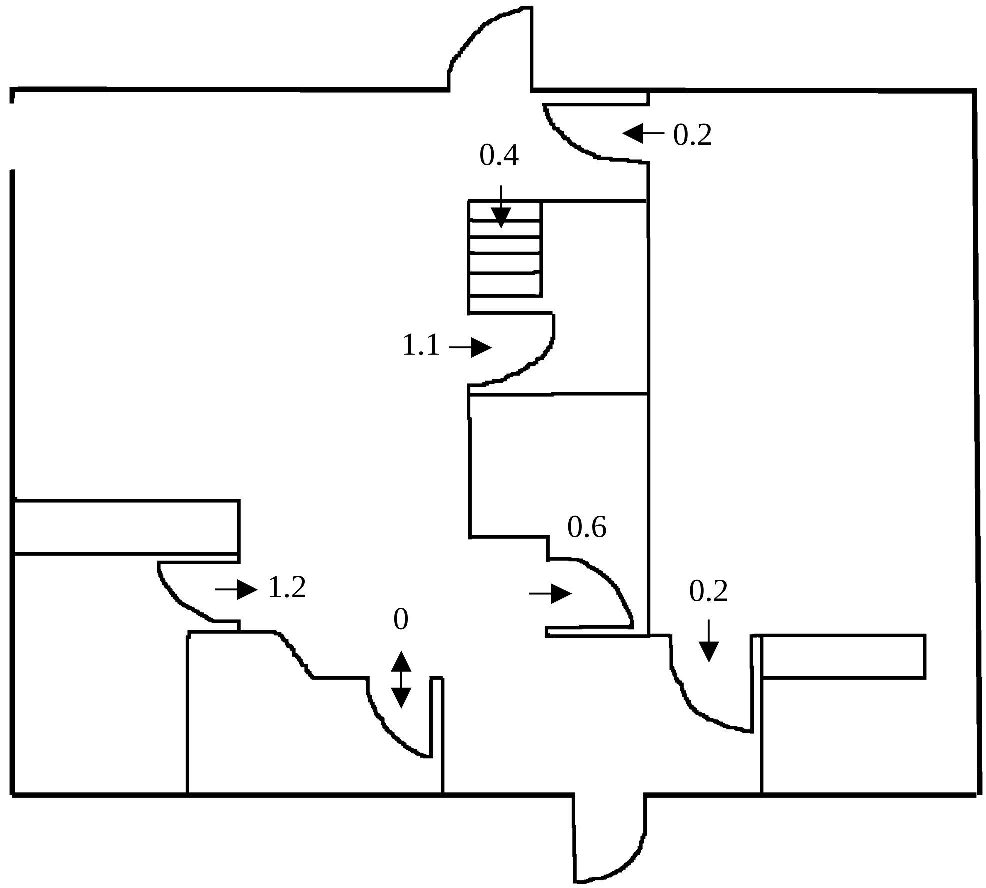

Figure A19-16. Pressure Differences between Rooms with AHU Fans On

Duct Leakage Measurements

No Duct leakage test was performed at this site because all the duct leakage area is inside the building envelope.

Space Conditions

The data for the space conditions was not collected.

Utility Bills

The NYSUT building utilizes natural gas for heating purposes. Cooling for the building is done with electrically powered condensers. The tables and graphs below show the gas and electric use trends for the facility. The building's utility bills are individually calculated for the two separate halves. Gas and electric use are evaluated for each building in the pages that follow and summarized in Table A19-6 below.

Table A19-6. Summary of Gas and Electric Use Indexes

	Gas Use (therms)	Electric Use (kWh)
Office	1,339	16,027
Conference	766	8,641
Total	2,105	24,668

	(therms/ft^2-y)	(kWh/ft^2-y)
Index	0.290	3.4

Notes: Floor area is 7,250 sq ft (first floor only)

Table A19-7. Summary of Electric Bills – Office Side

	NYSUT - Office - Electric Utility Data				
	Days in Month	Energy (kWh)	Demand (kW)	Elec. Use per Sq-Ft (kWh/sq ft)	Cost ($)
8/20/04	29	1,291	13	0.13	$289.21
9/20/04	31	1,585	14.2	0.16	$333.70
10/19/04	29	1,491	10.2	0.15	$290.80
11/17/04	29	1,358	6.4	0.14	$246.71
12/20/04	33	1,539	6.4	0.16	$255.99
1/21/05	32	1,371	6.7	0.14	$243.30
2/18/05	28	1,413	0	0.14	$222.00
3/22/05	32	1,469	0	0.15	$231.99
4/19/05	28	1,376	0	0.14	$206.04
5/18/05	29	1,317	0	0.13	$197.31
6/13/05	26	0	0	0.00	$20.98
7/15/05	30	1,817	0	0.19	$268.17
Most recent 12 Months	***356***	***16,027***	***14.2***	**1.64**	**$2,806.20**
Annualized	***365***	***16,423***	***14.2***	**1.68**	**$2,877.14**

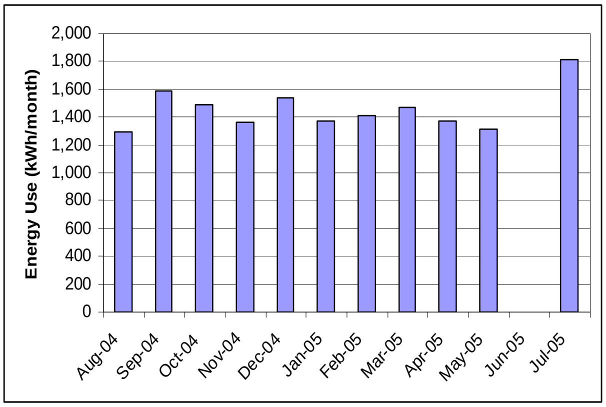

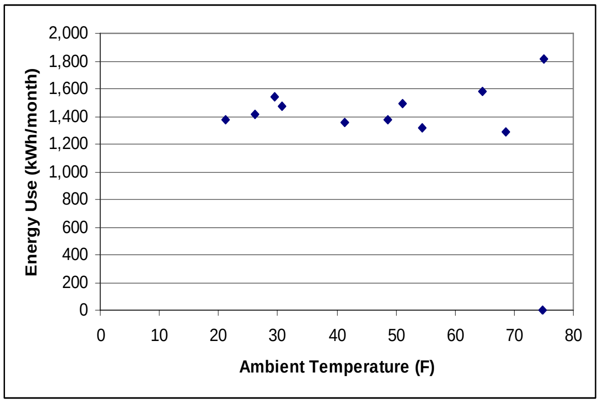

Figure A19-17. Monthly Electricity Use Trends – Office

Table A19-8. Summary of Electric Bills – Conference

	NYSUT - Conference - Electric Utility Data				
	Days in Month	Energy (kWh)	Demand (kW)	Elec. Use per Sq-Ft (kWh/sq ft)	Cost ($)
8/20/04	29	726	0	0.15	$118.25
9/20/04	31	731	0	0.16	$122.50
10/19/04	29	688	0	0.15	$117.31
11/17/04	29	752	0	0.16	$127.00
12/20/04	33	802	0	0.17	$130.11
1/21/05	32	763	0	0.16	$124.70
2/18/05	28	686	0	0.15	$118.40
3/22/05	32	669	0	0.14	$117.08
4/20/05	29	510	0	0.11	$89.54
5/18/05	28	694	0	0.15	$113.91
6/14/05	27	430	0	0.09	$78.52
7/15/05	31	1,190	0	0.25	$182.93
Most recent 12 Months	***358***	***8,641***	***0.0***	**1.84**	**$1,440.25**
Annualized	***365***	***8,811***	***0.0***	**1.87**	**$1,468.41**

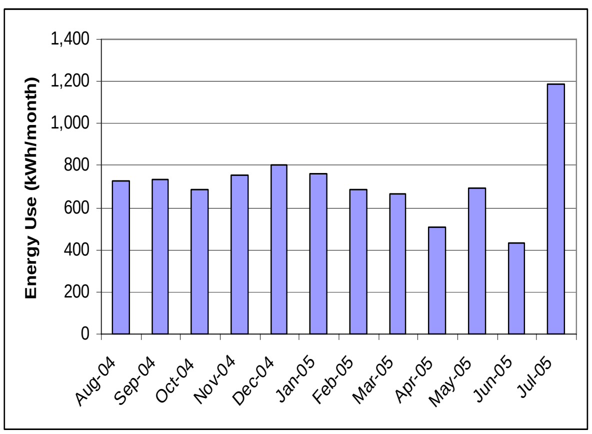

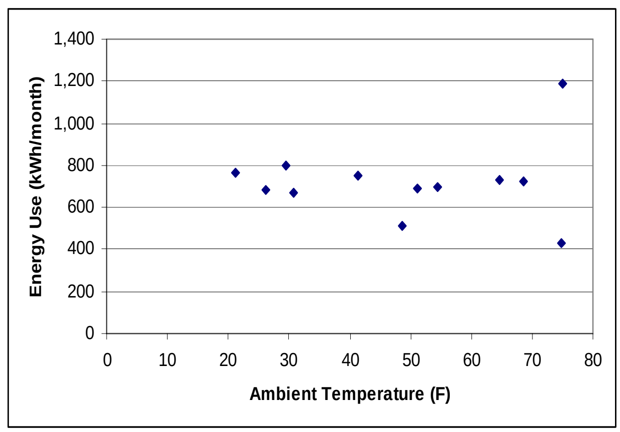

Figure A19-18. Monthly Electricity Use Trends – Conference

Table A19-9. Summary of Gas Bills – Office

	NYSUT - Office - Gas Utility Data			
	Days in Month	Gas Use (therms)	Gas Use per Sq-Ft (therm/sq ft)	Cost ($)
8/20/2004	30	8.0	0.0008	$29.53
9/20/2004	31	9.0	0.0009	$29.90
10/19/2004	29	25.0	0.0026	$45.71
11/17/2004	29	124.0	0.0127	$162.69
12/20/2004	31	205.0	0.0209	$278.80
1/21/2005	33	280.0	0.0286	$427.93
2/18/2005	28	236.0	0.0241	$296.50
3/22/2005	30	267.0	0.0272	$328.58
4/19/2005	32	113.0	0.0115	$160.32
5/18/2005	29	50.0	0.0051	$83.30
6/13/2005	26	14.0	0.0014	$36.82
7/15/2005	30	8.0	0.0008	$29.39
Most recent 12 Months	***358***	***1,339***	**0.1366**	**$1,909.47**
Annualized	***365***	***1,365***	**0.1393**	**$1,946.80**

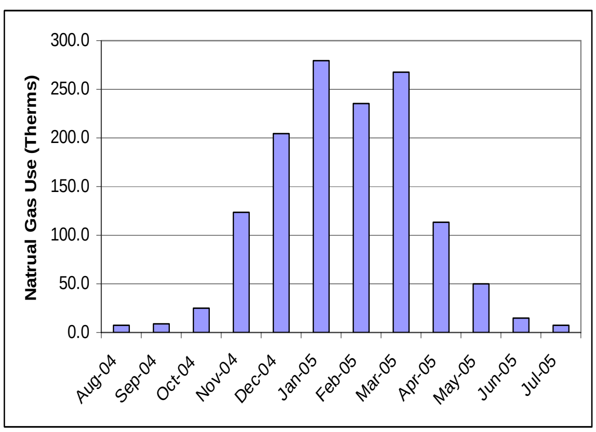

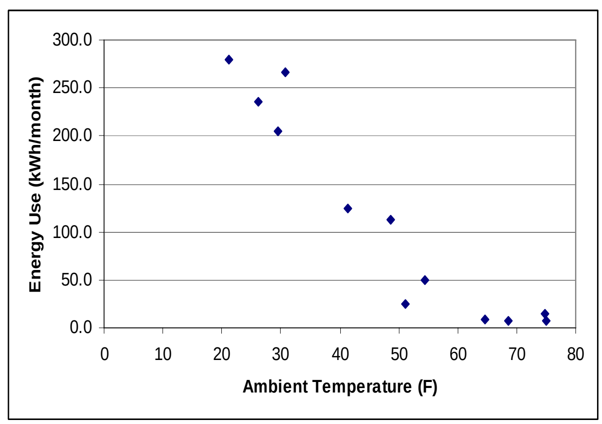

Figure A19-19. Monthly Gas Use Trends – Office

Table A19-10. Summary of Gas Bills – Conference

	NYSUT - Conference - Gas Utility Data			
	Days in Month	Gas Use (therms)	Gas Use per Sq-Ft (therm/sq ft)	Cost ($)
8/20/2004	29	0.0	0.0000	$21.05
9/20/2004	31	0.0	0.0000	$21.05
10/19/2004	31	9.0	0.0019	$29.34
11/17/2004	29	68.0	0.0145	$98.00
12/20/2004	31	100.0	0.0213	$146.32
1/21/2005	33	172.0	0.0366	$226.50
2/18/2005	28	131.0	0.0279	$173.50
3/22/2005	30	159.0	0.0338	$203.90
4/20/2005	32	66.0	0.0140	$102.11
5/18/2005	29	46.0	0.0098	$78.27
6/14/2005	26	15.0	0.0032	$38.00
7/15/2005	30	0.0	0.0000	$21.19
Most recent 12 Months	***359***	***766***	**0.1630**	**$1,159.23**
Annualized	***365***	***789***	**0.1679**	**$1,178.60**

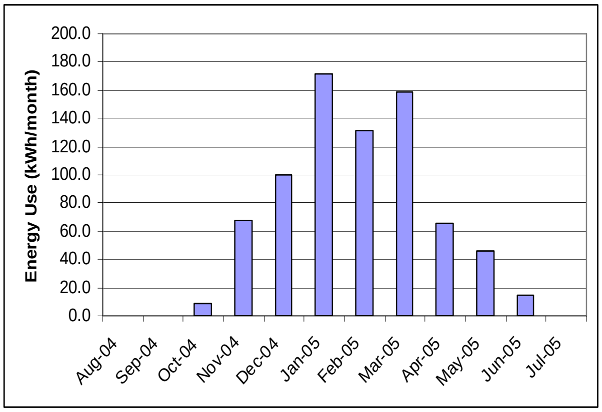

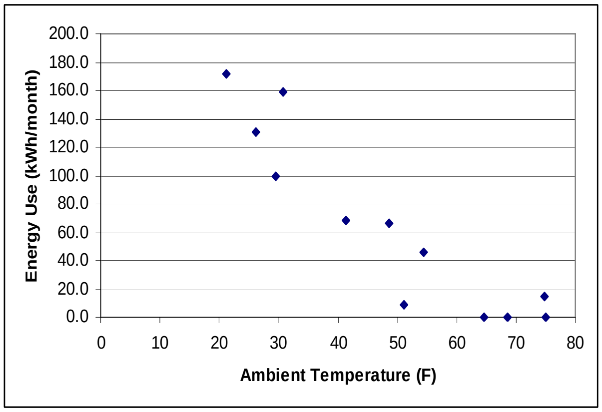

Figure A19-20. Monthly Gas Use Trends – Conference

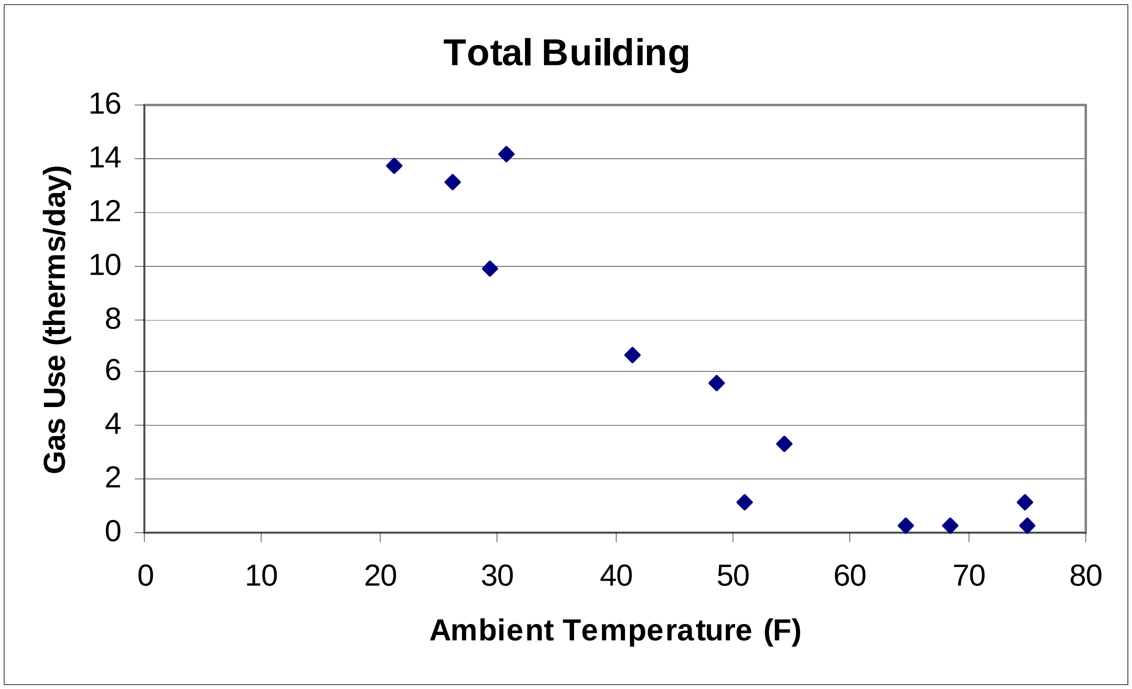

Figure A19-21. Gas Use Load Line, Both Meters Combined

The heat load line implies that the peak gas use at 0ºF is 22-24 therms per day or 90-100 MBtu/h. This implies that one of the 100 MBtu/h furnaces would be sufficient to heat the building under most conditions.

Summary and Recommendations

Electric/Gas Meters. The electric and gas meters for the two halves of the building are currently split because the building was originally built for the use of two tenants. The building is now only used by a single tenant, and will be like that for the foreseeable future. These meters cost money just for them to be in use.

Recommendation: Since only one meter is necessary, the amount paid in monthly fees for having the second meter can be eliminated if all the electrical lines and gas lines are run through a single meter.

Abandoned Outdoor Air. An abandoned outdoor air vent leads from the basement to the south side of the building. It is currently a large leak in the building, which causes hot air to leak into the building in the summer and cold air to leak in during the winter.

Recommendation. The abandoned vent should be sealed and insulated.

Condensate Leakage, Unit 2. The packed air handler unit 2 is leaking condensate onto the basement floor. This leak is likely caused by the drain being plugged or a leak in the piping to the condenser.

Recommendation. The unit likely just needs routine maintenance, and a repair service should be called in to look at the unit.

Field Test Site 20 – Cinemark Theaters, Rochester, NY

Figure A20-1. Photo of Main Entrance

CHARACTERISTICS

Building Description

The 96,000 sq-ft facility, built in 1996, is a large movie theater complex containing 16 standard theaters, an IMAX theater, a projections booth area, concession stands, four ticket booths, an arcade room, restrooms, and offices. The building has two floors. The first floor contains all of the theaters, restroom facilities, concession stands, ticket booths, and a gaming room. The second floor contains the offices, the projection booths, and secondary entrances and exits to the theaters. Figure A20-1 shows the building main entrance, which faces the parking lot to the north. Figure A20-2 shows the building floor plan.

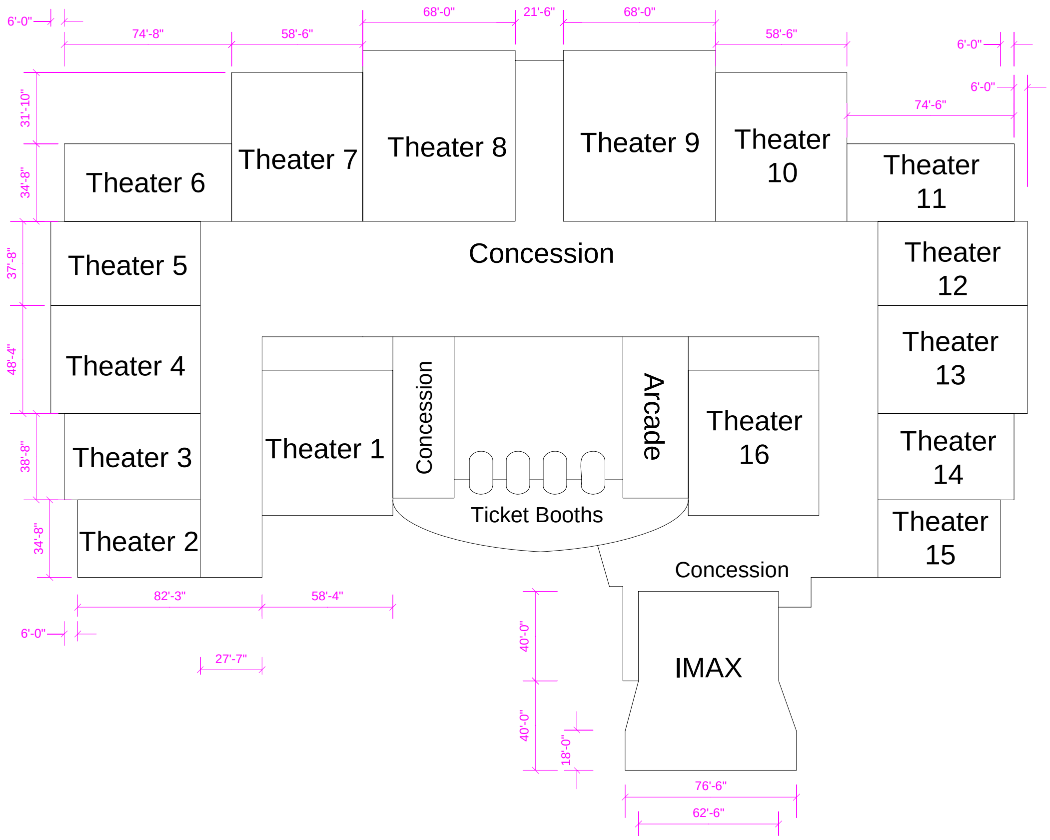

Figure A20-2. Floor Plan of Building

Construction Details

The walls are constructed with hollow core concrete blocks. Inside the bricks are 6" MTL Stud walls with batt-insulation and EIFS on board insulation EPDM 5/8". The roof is constructed of three-inch nominal ridged insulating board with EPDM flashing.

HVAC System

Table A20-1. Summary HVAC Equipment Installed at Site

HVAC Equipment	Manufacturer	Model	Heating Capacity (MBtu/h)	Cooling Capacity (tons)
AC-29, 25, 28	Trane	YCD075C4LABE	120	7½
AC-1, 8A, 8B, 9A, 9B, 13, 16, 17, 18, 19, 20, 23, 24, 26, 31	Trane	YCD241B4LODD	250	20
AC-2, 5, 12, 27, 30	Trane	YCD121B4LODD	150	10
AC-6, 11, 21, 22	Trane	YCD103B4LODD	150	8½
AC-3, 14	Trane	YCD151B4LODD	150	12½
AC-7, 10	Trane	YCD300B4LODD	250	25
AC-4	Trane	YCD181B4LODD	250	15
RTU-1	Trane	YCD241C4LGAB	250	20
RTU-2	Trane	YCD151C4LGAA	150	12½
RTU-3	Trane	YCD151C4LAAB	250	12½

Table A20-1 lists the equipment along with the heating and cooling capacity of each unit. The heating and cooling for the building is provided by 35 Trane Roof-Top Units (RTUs). These units range in heating capacity from 120 MBtu/h to 250 MBtu/h, and in cooling capacity from 7½ tons to 25 tons. The RTUs are computer controlled and the heating and cooling set points are set by the corporate office in Texas. All 35 units use gas for heating and electricity for cooling. The total heating capacity of the building is 7,160 MBtu/h. The total cooling capacity is 541.5 tons.

MEASUREMENTS

The test data below was taken on September 14 and 15, 2005. Test Personnel were John Carpenter and Mike Clarkin for both days of testing.

Building Envelope Airtightness

The leakage characteristics of the building enclosure were assessed using fan pressurization methods. Two blower doors were used for the test. We also ran the exhaust fan which added another 10,115 cfm of air flow for the depressurization test. All exterior doors and windows were closed. All interior doors were open. All exhaust and ventilation systems were left in their normal operating configuration. The building pressure was varied from 13 Pa to 20 Pa using two blower doors and the exhaust fans. Figure A20-3 shows the building leakage variation with building pressure. The linear regression predictred an exponent of 0.32, which not physically possible. Therefore we for the best fit to the data using a forced exponent of 0.5 (the dotted line in the figure). Table A20-2 shows the results of the blower door tests including model coefficients, effective leakage area (ELA), and air-changes-per-hour (ACH). The building has an effective leakage area of approximately 1.05 sq in per 100 sq ft of the total envelope area (including floor area). The building has an ACH_{50} of 0.82.

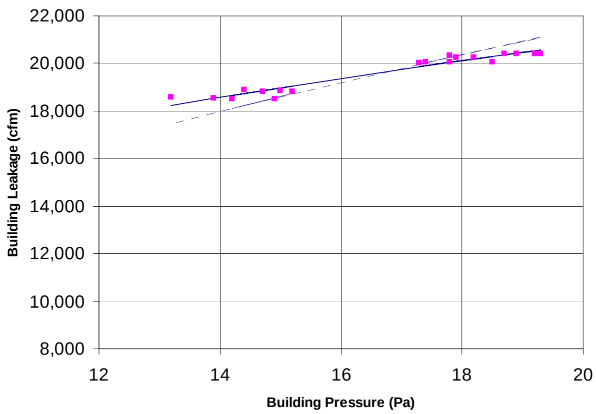

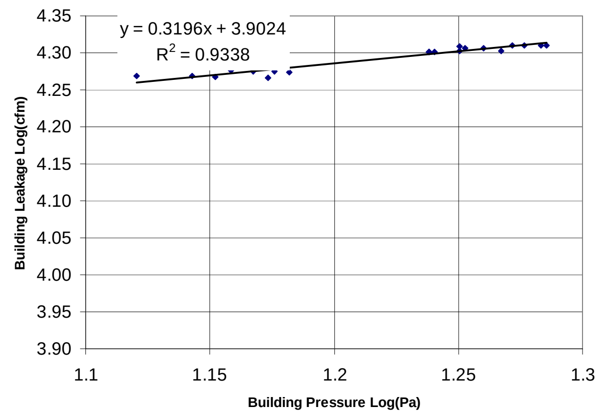

Depressurization Test

Figure A20-3. Variation of Building Leakage with Pressure: cfm = K(ΔP)^n

Table A20-2. Blower Door Test Data, Resulting Best-Fit Model Coefficients, and ELA

Test Results:

Flow Coefficient (K)	4802.0	94,550 sq ft, floor area
Exponent (n)	0.500	
Leakage area (LBL ELA @ 4 Pa)	2721.3 sq in	1.05 ELA / 100 sq ft
Airflow @ 50 Pa	33,955 cfm	0.82 ACH @ 50

Test Data:

Nominal Building Pressure (Pa)	Nominal Flow (cfm)	Ring
19.2	20,404	none
18.7	20,414	none
18.9	20,419	none
19.3	20,421	none
17.8	20,333	none
17.9	20,268	none
18.2	20,261	none
18.5	20,045	none
17.3	20,035	none
17.4	20,038	none
17.3	20,010	none
17.8	20,065	none
14.4	18,905	none
14.7	18,821	none
15.0	18,857	none
15.2	18,795	none
14.2	18,491	none
14.9	18,483	none
13.9	18,547	none
13.2	18,573	none
0.0	-	none
0.0	-	none
0.0	-	none
0.0	-	none
0.0	-	none
0.0	-	none
0.0	-	none
0.0	-	none
0.0	-	none

Nominal Airflow includes 10,115 cfm of exhaust flow (the exhaust flow is assumed to decrease by 2% for each 10 Pa of depressurization based typical fan curves)

Notes: ELA is leakage area (in square inches) at reference pressure of 4 Pa.
ELA per 100 sq ft is based on total building envelope surface area (ceiling, exterior walls and floor).

Pressure Mapping (Blower Door Testing)

Pressure readings in the building were taken using a digital micromanometer (DG 700) with the blower door operating. Pressure measurements were taken between interior rooms with doors closed. The measurements were taken with the building in the same configuration as the blower door test above.

The pressure difference across the building envelope was 20 Pa with the blower door operating. The pressure differences for a number of different locations are shown in Figure A20-4. A few of the theaters had slightly higher pressure than other theaters, which was likely caused by the RTU fans for those theaters running during the test.

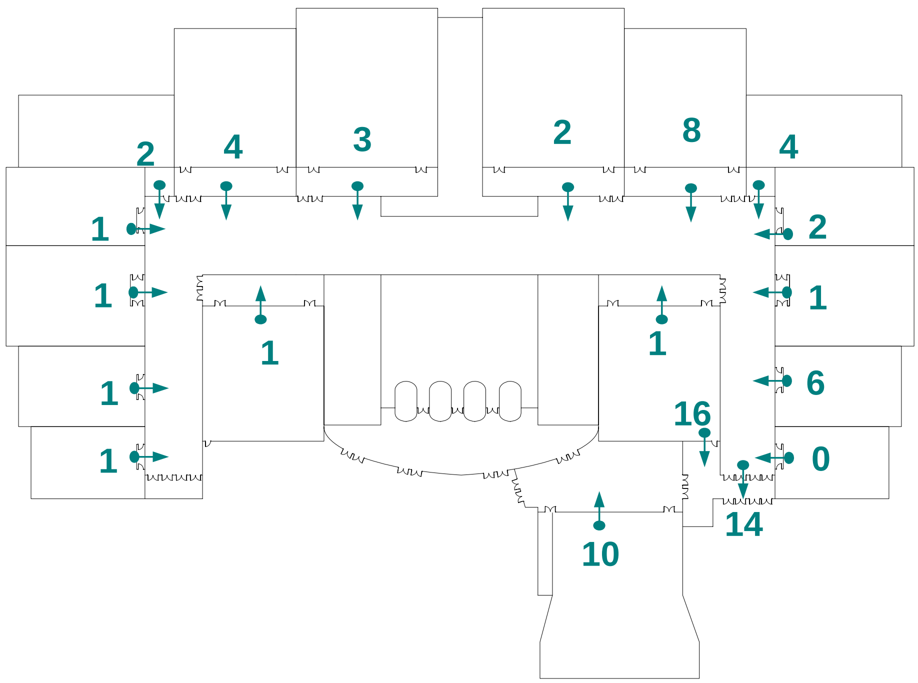

Figure A20-4. Pressure Mapping with Building Depressurized to 20 Pa

Pressure Mapping (AHU Fans On)

The air pressure relationships in the building were also determined with the roof top units on. Figure A20-5 shows the pressure differences induced across the doorways with RTU fans on and the doorways closed. Operation of the RTUs created small interior pressure differences. The building showed very little pressure differences with outdoors. The pressure differences amounted to less than 1 Pa. All the pressure readings for the IMAX theater area were neutral and a diagram of those readings is not included. It appears that the same theaters that showed higher pressure readings for the blower door pressure readings also showed higher pressures during normal operating conditions as well.

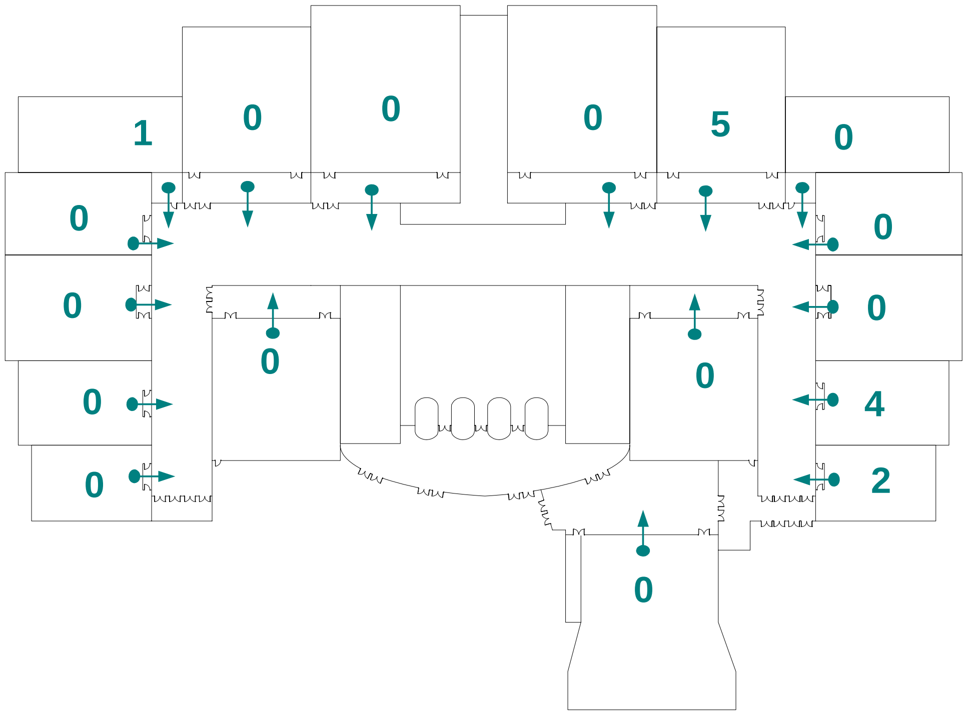

Figure A20-5. Pressure Differences between Rooms with <u>AHU Fans On</u>

<u>Duct Leakage Measurements</u>

No Duct leakage test was performed at this site because all the duct leakage area is inside the building envelope.

Projector Exhaust

Each of the 16 projectors in the theater had a large exhaust fan that lead up to a mushroom vent on the roof of the building. Flow readings for these exhaust fans were taken to determine the total airflow out of the building due to these exhaust fans. The flow rate for each individual fan ranges from 200 cubic feet per minute (cfm) to 1200 cfm. The flow rate was determined using the TSI Flow meter to determine the velocity of the flow, which was then multiplied by the area of the exhaust tube to calculate the total exhaust flow. These fans were off for the blower door and pressure mapping tests, and did not affect the readings.

Projector Airflow Measurements		
Projector #		cfm
1		400
2		350
3		250
4		900
5		515
6		450
7		1150
8		800
9		500
10		725
11		750
12		750
13		550
14		625
15		625
16		775
Total		**10115**

Utility Bills

No utility data was available.

Field Test Site 21 –Auto Accessories Retail, Clinton, NY

Main Entrance (North)


West Side of Building


East Side of Building


Back of Building (South)

Figure A21-1. Photos of Building

CHARACTERISTICS

Building Description

The 3,460 sq-ft facility is a one-story building. The building is used to sell and install aftermarket automotive accessories. It was built in the mid 1980s and was recently remodeled when its current tenants took over the facility in October of 2005. The building is heated and cooled by a 5 ton Carrier packaged unit. There are 14 supply diffusers, two return diffusers, and one exhaust fan. The building has a show room, a conference room, several offices, and a garage area for car servicing and storage. Figure A21-1 shows the building from various angles. The building entrance faces the parking lot to the north. Figure A21-2 shows the building floor plan.

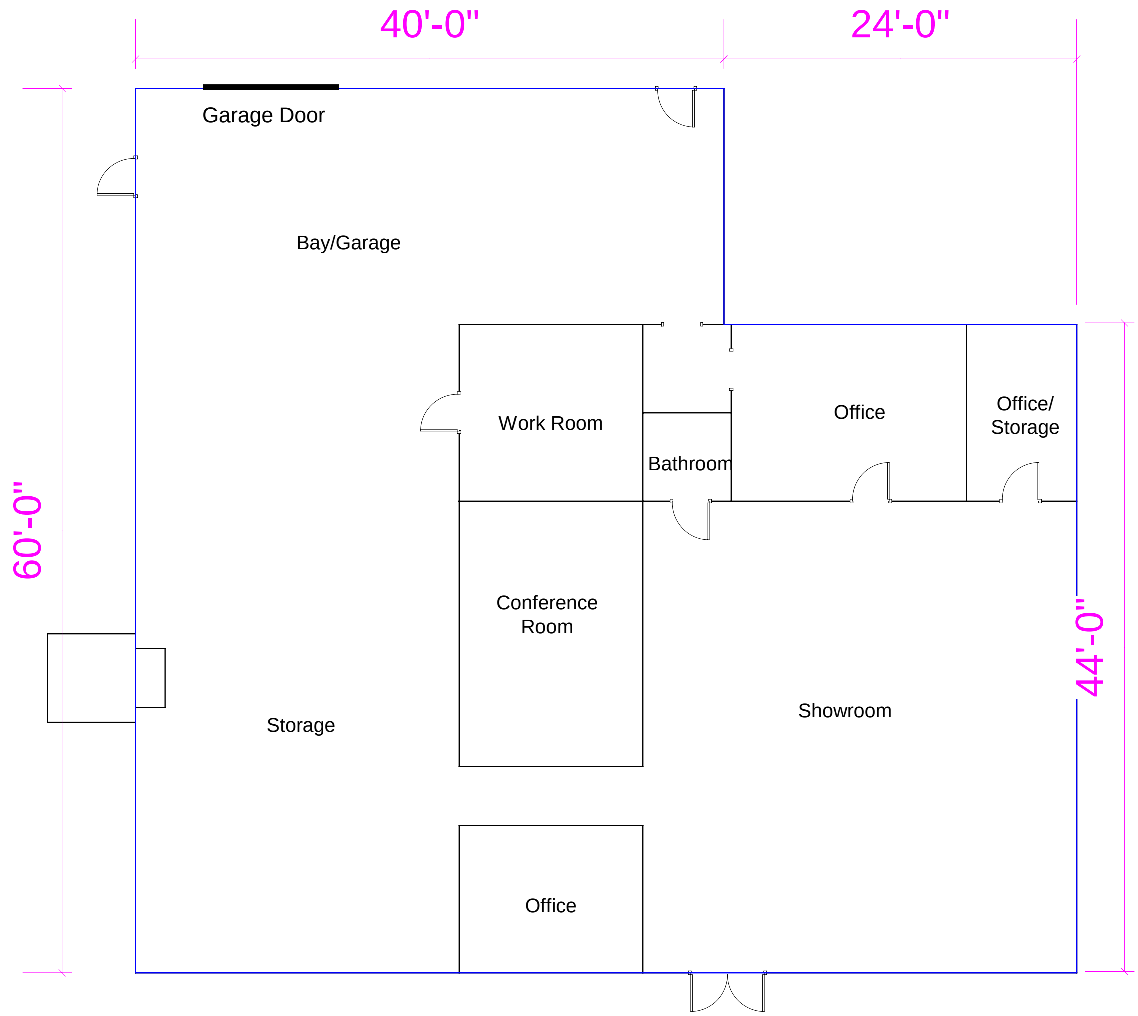

Figure A21-2. First Floor of Building

Construction Details

The building is wood frame construction with metal siding. The building is insulated with 6" batt-insulation. The interior walls are sheet rocked and painted. There is a drop ceiling with 4 in of unfaced insulation lying on top of the ceiling tiles. Six inches above the drop ceiling is a ceiling truss with 6 in of foil-faced fiberglass insulation. .

The edge of the roof has soffit vents that allow air to move freely into the attic area above the insulation. The roof also has a number of vents besides the soffits, which allow air to freely move in and out of the attic. The building has a significant amount of insulation, however, there is no true air barrier in the building, which causes thermal issues during the heating season.

In the shop, there is a bay door, on the west wall, to allow vehicles easy access to the building.

View of Ceiling Insulation and Ceiling Framework

Close up View of Ceiling

Roof Truss Framework

Figure A21-3. Photos of Ceiling and Roof Framework

HVAC System

Figure A21-4 show the locations of the HVAC equipment and supply/return grills in the building. Figure A21-5 shows pictures of various HVAC units for the building.

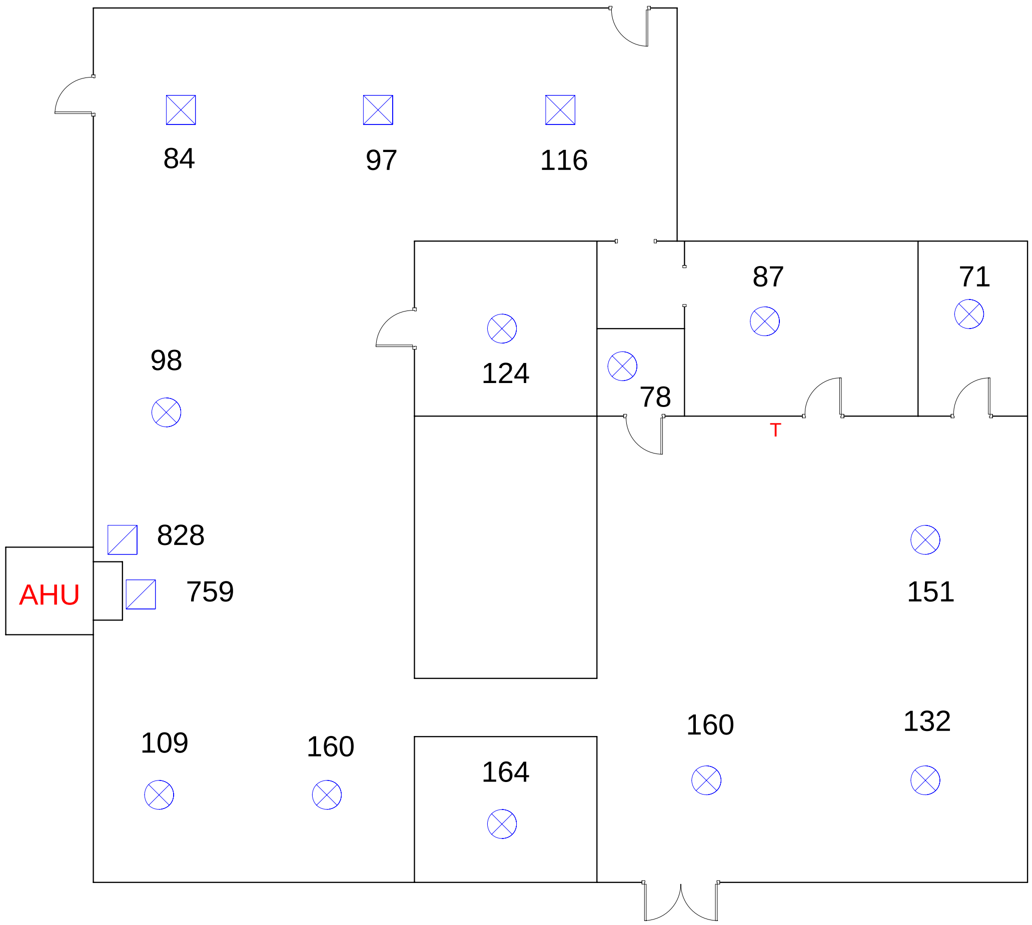

Figure A21-4. HVAC and Diffuser Location

The HVAC for the building is provided by a Carrier packaged unit. The ground-mounted packaged unit is outside on the east side of the building under a protective awning constructed of plywood. The unit provides 150,000 Btu/h for heating and 5 tons of cooling.

The ductwork for the unit runs inside the building, then up above both the drop ceiling. There a main duct trunk that runs across the building. This duct has 14 flex ducts that branch out from the main trunk to each of the diffusers that provide conditioned air to the space. At least one of the flex duct branches has its insulation starting to fall off. This insulation should be repaired in order to help prevent heat loss.

The packaged unit has a thermostat located in the show room. The thermostat is set to 68°F on the weekdays and 64°F on the weekends. The temperature is not turned down at nights because it takes a long time for the temperature in the Garage and storage area to recover back to a comfortable temperature.

Carrier Packaged Unit

Round Supply Diffuser

Square Supply Diffuser

Ductwork above insulated Ceiling Framework

Insulation coming off of the flex duct

Figure A21-5. HVAC Equipment and Ducts

MEASUREMENTS

The test data below was taken on January 19, 2006. Test Personnel were John Carpenter and Mike Clarkin. Temperature/RH sensors were left on site to obtain data (ask Mike??).

Building Envelope Airtightness

The leakage characteristics of the building enclosure were assessed using fan pressurization methods. A single blower door was installed for the test. The blower door was installed in the back door of the building right next to the garage door. All exterior doors were closed. The building has no windows that can be opened. To the extent possible, the building was tested in the following configuration:

- All interior doors open
- AHU off
- All exhaust fans sealed

The building was only able to be depressurized in the range of 3 to 7 Pa. The results of that blower door are summarized in Figure A21-6 and Table A21-1. Because the range of pressures was so small for this test, the resulting exponent was 1.0, which implies laminar flow through a long narrow crack. Generally we only see exponents greater than 0.6 in very tight buildings. The exponent near 1 in a very leaky building appears unlikely. However, it is also possible that airflow through perfectly placed fiberglass batts (with no gaps between the batts) could create laminar flow conditions. Though we observed various large gaps in the insulation.

As a check, we also determined the leakage statistics while forcing the exponent to 0.62. Table A21-2 compares the leakage statistics determined by the two methods. The equivalent leakage area at 4 Pa are very similar in both cases, at about 12 square inches per 100 square feet of envelope are (including the floor area). However, the ACH50, which is extrapolated to 50 Pa, were much different. The ACH50 determine with the exponent forced to 0.62 was 38 air changes per hour.

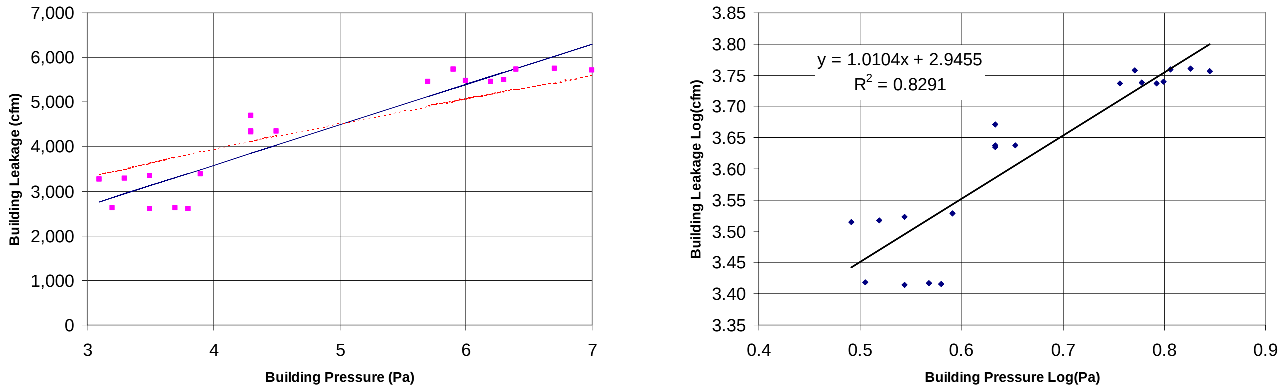

Depressurization Test

Figure A21-6. Variation of Building Leakage with Pressure: cfm = $K(\Delta P)^n$

Table A21-1. Blower Door Test Data, Resulting Best-Fit Model Coefficients, and ELA: Section 1

Test Results:

Flow Coefficient (K)	882.0	3,332 sq ft, floor area
Exponent (n)	1.010	
Leakage area (LBL ELA @ 4 Pa)	1014.1 sq in	11.45 ELA / 100 sq ft
Airflow @ 50 Pa	45,924 cfm	93.62 ACH @ 50

Test Data:

Nominal Building Pressure (Pa)	Nominal Flow (cfm)	Ring
5.9	5,723	a
6.4	5,738	a
6.7	5,754	a
7.0	5,710	a
5.7	5,456	a
6.2	5,455	a
6.0	5,482	a
6.3	5,494	a
4.3	4,684	a
4.3	4,341	a
4.5	4,345	a
4.3	4,315	a
3.9	3,380	a
3.5	3,339	a
3.1	3,271	a
3.3	3,288	a
3.7	2,611	a
3.5	2,597	a
3.2	2,621	a
3.8	2,607	a

Notes: ELA is leakage area (in square inches) at reference pressure of 4 Pa.
ELA per 100 sq ft is based on total building envelope surface area (ceiling, exterior walls and floor).

Table A21-2. Summary of Building Airtightness Results

	Flow Coeff. K	Exp. n	ELA (sq in)	ELA / 100 sq ft (sq in/sq ft)	Flow @ 50 Pa (cfm_{50})	ACH_{50}
Test Results	1,674.0	0.62	1120	12.65	18,929	38.6
Exponent Specified (n=0.62)	882.0	1.01	1014	11.45	45,924	93.6

Pressure Mapping (Blower Door Testing)

Pressure mapping for this building was done, however, all rooms had the same relative pressure. The building with the blower door on was 6 Pa depressurized to the outside.

HVAC Airflow Measurements

The airflow from each supply diffuser was measured using a Shortridge flow hood (compensated mode). The total supply airflow at the grilss as 1,631 cfm or 0.47 cfm per sq-ft of total floor area. This number is low for an office. Figure A21-7 displays the measured airflow at each diffuser and exhaust in the building.

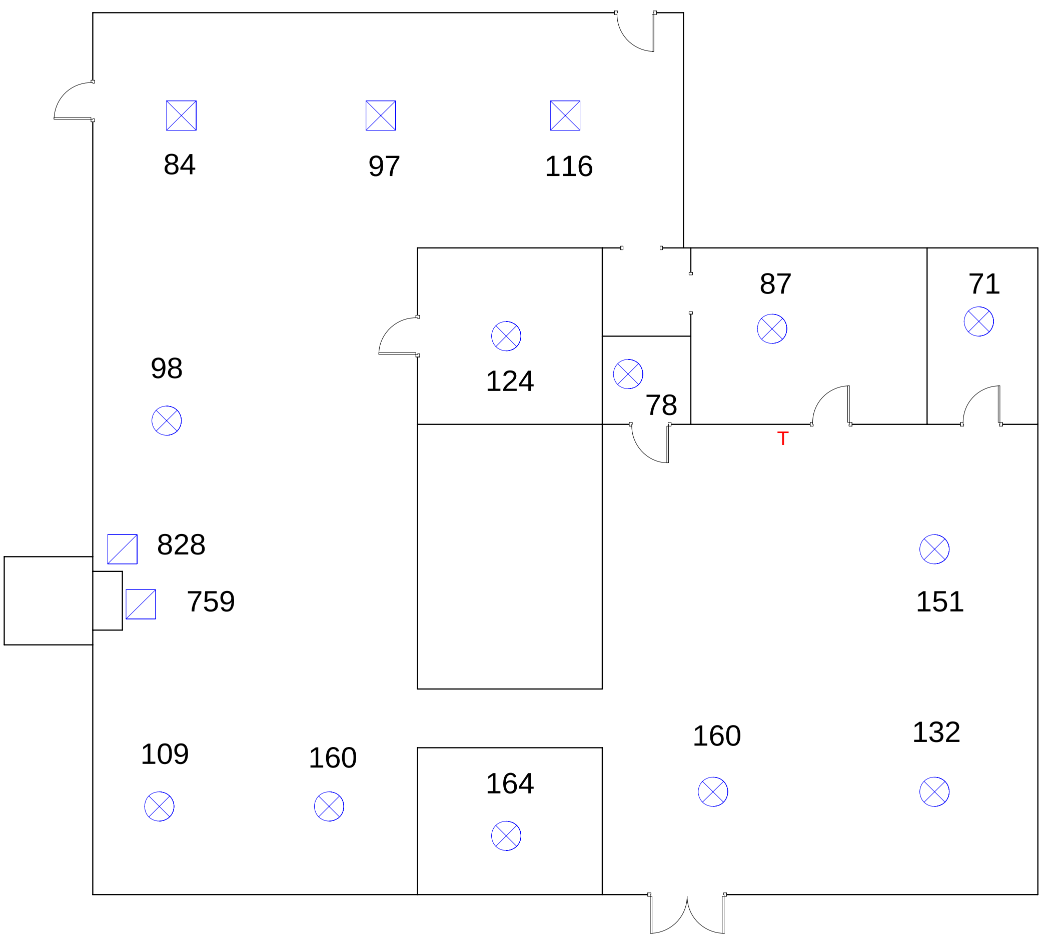

Figure A21-7. Supply and Return Airflow Measurements (cfm)

Table A21- 3 is a summary of the supply, return and exuast airflows for the HVAC units in the building. The supply and return airflow were very close, confirming that there was no ventation air explicitly provided. The negligible difference implies that there is little to no leakiness in either the supply ducts or the return ducts.

Table A21- 3. Comparison of Supply, Return and Ventilation Airflow Measurements

Supply/Return/Exhaust Airflow Measurements

Label	Measured (cfm)
S-1	84
S-2	97
S-3	116
S-4	109
S-5	160
S-6	164
S-7	160
S-8	132
S-9	151
S-10	71
S-11	87
S-12	124
S-13	78
S-14	98

Label	Measured (cfm)
R-1	828
R-2	759

Label	Measured (cfm)
EX-1	17

Flow Balance Summary

	cfm	cfm/ton	cfm/sq ft
Supply	1631	326	0.49
Return	1587		
Exhaust	17		
Net (S-R-E)	27		

Generally, the supply airflow rates through the equipment were lower than expected. Most packaged cooling systems run at 400 cfm per ton. This system runs at about 320 cfm/ton range.

Pressure Mapping (AHU Fans On)

Pressure mapping was also done while the AHU was on. All the rooms showed no pressure difference to the main space. The building was depressurized by 2 Pa with the AHU on. This pressure was probably due to stack effect.

Duct Leakage Measurements

No duct leakage test was performed.

Space Conditions

No data were collected.

Utility Bills

Table A21- 4. Electric Utility Bill Summary

	Days in Month	Energy (kWh)	Cost ($)	$/kWh
12/13/05	29	1,898	$305	0.16
1/13/06	31	2,281	$384	0.17
2/13/06	31	2,505	$477	0.19
3/15/06	30	2,238	$403	0.18
4/14/06	30	1,924	$353	0.18
5/15/06	31	1,702	$299	0.18
6/14/06	30	1,331	$246	0.18
7/14/06	30	1,297	$235	0.18
8/14/06	31	1,598	$295	0.18
10/12/06	59	2,107	$398	0.19
11/9/06	28	1,058	$196	0.19
Period	360	19,939	$3,590	0.18
Annual		20,216	$3,640	

Annual	6.1	kWh/ft^2-yr

Table A21- 5. Natural Gas Bill Summary

	Days in Month	Gas Use (therms)	Cost ($)	$/therm
11/09/05	8	47	$91	1.94
12/13/05	34	466	$790	1.70
01/13/06	31	509	$800	1.57
02/10/06	28	440	$677	1.54
03/14/06	32	470	$643	1.37
04/12/06	29	316	$450	1.42
05/12/06	30	2	$23	11.70
06/14/06	33	0	$21	0.00
07/14/06	30	0	$21	0.00
08/14/06	31	0	$21	0.00
09/13/06	30	0	$21	0.00
10/11/06	28	0	$21	0.00
11/11/06	31	161	$224	1.39
Annual	367	2,364	$ 3,713	1.57

Annual	70.9	MBtu/ft^2-yr

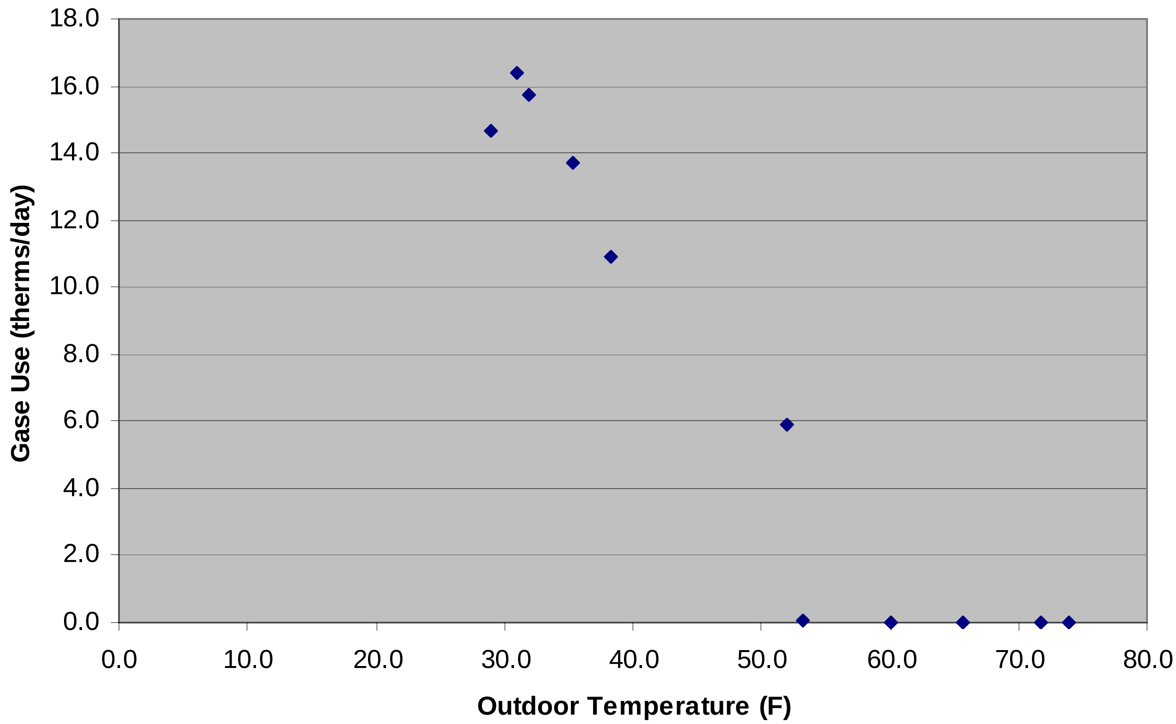

Figure A21-8. Heating Load Line

The load line implies the peak heating load at 0ºF is 122 MBtu/h. The capacity of the rooftop is 150 MBtu/h.

<u>**Summary and Recommendations**</u>

Installation of an Air Barrier. The building contains no true air barrier at the ceiling The result is very high leakage rate (ACH50 is 38) and high gas use (70 MBtu per square foot per year). The building has plenty of insulation, but needs to reduce the infiltration through the ceiling Annual gas costs are $3,700 per year. The creation of air barrier at the ceiling will result in a more comfortable store cut the gas costs by 50-70% per year.

Field Test Site 22 – Agricultural/Lawn & Garden Equipment, Clinton, NY

Main Entrance (North)

East Side of Building

Rear of Building (South)

West Side of Building

Figure A22-1. Photos of Building

CHARACTERISTICS

Building Description

The 4,128 sq-ft single-story retail building was facility was built in 1996 specifically for selling and servicing agricultural/ lawn and garden equipment. Figure A22-1 shows photos of the building from various angles. The building entrance faces the parking lot to the north. The front retail and part storage sections of the building is heated by a Lennox horizontal Gas Furnace. The repair shop area in the rear of the store is heated by a unit heater. The building does not have cooling . Figure A22-2 shows the building floor plan.

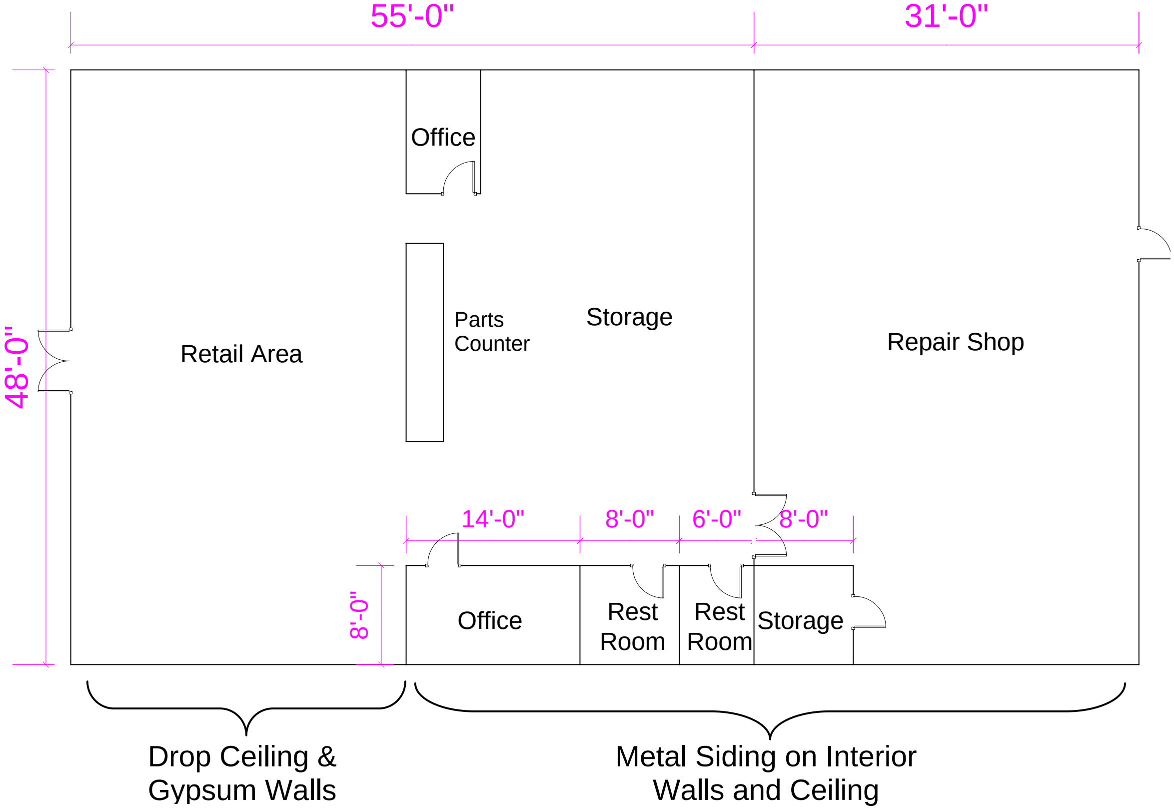

Figure A22-2. Building Floor Plan

Construction Details

The building is pole barn construction with fiberglass batt insulation and metal siding. The interior in the retail area is finished with gypsum board on the walls. The other areas of the building use metal siding for the interior finish. The building has a pitched roof with vented soffits and ridge venting. The roof is constructed with wooden trusses on 48 inch centers with metal roofing.

Retail Area with Drop Ceiling

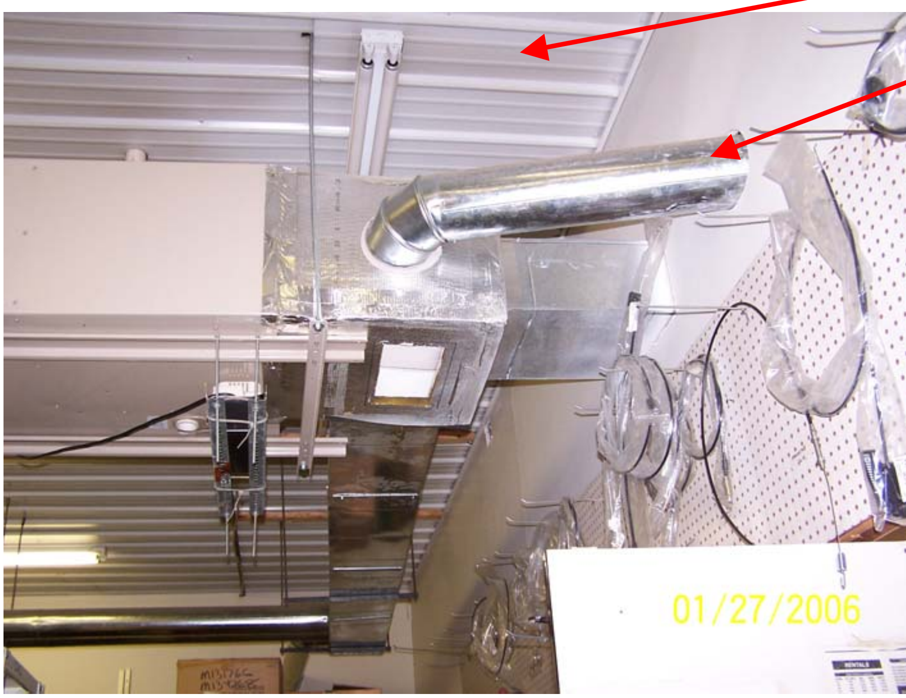

Metal Ceiling in Storage Area

Supply Ducts penetrate wall (above drop ceiling in Retail Area)

Furnace located above parts counter in storage area

Figure A22-3. Retail and Storage Areas

In the repair shop at the rear of the building there are two large overhead bay doors for getting equipment into shop. One door is located on the south wall (rear), the other is located on the east wall (side).

The roof truces have 6 in paper-faced fiberglass batt insulation. The trusses a 48 inches apart. So the fiberglass batts are installed perpendicular to the truss. The insulation is held in place using chicken wire. There are many large gaps to the attic.

Insulation held up by Chicken Wire (gaps exist in insulation)

Figure A22-4. Insulation above the Drop Ceiling and the missing Gypsum Board on the Walls

In the repair shop and storage area, metal siding is attached to the bottom of the trusses and to the walls. There is a small access opening in the ceiling in the repair shop. It appears that a hatch was never constructed for this opening. The dirt pattern on the insulation implies that air from the shop flows out though this hole into the attic during the winter (due to stack effect).

Figure A22-5. Uncovered Opening in Metal Ceiling in the Repair Shop

The Gypsum board in the retail area does not go all the way to the insulated trusses in all locations. Instead it ends only a few inches above the drop ceiling.

This building has severe ice dam issues. The employees at the shop said that they had to clear the ice dams off the building 2 or 3 times a year. This is likely caused by the loss of heat through insulation in the retail area. Air can travel freely through the drop ceiling, through the insulation, and hit the underside of the metal corrugated roof. The open access hole in the shop area may also be exacerbating the problem.

<u>**HVAC System**</u>

Figure A22-6 show the location of the HVAC equipment and supply/return grills in the building. Figure A22-7 shows pictures of HVAC equipment for the building.

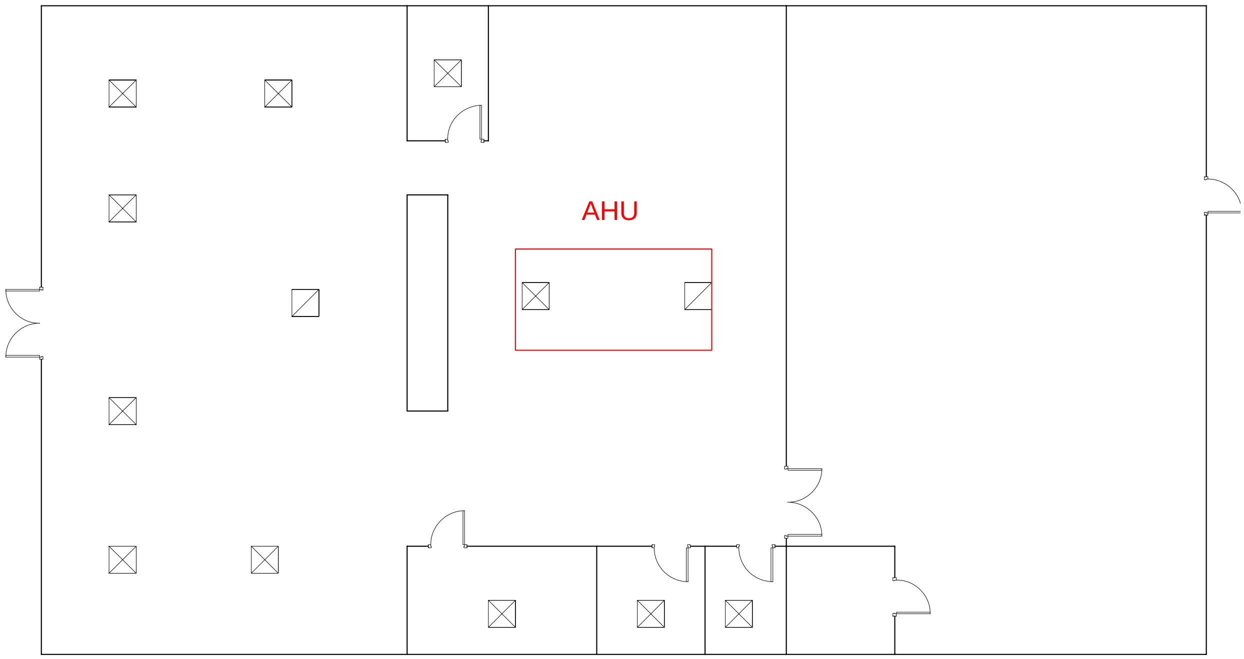

Figure A22-6. AHU, Supply Diffuser, and Returns within Building

The front retail area and storage area are heated by a Lennox Downdraft Gas Furnace. The horizontal hangs from the metal ceiling in the storage area. The ductwork is a combination of sheet metal ductwork and flex duct. There are 11 supply diffusers and 2 return ducts. The repair shop at the rear of the building is heated by a unit heater.

There are two manual thermostats in the building, one for the retail area and one for the shop area. The thermostat in the shop is kept at 64°F during the day, and is manually turned down to 60°F at night. The thermostat in the retail area is set to 68°F during the day and is manually set down to 60°F at night.
Employees at the store report that the front retail area tends to get much cooler on cold days then the back repair shop area.

Lennox Furnace

Supply Grill on Underside of Furnace

Return on Furnace

Supply Diffuser

Unit Heater

Exhaust Fan (South Wall)

Exhaust Damper (West Wall)

Figure A22-7. HVAC Equipment

In the repair shop, there was a manually-controlled exhaust fan. The fan is located on the south side of the building. When it is turned on, a damper on the west wall opens to allow fresh air in and to prevent the shop from becoming pressurized.

MEASUREMENTS

The test data below was taken on January 27, 2006. Test personnel were John Carpenter and Mike Clarkin.

Building Envelope Airtightness

The leakage characteristics of the building enclosure were assessed using fan pressurization methods. A single blower door was installed and used for all tests. All exterior doors and windows were closed. The blower door was placed in a exterior door in the repair shop at the rear of the building.

The building was tested in two parts. The first test evaluated only the repair shop (open hatch in the ceiling was left open). The doors that lead into the rest of the building (i.e., the storage area) were held closed. (the locking mechanism did not work correctly so they are manually held closed). The second test evaluated the entire building envelope. The doors into rest of the building were left open and all other interior were open for this test.

In the first test, building pressure was varied from 14 Pa to 36 Pa. Figure A22-8 shows the building leakage variation with building pressure. The pressure drop across the closed doors into storage area was nearly the same as the pressure across the exterior walls, implying that the leakage across the interior wall was small compared to the interior-to-exterior leaks for the front of the building. Table A22-1 shows the results of the blower door tests including model coefficients, effective leakage area (ELA), and air-changes-per-hour (ACH). The shop has an effective leakage area of approximately 8.10 sq in per 100 sq ft of the total envelope area (including floor area). The ACH_{50} for this section of the building was 23.8.

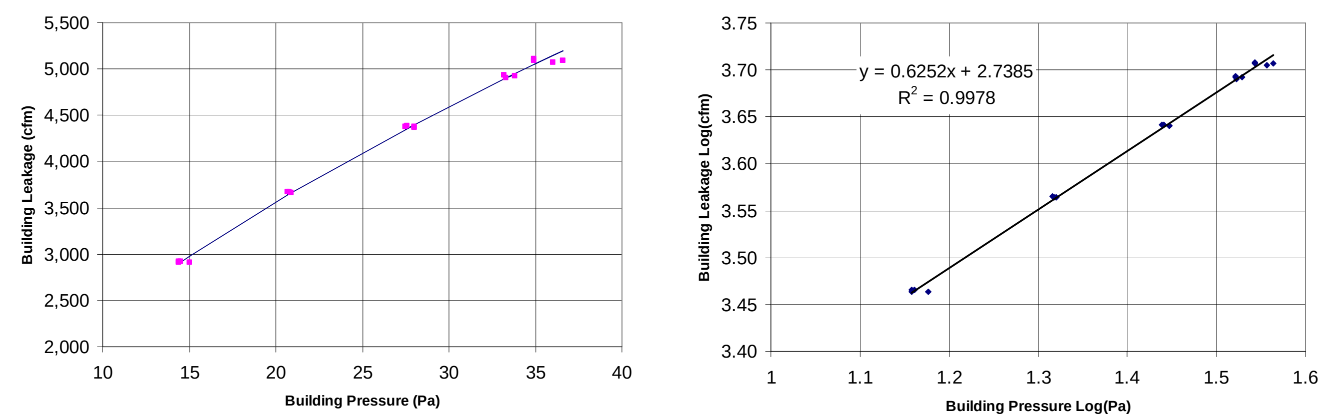

Depressurization Test – Rear Section

Figure A22-8. Variation of Building Leakage with Pressure: cfm = $K(\Delta P)^n$

Table A22-1. Blower Door Test Data, Resulting Best-Fit Model Coefficients, and ELA

Test Results:

Flow Coefficient (K)	547.6		1,330	sq ft, floor area
Exponent (n)	0.625			
Leakage area (LBL ELA @ 4 Pa)	369.1	sq in	8.10	ELA / 100 sq ft
Airflow @ 50 Pa	6,319	cfm	23.75	ACH @ 50

Test Data:

Nominal Building Pressure (Pa)	Nominal Flow (cfm)	Ring
34.9	5,091	Open
36.6	5,093	Open
36.0	5,073	Open
34.9	5,109	Open
33.2	4,933	Open
33.8	4,924	Open
33.2	4,929	Open
33.3	4,901	Open
27.5	4,376	Open
27.6	4,384	Open
28.0	4,371	Open
28.0	4,368	Open
20.9	3,663	Open
20.7	3,676	Open
20.9	3,663	Open
20.8	3,670	Open
15.0	2,909	Open
14.4	2,909	Open
14.4	2,918	Open
14.5	2,922	Open

Notes: ELA is leakage area (in square inches) at reference pressure of 4 Pa.
ELA per 100 sq ft is based on total building envelope surface area (ceiling, exterior walls and floor).

For the second test with the entire building, the building pressure was varied from 6 Pa to 13 Pa. Figure A22-9 shows the building leakage variation with building pressure. Table A22-2 shows the results of the blower door test including model coefficients, effective leakage area (ELA), and air-changes-per-hour (ACH). The whole building has an ELA of approximately 5.78 sq in per 100 sq ft of total envelope area. The ACH_{50} for the entire building was calculated to be 27.9.

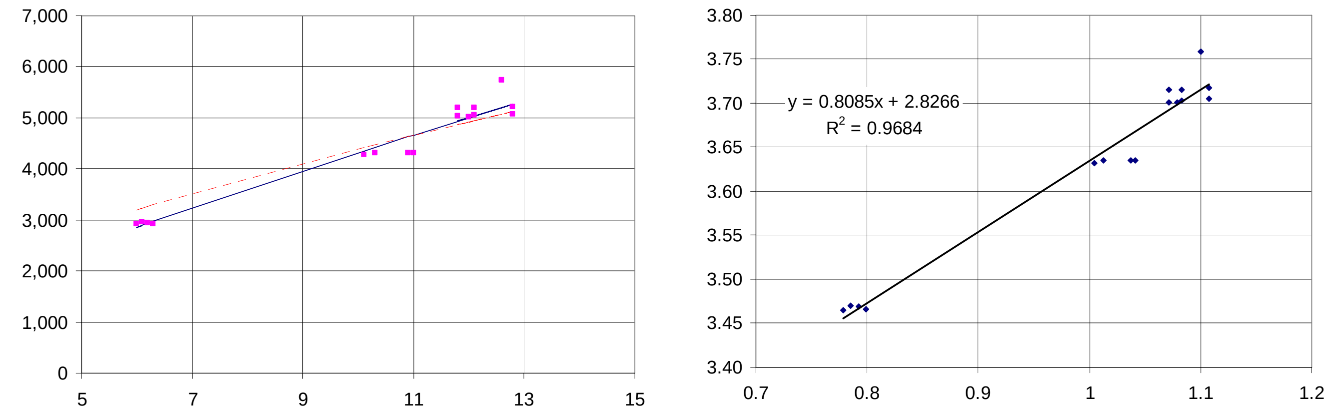

Depressurization Test 2 – Whole Building

Figure A22-9. Variation of Building Leakage with Pressure: cfm = K(ΔP)^n

Table A22-2. Blower Door Test Data, Resulting Best-Fit Model Coefficients, and ELA: Test 2

Test Results:

Flow Coefficient (K)	670.9	3,994 sq ft, floor area
Exponent (n)	0.808	
Leakage area (LBL ELA @ 4 Pa)	583.1 sq in	5.47 ELA / 100 sq ft
Airflow @ 50 Pa	15,857 cfm	23.82 ACH @ 50

Test Data:

Nominal Building Pressure (Pa)	Nominal Flow (cfm)	Ring
12.8	5,213	Open
12.6	5,738	Open
12.1	5,192	Open
11.8	5,197	Open
11.8	5,029	Open
12.0	5,020	Open
12.1	5,048	Open
12.8	5,075	Open
11.0	4,317	Open
10.9	4,320	Open
10.3	4,315	Open
10.1	4,283	Open
6.3	2,922	Open
6.2	2,947	Open
6.0	2,919	Open
6.1	2,950	Open

Notes: ELA is leakage area (in square inches) at reference pressure of 4 Pa.
ELA per 100 sq ft is based on total building envelope surface area (ceiling, exterior walls and floor).

The exponent for test 2 was higher than expected (0.82) most-likely because of the modest range of pressures. Therefore we also fit a model to the data using a specified exponent of 0.62. This model is shown is a dotted line in Figure A22-9. With this model theACH50 becomes 17.9

The leakage statistics for the all the tests are summarized in Table A22-3. The results imply that that the leakage was similar in the repair shop and the rest of the building. In the repair shop, the leakage is mostly due to the open access hole in the ceiling. In the remainder of the building the leakage is through the exposed insulation above the drop ceiling.

Table A22-3. Summary of Blower Door Test Data

	Flow Coeff. K	Exp. n	ELA (sq in)	ELA / 100 sq ft (sq in/sq ft)	Flow @ 50 Pa (cfm_{50})	ACH_{50}
Repair Shop Only	547.6	0.63	369	8.10	6,319	23.8
Entire Building	670.9	0.81	583	5.47	15,857	23.8
Entire Building (n=0.62)	1,053.0	0.62	705	6.61	11,907	17.9

Pressure Mapping (Blower Door Testing)

Pressure readings in the building were taken using a digital micromanometer (DG 700) with the blower door operating. Pressure measurements were taken between interior rooms with doors closed. During the blower door test, none of the rooms showed any difference between the pressure of the space and the pressure of the room. There was also no pressure difference between the pressure of the space and the pressure of the ceiling space.

HVAC Airflow Measurements

The airflow from each supply diffuser was measured using a Shortridge flowhood (compensated mode). The total supply airflow from the Lennox gas furnace is approximately 1,146 cfm or 0.43 cfm per sq-ft of total floor area (This only includes the front retail and storage area, and does not include the back shop, which uses its own heating system). Figure A22-10 displays the measured airflow at each diffuser and the location of the Lennox gas furnace, which is labeled as the AHU in the figure.

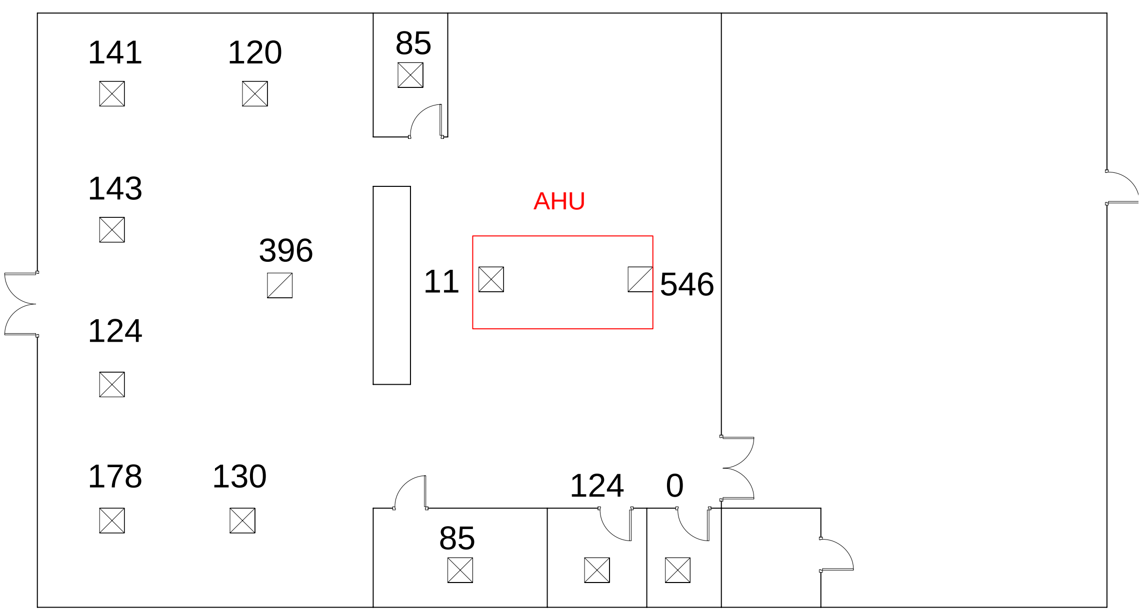

Figure A22-10. First Floor Supply and Return Airflow Measurements (cfm)

Table A22-4 is a summary of the supply, return and ventilation airflows for the HVAC units in the building. There is a small amount more supply flow than return flow. Which implies that about 200 cfm is being drawn in through the fresh air intake.

Table A22-4. Comparison of Supply, Return and Ventilation Airflow Measurements

Airflow Measurements			
Supply Flow		Return Flow	
Diffuser	Flow (cfm)	Diffuser	Flow (cfm)
S-1	178	R-1	396
S-2	124	R-2	546
S-3	143		
S-4	130		
S-5	120		
S-6	85		
S-7	85		
S-8	124		
S-9	0		
S-10	141		
S-11	16		
Total	1146	Total	942
Net Airflow Balance			204

The two bathroom exhaust fans removed about 70 cfm combined when they were on.

<u>Pressure Mapping (AHU Fans On)</u>

The air pressure relationships in the building were also determined with the air-handling unit on. Figure A22-11 shows the pressure differences induced across the doorways with the AHU fan on and the doorways closed. Operation of the AHUs created interior pressure differences up to 1 Pa. The building was pressurized with respect to outdoors was relatively small, only about 2 Pa. The differences are very modest and were partially induced by the slightly windy outdoor conditions.

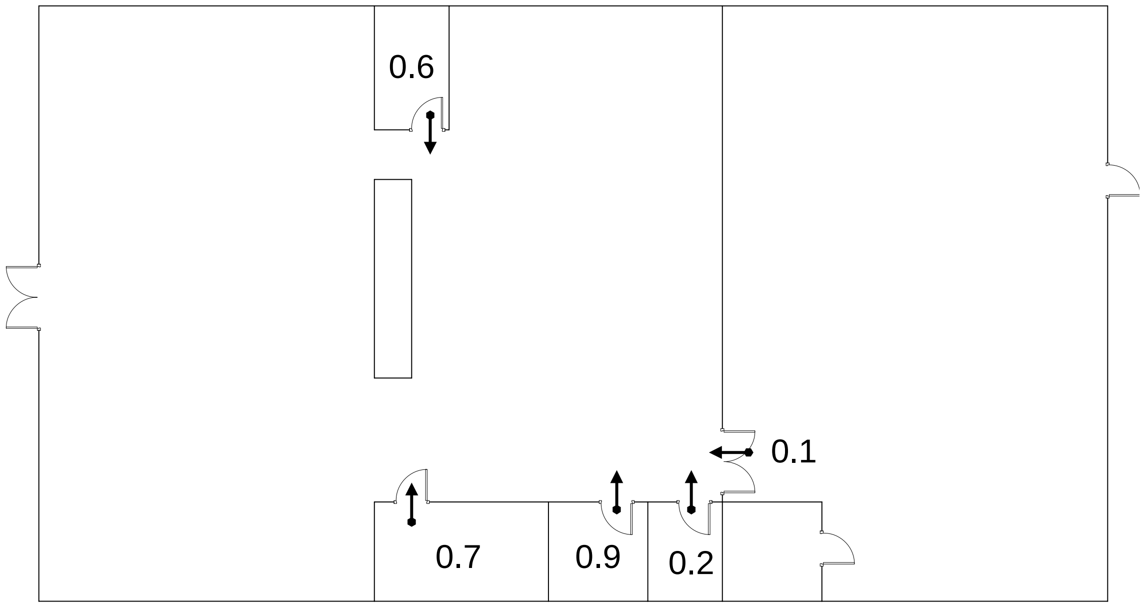

Figure A22-11. First Floor Pressure Differences between Rooms with <u>AHU Fans On</u>

If the shop exhaust fan is on, it depressurizes the space by 8 Pa compared to outside, and by 5 Pa compared to the to the storage area.

<u>Duct Leakage Measurements</u>

No Duct leakage test was performed at this site because all the duct leakage area is inside the building envelope.

<u>Space Conditions</u>

No space condition data has been obtained from the site at this time.

<u>Utility Bills</u>

The utility bills for this site were not available.

<u>Summary and Recommendations</u>

Air-Barrier in Ceiling of Front Room. There is no true air barrier in the front retail space. Air is able to flow freely through the drop ceiling around the cracks in the insulation and right through the soffits of the roof. The installation of an air barrier would help ease some of the thermal issues that are present in the front retail space as well as reducing the ice dam issues. There is an air barrier in the areas that do not have a drop ceiling. It is the metal sheeting just below the insulation. This means it is only necessary to make an adjustment in the areas with the drop ceilings.

<u>Recommendation:</u> There are a number of possible solutions to adding an air barrier that range in price and sophistication. Here are a few suggestions:

One solution would be to get a plastic sheet and staple it to the trusses that are holding up the insulation. It would be necessary to take care to insure that the plastic is air tight or reasonable close to air tight to as possible.

Another solution is to replace the drop ceiling with a gypsum board ceiling. This is a much more expensive and may reduce the aesthetics of the interior. A gypsum board ceiling would solve the air barrier issue, but the lighting fixtures and ductwork would need to be adjusted in order to install the drop ceiling while still maintain proper lighting and heating. To reduce the need to change the lighting and ductwork, the gypsum may be able to be installed above the current drop ceiling, however, it is hard to say how feasible this would be.

There is spray foam available that acts as both a thermal barrier and an air barrier. This can be very useful for certain situations where there is a continuous flat surface to spray the foam. In this building, it may be much hard to find a good surface to spray the foam to, additionally, the walls above where the drywall ends needs to be sprayed as well.

Programmable Thermostats. The thermostats currently installed in the building are manually set thermostats which are set in the morning and evening by employees.

<u>Recommendations:</u> Installing programmable thermostats in the place of the current thermostats would change the setback consistently at the intended time. The consistent reduction of the heating load at night could save money and the temperature setback increasing before the employees get to the store in the morning could increase store comfort in the early hours of the day.

Ice Dams. The building has some ice dam issues during the winter, where ice builds up on the edge of the sloped roof. This ice dam is caused by the loss of heat through the roof deck of the building. The creation of an air barrier that is mentioned in one of the recommendations above will greatly reduce the current ice dam issue. Additionally, there is also a vent in the ceiling, which is intended to allow air to flow into the shop when the exhaust fan is on.

<u>Recommendations:</u> Installing a damper on the ceiling vent would greatly reduce the infiltration and reduce the heat loss through the roof deck. This damper should be controlled by the same switch that currently controls the exhaust fan and the damper on the wall.

Field Test Site 23 – Large Retail Store, Oneonta, NY

Figure A23-1. Front of Store

CHARACTERISTICS

<u>Building Description</u>

The retail facility is located in Oneonta, NY and has 132,000 ft^2 of conditioned space. The facility opened in February 2006. The building is a "big box" facility with a large, open sales floor. The front of the store includes several smaller spaces such as rest rooms, a break area for the employees, a training room and offices. There is also a shipping and receiving area at the rear of the building. The west side of the building has a fenced in garden sales area that is partially covered.

The building is heated and cooled by 20 rooftop units (RTUs) with gas furnace sections. The main sales area and receiving area is served by 17 Carrier 48HG series units. The units are mostly 15 tons, except for the three units near the front entrances, which are 20 tons. Sales area RTUs all use an integrated supply/return air distribution system, or drop box, instead of duct work. The front areas are served three Carrier units with duct work above the drop ceiling. There is one exhaust fan removing air from the restrooms and other areas at the front of the store.

West Side of Store with Fenced Outdoor Garden Area.

Covered and Uncovered Areas in Outdoor Garden Section.

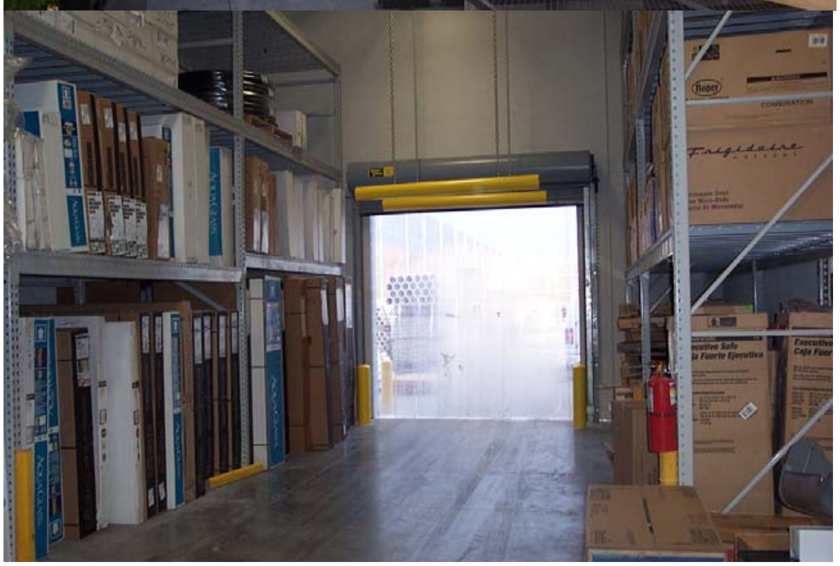

Door to Fenced Storage Yard at Rear East Side of Building.

Figure A23-2. Various Photos of Store Layout

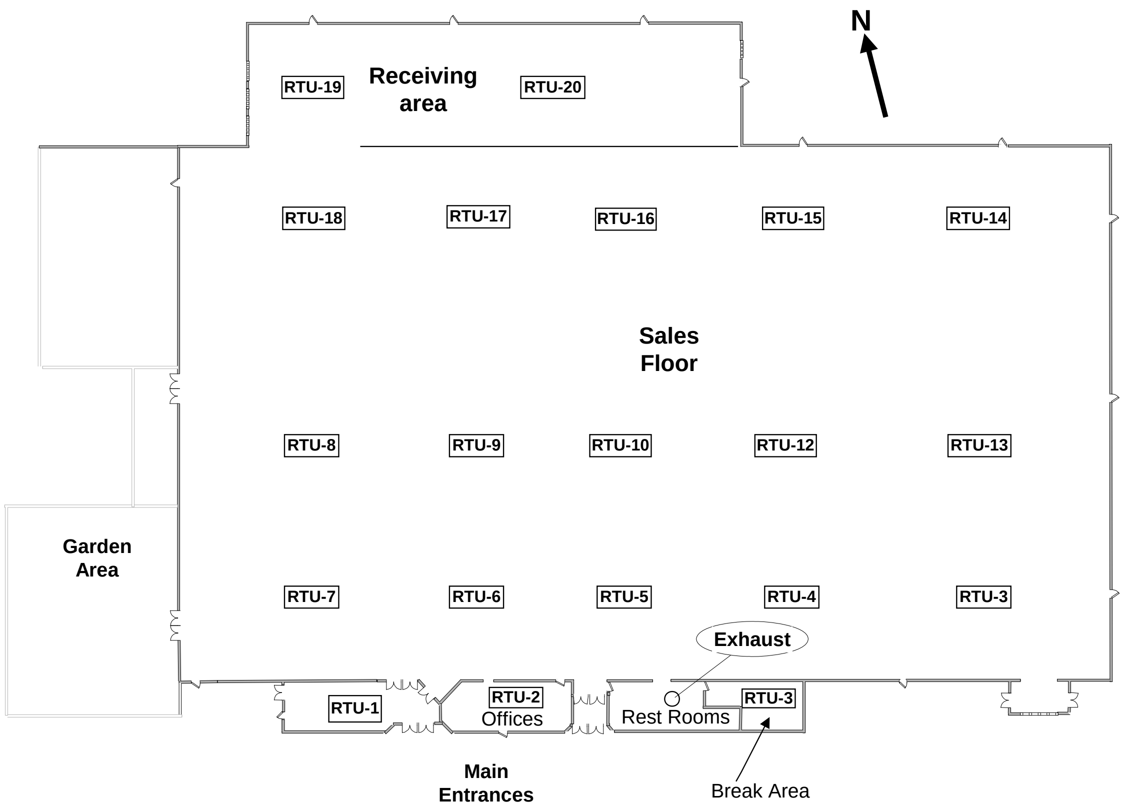

Figure A23-3. Facility Floor Plan

Construction Details

The exterior walls are constructed of 8 inch concrete block. The building has a metal roof deck with foam insulation and a white rubber membrane roof. The main sales area and the receiving area have an open ceiling. The office and restroom areas at the front of the store have a drop ceiling. Lighting to the sales area and the receiving area is provided with high bay fluorescent fixtures.

There are three main entrances at the front of the store each with a vestibule and automatic doors. In addition there are two automatic doors into the garden area. The east side of the storage area has a garage door that opens to fenced yard. That door opening has plastic screens to reduce airflow when the garage door is open. The receiving area on the west side of the store has air-tight docking doors to reduce infiltration when a trailer is unloading.

Roof-to-wall interface details

Walls are 37 blocks high.

Insulation stuffed into joist notches of block wall

Air-tight Loading Dock with Trailer in Place

Loading Dock Doors on West Side of Building

Figure A23-4. Facility Construction Details

<u>HVAC System</u>

Figure A23-3 shows the layout of the various RTUs on the building. The sizing of THE units is given in Table A23-1. The air flows and the measured ventilation through each RTU are given in Table A23-2. The RTUs serving the sales area use a drop down diffuser as shown in Figure A23-5. For the units 1 to 3 the conditioned air is distributed using ducts above the drop ceiling.

One of the biggest potential envelope leaks observed in the building was the hole in the roof deck that was made for the gas piping (see Figure A23-5). Since the roof curbs for the RTUs condenser area are not necessarily air tight, this was potentially are large (and high) opening to outdoors. We were not able to measure the impact of this leak.

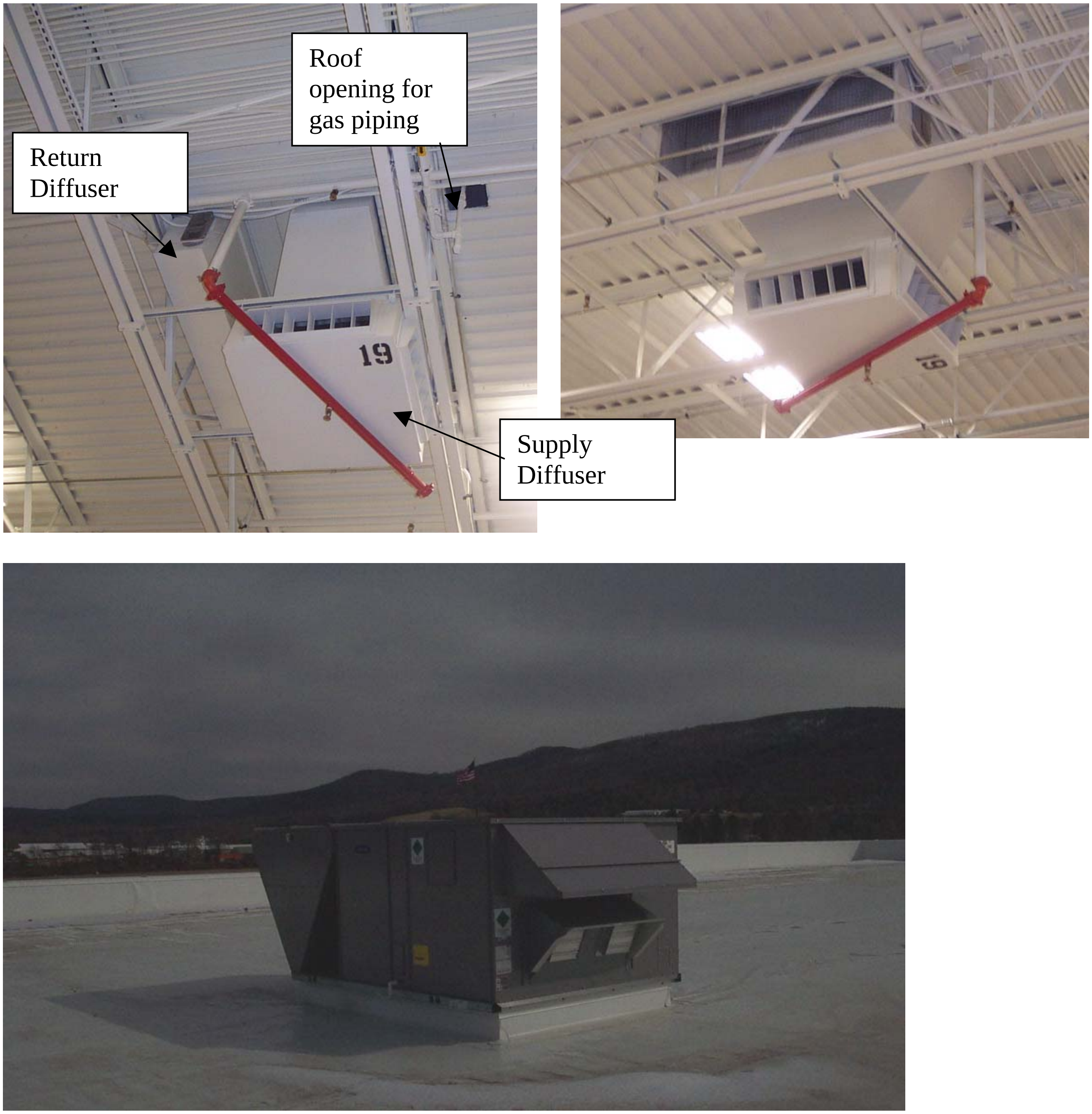

Figure A23-5. RTU Located on Roof / Dropdown Diffuser for an RTU Inside Store

Table A23-1. RTU Model Numbers and Sizes

Roof Top Unit	Carrier Model	RTU (Tons)
1	50HJ	3
2	48HJ	10
3	48HJ	10
4	48HG	20
5	48HG	15
6	48HG	20
7	48HG	20
8	48HG	15
9	48HG	15
10	48HG	15
11	48HG	15
12	48HG	15
13	48HG	15
14	48HG	15
15	48HG	15
16	48HG	15
17	48HG	15
18	48HG	15
19	48HG	15
20	48HG	15
Total		293
Floor area per ton		450

Table A23-2. RTU Unit Airflows

	Design			Measured		
RTU	Supply (cfm)	Ventilation (cfm)	Fan Motor (HP)	Ventilation (cfm)	Fan Power (KW)	Nominal Power (W/cfm)
1	1,200	200	0.75	-	na	na
2	3,750	450	3	-	0.16	0.04
3	4,100	1680	3	-	0.12	0.03
4	8,000	920	5	570	2.49	0.31
5	6,000	920	3	669	0.00	0.00
6	8,000	920	5	619	2.29	0.29
7	8,000	920	5	551	2.25	0.28
8	6,000	920	3	639	1.22	0.20
9	6,000	920	3	669	1.30	0.22
10	6,000	920	3	678	1.33	0.22
11	6,000	920	3	472	1.36	0.23
12	6,000	920	3	610	1.45	0.24
13	6,000	920	3	580	1.50	0.25
14	6,000	920	3	708	1.52	0.25
15	6,000	920	3	511	1.32	0.22
16	6,000	920	3	541	1.19	0.20
17	6,000	920	3	737	1.31	0.22
18	6,000	920	3	855	0.72	0.12
19	6,000	1048	3	629	1.39	0.23
20	6,000	1048	3	551	1.42	0.24
Total	117,050	18,226	64	10,589	24.34	0.21
Total/ft2	0.89	0.14		0.08		

Measurements

Pressure Mapping

The building pressures were measured with all the RTUs operating under normal conditions. A digital micro manometer (DG 700) was used to take the pressure measurements. Figure A23-6 shows the pressure measurements, with respect to indoors, at various points around the building taken on March 21 in the morning. The direction of the arrow indicates the direction of air flow and pressure difference. The average wind speed at this time was about 10 mph (see Figure A23-12). The impact of wind pressure on the building is apparent from the pressure readings. Figure A23-7 shows the operating pressures taken at about 9 pm on April 4 when conditions were very calm. The building was generally depressurized by about 3 Pa.

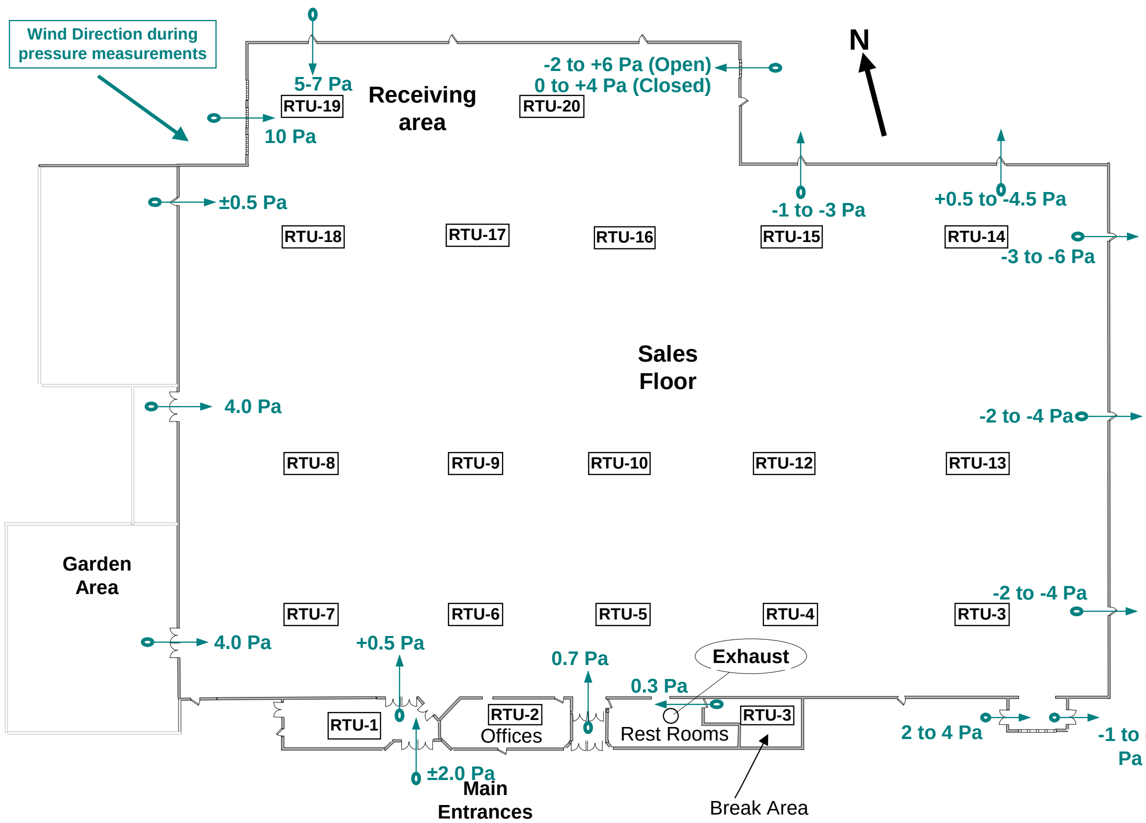

Figure A23-6. Operating Pressures Measured on March 21, 2006 – a Windy Day

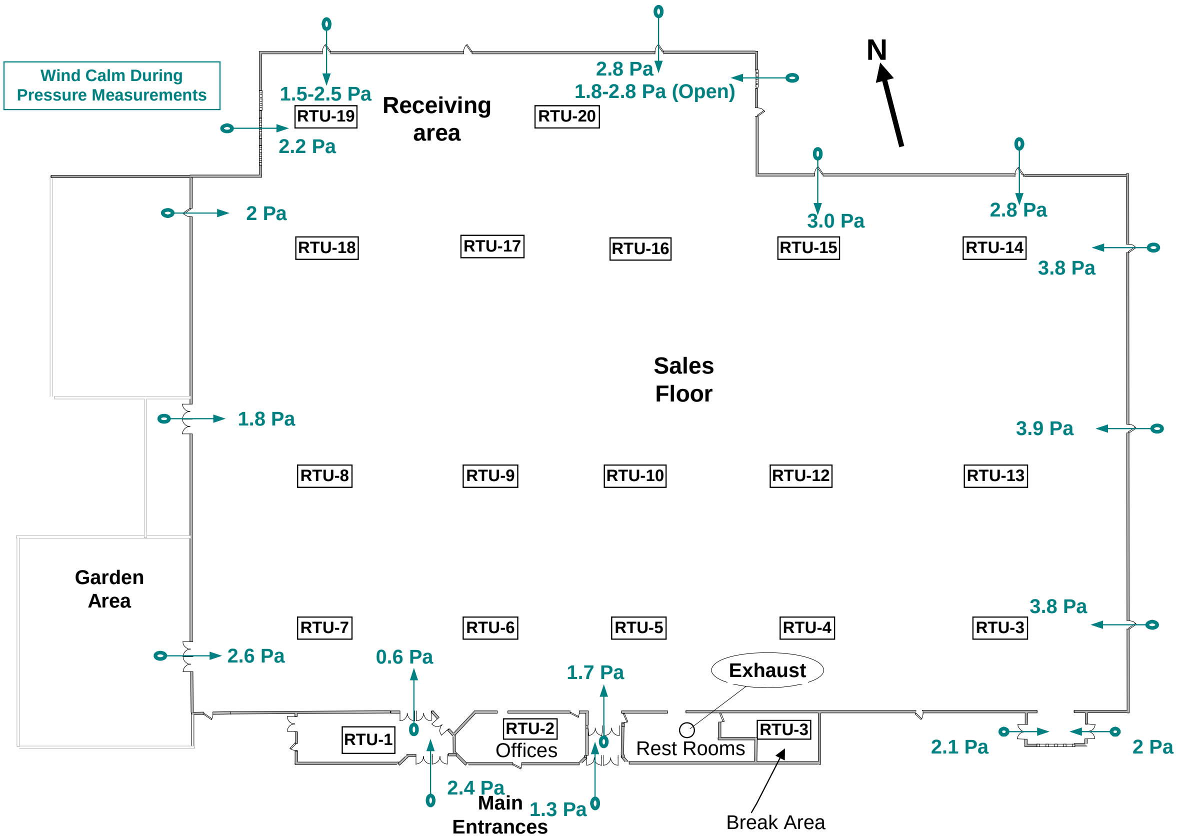

Figure A23-7. Operating Pressures Measured on April 4, 2006 – a Calm Night

HVAC Ventilation and Airflow Measurements

It was not possible to measure the total supply air flow rate for each unit, however we did measure the outdoor air flow into each RTU unit. The ventilation airflow was measured with a TSI Hot wire anemometer. The velocity measurements were taken at 9 different locations across the fresh air intake hood (see Figure A23-8) using an equal area method (i.e., three readings at the center of each filter). Each hood was 59” x 24”, or 9.83 ft^2.

The fresh air dampers were observed to be mostly closed on this cold day when ambient temperatures were less than 40°F (see Figure A23-9). The average velocity readings ranged from 48 to 87 standard fpm, corresponding to airflows of 472 to 855 scfm. The readings taken for each unit is listed in Table A23-2. These velocity readings are at the low end of the anemometer’s resolution and therefore have a significant amount of uncertainty associated with it. The total measured ventilation air flow was 10,589 cfm, or about 60% of the design value from the drawings.

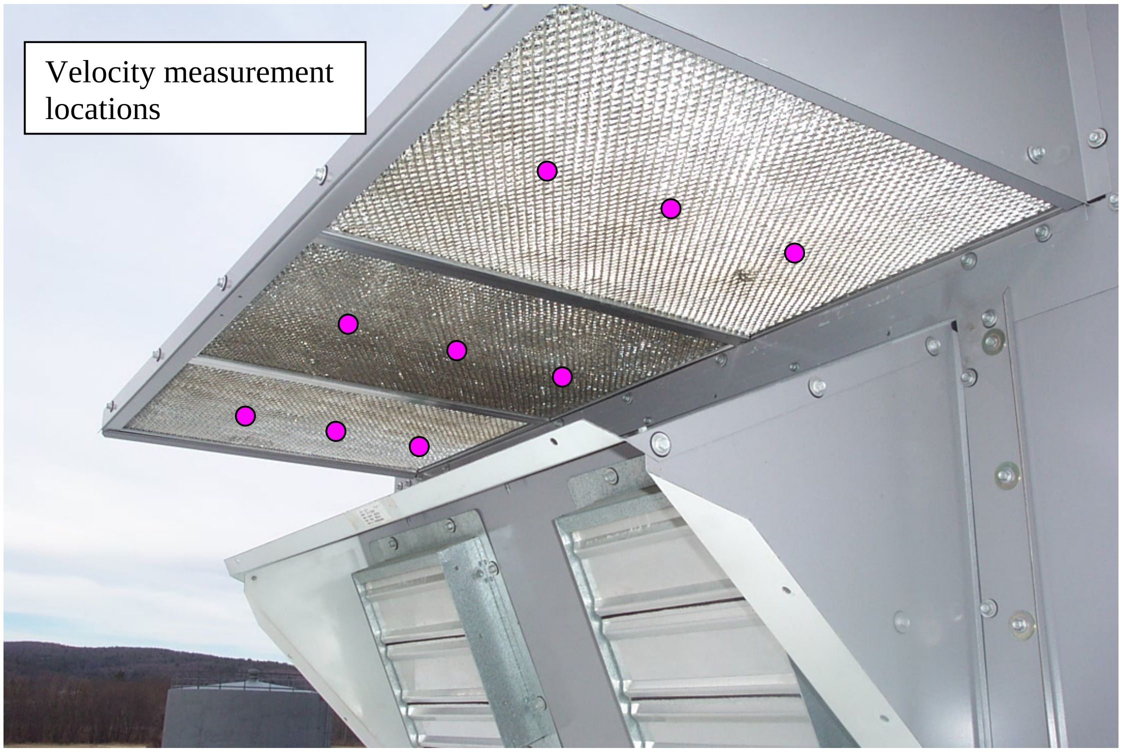

Figure A23-8. Fresh Air Intake Hood on each RTU

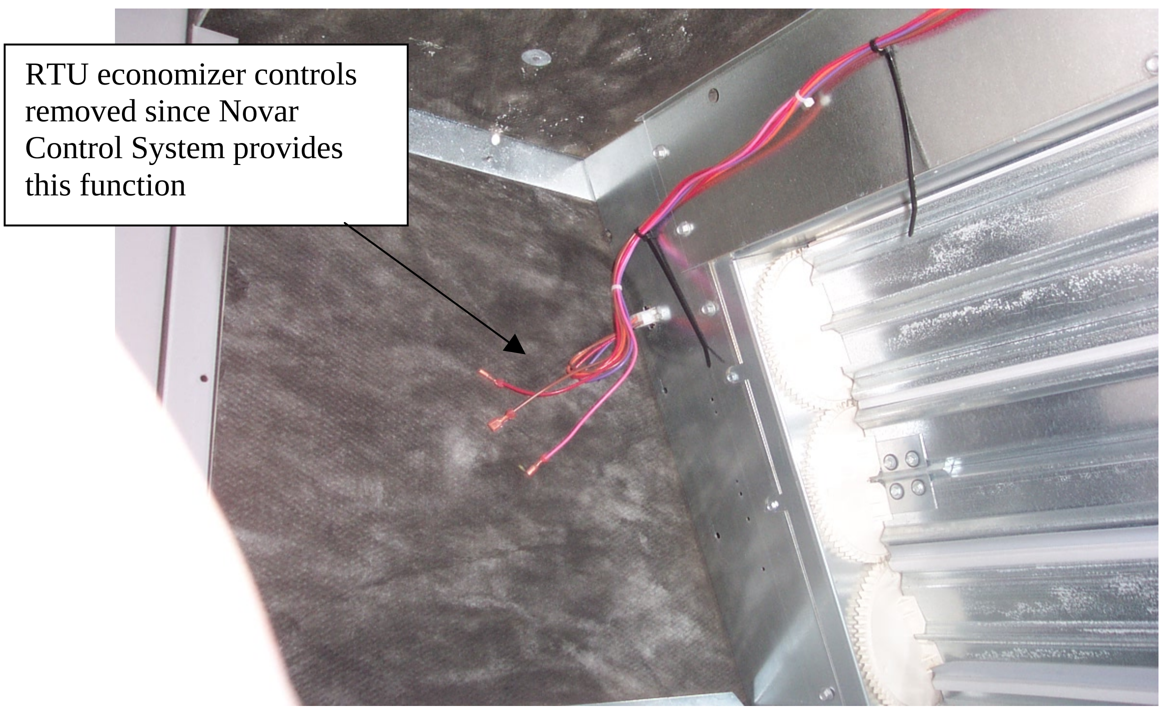

Figure A23-9. Fresh Air Damper Inside Fresh Air Intake Hood

The exhaust flow in the front areas of the store were measured with a Shortridge compensated flow hood. The measured values at each exhaust grill and given in Table A23-3. These exhaust flows total 887 cfm, which is about 53% of design flow for the exhaust fan. We also noticed a fair amount of airflow through a missing ceiling tile near the manager's office. The measured air through this 2 x 4 ft opening was about 332 cfm. This implies that the exhaust fan was depressurizing the area above the drop ceiling and pulling the balance of exhaust air from smaller areas at the front of the store.

Table A23-3. Measured Exhaust Air flows

Location	Design (cfm)	Measured (cfm)
Utility Closet		111
Unisex Restroom		94
Mens Restroom		340
Womens Restroom		342
Total	**1680**	**887**
		53%

Wind-Driven Infiltration/Airflow

The garden area doors on the west side of the building allow a significant amount of outdoor air to enter this store when open (see Figure A23-10). The wind blows through the exterior fencing and hits the building, pressurizing the garden area (see the pressure measurements in the previous section). In an effort to quantify the impact of this wind-driven airflow, we took flow measurements at three heights and on the left and right sides of the doorway.

Figure A23-10. Entrance to Garden Sales Area (Closest to Store Front)

There are two automatic doors into the garden area at the front and middle of the west wall. The door ways openings are both 111 inches high. The door closest to the front of the store opens 66.5 inches wide while the middle door into the garden area opens 54 inches. The total open area of the doors are 51.3 ft^2 and 41.6 ft^2, respectively. The automatic doors stay open for about 5-10 seconds.

The estimated air flow through the door closest to the front of the store given in Table A23-4. Measurements were taken on two different times: March 21 at 6 pm and April 4 at 6 pm. Figure A23-10, shows the typical velocity variation from the top to the bottom of the door and provides the measurement locations. At the time of the measurements, we also recorded the pressure across the door (with the door closed). We also show the corresponding stagnation pressure based on the recorded wind speed from regional weather stations[1] at approximately the same time. The recorded wind speeds for these two days are shown in Figure A23-12 and Figure A23-13.

Table A23-4. Measured Airflow through the Garden Area Door

Mar-21-2006 6pm

		Velocity Left Side (fpm)	Velocity Right Side (fpm)	Total Air Flow (CFM)
Reading 1	Average	141	86	5,818
Reading 2	Average	145	162	7,433
	Top		70	
	Mid		170	
	Bottom		320	

Measured Outdoor Wind Speed (at 6.pm)	10	mph	(4.4704	m/s)
Equivalent Stagnation Pressure	11.2	Pa		
Measured Pressure with Door Closed	3.0	Pa		

April-4-2006 at 7 pm

		Velocity Left Side (fpm)	Velocity Right Side (fpm)	Total Air Flow (CFM)
Reading 1	Average	121	68	6,203
	Top	78	50	
	Mid	85	55	
	Bottom	200	100	

Measured Outdoor Wind Speed (at 6.pm)	8	mph	(3.57632	m/s)
Equivalent Stagnation Pressure	7.2	Pa		
Measured Pressure with Door Closed	2.0	Pa		

Figure A23-11 shows the velocity profile down the door opening during the March 21 measurements. This profile was typical of the measurements taken at other times as well. The wind rose in Figure A23-14 shows that the wind predominately comes from the west and northwest, just as it did on these test days.

[1] Weather data was not available for Oneonta, so we used windspeed data from Albany, Binghamton, and Cooperstown.

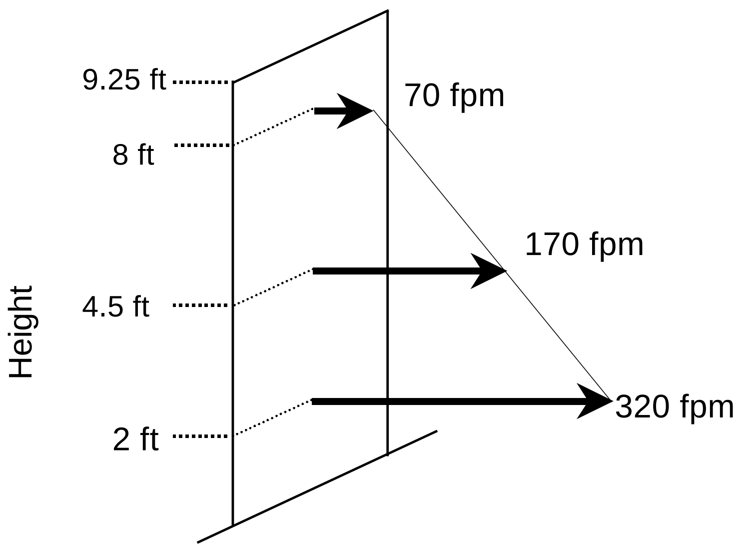

Figure A23-11. Representative Air Flow Profile Through Open Doorway – March 21

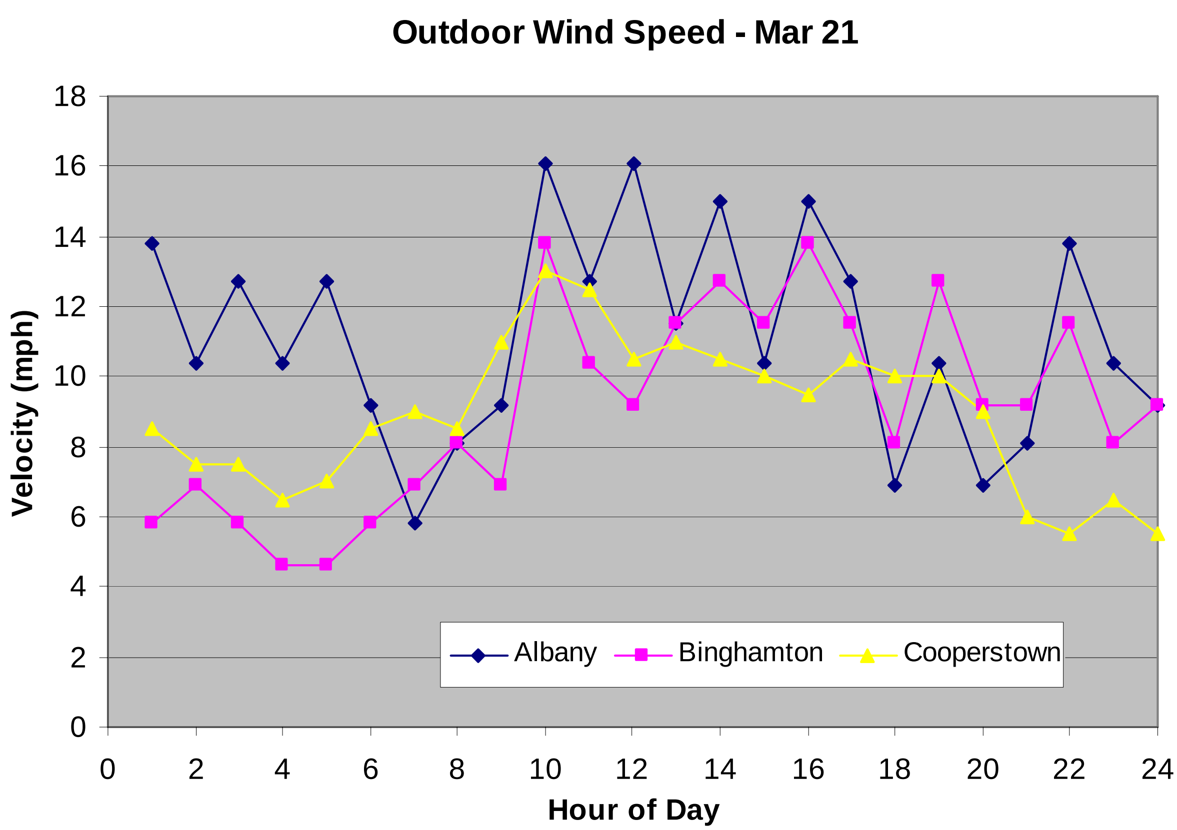

Figure A23-12. Outdoor Wind Speeds Recorded on March 21 for Nearby Locations

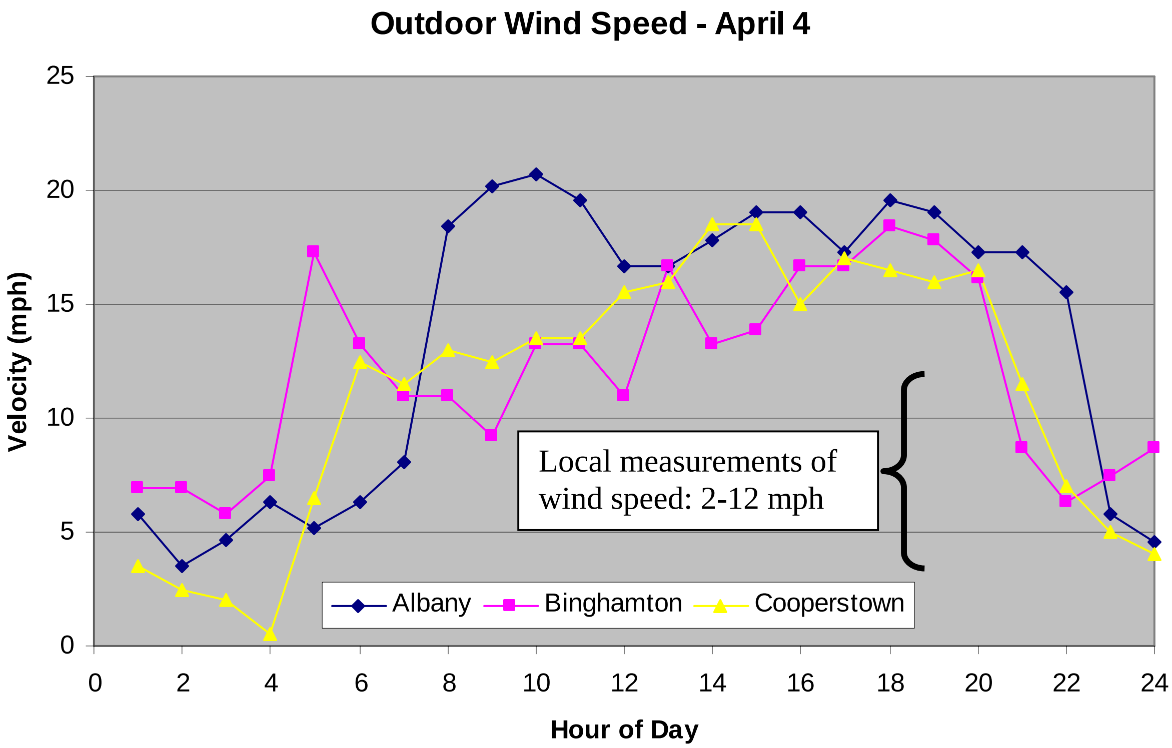

Figure A23-13. Outdoor Wind Speeds Recorded on April 4 for Nearby Locations

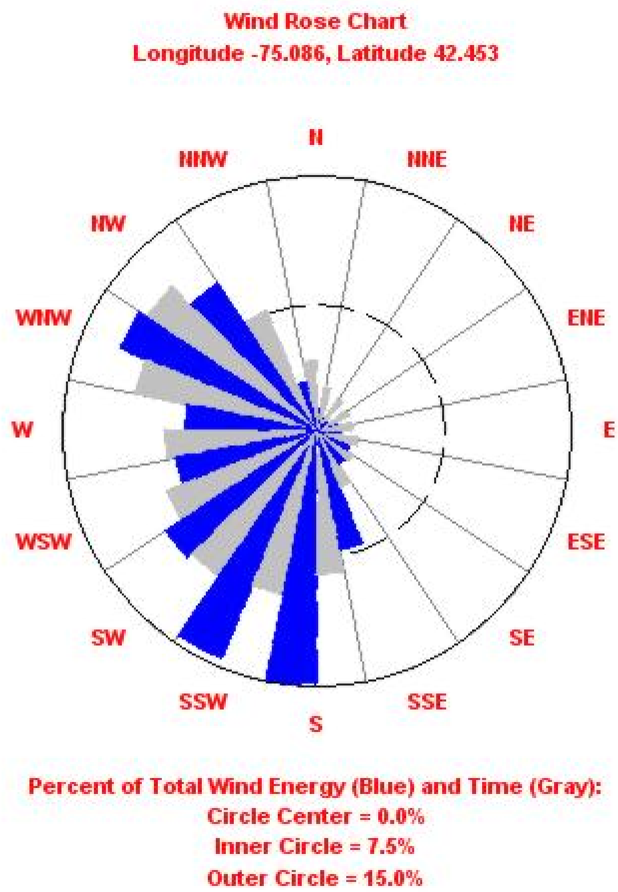

Wind Rose Chart showing probability wind coming from any direction in Oneonta, NY.

Figure A23-14. Wind Rose Chart for Oneonta, NY

Across the year, the amount of infiltration through the door depends on the amount of time the automatic door remains open. The door opens for 5-10 seconds every time a person goes through it. Based on our understanding of store traffic patterns, we estimated that at the busiest times of the year the door would be open about 10% of the time (or 6 minutes of every hour). The busiest times are assumed to 3 pm to 7 pm during April through October. Traffic at other times of the day in the season is slightly lower. In the winter, the traffic through the doors is assumed to only 20% of the spring/summer/fall pattern. The annual traffic pattern for the automatic door is shown by the shade plot in Figure A23-15. Each day is shown as a vertical stripe on the plot. Light gray indicates the opening fraction is zero. Darker shades indicate progressively more opening time.

The door opening schedule in Figure A23-15 was used with the linear relationship of airflow as function of wind speed that was determined using the data from Table A23-4. The simple linear model is shown as a line on Figure A23-16. The line is the best fit to the measurements taken on March 21 and April 4. This model was used with the hourly wind speed data from the TMY2 weather file for Binghamton, NY. While correlations were developed for the door closest to the front of the store, we assumed that that the air flow through middle door scales in proportion to its open area (i.e., its airflow is 81% of the tested door).

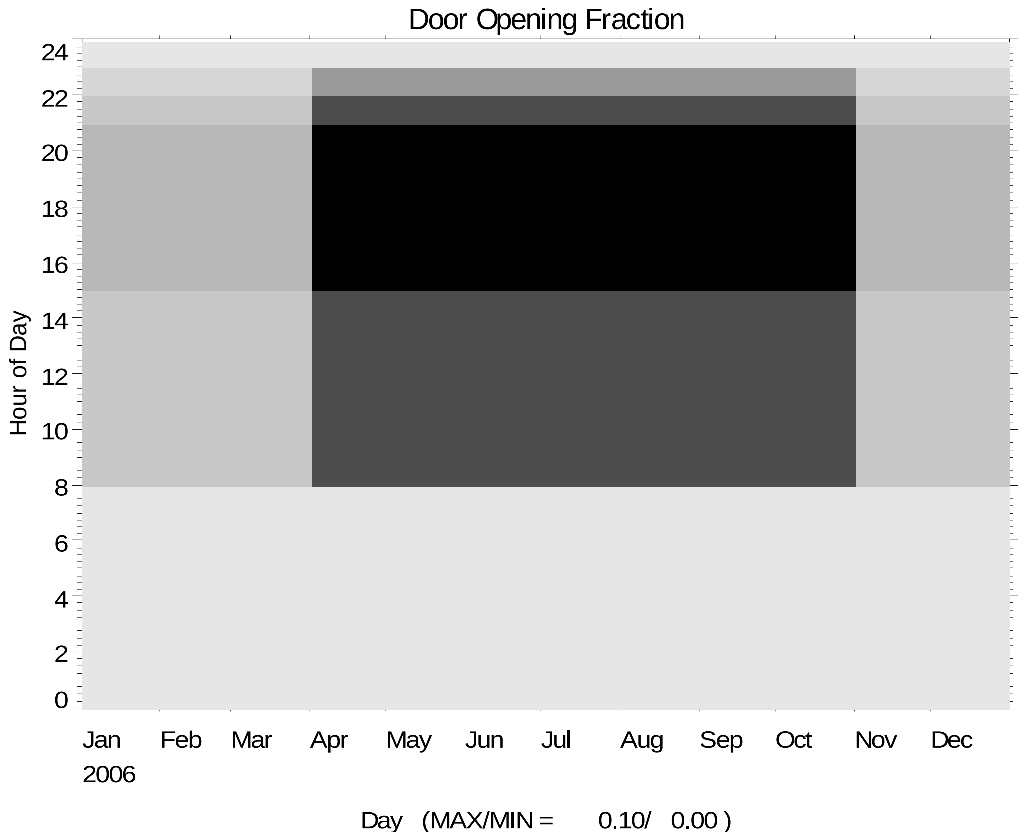

Figure A23-15. Shade Plot Showing the Assumed Fraction of each Hour that the Door is Open

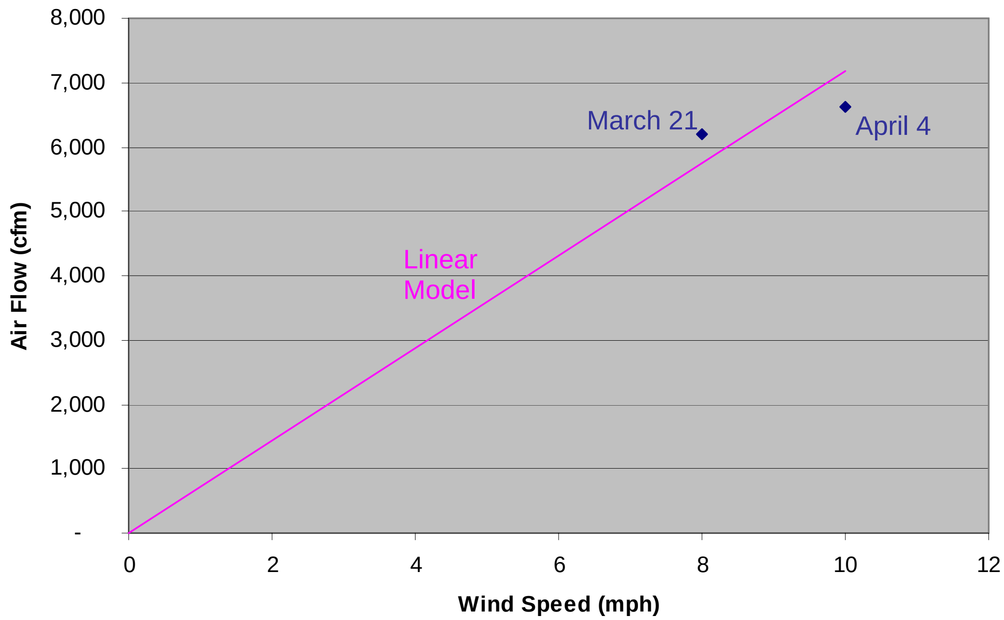

Figure A23-16. Linear Model Used to Predict Doorway Airflow Compared to Measured Airflows

Figure A23-17 shows the airflow predicted through both doors over the year using the TMY2 wind speed data for Binghamton, NY. On windy days in the spring the ventilation provided through the door reaches a daily average of 1300 cfm. The average of the Spring/Summer/Fall when the garden area is heavily used is about 650 cfm. Across the year the ventilation through the door averages 440 cfm. This compares to the 10,600 cfm measured for the facility and the 18,200 cfm specified on the drawings. So, while the peak infiltration through both open doors can be on the same order of the measured ventilation through the RTUs, the average across the summer season appears to be 5-7% of that value.

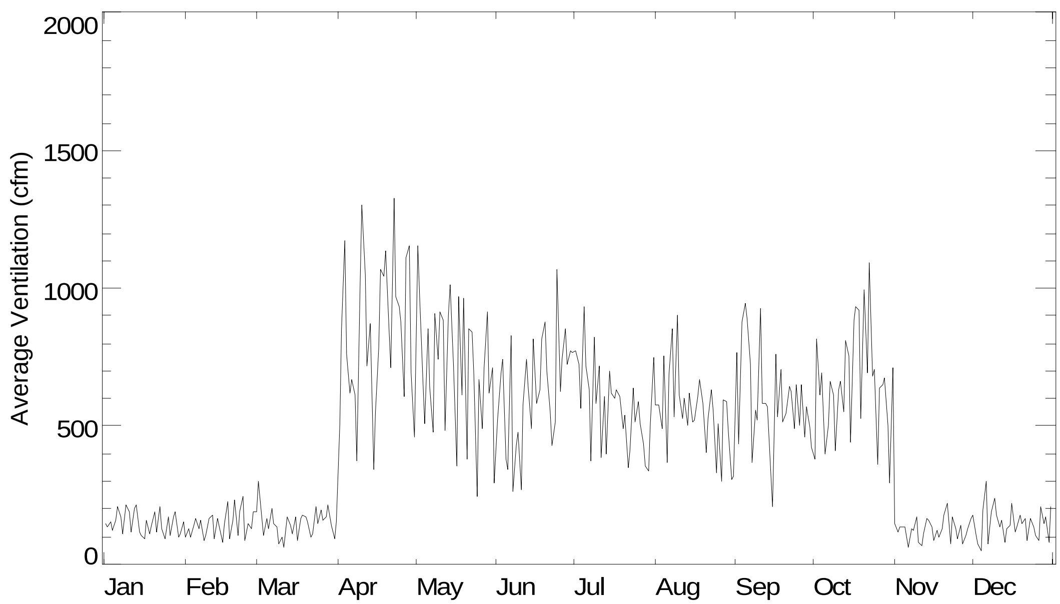

Figure A23-17. Average Airflow through Both Doors Using TMY2 Wind Speed Data for Binghamton, NY

Blower Door Testing

We setup two 5,000 cfm blower doors on March 21 in an attempt to pressurize the facility and measure the envelope leakage. The blower doors were both installed at the back of the building. With both doors exhausting 10,000 cfm from the building, we were not able to change the building pressure by more than 1 or 2 Pa – which was equivalent to the wind-induced pressure flutuations we were observing on that windy day.

Measured CO2 Levels

Two battery-powered CO_2 sensors were left in the facility from March 21 through April 4.   The sensors were left in the locations shown on Figure A23-18. One was installed in shelving behind the cashier's station in the garden area. The other sensor was installed in the lighting aisle (i.e., end of Aisle 9) near the center of the store. Both locations were selected based on the availability of 110 volt electrical outlet to power the infrared CO_2 sensor.

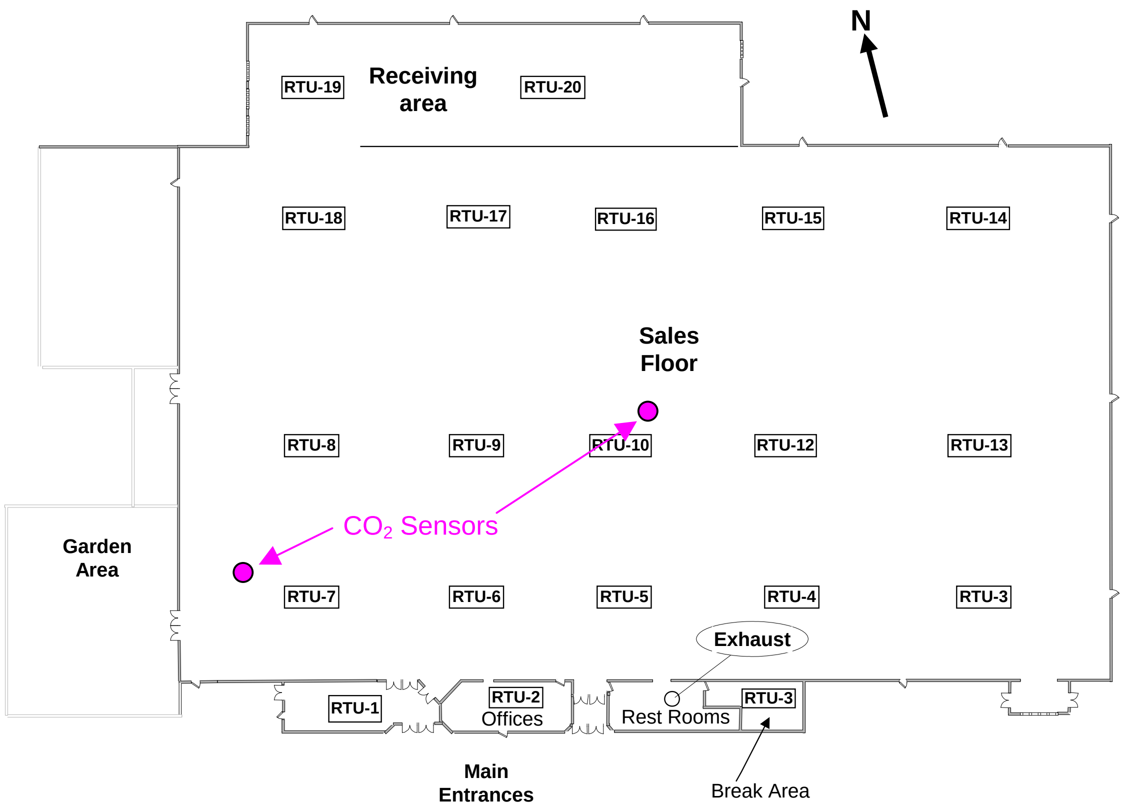

Figure A23-18. Location of CO_2 Dataloggers in the Facility

After retrieving the sensors and downloading the data, we realized that the outlet in the lighting section was turned off each night. The frequent powering on an off of these unit caused it to record erroneous readings. The sensor in the garden area was continuously powered, so it recorded valid readings. The measured CO_2 concentration for the garden area is shown in Figure A23-19. For this two week period, CO_2 levels ranged between 440 and 700 ppm. Figure A23-20 shows more detail for two periods when CO_2 levels were relatively high: April 25-26 and April 1-2. The daily profile typically peaks near 4 pm (16:00) each day and reaches a minimum overnight in the early morning hours.

CO_2 can be used as a tracer gas to infer the effective ventilation rate, assuming the space is well mixed. The decay of CO_2 levels can provide an indication of the air change rate when the space suddenly goes from occupied to unoccupied. In this large facility, the assumption that the space well mixed may be questionable. CO_2 produced in one local area of the store may decay because of inter-zone transfer instead of outdoor-to-indoor dilution.

Figure A23-21 and Figure A23-22 shows the decay of occupant-generated CO2 from 8 pm to 4 am on March 25 and April 1. In both cases the data were fit to an exponential decay to estimate the “local” air change (ACH) rate which is also equivalent to the mean age of the air in that location. The local ACH was 0.12 and 0.19 1/h with an assumed background concentration of 440 ppm. Assuming the facility was fully mixed overnight, this equates to an effective ventilation rate of 6,400 and 10,200 cfm for the 132,000 ft^2 facility. This inferred ventilation rate was inline with the measured ventilation values for the rooftop in the previous section.

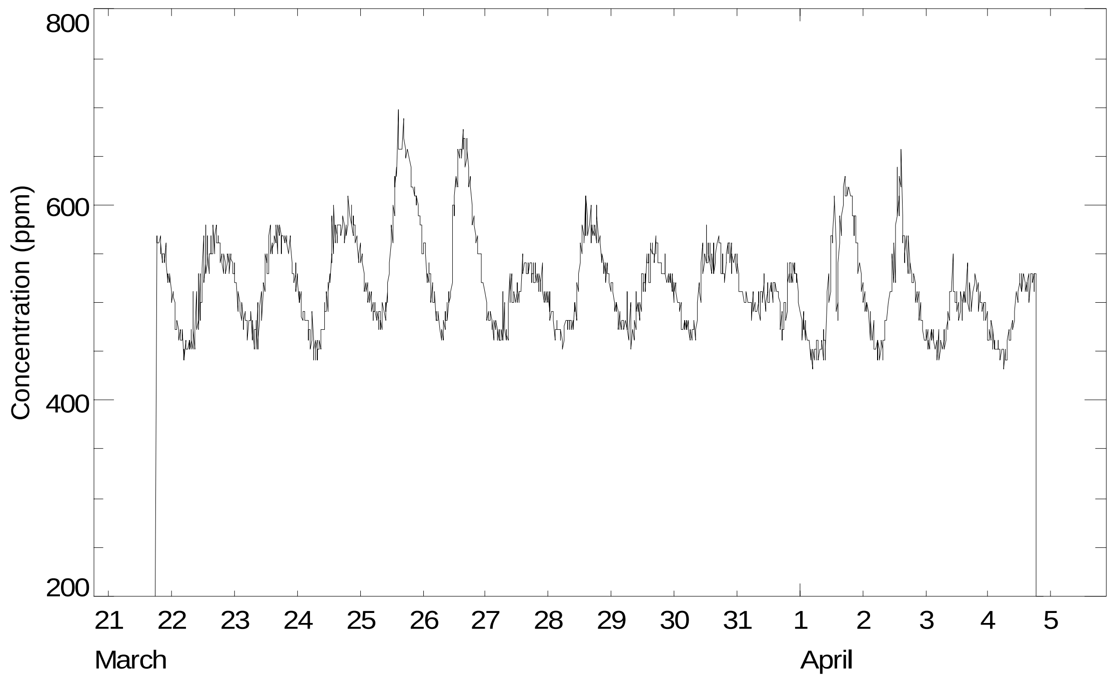

Figure A23-19. CO2 Levels Measured Near Garden Area Cashier's Station

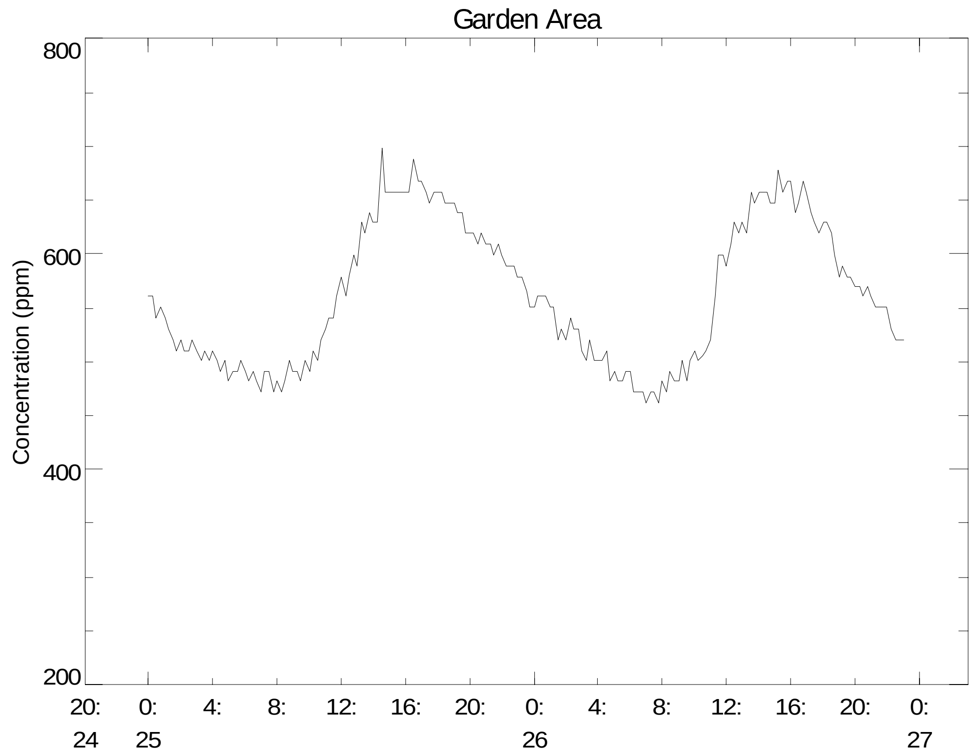

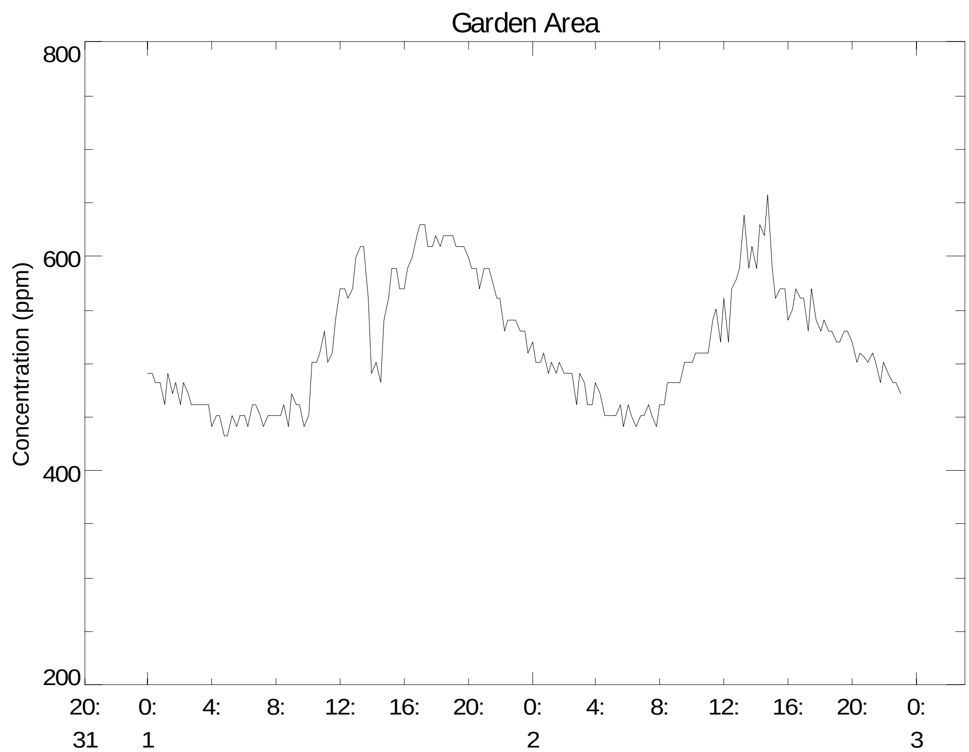

Figure A23-20. CO2 Levels Measured Near Garden Area on March 25-26 and April 1-2

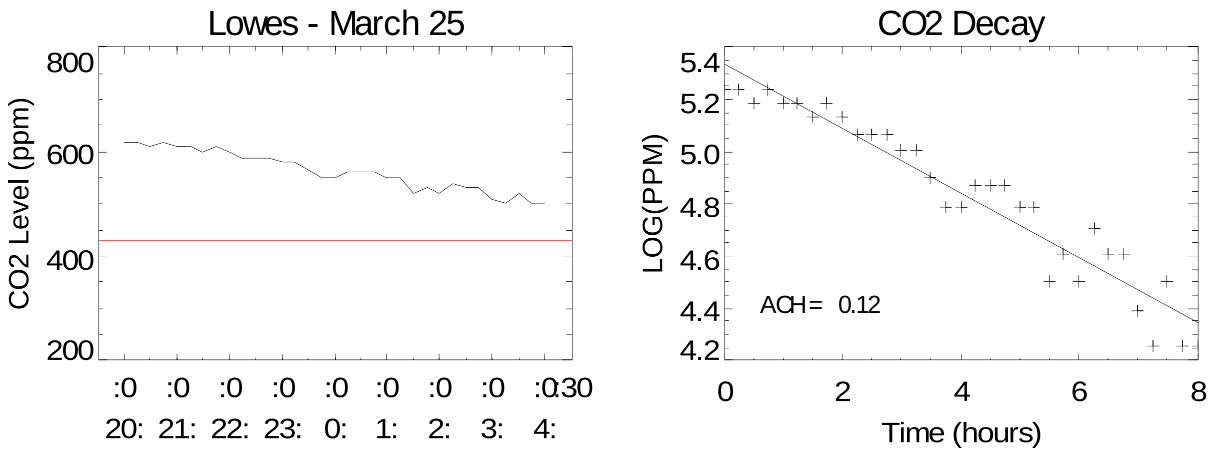

Figure A23-21. Decay of CO2 Concentration Near Garden Area on Overnight on March 25

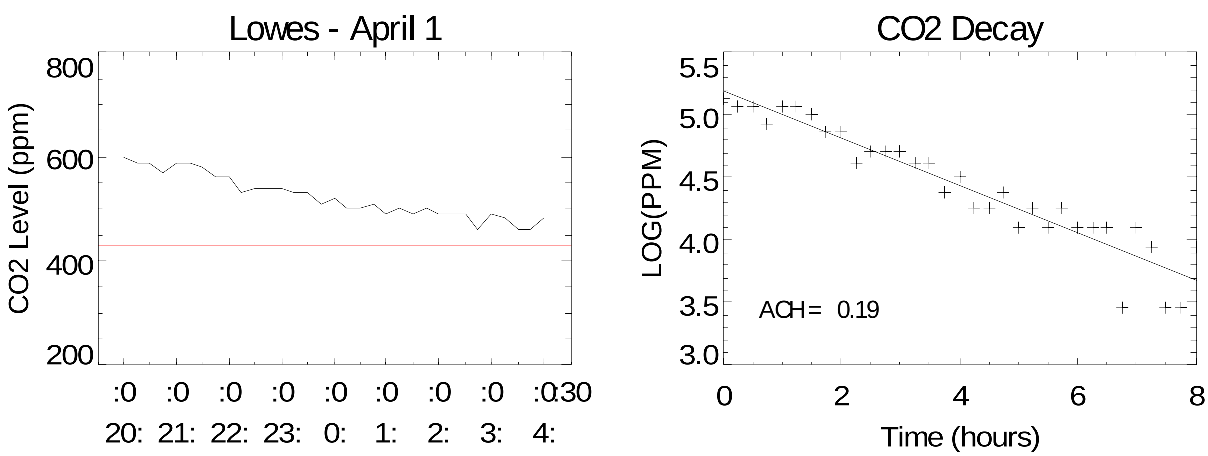

Figure A23-22. Decay of CO2 Concentration Near Garden Area on Overnight on April 1

Other Observations

The data considered in total are not consistent. While the store was observed to be negatively pressurized at 2-3 Pa, the measured net air flow into the build was positive (i.e., the ventilation in was greater than the exhaust out). This implies that the ventilation into the store was actually much lower than the measured ventilation determined from the measurements at each RTU. The other possibility was that much more exhaust is being provided by the front exhaust fan than implied by the design drawings.

Field Test Site 24 – Nursing Home, Waterville NY

Front of Building

Figure A24-1. Photo of Building

CHARACTERISTICS

Building Description

The 92 bed nursing home and extended care facility located in Waterville, NY. The 88,000 sq. ft. building is approximately 35 years old, and utilizes CMU block and brick façade construction, typical of institutional buildings of this age.

Construction Details

Building construction consists of 8-inch concrete masonry unit (CMU) construction and metal framed single pane operable windows. With the exception of a few resident rooms, no interior insulation is utilized. A spot inspection of doors and windows found most to be in appropriate operating condition given their age. Some visible light was observed through cracks around the exterior doors, and this should be addressed with weather stripping where appropriate. Because the HVAC system depressurizes the building, infiltration through cracks becomes a comfort issue, more than an energy issue. Sealing cracks will force fresh air to enter the building through the appropriate mechanical systems where it can be tempered, rather than directly mixing with space air. The roof has an appropriate level of rigid insulation (approximately 3-inches) applied prior to the most recent roof covering.

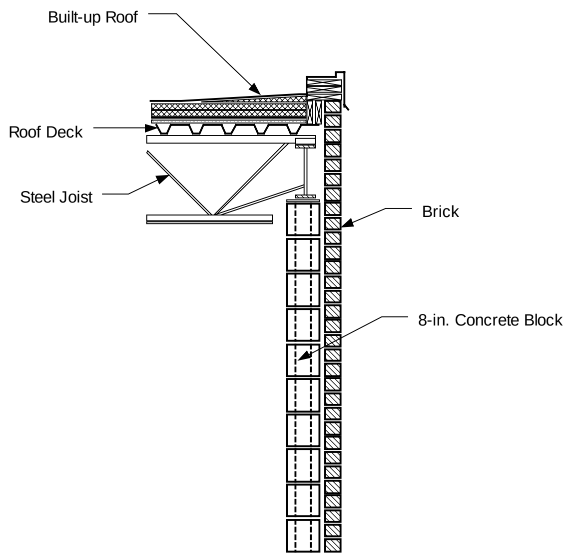

Figure A24-2. Roof and Wall Sections of the Building

HVAC System

Figure A24-3 displays typical HVAC equipment located on the rooftop, and Table A24-1 lists the model and size of the condensing units. The building has a total of 37-tons of cooling capacity installed, with an estimated maximum cooling power of 40 kW (based on 1.1 kW/ton).

Table A24-1. Rooftop Condensing Units

Unit #	Manuf.	Model	Tons
AC1	Trane XE 1200	TTP018C100A2	1.5
AC2	Trane	TTA036C300A0	3.0
AC3	Trane XE 1200	TTP030C100B0	2.5
AC4	Trane	TTA036C300A0	3.0
AC5	York	H1RA036525B	3.0
AC6	Mitsubishi Electric	PU24EK3	2.0
AC7	Mitsubishi Electric	PU24EK3	2.0
AC8	Trane XE 1200	TTP030C100B0	2.5
AC9	Mitsubishi Electric	PU18EK	1.5
AC10	Trane	TTA072C300A0	6.0
AC11	Mitsubishi Electric	PU18EK	1.5
AC12	Mitsubishi Electric	PU18EK	1.5
AC13	Trane	TTA048C300A0	4.0
AC14	York	H1RA036S256	3.0
Total			***37.0***

Trane 1.5 ton Condensing Unit (AC1)

York 3.0 ton Condensing Unit (AC5)

Mitsubishi Mini Split 1.5 ton Condensing Unit (AC11)

Figure A24-3. Typical Rooftop Condensing Units (3 of 14)

Figure A24-4 displays typical exhaust fan equipment located on the rooftop. No nameplate data were available, as the nameplates had been worn away. Actual airflow measurements were performed on each fan.

Exhaust Fan EF1 (1 of 4 typ) 1,000 – 2,600 SCFM

EF2 (1 of 2 typ) 130 – 160 SCFM

Exhaust Fan EF6 4,000 SCFM

Kitchen Hood Exhaust Fan EF5 3,400 SCFM

Figure A24-4. Typical Rooftop Exhaust Fans (4 of 10)

Figure A24-5 displays location of the equipment on the rooftop.

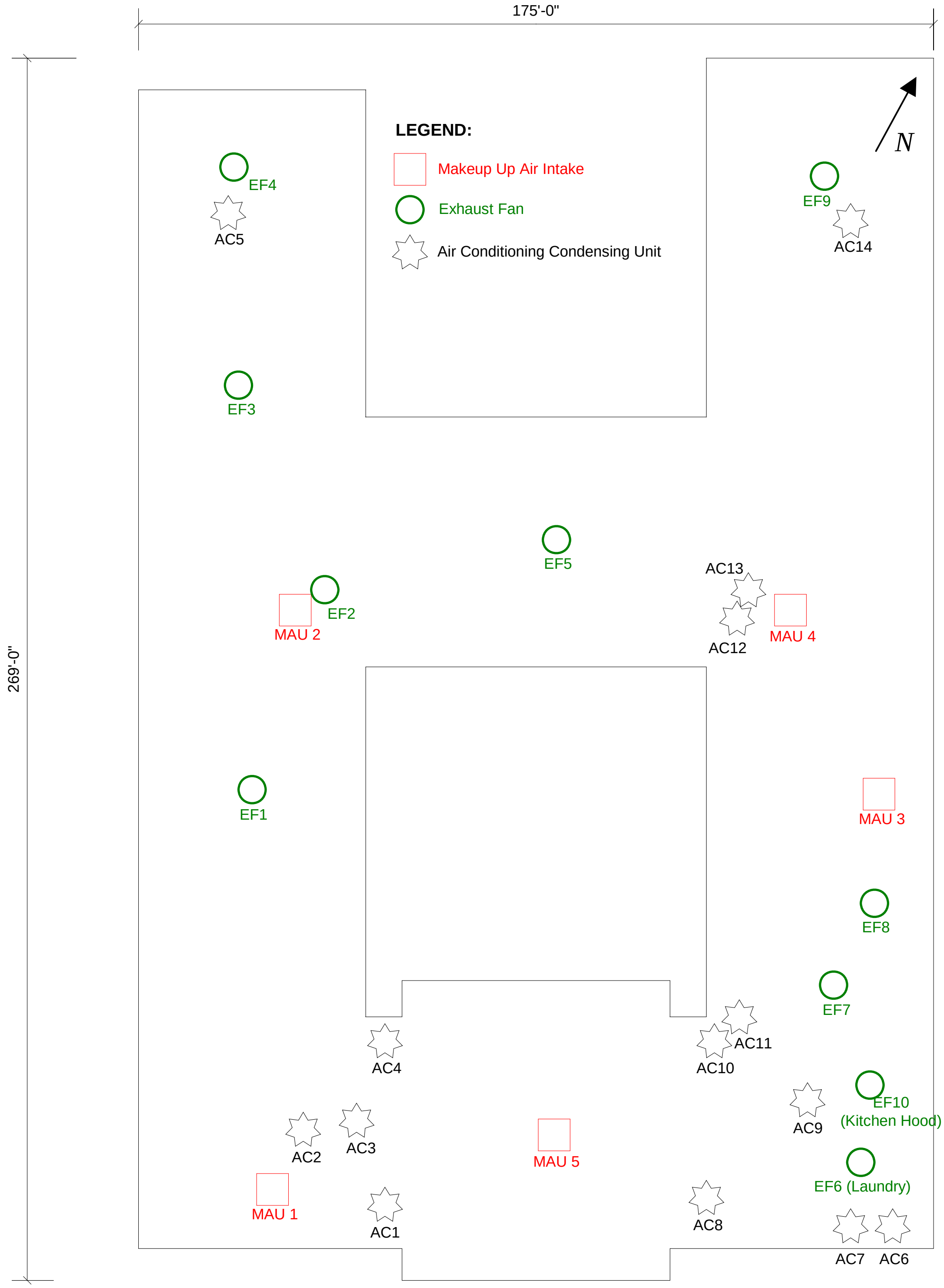

Figure A24-5. Rooftop Equipment Locations

MEASUREMENTS

A series of ventilation airflow measurements were performed on both the fresh air intakes and rooftop exhaust fans for the building, to determine the actual level of fresh air being introduced into the building. Mapping of the pressure differences from sampled zones was performed to identify any unusual airflow patterns in the building.

Pressure Mapping

Pressure differences between rooms and zones in the building were measured with all the air-handling equipment operating under normal conditions. A digital micro manometer (DG 700) was used to take the pressure measurements. Figure A24-6 and Figure A24-7 shows the locations where pressure measurements were taken. Mapping the pressure difference between zones allows for observation of the way air moves throughout the building.

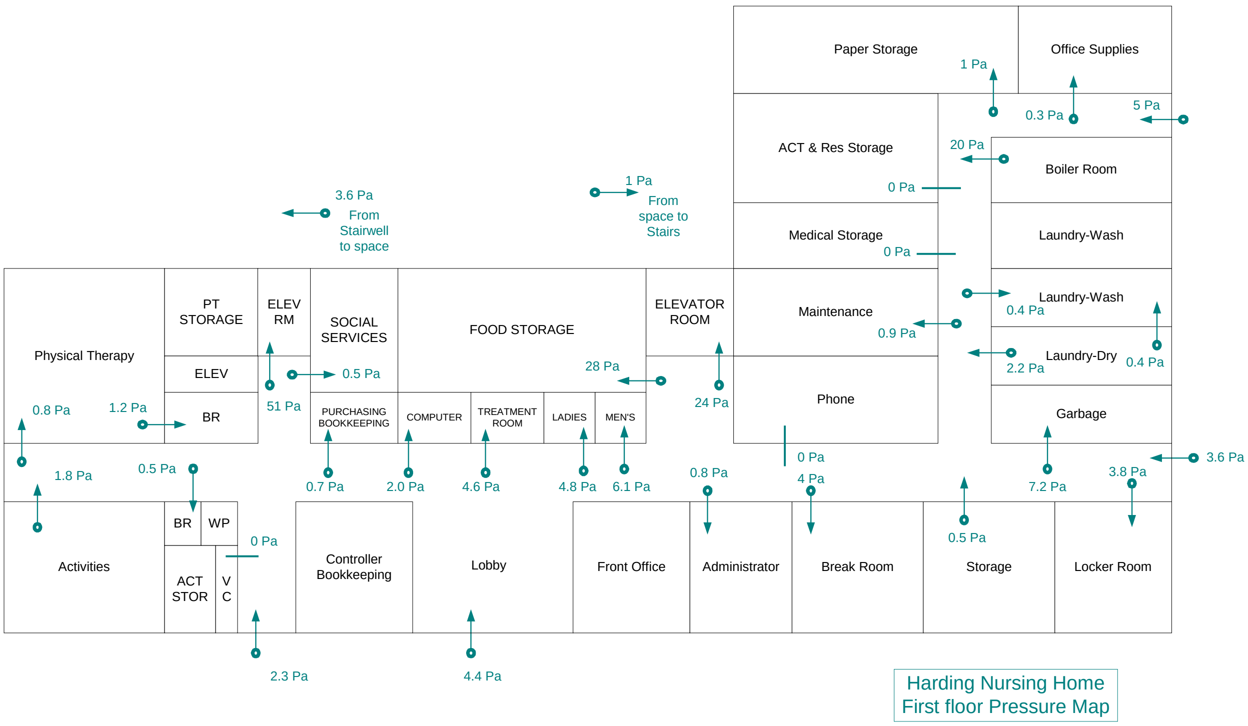

Figure A24-6. Pressure Differences on First Floor of Building

The pressure mapping indicates that the first floor of the building is under negative pressure compared to outdoors. This is consistent with the ventilation airflow balance calculation. The majority of the rooms are under negative pressure, compared to the hallway – indicating that most of the supply air from the AHU located in the food storage room is supplied to the hallway, and returned from the rooms. This is consistent with the building's original design intent.

The following zones on the first floor were observed to have unusual operation:

- Food Storage – The AHU in the food storage room does not use return ducting, but uses the entire food storage room as a plenum. This places this room under a large amount of negative pressure compared to the hallway. Cracks between the food storage room and adjacent elevator room are resulting in the pressure in the elevator room being depressed. This may result in the distribution of hydraulic oil fumes from the elevator sump being distributed throughout the building. This negative pressure is also observed to influence the adjacent treatment room and computer room.

- Boiler room – The boiler room is under high positive pressure compared to the hallway. This results from operation of sidewall ventilation fans that operate to maintain boiler room temperature within a reasonable range via ventilation. This may force fumes from the boiler operation into the adjacent occupied hallway areas.

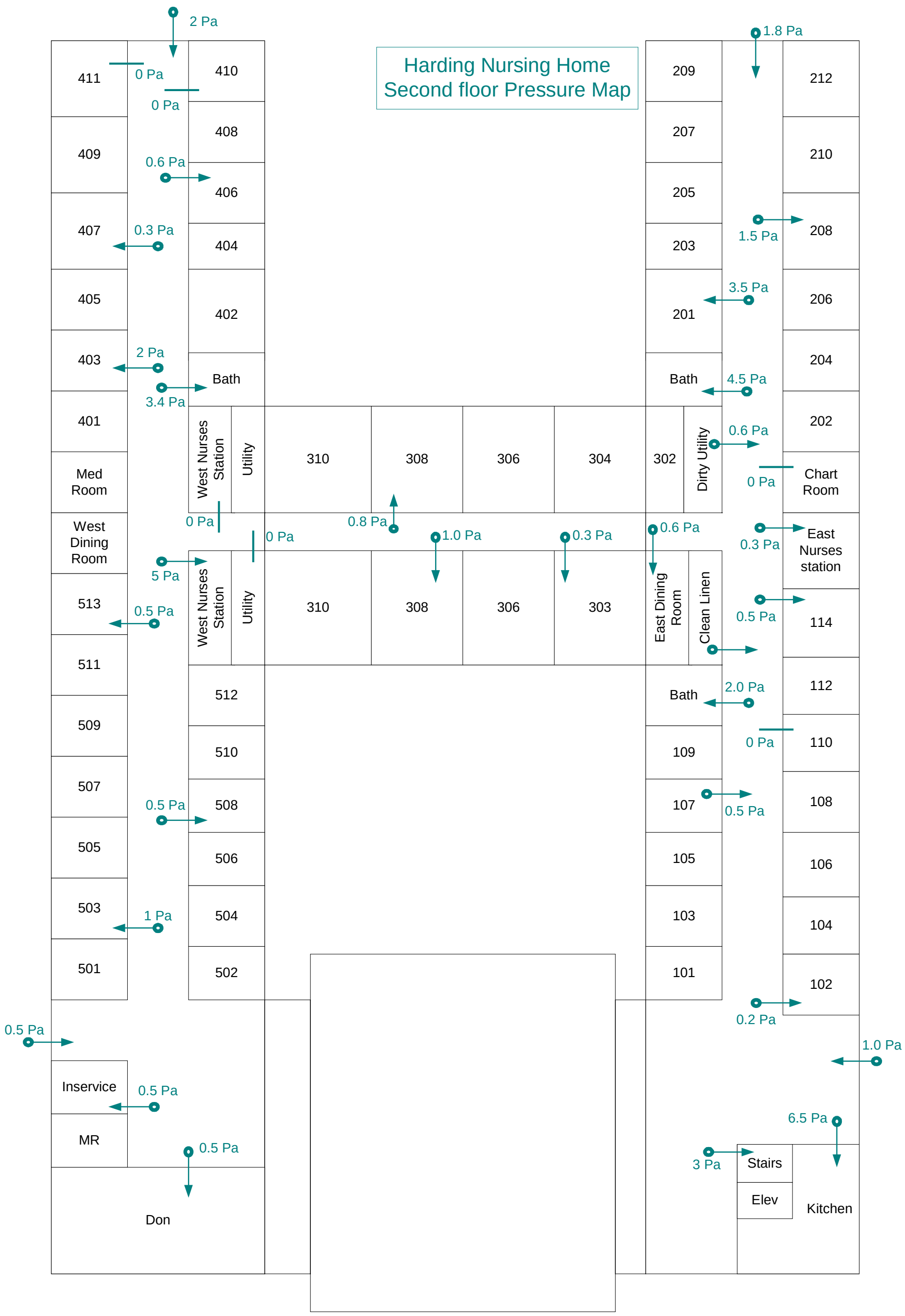

Figure A24-7. Pressure Differences on Second Floor of Building

The pressure mapping indicates that the second floor of the building is under negative pressure compared to outdoors, but the level of negative pressure is not as high as the first floor. Again, this is consistent with the ventilation airflow balance calculation. The majority of the patient rooms are under slight negative pressure, compared to the hallway. Negative pressure tends to increase with rooms closer to the bathrooms above which the exhaust fans are located. The kitchen is under a high degree of negative pressure due to the exhaust hood fan operation.

The following zones on the first floor were observed to have unusual operation:

- Clean Linen and Dirty Utility – Both rooms have positive pressure compared to the hallway. Care should be taken with storage of items in these rooms, as air is moved out of these rooms into the occupied hallway.

HVAC Ventilation and Airflow Measurements

A series of equal air traverse measurements were performed at each of the five makeup air intakes on the roof (Figure A24-8). Fresh air is induced through these makeup air intakes by the operation of an air handling unit (AHU) supply fan below. Fresh air is mixed with return air upstream of the heating and cooling coils where it is supplied to the hallways. The fraction of fresh air supplied is controlled by bypass dampers on the return side of the coil, which adjust the dampers proportionally using a manual pneumatic control. During the site visit, the typical damper setting was approximately 70% fresh air.

Figure A24-8. Makeup Air Intake Showing Traverse Points

Building Section: Green
MUA Unit # 2
Duct Length 34 in
Duct Width 34 in

	4 1/4"	12 3/4"	21 1/4"	29 3/4"	Average
4 1/4"	135	65	125	50	93.8
12 3/4"	230	200	210	55	173.8
21 1/4"	120	210	120	60	127.5
29 3/4"	85	205	45	45	95
					122.5 ft/min
					983.4 SCFM

Building Section: Pink
MUA Unit # 1
Duct Length 34 in
Duct Width 34 in

	4 1/4"	12 3/4"	21 1/4"	29 3/4"	Average
4 1/4"	45	50	55	55	51.3
12 3/4"	150	125	110	80	116.3
21 1/4"	130	70	125	50	93.8
29 3/4"	60	45	55	35	48.8
					77.5 ft/min
					622.2 SCFM

Building Section: Blue
MUA Unit # 3
Duct Length 34 in
Duct Width 22 in

	4 1/4"	12 3/4"	21 1/4"	29 3/4"	Average
8"	480	175	45	40	185
16"	410	295	70	45	205
					195 ft/min
					1012.9 SCFM

Building Section: Yellow/Purple
MUA Unit # 4
Duct Length 34 in
Duct Width 34 in

	4 1/4"	12 3/4"	21 1/4"	29 3/4"	Average
4 1/4"	160	215	250	125	187.5
12 3/4"	250	280	300	215	261.25
21 1/4"	110	275	225	230	210
29 3/4"	100	260	70	100	132.5
					197.8125 ft/min
					1588.0 SCFM

Table A24-2. MAU Traverse Data

EF1	
Pressure	Exhaust
(Pa)	(CFM)
5	2100
0	2160
-5	2200

EF2	
Pressure	Exhaust
(Pa)	(CFM)
5.2	149
0	133
-5	199

EF3	
Pressure	Exhaust
(Pa)	(CFM)
4.5	936
0	1043
5.1	1152

EF4	
Pressure	Exhaust
(Pa)	(CFM)
4.9	119
0	158
-5	188

EF5	
Pressure	Exhaust
(Pa)	(CFM)
5.1	718
0.4	747
-5	794

EF6	
Pressure	Exhaust
(Pa)	(CFM)
5.2	3845
0	4048
-5.2	4316

EF7	
Pressure	Exhaust
(Pa)	(CFM)
5.1	1557
0.1	1589
-5.1	1686

EF8	
Pressure	Exhaust
(Pa)	(CFM)
5	454
0	542
-5.1	595

EF9	
Pressure	Exhaust
(Pa)	(CFM)
5.1	2671
0.2	2632
-5.7	2783

EF10	
Pressure	Exhaust
(Pa)	(CFM)
4.9	3246
0.1	3495
-5.2	3525

Table A24-3. Exhaust Fan Flow Measurements – All Fans

EF1		
Pressure	Exhaust	Current
(Pa)	(CFM)	(Amp)
5	2100	6.7-6.8
0	2160	>6.7
-5	2200	6.7
		6.7-6.8 (open tent)

EF2		
Pressure	Exhaust	Current
(Pa)	(CFM)	(Amp)
4.5	936	6.7-6.8
0	1043	6.8
5.1	1152	6.8

Table A24-4. Exhaust Fan Flow Measurements Examining Impact of Adding Flow Tent to Backpressure

Traverse results for four of the makeup air intakes are summarized in Table A24-5. The fifth makeup air intake is located above the second floor dining area, and is not connected to an AHU. It strictly serves as a pressure relief for the building – but fresh air entering through this makeup air intake is not heated nor cooled.

Table A24-5. Makeup Air Intake Flows

Makeup Air Intake Number (From Figure A24-5)	**Wing**	*Fresh Air Flow*
MAU 1	Pink	622 SCFM
MAU 2	Green	983 SCFM
MAU 3	Blue	1,565 SCFM
MAU 4	Yellow/Purple	1,587 SCFM
Total		**4,759 SCFM**

The fresh air flow through the exhaust fans was measured by placing a capture tent over each exhaust fan and then running all the exhaust air through a duct-blaster fan, adjusting the duct-blaster to close to zero differential pressure across the tent. The duct-blaster fan is a calibrated fan which the pressure drop and flow relation are known. The airflow for each exhaust fan is shown in Figure A24-9.

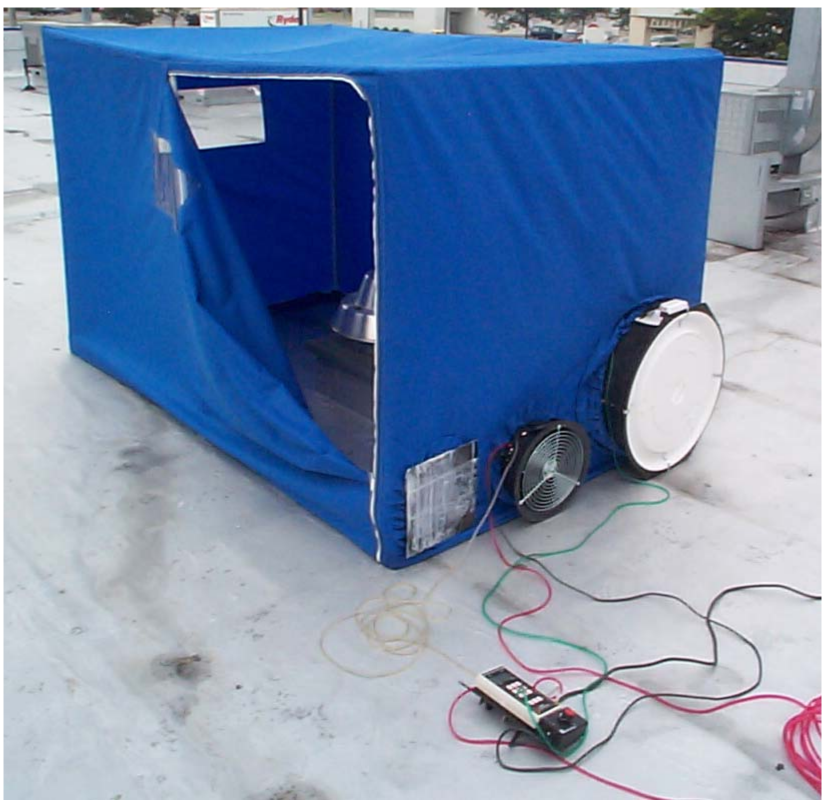

Figure A24-9. Exhaust Fan Capture Tent (Typical Installation)

Table A24-6. Exhaust Air Flows

Exhaust Fan Number (From Figure A24-5)	Wing	Exhaust Air Flow
EF1	Pink	2,160 SCFM
EF2	Pink	133 SCFM
EF3	Green	1,043 SCFM
EF4	Green	158 SCFM
EF5	Yellow	750 SCFM
EF6	First Floor (Laundry, garbage, locker rooms)	4,048 SCFM
EF7	Blue	1,590 SCFM
EF8	Blue	542 SCFM
EF9	Purple	2,634 SCFM
EF10	Kitchen	3,498 SCFM
Total		**16,556 SCFM**

The building exhausts a total of 16,556 SCFM, and the makeup air inlets on the AHUs introduce 4,759 SCFM of fresh air. This implies that 11,797 SCFM of fresh air enters the building through other means, including through the fresh air intakes on the fan-coil units located in each room, through cracks and around door openings, and through the pressure relief intake located above the dining room (Figure A24-10). The total exhaust air flow rate is from the building is 0.19 cfm per square foot of floor area.

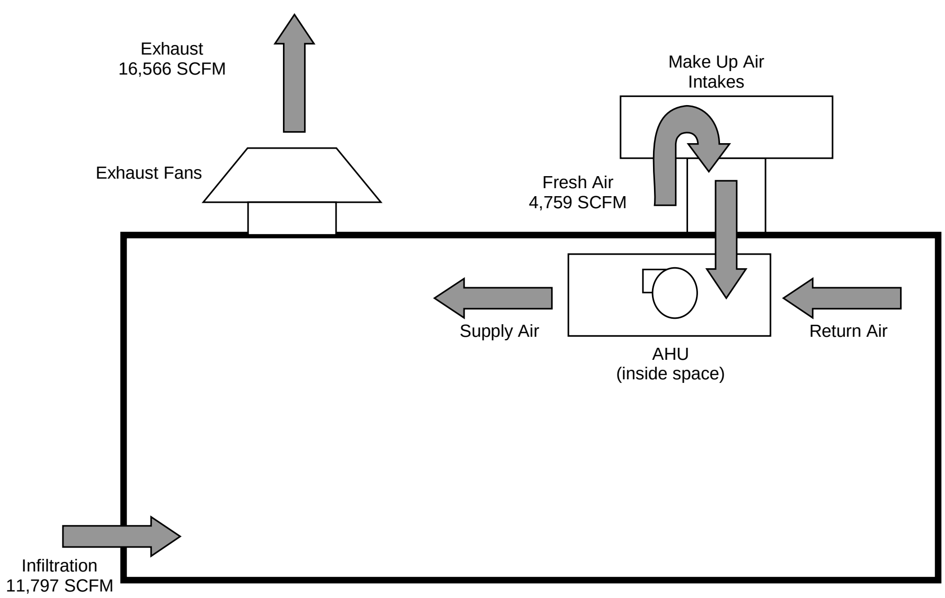

Figure A24-10. Airflow Balance on Building

Building Envelope Airtightness

Due to the nature of the building, we were not able to assess building leakage rates using fan depressurization methods. However, the leakage characteristics of the building envelope were inferred from the air flow imbalance and the operating pressure of the building. This single operating point is used with an assumed exponent of 0.58 to 0.62 to find the flow coefficient.

The resulting ACH_{50} was 5.0-7.1, assuming the range of measured pressures and exponents. This implies the building was fairly tight.

Flow Imbalance:	10,997 cfm (exhaust, assumes 400 cfm though 5^{th} MAU intake)
Pressure:	-2 to -3 Pa
Assumed Exponent (n):	0.58-0.62
Resulting cfm_{50}:	58,300-83,800 cfm
Resulting ACH_{50}:	5.0-7.1 1/h
Assumed Flow Equation:	$Q = 6577 \cdot \Delta p^{0.60}$

Space Conditions

Figure A24-11 shows the average temperature profiles and Figure A24-12 shows the relative humidity profiles for the office section of the building based on temperature readings taken with a HOBO data logger.

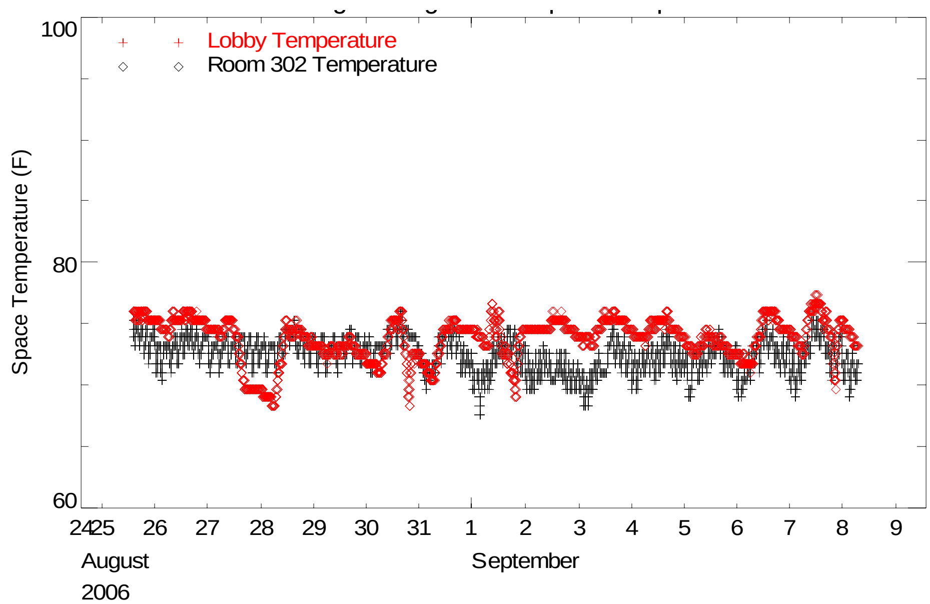

Figure A24-11. Measured Space Temperature Profile (August 25 to September 8)

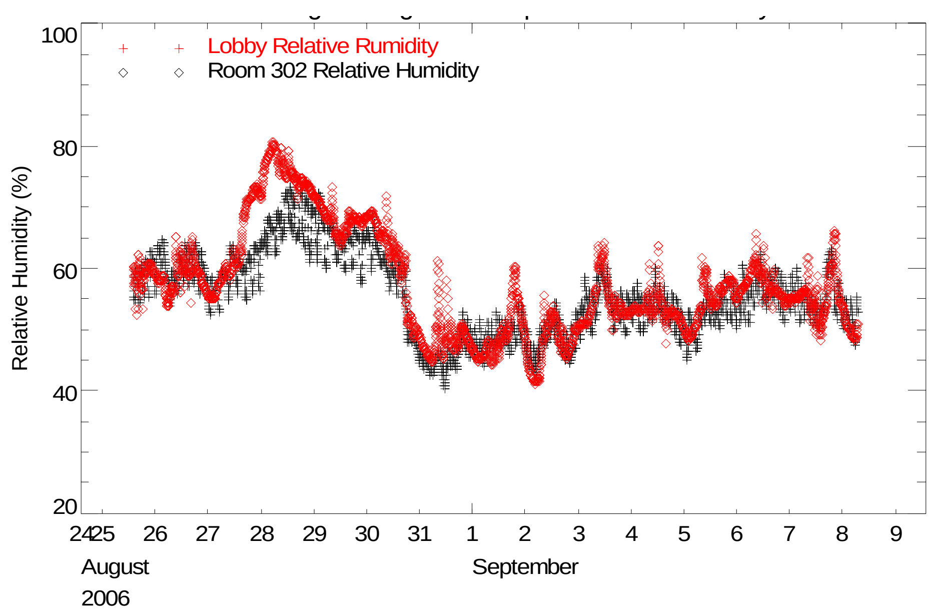

Figure A24-12. Measured Relative Humidity Profile (August 25 to September 8)

Measured CO2 Levels

Figure A24-13 shows the CO_2 concentration from the occupants in the lobby. Figure A24-14 shows the CO_2 concentration from the occupants in Room 302. The decay of the occupants CO_2 was measured after they had left the room.

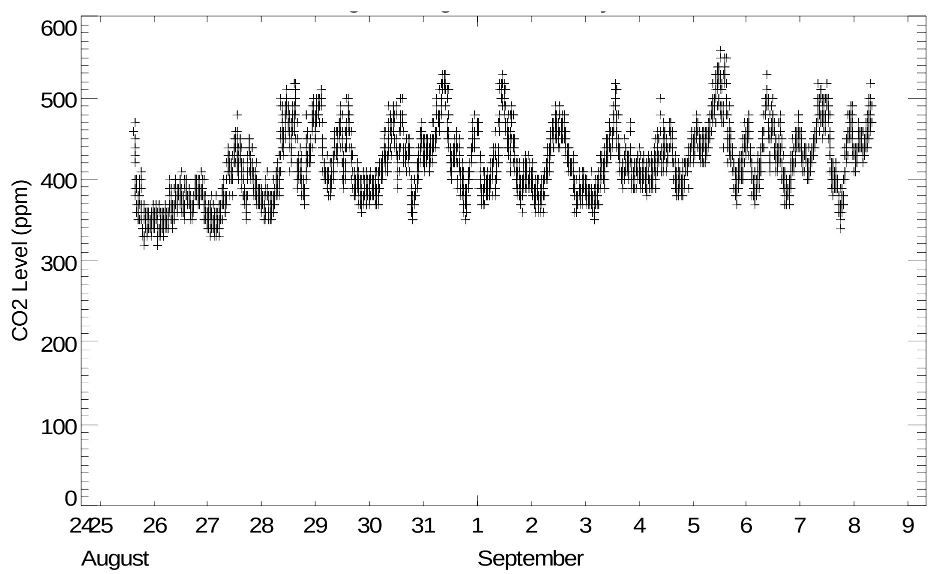

Figure A24-13. Measured CO2 Concentration for Lobby (August 25 to September 8)

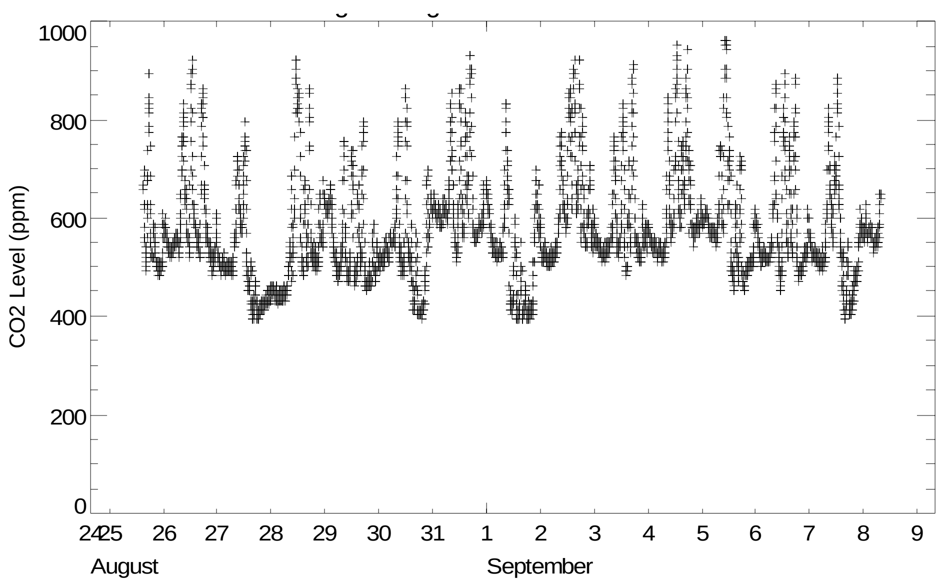

Figure A24-14. Measured CO2 Concentration for Room 302 (August 25 to September 8)

Figure A24-15 and Figure A24-16 show the resulting decay trends using CO_2 levels immediately after high occupancy periods. The predicted air change rate (ACH) is shown on each plot.

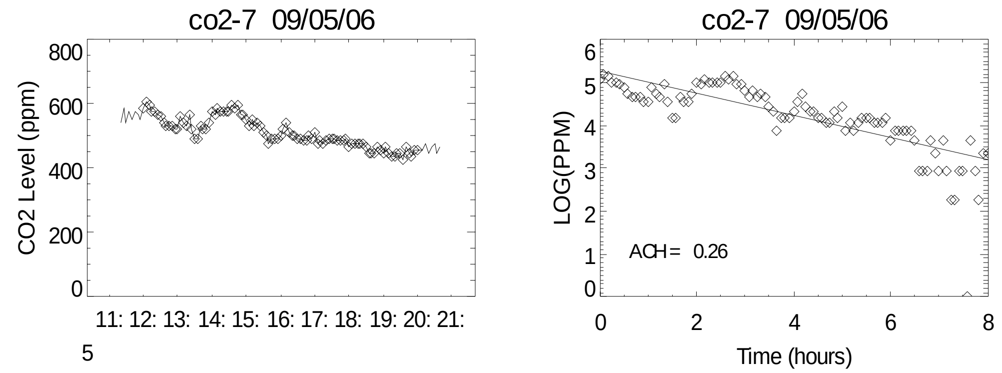

Figure A24-15. Tracer Gas Decay Using CO2 for Various Periods for the Lobby

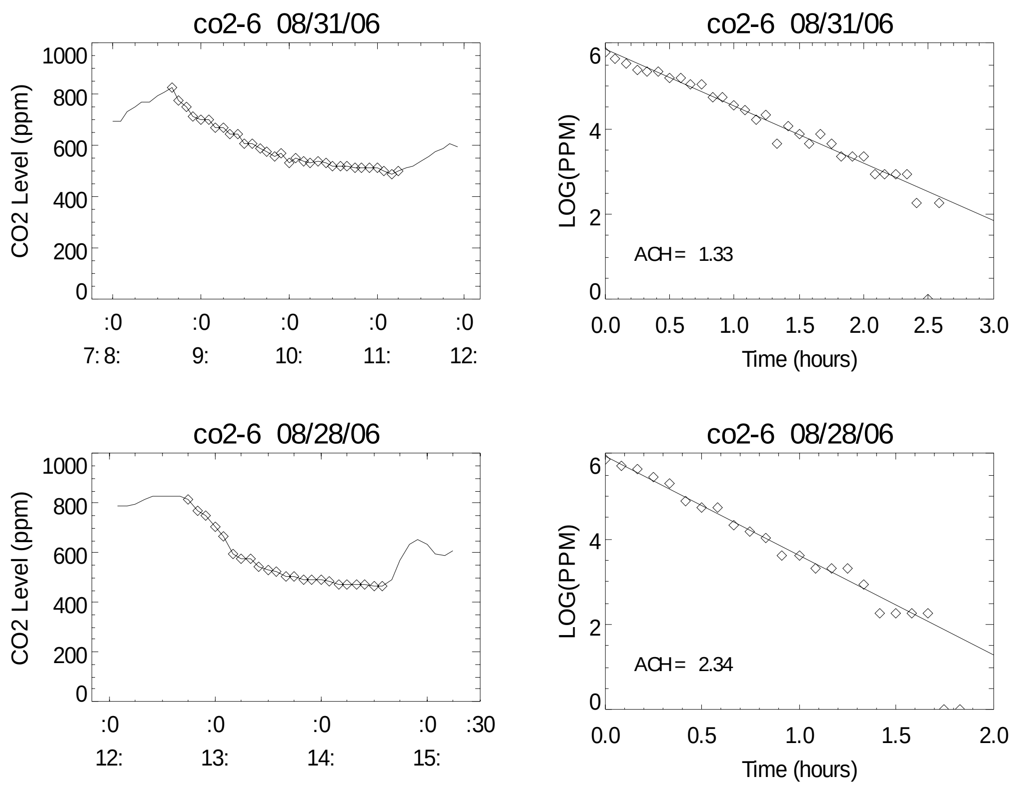

Figure A24-16. Tracer Gas Decay Using CO2 for Various Periods for Room 302

The implied ACH in these areas ranged from 1.3 to 2.3 air changes per hour. This is roughly in line with the measured exhaust of 16,556 cfm (or an average ACH or 1.4 for building).

Utility Bills

Table A24-7 displays the electric and natural gas utility data available for the facility. The building is billed under the NYSEG Non-residential time-of-use rate, which separates energy and demand consumption into on-peak and off-peak periods. The on-peak period spans from 7:00 AM to 11:30 PM each day, and all other times are off-peak. The facility has a nearly even split in energy consumption between the on and off-peak periods. The demand patterns also show only slight differences between the periods

Natural gas data showed use increasing during the winter months in response to higher heating loads, and decreasing to a base-load of approximately 2,500 therms/month during the summer months from hot water and kitchen operation. The

Table A24-7. Gas and Electric Utility Data

		Energy Use			Demand			Gas Use
End Date	No. Days	On-Peak (kWh)	Off-Peak (kWh)	Total (kWh)	On-Peak (kW)	Off-Peak (kW)	Total (kW)	Total (therms)
Sep-04								2,780
Oct-04								7,138
Nov-04								9,532
Dec-04	34	28,320	30,080	58,400	124.8	124.8	124.8	13,013
Jan-05	30	27,840	24,160	52,000	126.4	126.4	126.4	14,464
Feb-05	32	26,240	27,360	53,600	124.8	113.6	124.8	11,578
Mar-05	29	24,480	22,880	47,360	121.6	115.2	121.6	11,686
Apr-05	28	22,560	21,920	44,480	120.0	115.2	120.0	7,159
May-05	30	24,320	24,000	48,320	121.6	110.4	121.6	5,954
Jun-05	32	27,200	30,720	57,920	139.2	134.4	139.2	2,748
Jul-05	30	30,720	29,280	60,000	145.6	132.8	145.6	2,239
Aug-05	29	28,960	26,560	55,520	140.8	140.0	140.8	2,166
Sep-05	32	27,360	30,880	58,240	136.0	120.0	136.0	3,489
Oct-05	29	25,920	24,960	50,880	131.2	120.0	131.2	6,954
Nov-05	27	22,560	22,720	45,280	124.8	112.0	124.8	8,695
Dec-05	28	23,360	23,840	47,200	126.4	113.0	126.4	11,248
Jan-06	28	24,160	23,840	48,000	126.4	120.0	126.4	10,454
Feb-06	32	29,280	25,600	54,880	123.2	112.0	123.2	10,833
Mar-06	34	28,000	28,160	56,160	121.6	110.4	121.6	10,465
Apr-06	34	27,360	28,000	55,360	123.2	116.8	123.2	7,030
May-06	28	22,560	23,200	45,760	123.2	115.2	123.2	5,226
Jun-06	30	25,920	27,040	52,960	144.0	129.6	144.0	3,427
Jul-06	33	29,920	33,280	63,200	147.2	132.8	147.2	2,591
Past Year	***364***	***315,360***	***318,080***	***633,440***	***147.2***	***140.0***	***147.2***	***82,579***
		49.8%	50.2%	100.0%				

7.2	kWh/ft^2-yr	93.8	MBtu/ft^2-yr

The following figures display the variation in utility data with ambient temperature during that period. Ambient temperature is the single largest driving factor with the energy use variation at the facility, because the nursing home has continuous occupancy and a very regular operating schedule. Comparing the utility use trend versus ambient temperature allows us to separate the temperature dependant portions of the energy use from the base-load energy use.

Figure A24-17 and Figure A24-18 displays the variation in energy use and demand with ambient temperature. Both energy use and demand data were separated into on-peak and off-peak period. Total energy use for the facility is calculated by adding the on-peak and off-peak energy together. Total demand for the facility is determined by taking the maximum of the on-peak and off-peak demand for each billing cycle. For the Harding Nursing Home, the on-peak data is always higher than the off-peak demand data, by approximately 10 kW.

The energy trend indicates an increasing energy trend as ambient temperature moves away from 59ºF. The slightly increasing energy with decreasing ambient temperature occurs due to higher lighting runtimes during the darker, colder winter months. The increasing energy consumption with increasing ambient temperature occurs due to higher HVAC cooling operation. The trend indicates that there is a maximum of 590 kWh/day of HVAC operation (determined by evaluating the trend at 85ºF average daily temperature). By integrating the energy trend with daily typical meteorological year data, it was determined that cooling operation at the nursing home represents approximately 23,900 kWh/year, or 4% of the total energy use.

The utility data available is plotted against the ambient temperature during that period. The various plots below show the temperature dependent loads.

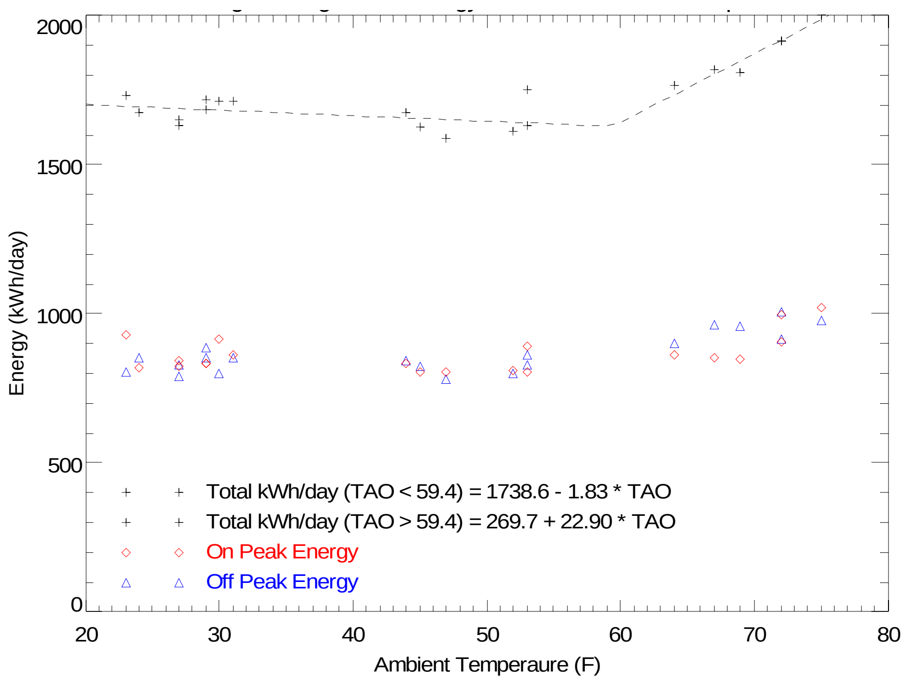

Figure A24-17. Energy Use Variation with Ambient Temperature

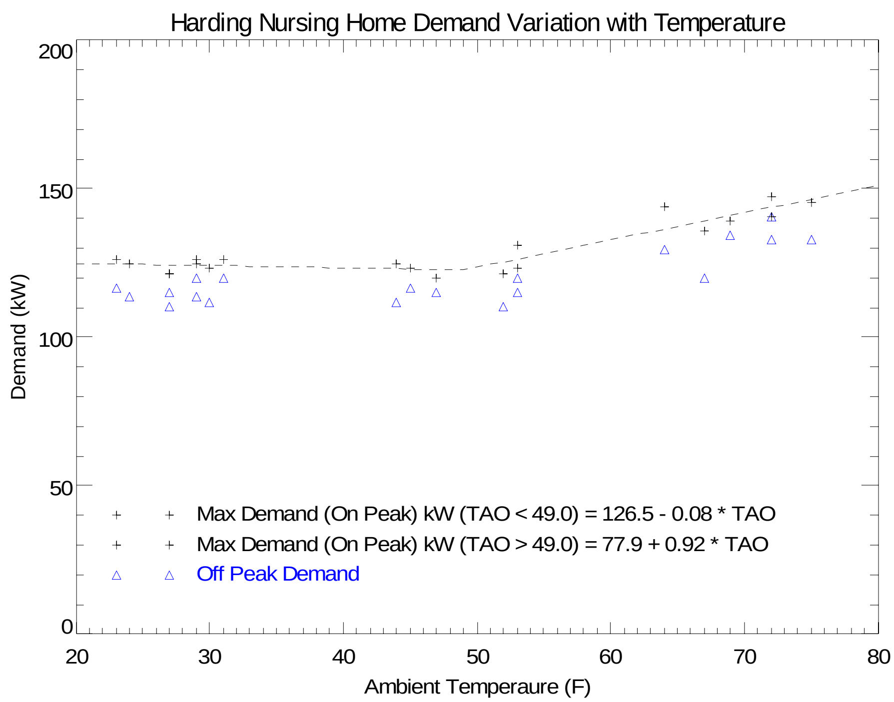

Figure A24-18. Demand Variation with Ambient Temperature

Figure A24-19 displays the natural gas use variation with ambient temperature. The natural gas use increases linearly with decreasing ambient temperature. The high ventilation rate for the facility results in little change between space heating gas use and domestic water heating (DHW) gas. It is assumed that the four months of data with average ambient temperature above 70ºF represents the temperature independent baseload. Baseload gas use (primarily used for DHW production, and some kitchen operation) consists of 24% of the total natural gas use.

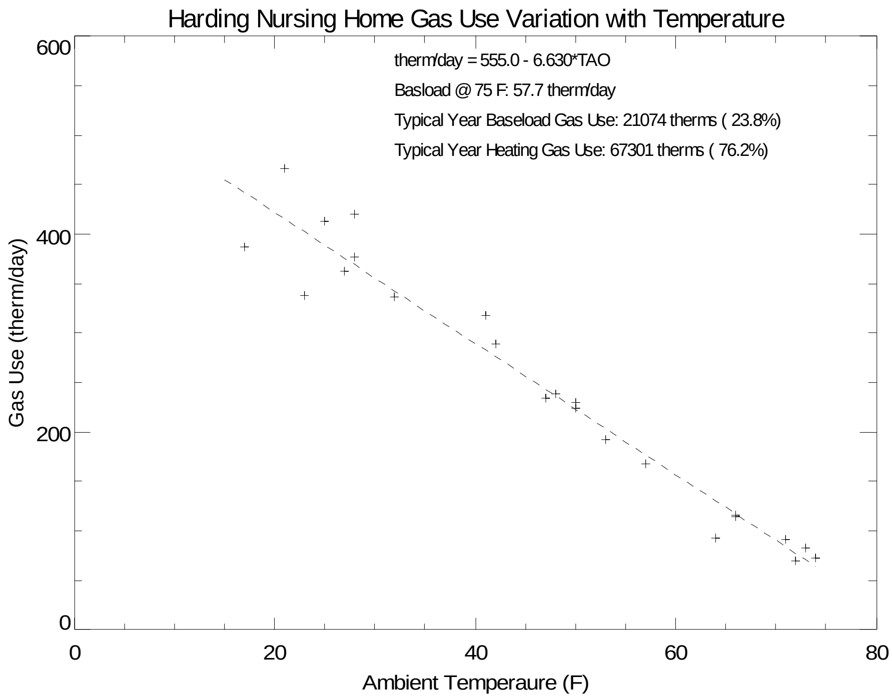

Figure A24-19. Natural Gas Use Variation with Ambient Temperature

Field Test Site 25 - Small Office Building/Apartment, Cazenovia NY

Apartment Entrance in Front (South)

Office Entrance on Side (North)

Figure A25-1. Photos of Building

CHARACTERISTICS

Building Description

The facility is a 2,010 square foot commercial office space with an attached 800 square foot apartment. Both the apartment and office space are accessible through the front door while the office has a separate door on the side of the building. The commercial space consists of five offices, two half-bathrooms and a conference room (with cathedral ceilings). There is a basement with 10-foot ceilings and concrete floors and walls, which is accessible through a open staircase at the back of the building. There is also a second unfinished basement that has a 5-foot ceiling and a hatch to outdoors.

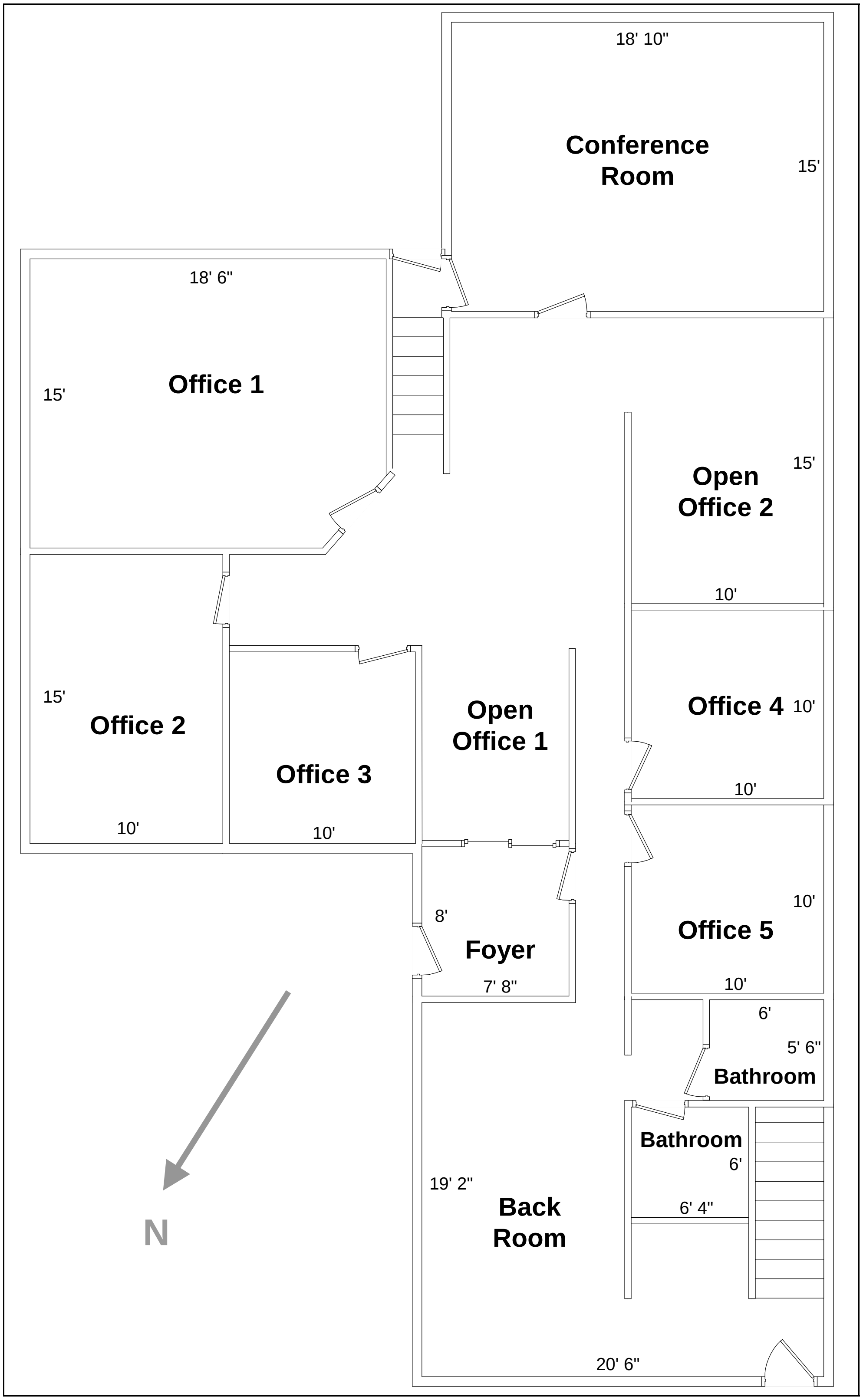

Figure A25-2. First Floor Plan (Office Section)

Construction Details

The structure was completed remodeled in 1997. The original farmhouse was built in the 19th century and used irregular-sized lumber in the construction. In 1997, the original farmhouse was "gutted to the studs" and additions were added on the front and back.

For the addition, the exterior walls are typical 2x6 stick frame construction with vinyl and Celtex insulation on the exterior. The interior has typical dry wall with a 5-mil poly vapor barrier to limit moisture transfer. The exterior walls contain 6-inch fiberglass batts. The roof on the addition is typical plywood decking with asphalt shingles supported by 2x6 wooden trusses. Ceiling insulation is provided by 6-in paper-backed fiberglass batts above fiberboard. There is an 8-inch plenum above a T-bar drop ceiling in the office area. The attic above the new structure in the back is partially finished with a plywood deck. The conference room at the front of the building has cathedral ceilings.

The old roof has a plywood deck on top of irregular 1-inch wooden boards and supported by 3x5 wooden beams. The old roof is mainly above the apartment with a small attic area that is connected by an open-air space to the attic over the addition.

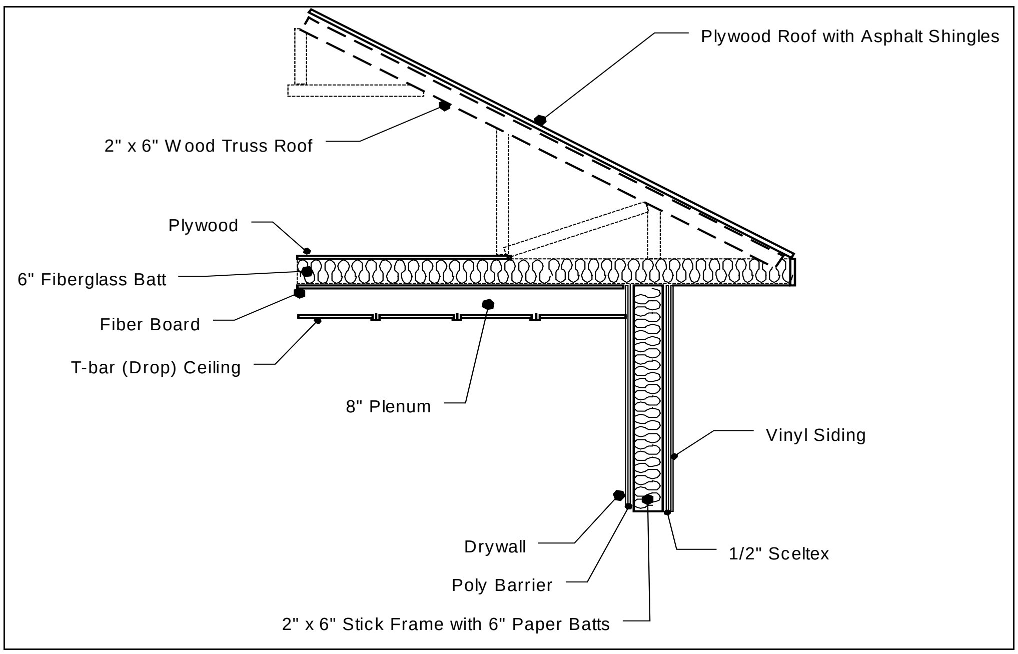

Figure A25-3. Roof and Wall Sections of the Addition along the Length of the Office Section of the Building

HVAC System

A conventional oil-fired boiler heats the office area by hot water baseboard radiators on the perimeter of the building. Cooling is provided by five window air conditioning units with two located in the main area and three smaller units located in three of the offices. In the summer, two A/C units in the main area of the office operate continuously to control moisture. The remaining three A/C units are operated manually by the occupants of these offices. These three units operate roughly 8am-5pm during the summer. These units are typically removed from the windows in late September and installed in early May.

Table A25-1 lists the installed HVAC equipment for both the office section and the restaurant.

Table A25-1. HVAC Equipment Installed at Site

Location	Equipment	Cooling Capacity (Btu)	EER (Btuh/W)	Power Rating (W)	Refrigerant / Pressure (psig)
Office 1	Haier HW-05CB12	5,000	8.8	568	R22 170 – 300
Office 2	General Electric AGW10ACG1	10,000	9.8	1,020	R22 150 – 350
Office 4	Samsung AW0516	5,000	8.0	625	R22 150 – 300
Open Office 2	Fedders A6Q10F2A	10,000	9.8	1,020	Unknown
Back Room	Goldstar LW-C1212CL	12,000	9.5	1,260	R22 150 – 350

MEASUREMENTS

The test data below was taken in September and October 2006. Blower door and pressure mapping measurements were taken on September 12 for building with the A/C units installed. The building was re-tested with the A/C units removed on October 3 and October 27.

Building Envelope Airtightness

The leakage characteristics of the enclosure were assessed using fan depressurization methods. For the depressurization testing, a Minneapolis Blower Door was used to depressurize the interior of the building. The external windows and doors were all closed to test the tightness of the building. We completed multiple tests while isolating parts of the office space to estimate the effects of leakage from different areas. Table A25-2 displays a summary of the blower door tests.

Table A25-2. Summary Table of Blower Door Depressurization Tests

Test No.	Date	Test Description	Flow Coeff. (K)	Exp. (n)	Leakage Area (in^2)	ACH @ 50
1	Sep 12	No basement sealing, door to upstairs apartment closed, depressurization, A/C Units Installed	715	0.598	464	23.5
2	Oct 3	Basement taped off at bottom of stairs, door to upstairs apartment closed, depressurization	622	0.593	401	25.1
3	Oct 3	Basement half door taped off, door to upstairs apartment closed, depressurization	677	0.611	448	23.4
4	Oct 3	No basement sealing, door to upstairs apartment closed, depressurization	670	0.609	441	23.0
5	Oct 3	No basement sealing, door to upstairs apartment open, depressurization	682	0.624	459	18.9
6	Oct 27	No basement sealing, door to upstairs apartment open, depressurization, gaskets installed	512	0.677	371	17.4
7	Oct 27	Basement half door taped off, door to upstairs apartment open, depressurization, gaskets installed	466	0.696	347	17.1

Comparing the results of the various blower door tests yield the following conclusions:

- The leakage area from having the A/C units installed (and the bathroom exhaust vents open) was 23 in^2 (comparing Tests 4 and 1).
- The basement half-door leakage area is about 24 in^2 (comparing Tests 7 and 6).
- By installing wall outlet gaskets, the leakage area of the office area was reduced by 88 in^2 (comparing Tests 6 and 5).

The following section gives details of each blower door test conducted at the site.

Test 1: A/C Units Installed, Basement Open, Apartment Closed (Sep 12)
The first test for the office section used the blower door to depressurize the building to several pressures between 10 and 40 Pa. The test was conducted with all interior doors open and all exterior doors and windows closed. The stairway to the basement was open and the door to the upstairs apartment was closed. Figure A25-5 shows the office section leakage variation with building pressure. The office section of the building has an effective leakage area of approximately 6.93 sq in per 100 sq ft of the total envelope and floor area of the first floor. The office section of the building has an ACH_{50} of 23.5

Test 2: A/C Units Removed, Basement Stairway Closed, Apartment Closed (Oct 3)
The second test for the office section used the blower door to depressurize the building to several pressure differences between 10 and 50 Pa. The test was conducted with all interior doors open and all exterior doors and windows closed. The bathroom exhaust fans were blocked off.

The stairway to the basement was taped off using a plastic sheet and duct mask (see Figure A25-4) and the door to the apartment was closed. The taped off basement setup only held for Test 2. Figure A25-6 shows the office section leakage variation with building pressure for this test. The ELA of the office section of the building has an effective leakage area of approximately 7.06 sq in per 100 sq ft of the total envelope and floor area. The office section of the building has an ACH_{50} of 25.1.

Figure A25-4. Entrance to Basement Sealed and Bathroom Exhaust Covered (Test 2)

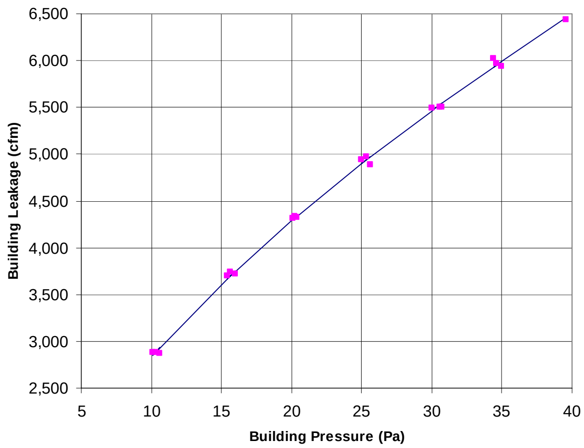

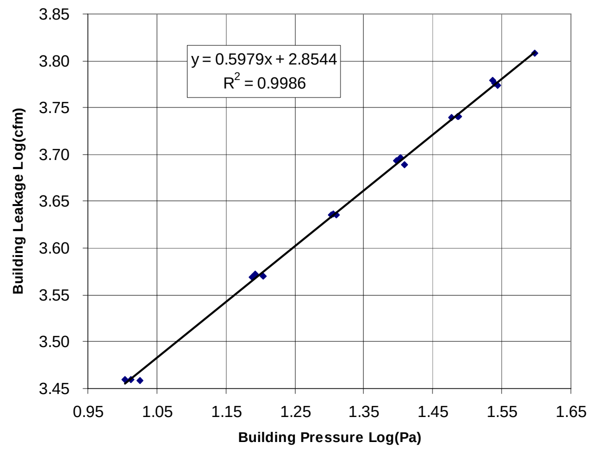

Flow Coefficient (K)	715.2	2524 sq ft. floor area
Exponent (n)	0.598	
Leakage area (LBL ELA @ 4 Pa)	464 sq in	6.93 ELA / 100 sq ft
Airflow @ 50 Pa	7,418 cfm	23.5 ACH @ 50

Test Data:

	Nominal Building Pressure (Pa)	Nominal Flow (cfm)	Ring
1	39.6	6,433	none
2	35.0	5,935	none
3	34.4	6,019	none
4	34.6	5,968	none
5	30.7	5,505	none
6	30.6	5,498	none
7	30.0	5,488	none
8	25.0	4,941	none
9	25.6	4,883	none
10	25.3	4,974	none
11	20.2	4,332	none
12	20.4	4,322	none
13	20.1	4,319	none
14	15.4	3,703	none
15	15.6	3,739	none
16	16.0	3,720	none
17	10.3	2,885	none
18	10.1	2,881	none
19	10.6	2,873	none

Notes: ELA is leakage area (in square inches) at reference pressure of 4 Pa.
ELA per 100 sq ft is based on total building envelope surface area (ceiling, walls and floor).

Figure A25-5. Test 1 Office Section – Blower Door Test Results

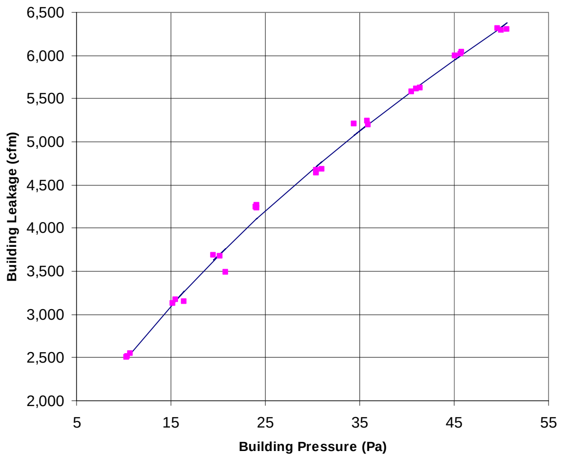

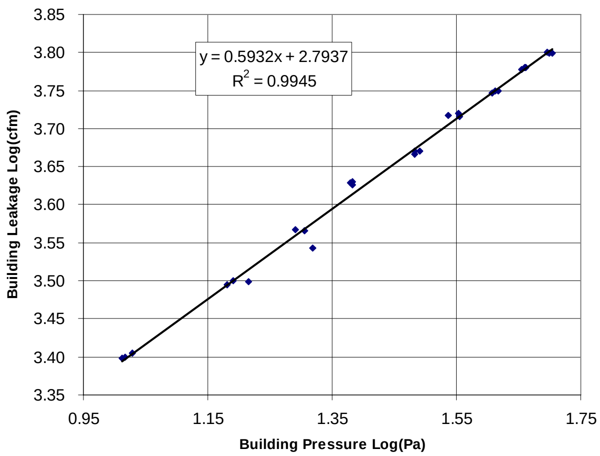

Flow Coefficient (K)	621.9		2016 sq ft. floor area
Exponent (n)	0.593		
Leakage area (LBL ELA @ 4 Pa)	401	sq in	7.06 ELA / 100 sq ft
Airflow @ 50 Pa	6,333	cfm	25.1 ACH @ 50

Test Data:

	Nominal Building Pressure (Pa)	Nominal Flow (cfm)	Ring
1	49.6	6,310	none
2	50.6	6,304	none
3	50.0	6,293	none
4	45.1	5,992	none
5	45.7	6,023	none
6	45.8	6,035	none
7	40.5	5,581	none
8	41.0	5,615	none
9	41.4	5,625	none
10	34.4	5,210	none
11	35.8	5,242	none
12	35.9	5,195	none
13	30.4	4,636	none
14	30.4	4,677	none
15	31.0	4,680	none
16	24.0	4,250	none
17	24.1	4,266	none
18	24.1	4,233	none
19	20.2	3,679	none
20	19.5	3,691	none
21	20.8	3,491	none
22	15.2	3,126	none
23	15.5	3,167	none
24	16.4	3,153	none
25	10.4	2,510	none
26	10.7	2,542	none
27	10.3	2,500	none

Notes: ELA is leakage area (in square inches) at reference pressure of 4 Pa.
ELA per 100 sq ft is based on total building envelope surface area (ceiling, walls and floor).

Figure A25-6. Test 2 Office Section – Blower Door Test Results

Test 3: A/C Units Removed, Basement Half-Door Taped Off, Apartment Closed (Oct 3)
The third test for the office section used the blower door to depressurize the building to several pressure differences between 10 and 40 Pa. The test was conducted with all interior doors open and all exterior doors and windows closed. The bathroom exhaust fans were blocked off.

The half-door from the full basement to the half basement was taped off using a plastic sheet and duct mask (similar to the full basement in Figure A25-4) and the door to the apartment was closed. Figure A25-7 shows the office section leakage variation with building pressure for this test. The ELA of the building has an effective leakage area of approximately 6.68 sq in per 100 sq ft of the total envelope and floor area. The office section of the building has an ACH_{50} of 23.4.

Test 4: A/C Units Removed, Basement Open, Apartment Closed (Oct 3)
The fourth test for the office section used the blower door to depressurize the building to several pressure differences between 10 and 40 Pa. The test was conducted with all interior doors open and all exterior doors and windows closed. The bathroom exhaust fans were blocked off.

Similar to Test 1, the basement half-door was not taped off and the apartment door was closed. However, for this test the air conditioners had been removed and the windows were shut. The bathroom exhaust fans were also blocked. Figure A25-8 shows the office section leakage variation with building pressure for this test. The ELA of the office section of the building has an effective leakage area of approximately 6.59 sq in per 100 sq ft of the total envelope and floor area. The office section of the building has an ACH_{50} of 23.0

Test 5: A/C Units Removed, Basement Open, Apartment Open (Oct 3)
The fourth test for the office section used the blower door to depressurize the building to several pressure differences between 10 and 35 Pa. Unlike the other tests, the door to the upstairs apartment was open the test the entire building. The test was conducted with all interior doors open and all exterior doors and windows closed.

The total building was depressurized to 35 Pa with the door open to the upstairs apartment. Including the basement, office and the apartment, the building total square footage for this test was approximately 3,324 ft^2. Figure A25-9 shows the office section leakage variation with building pressure for this test. The ELA of the building has an effective leakage area of approximately 5.02 sq in per 100 sq ft of the total envelope and floor area. The total building has an ACH_{50} of 18.9.

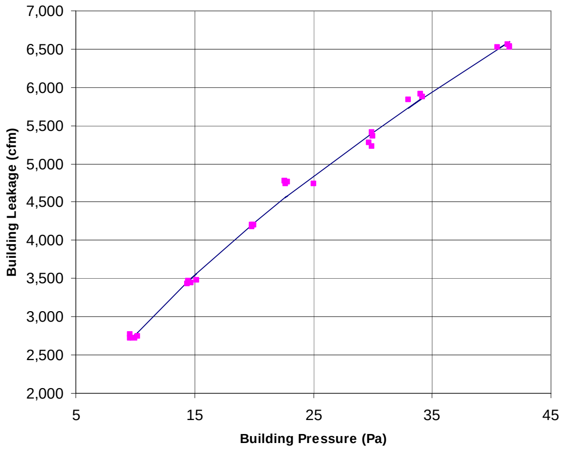

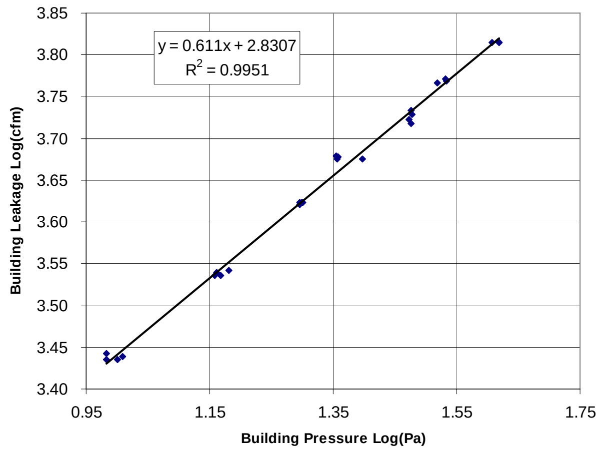

Flow Coefficient (K)	677.1	2524 sq ft. floor area
Exponent (n)	0.611	
Leakage area (LBL ELA @ 4 Pa)	448 sq in	6.68 ELA / 100 sq ft
Airflow @ 50 Pa	7,391 cfm	23.4 ACH @ 50

Test Data:

	Nominal Building Pressure (Pa)	Nominal Flow (cfm)	Ring
1	41.4	6,554	none
2	41.5	6,528	none
3	40.5	6,527	none
4	41.5	6,531	none
5	34.0	5,909	none
6	33.0	5,839	none
7	34.2	5,870	none
8	29.9	5,413	none
9	30.0	5,360	none
10	29.7	5,278	none
11	29.9	5,228	none
12	25.0	4,739	none
13	22.6	4,779	none
14	22.8	4,764	none
15	22.7	4,735	none
16	20.0	4,202	none
17	19.8	4,176	none
18	19.8	4,196	none
19	19.9	4,197	none
20	14.7	3,439	none
21	14.5	3,465	none
22	15.2	3,480	none
23	14.4	3,433	none
24	10.2	2,744	none
25	9.6	2,723	none
26	9.6	2,773	none
27	10	2,725	none

Notes: ELA is leakage area (in square inches) at reference pressure of 4 Pa.
ELA per 100 sq ft is based on total building envelope surface area (ceiling, walls and floor).

Figure A25-7. Test 3 Office Section – Blower Door Test Results

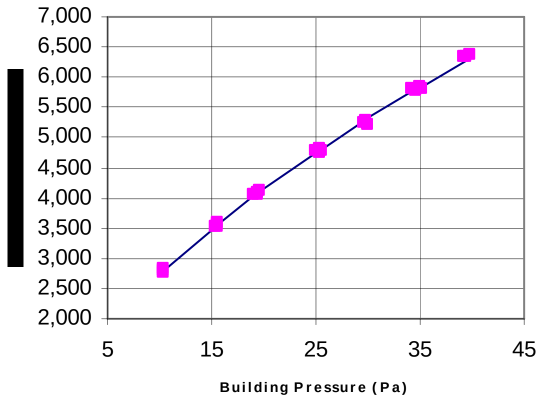

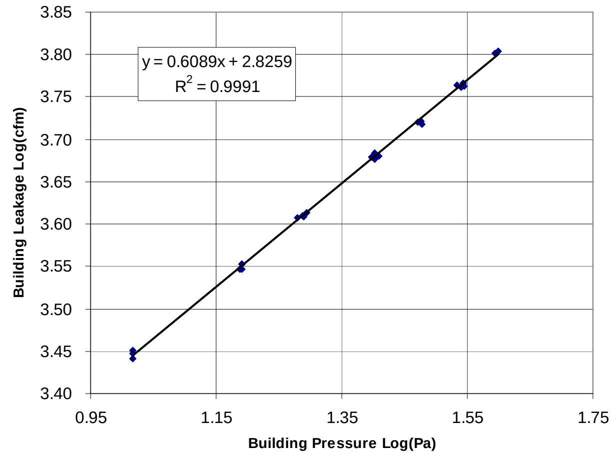

Flow Coefficient (K)	669.7	2524 sq ft. floor area
Exponent (n)	0.609	
Leakage area (LBL ELA @ 4 Pa)	441 sq in	6.59 ELA / 100 sq ft
Airflow @ 50 Pa	7,250 cfm	23.0 ACH @ 50

Test Data:

	Nominal Building Pressure (Pa)	Nominal Flow (cfm)	Ring
1	39.8	6,360	none
2	39.3	6,330	none
3	39.5	6,335	none
4	34.2	5,812	none
5	35.1	5,792	none
6	35.0	5,843	none
7	34.7	5,780	none
8	29.9	5,262	none
9	30.0	5,227	none
10	29.6	5,246	none
11	25.3	4,822	none
12	25.6	4,794	none
13	25.3	4,748	none
14	25.0	4,772	none
15	19.5	4,056	none
16	19.0	4,051	none
17	19.4	4,071	none
18	19.7	4,107	none
19	15.5	3,575	none
20	15.5	3,571	none
21	15.5	3,521	none
22	15.4	3526	none
23	10.4	2759	none
24	10.4	2802	none
25	10.4	2825	none

Notes: ELA is leakage area (in square inches) at reference pressure of 4 Pa.
ELA per 100 sq ft is based on total building envelope surface area (ceiling, walls and floor).

Figure A25-8. Test 4 Office Section – Blower Door Test Results

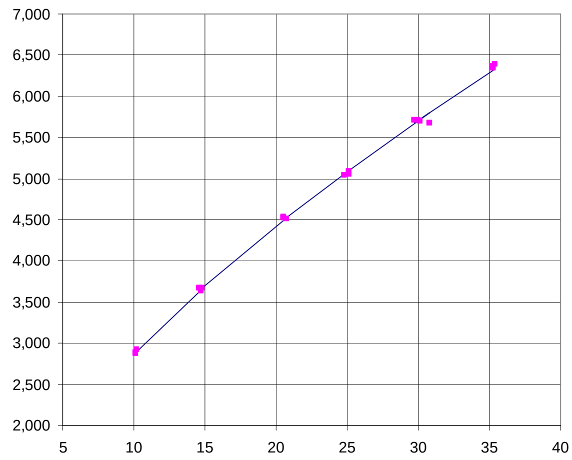

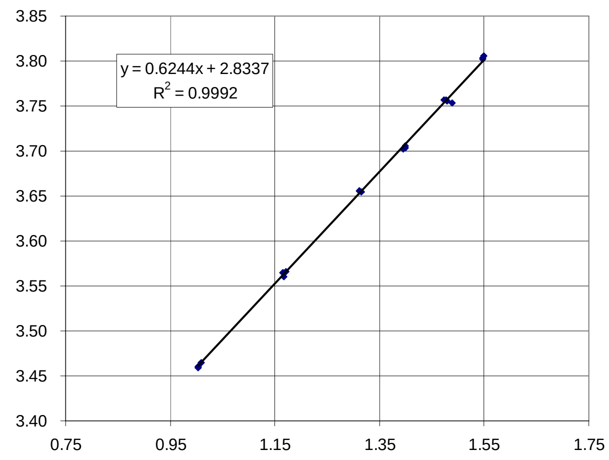

Flow Coefficient (K)	681.9	3324	sq ft. floor area
Exponent (n)	0.624		
Leakage area (LBL ELA @ 4 Pa)	459 sq in	5.02	ELA / 100 sq ft
Airflow @ 50 Pa	7,846 cfm	18.9	ACH @ 50

Test Data:

	Nominal Building Pressure (Pa)	Nominal Flow (cfm)	Ring
1	35.3	6,364	none
2	35.3	6,338	none
3	35.4	6,389	none
4	30.0	5,709	none
5	29.7	5,710	none
6	30.1	5,693	none
7	30.8	5,671	none
8	25.1	5,083	none
9	24.8	5,037	none
10	25.1	5,054	none
11	20.5	4,529	none
12	20.5	4,522	none
13	20.7	4,510	none
14	14.8	3,676	none
15	14.6	3,668	none
16	14.7	3,636	none
17	10.1	2,885	none
18	10.2	2,919	none
19	10.1	2,880	none

Notes: ELA is leakage area (in square inches) at reference pressure of 4 Pa.
ELA per 100 sq ft is based on total building envelope surface area (ceiling, walls and floor).

Figure A25-9. Test 5 Office & Apartment – Blower Door Test Results

Test 6: A/C Units Removed, Basement Open, Apartment Open, Gaskets Installed

The sixth test for the office section used the blower door to depressurize the building to several pressure differences between 10 and 40 Pa. Like Test 5, the door to the upstairs apartment was open. This test differs from test five because foam gaskets installed on about 100 outlets and light switches around the exterior of the building. The test was conducted with all interior doors open and all exterior doors and windows closed.

The total building was depressurized to 40 Pa with the door open to the upstairs apartment. Including the basement, office and the apartment, the building total square footage for this test was approximately 3,324 ft^2. Figure A25-11 shows the office section leakage variation with building pressure for this test. The ELA of the building has an effective leakage area of approximately 4.03 sq in per 100 sq ft of the total envelope and floor area. The total building has an ACH_{50} of 17.4.

Electrical Power Outlet

Communications Outlet (Phone and Internet)

Electrical Switch Outlet (Ceiling Lights)

Figure A25-10. Gaskets Installed on About 100 Outlets along Exterior Walls

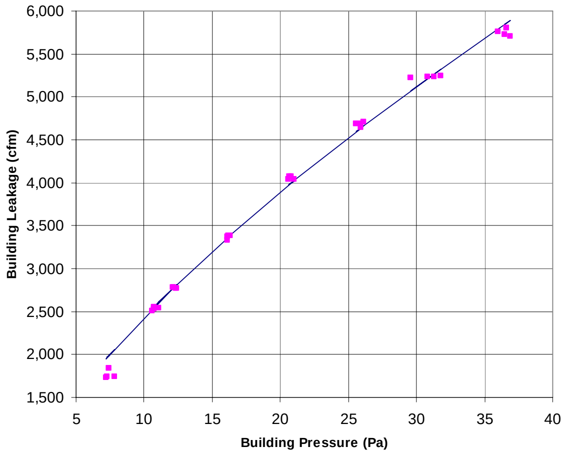

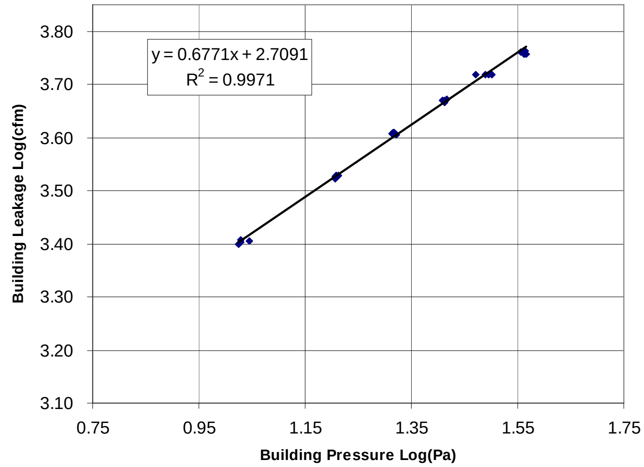

Flow Coefficient (K)	511.9	3324 sq ft. floor area
Exponent (n)	0.677	
Leakage area (LBL ELA @ 4 Pa)	371 sq in	4.05 ELA / 100 sq ft
Airflow @ 50 Pa	7,236 cfm	17.4 ACH @ 50

Test Data:

	Nominal Building Pressure (Pa)	Nominal Flow (cfm)	Ring
1	36.5	5,727	none
2	36.9	5,704	none
3	36.6	5,801	none
4	36.0	5,757	none
5	31.3	5,236	none
6	30.8	5,236	none
7	29.6	5,221	none
8	31.8	5,243	none
9	26.1	4,710	none
10	25.9	4,644	none
11	25.6	4,681	none
12	25.9	4,688	none
13	20.7	4,068	none
14	20.6	4,041	none
15	21.0	4,040	none
16	20.8	4,070	none
17	16.1	3,367	none
18	16.2	3,382	none
19	16.1	3,333	none
20	16.3	3,385	none
21	11.1	2,542	none
22	10.7	2,533	none
23	10.6	2,507	none
24	10.7	2,550	none

Notes: ELA is leakage area (in square inches) at reference pressure of 4 Pa.
ELA per 100 sq ft is based on total building envelope surface area (ceiling, walls and floor).

Figure A25-11. Test 6 Office & Apartment – Blower Door Test Results

Test 7: A/C Units Removed, Basement Half-Door Taped Off, Apartment Open, Gaskets Installed
The seventh test for the office section used the blower door to depressurize the building to several pressure differences between 10 and 40 Pa. The test was conducted with all interior doors open and all exterior doors and windows closed.

The half-door from the full basement to the half basement was taped off using duct mask and the door to the apartment was open. Figure A25-13 shows the office section leakage variation with building pressure for this test. The ELA of the building has an effective leakage area of approximately 3.79 sq in per 100 sq ft of the total envelope and floor area. The total building has an ACH_{50} of 17.1.

Figure A25-12. Basement Half Door Tapped Off (Left) and Exterior Basement Door (added for Tests 6 & 7)

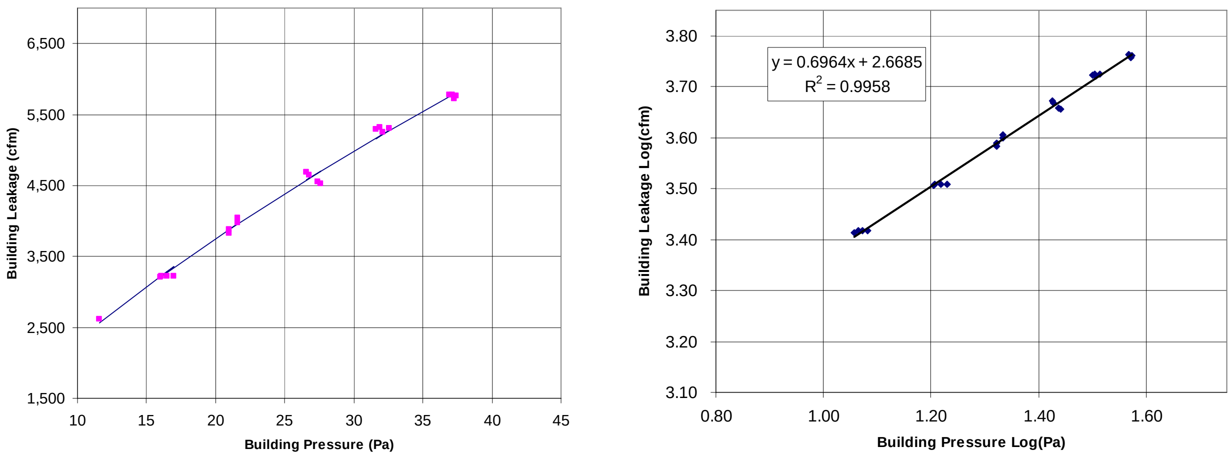

Flow Coefficient (K)	466.1	3324	sq ft. floor area
Exponent (n)	0.696		
Leakage area (LBL ELA @ 4 Pa)	347 sq in	3.79	ELA / 100 sq ft
Airflow @ 50 Pa	7,105 cfm	17.1	ACH @ 50

Test Data:

	Nominal Building Pressure (Pa)	Nominal Flow (cfm)	Ring
1	37.4	5,763	none
2	37.3	5,721	none
3	36.9	5,783	none
4	37.1	5,777	none
5	31.9	5,317	none
6	32.6	5,309	none
7	31.6	5,287	none
8	32.1	5,254	none
9	26.6	4,691	none
10	26.8	4,648	none
11	27.6	4,526	none
12	27.4	4,555	none
13	21.0	3,822	none
14	21.0	3,882	none
15	21.6	4,036	none
16	21.6	3,971	none
17	16.0	3,203	none
18	16.1	3,225	none
19	17.0	3,221	none
20	16.5	3,223	none
21	11.6	2,619	none
22	11.8	2,616	none
23	12.1	2,618	none
24	11.4	2,596	none

Notes: ELA is leakage area (in square inches) at reference pressure of 4 Pa.
ELA per 100 sq ft is based on total building envelope surface area (ceiling, walls and floor).

Figure A25-13. Test 7 Office & Apartment – Blower Door Test Results

<u>Pressure Mapping (Blower Door Testing)</u>

The air pressure relationships in the building were determined using a digital micro-manometer (DG 700) with the blower door operating. All interior doors were opened. The building was depressurized to around 40 pascals. Figure A25-14 shows the pressure drops across the interior doors when closed. The five office spaces had similar drops with the largest office at 14.4 pascals and the smallest offices around 11. The conference room had a very large pressure drop indicating the space is not closely coupled with the rest of the office when the door is closed.

We measured the pressure drop due to the exhaust fans in the bathroom by closing the doors and turning on the fans. The bathroom with an exterior wall was depressurized by1.5 Pa and the other bathroom had a drop of 1.4 Pa.

Figure A25-15 shows the pressure drops across the drop ceiling at several points in the office. The pressure drops were 2.5 to 5 pascals, indicating some degree of leakage above the ceiling.

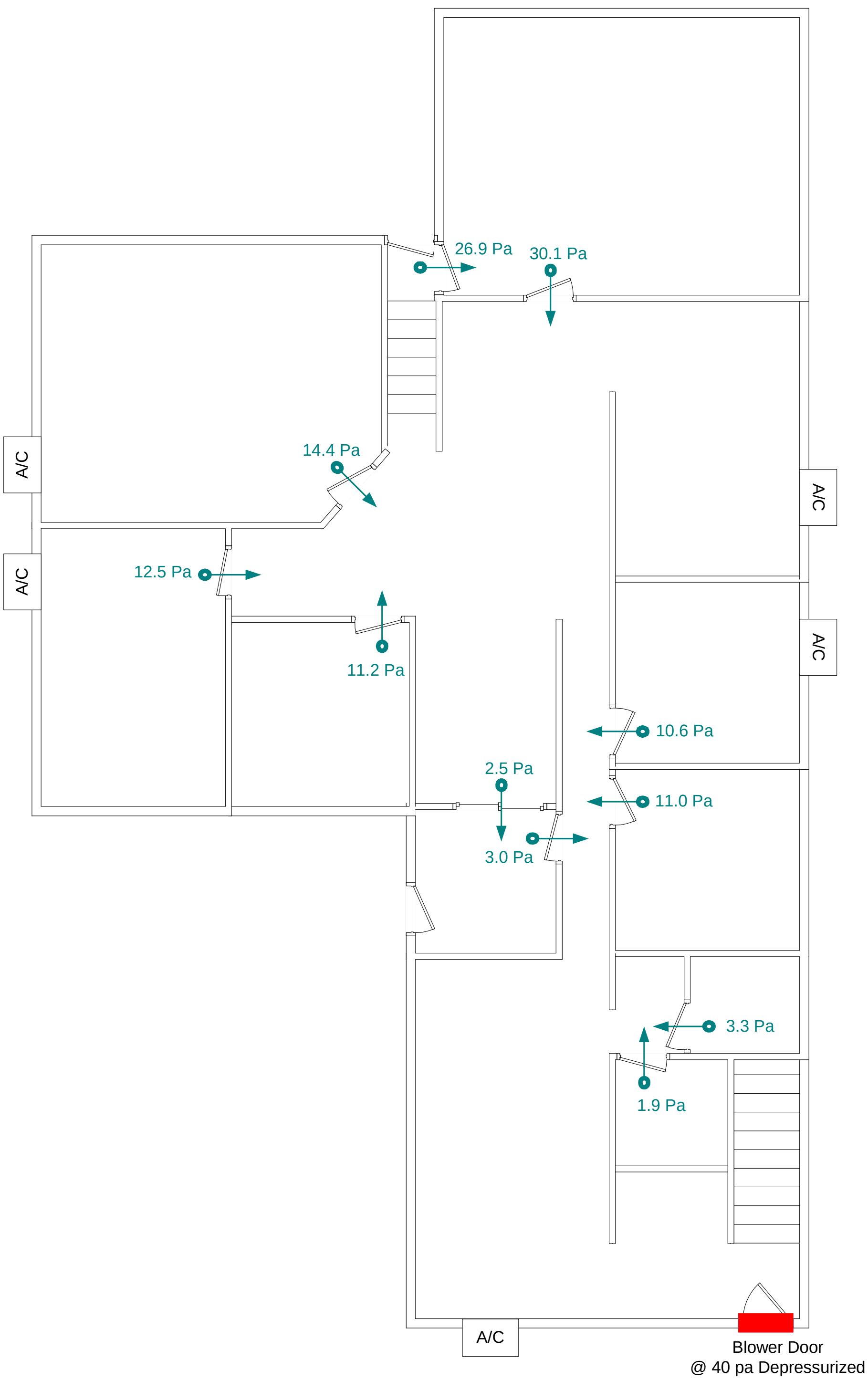

Office Depressurized 40 Pa - A/C Units Installed (Test 1)

Figure A25-14. Office Pressure Drops across Closed Doors

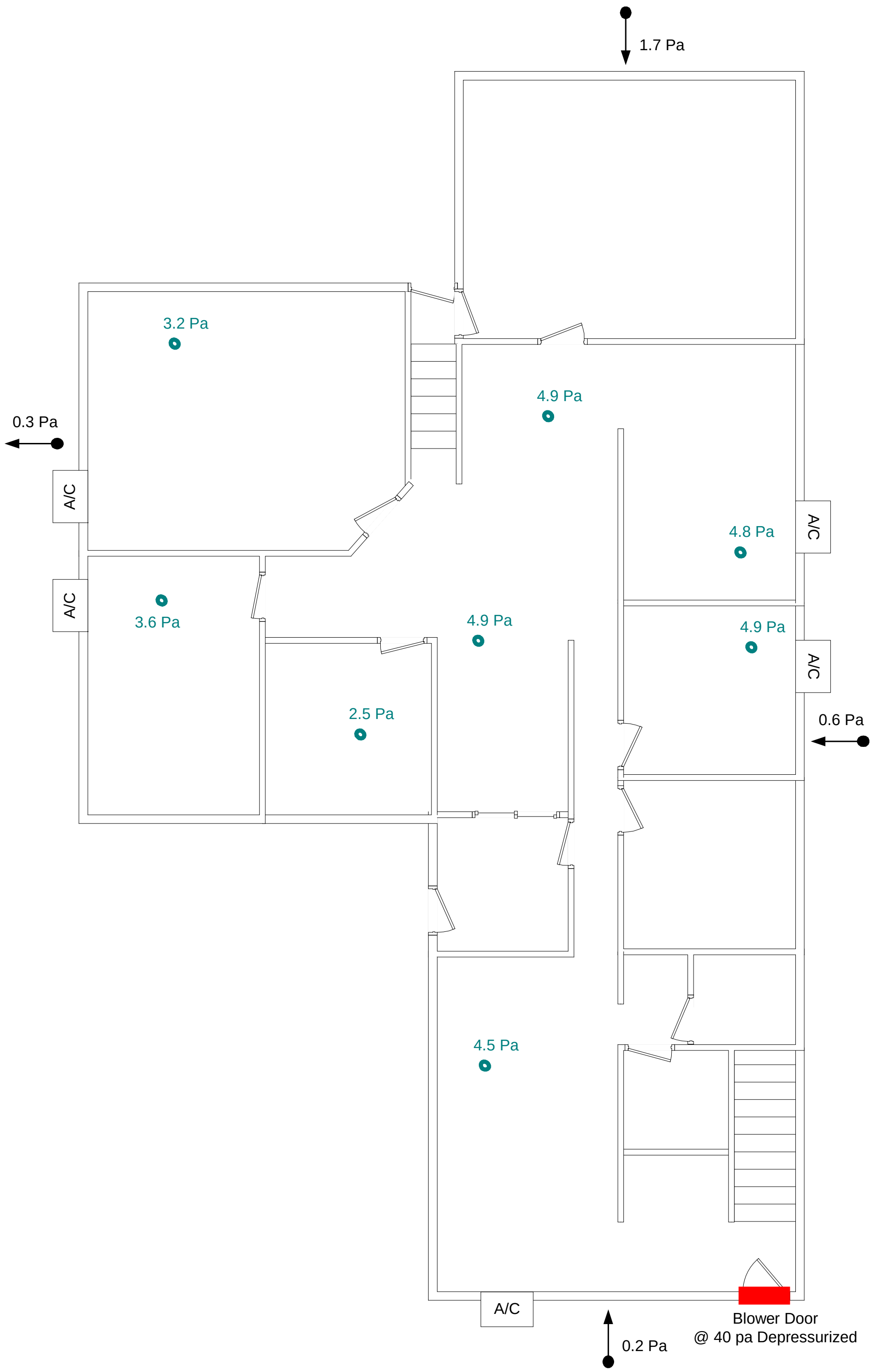

Office Depressurized 40 Pa - A/C Units Installed (Test 1)

Figure A25-15. Office Pressure Drops across Drop Ceiling

Space Conditions

Figure A25-16 shows the average temperature profiles for one small office in the building based on temperature readings taken with a HOBO data logger. The thick line shows the average for each hour while the shaded region corresponds to one standard deviation about the average. The dotted lines correspond to the minimum and maximum for each hour. A sensor was placed in the office on the west side of the building that was not adjacent to the bathrooms. The temperature profiles show that the temperature varies greater during weekdays (when occupied) than on the weekends.

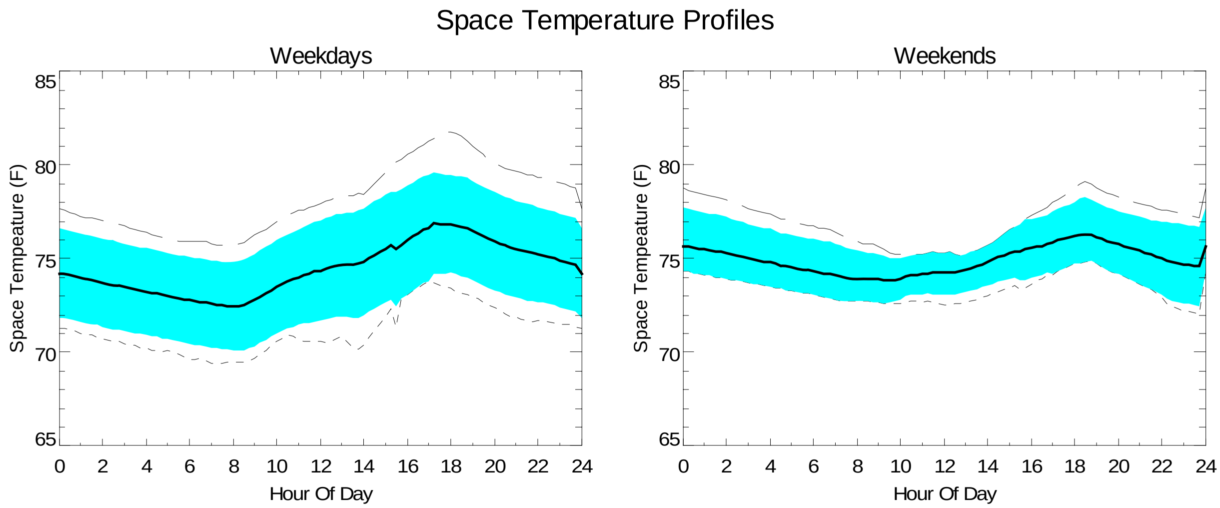

Figure A25-16. Measured Space Temperature Profile (September 5-21)

Figure A25-17 shows profile plots of the relative humidity in the office. A window air conditioner was installed in this office during the period. The occupant of the office runs the air conditioner based on personal comfort. Examining the relative humidity data, the space humidity was lower during the weekdays than weekends, from the use of the air conditioner during cooling periods. On the weekends, the RH remained around 50-55 %.

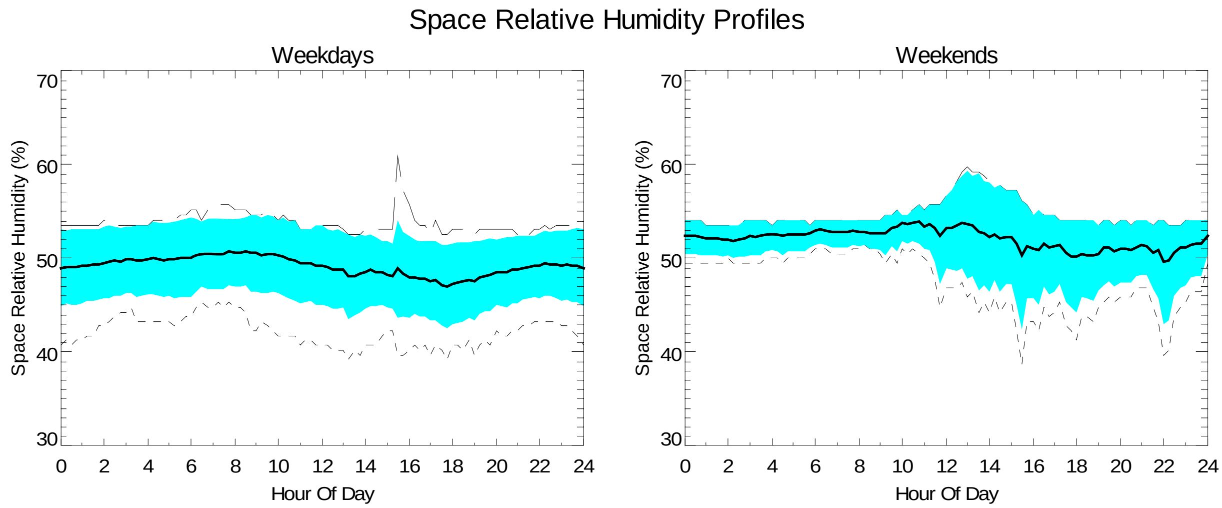

Figure A25-17. Measured Space Relative Humidity Profile (September 5-21)

Dynamic Building Pressure and Wind Speed

A private weather station is located ½ mile from this office (www.fenneralps.com). We gathered wind speed and direction data from this site at 10-minute intervals for several days from September 27 to October 4, 2006. For a portion of that period, we also collected building pressurization data. The interior pressure was measured in the Back Room of the office area (see Figure A25-2). Exterior pressure was measured at about 20 ft from the rear door (in vented canister to protect it from the wind). Pressure readings were collected at 1-minute intervals.

Figure A25-18 Shows the wind and pressure data for a 48 hour period starting at noon on September 29. The building pressure generally increases with wind speed, though the magnitude depends on the wind direction. In some cases the building pressure was negative when the wind came out of the South or Southwest. The instantaneous pressures reach as high as 14 Pa, though the 10-minute average never exceeded 4-5 Pa. Figure A25-19 shows a scatter plot of the 10-minute average data.

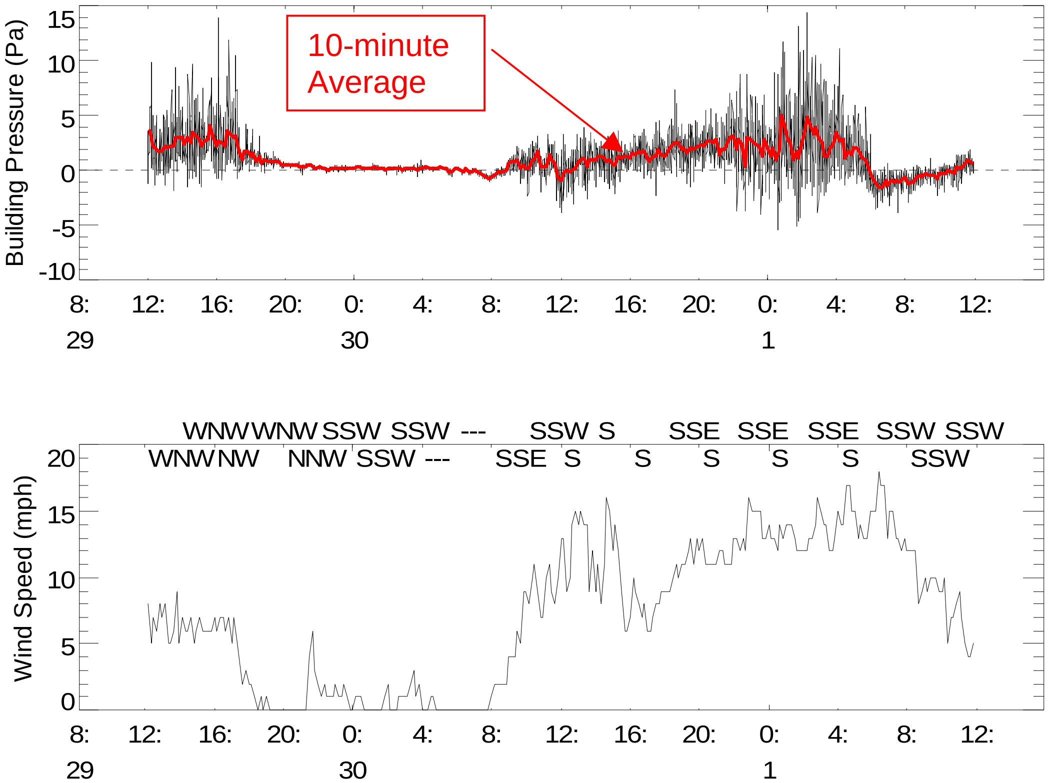

Figure A25-18. Measured Building Pressure and Local Wind Speed

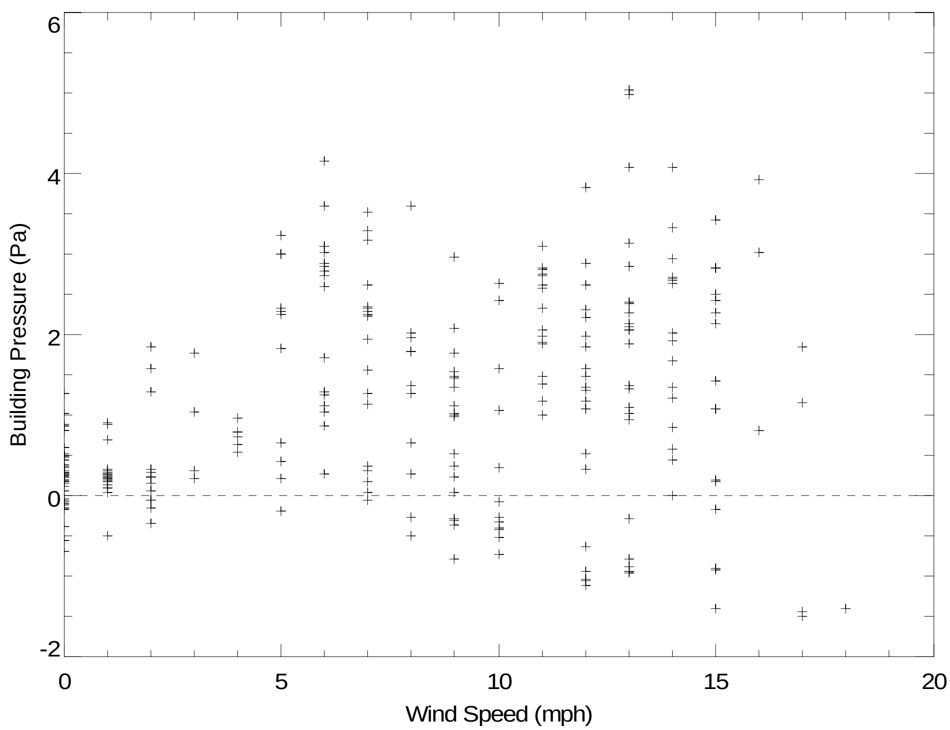

Figure A25-19. Measured Building Pressure vs. Wind Speed (10-minute Averages)

Utility Bills

Electric Bills are available starting on June 20, 2006. The commercial space has only been occupied since June 15, so the electric use in the first bill is artificially low. No. 2 fuel oil, used for water and space heating, has only been delivered three times. Since the current owners have only occupied the property since May 2006, there is insufficient data to complete a full utility bill analysis

Table A25-3. Utility Bills for Property

Electric Bills		No. 2 Fuel Oil Bills	
Date	**(kWh)**	**Date**	**(gals)**
Oct 18, 2006	1,473	Oct 27, 2006	205
Sep 17, 2006	1,712	Sep 5, 2006	150
Aug 16, 2006	2,700	May 31, 2006	100
Jul 18, 2006	2,352		
Jun 20, 2006	890		

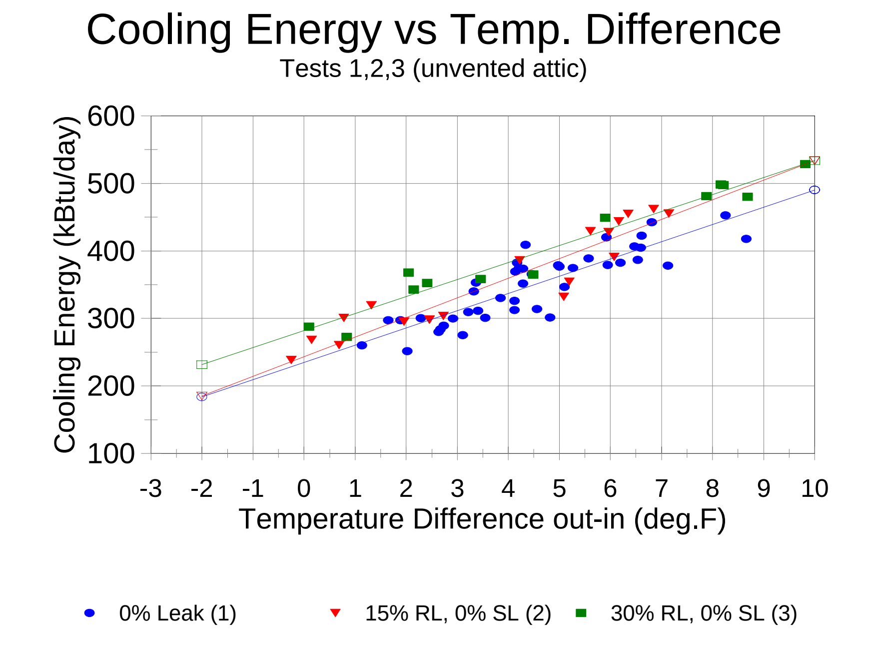

Figure B-1

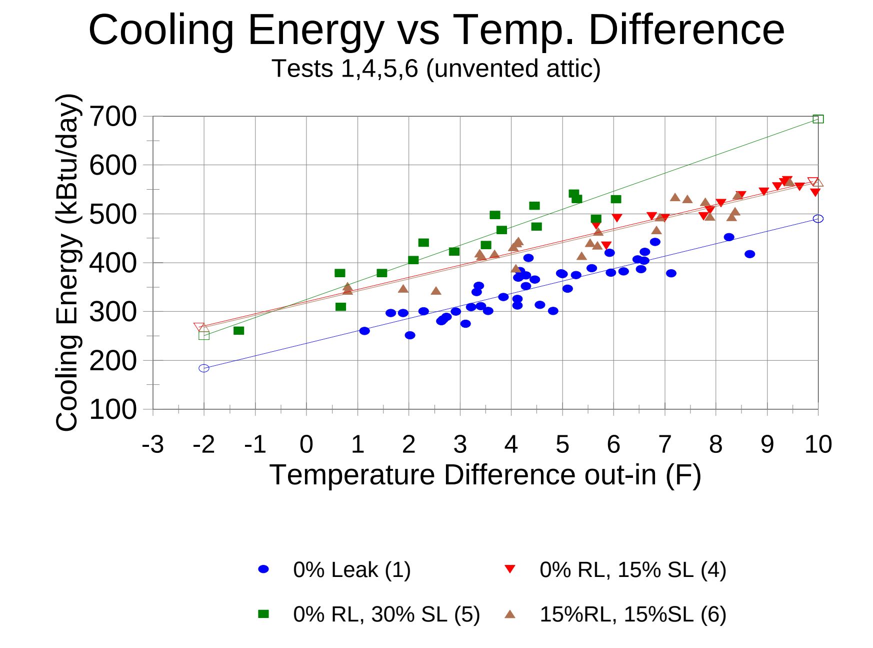

Figure B-2

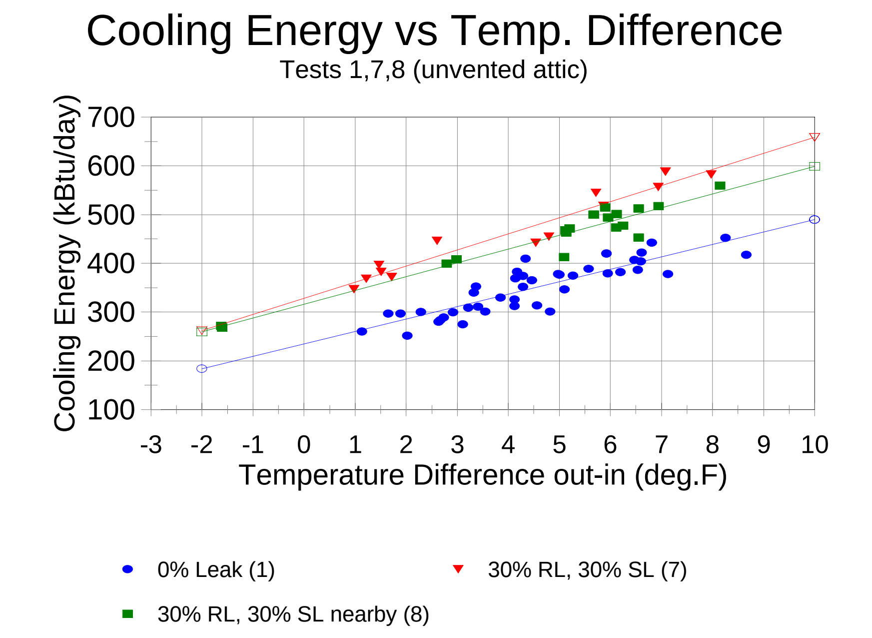

Figure B-3

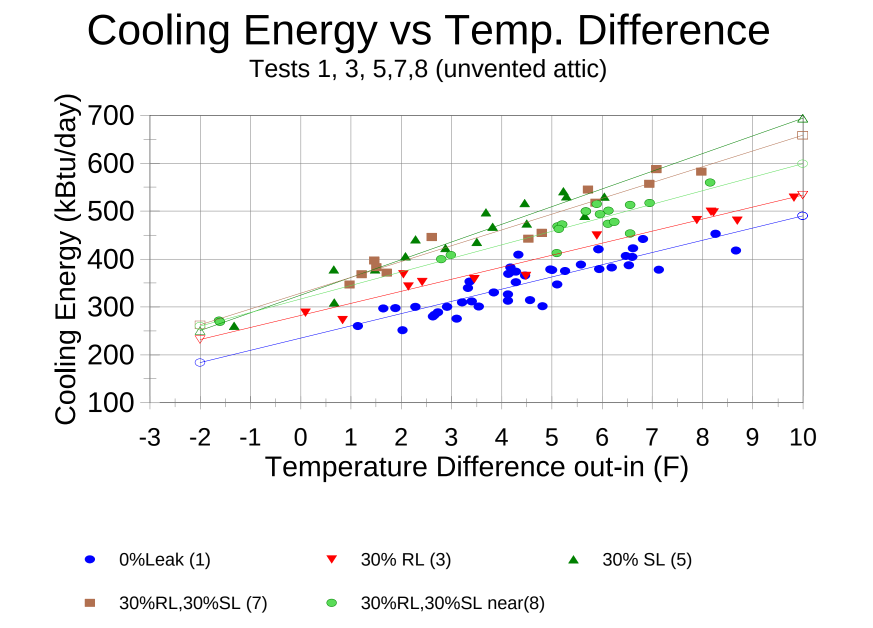

Figure B-4

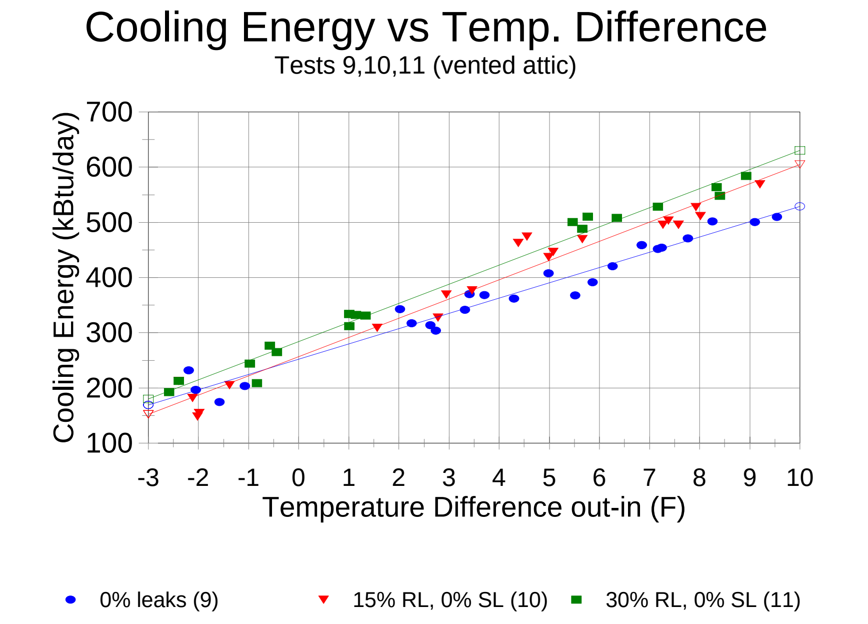

Figure B-5

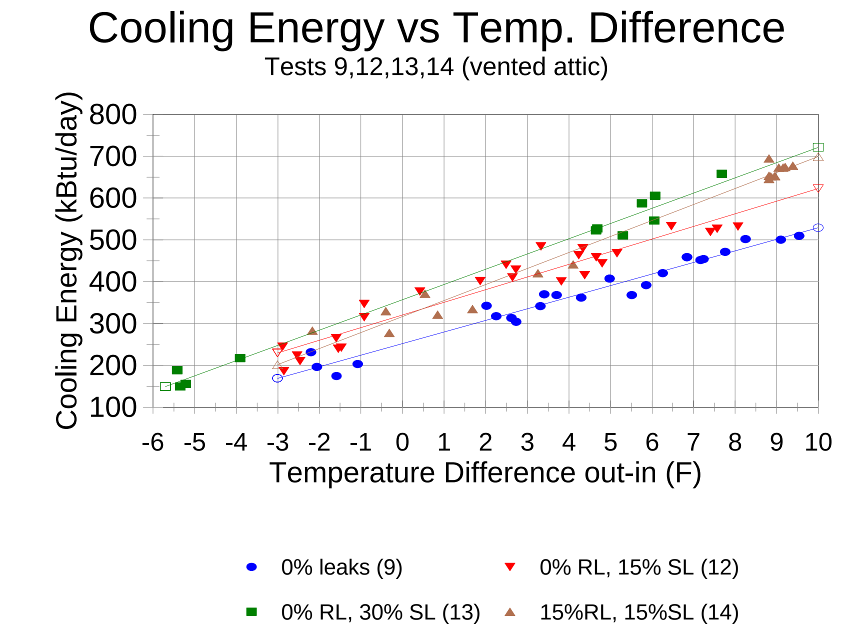

Figure B-6

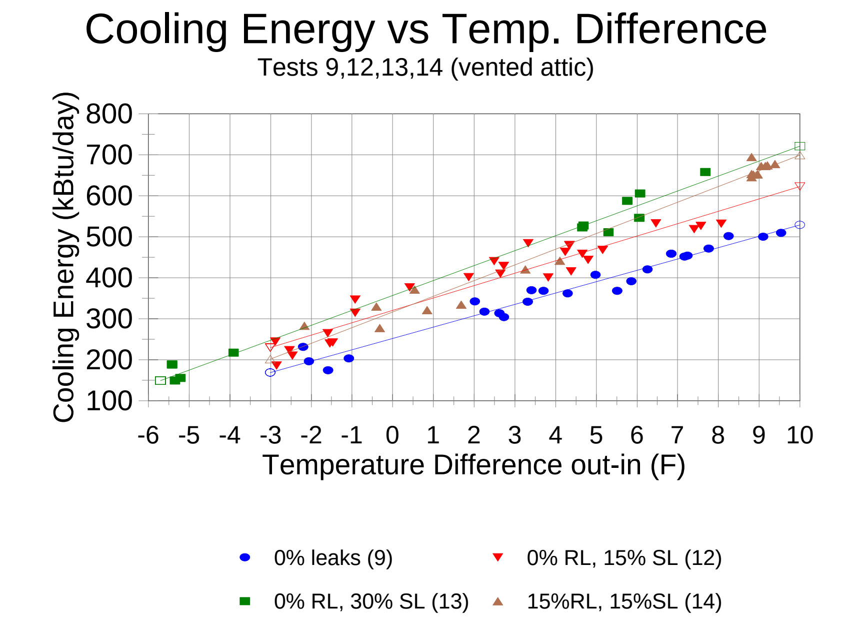

Figure B-7

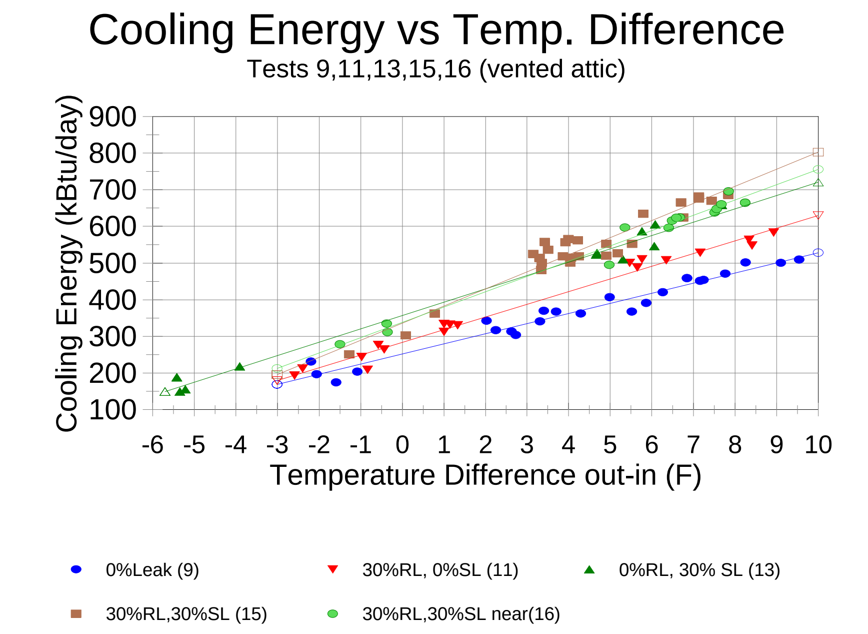

Figure B-8

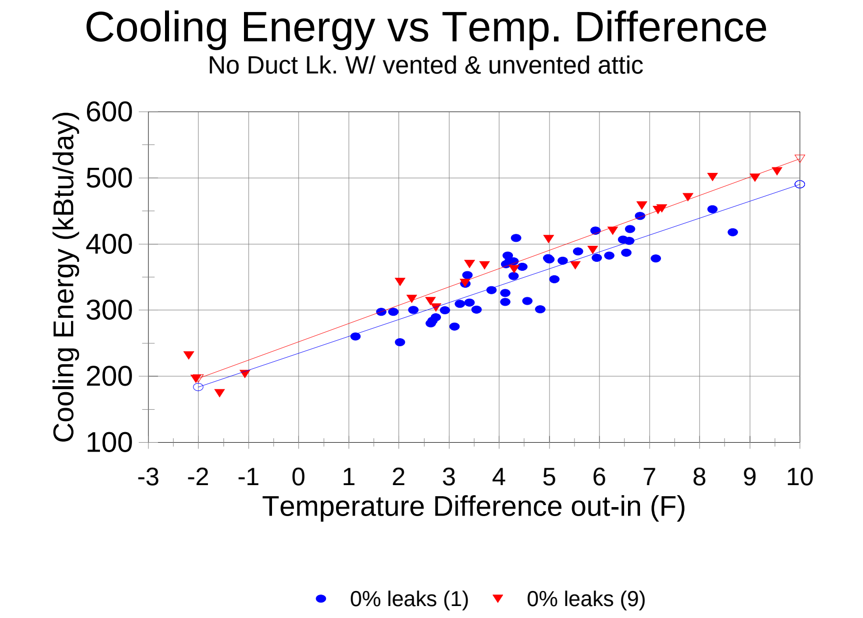

Figure B-9

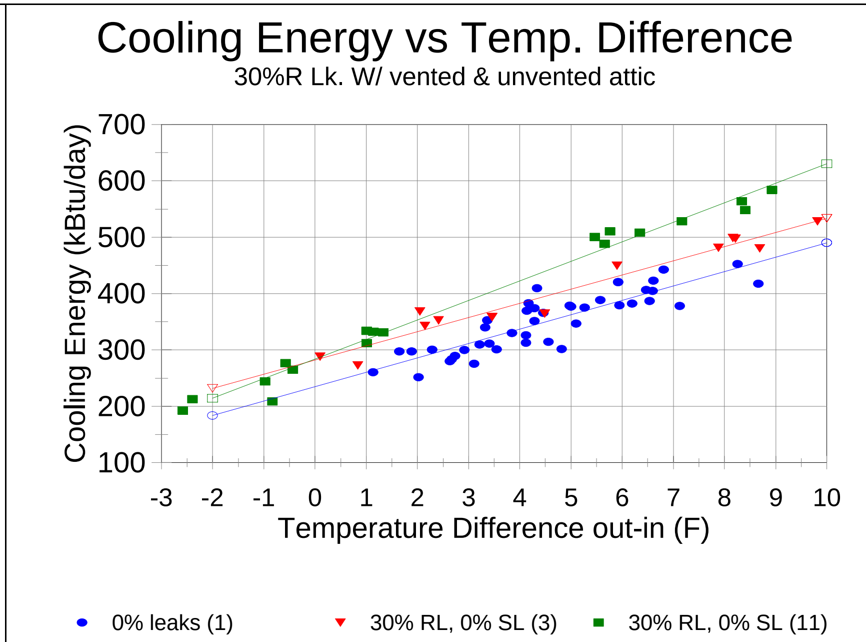

Figure B-10

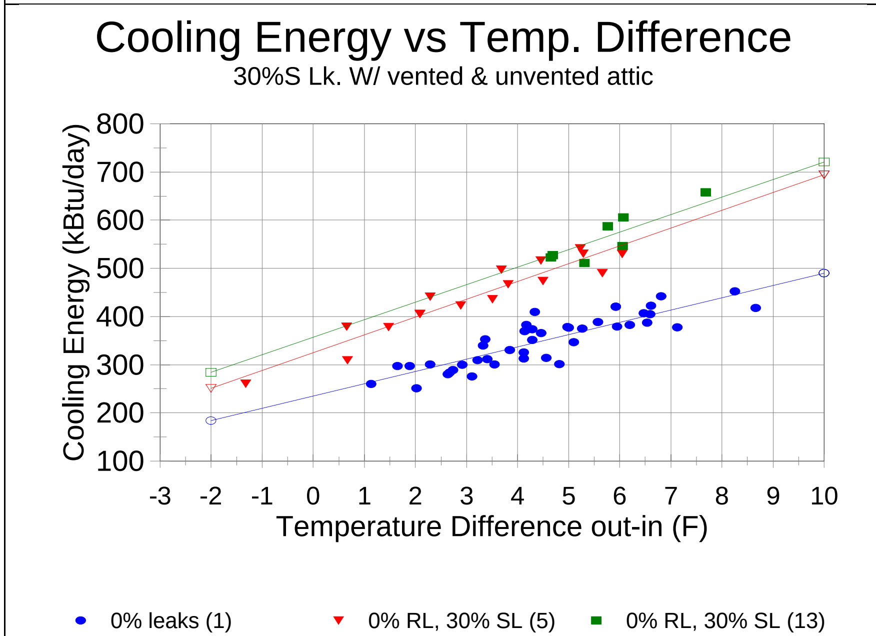

Figure B-11

THIS SPACE LEFT BLANK

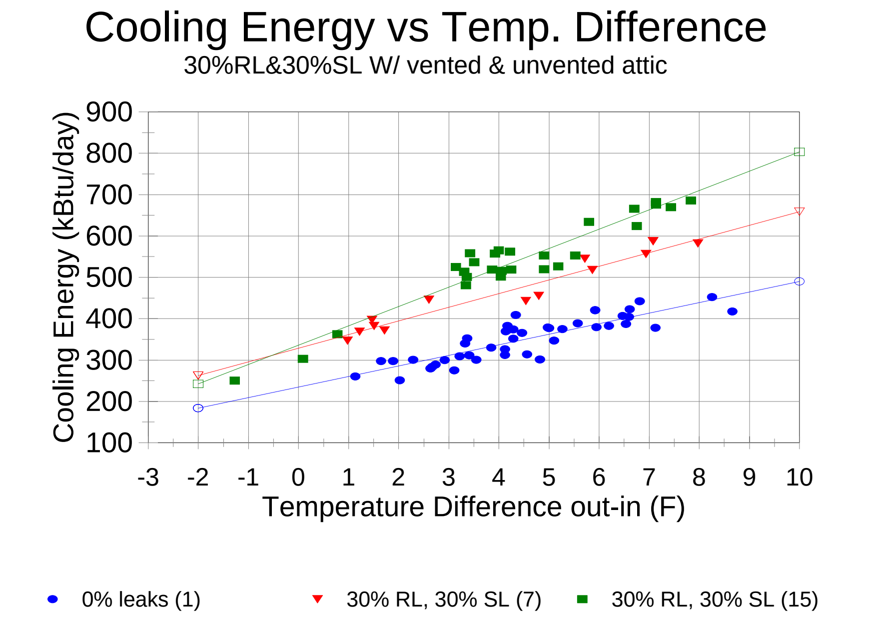

Figure B-12

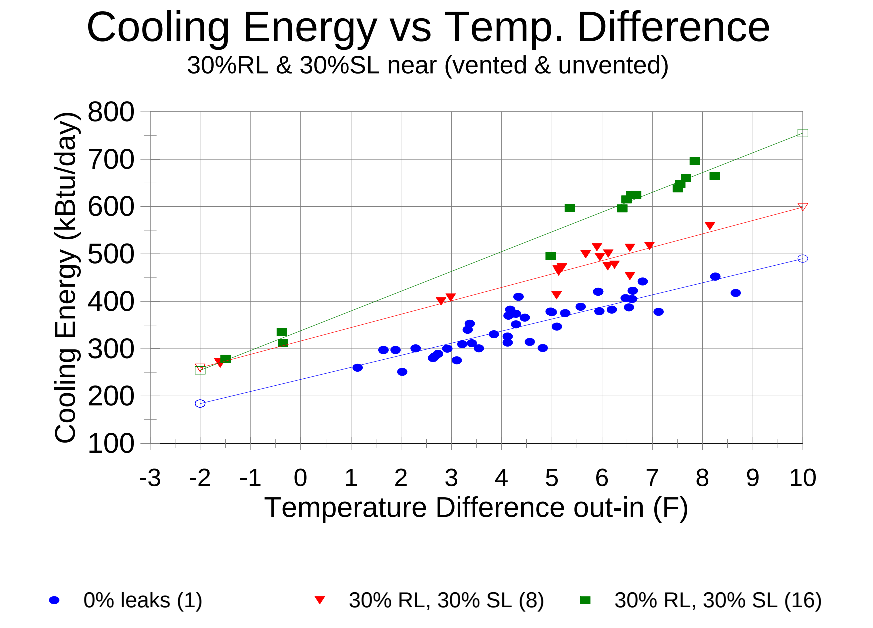

Figure B-13

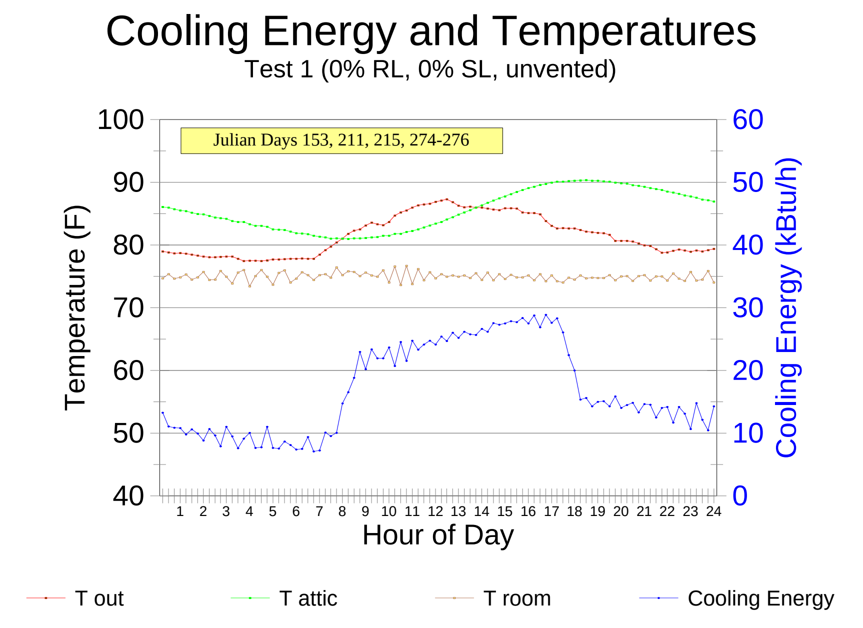

Figure B-14

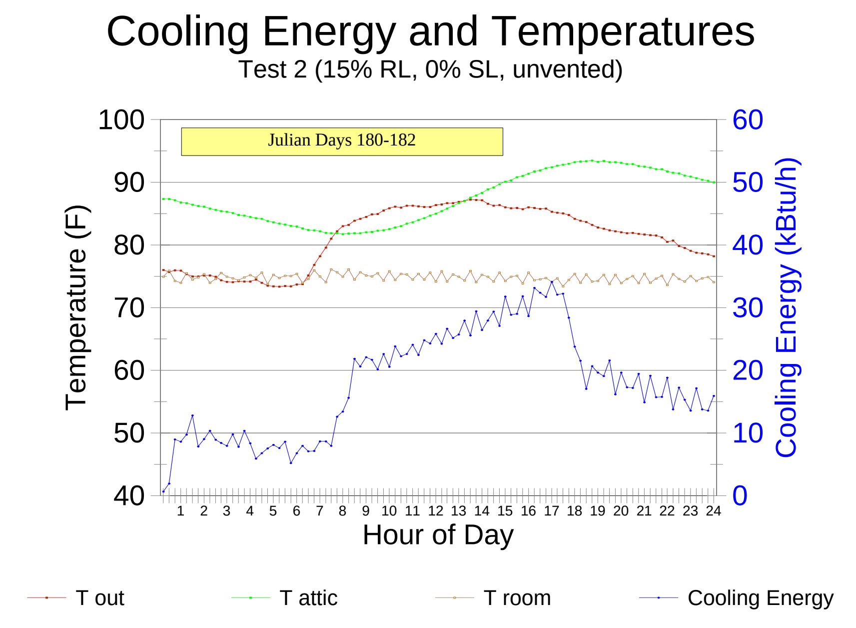

Figure B-15

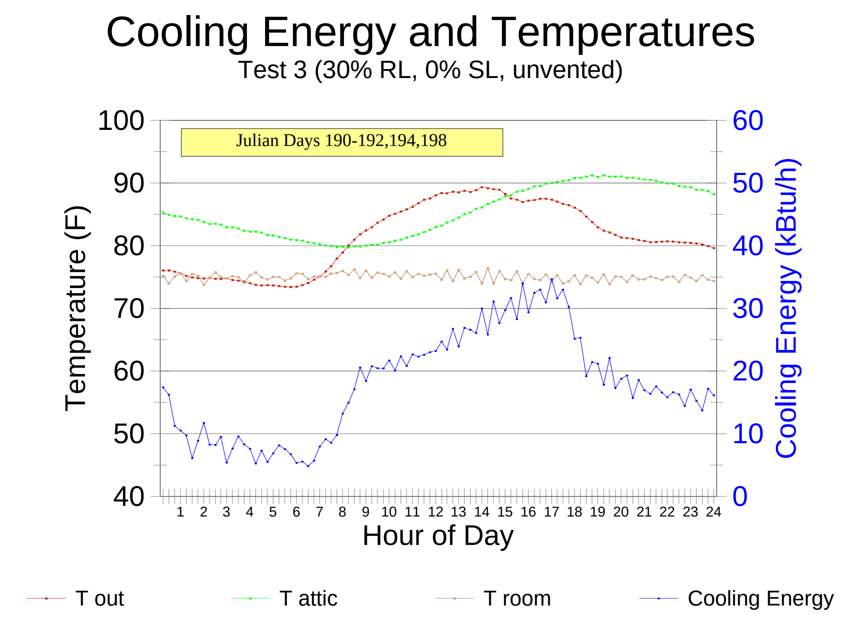

Figure B-16

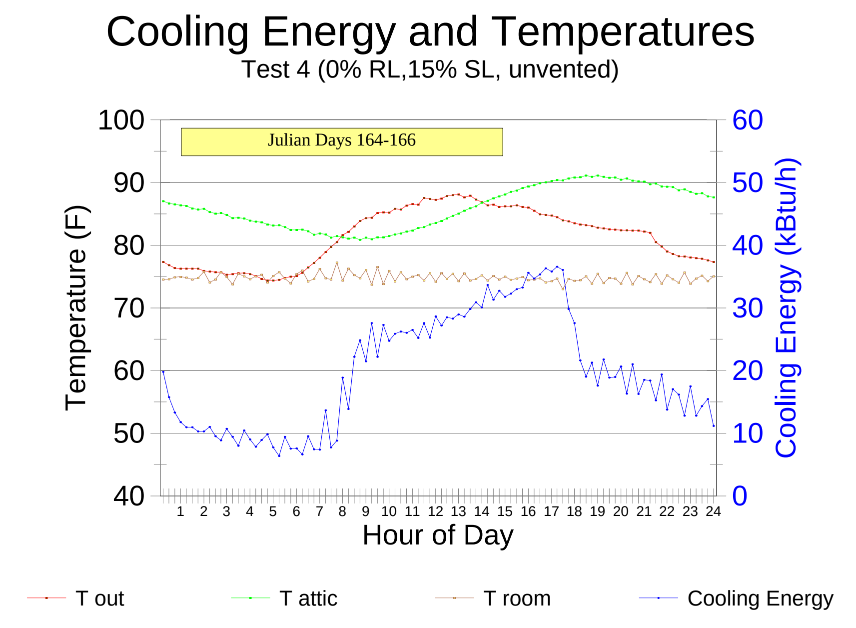

Figure B-17

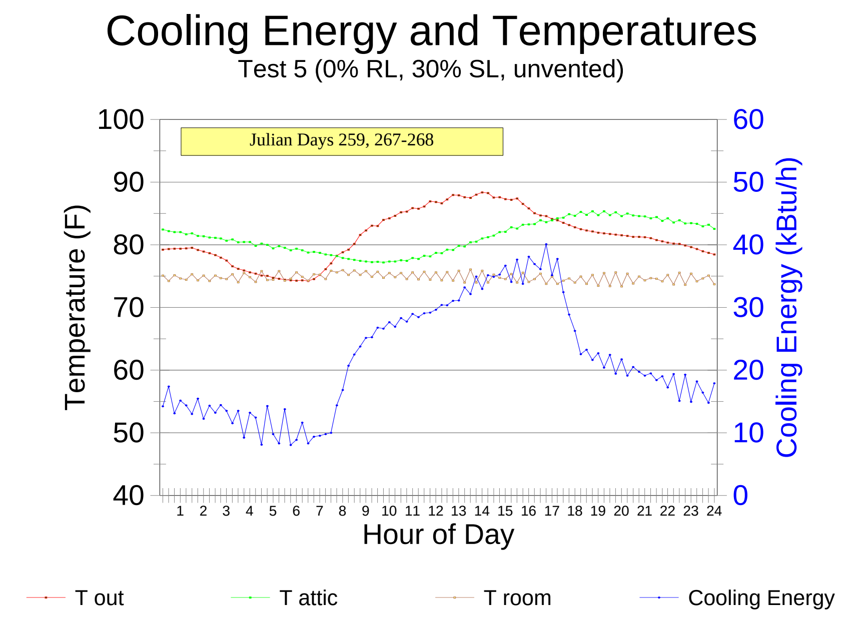

Figure B-18

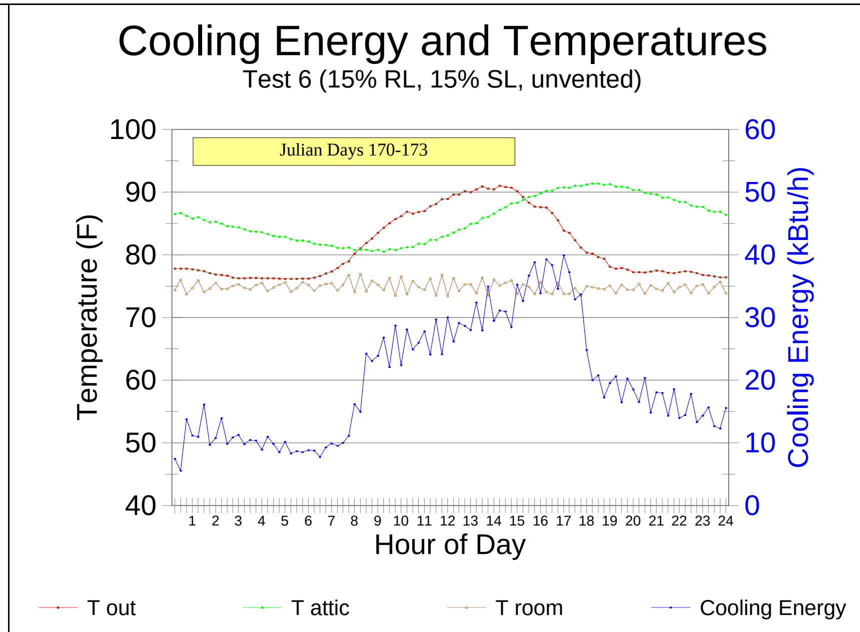

Figure B-19

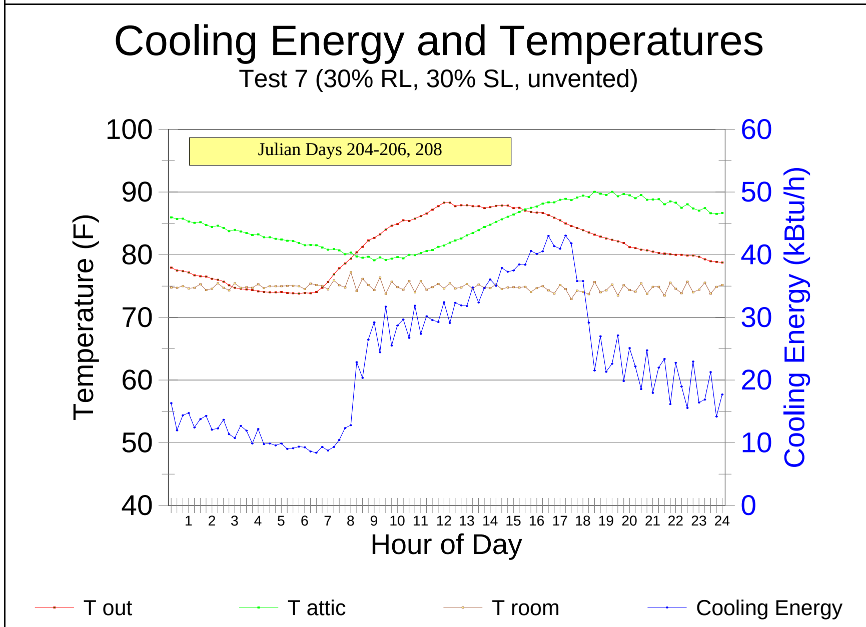

Figure B-20

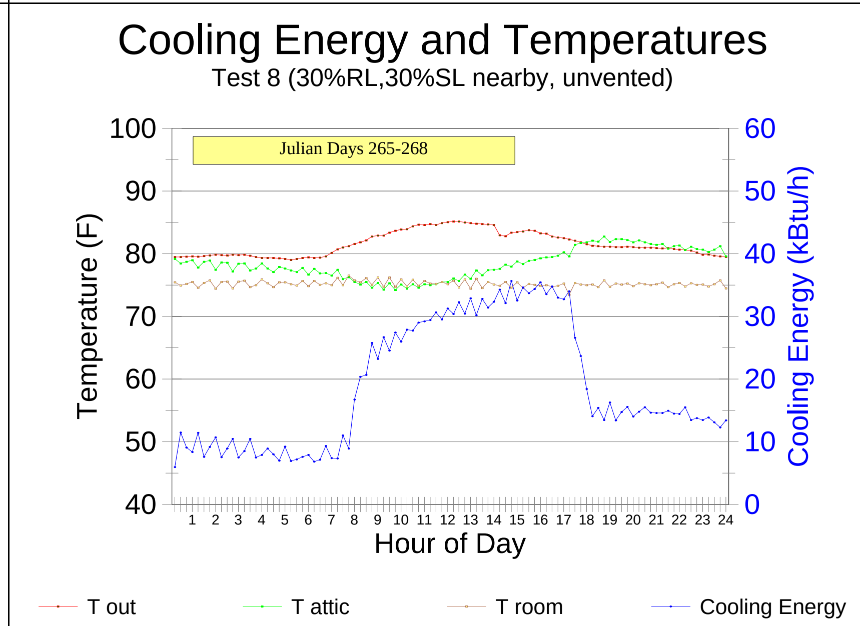

Figure B-21

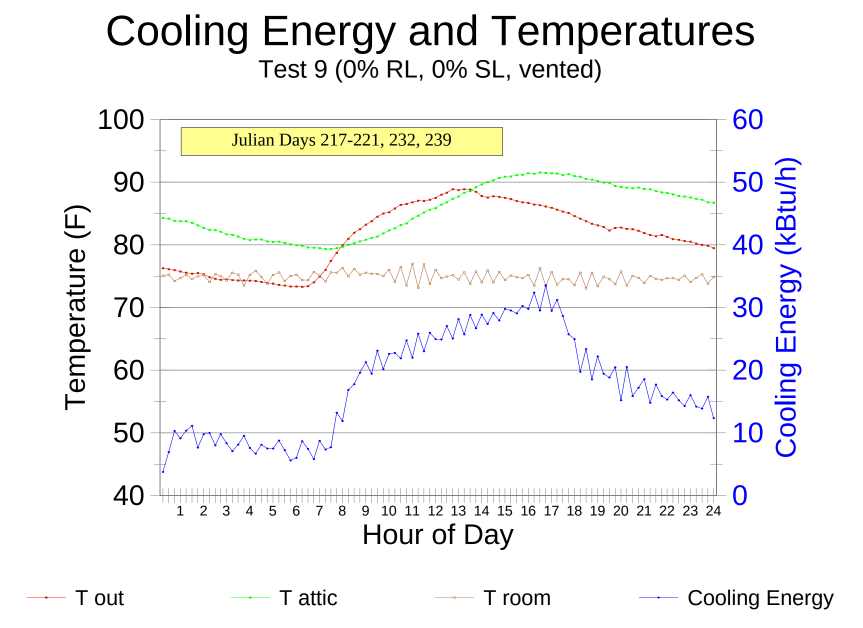

Figure B-22

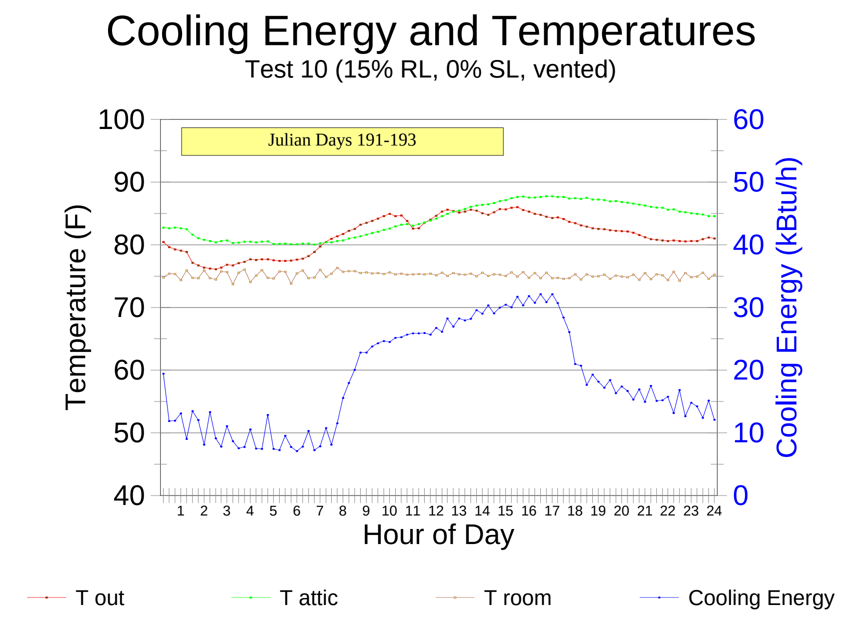

Figure B-23

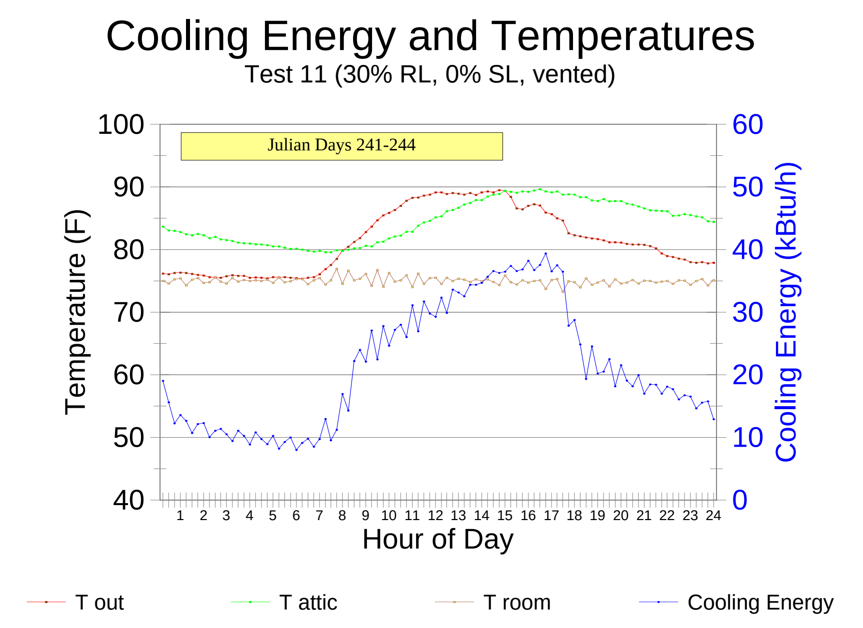

Figure B-24

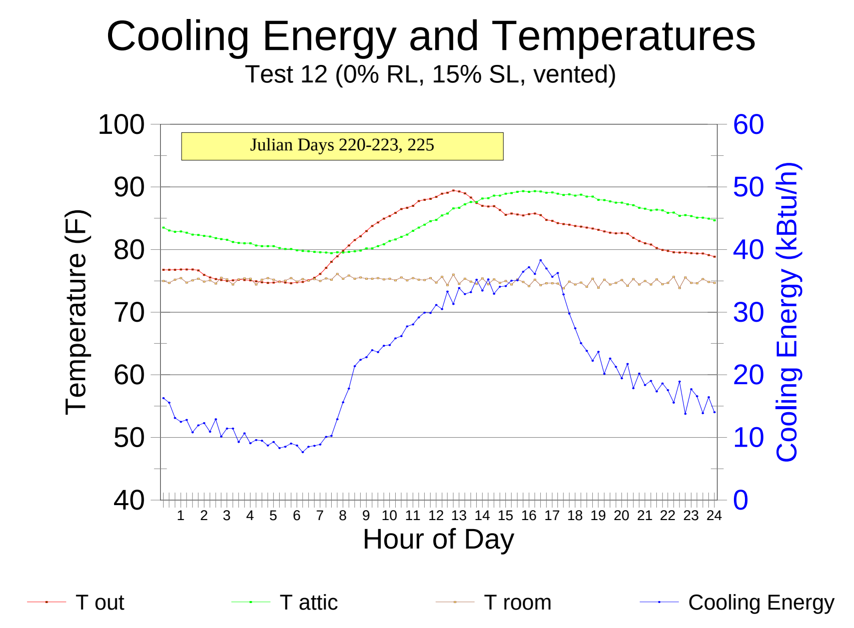

Figure B-25

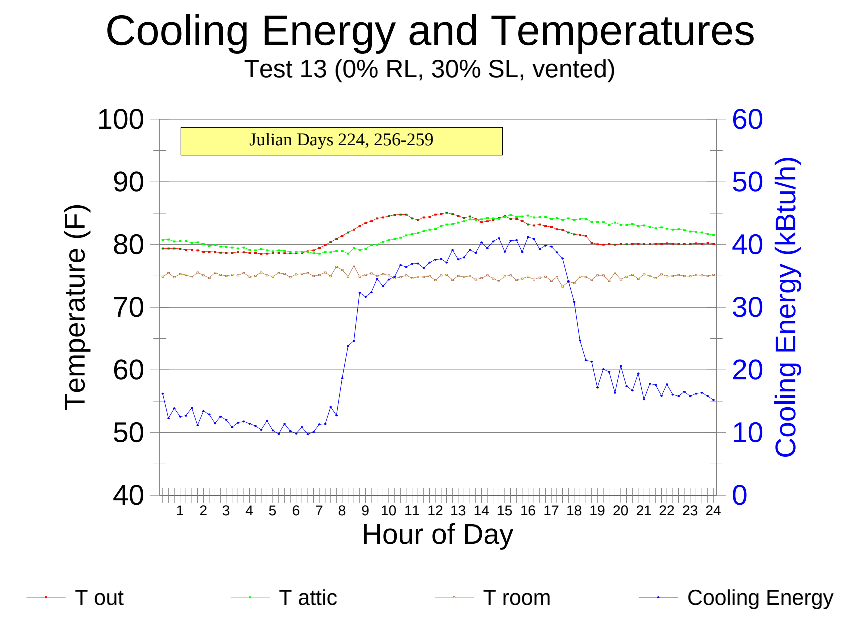

Figure B-26

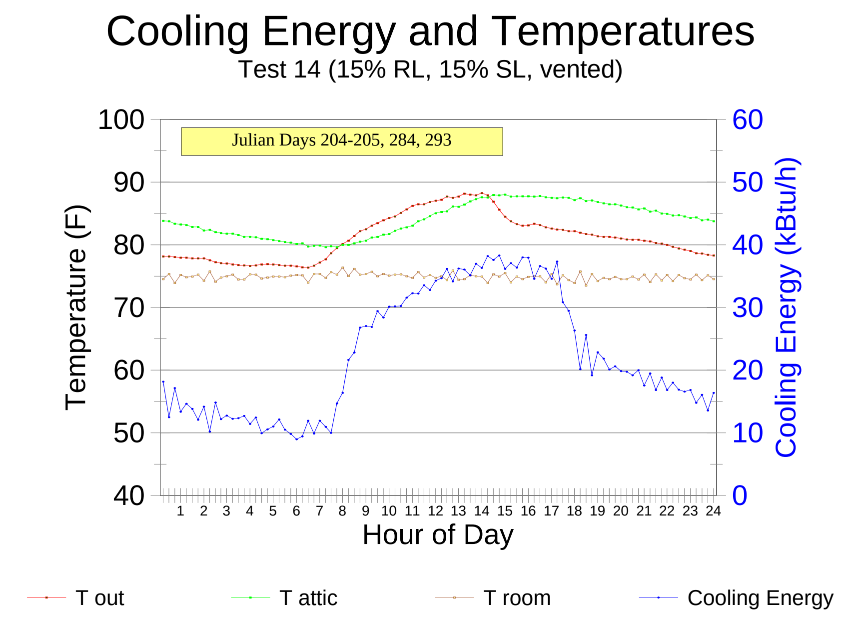

Figure B-27

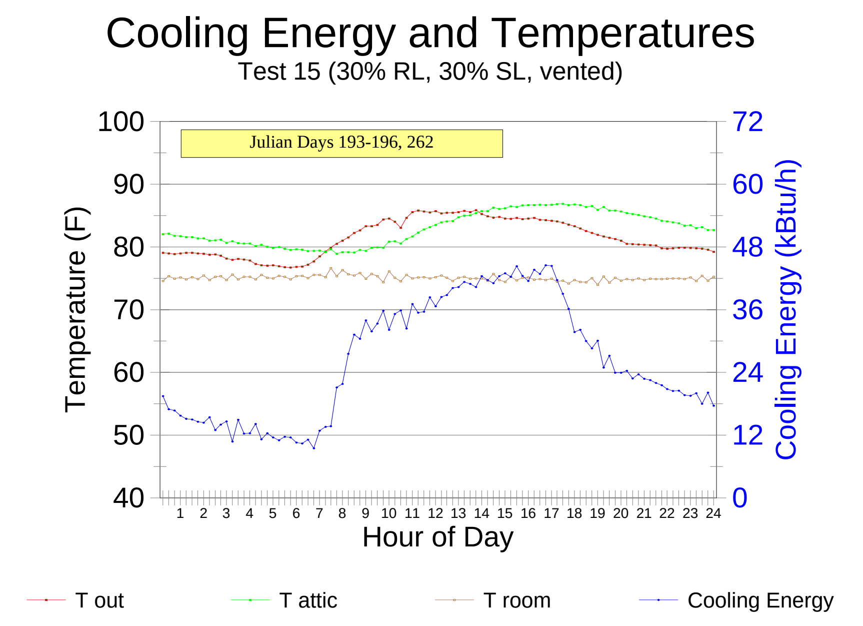

Figure B-28

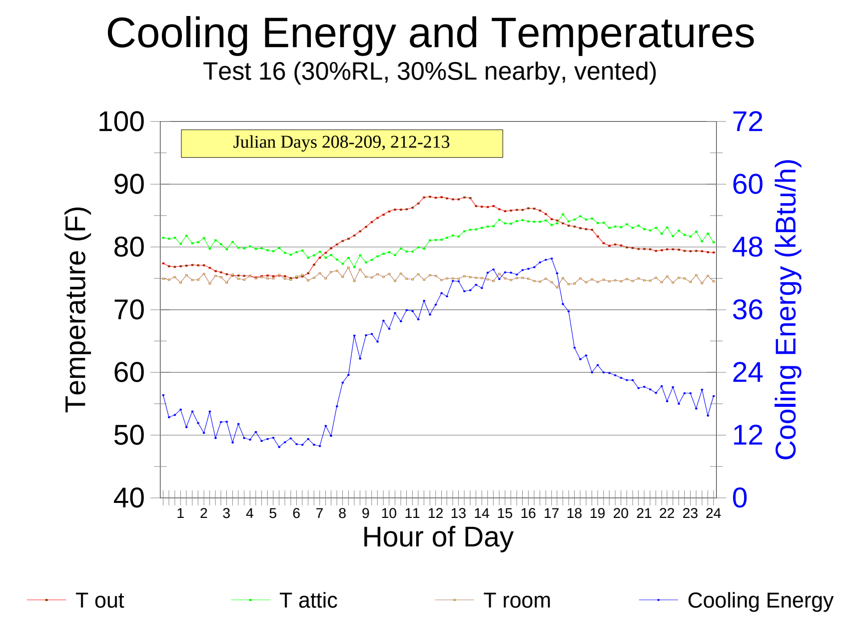

Figure B-29

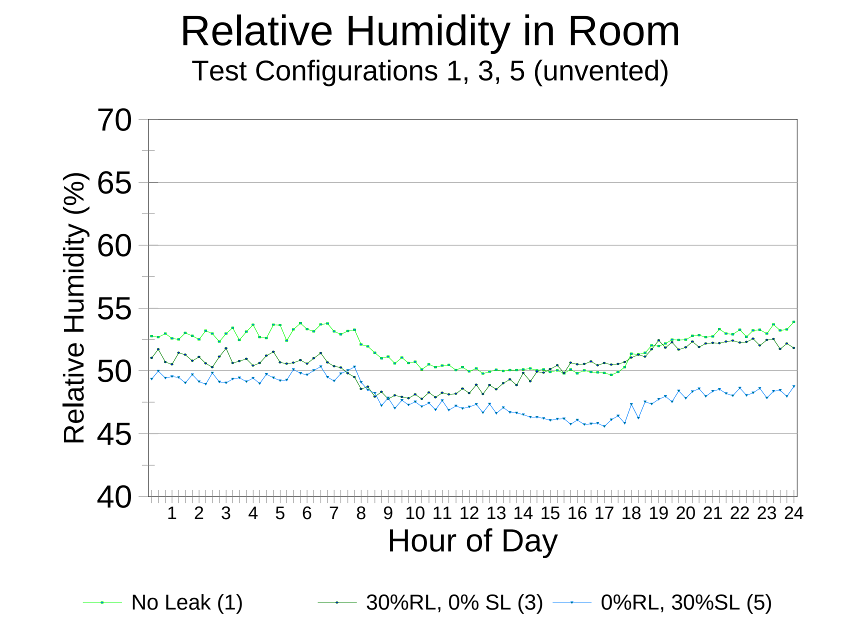

Figure B-30

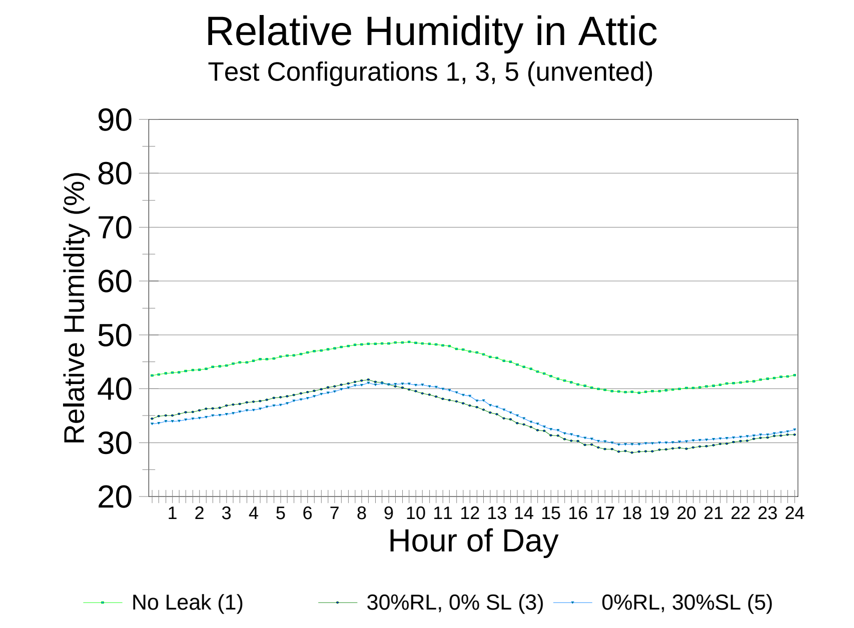

Figure B-31

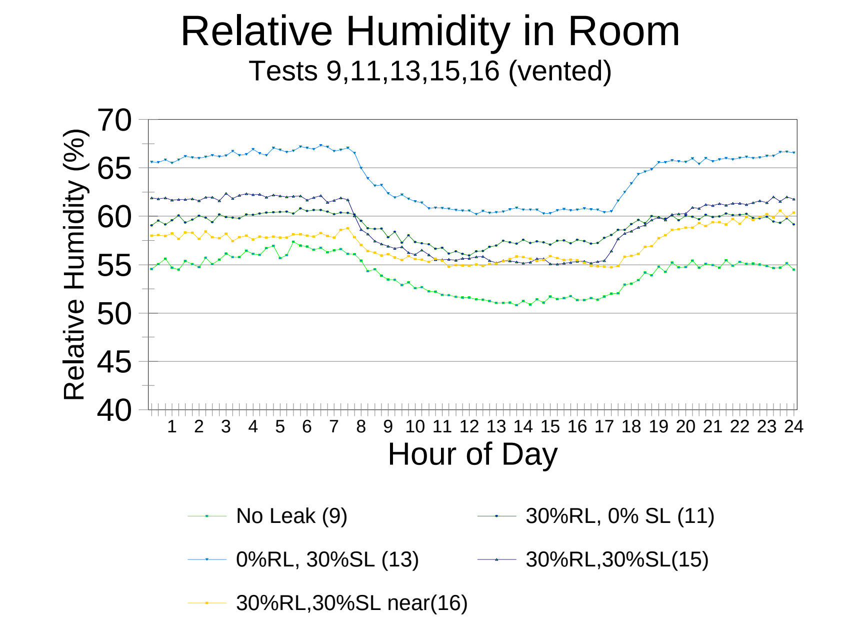

Figure B-32

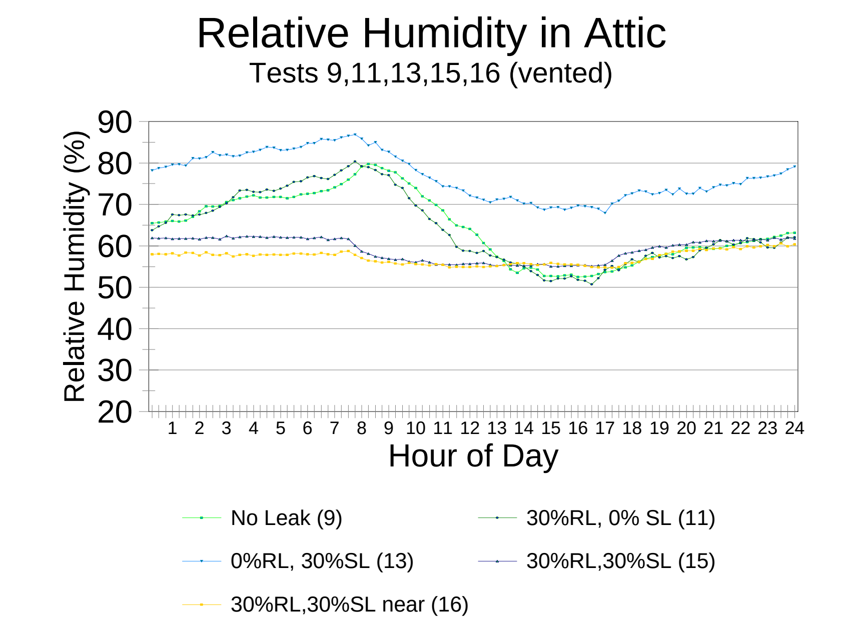

Figure B-33

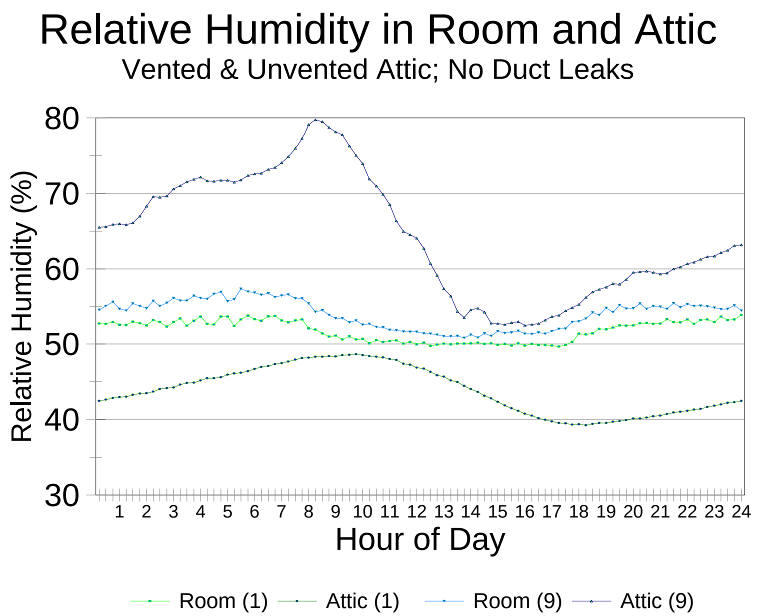

Figure B-34

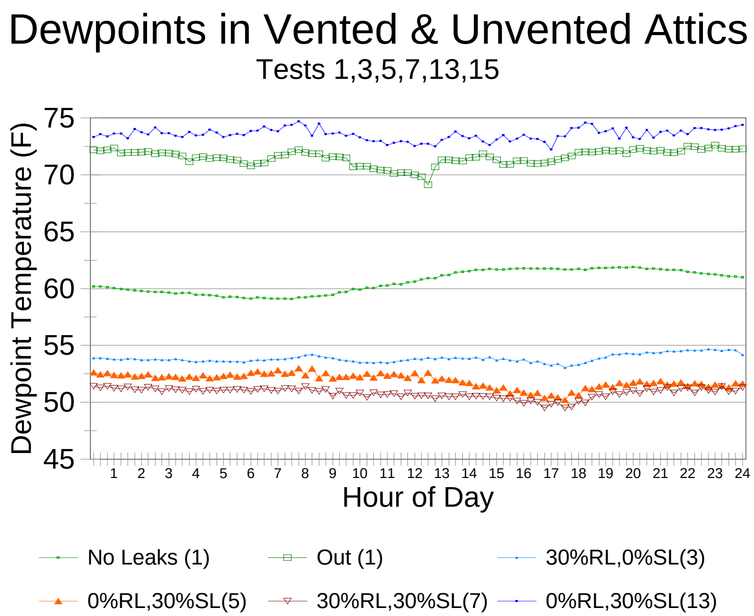

Figure B-35